Exhibit D20

Conceptual Site Model, Investigation and Remediation of Releases and Groundwater Protection and Evaluation, Red Hill Bulk Fuel Storage Facility

JOINT BASE PEARL HARBOR-HICKAM, O'AHU, HAWAI'I

Administrative Order on Consent in the Matter of Red Hill Bulk Fuel Storage Facility, EPA Docket Number RCRA 7003-R9-2015-01 and DOH Docket Number 15-UST-EA-01, Attachment A, Statement of Work Section 6.2, Section 7.1.2, Section 7.2.2, and Section 7.3.2

June 30, 2019
Revision 01

Comprehensive Long-Term Environmental Action Navy
Contract Number N62742-17-D-1800, CTO18F0126

This page intentionally left blank

Conceptual Site Model, Investigation and Remediation of Releases and Groundwater Protection and Evaluation, Red Hill Bulk Fuel Storage Facility

JOINT BASE PEARL HARBOR-HICKAM, O‘AHU, HAWAI‘I

Administrative Order on Consent in the Matter of Red Hill Bulk Fuel Storage Facility, EPA Docket Number RCRA 7003-R9-2015-01 and DOH Docket Number 15-UST-EA-01, Attachment A, Statement of Work Section 6.2, Section 7.1.2, Section 7.2.2, and Section 7.3.2

June 30, 2019
Revision 01

Prepared for:

Defense Logistics Agency Energy
8725 John J Kingman Rd Suite 4950
Fort Belvoir, VA 22060-6222

Prepared by:

AECOM Technical Services, Inc.
1001 Bishop Street, Suite 1600
Honolulu, HI 96813-3698

Prepared under:

Comprehensive Long-Term Environmental Action Navy
Contract Number N62742-17-D-1800, CTO18F0126

This page intentionally left blank

EXECUTIVE SUMMARY

This *Conceptual Site Model* (CSM) document is an iterative (evolving) representation of the Red Hill area based on all data obtained to date. The CSM thus provides a basis for evaluating groundwater flow, behavior of contaminants in the environment, contaminant transport pathways, and the potential for exposure of human receptors to potentially impacted drinking water in support of the Investigation and Remediation of Petroleum Product Releases and Groundwater Protection and Evaluation project, at Red Hill Bulk Fuel Storage Facility ("the Facility"), Joint Base Pearl Harbor-Hickam (JBPHH), Hawai'i. The Facility is owned by the United States (U.S.) Navy (DON; "Navy") and operated by Defense Logistics Agency (DLA).

This document has been prepared under Statement of Work Sections 6 and 7 of the *Administrative Order on Consent* (AOC) *In the Matter of Red Hill Bulk Fuel Storage Facility* (EPA Docket No: RCRA 7003-R9-2015-01; DOH Docket No: 15-UST-EA-01) (EPA Region 9 and DOH 2015). The AOC was issued by the U.S. Environmental Protection Agency (EPA) Region 9 and State of Hawai'i Department of Health (DOH) (EPA Region 9 and DOH 2015) to the Navy/DLA in response to a release of an estimated 27,000 gallons of Jet Fuel Propellant (JP)-8 from one of the Facility's underground fuel storage tanks (Tank 5) that was confirmed and reported to DOH on January 23, 2014. The tanks are located above a major groundwater aquifer, which is used to feed both Navy and City and County of Honolulu drinking water supply wells and shafts.

The initial CSM (Revision 00) (DON 2018g) was developed in accordance with the *CSM Development and Update Plan* (DON 2017i) to identify and evaluate the site-specific characteristics and processes that control the fate and transport of fuel (light non-aqueous-phase liquid [LNAPL]) and its constituent chemicals (petroleum hydrocarbons) from the source of a release (underground fuel storage tank[s] at the Facility), through the vadose and saturated zones, and on to potential receptors (e.g., residential receptors exposed via the drinking water pathway). The CSM is an evolving tool that will continue to be updated as new information becomes available.

Regulatory Agency Comments. The Regulatory Agencies identified their top ten concerns with previously submitted reports and presentations during an August 14, 2018 Technical Working Group meeting and further summarized those concerns in their October 29, 2018 letter to the Navy approving a revised schedule for forthcoming deliverables under AOC Statement of Work Sections 6 and 7. Since identification of those ten concerns, the Navy has been completing additional analyses and presenting results to the Regulatory Agencies to achieve alignment on these concerns. Some alignment has been achieved, while other technical issues remain unresolved. A summary of the status of each of the ten concerns, as well as the Navy's position regarding the concern, is provided in Appendix J. A primary goal of this CSM Revision 01 is to address the issues identified in these comments to the extent possible. This CSM Revision 01 incorporates additional data and evaluations accordingly.

Key Findings. Key findings from recently completed studies, field work, and computer simulations include:

- Long-term monitoring (LTM) and associated studies do not indicate that the 2014 release from Tank 5 impacted groundwater at Red Hill Shaft based on evaluation of multiple lines of evidence (LOEs).
- Based on thermal natural source-zone depletion (NSZD) studies, LTM, and other studies indicate that LNAPL is retained in the pore spaces of the rock within approximately 30 feet (ft) beneath the tanks and has not reached groundwater.

- Geologic information about the formation of lava tubes indicates that these will not act as preferential pathways for contaminants to flow between the Red Hill Facility and City and County of Honolulu Board of Water Supply (BWS) water supply wells or Red Hill Shaft.
- Seismic studies and borings (borings in South Hālawa only) indicate that extensive saprolite zones exist beneath stream valleys on both sides of Red Hill (including South Hālawa Stream and Moanalua Valley), and that these extend significantly below the water table. Where that occurs, they act as a barrier to groundwater flow and contaminant migration.
- While the heterogeneous geology beneath Red Hill results in locally variable hydraulic gradients, the overall groundwater flow direction is southwestward from the tank area, and flow appears to be highly influenced by clinker zones that might provide preferential pathways to Red Hill Shaft.
- Natural attenuation is occurring in both the unsaturated and saturated zones, and it acts to degrade petroleum contaminants in the environment.
- Risk-based decision criteria (RBDC) have been developed that are protective of human health in regard to chemicals of potential concern (COPCs) that may potentially impact public water supplies.
- COPCs detected in water development tunnel shafts have not exceeded the RBDC.
- Data collected as part of recent synoptic water level studies assisted with the development of aquifer hydraulic property estimates and evaluation of groundwater flow conditions in the site area.
- A transfer function-noise (TFN) analysis was completed using the recently collected synoptic water level data. The TFN analysis simulates the water level response to each hydraulic stress component (e.g., barometric pressure, pumping from shafts, tidal and other influences) through evaluation (convolution integration) of the hydraulic stress time series. The results of the TFN analysis indicate that pumping at Red Hill Shaft has the strongest influence on water level variability in the vicinity of Red Hill, relative to any other stresses evaluated. The TFN analysis allowed both development of step response functions (used to assist with groundwater model calibration) and estimation of aquifer hydraulic properties.

CSM Modules. This document is organized into seven detailed modules that describe the site-specific data and information, or LOEs, used to develop the current version of the CSM and evaluate remaining uncertainties. These seven modules are summarized in Table ES-1, which identifies the LOEs to date, the remaining uncertainties, and the activities planned to help fill existing data gaps and help address the uncertainties.

Table ES-1: Summary of CSM Modules

Conceptual Model
Module A: Physical Setting
The 144-acre underground fuel storage Facility is located in south-central O'ahu approximately 2–3 miles east of Pearl Harbor, within the Red Hill ridge that divides South Hālawa Valley from Moanalua Valley on southwest flank of O'ahu's Ko'olau Mountain Range. The Facility's twenty 250-ft-tall,12.5-million-gallon fuel storage tanks store and supply fuel for military operations in Hawai'i and throughout the Pacific. The tank bottoms are situated approximately 100–130 ft above an underlying basal aquifer that is a major municipal and military drinking water source and is considered an irreplaceable resource with a high vulnerability to contamination. Below the surface soil and saprolite of Red Hill ridge, geologic formations consist largely of basalt with varying layers of materials exhibiting high and low permeability and containing occasional voids. In the surrounding valleys, sedimentary deposits are underlain by weathered basalt (saprolite) and unweathered basalt. In the vicinity of Red Hill, the basal aquifer water table lies at approximately 20 ft above mean sea level, and regionally groundwater flows toward Pearl Harbor (Mauka to Makai), although potential exists for variability in localized flow directions depending on geologic formations and other factors.
Module B: Facility Construction and Operations
The Facility's 20 fuel storage tanks were field-constructed of steel-lined concrete in the early 1940s. They are connected to a fuel pumping station at Pearl Harbor via a tunnel system. Kerosene-based jet fuels stored at the Facility have included JP-5, JP-8, and NATO-grade F-24; the tanks currently contain kerosene-based JP-5 and F-24, and F-76 Diesel Fuel-Marine.
Module C: LNAPL Release Source Zone
During Tank 5 refilling operations following a routine 3-year inspection and refurbishment process conducted every 20 years, a release of approximately 27,000 gallons of JP-8 was confirmed and reported to DOH in writing on January 23, 2014. During that month, a fuel hydrocarbon seep confirmed to be JP-8 was observed on a tunnel wall below Tank 5, and soil vapor monitoring points installed beneath the tank exhibited a sharp increase in hydrocarbon vapor concentrations. Potential migration pathways include gaps between the tank's steel lining and inner side of its concrete shell, and cracks in the concrete shell into higher-permeability rock surrounding the concrete. Subsequent analysis indicated the cause of the release to be defective workmanship in welding by the tank refurbishment contractor, poor inspection, and ineffective quality control.
Module D: Vadose Zone
The Facility tanks are surrounded by rock in the vadose (i.e., unsaturated) zone, which consists primarily of basalt flows in complex, alternating layers. These heterogeneous layers vary from extremely high to extremely low permeability, with a corresponding varying ability to transmit and hold LNAPL depending on the layer's rock type and micro-pore structure (i.e., high ability in high-permeability a'ā and thin pāhoehoe flows; low ability in massive a'ā and massive pāhoehoe flows; limited transmissivity but high holding capacity in a'ā clinker zones). Geologic and water saturation characteristics in the rock surrounding the tanks could cause LNAPL to spread as it moves through the rock. As LNAPL moves through the larger pore spaces, some of it could be trapped in poorly connected fractures and blocked by surface tension and capillary forces of moisture, especially water held in the smaller pores. Hawaiian volcanic rocks vary in porosity and permeability depending on the emplacement process, lava type, genesis, flow thickness, flow rate, extent, cooling rate, and weathering. Permeability is typically highest in the relatively thick, unweathered rubbly a'ā clinker zones and intensely fractured zones or lava tubes of pāhoehoe flows. Permeability is much lower in the interior portions of massive flows, weathered interflows, intrusive rocks (dikes/sills), ash beds, and weathered rocks (saprolite)/soil horizons, which can impede vertical flow and horizontally flow across valleys. Generally, the bulk vertical permeability of the basalt is orders of magnitude lower than the bulk horizontal permeability. Horizontal permeability is higher in the direction that the lava flowed.

Conceptual Model
Module E: Saturated Zone
Groundwater flow and solute transport are controlled by hydraulic conditions (e.g., gradients) and physical properties of the hydrogeologic units (HGUs), including hydraulic conductivity, effective porosity, specific yield, specific storage, anisotropy, and dispersivity.
Fresh groundwater inflow originates as deep infiltration of precipitation and seepage from surface water features. According to the United States Geological Survey (USGS), estimates of recharge for O'ahu for recent conditions (2010 land cover and 1978–2007 rainfall) differ from predevelopment recharge values by only a few percent (Izuka et al. 2018). Spatial distribution of recharge mimics the orographic rainfall pattern—recharge is highest on windward slopes and mountain peaks below the top of the trade-wind inversion.
Groundwater outflow includes withdrawals from wells and natural groundwater discharge to springs, streams, wetlands, and submarine seeps. Data collected by the USGS for groundwater levels, saltwater/freshwater interface, spring flow, and stream base-flow indicate an overall reduction in aquifer storage for most areas where groundwater has been extracted; this has caused groundwater levels to decline (Izuka et al. 2018).
Regional groundwater levels decrease from areas of recharge (mauka) to areas of discharge (makai). Locally, water level gradients are extremely low and are influenced by geologic conditions as well as by variability in local pumping stresses from water development shafts and wells.
Module F: Fate and Transport of LNAPL and Dissolved COPCs in Groundwater
Attenuation studies, in the vadose zone as NSZD and in the dissolved groundwater plume as monitored natural attenuation (MNA), provide strong evidence of biodegradation. Occurrence of LNAPL is primarily limited to a depth of 30 ft beneath monitoring wells RHMW02 and RHMW03 and is being biodegraded based on thermal, soil vapor, and carbon trap studies. Attenuation of dissolved-plume COPCs in the saturated zone limits the extent of the existing small dissolved plume before reaching Red Hill Shaft under present conditions and within the context of historical releases. Spatial and temporal trends in COPCs, NAP data, and fuel studies provide strong evidence that active and robust attenuation processes are responsible for COPC degradation within groundwater plume under the tank farm.
Profiles of total petroleum hydrocarbons–diesel-range organics (TPH-d) from site data are consistent with soluble components of jet fuel. The available chromatograms from RHMW02 groundwater samples are all consistent with chromatograms for biodegraded kerosene-type fuels (e.g., JP-5 and JP-8). Petroleum fuels are composed primarily of hydrocarbons (nonpolar) that have distinctive chromatographic profiles. The majority of the fuel is not water soluble, and the chromatographic profiles are useful in distinguishing LNAPL from soluble fuel components and biodegraded material, Polar compounds are present in the groundwater, indicating ongoing biodegradation.
Module G : Exposure Model
Historical releases (prior to 2005) are considered the main source of impacts to groundwater at the Facility. Other releases (e.g., spills or leaks in the fuel system) may have occurred or may occur in the future. Potentially contaminated media are unconsolidated materials, volcanic rock within the tunnels, soil/rock vapor within the tunnels, tunnel air, groundwater beneath the Facility, and offsite surface water where groundwater may discharge. Human receptors that may contact onsite or offsite Facility-impacted media are Facility occupational workers, construction workers, and visitors, and offsite residents. Among the potentially complete exposure pathways identified, the primary one is offsite residents using tap water sourced from the Red Hill Shaft water supply well. These receptors could be exposed to chemicals in tap water via direct ingestion and dermal contact, and via inhalation while showering/bathing. Exposure by ecological receptors is considered incomplete or insignificant.

Overall, the current CSM indicates that LNAPL released from Red Hill fuel storage tanks has entered the vadose zone at various areas and times beneath Red Hill. Soil vapor monitoring data from beneath the tanks indicate that no significant releases have occurred since the monitoring program was initiated in 2008 with the exception of the January 2014 Tank 5 release.

Conceptual LNAPL Behavior. LNAPL entering the vadose zone encounters a complex geology in the surrounding volcanic layers that vary significantly in their permeability and overall geometry. Consequently, LNAPL will migrate laterally through high-permeability zones underlain by low-permeability layers. Vertical migration can occur through clinker bridges, and highly fractured zones within flows. As LNAPL moves through the pore spaces, some of it will be trapped in poorly connected intraflow fractures, voids, and pores. The LNAPL is expected to preferentially migrate along the predominant dip direction to the south-southwest. Once the LNAPL encounters the water table, its vertical migration potential is minimized due to the density difference between LNAPL and water. Soluble components (monitored by analyzing groundwater samples for COPCs) would enter the

groundwater through either dissolution from LNAPL in the vadose zone due to infiltrating water or through dissolution of LNAPL in the saturated zone close to the water table. Currently, no LNAPL has been measured in the water table monitoring wells. However, analytical data indicate the possible presence of LNAPL upgradient of Red Hill monitoring well RHMW02. The thermal profile study conducted in October 2017 shows evidence that residual LNAPL is primarily limited to a depth of 30 ft beneath the top of wells RHMW02 and RHMW03 (inside the lower access tunnel) and is being biodegraded.

Observed Behavior of COPCs. General transport of COPCs in the dissolved plume is expected to be in the southwest direction toward Red Hill Shaft, based on regional groundwater flow conditions, previous groundwater modeling by other researchers, ongoing groundwater modeling evaluations being conducted by the Navy, and the influence of Red Hill Shaft on groundwater conditions identified by a TFN analysis. The TFN analysis showed that pumping Red Hill Shaft was the primary factor influencing variability of water levels at Red Hill. Migration to the southeast and northwest is expected to be limited by the extent of lower-permeability materials (valley fill and saprolite) extending below the water table in the valleys bounding the Facility. Attenuation of COPCs in the dissolved plume in the saturated zone limits the extent of the existing dissolved plume before reaching Red Hill Shaft under present conditions and within the context of historical releases.

Uncertainties. CSM Revision 00 (July 27, 2018) identified uncertainties that have been partly or fully addressed by evaluation of new data that is documented in this CSM Revision 01. The primary uncertainties identified in CSM Revision 01 are:

- The nature of subsurface geology in North and South Hālawa Valleys
- Groundwater levels and hydraulic gradients in the site vicinity
- Extent of near-surface groundwater on the north side of Red Hill and the adjacent South Hālawa Valley floor
- Migration and retention of LNAPL following a release
- Groundwater flow directions and rates in the groundwater model domain
- Subsurface geologic features that may act as preferred groundwater flow pathways or barriers (e.g., lava tubes, clicker beds)
- Spatial distribution of COPC concentrations dissolved in groundwater between the Facility and water supply wells in North Hālawa Valley and Moanalua Valley

Ongoing new data collection, evaluations, and proposed activities to address remaining uncertainties include the following:

- *Groundwater levels and flow:* Incorporate in the modeling effort the results of Red Hill monitoring water level measurements from the progressively expanding monitoring well network. Assess groundwater level data from additional monitoring wells and test borings (RHMW11, RHTB01, and RHMW14) and augment with data from future wells currently being installed (RHMW12, RHMW13) at Red Hill and in North and South Hālawa Valleys. Continue to collect groundwater level data to represent both non-pumping conditions and various combinations of pumping of water supply wells in the area. Collect groundwater level measurements from intervals deeper below the water table.
- *Subsurface geology:* Collect additional hydrogeologic data and prepared detailed borehole geologic logs of deep borings in areas beneath North and South Hālawa Valleys.

- *COPC concentrations:* Continue to monitor for COPCs in the progressively expanding monitoring well network.
- *Biodegradation:* Evaluate recently collected thermal profiling data from key monitoring wells both in the tank area and outside and adjacent to the tank area for evidence of biodegradation. Continue collection and evaluation of natural attenuation parameter (NAP) data (e.g., dissolved oxygen and dissolved methane in groundwater and in the soil vapor monitoring points).
- *LNAPL migration and retention:* Inspect new cores for presence of LNAPL. Collect petrographic data on select cores from proposed new monitoring well RHMW01R, located within the tank farm.

CONTENTS

Executive Summary iii

Contents ix

Acronyms and Abbreviations xix

Well Name Cross-Reference Table xxiii

1. Conceptual Site Model Development and Structure 1-1

- 1.1 Purpose of the CSM 1-1
- 1.2 CSM Development Approach 1-2
- 1.3 Regulatory Issues and Resolution 1-3
- 1.4 CSM Updates and Refinement 1-3
- 1.5 Organization and Key Elements of the CSM 1-6

2. Module A: Physical Setting 2-1

- 2.1 Site Location 2-1
- 2.2 Surrounding Populations and Land Use 2-1
- 2.3 Climate 2-1
- 2.4 Vegetation and Wildlife 2-2
- 2.5 Archaeological Sites 2-2
- 2.6 Topography 2-2
- 2.7 Site Volcanic Rocks 2-3
- 2.8 Site Soils 2-4
- 2.9 Surface Water 2-5
- 2.10 Groundwater 2-5
- 2.11 Water Supply Wells 2-6
- 2.12 Red Hill Long-Term Monitoring System 2-7
  - 2.12.1 Soil Vapor Monitoring System 2-7
  - 2.12.2 Groundwater Monitoring Network 2-8
- 2.13 Uncertainty Analysis 2-10
- 2.14 Addressing Uncertainties 2-11

3. Module B: Facility Construction and Operations 3-1

- 3.1 Construction and Physical Characteristics of the Facility 3-1
- 3.2 Fuel Types 3-2
- 3.3 Uncertainty Analysis 3-5
- 3.4 Addressing Uncertainties 3-5

4. Module C: LNAPL Release Source Zone 4-1

- 4.1 Summary of Previous Investigations and Environmental Actions 4-1
- 4.2 Slop Tank (Facility No. S-355) 4-3
- 4.3 Former Oily Waste Disposal Facility 4-3
- 4.4 Surface Soil at RHMW14 4-3
- 4.5 History of January 2014 JP-8 Release from Tank No. 5 4-3
- 4.6 Construction Practices and Materials 4-4
  - 4.6.1 Bottom Drain 4-6
  - 4.6.2 Tunnel Floor Pipe Bedding and Sumps 4-6
  - 4.6.3 Recent Construction and Upgrades 4-6
  - 4.6.4 Current Conditions of Facility Infrastructure 4-6

4.7 Post-2014-Release Monitoring Results 4-7
4.8 2014 Release Conceptual Model 4-7
4.9 Uncertainty Analysis 4-8
4.10 Addressing Uncertainties 4-9

5. Module D: Vadose Zone 5-1

5.1 Geologic Features 5-1
5.1.1 Lava Flows 5-2
5.1.2 Geologic Cross Sections and Mapping 5-3
5.1.3 Gaussian Mixture Model 5-4
5.1.4 Assessment of Potential Preferential Pathways Related to Historical Lava Flow 5-5
5.1.5 Overall Occurrence of Rock Types 5-5
5.1.6 Permeability 5-10
5.1.7 Red Hill Geologic Framework Model 5-13
5.1.8 3D Regional Geologic Model 5-13
5.1.9 Assessment of Subsurface Heterogeneity 5-13
5.1.10 Geologic Features and LNAPL Movement 5-15
5.1.11 Petrographic Analyses 5-17
5.1.12 Infiltration Study of Surficial Saprolite Soils 5-20
5.1.13 Assessment of Geologic Features and Natural Processes Affecting LNAPL 5-20
5.2 Uncertainty Analysis 5-21
5.3 Addressing Uncertainties 5-21

6. Module E: Saturated Zone 6-1

6.1 Previous Groundwater Levels and Recently Collected Hydrogeologic Data 6-1
6.1.1 May 2006 Regional Aquifer Pumping Test 6-2
6.1.2 Quarterly Groundwater Monitoring 6-2
6.1.3 November 2016 Synoptic Monitoring 6-3
6.1.4 Recently Collected Hydrogeologic Data 6-3
6.1.5 2017 High-Precision Well Survey 6-6
6.1.6 Gyroscopic Corrections 6-6
6.1.7 2017–2018 Synoptic Monitoring 6-7
6.1.8 2017 Seismic Profiling Survey 6-9
6.1.9 TFN/Pair-Wise Analysis 6-10
6.2 Groundwater Flow Directions 6-13
6.2.1 May 2006 Pumping Test 6-13
6.2.2 May 2015 Pumping Test 6-14
6.2.3 November 2016 Synoptic Monitoring 6-14
6.2.4 2017–2018 Synoptic Monitoring 6-15
6.3 Hydraulic Properties of Hydrogeologic Units 6-26
6.3.1 Caprock 6-26
6.3.2 Valley Fill 6-26
6.3.3 Tuff 6-27
6.3.4 Saprolite 6-27
6.3.5 Basalt 6-27
6.3.6 Site-Area Aquifer Testing and Analysis of Hydraulic Parameters 6-29

6.4 General Groundwater Chemistry Distribution 6-30
6.5 Assessment of LOEs for Groundwater Flow 6-35
6.6 Uncertainty Analysis 6-36
6.7 Addressing Uncertainties 6-37
6.7.1 Groundwater Flow Directions and Rates 6-37
6.7.2 Thickness and Extent of Hydrogeologic Units 6-38
6.7.3 Preferential Pathways and Barriers 6-38
6.7.4 Groundwater Recharge and Discharge Rates 6-39

7. Module F: Fate and Transport of LNAPL and Dissolved COPCs in Groundwater 7-1

7.1 LNAPL Distribution, Fuel Type, and Evidence of Weathering 7-1
7.1.1 LNAPL Distribution in the Unsaturated Zone 7-1
7.1.2 LNAPL Distribution at the Water Table 7-2
7.1.3 Dissolved-Phase Fuel Type and Evidence of Weathering 7-3
7.2 Dissolved-Phase COPCs Detected in Groundwater 7-4
7.3 Natural Attenuation 7-8
7.3.1 Natural Source-Zone Depletion 7-8
7.3.2 Monitored Natural Attenuation 7-17
7.4 Groundwater Chemistry Lines of Evidence 7-24
7.4.1 Challenges with Organic Data Interpretation 7-24
7.4.2 Groundwater Chemistry as a Function of LNAPL Extent 7-25
7.4.3 Key Findings 7-25
7.5 Uncertainty Analysis 7-26
7.6 Addressing Uncertainties 7-27
7.6.1 Nature and Extent of Contamination 7-27
7.6.2 Source Area Extent, Mass Loading, and Natural Attenuation Rates 7-27

8. Module G: Exposure Model 8-1

8.1 Chemical Sources and Releases 8-1
8.2 Potentially Affected Media 8-1
8.3 Potential Receptors 8-2
8.3.1 Human Receptors 8-2
8.3.2 Ecological Receptors 8-3
8.4 Potentially Complete Exposure Pathways 8-3
8.5 Incomplete or Insignificant Pathways 8-3
8.6 Potential Exposure to LNAPL 8-4
8.7 Uncertainties 8-4
8.8 Addressing Uncertainties 8-5

9. References 9-1

APPENDIXES (included on CD-ROM)

A Cumulative Historical Groundwater Monitoring Results and COPC Concentration Graphs

B Fate and Transport Analyses

C Strike and Dip Data
D Evaluation of Potential Pāhoehoe Lava Flow Paths through Tank Farm Area
E Geologic Framework Model
F Petrographic Analytical Report
G Infiltration Study Report
H Transfer Function-Noise Analysis of 2017–2018 Synoptic Monitoring
I Multiple Impact Factors
J Regulatory Comments and Navy Responses

FIGURES

1-1 Red Hill Bulk Fuel Storage Facility and Vicinity 1-9
1-2 Pictorial CSM 1-11
2-1 County Land Use Ordinance Map 2-13
2-2 State Land Use Districts 2-15
2-3 Land Cover 2-17
2-4 Generalized Surficial Geology of O'ahu 2-19
2-5 Conceptual Cross Section View of O'ahu Hydrogeology 2-21
2-6 Aquifer Systems in the Groundwater Model Area 2-23
2-7 Water Supply Wells in the Groundwater Model Area 2-25
2-8 Soil Vapor Monitoring Point Construction Details 2-27
2-9 Existing and Proposed Groundwater Monitoring and Test Boring Locations 2-29
3-1 Location of Former Slop Tank S-355 and Slop Pump 3-1
4-1 Summary of Environmental Actions at Red Hill 4-11
4-2 Location of Oil-Tight Door and Sump Upgrades 4-13
4-3 Soil Vapor Measurements Prior to and Following 2014 Release 4-15
5-1 Geologic Cross Section Key Plan 5-23
5-2 Geologic Cross Section A–A′ 5-25
5-3 Geologic Cross Section A–A′ Extended 5-27
5-4 Geologic Cross Section B–B′ (View Looking East) 5-29
5-5 Cross Section B–B′ Extended (View Looking East) 5-31
5-6 Geologic Cross Section C–C′ 5-33
5-7 Geologic Cross Section D–D′ 5-35
5-8 Geologic Cross Section E–E′ 5-37
5-9 Cross Section F–F′ Āliamanu Crater Section 5-39

5-10	Cross Section of Red Hill Shaft Water Development Tunnel	5-41
5-11	Logs of Formations in Tank Excavations (Barrel Logs)	5-43
5-12	Plan of Lava Tubes Cut by Tank 18	5-45
5-13	Barrel Log Geology of Lava Tube and Loose Rock Interpolation	5-47
5-14	Geologic Mapping Points	5-49
5-15	Geologic Mapping Rose Diagram	5-51
5-16	Gaussian Mixture Model - Histograms of Dip Azimuth and Dip Magnitude	5-53
5-17	Polar Plot of Gaussian Mixture Modeling and Histogram	5-55
5-18	Glacioeustatic Fluctuations of Sea Level and Hawaiian Pleistocene Shorelines	5-57
5-19	Saprolite/Basalt Interface	5-59
5-20	Micro-Scale LNAPL Vadose Zone Mobility and Retention	5-61
6-1	Hydrographs of RHMW07 vs. RHMW02 and OWDFMW01	6-41
6-2	Hydrographs of RHMW07 vs. RHMW06 and HDMW2253-03	6-43
6-3	Cross Section B–B′ with Westbay Data (View Looking East)	6-45
6-4	RHMW11 Long-Term Water Level Elevations	6-47
6-5	TFN Analysis Results for RHMW08	6-49
6-6	Comparison of Observed and Computed Differences between Water Level at RHMW05 and RHMW10	6-51
6-7	Examples of Unit Step Response Functions Associated with Red Hill Shaft Pumping	6-53
6-8	Comparison of Transmissivity from TFN Analysis with Hantush and Thomas (1966)	6-55
6-9	Time-Series Plots of Water Level Data at Area Monitoring Wells during 2015 USGS Pumping Test at Red Hill Shaft and Hālawa Shaft	6-57
6-10	Groundwater Levels in RHMW04 and RHMW07 and Pumping Rates during May 2015	6-59
6-11	Possible Effects on Water Levels	6-61
6-12	BRF Corrected Water Levels and Selected Time Periods	6-63
6-13	Time 1: Red Hill Shaft Off (at Max Recovery), Hālawa Shaft Average Pumping 01/15/2018 6:00	6-65
6-14	Time 2: Red Hill Shaft at Max Pumping Hālawa Shaft Average Pumping 01/19/2018 21:10	6-67
6-15	Time 3: Red Hill Shaft Business as Usual Pumping, Hālawa Shaft Off 02/05/2018 19:00	6-69
6-16	Time 4: Red Hill Shaft Business as Usual Hālawa Shaft at Maximum Pumping 02/16/2018 5:00	6-71

6-17 Time 5: Red Hill Shaft Business as Usual Hālawa Shaft Average Pumping 02/19/2018 13:00 6-73

6-18 Head Differences Between Time 1 (Red Hill Shaft Off at Max Recovery, Hālawa Shaft Average Pumping, 01/15/2018 6:00) and Time 2 (Red Hill Shaft at Max Pumping, Hālawa Shaft Average Pumping, 01/19/2018 21:10) 6-75

6-19 Head Differences Between Time 3 (Red Hill Shaft Business as Usual Pumping, Hālawa Shaft Off, 02/05/2018 19:00) and Time 4 (Red Hill Shaft Business as Usual Pumping, Hālawa Shaft at Maximum Pumping, 02/16/2018 5:00) 6-77

6-20 Cooper-Jacob Drawdown and Recovery Plots at Time 2 (RHMW01, RHMW02, RHMW03, RHMW04, RHMW05, and RHMW06) 6-79

6-21 Cooper-Jacob Drawdown and Recovery Plots at Time 2 (RHMW07, RHMW08, RHMW09, RHMW10, RHMW11 Zones 1 and 2) 6-81

6-22 Cooper-Jacob Drawdown and Recovery Plots at Time 2 (RHMW11 Zones 3, 4, 5, 6, 7, and 8) 6-83

6-23 Cooper-Jacob Drawdown and Recovery Plots at Time 2 (Hālawa Deep Monitor Well [2253-03], Hālawa Deep Monitor Well Chase Tube, Ka'amilo Deep, Hālawa BWS Deep Monitor, OWDFMW01, and TAMC-MW2) 6-85

6-24 Cooper-Jacob Drawdown and Recovery Plots at Time 2 (Moanalua Deep, Moanalua DH43, 'Aiea Navy, Hālawa T45, Manaiki T24, and USGS RHMW11 Zone 8) 6-87

6-25 Aqtesolv Drawdown and Recovery Plots at Time 2 (RHMW01, RHMW02, RHMW03, RHMW04, RHMW05, RHMW06, RHMW08, RHMW09, RHMW10, OWDFMW01) 6-89

6-26 Aqtesolv Drawdown and Recovery Plots at Time 2 (RHMW11 Zones 1, 2, 3, 4, and 5, Moanalua Deep, Hālawa BWS Deep Monitor, Hālawa Deep Monitor Well [2252-03], Ka'amilo Deep, TAMC-MW2, and Manaiki T24) 6-91

6-27 Aqtesolv Drawdown and Recovery Plots at Time 2 (Hālawa T45 and Moanalua DH43) 6-93

6-28 Distance Drawdown at Time 2 6-95

6-29 Cooper-Jacob Drawdown and Recovery Plots at Time 4 (RHMW01, RHMW02, RHMW03, RHMW04, RHMW05, and RHMW06) 6-97

6-30 Cooper-Jacob Drawdown and Recovery Plots at Time 4 (RHMW07, RHMW08, RHMW09, RHMW10, RHMW11 Zones 1 and 2) 6-99

6-31 Cooper-Jacob Drawdown and Recovery Plots at Time 4 (RHMW11 Zones 3, 4, 5, 6, 7, and 8) 6-101

6-32 Cooper-Jacob Drawdown and Recovery Plots at Time 4 (Hālawa Deep Monitor Well (2253-03), Hālawa Deep Monitor Well Chase Tube, Ka'amilo Deep, Hālawa BWS Deep Monitor, OWDFMW01, and TAMC-MW2) 6-103

6-33 Cooper-Jacob Drawdown and Recovery Plots (Moanalua Deep, Moanalua DH43, 'Aiea Navy, Hālawa T45, Manaiki T24, and USGS RHMW11 Zone 8) 6-105

6-34 Logarithmic Plots Time 4 (RHMW01, RHMW02, RHMW03, RHMW04, RHMW05, RHMW06, RHMW08, RHMW09, RHMW10, RHMW11 Zone 1, and RHMW11 Zone 2) 6-107

6-35 Logarithmic Plots Time 4 (RHMW11 Zone 3 through Zone 8, Hālawa Deep Monitor Well [2253-03], Hālawa Deep Monitor Well Chase Tube, Ka'amilo Deep, Hālawa BWS Deep, OWDFMW01, and TAMC-MW2) 6-109

6-36 Logarithmic Plots Time 4 (Moanalua Deep, Moanalua DH43, 'Aiea Navy, Hālawa T45, Manaiki T24, and RHMW11 Zone 8 USGS) 6-111

6-37 Chemical Composition of Groundwater in Red Hill Monitoring Wells 6-113

6-38 Bivariate Plots 6-115

6-39 Estimated Local Meteoric Water Line 6-117

7-1 Range of VOC Concentrations and Fuel Weathering Observed in Below-Tank Soil Vapor Wells 7-29

7-2 Use of PID Monitoring Combined with Lab Analysis to Track Release and Subsequent Weathering of LNAPL Fuel for Tank 5 7-31

7-3 Conceptual Illustration of Carbon Dioxide Flux to Ground Surface and Tunnels 7-33

7-4 Net (Background Corrected) Temperature Profiles for Facility Wells (Well Air Temperatures Method), Highlighting Clinker Zones and Inferred LNAPL Intervals 7-35

8-1 Human Health Exposure Pathway Evaluation 8-7

TABLES

1-1 Summary of Updates to CSM Revision 01 1-4

2-1 Existing and Proposed Wells in the Red Hill Groundwater Monitoring Network 2-8

3-1 Types of Fuel Historically and Currently Stored in the Facility's Fuel Storage Tanks 3-3

4-1 Summary of Previous Red Hill Investigations 4-1

5-1 Geologic Media in Red Hill 5-15

5-2 Rock Type, Permeability, and Porosity Summary 5-18

5-3 Summary of Infiltration Test Results 5-20

6-1 RHMW11 Westbay Zone and Water Level Elevation Summary 6-4

6-2 RHMW11 Hydraulic Conductivity Estimates Derived from Pneumatic Testing and Laboratory Analyses 6-5

6-3 Summary of Gyroscopic Survey Results and Calculated Tape Correction Factors 6-7

6-4 Well and Transducer Information 6-8

6-5 Equivalent Regional-Scale Aquifer Hydraulic Properties for Step Response Functions at Red Hill Monitoring Wells with Red Hill Shaft and Hālawa Shaft Pumping 6-13

6-6 Summary of Cooper-Jacob Approximation Calculation Components from Red Hill Shaft Pumping 6-20

6-7 Summary of Cooper-Jacob Approximation Estimates of Transmissivity, Storativity, and Hydraulic Conductivity from Red Hill Shaft Pumping 6-22

6-8 Summary of Aqtesolv Approximation Estimates of Transmissivity, Storativity, and Hydraulic Conductivity from Red Hill Shaft Pumping 6-23

6-9 Summary of Distance vs. Drawdown Estimation of Transmissivity and Storativity, and Derived Hydraulic Conductivity from Red Hill Shaft Pumping 6-24

6-10 Summary of Aquifer Properties for Red Hill Shaft Pumping 6-25

6-11 TFN Computed Aquifer Properties for Hālawa Shaft Pumping 6-26

6-12 Hydraulic Parameters Developed from Local Numerical Flow Model Calibration at the Facility (DON 2007) 6-30

6-13 Major Ion Composition of Groundwater Samples Collected from Red Hill Monitoring Wells, November 2016 6-30

6-14 Groundwater Chemistry Data Compiled by the University of Hawai'i Water Resources Research Center for Geothermal Study 6-33

7-1 Findings and Conclusions of Soil Vapor Investigation 7-11

7-2 Summary of Total NSZD Rates (Gallons per Year) from the Tank Farm 7-15

7-3 Vertical Distribution of LNAPL Intervals Indicated by Net (Background-Corrected) Temperature Profiles from Three Facility Monitoring Wells 7-16

7-4 Summary of Microcosm and Microbial Study Preliminary Results by Monitoring Well 7-19

7-5 C vs. t Coefficients, Half-Lives, and First-Order Model Fit Parameters for the COPCs at RHMW02 (September 2005 to April 2018) 7-21

7-6 C vs. d Rate Attenuation Rates and Biodegradation Rates for COPCs along RHMW02-RHMW01 Transect for the Base Case Model (includes detected COPCs at both wells only) 7-21

7-7 C vs. d Rate Attenuation Rates and Biodegradation Rates for COPCs along RHMW02-RHMW01 Transect for the Clinker Model (includes detected COPCs at both wells only) 7-22

PHOTOGRAPHS

2-1 Aerial Photograph of Red Hill Area, ca. 1939–1940 2-31

2-2 A-Frame Derricks Installed atop Red Hill to Excavate the Pilot Shafts for the Fuel Storage Tank Chambers, August 1941 2-33

2-3 Aerial Photograph of Red Hill Area, 1952 2-35

1	5-1	Pāhoehoe Flows	5-63
2	5-2	Pāhoehoe Flows	5-65
3	5-3	Pāhoehoe Flows	5-67
4	5-4	Aʻā Permeability	5-69
5	5-5	Weathered Aʻā Clinker	5-71
6	5-6	Saprolite	5-73

This page intentionally left blank

ACRONYMS AND ABBREVIATIONS

[redacted]	redacted: Navy infrastructure
3D	three-dimensional
°F	degrees Fahrenheit
µg/L	micrograms per liter
AFFF	aqueous fire-fighting foam
Alk	alkanity
AOC	Administrative Order on Consent
AST	aboveground storage tank
Att.	Attachment
AVGAS	aviation gasoline
bgs	below ground surface
BP	before present
Br	bromide
BRF	Barometric Response Function
BTEX	benzene, toluene, ethylbenzene, and xylene
btoc	below top of casing
BWS	Board of Water Supply, City and County of Honolulu
C vs. d	concentration versus distance
C vs. t	concentration versus time
Ca	calcium
cc	cubic centimeter
CF&T	contaminant fate and transport
CH_4	methane
Cl	chloride
cm/s	centimeters per second
CO_3	carbonate
COPC	chemical of potential concern
CSM	conceptual site model
CWRM	Commission on Water Resource Management
DLA	Defense Logistics Agency
DLNR	Department of Land and Natural Resources, State of Hawai‘i
DO	dissolved oxygen
DOE	Department of Energy, United States
DOH	Department of Health, State of Hawai‘i
DON	Department of the Navy, United States
EAL	Environmental Action Level
EDA	exploratory data analyses
EPA	Environmental Protection Agency, United States
EPH	extractable petroleum hydrocarbon
EVS	Earth Volumetric Studio
F	fluoride
F-76	Diesel Fuel-Marine
Fe^{2+} or Fe(II)	ferrous iron
FID	flame ionization detector
ft	foot/feet
ft/d	feet per day
ft/ft	feet per foot
ft^2/d	square feet per day

g/cc	grams per cubic centimeter
gal/acre/yr	gallons per acre per year
gal/yr	gallons per year
GMM	Gaussian Mixture Modeling
GWPP	*Groundwater Protection Plan*
HART	Honolulu Area Rapid Transit
HCO_3	bicarbonate
HEER	Hazard Evaluation and Emergency Response
HGU	hydrogeologic unit
ID	identification
IRR	*Investigation and Remediation of Releases*
ITRC	Interstate Technology Regulatory Council
JBPHH	Joint Base Pearl Harbor-Hickam
JP	Jet Fuel Propellant
k	first-order rate coefficient
K	hydraulic conductivity [or potassium]
K_h	horizontal hydraulic conductivity
k_{point}	concentration vs. time attenuation rate coefficient
K_v	vertical hydraulic conductivity
KGS	Kansas Geologic Survey
LAT	lower access tunnel
LMWL	Local Meteoric Water Line
LNAPL	light non-aqueous-phase liquid
LOD	limit of detection
LOE	line of evidence
LTM	long-term monitoring
m	meter
m/s	meters per second
MADEP	Massachusetts Department of Environmental Protection
md	millidarcy
meq/L	milli-equivalents per liter
Mg	magnesium
mg/L	milligrams per liter
mgd	million gallons per day
MNA	monitored natural attenuation
MOGAS	motor gasoline
msl	mean sea level
n	number of samples
Na	sodium
NAD	North American Datum
NAP	natural attenuation parameter
NATO	North Atlantic Treaty Organization
NAVFAC	Naval Facilities Engineering Command
NGS	Next Generation Sequencing
NO_3	nitrogen
NPDES	National Pollutant Discharge Elimination System
NSFO	Navy Special Fuel Oil
NSZD	natural source-zone depletion
NWIS	National Water Information System

o/oo	parts per mil
ORP	oxidation-reduction potential
OSHA	Occupational Safety and Health Administration
OWDF	Oily Waste Disposal Facility
PAH	polynuclear aromatic hydrocarbon
PEST	Parameter Estimation
PIANO	paraffins, isoparaffins, aromatics, naphthenes, and olefins
PID	photoionization detector
ppbv	parts per billion by volume
psi	pounds per square inch
qPCR	polymerase chain reaction
R^2	coefficient of determination
RBDC	risk-based decision criteria
RCRA	Resource Conservation and Recovery Act
RI	remedial investigation
RQD	rock quality designation
RSL	Regional Screening Level
Sec.	Section
SiO_2	silica dioxide
SME	subject matter expert
SO_4, SO_4^{2-}	sulfate
SOW	scope of work
SSRBL	site-specific risk-based level
SVE	soil vapor extraction
SVM	soil vapor monitoring
SVOC	semivolatile organic compound
$t_{1/2}$	half-life for a given COPC
TAMC	Tripler Army Medical Center
TGM	*Technical Guidance Manual for the Implementation of the Hawaii State Contingency Plan*
TIC	tentatively identified compound
TIRM	Tank Inspection, Repair, and Maintenance
TOC	total organic carbon
TPH	total petroleum hydrocarbons
TPH-d	total petroleum hydrocarbons – diesel range organics
TPH-g	total petroleum hydrocarbons – gasoline range organics
TPH-o	total petroleum hydrocarbons – residual range organics (i.e., TPH-oil)
TUA	Tank Upgrade Alternatives
Turb	turbidity
U.S.	United States
UH	University of Hawaiʻi
UHM	University of Hawaiʻi at Mānoa
UIC	Underground Injection Control
USGS	United States Geological Survey
Vb	bulk volume
VOC	volatile organic compound
VPH	volatile petroleum hydrocarbon
WP	work plan
WRRC	Water Resources Research Center, University of Hawaiʻi

yr	year
λ	biodegradation rate coefficient
$\delta^{18}O_CORR$	ratio between the heavy and light isotopes of oxygen in the water sample to those ratios in an isotopic standard derived from seawater (corrected) in parts per mil (o/oo)
$\delta^{2}H_CORR$	ratio between the heavy and light isotopes of hydrogen in the water sample to those ratios in an isotopic standard derived from seawater (corrected) in parts per mil (o/oo)

WELL NAME CROSS-REFERENCE TABLE

Well ID	DLNR ID	USGS Site ID	Known Aliases
Fort Shafter Monitor	2053-10		
Moanalua Deep	2153-005	212123157535501	Moanalua Fresh Water Mon. Well
TAMC1	2153-007		
TAMC2	2153-008		
Manaiki T24	2153-009		Moanalua T24 (DLNR)
Moanalua 1	2153-010		
Moanalua 2	2153-011		
Moanalua 3	2153-012		
TAMC-MW2	2153-013	212144157534701	TAMC MW2 TAMC-MW-2
Moanalua DH43	2253-002	212225157533001	
Hālawa Deep Monitor Well (2253-03)	2253-003	212241157535501	Hālawa Deep HDMW HDMW2253-03
Hālawa Deep Monitor Well Chase Tube	2253-003	212241157535502	Hālawa Deep Chase Tube
RHMW06	2253-004	212226157534101	
RHMW07	2253-005	212222157535201	
RHMW08	2253-007	212216157535801	
RHMW09	2253-008	212209157535201	
RHMW10	2253-009	212213157533901	
RHMW11	2253-011	212226157535001	
Red Hill Shaft	2254-001	212225157542601	Red Hill Shaft (S11) RHMW2254-01 Navy Supply Well 2254-01
UMW-1	2254-02M	212229157541501	South Hālawa Alluvium MW-1 HCF shallow monitoring well Hālawa Correctional Facility MW 8067-01
ʻAiea Hālawa Shaft	2255-032	212253157554301	Hālawa Shaft (S5) Navy Hālawa Shaft
Hālawa T-45	2255-033		
Hālawa BWS Deep Monitor	2255-040	212233157552302	Hālawa TZ Well Hālawa deep monitor well near Hālawa T45 (2255-33)
ʻAiea Navy	2256-010	212238157561101	ʻAiea US Navy (187-B) ʻAiea boat harbor well
Pearl City III	2257-003		
Hālawa Shaft	2354-001	212305157542601	Hālawa Shaft (S12)
Kaʻamilo Deep	2355-015	212340157552301	Kaʻamilo Deep Monitor
OWDFMW01		212214157542601	MW08, OWDFMW08 (former names) OWDFMW1
RHMW01		212214157535401	
RHMW02		212216157534701	
RHMW03		212219157533901	
RHMW04		212231157532901	
RHMW05		212210157540201	

DLNR Department of Land and Natural Resources, State of Hawaiʻi
USGS United States Geological Survey

This page intentionally left blank

1. Conceptual Site Model Development and Structure

This *Conceptual Site Model* (CSM) is an iterative (evolving) representation of the Red Hill area based on data obtained to date. Thus, the CSM was developed to provide a basis for evaluating contaminant transport pathways and the potential for exposure of human receptors to potentially impacted drinking water in support of the Investigation and Remediation of Petroleum Product Releases and Groundwater Protection and Evaluation project, at Red Hill Bulk Fuel Storage Facility ("the Facility"), Joint Base Pearl Harbor-Hickam (JBPHH), Hawai'i. As shown on Figure 1-1, the Facility is located approximately 2.5 miles northeast of Pearl Harbor, on the low ridge (Red Hill) between South Hālawa and Moanalua Valleys. The Facility is owned by the United States (U.S.) Navy (DON; "Navy") and operated by Defense Logistics Agency (DLA).

The project is being performed under Statement of Work Sections 6 and 7 of the *Administrative Order on Consent* (AOC) *In the Matter of Red Hill Bulk Fuel Storage Facility* (EPA Docket No: RCRA 7003-R9-2015-01; DOH Docket No: 15-UST-EA-01) (EPA Region 9 and DOH 2015). The AOC was issued by the U.S. Environmental Protection Agency (EPA) Region 9 and State of Hawai'i Department of Health (DOH) to the Navy/DLA in response to a release of an estimated 27,000 gallons of Jet Fuel Propellant (JP)-8 from one of the Facility's underground fuel storage tanks (Tank 5) that was confirmed and reported to DOH on January 23, 2014. The bottoms of the Facility's tanks are located approximately 100–130 feet (ft) above a major groundwater aquifer, which is used to feed both Navy and City and County of Honolulu drinking water supply wells and shafts.

The AOC Statement of Work outlines eight sections that set forth the tasks and requirements the Navy/DLA will undertake to comply with the Order (EPA Region 9 and DOH 2015). The *Work Plan* (WP) */ Scope of Work* (SOW) (DON 2017a) for the current project presents the process, tasks, and deliverables that address the goals and requirements of Section 6 (Investigation and Remediation of Releases) and Section 7 (Groundwater Protection and Evaluation).

This CSM Revision 01 was prepared in accordance with the *CSM Development and Update Plan* (DON 2017i), one of the derivative deliverables prepared to supplement the project WP/SOW. It updates CSM Revision 00, published July 27, 2018 (DON 2018g).

1.1 PURPOSE OF THE CSM

The CSM (1) integrates and evaluates available regional and site-specific information and data as required to identify and (if possible) quantify the physical and chemical parameters and processes that control the nature, extent, fate, and transport of petroleum products (light non-aqueous-phase liquid [LNAPL]) and their constituent chemicals in the vadose and saturated zones at the Facility; (2) identifies exposure routes to potential human receptors as potentially complete, potentially complete but insignificant, or incomplete as required to assess risks to human receptors (ecological exposures are considered incomplete or insignificant); and (3) describes site-specific conditions that may affect the feasibility of alternatives for remediating groundwater and other environmental media (e.g., vadose zone soil and soil vapor) impacted by LNAPL or its constituent chemicals. Remedial alternatives will be evaluated per AOC Statement of Work Section 6.3 in the *Investigation and Remediation of Releases* (IRR) *Report*, anticipated for submittal in October 2019. This CSM also provides a basis for developing preliminary input parameters for numerical groundwater flow modeling; the groundwater flow model will be presented per AOC Statement of Work Section 7.1.3 in the *Groundwater Flow Model Report*, anticipated for submittal in October 2019 concurrent with the IRR Report.

The CSM is an evolving tool that will continue to be updated as new information (e.g., well, seismic, natural attenuation) becomes available. Refinements to the CSM will be used in ongoing modeling and remediation efforts.

The CSM presents currently available data to help evaluate site conditions, including LNAPL degradation and migration and dissolved-phase mass discharge (flux) in the subsurface. Factors related to attenuation of LNAPL (natural source-zone depletion [NSZD]) and dissolved-phase constituents (monitored natural attenuation [MNA]) are currently being evaluated, incorporating the concepts for NSZD as described by the Interstate Technology Regulatory Council (ITRC) (ITRC 2009a) and other references; results are presented in Appendix B. The groundwater modeling effort is focused on flow and does not directly rely on natural attenuation as part of various scenario evaluations, but currently available natural attenuation data and interpretations will be included for reference. As additional natural attenuation data become available, the data will be evaluated and included for support of the fate and transport modeling effort.

1.2 CSM DEVELOPMENT APPROACH

This CSM was developed using an evidence-based approach to identify and evaluate the site-specific characteristics and processes that control the fate and transport of jet fuel (LNAPL) and its constituent chemicals (petroleum hydrocarbons) from the source of release (an underground fuel storage tank at the Facility), through the vadose and saturated zones, and on to potential receptors (e.g., residential receptors exposed via the drinking water pathway). The graphical model presented on Figure 1-2 illustrates key elements of the CSM and cross-references to the seven detailed modules presented in subsequent sections of this document.

The CSM incorporates information about tank design, construction, fuel storage history, and potential pathways for migration of LNAPL and its constituent chemicals into the vadose and saturated zones to improve the understanding of LNAPL movement, retention, and degradation mechanisms. For example, the CSM describes how LNAPL releases would likely move from a tank leak point by characterizing the spatial distribution of interconnected pore spaces (e.g., clinker zones) and low-porosity, low-permeability massive a'ā and pāhoehoe flows. The CSM also contributes to the evaluation of the potential for lateral spreading, vertical transport, and retention of LNAPL in the subsurface, including the effects of capillary moisture in water-filled fractures and other voids and pore spaces within the thick sequence of massive a'ā basalt flows, volcanic tuff, valley fill deposits, saprolite, and clinker layers that form the vadose and saturated zones. These CSM components provide a basis for estimating the extent and volume of LNAPL that could be retained in the vadose zone, locating potential pathways for transport of LNAPL to the saturated zone, and for evaluating the fate and transport of dissolved petroleum product constituents in groundwater.

The CSM describes the hydrogeologic characteristics of geologic units in the vadose and saturated zones based on detailed geologic descriptions from barrel logs, boring logs, and published reports of other hydrogeologic investigations to estimate the direction(s) of flow and locations where LNAPL could accumulate in the vadose zone if released from one of the Facility's fuel storage tanks. The evaluation also includes:

- Review of Tank 5 release history, fuel types, leak rates, and volume estimates
- Assessment of potential leak locations and pathways for migration of LNAPL and its constituent chemicals from the fuel storage tanks into the vadose and saturated zones

- Evaluation of retention of LNAPL at both macro-scale (e.g., ponding on low-permeability units, retention on surface of individual clinkers/other clasts, lava tubes, boundaries of individual flows) and micro-scale (e.g., pore, micro-fractures retention)
- Studies of natural attenuation and degradation of jet fuels
- Evaluation of site-specific groundwater data (natural attenuation parameters [NAPs] and microbial analyses) (as described in DON 2017f)
- Evaluation of vertical flow velocities based on correlation between groundwater levels, precipitation, groundwater recharge rates, influence of pumping water supply wells, and soil vapor data

This CSM was prepared in accordance with current guidance, including but not limited to the following:

- *Standard Guide for Development of Conceptual Site Models and Remediation Strategies for Light Nonaqueous-Phase Liquids Released to the Subsurface*, ASTM E2531-06(2014) (ASTM 2014b)
- *Standard Guide for Developing Conceptual Site Models for Contaminated Sites,* ASTM E1689-95 (reapproved 2014) (ASTM 2014a)
- *Environmental Cleanup Best Management Practices: Effective Use of the Project Life Cycle Conceptual Site Model* (EPA 2011)
- *Evaluating Natural Source Zone Depletion at Sites with LNAPL, Interstate Technology Regulatory Council* (ITRC 2009a)
- *Evaluating LNAPL Remedial Technologies for Achieving Project Goals* (ITRC 2009b)
- LNAPL Conceptual Site Model module in: *LNAPL Training Part 2: LNAPL Characterization and Recoverability – Improved Analysis* (ITRC 2008)
- Section 3.3 Conceptual Site Models in: *Technical Guidance Manual for the Implementation of the Hawaii State Contingency Plan* (TGM) (DOH 2018)
- *Conceptual Site Model Tool,* Naval Facilities Engineering Command (NAVFAC) Technology Transfer, Environmental Restoration website (URL: http://t2.serdp-estcp.org/t2template.html#tool=CSM&page=S1)

1.3 REGULATORY ISSUES AND RESOLUTION

The Regulatory Agencies provided comments and technical input on the initial CSM Revision 00 (DON 2018g). Appendix J provides a summary of the Regulatory comments and Navy responses on the initial CSM. The Regulatory comments were provided in a letter dated October 29, 2018; the comments and Navy responses were summarized at a March 15, 2019 technical meeting; and follow-up comments from the Regulatory Agencies were provided in letter dated April 22, 2019. A primary goal of CSM Revision 01 is to address the issues identified in these comments. The changes to CSM Revision 01 identified in the following subsection are intended to address the Regulatory issues identified with the initial CSM.

1.4 CSM UPDATES AND REFINEMENT

As new data are obtained, the Red Hill CSM will be refined and updated on an as-needed basis through an iterative process designed to promote collaboration between the Navy, Regulatory Agencies, and AOC subject matter experts (SMEs). This iterative process is designed to ensure that the updated CSM

adequately represents current site-specific conditions and processes that affect the LNAPL degradation and migration in the subsurface. The refinement will continue until the investigative and data evaluation phases of the project are complete.

Since publication of CSM Revision 00 (July 27, 2018), the following new data have been obtained, evaluated, and integrated into this CSM Revision 01:

- Additional analytical data representing various media (e.g., vapor, soil, and LNAPL), NAPs, and general groundwater chemistry
- Data from additional monitoring wells and borings (e.g., subsurface geology, groundwater levels)
- Chemical distribution summary figures indicating the locations of chemical of potential concern (COPC) concentrations above project action levels and the estimated lateral and vertical extent of contamination
- Hydrogeologic data (2017–2018 synoptic water level study) and modeling results indicating the direction of groundwater flow
- Additional natural attenuation data
- Additional data from Facility investigations and construction upgrades (e.g., geotechnical investigation, release containment upgrades)

Table 1-1 summarizes the substantive updates to this document from CSM report Revision 00 (DON 2018g).

Table 1-1: Summary of Updates to CSM Revision 01

Document Section	Revisions
Module A: Physical Setting (Sec. 2)	• Revised Sec. 2.7 Volcanic Rocks discussion • Updated Sec. 2.12.2 Groundwater Monitoring Network with new and revised proposed well locations and rationale • Updated existing, proposed well locations (Figure 2-9) • Updated Uncertainties, Addressing Uncertainties
Module B: Facility Construction and Operations (Section 3)	• Updated Table 3-1 Types of Fuels Stored at Facility • Added description of Tank S-355 slop tanks to Sec. 3.1
Module C: LNAPL Release Source Zone (Sec. 4)	• Modified section title from "…Source-Zone Migration Model" to "LNAPL Release Source Zone" • Added Secs. 4.2 Slop Tank, Sec. 4.4.3 Recent Construction and Upgrades (oil-tight doors), and Sec. 4.4.4 Current Conditions of Facility Infrastructure (EPA 2017 system evaluation report) • Added Former OWDF to Table 4-1 and new Sec. 4.3 • Expanded discussion of saltwater corrosion in tanks (Sec. 4.4) • Updated Uncertainties, Addressing Uncertainties
Module D: Vadose Zone (Sec. 5)	• Merged Macro- and Micro-Scale subsections into Sec. 5.1 Geologic Features • Added or revised discussions on strike/dip and gaussian distribution (Appendix C), preferential pathways (Appendix D), tuff and caprock deposits, saprolite, and permeability • Added Secs. 5.1.7 Geologic Framework Model (Appendix E), 5.1.10 Petrographic Analyses (Appendix F), and 5.1.11 Infiltration Study (Appendix G) • Updated Uncertainties, Addressing Uncertainties

Document Section	Revisions
Module E: Saturated Zone (Sec. 6)	• Revised RHMW11 water elevations (Sec. 6.1.4) • Added Sec. 6.1.9 TFN/Pair-Wise Analysis (Appendix H) • Removed "Hydraulic Gradients and…" from title of Sec. 6.2 Groundwater Flow Directions • Incorporated barometric corrections to synoptic data, Cooper-Jacob approximations to Theis method, and Aqtesolv estimates (Sec. 6.2.4) • Removed Secs. 6.4 2005 USGS Regional SUTRA Model, 6.5 2007 Red Hill Groundwater Flow Model, and 6.6 Red Hill 2018 Groundwater Flow Model Area Groundwater Balance • Updated Uncertainties, Addressing Uncertainties
Module F: Fate and Transport of Dissolved COPCs in Groundwater (Sec. 7)	• Updated Sec. 7.2 Dissolved-Phase COPCs Detected in Groundwater with current monitoring results (Appendix A) • Updated Sec. 7.3 Natural Attenuation • Removed Sec. 7.4 Groundwater Flow and Contaminant Fate and Transport Modeling • Added Sec. 7.4 Groundwater Chemistry Lines of Evidence (Appendix B.8) • Updated Uncertainties, Addressing Uncertainties
Module G: Exposure Model (Sec. 8)	• Clarified definition of exposure model • Revised discussion on ecological receptors and on potential and incomplete/ insignificant pathways • Updated Uncertainties and Addressing Uncertainties
Appendix A: Cumulative Historical Groundwater Monitoring Results and COPC Concentration Graphs	• Updated with cumulative results as of First Quarter 2019 monitoring event (DON 2019) • Expanded Appendix A.1 tables to include EPA split sampling results
Appendix B: Fate and Transport Analyses:	
B.1: Thermal NSZD Analysis	• Revised discussion on background well, protocols and calculation method terminology and descriptions, and aerobic conditions observed • Revised results for Calculation Method 2 (Model-Correction) [formerly Thermal Profiles Method] and Calculation Method 3 (Groundwater Temperatures)
B.2: Carbon Trap NSZD Analysis	• Added Sec. 2.1.1 Reason for Difference in NSZD Rates between Tunnels
B.3: Soil Vapor Analysis	• Revised title and content of Table 4-5 Study Question 5 • Added current data (through January 2019) to Figure 4-3 Monthly PID Monitoring Results
B.4: MNA Primary Lines of Evidence and Rate Calculations	• Clarified reporting limit discussion (Sec. 2.1) • Revised discussion on methods for plume duration and plume attenuation and plume attenuation (Secs. 2.2–2.5) • Revised rate coefficients for plume duration and plume attenuation and associated discussion of results (Secs. 3.1–3.5) • Revised estimated plume bulk attenuation rates (Sec. 4)
B.5: MNA Secondary Lines of Evidence	• Clarified data qualifications and reporting limits (Sec. 2.1) • Updated time-series figures and X-Y plots using current (January/February 2019) monitoring data • Moved COPC time-series figures (Att. B.5.1) to new Appendix B.8, added DO and ORP to plots (Att. B.5.1, B.5.2)
B.6: Microcosm Study and Microbial Parameter Analysis	• *Microcosm study:* updated incubation periods (Sec. 2.3.1), revised constituent-specific rate coefficients (Table 3-1), and expanded discussion of findings (Sec. 3.1) • *Microbial parameter analysis:* updated discussion of findings and added laboratory reports (Att. B.6.2)

Document Section	Revisions
B.7: Forensics and Data Evaluation - Groundwater	• Revised text to limit discussion to jet fuel chemistry (Sec. 2) and evaluation of dissolved material measured as TPH-d (Sec. 3) • Revised Section 3 title and discussion of dissolved material measured as TPH-d in groundwater • Incorporated former discussion assessing potential impact to groundwater from the 2014 fuel release (Sec. 4), evidence of impact to outlying wells from fuel releases/site operations (Sec. 5), and associated attachments (B.7.2, B.7.3, and B.7.4) into new Appendix B.8
New appendixes:	Description
B.8: Comprehensive Evaluation of Groundwater Chemistry	• Development of multiple LOEs to assess potential impact to groundwater after the 2014 Tank 5 release and evidence of impact to outlying wells from fuel releases/site operations
Appendix C: Strike and Dip Data	• Strike/dip, azimuth field measurements
Appendix D: Evaluation of Potential Pāhoehoe Lava Flow Paths through Tank Farm Area	• Random walk modeling of potential historical lava flow paths
Appendix E: Geologic Framework Model	• Description of current stratigraphic model: geophysical investigation, new cross sections, tuff complex, marine sediments, and alternative saprolite evaluation/interpretation for South Hālawa Valley
Appendix F: Petrographic Analytical Report	• Petrographic laboratory analytical report
Appendix G: Infiltration Study Report	• Geotechnical results of infiltration testing
Appendix H: Transfer Function-Noise Analysis of 2017–2018 Synoptic Monitoring	• Analysis of selected 2017–2018 synoptic monitoring data to extract information for numerical groundwater model calibration and estimate equivalent regional-scale aquifer hydraulic properties and anisotropy
Appendix I: Multiple Impact Factors	• Comparison of dissolved oxygen concentrations between Red Hill and other sites, analysis of potential drilling impacts on TPH-d detections in groundwater, and a multiple impact factor analysis to provide additional LOEs
Appendix J: Regulatory Comments and Navy Responses	• Regulatory Agency comments on CSM Revision 00 (July 27, 2018) and Navy responses

Att.	Attachment
DO	dissolved oxygen
LOE	line of evidence
ORP	oxidation-reduction potential
OWDF	Oily Waste Disposal Facility
PID	photoionization detector
Sec.	Section
TFN	transfer function-noise
TPH-d	total petroleum hydrocarbons – diesel range organics

1.5 ORGANIZATION AND KEY ELEMENTS OF THE CSM

The CSM is organized into seven modules that describe the site-specific data and information, or lines of evidence (LOEs), used to develop the current version of the CSM, and evaluate remaining uncertainties:

- Module A: Physical Setting (Section 2)
- Module B: Facility Construction and Operations (Section 3)
- Module C: LNAPL Release Source Zone (Section 4)
- Module D: Vadose Zone (Section 5)
- Module E: Saturated Zone (Section 6)
- Module F: Fate and Transport of LNAPL and Dissolved COPCs in Groundwater (Section 7)

- Module G: Exposure Model (Section 8)

Each module concludes by identifying uncertainties and describing additional investigation activities needed to fill data gaps and address the uncertainties. The results will be used to refine and update the CSM in future updates, in turn supporting the groundwater modeling effort.

This page intentionally left blank

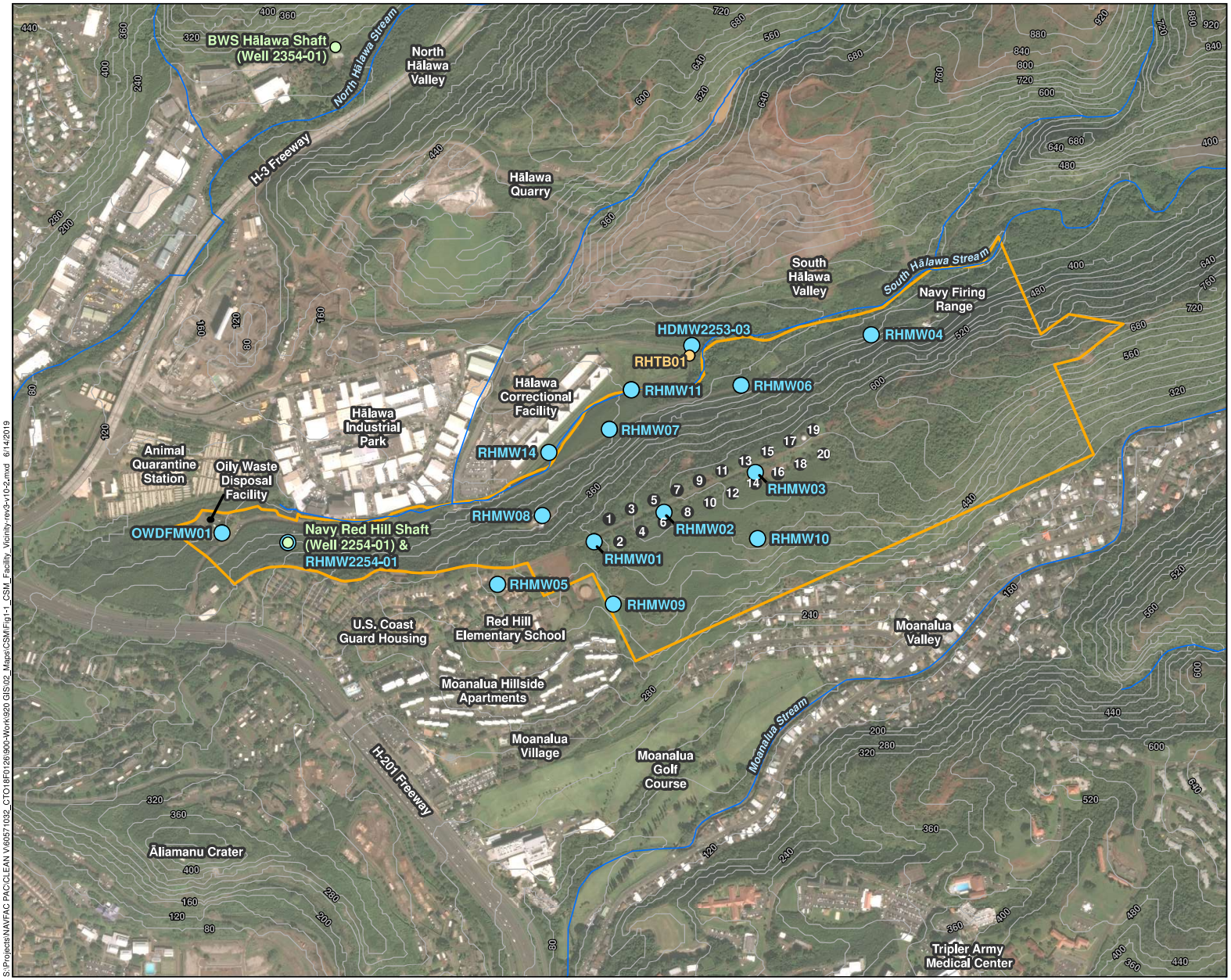

Location Map

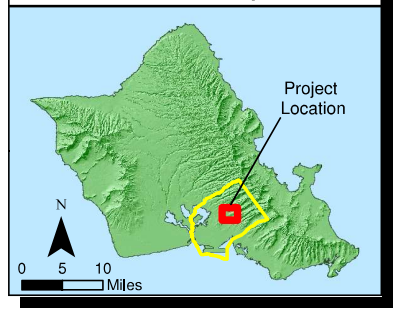

Legend

- Groundwater Monitoring Location
- Water Supply Well
- Test Boring
- Stream
- Topographic Contour (feet mean sea level)
- Red Hill Facility Boundary
- Red Hill Fuel Storage Tank
- Groundwater Model Area

Notes

1. Map projection: NAD 1983 Hawaii State Plane Zone 3 feet
2. Base Map: DigitalGlobe, Inc. (DG) and NRCS. Publication_Date: 2015

N

0 500 1,000 2,000 Feet

S:\Projects\NAVFAC PAC\CLEAN V\60571032_CTO18F0126\900-Work\920 GIS\02_Maps\CSM\Fig1-1_CSM_Facility_Vicinity-rev3-v10-2.mxd 6/14/2019

Figure 1-1
Site Location Map
Conceptual Site Model Rev. 01
Investigation and Remediation of Releases and Groundwater Protection and Evaluation
Red Hill Bulk Fuel Storage Facility
JBPHH, O'ahu, Hawai'i

This page intentionally left blank

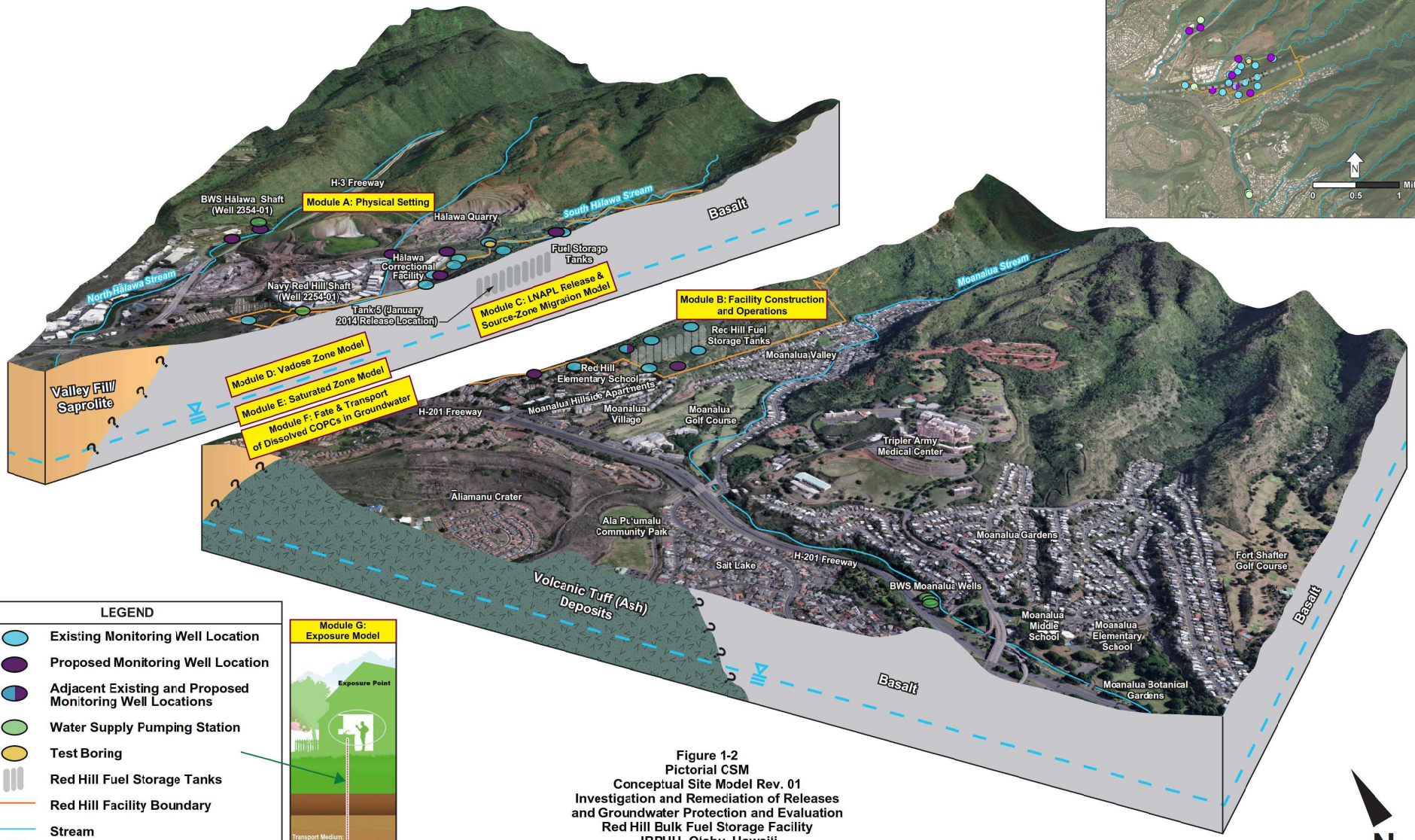

Figure 1-2
Pictorial CSM
Conceptual Site Model Rev. 01
Investigation and Remediation of Releases
and Groundwater Protection and Evaluation
Red Hill Bulk Fuel Storage Facility
JBPHH, Oʻahu, Hawaiʻi

S:\Projects\NAVFAC PAC\CLEAN IV\60481245\CTO 0053\900-Work\921 Graphics\CSM Native\Red Hill_RI_ACrater Moanalua Hills_Valley_Gardens.ai 04/02/2019

This page intentionally left blank

2. Module A: Physical Setting

2.1 SITE LOCATION

The 144-acre Facility is located in south-central O'ahu, approximately 2–3 miles east of Pearl Harbor, within the Red Hill ridge that divides South Hālawa Valley from Moanalua Valley on the southwest flank of O'ahu's Ko'olau Mountain Range (Figure 1-1). The Facility contains 20 large-capacity fuel storage tanks installed underground within Red Hill; these tanks are collectively referred to as the tank farm.

2.2 SURROUNDING POPULATIONS AND LAND USE

Populated areas closest to the Facility are 'Aiea to the west and Honolulu to the south and east. Honolulu is heavily urbanized and densely populated.

Figure 2-1 shows zoning established by County land use ordinance, and Figure 2-2 shows State land use districts. As shown on Figure 2-1, the Facility is located on land zoned by the County as a mix of F-1 Federal and Military and P-1 Restricted Preservation districts. All major structures at the Facility are located underground.

Preservation land is located east and northeast of the Facility boundary. To the southeast are residential single-family homes in Moanalua Valley; a high cliff face with a 100–200 ft elevation difference exists between the Facility and this residential area. Southwest of the tank farm area on the lower southwest flank of Red Hill are the public Red Hill Elementary School and residential apartments, and further west is U.S. Coast Guard Housing on F-1 Military land. North of the western segment of the Facility boundary in South Hālawa Valley is the State Animal Quarantine Station, private businesses in Hālawa Industrial Park, and the State-operated Hālawa Correctional Facility (see Figure 1-1). To the north of the Correctional Facility at the lower reaches of an inter-valley ridge that forms the north wall of South Hālawa Valley is the open-pit Hālawa Quarry operated by the Hawaiian Cement Company.

The H-201 Moanalua Freeway transits approximately 350–700 ft beyond the Facility's southwest boundary and intersects with the H-1 and H-3 Freeways at the Hālawa Interchange, approximately 1,800 ft west. The H-3 Freeway transits northeast from the interchange through North Hālawa Valley and on to O'ahu's windward side.

Historical Land Use. Prior to construction of the tank farm, the surface of Red Hill supported cane and pineapple agriculture, as reported in Woodbury (1946) and shown in an aerial photograph ca. 1939–1940 (Photo 2-1). Navy archive images show that the Red Hill ground surface was exposed and modified during construction of the tank farm beginning in 1940 (Photo 2-2). An aerial photograph taken in 1952 shows unmaintained land on the ridge of Red Hill and agriculture on the lower reaches of Red Hill north of the Moanalua Golf Course (Photo 2-3).

2.3 CLIMATE

The subtropical climate of O'ahu is warm and humid; prevailing northeast trade winds and ocean currents are dominating factors in the climate. Ocean temperatures are approximately 75–85 degrees Fahrenheit (°F) at Honolulu, and air temperatures in O'ahu average 70°–85°F, with the warmest months being June–October. Northeasterly winds persist most of the year, and the northeastern (windward) sides of the island are commonly the wettest due to orographic lifting and cooling of marine air, producing precipitation.

O'ahu has two general seasons for precipitation: October–April is considered the wet season and May–September the dry season. Although precipitation can be as high as 300 inches per year in some places on the island, most of O'ahu receives 20–75 inches per year. Precipitation is most commonly in the form of rain and is at a maximum between 2,000 ft and 4,000 ft mean sea level (msl).

On the Ko'olau Range's leeward slopes, precipitation generally increases up-valley as elevation increases, and decreases down-valley. Average annual precipitation in upper North Hālawa Valley and Moanalua Valley, near the ridge line of the Ko'olau Mountains, is approximately 139 and 137 inches, respectively (USGS 2017b, 2017a). Downgradient in North Hālawa Valley near municipal water supply well Hālawa Shaft, formerly active precipitation gages (2005–2009) have recorded average annual precipitation of 35–41 inches (USGS 2017c, 2017d).

2.4 VEGETATION AND WILDLIFE

The aboveground portion of the site is inhabited by non-native vegetation, including koa haole scrub, disturbed habitat, and landscaped areas (Figure 2-3). Koa haole grows throughout O'ahu, primarily in areas that have been disturbed by grazing or human activities. The scrub community on Red Hill is dominated by koa haole (*Leucaena leucocephala*), guinea grass (*Panicum maximum*), and Chinese violet (*Asystasia gangetica*). The disturbed habitat is composed of weedy plant species that can withstand frequent disturbance by human activities or natural events. Although this vegetation does support some wildlife species, the habitat is considered very low quality and is primarily used by introduced, common urban species. The onsite habitat is not considered sensitive and is dominated by introduced plant and animal species that have replaced native species. No native or sensitive species were observed in a 1995 biological survey of the area (DON 1996a); while no subsequent threatened or endangered species surveys are known to have been conducted at the Facility, anticipated federal- or state-listed threatened or endangered species are not known or expected to be present on site (DON 2005). The endangered Hawaiian hoary bat (*ōpe'ape'a*; *Lasiurus cinereus semotus*) could conceivably use the trees; therefore, requirements stipulated in the Categorical Exclusions are followed, and field personnel coordinate with the Navy's Natural and Cultural Resources personnel to obtain clearance prior to mobilizing for field work in areas containing trees.

2.5 ARCHAEOLOGICAL SITES

An archeological survey report prepared for the Facility (DON 2015b) included an inventory-level pedestrian survey of 170 acres and a line-of-sight survey of 77 acres where the terrain was too steep or otherwise inaccessible. The report concluded that ranching and military activities in the 20th century had a substantial impact across much of the Facility area, although limited areas with intact traditional Hawaiian sites still persist. Fourteen historical sites were identified within the Facility boundaries, including Hawaiian residential, cultural, religious, and agricultural areas, plantation and ranching sites, and military sites. Ten of these sites were recommended for listing on the National Registry of Historic Places. Locations and access routes for field work (e.g., monitoring well installation) are checked for proximity to identified archaeological sites prior to commencing field work, and field personnel are instructed to stop work and notify the Navy's Natural and Cultural Resources and/or pertinent State (e.g., State Historic Preservation Office) personnel if any indications of possible archaeological findings are encountered during field work.

2.6 TOPOGRAPHY

Four major geomorphic provinces define the island of O'ahu: two volcanic mountain ranges (Wai'anae and Ko'olau), the Schofield Plateau, and the coastal plains, which form the northwest and south island margins (Stearns and Vaksvik 1935). The Ko'olau volcano is a shield (dome) volcano; the east (windward) half of it is "missing" because of collapse due to catastrophic mass wasting (Walker 1990).

The pali (cliff line) on the windward side of the range defines the predominantly stream-eroded, back-collapsed scarp. In the south/central part of the range, the leeward flank of the shield volcano is eroded into a series of parallel ridges and stream-carved valleys extending generally perpendicular from the Koʻolau crest, which trends northwest–southeast.

Red Hill is one such leeward ridge, descending 5 miles from the Koʻolau crest at approximately 2,200 ft msl southwest to the coastal plain. The surface elevation of Red Hill in the tank farm area is approximately 420–560 ft msl. The ridge's northwest and southeast flanks drop steeply to South Hālawa Valley and Moanalua Valley, where valley floor elevations in the tank farm area are approximately 200 ft msl and 100–160 ft msl, respectively. North Hālawa Valley lies north of South Hālawa Valley and a low inter-valley ridge, site of Hālawa Quarry.

2.7 SITE VOLCANIC ROCKS

As indicated on Figure 2-4, the Facility is located within the Koʻolau Volcanic series. The Koʻolau formation at Red Hill consists of the basaltic lava flows that erupted from a fissure line approaching 30 miles in length and trending in a northwest rift zone (Wentworth and MacDonald 1953). Pāhoehoe and aʻā lava flows are present in the Koʻolau formation. The valleys on either side of Red Hill ridge were formed as a result of fluvial erosion and are filled with sedimentary deposits (alluvium and colluvium), also known as valley fill, underlain by residual (weathered basalt), also known as saprolite. Saprolite zones in Hawaiʻi are typically around 75 ft thick but can be 300 ft thick or greater beneath the valley floors or in areas of high precipitation. The results of a recently conducted seismic survey in North and South Hālawa Valleys, Red Hill, and Moanalua Valley (DON 2018c) found that valley fill and saprolite to extend much deeper in the valleys surrounding Red Hill, particularly in the center of the valleys and below the streambeds. The role of saprolite as a low-permeability barrier that can impede the flow of groundwater and transport of dissolved constituents is discussed in Module D: Vadose Zone (Section 5).

The southeastern third of Koʻolau volcano's remnant shield (which includes the site vicinity) experienced a rejuvenation stage of volcanism. Most rejuvenation-stage volcanoes lie south of the erosional valleys carved out of the Koʻolau shield and are interbedded with alluvial and marine sediments. These rejuvenation-stage vents and associated flows and ash deposits compose the Honolulu volcanic series. These eruptions did not occur in rapid succession, but were scattered over the last 900,000 years (Walker 1990). Salt Lake Tuff, named for Salt Lake Crater east of Pearl Harbor, consists of subaerial gray to brown tuff containing nodules of dunite (Stearns and Vaksvik 1935). It is as thick as 300 ft, contains upright tree molds, and passes beneath sea level. It overlies Āliamanu Tuff. The Āliamanu Tuff, named for Āliamanu Crater east of Pearl Harbor, is composed of water-laid gray to black or grayish-brown tuff, rounded gravel, and (in tunnels) large vesicular bombs and spatter (Stearns and Vaksvik 1935). It is separated from the overlying Salt Lake Tuff by red soil and typically overlies older alluvium.

The presence of nearly horizontal beds of lava flows with variable strike and dip and alternately greater and lesser resistance to erosion at the site has been described in previous investigations and observed during site reconnaissance activities. Rapid erosion of the less-resistant beds, such as aʻā clinker, has resulted in undercutting of the more resistant massive aʻā and pāhoehoe layers. The flows vary from evenly bedded, relatively flat, and continuous to undulating and uneven.

Aʻā clinker is composed of gravel- and cobble-size rubble that resembles a conglomerate. It is usually loosely held together unless it has been welded together by heat. Aʻā clinker is extremely permeable and is subject to more rapid chemical weathering processes. Vertical fractures present within individual lava flows of aʻā are also subject to rapid weathering. Similarly, the nearly horizontal

contacts between pāhoehoe lava flows, which are absent of a'ā clinker, are susceptible to weathering. Rock layers with denser, more closely spaced intraflow fracturing appear more extensively weathered.

Caprock. West and southwest of the Facility, substantial thicknesses of heterogeneous sediments occur on the coastal plains in southern O'ahu around Pearl Harbor. These terrestrial and marine sediments and reef limestone deposits form a wedge up to 1,000 ft thick, commonly referred to as caprock, and overlie the lava flows of the basaltic aquifer. Overall, the caprock has lower hydraulic conductivity than the basaltic rocks, and it confines the underlying basal aquifer in the Pearl Harbor and Honolulu areas. Rejuvenation stage volcanics, caprock deposits, deep-stream valley fill sediments, and saprolite all have the potential to impede groundwater flow.

Pyroclastic Deposits. Pyroclastic (airfall) deposits were encountered in rock cores at Red Hill. None have been observed in rock outcrops along Red Hill, but deposits were observed at Moanalua Golf Course and in the BWS Moanalua Water Tunnel that runs south through the lower end of Red Hill from Hālawa Valley to Moanalua Valley. These deposits are granular in nature and include ash, cinder, spatter, and larger blocks (i.e., tuff). Due to the highly weathered nature of pyroclastic deposits proximal to Red Hill, their porosity and permeability are similar to those of fine-grained consolidated granular sediments, with similar grain size and degree of sorting.

Valley Fill. The deposits within and near the base of the valleys generally consist of fill of highly weathered and compact older alluvium that is mantled with more recent unconsolidated alluvium and colluvium (Oki 2005). The older alluvium consists of terrestrial sediments that vary in size from fine-grained particles to boulders, and is less permeable. The older alluvium has been weathered and compacted into a soft coherent mass (Wentworth 1951). The older alluvium may be hundreds of feet thick at lower altitudes, but at altitudes above approximately 400–600 ft, older alluvium may be nonexistent. These materials overlay highly weathered saprolite.

Saprolite. Based on previously collected rock samples and cores from borings, the horizon of soils and highly weathered basalt described as saprolite on the Red Hill ridge is approximately 15–25 ft thick. Saprolite is weathered rock material that retains textural features of the parent rock. Intense weathering of basaltic rocks can significantly reduce the permeability of the parent rock by transforming igneous minerals to clays and oxides (Hunt Jr. 1996). The saprolite zone beneath valley fill in stream valleys creates a barrier to groundwater flow because of the lower hydraulic conductivity of the clayey weathered basalt material. Saprolite most likely formed beneath a deeply incised paleo-valley that lies below the present-day South Hālawa Stream.

A detailed description of site-specific geology and hydrogeology, including hydraulic characteristics of volcanic rock and the nature of valley fill, is presented in Module D: Vadose Zone and Module E: Saturated Zone (Sections 5 and 6, respectively).

2.8 SITE SOILS

Soils in the vicinity of the Facility are mapped as Helemano-Wahiawā association consisting of well-drained, moderately fine textured and fine textured soils (USDA SCS 1972). The surfaces of the basaltic flows have been weathered to form reddish-brown clayey silt, which is the basis for the local name "Red Hill." These soils typically range from nearly level to moderately sloping and occur in broad areas dissected by very steep gulches. They formed in material weathered from basalt to a depth of approximately 10 ft below ground surface (bgs). Along the slopes, the basaltic bedrock is covered with approximately 10–30 ft of Ko'olau residuum. These soils were derived from weathering of the underlying basalt bedrock or were deposited as alluvium/colluvium. The younger alluvium/colluvium deposits were derived from fractured basalts and tuff. Beneath the surficial soils, alternating layers of

clay and basalts are encountered at depth. The northwestern slope of Red Hill is generally barren of soil and consists of outcropping basalt lava flows to the valley floor.

2.9 SURFACE WATER

Surface water features in the vicinity of the tank farm include South Hālawa Stream (approximately 600–800 ft to the north), North Hālawa Stream (approximately 4,000–4,500 ft to the northwest), and Moanalua Stream (approximately 1,700–2,000 ft to the south) (Figure 1-1). Potential recharge (runon and operational water use) from the Hālawa Quarry north of the tank farm area may also impact groundwater flow in this area. In the area of Hālawa Valley, stream flow is isolated from the basal groundwater table and is over deeply weathered rock. These flows may contribute water to perched groundwater within alluvial material (valley fill). Most precipitation percolates to the freshwater-lens aquifer and does not maintain base flows in the streams (Izuka 1992). Groundwater that flows beneath the Facility does not intercept surface water inland of the ocean shoreline (DON 2007). Both South Hālawa Stream and Moanalua Stream (to the north and south of Red Hill ridge, respectively) are located approximately 100 ft or more above the groundwater table in the vicinity of the Facility. The bottoms of the Facility's fuel storage tanks are located at least 50 ft below the bottom of these streams.

2.10 GROUNDWATER

Groundwater in Hawai'i exists in two principal aquifer types: basal and caprock. Perched groundwater has also been reported in the Facility area. A conceptual cross section view of O'ahu hydrogeology depicting the basal groundwater freshwater–saltwater interface, low-permeability caprock, and perched water zones is presented on Figure 2-5.

The basal aquifer exists as a lens of fresh water floating on and displacing seawater within the pore spaces, open fractures, and voids of the basalt that forms the underlying mass of each Hawaiian island. Near the shoreline and at lower elevations within the coastal plains, groundwater in the basal aquifer is typically confined by the overlying caprock and is under pressure. Waters that flow freely to the surface from wells that tap the basal aquifer are referred to as artesian. The basal aquifer beneath the Facility is included in the Oahu Sole Source Aquifer (also known as the Southern Oahu Basal Aquifer), designated a Sole Source Aquifer in 1987 under Section 1424(e) of the Safe Drinking Water Act (61 Fed. Reg. 47752). Sole Source Aquifers are those that are the sole or principal drinking water source for an area and that, if contaminated, would create a significant hazard to public health. Groundwater in the area of the Facility is on the boundary of the Waimalu and Moanalua Aquifer Systems of the Pearl Harbor and Honolulu Aquifer Sectors, respectively. The aquifers are classified as basal, unconfined, flank-type and are currently used as a drinking water source. The aquifers are considered fresh, with less than 250 milligrams per liter (mg/L) of chloride, and are considered an irreplaceable resource with a high vulnerability to contamination (Mink and Lau 1990). These aquifer systems underlie the Waimalu, North Hālawa, South Hālawa, Moanalua, and Kalihi Valleys, as shown on Figure 2-6. Red Hill ridge is an administrative boundary between these aquifer systems, but is not actually a hydrogeologic boundary because there are no geochemical or physical attributes that distinguish between these two aquifer systems at this location (DON 2007).

The second type of aquifer is the caprock aquifer, which consists of various kinds of sediments and sedimentary and volcanic rock containing groundwater under unconfined and semi-confined conditions. Commonly, the caprock consists of a thick sequence of nearly impermeable clays, coral, volcanic ash, and basalt that separates the caprock aquifer from the basal aquifer. The impermeable nature of these materials and the artesian nature of the basal aquifer severely restrict the downward migration of groundwater from the upper caprock aquifer. However, the caprock is located downgradient of the Facility and the surrounding valleys; therefore, this aquifer is not present in the

site vicinity. While the caprock aquifer does not extend to the Red Hill Shaft drinking water supply well or the tank farm area, it is present in makai (seaward) portions of the study area and may influence the flow of groundwater.

Groundwater elevations in the southern O'ahu region range from 0 ft msl near the shoreline to approximately 30 ft msl at the southern O'ahu and Schofield water region boundary. The groundwater elevation in the project vicinity is approximately 20 ft msl. Nearshore, the water is typically under artesian pressure because it is confined by caprock, unless hydraulic heads are decreased by pumping or dry climatic conditions. Groundwater in the vicinity of Pearl Harbor, including Red Hill, generally flows toward the harbor, but the potential exists for variances in the localized flow directions from the anticipated regional flow pattern.

The Facility is located inland and to the east of the Hawai'i State Underground Injection Control (UIC) Line, as indicated on Figure 2-6. The UIC Line indicates the border between groundwater that is or is not (i.e., aquifers shoreward of the line) considered a potential source of drinking water by the State of Hawai'i. The EPA, however, does not recognize this boundary and considers the area shoreward of the UIC Line to be a potential source of drinking water.

Shallow groundwater (at times identified as a perched zone) has been encountered in the site vicinity. A shallow perched water-bearing zone was encountered during investigations conducted at the former Oily Waste Disposal Facility (OWDF) (DON 1996a), Hālawa Correctional Facility (Dames & Moore 1991; EKNA 1999), the City and County of Honolulu Hālawa Bus Facility (Kimura 2000), and Tripler Hospital (ECC 2000) (see Table 2-13 in DON [2017b]). Shallow perched water-bearing zones were also encountered during drilling of onsite monitoring wells RHMW04 at approximately 183–228 ft msl (DON 2007), and RHMW08 in two zones at approximately 214–217 and 193–198 ft msl. Shallow groundwater was observed at monitoring well RHMW11 on the South Hālawa Valley floor at approximately 110–115 ft msl with continuous saturation within the saprolite (perched conditions not observed) (DON 2018b). The saprolite zone beneath valley fill creates a barrier to groundwater flow because of the lower hydraulic conductivity of the clayey weathered basalt material and higher groundwater levels.

As indicated conceptually on Figure 2-5, dikes are not expected to occur in the Facility area but do occur further inland. Where present, the dikes' low permeability can impede the flow of groundwater and confine groundwater in localized compartments, resulting in localized deviances from average groundwater levels. Dikes are often less than 10 ft wide but can extend vertically and laterally for long distances. Furthermore, dike complexes can form where individual dikes intersect at various angles. Dikes and dike complexes can intersect similarly low-permeability, nearly horizontal lava flows, collectively inhibiting lateral and vertical groundwater flow and resulting in high-level groundwater impoundments.

Details on site-specific hydrogeology are presented in Module D: Vadose Zone and Module E: Saturated Zone (Sections 4 and 6, respectively).

2.11 WATER SUPPLY WELLS

Locations of water supply wells in the groundwater model area are shown on Figure 2-7; additional detail on these wells is presented in the *Groundwater Model Evaluation Plan* (DON 2017h). The Hālawa/Red Hill/Moanalua area provides approximately 25 percent of the drinking water for urban Honolulu. Drinking water supply wells of primary concern for the investigation due to their proximity to the Facility tanks and pumping capacities are Red Hill Shaft, Hālawa Shaft, and Moanalua Wells (see Figure 2-7):

- The Navy's Red Hill Shaft (Hawai'i Well Identification [ID] 2254-01) is a potable water pumping station operated by NAVFAC Hawaii, Utilities and Energy Division. The pumping station is located within the Facility's lower tunnel system approximately 2,600 ft makai (seaward) of the Facility tanks. The station pumps groundwater from a water development tunnel (also called an infiltration gallery) that extends from the pumping station approximately 1,200 ft east and southeast to within 1,530 ft of Tank 1, the nearest fuel storage tank. The pumping station supplies the JBPHH water distribution system, which serves approximately 65,200 military customers. The average pumping rate at Red Hill Shaft is [redacted] million gallons per day (mgd).
- Hālawa Shaft (2354-01) is located approximately 4,400 ft northwest of the tank farm. It is a municipal water supply well operated by the City and County of Honolulu Board of Water Supply (BWS). The pumping station is located in an underground pump room approximately 150 ft bgs. Groundwater is pumped from a water development tunnel to provide municipal drinking water for O'ahu. The tunnel extends from the pumping station 919 ft northeast, and comes within 4,600 ft of the Facility tanks at the closest point between the two. The average pumping rate is 7.0–12.1 mgd.
- Moanalua Wells Moanalua 1 (2153-10), Moanalua 2 (2153-11), and Moanalua 3 (2153-12) are located approximately 6,650 ft south of the Facility tanks and are operated by BWS. Groundwater pumped from these wells also supplies municipal drinking water for O'ahu. The average pumping rate (as channeled and measured at Moanalua 1) is 1.0–4.3 mgd.

Currently, it is presumed that the above wells represent key components in the most significant exposure pathway to human receptors from a Facility fuel release due to their known or suspected pumping influence on the aquifer beneath the Facility, the size of their drinking water distribution system(s), proximity to the Facility, and the potential groundwater flow direction relative to the Facility. BWS has projected an increase of 15–21 percent in water use in central O'ahu from 2012 demand levels of 17.2 mgd (BWS 2016).

2.12 RED HILL LONG-TERM MONITORING SYSTEM

The Facility has a network of soil vapor and groundwater monitoring points that are sampled periodically in accordance with the Red Hill *Groundwater Protection Plan* (GWPP) (DON 2014b) and long-term monitoring (LTM) *Work Plan/Sampling and Analysis Plan* (DON 2015c); all results are reported to DOH.

2.12.1 Soil Vapor Monitoring System

The Facility's soil vapor monitoring (SVM) system consists of 47 probes installed during previous investigations in angle boreholes beneath each of the 18 active Facility tanks (Tanks 1 and 19 are inactive). One angle boring is located under each tank, and two to three probes are installed in each boring. The three probe positions are referred to as shallow (near tank access), middle (near centerline of tank), and deep (near outer opposite edge of the tank). Construction details are shown on Figure 2-8. Each probe is used to withdraw vapor from these three isolated segments of the borehole via a pump and sampled in the field using a hand-held organic compound photoionization detector (PID). Total volatile organic vapors are measured down to 1 part per billion by volume (ppbv) and compared to baseline measurements from the same location. Increasing concentrations over time have been used as an indication of fuel leaks at the tested tank. SVM points have been monitored on a monthly basis at a minimum since 2008 (DON 2008a). The monitoring reports are currently included as Appendix B of the Navy's *Quarterly Release Response Reports* to DOH (DON 2014a).

2.12.2 Groundwater Monitoring Network

The Red Hill groundwater LTM program began in February 2005, when the network consisted of three wells; additional wells have subsequently been added to the network both before and after the 2014 Tank 5 release. As of the First Quarter 2019 groundwater monitoring event, 14 groundwater monitoring locations are included in the network (see Figure 2-9 and Table 2-1): one sampling point adjacent to the Red Hill Shaft water supply well (2254-01) and 14 groundwater monitoring wells (RHMW01 through RHMW14, HDMW2253-03, and OWDFMW01) installed in the basal aquifer within or near the Facility. Multilevel monitoring well RHMW14 and test boring RHTB01 (with grouted-in-place piezometers; see Section 5.1) were installed in early 2019. An additional eight monitoring wells are proposed for installation or undergoing installation within the Facility boundaries and in North and South Hālawa Valleys to extend the network and improve understanding of regional geology, hydrogeology, and local groundwater flow in support of the investigation's groundwater modeling efforts (DON 2017f).

Groundwater monitoring has been conducted on a quarterly basis at a minimum since 2005. Each monitoring event's sampling program, the screening criteria, and analytical results are presented in quarterly groundwater monitoring reports to DOH. Analytical parameters and discussion of COPC trends in groundwater are presented in Section 7.2.

Well elevation and gyroscopic surveys were recently conducted at the Red Hill monitoring locations to improve the accuracy of groundwater elevation measurements, which are critical to the groundwater modeling effort due to the regional aquifer's extremely low gradients. Elevations of all existing monitoring locations were resurveyed in Summer 2017 using high-precision Second Order, Class I techniques (DON 2018a) to (1) establish accurate top-of-casing elevations, for which variable data had been reported by previous surveys, and (2) establish standard measuring point(s) for each monitoring location. For wells existing during the 2007 Facility investigation (DON 2007), corrections based on the resurveyed measurement point elevations were all less than -0.5 ft except for RHMW2254-01 (-5.0 ft). Additionally, field gyroscopic directional surveys were conducted at all existing monitoring wells (except RHMW01 due to its small diameter) to determine whether any wells deviate from true vertical; tape correction factors calculated for all wells based on three-dimensional modeling of the field data were less than -0.1 ft except for RHMW09 (-0.24 ft) (DON 2018d). Gyroscopic correction factors for manually collected depth to water measurements have been provided to stakeholders.

Existing and proposed monitoring wells in the Red Hill groundwater monitoring network are summarized in Table 2-1.

Table 2-1: Existing and Proposed Wells in the Red Hill Groundwater Monitoring Network

Monitoring Well / Sampling Point	Location and Approximate Distance from Tank Farm	Installation Date	Rationale for Inclusion in Network
Existing [a]			
RHMW2254-01	Inside Adit 3 lower access tunnel near Red Hill Shaft; 2,600 ft W of Tank 1	2005	Monitor groundwater at Red Hill Shaft (Navy Supply Well 2254-01).
RHMW01	Inside lower access tunnel SW of Tanks 1–2	2001	Monitor groundwater directly under tank farm.
RHMW02	Inside lower access tunnel near Tank 6	2005	Monitor groundwater directly under tank farm.
RHMW03	Inside lower access tunnel near Tank 14	2005	Monitor groundwater directly under tank farm.
RHMW04	Northeast of tank farm; 850 ft NE of Tank 19	2005	Monitor background conditions in basal aquifer.
RHMW05	Inside lower access tunnel between tank farm and Red Hill Shaft; 1,000 ft SW of Tank 2 (1,700 ft SE of Red Hill Shaft)	2009	Monitor groundwater between tank farm and Red Hill Shaft.

Monitoring Well / Sampling Point	Location and Approximate Distance from Tank Farm	Installation Date	Rationale for Inclusion in Network
RHMW06	North of tank farm, between tank farm and Hālawa Quarry; 550 ft NE of Tank 15	2014	Monitor groundwater between tank farm and Hālawa Shaft (BWS Supply Well 2354-01).
RHMW07	North of tank farm, between tank farm and Hālawa Correctional Facility; 600 ft NW of Tank 3	2014	Monitor groundwater between tank farm and Hālawa Shaft.
RHMW08	West of tank farm, between tank farm and Hālawa Industrial Park; 550 ft W of Tank 1	2016	Monitor groundwater west of tank farm, in general area between tank farm and Red Hill Shaft.
RHMW09	Between tank farm and Moanalua Valley residential area; 450 ft S of Tank 2	2016	Monitor groundwater southwest of tank farm.
RHMW10	Between tank farm and Moanalua Valley residential area; 400 ft S of Tank 14	2017	Monitor groundwater south of tank farm.
RHMW11 [b]	North side of South Hālawa Stream; 900 ft N of Tank 5 (multilevel well)	2017	Determine if valley fill and saprolite extend below the water table in South Hālawa Valley. Evaluate groundwater flow directions in South Hālawa Valley, groundwater quality between Red Hill and Hālawa Shaft, and potential presence for perched groundwater conditions throughout the entire thickness of the vadose zone in South Hālawa Valley.
RHMW14 [b]	At Hālawa Correctional Facility near concrete-lined bank of South Hālawa Stream; 700 ft NW of Tank 1 (multilevel well)	2019	Determine extent of valley fill and saprolite in the area. Evaluate groundwater quality and groundwater flow directions in South Hālawa Valley, and the potential presence for perched groundwater conditions throughout the entire thickness of the vadose zone in the area.
HDMW2253-03 (Hālawa Deep Monitor Well)	East of Hālawa Correctional Facility; 1,000 ft N of Tank 13	2000	Monitor groundwater between tank farm and Hālawa Shaft.
OWDFMW01	At OWDF in western portion of Facility; 3,100 ft W of Tank 1 (550 ft W of Red Hill Shaft)	1998	Monitor groundwater west of Red Hill Shaft.
Proposed [c]			
RHMW01R	Inside lower access tunnel adjacent to RHMW01, SW of Tanks 1–2	[2019]	Provide capability to detect LNAPL at the groundwater surface, which cannot be achieved by RHMW01 since it is screened below the water table surface.
RHMW07D	At foot of Red Hill on opposite side of RHMW14 near concrete-lined bank of South Hālawa Stream; 600 ft NW of Tank 1	[2019]	Evaluate water level elevations in discrete vertical zones to further evaluate the basal aquifer groundwater table elevation at this location and evaluate the potential for preferential pathways in both shallow and deeper portions of the basal aquifer between Red Hill tank farm and Hālawa Shaft.
RHMW12	In South Hālawa Valley north of Hālawa Correctional Facility; 1,600 ft N of Tank 2 (multilevel well currently under construction)	[2019]	Evaluate groundwater flow north of tank farm in South Hālawa Valley, and groundwater recharge southeast of the former quarry pit where water used by the quarry is discharged. Further define geometry of valley fill sediments and saprolite layers in South Hālawa Valley.
RHMW13	In South Hālawa Valley at foot of Red Hill near RHMW04; 800 ft NW of Tank 19 (multilevel well currently under construction)	[2019]	Evaluate groundwater flow north of the tank farm in upper South Hālawa Valley, and groundwater quality to the northwest of Tank 5. Further define geometry of valley fill sediments and saprolite layers in South Hālawa Valley.

Monitoring Well / Sampling Point	Location and Approximate Distance from Tank Farm	Installation Date	Rationale for Inclusion in Network
RHMW15	West of RHMW05 in the upper extent of the Red Hill Shaft; 1,550 SW of Tank 1	[2019]	Improve assessment of the effects of pumping at Red Hill Shaft. Further characterize lithology and evaluate groundwater quality adjacent to the upper reaches of the Red Hill Shaft water development tunnel.
RHMW17	Northwest of North Hālawa Stream and just southeast of Hālawa Shaft; 4,040 ft NW of Tank 1 (400 ft S of BWS Hālawa Shaft)	[2019]	Determine if valley fill and saprolite extend below the water table in North Hālawa Valley. Evaluate groundwater quality and (with RHMW18) groundwater flow directions in North Hālawa Valley. Assess effects of pumping at Hālawa Shaft on surrounding water table. Evaluate potential presence for perched groundwater conditions throughout the entire thickness of the vadose zone in the area.
RHMW18	Northwest of North Hālawa Stream; 4,300 ft NW of Tank 1 (950 ft SW of BWS Hālawa Shaft)	[2019]	Determine if valley fill and saprolite extend below the water table in North Hālawa Valley. Evaluate groundwater quality and (with RHMW17) groundwater flow directions in North Hālawa Valley. Assess effects of pumping at Hālawa Shaft on the surrounding water table. Evaluate potential presence for perched groundwater conditions.
RHMW19	Between tank farm and Moanalua Valley, between RHMW09 and RHMW10; 550 ft SE of Tank 6	[2019]	Evaluate groundwater flow directions in the area, and groundwater quality toward Moanalua Valley.

[a] All existing locations except RHMW2254-01, RHMW01, and HDMW2253-03 are screened across the water table surface. RHMW2254-01 is an unscreened sampling point in the water development tunnel near the input to the Red Hill Shaft pumping station. RHMW01's screened interval is below the water table surface. HDMW2253-03 is an open-hole deep monitor well operated by the State of Hawai'i Department of Land and Natural Resources (DLNR).

[b] RHMW11 and RHMW14 were installed as a multilevel Westbay-system well, with eight discrete sampling zones extending from the elevation of the basal water table surface to approximately 300 ft below that elevation.

[c] Completion type of the proposed wells (i.e., conventional well with standard casing and slotted screen or multilevel Westbay-system well) is currently under review. Installation dates for proposed wells are projected (DON 2017f); exact locations are subject to change.

In addition, recent installation of test boring RHTB01 adjacent to monitoring well HDMW2253-03 has provided lithologic data and water level data via grouted-in-place piezometers to support evaluation of hydrogeologic conditions in South Hālawa Valley.

2.13 UNCERTAINTY ANALYSIS

Although uncertainty remains regarding groundwater levels and hydraulic gradients in the site vicinity due to a nearly flat groundwater table surface, which creates very small and variable hydraulic gradients, the unreliability of previously available well elevation data for the Red Hill groundwater monitoring wells has been mitigated by the recently completed high-precision well elevation survey (DON 2018a) and development of water level tape correction factors based on the gyroscopic survey. The extent of shallow groundwater encountered above the water table on the north side of Red Hill and the adjacent South Hālawa Valley floor is unknown: it may be semi-contiguous or contiguous along the flank of Red Hill and/or the valley floor, or may occur only in isolated areas, as has been observed in the few well locations where it has been reported (see Section 2.10). There is uncertainty about the degree to which recharge from the Hālawa Quarry and cement plant affects this shallow groundwater and the groundwater table.

Uncertainty regarding the total depth of saprolite in North and South Hālawa Valleys exists because the seismic surveys completed along several transects provide estimated rather than directly measured depths to the top and bottom of saprolite. Data collected from RHMW11 are consistent with the interpreted saprolite depths at nearby transect locations. However, because RHMW11 is not collocated with any of the seismic survey transects, the ability to directly correlate with seismic survey interpretations is limited. Uncertainty has been further resolved with continuous coring and geophysical logging of RHMW14 and test boring RHTB01, the latter located adjacent to seismic survey Transect E (Figure 2-9) to allow direct correlation of observed geologic conditions with seismic survey interpretation at that location (DON 2018c).

2.14 ADDRESSING UNCERTAINTIES

The following ongoing, planned, or proposed activities are designed to help resolve the uncertainties described in Section 2.13.

The planned installation of several monitoring wells in North and South Hālawa Valleys will include collection of continuous rock core samples (DON 2017f). A detailed geologic boring log of each new monitoring well will be generated. As part of this effort, RHMW14 has recently been installed as a multilevel Westbay-system well and is completed approximately 300 ft below the water table surface. Newly proposed wells will be installed as either a multilevel Westbay-system well or conventional monitoring well (i.e., standard casing and slotted screen) based on input from the Regulatory and permitting agencies. Following completion of coring for a multilevel Westbay-system well, a borehole geophysical logging program consisting of caliper tool, acoustic televiewer, and gyroscopic survey will be conducted within each borehole. Video logging will be performed in all boreholes regardless of well construction type. The results will be used to better define the nature of subsurface geology in the valleys and support the groundwater flow and contaminant fate and transport (CF&T) modeling efforts.

Resolving uncertainty regarding groundwater levels and hydraulic gradients in the site vicinity is an important objective of recently completed, ongoing, and planned investigations. These investigations include the well elevation survey (DON 2018a) and gyroscopic survey (DON 2016b) for Red Hill groundwater monitoring wells, synoptic water level measurements recently collected by the U.S. Geological Survey (USGS) (USGS 2017e), and installation of new monitoring wells at Red Hill and in North and South Hālawa Valleys (DON 2017f). These new data will be used to develop input parameters for groundwater flow modeling. The synoptic water level study will also improve understanding of flow resulting from various pumping conditions. The results will help further define actual groundwater flow directions and assess the potential for transport of contaminants to potential downgradient exposure points.

This page intentionally left blank

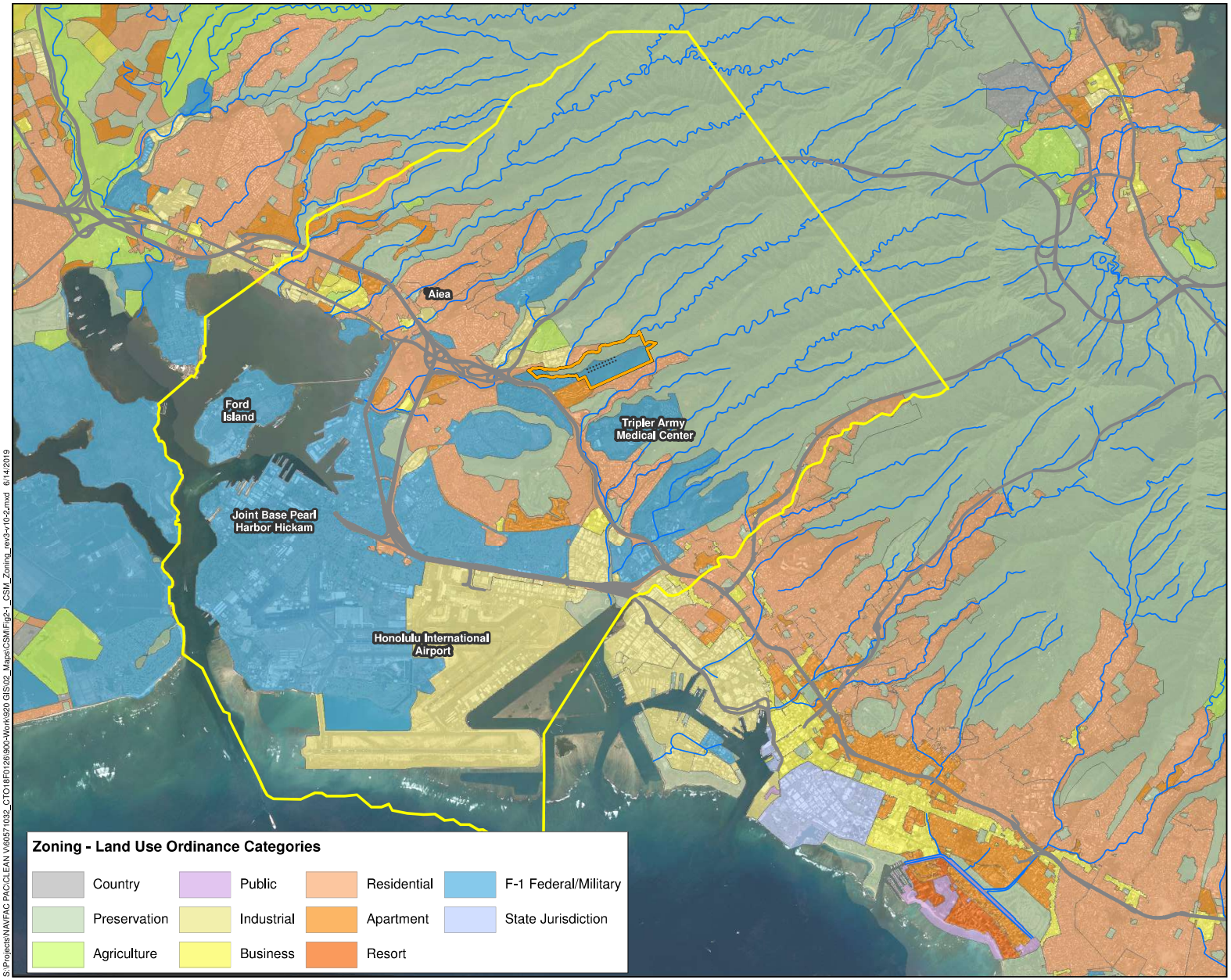

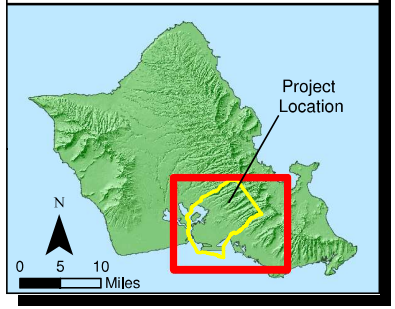

Legend

- Groundwater Model Domain
- Red Hill Facility Boundary and Fuel Storage Tanks
- Highway or Freeway
- Stream

Notes

1. Map projection: NAD 1983 Hawaii State Plane Zone 3 feet
2. Base Map: DigitalGlobe, Inc. (DG) and NRCS. Publication_Date: 2015
3. Land Use Ordinance Data Source: Honolulu Land Information System (HoLIS): Zoning - Land Use Ordinance, 9/26/2017.

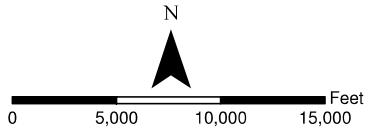

S:\Projects\NAVFAC PAC\CLEAN V\60571032_CTO18F0126\900-Work\920 GIS\02_Maps\CSM\Fig2-1_CSM_Zoning_rev3-v10-2.mxd 6/14/2019

Figure 2-1
County Land Use Ordinance Map
Conceptual Site Model Rev. 01
Investigation and Remediation of Releases and Groundwater Protection and Evaluation
Red Hill Bulk Fuel Storage Facility
JBPHH, O'ahu, Hawai'i

This page intentionally left blank

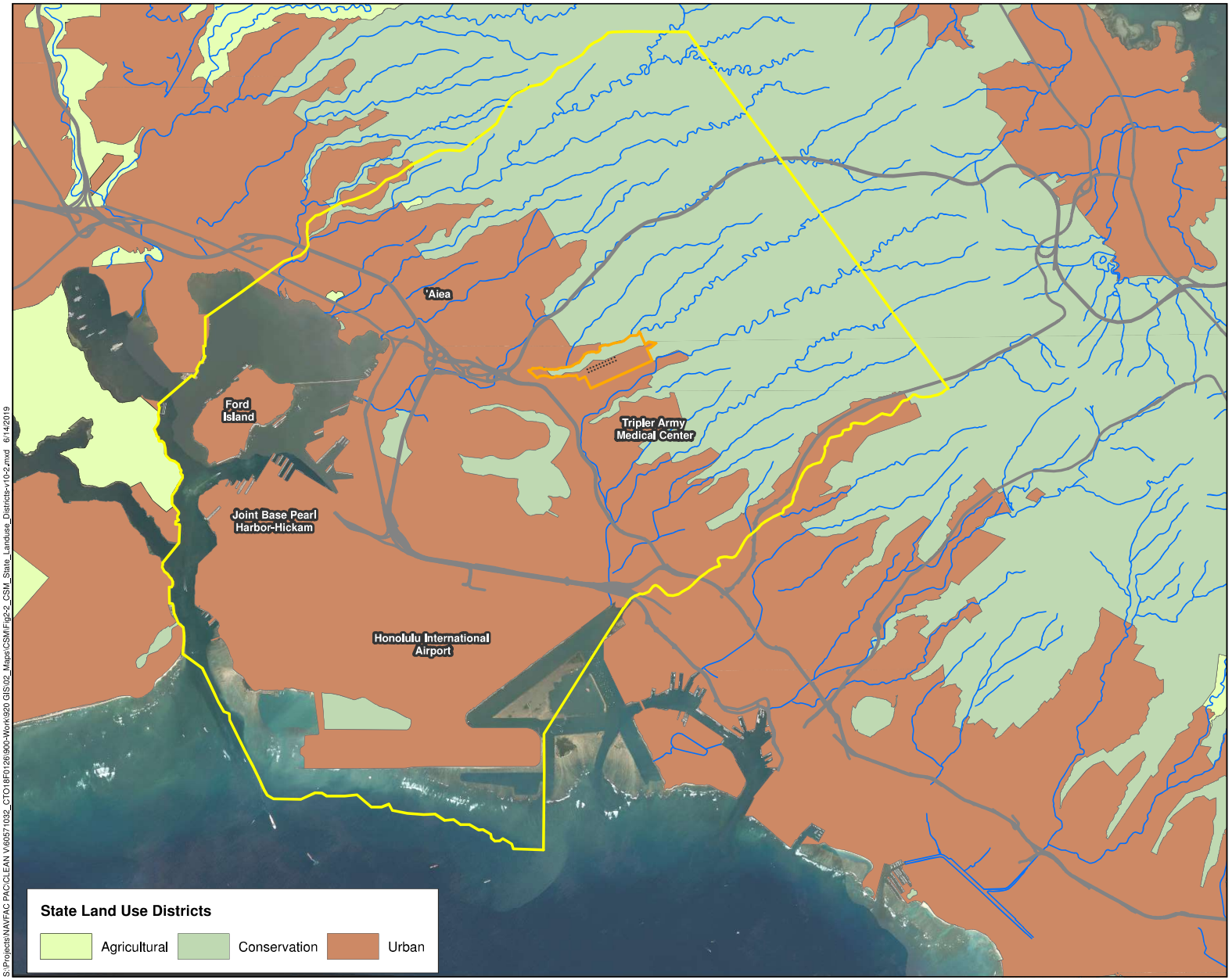

S:\Projects\NAVFAC PAC\CLEAN V\60571032_CTO18F0126\900-Work\920 GIS\02_Maps\CSM\Fig2-2_CSM_State_Landuse_Districts-v10-2.mxd 6/14/2019

Location Map

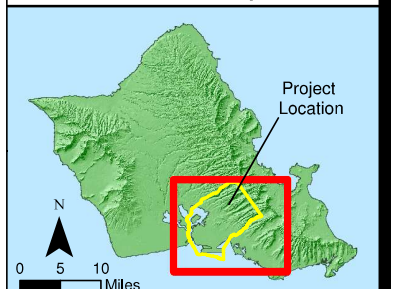

Legend

- Groundwater Model Domain
- Red Hill Facility Boundary and Fuel Storage Tanks
- Highway or Freeway
- Stream

Notes

1. Map projection: NAD 1983 Hawaii State Plane Zone 3 feet
2. Base Map: DigitalGlobe, Inc. (DG) and NRCS. Publication_Date: 2015
3. State Land Use Districts Data Source: Honolulu Land Information System (HoLIS): State Land Use Districts, 9/26/2017

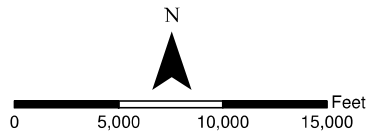

Figure 2-2
State Land Use Districts
Conceptual Site Model Rev. 01
Investigation and Remediation of Releases and Groundwater Protection and Evaluation
Red Hill Bulk Fuel Storage Facility
JBPHH, O'ahu, Hawai'i

This page intentionally left blank

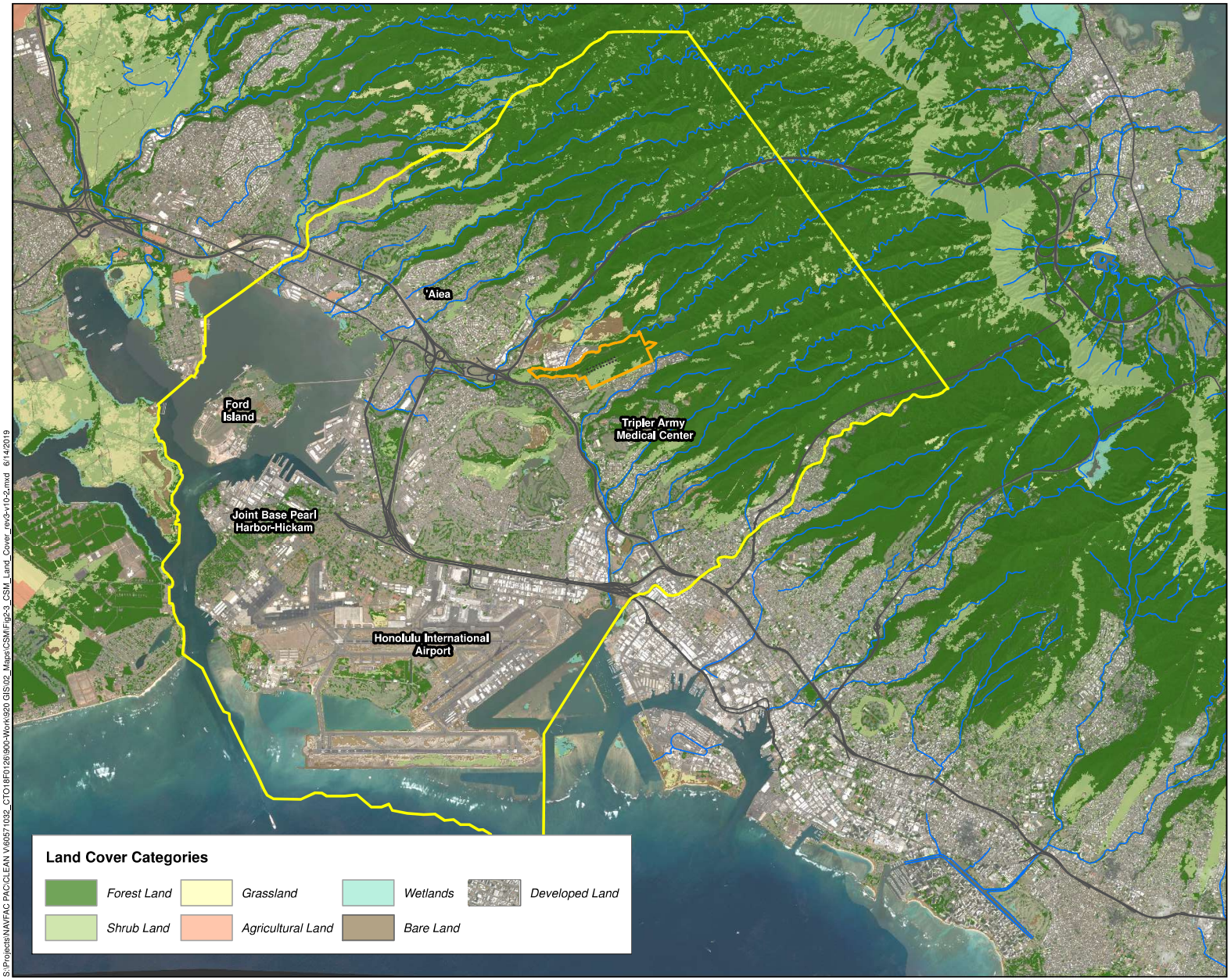

Location Map

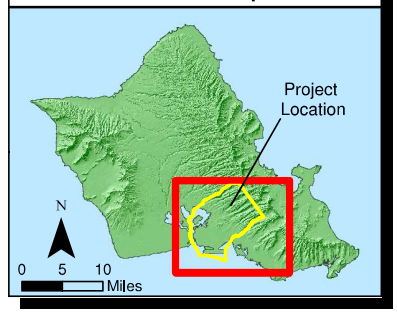

Legend

- Groundwater Model Domain
- Red Hill Facility Boundary and Fuel Storage Tanks
- Highway or Freeway
- Stream

Notes

1. Map projection: NAD 1983 Hawaii State Plane Zone 3 feet
2. Base Map: DigitalGlobe, Inc. (DG) and NRCS. Publication_Date: 2015
3. Land cover imagery source: NOAA Office for Coastal Management: Digital Coast - 2011 C-CAP Land Cover of Oahu, Hawaii (coast.noaa.gov)

N

0 5,000 10,000 15,000 Feet

S:\Projects\NAVFAC PAC\CLEAN V\60571032_CTO18F0126\900-Work\920 GIS\02_Maps\CSM\Fig2-3_CSM_Land_Cover_rev3-v10-2.mxd 6/14/2019

Figure 2-3
Land Cover
Conceptual Site Model Rev. 01
Investigation and Remediation of Releases and Groundwater Protection and Evaluation
Red Hill Bulk Fuel Storage Facility
JBPHH, O'ahu, Hawai'i

This page intentionally left blank

S:\Projects\NAVFAC PAC\CLEAN IV\60477080CTO 0053\900-Work\921 Graphics\PID_Wp\Fig3_GenSurficial_Geology.ai

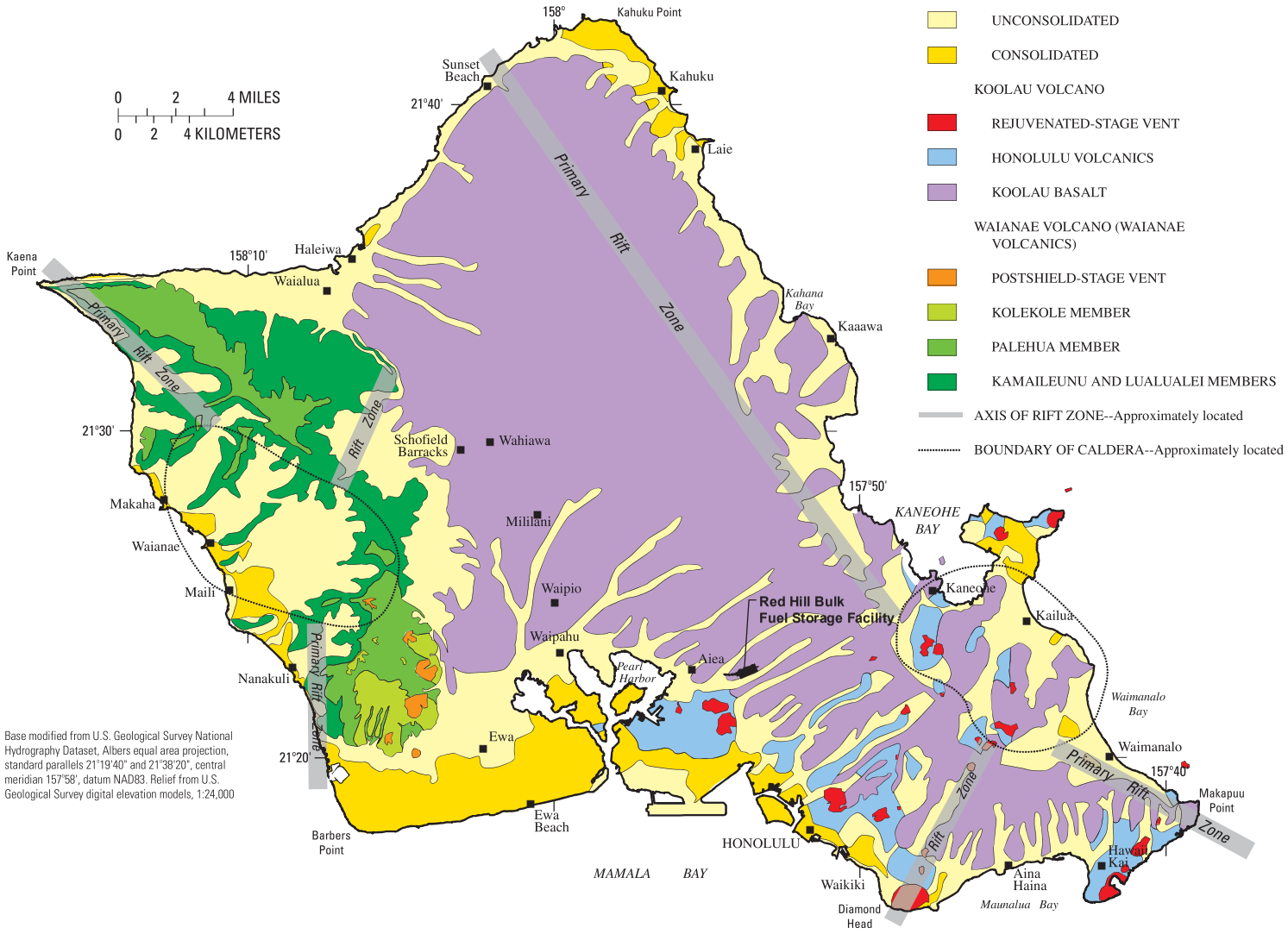

Note:
Modified from Stearns (1939); Langenheim and Clague (1987); Presley et al. 1997.

Figure 2-4
Generalized Surficial Geology of O'ahu
Conceptual Site Model Rev. 01
Investigation and Remediation of Releases and Groundwater Protection and Evaluation
Red Hill Bulk Fuel Storage Facility
JBPHH, O'ahu, Hawai'i

This page intentionally left blank

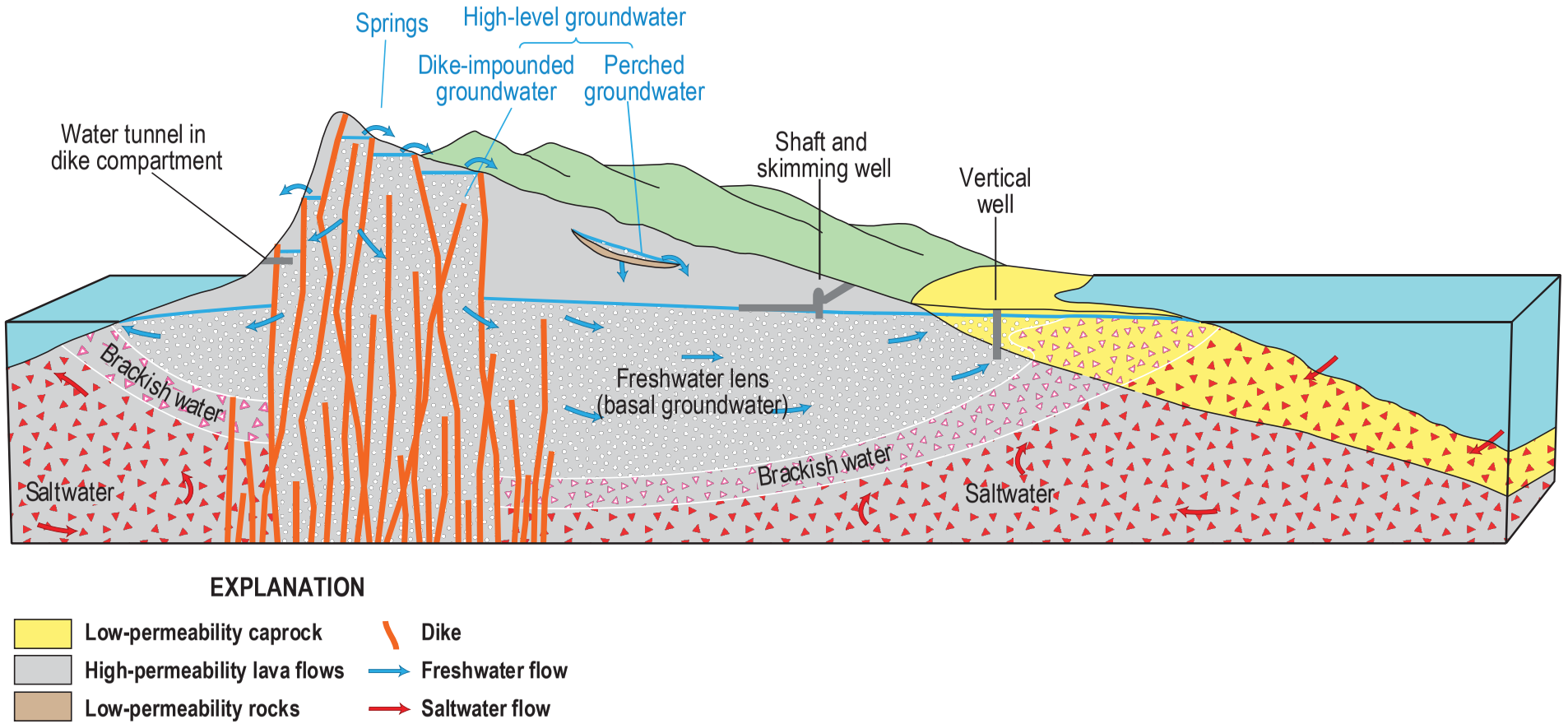

Source: Izuka et al. (2016 [2018]), Figure 21; as modified from Oki et al. (1999)

Figure 2-5
Conceptual Cross Section View of O'ahu Hydrogeology
Conceptual Site Model Rev. 01
Investigation and Remediation of Releases and Groundwater Protection and Evaluation
Red Hill Bulk Fuel Storage Facility
JBPHH, O'ahu, Hawai'i

This page intentionally left blank

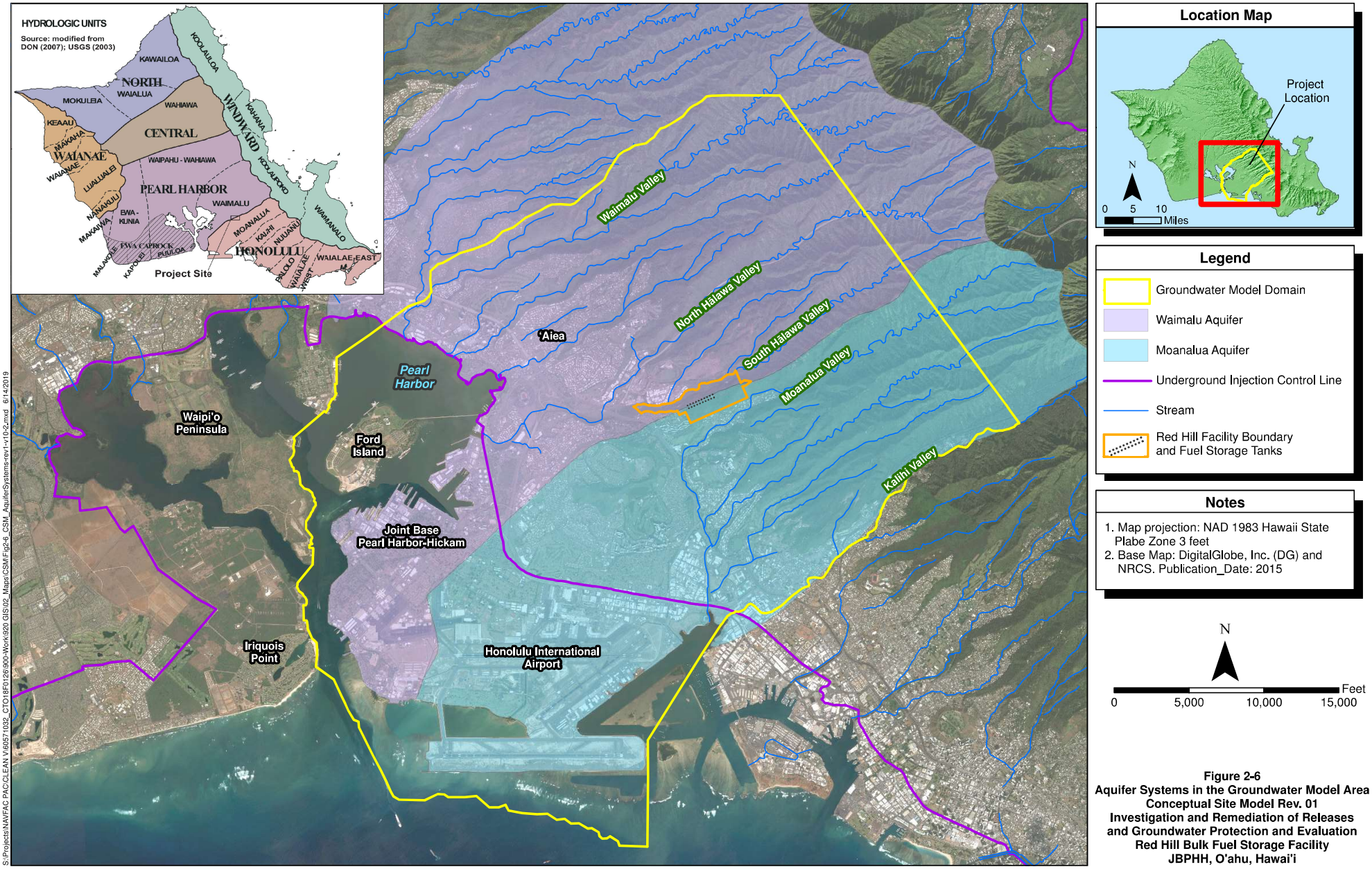

Location Map

Legend

- Groundwater Model Domain
- Waimalu Aquifer
- Moanalua Aquifer
- Underground Injection Control Line
- Stream
- Red Hill Facility Boundary and Fuel Storage Tanks

Notes

1. Map projection: NAD 1983 Hawaii State Plabe Zone 3 feet
2. Base Map: DigitalGlobe, Inc. (DG) and NRCS. Publication_Date: 2015

N

0 5,000 10,000 15,000 Feet

S:\Projects\NAVFAC PAC\CLEAN V\60571032_CTO18F0126\900-Work\920 GIS\02_Maps\CSM\Fig2-6_CSM_AquiferSystems-rev1-v10-2.mxd 6/14/2019

Figure 2-6
Aquifer Systems in the Groundwater Model Area
Conceptual Site Model Rev. 01
Investigation and Remediation of Releases and Groundwater Protection and Evaluation
Red Hill Bulk Fuel Storage Facility
JBPHH, O'ahu, Hawai'i

This page intentionally left blank

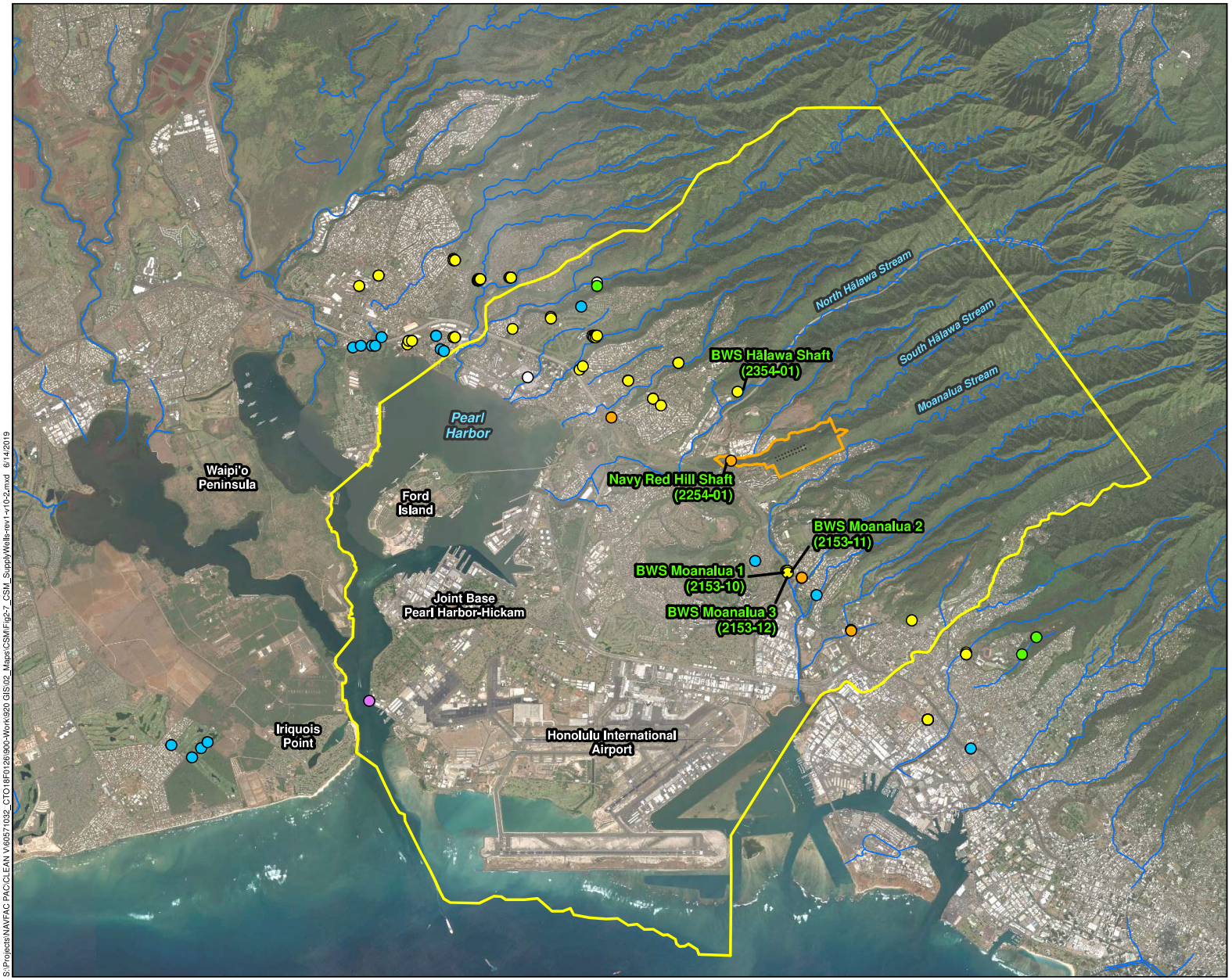

Location Map

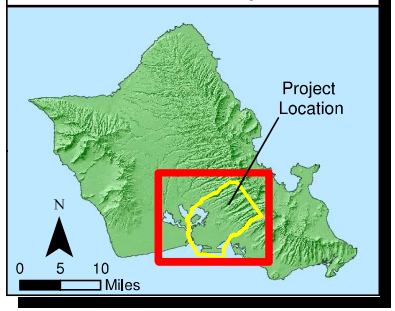

Legend

Supply Well

- Agriculture
- Domestic
- Industrial
- Irrigation
- Military
- Municipal
- Groundwater Model Domain
- Red Hill Facility Boundary and Fuel Storage Tanks
- Stream

Notes

1. Map projection: NAD 1983 Hawaii State Plabe Zone 3 feet
2. Base Map: DigitalGlobe, Inc. (DG) and NRCS. Publication_Date: 2015

N

0 4,000 8,000 12,000 Feet

Figure 2-7
Water Supply Wells
in the Groundwater Model Area
Conceptual Site Model Rev.01
Investigation and Remediation of Releases
and Groundwater Protection and Evaluation
Red Hill Bulk Fuel Storage Facility
JBPHH, O'ahu, Hawai'i

S:\Projects\NAVFAC PAC\CLEAN V\60571032_CTO18F0126\900-Work\920 GIS\02_Maps\CSM\Fig2-7_CSM_SupplyWells-rev1-v10-2.mxd 6/14/2019

This page intentionally left blank

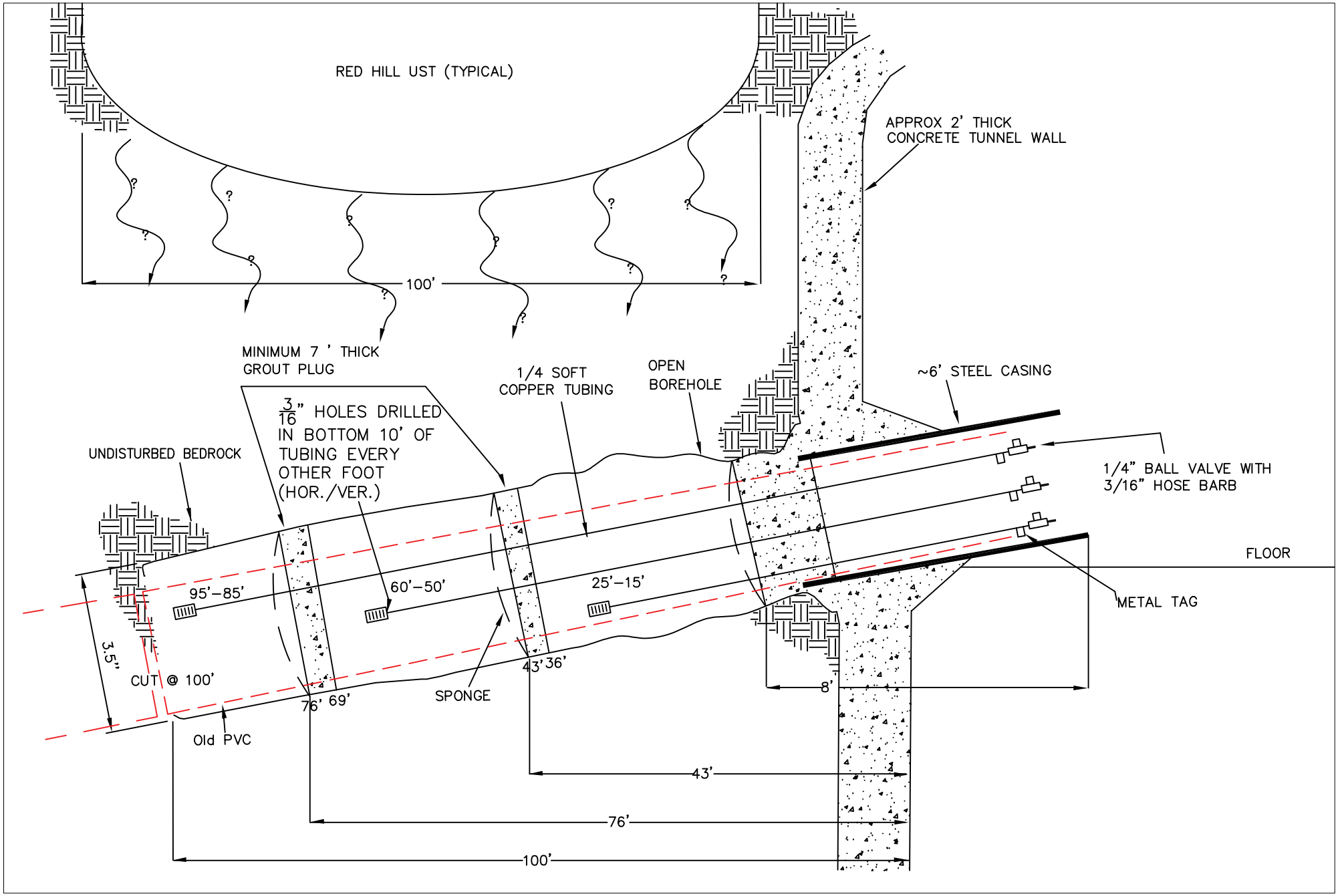

Source: DON (2007), Figure 2-2

Figure 2-8
Soil Vapor Monitoring Point Construction Details
Conceptual Site Model Rev. 01
Investigation and Remediation of Releases and Groundwater Protection and Evaluation
Red Hill Fuel Storage Facility
O'ahu, Hawai'i

This page intentionally left blank

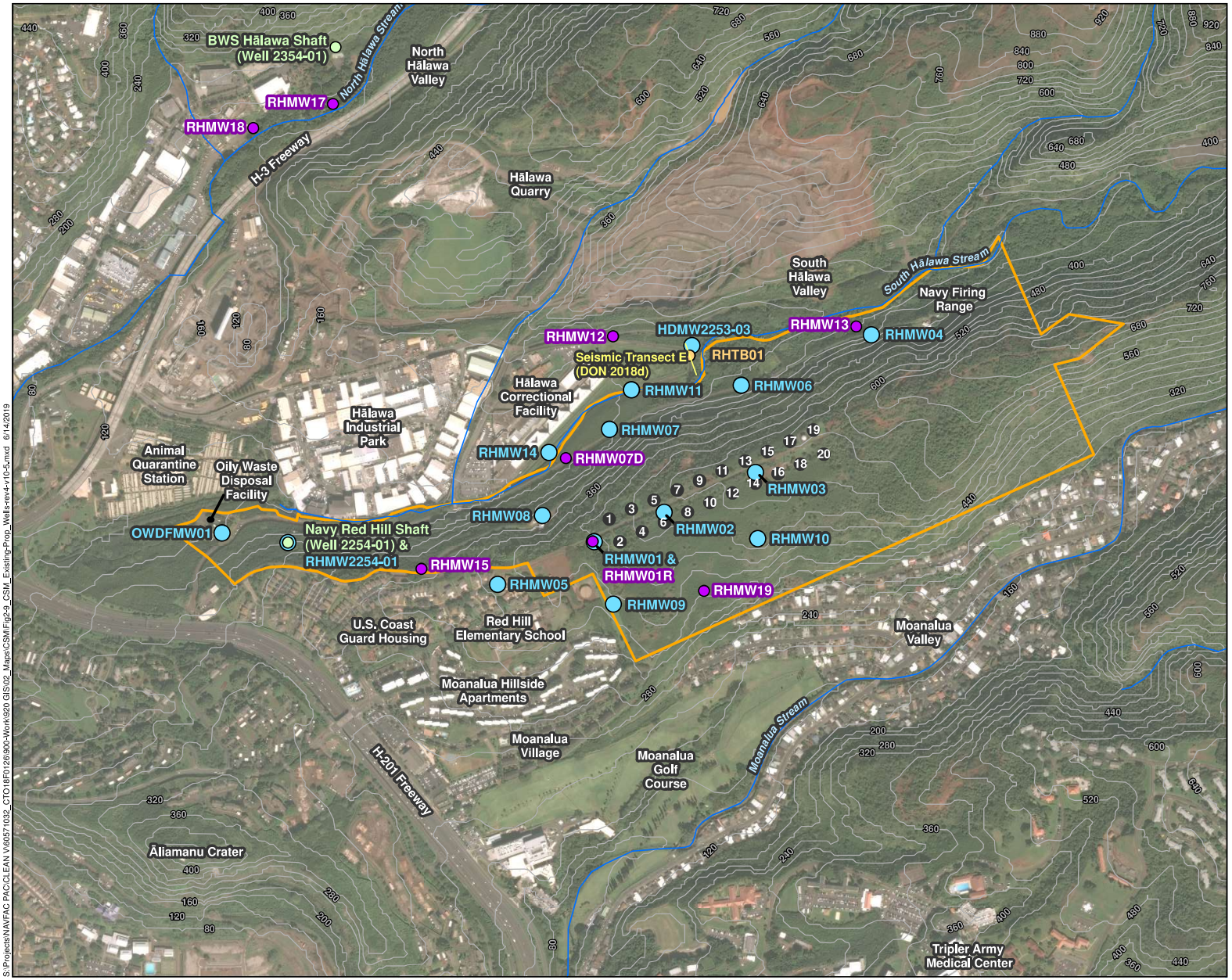

Location Map

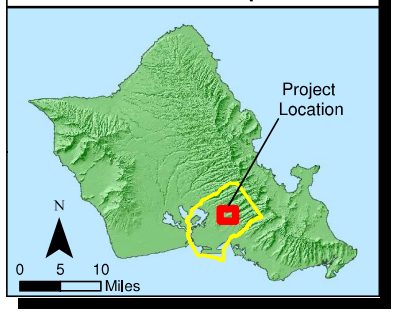

Legend

- Existing Monitoring Location
- Proposed Monitoring Well
- Water Supply Well
- Test Boring - Seismic Transect 'E'
- Stream
- Topographic Contour (feet mean sea level)
- Red Hill Facility Boundary
- Red Hill Fuel Storage Tank
- Groundwater Model Area

Notes

1. Map projection: NAD 1983 Hawaii State Plabe Zone 3 feet
2. Base Map: DigitalGlobe, Inc. (DG) and NRCS. Publication_Date: 2015

N

0 500 1,000 2,000 Feet

Figure 2-9
Existing and Proposed Groundwater Monitoring and Test Boring Locations
Conceptual Site Model Rev. 01
Investigation and Remediation of Releases and Groundwater Protection and Evaluation
Red Hill Bulk Fuel Storage Facility
JBPHH, O'ahu, Hawai'i

S:\Projects\NAVFAC PAC\CLEAN V\60571032_CTO18F0126\900-Work\920 GIS\02_Maps\CSM\Fig2-9_CSM_ExistingProp_Wells-rev4-v10-5.mxd 6/14/2019

This page intentionally left blank

Historical Photographs:

Orange line: Red Hill Bulk Fuel Storage Facility Boundary
Source: Hawai'i State Archives; photo M-56.45

Photo 2-1: Aerial Photograph of Red Hill Area, ca. 1939–1940

This page intentionally left blank

Source: Navy historical photograph

Photo 2-2: A-Frame Derricks Installed atop Red Hill to Excavate the Pilot Shafts for the Fuel Storage Tank Chambers, August 1941

This page intentionally left blank

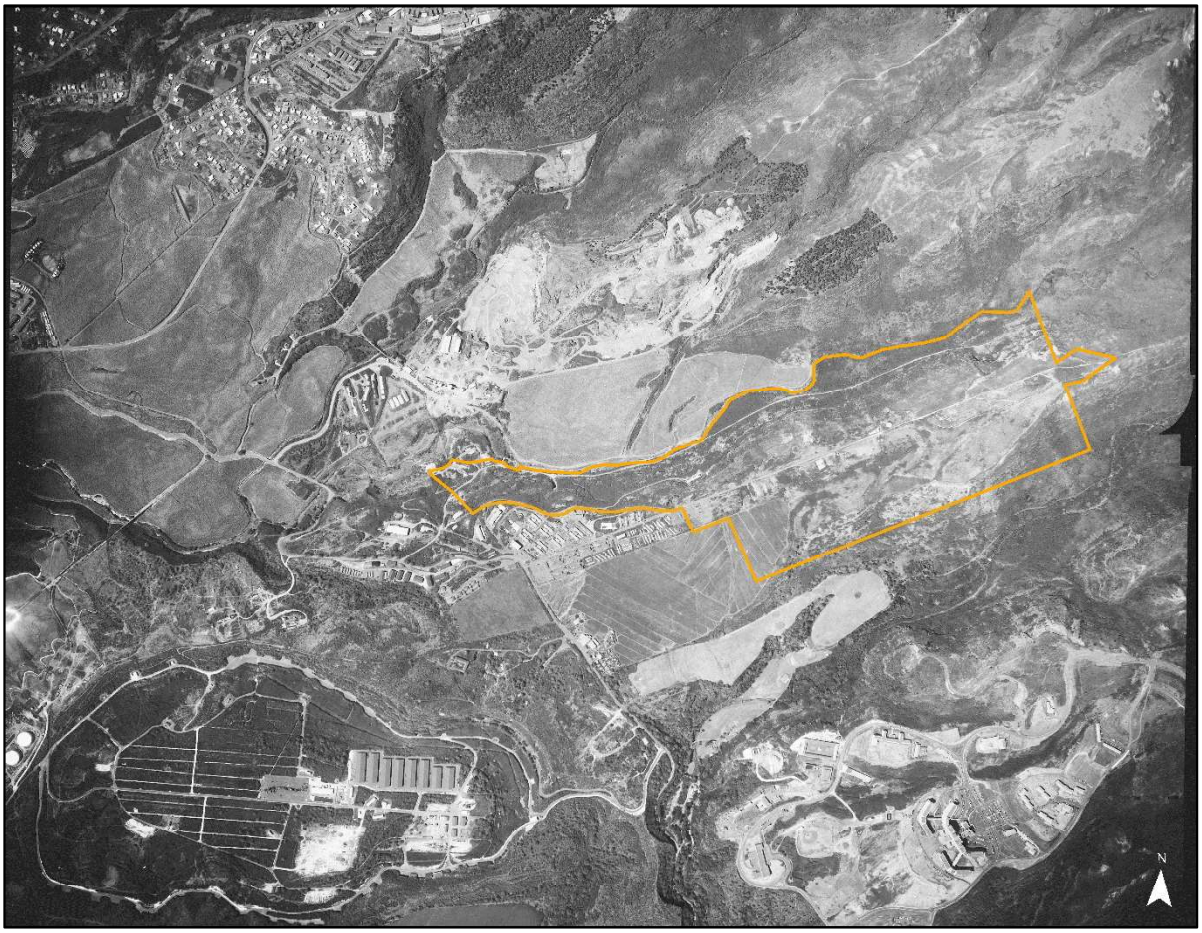

Orange line: Red Hill Bulk Fuel Storage Facility Boundary
Source: USGS aerial photo; 4-3-52, 2-67, GS-MFY (2400)

Photo 2-3: Aerial Photograph of Red Hill Area, 1952

This page intentionally left blank

3. Module B: Facility Construction and Operations

As shown on Figure 1-2, the Facility's complex of 20 fuel storage tanks were constructed underground within the thick sequence of volcanic rocks that form Red Hill. The tanks are currently used to store fuel for JBPHH operations, and have provided fuel for military operations in Hawai'i and throughout the Pacific since the Facility was completed in the early 1940s. Each tank is approximately 250 ft in height and 100 ft in diameter, with a capacity of approximately 12.5 million gallons. The tanks are constructed of concrete shell lined by steel, and 18 of them are currently active (Tanks 1 and 19 are inactive). The Facility tanks extend vertically through a 250-ft-thick sequence of massive basalt layers, inter-bedded tuff deposits, and breccia zones. The Facility was declared a National Historic Civil Engineering Landmark by the American Society of Civil Engineers in 1995.

3.1 Construction and Physical Characteristics of the Facility

The tanks were constructed in two parallel rows of ten tanks, i.e., ten pairs of tanks, connected by short tunnels to the main upper and lower access tunnels that transit between the two parallel rows of tanks. These main access tunnels contain light rail systems, water and electrical facilities, and fuel pipelines. In the lower tunnel, each short tunnel branches off from the main service tunnel and terminates at a "face-wall" under each tank. Ancillary piping extends from each face-wall to connect to fuel transmission lines that run approximately 2.5 miles from the Facility to a fuel pumping station at Pearl Harbor. The configuration of these fuel transmission lines (since the mid-2000s) is as follows (HAER 2015):

- 32-inch-diameter – Diesel Fuel-Marine (F-76)
- 18-inch-diameter – JP-5
- 16-inch-diameter – JP-8/F-24
- 16-inch-diameter between Red Hill and Pearl City – out of service, decommissioned, and abandoned in place (formerly JP-5, aviation gasoline [AVGAS], and motor gasoline [MOGAS])

The tanks are spaced 200 ft on center, separated from each other by 100 ft of basalt rock. The tops of the tanks are approximately 110–175 ft bgs, and the bottoms of the tanks are approximately 350–450 ft bgs (123–151 ft msl) (DON 2016a) and approximately 100–130 ft above the basal aquifer water table (the tanks are installed at slightly increasing elevations moving upslope; i.e., the bottoms of Tanks 1–2 are approximately 30 ft lower than the bottoms of Tanks 19–20).

Each tank was constructed by excavating the igneous rock formation of Red Hill to create a chamber for the tank, which was then lined with reinforced concrete and a ¼-inch-thick steel liner. The primary structure of each tank consists of an upper dome, barrel, and lower dome. The upper dome was constructed first. Rock was excavated to create a cavity for the upper dome. Steel framing and liner plates were then installed, followed by filling the cavity between the liner plates and lava rock with reinforced concrete, 4 ft thick. After the upper dome was constructed, the barrel and lower dome were excavated, and the rock face was sealed with spray-applied concrete (gunite). The barrel is constructed of reinforced concrete (2.5 ft thick minimum at the top, 4 ft thick minimum at the bottom). Steel angles were cast into the concrete for installation of the steel liner. The concrete tank was lined with ¼-inch-thick steel plates, which were attached by welding to the imbedded steel, and butt welded together at all plate edges. After the barrel was constructed, it was pre-stressed by injecting grout between the reinforced concrete and lava rock. The lower dome is similarly constructed of reinforced concrete and lined with ¼-inch-thick steel plates. The floor of the lower dome is flat and consists of ½-inch-thick

steel plates (DON 2016a). During construction, all lava tubes were carefully sealed with concrete plugs to help eliminate potential preferential pathways.

The pressurized grouting procedure is further detailed in a Red Hill Facility construction report prepared by the Historic American Engineering Record (HAER 2015):

> "*The bedrock sides of the tank excavation were coated with Gunite, approximately 6" thick, consolidating 'any loose rock to protect the workers excavating the vault and building the tank inside the vault.' The original contractors filled the joint between the reinforced-concrete shell and the Gunite on the bedrock with pressurized grout, after the concrete shell had cured. A former Supply Center Fuel Department Superintendent* [James Gammon] *provided further explanation about the purpose and steps of Gunite and grout placement:*
>
> > "*The purpose of grouting was to seal any cold joints in the reinforced concrete shell or in the gunited rock, … AND to pre-stress the tank structure with a compressive force that would counter the force of the hydrostatic pressure when the tank was filled with fuel…. [In] some areas of the vault that were not gunited during excavation [the step of] grouting would have consolidated the rock as well as sealed the joint between the rock and the reinforced concrete.*"

During the same period as tank construction, the Red Hill Shaft water development tunnel was constructed (see Section 2.11).

Additional construction in the early 1960s included oily waste piping and storage and fuel handling infrastructure. The Adit 6 tunnel contained a 16-inch-diameter fuel pipeline to the Pearl City Fuel Annex and an 8-inch-diameter oily waste line to a former 5,000-barrel-capacity slop tank (Facility No. S-355) located outside Adit 6 (HAER 2015). The slop tank was demolished, associated piping was cut and plugged, and the adjacent slop pump was removed in 2008 (Shaw 2009). The location and layout of slop tank No. S-355 and an adjacent slop tank pump are depicted on Figure 3-1. Boring no. 5 on Figure 3-1 is discussed in Section 4.2.

3.2 FUEL TYPES

Historically, types of fuel stored at the Facility have included Diesel Oil, Navy Special Fuel Oil (NSFO), Navy Distillate, F-76, AVGAS, and MOGAS. Originally, Tanks 3–20 contained NSFO and Tanks 1 and 2 stored diesel oil. Over time, each tank has been converted to store a variety of different fuel types (DON 2002). Conversion of tanks to store aviation fuel (jet fuel and AVGAS) began in the early 1960s (HAER 2015). Kerosene-based jet fuels stored at the Facility have included JP-5, JP-8, and North Atlantic Treaty Organization (NATO)-grade F-24. Based on discussions with Navy Region Hawai'i, there is no intent to store volatile fuels (such as MOGAS or AVGAS) in the future.

As indicated in Table 3-1, the fuel storage tanks currently contain JP-5, F-24, and F-76.

Table 3-1: Types of Fuel Historically and Currently Stored in the Facility's Fuel Storage Tanks

Tank ID	Date (Current Status [a])	Fuel Type
F-1	10/26/1942	Diesel Oil
	01/20/1947	Empty
	02/21/1947	Diesel Oil
	08/20/1953	Empty
	05/12/1954	Diesel Oil
	09/01/1999	Empty
	02/04/1970	JP-5
	11/30/2006	Empty (declared permanently out of service)
	Current (Inactive)	Empty
F-2	01/26/1942	Diesel Oil
	02/26/1948	Empty
	05/24/1948	Diesel Oil
	1962	JP-5
	2008	F-24 Jet Fuel
	Current (Active)	F-24 Jet Fuel
F-3	11/15/1942	Navy Special Fuel Oil
	08/27/1970	Navy Distillate
	04/03/1973	F-76 Diesel Fuel-Marine
	12/26/1973	JP-5
	early 2000s	JP-8
	2016	F-24 Jet Fuel
	Current (Active)	F-24 Jet Fuel
F-4	11/15/1942	Navy Special Fuel Oil
	02/17/1971	Navy Distillate
	06/06/1973	F-76 Diesel Fuel-Marine
	01/26/1974	JP-5
	early 2000s	JP-8
	2016	F-24 Jet Fuel
	Current (Active)	F-24 Jet Fuel
F-5	12/19/1942	Navy Special Fuel Oil
	04/06/1970	Empty
	12/29/1971	Navy Distillate
	08/08/1974	Empty
	10/1974	JP-5
	01/01/1976	Empty
	01/10/1983	JP-5
	early 2000s	JP-8
	10/2009	Empty
	Current (Active)	Empty
F-6	12/30/1942	Navy Special Fuel Oil
	03/29/1970	Empty
	02/29/1972	Navy Distillate
	10/1974	JP-5
	01/15/1982	F-76 Diesel Fuel-Marine
	07/22/1994	Empty
	05/19/1995	JP-5
	04/15/1998	Empty
	early 2000s	JP-8
	2016	F-24 Jet Fuel
	Current (Active)	F-24 Jet Fuel
F-7	03/16/1943	Navy Special Fuel Oil
	03/18/1971	Empty
	05/04/1971	Navy Distillate
	06/22/1973	Empty
	09/11/1973	F-76 Diesel Fuel-Marine
	05/22/1978	Empty
	02/29/1980	F-76 Diesel Fuel-Marine
	04/24/1995	Empty
	1996	JP-5
	Current (Active)	JP-5
F-8	03/02/1943	Navy Special Fuel Oil
	05/21/1971	Navy Distillate
	09/12/1973	F-76 Diesel Fuel-Marine
	04/13/1995	Empty
	1996	JP-5
	Current (Active)	JP-5
F-9	02/14/1943	Navy Special Fuel Oil
	06/23/1972	Navy Distillate
	09/13/1973	F-76 Diesel Fuel-Marine
	09/14/1995	Empty
	05/30/1996	JP-5
	Current (Active)	JP-5
F-10	01/26/1943	Navy Special Fuel Oil
	06/29/1972	Navy Distillate
	09/01/1973	F-76 Diesel Fuel-Marine
	10/03/1995	Empty
	1996	JP-5
	Current (Active)	JP-5

Tank ID	Date (Current Status [a])	Fuel Type	Tank ID	Date (Current Status [a])	Fuel Type
F-11	02/11/1943	Navy Special Fuel Oil	**F-12**	03/19/1943	Navy Special Fuel Oil
	06/29/1972	Navy Distillate		04/28/1970	Empty
	10/1973	F-76 Diesel Fuel-Marine		05/26/1972	Navy Distillate
	late 1990s	JP-5		01/29/1981	F-76 Diesel Fuel-Marine
				08/24/1994	Empty
				07/25/1995	F-76 Diesel Fuel-Marine
				late 1990s	JP-5
	Current (Active)	JP-5		Current (Active)	JP-5
F-13	03/23/1943	Navy Special Fuel Oil	**F-14**	03/21/1943	Navy Special Fuel Oil
	04/21/1976	F-76 Diesel Fuel-Marine		03/13/1973	Navy Distillate
	12/01/1994	Empty		10/25/1973	Navy Special Fuel Oil
	10/04/1995	JP-5		08/26/1975	Navy Distillate
	2000	F-76 Diesel Fuel-Marine		04/12/1981	F-76 Diesel Fuel-Marine
	06/2016	Empty		01/19/1995	Empty
				04/29/1996	JP-5
				2000	Diesel Fuel-Marine
				07/2012	Empty
	Current (Active)	Empty		Current (Active)	Empty
F-15	04/29/1943	Navy Special Fuel Oil	**F-16**	05/08/1943	Navy Special Fuel Oil
	10/27/1972	Navy Distillate		11/10/1971	Navy Distillate
	09/14/1973	F-76 Diesel Fuel-Marine		06/15/1975	F-76 Diesel Fuel-Marine
	10/02/1998	Empty		05/25/1994	Empty
	1998	F-76 Diesel Fuel-Marine		10/01/1998	JP-5
				11/04/1998	Empty
				1998	F-76 Diesel Fuel-Marine
	Current (Active)	F-76 Diesel Fuel-Marine		Current (Active)	F-76 Diesel Fuel-Marine
F-17	5/23/1943	Navy Special Fuel Oil	**F-18**	06/13/1942	Navy Special Fuel Oil
	03/30/1960	Empty		03/30/1960	Empty
	12/11/1964	AVGAS		05/1963	JP-5 (for leak tests)
	08/29/1968	MOGAS		08/18/1964	AVGAS
	01/15/1969	JP-5		10/30/1968	Empty
	02/2010	Empty		01/10/1969	JP-5
	Current (Active)	Empty		Current (Active)	JP-5
F-19	06/13/1943	Navy Special Fuel Oil	**F-20**	07/20/1943	Navy Special Fuel Oil
	03/30/1960	Empty		03/30/1960	Empty
	01/17/1964	JP-5		06/14/1964	JP-5
	10/1985	Empty		12/28/1971	Empty
	11/2006	Empty (removed from service)		04/04/1972	JP-5
	Current (Inactive)	Empty		Current (Active)	JP-5

Sources: DON (2005), Red Hill Groundwater LTM reports (DON 2018f), Tank Inspection Reports, and CIV NAVSUP review 2019-06-18.

[a] Active status indicates a tank is currently available for use, but does not necessarily indicate the tank is currently filled. Inactive status indicates a tank is currently not available for use.

3.3 UNCERTAINTY ANALYSIS

As noted in Section 3.2, the Navy has no plans to alter the types of fuels stored at the Facility. Issues related to tank integrity and upgrade alternatives are being addressed by other sections of the AOC Statement of Work (EPA Region 9 and DOH 2015).

3.4 ADDRESSING UNCERTAINTIES

Future activities relevant to Facility construction and operation are being addressed by AOC Statement of Work (EPA Region 9 and DOH 2015) Section 2 Tank Inspection, Repair, and Maintenance (TIRM); Section 3 Tank Upgrade Alternatives (TUA); Section 4 Release Detection / Tank Tightness Testing; Section 5 Corrosion and Metal Fatigues Practices; and Section 8 Risk/Vulnerability Assessment.

This page intentionally left blank

S:\Projects\NAVFAC PAC\CLEAN V\60571032_CTO18F0126\900-Work\920 GIS\02_Maps\CSM\Fig3-1 Slop Tank Location 2013b.mxd 6/20/2019

Location Map

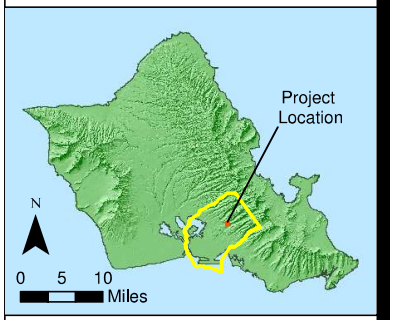

Site Location Map

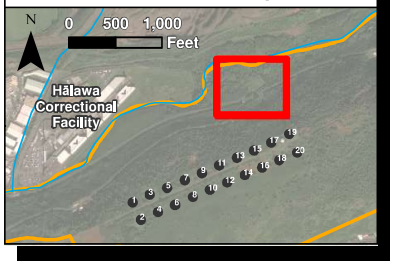

Legend

- Boring Location
- Red Hill Monitoring Well RHMW06
- Stream
- Groundwater Model Domain
- Red Hill Installation Boundary

Notes

1. Map projection: NAD_1983_StatePlane_Hawaii_3_FIPS_5103_Feet
2. Base Map: Google earth, © 2017 Google
3. Location of Former Slop Tank features are estimated from U.S. Naval Supply Center Pearl Harbor, Yards & Docks Drawing No. 890473 -Conversion of POL Storage Facilities, Red Hill Storage 5000 BBL Slop Tank Plan, dated 6/28/60. Location of Boring B-5 from PGE (2015).

Figure 3-1
Location of Former
Slop Tank S-355 and Slop Pump
Conceptual Site Model Rev. 01
Investigation and Remediation of Releases
and Groundwater Protection and Evaluation
Red Hill Bulk Fuel Storage Facility
JBPHH, O'ahu, Hawai'i

This page intentionally left blank

4. Module C: LNAPL Release Source Zone

This module provides appropriate models for evaluating possible release scenarios. Understanding how fuel could leak and migrate into the surrounding rock formations from the 2014 Tank 5 release can provide insights on how fuel that may be released at other tanks within the tank farm could migrate in the source-zone area. The release source-zone model presented below includes specific detail about the causes of the Tank 5 release in January 2014 and assessment of potential migration pathways intrinsic to the construction of the tanks and surrounding facilities; it includes:

- Previous investigations and the Red Hill LTM network
- Location of possible release point(s) within the tank based on construction, measurements, and observations
- Possible locations and means that leaking fuel could enter the surrounding rock formation

Migration pathways for fuel/LNAPL from the tank source to the surrounding rock formation were assessed by reviewing the following:

- Tank designs and plans
- Construction "as built" plans
- Documented construction practices
- Modifications and upgrades
- Documented leaks in and around the Red Hill tank farm

4.1 Summary of Previous Investigations and Environmental Actions

Previous environmental investigations at the Facility since 1996 are summarized in Table 4-1.

Table 4-1: Summary of Previous Red Hill Investigations

Investigation	Summary	COPCs and Other Parameters Investigated
Remedial Investigation Phase I and II, Red Hill Oily Waste Disposal Facility (DON 1996a, 2000)	A two-phase remedial investigation (RI) was initiated in the early 1990s at a site where oily waste from cleaning of the Facility's fuel storage tanks was historically disposed of (first in an unlined pit and later in a lined stilling basin that subsequently cracked and was repaired). In 1995, an interim removal action was initiated to remove the stilling basin and underlying soil contamination and install a low-permeability geosynthetic cap over the backfilled excavation to reduce infiltration (DON 1996b). The Phase II RI further characterized the vertical extent of petroleum hydrocarbon contamination. The investigation concluded that although the contaminant transport pathway to the basal aquifer was potentially complete, any potential transport that could occur would be insignificant due to the removal action, reduction of infiltration, and documented major hydrogeologic barriers. DOH issued a concurrence letter for a No Further Action determination for the OWDF in 2005 (DOH 2005). Due to anomalous data reported in recent years at basal groundwater monitoring well OWDFMW01 (installed during the investigation as MW08), the site has been re-opened by the Navy and is being re-evaluated under the DOH Hazard Evaluation and Emergency Response (HEER) Office.	TPH, PAHs, and VOCs

Investigation	Summary	COPCs and Other Parameters Investigated
Facility Site Characterization and Investigation (DON 1999, 2002)	A two-phase investigation was initiated in 1998 to evaluate presence of petroleum constituents. The investigation included drilling and sampling of slant borings under all 20 Facility tanks and two vertical borings within the lower access tunnel west of the tanks; installation and sampling of one groundwater monitoring well (since renamed as RHMW01); and a screening-level risk assessment. Results indicated that petroleum had been released from several Facility tanks, as observed in core samples and indicated by the groundwater data. The Phase II report recommended a comprehensive assessment of human health risks potentially associated with the Facility. The DOH Solid Waste Branch requested that quarterly groundwater monitoring be conducted, a Tier 3 risk assessment be conducted to evaluate the risk to Red Hill Shaft (Navy Supply Well 2254-01), and a contingency plan be developed to protect the well from future contamination.	TPH-g, TPH-d, TPH-o, TPH-kerosene, VOCs, PAHs, SVOCs, and hydrocarbon fingerprint
Technical Report (DON 2007)	An environmental investigation and risk assessment initiated in 2004 included installation of SVM points in angle borings drilled under the Facility tanks and three groundwater monitoring wells (RHMW02, RHMW03, and RHMW04) in the lower tunnel. Rock core, groundwater, and soil vapor samples were collected and analyzed; a three-dimensional groundwater model was developed to simulate CF&T; and a Tier 3 human health risk assessment was conducted. The risk assessment found the primary potential risk to be from a hypothetical future scenario where groundwater beneath the tank farm was extracted for residential tapwater use. The CF&T modeling estimated the quantity, time, and distance a release of JP-5 fuel would result in benzene exceeding federal and state criteria at the Red Hill Shaft water supply well. The report recommended developing mitigation steps for a contingency plan, which was subsequently developed as the Red Hill GWPP (DON 2008b).	VOCs, alkalinity, fixed gases, metals, anions, MADEP VPH/EPH fractions, TPH-g, TPH-d, TPH-o, and percent solids
Tank 17 Removal Action Report (DON 2008c)	A limited removal action and site characterization investigation was conducted in June 2008 after approximately 4 gallons of JP-5 fuel were released from overhead piping in the Facility tunnel. Following the removal action, the report's Environmental Hazard Analysis determined that the release posed no further significant environmental hazards.	TPH-g, TPH-d, VOCs, PAHs, and flashpoint
Type 1 Letter Report (DON 2010)	After a reported TPH-d concentration in an October 2008 groundwater sample from RHMW02 exceeded the SSRBL, an investigation was conducted to provide a report to DOH in accordance with the Red Hill GWPP (DON 2008b). The 2010 investigation re-evaluated the DON (2007) groundwater model assumptions/results and the Tier 3 risk assessment results. The re-evaluation of the 2007 groundwater model found local groundwater flow direction to be from the tank farm toward Red Hill Shaft, and a regional component flowing toward the northwest. The re-evaluation of the 2007 risk assessment found that its conclusions remained valid. An additional groundwater monitoring well (RHMW05) was installed west of the tank farm and added to the Red Hill groundwater monitoring network.	TPH-g, TPH-d, VOCs, MADEP VPH/EPH fractions, PAHs, and lead

EPH extractable petroleum hydrocarbon
MADEP Massachusetts Department of Environmental Protection
PAH polynuclear aromatic hydrocarbon
SSRBL site-specific risk-based level
SVOC semivolatile organic compound
TPH-d TPH-diesel range organics
TPH-g TPH-gasoline range organics
TPH-o TPH-residual range organics (i.e., TPH-oil)
VOC volatile organic compound
VPH volatile petroleum hydrocarbon

A summary of all key environmental actions and milestones is provided on Figure 4-1.

A chronological listing of regulatory issues and submitted documents regarding Facility tank petroleum releases as of August 21, 2014, is presented in Appendix A of the 2014 *Interim Update* to the Red Hill GWPP (DON 2014b).

4.2 SLOP TANK (FACILITY NO. S-355)

From 1964 to the present, the Adit 6 tunnel has contained a 16-inch-diameter fuel pipeline to Pearl City Fuel Annex and an 8-inch-diameter oily waste line to a former 5,000-barrel-capacity jet fuel slop tank (Facility No. S-355) located outside Adit 6 (HAER 2015). The slop tank and the adjacent slop pump was removed and associated piping was cut and plugged in 2008 (Shaw 2009). TPH results from samples collected directly beneath the tank at the time of tank removal did not exceed DOH Environmental Action Levels (EALs). However, during a geotechnical investigation (*Red Hill Fire Suppression and Ventilation System PGE Job No.3773-008, June 2013*) (PGE 2015), one of ten borings (boring B-5, of B-4 through B-13) drilled proximal to the former slop tank encountered a "strong hydrocarbon odor" in the weathered clinker and basalt from approximately 26 ft bgs to the total boring depth at 41.5 ft bgs). No samples were submitted for laboratory analysis of petroleum hydrocarbon contamination. The location and layout of slop tank No. S-355, adjacent slop tank pump, and boring B-5 are depicted on Figure 3-1.

4.3 FORMER OILY WASTE DISPOSAL FACILITY

The former OWDF, located within the Red Hill Bulk Fuel Storage Facility boundaries approximately 600 ft west of Red Hill Shaft (Figure 1-1), was built in the 1940s as a collection point for oily wastewater generated by periodic cleaning of the Facility's fuel storage tanks. The wastewater was collected originally in an unlined pit and later in a concrete-lined stilling basin that subsequently cracked and was repaired. During a two-phase site investigation conducted by the Navy in the 1990s (described in Table 4-1), petroleum waste was found to have infiltrated to a perched water-bearing zone beneath the stilling basin but was not detected in the underlying basal aquifer. The investigation found that the basal aquifer beneath the OWDF was locally confined by low-permeability massive basalt and overlain by saprolite/alluvium with multiple perched horizons that presented hydrogeologic barriers to downward COPC transport (DON 2000).

The stilling basin was removed and the excavation was capped in 1995 (DON 1996b); tank-cleaning wastewater is now collected in a 40,000-gallon aboveground storage tank (AST) installed at the site, where it is removed and transported off site for processing. One of the basal groundwater monitoring wells installed during the OWDF investigation was incorporated into the Red Hill groundwater monitoring network in 2009, renamed as OWDFMW01.

4.4 SURFACE SOIL AT RHMW14

Initial drilling of multilevel monitoring well RHMW14 at the Hālawa Correctional Facility (Figure 1-1) was temporarily suspended in late November 2018 due to hydrocarbon odors noted in shallow soil at approximately 12 ft bgs. The landowner officially notified DOH on November 28, 2018. Suspected impacted soil appeared to be shallow and vertically localized (less than 20 ft bgs) based on follow-up analytical samples. No samples exceeded current DOH Tier 1 EALs. Shallow soils were isolated via surface casing, and drilling and installation of RHMW14 resumed as planned.

4.5 HISTORY OF JANUARY 2014 JP-8 RELEASE FROM TANK NO. 5

During Tank 5 refilling operations following a routine 3-year inspection and refurbishment process, a fuel release was discovered and verbally reported to DOH on January 13, 2014. A release of JP-8 from Tank 5 was confirmed and reported to DOH in writing on January 23, 2014. The volume of fuel lost from Tank 5 was estimated at 27,000 gallons. The following timeline of the 2014 release was compiled

from the AOC Section 2.2 *Tank Inspection, Repair, and Maintenance* (TIRM) *Report* (NAVFAC EXWC 2016), the Tank 5 *Initial Release Response Report* (DON 2014a), and the Navy's Energy & Environmental Magazine *Currents* (Isobe 2016):

- Following the 3-year inspection and refurbishment completed in accordance with a process conducted every 20 years, Tank 5 was placed back into service on December 9, 2013, and the Navy commenced filling it with JP-8 fuel.
- Alarms were activated when initially filling Tank 5 following the tank refurbishment.
- Operators observed an unscheduled fuel movement on January 11, 2014 and confirmed a 3/16-inch drop in fuel with manual gauges by January 13, 2014. Product from Tank 5 was drained.
- A fuel hydrocarbon seep was observed below Tank 5 on the evening of January 12, 2014 in the lower cross tunnel wall near the exterior of the material encasing the lower part of the tank. A sample showed that the liquid was JP-8 fuel.
- The SVM points under Tank 5 exhibited a sharp increase in hydrocarbon vapor concentrations from previously measured December 15, 2013 levels, and concentrations also increased significantly in nearby SVM points at Tanks 3, 6, 7, 8, and 9 (see Section 4.7).
- Subsequent analysis indicated faulty work by a contractor, specifically:
  - Defective workmanship in welding by the contractor was found in Tank 5.
  - Defective welds had not been discovered and corrected by the contractor due to poor inspection and ineffective quality control.
  - Seventeen unrepaired ¼-inch gas test holes drilled through the tank shell were found. These, along with defective welds on patch plates that covered the gas test holes, were deemed the underlying cause of the release. As noted in the TIRM Report (NAVFAC EXWC 2016): "*When Tank 5 was filled with fuel, the typical leak path was through defects in the seal weld, through the joint between a patch plate and the tank shell, and through the gas test hole*" (Section 9-2.1.4).

4.6 CONSTRUCTION PRACTICES AND MATERIALS

Review of Red Hill construction practices and "as-built" plans indicate potential migration pathways related to the practices and materials used.

The AOC Section 2.2 TIRM Report (NAVFAC EXWC 2016) indicates that "*Areas of* [Tank 5's] *internal steel liner appear to have separated from the concrete encasement surrounding the tank. This condition can allow water, fuel, liquid or vapor, to be trapped in a localized area between the two surfaces*" (TIRM Report Appendix AN, Section 2.1; 10/3/2014). The purpose of the gas test holes drilled in the tank shell was to "*sample for hydrocarbon vapor due to fuel which may have been in the tank shell to concrete interstice"* (TIRM Report Chapter 5-6.1), which is an industry-standard safety requirement prior to conducting welding activities *"…since hydrocarbons have been found in contact with the back wall surfaces in the past tanks*" (contractor's 2010 pre-refurbishment Tank 5 Inspection Report; TIRM Report Appendix T, Table 7-1, Note 3). In addition, the AOC Statement of Work Section 3.2 TUA *Scope of Work* (DON 2016a) notes that typical historical structural and integrity issues with the Red Hill fuel storage tanks relevant to repairing them for a future use include "*corrosion and pitting,*" "*holes in the steel liner,*" and "*defective welds in the barrel and upper and lower domes*" (TUA Scope of Work, Section 2.3).

The following summary of the design, construction, and modification of the tanks' tell-tale system

from a Red Hill construction report published by the Historic American Engineering Record can provide insight to potential leak points (HAER 2015):

- The original tell-tale leak-detection system consisted of a series of 12 vertical pipes, equally spaced around the perimeter of each tank.
- The pipes ran vertically down the inside tank wall, penetrated the lower dome, ran through the concrete plug under the tank, and ended at a monitoring station in the lower access cross tunnel near the skin valves for each tank.
- Tell-tale pipes were designed to collect any fuel that leaked through a hole in a shell plate (or through a hole in a shell-plate weld):
  - Fuel leaks to the space between the back side of the steel shell plates and the inner side of the reinforced concrete wall.
  - The tell-tale pipe would then deliver the collected fuel to the lower access cross tunnel, to indicate the presence of a leak.
  - During service intervals, the tell-tale pipes at or near the bottom of the tanks experienced significant corrosion on the external surfaces of the piping due to saltwater in the bottom of the tanks. Many tell-tale leak indications were found to be false due to holes corroded through the telltale piping itself (TIRM Report, Chapter 1-3.2) (NAVFAC EXWC 2016). From the time the Facility began operation in 1942 until the Chevron refinery was built on O'ahu in the early 1960s, all fuel was delivered to Pearl Harbor by tanker ships. Waves washing over the deck of a fully loaded tanker ship would result in seawater entering the cargo tanks through vents. The rolling of the ship helped to mix the seawater with the fuel, and when a tanker docked at Pearl Harbor, the saltwater was offloaded along with the fuel. The saltwater settled to the bottom of a Red Hill tank and exposed the tell-tale piping to increased corrosion rates (HAER 2015).
- During 1960–1963, the tell-tales in Tanks 17–20 were modified and improved:
  - The pipe diameter was increased to prevent clogging, and the pipe wall thickness was increased to Schedule 80, to provide corrosion allowance.
  - Tank 19 retains these tell-tale pipe improvements from the period 1960–1963. It is not known if any of the improved tell-tales remain in Tanks 17, 18, or 20.
- During 1971–1973, two additional improvements to the tell-tale design were installed in Tanks 5, 6, and 12:
  - The pipes up into the Gauging Gallery at the top of the tank were extended to where they could be readily accessed for flushing and cleaning.
  - The exit point of the tell-tale pipes was relocated by routing through the side of the hemispherical lower tank section above the previous bottom exit point, so they would not be exposed to the corrosive effect of the tank bottom water.
- A 1977 design decision (MILCON P-060) removed the tell-tale systems from Tanks 1–16 altogether. Removal of the tell-tale systems created two problems:
  - It removed a tool for potentially identifying and locating fuel leaks.
  - It eliminated a way to drain off any rainwater that percolates down through the lava rock and finds its way into the space between the back side of the steel shell plates and the inner side of the concrete wall. The standing water could cause accelerated corrosion of the back side of the steel shell plate.

- Hundreds of small steel plates are welded to the tank walls to cover small holes through the liner plates that remained when the tell-tale pipes were removed under Project P-060.

4.6.1 Bottom Drain

The bottom drain pipe originally installed in each tank has been identified as a source of possible leaks: "*As the 8-inch-diameter pipe 'daylights' through the concrete wall at the end of the LAT* [lower access tunnel] *cross tunnel, it connected to a manually operated 8-inch gate valve, the skin valve. Due to the constant exposure to tank bottom water, holes corroded through the pipe walls of several of the bottom drain pipes; these rusted pipes were removed from service*" (HAER 2015).

4.6.2 Tunnel Floor Pipe Bedding and Sumps

Lower tunnels could have potential migration pathways for LNAPL migration through the following:

- Contraction of the gunite during curing could create space between the gunite and rock formations around the tunnel exterior.
- Sumps, vent lines, grates, and drains.

4.6.3 Recent Construction and Upgrades

The Navy/DLA recently installed or upgraded six oil-tight doors in the lower access tunnel to contain fuel migration in the event of an emergency, along with a new fire suppression system to reduce the threat of a release caused by fire (Atlas et al. 2017). The project included repair of inoperable doors that could open and close reliably with remote capability during fuel release and fire events. The electro-mechanical system replaced previously inoperable mechanical- and pneumatic-powered systems. Additionally, five new sumps were installed in proximity to each door. Each sump is capable of pumping released hydrocarbon fuel, aqueous fire-fighting foam (AFFF), or water to a 150,000-gallon retention tank located outside of Adit 3 in the event of a release or flood. Locations of the oil-tight doors and sumps are presented on Figure 4-2.

4.6.4 Current Conditions of Facility Infrastructure

A 2017 evaluation of the Facility conducted for EPA (Atlas et al. 2017) found the following:

- Piping components in the tunnel system between the Red Hill Facility storage tanks and the pumphouse and piping components from the surge tank into the pump manifolds appear to be in generally good condition, with minor surface defects and pitting on the pipeline in some areas.
- No major issues were observed on the piping.
- Any potential leak paths in these areas would likely be contained by the tunnel system and the oil-tight doors and would likely be detected by pressure drops monitored in the control room.
- Piping systems at the upper tank farm area (where the system's ASTs are located) are in generally good shape and have been designed and maintained to modern standards.
- Any potential product loss in this area would likely be contained by the liner located beneath the upper tank farm ASTs and equipment and would likely be detectable with a pressure drop in the piping system.

4.7 POST-2014-RELEASE MONITORING RESULTS

Soil Vapor. Following the 2014 release, soil hydrocarbon vapor levels were collected from the three-point SVM system under the tanks. Concentrations under Tank 5 measured on December 23, 2013 and on January 15, 2014 increased as follows: from 50 to 96 ppbv (shallow), from 622 to 225,000 ppbv (middle), and from 794 to 204,000 ppbv (deep). The high concentration of 225,000 ppbv measured on January 15, 2014 initially decreased to 100,000 ppbv on February 24, 2014, but later increased even higher to 450,000 ppbv on May 1, 2014 (see Figure 4-3). This suggests that Tank 5 releases may have occurred along multiple migration pathways to the tank bottom, with some pathways taking longer than others. This concept would be consistent with the forensic analysis of the release from multiple release locations via gas test holes as the primary cause of the release, as described above in Section 4.5 (NAVFAC EXWC 2016).

Vapor concentrations also increased over pre-January 2014 conditions in nearby SVM points at Tanks 3, 6, 7, 8, and 9 but generally exhibited average vapor concentrations less than 10 percent of the Tank 5 vapor concentration over the next year (Figure 4-3, lower panel). The detection of the Tank 5 release in a large number of SVM points indicates that the existing SVM network provides a robust system for detection of this type of release. There were also less-significant responses in tanks as distant as Tank 15 to the north during vapor monitoring on January 30, 2014. The SVM points for the tanks around the Tank 5 release are located at elevations between ~80 and ~110 ft msl, are well under the elevation of the release (~180–250 ft msl), and are below the elevation of the bottom of Tank 5 (~115 ft msl). Thus, some combination of lateral/downward LNAPL migration and diffusion/advective vapor migration could explain the migration of vapors from the Tank 5 release to the SVM points under the nearby tanks. The low vapor pressure of the jet fuel constituents will likely preclude any density-driven migration of jet fuel vapors.

Groundwater. Following the 2014 release, water samples were collected from drinking water supply wells Navy Red Hill Shaft, BWS Hālawa Shaft, Hālawa Wells, ʻAiea Wells, ʻAiea Gulch Wells, and Moanalua Wells. Test results indicated that no petroleum constituents had reached the groundwater drinking water supply wells in the months following the release (RHSF Task Force 2014).

Cumulative concentration graphs of Red Hill groundwater monitoring results for current COPCs dating from 2005 onward are presented in Appendix A (and further discussed in Section 7.2); the date of the 2014 release is indicated on the graphs. The graphs, current as of the January 2019 monitoring event (see Appendix B.3 Figure 4-3), show that exceedances of screening criteria (DOH Tier 1 EALs) for total petroleum hydrocarbons (TPH) and/or naphthalenes have occurred in the monitoring wells closest to the tanks (RHMW01, RHMW02, and RHMW03) both before and after the 2014 Tank 5 release. No confirmed floating free product has been measured at any monitoring location, and no exceedances of the COPC screening criteria have been observed at sampling point RHMW2254-01 located adjacent to Red Hill Shaft (Navy Supply Well 2254-01). Further discussion of dissolved-phase COPCs detected in groundwater is presented in Section 7.2.

Since the 2014 release, seven additional groundwater monitoring wells to date have been added to the Red Hill network (see Table 2-1).

4.8 2014 RELEASE CONCEPTUAL MODEL

Release Point:

- Multiple breaches in the wall of Tank 5 into the space between the back side of the steel shell plates and the inner side of the reinforced concrete.

- Seventeen unrepaired gas test holes through the tank shell were found and were deemed the underlying cause of the release.
- Defective workmanship in welding by the contractor was found in Tank 5.
- Corrosion and pitting in interior and exterior steel tank wall.
- Multiple migration pathways from different areas, some taking different and possibly longer routes.

Release Point LOEs:

- Results of forensic analysis of the release as detailed in NAVFAC EXWC (2016)
- Historical observations of space between the back side of the steel shell plates and the inner side of the reinforced concrete (NAVFAC EXWC 2016)
- Areas of weakness or corrosion potential such as the bottom drain pipe and tell-tale pipe penetrations (NAVFAC EXWC 2016)

Migration Pathways:

- LNAPL migrates down along the space between the back side of the steel shell plates and the inner side of the reinforced concrete to lower tank bottom.
- Some LNAPL may potentially exit into cracks in the concrete shell into higher-permeability rock types surrounding the concrete or to space between the inner side of the reinforced concrete and outer gunite-covered rock formations.
- Contraction of the gunite after curing could create space between the gunite and rock formations around the tunnel exterior.
- Potential damage to concrete and gunite associated with tank metal plate reinforcement.
- Sumps, vent lines, grates, and drains.

Migration Pathway LOEs:

- Construction design supports potential development of LNAPL migration pathways due to cold joints, contraction, and cracking in the concrete and gunite.
- Historical observations of space between the back side of the steel shell plates and the inner side of the reinforced concrete (NAVFAC EXWC 2016).
- Appearance of a fuel hydrocarbon seep observed below Tank 5 on the evening of January 12, 2014 in the lower cross tunnel wall near the exterior of the material encasing the lower part of Tank 5.
- Monitored results of increasing soil vapor levels directly below and adjacent to Tank 5.

4.9 UNCERTAINTY ANALYSIS

Migration of the 2014 JP-8 release down along the space between the back side of the steel liner plates and the inner side of the reinforced concrete to lower tank bottom has not been verified but is based on strong evidence (e.g., historical construction documentation, forensic studies, and observation of leaking fuel near the bottom of the Tank 5 tunnel wall). Other suspected release points from corrosion and pitting in the interior and exterior steel tank wall have not been verified. Other suspected migration

routes, including migration to permeable rock formations outside the gunite/concrete wall, around tunnel linings, and through grates, drains, vent lines, or sumps, have not been verified.

Soil vapor result uncertainties arise from the period frequency of sampling during and following the 2014 release, and from the fact that most vapor measurements have been collected with a PID that yields aggregate hydrocarbon results.

Previous hydrocarbon releases have been documented to have impacted the shallow perched zones underlying the Hālawa Correctional Facility adjacent to Red Hill (Dames & Moore 1991; EKNA 1999, 2000) and may complicate hydrocarbon source attribution in this area.

4.10 ADDRESSING UNCERTAINTIES

The following ongoing, planned, or proposed activities are designed to help resolve the uncertainties described in Section 4.9:

- Sampling of potential fuel-hydrocarbon-stained walls was conducted in April 2019 at five locations in the lower tunnel and at one location in the upper tunnel near Tank 19. The results are currently being evaluated.
- Vertical temperature profiles have been measured in key monitoring wells. Because LNAPL biodegradation releases heat, increases in temperature over background conditions are being used to indicate the vertical distribution of LNAPL beneath select tanks at the Facility. In April 2019, vertical temperature profiles of monitoring wells previously sampled in the lower tunnel were re-collected along with profiles of existing monitoring wells outside the tunnel. The April 2019 data are currently being evaluated. The new data will support an assessment of repeatability of the previous tunnel well results as well as facilitate a more comprehensive evaluation of temperature contrast in areas within and outside the tank farm.
- NAP data, particularly dissolved oxygen (DO) and dissolved methane in groundwater and in the SVM points, have been collected and are being used to better understand where LNAPL biodegradation is occurring.
- The lack of sheen observations in the Facility monitoring wells is being used to help constrain the location of any saturated-zone LNAPL lenses at the Facility.

This page intentionally left blank

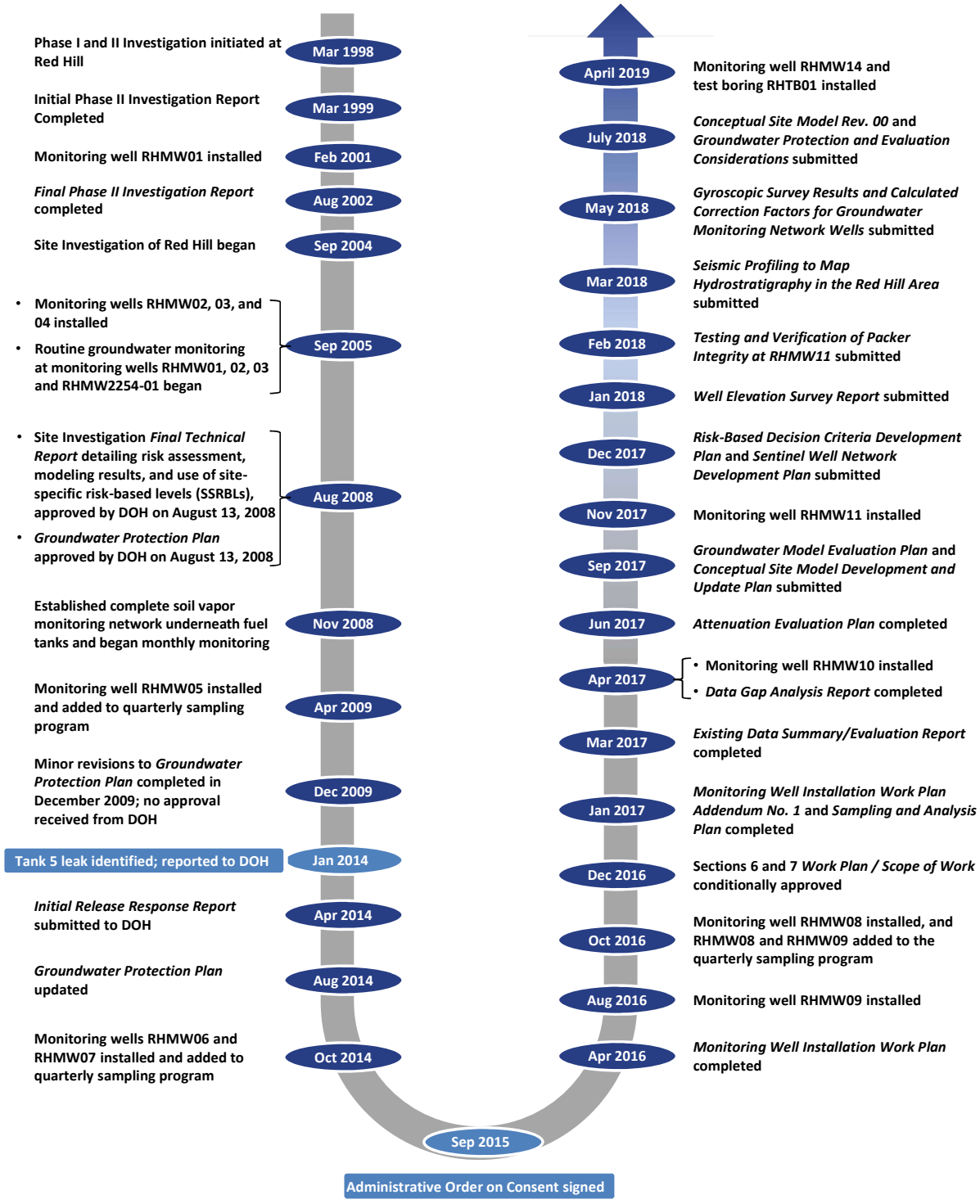

Figure 4-1
Summary of Environmental Actions at Red Hill
Conceptual Site Model Rev. 01
Investigation and Remediation of Releases and Groundwater Protection and Evaluation
Red Hill Bulk Fuel Storage Facility, JBPHH, O'ahu, Hawai'i

This page intentionally left blank

Legend	
○	Approximate Location of Oil-Tight Door
●	Approximate Location of Sump

Notes
Locations are Approximate

Source: NAVFAC Drawing No. 19049143
Dated October 28, 2014

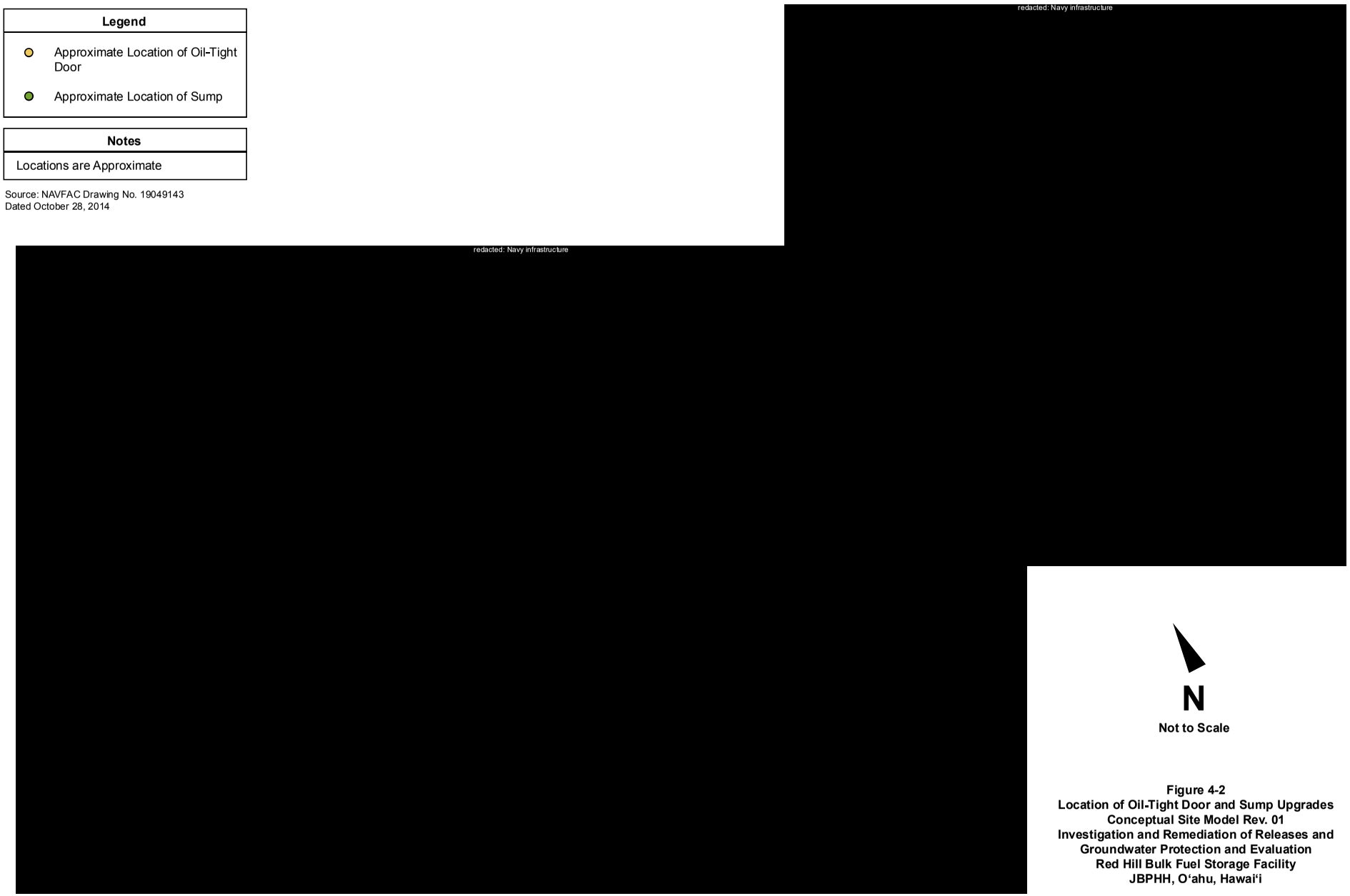

N

Not to Scale

Figure 4-2
Location of Oil-Tight Door and Sump Upgrades
Conceptual Site Model Rev. 01
Investigation and Remediation of Releases and Groundwater Protection and Evaluation
Red Hill Bulk Fuel Storage Facility
JBPHH, O'ahu, Hawai'i

This page intentionally left blank

Linear Scale Graph of Monthly PID Monitoring Results for Below Fuel Tank Soil Vapor Wells:

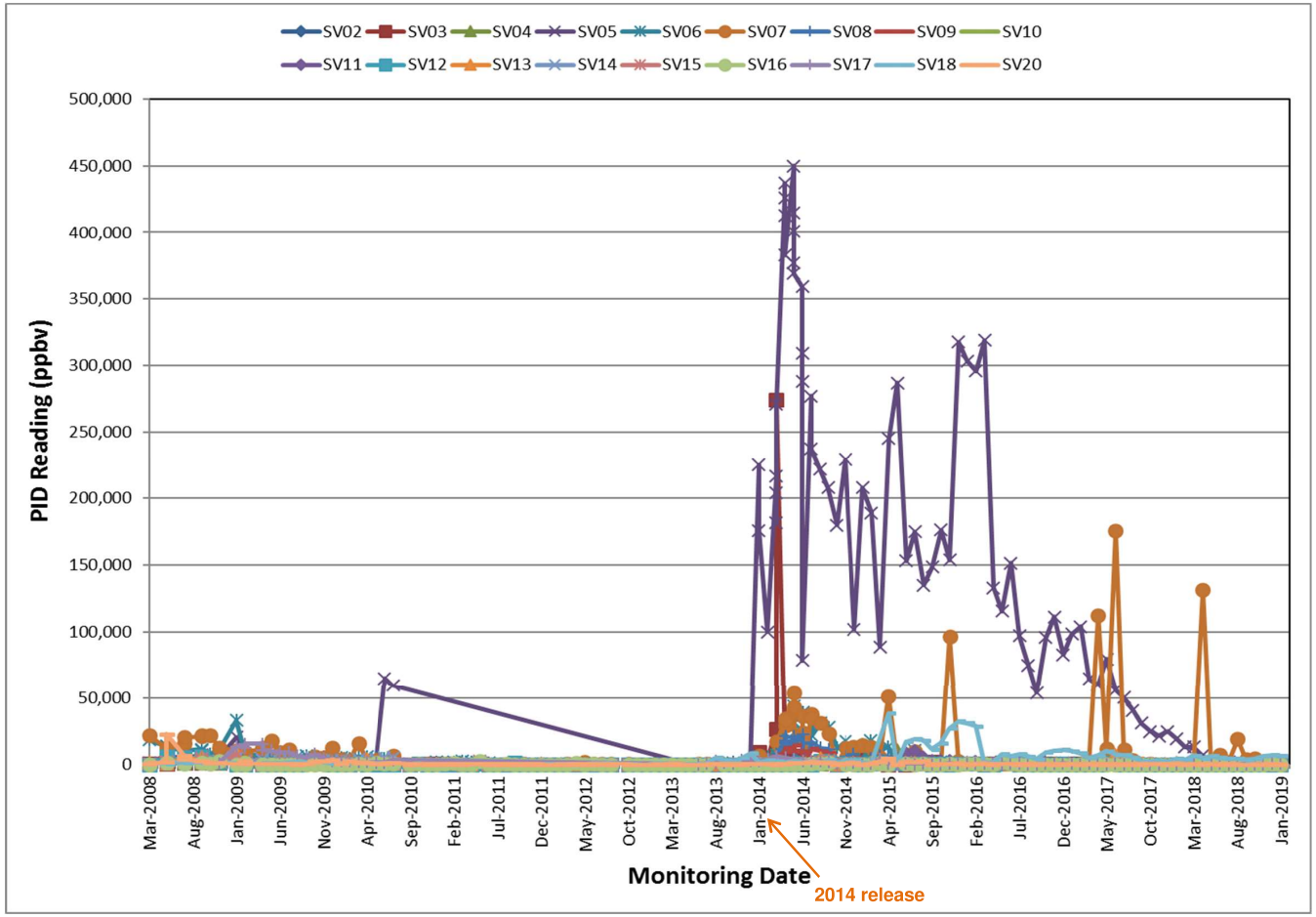

Average Yearly Total Organic Soil Vapor Concentrations by Tank, 2013 and 2014:

Tank Farm	1	3	5	7	9	11	13	15	17	19
	2	4	6	8	10	12	14	16	18	20
2013		158	203	310	156	172	132	153	1,733	
	188	188	507	226	177	128	135	127	1,328	263
2014		7,093	200,938	19,400	5,577	926	992	750	2,603	
	328	1,125	16,048	9,503	1,941	704	573	352	2,377	942

Parts per Billion by Volume

	No Data	7	5,001 - 10,000
1	< 50	8	10,001 - 20,000
2	51 - 100	9	20,001 - 50,000
3	101 - 500	10	50,001 - 100,000
4	501 - 1,000	11	100,001 - 200,000
5	1,001 - 2,000	12	200,001 - 450,000
6	2,001 - 5,000		

Figure 4-3
Soil Vapor Measurements Prior to and Following 2014 Release
Conceptual Site Model Rev. 01
Investigation and Remediation of Releases and Groundwater Protection and Evaluation
Red Hill Bulk Fuel Storage Facility, JBPHH, O'ahu, Hawai'i

This page intentionally left blank

5. Module D: Vadose Zone

The Facility tanks are surrounded by rock in the vadose (i.e., unsaturated) zone, which consists primarily of layered basalt. Although fuel was likely released into the vadose zone as a result of the January 2014 Tank 5 release, LNAPL has not been measured in any of the monitoring wells beneath the Facility or in water supply wells in the area. As fuel migrates through the vadose zone, several processes redistribute and/or degrade the contaminant mass:

- *Volatilization:* Fuel releases undergo evaporative weathering by losing volatile compounds to gas-filled pore space in the vadose zone.
- *Capillary Forces:* As LNAPL migrates through the vadose zone, some mass is retained within the basalt matrix by surface tension and capillarity. The retention capacity of the vadose zone basalt is influenced by a number of factors including the characteristics of the basalt (discussed in detail within this section), the viscosity of the LNAPL, and the presence or absence of other liquids such as water. Weathering or dissolution of LNAPL in the vadose zone could also impact viscosity and LNAPL retention.
- *Dissolution:* Compounds in fuels transfer from the LNAPL into pore water that contacts the fuel.
- *Microbial degradation:* Indigenous microbial populations degrade petroleum fuels under both aerobic and anaerobic conditions.

The following subsections describe elements that may influence the migration and fate of LNAPL.

5.1 GEOLOGIC FEATURES

In the Facility area, the vadose zone surrounding the fuel tanks is heterogeneous and composed of a series of alternating layers of basalt flows that vary from high to extremely low permeability. The spatial distribution of the interconnected pore space (effective porosity) is complex and controls the migration pathways. Geologic logs and data from existing reports, new wells, and geologic mapping have been used to better define the permeable pathways of higher effective porosity as well as low-permeability barriers to LNAPL movement. Additionally, porosity values were derived by petrographic laboratory testing, and permeabilities have been derived by transfer function-noise (TFN) modeling and hydraulic testing in the multilevel wells (Section 6). Generally, the permeability of volcanic rocks is variable and depends on the mode of emplacement, amount of weathering, and thickness of the rocks (Gingerich and Oki 2000).

Basalt flow layers are also present below the groundwater table in the Facility area. Information in geologic logs has been used to assess the nature and extent of low-permeability dense a'ā basalt layers, as well as high-permeability a'ā clinker zones and interflow voids between thin pāhoehoe lava flows and discontinuous fractures and cooling joints that occur within individual lava flows (i.e., intraflow fractures), which may create preferred flow pathways for groundwater and LNAPL movement in the Facility source area.

Geologic mapping and correlation of borehole geologic logs have better defined the strike and dip of the lava flows and presence of interbedded clinker units. Information from barrel logs prepared during tank construction (DON 1943) was also used to develop geologic cross sections of the tank area. These logs describe the excavated surface of the cylindrical spaces mined for the tanks and are relatively coarse descriptions. Relative to boring log information, the barrel logs provide less detail and indicate significantly thicker sections of clinker when compared to logs from nearby borings at Red Hill. As such, there are limitations to the use of data from the barrel logs. The porosity and permeability of

each different geologic unit is estimated based on the geologic descriptions from the barrel logs, boring logs, and published reports from other hydrogeology investigations of the basalt. This information was evaluated to better define the thickness and locations of permeable layers or zones, then used to estimate likely directions and locations where LNAPL could migrate if released from a tank.

In the neighboring valleys, alluvium (valley fill) is present near the ground surface. Below the alluvium, intense weathering of basaltic rocks reduces the permeability of the parent rock by altering igneous minerals to clays and oxides (saprolite). These valley fills and underlying saprolitic formations can influence groundwater flow and contaminant transport. Site-specific saprolite identification, based on data available to date, is detailed below.

5.1.1 Lava Flows

As described by Macdonald's (1941) report on the geology of the Red Hill and Waimalu Areas, O'ahu, "*The lava flows form sheets 3 to 50 feet thick, with very irregular tops and bottoms, sloping gently southwestward. Many of them thin toward the southwest. The lavas moved down the slope toward the southwest as relatively narrow streams. Their continuity along the ridge at Red Hill is therefore greater than across the ridge.*"

Hunt Jr. (1996) describes that "*Wentworth and Macdonald (1953) listed measurements for 22 historical flows on Mauna Loa and Kilauea on the island of Hawaii, which presumably are typical of flows on Oahu as well. The flows on Hawaii average about 15 miles in length and about one-half mile in width.*" Given that the distance from the Northwest Rift Zone of Ko'olau volcano to Red Hill is approximately 6–7 miles, a'ā lava flow core widths could be significantly less than one-half mile wide, potentially hundreds of feet wide.

According to Macdonald (1941), many flows thicken or thin rapidly across the ridge, and some pinch out altogether at Red Hill. This implies the existence of relatively narrow flows. If clinker bridges are present, they would be pathways for lateral and vertical flow at the edges of a lava flow but would be limited in areal extent perpendicular to lava flow direction.

Lava flows are controlled by topography and follow natural drainage patterns. Recent (May 2018) thermal imagery of the flows occurring in the eastern region of Hawai'i Island shows that flows do meander typically at 30–45 degrees relative to the baseline flow direction (fall line). Because lava tubes occur in pāhoehoe lava and are generally oriented along the axis of flow within individual beds, it is unlikely that continuous lava tubes would exist between Red Hill Shaft and Hālawa Shaft, as the orientation of such a tube would be oriented transverse to the lava flow axis and would have to remain open in subsequently weathered basalt (e.g., saprolite). If the meander (in the lava flow) were fed by a lava tube, this would imply that the lava tube would need to exceed 1 mile approximately perpendicular to the axis of the flow to intercept Hālawa Shaft. Such a lava tube would also need to dip at a very shallow angle to continuously intercept the upper portions of the regional basal aquifer water table, which is unlikely. An angle of less than 1 degree would be required to create a hydraulic connection via a lava tube between Red Hill and Hālawa Shaft, near the water table. This dip and orientation of a lava tube is inconsistent with conditions reported and observed in the Hawaiian islands. Hālawa Shaft is oriented at approximately 305 degrees from the Red Hill Facility. This conceptual lava tube would also have to stay open and remain competent long after the lava flow had ended. Fresh lava tubes sometimes collapse following drainage of lava from the tube and cooling. Relict lava tubes in saprolite, such as what is observed in South Hālawa Valley as well as North Hālawa Valley, are expected to collapse and/or become infilled (D. Thomas, University of Hawai'i [UH] Hilo and DOH, pers. comm. 2018).

Macdonald (1941) writes: "*The pahoehoe flows are fed by lava moving through tubes in the interior of the flow, most of them only a foot or two across but a few reaching diameters of tens of feet. Sometimes the liquid lava drains away from these tubes leaving them partly or entirely empty.*" In highly weathered basalt and saprolite sequences, such as those found below valley fill deposits in South Hālawa Valley, lava tube structures, if present, would generally fail and collapse. Based on the drilling of thousands of feet through similar volcanic materials on Hawai'i Island, the occurrence of lava tubes was described as "rare" (D. Thomas, UH Hilo and DOH, pers. comm. 2018). Lava tubes are constrained by the width of the lava flow they are contained within. With that, it is highly unlikely that there may be lava tubes from Red Hill area that would provide a conduit or pathway toward Hālawa Shaft (i.e., the unlikely geometry that would allow a lava tube somewhere near the water table under the Red Hill Facility to be oriented all the way across [under or around] the saprolite in modern day North and South Hālawa Valleys, and then extend all the way to Hālawa Shaft).

5.1.2 Geologic Cross Sections and Mapping

Geologic cross sections have been prepared from available geologic logs of rock cores and from field mapping (Figure 5-1 through Figure 5-9). Geologic logs from the Red Hill groundwater monitoring network, from Macdonald (1941), and from Stearns (1943) (Figure 5-10) were used to correlate the stratigraphy of the basalt flows at Red Hill. Barrel logs developed during construction of the tanks also depict the stratigraphy of the rock formation (Figure 5-11). These logs encompass the 150-ft-tall cylinder interval of the tanks below the base of the upper dome and above the top of the lower dome, i.e., the middle 150 ft of the 250-ft-tall tanks.

In general, the upper stratigraphic section in Red Hill is composed predominantly of a'ā flows with some interbedded pāhoehoe flows (Figure 5-2). Field mapping also indicated a predominance of a'ā flows in exposed cliff-forming outcrops that correlate with the upper stratigraphic section. The lower section is composed primarily of thinner bedded pāhoehoe flows (see Photo 5-1). Correlation of boring logs at Red Hill indicates the presence of one or more intervals of a'ā flows (composed of several flows with a'ā clinker layers) within the pāhoehoe section that are approximately 30–60 ft thick.

A 1943 Navy as-built drawing, "Plan of Lava Tubes Cut by Tank 18," maps lava tubes connecting from Tank 20 to Tank 18 that were compass-surveyed (Figure 5-12). The survey shows these lava tubes are oriented downgradient in a south-southwest direction ranging from 187 to 241 degrees. These bounding orientations have a middle orientation of 214 degrees. Kriging correlation of lava tube and loose rock from barrel log data also presents similar orientations to the south-southwest (Figure 5-13).

Geologic mapping indicates the predominant dip direction (i.e., dip azimuth) is toward the south-southwest in the Red Hill area. Regionally, flows commonly dip 3–10 degrees from horizontal (i.e., dip magnitude) in the direction away from the eruptive axis of the volcano (Hunt Jr. 1996), and the dip direction is generally to the southwest. The average dip directions from geologic mapping in the Red Hill area are:

- Hālawa side of Red Hill: 194 degrees
- Active pit at Hālawa Quarry: 194 degrees
- Moanalua Water Tunnel: 206 degrees
- Moanalua side of Red Hill and Moanalua Golf Course: 209 degrees
- Moanalua side of Red Hill from Tripler Ridge and Moanalua Valley: 186 degrees

Geostatistical evaluation of dip azimuth and magnitude data collected during geologic mapping included generation of rose diagrams and Gaussian mixing models. To derive true dip, data included discrete field dip azimuth and dip magnitude (true dip) measurements as well as common plane-derived measurements using two apparent dips measured in the field (see Appendix C). Discrete measurements were collected from the Hālawa side of Red Hill, Moanalua Water Tunnel, Moanalua side of Red Hill, and Moanalua Golf Course (Figure 5-14).

Apparent dip data were collected in the active pit area at Hālawa Quarry and from the Moanalua side of Red Hill from Tripler Ridge and Moanalua Valley. Additional apparent dip azimuth and magnitude data were derived from clinker correlation, kriging correlation, and a Lower Beds correlation feature between Tanks 9–16 developed from models of three-dimensional (3D) barrel log data. Additionally, one dip azimuth and dip magnitude value was provided by DOH.

Weighting was applied to the mapping data as follows:

- All discrete field measurements (Hālawa side, Moanalua side, and Golf Course, Moanalua Tunnel) were weighted 1 point each (39 measurements).
- Common Plane measurements in Hālawa Quarry were weighted 10 points each (6 measurements).
- Common Plane measurements of Moanalua side of Red Hill from Tripler Ridge and Moanalua Valley were weighted 3 points each (9 measurements).
- Common Plane measurement of barrel log clinker correlation was weighted 5 points (1 measurement).
- Common Plane measurement of barrel log kriging correlation was weighted 5 points (1 measurement).
- Common Plane measurement of barrel log Lower Beds Tanks 9–16 was weighted 3 points (1 measurement).
- DOH dip azimuth and dip magnitude was weighted 10 points (1 measurement).

All data using weighting factors yielded an average dip azimuth of 197.4 degrees and an average dip magnitude of 6.5 degrees. With the objective to derive a range of dip azimuth and magnitude data and a best-estimate value, further review of that data set shows multiple dip-azimuth populations. Rose diagram plots of these data show what appear to be approximately 217- and 183-degree dip azimuths—an indication of a bi-modal distribution (Figure 5-14).

These azimuths have a slightly farther spread than what Gaussian distributions indicate (Section 5.1.3).

5.1.3 Gaussian Mixture Model

At least two subpopulations of dip azimuth were apparent in histograms of field measurements, and those two subpopulations appeared to overlap, preventing the separation of readings so that the mean dip azimuth of each subpopulation could be computed. Weighted pairs of dip azimuth and dip magnitude were analyzed using two-dimensional Gaussian Mixture Modeling (GMM), which estimates a separate mean and standard deviation for each subpopulation, in addition to evaluating the number of subpopulations present in the data. A common statistical analysis package was used to complete the analysis of the dip measurements (scikit-learn, implemented in Python at https://scikit-learn.org/stable/modules/mixture.html).

An evaluation of the GMM results indicated that the simplest combination of Gaussian models that fit the dip field measurements had three components, two of which were visually apparent when examining histograms of site data (Figure 5-16). The three components composing the GMM were (mean +/- standard deviation):

- Dip azimuth of 184.6 +/- 7.1 degrees, with a dip magnitude of 5.9 +/- 1.4 degrees
- Dip azimuth of 213.6 +/- 4.8 degrees, with a dip magnitude of 2.9 +/- 0.5 degrees
- Dip azimuth of 200.5 +/- 29.7 degrees, with a dip magnitude of 11.2 +/- 5.2 degrees

These components are illustrated on a polar plot of the GMM data analysis, Figure 5-17. The probability that dip azimuth will take a particular value is shown as unitless (see "p(Dip Azimuth)" on Figure 5-17); integrating under the blue curve will sum to a total probability of 1.0. The first two contributors to the GMM showed tall, narrow peaks with relatively small standard deviations, and the third component was a minor contributor with a broad peak (i.e., a comparatively large standard deviation) (Figure 5-16).

The bi-modal separation between the two major components (184.6 and 213.6 degrees) of the GMM is 29.0 degrees (see Figure 5-11 and Figure 5-17).

5.1.4 Assessment of Potential Preferential Pathways Related to Historical Lava Flow

Random walk modeling was performed using a recently developed probabilistic model, MrLavaLoba (Vitturi and Tarquini 2018), to evaluate the potential historical lava flow paths passing through the vicinity of the Red Hill tank farm. The purpose was to evaluate the likelihood of a flow path present from the tank farm area to Red Hill Shaft. Results are presented in Appendix D.

The model parameters used were based on Vitturi and Tarquini (2018) for simulating a Kilauea volcano eruption. The downslope was represented by a digital elevation model generated based on a dip orientation with an azimuth of 213.6 degrees and a dip angle of 2.9 degrees. A fractal dimension range between 1.13 and 1.23 was adopted (Bruno et al. 1992) to simulate pāhoehoe lava flow. The lava flow pathlines were simulated from a location upgradient from the tank farm.

A total of 10,000 Monte Carlo simulations of random lava flow pathlines were generated. Of these 10,000 simulated pathlines, 3,635 pathlines passed through the tank farm area with fractal dimensions in the range of 1.13–1.23. None of the pathlines through the tank farm area passed through the Red Hill Shaft area. Even if a pathline passes through the tank farm area and the Red Hill Shaft area, it might not pass through the elevation intervals of concern. In addition, a lava flow path does not imply a continuous channel that forms a preferential pathway for contaminant transport. Therefore, the results indicate that a preferential pathway occurring between the tank farm area and the Red Hill Shaft area in relation to historical lava flow is unlikely.

5.1.5 Overall Occurrence of Rock Types

The presence of nearly horizontal to gently dipping lava flows with layers (i.e., beds) of alternately greater and lesser resistance to erosion at the site were observed during rock coring for installation of Red Hill groundwater monitoring wells and site reconnaissance activities. No dikes were apparent in recovered cores or in observed outcrops at Red Hill.

Erosion of the less-resistant beds, such as a'ā clinker, has resulted in undercutting of the more resistant massive a'ā and pāhoehoe flows (Photo 5-2). Thinner bedded pāhoehoe flows are less resistant than

massive a'ā flows (Photo 5-3). In general, flows vary from evenly bedded, relatively flat to gently dipping, and continuous to undulating and uneven.

Features or media with a high surface area to volume ratio, such as a'ā clinker and high-angle intraflow fractures, are also subject to weathering. Similarly, the nearly horizontal contacts between pāhoehoe lava flows, which do not contain a'ā clinker, are susceptible to weathering. Rock layers with denser, more closely spaced fracturing also can be more extensively weathered. Vertical fractures and cooling joints are limited or bound within each pāhoehoe or a'ā flow; i.e., they do not continue into the overlying or underlying flows.

5.1.5.1 PĀHOEHOE

Pāhoehoe flow beds are typically thin and formed from relatively rapidly flowing basaltic lavas that tend to spread out laterally before cooling and solidification. These flow beds have a smooth or rope-like surface texture and highly vesicular interiors (vesicles are pore spaces in the lava caused by degassing of the molten pāhoehoe lava). Lava tubes are associated with pāhoehoe lava flows. Along the ridge of Red Hill, lava tubes were not encountered during coring and rates of core recovery were high with the exception of a large void encountered in the bottom of RHMW09. A 1.5-ft-thick void (potentially a lava tube) was encountered during drilling at RHMW11 situated in South Hālawa Valley (DON 2018b). Pāhoehoe flows contain voids of various sizes and are cracked and collapsed in places. These cracks occur within individual layers and are not vertically continuous across multiple flows. Ponding of pāhoehoe lava in depressions or on gentle slopes can result in thick accumulations of massive pāhoehoe. Interflow voids form where the irregular upper surface of a flow is not completely filled in by the viscous lava of a subsequent flow.

Discerning massive pāhoehoe flows from high-permeability thin pāhoehoe flows in boring logs is difficult. As Hunt Jr. (1996) states, most pāhoehoe flows are thin. Given that flows dip at approximately 3–12 degrees in the Red Hill area, the likelihood of ponding of pāhoehoe (i.e., resulting in massive pāhoehoe) would be low. This indicates that thin pāhoehoe flows are predominant at Red Hill (i.e., most, > 90 percent). Exposed outcrops of pāhoehoe on the South Hālawa Valley side of Red Hill reveal primarily thin-bedded flows, which are accentuated by differing weathering resistance of flows at this outcrop (Photo 5-1). These accumulations of pāhoehoe flows may represent a flow field that is divided into a number of lava flows, which at any one time form flow units with specific orientation (T. Thordarson, University of Iceland-Reykjavik, pers. comm. 2017). In addition, each lava flow can branch and is always composed of multiple lava lobes (often in the thousands). As such, pāhoehoe lava flow fields are continuous and can cover very large areas.

On an outcrop scale (or in a drill hole), each pāhoehoe flow field is composed of multiple units defined by chilled outer margins. It can be highly difficult to define the thickness (and extent) of a flow field from outcrop patterns and even more so from drill holes.

Although vesicles are seen as small rounded holes in pāhoehoe, these pore spaces are not interconnected (Mink 1980; Hunt Jr. 1996). Thus, the total porosity of vesicular pāhoehoe may be high, but it has very low effective porosity because the vesicles are not connected and do not transmit fluids. Clinker layers are generally absent from pāhoehoe flows (Izuka et al. 2018). Although less common, lava tubes a few inches to several feet in diameter have been reported in pāhoehoe flows (Izuka et al. 2018). Larger lava tubes have also been discovered in tunneling (Hunt Jr. 1996), and are recorded in barrel logs generated during construction of the Facility tanks. With the exception of what may be small lava tubes encountered during coring of RHMW11 and RHMW09, no other lava tubes were encountered during coring of boreholes for monitoring wells recently installed at the Facility, and core recovery rates were high.

5.1.5.2 Aʻā

Aʻā flows are composed of thick, massive layers of dense, hard, competent basalt flows with few intraflow fractures. Aʻā lava flows form from more viscous lava and have a rubbly surface. Aʻā lava flows are characterized by an interior or core of solid, dense, massive rock with exterior top and bottom coarse rubble or clinker zones (Photo 5-4). Massive dense aʻā core in outcrops and in cores are characterized by stretched vesicles and the absence of open fractures. The massive rock in the interior of a flow is virtually impermeable and typically has few fractures of small aperture, as reflected by high rock quality designation (RQD) values and high core recovery rates. These high-angle intraflow fractures and cooling joints are limited or bound within each aʻā core flow; i.e., they do not continue into the overlying or underlying flows. Fracture apertures have also been mapped as relatively thin (and weathered in many cases), which further reduces the potential for significant vertical migration of fluids.

However, along the tops and bottoms of these dense basalt flows are zones of aʻā clinker (highly fractured or fragmented rock). The thicker aʻā clinker zones are typically composed of unconsolidated rubble with much larger pore spaces between the brittle, fragmented rock compared to the dense, hard interior portions of massive aʻā basalt flows. Clinker zones are similar to layers of coarse, well-sorted gravel, where layered sequences of flows can result in widespread beds with high horizontal permeability. Clinker zones characteristically have a high proportion of pore space and surface area and are prone to weathering quickly, while the weathering of dense massive rock proceeds more slowly. Weathered clinker has been frequently observed in recovered rock cores underlying Red Hill.

Based on outcrop exposures and rock cores, approximately 60 percent of aʻā clinker is weathered, has a high content of fine-grained material, and is of relatively low permeability at Red Hill (Photo 5-5).

5.1.5.3 Pyroclastic Deposits

Pyroclastic (airfall) deposits were encountered in rock cores at Red Hill. None have been observed in rock outcrops along Red Hill, but deposits were observed at Moanalua Golf Course and in the BWS Moanalua Water Tunnel that runs south through the lower end of Red Hill from Hālawa Valley to Moanalua Valley. These deposits are granular in nature and include ash, cinder, spatter, and larger blocks (i.e., tuff). Deposits recovered in cores are highly weathered.

Situated immediately to the south and southwest of Red Hill, the Salt Lake Tuff consists of subaerial gray to brown tuff containing nodules of dunite (Stearns and Vaksvik 1935). It is as thick as 300 ft and passes beneath sea level. It overlies Āliamanu Tuff to its northwest, which is composed of water-laid gray to black or grayish-brown tuff, rounded gravel, and (in tunnels) large vesicular bombs and spatter (Stearns and Vaksvik 1935). It is separated from the overlying Salt Lake Tuff by red soil and typically overlies older alluvium (Figure 5-9).

Pankiwskyj (1972) mapped the Salt Lake and Āliamanu tuff deposits and found that they are areally extensive and mantle a significant area of Pearl Harbor to the west and southwest of the Salt Lake and Āliamanu Crater areas. For the 3D geologic framework model (see Section 5.1.7), the extent of the tuff deposits was based on work by Pankiwskyj (1972) as well as data from Honolulu Authority for Rapid Transportation (HART) study borings (HART 2014). The tuff cone vents and associated throat or root structure were interpreted based on academic research papers on other similar Honolulu Volcanic Series tuff cones (Wentworth 1938) as well as tuff cones outside of Hawaiʻi (Sohn and Park 2005; White and Ross 2011).

5.1.5.4 CAPROCK DEPOSITS

The caprock units within the peripheral valleys have a character distinct from the lower portion of the valleys and plateaus, where the deposits often consist of terrestrial sediments that interfinger with marine sediments and limestone units, described as follows:

- *Valley Fill.* The deposits within and near the base of the valleys generally consist of fill of highly weathered and compact older alluvium that is mantled with more recent unconsolidated alluvium and colluvium (Oki 2005). The older alluvium consists of terrestrial sediments that vary in size from fine-grained particles to boulders and is generally less permeable than the overlying unconsolidated alluvium and colluvium. The older alluvium has been weathered and compacted into a soft coherent mass (Wentworth 1951). The older alluvium may be hundreds of feet thick at lower elevations, but at elevations above approximately 400–600 ft msl, older alluvium may be nonexistent. These materials overlay highly weathered saprolite.

  Drilling at monitoring well RHMW11 encountered valley fill deposits to a depth of 67 ft bgs (DON 2018b). Recent drilling at monitoring well RHMW14 and test boring RHTB01 encountered valley fill deposits to depths of 72 ft bgs and 89 ft bgs, respectively. These depths are consistent with stream valley incision or erosion during prior glacio-eustatic stands of sea level. Stearns (1978) described that the Waipio low stand of the sea was approximately minus 350 ft msl and lasted long enough for deep erosion along major streams (Figure 5-18). The Waipio low stand correlates with the Illinoian glacial period, about 500,000 years before present (BP), during the Pleistocene age (Stearns 1978). Deep valleys were cut during the Nebraskan glacial period (1.4 million years BP), the Kahipa low stand (Kansan glacial period; 800,000 BP), and the Waipio low stand described above, prior to subsidence of the islands. All these low stands of the sea were of relatively long duration.

  On a regional basis, Stearns (1978) notes that "*The Waipio low stand exposed broad marine flats on which sand was abundant in many places. The drop in sea level lasted long enough for all major streams to cut their channels to levels well below present sea level along the coasts. Considerable erosion of the sedimentary caprock of the Honolulu artesian basin took place, resulting in numerous leaks, now the sites of artesian springs.*" Sherrod et al. (2007) has mapped (after the original mapping by Stearns) the valley fill deposits as 'Older Alluvium.'

- *Coastal Caprock.* A wedge of calcareous and volcanogenic sediment overlies the basal volcanics that ranges from nearly 1,000 ft thick near the coast and gradually thins and interfingers with increasing volcanogenic-sediments consisting of older weathered consolidated alluvium and more recent unconsolidated alluvium and colluvium near the valley mouths. The confining, less-permeable properties of the coastal caprock are due primarily to the presence of fine-grained layers and weathering of basalt-derived material (Hunt Jr. 1996).

Interpretation of the marine limestone caprock geometry in the 3D geologic framework model (Section 5.1.7) was based largely on borings from Stearns and Chamberlain (1967) and geologic maps showing the caprock thickness and elevation of the top of the basalt published in recent a USGS study (Izuka et al. 2018).

5.1.5.5 SAPROLITE

Based on previously collected rock samples and cores from borings noted in this document and logs from a geotechnical investigation (PGE 2015), the horizon of soils and highly weathered basalt described as saprolite on the Red Hill ridge is approximately 15–25 ft thick (Photo 5-6); see Figure 5-2 through Figure 5-8. Saprolite is weathered rock material that retains textural features of the parent

rock. Intense weathering of basaltic rocks can significantly reduce the permeability of the parent rock by transforming igneous minerals to clays and oxides (Hunt Jr. 1996). Site soils on the ridges and side slopes are mapped as Helemano-Wahiawā association, consisting of well-drained, moderately fine-textured and fine-textured clay-rich soils derived from basalt parent rock that give the soils its characteristic red color (USDA SCS 1972). These soils are identified throughout the confines of the Facility and extend more than one-half mile upslope from Tanks 19 and 20.

The depth of valley fill and saprolite in the valleys surrounding Red Hill, particularly in the center of the valleys and below the streambeds, is not yet well defined. However, important geologic information has been obtained from core borings recently completed for this project (see Figure 1-1 for well and boring locations):

- During coring of monitoring well RHMW11, located in South Hālawa Valley, saprolite was encountered at approximately 68 ft bgs and extended to a depth of 279 ft bgs, or approximately 87 ft below the expected depth of the regional basal groundwater table (approximately 20 ft msl); see Figure 5-4 and Figure 5-5) (DON 2018b). This depth is consistent with the description in Section 2.7 that saprolite zones are typically around 75 ft thick but can be 300 ft thick or greater beneath the valley floors or in areas of high precipitation.
- During coring of monitoring well RHMW14, located approximately 850 ft west-southwest of RHMW11 in South Hālawa Valley, saprolite was encountered at approximately 72 ft bgs and extended to a depth of 101 ft bgs, or approximately 60 ft above the expected depth of the regional basal groundwater table. This indicates that RHMW14 is located on the south side of the valley instead of along the axis or center of the valley, where valley fill deposits and underlying saprolite zones are expected to be thicker.
- During coring of test boring RHTB01, located approximately 60 ft from Hālawa Deep Monitor Well (HDMW2253-003) in South Hālawa Valley, saprolite was encountered at approximately 89 ft bgs and extended to a depth of 242 ft bgs, or approximately 37 ft below the expected depth of the regional basal groundwater table.

An inspection and interpretation of the logs of cuttings (not cores) conducted for Hālawa Deep Monitor Well (HDMW2253-003) and Waimalu Deep Monitor Well (2456-005) found the following:

- Hālawa Deep Monitor Well (HDMW2253-003): Alluvium (cuttings with clay) at 0–60 ft bgs, saprolite (weathered basalt) at 60–285 ft bgs, and less-weathered to unweathered basalt from 285 ft bgs to total depth.
- Waimalu Deep Monitor Well (2456-005): Alluvium (basalt boulder with dark brown silty sand) at 0–30 ft bgs, saprolite (weathered basalt) at 30–350 ft bgs, and less-weathered basalt at 350 ft to total depth.

Based on data developed from those two well locations, the thickness of saprolite beneath alluvium/valley fill deposits is on the order of 225–320 ft thick with an average of approximately 270 ft. These numbers are consistent with and compare to those of Oki (2005, Figures 21 and 22).

A 3D geologic framework model was developed that describes the lateral and vertical extent of saprolite (as well as caprock, marine sediments, tuffs, and basalt) in the vicinity of Red Hill; see Section 5.1.7 for discussion. This model is based on (a) the seismic study conducted by Boise State (DON 2018c), (b) previous geologic studies in the area, and (c) interpretation of boring logs from key well locations within the area. Two bounding interpretations of the Hālawa Deep Monitor Well (HDMW2253-03) boring log for the saprolite/basalt interface are presented here: (1) an upper bound

interpretation of -5 ft msl and (2) a lower bound interpretation of -55 ft msl. The location where the surface of each saprolite/basalt interface would cross or intersect the air/groundwater interface (piezometric surface) of the regional basal aquifer in South Hālawa Valley was extrapolated by projecting the base of saprolite up-valley using a 3% slope, which is based on the Oki (2005) estimated projection for base of valley fill/saprolite in nearby valleys including North Hālawa and Waimalu Valleys. Figure 5-19 presents where each saprolite/basalt surface crosses the air/groundwater interface (piezometric surface) of the regional basal aquifer along the axis or center of the valley.

According to Hunt Jr. (1996), the effectiveness of steep geohydrologic barriers:

> "*may diminish inland from the coast with increasing altitude and decreasing penetration of the valleys into the underlying basalt. The boundary between the Pearl Harbor and Moanalua areas has been revised from South Halawa Valley to North Halawa Valley (fig. 5) following Eyre (P.R. Eyre, U.S. Geological Survey, written commun., 1991). Eyre reasoned that North Halawa Valley is deeper than South Halawa Valley and, therefore, is a more appropriate boundary between the two areas. This interpretation is consistent with Wentworth (1951). The curved trend of this barrier reflects an assumed paleodrainage pattern in southern Oahu before island subsidence and sediment infilling of the valleys. The Kaimuki area is bounded on the east by the Kaau rift zone and, perhaps, by valley fill in Palolo Valley (fig. 5).*"

Borehole geophysical data collected in RHMW11 and in Hālawa Deep Monitor Well (HDMW2253-03) are consistent with each other and indicate the presence of saprolite or highly weathered basalt to a depth of approximately 279 ft bgs. Review of the HDMW2253-03 geologic log based on drill cuttings indicates clays consistent with saprolite development from 68.5 to 279 ft bgs. Additionally, the geologic core logs of RHMW11 (DON 2018b) and RHTB01 illustrate saprolite consistent with the interpreted saprolite depth at HDMW2253-03.

2017 Seismic Profiling Survey. A survey was conducted in December 2017 along nine transects in the Red Hill area to map stratigraphy and hydrogeologic boundaries beneath North Hālawa Valley, South Hālawa Valley, and Moanalua Valley (DON 2018c). Seismic reflection results show the geometry and depth to key hydrostratigraphic boundaries within the upper 1,000 ft bgs. Key reflectors include the base of alluvium or top of saprolite, top of water-saturated (possibly perched) sediments, and the contact between weathered basalt (saprolite) and unweathered basalt. Review of seismic velocity data obtained from HART (1951) shows they correlate well with seismic velocities used for the seismic profiling survey. These nine transects and interpretations were used to refine the CSM; see Section 6.1.8 for detail.

5.1.6 Permeability

As described above, the site geology exhibits a wide range variability and the vadose zone is heterogeneous and composed of a series of alternating layers of basalt flows that vary from high to extremely low permeability. See Section 6.1 for permeability and hydraulic conductivity data that have been derived by TFN modeling and hydraulic testing in the multilevel Westbay systems.

5.1.6.1 Pāhoehoe Permeability

In general, thin pāhoehoe lava flows have porosity fractures that result in high permeability, whereas thicker pāhoehoe flows are more massive with much lower effective porosity and permeability. The interconnected void spaces in a sequence of pāhoehoe flows may lead to high permeability according to Gingerich and Oki (2000). According to Hunt Jr. (1996):

> *"The mixture of voids and fractures in pahoehoe flows imparts high intrinsic permeability similar to that of carbonate rocks. Vertical permeability elements in pahoehoe include cooling joints; collapse features; skylights or holes in the roofs of large lava tubes; and large, open cracks where lava is pushed up into humps and pressure ridges. Lateral permeability elements in pahoehoe include drained lava tubes and interflow voids (small depressions in the irregular upper surface of a lava flow that are not filled in by the viscous lava of the subsequent flow)."*

5.1.6.2 *AʻĀ PERMEABILITY*

The smaller effective porosity of massive aʻā cores can result in extremely low vertical permeability, especially when the rock is not fractured. The principal vertical permeability of a massive aʻā core is imparted by wide, regularly spaced intraflow cooling joints, which are typically low-permeability features. The aʻā lava flows may also act as localized confining layers in the basal aquifer system. The smaller effective porosity of massive aʻā cores suggests permeability several orders of magnitude less than aʻā clinker or thin-bedded pāhoehoe. Hunt Jr. (1996) describes marginal clinker at the periphery of an aʻā flow may provide local avenues of high vertical permeability in lava sequences and that such flow-margin clinker bridges may be more prevalent in sequences of thinner flows than in thicker flows.

Aʻā clinker is composed of gravel- and cobble-size rubble that resembles a conglomerate. It is usually loosely held together unless it has been welded together by heat. Borehole geologic logs and core photos from the Facility area show the aʻā clinkers are loose fragmented rock, evidenced by much lower RQD values and low rates of core recovery that are attributable to erosion of unconsolidated rock fragments and sediment by water circulating around the core bit during drilling.

The thicker, unweathered aʻā clinker zones have large interconnected pore spaces (macro-pores), high effective porosity, and high permeability. Aʻā clinker is subject to more rapid chemical weathering processes, and once it has significantly weathered, its permeability is reduced. Often the thinner clinker beds are found to be highly weathered and clayey.

Clinker zones that are unweathered characteristically have high horizontal permeability. Based on outcrop exposures and rock cores, approximately 60 percent of aʻā clinker is weathered, has a high content of fine-grained material, and is of relatively low permeability at Red Hill (Photo 5-5). From Hunt Jr. (1996):

> "*The areal extent of lava flows is much larger than their typical thickness of about 10 ft. Wentworth and Macdonald (1953, p. 31) listed measurements for 22 historical flows on Mauna Loa and Kilauea on the island of Hawaii (fig. 8), which presumably are typical of flows on Oahu as well. The flows on Hawaii average about 15 mi in length and about one-half mile in width. Individual flows can be traced and mapped on the surface of young, unweathered volcanoes. Areal correlation of flows in the subsurface requires careful drilling and collection of core samples or drill cuttings, detailed description and petrographic study of the samples, and borehole geophysical logging. These data are not collected routinely in Hawaii, and there are few instances when data are sufficient for lateral tracing of subsurface flows.*"

5.1.6.3 *PERMEABILITY OF PYROCLASTIC DEPOSITS*

Weathering processes in Hawaiʻi affect the hydraulic properties of ash and tuff, as their permeability can be greatly reduced by chemical weathering; original pore spaces are closed by swelling of mineral particles as chemical changes cause the deposits and rocks to disintegrate (Oki, Gingerich, and Whitehead 1999). The Honolulu volcanics are found to have varying hydraulic conductivities due to the different rock types and degrees of weathering; they can contain units of cinders, ash, tuff, and

weathered rocks, which alter the hydraulic conductivity of the material (Okuhata et al. 2017; Izuka et al. 2018). Weathering processes in Hawai'i affect the hydraulic properties of ash and tuff as their permeability can be greatly reduced by chemical weathering; original pore spaces are closed by swelling of mineral particles as chemical changes cause the deposits and rocks to disintegrate (Oki, Gingerich, and Whitehead 1999).

Due to the highly weathered nature of pyroclastic deposits proximal to Red Hill, their porosity and permeability are similar to those of fine-grained consolidated granular sediments, with similar grain size and degree of sorting. Fine-grained ash is less permeable than coarser pyroclastic deposits, and its permeability may be reduced further by degree of welding, weathering, or compaction (Visher and Mink 1964; Hunt Jr. 1996). According to Visher and Mink (1964), volcanic tuffs of the Honolulu volcanic series are among the most impervious rocks.

Hydraulic conductivity values for tuffs (part of the Honolulu Volcanic Series) have been reported to range from < 1 to 490 feet per day (ft/d) (Hunt Jr. 1996). In an O'ahu groundwater model of the Nu'uanu and Kalihi aquifer systems developed by Okuhata et al. (2017), hydraulic conductivities of 10 ft (3 meters [m]) (horizontal, latitudinal) and 3 ft (1 m) (horizontal, transverse) and 0.1 ft (0.03 m) per day were used for the for the Honolulu volcanics. Belcher et al. (2001) provides a range of Death Valley, CA hydraulic conductivities for tuff breccia and ash-flow tuff, as well as for bedded ash-fall and reworked tuff and ash-flow tuff, all between < 1 and 45 ft/d; these types of tuffs and ash flows are similar to the Honolulu Volcanic Series deposits. Section 6.3 further develops hydraulic properties.

The position of the Salt Lake and Āliamanu Tuffs situated immediately to the south and southwest of Red Hill may have significant influence on groundwater flow in the Red Hill area. The Salt Lake Tuff is as thick as 300 ft and passes beneath sea level, and the underlying Āliamanu Tuff to its northwest was water-laid and typically overlies older alluvium. Additionally, the tuff cone vents and associated throat or root structures are interpreted to extend to depths of hundreds of feet to greater than 1,000 ft.

5.1.6.4 PERMEABILITY OF SAPROLITE

Hunt Jr. (1996) reports the hydraulic conductivity of saprolite at less than 1 ft/d. Low-permeability saprolite consisting of clay-rich materials and highly weathered basalt was encountered beneath valley fill deposits at locations RHMW11, RHMW14, and RHTB01 (see Figure 1-1). The saprolite zone encountered at RHMW11 creates a barrier to groundwater flow because of the lower hydraulic conductivity of the clayey weathered basalt material and higher piezometric heads, as also evidenced by seismic refraction and reflection profiles obtained in the valley, as discussed in Section 6. This saprolite most likely formed beneath a deeply incised paleo-valley that lies below the present-day South Hālawa Stream.

5.1.6.5 INFLUENCE OF HĀLAWA QUARRY

As shown on Figure 5-5, rock quarrying operations over decades have removed considerable quantities of material. The active quarry pit immediately north of South Hālawa Valley currently has a floor elevation of approximately 196 ft msl. To the west of the active pit lies a formerly active quarry pit, which is now partially filled with sediment and used as a sedimentation/runoff control basin for the cement plant operation. The active pit is separated from South Hālawa Valley by a ridge approximately 300 ft msl. With this configuration, the approximately 500-ft-wide by 1,200-ft-long active quarry pit acts as a collection basin during high rainfall events that could potentially increase the natural groundwater recharge rate in that area and may, along with other local sources of recharge, cause short-term or temporary effects on groundwater levels in the basal aquifer beneath the pit.

5.1.7 Red Hill Geologic Framework Model

A geologic framework model was generated using CTECH's Earth Volumetric Studio (EVS) software. The lithologic information used to generate the model was derived from available borehole lithology and from a series of geologic cross sections in the vicinity of Red Hill. Interpolation of lithologic contacts from borehole lithology and cross sections was achieved via adaptive indicator kriging. The framework model was used to visualize the extent of clinker beneath the water table. Groundwater data from the November 2016 synoptic gauging event was incorporated into the model to serve as an upper domain relative to the model's geologic block.

The geologic framework model was also used to compute the estimated volume of clinker and pahoehoe within user-specified domains. The EVS volumetric module was used to compute the volume of clinker and pāhoehoe within each zone against the overall geometric volume to achieve a percent total. In addition to use in groundwater modeling, this geologic evaluation was also incorporated into the holding capacity analysis included in the *Groundwater Protection and Evaluation Considerations* report (DON 2018h).

Details are presented in Appendix E.

5.1.8 3D Regional Geologic Model

Geologic information from borehole logs, seismic profiles, developed cross sections, and relevant publications were incorporated into the development of a 3D regional geologic model of Red Hill and surrounding environs including North and South Hālawa Valleys, Moanalua Valley, the Salt Lake area, and Pearl Harbor. The model encompasses both the vadose and saturated zones and includes the various rock types present: unweathered basalt (undifferentiated), pyroclastic deposits, caprock deposits, and weathered basalt or saprolite. The 3D regional geologic model was developed to provide stratigraphic support for the Red Hill groundwater flow model; the model extent mirrored the extent of the groundwater flow model domain.

Several data sources were used to develop the 3D regional geologic model. These sources included:

- USGS caprock thickness structural contour data sets
- Regional geologic cross sections
- Geophysical investigation study
- Volcanic tuff and pyroclastic mapping
- Marine sediment mapping
- South Hālawa Valley base of saprolite interpretations

Details are presented in Appendix E.

5.1.9 Assessment of Subsurface Heterogeneity

Geologic logs and photographs of basalt cores from the Red Hill area show that the vadose zone surrounding the fuel tanks is composed of a heterogeneous series of layered basalt flows. Both types of basalt, pāhoehoe and a'ā, are present.

Within the heterogeneous layered basalt formation that composes the vadose zone surrounding the fuel tanks, the spatial distribution of interconnected pore spaces (effective porosity) is the result of the basalt lava flow genesis and subsequent sub-aerial weathering that may occur prior to the next flow.

Viewed within a smaller area, the movement of molten lava is complex and unpredictable, but the flows generally move downhill due to gravitational force. Nonetheless, the available geologic information from boring logs and core photos can be integrated with geologic observations of local basalt outcrops, as well as photos of active lava flows on Hawai'i Island, to generally characterize the physical properties of basalt that affect LNAPL movement and groundwater migration at a large scale where local heterogeneity is not considered.

Clinker that forms along the base, top, and sides of a'ā flows may have high permeability and porosity similar to a gravel aquifer. Clinker at the periphery of an a'ā flow may form bridges between the massive interior zones of two adjacent flows and provide local avenues of high vertical permeability (Hunt Jr. 1996). Sequences of thin lava flows in Hawai'i typically form highly permeable aquifers, with horizontal hydraulic conductivity (K_h) values of hundreds to tens of thousands of ft/d (Izuka et al. 2018). Hunt Jr. (1996) compared the permeability of massive a'ā vs. high permeability lava flows and concluded: "*In contrast, the smaller effective porosity of massive aa cores suggests permeability several orders of magnitude less than aa clinker or thin-bedded pahoehoe."* Most of the O'ahu pāhoehoe flows are thin (Hunt Jr. [1996]; J. Kronen, AECOM, pers. comm,, 2017) and therefore are likely to exhibit higher permeability.

Geologic observations and reports by the USGS also reveal that the interior portions of the dense, massive a'ā basalt flows typically have very low primary porosity, low permeability (hydraulic conductivity), and low effective porosity. Within the dense basalt flow interiors, a small amount of secondary porosity is attributable to fractures formed during cooling. These cooling fractures are typically short in length and confined within an individual flow. Borehole logs and core photos from Red Hill monitoring well borings reveal that the cooling fractures typically have very narrow apertures, and most are just hairline cracks. On the other hand, more intensely fractured zones and loose rubble logged as a'ā clinker occur along the exterior portions of basalt flows, due to rapid cooling and fragmentation of the lava flow surface as it solidifies from the molten lava material (Hunt Jr. 1996).

The heterogeneous nature of the basalt is revealed in the geologic log of the Red Hill Shaft water development tunnel prepared by the USGS (Stearns 1943). That log, reproduced as Figure 5-10, recorded water inflow rates measured by the USGS as the tunnel was being constructed. The log shows that flow rates increased dramatically as the tunnel penetrated beyond 550 ft, which is attributable to a large increase in permeability of the basalt formation. On Figure 5-10, the relatively thin "top clinker" logged in the first 550 ft of the tunnel's upper lift produced essentially no groundwater. The tunnel was described as "dry" during tunneling out to about 480 ft from the shaft. Subsequent tunneling of this section, but at a lower level (lift), produced about [redacted]. Progressing beyond 480 ft, the tunnel produced greater water inflows. At 730 ft the flow was recorded to be [redacted]. After reaching 980 ft, the flow recorded was [redacted]. Tunneling from that point forward, the rate of inflow encountered in the tunnel became much larger. In the last 200 ft of the tunnel, 980–1,180 ft from the shaft, the groundwater inflows increased from [redacted] to [redacted]. The thicker clinker zone shown on the geologic log (Stearns 1943) produced the majority of the groundwater. This 200-ft section of clinker penetrated by the tunnel produced about eight times more water than the clinker and pāhoehoe logged in the initial 480 ft of the tunnel. In summary, by the end of the Red Hill water development tunneling project, the groundwater inflow had increased from approximately [redacted] to [redacted] in the last 500 ft of that tunnel. The distal end of this water development tunnel is located near RHMW05.

Lying beneath the vadose zone, this same basalt formation comprises the volcanic rock aquifer described in several hydrogeology reports. The hydraulic conductivity of flank lavas is dependent on such features as thickness of the flows, thickness of clinker zones associated with a'ā flows, frequency and extension of fractures, and occurrence of lava tubes associated with pāhoehoe flows. Hydraulic

conductivity ranges from several hundred to several thousand ft/d in highly permeable dike-free flank lavas, and is typically orders of magnitude higher in the horizontal direction than in the vertical direction (DON 2007). Significant differences in geologic features that occur in the vadose zone versus the upper 50 ft of the saturated zone are not expected.

The horizontal hydraulic conductivity (K_h) tends to be several times greater parallel to the direction of lava flows (i.e., downslope) than perpendicular to the flows (Nichols, Shade, and Hunt Jr. 1996). On a regional scale, USGS reports indicate the volcanic rock aquifer has high K_h, 1,500–4,500 ft/d. However, this aquifer has much lower vertical hydraulic conductivity (K_v), 7.5 ft/d, which is about 200–600 times lower than the K_h. Total porosity of the volcanic rock aquifer ranges between 5 and 50 percent, but the effective porosity is approximately 4–5 percent (Oki 1998; Whittier et al. 2004; Oki 2005; Izuka et al. 2018). See Section 6.1 for permeability and hydraulic conductivity data that have been derived by TFN modeling and hydraulic testing in the multilevel Westbay systems.

Rotzoll, El-Kadi, and Gingerich (2007) analyzed 238 aquifer tests of wells in Hawai'i basalt and found that hydraulic conductivity is lognormally distributed and ranges over several orders of magnitude, from 1 to 8,000 ft/d. The arithmetic mean, geometric mean, and median values of hydraulic conductivity for dike-free volcanic rocks were respectively 1,700, 900, and 1,200 ft/d.

5.1.10 Geologic Features and LNAPL Movement

To evaluate LNAPL movement at the Facility, the geologic media were divided into five classes, as indicated in Table 5-1.

Table 5-1: Geologic Media in Red Hill

Media Type	Ability to Transmit, Hold LNAPL
Massive a'ā flows	Limited
A'ā clinker with fine-grained sediments	Limited LNAPL transmissivity but high holding capacity
High-permeability a'ā clinker	High
Massive pāhoehoe flows	Limited
High-permeability thin pāhoehoe flows	High

Geologic logs of core collected from the Facility often indicate that thin clinker zones were weathered as the top of a flow was exposed at ground surface. Considering the weathering processes reported by the USGS (Hunt Jr. 1996), fine-grained residuum would be created as the lava flow top and side clinkers were weathered at land surface for extensive periods. This weathering, including erosion and saprolitic development of clays, would cause the surfaces of clinkers formed along the top and sides of a'ā flows to have lower permeability and lower effective porosity than non-weathered clinkers. Thinner clinker beds are often highly weathered throughout the entire thickness of the bed. The eroded fines and clay-rich matrix in the weathered clinkers would have a high capillary threshold entry pressure because water is tightly held by surface tension and capillary forces. The high threshold entry pressure must be overcome to allow LNAPL to enter water-saturated fine-grained residuum.

Conversely, the interior portions of larger, thicker clinker zones would be less affected by the weathering processes described by the USGS (Hunt Jr. 1996) because those clinkers would be more distant from subaerial exposure at the land surface. Thus, interior portions of larger, thicker clinker zones would contain little eroded and clay-rich materials, and thus may have extremely high permeability and high effective porosity. Intergranular porosity of such clinker zones is analogous to well-sorted, coarse gravel deposits (Hunt Jr. 1996). Widespread beds of clinker contribute high

horizontal permeability to a layered sequence of lava flows (Hunt Jr. 1996). As a site-specific example, the high rates of water inflow logged by the USGS in the Red Hill Shaft water development tunnel (Figure 5-10) show that the thick clinker zone encountered at the end of the tunnel has extremely high hydraulic conductivity. Additionally, clinker zones formed along the sides of lava flows may provide conduits or "clinker bridges." Where unweathered, such clinker bridges may allow LNAPL to migrate vertically between massive basalt flow layers.

Directly beneath the Facility's fuel storage tanks, the relatively dense, low-permeability massive basalt layers and the weathered layers as noted above would impede downward migration of LNAPL and water. But the thicker, non-weathered, high-permeability clinker zones create preferred flow pathways for fluids to move laterally. LNAPL would move primarily in down-dip directions, while a gas or vapor lighter than air would move primarily in up-dip directions, although if the release had significant hydraulic head, the head may be sufficiently high to drive some LNAPL up-dip and cross-dip as well. Although the jet fuel vapors are heavier than air, the low vapor pressure of the jet fuel constituents limits the amount of partitioning into the vapor phase, and further limits any density-driven migration of the vapors. The LNAPL released from a fuel tank would likely move from the leak point(s) along interconnected void spaces that may exist immediately outside the tank, and then into the surrounding rock with permeable zones. The available data show the geometry of the geologic features that contain large interconnected pore spaces (macro-pores) where LNAPL is most likely to move. In addition, because the Facility's ventilation system operates under a slight vacuum, vapors within the vadose zone are expected to move toward the tunnel and be expelled through the tunnel exhaust system.

Cooling fractures or joints exist within interior portions of both types of lava flows; and they are not continuous across flow boundaries. In a fracture filled with LNAPL, the pressure head of the LNAPL is equal to the connected vertical height of the LNAPL in the fracture and other fractures directly connected with it. However, where thin fractures contain moisture or water droplets, the water will impede the influx of LNAPL and reduce the relative permeability for LNAPL. Moisture held in fine-grained materials within weathered clinker will also cause very low relative permeability for the LNAPL. As previously described, fractures are generally limited to individual flows and often have small apertures, contain weathered materials, and have been subjected to secondary mineralization. Compared to water, the higher viscosity of jet fuel will impede LNAPL movement through small pore spaces, especially small water-filled fractures within the massive dense a'ā basalt layers (Figure 5-20).

Thus, LNAPL would enter and move preferentially through clinker zones and/or thin pāhoehoe flows that have relatively high permeability and high effective porosity. Macro-pores pose the least capillary water resistance and thus are the preferred pathways. After LNAPL moves downward through macro-pores to the top of a dense, low-porosity, low-permeability lava bed, the LNAPL would move down-dip and spread laterally along the base of the permeable zones.

As LNAPL moves through interconnected macro-pores, such as those in the larger, thicker non-weathered clinker zones or thin pāhoehoe, some of the LNAPL will be retained in the pore spaces. Surface tension and capillary forces of water in the smaller pore spaces of small fractures and other pore spaces filled with fine-grained residuum will impede and trap the LNAPL. The LNAPL volume permanently retained in the pore space is defined as "residual saturation."

If LNAPL moving in a fracture were to reach the groundwater level, the accumulated weight of LNAPL in the fracture within the individual a'ā flow will depress the LNAPL–water interface within the fracture. At Red Hill, this is likely minimal due to limited vertical extent of fractures observed in core samples and outcrops. In rock that has been wetted by water first, LNAPL will enter a given fracture only if the pressure of LNAPL exceeds the capillary pressure of water in the fracture entrance.

Where a fracture containing LNAPL penetrates below the groundwater surface, the LNAPL is proportional to the connected vertical height of LNAPL in the fracture above the groundwater level. This LNAPL pressure is balanced by the buoyancy of the LNAPL created by the greater density of the groundwater below.

5.1.11 Petrographic Analyses

Petrographic laboratory analyses were conducted on core samples from Red Hill monitoring well borings to characterize the LNAPL retention and mobility characteristics of the basalt. Laboratory samples were analyzed by Core Laboratories in Bakersfield, CA. The analyses were conducted to support characterization of the vadose zone and fluid properties that affect LNAPL movement, in accordance with the *Attenuation Evaluation Plan* (DON 2017g). Twenty-three samples were selected and submitted for mobility analysis from archived core sections from borings at the Facility. The cores were selected by project geologists to represent various rock types including pāhoehoe, a'ā, and clinker. One of the 23 samples was found unsuitable for testing at the laboratory. The Navy provided the laboratory Jet Fuel (NAPL) to be used for saturating the samples along with viscosity, density, and interfacial surface tension analyses. Appendix F presents the laboratory mobility report, and Table 5-2 presents a summary table of permeability and mobility characteristics.

Petrographic results may be used to inform future LNAPL evaluations and groundwater transport modeling. Additional petrographic analysis may be employed during the drilling of RHMW01R, proposed in DON (2017f) for installation adjacent to existing monitoring well RHMW01.

Table 5-2: Rock Type, Permeability, and Porosity Summary

Monitoring Well ID - Core ID	Laboratory Sample ID	Depth of Sample (ft)	Measured at 250psi Net Confining Stress [a]			Helium Grain Volume (cc)	Grain Density (g/cc)	Core Description Provided by AECOM
			Permeability to Air (Kair) (md)	Total Porosity (%Vb)	Helium Pore Volume (cc)			
Pāhoehoe								
RWMW09-BS03	ERH 511	155.30	7.1	41.2	23.35	33.35	3.05	Pāhoehoe
RWMW08-BS02	ERH 516	242.70	0.2	40.9	22.41	32.44	3.05	Pāhoehoe
RWMW08-BS03	ERH 517	341.40	53.3	42.9	24.36	32.42	3.06	Pāhoehoe
RWMW08-BS04	ERH 521	171.35	1.8	37.4	21.67	36.29	3.05	Pāhoehoe
RWMW08-BS07	ERH 524	249.00	16453.0 [b]	48.3	28.25	30.21	3.00	Pāhoehoe
RWMW08-BS08	ERH 525	289.25	0.4	29.9	16.28	38.10	3.08	Pāhoehoe
RWMW10-BS04	ERH 529	177.40	0.3	29.2	16.26	39.47	3.07	Pāhoehoe
RWMW10-BS06	ERH 531	296.95	4529.0 [b]	51.3	30.08	28.60	3.02	Pāhoehoe - oxidized dark reddish brown, highly vesicular 50%, small vesicles
RWMW10-BS07	ERH 532	325.35	0.1	23.3	13.35	44.01	3.01	Pāhoehoe - gray, large vesicles 15%, some infilling in vesicles
RWMW10-BS08	ERH 533	393.60	0.1	13.3	7.70	49.99	3.00	Pāhoehoe - gray, vesicular 25%, small to medium vesicles
RWMW10-BS09	ERH 534	489.65	11716.0 [c]	35.10	20.18	37.32	3.04	Pāhoehoe - sl. oxidized reddish brown, vesicular 25%, small to medium vesicles
		Max	*16453.0*	*51.3*	*30.1*	*50.0*	*3.1*	
		Min	*0.1*	*13.3*	*7.7*	*28.6*	*3.0*	
		Avg	*2978.3*	*35.7*	*20.4*	*36.6*	*3.0*	
Massive A'ā								
RWMW09-BS02	ERH 510	81.10	0.018	5.11	3.04	56.38	3.00	Massive a'ā
RWMW09-BS06	ERH 514	162.95	0.097	21.1	11.93	44.70	3.04	Massive a'ā
RWMW10-BS02	ERH 527	137.80	0.050	13.3	5.64	36.81	3.00	Massive a'ā
RWMW10-BS05	ERH 530	215.50	0.089	11.82	7.32	54.60	2.99	Massive a'ā
		Max	*0.097*	*21.1*	*11.9*	*56.4*	*3.0*	
		Min	*0.018*	*5.1*	*3.0*	*36.8*	*3.0*	
		Avg	*0.064*	*12.8*	*7.0*	*48.1*	*3.0*	

Monitoring Well ID - Core ID	Laboratory Sample ID	Depth of Sample (ft)	Measured at 250psi Net Confining Stress [a]			Helium Grain Volume (cc)	Grain Density (g/cc)	Core Description Provided by AECOM
			Permeability to Air (Kair) (md)	Total Porosity (%Vb)	Helium Pore Volume (cc)			
Welded A'ā Clinker								
RWMW09-BS05	ERH 513	133.20	21.8	28.9	16.19	39.84	2.99	Welded a'ā clinker
RWMW08-BS06	ERH 523	218.80	31.8	17.6	7.24	33.94	3.00	Massive a'ā
RWMW10-BS01	ERH 526	108.70	5.0	29.42	17.25	41.38	3.02	Welded a'ā clinker
		Max	*31.8*	*29.4*	*17.2*	*41.4*	*3.0*	
		Min	*5.0*	*17.58*	*7.24*	*33.94*	*2.99*	
		Avg	*19.5*	*25.3*	*13.6*	*38.4*	*3.0*	
Weathered A'ā Clinker								
RWMW09-BS01	ERH 509	65.90	618.9	41.8	21.94	30.57	2.94	Weathered a'ā clinker
RWMW09-BS04	ERH 512	106.10	302.0 [b]	44.7	18.33	22.69	2.98	Weathered a'ā clinker
RWMW08-BS01	ERH 515	Unable to obtain sufficient sample for testing						Weathered a'ā clinker
RWMW08-BS05	ERH 522	200.30	614.0 [b]	39.0	19.67	30.80	2.95	Weathered a'ā clinker
RWMW10-BS03	ERH 528	155.60	2.7	26.16	15.99	45.12	3.00	Weathered a'ā clinker
		Max	*618.9*	*44.7*	*21.9*	*45.1*	*3.0*	
		Min	*2.7*	*26.2*	*16.0*	*22.7*	*2.9*	
		Avg	*384.4*	*37.9*	*19.0*	*32.3*	*3.0*	

Notes: Methodology: API RP40
cc cubic centimeter
g/cc grams per cubic centimeter
md millidarcy
psi pounds per square inch
Vb bulk volume
[a] 250 psi confining stress to minimize bypass around sample
[b] Lowest value of the post-test run used
[c] Post-test value remained unchanged

5.1.12 Infiltration Study of Surficial Saprolite Soils

Infiltration testing was performed at the Facility to characterize water infiltration rates in the surficial saprolite soils overlying much of the ridgetop area at the site overlying the tank farm. The infiltration study was conducted by Geolabs, Inc. The report is presented in Appendix G.

Water infiltration rates into the subsurface soils were tested by performing double-ring infiltrometer tests at three prepared test locations (identified on Plate 2 of Appendix G) in general accordance with ASTM D3385. The tests were performed by driving two open-top and -bottom concentric cylinders into the ground, partially filling the rings with water, and maintaining a near-constant water level for the duration of the test. The double-ring infiltrometer test estimates the vertical rate of movement of water through the bottom of the inner cylinder, while the outer ring helps to reduce the lateral movement of water in the soil. This is done to help constrain water movement to nearly vertical. The volume of water added to the inner ring was measured as the infiltrated water volume. The tests were carried out in several increments until achieving a steady-state condition with a relatively constant water infiltration rate.

Test locations IF-1 and IF-2 were performed in vegetated areas that were cleared of vegetation and excavated generally below the grass root line, approximately 0.5–1 ft below the existing grade. IF-3 was performed on a leveled pad excavated near the toe of a barren saprolite outcrop. However, because of past disturbance on Red Hill as a result of historical agriculture in the area (see Section 2.2) and tank, tunnel, and ventilation system construction (see Section 3.1), it is unknown if these locations/outcrops are intact or disturbed. Laboratory Atterberg Limit tests conducted on the soil samples from each of the test locations indicate that the near-surface soils at IF-1 and IF-2 are classified as Silty Clay (CH), while the soil sample for IF-3 is classified as Clayey Silt (MH).

Results of the soil classification and double-ring infiltrometer tests are summarized in Table 5-3.

Table 5-3: Summary of Infiltration Test Results

	Final Infiltration Rate		Soil Classification
Test No.	(cm/hour)	(inch/hour)	(USCS)
IF-1	20.6	8.11	Silty Clay (CH)
IF-2	10.7	4.21	Silty Clay (CH)
IF-3	22	8.66	Clayey silt (MH)

Results of the soil classification and infiltration study inform understanding of local recharge potential.

5.1.13 Assessment of Geologic Features and Natural Processes Affecting LNAPL

The updated geologic CSM described in this section has better defined the spatial distribution, orientation, and physical characteristics of the basalt layers, and thus provides a basis for evaluating the LNAPL movement beneath the Facility tanks. The available geologic logs and core photos from the Facility area reveal that thick, unweathered clinker layers in the basalt composed of loose rubble and large interconnected macro-pores are the principal zones that can transmit fluids. Although much less common, open fractures with substantial aperture thickness and lava tubes may also exist as potential conduits, but these are not expected to be laterally continuous or extend between flows. Geologic features with extensive interconnected macro-pores, such as thick, non-weathered clinker beds, clinker bridges, and thin pāhoehoe flows, appear to be the primary pathways for LNAPL movement.

Future potential LNAPL releases would likely move from a fuel tank leak point into basalt layers containing macro-pores (e.g., thick, non-weathered clinker zones, lava tubes, and interflow voids), then the LNAPL would move primarily downward and down-dip through clinker or an open fracture until being impeded by the top of a dense massive layer of low-porosity, low-permeability basalt (or until LNAPL had reached residual saturation). The LNAPL would then spread horizontally on top of lower permeability flow beds until reaching fractures, clinker bridges or other vertical conduits. Once entering a permeable feature that allows downward movement, the LNAPL may penetrate deeper until a fracture ends at the base of a flow, or the LNAPL encounters a low-permeability bed. Based on available information, the dense interiors of the basalt flows may have an effective porosity of 1–2 percent, whereas the thick, non-weathered clinkers may have an effective porosity of 20–30 percent. Interconnected macro-pores appear to be more prevalent in the thicker non-weathered clinker beds. Thus, most of the LNAPL would move within those thicker clinker zones, and in the same direction as the dip of the low-permeability lava beds. The LNAPL would also spread laterally in the clinker zones and thin pāhoehoe flows, but the movement would be primarily down the dip of the lava beds. If LNAPL entered a pāhoehoe lava tube, it would move within the confined walls of the lava tube, generally downslope.

Movement of LNAPL through thin, weathered clinker layers and fractures containing fine-grained sediments or infill would be restricted by capillary forces created by moisture in the smaller pore spaces. Water held by surface tension and capillary forces in those small pore spaces would cause the relative permeability for LNAPL to be very low. Compared to water, the higher viscosity of jet fuel would also restrict LNAPL movement through small pore spaces. Collection of additional residual saturation data is planned during the drilling of proposed monitoring well RHMW01R adjacent to existing well RHMW01 in the Facility's lower access tunnel (DON 2017f) to enable estimates of volume of LNAPL potentially retained and extent of LNAPL in the vadose zone beneath the tanks (DON 2017g).

5.2 UNCERTAINTY ANALYSIS

At this point in the study, the main uncertainty is the potential extent of LNAPL movement away from the Facility fuel tanks. Historically, no LNAPL has been measured in monitoring wells at the site, only isolated odors and staining have been observed in cores collected adjacent to the tanks within borings, and no LNAPL seeps/staining have been observed during field surface mapping at the site. RHMW02, however, has had historical levels of TPH-d exceeding solubility limits, indicating a potential for the occurrence of LNAPL.

5.3 ADDRESSING UNCERTAINTIES

The following ongoing, planned, or proposed activities are designed to help resolve the uncertainties described in Section 5.2.

To help determine the potential extent of LNAPL movement away from the Facility fuel tanks, additional core samples are planned for petrographic analyses of the capacity of the basalt to retain LNAPL. A core boring will be drilled to install a proposed new monitoring well (RHMW01R) adjacent to RHMW01 inside the Facility tunnel system, which will have a screen interval intersecting the water table (DON 2017f). A detailed geologic log will be prepared during the core drilling. Core samples from this boring will be inspected for the presence of LNAPL on site during drilling, then planned for preservation and shipping for laboratory petrographic analyses. If no LNAPL is detected, then selected core samples will be saturated in the laboratory to measure residual saturation values that reasonably represent the geologic units beneath the Facility.

This page intentionally left blank

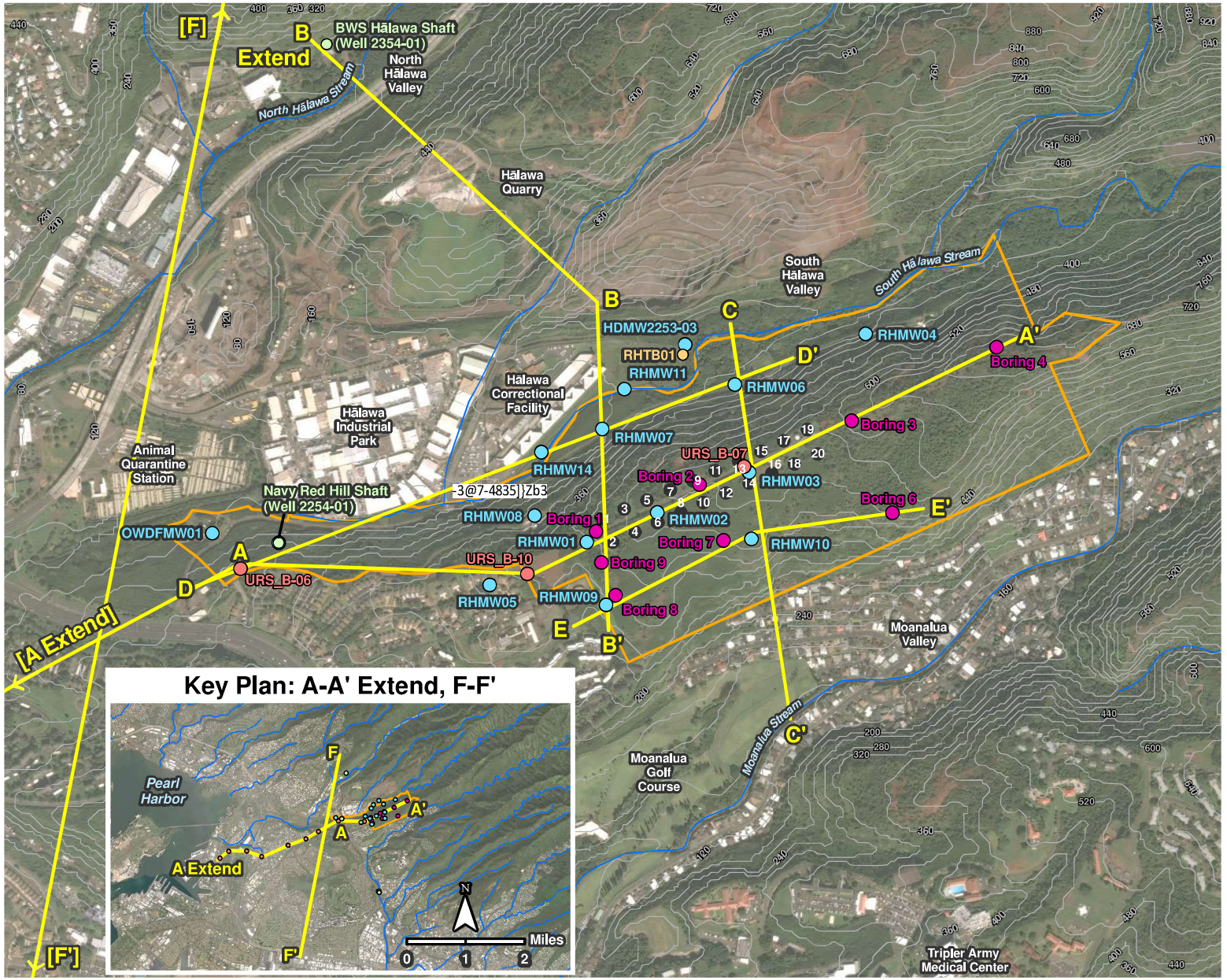

Location Map

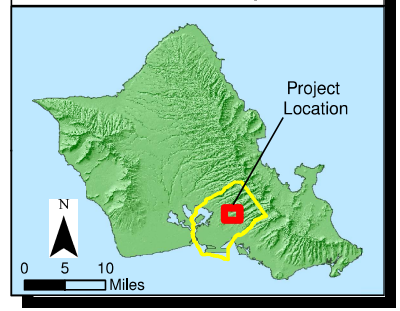

Legend

- Macdonald 1941 Boring
- URS 2012 Geotechnical Boring
- Red Hill Monitoring Well Boring
- Red Hill Test Boring
- Water Supply Well
- Stream
- Topographic Contour (feet above mean sea level)
- Red Hill Facility Boundary and Fuel Storage Tanks
- Groundwater Model Domain

Notes

1. Map projection: NAD 1983 Hawaii State Plane Zone 3 feet.
2. Base Map: DigitalGlobe, Inc. (DG) and NRCS. Publication_Date: 2015
3. Yellow lines correspond to geologic cross sections presented on Figures 5-2 (A-A'), 5-3 (A-A' Extended), 5-4 (B-B'), 5-5 (B-B' Extended), 5-6 (C-C'), 5-7 (D-D'), 5-8 (E-E'), 5-9 (F-F'), and 5-10 (K-K').

N

0 400 800 1,600 Feet

Figure 5-1
Geologic Cross Section Key Plan
Conceptual Site Model Rev. 01
Investigation and Remediation of Releases and Groundwater Protection and Evaluation
Red Hill Bulk Fuel Storage Facility
JBPHH, O'ahu, Hawai'i

S:\Projects\NAVFAC PACOM\EAN V\60571032_CTO18F0126\900-Work\920 GIS\02_Maps\CSM\Fig5-1_Xsection_KeyPlan_rev4v10-5.mxd 6/14/2019

This page intentionally left blank

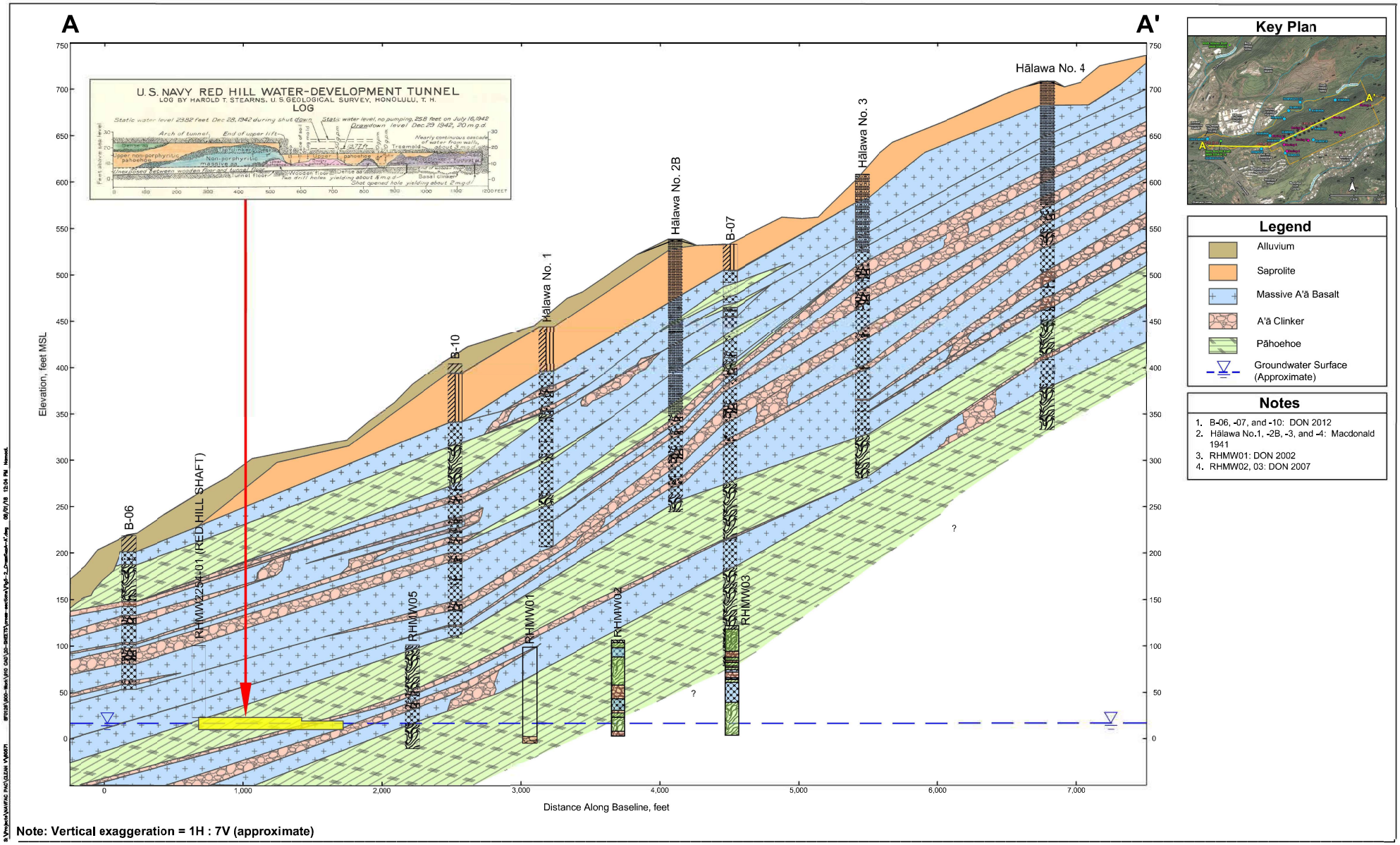

Note: Vertical exaggeration = 1H : 7V (approximate)

Figure 5-2
Cross Section A-A'
Conceptual Site Model Rev. 01
Investigation and Remediation of Releases and Groundwater Protection and Evaluation
Red Hill Bulk Fuel Storage Facility, JBPHH, O'ahu, Hawai'i

This page intentionally left blank

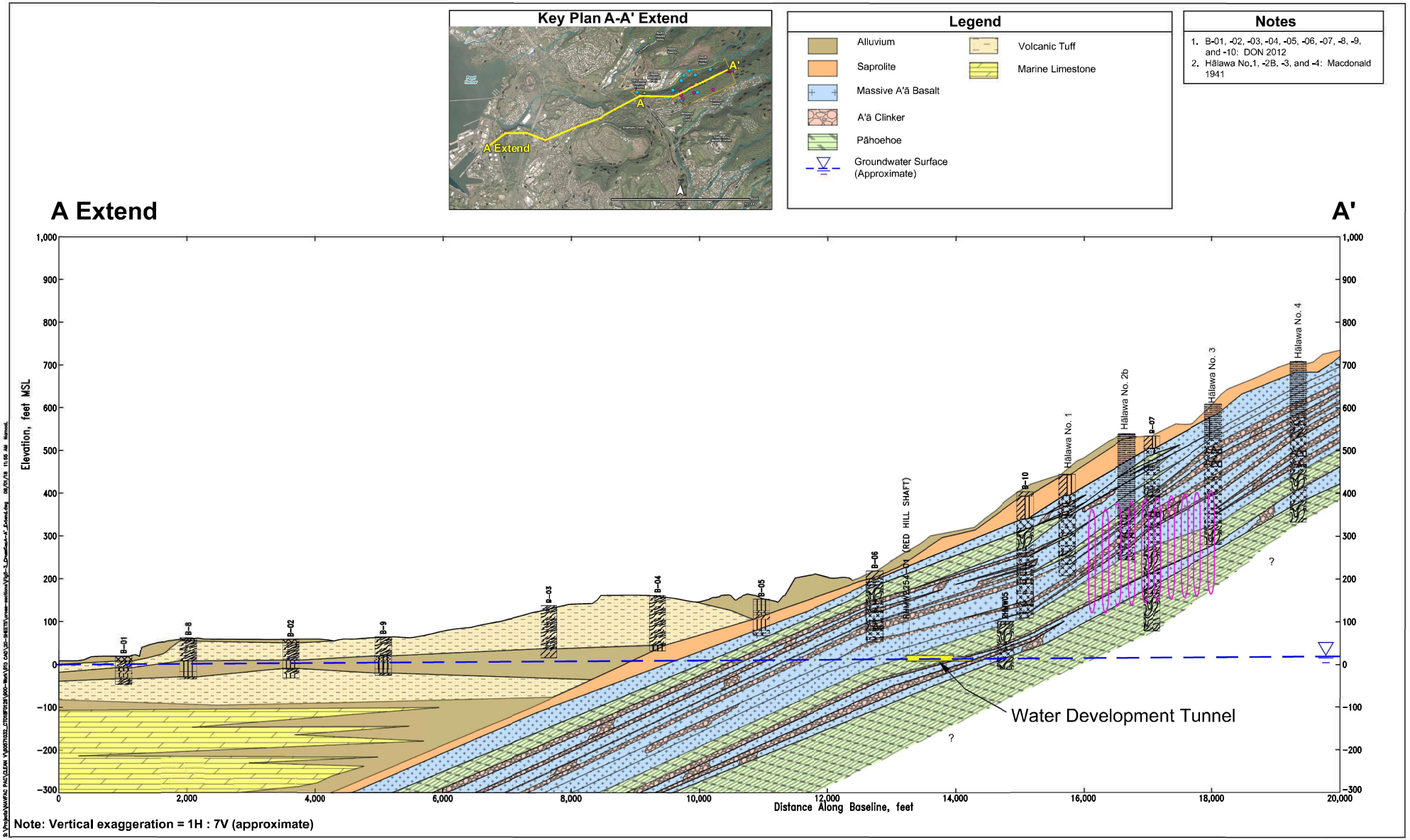

Figure 5-3
Cross Section A-A' Extended
Conceptual Site Model Rev. 01
Investigation and Remediation of Releases and Groundwater Protection and Evaluation
Red Hill Bulk Fuel Storage Facility, JBPHH, O'ahu, Hawai'i

This page intentionally left blank

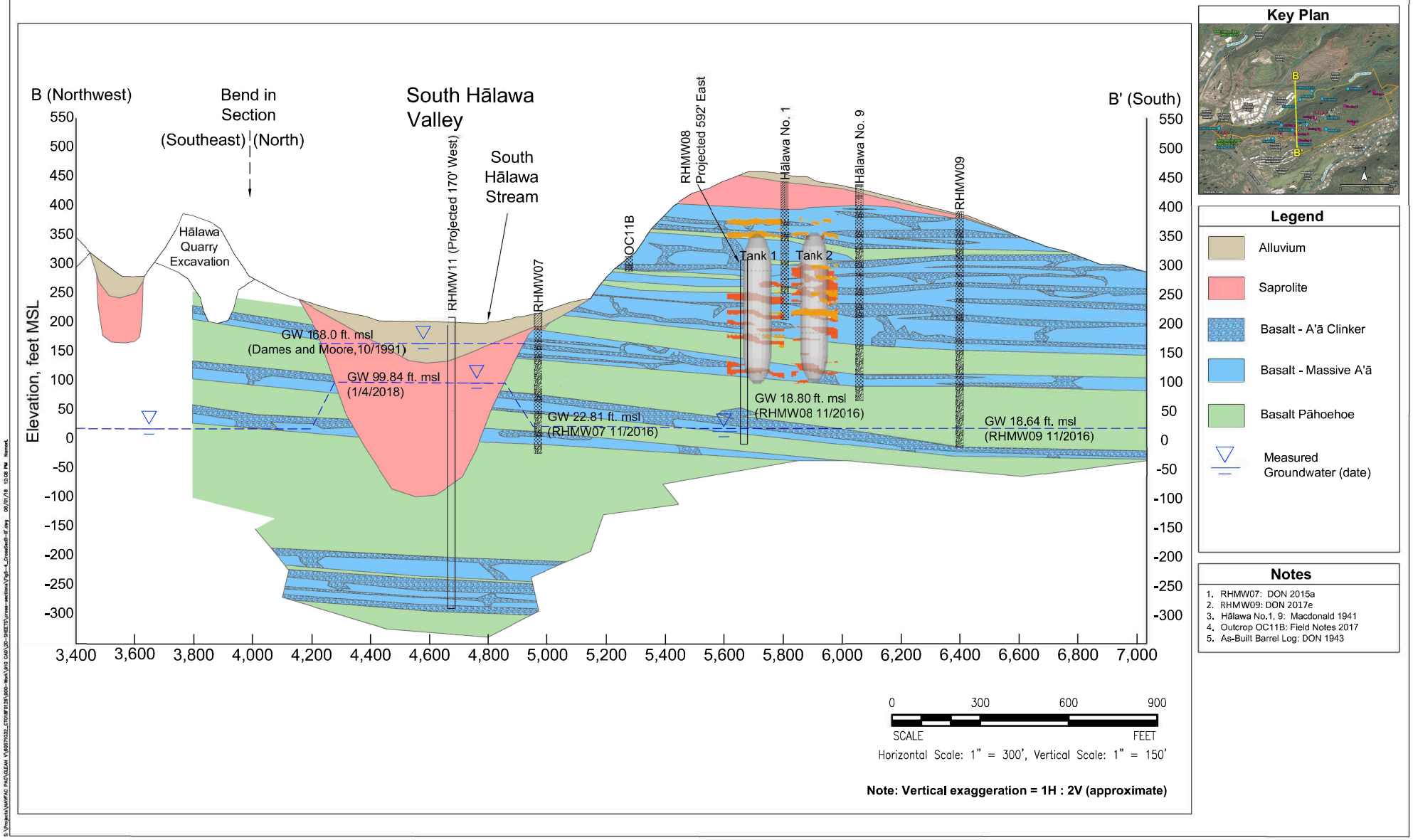

Key Plan

Legend

- Alluvium
- Saprolite
- Basalt - A'ā Clinker
- Basalt - Massive A'ā
- Basalt Pāhoehoe
- Measured Groundwater (date)

Notes

1. RHMW07: DON 2015a
2. RHMW09: DON 2017e
3. Hālawa No.1, 9: Macdonald 1941
4. Outcrop OC11B: Field Notes 2017
5. As-Built Barrel Log: DON 1943

Figure 5-4
Cross Section B-B' (View Looking East)
Conceptual Site Model Rev. 01
Investigation and Remediation of Releases and Groundwater Protection and Evaluation
Red Hill Bulk Fuel Storage Facility, JBPHH, O'ahu, Hawai'i

This page intentionally left blank

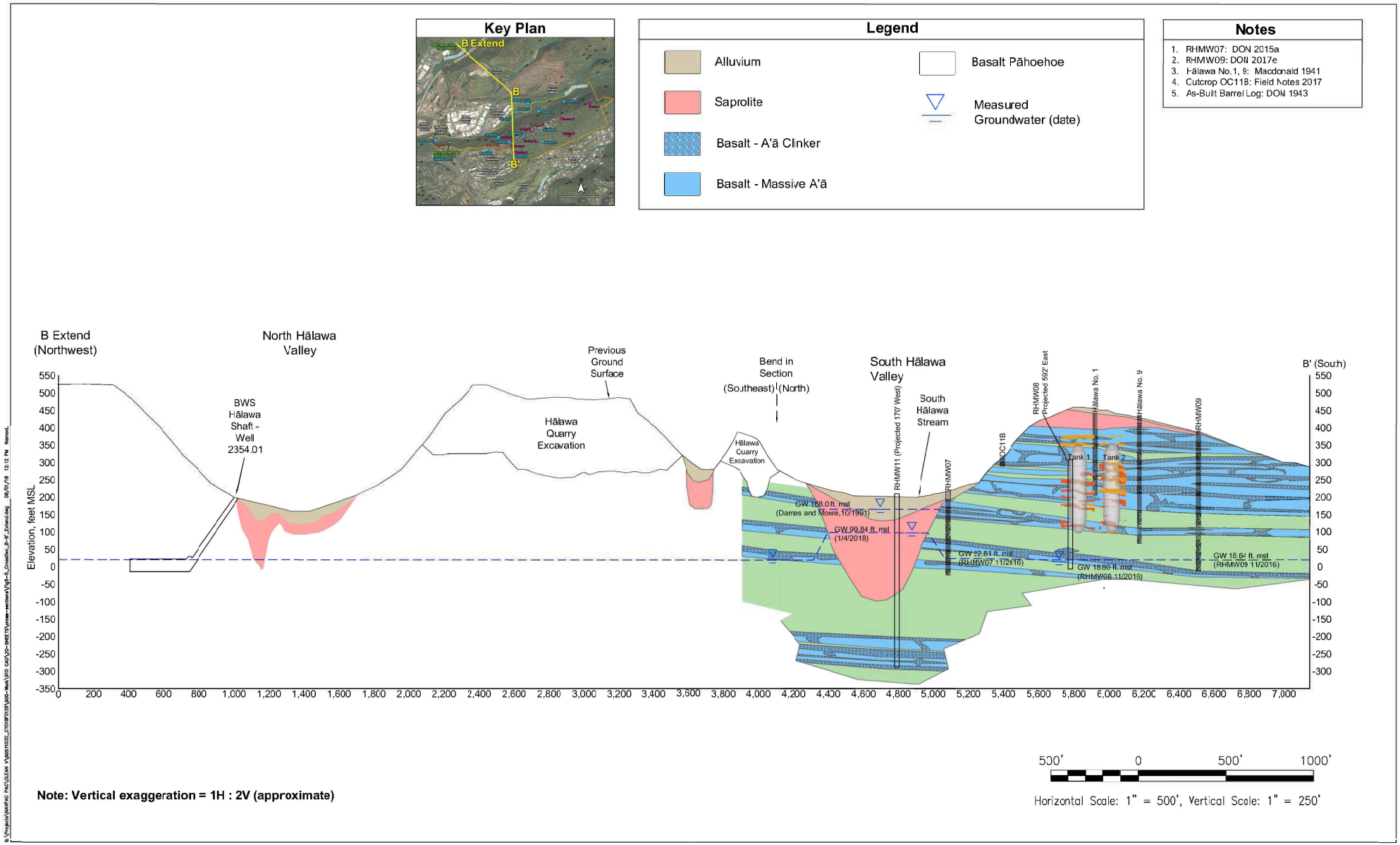

Figure 5-5
Cross Section B-B' Extended (View Looking East)
Conceptual Site Model Rev. 01
Investigation and Remediation of Releases and Groundwater Protection and Evaluation
Red Hill Bulk Fuel Storage Facility, JBPHH, O'ahu, Hawai'i

This page intentionally left blank

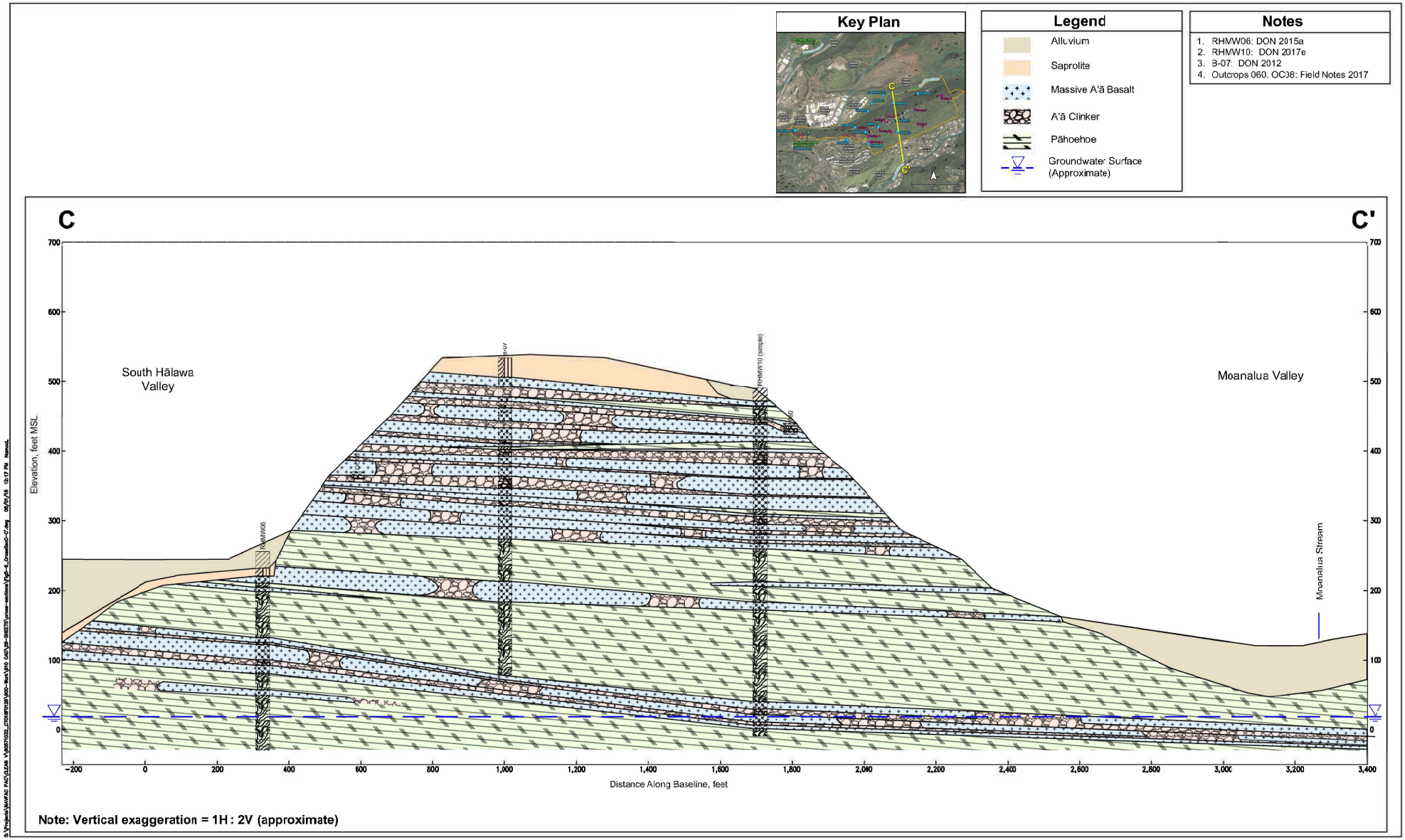

Figure 5-6
Cross Section C - C'
Conceptual Site Model Rev. 01
Investigation and Remediation of Releases and Groundwater Protection and Evaluation
Red Hill Bulk Fuel Storage Facility, JBPHH, O'ahu, Hawai'i

This page intentionally left blank

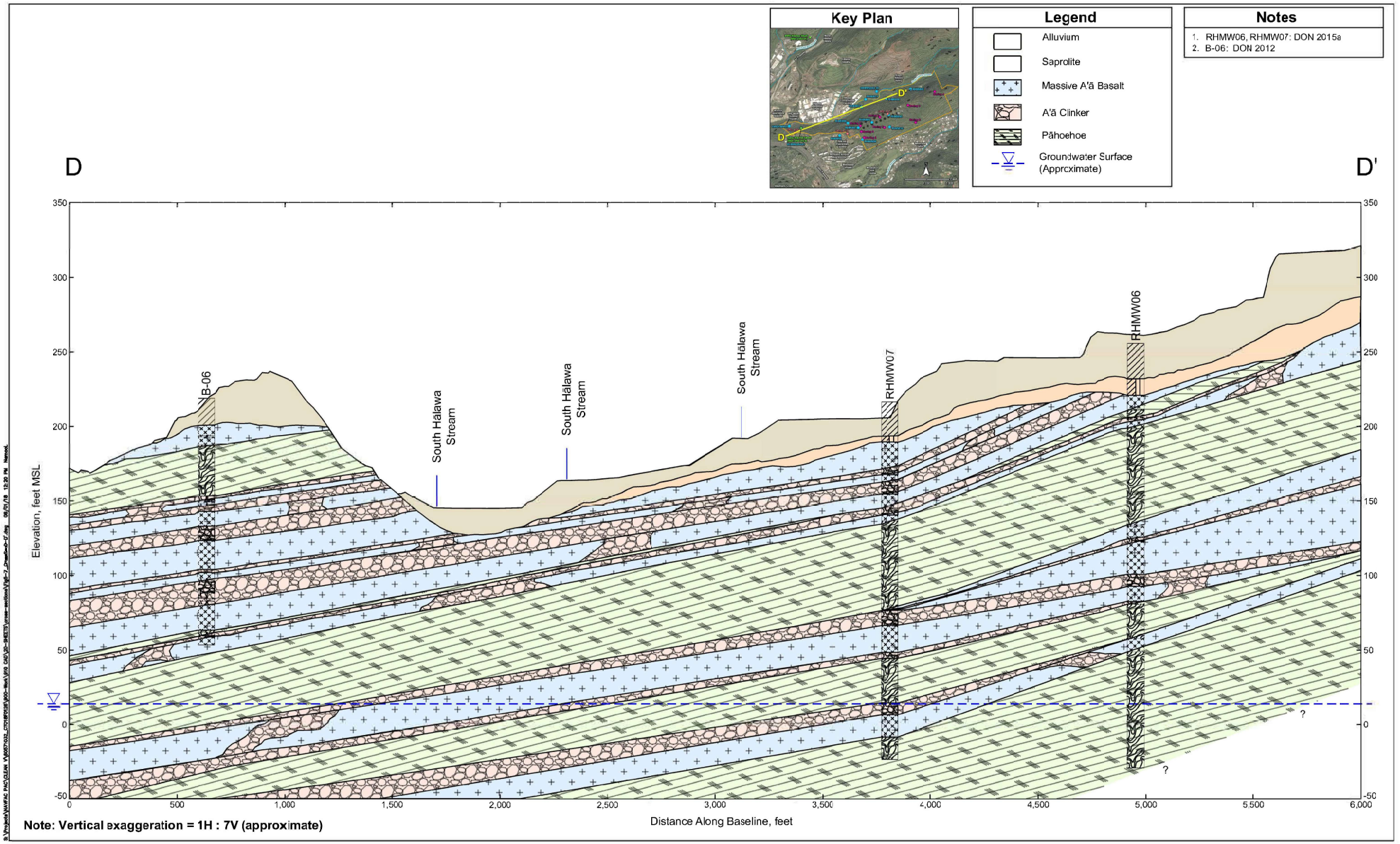

Figure 5-7
Cross Section D-D'
Conceptual Site Model Rev. 01
Investigation and Remediation of Releases and Groundwater Protection and Evaluation
Red Hill Bulk Fuel Storage Facility, JBPHH, O'ahu, Hawai'i

This page intentionally left blank

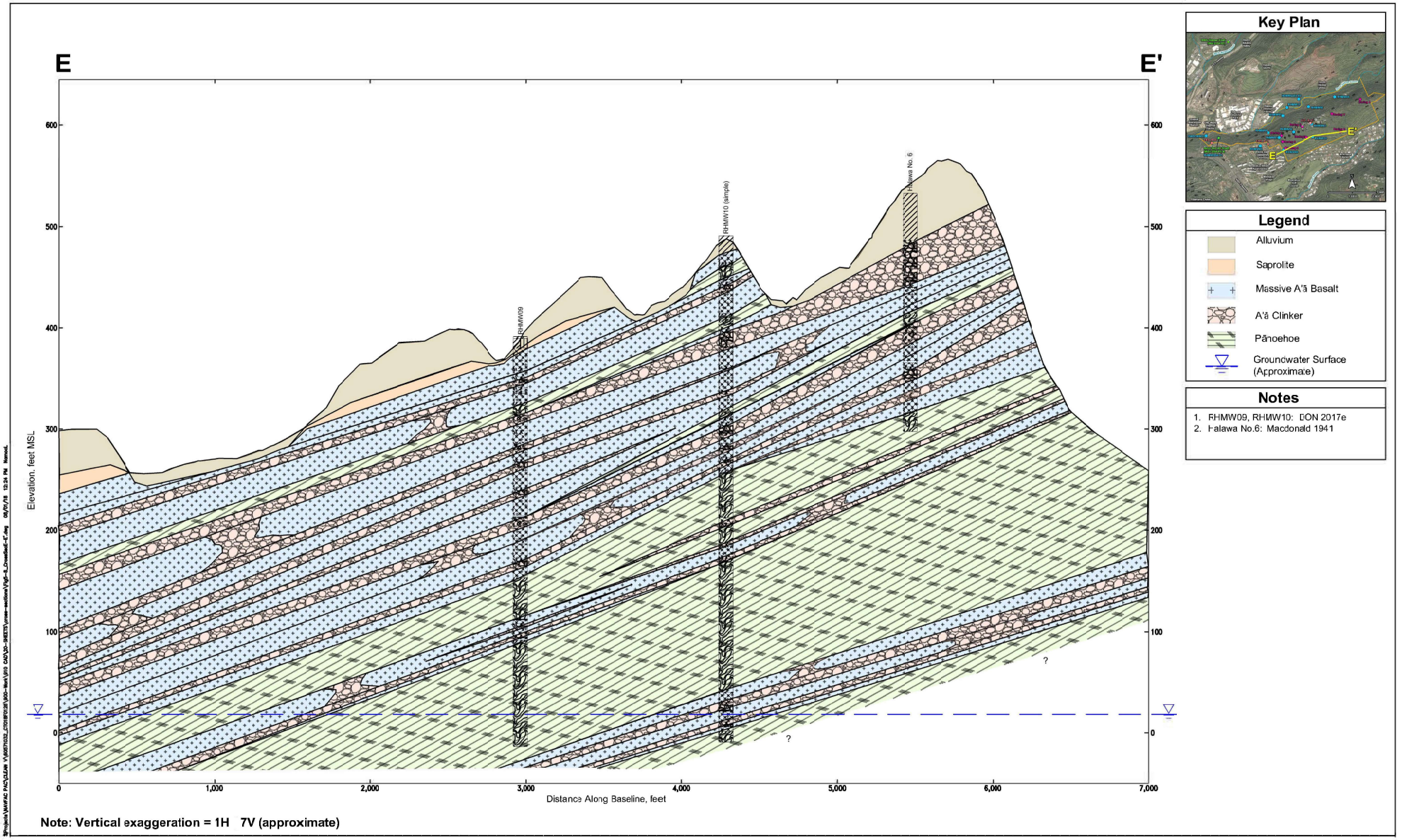

Figure 5-8
Cross Section E-E'
Conceptual Site Model Rev. 01
Investigation and Remediation of Releases and Groundwater Protection and Evaluation
Red Hill Bulk Fuel Storage Facility, JBPHH, O'ahu, Hawai'i

This page intentionally left blank

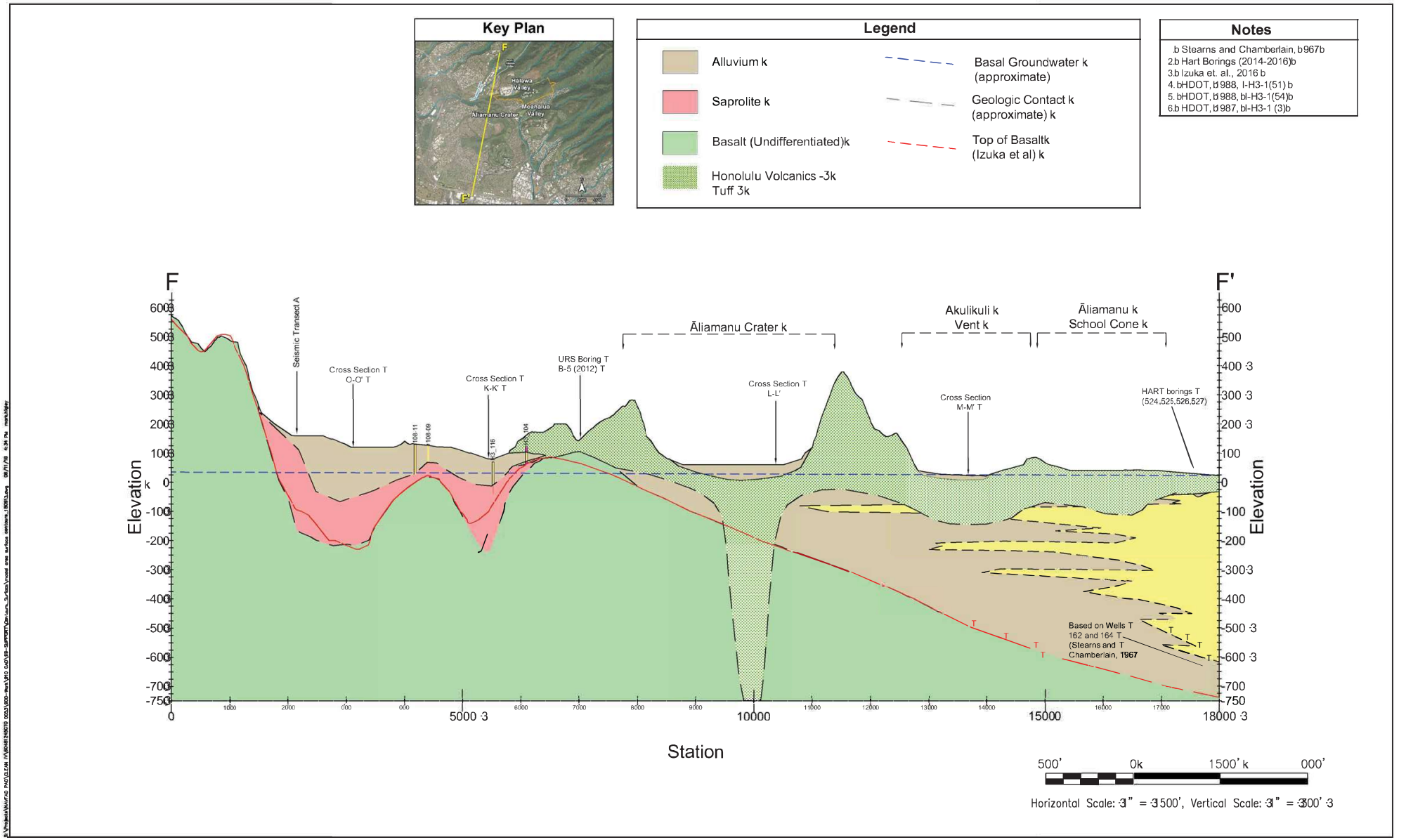

Figure 5-9
Cross Section F-F' Āliamanu Crater Section
Conceptual Site Model Revision 01
Investigation and Remediation of Releases and Groundwater Protection and Evaluation
Red Hill Bulk Fuel Storage Facility, JBPHH, O'ahu, Hawai'i

This page intentionally left blank

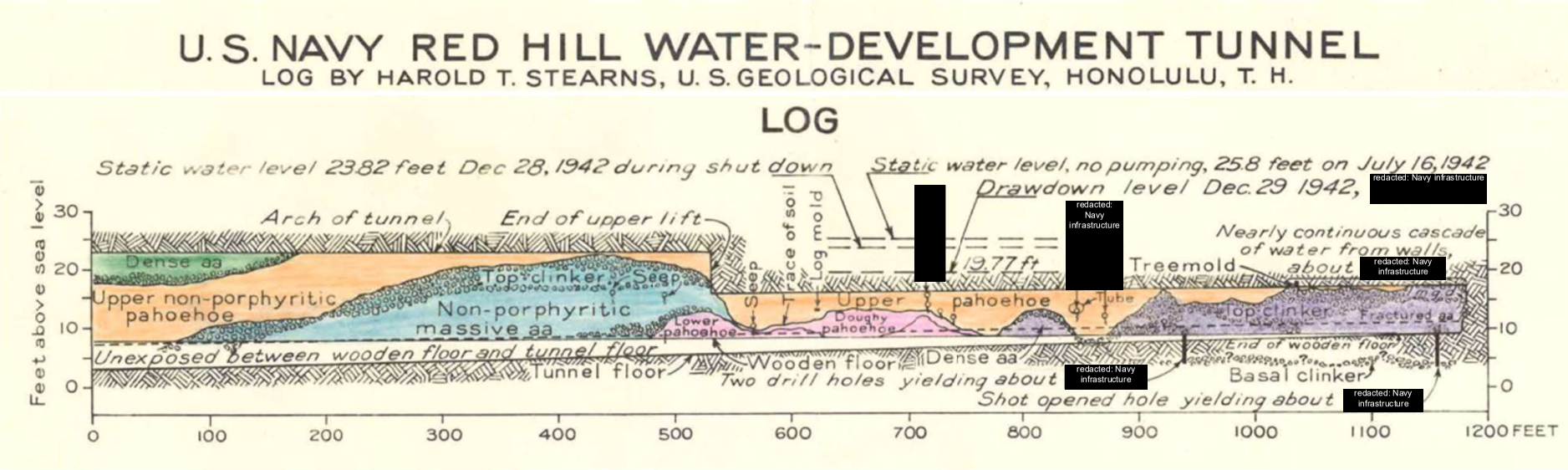

The heterogeneous nature of the basalt is revealed in the geologic log of the Red Hill Shaft water development tunnel (i.e., the infiltration gallery) prepared by the USGS (Stearns 1943).

Figure 5-10
Cross Section of Red Hill Shaft Water Development Tunnel
Conceptual Site Model Rev. 01
Investigation and Remediation of Releases and Groundwater Protection and Evaluation
Red Hill Bulk Fuel Storage Facility, JBPHH, O'ahu, Hawai'i

This page intentionally left blank

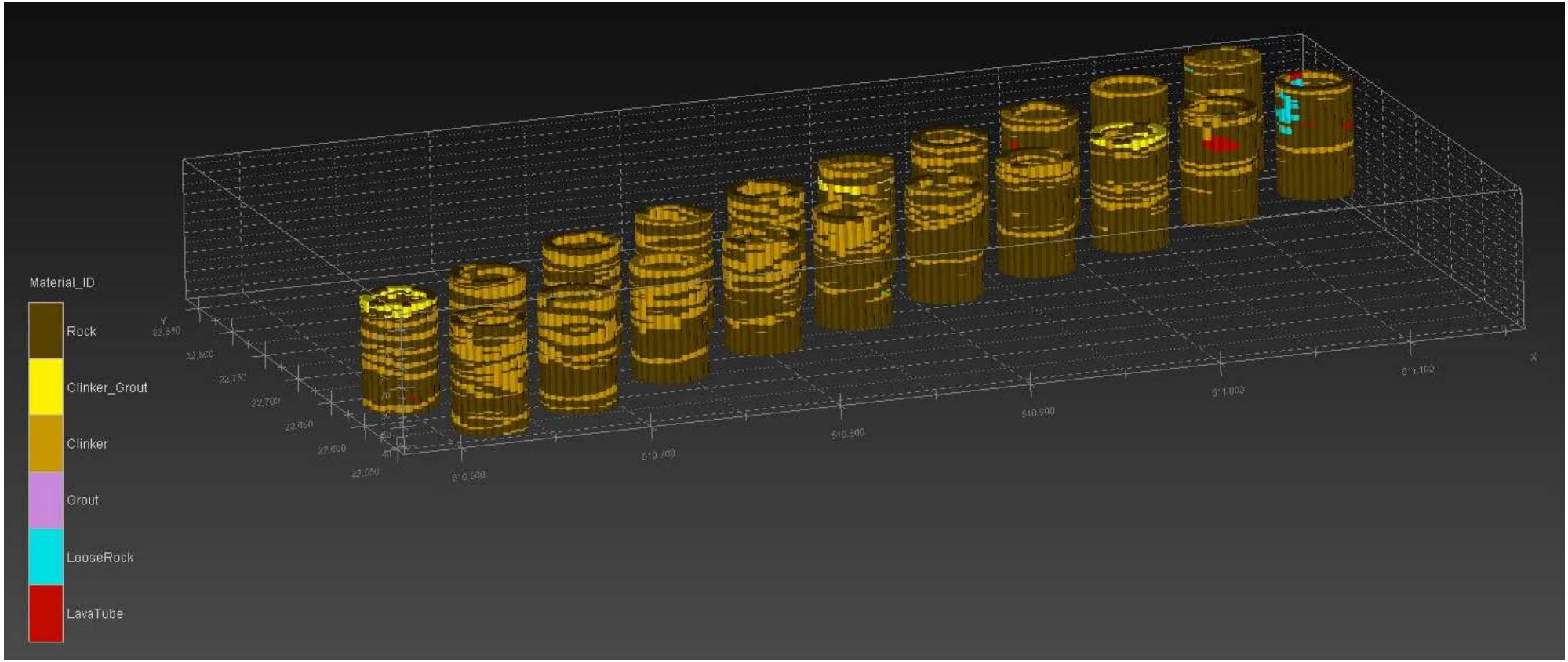

Figure 5-11
Logs of Formations in Tank Excavations (Barrel Logs)
Conceptual Site Model Rev. 01
Investigation and Remediation of Releases and Groundwater Protection and Evaluation
Red Hill Bulk Fuel Storage Facility, JBPHH, O'ahu, Hawai'i

This page intentionally left blank

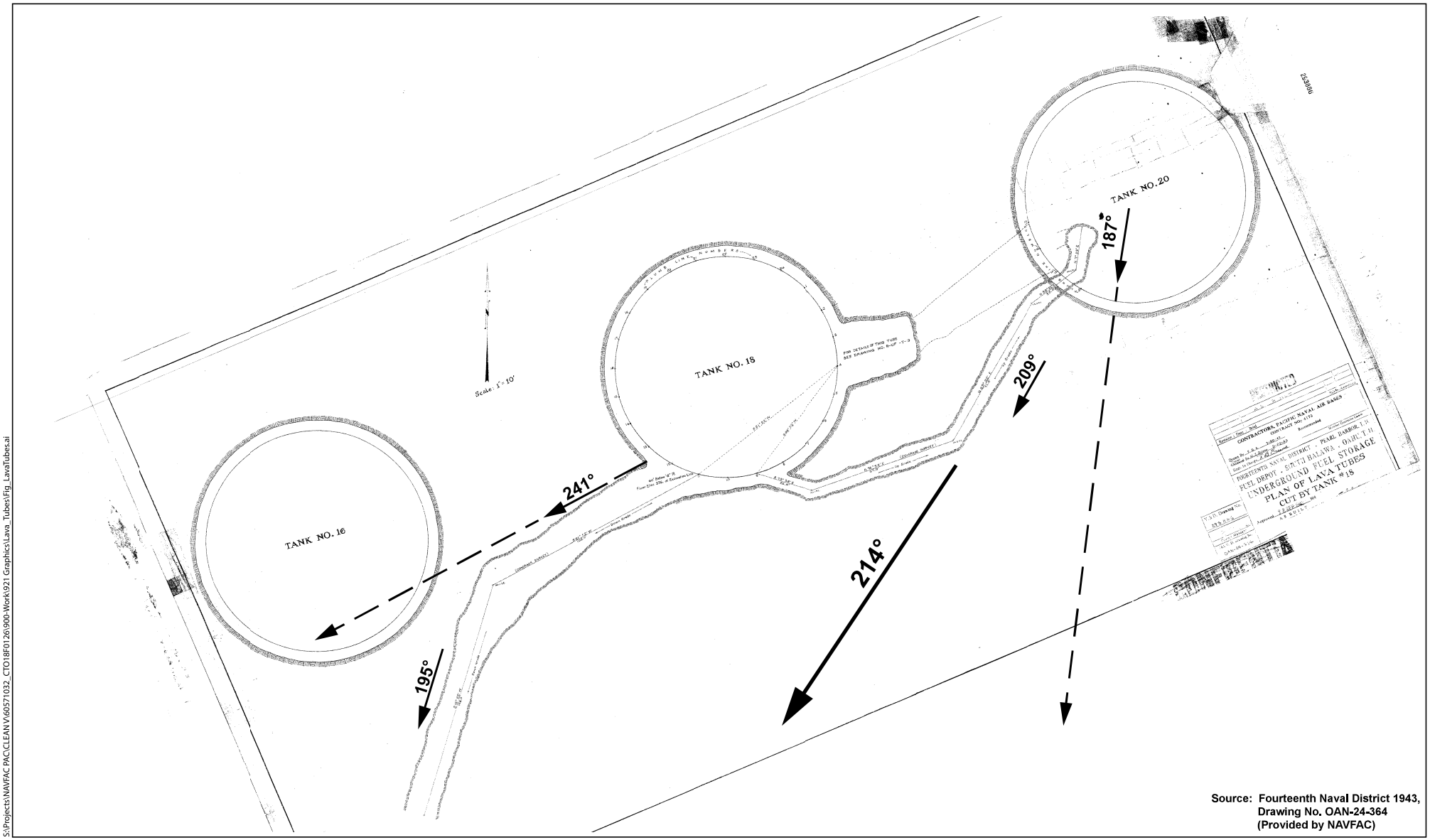

S:\Projects\NAVFAC PAC\CLEAN V\60571032_CTO18F01260900-Work\921 Graphics\Lava_Tubes\Fig_LavaTubes.ai

Figure 5-12
Plan of Lava Tubes Cut by Tank 18
Conceptual Site Model Rev. 01
Investigation and Remediation of Releases and Groundwater Protection and Evaluation
Red Hill Bulk Fuel Storage Facility
JBPHH, Oʻahu, Hawaiʻi

This page intentionally left blank

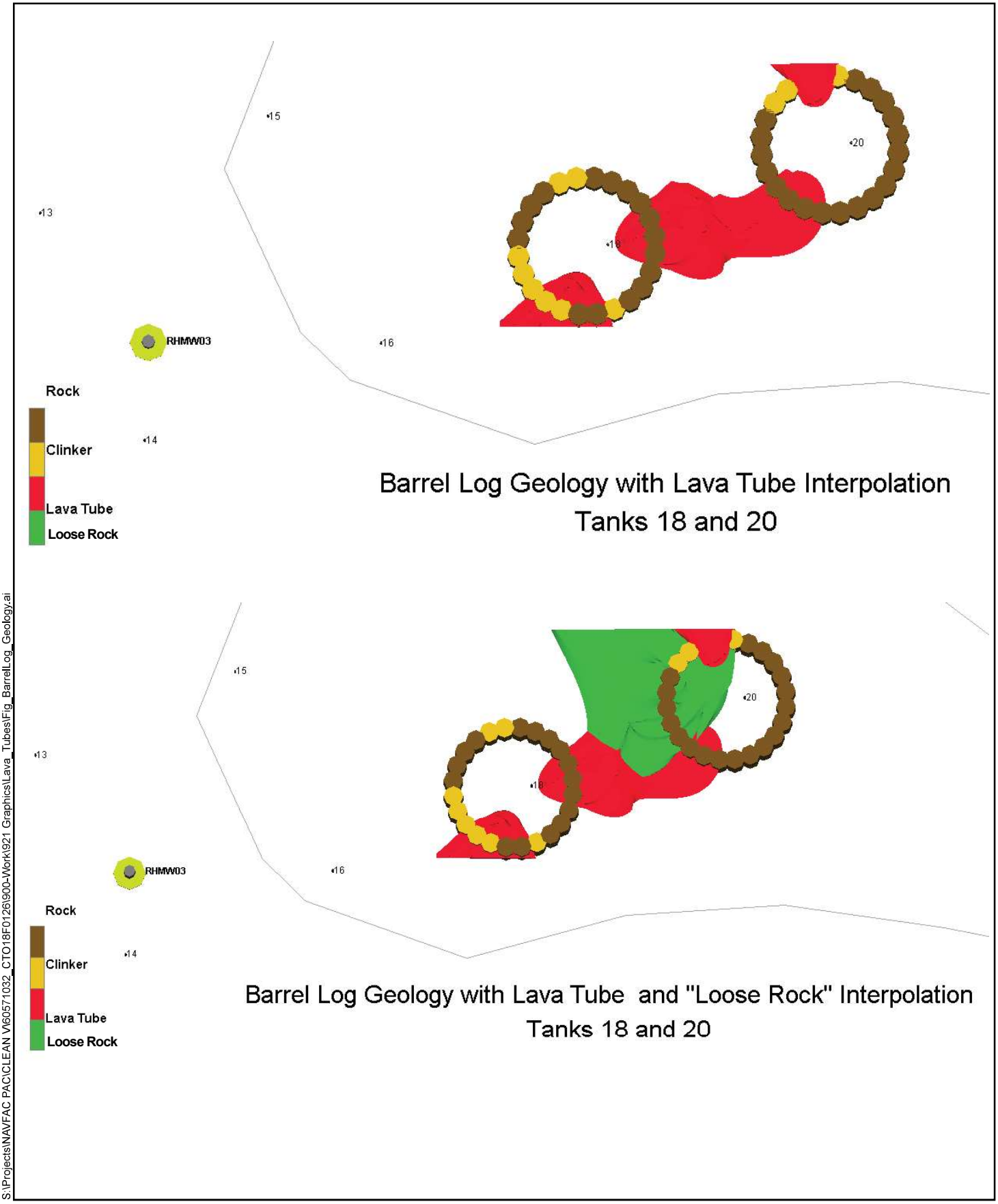

S:\Projects\NAVFAC PACIFIC\CLEAN V\60571032_CTO18F01261900-Work\921 Graphics\Lava_Tubes\Fig_BarrelLog_Geology.ai

Figure 5-13
Barrel Log Geology of Lava Tube and Loose Rock Interpolation
Conceptual Site Model Rev. 01
Investigation and Remediation of Releases and Groundwater Protection and Evaluation
Red Hill Bulk Fuel Storage Facility
JBPHH, Oʻahu, Hawaiʻi

This page intentionally left blank

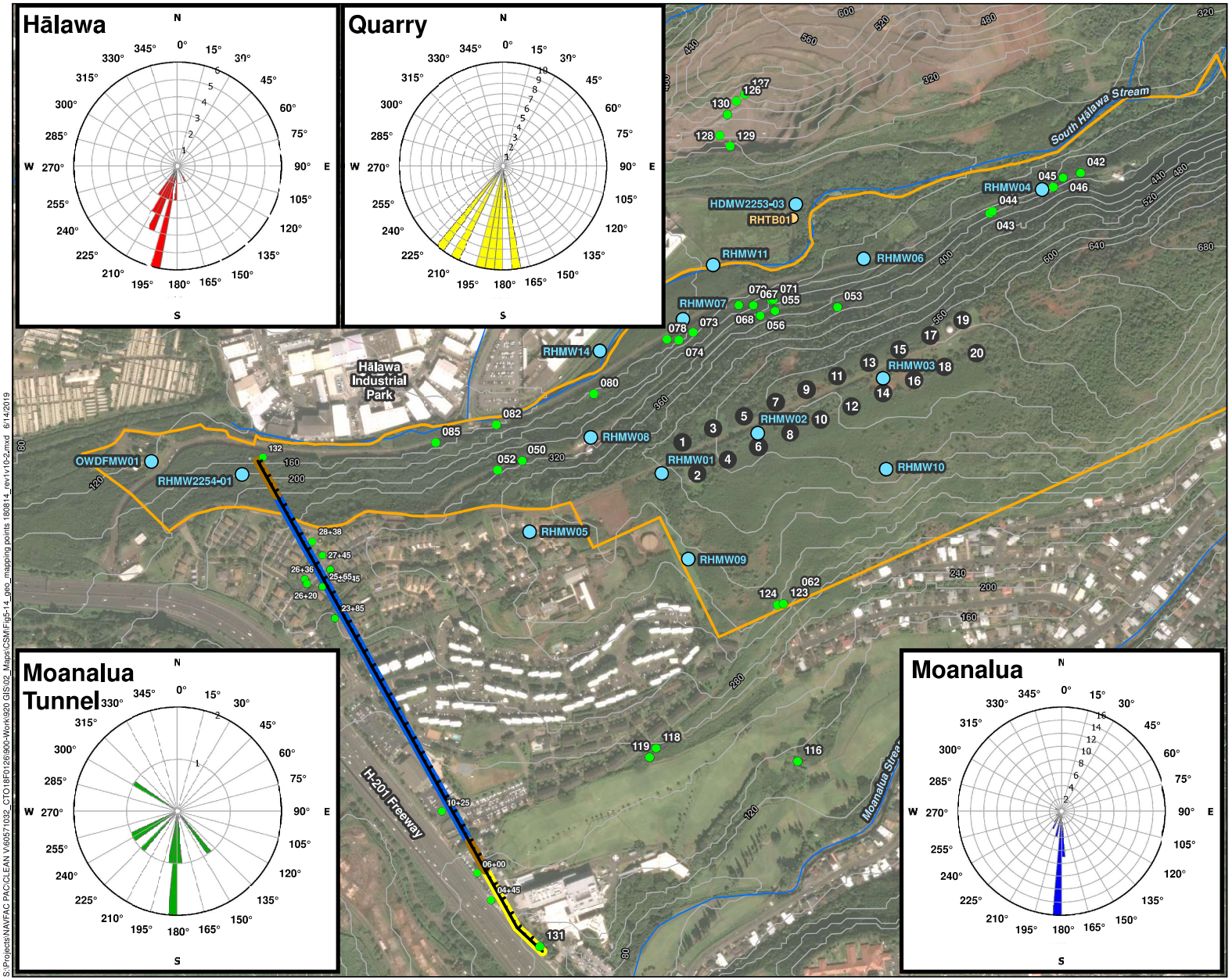

Location Map

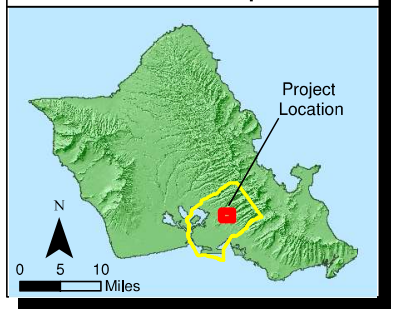

Legend

- 28+38 — Geologic Field Mapping Point (dip azimuth in degrees)
- Gunite (Moanalua Tunnel)
- A'ā Basalt (Moanalua Tunnel)
- Tuff (Moanalua Tunnel)
- Groundwater Monitoring Location
- Test Boring
- Stream
- 400 — Topographic Contour (feet above mean sea level)
- Red Hill Facility Boundary and Fuel Storage Tanks
- Groundwater Model Domain

Notes

1. Map projection: NAD 1983 Hawaii State Plane Zone 3 feet
2. Base Map: DigitalGlobe, Inc. (DG) and NRCS. Publication_Date: 2015

N

0 500 1,000 Feet

Figure 5-14
Geologic Mapping Points
Conceptual Site Model Rev. 01
Investigation and Remediation of Releases and Groundwater Protection and Evaluation
Red Hill Bulk Fuel Storage Facility
JBPHH, O'ahu, Hawai'i

S:\Projects\NAVFAC PAC\CLEAN V\60571032_CTO18F0126\900-Work\920 GIS\02_Maps\CSM\Fig5-14_geo_mapping points 180814_rev1v10-2.mxd 6/14/2019

This page intentionally left blank

S:\Projects\NAVFAC PAC\CLEAN V\60571032_CTO18F0126\900-Work\921 Graphics\Fig5-15_Geologic Mapping Rose Diagram.ai

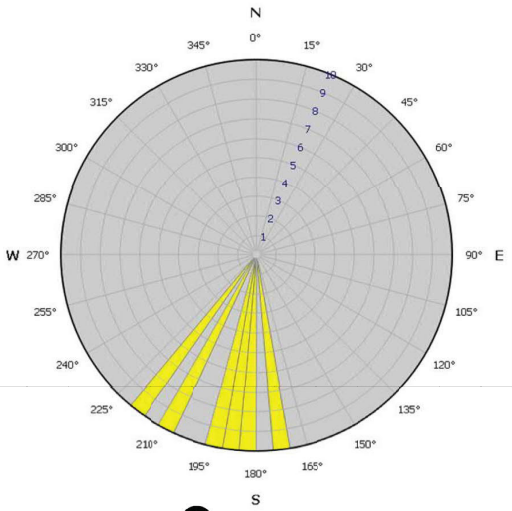

Quarry

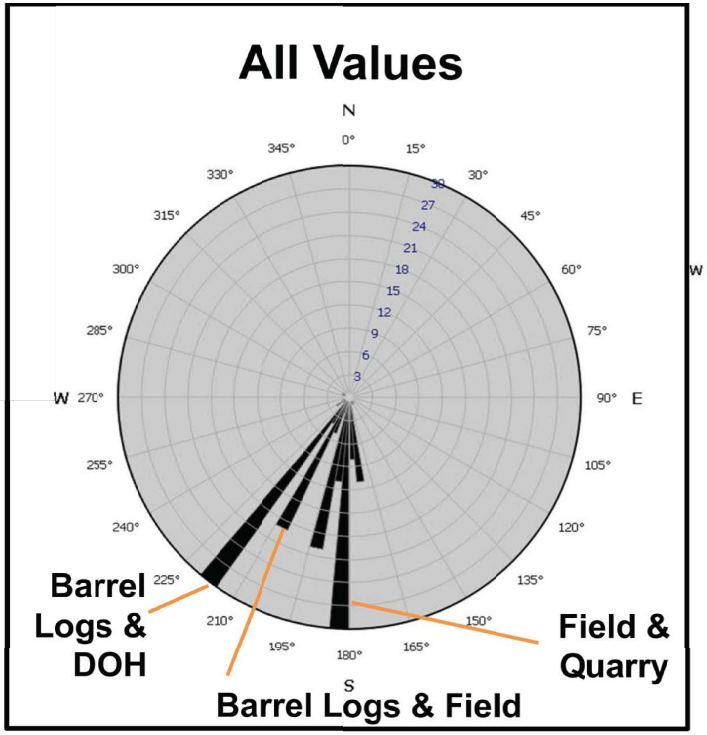

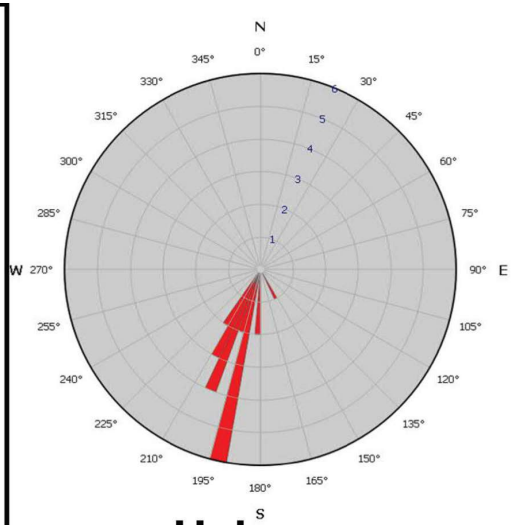

Halawa

Moanalua Tunnel

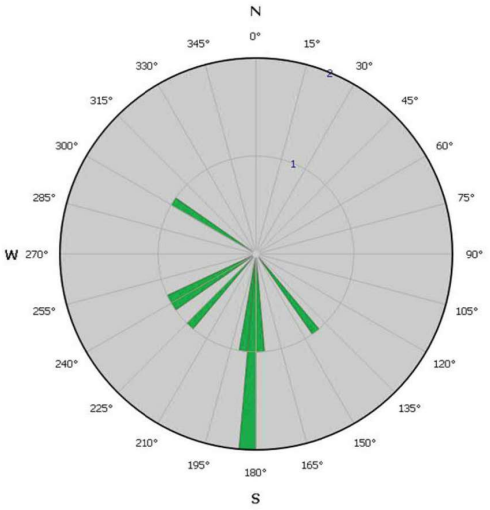

- All field measurements (Halawa, Moanalua, Moanalua Tunnel) (N = 39): 1 pt
- Common Plane measurements (Quarry) (N = 6): 10 pts
- Common Plane (Moanalua) (N = 9): 3 pts
- Barrel logs
  - Clinker (N = 1): 5 pts
  - Kriging (N = 1): 5 pts
  - Lower Beds Tanks 9-16 (N = 1) : 3 pts
- DOH 217˚, 3˚ dip magnitude (N = 1): 10 pts

Average azimuth: 197.4˚; average dip: 6.5˚

Moanalua

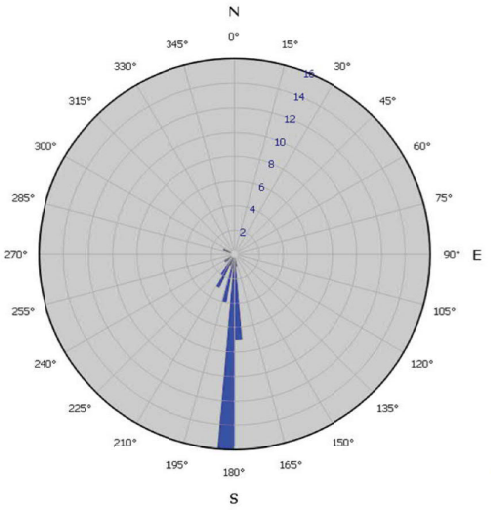

Figure 5-15
Geologic Mapping Rose Diagram
Investigation and Remediation of Releases and Groundwater Protection and Evaluation
Red Hill Bulk Fuel Storage Facility
JBPHH, Oʻahu, Hawaiʻi

This page intentionally left blank

S:\Projects\NAVFAC PAC\CLEAN V\60571032_CTO18F0126\900-Work\921 Graphics\Fig5-16_Gaussian Mixture_Histogram.ai

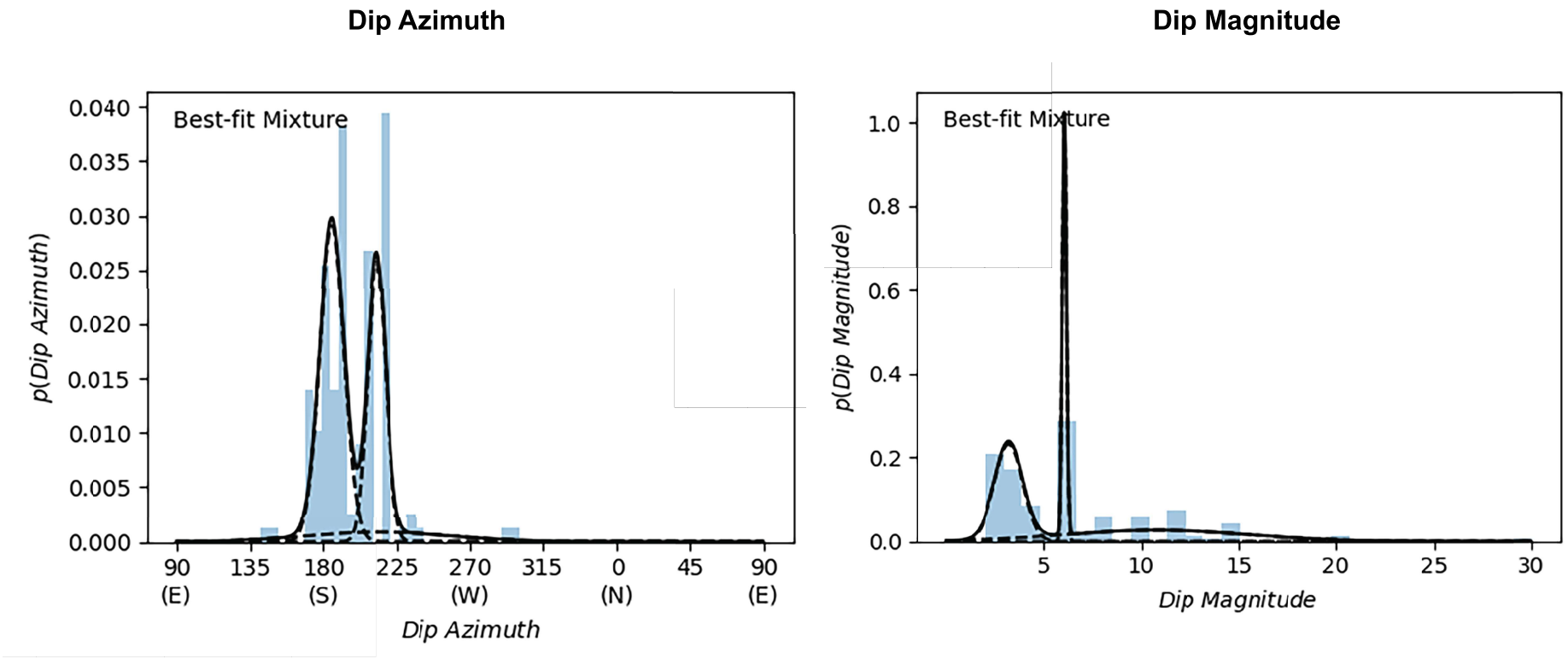

- 3-component solution
- Large peaks at 184.6° and 213.6°
- Smaller peak at 200.5°

- 3-component solution
- Large peaks at 2.9° and 213.6°
- Large peak with no variance at 5.9°
- Smaller peak at 11.2°

Figure 5-16
Gaussian Mixture Model - Histograms of Dip Azimuth and Dip Magnitude
Investigation and Remediation of Releases and Groundwater Protection and Evaluation
Red Hill Bulk Fuel Storage Facility
JBPHH, Oʻahu, Hawaiʻi

This page intentionally left blank

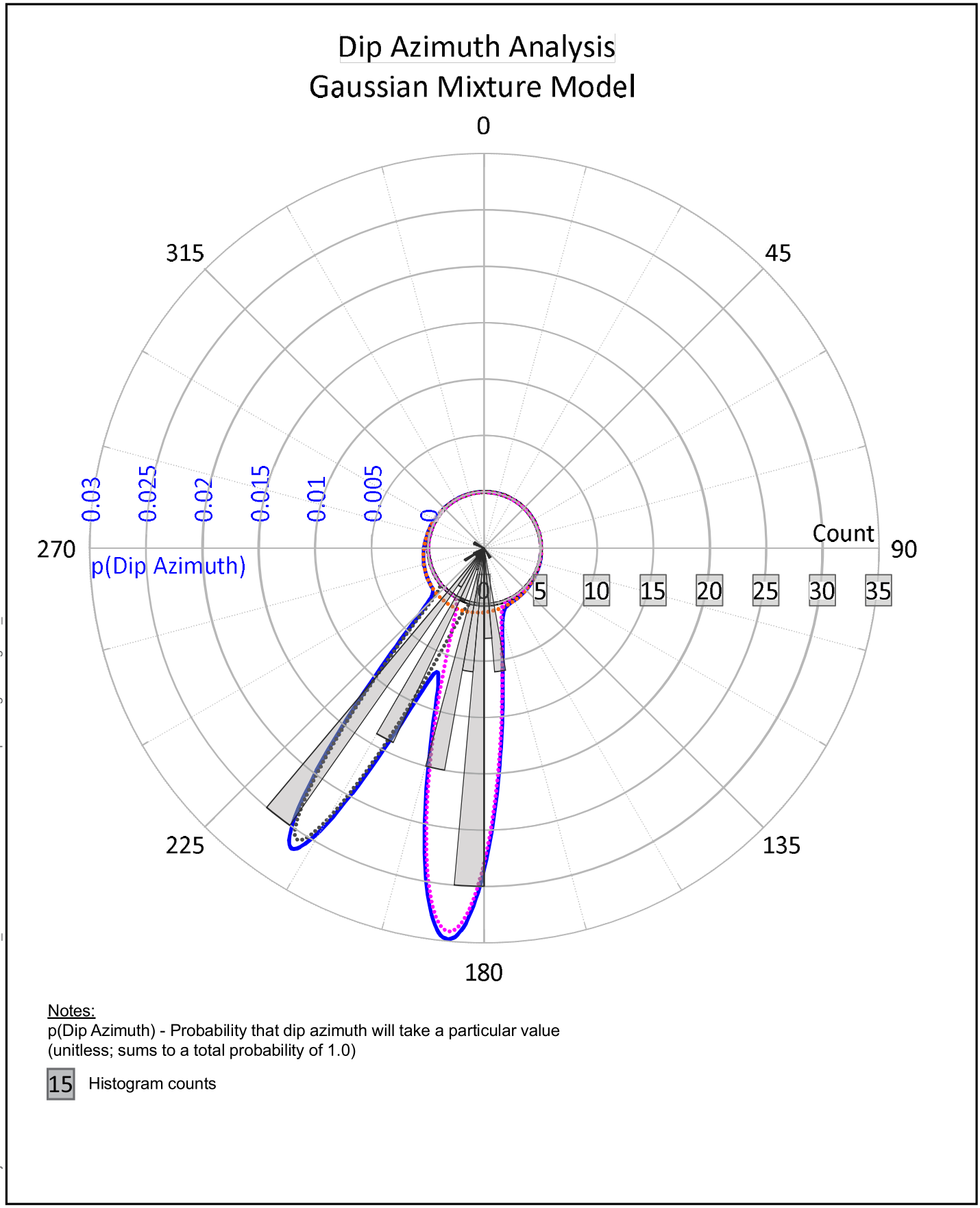

Notes:
p(Dip Azimuth) - Probability that dip azimuth will take a particular value (unitless; sums to a total probability of 1.0)

15 Histogram counts

S:\Projects\NAVFAC PAC\CLEAN V\60571032_CTO18F0126\900-Work\921 Graphics\Fig5-13\Fig5-17_Polar Plot.ai

Figure 5-17
Polar Plot of Gaussian Mixture Modeling
Conceptual Site Model Rev. 01
Investigation and Remediation of Releases and Groundwater Protection and Evaluation
Red Hill Bulk Fuel Storage Facility
JBPHH, O‘ahu, Hawai‘i

This page intentionally left blank

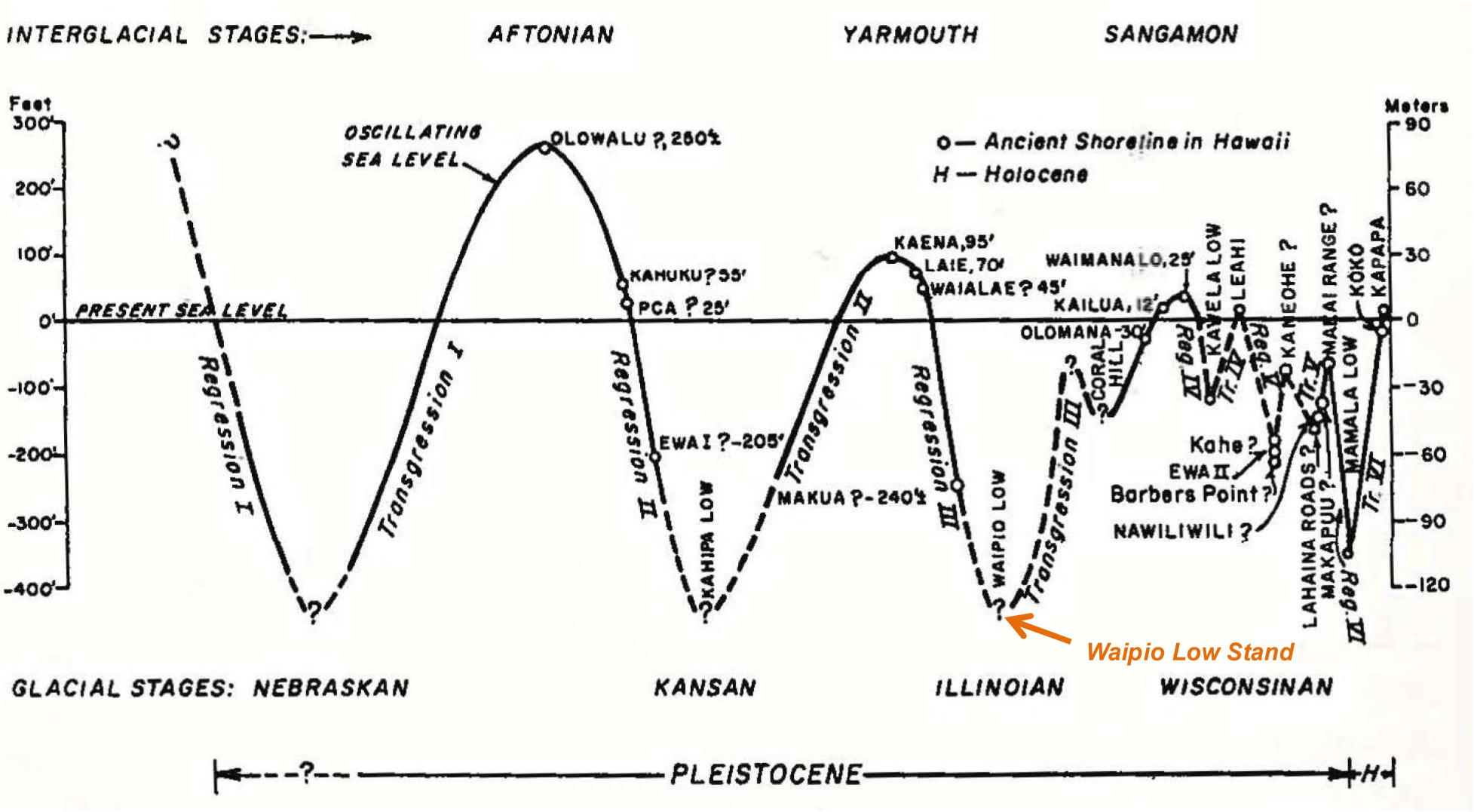

Source: Stearns (1978 Figure 1). The Waipio low stand of the sea was minus 350± feet and lasted long enough for deep erosion along major streams. It correlates with the Illinoian glacial period, about 500,000 years before present, Pleistocene age. **The drop in sea level lasted long enough for all major streams to cut their channels to levels well below present sea level along the coasts**." Stearns (1978)
Note: Sherrod et al. (2007) has mapped (after the original mapping by Stearns) the valley fill deposits as 'Older Alluvium.'

Figure 5-18
Glacioeustatic Fluctuations of Sea Level and Hawaiian Pleistocene Shorelines
Conceptual Site Model Rev. 01
Investigation and Remediation of Releases and Groundwater Protection and Evaluation
Red Hill Bulk Fuel Storage Facility, JBPHH, O'ahu, Hawai'i

This page intentionally left blank

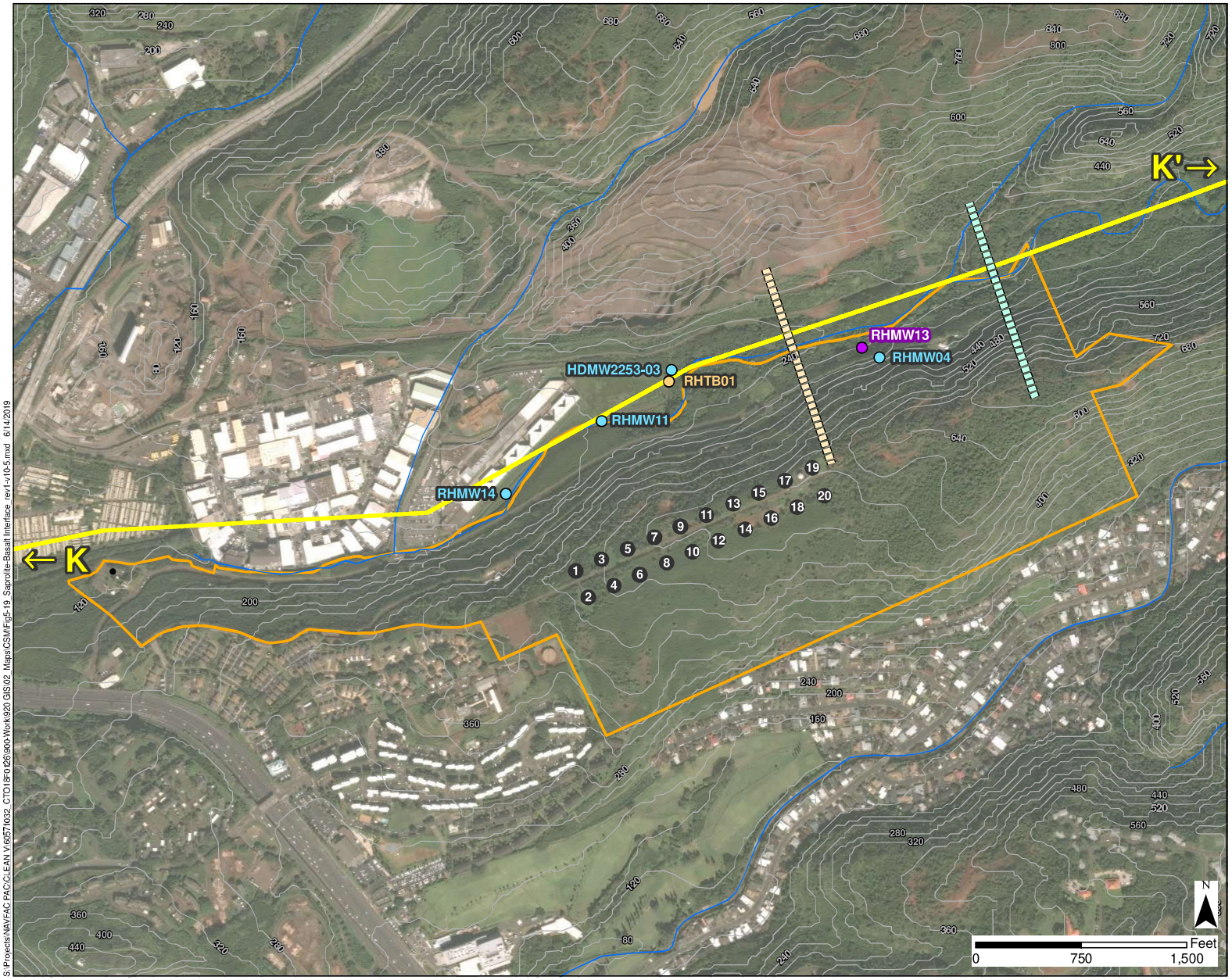

Location Map

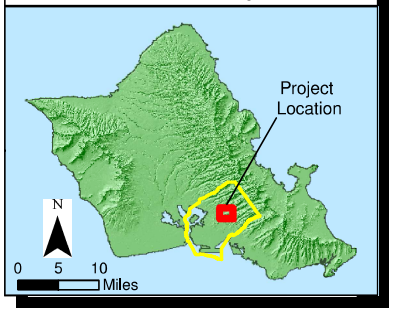

Legend

Where saprolite/basalt interface crosses water table using a 3% slope projected upvalley from:

- -5 ft msl at HDMW2253-003
- -55 ft msl at HDMW2253-003
- K-K' South Hālawa Valley Geologic Cross Section (see Appendix E)
- Existing Monitoring Well
- Proposed Monitoring Well
- Test Boring
- Stream
- Topographic Contour (feet mean sea level)
- Red Hill Facility Boundary
- Red Hill Fuel Storage Tank
- Groundwater Model Domain

Notes

1. Map projection: NAD 1983 Hawaii State Plane Zone 3 feet
2. Base Map: DigitalGlobe, Inc. (DG) and NRCS. Publication_Date: 2015
3. Coordinates: NAD 1983 UTM Zone 4N
4. Saprolite/basalt interface slope of 3% based on Oki 2005; -5 ft msl and -55 ft msl are relative to HDMW2253-003.

Figure 5-19
Saprolite/Basalt Interface
Conceptual Site Model Rev. 01
Investigation and Remediation of Releases and Groundwater Protection and Evaluation
Red Hill Bulk Fuel Storage Facility
JBPHH, O'ahu, Hawai'i

S:\Projects\NAVFAC PAC\CLEAN V\60571032_CTO16F01\26\900-Work\920 GIS\02_Maps\CSM\Fig5-19_Saprolite-Basalt Interface _rev1-v10-5.mxd 6/14/2019

This page intentionally left blank

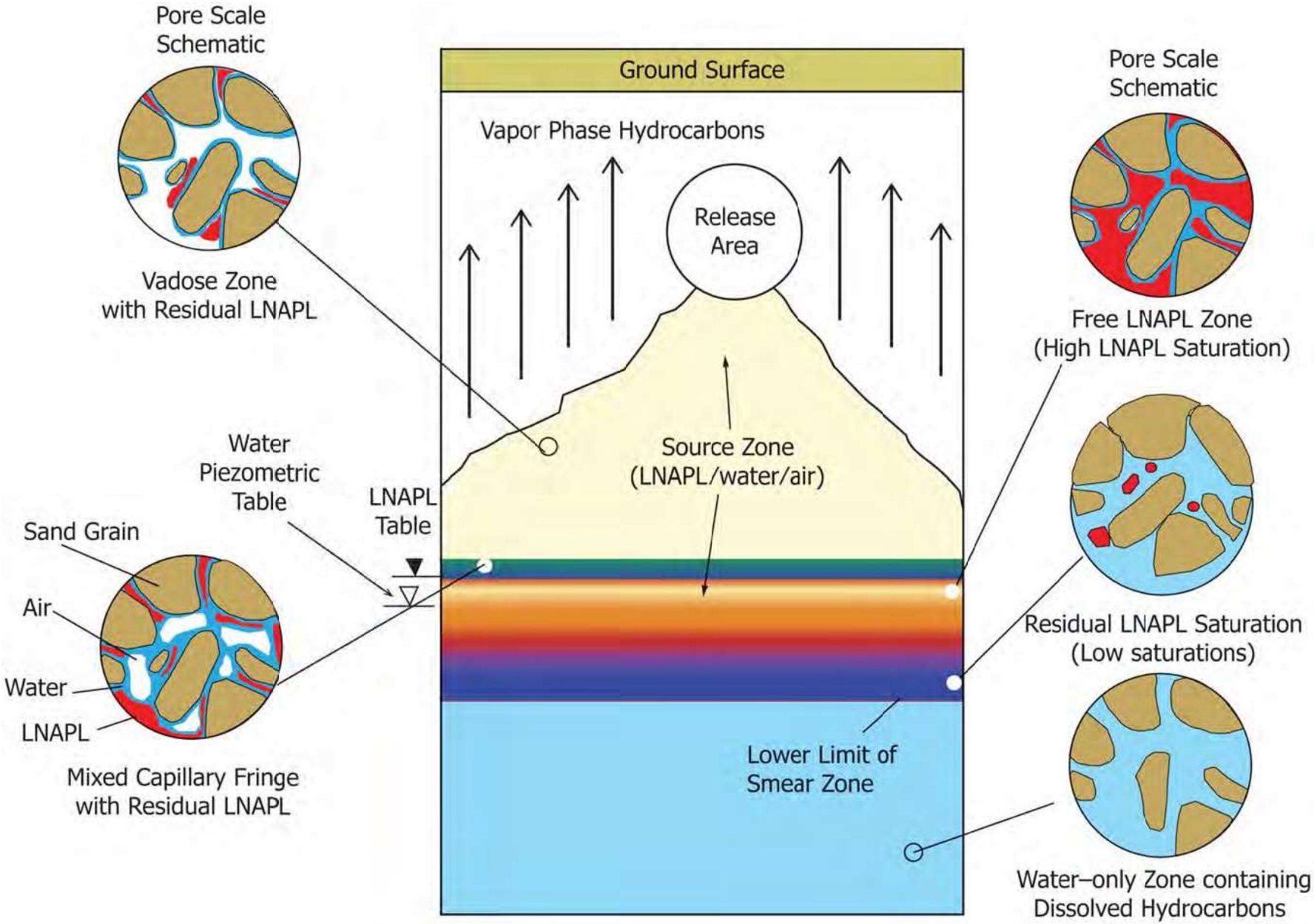

NOTE 1—During the early stages of an LNAPL release, LNAPL can be mobile (free) in all zones.
NOTE 2—The schematic is intended to convey generalized zones, not the dynamics of an active LNAPL release.

LPANL= light non-aqueous-phase liquid
COC = chemical of concern
(From Huntley and Beckett 2002)

Source: ASTM (2014b)

Figure 5-20
Micro-Scale LNAPL Vadose Zone Mobility and Retention
Conceptual Site Model Rev. 01
Investigation and Remediation of Releases and Groundwater Protection and Evaluation
Red Hill Bulk Fuel Storage Facility
JBPHH, O'ahu, Hawai'i

Copyright ASTM International
Provided by IHS under license with ASTM
No reproduction or networking permitted without license from IHS
Licensee=AECOM EW & Canada/5906698006; 04/24/2017 19:54:08 MDT

This page intentionally left blank

Thin bedded pāhoehoe flows are predominant in the lower section at Red Hill.

Photo 5-1
Local Geology – Pāhoehoe Flows
Conceptual Site Model Rev. 01
Investigation and Remediation of Releases and Groundwater Protection and Evaluation
Red Hill Bulk Fuel Storage Facility, JBPHH, O'ahu, Hawai'i

This page intentionally left blank

Erosion of the less-resistant beds, such as a‘ā clinker, has resulted in undercutting of the more resistant massive a‘ā and pāhoehoe layers.

Photo 5-2
Local Geology – Pāhoehoe Flows
Conceptual Site Model Rev. 01
Investigation and Remediation of Releases and Groundwater Protection and Evaluation
Red Hill Bulk Fuel Storage Facility, JBPHH, O'ahu, Hawai'i

This page intentionally left blank

Thinner bedded pāhoehoe flows are overlain by thicker, more resistant aʻā flows.

Photo 5-3
Local Geology – Pāhoehoe Flows
Conceptual Site Model Rev. 01
Investigation and Remediation of Releases and Groundwater Protection and Evaluation
Red Hill Bulk Fuel Storage Facility, JBPHH, O'ahu, Hawai'i

This page intentionally left blank

Base of aʻā lava flow

aʻā lava flows are characterized by an interior or core of solid, dense, massive rock with exterior top and bottom coarse rubble or clinker zones. Clinker zones are similar to layers of coarse well-sorted gravel, where layered sequences of flows can result in widespread beds with high horizontal permeability. The smaller effective porosity of massive aʻā cores can result in extremely low vertical permeability. The principal vertical permeability of a massive aʻā core is imparted by wide, regularly spaced cooling joints, which are typically low-permeability features.

Massive core and top of aʻā lava flow

Photo 5-4
Local Geology – Aʻā Permeability
Conceptual Site Model Rev. 01
Investigation and Remediation of Releases and Groundwater Protection and Evaluation
Red Hill Bulk Fuel Storage Facility, JBPHH, O'ahu, Hawai'i

This page intentionally left blank

Approximately 60% of aʻā clinker is weathered and of relatively low permeability at Red Hill.

Photo 5-5
Local Geology – Weathered Aʻā Clinker
Conceptual Site Model Rev. 01
Investigation and Remediation of Releases and Groundwater Protection and Evaluation
Red Hill Bulk Fuel Storage Facility, JBPHH, O'ahu, Hawai'i

This page intentionally left blank

Saprolite outcrops in several locations on the ridge at Red Hill.

Photo 5-6
Local Geology – Saprolite
Conceptual Site Model Rev. 01
Investigation and Remediation of Releases and Groundwater Protection and Evaluation
Red Hill Bulk Fuel Storage Facility, JBPHH, O'ahu, Hawai'i

This page intentionally left blank

6. Module E: Saturated Zone

The hydrogeologic CSM provides a framework for assessing the hydrogeology of the Facility and surrounding area, and for evaluating the feasibility of investigation methodologies and potential remedial alternatives. To evaluate potential COPC migration in groundwater, the CSM describes groundwater conditions in the Facility area as well as the surrounding areas that may be potentially impacted from fuel releases and includes water supply wells and shafts. Accordingly, the CSM provides the conceptual hydrogeologic basis for the numerical groundwater modeling. Specific hydrogeologic information needed for site characterization and modeling includes:

- Hydrogeologic unit (HGU) characteristics:
  - Basalt (including zones of weathered basalt/saprolite), Caprock and Valley Fill HGU geometry, and hydraulic properties
  - Perched/elevated groundwater zone areas, genesis, and potential effects on contaminant migration
  - Geologic structures that may affect groundwater flow
  - Preferential pathways for groundwater flow (e.g., a'ā clinker and lava tubes)
- Hydraulic heads, gradients, and groundwater flow:
  - Synoptic monitoring data to evaluate pumping and non-pumping conditions
  - Time-series hydrographs and potentiometric maps
  - External factors such as seasonal changes, barometric pressure fluctuations, ocean tides, earth tides, recharge at model boundary, and direct rainfall recharge
- Water balance for groundwater model domain:
  - Groundwater flow rates (mass flux rates) along each model boundary
  - Groundwater recharge and discharge locations and rates
  - Pumping well/shaft locations, construction, and withdrawal rates

The following subsections describe the hydrogeologic CSM based on currently available data. The HGU characteristics are detailed in Section 5.

6.1 Previous Groundwater Levels and Recently Collected Hydrogeologic Data

Although useful information was provided by previous groundwater studies for the Facility, there is some uncertainty in the groundwater levels and hydraulic gradients in the site vicinity (due to extremely flat gradients and measurement error), as detailed in the *Existing Data Report* (DON 2017b) and *Data Gap Analysis Report* (DON 2017d). Resolving this uncertainty is an important objective of the site investigations now underway and the recent 2017–2018 synoptic monitoring. The following discussion is based on the data currently available. This section discusses previously collected data and data collected as part of the current investigation including:

- Aquifer pumping tests and synoptic water level studies
- Water levels measured during quarterly sampling events
- 2017 high-precision survey of water level measuring point elevations

- 2017 gyroscopic survey
- 2017 seismic survey

These data are evaluated collectively and are used to better understand the groundwater flow conditions in and around the site.

6.1.1 May 2006 Regional Aquifer Pumping Test

A regional groundwater aquifer pumping test conducted in May 2006 (DON 2007) showed that pumping of Red Hill Shaft (Navy Supply Well 2254-01) for approximately 1 week at above-average rates (approximately [redacted]) lowered groundwater elevations substantially near the pumping well and created a hydraulic capture zone along the RHS water development tunnel. This pumping increased the generally gentle southwesterly gradient in the Facility area, but no response was noted in the Hālawa Deep Monitor Well (HDMW2253-03) located approximately 3,700 ft northeast from Red Hill Shaft. However, HDMW2253-03 is a deep open borehole that is used to monitor the freshwater / saltwater interface in the area, and this well may not respond in a manner similar to shallow water table wells in the vicinity. Other wells monitored near the Facility did show a clear hydraulic response to pumping of Red Hill Shaft. Additional discussion of the 2006 regional groundwater aquifer pumping test is presented in Sections 6.1.9 and 6.3.6.

During this test, the highest pumping rates reported for Red Hill Shaft approached [redacted] for several periods as long as 1 day. During those periods, the largest drawdown measured at Red Hill Shaft was approximately 7 ft (DON 2007). Due to the construction of these types of tunnel wells (including both Red Hill and Hālawa Shaft), drawdown in the pools or wet wells (which are fed by water infiltration tunnels) may not be indicative of actual drawdown or heads in the aquifer. This must be considered during evaluation of data. In addition to traditional methods of aquifer testing evaluation, analysis of synoptic pumping using analytical methods, which represent line sinks, will also be considered.

6.1.2 Quarterly Groundwater Monitoring

Monitoring began in June 2008, with quarterly or monthly measurements of depth to groundwater in wells RHMW01 through RHMW03. Monitoring wells RHMW04, RHMW05, OWDFMW01, HDMW2253-03 and sampling point RHMW2254-01 were subsequently added to the groundwater monitoring program. Data from the more recently installed wells are available beginning in October 2014 for RHMW06 and RHMW07, October 2016 for RHMW08 and RHMW09, May 2017 for RHMW10, and December 2017 for the new multilevel well RHMW11. Farther away from the Facility, water levels in other wells in the model domain have also been measured at various times by other agencies, including USGS and BWS.

Time-series graphs of groundwater levels (hydrographs) for select Red Hill monitoring network wells are provided on Figure 6-1 and Figure 6-2, which show temporal fluctuations attributable to seasonal variations in recharge rates and pumping of large water supply wells/shafts. Of particular interest are the plots showing the water levels in RHMW07 relative to those in other monitoring wells because the RHMW07 levels initially seemed to be unusually high. However, resurveying of all the wellhead measurement points has verified the accuracy of the data. Now that a sufficient period of monitoring data is available, it is clear the RHMW07 data reflect similar fluctuations over seasonal time scales, and therefore, RHMW07 appears to be hydraulically connected with the basal aquifer over long-term cycles (Figure 6-1 and Figure 6-2). But as discussed later, RHMW07 did not respond to short-term 2017–2018 synoptic monitoring pumping or recovery as did the other Red Hill area wells. RHMW07 also had a different barometric response than the other Red Hill area wells.

Groundwater levels at RHMW07 are higher than at wells further south in the Facility area. As evidenced by barometric responses and water level responses during the 2017–2018 synoptic water monitoring period, there may be attenuated hydraulic communication between this well and the basal aquifer in which the surrounding Red Hill monitoring wells are completed.

Groundwater elevations in HDMW2253-03 do not represent water table conditions because this well is constructed as an open borehole that extends deep below the freshwater lens. HDMW2253-03 was purposely constructed with an open zone from 250 to 1,575 ft bgs to monitor the depth and thickness of the saltwater/freshwater transition zone. Water levels in HDMW2253-03 are typically a few tenths of a foot higher than the "chase tube" completed with an open pipe in the annular space between the inner casing and the borehole, at an elevation approximately equal to the regional basal aquifer water level. Also, as described in Section 6.4, the water in the deep monitoring well is saltier than in the surrounding groundwater. These factors indicate that deeper, saltier groundwater may be rising up through HDMW2253-03 and mixing/discharging into the fresh basal aquifer.

6.1.3 November 2016 Synoptic Monitoring

In November 2016, wells in the primary area of interest were measured during a synoptic monitoring event by the USGS and the Navy (Oki 2017). Red Hill Shaft had been shut down in February 2016 due to mechanical problems, and through November 2016, only occasional, very limited-duration pumping was reported by the Navy. Thus, these synoptic data reflect non-to-minimal-pumping conditions for Red Hill Shaft, while Hālawa Shaft pumping continued at relatively low operational rates, typical for November (likely related to lower seasonal customer demand).

6.1.4 Recently Collected Hydrogeologic Data

New multilevel monitoring well RHMW11 was drilled and constructed in late 2017 in accordance with the Red Hill *Monitoring Well Installation Work Plan* (DON 2016b). At the well location, low-permeability saprolite, which consists of clay-rich materials and weathered basalt, extends to a depth of approximately 87 ft below the regional basal groundwater table (as recorded at the time of drilling). RHMW11 was completed with eight discrete monitoring intervals (also referred to as zones) that are independently sealed and isolated using a series of Westbay System packers (as illustrated on Figure 6-3). The well is constructed with Zone 1 as the deepest zone, each subsequent zone completed at a shallower depth, and Zone 8 as the uppermost or shallowest zone (DON 2018b).

The five deeper sampling intervals (Zone 1 through Zone 5) in RHMW11 are completed in unweathered basalt below the shallower saprolite. Hydraulic head measurements in those zones are approximately 18–19 ft msl (Figure 6-4). The hydraulic head data from RHMW11 generally show a pronounced downward hydraulic gradient, which is much stronger downward within the saprolite zone than in the unweathered basalt aquifer. The upper three sampling intervals (Zone 6 through Zone 8) show there is a continuously saturated zone within the saprolite (Figure 6-4). Potentiometric head data have been obtained from RHMW11 that show the potentiometric surface in the upper saprolite is actually much higher than previously estimated at that location. When water levels were first recorded in December 2017, Zones 6, 7, and 8 had water level elevations of 35.51, 58.21, and 88.59 ft msl, respectively, indicating that these zones were not in hydraulic equilibrium with their surroundings at that time. As of January 2019, the water levels in Zones 6, 7, and 8 were measured at 57.06, 65.37, and 114.35 ft msl, respectively. By monitoring the water levels in these three upper zones and comparing them to synoptic water levels (Section 6.2.4) measured at monitoring well UMW-1, it was determined that these zones came into hydraulic equilibrium between October 2018 and January 2019. UMW-1 is a shallow monitoring well located at the Hālawa Correctional Facility that was installed as part of a previous investigation (Unitek 1988) and is screened in the valley fill alluvium overlying saprolite at that location. Water level elevations from RHMW11 are presented in Table 6-1.

Table 6-1: RHMW11 Westbay Zone and Water Level Elevation Summary

Zone Identifier	Zone Top (ft bgs)	Zone Bottom (ft bgs)	Zone Top (elevation ft msl)	Zone Bottom (elevation ft msl)	Generalized Geology	Zone Water Level (elevation ft msl)
Zone 8	159.3	204.5	51.06	5.86	Saprolite	114.35
Zone 7	209.8	239.8	0.56	-29.44	Saprolite	65.37
Zone 6	245.0	255.5	-34.64	-45.14	Saprolite	57.06
Zone 5	277.3	290.3	-66.94	-79.94	Basalt	19.91
Zone 4	330.5	342.8	-120.14	-132.44	Basalt	19.85
Zone 3	347.8	367.0	-137.44	-156.64	Basalt	19.62
Zone 2	394.0	420.3	-183.64	-209.94	Basalt	19.52
Zone 1	450.3	469.5	-239.94	-259.14	Basalt	19.22

Notes: Approximate land surface elevation = 210.36 ft msl.
Piezometric heads reported in zones measured on 1/28/2019 during the First Quarter 2019 quarterly groundwater monitoring (DON 2019).

The saprolite zone encountered at RHMW11 creates a barrier to groundwater and LNAPL flow because of the lower hydraulic conductivity of the clayey weathered basalt material and higher piezometric heads, as also evidenced by seismic refraction and reflection profiles obtained in the valley as discussed in Section 6.1.8 (DON 2018c). Pneumatic testing of select zones in RHMW11, including Zones 6, 7, and 8, was conducted following well construction (DON 2018b). Pneumatic test data from RHMW11 Zones 6, 7, and 8 approximated slug withdrawal tests and were analyzed using three different techniques (Hvorslev 1951; Bouwer and Rice 1976; Cooper, Bredehoeft, and Papadopulos 1967). Tests in Zones 6, 7, and 8, as well as laboratory analysis of cores collected during drilling from the borehole in Zone 8, show that the hydraulic conductivity of saprolite and weathered basalt in the upper three sampling intervals is very low compared to unweathered basalt (see Table 6-2). The subsurface extent of this saprolite barrier away from RHMW11 and the seismic transects is not well known. However, this saprolite zone most likely formed beneath a deeply incised paleo-valley below the present-day South Hālawa Stream. Thus, the deep saprolite zone of RHMW11 likely trends generally east to west, which is consistent with the geologic log of HDMW2253-03 that also shows deep weathered basalt (saprolite) extending to a roughly similar depth (-5 ft msl or -55 ft msl depending on interpretation) as at RHMW11. Recharge rates are higher in the upslope areas of the Ko'olau Mountains, where precipitation rates increase and low-permeability saprolite layers over the basalt are absent or thin.

Table 6-2: RHMW11 Hydraulic Conductivity Estimates Derived from Pneumatic Testing and Laboratory Analyses

Pneumatic Test Results

Slug Test Zone	K (Hvorslev 1951) ft/d	K (Hvorslev 1951) cm/s	K (Bouwer and Rice 1976) ft/d	K (Bouwer and Rice 1976) cm/s	K (Cooper, Bredehoeft, and Papadopulos 1967) ft/d	K (Cooper, Bredehoeft, and Papadopulos 1967) cm/s	Date	Zone Geology / Feature
Zone 8	9.2E-02	3.2E-05	1.0E-01	3.5E-05	7.1E-02	2.5E-05	12/13/2017	Saprolite
Zone 7	1.2E-01	4.2E-05	1.3E-01	4.6E-05	1.1E-01	3.8E-05	12/9/2017	Saprolitic clinker zone
Zone 7	2.6E-01	9.2E-05	2.8E-01	9.9E-05	2.7E-01	9.7E-05	12/11/2017	Saprolitic clinker zone
Zone 6	3.4E-01	1.2E-04	2.8E-01	9.9E-05	1.7E-01	6.0E-05	12/7/2017	Saprolite
Zone 5	—	—	—	—	—	—	—	Lava tube
Zone 4	—	—	—	—	—	—	—	Pāhoehoe
Zone 3	—	—	—	—	—	—	—	Pāhoehoe
Zone 2	—	—	—	—	—	—	—	Clinker zone
Zone 1	—	—	—	—	—	—	—	Clinker zone
Minimum	*9.2E-02*	*3.2E-05*	*1.0E-01*	*3.5E-05*	*7.1E-02*	*2.5E-05*		
Maximum	*3.4E-01*	*1.2E-04*	*2.8E-01*	*9.9E-05*	*2.7E-01*	*9.7E-05*		

RHMW11 Laboratory Test Results

Tested Zone	Core Depth (ft bgs)	K (ft/d)	K (cm/s)	Sample ID	Zone Geology / Feature
Zone 8	162.6–163.6	2·49E-05	8.8E-09	ERH443B-V	Saprolite
Zone 8	162.6–163.6	2·21E-05	7.8E-09	ERH443B-H	Saprolite
Zone 8	174.3–175.0	1.26E-05	4.5E-09	ERH443C-V	Saprolite
Zone 8	174.3–175.0	1.57E-05	5.5E-09	ERH443C-V	Saprolite
Zone 8	189.5–190.0	8.50E-05	3.00E-08	ERH443D-V	Saprolite
Zone 8	189.5–190.0	7.99E-06	2.82E-09	ERH443D-H	Saprolite
	Minimum	*7.99E-06*	*2.8E-09*		
	Maximum	*8.50E-05*	*3.0E-08*		

— no data; slug test data from these intervals could not be evaluated due to high hydraulic conductivity of the basalt.
cm/s centimeters per second
K hydraulic conductivity

Based on the existence of the saprolite in the upper three zones at RHMW11, it is concluded that the unweathered basalt basal aquifer beneath the saprolite is under confining conditions. While the majority of the monitoring wells within the Red Hill monitoring network appear to be in unconfined conditions, there are a few notable exceptions in addition to RHMW11. These exceptions are:

- RHMW07
- OWDFMW01
- Hālawa Deep Monitor Well (2253-03)

Wells completed in neighboring valleys (e.g., Moanalua) may also be completed in confined conditions beneath saprolite, but there are few data to support a definitive conclusion. Wells completed in the caprock closer to the coast may also be in confined conditions but are not the principle focus of this analysis.

Other wells have uncertain completion, impacting the quality of data collected, and therefore, it is difficult to draw conclusions from their associated data. These wells include:

- Moanalua DH43: Based on a 2014 video survey of this well (Juturna LLC 2014), it is constructed with 2-inch pipe. At 244 ft bgs, the camera was stopped by an obstruction immediately below the pipe. Based on a sounding of the well with a water level probe, it was approximately 276 ft deep from the top of the 2-inch pipe. It is unknown if the lower 32 ft of the well is open hole or cased. No screen or slots were observed in the pipe.
- HDMW2253-03 Chase Tube: This well was installed inside the annular space between the drilled borehole and the well casing of Hālawa Deep Monitor Well. The Well Completion Report (CWRM 2001) indicates that the monitor tube extends to a depth of 210 ft bgs and is slotted in the last 10 ft. However, since the as-built conditions of the monitor tube were not confirmed, a video survey was conducted in 2014 (Juturna LLC 2014). At the time of the survey, water was encountered at a depth of approximately 208 ft below the top of pipe. The video shows that the 2-inch pipe actually extended to a depth of approximately 237 ft. The camera would not extend beyond that depth. Therefore, it is unknown what existed below that. No well screen or slots were observed in the video.

6.1.5 2017 High-Precision Well Survey

At least four wellhead surveys have been conducted for the Red Hill monitoring wells at different times. In addition, the measuring (or reference) points used over the years to determine water elevations may have changed for individual wells, and there may be differences in measuring points used by various investigators. Results of the high-precision survey conducted in summer–fall 2017 address this issue for subsequent monitoring (DON 2018a, 2018e). However, past groundwater elevations should be used with caution when evaluating absolute groundwater elevations, although they may be appropriate for evaluating shorter-term trends.

6.1.6 Gyroscopic Corrections

Well gyroscopic field surveys, 3D modeling of gyroscopic data, and evaluation of gyroscopic data were conducted to determine how the wells deviate from true vertical and to calculate correction factors that can be applied to groundwater level measurements for true vertical depths. As depicted on Figure 10.66 in Driscoll (1986), wells are typically neither perfectly plumb nor perfectly aligned. Assessment of the plumbness and alignment of each well is required to determine the degree to which a well's apparent depth deviates from its actual depth (vertical distance along a plumb line from the surface). Because the hydraulic conductivity of the regional basal aquifer in the Red Hill area is so high, a nearly horizontal and flat groundwater surface is manifest. Since groundwater flows from high to low hydraulic head as influenced by hydraulic conductivity distributions/orientations, highly accurate water level elevations are needed to develop an understanding of local and regional gradients. The following wells are evaluated in this CSM: RHMW02 through RHMW10, HDMW2253-03, OWDFMW01, and RHMW11 (multilevel well). The calculated correction factors (Table 6-3) were provided to USGS on May 1, 2018 (DON 2018d). The tape correction factors are applied to measured groundwater depths to correct them to true vertical depths. The correction factors for all wells except RHMW09 are less than 0.1 ft. The USGS used the results of the high-precision survey and gyroscopic corrections in the water level elevations on the National Water Information System (NWIS) website for the 2017–2018 synoptic monitoring. No tape corrections were made to other wells.

Table 6-3: Summary of Gyroscopic Survey Results and Calculated Tape Correction Factors

Well ID	Survey Y (State Plane Zone 3 NAD 1983 ft) [a]	Survey X (State Plane Zone 3 NAD 1983 ft) [a]	Survey Top of Casing (Z) (ft msl) [a]	Inside Diameter of Well (inches) [b]	Measured Depth to Water with Tape from Top of Casing (ft bgs) [c]	3D Model of Vertical Plumb Depth (ft bgs)	Tape Correction Factor (ft) [d]
RHMW02	74282.05	1675639.24	104.60	1.94	84.96	85.48	-0.06
RHMW03	74610.90	1676391.37	120.90	1.94	101.22	101.74	-0.04
RHMW04	75742.78	1677345.53	312.11	3.83	81.66	293.01	-0.02
RHMW05	73690.63	1674268.20	101.31	1.93	81.80	82.17	-0.01
RHMW06	75327.62	1676274.46	259.09	3.81	239.57	240.27	-0.01
RHMW07	74964.68	1675189.75	220.39	3.81	196.99	197.57	-0.01
RHMW08	74257.02	1674635.42	310.43	3.81	290.98	291.60	-0.03
RHMW09	73527.70	1675221.52	395.37	3.81	375.99	376.49	-0.24
RHMW10	74066.93	1676410.03	495.59	3.81	476.15	476.36	-0.09
HDMW2253-03	75654.10	1675867.45	226.68	8.00	205.81	206.79	-0.01
OWDFMW01	74112.72	1671997.20	138.14	3.81	118.85	119.04	-0.03
RHMW11 (multilevel) Zones 1–5	75290.37	1675370.69	211.26	1.40	—	191.28	-0.09
RHMW11 (multilevel) Zone 6	75290.37	1675370.69	211.26	1.40	—	139.19	-0.07
RHMW11 (multilevel) Zone 7	75290.37	1675370.69	211.26	1.40	—	135.97	-0.07
RHMW11 (multilevel) Zone 8	75290.37	1675370.69	211.26	1.40	—	107.08	-0.05

— no data

NAD North American Datum

[a] Source: *Well Elevation Survey Report, Red Hill Bulk Fuel Storage Facility, Joint Base Pearl Harbor-Hickam, O'ahu, Hawai'i*; and *Well Elevation Surveys for Red Hill Monitoring Well RHMW11 and Navy 'Aiea Halawa Shaft 2255-032, Honolulu, O'ahu, Hawai'i* (DON 2018a, 2018e)

[b] Source: Monitoring well construction logs

[c] Source: *Final First Quarter 2019 - Quarterly Groundwater Monitoring Report* (DON 2019) and recently collected field data for RHMW11

[d] Source: *Technical Memorandum, Gyroscopic Survey Results and Calculated Correction Factors for Groundwater Monitoring Network Wells at the Red Hill Bulk Fuel Storage Facility, Joint Base Pearl Harbor-Hickam, O'ahu, Hawai'i* (DON 2018d)

6.1.7 2017–2018 Synoptic Monitoring

From July 2017 through March 2018, depth to water in wells in the primary area of interest were measured during a synoptic monitoring event by the USGS, BWS, and Navy. The *Final Synoptic Water Level Study Work Plan* dated August 10, 2017 from the USGS lays out this program (USGS 2017e). The purpose of the continuous water-level monitoring was to provide data that will lead to an improved understanding of the groundwater flow system in the Hālawa area. Groundwater levels were monitored in 23 wells to document spatial and temporal variations in groundwater levels under typical and controlled withdrawal conditions. An attempt was made to coordinate controlled withdrawal conditions designed to provide data that can be used to interpret the short-term, aquifer-wide response of the aquifer to withdrawals. However, the USGS could not mandate specific withdrawal conditions because overriding water-purveyor constraints related to meeting water demand limited the water-purveyors' ability to maintain the exact planned rates of withdrawal. Most groundwater-level data collected as part of this effort were made publicly available online through the NWIS database. Groundwater levels were monitored for multiple months in 23 wells in the Hālawa, Moanalua, and

'Aiea areas. Data were recorded at 10-minute intervals. Details of the monitoring plan are provided below.

The pumping scenarios were as follows:

1. Withdrawing water from Moanalua Wells 1, 2, and 3 at a high rate while both Hālawa Shaft and Red Hill Shaft withdrew water at typical rates.
2. Allowing Red Hill Shaft to recover for approximately 5 days while Hālawa Shaft pumped at a near constant rate.
3. Withdrawing water from Red Hill Shaft at a nearly steady rate for approximately 4.5 days while Hālawa Shaft withdrew water at a typical and near-constant rate.
4. Allowing Hālawa Shaft to recover for approximately 10 days while Red Hill Shaft was pumping under normal operational conditions (on and off in response to water system demands).
5. Withdrawing water from Hālawa Shaft at a high rate for 10 days while Red Hill Shaft was pumping under normal operational conditions.
6. Withdrawing water from Hālawa Shaft at a normal rate while Red Hill Shaft was pumping under normal operational conditions.

Groundwater levels were monitored in 23 existing wells in the Red Hill groundwater flow model domain. The 23 wells include two wells that are actively being monitored for groundwater levels by BWS using shaft encoders. Near the end of the synoptic monitoring period, transducers were also installed in a shallow monitoring well (UMW-1) at the Hālawa Correctional Facility. This well is completed and screened within valley fill alluvium perched above saprolite. Monitoring in RHMW11 consisted of Westbay pressure transducers in all eight zones, and a vented pressure transducer in the Westbay center tube with pumping port 8 open from January 12 to February 23, 2018, and with pumping port 5 open from August 10, 2018 to January 2019, monitored by the USGS. Based on the *Final Synoptic Water Level Study Work Plan* (USGS 2017e), the USGS issued a draft report documenting the data collected during the monitoring period. The non-interpretive report was provided to SMEs for comment (2-week comment period) and followed the standard USGS review, approval, and publication process. The final report was published in 2018 (Mitchell and Oki 2018).

The well and transducer information is summarized in Table 6-4.

Table 6-4: Well and Transducer Information

DLNR ID	USGS Site ID	Well ID	Transducer
3-2153-05	212123157535501	Moanalua Deep	700H vented
3-2153-13	212144157534701	TAMC-MW2	700H vented
3-2253-02	212225157533001	Moanalua DH43	700H vented
3-2253-03	212241157535502	HDMW2253-03Chase Tube	700H vented
3-2253-03	212241157535501	HDMW2253-03 (Hālawa Deep Monitor Well)	700H vented
3-2253-04	212226157534101	RHMW06	700H vented
3-2253-05	212222157535201	RHMW07	700H vented
3-2254-01	212225157542601	Red Hill Shaft	700H vented (2 transducers)
3-2254-02M	212229157541501	UMW-1	700H vented
3-2255-32	212253157554301	'Aiea Hālawa Shaft	700H vented

DLNR ID	USGS Site ID	Well ID	Transducer
3-2255-40	212233157552302	Hālawa BWS Deep Monitor	700H vented
3-2256-10	212238157561101	'Aiea Navy	700H vented
3-2354-01	212305157542601	Hālawa Shaft	700H vented
3-2355-15	212340157552301	Ka'amilo Deep	700H vented
—	212214157542601	OWDFMW01	700H vented
—	212214157535401	RHMW01	700 non-vented
—	212216157534701	RHMW02	700H vented
—	212219157533901	RHMW03	700H vented
—	212231157532901	RHMW04	700H vented
—	212210157540201	RHMW05	700H vented
—	212216157535801	RHMW08	700H vented
—	212209157535201	RHMW09	700H vented
—	212213157533901	RHMW10	700H vented
3-2253-11	212226157535001	RHMW–1 - Zone 8 [a]	700H vented
3-2253-11	212226157535001	RHMW–1 - Zone 8	nonvented MOSDAX
3-2253-11	212226157535001	RHMW–1 - Zone 7	nonvented MOSDAX
3-2253-11	212226157535001	RHMW–1 - Zone 6	nonvented MOSDAX
3-2253-11	212226157535001	RHMW–1 - Zone 5 [a]	700H vented
3-2253-11	212226157535001	RHMW–1 - Zone 5	nonvented MOSDAX
3-2253-11	212226157535001	RHMW–1 - Zone 4	nonvented MOSDAX
3-2253-11	212226157535001	RHMW–1 - Zone 3	nonvented MOSDAX
3-2253-11	212226157535001	RHMW–1 - Zone 2	nonvented MOSDAX
3-2253-11	212226157535001	RHMW–1 - Zone 1	nonvented MOSDAX
2255-033	—	Hālawa T-45	shaft encoder
2153-009	—	Manaiki T24	shaft encoder
2-2153-10	—	Moanalua 1	—
3-2153-11	—	Moanalua 2	—
3-2153-12	—	Moanalua 3	—
3-2153-07	—	TAMC1	—
3-2153-08	—	TAMC2	—

— no data available or not applicable
[a] USGS installed a 700H vented transducer to monitor Zone 8 from January 12 to February 23, 2018, and a 700H vented transducer to monitor Zone 5 from August 10, 2018 through January 2019.

Data from the transducers were evaluated by the USGS, and those that did not meet their acceptance criteria were not released in the final approved data set. Unfortunately, the data from both the primary and backup transducers in Red Hill Shaft did not meet USGS acceptance criteria during the period of recovery and pump testing of Red Hill Shaft, and therefore, no data are available from the shaft for that period.

6.1.8 2017 Seismic Profiling Survey

Nine seismic profiles were acquired in the Red Hill area over 9 days in December 2017 (DON 2018c). The objectives were to map stratigraphy and hydrogeologic boundaries beneath three valleys: North Hālawa Valley (Transects A, B, and C); South Hālawa Valley (Transects D, E, F, and G); and Moanalua Valley (Transects H and I). Seismic data quality was generally very good with: (1) clear first arrivals needed to obtain shallow seismic velocity distributions and (2) observable reflections noted between surface wave and seismic refraction signals to map large-contrast subsurface

boundaries. Seismic refraction results constrain seismic velocities for the upper 100 ft and tie those velocities to nearby well logs and to other published results from Hawai'i to help constrain travel time to depth conversions for the seismic reflection results. Seismic reflection results show the geometry and depth to key hydrostratigraphic boundaries within the upper 1,000 ft below land surface. Key reflectors include the base of alluvium or top of saprolite, top of water saturated (possibly perched) sediments, and the contact between highly weathered basalt (saprolite) and unweathered basalt.

Valley fill sediments are constrained to the upper ~60 ft below land surface in all three valleys. Saturated and/or competent saprolite is mapped from the surface to hundreds of feet bgs. Those conceptualizations are consistent with V- and/or U-shaped saprolite base geometries across the valleys, with the maximum saprolite thickness below surface stream flow locations. The saprolite base extends to hundreds of feet below sea level in portions of North and South Hālawa Valleys. The depth to the base of the saprolite was constrained by only one short profile beneath Moanalua Valley. The depth to these key hydrostratigraphic boundaries in South Hālawa Valley is generally consistent with lithologic logs from nearby monitoring wells. The seismic profiles could not detect the geometry or depth of the regional basal water table, in part due to shallow and confined perched water systems and the lack of large physical property contrasts (seismic velocity and density) at this basal water system boundary. The seismic profiles also do not constrain volcanic stratigraphy (e.g., individual volcanic flows, lava tubes) beneath the top of unweathered basalt unit due to complexities in the seismic wavefield within this layered basalt system.

The Red Hill seismic survey yielded information on key hydrostratigraphic boundaries in the valleys. The seismic velocity and reflection results from this study allow definition of four hydrostratigraphic units. Seismic velocities that are consistent with dry alluvium, as measured by seismic velocities less than 1,000 meters per second (m/s), extend up to 60 ft deep in all three valleys. These shallow alluvial sediments overlie saprolite, as defined by velocities between 1,000 and 1,500 m/s. The thickness of dry saprolite layer ranges from 0 to 100 ft thick. With increasing depth and rock density, saprolite increases in seismic velocity to greater than 1,500 m/s. Also, with saturation, seismic velocities in both alluvium and saprolite exceed 1,500 m/s. These zones extend in depth for a few hundred feet beneath portions of all three valleys. Unaltered basalts exceed a seismic velocity of 3,000 m/s. These velocities are observed along the valley margins and at depth beneath each valley. The highly weathered volcanic rocks extend to approximately 300 ft below sea level beneath portions of North Hālawa and South Hālawa valleys. The depth and saprolite base geometry is less constrained beneath Moanalua Valley. The greatest depth to saprolite base is consistent with the surface expression of the streams that drain the valleys. These transects and interpretations were used to refine the CSM. As described in Section 5, the seismic velocity assumptions used for this analysis are in general correlation with the HART boring data.

6.1.9 TFN/Pair-Wise Analysis

The water level at a monitoring well changes with time responding to fluctuations in hydraulic stresses due to groundwater extraction, barometric pressure, tidal influences, recharge, and regional head changes. Selected 2017–2018 synoptic monitoring data were analyzed using transfer function-noise (TFN) modeling to address the following specific objectives:

- Estimation of the unit step-response functions (i.e., the transient drawdown responses caused by unit pumping) associated with different monitoring wells and pumping from Red Hill Shaft and Hālawa Shaft individually for direct use as numerical groundwater model calibration targets
- Estimation of the individual contributions of major hydraulic stress changes to the monitored water level changes

- Estimation of equivalent regional-scale hydrogeologic parameters for comparison with results from other aquifer test data analyses
- Estimation of the magnitude of the water level fluctuations that are not accounted for by the potential hydraulic stresses considered by TFN modeling (i.e., the residual)

TFN modeling is a well-established technique for estimating the source-response relationship of a linear system using time series data (e.g., Box and Jenkins 1970). It has been applied to many disciplines, including hydrology (e.g., Asmuth and Knotters 2004).

The TFN analysis was performed based on an hourly time step size. Details are presented in Appendix H. The time series data were aggregated based on hourly averaging. The sources of hydraulic stresses initially considered included (1) groundwater extraction from Red Hill Shaft, Hālawa Shaft, 'Aiea Hālawa Shaft, and Moanalua Wells; (2) barometric pressure; (3) rainfall; (4) ocean tide; and (5) earth tide. Exploratory data analyses (EDA) were first performed to examine the characteristics of the time series of the water levels in the monitoring wells. The characteristics examined included the power density spectra, auto-correlation functions, cross-correction functions, and signature/patterns. The EDA results indicated that:

- The effect of the groundwater extraction at 'Aiea Hālawa Shaft and Moanalua Wells on the water levels at the monitoring wells is negligible.
- The ocean tide and earth tide time series are highly correlated with similar frequency characteristics.
- Using an hourly time step size is reasonable since the predominant frequencies of variations are lower than approximately two cycles per day.
- The correlation between the water levels at the monitoring wells and daily rainfall is low. The correlation with weekly averaged rainfall is also low. The correlation with 30-day-averaged rainfall slightly increased. However, the magnitude of influence of the 30-day-averaged rainfall on the residual signal was insignificant.

Therefore, the TFN analysis included the hydraulic stresses due to groundwater extractions from Red Hill Shaft and Hālawa Shaft, barometric pressure, tidal influence, and rainfall. The earth tide time series was selected as the surrogate representing the tidal influence. The 30-day-averaged rainfall was initially included as a source for consistency with the duration of the synoptic data period considered.

An exploratory TFN analysis was performed to compute the transfer function empirically from data. The shapes of the empirically derived transfer functions resemble the analytical drawdown response solution based on Hantush (1956). Subsequently, the TFN analysis was performed using a Hantush (1956) functional form to represent the transfer functions. The actual locations of the pumping shafts and monitoring wells were used to calculate the distance used in the Hantush equation. In a heterogeneous and anisotropic aquifer, a monitoring well responds to pumping from a shaft as if the pumping is from an image location in an equivalent homogeneous and isotropic aquifer. It is analogous to an underwater object appearing to be shallower when it is viewed from above water. Therefore, in the final TFN analysis, the equivalent image location of the pumping center associated with each shaft was estimated by optimization to further improve TFN calibration to the observed water level time series. The optimized distances are generally less than 10 percent different from the actual geographical distance. In addition, the results of the preliminary analysis showed that the contribution from the 30-day-averaged rainfall is negligibly small, suggesting that there was no significant contribution from direct rainfall recharge in the vicinity of the monitoring well during the analysis period. The rainfall effect likely occurred at a timescale much longer than 30 days, as delayed and

extended response to recharge from upgradient regions. Therefore, the final TFN analysis was performed without the 30-day-averaged rainfall.

The TFN analysis was applied to monitoring well data that show responses to Red Hill Shaft and Hālawa Shaft pumping. As an example, Figure 6-5 shows the results from TFN analysis of the water level data at monitoring well RHMW08 for the Red Hill Shaft shutdown/restart period and the Hālawa Shaft shutdown/restart period, respectively. The simulated water level responses closely match the observed water level responses. The contribution of Hālawa Shaft pumping to the water level changes during the Red Hill Shaft shutdown/restart period is small because the Hālawa Shaft pumping rate was steady. The time series plot of TFN residuals do not show correlation with shaft pumping, barometric pressure, or tidal fluctuations. Rather, the TFN residuals are likely attributable to seasonal and background fluctuations caused by rainfall recharge in distal upgradient areas.

Figure 6-6 shows the observed and TFN model-simulated differences between the water levels at monitoring wells RHMW05 and RHMW10. The TFN simulated drawdown difference in the monitoring wells is in good agreement with the observed drawdown difference. Figure 6-7 shows several examples of the unit step response functions associated with Red Hill Shaft pumping for use as numerical model calibration targets. The observed differential head time series do not show a trend, suggesting that the residuals from the TFN analysis for the selected wells are similar when Red Hill Shaft is off or on. Therefore, the impacts due to ambient fluctuations are spatially uniform, and the induced differential head is small. Differential head is dominated by the pumping influence of Red Hill Shaft.

The TFN analysis was also applied to the water level data collected from Red Hill Shaft and Hālawa Shaft. In addition to the step response function based on Hantush (1956), a zero-lag (i.e., instantaneous response) term was added. The results indicated that ratios of the zero-lag terms to the total long-term drawdowns are approximately 2–4 percent for Red Hill Shaft and Hālawa Shaft. As an example, Figure 6-8 shows the TFN results for Red Hill Shaft.

The equivalent regional-scale, homogeneous, and isotropic parameters (Hantush 1956) associated with the step response functions at different monitoring wells for Red Hill Shaft and Hālawa Shaft pumping are summarized in Table 6-5. Monitoring well RHMW07 was excluded from the analysis since it responds primarily to barometric pressure.

In summary, the TFN analysis provided (1) insight into aquifer response to multiple stresses occurring at different frequencies and magnitudes, (2) estimation of equivalent regional-scale aquifer hydraulic properties, and (3) well-specific step- and impulse-response functions that will be used for groundwater model calibration.

Table 6-5: Equivalent Regional-Scale Aquifer Hydraulic Properties for Step Response Functions at Red Hill Monitoring Wells with Red Hill Shaft and Hālawa Shaft Pumping

	Red Hill Shaft Pumping		Hālawa Shaft Pumping	
Monitoring Well	Equivalent Transmissivity (ft^2/d)	Equivalent Storativity	Equivalent Transmissivity (ft^2/d)	Equivalent Storativity
OWDFMW01	513,000	0.10	1,670,000	0.14
RHMW01	565,000	0.07	1,470,000	0.08
RHMW02	521,000	0.04	1,520,000	0.08
RHMW03	532,000	0.02	1,430,000	0.08
RHMW04	548,000	0.03	1,080,000	0.10
RHMW05	550,000	0.18	1,620,000	0.06
RHMW06	580,000	0.02	1,430,000	0.08
RHMW08	548,000	0.05	1,610,000	0.05
RHMW09	553,000	0.05	1,650,000	0.07
RHMW10	520,000	0.02	1,710,000	0.08
RHMW11 Z1	667,000	0.04	1,390,000	0.09
RHMW11 Z2	756,000	0.05	641,000	0.11
RHMW11 Z3	652,000	0.05	1,300,000	0.14
RHMW11 Z4	784,000	0.04	627,000	0.14
RHMW11 Z5	810,000	0.04	1,270,000	0.15

ft^2/d square feet per day

6.2 GROUNDWATER FLOW DIRECTIONS

Groundwater levels near the Facility are strongly influenced by local heterogeneities and the pumping rates and locations of large-capacity supply wells, as indicated by the results of three regional pumping tests conducted in May 2006, May 2015, and July 2017 through March 2018. Notwithstanding the local heterogeneities, in a larger sense, groundwater flow follows the regional flow patterns.

6.2.1 May 2006 Pumping Test

The results from the regional groundwater pumping test of Red Hill Shaft conducted in May 2006 did not indicate any hydraulic response in HDMW2253-03, located on the northern edge of South Hālawa Valley, during pumping of Red Hill Shaft (DON 2007); however, monitoring points in that area were sparse. Conversely, wells monitored near the Facility did show a clear hydraulic response to pumping of Red Hill Shaft. Even though data points were sparse to the north of the Facility, the evaluation of the May 2006 pumping test suggested that a groundwater barrier may exist beneath South Hālawa Valley (DON 2007).

In 2010, the Navy re-evaluated the groundwater level measurements from May 2006 (DON 2007) to prepare revised water table potentiometric maps for the site area for pumping and non-pumping conditions (DON 2010). Those data show that when the Navy was operating Red Hill Shaft at normal capacity (pumping approximately [redacted]), the principal hydraulic gradient was toward the southwest from the tank farm area toward Red Hill Shaft. The report also suggested the hydraulic gradient from the area just north of the Facility may be toward the west-northwest (DON 2010). The report also indicated the southwesterly gradient was approximately 0.00022 foot per foot (ft/ft), and the northwesterly gradient appeared to be less.

6.2.2 May 2015 Pumping Test

During May 2015, the USGS and BWS conducted a pumping test of Hālawa Shaft while monitoring water level elevations in a number of monitoring wells. These wells included Hālawa T-45, OWDFMW01, RHMW04, RHMW07, Moanalua DH43, TAMC-MW2, and Moanalua Deep. Pumping rates at Hālawa Shaft and Red Hill Shaft during May 2015 and time-series plots of water level data available from monitoring wells are shown on Figure 6-9.

For the May 2015 test, pumping of BWS Hālawa Shaft was suspended during the period May 8–13, 2015. Subsequently, Hālawa Shaft was pumped at a much higher rate, approximately 14 mgd, for the period May 14–20, 2015. The pumping rate decreased starting on May 21 to approximately 8–9 mgd, then decreased to approximately 6 mgd during May 23–28. Red Hill Shaft pumping rates varied substantially on a daily basis throughout May 2015, as shown on Figure 6-10.

Variations in pumping rates at Hālawa Shaft and Red Hill Shaft during the May 2015 pumping test tend to complicate and obscure relationships between pumping rates and the measured drawdowns. Data were not collected from RHMW01, RHMW02, RHMW03, RHMW05, and RHMW06 in the Red Hill area, nor from Ka'amilo Deep, 'Aiea Navy, or Hālawa BWS Deep Monitor. Both of these limitations create uncertainty in evaluating the available data. Nonetheless, the following observations were made related to data collected during the May 2015 pumping test:

- Groundwater levels fluctuated daily by small amounts (approximately 0.1 ft) in both Red Hill monitoring wells located adjacent to South Hālawa Valley (RHMW04 and RHMW07).
- There appear to be water level fluctuations attributable to barometric pressure changes at both RHMW04 and RHMW07. However, other factors may also cause such minor fluctuations, such as transducer properties and electronic/strain gauge drift.
- The largest groundwater level increase during this period was about 0.35 ft (RHMW04), when the pumping rate at Hālawa Shaft stopped during May 7–14 and Red Hill Shaft was pumping daily at rates varying from [redacted].
- The largest water level decline was about 0.45 ft (RHMW04) between May 14 and May 21, 2015 when Hālawa Shaft was pumping the maximum rate of approximately 14 mgd and Red Hill Shaft was pumping daily at rates varying from [redacted].

Overall, the data from the May 2015 pumping test indicate that pumping both these water supply sources (Hālawa Shaft and Red Hill Shaft) affect groundwater levels in the South Hālawa Valley area. These water level changes were relatively small in magnitude.

6.2.3 November 2016 Synoptic Monitoring

Observations related to water level elevations calculated for this synoptic monitoring event are consistent with observations for other similar monitoring events. The absence of steep gradients at the site and near the vicinity is consistent with the presence of very high hydraulic conductivity zones in the regional basal aquifer. With the exception of wells RHMW07, HDMW2253-03, and DH43, the data reflect a very low hydraulic gradient along and in the vicinity of Red Hill ridge (RHMW01 through RHMW05 and OWDFMW01) with groundwater elevations of approximately 19 ft msl with slightly lower elevations immediately to the north (RHMW06 and RHMW08) and south (RHMW09) of the tank farm. The groundwater elevations decrease to the west toward Pearl Harbor to approximately 17 ft msl. Because pumping from Red Hill Shaft had been minimal in the preceding months, this distribution of hydraulic heads at the site represents a minimally stressed system. However, in the absence of strong gradients, the groundwater flow direction cannot be determined

with great confidence. Rather, the observation for other events also holds true for this event: hydraulic heads along the ridge are slightly higher than the adjacent flanks.

6.2.4 2017–2018 Synoptic Monitoring

Data from the 2017–2018 synoptic study are published on NWIS. All the wells were monitored with vented (i.e., gauged on differential) transducers except RHMW01, which was too small in diameter to accommodate a vented transducer. Instead, a smaller-diameter non-vented (i.e., absolute or total) transducer was used in RHMW01. The USGS installed a vented transducer in the center tube of RHMW11, which was opened to the Zone 8 pumping port. Separately, non-vented transducers were locked into each of the eight zones intermittently from December 2017 to January 2019. Measurements in these zones are different from all the other wells because the other wells are open to atmosphere at the top. For the synoptic water level study, the pumping port in either Zone 8 or Zone 5 was open to allow monitoring with a USGS transducer; water level data derived from the Westbay MOSDAX transducer in Zone 8 and in Zone 5 do not represent "shut-in" conditions.

6.2.4.1 Barometric Efficiency and Other Possible Effects

The first step in analyzing the data was to look for effects of barometric pressure, seasonal water level changes, earth tides, ocean tides, precipitation/recharge, and pumping from various wells and shafts. Synoptic data were plotted along with ocean tides, earth tides, streamflow, and precipitation. Visually, the latter three do not appear to correlate with water levels in the Red Hill area wells (near-field) (Figure 6-11).

While the skeletal structure of an aquifer may restrict some of the increase in barometric pressure at the land surface from translating to the water in the aquifer, an open-top well will allow the full increase to load onto the water level inside the well. This will produce an imbalance in pressure. The ratio of the barometric pressure change to the change in water level is termed barometric efficiency. In a confined aquifer, an increase in barometric pressure will typically cause a decrease in water level inside the well. In an unconfined aquifer, there may be a time lag between increased barometric pressure at the surface and a change at the water level. This is primarily governed by hydraulic diffusivity (transmissivity divided by storativity). Other factors that can affect barometric efficiency are well-skin (or clogged well screen) and well-bore storage.

Numerous methods have been developed to determine barometric efficiency. The Kansas Geologic Survey (KGS) Barometric Response Function (BRF) software (Bohling, Jin, and Butler 2011) was used for this study. The KGS BRF software consists of a Microsoft Excel worksheet and a compiled program (executable). The user inputs a set of water level values and corresponding barometric pressure data, from which the software can compute a BRF and subsequently a set of corrected water level values. The KGS BRF software also allows the user to correct for the influence of earth tides.

Because the majority of the transducers in this synoptic study are vented to the atmosphere via a tube, the effects of barometric pressure change do not affect measured pressures. However, the unvented transducers typically do require barometric correction. Barometric pressure was monitored and reported by the USGS at five locations, and the data were input into the KGS BRF software. Passing storm fronts should theoretically result in many series of sub-parallel loops. By convention, a slope of -1.0 for these loops translates to a 100% barometric efficiency in a classic confined aquifer response. While this is not traditionally performed with vented transducers, this analysis was performed for all wells in the synoptic monitoring program.

An enigmatic response is observed in RHMW07 data. Although this well was monitored with a vented transducer, it responded with a relatively high (~70%) efficiency, which is typical of the response seen

in an aquitard or a confined aquifer. There was no observed evidence of a time lag in the water level barometric pressure versus time plots.

One explanation for this type of response could be a plugged vent tube. In the May 2015 pumping test, there were water level fluctuations at both RHMW04 and RHMW07 potentially attributable to barometric pressure changes. In 2015, the barometric effects appeared to be larger at RHMW07 than at RHMW04; however, other yet-unexplained factors may have caused these fluctuations.

Following the evaluation of barometric efficiency, synoptic data were plotted against ocean tides. Ocean tide data were recorded at the NOAA tide gauge 1612340, which is the active station located closest to the area of interest. Most of the wells appear to be tidally influenced. A tidal response was not observed in Ka'amilo Deep, Hālawa Deep Monitor Well (HDMW2253-03), or the HDMW2253-03 Chase Tube. This is likely due to well construction (open vertical holes) and distance from the shoreline. Most wells saw a typical time lag between a change in ocean tides and a change at the water level, with wells located farther onshore experiencing a longer delay before water levels were impacted.

After determining that barometric pressure and ocean tides both had some influence on the synoptic data, the KGS BRF software (Bohling, Jin, and Butler 2011) was used to remove the barometric pressure and ocean tidal influence from the synoptic data. For this study, ocean tides were used in place of earth tides. Barometric pressure recorded in Red Hill Shaft and ocean tide data from NOAA tide gauge 1612340 were input into the software to compute a BRF for each set of water levels in the synoptic monitoring program. The BRF for each well was then used to calculate a corrected set of synoptic data.

6.2.4.2 CORRECTED WATER LEVEL DATA

BRF corrected water levels were plotted for five different periods listed below, as shown on Figure 6-12:

- Time 1 – Red Hill Shaft off for ~5 days, Hālawa Shaft average pumping (0600 January 15, 2018)
- Time 2 – Red Hill Shaft on steady for ~4 days, Hālawa Shaft average pumping (2110 January 19, 2018)
- Time 3 – Red Hill Shaft business as usual, Hālawa Shaft off (1900 February 5, 2018)
- Time 4 – Red Hill Shaft business as usual, Hālawa Shaft maximum pumping (0500 February 16, 2018)
- Time 5 – Red Hill Shaft business as usual, Hālawa Shaft average pumping (1300 February 18, 2018)

Groundwater elevations (corrected for barometric and tidal fluctuations) for these five times are plotted on Figure 6-13 through Figure 6-17. A description of each period is provided below:

Time 1

Time 1 represents a period when Red Hill Shaft had been offline and water levels had been allowed to recover for approximately 5 days. During this time, Hālawa Shaft was pumping steadily at average rates. On Figure 6-13, groundwater elevations along the ridge of the Facility ranged from 18.66 ft msl at RHMW03, to 18.63 ft at RHMW01 and RHMW02, and to 18.51 ft at OWDFMW01. With the

exception of RHMW07 (22.64 ft), RHMW11 Zones 6 through 8 (71.17–98.77 ft), HDMW2253-03 (19.50 ft), and HDMW2253-03 Chase Tube (19.13), the heads generally decline off the two flanks of the ridge (to the northwest and southeast). In general, water levels are higher to the south in Moanalua Valley (Moanalua DH43, TAMC-MW2 and Moanalua Deep). Water levels shown in the northwest corner of Figure 6-13 range from 15.82 ft at 'Aiea Hālawa Shaft (an active pumping shaft) to 16.77 ft at Hālawa BWS Deep Monitor. While the general water level trend across the entire area is from the south and east toward the northwest, the trends are more complicated around the Facility. This may be a product of well purpose (e.g., water supply, shallow groundwater monitoring, and deep saltwater/freshwater interface monitoring), well construction (e.g., open vertical hole, horizontal shaft, filter-packed and cased), and the density of wells in the Facility area. Water levels gently slope toward the west-southwest along the ridge, but as mentioned above, dip away at the flanks (sub-parallel with surface topography). The water levels in the unweathered basalt in RHMW11 (Zones 1 through 5) comport with the majority of the other Red Hill monitoring wells; however, the water levels in the saprolite zone stand much higher than the regional water levels in the basal aquifer. This suggests a continuously saturated saprolite zone underlying a perched valley fill alluvium aquifer. RHMW07 water levels stand about 4 ft above the others nearby in the basal aquifer. Water levels in HDMW2253-03 and HDMW2253-03 Chase Tube display an upward vertical gradient, possibly indicating that deeper saltier water may be rising up through the long-open-hole monitoring well and discharging to create a mound of saltier water in the fresh basal aquifer. Water levels at the principal production shafts (Red Hill Shaft and Hālawa Shaft) are depicted in green on Figure 6-13. Because of the lengths of the shafts, these levels likely represent a composite of the heads in the aquifer along the length of the open shaft. Water levels measured during pumping often need to consider frictional losses associated with filter pack and screen, but these may not be important in these unlined shafts. Other wells and shafts in the area were potentially pumping during this period; these include 'Aiea Hālawa Shaft, the BWS Moanalua Wells 1, 2, and 3, and Tripler Army Medical Center (TAMC) water supply wells located in the vicinity of Moanalua Elementary School. These may all complicate interpretation of these water levels. Because of the heterogeneities in geology, well depth, and construction, no attempt has been made to contour the water levels. The patterns depicted on Figure 6-13 represent an extremely gentle groundwater gradient, and despite the considerable effort to reduce errors, the remaining residual errors are probably on the order of a few tenths of a foot. Therefore, making further interpretations in the Red Hill area may not provide a better understanding of groundwater conditions in the area.

Time 2

Time 2 represents a period when Red Hill Shaft had been pumping steadily for about 4.5 days at approximately [redacted]. During this time, Hālawa Shaft was pumping steadily at an average rate. On Figure 6-14, groundwater elevations along the ridge of the Facility ranged from 18.22 ft at RHMW03, to 18.17 ft at RHMW02, to 18.14 ft at RHMW01, and to 18.00 ft at OWDFMW01. Again, water levels generally decline off to the flanks of the ridge. The same patterns observed at RHMW07, RHMW11 Zones 6, 7, and 8, and HDMW2253-03 Chase Tube at Time 1 continue in Time 2 (as well as Times 3, 4, and 5). The differences between Time 1 and Time 2 are discussed below.

Head Differences between Time 1 and Time 2

The water levels displayed on Figure 6-18 represent the water level fluctuations observed in response to pumping Red Hill shaft steadily at approximately [redacted] for about 4.5 days. Drawdowns associated with this pumping are also contoured into ovals of approximately equal drawdown for interpretation to be discussed below. The drawdown is greatest in the wells that are nearest to Red Hill Shaft, and drawdown declines away from Red Hill Shaft. The drawdown contours generally describe nearly concentric ovals with the primary orientation approximately northeast to southwest. Not all the indicated fluctuation in wells (especially the distal wells) is thought to be associated with pumping at

Red Hill Shaft, nor are the changes observed in RHMW07, RHMW11 (Zones 6, 7, and 8), or the HDMW2553-03 Chase Tube. Across the rest of the area depicted on Figure 6-18, water levels generally decline on the order of 0.1–-0.2 ft, but this may be due to effects other than the pumping of Red Hill Shaft, and they are within the range of probable error.

Time 3

Time 3 represents a period when Red Hill Shaft was pumping in response to demands and typically turned off and on several times per day. This was termed "business as usual." During this time, Hālawa Shaft had been shut off for approximately 9 days. On Figure 6-15, groundwater elevations along the ridge of the Facility ranged from 18.60 ft at RHMW03, to 18.54 ft at RHMW02, to 18.55 ft at RHMW01, and to 18.36 ft at OWDFMW01. With the exceptions noted in Time 1, the water levels generally decline off the two flanks of the ridge (to the northwest and southeast). In general, water levels are higher to the south in Moanalua Valley (Moanalua DH43, TAMCMW-2, and Moanalua Deep) and lower in the northwest area. Again, while the general water level trend across the entire area depicted on Figure 6-15 is toward the northwest, the trends are more complex around the Facility.

Time 4

Time 4 represents a period when Red Hill Shaft was pumping business as usual. During this time, Hālawa Shaft was pumping steadily at approximately 12 mgd for about 10 days. On Figure 6-16, groundwater elevations along the ridge of the Facility ranged from 18.39 ft at RHMW03, to 18.34 ft at RHMW02, to 18.32 ft at RHMW01, and to 18.14 ft at OWDFMW01. The other general patterns noted above continue in Time 4. Lower water level (12.32 ft) was noted at Hālawa Shaft during this period of heavy pumping. The differences between Time 3 and Time 4 are discussed below.

Head Differences between Time 3 and Time 4

The water levels displayed on Figure 6-19 represent the water level fluctuations observed in response to heavier-than-normal pumping of Hālawa Shaft as compared to Time 3, when this well was offline for several days. Although there is significant drawdown in Hālawa Shaft itself, it is unclear whether the drawdown indicated at Hālawa BWS Deep Monitor, Hālawa T45, OWDFMW01, RHMW01, RHMW02, RHMW03, RHMW04, RHMW06, RHMW08, RHMW09, RHMW10, and the five deeper zones in RHMW11 is due to pumping at Hālawa Shaft or Red Hill Shaft. However, a pattern of nearly concentric ovals is not apparent at the end of Time 4 as it was for the end of Time 2 (Red Hill Shaft pumping). The results are non-unique, and additional analysis will not be pursued.

Time 5

Time 5 represents a period when Red Hill Shaft was pumping business as usual. During this time, Hālawa Shaft was pumping steadily at an average rate. On Figure 6-17, groundwater elevations along the ridge of the Facility ranged from 18.51 ft at RHMW03, to 18.47 ft at RHMW02, to 18.50 ft at RHMW01, and to 18.34 ft at OWDFMW01. The other local and regional trends noted above continued for Time 5.

6.2.4.3 PUMP TEST ANALYSES FOR RED HILL SHAFT PUMPING

Initial analysis of the synoptic data was performed using the Cooper-Jacob (1946) method because of its ease of operation. The Cooper-Jacob approximation to the Theis method is operationally elegant and appropriate at late pumping times, specifically when $(r^2S)/(4Tt)$ is less than 0.05. This analysis was performed for Red Hill pumping (Time 2, discussed in Section 6.2.4.4). The various methodologies used in this study and the resulting aquifer parameters are discussed below.

Cooper-Jacob Approximation to the Theis Method – Drawdown vs. Time

Drawdown was plotted versus the logarithm of pumping time at Red Hill Shaft (or the ratio of time since pumping started divided by time since pumping stopped for recovery) (Figure 6-20 through Figure 6-24). The slopes of these semi-logarithmic lines and the x-intercepts were recorded. These values were then used to calculate transmissivity and storativity using the Cooper-Jacob approximation to the Theis equation (Cooper and Jacob 1946). To convert transmissivity to hydraulic conductivity, it is first necessary to know the aquifer thickness. Because of the depth of the basalt (thousands of feet deep), the high horizontal to vertical anisotropy, and the shallow depths of most wells and shafts, this value would not meet the classic definition of aquifer thickness. Instead, three different values of aquifer thickness are assumed for this conversion. The results from Red Hill Shaft pumping are presented in Table 6-6 and Table 6-7.

For Red Hill Shaft pumping, the Cooper-Jacob criterion (presented earlier in this section, i.e., $[(r^2S)/(4Tt)]$ is generally met. Data from Hālawa Shaft generally did not meet this criterion. Because of the high hydraulic conductivities in the basalt and the relatively modest drawdowns observed in the monitoring wells, the Cooper-Jacob approximation is appropriate due to the flow being essentially horizontal and laminar (non-turbulent). Turbulent losses may, however, need to be considered when evaluating data from the pumping wells themselves.

Theis Solution in Aqtesolv – Drawdown vs. Time

Aqtesolv (Duffield 2007) is an aquifer test software program that allows the user to fit a type-curve to the logarithmic drawdown versus time plot Figure 6-25 to Figure 6-27). For this analysis, the Theis solution was used to compute transmissivity and storativity parameters. For Red Hill Shaft pumping, curve-fitting on logarithmic plots was computed separately, first for recovery and then for drawdown. The analysis was performed this way because the pumps at Red Hill shaft were turned off first (Time 1), allowing water levels to recover, after which the pumps were turned back on (Time 2). The resulting parameters are presented in Table 6-8.

Table 6-6: Summary of Cooper-Jacob Approximation Calculation Components from Red Hill Shaft Pumping

Well ID	Distance to Red Hill Shaft (ft)	Drawdown			Recovery		Comments
		Δs (ft)	t_0 (min)	t_0 (day)	Δs' (ft)	Residual Drawdown	
RHMW01	1,600	0.26	80	0.056	0.17	0	
RHMW02	2,300	0.28	140	0.097	0.16	0	
RHMW03	3,100	0.28	180	0.125	0.17	0	
RHMW04	4,400	0.30	290	0.201	0.16	0	
RHMW05	810	0.26	60	0.042	0.17	0	
RHMW06	3,300	0.26	210	0.146	0.10	0	
RHMW07	2,200	N/A	N/A	N/A	N/A	N/A	No clear trend
RHMW08	1,300	0.30	80	0.056	0.15	0	
RHMW09	1,800	0.28	120	0.083	0.16	0	
RHMW10	3,000	0.23	190	0.132	0.17	0	
RHMW11 Zone 1	2,500	0.23	190	0.132	0.17	0	
RHMW11 Zone 2	2,500	0.23	240	0.167	0.16	0	
RHMW11 Zone 3	2,500	0.22	200	0.139	0.15	0	
RHMW11 Zone 4	2,500	0.23	240	0.167	0.16	0	
RHMW11 Zone 5	2,500	0.23	155	0.108	0.18	0	
RHMW11 Zone 5	2,500	N/A	N/A	N/A	N/A	N/A	No USGS transducer during this period
RHMW11 Zone 6	2,500	N/A	N/A	N/A	N/A	N/A	No clear trend
RHMW11 Zone 7	2,500	N/A	N/A	N/A	N/A	N/A	No clear trend
RHMW11 Zone 8	2,500	N/A	N/A	N/A	N/A	N/A	No clear trend related to pumping, heads rose throughout monitoring period
RHMW11 Zone 8	2,500	N/A	N/A	N/A	N/A	N/A	USGS Transducer. No clear trend, heads rose during pumping
HDMW2253-03	3,100	0.17	600	0.417	N/A	N/A	No apparent recovery trend
HDMW2253-03 Chase Tube	3,100	N/A	N/A	N/A	N/A	N/A	No clear trend
OWDFMW01	1,500	0.30	120	0.083	0.21	0	
Hālawa BWS Deep Monitor	6,400	0.14	1,000	0.694	N/A	N/A	No apparent recovery trend
Ka'amilo Deep	9,900	0.11	800	0.556	N/A	N/A	No apparent recovery trend

Well ID	Distance to Red Hill Shaft (ft)	Drawdown			Recovery		Comments
		Δs (ft)	t_0 (min)	t_0 (day)	$\Delta s'$ (ft)	Residual Drawdown	
TAMC-MW2	3,400	0.19	600	0.417	N/A	N/A	No apparent recovery trend
Moanalua Deep	6,300	0.18	700	0.486	N/A	N/A	No apparent recovery trend
Moanalua DH43	4,800	N/A	N/A	N/A	N/A	N/A	
Hālawa Shaft	4,500	N/A	N/A	N/A	N/A	N/A	Operating production well
ʻAiea Navy	10,600	N/A	N/A	N/A	N/A	N/A	No clear drawdown trend
ʻAiea Hālawa Shaft	8,500	N/A	N/A	N/A	N/A	N/A	Operating production well
Manaiki T24	6,000	0.16	700	0.486	N/A	N/A	No apparent recovery trend
Hālawa T45	7,900	0.11	570	0.396	N/A	N/A	Missing portion of synoptic data set

1 N/A not applicable

Table 6-7: Summary of Cooper-Jacob Approximation Estimates of Transmissivity, Storativity, and Hydraulic Conductivity from Red Hill Shaft Pumping

	Drawdown					Recovery			
Well ID	Transmissivity (ft^2/d)	K (ft/d) - 20 ft	K (ft/d) - 50 ft	K (ft/d) - 100 ft	Storativity	Transmissivity (ft^2/d)	K (ft/d) - 20 ft	K (ft/d) - 50 ft	K (ft/d) - 100 ft
RHMW01	724,000	36,200	14,500	7,240	0.04	520,000	26,000	10,400	5,200
RHMW02	672,000	33,600	13,400	6,720	0.03	552,000	27,600	11,000	5,520
RHMW03	672,000	33,600	13,400	6,720	0.02	520,000	26,000	10,400	5,200
RHMW04	627,000	31,400	12,500	6,270	0.02	552,000	27,600	11,000	5,520
RHMW05	724,000	36,200	14,500	7,240	0.10	520,000	26,000	10,400	5,200
RHMW06	724,000	36,200	14,500	7,240	0.02	883,000	44,200	17,700	8,830
RHMW08	627,000	31,400	12,500	6,270	0.05	589,000	29,500	11,800	5,890
RHMW09	672,000	33,600	13,400	6,720	0.04	552,000	27,600	11,000	5,520
RHMW10	818,000	40,900	16,400	8,180	0.03	520,000	26,000	10,400	5,200
RHMW11 Zone 1	818,000	40,900	16,400	8,180	0.04	589,000	29,500	11,800	5,890
RHMW11 Zone 2	818,000	40,900	16,400	8,180	0.05	552,000	27,600	11,000	5,520
RHMW11 Zone 3	855,000	42,800	17,100	8,550	0.04	589,000	29,500	11,800	5,890
RHMW11 Zone 4	818,000	40,900	16,400	8,180	0.05	552,000	27,600	11,000	5,520
RHMW11 Zone 5	818,000	40,900	16,400	8,180	0.03	491,000	24,600	9,820	4,910
OWDFMW01	627,000	31,400	12,500	6,270	0.05	421,000	21,100	8,420	4,210
TAMC-MW2	990,000	49,500	19,800	9,900	0.08	N/A	N/A	N/A	N/A
Moanalua DH43	649,000	32,500	13,000	6,490	0.06	680,000	34,000	13,600	6,800
HDMW2253-03	1,710,000	85,600	34,200	17,100	0.14	N/A	N/A	N/A	N/A
Hālawa BWS Deep Monitor	1,340,000	67,200	26,900	13,400	0.05	N/A	N/A	N/A	N/A
Ka'amilo Deep	1,710,000	85,600	34,200	17,100	0.02	N/A	N/A	N/A	N/A
Moanalua Deep	1,045,000	52,300	20,900	10,500	0.03	N/A	N/A	N/A	N/A
Manaiki T24	1,180,000	58,800	23,500	11,800	0.04	N/A	N/A	N/A	N/A
Hālawa T45	1,710,000	85,600	34,200	17,100	0.02	N/A	N/A	N/A	N/A

K hydraulic conductivity
N/A not applicable

Table 6-8: Summary of Aqtesolv Approximation Estimates of Transmissivity, Storativity, and Hydraulic Conductivity from Red Hill Shaft Pumping

	Drawdown					Recovery				
Well ID	Transmissivity (ft^2/d)	K (ft/d) - 20 ft	K (ft/d) - 50 ft	K (ft/d) - 100 ft	Storativity	Transmissivity (ft^2/d)	K (ft/d) - 20 ft	K (ft/d) - 50 ft	K (ft/d) - 100 ft	Storativity
RHMW01	615,000	30,800	12,300	6,200	0.04	1,138,000	56,900	22,800	11,400	0.01
RHMW02	596,000	29,800	11,900	6,000	0.04	1,453,000	72,600	29,000	14,500	0.001
RHMW03	607,000	30,400	12,100	6,100	0.02	1,437,000	71,800	28,700	14,400	0.001
RHMW04	527,000	26,400	10,600	5,300	0.03	1,610,000	80,500	32,200	16,100	0.001
RHMW05	590,000	29,500	11,800	5,900	0.14	1,410,000	70,500	28,200	14,100	0.02
RHMW06	678,000	33,900	13,600	6,800	0.02	1,541,000	77,100	30,800	15,400	0.001
RHMW08	613,000	30,600	12,300	6,100	0.05	1,449,000	72,500	29,000	14,500	0.001
RHMW09	618,000	30,900	12,400	6,200	0.05	1,648,000	82,400	33,000	16,500	0.001
RHMW10	577,000	28,800	11,500	5,800	0.02	1,569,600	78,500	31,400	15,700	0.001
RHMW11 Zone 1	824,000	41,200	16,500	8,200	0.05	1,248,000	62,400	25,000	12,500	0.01
RHMW11 Zone 2	734,000	36,700	14,700	7,300	0.06	1,106,000	55,300	22,100	11,100	0.02
RHMW11 Zone 3	685,000	34,300	13,700	6,900	0.06	1,189,000	59,400	23,800	11,900	0.01
RHMW11 Zone 4	805,000	40,200	16,100	8,000	0.06	1,527,000	76,400	30,500	15,300	0.01
RHMW11 Zone 5	787,000	39,400	15,700	7,900	0.05	1,298,000	64,900	26,000	13,000	0.01
OWDFMW01	613,000	30,700	12,300	6,100	0.05	1,367,000	68,400	27,300	13,700	0.002
TAMC-MW2	1,110,000	55,400	22,200	11,100	0.09	1,496,000	74,800	29,900	15,000	0.02
Moanalua DH43	No drawdown response					718,000	35,900	14,400	7,200	0.13
HDMW2253-03	1,600,000	80,000	32,000	16,000	0.09	1,447,000	72,000	30,000	14,500	0.12
Hālawa BWS Deep Monitor	744,000	37,000	14,900	7,400	0.07	2,255,000	113,000	45,100	22,600	0.04
Ka'amilo Deep	1,700,000	85,000	34,000	17,000	0.03	1,209,000	60,400	24,200	12,100	0.03
Moanalua Deep	637,000	31,800	12,700	6,400	0.04	1,568,000	78,400	31,400	15,700	0.03
Manaiki T24	1,480,000	73,800	29,500	14,800	0.06	1,522,000	76,100	30,400	15,200	0.02
Hālawa T45	1,070,000	53,600	21,400	10,700	0.03	Missing water level data for portions of the recovery period				

K hydraulic conductivity

Cooper-Jacob Approximation to the Theis Method – Drawdown vs. Distance

Logarithm of distance versus drawdown (at Time 2) was plotted on a single X:Y scatter plot, and a linear trend was manually fitted (Figure 6-28). Distance of each of these wells was computed from the center of the clinker zones from the last 200 ft of Red Hill Shaft. The slope of this line and x-intercept were recorded and used in the Cooper-Jacob distance-drawdown method, and then the following parameters were calculated:

T 744,000 square feet per day (ft^2/d)

S 0.019

RHMW11 Zones 6, 7, and 8; Moanalua DH43; RHMW07; and HDMW2253-03 Chase Tube are all outliers for this general trend. This suggests that they are all distinct from the other wells completed in the unweathered basalt basal aquifer. This could be due to well construction, fine-grained material (saprolite or valley fill) in the screen interval, and/or hydraulic barriers. The RHMW07 time drawdown plot did not indicate it was responding to pumping of Red Hill Shaft.

Anisotropic Evaluation

Two additional distance-drawdown analyses were performed on the near field wells (RHMW01, RHMW02, RHMW03, RHMW04, RHMW05, RHMW06, RHMW08, RHMW09, RHMW10, RHMW11 Zone 5, and OWDFMW01) to account for anisotropy (Mutch, Jr. 2005; Hantush and Thomas 1966). The oval of equal drawdown, centered on the clinker zone in Red Hill Shaft on Figure 6-18, represents the principal direction of anisotropy. A geographic transformation was applied to the wells, based on the oval's orientation: 62 degrees from north (the same orientation as 242 degrees from north; this is in general agreement with the primary dip azimuth discussed in Appendix C). This was used to calculate the following parameters presented in Table 6-9. The TFN analysis (Section 6.1.9) is more mathematically rigorous than the analytical solutions presented below.

Table 6-9: Summary of Distance vs. Drawdown Estimation of Transmissivity and Storativity, and Derived Hydraulic Conductivity from Red Hill Shaft Pumping

Major Axis				Minor Axis				
Transmis-sivity (ft^2/d)	K (ft/d) - 20 ft	K (ft/d) - 50 ft	K (ft/d) - 100 ft	Transmis-sivity (ft^2/d)	K (ft/d) - 20 ft	K (ft/d) - 50 ft	K (ft/d) - 100 ft	Storativity
Mutch (2005)								
3,837,000	191,850	76,740	38,370	319,000	15,950	6,380	3,290	0.141
Hantush and Thomas (1966)								
2,531,000	126,550	50,620	25,310	210,000	10,500	4,200	2,100	0.093

Comparison of Aquifer Properties for Red Hill Shaft Pumping

Review of the distance drawdown evaluation associated with Time 2 yields similar values as the time drawdown evaluation for transmissivity and storativity. The parameters calculated from the TFN analysis (Section 6.1.9), are also consistent with the values derived from the Theis and Cooper-Jacob analytical solutions. Table 6-10 presents a summary of the parameters computed for the near-field wells derived by the methods described throughout this subsection.

Table 6-10: Summary of Aquifer Properties for Red Hill Shaft Pumping

	Drawdown					Recovery				
	Transmissivity (ft^2/d)	K (ft/d) - 20 ft	K (ft/d) - 50 ft	K (ft/d) - 100 ft	Storativity	Transmissivity (ft^2/d)	K (ft/d) - 20 ft	K (ft/d) - 50 ft	K (ft/d) - 100 ft	Storativity
Cooper-Jacob – Time Drawdown										
Mean	734,289	36,713	14,685	7,343	0.040	560,133	36,713	14,685	7,343	NA
Minimum	627,000	31,350	12,540	6,270	0.015	421,000	31,350	12,540	6,270	NA
Maximum	855,000	42,750	17,100	8,550	0.103	883,000	42,750	17,100	8,550	NA
Theis (Aqtesolv) – Time Drawdown										
Mean	658,000	32,900	13,160	6,580	0.048	1,399,400	69,970	27,988	13,994	0.006
Minimum	527,000	26,350	10,540	5,270	0.024	1,106,000	55,300	22,120	11,060	0.001
Maximum	824,000	41,200	16,480	8,240	0.135	1,648,000	82,400	32,960	16,480	0.019

Cooper-Jacob – Distance Drawdown									
Standard	Transmissivity (ft^2/d)		K (ft/d) - 20 ft		K (ft/d) - 50 ft		K (ft/d) - 100 ft		Storativity
	744,000		37,200		14,880		7,440		0.190
	Major Axis				Minor Axis				Storativity
	Transmissivity (ft^2/d)	K (ft/d) - 20 ft	K (ft/d) - 50 ft	K (ft/d) - 100 ft	Transmissivity (ft^2/d)	K (ft/d) - 20 ft	K (ft/d) - 50 ft	K (ft/d) - 100 ft	
Mutch (2005)	3,837,000	191,850	76,740	38,370	319,000	15,950	6,380	3,290	0.141
Hantush and Thomas (1966)	2,531,000	126,550	50,620	25,310	210,000	10,500	4,200	2,100	0.093

TFN/Pair-Wise Analysis					
	Transmissivity (ft^2/d)	K (ft/d) - 20 ft	K (ft/d) - 50 ft	K (ft/d) - 100 ft	Storativity
Mean	607,000	30,300	12,100	6,070	0.05
Minimum	513,000	25,700	10,300	5,130	0.02
Maximum	810,000	40,500	16,200	8,100	0.18

The hydraulic conductivity values are highly dependent on the assumption of aquifer thickness, so those estimates should be used with caution and with an understanding of this limitation.

6.2.4.4 PUMP TEST ANALYSES FOR HĀLAWA SHAFT PUMPING

Similar analyses were repeated for the synoptic data collected during Hālawa Shaft maximum sustained pumping (Time 4). The distance to each well was computed from the center of Hālawa Shaft, in a clinker zone. As with Time 2, drawdown was plotted versus the logarithm of pumping time at Hālawa Shaft (or the ratio of time since pumping stopped for recovery (Figure 6-29 through Figure 6-33). A semi-logarithmic line could not be fit to the data set. Logarithmic-logarithmic plots of drawdown versus time are also presented on Figure 6-34 through Figure 6-36. Theis-type curves could not be fit to these data. The logarithm of distance versus drawdown was also plotted on a single X:Y scatter plot versus distance; a straight line could not be fit to this plot.

No clear trend was apparent for any of these analyses. These classical analytical solutions could not be applied to Time 4. This may be due to the significant distance between Hālawa Shaft and the wells, as well as the varying geology between the valleys. However, it was possible to compute equivalent hydraulic parameters for Hālawa Shaft pumping derived from the TFN analysis (Table 6-11).

Table 6-11: TFN Computed Aquifer Properties for Hālawa Shaft Pumping

	Equivalent Transmissivity (ft^2/d)	K (ft/d) - 20 ft	K (ft/d) - 50 ft	K (ft/d) - 100 ft	Equivalent Storativity
Mean	1,360,000	68,000	27,200	13,600	0.10
Minimum	627,000	31,300	12,500	6,270	0.05
Maximum	1,710,000	85,500	34,200	17,100	0.15

Continued monitoring of the well network is ongoing.

6.3 HYDRAULIC PROPERTIES OF HYDROGEOLOGIC UNITS

Groundwater flow and solute transport are controlled by the hydraulic and physical properties of the HGUs, including hydraulic conductivity, effective porosity, specific yield, specific storage, and dispersivity. For sites in O'ahu, estimated parameter values have been reported in Nichols, Shade, and Hunt Jr. (1996), Hunt Jr. (1996), Oki (1998, 2005), Izuka et al. (2018), and others. The following is a summary of the information provided in those reports.

6.3.1 Caprock

Hydraulic conductivity of the caprock spans several orders of magnitude depending on material type. The older alluvium, including fine-grained muds and saprolite (thoroughly weathered volcanic rock), have hydraulic conductivities ranging from approximately 0.01 to 1 ft/d (Wentworth 1938). Sands have an estimated hydraulic conductivity ranging from 1 to 1,000 ft/d (Hutcheson et al. 1996). Coral gravels and reef limestone deposits have hydraulic conductivities of several thousands of ft/d (Oki 1998). Souza and Voss (1987) estimated an effective K_h of 0.15 ft/d for caprock. Although the permeability varies greatly with material type, in general, the caprock acts as a low-permeability confining unit atop the basal aquifer near the coastline (Visher and Mink 1964).

The 2005 USGS groundwater model (Oki 2005) used a range of values for hydraulic conductivity of the caprock, depending on location and rock type. For the upper limestone unit in the caprock, the K_v was 25 ft/d and the K_h was 2,500 ft/d. For the low-permeability units of the caprock, the USGS study used hydraulic conductivities ranging from 0.01 to 0.6 ft/d (Oki 2005). A more recent USGS groundwater model (Rotzoll 2012) of the Pearl Harbor area distinguished K_h along the general lava-flow direction (longitudinal K_h) from K perpendicular to the general lava-flow direction (transverse K_h). The model used the following hydraulic conductivity values for the caprock: 0.3 ft/d, 0.2 ft/d, and 0.3 ft/d (K_h longitudinal, K_h transverse, and K_v, respectively).

6.3.2 Valley Fill

Hydraulic conductivity estimates of valley fill deposits range from 0.019 to 0.37 ft/d (Wentworth 1938). In the Pearl Harbor area, the 2005 USGS groundwater model (Oki 2005) used 0.058 ft/d for both K_h and K_v of this unit. The valley fill deposits are underlain by weathered basalt (saprolite) of low permeability that also impedes groundwater flow (Oki 2005).

According to the most recent pertinent USGS report (Izuka et al. 2018), specific-yield values used in numerical models for the Caprock HGU, which includes valley fill deposits, have ranged between 0.04 and 0.2 (Souza and Voss 1987; Oki 1998; Gingerich and Voss 2005; Oki 2005; Rotzoll, El-Kadi, and Gingerich 2007; Rotzoll 2012).

6.3.3 Tuff

Visher and Mink (1964) found that volcanic tuffs of the Honolulu volcanic series are among the most impervious rocks. Hydraulic conductivity values for tuffs (part of the Honolulu Volcanic Series) have been reported to range from < 1 to 490 ft/d (Hunt Jr. 1996). Porosity values have been listed as 0.01 to 0.16 (Oki 2005). In an O'ahu groundwater model of the Nu'uanu and Kalihi aquifer systems developed by Okuhata et al. (2017), hydraulic conductivities of 10 ft (3 m) (horizontal, latitudinal) and 3 ft (1 m) (horizontal, transverse) and 0.1 ft (0.03 m) per day were used for the for the Honolulu volcanics. Belcher et al (2001) provides a range of hydraulic conductivities for tuff breccia and ash-flow tuff, as well as, bedded ash-fall and reworked tuff and ash-flow tuff all between < 1 and 45 ft/d. These types of tuffs and ash flows from Death Valley, CA are similar to the Honolulu volcanic series deposits.

According to Oki et al (1999), sedimentary and pyroclastic deposits are commonly confining units or relatively poor aquifers in the Hawaiian islands. They found that weathered ash and tuff beds are generally are of low permeability and impede the seaward and lateral movement of freshwater.

6.3.4 Saprolite

Hydraulic conductivity estimates for K_h saprolite deposits range from < 0.1 to 1 ft/d (Nichols, Shade, and Hunt Jr. 1996; Rotzoll and El-Kadi 2007). Hunt Jr. (1996) reports the hydraulic conductivity of saprolite at less than 1 ft/d. Recent December 2017 preliminary hydraulic conductivities derived from pneumatic slug testing within saprolite layers of the packered zones (Zones 6, 7, and 8) of RHMW11 (multilevel well with eight zones) ranged from 0.0033 to 0.026 ft/d, and hydraulic conductivities derived from laboratory core tests within the upper zone of the saprolite ranged from 7.99E-06 to 8.50E-05 ft/d. Pneumatic test data from RHMW11 Zones 6, 7, and 8 approximated slug withdrawal tests and were analyzed using three different techniques (Hvorslev 1951; Bouwer and Rice 1976; Cooper, Bredehoeft, and Papadopulos 1967); results are presented in Table 6-2.

6.3.5 Basalt

The diverse rock textures encompassed by the three types of lava that comprise the basal aquifer in the immediate vicinity of the site (massive a'ā, pāhoehoe, a'ā clinker) impart a complex porosity distribution to the lavas (Hunt Jr. 1996). In a layered sequence of lava flows, several types of primary porosity are present:

- Vesicular – small isolated gas vesicles that form in molten lava
- Fracture – joints, cracks, and bedding-plane separations
- Intergranular – fragmental rock, including cinders, rubble, and clinkers
- Conduits – large openings such as lava tubes and interflow voids

Vesicles are poorly connected and contribute little to effective porosity. Estimates of the total porosity of various volcanic rocks on O'ahu range from 5 to 51 percent, with a median value of approximately 43 percent; values of effective porosity may be lower by as much as a factor of 10 (Hunt Jr. 1996). Fracture and intergranular porosity can form a pervasive network of small openings that facilitates diffuse groundwater flow. Conduits such as lava tubes provide avenues for highly channelized flow. However, these conduits may be impeded by collapse and infilling of the more rapidly weathering lava tubes. Intact lava tubes are quite rare and are discussed in further detail in Section 5.1.1.

Hawaiian volcanic rocks vary in porosity and permeability depending on the emplacement process, lava type, genesis, flow thickness, flow rate, extent, cooling rate, and weathering. Permeability is

typically highest in the relatively thick, unweathered rubbly a'ā clinker zones and intensely fractured zones or lava tubes of pāhoehoe flows. Permeability is much lower in the interior portions of massive flows, weathered interflows, intrusive rocks (dikes/sills), ash beds, and weathered rocks (saprolite)/soil horizons, which can impede vertical flow. Even slight weathering of the basalt along flow tops and fractures results in clay mineral formation and low permeability.

The permeability of lava flows in the Pearl Harbor area generally is high. The main elements of lava flows contributing to the permeability are a'ā clinker zones, voids along the contacts between flows, intraflow cooling joints perpendicular to flow surfaces, and lava tubes developed in pāhoehoe flows. Consequently, the regional K_h of these volcanic rocks generally ranges from hundreds to thousands of ft/d (Hunt Jr. 1996; Oki 2005). Because of the extremely high-permeability, horizontal water-table gradients in these rocks are small (typically on the order of 1 ft/mile). K_h in the lava flows is often anisotropic. Hydraulic conductivity is often much greater parallel to the lava flows than perpendicular to the flows (Oki 2005).

According to the most recent regional USGS report (Izuka et al. 2018), estimates of K_h for dike-free lava-flow aquifers on O'ahu range between 500 and 5,000 ft/d (Hunt Jr. 1996). Aquifer test results show K_h values of 26–5,000 ft/d, with the majority of results between 200 and 1,500 ft/d (Wentworth 1938; Visher and Mink 1964; Takasaki and Valenciano 1969; Izuka et al. 2018; Rosenau, Lubke, and Nakahara 1971; Soroos 1973; Williams and Soroos 1973; Dale 1978; Mink 1980; Eyre 1983; Eyre, Ewart, and Shade 1986). Values of K_h used in calibrated numerical models range from approximately 100 to 7,500 ft/d (Eyre, Ewart, and Shade 1986; Souza and Voss 1987; Oki 1998; Gingerich and Voss 2005; Whittier et al. 2004; Rotzoll, El-Kadi, and Gingerich 2007).

Where the basalt has not been intruded by dikes (as in the study area), K_h values generally range from hundreds to thousands of ft/d (Soroos 1973; Mink 1980; Hunt Jr. 1996). Souza and Voss (1987) estimated the ratio of K_v to K_h is 0.05. For the volcanic rock aquifer in the Pearl Harbor area, the 2005 USGS regional groundwater model (Oki 2005) used a value of 4,500 ft/d for K_h along the general lava-flow direction (longitudinal K_h) and 1,500 ft/d for K perpendicular to the general lava-flow direction (transverse K_h). The same model used 7.5 ft/d for K_v of the volcanic rock aquifer (Oki 2005). A more recent USGS groundwater model of the Pearl Harbor area (Rotzoll 2012) used 1,350 ft/d for longitudinal K_h, 675 ft/d for transverse K_h, and 6.8 ft/d for K_v.

Weathering reduces the hydraulic conductivity of volcanic rocks (Mink 1980). Saprolite (thoroughly weathered volcanic rock) is soft and rich in clay minerals, may be found in deposits 100–300 ft thick, and has very low hydraulic conductivity (DON 2007). According to the USGS (Oki 2005), the R.M. Towill Corporation reported a hydraulic conductivity of 0.058 ft/d for weathered basalt beneath Waiawa Stream Valley based on an injection test. Wentworth (1938) estimated the hydraulic conductivity of weathered basalt to be between 0.083 and 0.128 ft/d based on laboratory parameter tests on core samples. Recent December 2017 preliminary hydraulic conductivities derived from pneumatic slug testing within saprolite layers of the packered zones of RHMW11 (multilevel well with eight zones) ranged from 0.0033 to 0.026 ft/d, and hydraulic conductivities derived from laboratory core tests within the upper zone of the saprolite ranged from 7.99E-06 to 8.50E-05 ft/d.

Specific storage is the volume of water released from storage per unit decline in hydraulic head in the aquifer, per unit area of the aquifer. In the Pearl Harbor area, specific storage was estimated to range from 10^{-4} to 10^{-7} per foot (Williams and Soroos 1973). For unconfined parts of aquifers, specific yield plays a more significant role than specific storage. Specific yield is defined as the volume of water that a saturated rock or soil will yield by gravity drainage divided by the total volume of rock or soil, and

is usually expressed as a percentage. Specific yield is less than the effective porosity because some portion of the water is held by surface tension and capillary forces and will not drain by gravity.

Specific yield values used for the volcanic-rock aquifer in regional groundwater models and reported by the USGS (Izuka et al. 2018) range between 0.03 and 0.1 percent (Eyre, Ewart, and Shade 1986; Souza and Voss 1987; Oki et al. 1996; Oki 1998; Gingerich and Voss 2005; Oki 2005; Rotzoll, El-Kadi, and Gingerich 2007; Whittier et al. 2010; Rotzoll 2012). In the Facility area, reported values for specific storage and specific yield values were derived from numerical modeling analysis of the regional aquifer pumping test conducted in May 2006, the results of which are summarized in the following subsection (DON 2007).

6.3.6 Site-Area Aquifer Testing and Analysis of Hydraulic Parameters

Hydraulic conductivity values for the Basalt HGU in the Facility area were recently obtained from hydraulic tests performed in RHMW11, which augment the hydraulic parameter values derived from previous numerical modeling analysis of data collected from the regional groundwater aquifer pumping test conducted in May 2006 (see also Sections 6.1 and 6.1.9). Section 6.1 describes the results of hydraulic tests conducted in RHMW11 (Table 6-2). These tests show that the saprolite and weathered basalt have extremely low hydraulic conductivities, but the deeper unweathered basalt has very high hydraulic conductivity. The May 2006 numerical analysis was conducted using the local groundwater flow model for the 2007 Red Hill project (DON 2007). The aquifer pumping test was conducted in May 2006 by the Navy in coordination with BWS, the State of Hawai'i Department of Land and Natural Resources (DLNR) and its Commission on Water Resource Management (CWRM), and the U.S. Army Corps of Engineers. For the 2006 test, the primary pumping well was Red Hill Shaft. Groundwater level monitoring was performed via transducers and data loggers in several wells in the Red Hill area, including the Red Hill monitoring wells and other wells near Red Hill Shaft and Hālawa Shaft. The collected field data were compared to simulated water levels from corresponding wells to calibrate hydraulic conductivity and other hydrogeologic properties for a local groundwater flow model.

The 2006 pumping test period covered approximately 1 month, from May 10 to June 1, 2006, although some data loggers recorded water levels earlier. The main pumping test was initiated by completely shutting off Red Hill Shaft between May 12 and May 19, which allowed the water levels near the well to recover from pumping stresses. During this same period, BWS Hālawa Shaft and the BWS Moanalua Wells maintained their regular pumping schedules and rates. After the recovery period, Red Hill Shaft was subjected to a period of above-average pumping between May 19 and May 26; the 10-year average pumping rate for the well is approximately [redacted], and during the above-average pumping period the pumping rate alternated between [redacted].

The local groundwater flow model for the 2007 Red Hill project was calibrated for both steady-state and dynamic, or "transient," conditions (DON 2007 Appendix L). The steady-state calibration was conducted by (1) selecting representative hydraulic parameters of the major stratigraphic units from literature values, (2) simulating water table elevations using average recharge and pumping conditions for the period between 1996 and 2005, and (3) iteratively running the groundwater flow model, using a Parameter Estimation (PEST) algorithm (Doherty 2000), until the differences between the measured and simulated groundwater elevations were minimized. Thirty wells located in the local model area were used to define the steady-state water table elevations. Table 6-12 provides the hydraulic parameters derived using this modeling approach with PEST; these hydraulic parameter values are specified in the final 2007 calibrated numerical flow model (DON 2007).

Table 6-12: Hydraulic Parameters Developed from Local Numerical Flow Model Calibration at the Facility (DON 2007)

Hydrogeologic Unit	Horizontal, Longitudinal K (ft/d)	Horizontal, Transversal K (ft/d)	Vertical K (ft/d)	Effective Porosity	Specific Storage (per ft)	Specific Yield
Caprock	115	115	115	0.10	3.05 × 10-5	0.10
Valley Fill	0.066	0.066	0.066	0.15	1.52 × 10-5	0.12
Basalt	4,428	1,476	7.4	0.05	1.07 × 10-5	0.031

K hydraulic conductivity

6.4 GENERAL GROUNDWATER CHEMISTRY DISTRIBUTION

The major ion composition of groundwater samples collected from Red Hill area monitoring wells in November 2016 is shown in Table 6-13. Values in the table are provided in mg/L and expressed as milli-equivalents per liter (meq/L). Major ion composition of the groundwater is shown on Figure 6-37, which is a trilinear plot of the data in Table 6-13 along with results for RHMW09, RHMW10, and RHMW11 (Zones 1 through 5) that were collected in February 2017, October 2017, and March 2018, respectively. On the trilinear plot, the colored dots indicate the well location from which samples were collected.

Table 6-13: Major Ion Composition of Groundwater Samples Collected from Red Hill Monitoring Wells, November 2016

Monitoring Well / Sampling Point	Unit	Ca	Mg	Na	K	CO_3	HCO_3	Cl	SO_4
RHMW2254-01	mg/L	15.8	15.4	42.2	2.23	1.7	67.4	72.3	18.5
	meq/L	0.788	1.27	1.84	0.057	0.056	1.11	2.04	0.385
RHMW01	mg/L	11.5	9.88	35.2	1.9	1.7	94.4	39.4	4.5
	meq/L	0.574	0.813	1.53	0.049	0.056	1.55	1.11	0.094
RHMW02	mg/L	12.6	24.8	53.6	2.44	1.7	196	39	1.2
	meq/L	0.629	2.04	2.33	0.062	0.056	3.21	1.10	0.025
RHMW03	mg/L	25	33.4	104	3.7	1.7	285	47.2	45.7
	meq/L	1.25	2.75	4.52	0.095	0.056	4.67	1.331	0.951
RHMW04	mg/L	16.9	18.6	34.7	1.96	1.7	75.2	72.8	9.8
	meq/L	0.843	1.53	1.51	0.050	0.056	1.23	2.05	0.204
RHMW05	mg/L	7.85	13.2	136	4.93	1.7	98.1	157	46.5
	meq/L	0.392	1.07	5.92	0.126	0.056	1.61	4.43	0.967
RHMW06	mg/L	35.1	54.9	165	2.33	1.7	108	365	81.8
	meq/L	1.75	4.52	7.18	0.060	0.056	1.77	10.3	1.70
RHMW07	mg/L	55.5	71.9	150	3.04	1.7	119	411	67.9
	meq/L	2.77	5.92	6.53	0.078	0.056	1.95	11.6	1.41
RHMW08	mg/L	32.7	12	109	5.68	1.7	50.8	169	58.2
	meq/L	1.63	0.988	4.74	0.145	0.056	0.833	4.77	1.21
RHMW09	mg/L	12.9	11.6	36.6	2.11	1.7	66.5	51.5	10.1
	meq/L	0.644	0.955	1.59	0.054	0.056	1.09	1.45	0.211
HDMW2253-03	mg/L	12.9	17.5	57.1	0.608	1.7	50	84.7	27.6
	meq/L	0.644	1.44	2.48	0.016	0.056	0.82	2.39	0.574

Monitoring Well / Sampling Point	Unit	Ca	Mg	Na	K	CO_3	HCO_3	Cl	SO_4
OWDFMW01	mg/L	115	220	350	7.64	1.7	161	1070	368
	meq/L	5.74	18.1	15.2	0.196	0.056	2.64	30.2	7.65

Ca calcium
Cl chloride
CO_3 carbonate
HCO_3 bicarbonate
K potassium
meq/L milli-equivalents per liter
Mg magnesium
mg/L milligrams per liter
Na sodium
SO_4 sulfate

A trilinear plot is useful for interpreting groundwater data because it facilitates visual comparison of the major ion composition in water samples that may reflect the effects of recharge, aquifer interactions, and chemical sources on natural groundwater. Each data point on the trilinear plot shows the composition of the water sample as a percentage of total ions, in meq/L. A plot of several samples from different locations in a study area is often useful to identify mixtures of different water types (Hem 1985). Mixing of two distinct water types is seen as a linear trend in the data points on the Figure 6-37 trilinear diagram for samples lying between the two distinct water-type endpoints.

Additional groundwater chemistry data compiled by the University of Hawai'i at Mānoa (UHM) Water Resources Research Center (WRRC) as part of a Department of Energy (DOE)-funded geothermal assessment study and provided to the Navy by UHM are presented in Table 6-14. These groundwater samples were collected as part of statewide geothermal resource assessment funded by the DOE. As part of that effort, the Navy (NAVFAC) facilitated the collection of water samples from a suite of monitoring wells located on Navy facilities. Samples were collected at 12 wells in the NAVFAC monitoring network and were analyzed for major ions, trace metals, and oxygen and hydrogen isotopes. UHM also compared these data from the Red Hill area with four samples collected elsewhere on O'ahu by UHM and with data collected by the USGS for the National Water Quality Assessment 2001 (https://pubs.usgs.gov/wri/wri034305/). Overall the major ion concentrations reported in the UHM groundwater data are comparable to the general water chemistry data in Table 6-13 and consistent with Figure 6-37.

One of the most meaningful natural geochemical parameters in groundwater is chloride because it is less reactive than other major ions with the crystalline rock, sediment, and soils through which groundwater moves, and is relatively unaffected by bacterial reactions and biodegradation processes. Samples from wells nearest the Red Hill fuel tanks show the lowest chloride concentrations, which range from 37 to 47 mg/L in RHMW02, RHMW01, and RHMW03 (see Table 6-13 and Table 6-14). In contrast, chloride concentrations of 365 mg/L and 431 mg/L were observed at RHMW06 and RHMW07, respectively. The deep-water sample from HDMW2253-03 (624 ft) contained chloride at 1,874 mg/L, while the shallow sample from the same well collected at 50 ft depth contained chloride at only 88 mg/L. For comparison, the sample from Hālawa Shaft contained chloride at 120 mg/L. Bivariate plots were developed to evaluate conductivity in groundwater (Figure 6-38) HDMW2253-03 has a relatively high chloride signature (along with associated ions) that may be influencing surrounding wells such as RHMW06 and RHMW07.

The spatial distribution of the chloride concentrations are consistent with, and provide additional support for, the conceptual model of the groundwater flow pattern in the Facility area described above (Sections 6.1 and 6.1.9). Specifically, the pattern of chloride concentrations suggests that chloride is

being added to the relatively fresh groundwater flow system in the area north of South Hālawa Stream. As this higher-chloride groundwater flows southward, it is being diluted by lower-chloride groundwater flowing southwestward beneath South Hālawa Stream and the Facility. Mixing of the higher chloride water flowing from the north with the lower chloride water flowing from the northeast and east, the resulting chloride concentration is reflected in the sample of Red Hill Shaft, approximately 90 mg/L.

A principal component analysis (PCA) was conducted with select geochemical parameters (details are presented in Appendix B.8), including chloride and sulfate. Additional discussion of the PCA results is presented in Appendix B Attachment B.8.3.

UHM also provided stable isotopic measurements of oxygen and hydrogen for the groundwater samples. In particular, these data include (1) the ratio of the "heavy" isotope of hydrogen ^{2}H to the common and "lighter" isotope ^{1}H; and (2) the ratio of the heavy isotope of oxygen ^{18}O to the common and lighter isotope ^{16}O. The values are expressed as a ratio between the heavy and light isotopes in the water sample to those ratios in an isotopic standard derived from seawater. The units are parts per mil (o/oo) and designated $\delta^{2}H$ for hydrogen and $\delta^{18}O$ for oxygen. To facilitate interpretation, these isotopic data are typically plotted on an X-Y graph with $\delta^{18}O$ on the X axis and $\delta^{2}H$ on the Y axis. Factors affecting the isotopic composition of water include the temperature of precipitation, the distance the water vapor travels before precipitation, latitude, and amount of evaporation. Nonetheless, most groundwater samples for $\delta^{18}O$ and $\delta^{2}H$ plot closely to the Global Meteoric Water Line where: $\delta^{2}H = 8*\delta^{18}O+10$. However, there is also some regional variability in the relationship between $\delta^{2}H$ and $\delta^{18}O$, which is referred to as the Local Meteoric Water Line (LMWL). The estimated LMWL for the site is shown on Figure 6-39, along with data from several Red Hill monitoring network wells.

In the preliminary UHM analyses of these data provided to the Navy, UHM performed a regression analysis to provide a preliminary LMWL based on reasonable assumptions and the available data. This preliminary LMWL is very similar to the LMWL developed by UHM and the USGS for Hawai'i and Maui Islands. The RHMW well samples generally plot along the LMWL except for OWDFMW01, which falls well to the right of the LMWL.

Table 6-14: Groundwater Chemistry Data Compiled by the University of Hawai'i Water Resources Research Center for Geothermal Study

Well No.	Name	Date	Specific Conduc-tivity	pH	ORP	Alk	DO (mg/L)	Turb	NO_3	Ca	Mg	K	Na	Br	Cl	F	SiO_2	SO_4	HCO_3	CO_3	Hydrogen 2/1 ratio	Oxygen 18/16 ratio	$\delta^{18}O$_CORR	$\delta^{2}H$_CORR
HDMW2253-03 Deep Sample																								
3-2253-003	HDMW@-624ft	3/6/2017	5,500	7.15	41	31	7.2	—	0.2	320.9	279.4	15.9	473.8	6.4	1,874.0	0.01	39.2	247.2	37.8	18.6	-11.45	-3.06	-12.98	-3.41
Red Hill Outside Wells																								
OWDFMW1	OWDFMW1	7/19/2016	4,042	8.02	117	166	4.0	67.0	1.6	106.1	244.9	7.3	368.5	3.0	1,059.0	0.05	51.4	321.1	202.5	99.6	-20.14	-3.40	-21.59	-3.61
3-2253-005	RHMW07	7/19/2016	1,869	7.26	152	97	2.6	1.7	0.9	61.2	82.6	3.0	162.3	1.4	431.0	0.06	76.2	72.6	118.3	58.2	-13.22	-2.96	-13.81	-3.04
3-2253-007	RHMW08	1/11/2017	1,001	8.20	168	56	4.7	2.0	0.5	32.4	18.9	5.6	108.6	0.6	169.0	0.23	45.6	79.0	68.3	33.6	-16.70	-3.60	-17.13	-3.65
3-2253-003	HDMW@-50ft	3/6/2017	485	6.71	56	45	5.1	—	0.2	11.8	15.5	0.4	50.7	0.2	88.0	0.06	65.0	27.6	54.9	27.0	-11.80	-2.90	-12.14	-2.93
3-2253-004	RHMW06	7/19/2016	1,568	6.93	193	100	6.3	4.2	0.6	45.2	74.2	2.4	198.9	1.3	416.0	0.06	74.3	94.6	122.0	60.0	-12.85	-3.01	-13.42	-3.09
RHMW04	RHMW04	7/19/2016	437	6.50	201	56	8.6	6.0	0.6	18.6	18.8	2.3	33.8	0.3	74.0	0.06	57.1	10.9	68.3	33.6	-11.61	-3.03	-11.94	-3.06
Red Hill Tunnel Wells																								
3-2254-001	RHMW2254-01	1/9/2017	450	7.54	171	54	8.6	-4.4	0.0	16.7	15.7	2.5	41.8	0.3	89.0	0.07	49.1	15.2	65.9	32.4	-10.30	-3.20	-10.64	-3.23
RHMW05	RHMW05	2/7/2017	844	7.91	119	90	8.3	-2.2	1.0	7.8	12.8	4.9	138.8	0.5	148.0	0.33	86.5	46.2	109.8	54.0	-13.00	-3.30	-13.39	-3.34
RHMW01	RHMW01	2/6/2017	333	6.87	-19	92	0.5	-5.8	0.4	—	—	—	—	—	40.9	—	—	4.6	112.0	—	—	—	—	—
RHMW02	RHMW02	2/7/2017	519	6.54	-37	188	0.1	-2.1	0.4	13.4	25.7	2.3	53.0	0.1	37.0	0.64	91.3	0.4	229.4	112.8	-11.80	-3.20	-12.11	-3.22
RHMW03	RHMW03	1/12/2017	802	6.77	198	252	3.0	-0.5	1.8	24.5	32.2	3.3	98.2	0.2	47.0	0.18	86.2	44.2	307.4	151.2	-17.90	-3.70	-18.22	-3.72
BWS Wells																								
3-2354-001	Hālawa Shaft	3/6/2017	560	—	—	52	—	—	0.5	27.0	23.0	2.5	38.0	0.4	120.0	—	—	—	—	—	—	—	—	—

— no data

$\delta^{18}O$_CORR ratio between the heavy and light isotopes of oxygen in the water sample to those ratios in an isotopic standard derived from seawater (corrected) in parts per mil (o/oo)

$\delta^{2}H$_CORR ratio between the heavy and light isotopes of hydrogen in the water sample to those ratios in an isotopic standard derived from seawater (corrected) in parts per mil (o/oo)

Alk alkalinity
Br bromide
Ca calcium
Cl chloride
CO_3 carbonate
DO dissolved oxygen
F fluoride
HCO_3 bicarbonate
K potassium
Mg magnesium
NO_3 nitrogen
ORP oxidation-reduction potential
SiO_2 silica dioxide
SO_4 sulfate
Turb turbidity

This page intentionally left blank

As described in the UHM evaluation, these isotopic data for groundwater are useful for estimating the effective (volume-weighted average) elevation that the groundwater recharge occurred. Studies done by the USGS and UHM have shown a strong correlation between the isotopic composition of rainfall and the elevation where that rainfall reached the ground surface. The relationship between the isotopic composition of rainfall and elevation varies depending on whether or not the rainfall occurred above the trade wind inversion elevation, and whether the rainfall occurred on the windward or leeward slope of an island. For East Maui, it was found that for elevations less than 1,900 m (6,200 ft), the following relationship between recharge elevation and the $\delta^{18}O$ values:

- Windward slopes: Recharge Elevation (m msl) = $-860*\delta^{18}O$
- Leeward slopes: Recharge Elevation (m msl) = $-810*\delta^{18}O$

Using this relationship, the Red Hill area monitoring well data were used by UHM to estimate that groundwater recharge occurred over an elevation range of approximately 2,100 ft. This estimate is based on the difference in the $\delta^{18}O$ value at HDMW2253-03 (-2.93 in a shallow sample from 50 ft depth) and RHMW03 (-3.72). UHM found that $\delta^{18}O$ values for RHMW04, RHMW06, RHMW07, and HDMW2253-03 are consistent with lower-elevation recharge, while the $\delta^{18}O$ values for the other Red Hill area wells and wells at the Moanalua and Honolulu International Country Club are consistent with middle- to higher-elevation recharge. These and other data (including the TFN analysis) may suggest recharge from various locations/elevations is flowing along different flow paths generally paralleling the primary lava flows from the Ko'olau range during the shield-building phase. In summary, the stable isotope groundwater data for oxygen and hydrogen are consistent with the conceptual model of the groundwater recharge and flow pattern in the Red Hill Facility area that is described above (Sections 6.1 and 6.1.9).

In addition, isotopic analysis of $^{14}C/^{15}C$-nitrogen ($\delta^{15}N$) and $^{34}C/^{32}C$-sulfur ($\delta^{34}S$) was conducted during the Fourth Quarter 2017 Red Hill groundwater sampling event. Enrichment of heavier isotopes of nitrogen and sulfur would be indicative of biodegradation (see Section 7 for additional discussion of biodegradation). Trends were inconclusive; results are presented in Appendix B.8.3.

6.5 ASSESSMENT OF LOEs FOR GROUNDWATER FLOW

The regional groundwater head gradients are from east to west within the study domain. Local-scale heterogeneities including clinker zones with large contrasts in hydraulic properties cause local variations in these flow gradients. Multiple LOEs exist for the conceptual model of groundwater flow directions in the Facility area, including:

- Groundwater levels measured throughout the Facility area of interest are consistent with the regional groundwater levels and flow directions reported in previous studies, which include those by the USGS (Oki 2005) and DON (2007, 2010).
- Spatial distributions of groundwater level elevations measured in the Red Hill area monitoring wells show hydraulic gradients are generally southwestward beneath the Facility, even when Red Hill Shaft was not pumping in November 2016. However, the gradient at Red Hill is extremely gentle and is also affected by local heterogeneities.
- Borehole geologic logs show a deep saprolite zone occurs beneath South Hālawa Valley and forms a low-permeability barrier to groundwater flow. At monitoring well RHMW11, this saprolite extends to approximately 87 ft below the regional basal groundwater table. New data from multiple intervals in RHMW11 show the saprolite zone is continuously saturated and the groundwater levels in the saprolite are still equilibrating, but indicate a downward vertical

hydraulic gradient, and the potentiometric surface is much higher than at nearby RHMW07 and other Red Hill wells. However, the lateral and vertical extent of the saprolite has not been completely delineated, particularly in the upper portion of South Hālawa Valley.

- Groundwater flows from areas of higher recharge (which, based on the TFN, is occurring at higher elevations) to areas of lower recharge or discharge. Recharge occurs as a result of direct infiltration of rainfall, seepage from streams, and other water sources at the land surface. Recharge rates are spatially distributed throughout the groundwater model area such that higher recharge occurs at higher land surface elevations as recently estimated by the USGS (Engott et al. 2015).
- The geologic log of the Red Hill water development tunnel (i.e., Red Hill Shaft) (Stearns 1943) shows a highly permeable clinker zone in the last couple hundred feet of the tunnel (see Figure 5-10). Groundwater contours may be indicative of a converging flow pattern toward the eastern end of the water tunnel.
- Time-series water level data from the May 2006 pumping test of Red Hill Shaft and the USGS/BWS May 2015 pumping test of Hālawa Shaft suggest there is a hydraulic barrier located north of monitoring well RHMW07.
- Pump test data from the 2017–2018 synoptic monitoring indicate that RHMW07, RHMW11 (Zones 6, 7, and 8), HDMW2253-03 Chase Tube, and others do not respond to pumping from Red Hill Shaft or Hālawa Shaft.
- Trends in major chemical components in groundwater from monitor wells indicate mixing of two main groundwater types, a sodium-chloride type water from the area north of South Hālawa Valley and sodium-bicarbonate type from the southeast.
- Groundwater chemistry data from Red Hill area wells compiled and evaluated by UHM, which include major ions and stable isotopes of oxygen and hydrogen, support the conceptual model of the groundwater recharge and flow pattern in the Red Hill Facility area described above.

Groundwater levels measured throughout the Facility area of interest are consistent with the regional groundwater levels and flow directions reported in previous studies, which include those by the USGS (Oki 2005) and DON (2007, 2010).

6.6 UNCERTAINTY ANALYSIS

Uncertainties associated with the Saturated Zone model include insufficient data and information regarding:

- *Groundwater flow directions and rates in the groundwater model area.* Recently, the direction and rate of migration of groundwater potentially impacted by COPCs from the Facility has been better defined. Accurate hydraulic heads (groundwater levels) and hydraulic gradients in the area of existing Red Hill groundwater monitoring wells were recently established by the high-accuracy survey of wellhead elevations (DON 2018a). Nonetheless, some uncertainty remains in the spatial distribution of hydraulic heads and hydraulic gradients in the area extending northward to Hālawa Shaft and in the area extending from the Facility southward to the Moanalua and TAMC Wells. In addition, it is unclear what the reported Hālawa Shaft water levels represent, because details on the measuring point used for water level measurements have not been obtained.
- *The thickness and extent of HGUs in the groundwater model area.* In particular, better definition of the depths of older alluvial sediment fill and saprolite in areas beneath North and South Hālawa Valleys is needed.

- *Geologic features that may act as preferred groundwater flow pathways or barriers.* Clinker zones, paleo-channels, faults, dense low-permeability lava flows, and lava tubes in the primary area of interest result in heterogeneities that may affect local gradients. Sensitivity analyses help bound many of these factors.
- *Hydraulic properties of the Basalt HGU (the basal aquifer).* Additional data are needed to calibrate the groundwater flow model and refine aquifer hydraulic properties, including transmissivity, hydraulic conductivity, heterogeneity, anisotropy, storativity, and specific yield. These are being developed from the 2017–2018 synoptic monitoring data set.
- *Groundwater recharge and discharge rates.* Recharge and discharge rates at Red Hill, the cement plant, crushing facility, and quarry to the north are not yet defined. The degree to which recharge rates are reduced by the thick clayey saprolitic soil overlying the Facility is also not well defined. Total groundwater discharge flux out of the model area is currently unknown. Flow monitoring of larger springs in the Pearl Harbor area is being conducted by the USGS, and these data are available from the USGS website, but total groundwater discharge flux out of the model area is not being measured and is not reported in recent USGS reports (Engott et al. 2015; Izuka et al. 2018).

6.7 ADDRESSING UNCERTAINTIES

The following ongoing, planned, or proposed activities are designed to help resolve the uncertainties described in Section 6.6.

6.7.1 Groundwater Flow Directions and Rates

A high-precision well elevation survey has recently been completed to more accurately determine the measuring point elevations of all wells in the Red Hill groundwater monitoring network (DON 2018a). Data from this survey will enable more accurate determinations of hydraulic heads and hydraulic gradients using the available groundwater level measurements.

Similar groundwater level data from additional monitoring well locations are needed to better define the direction and rate of migration of groundwater potentially impacted by COPCs from the Facility, and to further define the spatial distribution of hydraulic heads (groundwater levels) and hydraulic gradients in the areas extending northward to Hālawa Shaft, near the Red Hill Shaft water development tunnel, and in the area extending southward to the Moanalua and TAMC Wells. Accordingly, additional monitoring wells are planned or currently being installed at selected key locations to provide these data (see Figure 2-9) (DON 2017f). Furthermore, the numerical-model-simulated water levels at wells that are currently monitored for regional flow conditions will be evaluated in a similar manner to the monitoring data to establish if the simulations are consistent with observations.

Groundwater level elevation data are needed to represent both non-pumping conditions and various combinations of pumping these wells. The additional monitoring wells will need to be completed with intake intervals that measure groundwater levels (hydraulic heads) to define the potentiometric surface, which will reflect horizontal hydraulic gradients at the water table. Hydraulic head measurements are also needed from intervals deeper below the water table to measure the vertical hydraulic gradient at the selected locations. Pumping and water level monitoring data from the 2017–2018 USGS synoptic study are being analyzed to establish the aquifer response to non-pumping and various pumping conditions to help better define the hydraulic properties that affect regional groundwater flow.

To define hydraulic heads and gradients, additional data have been collected from the multilevel system in RHMW11, where a shallow saturated zone appears to extend to the water table within

saprolite. Data will also be collected from additional monitoring wells in the area south of Hālawa Shaft and elsewhere in Hālawa Valley.

Groundwater data obtained from the new monitoring wells will be used to further define the actual groundwater flow directions, and the updated groundwater model will be calibrated to reflect those new data. As part of the investigation, the potential for transient and/or local groundwater flow northwestward from the Facility (see Section 6.6) will also be evaluated.

6.7.2 Thickness and Extent of Hydrogeologic Units

Geologic maps showing the Caprock HGU thickness and elevation of the top of the Basalt HGU were published in recent USGS studies (Izuka et al. 2018). For these maps, the geospatial data sets have been obtained from the USGS and are now being evaluated to estimate the extent and thickness of the HGUs in the model area. However, additional hydrogeologic data are needed to better define the depths of older alluvial sediment fill and saprolite in areas beneath North and South Hālawa Valleys. Detailed borehole geologic logs of deep borings in those areas would reduce this uncertainty. Borings from Honolulu Authority for Rapid Transportation (HART) studies (HART 2014) were evaluated for integration into cross sections within the groundwater model domain to further improve the geologic model. Valley fill/saprolite may locally affect groundwater movement, and additional data will help improve the understanding of hydraulic gradients and groundwater flow directions. One of the sensitivity models prepared during the interim groundwater flow modeling evaluated the existence and effect of saprolite in the North and South Hālawa Valley. The results indicate that groundwater flow is not sensitive to the existence of saprolite in South Hālawa Valley based on the assumptions used in this analysis. The Navy is currently planning at least one new boring for installing a monitoring well in North Hālawa Valley to provide geologic data to define the valley fill and saprolite thickness immediately south of Hālawa Shaft.

6.7.3 Preferential Pathways and Barriers

Hydrogeologic data are being collected from the additional Red Hill area monitoring wells currently being installed. These data will support further evaluation of geologic features that may act as preferred groundwater flow pathways or barriers. Similar data will also be needed from additional monitoring well locations. Together, these data will be evaluated to better define the spatial distribution of clinker zones, paleo-channels, faults, dense low-permeability lava flows, and dikes in the primary area of interest for groundwater modeling. Recent analysis of primary basalt flow directions relative to the formation of lava tubes in pāhoehoe at Red Hill (see further discussion in Section 5) indicate that it would be highly unlikely for a lava tube to extend in the direction of Hālawa Shaft from Red Hill. In addition, any such tube would be intersected by valley fill and saprolite in South and North Hālawa Valleys, which would prevent it from acting as a preferential pathway from Red Hill to Hālawa Shaft.

Random walk modeling was performed to evaluate the potential historical lava flow paths passing through the vicinity of the tanks. Lava flows were simulated using a probabilistic model recently developed by Vitturi and Tarquini (2018), as described in Appendix D. Results indicate that it is unlikely that a preferential pathway exists between the tank farm area and Red Hill Shaft area in relation to historical lava flows.

Hydraulic Properties of Basalt HGU. The new monitoring wells being installed will include borehole geologic/geophysical logs and core samples for further characterizing the physical properties of the Basalt HGU (basal aquifer), such as was recently obtained from monitoring well RHMW11. However, additional data are needed for calibrating the groundwater flow model to refine aquifer hydraulic properties, which include transmissivity, hydraulic conductivity, heterogeneity, anisotropy, storativity, and specific yield.

The existing 2007 groundwater model was calibrated using pumping test data from May 2006, when fewer monitoring wells were available near the Facility. Since 2007, the only new information relevant to aquifer hydraulic properties in the modeling area is the USGS data set collected in May 2015 while BWS Hālawa Shaft pumping was pumping and the 2017–2018 synoptic monitoring under various pumping conditions. Other wells in the Hālawa and Moanalua area were also being pumped during that time, but the pumping data appear to be incomplete. Variable pumping rates add further uncertainty in evaluating the data.

To address the uncertainty, a regional-scale aquifer test with synoptic monitoring of groundwater levels in monitoring wells and pumping rates of supply wells located near the Facility was recently completed. As requested by the Navy, the USGS performed synoptic monitoring of 23 monitoring wells while the supply wells are pumped in sequence at controlled flow rates and continuously monitored (USGS 2017e). Using these regional pumping test data, the groundwater flow model will be calibrated using an iterative process to reasonably match these data by adjusting the aquifer hydraulic properties in the model within the range of reported values from other studies. The flow model calibration will be complete when the refined model simulations reasonably match the time-series drawdown and recovery data, the measured hydraulic gradients, and groundwater level contour maps for non-pumping and pumping conditions.

6.7.4 Groundwater Recharge and Discharge Rates

A water balance analysis was performed and integrated along with refined groundwater recharge rates into the numerical groundwater model.

A number of monitoring wells in South Hālawa Valley and to the north have encountered shallow, possibly perched, groundwater, which is further indication of the increase in local groundwater recharge rates and/or an indicator of lower-permeability materials. A pressure transducer was placed in one of the shallow monitoring wells at the Hālawa Correctional Facility. Based on review of the most recent data on the USGS website, the water table elevation in this well is approximately 155 ft above msl. In context, the heads in the basal aquifer are generally 18–20 ft above msl, while the saprolite zones in RHMW11 are 70–115 ft above msl, and are considered to have reached approximate hydraulic equilibrium sometime between October 2018 and January 2019. As described in Module A: Physical Setting (Section 2), further evaluation of new and existing data will be conducted to help define the contiguous or isolated nature of this shallow water zone. The CSM will be updated to describe the perched water locations and depths (elevations).

Natural groundwater discharge also occurs along the coast, and thus the groundwater model update needs to specify the rate of this flux. Updated estimates of groundwater recharge and discharge may become available from the USGS modeling studies currently underway. If not, however, the impact of these data gaps will be further evaluated during the modeling.

This page intentionally left blank

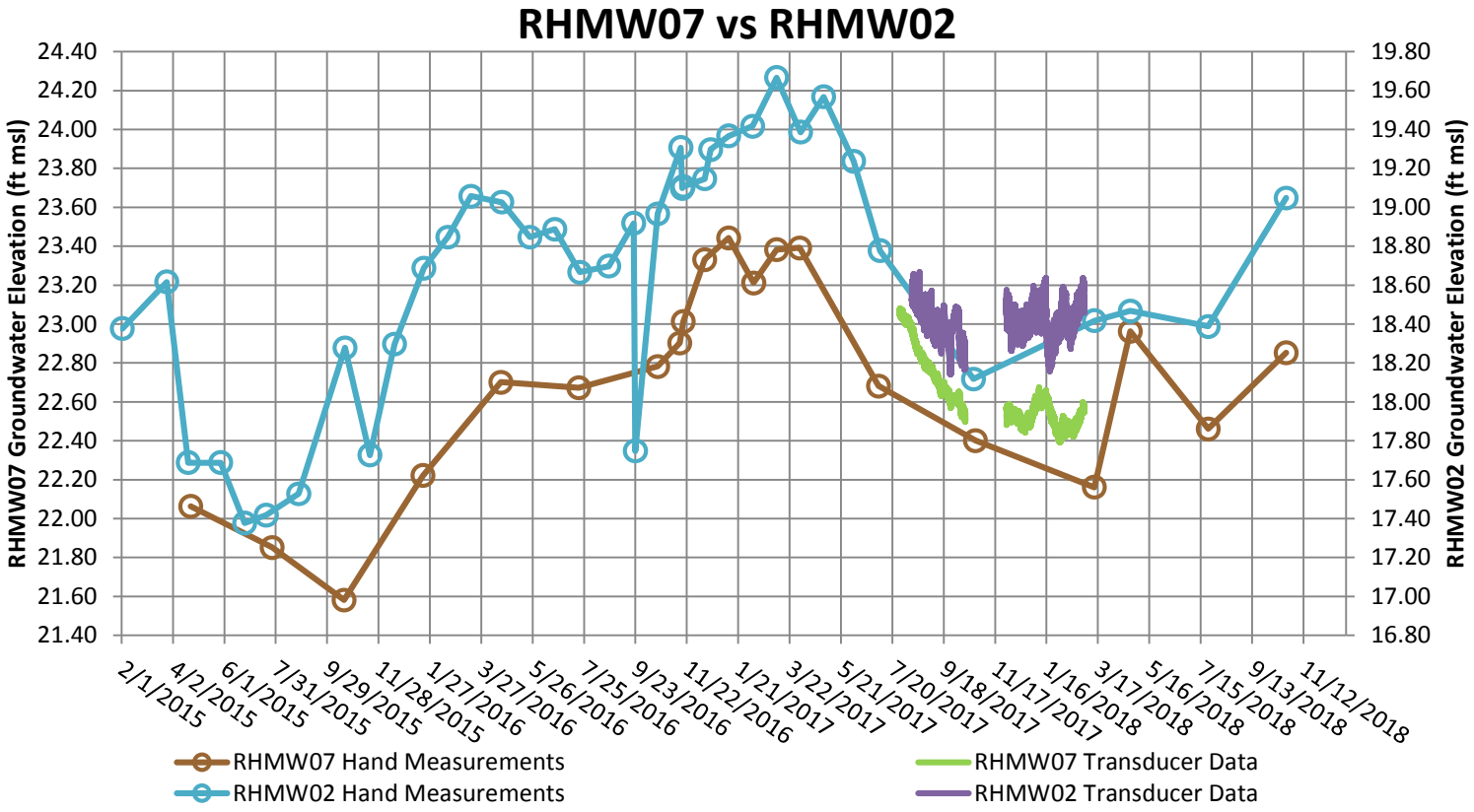

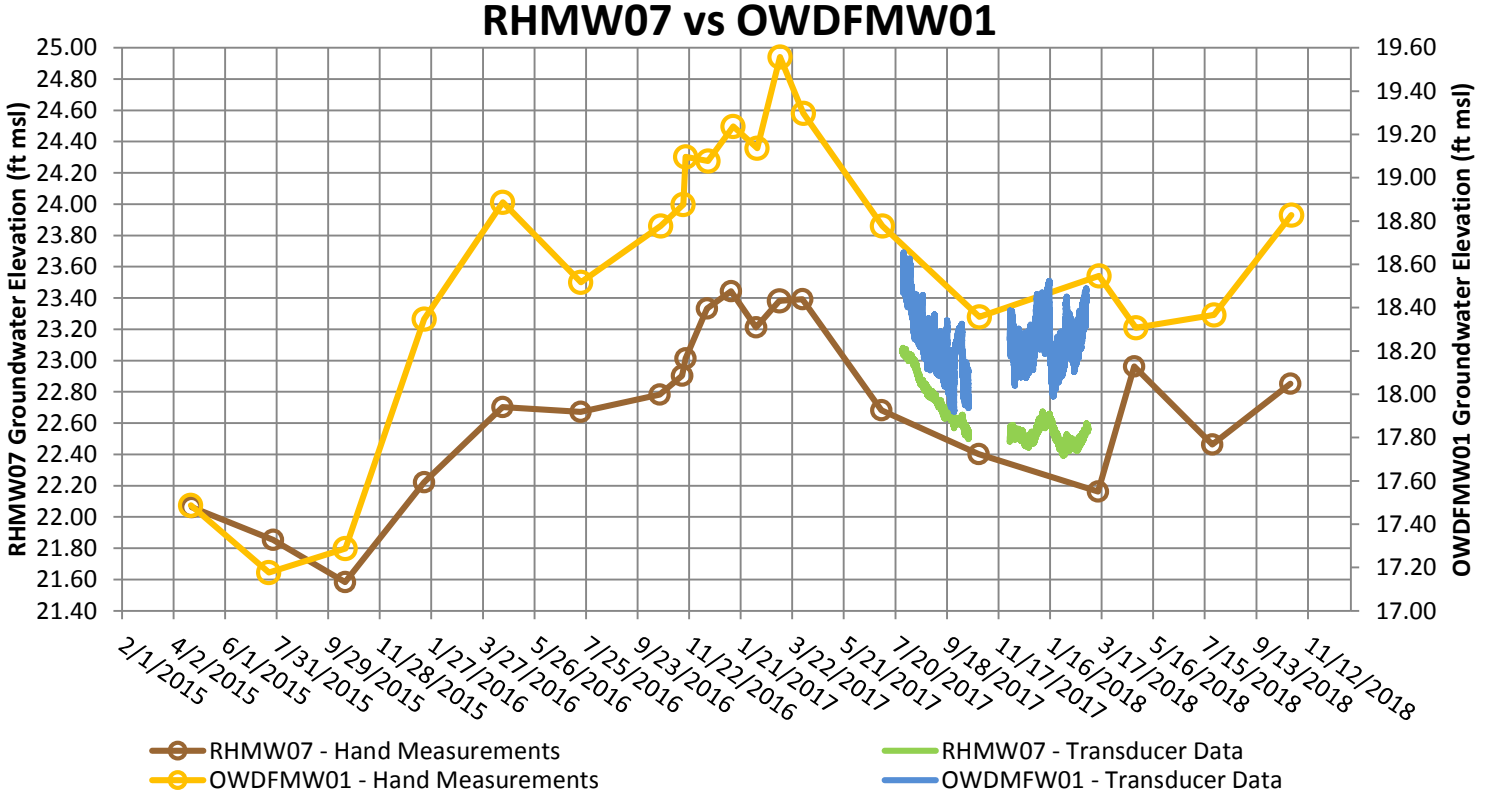

Notes:

- Synoptic water level data were corrected using the method prescribed by KGS BRF software (Bohling, Jin, and Butler 2011).
- Hand measurements were taken during groundwater LTM events. All hand measurements after 2017 were corrected using the *Well Elevation Survey* results and corrections from the gyroscopic survey (DON 2018a, 2018c).

Figure 6-1
Hydrographs of RHMW07 vs. RHWM02 and OWDFMW01
Conceptual Site Model Rev. 01
Investigation and Remediation of Releases and Groundwater Protection and Evaluation
Red Hill Bulk Fuel Storage Facility, JBPHH, O'ahu, Hawai'i

This page intentionally left blank

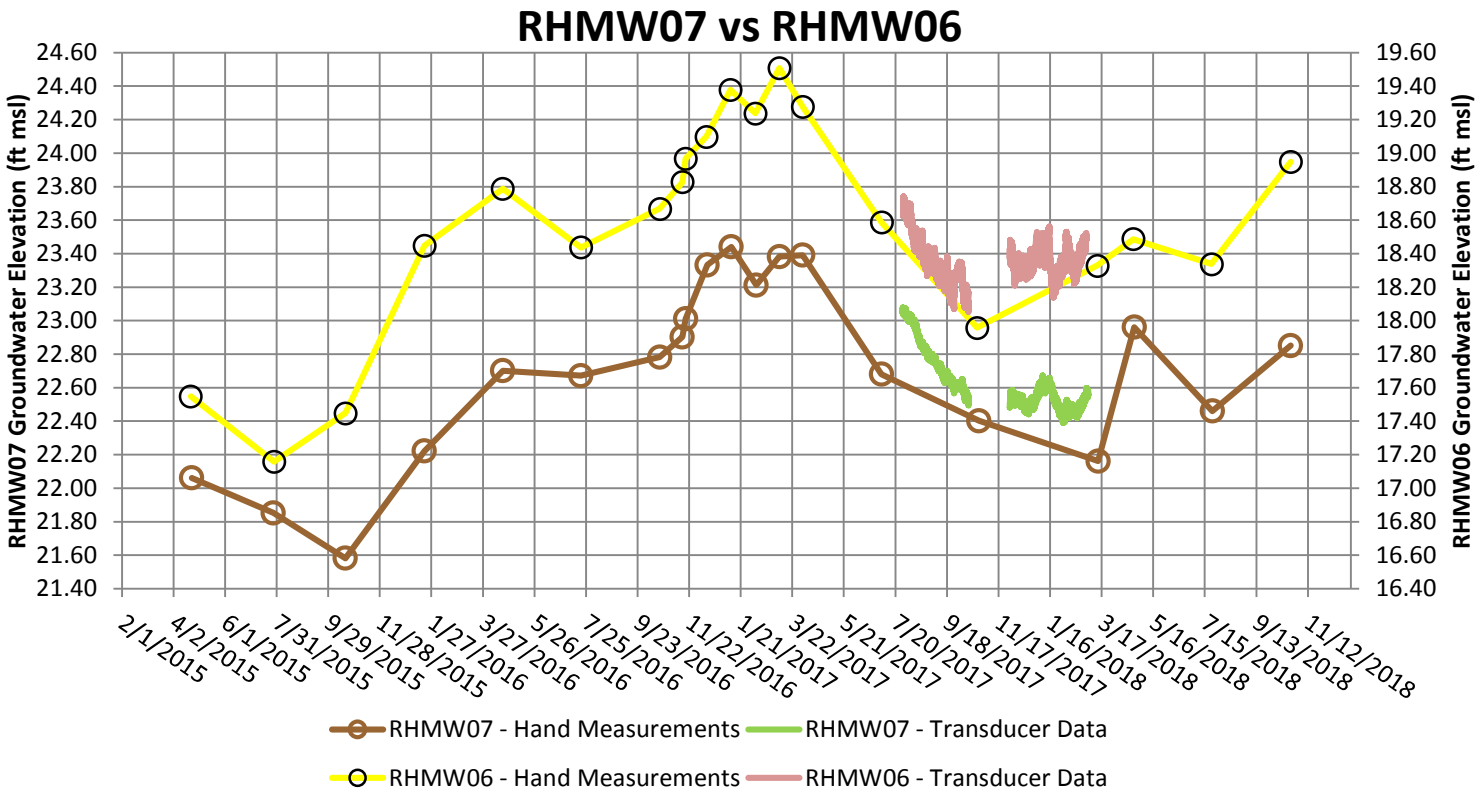

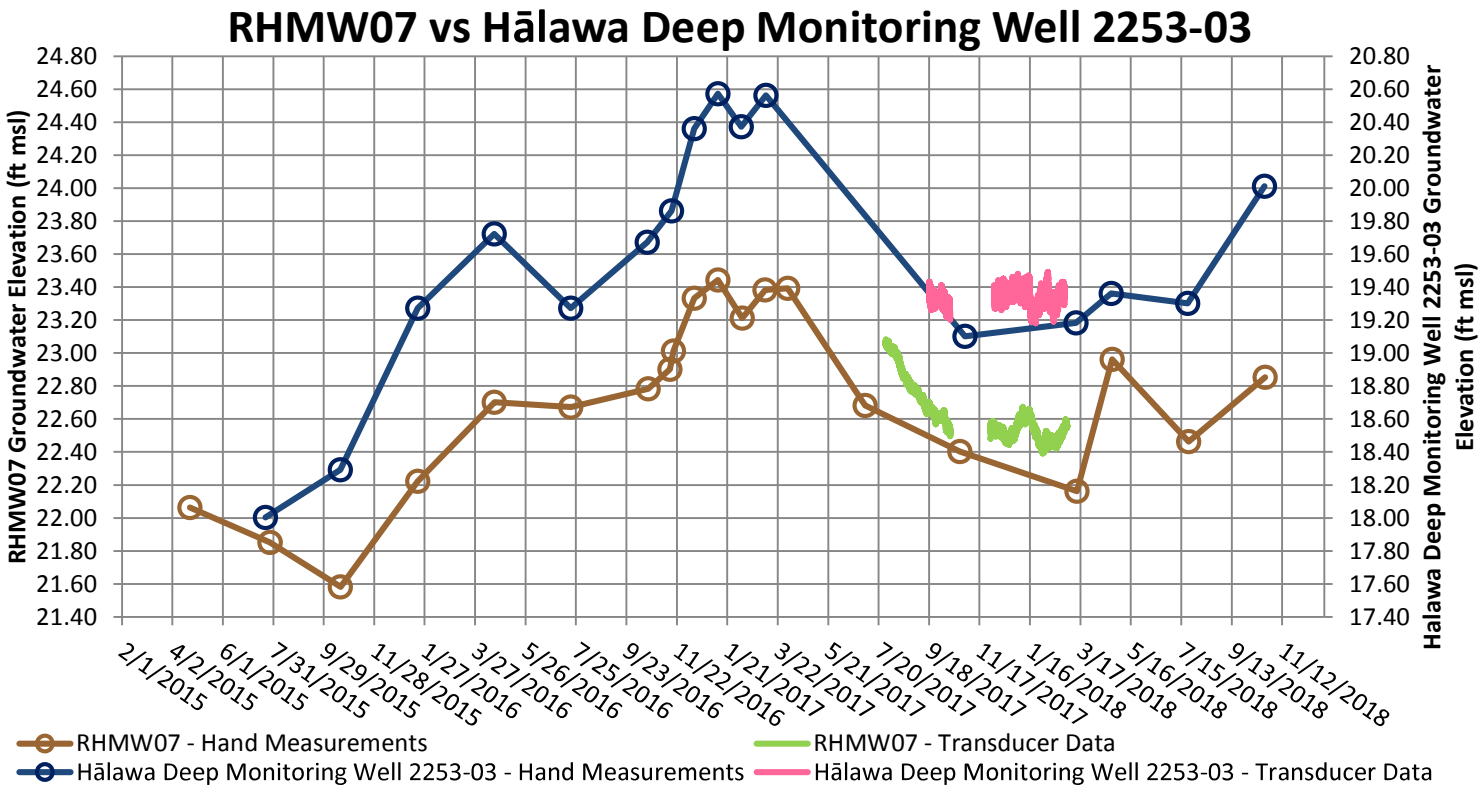

Notes:

- Synoptic water level data were corrected using the method prescribed by KGS BRF software (Bohling, Jin, and Butler 2011).
- Hand measurements were taken during groundwater LTM events. All hand measurements after 2017 were corrected using the *Well Elevation Survey* results and corrections from the gyroscopic survey (DON 2018a, 2018c).

Figure 6-2
Hydrographs of RHMW07 vs. RHWM06 and HDMW2253-03
Conceptual Site Model Rev. 01
Investigation and Remediation of Releases and Groundwater Protection and Evaluation
Red Hill Bulk Fuel Storage Facility, JBPHH, O'ahu, Hawai'i

This page intentionally left blank

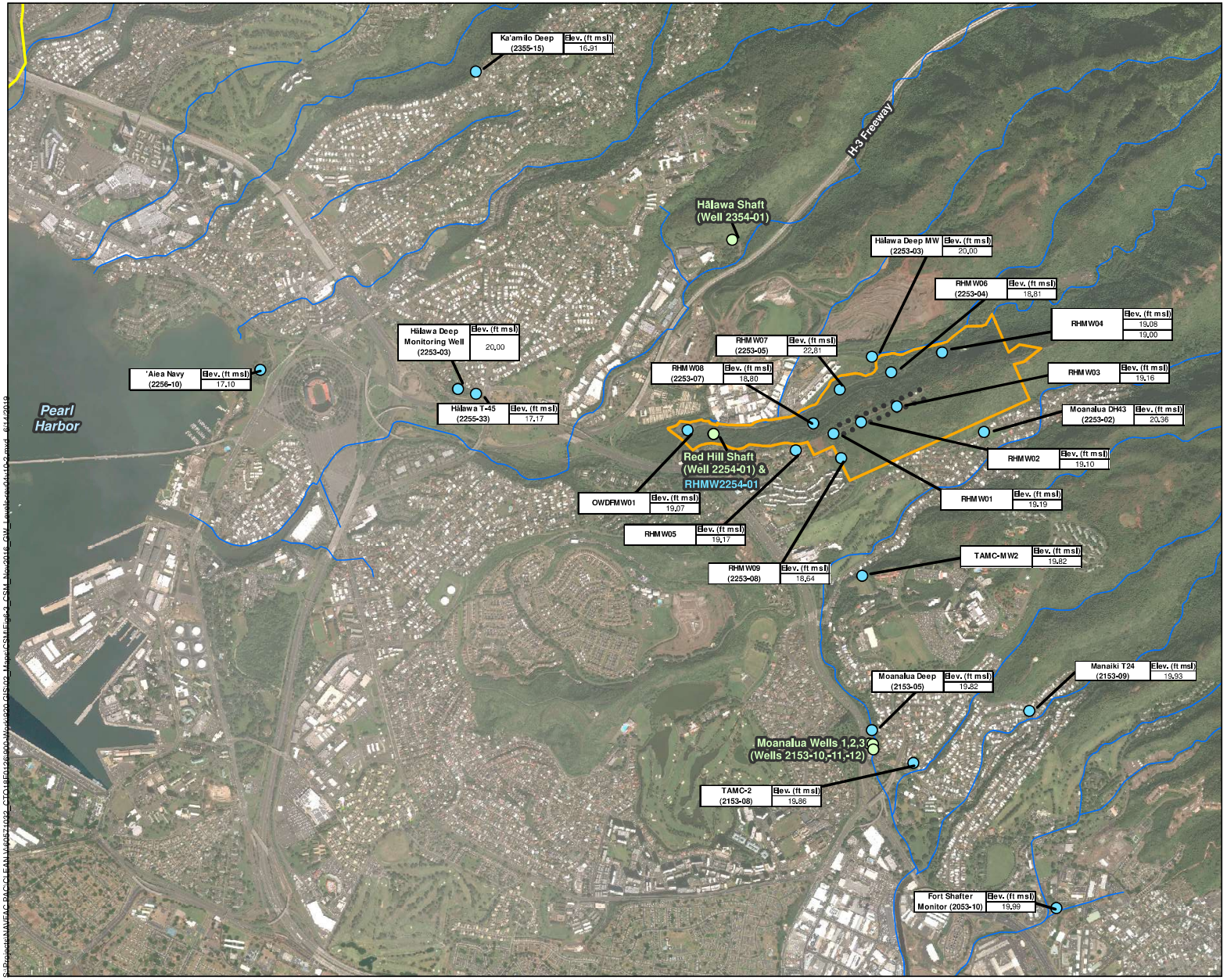

Location Map

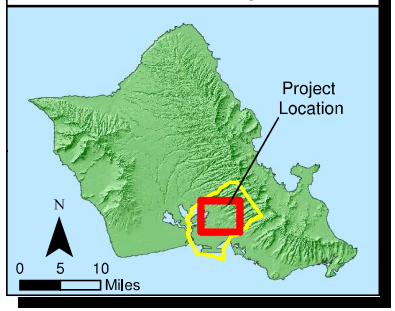

Legend

- Groundwater Monitoring Location
- Water Supply Well
- Groundwater Model Domain
- Red Hill Facility Boundary and Fuel Storage Tanks
- Stream

Notes

1. Map projection: NAD 1983 Hawaii State Plane Zone 3 feet
2. DigitalGlobe, Inc. (DG) and NRCS. Publication_Date: 2015
3. Definitions:
   - BWS Honolulu Board of Water Supply
   - ft foot or feet
   - msl mean sea level
   - MW monitoring well
   - NM not measured
4. All water levels were measured on 11/18/2016. Measurements were collected between 8:00am and 11:20am.

N

0 1,250 2,500 5,000 Feet

Figure 6-3
November 2016 Groundwater Levels
Conceptual Site Model Rev. 01
Investigation and Remediation of Releases and Groundwater Protection and Evaluation
Red Hill Bulk Fuel Storage Facility
JBPHH, O'ahu, Hawai'i

S:\Projects\NAVFAC_PAC\CLEAN\605721029_CTO11\FIG\105\00\Work\2020\GIS\02_Maps\GSM\Fig6-3_GSM_Nov2016_GW_Levels_rev04\10-2.mxd 8/14/2019

This page intentionally left blank

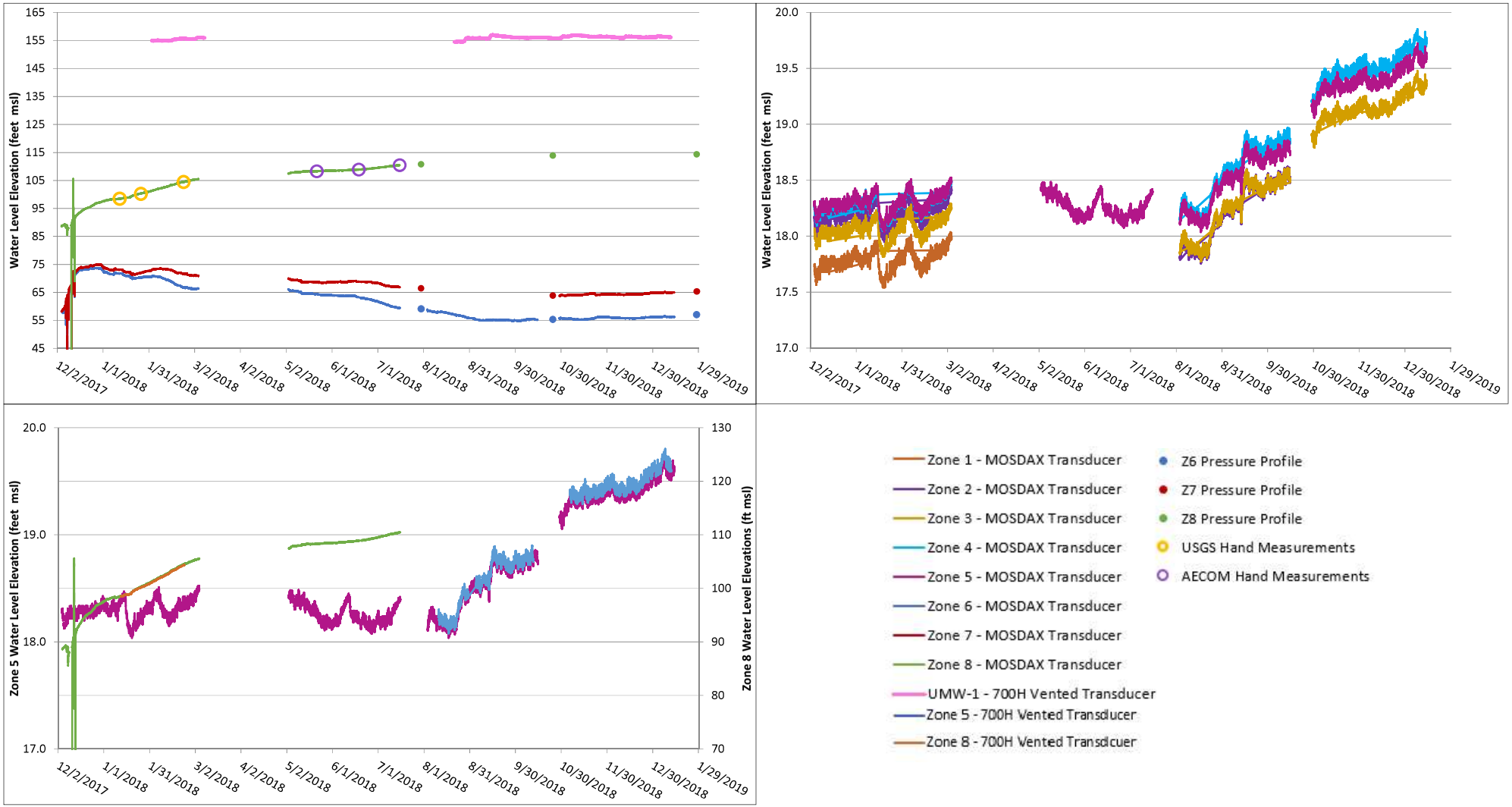

Figure 6-4
RHMW11 – Long-Term Water Level Elevations
Conceptual Site Model Rev. 01
Investigation and Remediation of Releases and Groundwater Protection and Evaluation
Red Hill Bulk Fuel Storage Facility
JBPHH, O'ahu, Hawai'i

This page intentionally left blank

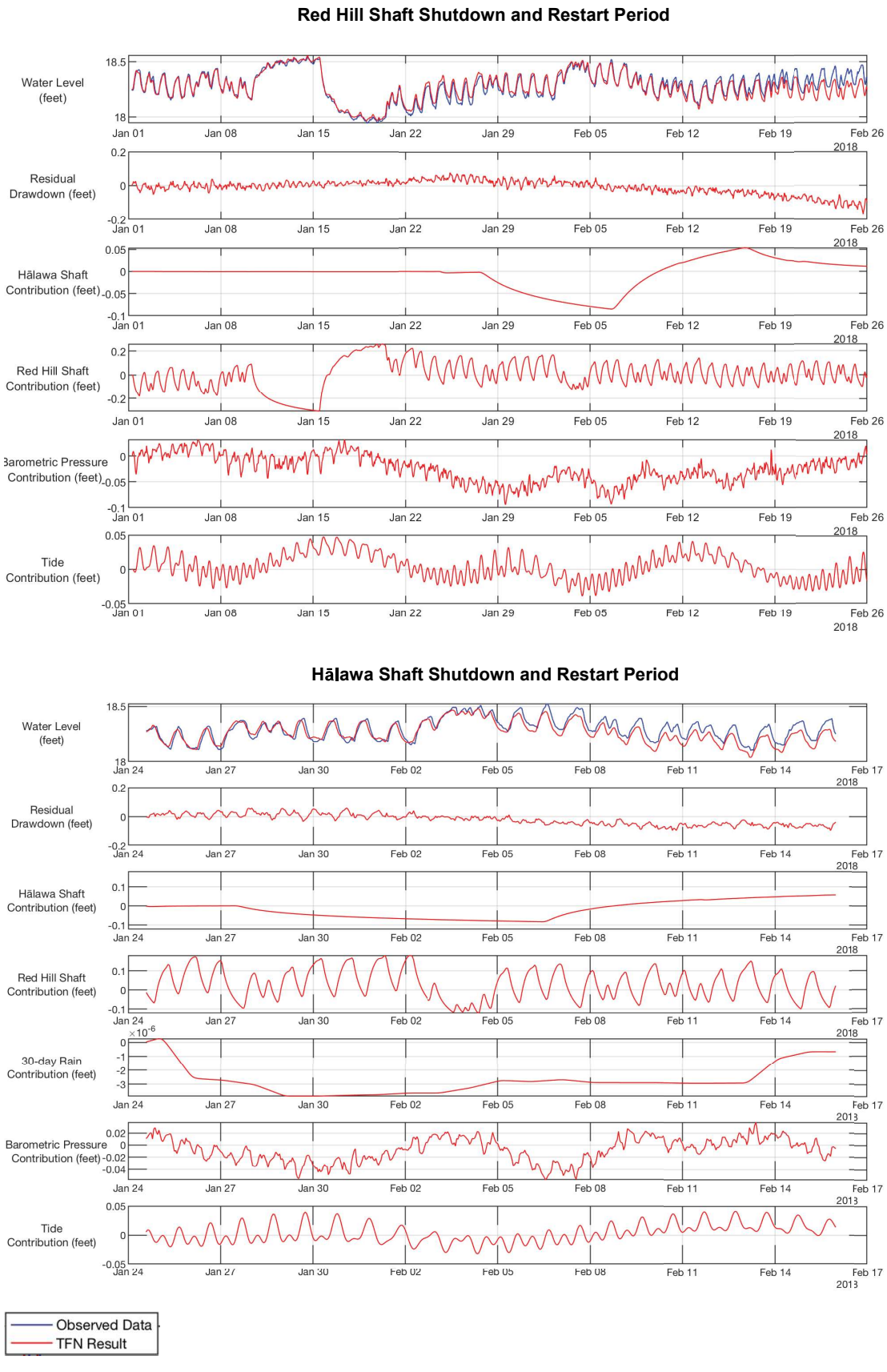

Figure 6-5
TFN Analysis Results for RHMW08
Conceptual Site Model Rev. 01
Investigation and Remediation of Releases and Groundwater Protection and Evaluation
Red Hill Bulk Fuel Storage Facility
JBPHH, O‘ahu, Hawai‘i

This page intentionally left blank

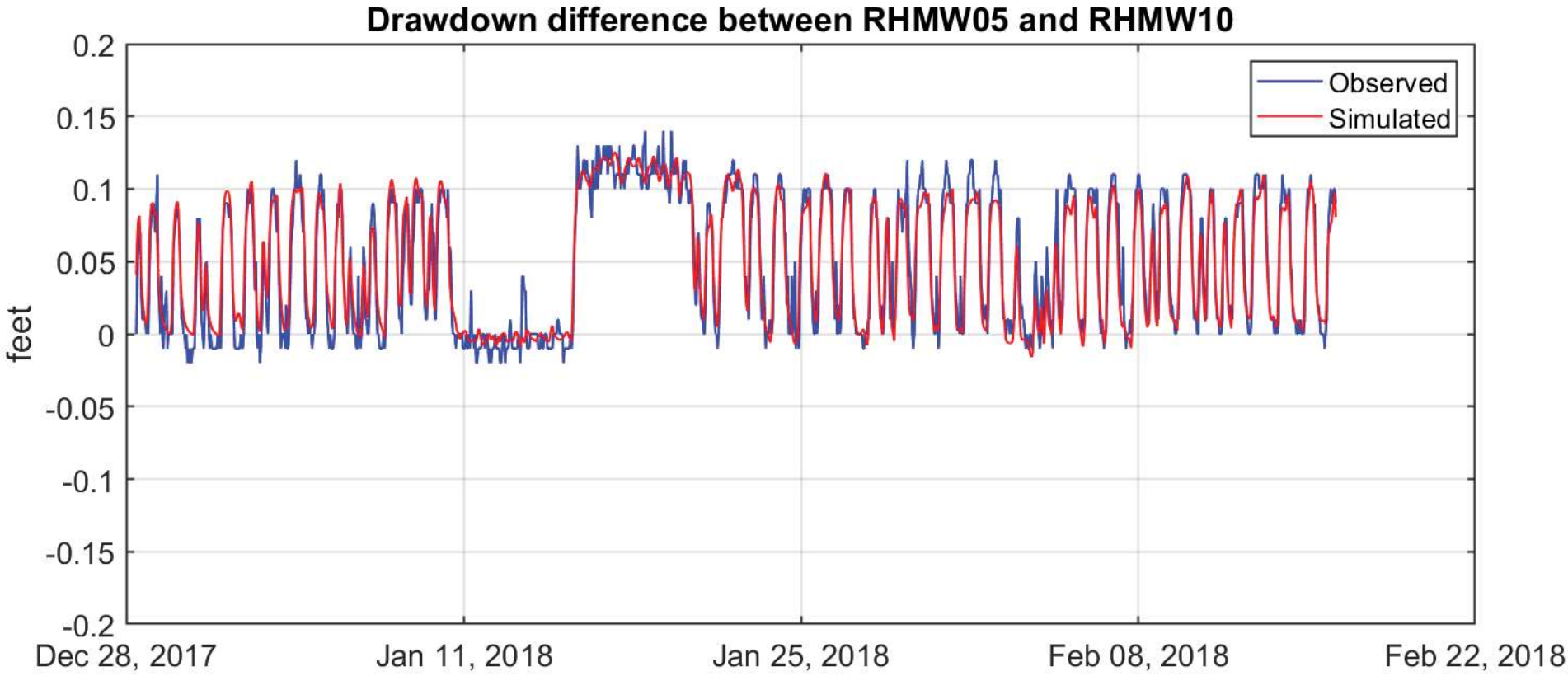

Figure 6-6
Comparison of Observed and Computed Differences between Water Level at RHMW05 and RHMW10
Conceptual Site Model Rev. 01
Investigation and Remediation of Releases and Groundwater Protection and Evaluation
Red Hill Bulk Fuel Storage Facility
JBPHH, Oʻahu, Hawaiʻi

This page intentionally left blank

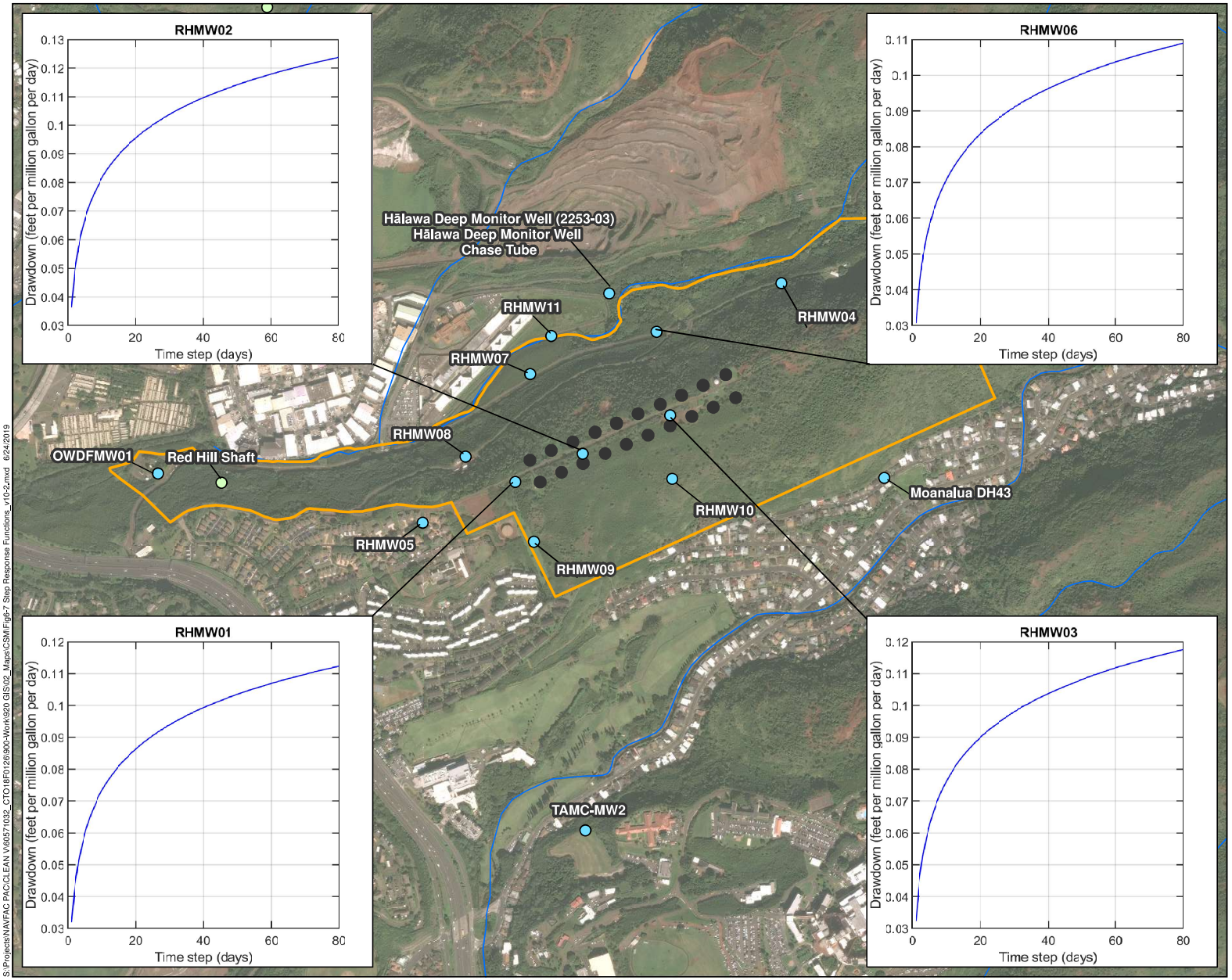

S:\Projects\NAVFAC PAC\CLEAN V\60571032_CTO18F0126\900-Work\920 GIS\02_Maps\CSM\Fig6-7 Step Response Functions_v10-2.mxd 6/24/2019

Location Map

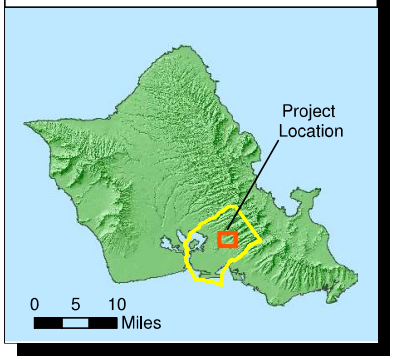

Legend

- Red Hill Fuel Storage Tank
- Supply Well
- Monitoring Well
- Groundwater Model Domain
- Red Hill Facility Boundary
- Stream

Notes

1. Map projection: NAD 1983 Hawaii State Plane Zone 3 (feet)
2. DigitalGlobe, Inc. (DG) and NRCS. Publication_Date: 2015

N

0 500 1,000 2,000 Feet

Figure 6-7
Examples of Unit Step Response Functions Associated with Red Hill Shaft Pumping
Conceptual Site Model Rev. 01
Investigation and Remediation of Releases and Groundwater Protection and Evaluation
Red Hill Bulk Fuel Storage Facility
JBPHH, O'ahu, Hawai'i

This page intentionally left blank

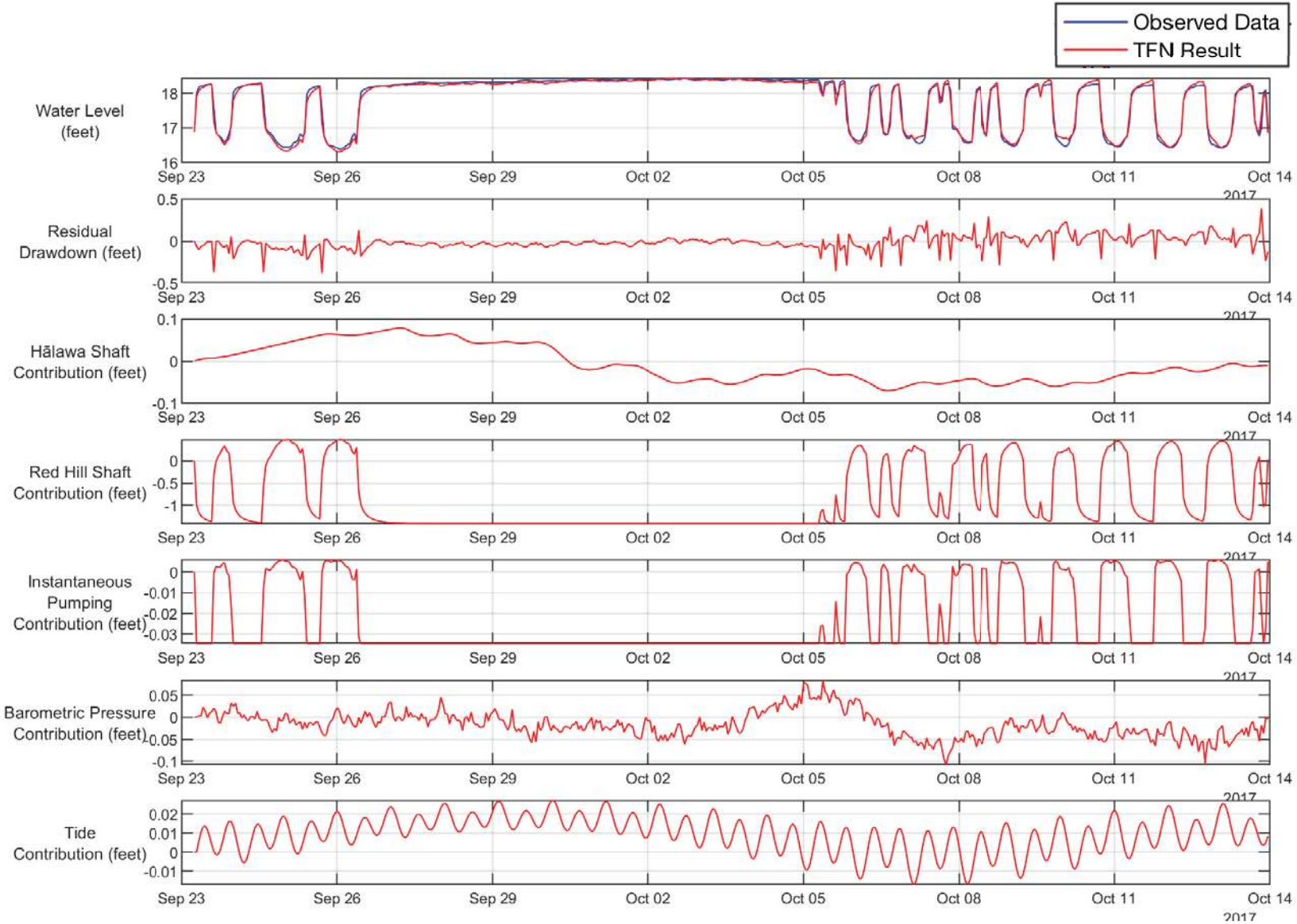

Figure 6-8
TFN Analysis Results for Red Hill Shaft
Conceptual Site Model Rev. 01
Investigation and Remediation of Releases and Groundwater Protection and Evaluation
Red Hill Bulk Fuel Storage Facility
JBPHH, O‘ahu, Hawai‘i

This page intentionally left blank

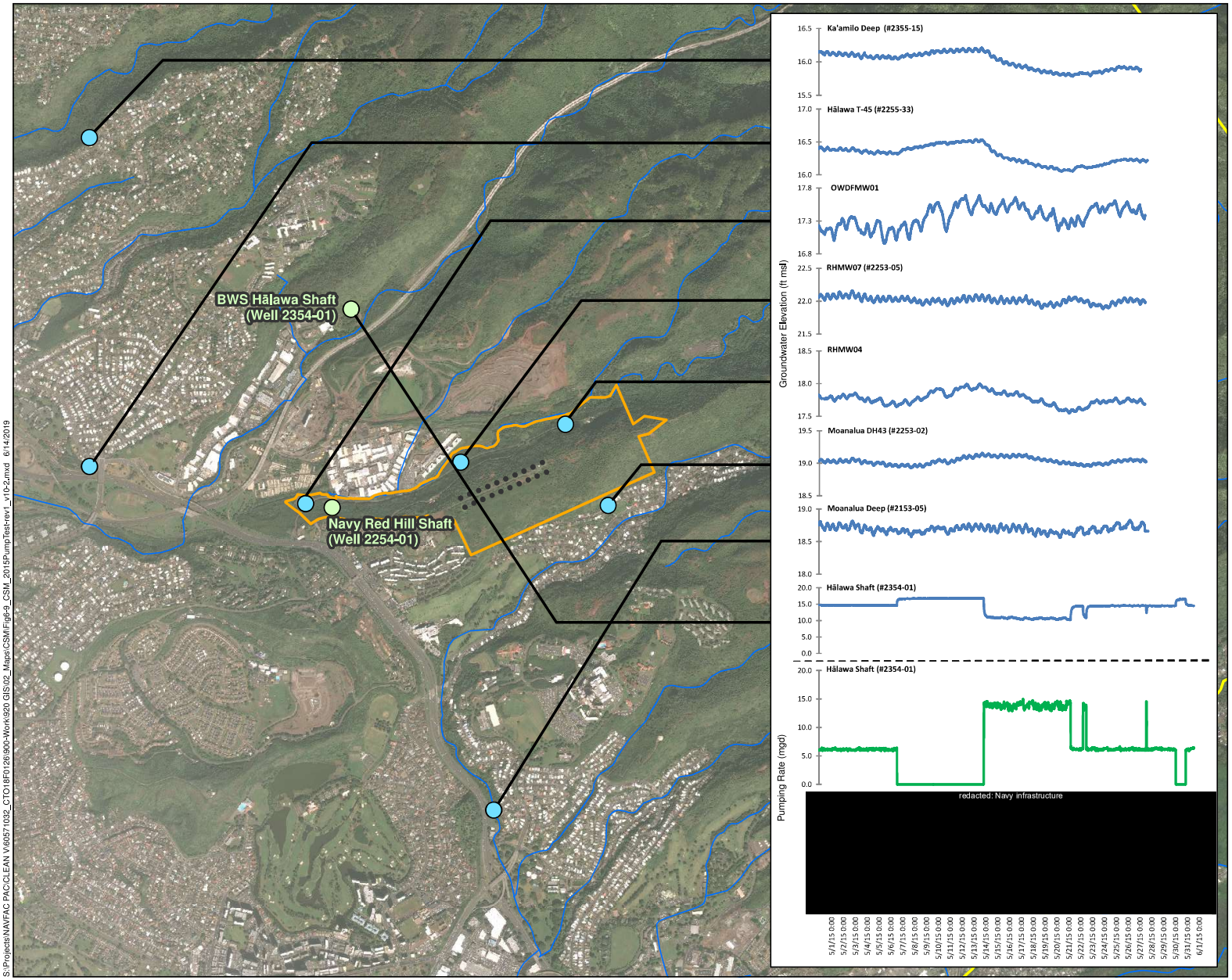

Location Map

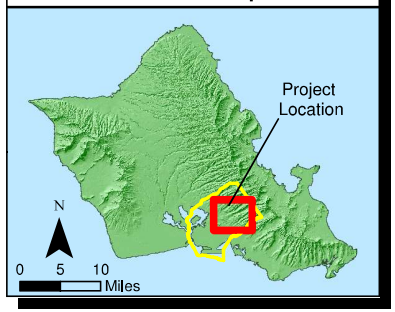

Legend

- Monitoring / Observation Well
- Water Supply Well
- Groundwater Model Domain
- Red Hill Facility Boundary and Fuel Storage Tanks
- Stream

Notes

1. Map projection: NAD 1983 Hawaii State Plane Zone 3 (feet)
2. DigitalGlobe, Inc. (DG) and NRCS. Publication_Date: 2015

N

0 1,250 2,500 5,000 Feet

S:\Projects\NAVFAC PAC\CLEAN V\60571032_CTO18F0126\900-Work\920 GIS\02_Maps\CSM\Fig6-9_CSM_2015PumpTest-rev1_v10-2.mxd 6/14/2019

Figure 6-9
Time-Series Plots of Water Level Data at Area Monitoring Wells during 2015 USGS Pumping Test at Red Hill Shaft and Hālawa Shaft
Conceptual Site Model Rev. 01
Investigation and Remediation of Releases and Groundwater Protection and Evaluation
Red Hill Bulk Fuel Storage Facility
JBPHH, O'ahu, Hawai'i

This page intentionally left blank

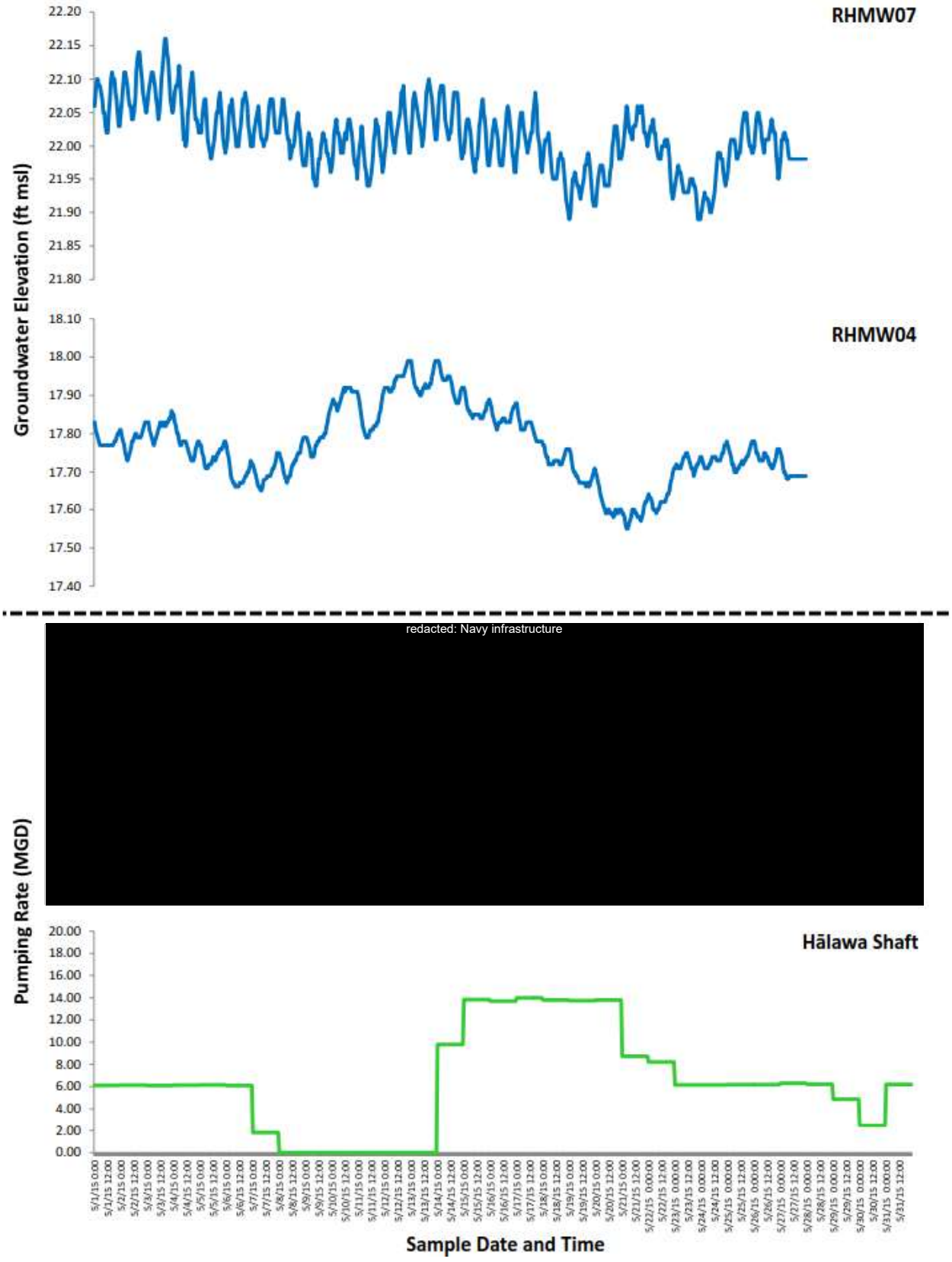

Figure 6-10
Groundwater Levels in RHMW04 and RHMW07 and Pumping Rates during May 2015
Conceptual Site Model Rev. 01
Investigation and Remediation of Releases and Groundwater Protection and Evaluation
Red Hill Bulk Fuel Storage Facility, JBPHH, O'ahu, Hawai'i

This page intentionally left blank

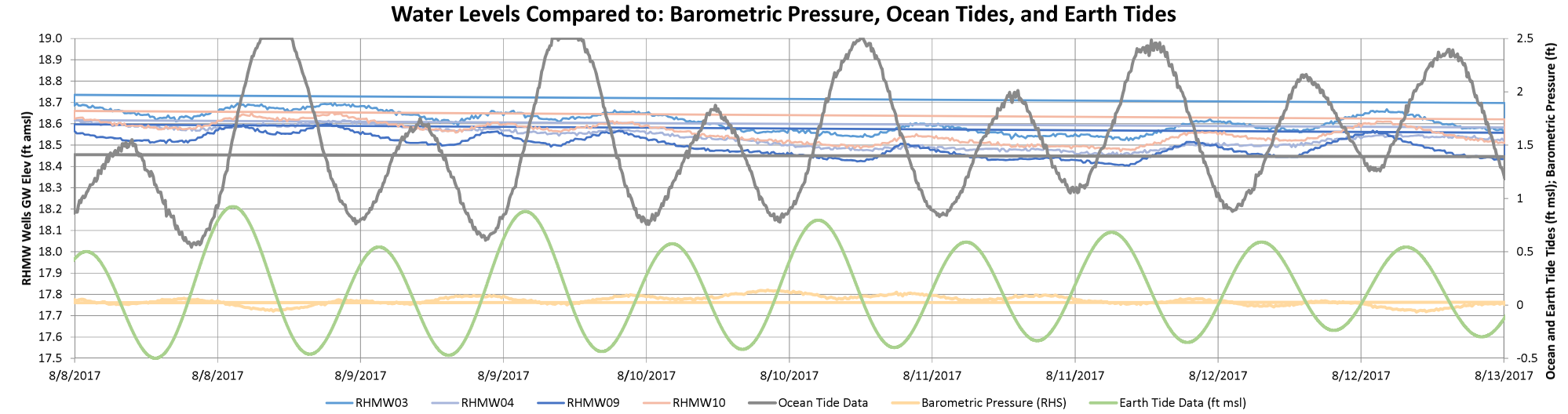

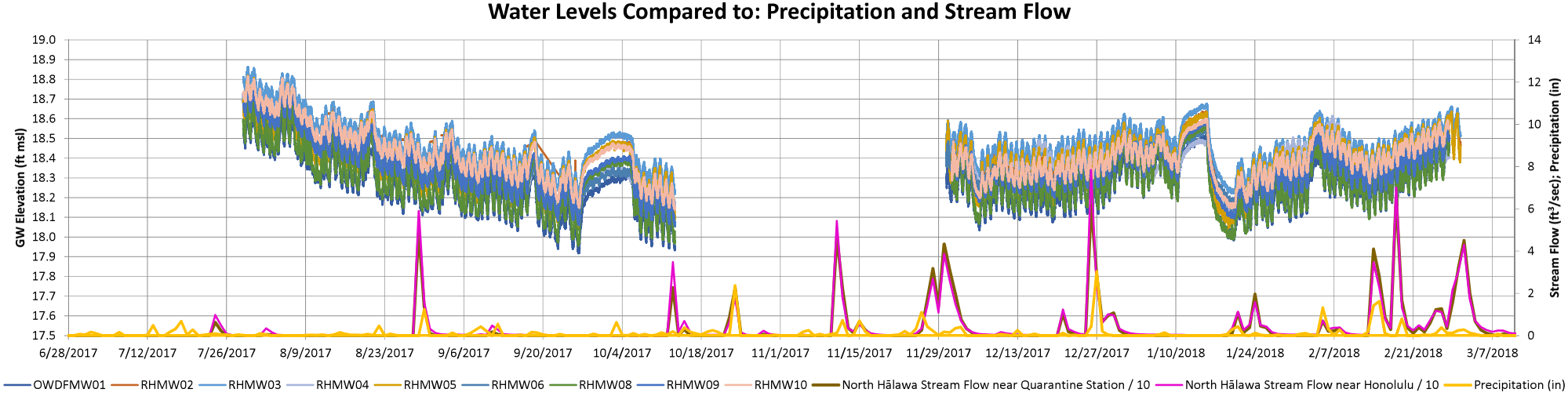

Figure 6-11
Possible Effects on Water Levels
Conceptual Site Model Rev. 01
Investigation and Remediation of Releases and Groundwater Protection and Evaluation
Red Hill Bulk Fuel Storage Facility
JBPHH, O'ahu, Hawai'i

This page intentionally left blank

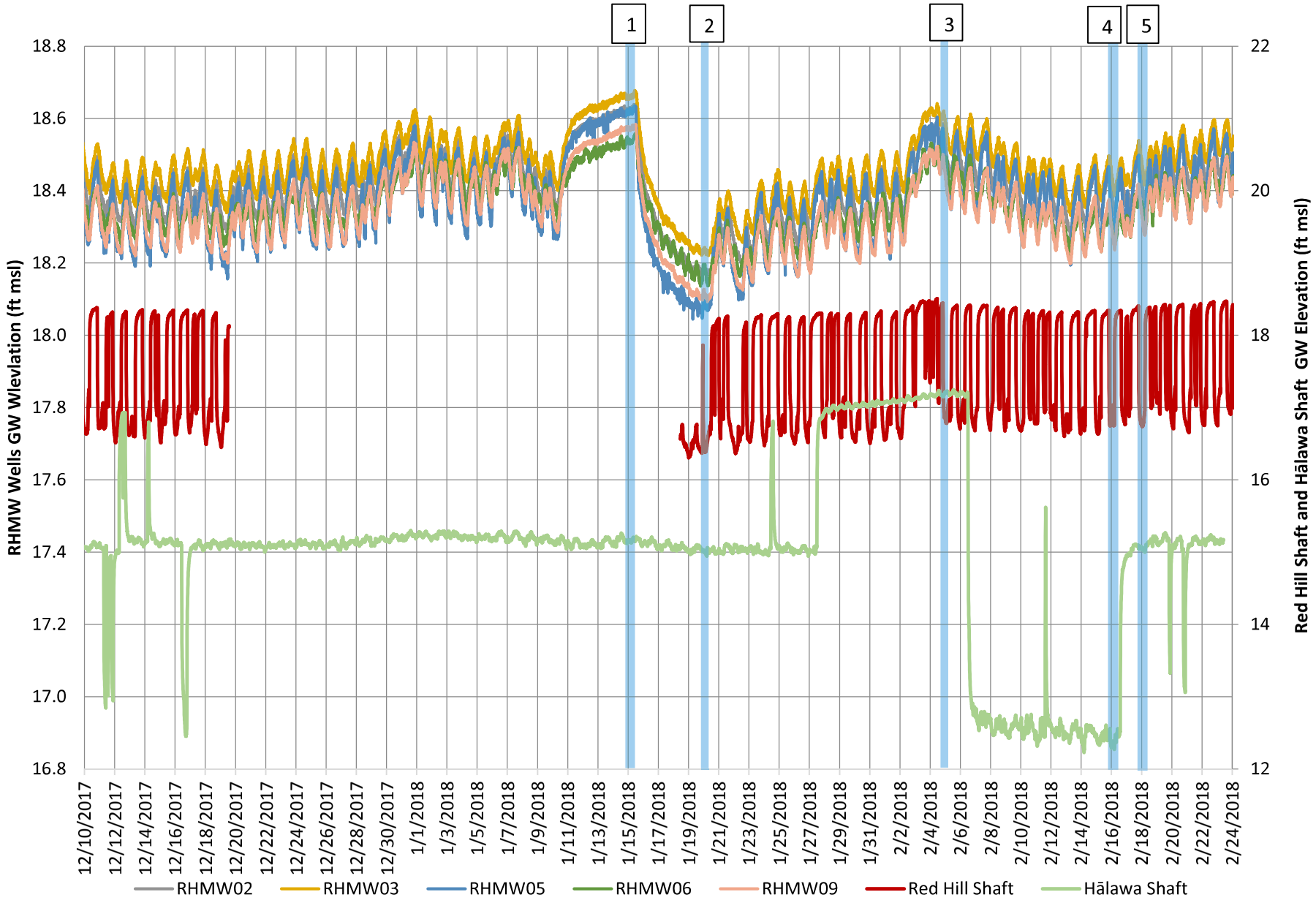

Figure 6-12
BRF Corrected Water Levels and Selected Time Periods
Conceptual Site Model Rev. 01
Investigation and Remediation of Releases and Groundwater Protection and Evaluation
Red Hill Bulk Fuel Storage Facility
JBPHH, O‘ahu, Hawai‘i

This page intentionally left blank

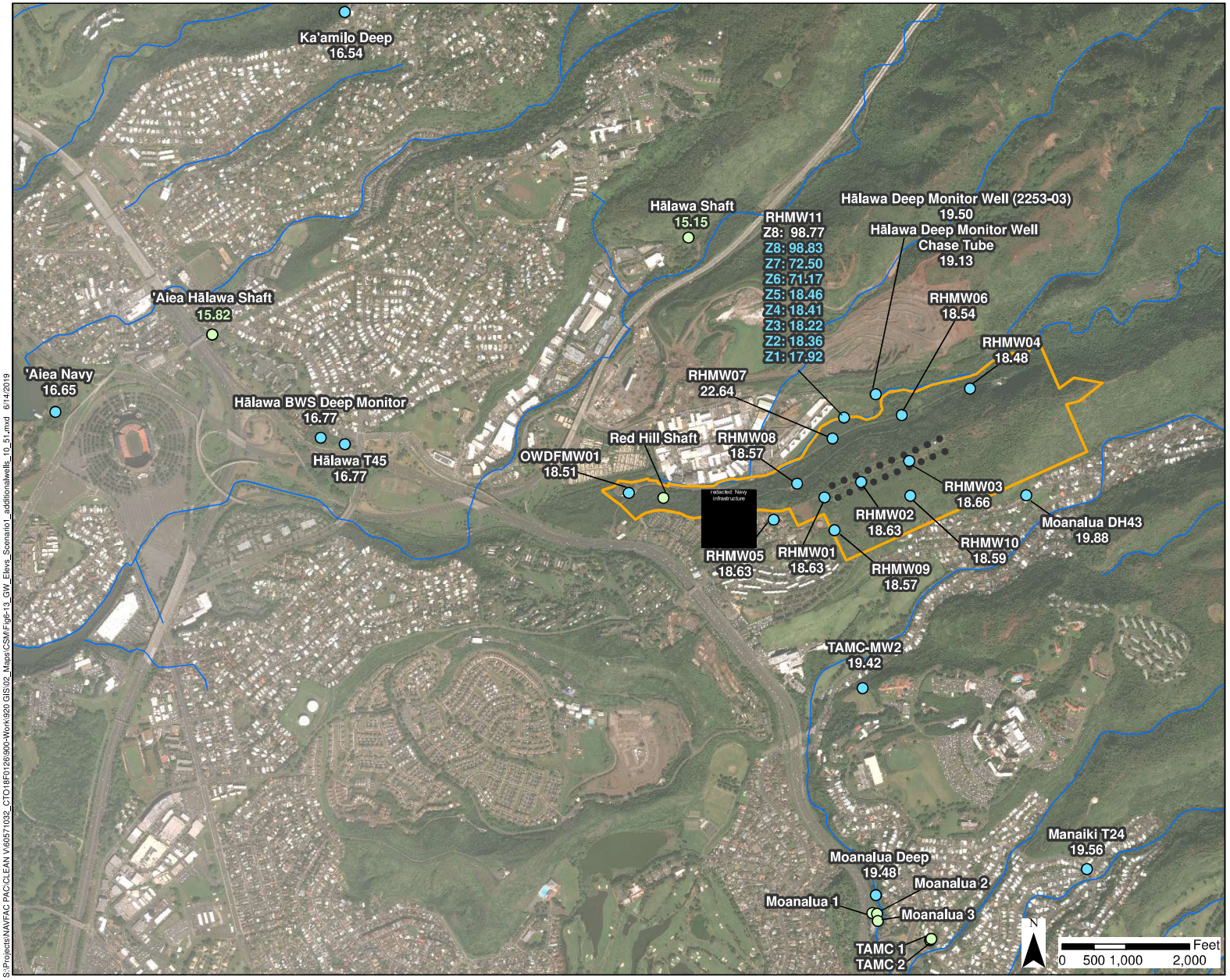

Location Map

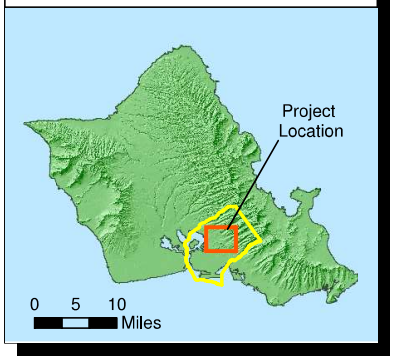

Legend

- Clinker
- Red Hill Fuel Storage Tank
- Supply Well
- Monitoring Well
- Groundwater Model Domain
- Red Hill Facility Boundary
- Stream

Notes

1. Map projection: NAD 1983 Hawaii State Plane Zone 3 (feet)
2. DigitalGlobe, Inc. (DG) and NRCS. Publication_Date: 2015
3. BRF corrections were applied to all water levels, but excluded RHMW11 Z6, Z7, Z8, and supply wells.

Z1: 17.91 indicates measurement was made in a Westbay sampling port

15.15 indicates measurement was made in a pumping well

Figure 6-13
Time 1: Red Hill Shaft Off (At Max Recovery), Hālawa Shaft Average Pumping 01/15/2018 6:00
Conceptual Site Model Rev. 01
Investigation and Remediation of Releases and Groundwater Protection and Evaluation
Red Hill Bulk Fuel Storage Facility
JBPHH, O'ahu, Hawai'i

S:\Projects\NAVFAC PAC\CLEAN V\60571032_CTO18F0126\900-Work\920 GIS\02_Maps\CSM\Fig6-13_GW_Elevs_Scenario1_additionalwells_10_51.mxd 6/14/2019

This page intentionally left blank

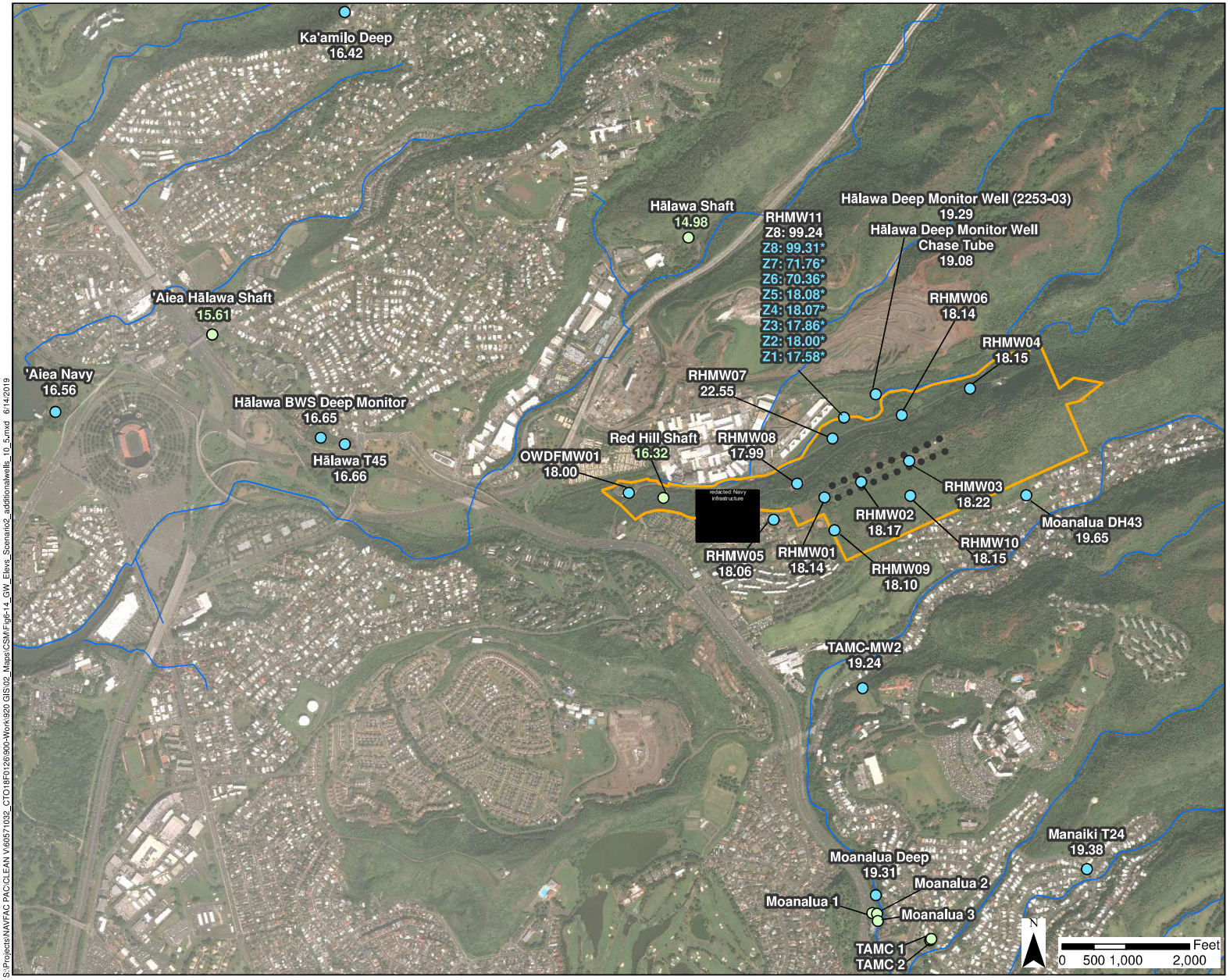

S:\Projects\NAVFAC PAC\CLEAN V\60571032_CTO18F0126\900-Work\920 GIS\02_Maps\CSM\Fig6-14_GW_Elevs_Scenario2_additionalwells_10_5.mxd 6/14/2019

Location Map

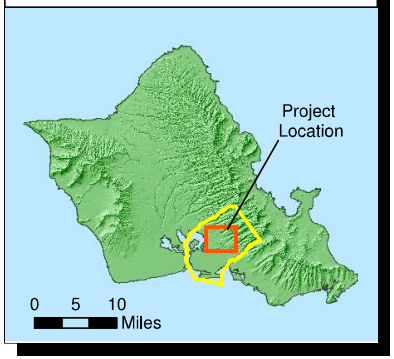

Legend

- Clinker
- Red Hill Fuel Storage Tank
- Supply Well
- Monitoring Well
- Groundwater Model Domain
- Red Hill Facility Boundary
- Stream

Notes

1. Map projection: NAD 1983 Hawaii State Plane Zone 3 (feet)
2. DigitalGlobe, Inc. (DG) and NRCS. Publication_Date: 2015
3. BRF corrections were applied to all water levels, but excluded RHMW11 Z6, Z7, Z8, and supply wells.

* Measurment recorded at 21:00

Z1: 17.91 indicates measurement was made in a Westbay sampling port

15.15 indicates measurement was made in a pumping well

Figure 6-14
Time 2: Red Hill Shaft At Max Pumping
Hālawa Shaft Average Pumping 01/19/2018 21:10
Conceptual Site Model Rev. 01
Investigation and Remediation of Releases and Groundwater Protection and Evaluation
Red Hill Bulk Fuel Storage Facility
JBPHH, O'ahu, Hawai'i

This page intentionally left blank

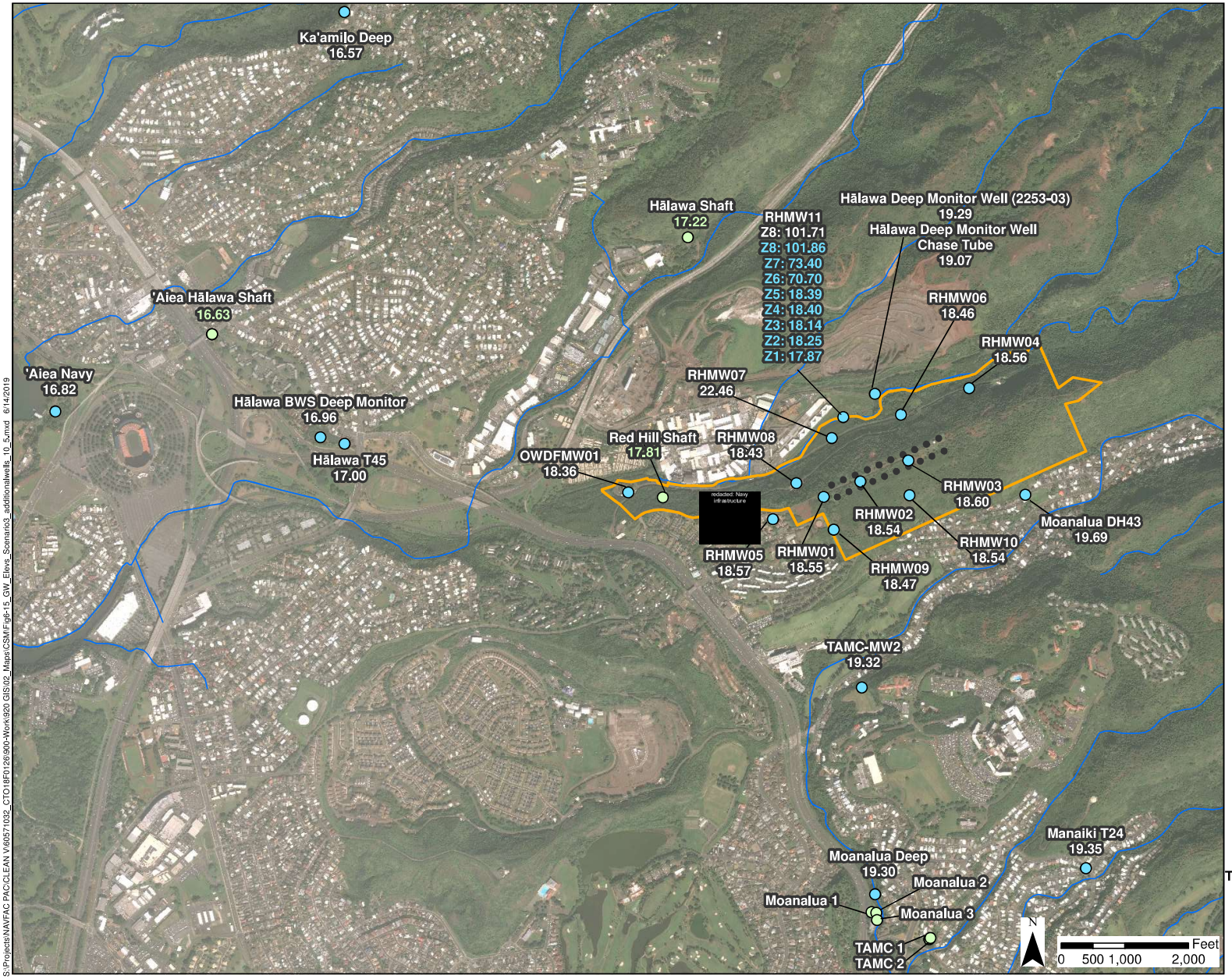

Location Map

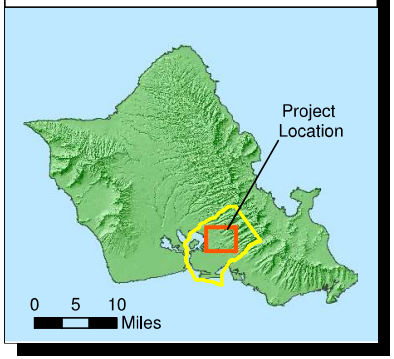

Legend

- Clinker
- Red Hill Fuel Storage Tank
- Supply Well
- Monitoring Well
- Groundwater Model Domain
- Red Hill Facility Boundary
- Stream

Notes

1. Map projection: NAD 1983 Hawaii State Plane Zone 3 (feet)
2. DigitalGlobe, Inc. (DG) and NRCS. Publication_Date: 2015
3. BRF corrections were applied to all water levels, but excluded RHMW11 Z6, Z7, Z8, and supply wells.

Z1: 17.91 indicates measurement was made in a Westbay sampling port

15.15 indicates measurement was made in a pumping well

Figure 6-15
Time 3: Red Hill Shaft Business as Usual Pumping
Hālawa Shaft Off 02/05/2018 19:00
Conceptual Site Model Rev. 01
Investigation and Remediation of Releases and Groundwater Protection and Evaluation
Red Hill Bulk Fuel Storage Facility
JBPHH, O'ahu, Hawai'i

S:\Projects\NAVFAC PAC\CLEAN V\60571032_CTO18F0126\900-Work\920 GIS\02_Maps\CSM\Fig6-15_GW_Elevs_Scenario3_additionalwells_10_5.mxd 6/14/2019

This page intentionally left blank

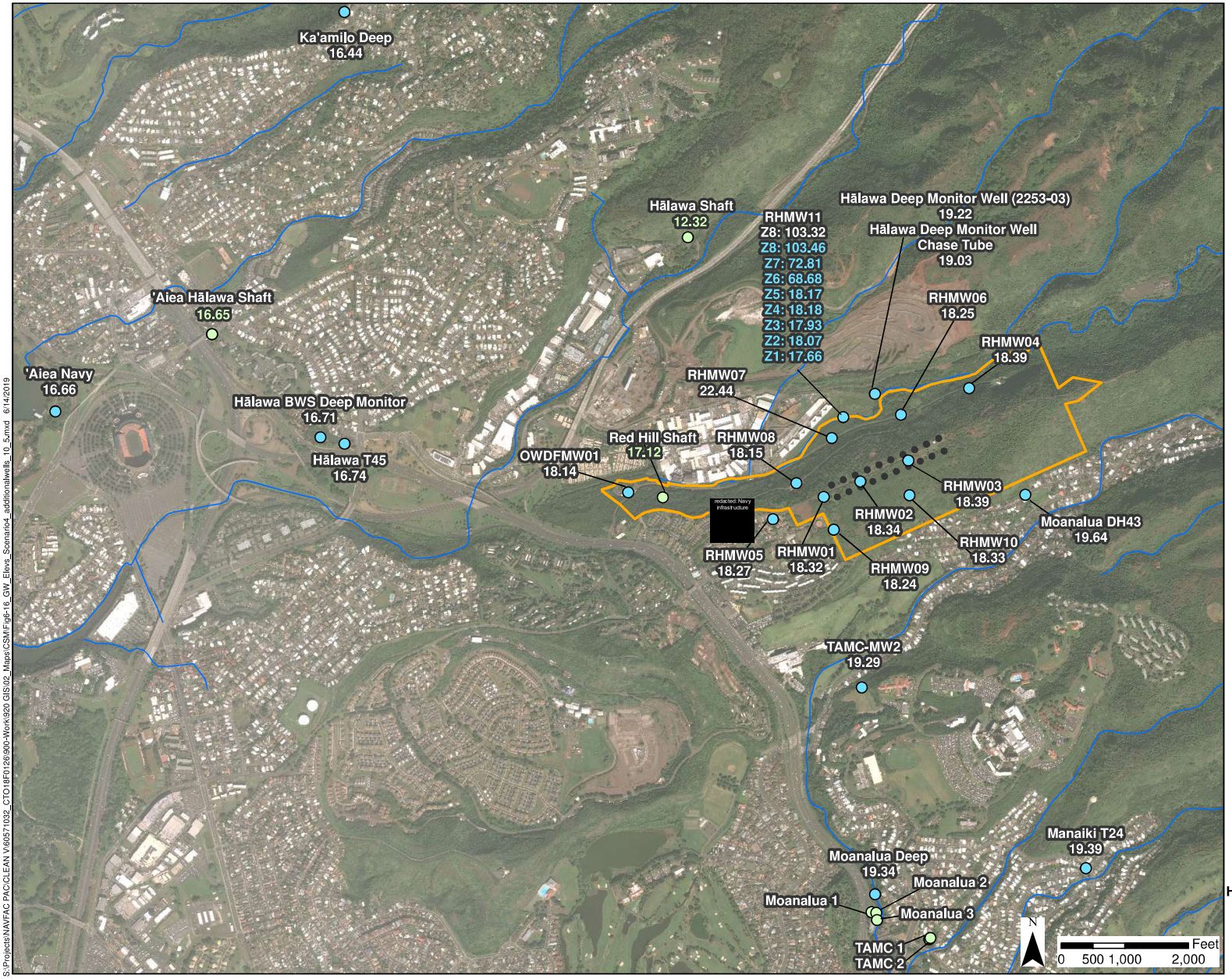

S:\Projects\NAVFAC PAC\CLEAN V\60571032_CTO18F0126\900-Work\920 GIS\02_Maps\CSM\Fig6-16_GW_Elevs_Scenario4_additionalwells_10_5.mxd 6/14/2019

Location Map

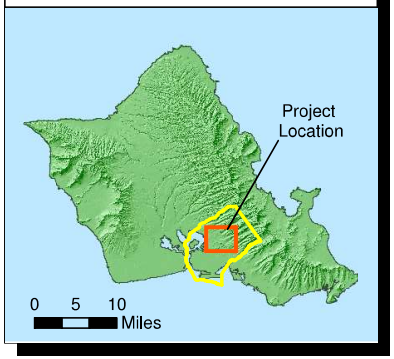

Legend

- Clinker
- Red Hill Fuel Storage Tank
- Supply Well
- Monitoring Well
- Groundwater Model Domain
- Red Hill Facility Boundary
- Stream

Notes

1. Map projection: NAD 1983 Hawaii State Plane Zone 3 (feet)
2. DigitalGlobe, Inc. (DG) and NRCS. Publication_Date: 2015
3. BRF corrections were applied to all water levels, but excluded RHMW11 Z6, Z7, Z8, and supply wells.

Z1: 17.91 indicates measurement was made in a Westbay sampling port

15.15 indicates measurement was made in a pumping well

Figure 6-16
Time 4: Red Hill Shaft Business as Usual
Hālawa Shaft at Maximum Pumping 02/16/2018 5:00
Conceptual Site Model Rev. 01
Investigation and Remediation of Releases and Groundwater Protection and Evaluation
Red Hill Bulk Fuel Storage Facility
JBPHH, O'ahu, Hawai'i

This page intentionally left blank

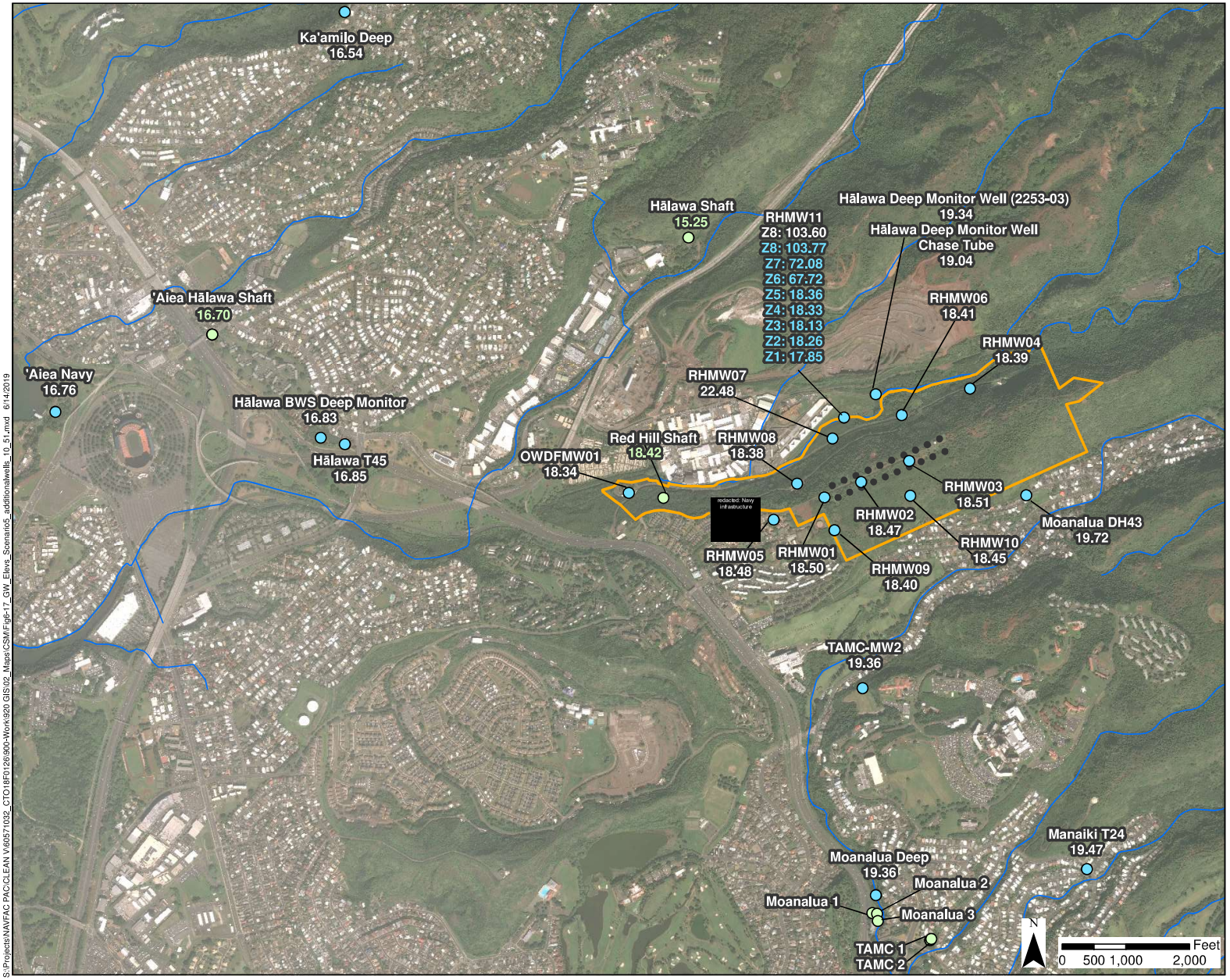

Location Map

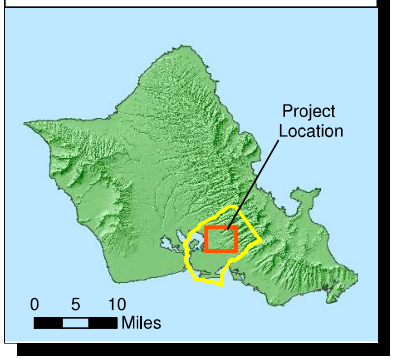

Legend

- Clinker
- Red Hill Fuel Storage Tank
- Supply Well
- Monitoring Well
- Groundwater Model Domain
- Red Hill Facility Boundary
- Stream

Notes

1. Map projection: NAD 1983 Hawaii State Plane Zone 3 (feet)
2. DigitalGlobe, Inc. (DG) and NRCS. Publication_Date: 2015
3. BRF corrections were applied to all water levels, but excluded RHMW11 Z6, Z7, Z8, and supply wells.

Z1: 17.91 indicates measurement was made in a Westbay sampling port

15.15 indicates measurement was made in a pumping well

Figure 6-17
Time 5: Red Hill Shaft Business as Usual
Hālawa Shaft Average Pumping 02/19/2018 13:00
Conceptual Site Model Rev. 01
Investigation and Remediation of Releases and Groundwater Protection and Evaluation
Red Hill Bulk Fuel Storage Facility
JBPHH, O'ahu, Hawai'i

S:\Projects\NAVFAC PAC\CLEAN V\60571032_CTO18F0126\900-Work\920 GIS\02_Maps\CSM\Fig6-17_GW_Elevs_Scenario5_additionalwells_10_51.mxd 6/14/2019

This page intentionally left blank

Location Map

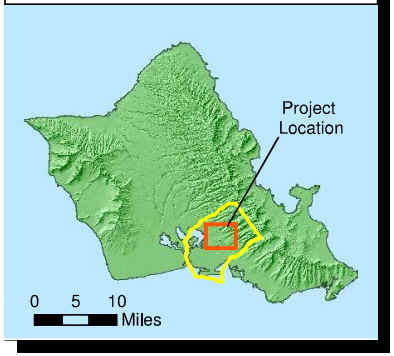

Legend

- Clinker
- Red Hill Fuel Storage Tank
- Supply Well
- Monitoring Well
- Contour of Equal Drawdown (feet)
- Groundwater Model Domain
- Red Hill Facility Boundary
- Stream

Notes

1. Map projection: NAD 1983 Hawaii State Plane Zone 3 (feet)
2. DigitalGlobe, Inc. (DG) and NRCS. Publication_Date: 2015

Z1: 17.91 indicates measurement was made in a Westbay sampling port

15.15 indicates measurement was made in a pumping well

Figure 6-18
Head Differences Between - Time 1 (Red Hill Shaft Off at Max Recovery, Hālawa Shaft Average Pumping, 01/15/2018 6:00) and Time 2 (Red Hill Shaft at Max Pumping, Hālawa Shaft Average Pumping, 01/19/2018 21:10)
Conceptual Site Model Rev. 01
Investigation and Remediation of Releases and Groundwater Protection and Evaluation
Red Hill Bulk Fuel Storage Facility
JBPHH, O'ahu, Hawai'i

S:\Projects\NAVFAC PAC\CLEAN V\60571032_CTO18F01126\900-Work\920 GIS\02_Maps\CSM\Fig6-18_GW_Drawdowns_Scenarios1_2_distances_10-51.mxd 6/14/2019

This page intentionally left blank

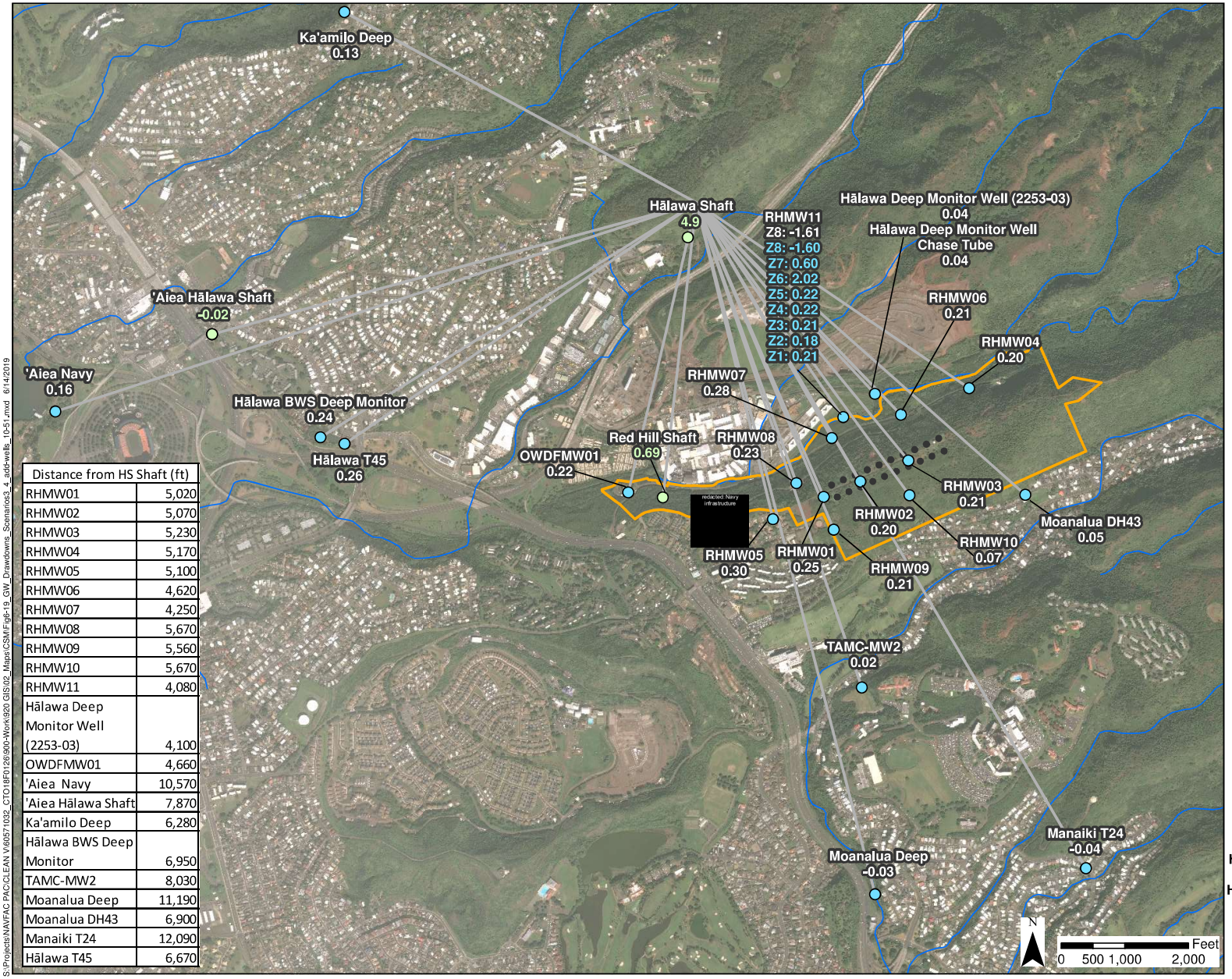

Distance from HS Shaft (ft)	
RHMW01	5,020
RHMW02	5,070
RHMW03	5,230
RHMW04	5,170
RHMW05	5,100
RHMW06	4,620
RHMW07	4,250
RHMW08	5,670
RHMW09	5,560
RHMW10	5,670
RHMW11	4,080
Hālawa Deep Monitor Well (2253-03)	4,100
OWDFMW01	4,660
'Aiea Navy	10,570
'Aiea Hālawa Shaft	7,870
Ka'amilo Deep	6,280
Hālawa BWS Deep Monitor	6,950
TAMC-MW2	8,030
Moanalua Deep	11,190
Moanalua DH43	6,900
Manaiki T24	12,090
Hālawa T45	6,670

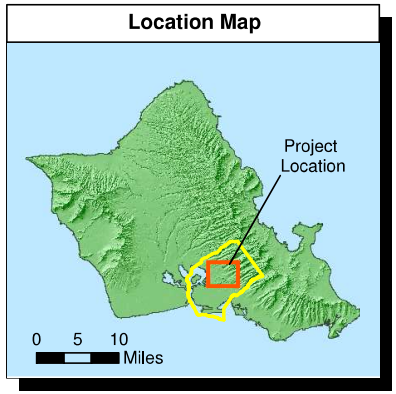

Legend

- Clinker
- Red Hill Fuel Storage Tank
- Supply Well
- Monitoring Well
- Groundwater Model Domain
- Red Hill Facility Boundary
- Stream

Notes

1. Map projection: NAD 1983 Hawaii State Plane Zone 3 (feet)
2. DigitalGlobe, Inc. (DG) and NRCS. Publication_Date: 2015

Z1: 17.91 indicates measurement was made in a Westbay sampling port

15.15 indicates measurement was made in a pumping well

Figure 6-19
Head Differences Between Time 1 (Red Hill Shaft Off at Max Recovery, Hālawa Shaft Average Pumping, 01/15/2018 6:00) and Time 2 (Red Hill Shaft at Max Pumping, Hālawa Shaft Average Pumping, 01/19/2018 21:10)
Conceptual Site Model Rev. 01
Investigation and Remediation of Releases and Groundwater Protection and Evaluation
Red Hill Bulk Fuel Storage Facility
JBPHH, O'ahu, Hawai'i

S:\Projects\NAVFAC PAC\CLEAN V\60571032_CTO18F01126\900-Work\920 GIS\02_Maps\CSM\Fig6-19_GW_Drawdowns_Scenarios3_4_add-wells_10-51.mxd 6/14/2019

This page intentionally left blank

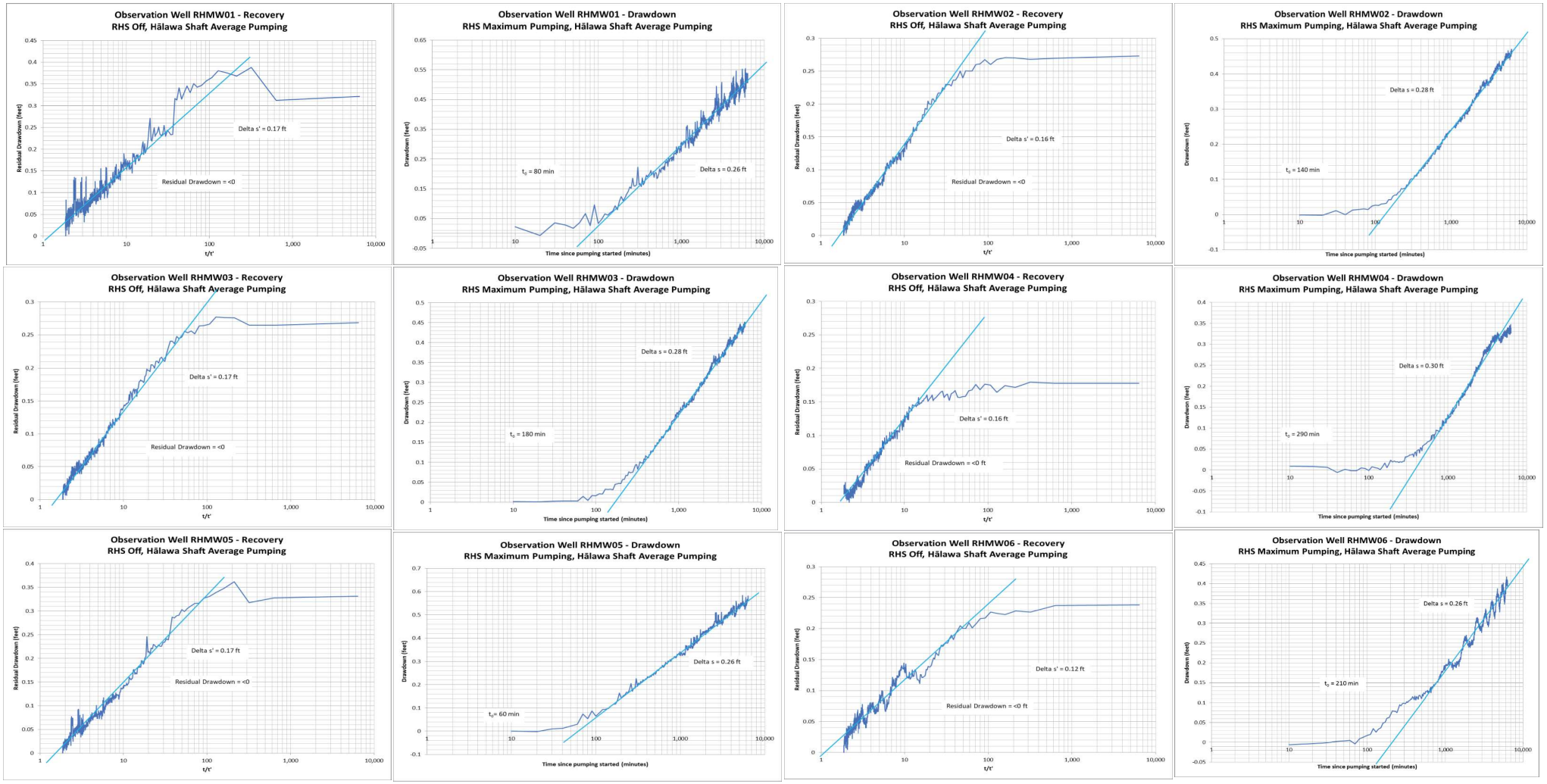

Figure 6-20
Cooper-Jacob Drawdown and Recovery Plots Time 2 (RHMW01, RHMW02, RHMW03, RHMW04, RHMW05, and RHMW06)
Conceptual Site Model Rev. 01
Investigation and Remediation of Releases and
Groundwater Protection and Evaluation
Red Hill Bulk Fuel Storage Facility
JBPHH, O'ahu, Hawai'i

This page intentionally left blank

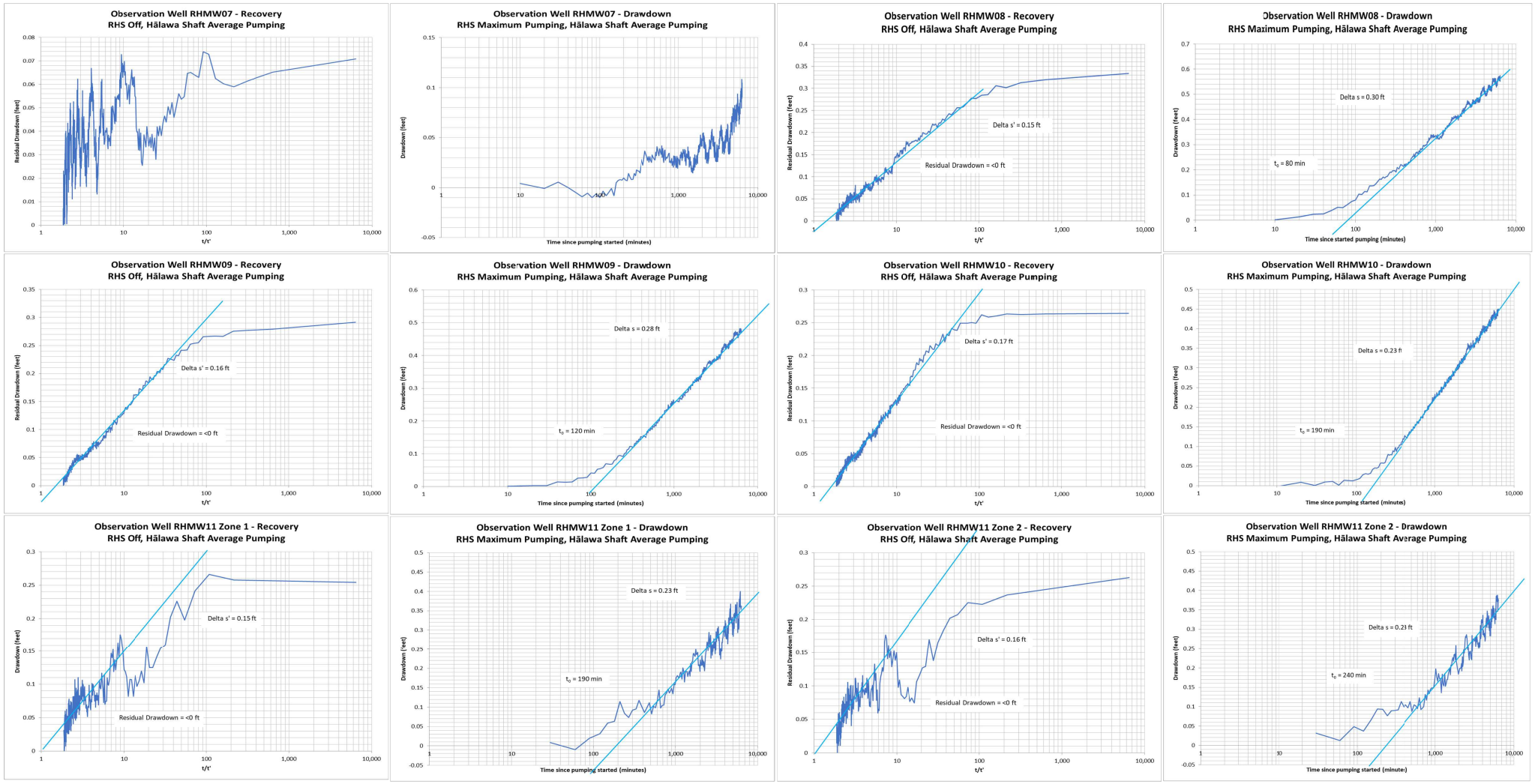

Figure 6-21
Cooper-Jacob Drawdown and Recovery Plots Time 2 (RHMW07, RHMW08, RHMW09, RHMW10, RHMW11 Zones 1 and 2)
Conceptual Site Model Rev. 01
Investigation and Remediation of Releases and
Groundwater Protection and Evaluation
Red Hill Bulk Fuel Storage Facility
JBPHH, Oʻahu, Hawaiʻi

This page intentionally left blank

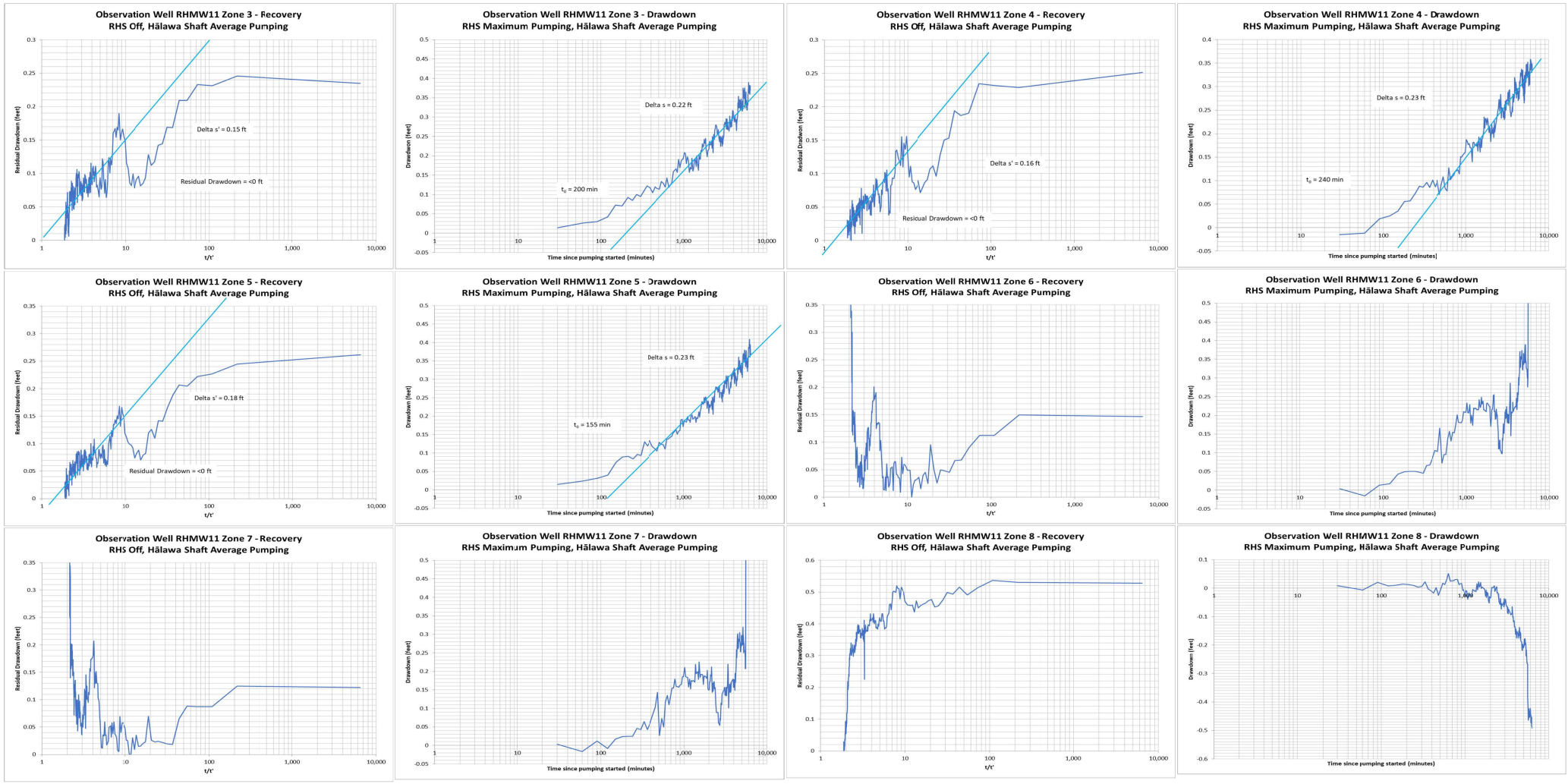

Figure 6-22
Cooper-Jacob Drawdown and Recovery Plots Time 2 (RHMW11 Zones 3, 4, 5, 6, 7, and 8)
Conceptual Site Model Rev. 01
Investigation and Remediation of Releases and
Groundwater Protection and Evaluation
Red Hill Bulk Fuel Storage Facility
JBPHH, O'ahu, Hawai'i

This page intentionally left blank

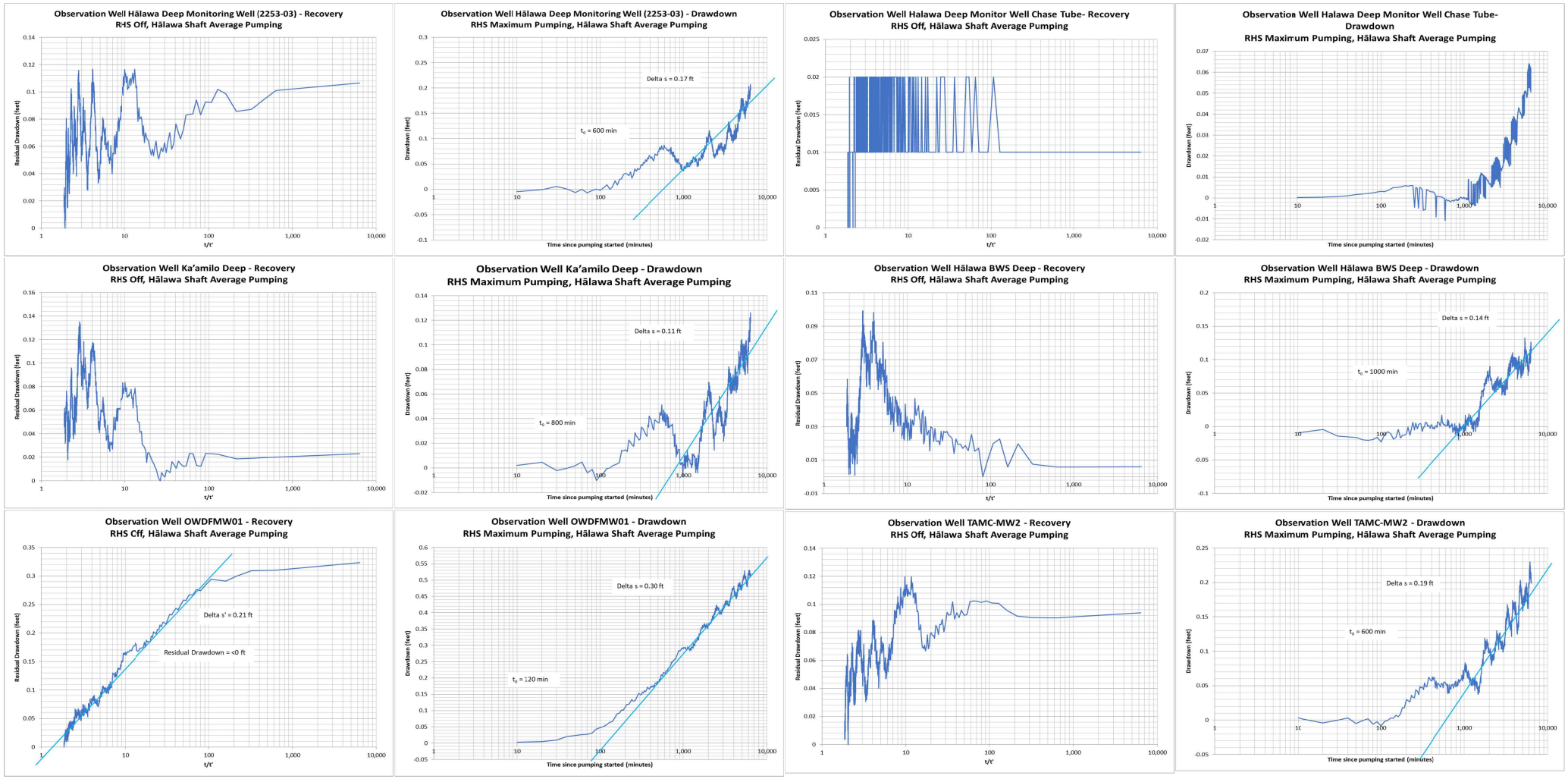

Figure 6-23
Cooper-Jacob Drawdown and Recovery Plots Time 2
(Hālawa Deep Monitor Well [2253-03], Hālawa Deep Monitor Well Chase Tube, Ka'amilo Deep, Hālawa BWS Deep Monitor, OWDFMW01, and TAMC-MW2)
Conceptual Site Model Rev. 01
Investigation and Remediation of Releases and Groundwater Protection and Evaluation
Red Hill Bulk Fuel Storage Facility
JBPHH, O'ahu, Hawai'i

This page intentionally left blank

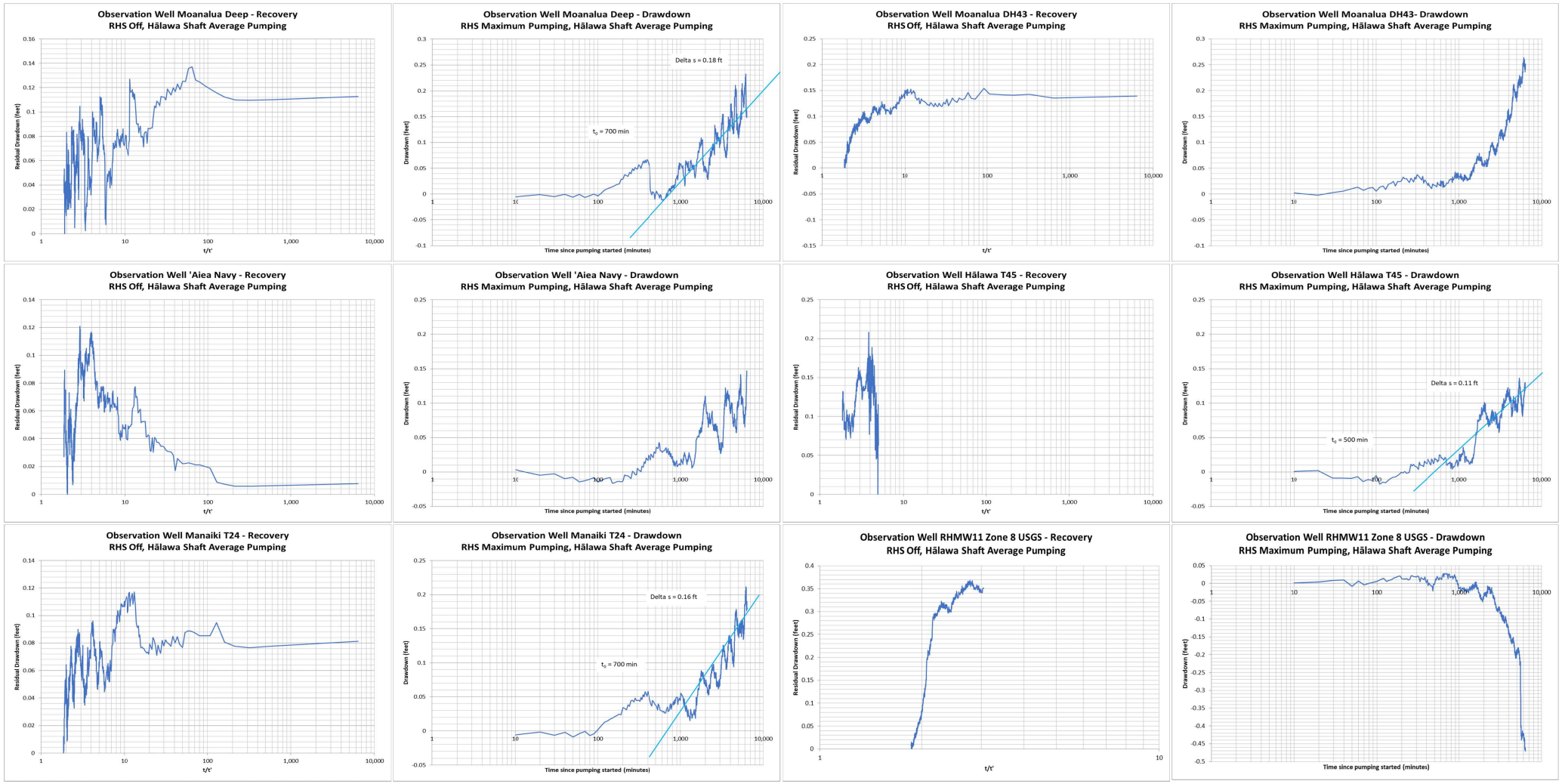

Figure 6-24
Cooper-Jacob Drawdown and Recovery Plots Time 2
(Moanalua Deep, Moanalua DH43, ʻAiea Navy, Hālawa T45, Manaiki T24, and USGS RHMW11 Zone 8)
Conceptual Site Model Rev. 01
Investigation and Remediation of Releases and Groundwater Protection and Evaluation
Red Hill Bulk Fuel Storage Facility
JBPHH, Oʻahu, Hawaiʻi

This page intentionally left blank

Observation Well RHMW01 – Recovery
RHS Off,
Hālawa Shaft Average Pumping

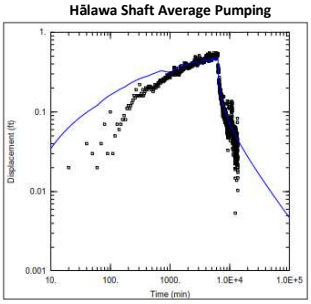

Observation Well RHMW01 – Drawdown
RHS Maximum Pumping,
Hālawa Shaft Average Pumping

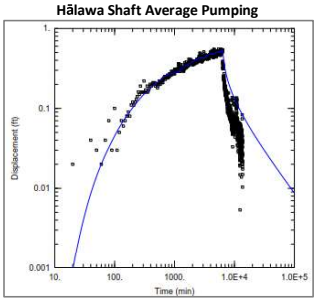

Observation Well RHMW02 – Recovery
RHS Off,
Hālawa Shaft Average Pumping

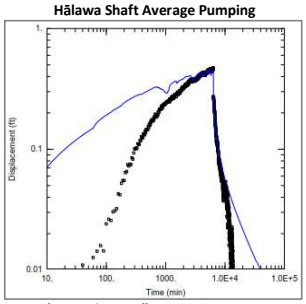

Observation Well RHMW02 – Drawdown
RHS Maximum Pumping,
Hālawa Shaft Average Pumping

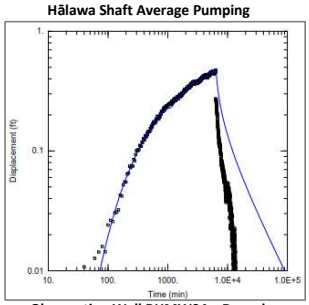

Observation Well RHMW03 – Recovery
RHS Off,
Hālawa Shaft Average Pumping

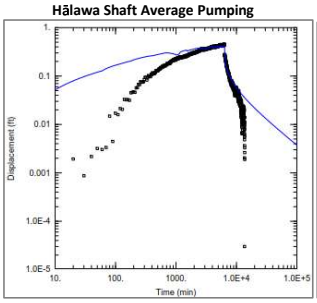

Observation Well RHMW03 – Drawdown
RHS Maximum Pumping,
Hālawa Shaft Average Pumping

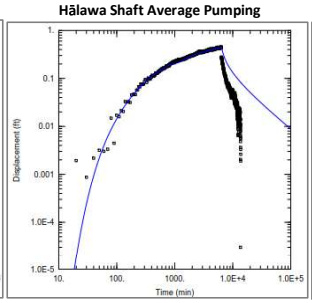

Observation Well RHMW04 – Recovery
RHS Off,
Hālawa Shaft Average Pumping

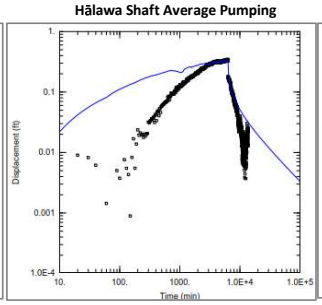

Observation Well RHMW04 – Drawdown
RHS Maximum Pumping,
Hālawa Shaft Average Pumping

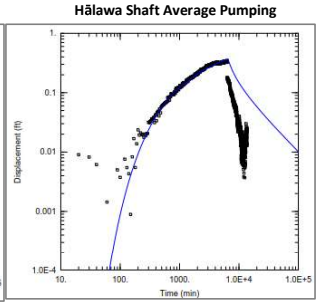

Observation Well RHMW05 – Recovery
RHS Off,
Hālawa Shaft Average Pumping

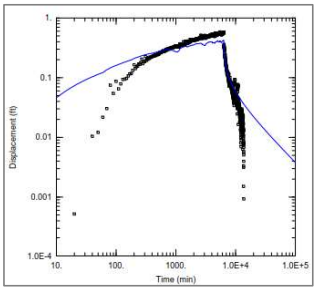

Observation Well RHMW05 – Drawdown
RHS Maximum Pumping,
Hālawa Shaft Average Pumping

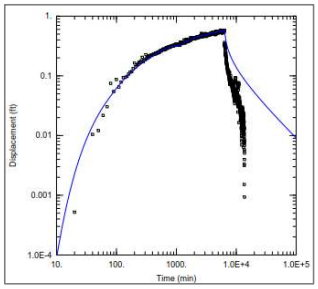

Observation Well RHMW06– Recovery
RHS Off,
Hālawa Shaft Average Pumping

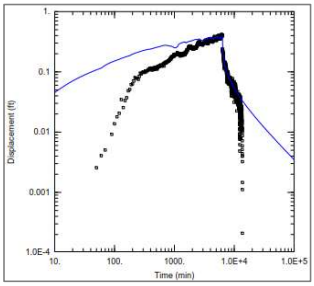

Observation Well RHMW06 – Drawdown
RHS Maximum Pumping,
Hālawa Shaft Average Pumping

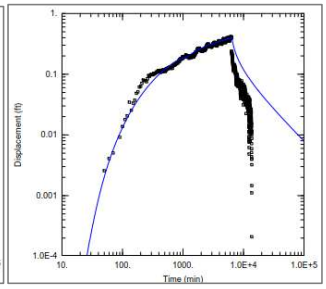

Observation Well RHMW08 – Recovery
RHS Off,
Hālawa Shaft Average Pumping

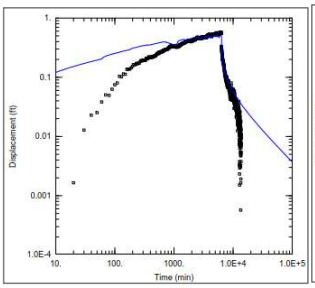

Observation Well RHMW08 – Drawdown
RHS Maximum Pumping,
Hālawa Shaft Average Pumping

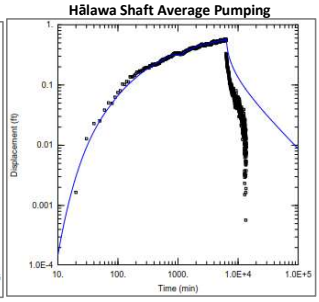

Observation Well RHMW09– Recovery
RHS Maximum Pumping,
Hālawa Shaft Average Pumping

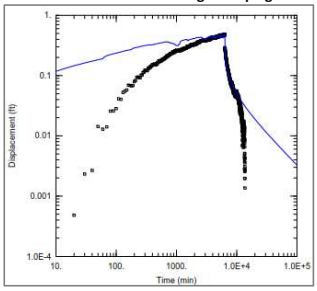

Observation Well RHMW09 – Drawdown
RHS Maximum Pumping,
Hālawa Shaft Average Pumping

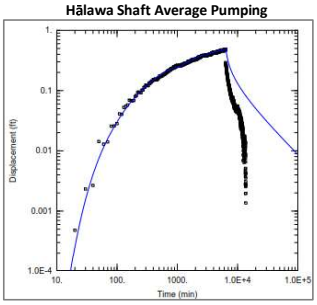

Observation Well RHMW10 – Recovery
RHS Off,
Hālawa Shaft Average Pumping

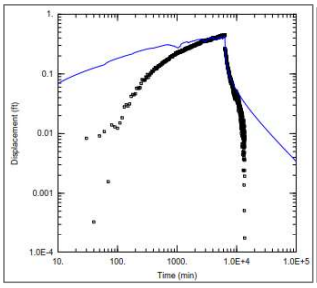

Observation Well RHMW10 – Drawdown
RHS Maximum Pumping,
Hālawa Shaft Average Pumping

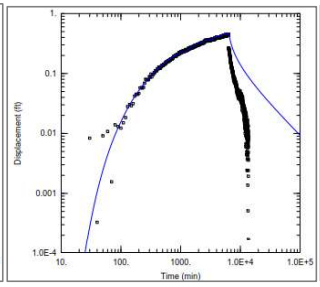

Observation Well OWDFMW01– Recovery
RHS Off,
Hālawa Shaft Average Pumping

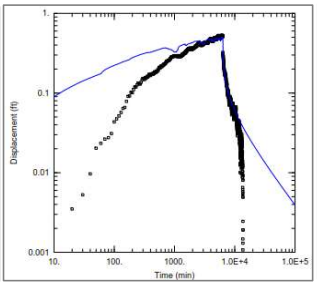

Observation Well OWDFMW01 – Drawdown
RHS Maximum Pumping,
Hālawa Shaft Average Pumping

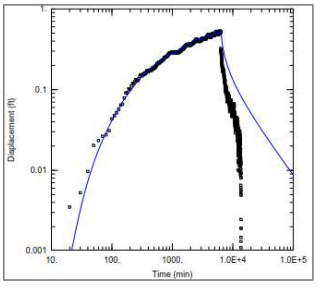

Figure 6-25
Aqtesolv Drawdown and Recovery Plots Time 2
(RHMW01, RHMW02, RHMW03, RHMW04, RHMW05, RHMW06, RHMW08, RHMW09, RHMW10, OWDFMW01)
Conceptual Site Model Rev. 01
Investigation and Remediation of Releases and
Groundwater Protection and Evaluation
Red Hill Bulk Fuel Storage Facility
JBPHH, Oʻahu, Hawaiʻi

This page intentionally left blank

Observation Well RHMW11 Zone 1 – Recovery, RHS Off, Hālawa Shaft Average Pumping

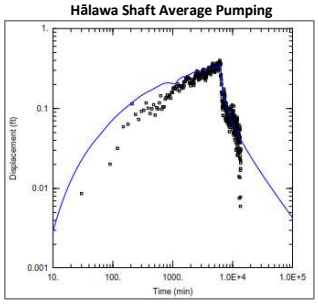

Observation Well RHMW11 Zone 1 – Drawdown, RHS Maximum Pumping, Hālawa Shaft Average Pumping

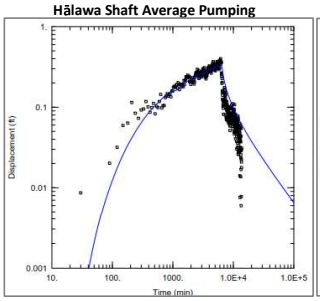

Observation Well RHMW11 Zone 2 – Recovery, RHS Off, Hālawa Shaft Average Pumping

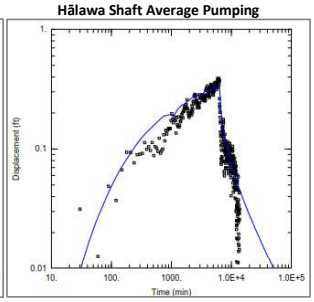

Observation Well RHMW11 Zone 2 – Drawdown, RHS Maximum Pumping, Hālawa Shaft Average Pumping

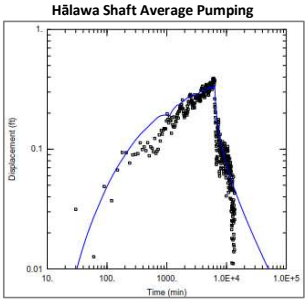

Observation Well RHMW11 Zone 3 – Recovery, RHS Off, Hālawa Shaft Average Pumping

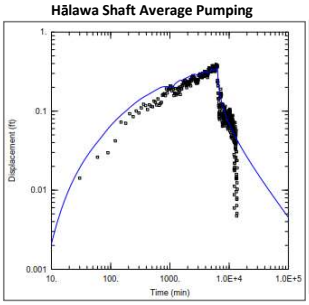

Observation Well RHMW11 Zone 3 – Drawdown, RHS Maximum Pumping, Hālawa Shaft Average Pumping

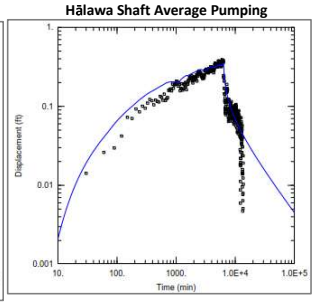

Observation Well RHMW11 Zone 4 – Recovery, RHS Off, Hālawa Shaft Average Pumping

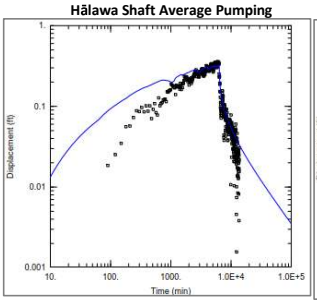

Observation Well RHMW11 Zone 4 – Drawdown, RHS Maximum Pumping, Hālawa Shaft Average Pumping

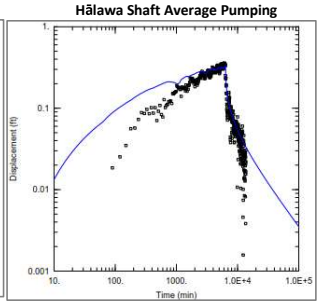

Observation Well RHMW11 Zone 5 – Recovery, RHS Off, Hālawa Shaft Average Pumping

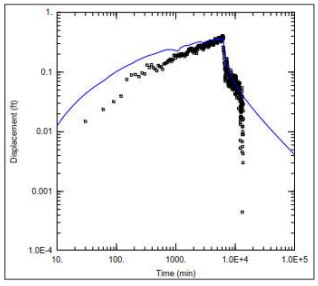

Observation Well RHMW11 Zone 5 – Drawdown, RHS Maximum Pumping, Hālawa Shaft Average Pumping

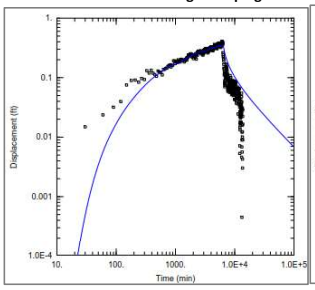

Observation Well Moanalua Deep – Recovery, RHS Off, Hālawa Shaft Average Pumping

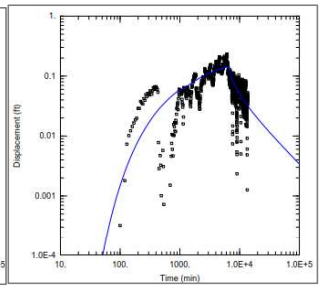

Observation Well Moanalua Deep – Drawdown, RHS Maximum Pumping, Hālawa Shaft Average Pumping

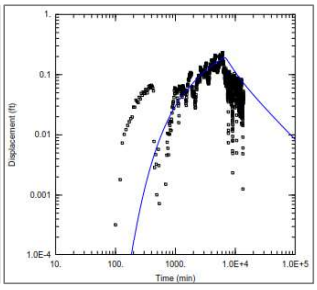

Observation Well Hālawa BWS Deep Monitor – Recovery, RHS Off, Hālawa Shaft Average Pumping

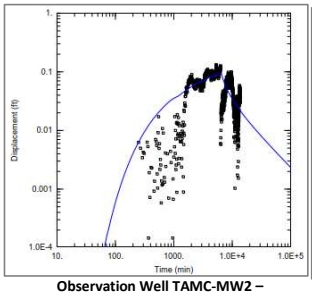

Observation Well Hālawa BWS Deep Monitor – Drawdown, RHS Maximum Pumping, Hālawa Shaft Average Pumping

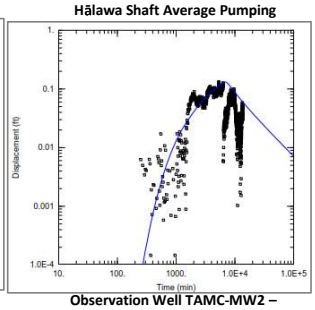

Observation Well Hālawa Deep Monitor Well (2253-03) – Recovery, RHS Off, Hālawa Shaft Average Pumping

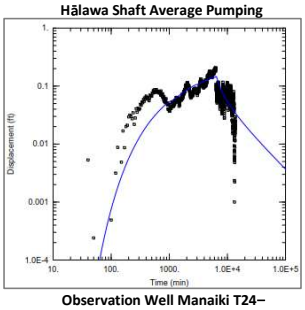

Observation Well Hālawa Deep Monitor Well (2253-03) – Drawdown, RHS Maximum Pumping, Hālawa Shaft Average Pumping

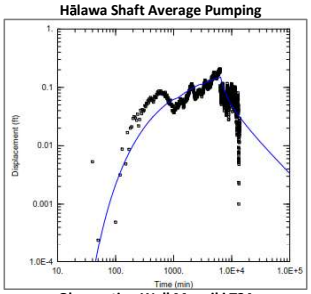

Observation Well TAMC-MW2 – Recovery, RHS Off, Hālawa Shaft Average Pumping

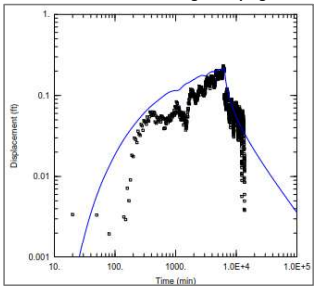

Observation Well TAMC-MW2 – Drawdown, RHS Maximum Pumping, Hālawa Shaft Average Pumping

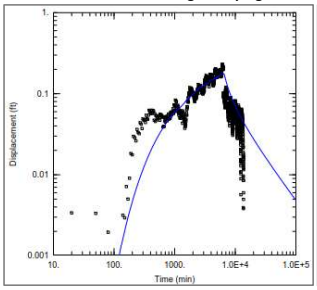

Observation Well Manaiki T24– Recovery, RHS Off, Hālawa Shaft Average Pumping

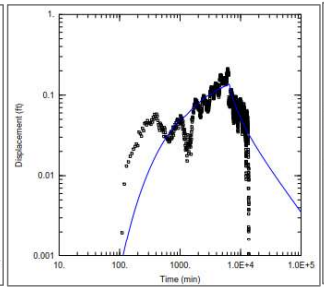

Observation Well Manaiki T24 – Drawdown, RHS Maximum Pumping, Hālawa Shaft Average Pumping

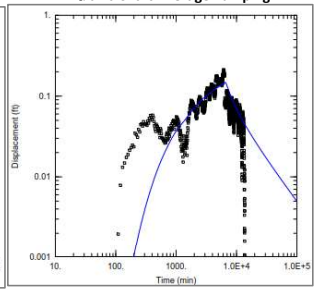

Figure 6-26
Aqtesolv Drawdown and Recovery Plots Time 2
(RHMW11 Zone 1, 2, 3, 4, and 5, Moanalua Deep, Hālawa BWS Deep Monitor, Hālawa Deep Monitor Well [2252-03], TAMC-MW2, and Manaiki T24)
Conceptual Site Model Rev. 01
Investigation and Remediation of Releases and Groundwater Protection and Evaluation
Red Hill Bulk Fuel Storage Facility
JBPHH, O'ahu, Hawai'i

This page intentionally left blank

Observation Well Hālawa T45
– Drawdown, RHS Maximum Pumping,
Hālawa Shaft Average Pumping

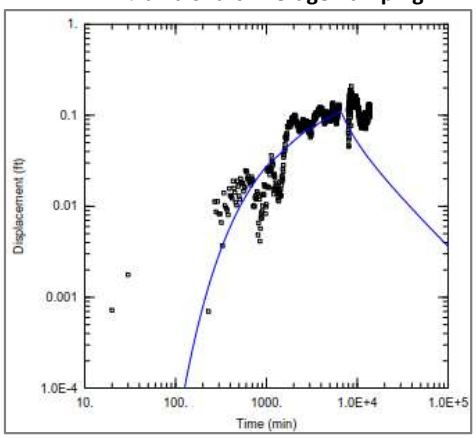

Observation Well Moanalua DH43
– Recovery, RHS Off,
Hālawa Shaft Average Pumping

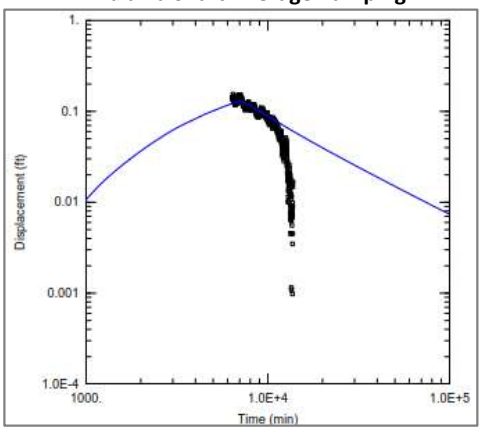

Observation Well Kaʻamilo Deep
– Recovery, RHS Off,
Hālawa Shaft Average Pumping

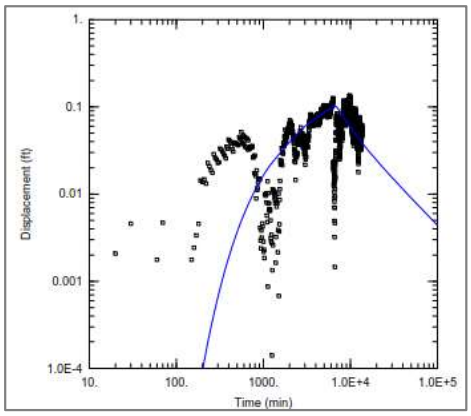

Observation Well Kaʻamilo Deep
– Drawdown, RHS Maximum Pumping,
Hālawa Shaft Average Pumping

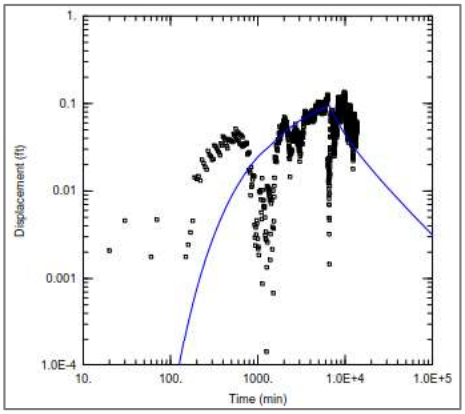

Figure 6-27
Aqtesolv Drawdown and Recovery Plots Time 2 (Hālawa T45, Moanalua DH43, and Kaʻamilo Deep)
Conceptual Site Model Rev. 01
Investigation and Remediation of Releases and
Groundwater Protection and Evaluation
Red Hill Bulk Fuel Storage Facility
JBPHH, Oʻahu, Hawaiʻi

This page intentionally left blank

Figure 6-28
Distance Drawdown at Time 2
Conceptual Site Model Rev. 01
Investigation and Remediation of Releases and Groundwater Protection and Evaluation
Red Hill Bulk Fuel Storage Facility
JBPHH, Oʻahu, Hawaiʻi

This page intentionally left blank

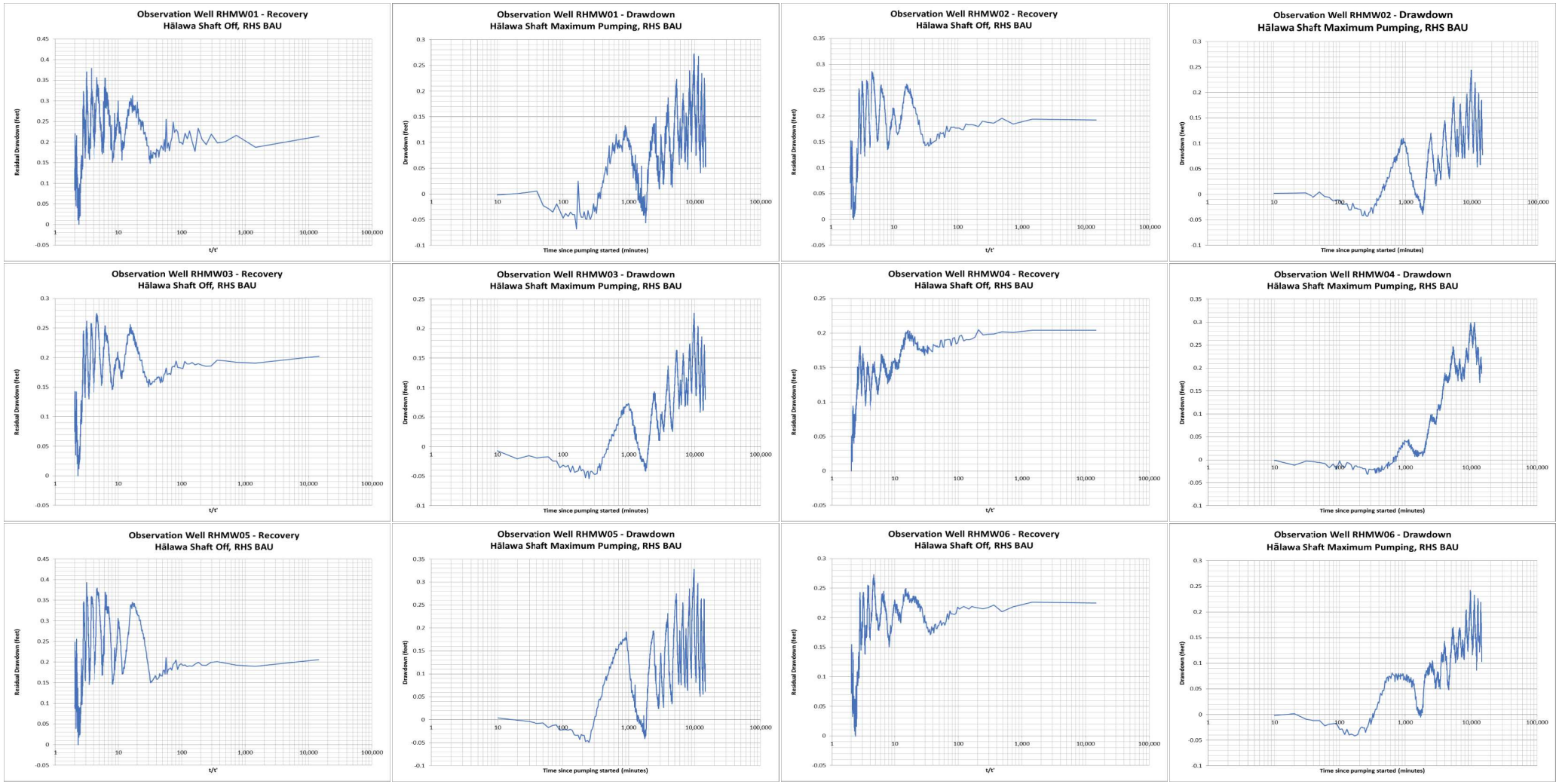

Figure 6-29
Cooper-Jacob Drawdown and Recovery Plots Time 4 (RHMW01, RHMW02, RHMW03, RHMW04, RHMW05, and RHMW06)
Conceptual Site Model Rev. 01
Investigation and Remediation of Releases and
Groundwater Protection and Evaluation
Red Hill Bulk Fuel Storage Facility
JBPHH, Oʻahu, Hawaiʻi

This page intentionally left blank

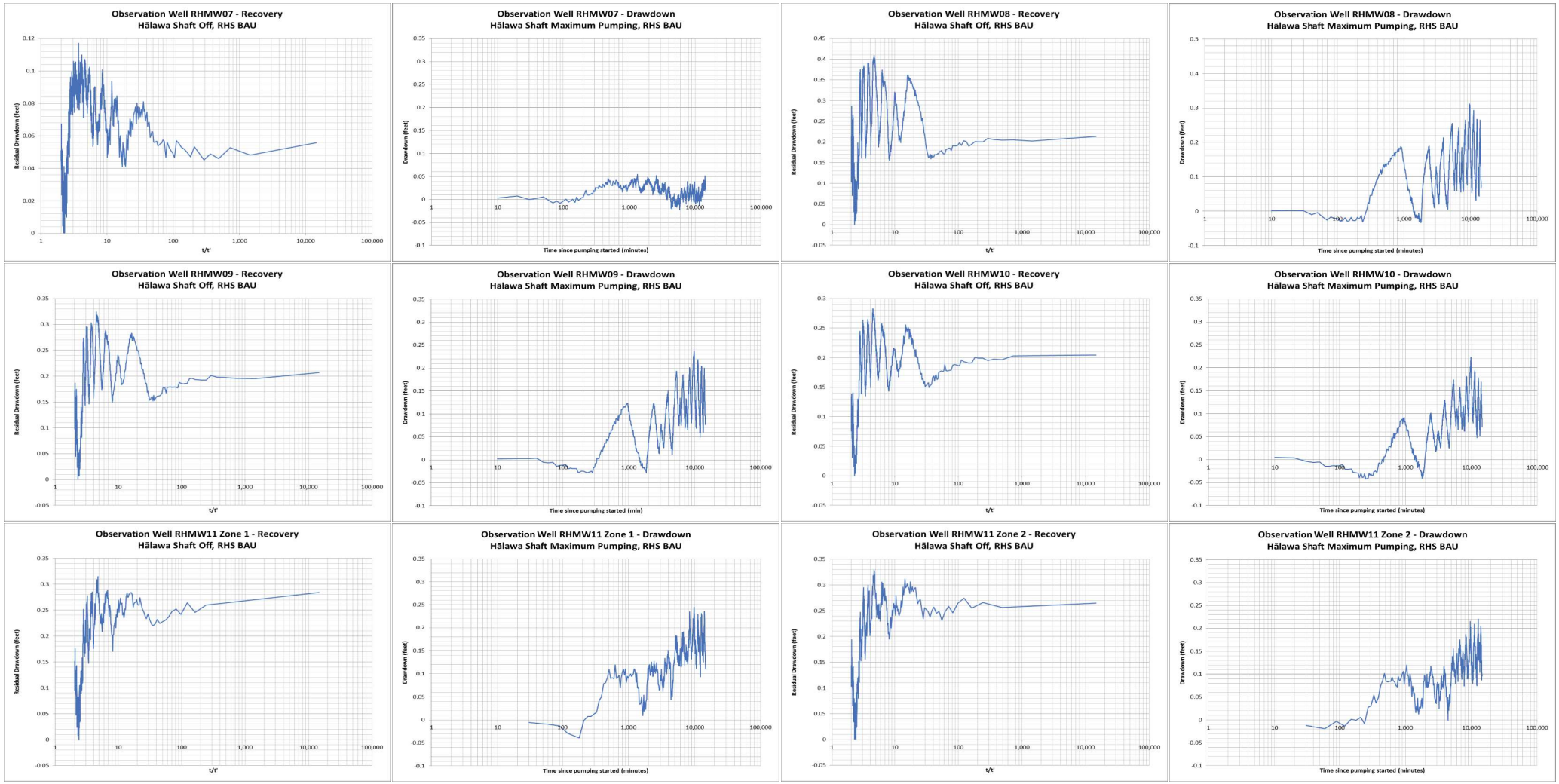

Figure 6-30
Cooper-Jacob Drawdown and Recovery Plots Time 4 (RHMW07, RHMW08, RHMW09, RHMW10, RHMW11 Zones 1 and 2)
Conceptual Site Model Rev. 01
Investigation and Remediation of Releases and
Groundwater Protection and Evaluation
Red Hill Bulk Fuel Storage Facility
JBPHH, Oʻahu, Hawaiʻi

This page intentionally left blank

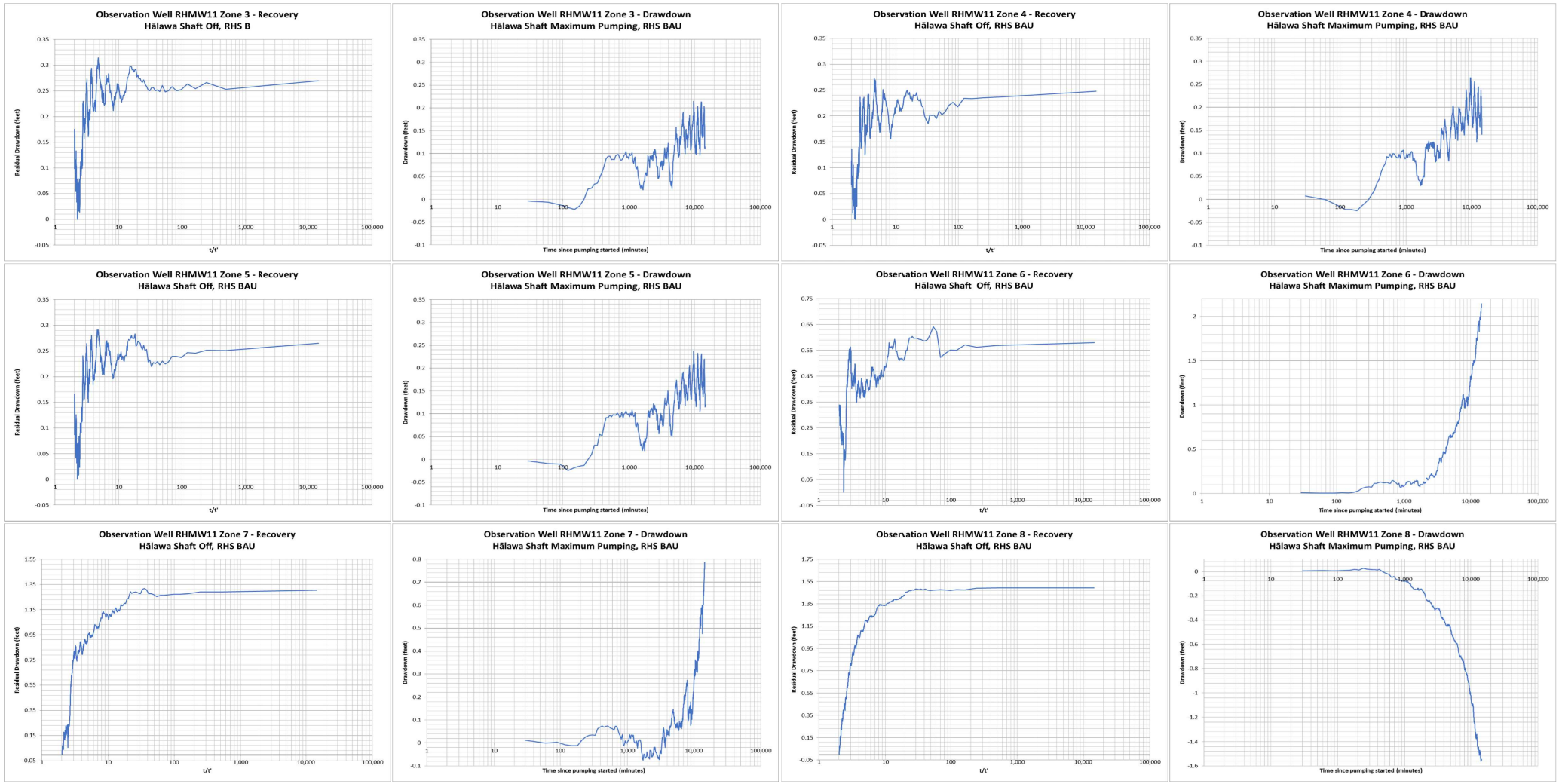

Figure 6-31
Cooper-Jacob Drawdown and Recovery Plots Time 4 (RHMW11 Zones 3, 4, 5, 6, 7, and 8)
Conceptual Site Model Rev. 01
Investigation and Remediation of Releases and
Groundwater Protection and Evaluation
Red Hill Bulk Fuel Storage Facility
JBPHH, Oʻahu, Hawaiʻi

This page intentionally left blank

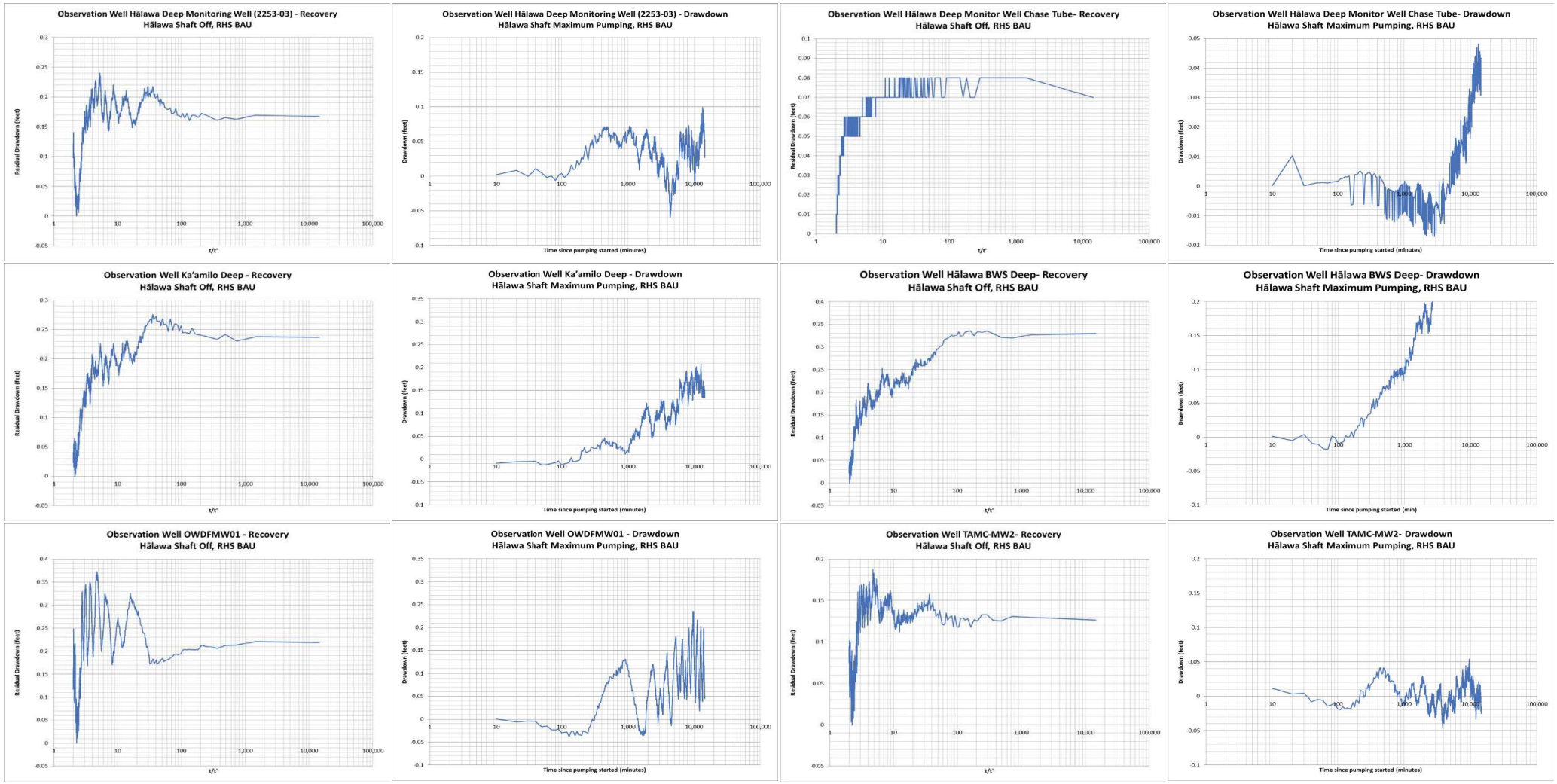

Figure 6-32
Cooper-Jacob Drawdown and Recovery Plots Time 4
(Hālawa Deep Monitor Well [2253-03], Hālawa Deep Monitor Well Chase Tube, Ka'amilo Deep, Hālawa BWS Deep Monitor, OWDFMW01, and TAMC-MW2)
Conceptual Site Model Rev. 01
Investigation and Remediation of Releases and Groundwater Protection and Evaluation
Red Hill Bulk Fuel Storage Facility
JBPHH, O'ahu, Hawai'i

This page intentionally left blank

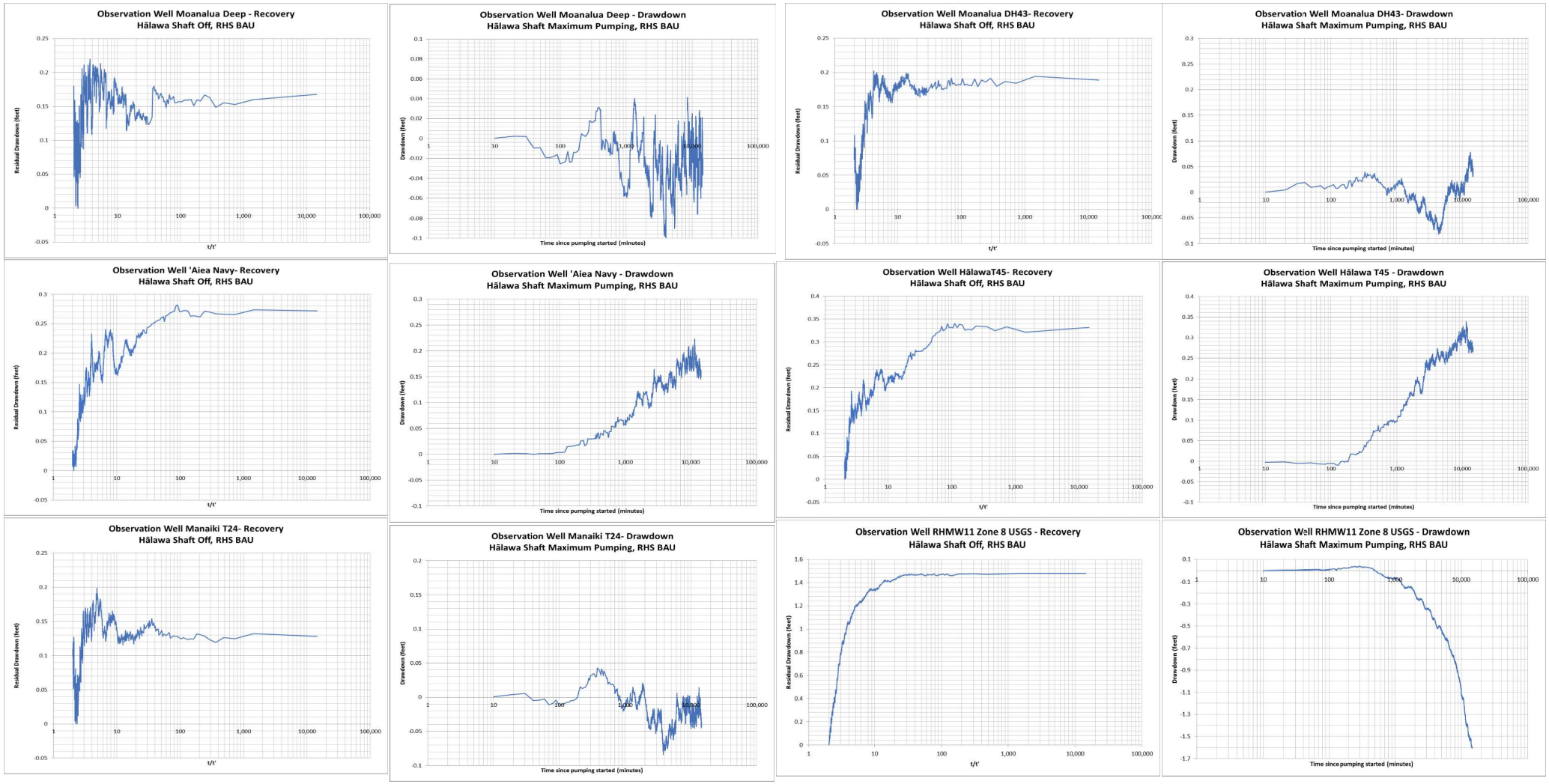

Figure 6-33
Cooper-Jacob Drawdown and Recovery Plots Time 4
(Moanalua Deep, Moanalua DH43, ʻAiea Navy, Hālawa T45, Manaiki T24, and USGS RHMW11 Zone 8)
Conceptual Site Model Rev. 01
Investigation and Remediation of Releases and Groundwater Protection and Evaluation
Red Hill Bulk Fuel Storage Facility
JBPHH, Oʻahu, Hawaiʻi

This page intentionally left blank

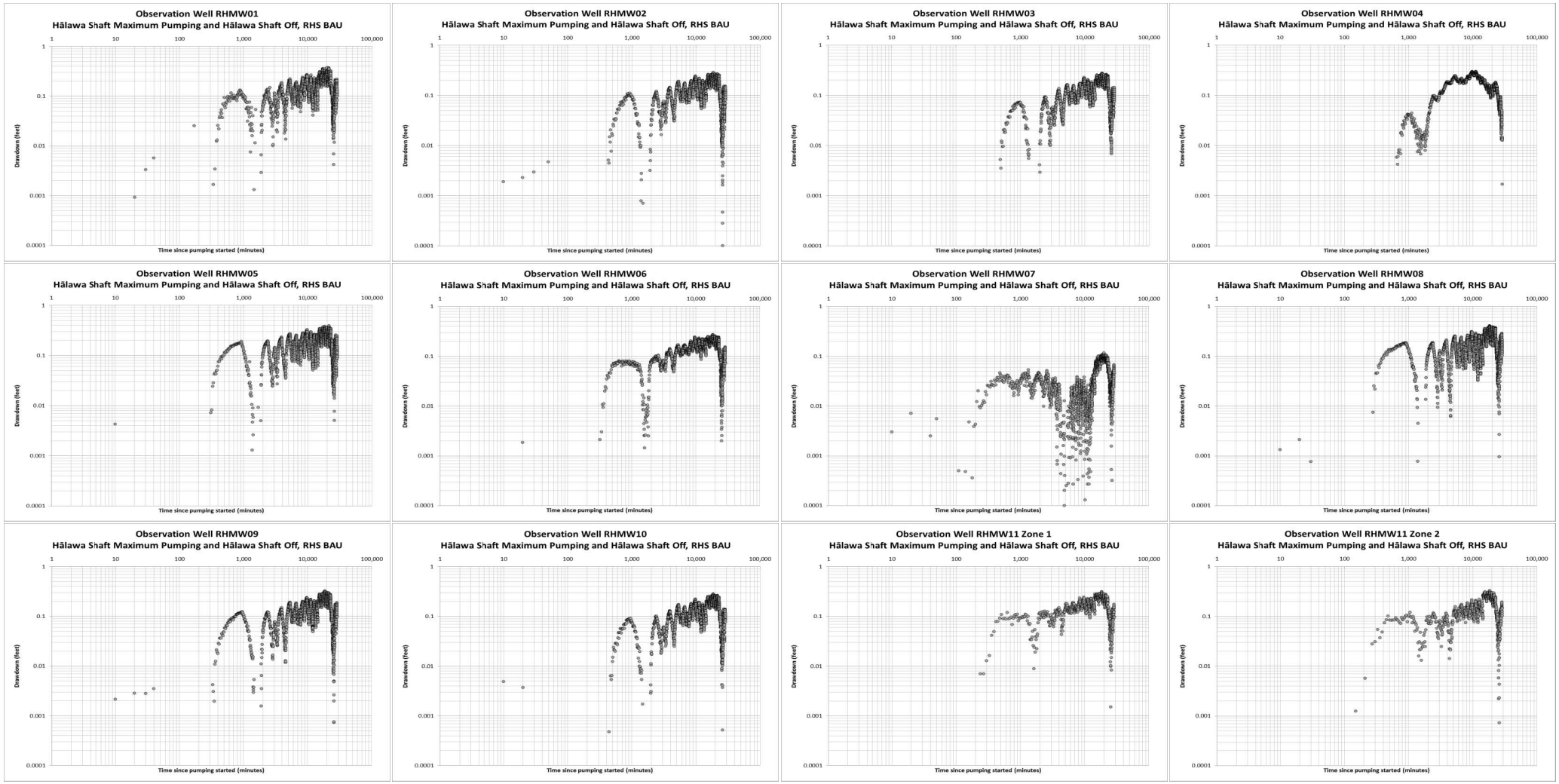

Figure 6-34
Logarithmic-Logarithmic Plots of Water Level vs Time, Time 3 and Time 4
(RHMW01, RHMW02, RHMW03, RHMW04, RHMW05, RHMW06, RHMW07, RHMW08, RHMW09, RHMW10, RHMW11 Zone 1, and RHMW11 Zone 2)
Conceptual Site Model Rev. 01
Investigation and Remediation of Releases and Groundwater Protection and Evaluation
Red Hill Bulk Fuel Storage Facility
JBPHH, O'ahu, Hawai'i

This page intentionally left blank

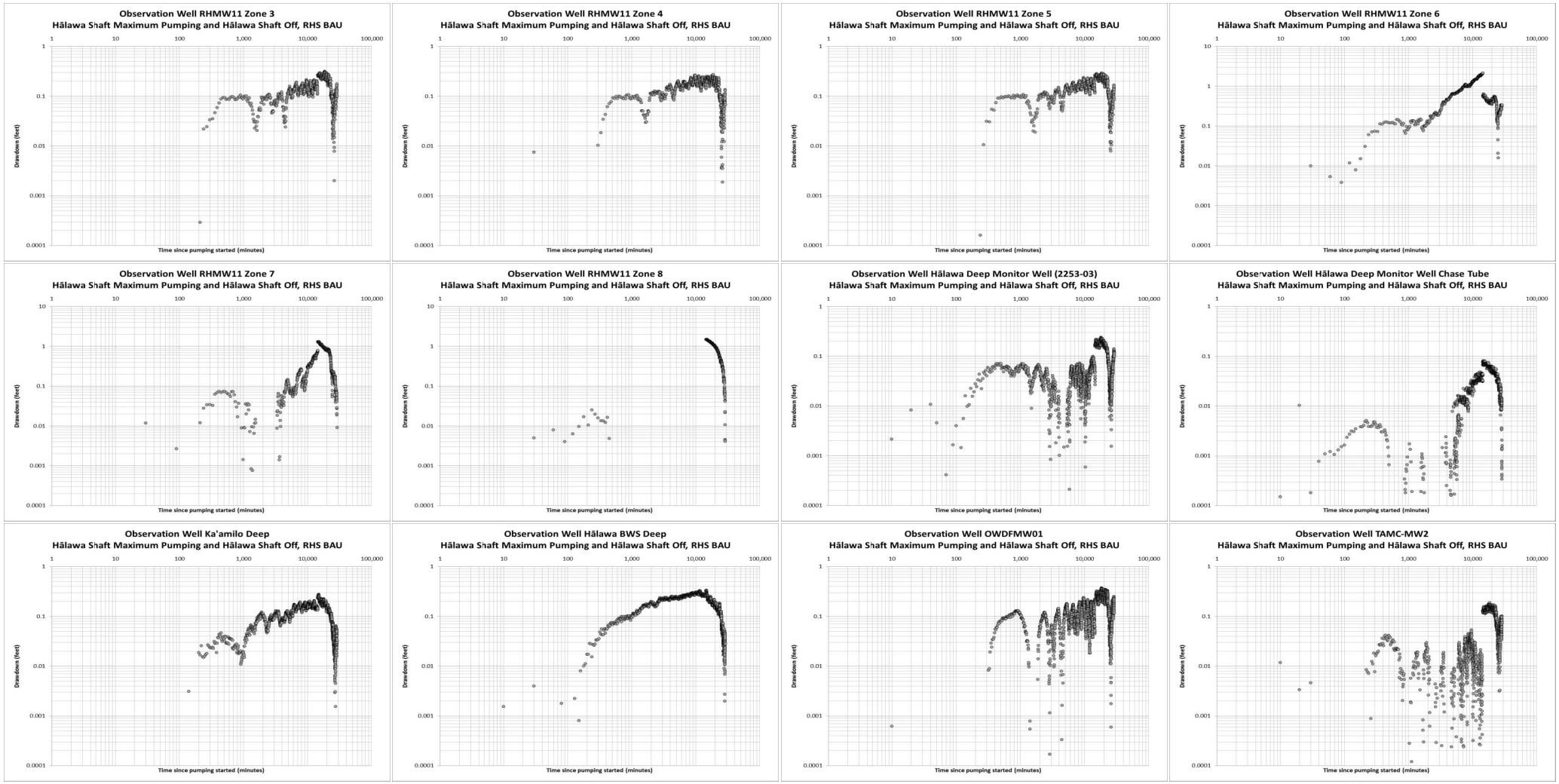

Figure 6-35
Logarithmic-Logarithmic Plots of Water Level vs Time, Time 3 and Time 4
(RHMW11 Zone 3 through Zone 8, Hālawa Deep Monitor Well [2253-03], Hālawa Deep Monitor Well Chase Tube, Ka'amilo Deep, Hālawa BWS Deep, OWDFMW01, and TAMC-MW2)
Conceptual Site Model Rev. 01
Investigation and Remediation of Releases and Groundwater Protection and Evaluation
Red Hill Bulk Fuel Storage Facility
JBPHH, O'ahu, Hawai'i

This page intentionally left blank

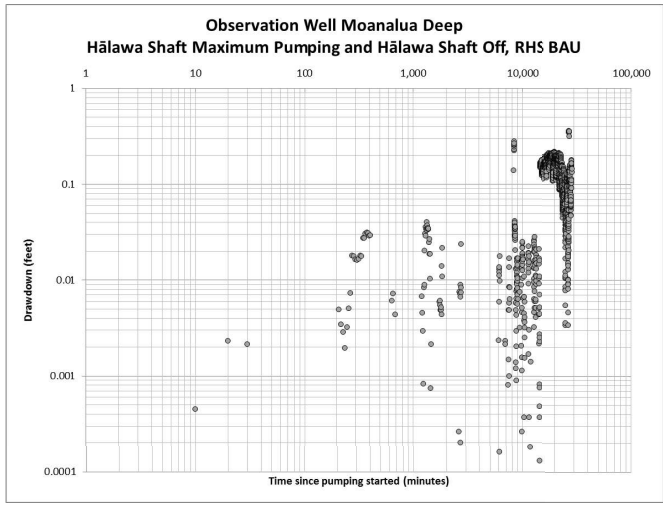

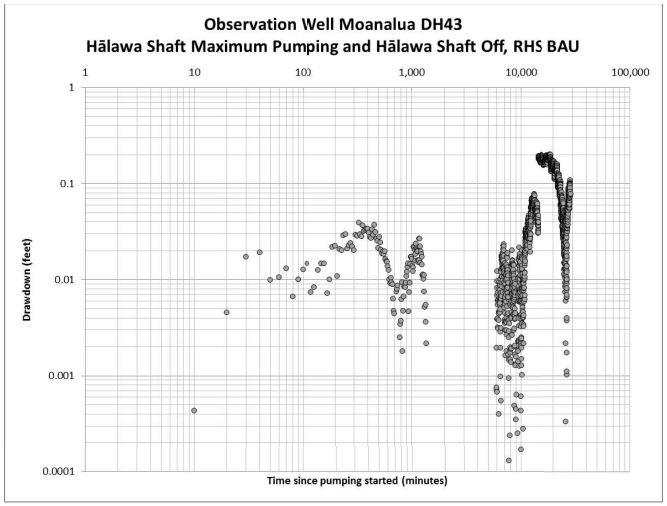

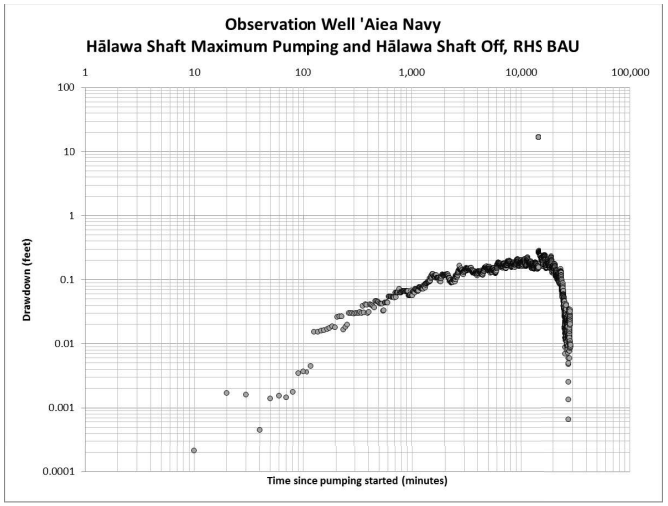

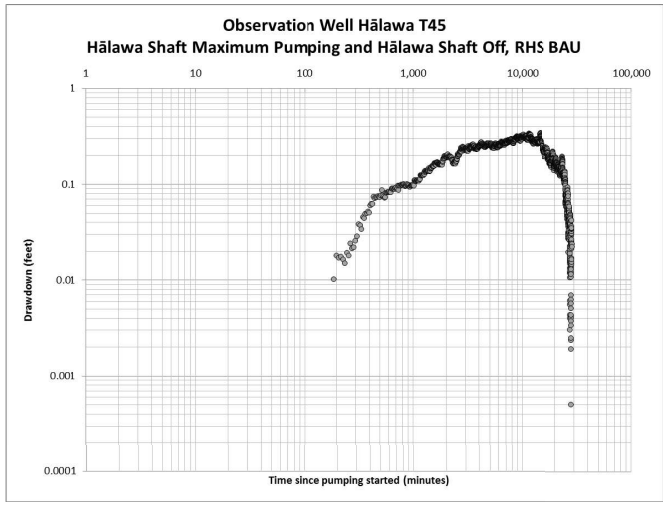

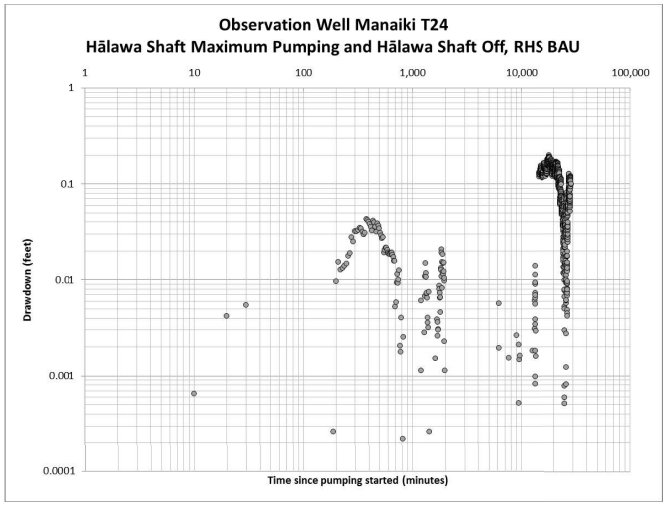

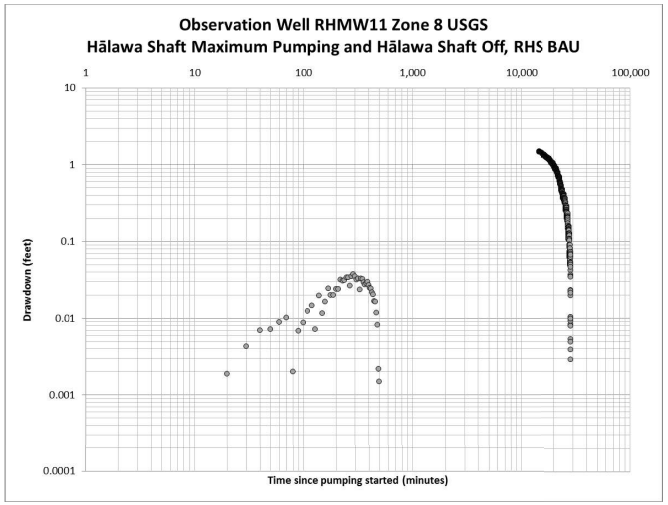

Figure 6-36
Cooper-Jacob Drawdown and Recovery Plots Time 2
(Moanalua Deep, Moanalua DH43, ʻAiea Navy, Hālawa T45, Manaiki T24, and RHMW11 Zone 8 USGS)
Conceptual Site Model Rev. 01
Investigation and Remediation of Releases and Groundwater Protection and Evaluation
Red Hill Bulk Fuel Storage Facility
JBPHH, Oʻahu, Hawaiʻi

This page intentionally left blank

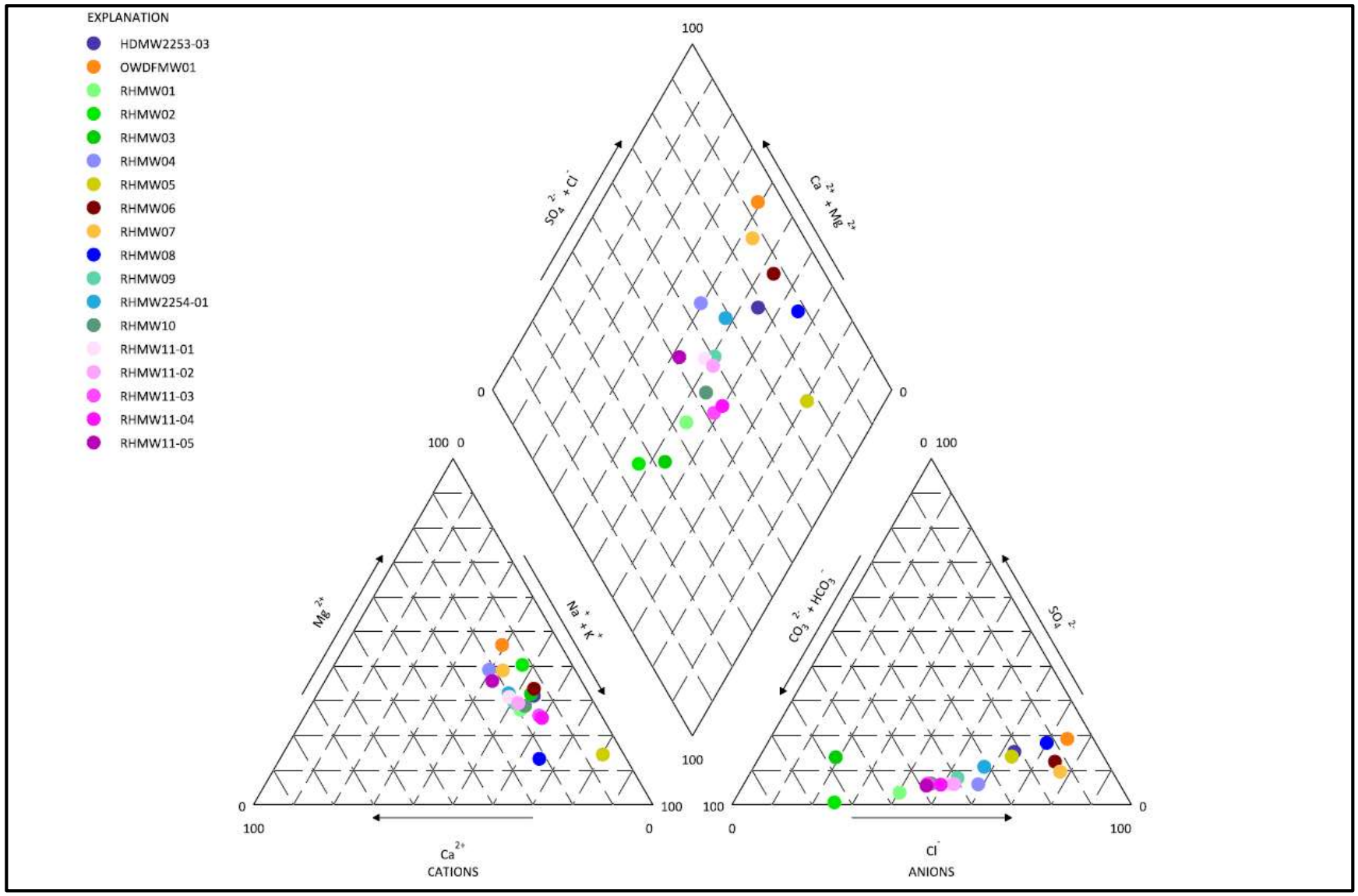

Figure 6-37
Chemical Composition of Groundwater in Red Hill Monitoring Wells
Conceptual Site Model Rev. 01
Investigation and Remediation of Releases and Groundwater Protection and Evaluation
Red Hill Bulk Fuel Storage Facility
JBPHH, Oʻahu, Hawaiʻi

This page intentionally left blank

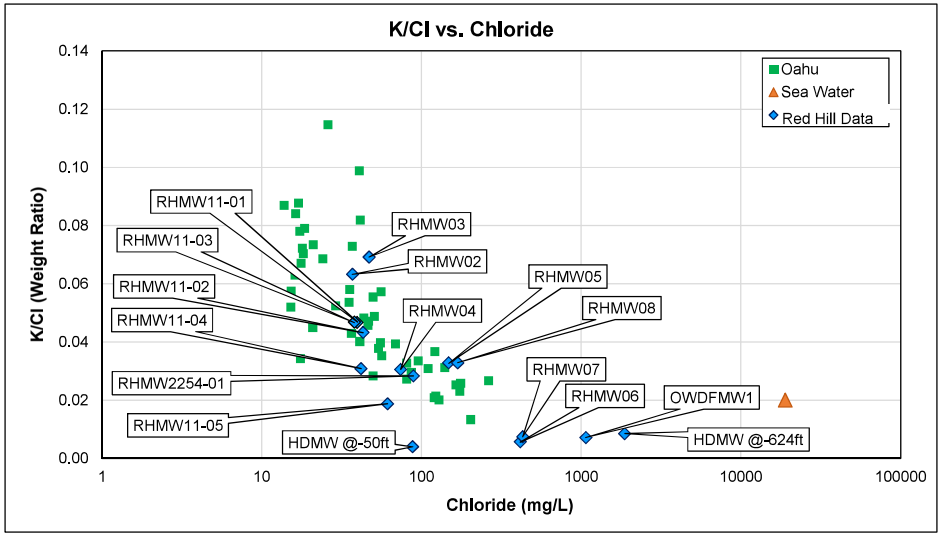

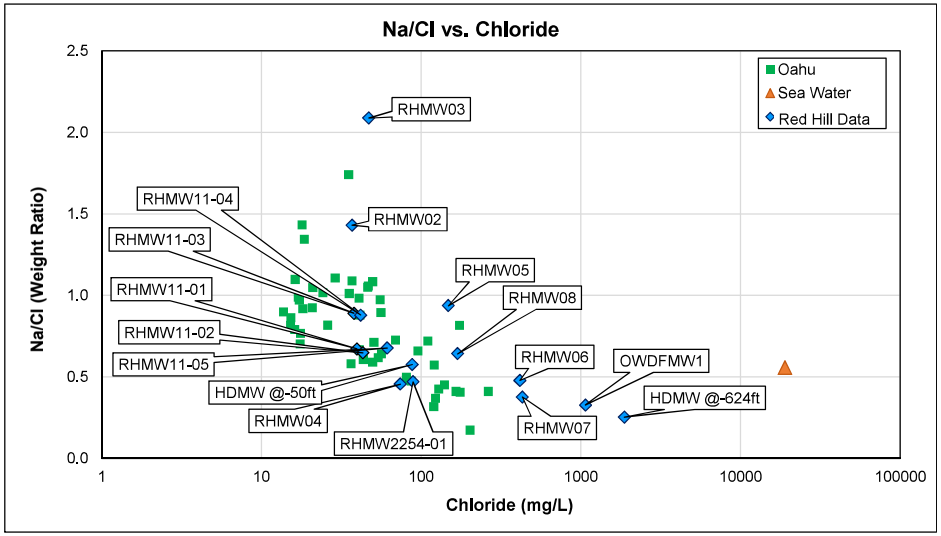

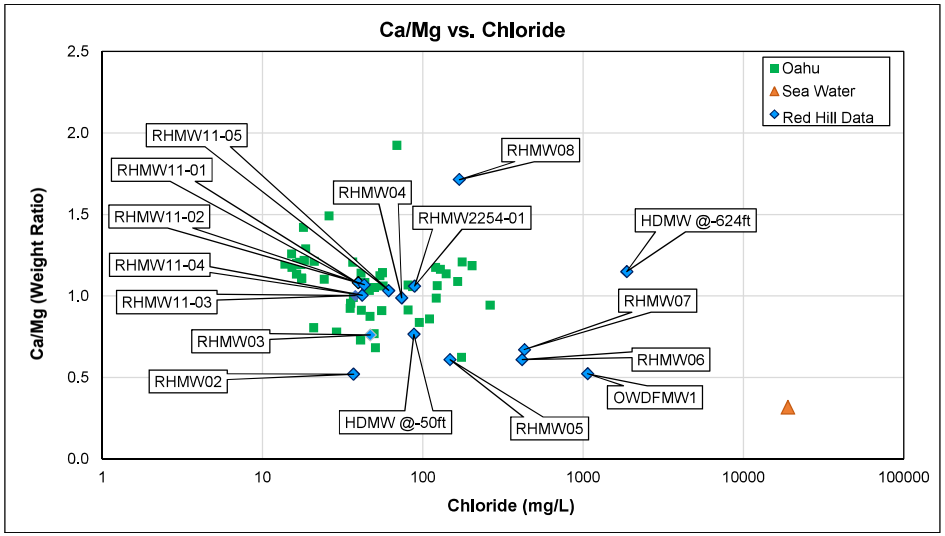

Figure 6-38
Bivariate Plots
Conceptual Site Model Rev. 01
Investigation and Remediation of Releases and Groundwater Protection and Evaluation
Red Hill Bulk Fuel Storage Facility
JBPHH, O‘ahu, Hawai‘i

This page intentionally left blank

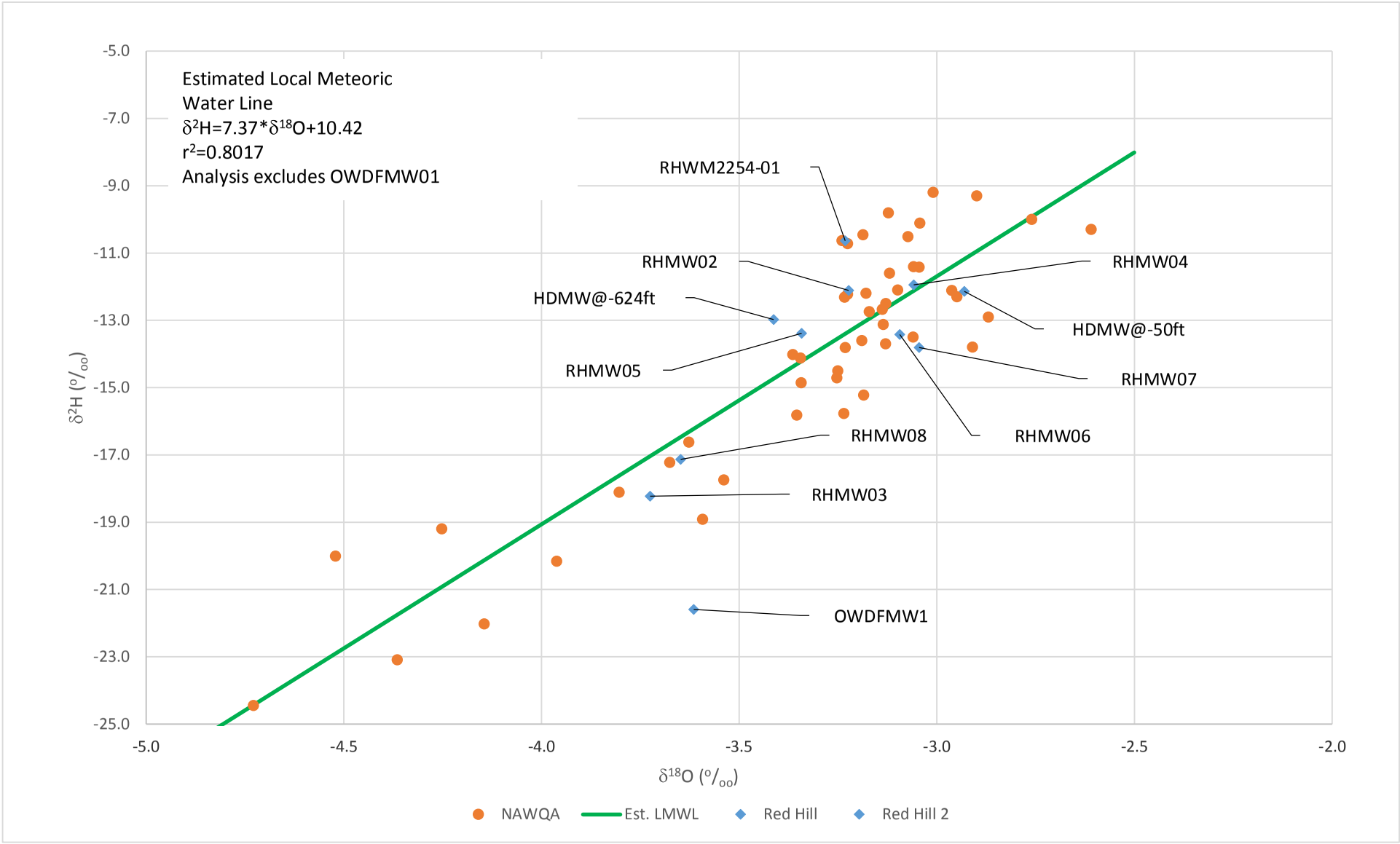

Figure 6-39
Estimated Local Meteoric Water Line
Conceptual Site Model Rev. 01
Investigation and Remediation of Releases and Groundwater Protection and Evaluation
Red Hill Bulk Fuel Storage Facility
JBPHH, O‘ahu, Hawai‘i

This page intentionally left blank

7. Module F: Fate and Transport of LNAPL and Dissolved COPCs in Groundwater

Potential vadose zone and groundwater transport pathways are identified based on the spatial and temporal trends of COPCs in groundwater from historical sampling conducted at the site. Evaluations of LNAPL migration are based on direct observation in core samples, and indirectly based on vapor monitoring and samples, temperature surveys, and petrographic studies. Fate is discussed within the context of fuel properties and attenuation studies both in the vadose zone as NSZD and in the dissolved groundwater plume as MNA processes.

7.1 LNAPL Distribution, Fuel Type, and Evidence of Weathering

This subsection documents the available information for characterizing the distribution of LNAPL in the subsurface at the Facility, the evidence concerning the type of fuel released, and the weathering of that fuel. A thorough discussion of LNAPL release in the source zone based on the construction of the tank farm and influence of the complex underlying geology (geometry, rock characteristics, volcanic features) is presented in Module C: LNAPL Release Source Zone (Section 4) and Module D: Vadose Zone (Section 5), respectively.

7.1.1 LNAPL Distribution in the Unsaturated Zone

Data collected in accordance with the *Attenuation Evaluation Plan* (DON 2017g) have been used to evaluate the distribution of LNAPL within the vadose zone at the Facility. Specifically, (1) the thermal NSZD investigation has been used to evaluate the vertical distribution of LNAPL in the unsaturated zone (see Section 7.3.1.4 and Appendix B.1), and (2) observations of soil/rock contamination while drilling angle borings under the tanks between 1998 and 2002 (DON 1999, 2002) have been used to evaluate the presence of LNAPL below individual tanks (Appendix B.1 Figure 3-3). These data suggest the following LNAPL distribution in the vadose zone:

- Based on the temperature profiles for Facility wells, LNAPL is inferred to be present within the top one-third of the unsaturated zone between the lower access tunnel and the water table (i.e., within the elevations of 70–110 ft msl (see Section 7.3.1.4).
- Based on the angle boring investigations conducted between 1998 and 2002, LNAPL staining and/or sheens were observed in unsaturated-zone soils below Tanks 1, 9, 11, 13, 14, and 16. For example, "hydrocarbon odor and sheen" was observed at 88 ft msl in an angle boring under Tank 14.
- Based on the angle boring investigations conducted between 1998 and 2002, petroleum odors (but no staining or sheens) were noted below Tanks 2–8, 12, and 18–20. For example, odors were observed at 80 ft msl in an angle boring under Tank 2.
- No evidence of petroleum impacts was observed below Tanks 10, 15, and 17 during the angle boring investigations.
- Based on the angle boring investigations conducted between 1998 and 2002, TPH concentrations up to 43,000 milligrams per kilogram were measured in soil samples collected as part of this investigation (DON 2002 Table 4-2).
- Based on monthly SVM conducted since 2008, there has been no significant release of LNAPL from any tank since 2008 except for the 2014 release from Tank 5 (see Section 7.3.1.4 and Appendix B.3).
- Based on available data, LNAPL present in the vicinity of Tank 5 has penetrated only the upper portion of the unsaturated zone. Previous investigations have confirmed that (1) the

vadose zone and saturated zone beneath the Facility are composed of zones of high horizontal permeability, interconnected at the site scale; (2) low-permeability zones of unfractured basalt may be barriers to the movement of fluids through the vadose zone and groundwater flow; and (3) valley fill sediments are fine grained and have the potential to form low-permeability flow barriers. Saprolite occurring beneath valley fill sediments also has the potential to form a low-permeability flow barrier, which could further impede the flow of fluids or groundwater. Dikes may be barriers but have not been observed at the site.

7.1.2 LNAPL Distribution at the Water Table

Historical observations and monitoring data from Facility monitoring wells have been used to evaluate LNAPL distribution at the water table.

7.1.2.1 Observation of LNAPL in Monitoring Wells

No LNAPL has been observed in any Facility monitoring well since 2014 (i.e., after the January 2014 Tank 5 release event). Prior to 2014, the available records regarding LNAPL monitoring do not provide a clear indication of the presence or absence of LNAPL in individual wells. Discussions with DOH (Whittier 2018) indicated that a yellow tint and naphthalene odor were noted in an early sampling event for RHMW02 prior to the 2014 release. A follow-up record search did not uncover documentation of this in RHMW02 sampling logs or reports. Assessment of the presence of LNAPL by comparing COPC concentrations to ideal effective solubilities is presented in Appendix B.7.

7.1.2.2 Evidence of LNAPL Based on COPC Concentrations in Monitoring Wells

Dissolved-phase concentrations of COPCs in groundwater and chromatographic profiles of TPH analysis may be useful as indirect indicators in evaluating the presence of LNAPL in groundwater, when used collectively as multiple LOEs. Based on evaluation of chromatograms, there is no evidence of the presence of LNAPL in any of the groundwater samples collected from monitoring wells at the Facility. For the four monitoring wells located adjacent to or immediately downgradient from the tanks, the dissolved-phase COPC concentrations support the following observations:

- In monitoring well RHMW03, total dissolved-phase concentrations of fuel constituents are relatively low (< 0.5 mg/L since 2005), with limited depletion of groundwater electron acceptors nitrate and sulfate and no measurable methane production. The groundwater data in this area suggest the presence of a low-concentration dissolved plume, potentially one that is driven by infiltration/leaching processes, and do not indicate the presence of LNAPL in the saturated zone upgradient of RHMW03.
- Monitoring well RHMW02 exhibits the highest concentrations of total dissolved-phase fuel constituents among the Facility monitoring wells (approximately 1–7 mg/L since 2005). Many of these concentrations are in the form of polar compounds often associated with the biodegradation of petroleum. The concentrations of naphthalene, 1-methylnaphthalene, and 2-methylnaphthalene are equal to or greater than the expected concentration based on the effective solubility of these compounds in jet fuel. However, concentrations of benzene, toluene, ethylbenzene, and xylene (BTEX) are very low (generally less than 1 microgram per liter [µg/L]). Although COPC concentrations have varied over time, the observed concentration ranges are similar for the monitoring periods before and after the 2014 Tank 5 release. The MNA sampling parameters indicate high levels of biodegradation occurring in the vicinity of this well, as key electron acceptors are depleted and high concentrations of dissolved methane are present (sometimes greater than 10 mg/L). Taken together, these data suggest the presence of weathered LNAPL (i.e., pre-2005 release) within the saturated zone upgradient from this well. Based on the angle boring investigations conducted during 1998–

2002 (DON 1999, 2002), this LNAPL may have originated from Tank 9, 11, or 13. Based on a comprehensive evaluation of all monitoring data and LOEs, the monitoring data do not indicate that the 2014 Tank 5 release impacted groundwater, and that the observed detections in groundwater are more likely attributable to historical releases.

- Monitoring well RHMW01 exhibits the next-highest dissolved-phase fuel constituent concentrations (ranging from not detected to approximately 1.5 mg/L since 2005), which may have some hydraulic connection to monitoring well RHMW02 located upgradient. Since 2005, electron acceptors are depleted, and methane is present in the 0.06–7.5 mg/L range. These data are consistent with the natural attenuation of dissolved petroleum constituents in groundwater and do not suggest the presence of LNAPL within the saturated zone between RHMW02 and RHMW01.
- Monitoring well RHMW05 is located between the tank farm area and the Red Hill Shaft water development tunnel. Groundwater at this location exhibits no or extremely low concentrations of fuel hydrocarbons (typically less than 0.05 mg/L). These data do not suggest the presence of LNAPL within the saturated zone between RHMW01 and RHMW05.

7.1.3 Dissolved-Phase Fuel Type and Evidence of Weathering

Appendix B.7 includes a description of jet fuel composition, partitioning into water, and biodegradation, as well as an assessment of what composes the TPH in groundwater from monitoring location RHMW02, the only well with current concentrations of TPH-d exceeding Hawai'i DOH EALs (DON 2019). The analysis, presented in Appendix B.7, is summarized below. No measurable LNAPL has been documented in the monitoring wells at the Facility. Consequently, the evaluation of fuel type and weathering has relied on the available dissolved-phase COPC monitoring results, particularly the dissolved TPH-d results and chromatograms.

The mixture of individual constituents in TPH-d in monitoring well RHMW02 is consistent with a jet fuel release. The TPH-d is composed of soluble components of jet fuels or kerosene (i.e., the base fuel for jet fuels), which include:

- Substituted benzenes (primarily C3- and C4-benzenes: substituted benzenes with side chains containing three and four carbons)
- Naphthalene and C1-substituted naphthalenes (i.e., 1-methylnaphthalene and 2-methylnaphthalene)
- C2+ substituted naphthalenes

It is evident that the dissolved TPH-d in RHMW02 is from a jet fuel release that is weathered based on the aromatic hydrocarbons found in the groundwater and the predominance of polar compounds/metabolites. Appendix B.7 includes more-detailed discussions of what constituents compose the aromatic hydrocarbons in the groundwater and associated metabolites.

7.1.3.1 Evidence of Dissolved-Phase TPH Weathering

The TPH chromatographic profiles or "fingerprints" show the following evidence of weathering:

- Profiles consistent with soluble components of jet fuel. The presence of naphthalene, C1-naphthalenes, as well as C2+naphthalenes is evident. There is also evidence of C4-benzenes. Lighter components are partially lost in the extraction and concentration of the extract prior to analysis; thus, lighter substituted benzenes, if present, would not be detected in the TPH-d analysis.

- Presence of a "hump" in the chromatograms that extends beyond the end of the jet/kerosene carbon range (C16+) (see Appendix B.7 Figure 2-11, Figure 3-2, and associated discussion). Unweathered petroleum fuels are composed primarily of hydrocarbons (nonpolar) that have distinctive chromatographic profiles seen as evenly distributed peaks spanning the carbon range of the fuel. The presence of a hump with unevenly distributed peaks beyond the fuel carbon range is likely due to polar matter that could be metabolites from biodegradation. Silica gel treatment (used to remove polar material) of the groundwater extract used for measuring TPH-d removes between 43% and 86% of the RHMW02 dissolved TPH-d concentration, indicating that a significant amount of polar compounds is present in the groundwater. The dissolved organics in RHMW02 are a mixture of hydrocarbons and polar compounds/metabolites, indicating ongoing biodegradation.
- Certain compounds that are relatively resistant to biodegradation are typically found in low concentrations in unweathered fuel, but become relatively enriched in the weathered fuels as the more degradable compounds are consumed. Some of the compounds detected as tentatively identified compounds (TICs) in RHMW02 are these more recalcitrant compounds (e.g., naphtheno-benzenes); these compounds would likely not be detectable in a plume originating from an unweathered fuel release. The detection of these compounds in RHMW02 indicates that the dissolved-phase plume is originating from weathered fuel (see Appendix B.7 Section 3.2 and Table 3-3).
- Methane is consistently detected in RHMW02, indicating anaerobic (i.e., methanogenic) biodegradation of fuel constituents.

7.2 DISSOLVED-PHASE COPCS DETECTED IN GROUNDWATER

The Red Hill groundwater monitoring network is described in Section 2.12.2. Groundwater samples are currently analyzed for the following constituents: COPCs (including TPH-gasoline range organics [TPH-g], TPH-d, TPH-residual or oil range organics [TPH-o], BTEX, 1-methylnaphthalene, 2-methylnaphthalene, and naphthalene); fuel additives (including phenol and 2-[2-ethoxymethoxy]-ethanol); lead scavengers (including 1,2-dichloroethane and 1,2-dibromoethane; for newly installed monitoring wells only); and NAPs (including nitrate, sulfate, chloride, nitrate-nitrite as nitrogen, alkalinity, ferrous iron, methane, DO, oxidation-reduction potential [ORP], total organic carbon [TOC], dissolved organic carbon [DOC], and TPH-d/o with silica gel cleanup). Groundwater samples have also been analyzed for general groundwater chemistry, which is further discussed in Section 6.4.

Current and historical COPCs, fuel additives, and lead scavenger results are compared against the screening criteria, which are partially based on the most current DOH (2017) Table D-1b EALs (i.e., groundwater EALs for sites where groundwater is a current or potential drinking water resource and the nearest surface water body is greater than 150 m from release site) where available. For analytes without EALs, the screening criteria are based on most current EPA Regional Screening Levels (RSLs) (EPA 2019). TPH-d and benzene results from select monitoring wells (i.e., RHMW01, RHMW02, and RHMW03) are also compared to Site-Specific Risk-Based Levels (SSRBLs), which were established in the latest Red Hill GWPP (DON 2014b) and subsequently presented in the AOC Statement of Work Sections 6 and 7 scoping completion letter (EPA Region 9 and DOH 2016) (DON 2017i). New risk-based decision criteria (RBDC) were proposed in the *Risk-Based Decision Criteria Development Plan* (DON 2017i, Table 5-1).

One approach for evaluating COPC plume trends is plotting COPC concentrations over time at each monitoring location, as well as spatial graphing of contaminant concentrations versus distance downgradient along the plume flow path over multiple sampling events. Historical Red Hill groundwater monitoring results indicate that most COPCs, and in general the highest detected COPC

concentrations, occur in well RHMW02. Seasonal variations (i.e., wet and dry season effects) are not evident. Cumulative results of historical groundwater monitoring and graphs of COPC concentrations over time (2005–January 2019) are presented in Appendix A. Additional discussions of COPC and NAP results are discussed in the Red Hill quarterly groundwater monitoring reports (DON 2019).

A more detailed evaluation of the data is presented in Appendix B.7, Appendix B.8, and Appendix I. It is good practice to consider multiple LOEs to assess potential impacts to groundwater from Facility operations when COPCs are reported sporadically and at concentrations below varying reporting limits. Limitations of sampling and analysis as well as the use of multiple laboratories over time can have significant impact to data quality.

Lead scavengers 1,2-dibromoethane (used in leaded gasoline and aviation gasoline) and 1,2-dichloroethane (used in leaded gasoline) have not been detected in any monitoring location except RHMW08, where 1,2-dichloroethane was detected by the EPA Region 9 laboratory in 2017. Leaded fuel has not been stored on site since 1968.

Other than for RHMW02 and RHMW01, most COPC detections are sporadic and are estimates below reporting limits. Appendix B.8 includes a review of low-level detections of COPCs and other compounds analyzed along with COPCs. Naphthalenes were historically detected at similar concentrations in multiple wells during the same sampling events when two particular laboratories were used. More than half of all detections of naphthalenes in outlying wells (i.e., all monitoring network wells other than near-tank wells RHMW01, RHMW02, and RHMW03) were reported by these two laboratories. These occurrences are considered suspect, and the results should be interpreted with caution.

Quarterly groundwater monitoring analytical results through January 2019 for the 14 monitoring locations are summarized below.

- *RHMW2254-01* is a sampling point located inside the infiltration gallery (i.e., the water development tunnel) of Navy Supply Well 2254-01 (Red Hill Shaft). Detections of TPH-g, TPH-d, TPH-o, ethylbenzene, toluene, xylenes, 1-methylnaphthalene, 2-methylnaphthalene, and naphthalene occurred occasionally during monitoring events since this sampling point was installed in 2005. No COPC has been detected above the screening criteria, with most detections reported as estimated values below quantitation limits. The highest TPH-d concentration (100 µg/L) was detected by EPA Region 9 laboratory analysis of a split sample in March 2017, which was not confirmed in the duplicate sample analyzed by EPA (reported as non-detect at < 100 µg/L) or in the primary and duplicate split samples analyzed by the Navy- contracted laboratory (reported as non-detect at < 25 µg/L). Toluene, ethylbenzene, and xylenes were detected below screening criteria in groundwater samples collected during the Fourth Quarter (October) 2018 monitoring event, but non-detect during subsequent monthly and quarterly monitoring events. Fuel additives have never been detected at this sampling point. Naphthalenes have not been detected since March 2014.
- *RHMW01*, a monitoring well located inside the lower access tunnel southwest of the tank farm, was installed in 2001 (DON 2002). TPH-d is consistently detected at RHMW01, with the most recent DOH screening criterion (400 µg/L) exceedance during the First Quarter (January) 2016 monitoring event. TPH-d has never exceeded the SSRBL (4,500 µg/L). Evaluation of the chromatographic profiles indicates the likely presence of biodegradation by-products. TPH-o was detected occasionally, and TPH-o last exceeded its screening criterion (500 µg/L) during monitoring events in 2005. TPH-g, benzene, and toluene were detected occasionally at concentrations below the screening criteria during monitoring events between 2005 and 2017.

Naphthalene, 1-methylnaphthalene, and 2-methylnaphthalene were periodically detected below the respective screening criteria (17, 10, and 10 µg/L).

- *RHMW02*, an in-tunnel monitoring well located next to Tank 6, was installed in 2005 (DON 2007). TPH-g is regularly detected at RHMW02 and exceeded the screening criterion (300 µg/L) during 2012 and 2013 monitoring events. TPH-d is always detected; concentrations exceeded the screening criterion in all monitoring events and exceeded the SSRBL (4,500 µg/L) in 2008, 2014, 2015, and 2016, with a maximum concentration of 6,500 µg/L detected in January 2016. TPH-d concentrations have exceeded at times the effective solubility of undegraded jet fuel in water (~5,000 µg/L). The TPH-d chromatographic signature and the results of the TPH-d with silica gel cleanup analysis indicate that the reported TPH-d results are a mixture of jet-fuel-soluble components (substituted benzenes and naphthalenes) and biodegradation by-products (see additional discussion in Appendix B.7 Section 4.2). Based on TPH-d with silica gel cleanup data, approximately 80% of the TPH-d concentrations are in the form of polar compounds/metabolites associated with the biodegradation of hydrocarbons. TPH-o was detected below the 500 µg/L screening criterion in most monitoring events from April 2015 to April 2017 but has not been detected since. Benzene, ethylbenzene, toluene, and total xylenes were also detected in many events from 2005 onward at trace concentrations below the screening criteria. 1-methylnaphthalene, 2-methylnaphthalene, and naphthalene regularly exceeded their respective screening criteria (10, 10, and 17 µg/L) during monitoring events from 2005 onward. Maximum concentrations of 1-methylnaphthalene, 2-methylnaphthalene, and naphthalene were 142 (detected in 2006), 88.5 (detected in 2005), and 343 µg/L (detected in 2006), respectively.
- *RHMW03*, an in-tunnel monitoring well located next to Tank 14, was installed in 2005 (DON 2007). TPH-d and TPH-o have been regularly detected, but always at concentrations below the respective screening criteria (400 and 500 µg/L). TPH-g, toluene, 1-methylnaphthalene, 2-methylnaphthalene, and naphthalene were occasionally detected at trace concentrations below screening criteria between 2005 and 2017. Benzene, ethylbenzene, and xylenes have never been detected.
- *RHMW04*, an outside-tunnel monitoring well located northeast of the tank farm, was installed in 2005 as a background monitoring location (DON 2007). TPH-d, benzene, xylenes, 1-methylnaphthalene, 2-methylnaphthalene, and naphthalene were detected at trace levels below screening criteria sporadically, typically not in the same sampling events. The first sample from RHMW04 collected September 2005 had TPH-d detected at 338 µg/L. This TPH-d result may have been due to well drilling and installation activities (see Appendix I for further discussion). The only other two detections of TPH-d were reported during July 2014 (17 J µg/L) and January 2015 (10 J µg/L) groundwater monitoring events. Review of the chromatograms from the analyses of these two samples indicate that the reported numerical results are from non-petroleum-like individual peaks in the 2014 sample and integration of the baseline in the 2015 sample; neither are due to impact from fuels.
- *RHMW05,* an inside-tunnel monitoring well located southwest of the tank farm and southeast of sampling point RHMW2254-01, was installed in 2009. Benzene, ethylbenzene, and xylenes have never been detected. TPH-g, TPH-o, toluene, 1-methylnaphthalene, 2-methylnaphthalene, and naphthalene have been detected occasionally below screening criteria. TPH-d was detected occasionally between 2005 and 2016, exceeded the screening criterion of 400 µg/L during monitoring events in 2009 (491 and 673 µg/L) and 2010 (2,060 µg/L), but since then has had detections below screening criteria until January 2016. No COPCs have been detected after January 2016.

- *RHMW06 & RHMW07*, outside-tunnel monitoring wells located north of the tank farm, were installed in 2014 in response to the January 2014 release (DON 2015a). TPH-g, benzene, ethylbenzene, toluene, and xylenes have never been detected. TPH-d, TPH-o, and 2-methylnaphthalene were occasionally detected in both wells below screening criteria. Most TPH detections occurred within 1 year of well construction and may be associated with drilling and well installation. 1-methylnaphthalene and naphthalene were detected in RHMW07 below screening criteria. No COPCs have been detected after March 2017.

- *RHMW08 & RHMW09*, outside-tunnel monitoring wells located northwest and south of Tank 1, respectively, were installed in 2016 as part of the AOC Statement of Work Sections 6 and 7 investigation (DON 2017a). No COPCs have been detected at RHMW09. TPH-d and TPH-o have been detected at RHMW08, both at estimated values below the respective screening criteria (400 and 500 µg/L) both occurring within 1 year of well construction; these detections may be associated with drilling and well installation activities (additional discussion of drilling impacts presented in Appendix I). 1,2-dichloroethane was detected by the EPA Region 9 laboratory in 2017 in RHMW08 (0.003–0.004 µg/L), well below its screening criterion (5 µg/L).

- *RHMW10,* an outside-tunnel monitoring well located south of Tank 14, was installed in April 2017 as part of the AOC Statement of Work Sections 6 and 7 investigation (DON 2017a). TPH-d and TPH-o were occasionally detected at concentrations below their respective screening criteria. Evaluation of the groundwater and drilling source water TPH results from that event indicates potential contamination from drilling activities in the May and October 2017 samples (see Appendix I for additional details), and laboratory contamination in the November 2018 sample. No other COPCs have been detected.

- *RHMW11,* an outside-tunnel multilevel well located north of the tank farm at the Hālawa Correctional Facility, was installed in November 2017 as part of the AOC Statement of Work Sections 6 and 7 investigation (DON 2017a). Five of the eight multilevel monitoring zones (RHMW11-01, -02, -03, -04, and -05) were sampled during the First, Second, and Third Quarter 2018 events, and only one of eight monitoring zones (RHMW11-05) was sampled during the Fourth Quarter 2018 and First Quarter 2019 events. No COPCs have been detected at any sampled monitoring zone. Sampling was not performed in the monitoring zones located in the saprolite formation (RHMW11-06, -07, and -08) due to low hydraulic conductivity. Sampling RHMW11-06, -07, and -08 would cause additional stress in the formation, requiring another extensive period for water level recovery and equilibration at these zones.

- *HDMW2253-03* (Hālawa Deep Monitor Well 2253-03), an outside-tunnel well located north of the tank farm at the Hālawa Correctional Facility, was installed in 2000 by DLNR. HDMW2253-03 was designed and constructed to monitor the saltwater/freshwater interface, and draws water from 40 ft below the water table and deeper. TPH-g, benzene, toluene, 2-methylnaphthalene, and naphthalene have been detected below screening criteria. TPH-d (600 µg/L) was detected above the screening criterion (400 µg/L) during the January 2013 quarterly monitoring event. No COPCs have been detected since July 2016. HDMW2253-03 was not sampled during quarterly and monthly monitoring events from April to July 2017 due to experimental testing conducted by CWRM and UH.

- *OWDFMW01*, located at the former OWDF west of Navy Supply Well 2254-01 (Red Hill Shaft), was installed in 1998 as part of an environmental investigation (DON 2000) and added to the Red Hill groundwater monitoring network in 2009. TPH-d exceeded the screening criterion during quarterly monitoring events in 2010, 2012, 2013, and 2015. TPH-d, TPH-o, 1-methylnaphthalene, 2-methylnaphthalene, and naphthalene were occasionally detected at concentrations below the respective screening criteria. Evaluation of the analytical

chromatograms indicates that the reported TPH-d and TPH-o detections are from non-petroleum sources, based on the chromatograms exhibiting a non-petroleum chemical signature.

Appendix B.7 presents a detailed evaluation of jet fuel chemistry, composition of site dissolved-phase hydrocarbons, and attenuation in RHMW02. Appendix B.8 includes a comprehensive evaluation of groundwater chemistry, spatial and temporal trends, and usability of analytical data. Multiple LOEs are used to assess impact of the 2014 JP-8 release to the site groundwater and impact to groundwater in outlying wells from fuel releases/site operations in general. Appendix I presents a comparison of dissolved oxygen concentrations between Red Hill and other sites, an analysis of potential drilling impacts on TPH-d detections in groundwater, and a multiple impact factor analysis to provide additional LOEs.

It was concluded that impacts to groundwater from the jet fuel release seem to be localized in the area of RHMW02, and that natural attenuation is occurring at the site based on groundwater COPC and NAP concentrations at RHMW02 and to a lesser extent at RHMW01 and RHMW03. The available data suggest the presence of weathered LNAPL (i.e., pre-2005 release) in the immediate vicinity of RHMW02 or within the saturated zone upgradient of this well. The groundwater monitoring data indicate it is likely that the 2014 Tank 5 release did not impact groundwater and impacts to groundwater are more likely attributable to historical releases.

There is currently no evidence that the 2014 JP-8 release reached the Red Hill Shaft supply well or any of the outlying wells. Any impacts to groundwater (RHMW02, RHMW01, and RHMW03) are more likely attributable to historical leaks. Evaluation of the data indicates that low-level detections (i.e., less than 0.1 µg/L) of naphthalene in outlying wells are not consistent with LNAPL transport through either the vadose or saturated zones. Due to the uncertainties in the data, these low-level detections are not considered as evidence of impacts from the Facility without additional supporting LOEs.

7.3 NATURAL ATTENUATION

This subsection summarizes natural attenuation studies being conducted at Red Hill. As additional data become available, the natural attenuation text will be updated to reflect current knowledge.

The *Attenuation Evaluation Plan* (DON 2017g) describes the technical approach and additional data used to further evaluate natural attenuation processes for petroleum source depletion. These additional data are being evaluated and integrated to refine the CSM of natural attenuation and source depletion processes. Two different types of attenuation were identified in the *Attenuation Evaluation Plan* (DON 2017g): NSZD (Section 7.3.1) and MNA (Section 7.3.2). NSZD guidance generally addresses LNAPL source zones, while MNA guidance (e.g., Wiedemeier et al. 1999a,b) primarily addresses attenuation of dissolved plumes emanating from a source zone.

7.3.1 Natural Source-Zone Depletion

In 2009, the ITRC published a document describing the NSZD approach, which is a straightforward, quantitative mass balance method to estimate the rates at which quantities of liquid fuels (LNAPLs) are being naturally lost from a petroleum source zone due to the combined effects of sorption, volatilization, dissolution, and aerobic and anaerobic biodegradation (ITRC 2009a).

NSZD is the active process whereby LNAPL is degraded in the subsurface by biological and other naturally occurring processes. For this CSM, LNAPL consists of petroleum hydrocarbons in the form of various fuels. NSZD rates have been measured at many LNAPL sites and can be quantified by

measuring the magnitude and distribution of subsurface temperatures and then calculating the net heat flux being generated by biodegradation processes.

In NSZD, fuel hydrocarbons (LNAPLs) are attenuated by natural processes, primarily aerobic and anaerobic biodegradation. NSZD processes are active both in the unsaturated and saturated zone. These biodegradation processes are not limited to highly soluble hydrocarbon compounds in the LNAPL but can also remove relatively insoluble compounds from the LNAPL. NSZD rates can be measured using several different methods, and the resulting rates can be in the range of a few hundred to a few thousand gallons of LNAPL biodegraded per acre per year.

NSZD is now emerging as an important remediation approach for petroleum hydrocarbon sites. NSZD is a well-accepted technology described by hundreds of technical papers, guidance documents, and patents. The ITRC, an industry group directed by state environmental regulators, issued the first NSZD guidance in 2009 and in 2018 updated it to represent new technologies, including thermal NSZD. Key publications summarizing this technology include *Overview of Natural Source Zone Depletion: Processes, Controlling Factors, and Composition Change* (Garg et al. 2017) and *Light Non-Aqueous Phase Liquid (LNAPL) Site Management: LCSM Evolution, Decision Process, and Remedial Technologies, Appendix B—Natural Source Zone Depletion (NSZD)* (ITRC 2018). As described in Garg et al. (2017), a variety of methods have been used to obtain NSZD rates, as summarized below.

7.3.1.1 Migration of LNAPL and Dissolution

Geologic and water saturation characteristics in the rock surrounding the tanks will cause LNAPL to spread as it moves through the rock. As LNAPL moves through the larger pore spaces, some of it will be trapped in poorly connected fractures and blocked by surface tension and capillary forces of moisture, especially water held in the smaller pores. Hydrocarbon constituents dissolve from a LNAPL source and are transported in solution by groundwater, as described by the ITRC (2009a).

Even though it is possible to recover LNAPL from a source zone, LNAPL below the point of residual saturation will remain, and dissolution by water contact will continue to the solubility limits of compounds in the LNAPL (ITRC 2009a). Effective solubility represents the maximum equilibrium concentration of a constituent from a multicomponent LNAPL mixture in groundwater at a specific temperature and pressure (EPA 1995). Effective solubility of an individual LNAPL constituent is a product of its mole fraction in the LNAPL and solubility of the constituents in its pure non-aqueous phase (ITRC 2009a). Solubility of jet fuel is a focus of Appendix B.7 Forensics and Data Evaluation - Groundwater (summarized in Section 7.1.3.1).

7.3.1.2 Volatilization and Diffusion in the Unsaturated Zone

Petroleum constituents in LNAPL also volatilize and biodegrade by microbial and/or enzymatic activity (ITRC 2009a). Volatile constituents move by diffusion from areas of higher concentration to areas of lower concentration. Hydrocarbon vapors preferentially migrate from the LNAPL source toward the ground surface but are typically biodegraded aerobically in the presence of oxygen before they reach the surface. Diffusion is usually the dominant mechanism for vapor-phase transport in unsaturated porous media under most conditions (Rockhold, Yarwood, and Selker 2004) and is a function of a constituent's air diffusion coefficient and the air-filled porosity of the soil. Diffusion and advective vapor migration are faster in soils and rock with more air-filled effective porosity (ITRC 2009a). Sites with more air-filled porosity will have higher diffusion rates, more oxygen influx, and more aerobic biodegradation compared to anaerobic biodegradation.

7.3.1.3 NEW CONCEPTUAL MODEL FOR BIODEGRADATION AT LNAPL SITES

A 2017 report in the journal *Groundwater Monitoring & Remediation* reviewed extensive research on natural attenuation and petroleum source depletion processes during the last 35 years and presented the key findings related to natural attenuation of petroleum (Garg et al. 2017). That report includes results of long-term research studies of petroleum degradation that were initiated in 1983 by the USGS and subsequent studies of natural attenuation processes by Arizona State University and Colorado State University. Those in-depth research studies were integrated to develop a comprehensive mass-balance and reactive-transport model (Ng et al. 2014, 2015). The paper by Garg et al. (2017) indicates that methanogenic processes are likely responsible for most of the NSZD at sand/silt/clay sites impacted by LNAPL. This is because the sand/silt/clay impedes rapid diffusion of oxygen and creates anaerobic zones where methanogenic processes are active.

While methanogenesis is likely the dominant process for degradation of petroleum LNAPL in the saturated and smear zones (Garg et al. 2017), it may not be as important in the unsaturated zone at the Facility because the unsaturated zone underlying the tank farm area contains permeable media that allows oxygen to enter and drive aerobic biodegradation rather than anaerobic biodegradation processes. The NSZD measurements described below have been performed at the Facility, and helped determine if biodegradation is occurring, determine where aerobic vs. anaerobic processes dominated, and provided NSZD rate information for the Facility. As described below, both the shallow and deep unsaturated zone at the Facility are characterized by non-detect methane concentrations and high oxygen concentrations indicating that NSZD occurs through direct aerobic degradation of LNAPL rather than methanogenesis followed by aerobic degradation of methane at a shallower depth.

7.3.1.4 MEASURING NSZD AT THE FACILITY

Biodegradation of petroleum in the unsaturated zone generates carbon dioxide, potentially methane, and heat and will deplete oxygen. To further evaluate this, studies of natural attenuation and source depletion processes were conducted that included (1) a soil vapor study, (2) a carbon trap study, and (3) a thermal NSZD investigation. These studies, presented in Appendix B.3, B.2, and B.1, respectively, are summarized below.

Soil Vapor Study. A soil vapor study was conducted that involved collection of soil vapor samples from the shallow, middle, and deep soil vapor probes that currently exist underneath the tanks; from vapor pins installed in the upper access tunnel; and from sampling points on the surface of Red Hill. The samples were analyzed for concentrations of oxygen, carbon dioxide, volatile organic compounds (VOCs), and methane. The soil vapor study was designed to help address the following study questions:

1. Is there evidence of recent or historical fuel releases at one or more of the tanks?
2. Is LNAPL present below the tanks?
3. Is NSZD occurring?
4. Can vapor monitoring help quantify the magnitude of NSZD?
5. Can vapor monitoring be used to track NSZD progress over time?
6. Are vadose zone petroleum vapors a significant source of impacts in the tunnels?

Field monitoring and laboratory analysis of soil vapors was conducted in October/November 2017. Investigation results support evidence of releases and NSZD, an evaluation of the utility of SVM to

track releases, the NSZD of LNAPL fuel as expressed in the vapor emissions, and insights as to the source of petroleum VOCs in the tunnels. Soil vapor study results are summarized in Table 7-1.

Table 7-1: Findings and Conclusions of Soil Vapor Investigation

Question	Answer	Discussion
Evidence of Releases and NSZD		
1. Is there evidence of recent or historical fuel releases at one or more of the tanks?	YES. The soil vapor results suggest a historical release of LNAPL fuel at Tank 5 and, at the other tanks, low-level vapor-phase releases associated with ongoing Facility operations.	As shown on Figure 7-1, the SVM showed a range of total VOC concentrations and differences in alkane composition for the below-tank SVM points. Together, these data indicate the presence of weathered LNAPL fuel below Tank 5. For the other tanks, the target analyte results along with visual evaluation of the FID chromatograms indicate low levels of unweathered or lightly weathered petroleum vapors likely associated with ongoing Facility operations combined with less volatile compounds likely associated with highly weathered historical releases. The low levels of unweathered petroleum vapors are consistent with minor vapor-phase emissions typical of any fuel storage operation.
2. Is LNAPL present below the tanks?	YES. The soil vapor results suggest the presence of weathered LNAPL fuel below Tank 5.	Angle borings completed below some of the other tanks provided visual evidence of LNAPL at the time the borings were installed (1998–2002) (DON 1999, 2002). For these other tanks, the presence of LNAPL is not reflected in the quantitative analysis of soil vapor samples collected in October/November 2017; however, many of the FID chromatograms show an unresolved hump of less-volatile compounds potentially consistent with the presence of highly weathered LNAPL (see Appendix B.3 Attachment B.3.2).
3. Is NSZD occurring?	YES. As discussed above, the soil vapor results suggest that significant biological weathering of the LNAPL below Tank 5 has occurred since the 2014 release. This is consistent with other LOEs supporting biological NSZD.	The conclusion of biological weathering of LNAPL releases is supported by the following observations: • The petroleum vapor fingerprint from below Tank 5 is consistent with weathered LNAPL associated with the 2014 release. • The vapor testing below other tanks indicates that the LNAPL visually observed in borings completed below these tanks in 1998–2002 (DON 1999, 2002) is depleted in VOCs. • Field monitoring and laboratory analysis indicate high oxygen concentrations (13.7–20.6%) in all the below-tank SVM points, supporting aerobic biodegradation. • Thermal monitoring indicates ongoing biological NSZD (see Appendix B.1). • Carbon trap data provide an additional, independent LOE of ongoing biological NSZD (see Appendix B.2).
Utility of Soil Vapor Monitoring Data		
4. Can vapor monitoring help detect new LNAPL fuel releases?	YES. Monthly PID screening of the soil vapor monitoring points with laboratory confirmation for those with elevated PID readings is likely to be a reliable method for detecting any new LNAPL releases of jet fuel.	As shown on Figure 7-2, monthly PID monitoring clearly reflects the LNAPL fuel release from Tank 5 that occurred in January 2014. If future PID monitoring suggests a new release, laboratory analysis by TO-15 PIANO can be used to confirm that the observed PID spike is associated with a new release. Following the Tank 5 release, elevated PID readings (> 25,000 ppbv) were observed in nine SVM points (below Tank 5 and three adjacent tanks), indicating that the existing soil vapor network provides a robust system for release detection. Evaluation of the available PID monitoring data (2008–present) (DON 2008a) indicates that the 2014 Tank 5 release was the only significant release event during that monitoring period.

Question	Answer	Discussion
5. Can vapor monitoring be used to track NSZD progress over time?	YES. Monthly PID monitoring appears to track decreases in petroleum vapor concentration over time associated with weathering of LNAPL releases. The TO-15 PIANO analysis provides detailed information on the petroleum VOC vapor composition that can be used to evaluate the degree of biological weathering.	As shown on Figure 7-2, the monthly PID monitoring shows a decrease in PID readings at Tank 5 from 2014 to 2018 following the 2014 release event. The TO-15 PIANO analysis in November 2017 indicated a depletion of n-alkanes resulting in a relative enrichment of cycloalkanes confirming the occurrence of biological weathering (Figure 7-2, right panel). These data indicate that monthly PID monitoring combined with periodic laboratory analyses can serve to document both the magnitude and mechanism of NSZD. Results presented in Appendix B.3 Section 4 show that monthly PID monitoring conducted since 2008 has also documented the occurrence of NSZD below Tanks 3, 6, 7, 8, and 9. When averaged across all wells, PID readings show a clear decreasing concentration from 2008 to 2013 and from 2014 to 2018, documenting ongoing NSZD processes (Appendix B.3 Figure 4-4).
Risk Assessment		
6. Are vadose zone petroleum vapors a significant source of impacts in the tunnels?	NO. Facility operations are the primary source of petroleum vapors in the tunnels. Any soil vapors entering the tunnel are highly diluted by the tunnel ventilation system.	The magnitude and sources of petroleum vapors in the tunnels were evaluated using PID readings and qualitative observations. These data suggest that: • Petroleum vapor concentrations in the tunnels are higher than in outdoor air. • Although vapor flow is from the vadose zone into the tunnel, any soil vapors entering the tunnels are highly diluted by ambient air from the tunnel ventilation system. • The primary source of the petroleum vapors in the tunnels is active operations at the Facility.

FID flame ionization detector
PIANO paraffins, isoparaffins, aromatics, naphthenes, and olefins

For locations where the monitoring well screen extends above and below the water table, concentrations of VOCs and NAPs (i.e., oxygen, carbon dioxide, and methane) can be used to monitor biodegradation of petroleum at the water table. Thus, to further evaluate biodegradation activity at and near the water table, vapor samples were collected from selected wells. The selected locations included monitoring wells in the source area where the screen straddles the groundwater table. At each monitoring well, a vapor sample was collected at a point directly above the groundwater level in the well and analyzed for the same gases analyzed from the SVM probes, described above. These vapor concentration data continue to be evaluated in conjunction with the vapor data from the SVM points and the other groundwater COPC and NAP analysis data.

Carbon Trap Study. LNAPL biodegradation generates carbon dioxide, which was measured using a chamber-based sampling device or carbon traps at the surface, and by analyzing the vertical concentration gradient and applying diffusion calculations.

The carbon dioxide efflux method (or "carbon trap" method) is one of a variety of methods (as described in Garg et al. (2017) that have been used to obtain NSZD rates. This method measures the amount of carbon dioxide being generated through the biodegradation of LNAPL. The carbon dioxide is captured using two carbon dioxide sorbent elements composed of soda lime (consisting primarily of calcium hydroxides), which are contained in a canister, over potential LNAPL zones (McCoy et al. 2014). The carbon dioxide generated by LNAPL biodegradation is transported to the surface by diffusion, and in some cases advection, and is trapped in one sorbent element. The other sorbent element prevents atmospheric carbon dioxide from being captured by the first sorbent element. Traps are typically deployed in receivers in the field for 14 days and then sent to the laboratory. The carbon-14 fraction (^{14}C correction) is also measured in the laboratory so that "modern carbon" (e.g., carbon dioxide generated from biodegradation of recent plant material) can be separated from "ancient

carbon" (carbon dioxide associated with the biodegradation of fossil fuel). The efflux rate of ancient carbon is used to calculate a NSZD rate in units of gallons per acre per year (gal/acre/yr). Due to the unique construction of the Facility, conventional carbon traps were used to measure carbon dioxide flux at the ground surface, and modified carbon cartridges were used to measure carbon dioxide flux from the basalt into the tunnels.

*NSZD Rate Based on Tunnel Carbon Dioxide Flux***.** The ventilation system in the upper and lower access tunnels creates a negative pressure gradient within the tunnels (i.e., a pressure gradient from the basalt into the tunnel), so that any advective gas flow is from the unsaturated zone into the tunnels (see Appendix B.3). As a result, the tunnels act like a soil vapor extraction (SVE) system and can capture ancient (i.e., petrogenic) carbon dioxide generated through biological NSZD occurring in the unsaturated zone.

Carbon dioxide concentrations in the tunnels were measured through the collection of 24-hour air samples pumped through carbon trap cartridges. The concentration of ancient carbon in each sample was determined using two methods: either (1) assuming a standard fraction of modern carbon in contemporary living material (Hua, Barbetti, and Rakowski 2013) or (2) using a site-specific value. This ancient carbon was attributed to petroleum NSZD. The flux of ancient carbon through the tunnel was calculated by multiplying the excess ancient carbon concentration by the tunnel air flow. Tunnel air flow was estimated using either (1) the design air flow rate in the tunnels or (2) a modified flow rate accounting for ventilation system maintenance (based on communications with the Navy: December 5, 2017 email message from John Floyd to Curtis C. Stanley, GSI Environmental, "RE: 4671 Tunnel Ventilation Questions for Navy"). Based on this range of calculation inputs, the NSZD rate attributable to ancient carbon entering the tunnels was calculated at between 3,400 and 6,400 gallons per year (gal/yr).

NSZD Rate Based on Ground Surface Carbon Dioxide Flux. Carbon traps were also installed on the top and sides of the tank farm (transverse to the tank farm) either near known impact areas or on clinker zone outcrops. All ground surface carbon traps showed low or zero NSZD based on the ancient carbon captured, indicating that carbon dioxide flux to the ground surface is low and variable. The NSZD rates estimated using individual carbon traps ranged from zero gal/acre/yr to 84 gal/acre/yr. Based on the trap data and the total ground surface area for carbon dioxide efflux, the NSZD rate attributable to ground surface carbon dioxide flux from the top and sides of the tank farm is estimated at 1,000 gal/yr.

Conclusions. The majority of the NSZD is from the tunnel acting like a partial SVE system, pulling carbon dioxide from the basalt into the tunnels (Figure 7-3). Thicker arrows on Figure 7-3 indicate greater flux; location of tanks, traps, and biodegradation zones are approximate. The two NSZD rates (flux to the tunnels and flux to the ground surface) are additive, so the total NSZD rate at the tank farm is estimated at 4,400–7,400 gal/yr.

Furthermore, if less than 0.5% of the air flow through the tunnel originates from the vadose zone (rather than the tunnel entrances and ventilation system intakes), then the resulting ventilation of the vadose zone would be sufficient to provide 100% of the oxygen needed to support the observed NSZD while maintaining vadose zone oxygen concentrations above 19%. Thus, only a small amount of leakage through the tunnel walls is required to provide sufficient air flow through the unsaturated zone to sustain aerobic biodegradation. Differential pressure measurements between the soil vapor wells and the lower tunnel confirmed a pressure gradient that support air flow from the basalt into the lower tunnel (see Appendix B.3)

Thermal NSZD Investigation. A thermal NSZD investigation was conducted using two protocols in the field to measure vertical temperature profiles in wells in the Facility, with both protocols producing

similar data. These data were then used to determine the general vertical location of LNAPL at each location and the corresponding NSZD rates for that LNAPL.

Vertical temperature profiles were obtained in October–November 2017 from three existing monitoring wells (RHMW01, RHMW02, and RHMW03) and one background well (RHMW05). These profiles were then used to quantify NSZD rates at the tank farm. Additional thermal profiles were collected in May 2019 in the previously profiled wells and in unprofiled wells outside the tank farm area. These new thermal profile data will facilitate evaluation of the stability of the thermal data in wells underlying the tank farm and how they may contrast with areas outside the tank farm. Data are currently under evaluation and will be reported later.

Two protocols were employed to obtain temperature measurements: Well Air Temperature Measurements and Wall Temperature Measurements. In the Well Air Temperature Measurements configuration, the thermocouple for temperature measurement was fed through a hole in a well plug, a weight was attached to a line attached to the end of the thermocouple, and the assembly was fed down the well. In the Wall Temperature Measurements configuration, the thermocouple was attached to a pipe test ball plug, which was fed down the well and inflated, thus pressing the thermocouple against the inside wall of the monitoring well. Both configurations provided similar thermal profiles, so the NSZD rates were calculated for both methods and averaged.

By performing two different calculations, a range in the NSZD rates was obtained:

- Calculation Method 1 (Background-Correction) used the net (background-corrected) temperature profiles to remove seasonal and tunnel heating effects to calculate heat fluxes going upward into the tunnel and downward into the groundwater, and then these heat fluxes were used to calculate a total NSZD rate. This is the most common method used to calculate NSZD rates using temperature.
- Calculation Method 2 (Model-Correction) is an alternate method where Hillel (1982) model-corrected temperatures were used to correct for minor seasonal effects in the temperature data.

NSZD Results. The NSZD rates for both calculation methods were relatively similar, which increases the confidence in the accuracy of these results. Measured NSZD rates using Calculation Method 1 (Background-Correction) for each calculation and averaged results from Well Air Temperature and Wall Temperature Measurements are shown below; these are considered the more accurate calculations for NSZD rates of all the methods:

- RHMW01: 140 gal/acre/yr of NSZD
- RHMW02: 640 gal/acre/yr of NSZD
- RHMW03: 1,500 gal/acre/yr of NSZD

Typical NSZD rates measured at other hydrocarbon release sites range from hundreds to thousands of gal/acre/yr (Garg et al. 2017), so these values are consistent with other hydrocarbon releases that are being biodegraded by NSZD biodegradation processes.

The distribution matches the site conceptual model where known past releases have been associated with the tanks near RHMW02 and RHMW03 (DON 1999, 2002; see Section 4.1). RHMW01 is located just southwest of the tank farm. RHMW05 showed virtually no NSZD, which was expected since it was the background well and was farthest from the tank farm.

In addition to measuring NSZD rates from the temperature profiles using Calculation Method 1 (Background-Correction) and Calculation Method 2 (Model-Correction), a supporting calculation was done to estimate the NSZD rate indicated by the increase in temperature seen in groundwater underlying the tank farm—Calculation Method 3 (Groundwater Temperatures). The lower range of this calculation was of the same magnitude as the vertical heat flux moving into groundwater from the vertical temperature profiles, again increasing the confidence in the NSZD calculation methods.

Assuming the three thermal NSZD measurements are representative samples of NSZD within the tank farm, an average NSZD rate for the entire tank farm was calculated in gal/yr. Taking an average of all Calculation Method 1 (Background-Correction) NSZD rates (759 gal/acre/yr) and multiplying this by the area encompassed by the tank farm (13.1 acres), the total NSZD rate comes to 9,935 gal/yr or about 10,000 gal/acre/yr. To establish a range of values for the total NSZD at the tank farm, the standard deviation of the total NSZD rate of all three wells using Calculation Method 1 (Background-Correction) was calculated. This value is 7,300 gal/yr. Therefore, the average total NSZD rate at the tank farm is estimated at 2,600–17,300 gal/yr. Total NSZD rates in units of gal/yr are shown in Table 7-2. The Bottom Heat Flux NSZD rate is calculated based on the downward heat flux from the reaction zone to groundwater that increases the groundwater temperature. The Top Heat Flux NSZD rate is calculated based on the upward flux from the reaction zone to the lower tunnel at the Facility where the shallowest temperatures were measured at the three monitoring well locations.

Table 7-2: Summary of Total NSZD Rates (Gallons per Year) from the Tank Farm

Well	Calculation Method 1 (Background-Correction)	Calculation Method 2 (Model-Correction)	Calculation Method 3 (Groundwater Temperatures)
Bottom Heat Flux NSZD Rate (gal/yr)			
RHMW01	1,600	2,200	N/A
RHMW02	2,100	2,500	N/A
RHMW03	2,500	3,900	N/A
Average	*2,000*	*2,800*	*2,300–51,600*
Top Heat Flux NSZD Rate (gal/yr)			
RHMW01	220	600	N/A
RHMW02	6,300	6,700	N/A
RHMW03	17,000	17,500	N/A
Average	*7,900*	*8,200*	*N/A*
Total NSZD Rate (gal/yr)			
RHMW01	1,900	2,700	N/A
RHMW02	8,400	9,100	N/A
RHMW03	20,000	21,400	N/A
Average	*9,900*	*11,100*	*N/A*

Note: Values are rounded. Calculations were performed using unrounded values.
N/A not applicable

Although there is some uncertainty regarding how NSZD rates change over time at an individual site, there is a general conceptual model that NSZD rates may be relatively constant provided there is a continuing source term. Even as biodegradation acts first on easily biodegradable compounds and then progresses to less-biodegradable compounds, the overall NSZD rate (i.e., mass of petroleum degraded per year) may remain relatively constant (e.g., Garg et al. 2017). For example, for the purpose of evaluating past and future attenuation, USGS researchers at the Bemidji National Crude Oil Release

site in Minnesota assumed constant NSZD rates over the lifetime of the crude oil release that occurred at that site in 1979 (Ng et al. 2014, 2015).

Vertical LNAPL Distribution Inferred from Temperature Profiles. In addition to providing NSZD rates, the temperature data also indicate the general location of biodegradation reactions occurring in the subsurface. Because high oxygen levels were observed at all depths within the unsaturated zone (see Appendix B.3), the heat-generating degradation reactions were assumed to be occurring with the LNAPL intervals. Thus, the LNAPL intervals in each well were determined by analyzing the temperature gradients in the net (background-corrected) temperature profiles (profiles of the difference between the raw temperature recorded at each depth for a well minus the raw temperature calculated at the same depth for the background well, RHMW05). From these data, the general location of LNAPL biodegradation reactions in these wells was in the intervals shown in Table 7-3 and on Figure 7-4. On Figure 7-4, each scale shows depth below the tunnel floor, with the elevation scale (ft msl) on the far left. As shown on this figure, the interval of the LNAPL does not correspond directly with the location of the clinker zones at these locations. This indicates that other geologic media, such as thin pāhoehoe layers, are able to transmit and hold LNAPL.

Table 7-3: Vertical Distribution of LNAPL Intervals Indicated by Net (Background-Corrected) Temperature Profiles from Three Facility Monitoring Wells

Monitoring Well	Top of Casing Elevation (ft msl)	Approximate Top of LNAPL (ft btoc)	Approximate Bottom of LNAPL (ft btoc)	Approximate Top of LNAPL (ft msl)	Approximate Bottom of LNAPL (ft msl)
RHMW01	102.0	20	30	82	72
RHMW02	104.6	0	30	105	75
RHMW03	121.9	10	45	111	76

Note: All three wells are installed in the lower access tunnel of the Facility.
btoc below top of casing

At many NSZD sites in unconsolidated media, the intervals of the LNAPL and the intervals of the heat generation are not collocated because methanogenic processes degrade the LNAPL near and in the water table, and then methane is produced. This methane then diffuses toward the surface but is oxidized by naturally occurring bacteria in a reaction zone between the top of the LNAPL and the surface. This methane oxidization zone is where the heat is generated in this type of system.

Within the tank farm area, however, the unsaturated zone is characterized by high oxygen concentrations and no detectable methane both in well headspace samples collected immediately above the water table and soil vapor samples collected from 10 to 30 ft below the fuel tanks (see Appendix B.3). These results indicate that heat generation within the unsaturated zone at the tank farm area is attributable to direct aerobic degradation of petroleum constituents within LNAPL-impacted intervals.

Note that the LNAPL distribution shown by the thermal profile at RHMW03, between 10 and 45 ft below the lower access tunnel floor (76–111 ft msl) (Figure 7-4), corresponds to the observed LNAPL distribution below Tank 14 observed in the 2000 timeframe, where LNAPL was observed between 88.83 and 98.15 ft msl in angle boring B-14, as shown on Appendix B.2 Figure 4-3. This indicates that the thermal NSZD method is a robust approach to delineating vertical LNAPL distributions in the aerobic system.

The net temperature signal at RHMW02 measured in the 0–30 ft segment of the thermal profile below the lower access tunnel floor is consistent with a release of LNAPL from Tank 5 in 2014 that did not reach the water table.

7.3.2 Monitored Natural Attenuation

Several processes are known to cause a reduction in the concentration and/or mass of a contaminant dissolved in groundwater via MNA. Processes that result in a change in a contaminant's aqueous-phase concentration, but not of the total contaminant mass in groundwater, are termed nondestructive. Processes that result in the reduction of contaminant mass are referred to as destructive. Nondestructive processes include advection, hydrodynamic dispersion (mechanical dispersion and diffusion), sorption, dilution, and volatilization. Destructive processes include aerobic and anaerobic biodegradation, and in some cases, abiotic degradation. A key concept is that MNA methods focus on the attenuation of dissolved groundwater plumes or vapor plumes, while NSZD methods focus on measuring attenuation in source zones.

7.3.2.1 KEY MNA PROCESSES

Hydrodynamic dispersion is the process whereby a groundwater plume mixes with clean water as the plume migrates through a porous medium. This mixing occurs as a result of two processes: mechanical dispersion due to the change in groundwater flow paths as groundwater migrates through a porous medium, and molecular diffusion of contaminants from high-concentration to low-concentration zones. There is currently a re-evaluation of the importance of both the mechanical dispersion versus diffusion process, but in general, dispersion is a second-order process (i.e., typically does not serve as the primary natural attenuation process).

Sorption is a non-destructive process in which organic compounds are sorbed to the matrix of the water-bearing unit and is represented by a retardation factor (Wiedemeier, Rifai, et al. 1999). Sorption is controlled by both the characteristics of the chemicals (chemicals that are more hydrophobic will exhibit more sorption) and the soil (soils with more organic material will be able to sorb more chemicals). The amount of sorption is described using a "retardation factor" that reflects two key factors: (1) the degree to which a particular constituent moves slower than groundwater seepage velocity, and (2) the ratio of total constituent mass per volume of aquifer matrix to the volume of dissolved constituents.

Back-diffusion occurs where porous, low-permeability geologic material is in long-term contact with LNAPL or dissolved plumes. First, dissolved contaminants enter porous, low-permeability materials such as clays (or fine-grained material in weathered clinker) by the physical process of diffusion (movement of dissolved constituents from areas of high to low concentration). When matrix diffusion is active over several years, significant contaminant mass can be stored in low-permeability zones. Then, after source material (e.g., LNAPL) is removed by remediation and/or NSZD, back-diffusion from these fine-grained units can serve as long-term ongoing sources of dissolved constituents to groundwater.

In MNA, biodegradation is the process where naturally occurring bacteria biodegrade fuel constituents to end-products such as carbon dioxide. Bacteria typically will utilize an electron acceptor that is present in groundwater, soil, or the air and will then produce carbon dioxide. Common electron acceptors for MNA reactions in the unsaturated and saturated zones include oxygen for aerobic reactions and nitrate, sulfate, and/or ferric iron for anaerobic reactions. Another reaction is methanogenic, where one class of fermenting bacteria can ferment hydrocarbons to dissolved hydrogen and/or acetate, and then the hydrogen/acetate is utilized by methanogens to produce methane and carbon dioxide.

7.3.2.2 MICROBIAL INVESTIGATIONS

Two microbial studies of natural attenuation capacity at Red Hill due to biodegradation were performed:

- A microcosm study designed to estimate the bulk attenuation rate due to biodegradation for several constituents of concern under aerobic and anaerobic conditions. Microcosms were constructed with site groundwater from RMHW01 and RHMW02 and were monitored over an extended period (approximately 1 year) to assess degradation rates.
- A microbial parameter study to assess levels of several functional genes associated with aerobic and anaerobic degradation of BTEX, alkane, and/or PAH degradation that can be used as an indicator for biodegradation capacity of petroleum hydrocarbon degradation. The tests involve polymerase chain reaction (qPCR)-based analyses of site groundwater from RHMW01, RHMW02, RHMW03, and RHMW04. The results provide a snapshot of the microbial community present at the Facility, including those capable of petroleum hydrocarbon degradation. Data from a single sampling event (October 25, 2017) are available for evaluation.

Collectively, the results of these tests help to establish if key organisms are present, active, and degrading hydrocarbons at rates that help to limit migration. These data not only serve as a LOE for attenuation but also provide insight on rates. The data and analysis of these studies are presented in Appendix B.6 and summarized below.

Microcosm Results. Rate coefficients were calculated for individual constituents using available time-series concentration data and assuming that degradation fits a first-order relationship. Rapid biodegradation under aerobic conditions was observed in the microcosms from RHMW02; all constituents were degraded with half-lives of less than 1 week, and several less than 1 day. Aerobic biodegradation rates at this location are consistent with those reported by Kao et al. (2006) for benzene, toluene, and xylene and 1,2,4-trimethylbenzene (half-lives ranging from 0.8 to 6 days) and Landmeyer et al. (1998) for naphthalene (half-life of 0.8 day). The data indicate that strong degradation capacity can be stimulated at this location when oxygen is present. Slower biodegradation rates were observed in the aerobic microcosms from RHMW01, although all constituents exhibited a concentration decrease over the monitoring period. Complete degradation of all constituents was observed in microcosms from RHMW01 and RHMW02. Aerobic half-life estimates at RHMW01 for the constituents included in the test range from 3 days (2-methylnaphthalenene) to 25 days (benzene); all half-lives from RHMW02 were < 1 week.

Based on the microcosm results, degradation of these petroleum hydrocarbons is slower under anaerobic conditions, with half-lives generally on the order of 101 to > 10,000 days depending on the compound. Anaerobic degradation rates observed in RHMW01 were faster than those observed in RHMW02. Degradation of several compounds could not be established in RHMW02, and no degradation of benzene could be established in microcosms from either well. When degradation was observed under anaerobic conditions, it occurred after a lag period, indicating that native microbial populations were acclimating to the test conditions.

Microbial Parameters (QuantArray-Petro and Next Generation Sequencing [NGS]). Samples from all four wells contained measurable levels of several functional genes associated with aerobic and anaerobic degradation of BTEX, alkane, and/or PAHs based on the QuantArray-Petro analysis. This is a strong indicator for biodegradation capacity. In general, the measured levels of these biomarkers were considered low to moderate (based on a comparison to sample results in the database

maintained by the performing laboratory). This is consistent with the relatively low biomass concentrations that were also observed in these wells.

RHMW02, RHMW03, and RHMW04 had several aerobic biomarkers, including the highest levels of PM1, which is associated with BTEX. RHMW04 is located outside the area of groundwater impacts and is screened in an aerobic portion of the groundwater-bearing unit. RHMW02 is screened in a much more reducing portion of the groundwater-bearing unit based on low DO levels (historically below 1 mg/L) and elevated methane levels (4.5 mg/L during the October 2017 monitoring event). In addition, the microcosm study showed that the RHMW02 microbial community could be easily stimulated to degrade petroleum hydrocarbons aerobically when oxygen was added to the bottles. Low DO levels are also observed in RHMW03, but based on data from historical monitoring events, RHMW03 does not show geochemical indicators of intense anaerobic activity, with relatively little sulfate depletion and no methane production over the past 2 years. Relative to the other wells, RHMW01 generally had lower levels of aerobic biomarkers and higher levels of anaerobic biomarkers, consistent with the existing groundwater sampling data showing dissolved petroleum constituents and low DO concentrations at these locations.

Samples from all four wells had moderate to high levels of benzyl coenzyme, which is a biomarker of anaerobic BTEX degradation, while RHMW01 and RHMW02 had measurable levels of biomarkers associated with anaerobic PAH degradation (e.g., naphthalenes). RHMW01 and RHMW02 also had the highest levels of eubacteria, which can be used as a bulk indicator of microbial abundance. This is consistent with the results of the microbial community analysis (NGS data), as well as the diversity of aerobic and anaerobic biomarkers measured in samples from these wells. Collectively, these data provide significant evidence that biodegradation of petroleum hydrocarbons can occur at these locations.

Conclusions. The results of these microbial studies are largely consistent with concentration trends and geochemical conditions at the Facility. Specifically, petroleum hydrocarbon concentrations are relatively high at RHMW02 and then attenuate significantly moving away from this well. The molecular data suggest that a combination of anaerobic and aerobic processes is responsible for this attenuation, although the potential for rapid aerobic degradation (as observed in the microcosms) is restricted somewhat by the availability of oxygen in the vicinity of RHMW02 and the relatively low initial concentration of biomass. Degradation rates are apparently slower at RHMW01 based on the available microcosm data, but the molecular data provide another LOE that biodegradation within the plume is contributing to the attenuation observed at RHMW01.

Study results for the four monitoring wells are summarized in Table 7-4.

Table 7-4: Summary of Microcosm and Microbial Study Preliminary Results by Monitoring Well

Monitoring Well	Range of Aerobic Biodegradation Half-Lives (days) (from Microcosm Study)	Range of Anaerobic Biodegradation Half-Lives (days) (from Microcosm Study)	Presence and Abundance of Biomarkers for Aerobic Biodegradation?	Presence and Abundance of Biomarkers for Anaerobic Biodegradation?
RHMW01	8 days to 25 days	101 days to 1,732 days	Yes	Yes
RHMW02	< 1 day to 7 days	495 days to > 10,000 days; degradation not observed for several compounds	Yes	Yes
RHMW03	Not included in study	Not included in study	Yes	Yes (limited)
RHMW04	Not included in study	Not included in study	Yes	Yes (limited)

7.3.2.3 MNA MEASUREMENT METHODS

MNA protocols divide MNA measurement methods into three different LOEs described in the EPA's (1999) MNA Directive:

- *MNA-LOE 1 (primary data).* Demonstrate a loss of contaminant mass or reduction in concentration in groundwater.
- *MNA-LOE 2 (secondary data).* Show conditions are conducive to MNA success using geochemical data.
- *MNA-LOE 3.* Use special microcosm or field studies to demonstrate "proof of concept" of a particular attenuation process. The microcosm study and microbial parameters fit in this category and are described in Section 7.3.2.2 and Appendix B.6.

According to this directive, the first LOE is always used to demonstrate MNA, the second LOE is often used, and the third LOE is used less frequently. Since publication of the EPA MNA directive in 1999, new technologies and approaches have blurred the lines on which MNA measurement methods fit under which LOEs.

Chemical fingerprinting of both groundwater and vapor samples has been performed to determine if and how much weathering has occurred in areas impacted by hydrocarbon vapors and dissolved constituents as well as provide forensic data to better understand LNAPL releases. These analyses are presented in Appendix B.7 and Appendix B.3.

7.3.2.4 EVALUATION USING NATURAL ATTENUATION PARAMETERS

Primary (#1), secondary (#2), and tertiary (#3) LOEs were evaluated to demonstrate whether natural attenuation processes are occurring at the Facility. The evaluations, presented in Appendix B.4, B5, and B.6 respectively, are summarized below.

Analysis of Primary MNA Data. Natural attenuation processes at the Facility were evaluated using primary LOEs (i.e., temporal and spatial contaminant concentrations) from the Facility groundwater monitoring network. Where data are available, first-order rate coefficients and associated half-lives were calculated for monitoring wells RHMW01 and RHMW02 at the Facility. COPCs include 1-methylnaphthalene, 2-methylnaphthalene, and naphthalene. These data serve as a LOE for COPC attenuation and will provide site-specific input values for ongoing fate and transport modeling at the Facility.

BTEX data were not analyzed in this study, given their low concentrations and/or limited data sets (i.e., benzene and toluene). TPH-d was included in the analysis; however, due to laboratory analytical issues associated with the TPH-d method such as variations in extraction efficiency and absence of silica gel cleanup (see Appendix B.7 and B.8), the TPH-d results have high uncertainty.

Two types of first-order attenuation rate coefficients were calculated to evaluate LOE 1 MNA processes at the Facility:

- *Plume Duration (Concentration vs. Time [C vs. t] analysis):* Based on analysis of COPC concentrations over time, concentration trends (increasing, stable, or decreasing) and effects of attenuation processes on plume duration were evaluated.
- *Plume Attenuation (Concentration vs. Distance [C vs. d] analysis):* Based on changes in COPC concentrations between different monitoring locations, COPC attenuation (which

includes both dispersion and biodegradation) within the groundwater flow system was evaluated.

*Plume Duration***:** *C vs. t Attenuation Rate Coefficient (k_{point}).* C vs. t first-order rate coefficients were calculated at monitoring well RHMW02. Full results are presented in Appendix B.4, and results for RHMW02 are summarized in Table 7-5. C vs. t rate coefficients were not calculated for TPH-d due to issues with the laboratory analysis for this parameter. During the monitoring period 2005–2018, several different laboratories were used for analysis of groundwater samples. Some of the increases and decreases in TPH-d concentrations over time appear to be related to analytical differences between laboratories (see Appendix B.7 for more information). As a result, a C vs. t attenuation rate for this parameter would not accurately reflect the true rate of COPC concentration change over time in individual monitoring wells.

Table 7-5: C vs. t Coefficients, Half-Lives, and First-Order Model Fit Parameters for the COPCs at RHMW02 (September 2005 to April 2018)

COPC	k (yr^{-1})	$t_{1/2}$ (yr)	n	R^2	p-value
1-Methylnaphthalene	-0.05	*	66	0.0167	0.916
2-Methylnaphthalene	0.04	**	66	0.0076	0.465
Naphthalene	0.03	**	66	0.0078	0.314

* Half-life for 1-methylnaphthalene is not reported because there is no statistically significant trend with time.
** Half-lives are not reported for 2-methylnaphthalene and naphthalene because attenuation rates were positive.
Bold italics: p-value = less than 0.05 (reject null hypothesis H_o: slope = 0)
k first-order rate coefficient
n number of samples
R^2 coefficient of determination
$t_{1/2}$ half-life
yr year

Plume Attenuation: C vs. d. For monitoring wells RHMW02 and RHMW01, C vs. d first-order bulk attenuation rates (k) and half-lives were calculated using the entire historical groundwater data set (2005 to January/February 2019). The locations of these monitoring wells align with the expected direction of groundwater flow through the tank farm (west-southwesterly direction), and the current groundwater model indicates that they are on the same flow path. However, the flow path is not precisely known, and therefore there is some uncertainty in the calculated attenuation rates. First-order attenuation rates were calculated for each monitoring event where a COPC was detected in both monitoring wells. The average attenuation rate and standard deviation are presented in Table 7-6 for the Base Case Model and in Table 7-7 for the Clinker Model. In addition, for each paired measurement, a biodegradation rate was calculated using the method of Buscheck and Alcantar (1995) method to separate the contributions of biodegradation and dispersion in the overall C vs. d attenuation rates. These results are also presented in Table 7-6 and Table 7-7.

Table 7-6: C vs. d Rate Attenuation Rates and Biodegradation Rates for COPCs along RHMW02-RHMW01 Transect for the Base Case Model (includes detected COPCs at both wells only)

COPC	n	k (per day) [a]	$t_{1/2}$ (day)	λ (per day)	$t_{1/2}$ (day)
TPH-d	58	-0.16 ± 0.04	4.2	-0.16 ± 0.04	4.6
1-Methylnaphthalene	10	-0.44 ± 0.17	1.6	-0.34 ± 0.18	2.0
2-Methylnaphthalene	13	-0.40 ± 0.16	1.7	-0.32 ± 0.17	2.2
Naphthalene	25	-0.37 ± 0.12	1.9	-0.30 ± 0.13	2.3

λ biodegradation rate coefficient
[a] Attenuation rates are presented as mean ± standard deviation.

Table 7-7: C vs. d Rate Attenuation Rates and Biodegradation Rates for COPCs along RHMW02-RHMW01 Transect for the Clinker Model (includes detected COPCs at both wells only)

COPC	n	k (per day) [a]	$t_{1/2}$ (day)	λ (per day)	$t_{1/2}$ (day)
TPH-d	58	-0.11 ± 0.03	6.6	-0.10 ± 0.03	7.2
1-Methylnaphthalene	10	-0.28 ± 0.11	2.5	-0.22 ± 0.11	3.2
2-Methylnaphthalene	13	-0.25 ± 0.10	2.7	-0.20 ± 0.11	3.4
Naphthalene	25	-0.23 ± 0.08	3.0	-0.19 ± 0.08	3.6

[a] Attenuation rates are presented as mean ± standard deviation.

A similar analysis was conducted using all paired measurements where a COPC was detected in either RHMW02 or RHMW01. For this analysis, the reported limit was used in place of non-detect results. This approach increased the number of paired measurements that could be used to calculate C vs. d attenuation rates and biodegradation rates. However, this approach resulted in little change (< 21%) in the average attenuation rate for each COPC (see Appendix B.4). For TPH-d, C vs. d attenuation rates were calculated using TPH-d results, TPH-d with silica gel cleanup, and TOC results. C vs. d attenuation rates were similar (-0.7 to -0.11 per day) for all three analytical methods (see Appendix B.4).

Plume Attenuation: RHMW02 to Red Hill Shaft. Similar to the analysis of COPC concentrations in RHMW02 and RHMW01, the change in COPC concentration between RHMW02 and Red Hill Shaft can be used to estimate COPC attenuation rates. As Red Hill Shaft is a pumping well that induces flow, there is greater confidence in the flow path between RHMW02 and Red Hill Shaft than between RHMW01 and RHMW02. However, because Red Hill Shaft captures groundwater flow from a large area, a modified evaluation method is required to account for dilution of COPCs caused by mixing of the plume with clean water. This calculation method is presented in Appendix B.4 The C vs. d attenuation rate coefficient for COPC migration from RHMW02 to Red Hill Shaft was evaluated only for naphthalene, because naphthalene has been the most commonly detected individual COPC at Red Hill Shaft (detections for 12 of 66 monitoring events from 2005 to January/February 2019). Two attenuation rates were calculated based on two estimates of travel time from RHMW02 to Red Hill Shaft: (1) the travel time from the base case groundwater flow model (64 days) and (2) the travel time for the base case model including a clinker zone connecting the Facility source area to the Red Hill Shaft (45 days). The resulting attenuation rates were 0.03 per day and 0.09 per day, respectively, corresponding to a half-life of 8–24 days. These half-lives are much larger than the half-life calculated for naphthalene between RHMW02 and RHMW01 (2.3 and 3.6 days; see Table 7-6 and Table 7-7).

Conclusions. Groundwater monitoring data from the Facility over the monitoring period 2005–April 2018 have been used to evaluate plume duration and plume attenuation. These evaluations support the following observations:

- *Plume Duration:* COPC concentrations at individual monitoring locations vary over time, exhibiting both increases and decreases in concentration. However, at RHMW02, the monitoring location with the highest COPC concentrations, most of the COPCs show no overall long-term concentration trend (i.e., the overall concentration trend is stable over the monitoring period). This suggests the presence of a weathered source of COPCs upgradient, present prior to the 2014 Tank 5 release.
- *Plume Attenuation:* COPC concentrations generally decrease from the source area (represented by RHMW02) to downgradient monitoring locations (RHMW01 and Red Hill Shaft). C vs d attenuation half-lives range from 1.6 to 7 days for the analysis of concentration

changes from RHMW02 to RHMW01, while half-lives range from 5 to 24 days for the analysis of concentration changes from RHMW02 to Red Hill Shaft. Although both analyses support the conclusion that biodegradation is contributing to the natural attenuation of COPCs within groundwater, the estimated attenuation rate is approximately three times slower for analysis of concentration changes from RHMW02 to Red Hill Shaft compared to RHMW02 to RHMW01.

- Both evaluations of C vs d attenuation rates depend on important assumptions:
  - *RHMW02 to RHMW01:* This analysis assumes that RHMW02 and RHMW01 are in the same flow path (i.e., the COPCs present in RHMW01 originated in the vicinity of RHMW02). If the COPCs in RHMW01 actually originate from a lower-strength source (or a more distant source), then the analysis would overestimate true attenuation rate.
  - *RHMW02 to Red Hill Shaft:* This analysis assumes that the very low naphthalene concentrations detected in Red Hill Shaft (i.e., < 0.1 µg/L) reflect the actual naphthalene concentration in the Red Hill Shaft water rather than false-positive artifacts of laboratory analysis. For example, for a number of sampling events in 2013 and 2014, low concentrations of naphthalene (< 0.1 µg/L) were detected in most or all of the groundwater samples, including those from wells upgradient of the Facility source area (see Appendix B.8 for additional discussion of the uncertainty associated with the low concentration detections of naphthalene). If the actual naphthalene concentrations in Red Hill Shaft are lower than those indicated by the laboratory detections, then the analysis would underestimate the true attenuation rate.
- Taken together, analysis of RHMW02 to RHMW01 and RHMW02 to Red Hill Shaft likely represents an estimated range of plume bulk attenuation rates for COPCs in groundwater at the Facility (i.e., an attenuation half-life of 1.6–7 days or 8–24 days). These rate calculations demonstrate that robust attenuation processes are present in the groundwater underlying the Facility and provide a starting point for the groundwater fate and transport model; they will be fine-tuned in the groundwater fate and transport model.

Analysis of Secondary MNA Data. Natural attenuation processes at the Facility were also evaluated using secondary LOEs (i.e., geochemical data; electron acceptor concentrations) from the Facility groundwater monitoring network. Concentrations of the following analytes were considered: total alkalinity, nitrate as nitrogen (NO_3^-), ferrous iron (Fe^{2+} or Fe[II]), sulfate (SO_4^{2-}), and methane (CH_4). In addition, field measurements of DO (O_2) and ORP were incorporated in the MNA analysis. COPCs considered for this study were TPH-d, 1-methylnaphthalene, 2-methylnaphthalene, and naphthalene. Where sufficient data are available, relationships between electron acceptor concentrations (and field parameters) and COPC concentrations were identified using time-series and X-Y plots for all monitoring wells.

Spatial and temporal concentration trends for electron acceptors (O_2, NO_3^-, SO_4^{2-}) and metabolic byproducts (Fe^{2+}, CH_4) provide strong evidence for aerobic and anaerobic petroleum hydrocarbon degradation within the tank farm area. In the area of the highest COPC concentrations (RHMW01 and RHMW02), electron acceptors (O_2, NO_3^-, SO_4^{2-}) are depleted (or have low concentrations) and concentrations of metabolic byproducts (Fe^{2+}, CH_4) are elevated relative to the monitoring locations outside the tank farm area (Appendix B.5). As expected from MNA processes, higher TPH-d concentrations correspond to (1) lower DO, nitrate, and sulfate concentrations and (2) higher dissolved methane and ferrous iron concentrations. Negative ORP values further support the presence of anaerobic conditions within the tank farm area. These secondary LOEs, combined with COPC

attenuation rates and half-lives (see Appendix B.4), provide strong evidence of active and robust biodegradation of COPCs within the tank farm area.

Analysis of Tertiary MNA Data. Results from the microcosm studies demonstrated naturally occurring microorganisms could achieve rapid degradation of relevant petroleum hydrocarbons under aerobic conditions. These degradation rates were consistent with those observed in literature, as well as those estimated using site-specific C vs. d data from within the plume (i.e., primary LOE). Rates were slower in microcosms maintained under strictly anaerobic conditions, but electron acceptor availability within the aquifer is unlikely to be limited to the same extent as the microcosm bottles. The abundance of aerobic and anaerobic biomarkers for degradation at multiple locations confirms that indigenous populations with the desired metabolic capabilities are present within the aquifer. Collectively, these results support the other LOE and suggest that biodegradation is contributing to the natural attenuation of petroleum hydrocarbons at the Facility.

7.4 GROUNDWATER CHEMISTRY LINES OF EVIDENCE

A comprehensive evaluation was conducted with all available groundwater data for all wells (except OWDFMW01) using LOEs to assess two overall key issues:

- Potential impact to groundwater after the 2014 JP-8 release from Tank 5
- Evidence of impact to outlying wells from fuel releases/site operations

Data used for this evaluation are COPCs, inorganic groundwater chemistry parameters, organic compounds targeted by the same methods used for COPCs but not required by the LTM program (non-COPCs), and organic TICs that are seen in the analysis of COPCs but are not targets of the methods.

The specific objectives of this study are:

- Evaluate all available Red Hill investigation and groundwater LTM chemistry data as an extension of prior chemistry analyses.
- Use multiple LOEs utilizing temporal and spatial trends to support development of the key findings.
- Evaluate whether the sporadic detections of various chemicals in outlying wells are associated with releases from the Red Hill Facility.
- Evaluate data with respect to potential LNAPL extent.
- Evaluate whether the 2014 Tank 5 fuel release contributed to groundwater contamination.

A summary of the key findings from the groundwater chemistry LOEs is presented in Section 7.4.3; the full analysis with discussion for each LOE is presented in Appendix B.8, with the multiple LOEs compiled in Appendix B.8 Table 6-1. Additionally, a multiple impact factor analysis using COPCs and geochemical parameters is presented in Appendix I.

7.4.1 Challenges with Organic Data Interpretation

There are several concerns regarding the data quality and density with respect to interpretation of trends in organic constituents, including:

- Wells were installed at different times and sampled at different frequencies.

- Analytical laboratories and detection/reporting limits have varied throughout the monitoring program.
- Very low concentrations push laboratory abilities and may result in laboratory quality assurance/quality control (QA/QC) issues. For example, sampling/laboratory contamination and inappropriate chemical/compound determination can result in "detections" that are not real.
- Other concerns presented in Appendix B.8

If site data are assessed at face value without taking into account the limitations and validity of these data, there can be misleading interpretations of site impacts. Examining these data in-depth and developing multiple LOEs provide a strong basis for the key findings discussed below.

7.4.2 Groundwater Chemistry as a Function of LNAPL Extent

As discussed in Section 7.1.2, no measurable LNAPL at the water table has been documented in Red Hill monitoring wells. An analysis of dissolved-phase constituents can be used as LOEs to determine the presence and extent of LNAPL in the groundwater at the site. If LNAPL is present near a monitoring well, it would be expected to:

- Exhibit both an organic and inorganic/geochemical footprint (as seen relative to RHMW02).
- Result in a continuing impact (i.e., chemical signature) to the well rather than random, sporadic, low-level detections.
- Exhibit an organic signature consistent with the fuel type (e.g., jet fuel) and representative of the dissolution of the LNAPL source over time as well as weathering.
- Exhibit an inorganic chemical signature demonstrating biodegradation (e.g., low DO).

Wells farther downgradient from an LNAPL source would still see reduced concentrations of chemicals based on the factors mentioned above. The chemical signature would be significantly influenced by relative biodegradation of chemical constituents in the dissolved-phase plume. Even in this case, it is highly unlikely that the chemical signature would result in random sporadic detections.

7.4.3 Key Findings

Monitoring Wells in Tank Area: Consistent and coinciding detections of COPCs and fuel-related non-COPCs and TICs have been reported in RHMW02 over time. These detections are consistent with a nearby LNAPL source in the unsaturated zone. Coinciding detections are observed to a lesser extent in RHMW01, indicating that RHMW01 may have some hydraulic connection to RHMW02 located upgradient. Coinciding detections are not observed in RHMW03.

2014 Tank 5 Release: There is evidence of a pre-2006 LNAPL release impacting groundwater upgradient of RHMW02. The lower concentrations of COPCs at RHMW01 and RHMW03 compared to RHMW02 are not indicative of LNAPL release to groundwater in the vicinity of these two wells. There are indications of biodegradation at RHMW02 and RHMW01 and marginal indications at RHMW03.

The steady BTEX trends and consistent naphthalenes weathering ratio at RHMW02 before and after the 2014 fuel release do not support impact at RHMW02 from the 2014 fuel release. Similarly, there are no consistent observable changes in COPC or non-COPC detections in site wells before and after the 2014 fuel release.

In summary, a comprehensive evaluation of the entire monitoring data set does not indicate that the 2014 JP-8 release from Tank 5 impacted groundwater. The observed impacts to groundwater in some of the near-tank wells (i.e., RHMW01, RHMW02, and RHMW03) are likely attributable to historical leaks.

Impacts to Outlying Wells: There are inconsistent and noncoinciding detections of COPCs and fuel-related non-COPCs and TICs in outlying wells. As previously discussed, the presence of LNAPL in the area of the wells would result in a continuing, much more consistent impact to wells.

In addition, a wide variety of constituents were reported in outlying wells that were not related to petroleum hydrocarbons, such as phthalates and halogenated compounds. These compounds are not associated with fuel and may be indicators of sample or laboratory issues.

Overall, the detection signatures at outlying wells are not consistent with fuel releases. The detections of compounds are sporadic and at very low concentrations. There is a similar detection pattern observed across a diverse set of monitoring locations (e.g., Red Hill Shaft, RHMW05, Hālawa Deep Monitor Well). As these wells have different constructions and are operated differently, the similarity in the detection patterns for some COPCs (e.g., naphthalenes) brings into question the reliability of those data as an indicator of a hydrocarbon release.

In summary, a comprehensive evaluation of the entire monitoring data set does not indicate impacts to outlying wells associated with a nearby LNAPL source.

7.5 UNCERTAINTY ANALYSIS

Recent investigation activities and a comprehensive review of historical investigation results have significantly improved the conceptual model for the fate and transport of LNAPL and dissolved COPCs at the Facility. However, remaining key uncertainties include:

- *LNAPL distribution at the water table:* measurable LNAPL has not been documented in any of the existing monitoring wells; however, a yellow tint and naphthalene odor may have been noted at an early sampling event prior to the 2014 release at RHMW02 (Whittier 2018). The presence and distribution of LNAPL at the water table at other locations within the vicinity of the tanks is less certain.
- *Plume attenuation rates:* Plume attenuation rates (C vs. d rates) have been estimated based on data from limited paired locations (i.e., RHMW02, RHMW01, and Red Hill Shaft). The small number of monitoring locations available for this analysis increases the uncertainty in the results.
- *Accuracy of very low COPC detections:* The historical groundwater monitoring data set includes sporadic detections on some COPCs at some locations at very low concentrations (e.g., less than 0.1 µg/L for individual COPCs; less than 50 µg/L for TPH analyses). During some monitoring events, these low-level detections have occurred in most or all wells sampled, including wells upgradient from the active parts of the Facility. The reliability of these very low detections is uncertain (see Appendix B.8).
- *Applicability of RBDC as final decision criteria:* RBDCs have been developed and proposed as screening levels for the initial evaluation of Facility monitoring results (DON 2017i, Table 5-1). Some RBDCs (e.g., naphthalene) are close to the limit of detection (LOD) for sample analytical results. Final decision criteria for Facility COPCs will be developed in the future.

- *Different interpretations of site data:* Different interpretations of site data result in differing conclusions as to the presence of LNAPL on site. Assessment of individual data points, e.g., a single COPC detection, may lead to different conclusions compared to an analysis of multiple COPCs and data trends.

In addition, the spatial distribution of COPC concentrations dissolved in groundwater between the Facility and the water supply wells in North Hālawa Valley and Moanalua Valley is not well understood. Previous hydrocarbon releases documented to have impacted the shallow perched zones underlying the Hālawa Correctional Facility (Dames & Moore 1991; EKNA 1999, 2000) may complicate hydrocarbon source attribution in this area.

The extent of the source area, COPC mass loading rates, and site-specific values for natural attenuation rates of the COPCs are uncertain. Compositional changes in released kerosene-based fuels over time are unknown. Site-specific values for COPC sorption and degradation rates are not currently available.

7.6 ADDRESSING UNCERTAINTIES

The following ongoing, planned, or proposed activities are designed to help resolve the uncertainties described in Section 7.5. Additional hydrogeologic and chemical data are currently being collected as described in the project WP/SOW (DON 2017a) and subsequent derivative deliverables.

7.6.1 Nature and Extent of Contamination

Additional data are being collected to better define the spatial distribution of COPC concentrations dissolved in groundwater surrounding the Facility. To fulfill these data needs, additional monitoring wells are being installed and sampled for detailed groundwater quality analyses to characterize the spatial distribution of COPC concentrations. Similar groundwater quality data from additional monitoring well locations, which were recently planned (DON 2017f), will better define the nature and extent of COPCs between the Facility and the water supply wells.

7.6.2 Source Area Extent, Mass Loading, and Natural Attenuation Rates

To reduce potential uncertainties, additional data collection activities have been undertaken, including:

- *Recharge to Groundwater Measurements:* A better understanding of vadose zone LNAPL dissolution rates was needed. While a recharge study showed high potential recharge rates under ponded conditions, the TFN study (Section 6.1.9 and Appendix H) provides insights on the relatively low amount of direct recharge to groundwater in the Facility area.
- *Thermal NSZD Analysis:* The vertical temperature profiles were measured in all outlying monitoring wells at the Facility in April 2019 to confirm that large LNAPL bodies are not present on the water table or in the vadose zone in the vicinity of these wells.
- *Numerical LNAPL Release Model:* A numerical 3D LNAPL release model may be developed to bound the hypothetical impact area for several different LNAPL release scenarios.

This page intentionally left blank

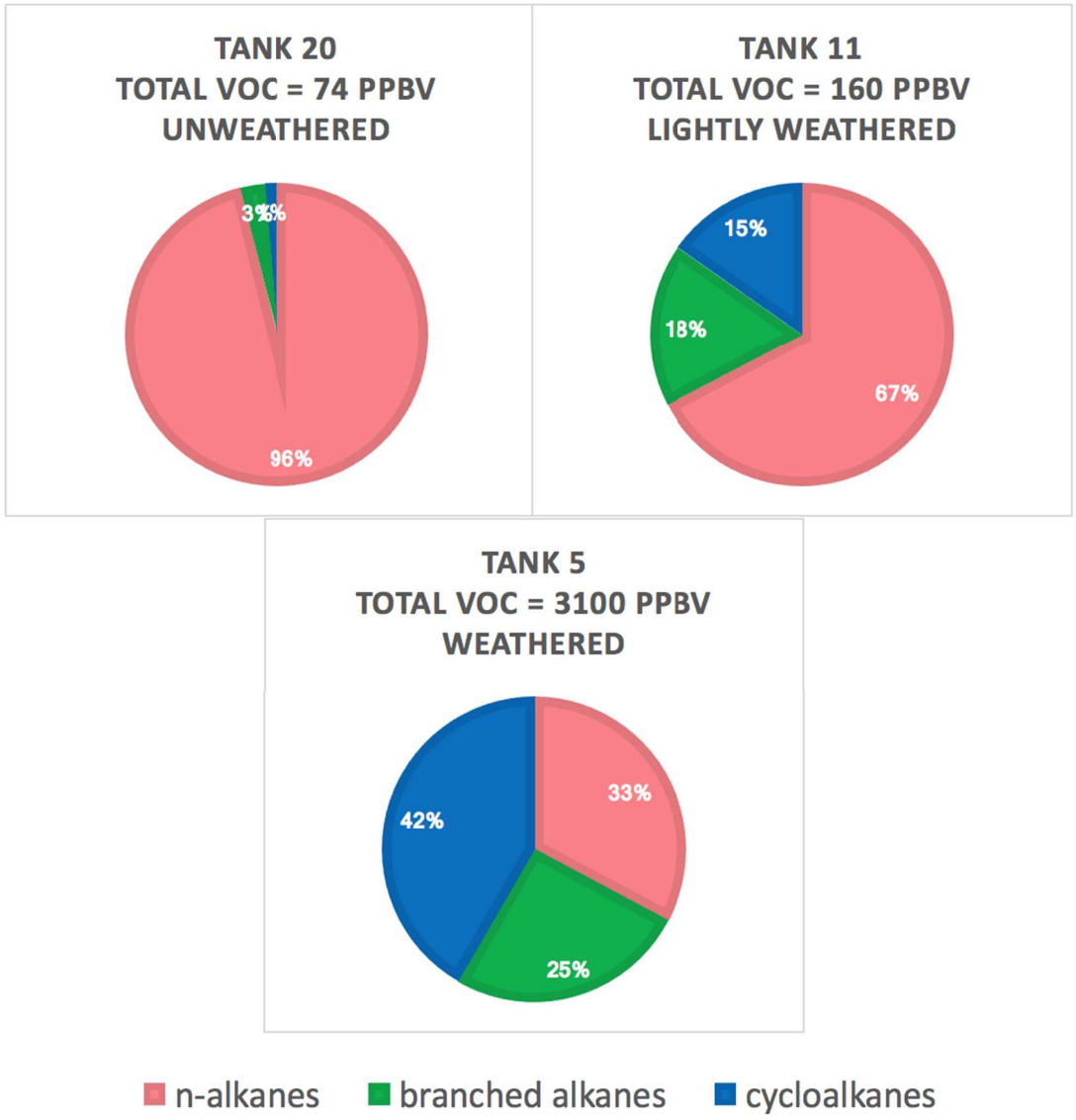

Figure 7-1
Range of VOC Concentrations and Fuel Weathering Observed in Below-Tank Soil Vapor Monitoring Points
Conceptual Site Model Rev. 01
Investigation and Remediation of Releases
and Groundwater Protection and Evaluation
Red Hill Bulk Fuel Storage Facility
JBPHH, Oʻahu, Hawaiʻi

This page intentionally left blank

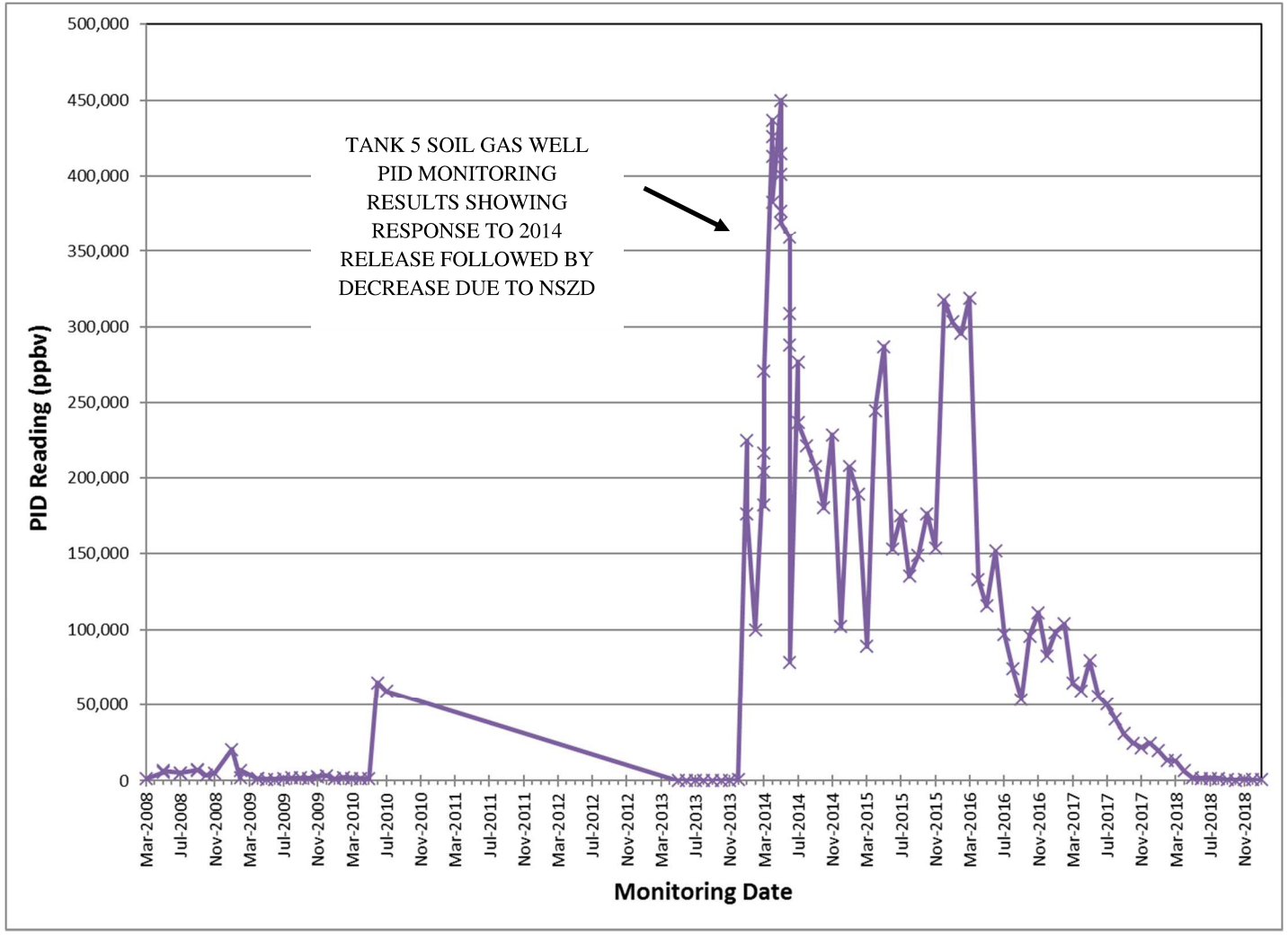

LAB ANAYSIS OF VAPORS
BELOW TANK 5
COLLECTED IN NOV. 2017
SHOWING BIOLOGICAL
WEATHERING
(I.E., ENRICHMENT IN
CYCLOALKANES)

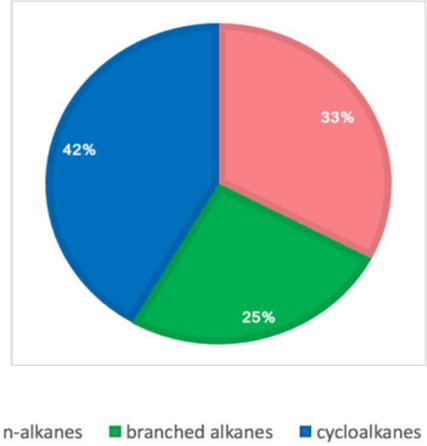

Figure 7-2
Use of PID Monitoring Combined with Lab Analysis to Track Release and Subsequent Weathering of LNAPL Fuel for Tank 5
Conceptual Site Model Rev. 01
Investigation and Remediation of Releases
and Groundwater Protection and Evaluation
Red Hill Bulk Fuel Storage Facility
JBPHH, Oʻahu, Hawaiʻi

This page intentionally left blank

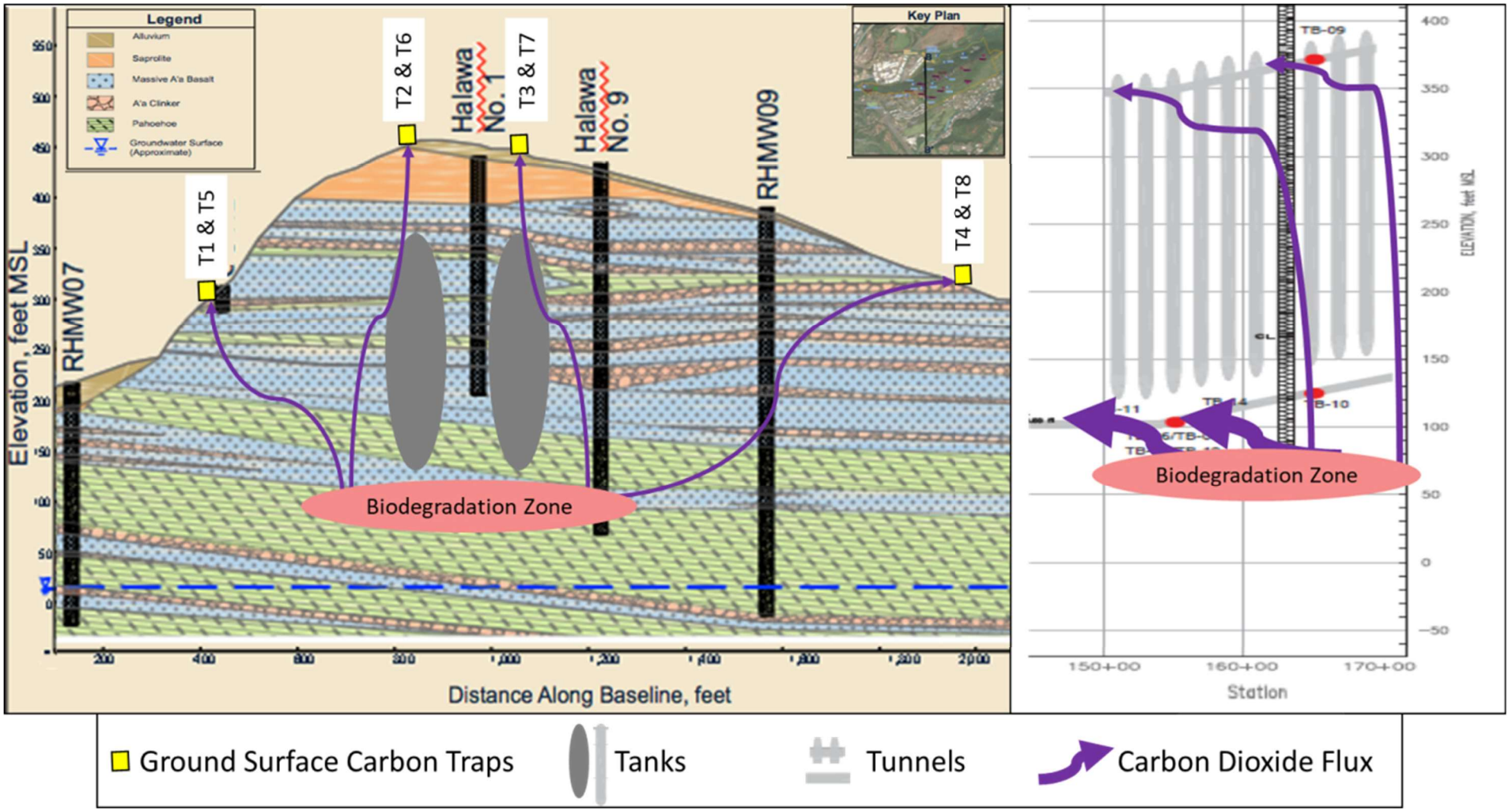

Figure 7-3
Conceptual Illustration of Carbon Dioxide Flux to Ground Surface and Tunnels
Conceptual Site Model Rev. 01
Investigation and Remediation of Releases
and Groundwater Protection and Evaluation
Red Hill Bulk Fuel Storage Facility
JBPHH, Oʻahu, Hawaiʻi

This page intentionally left blank

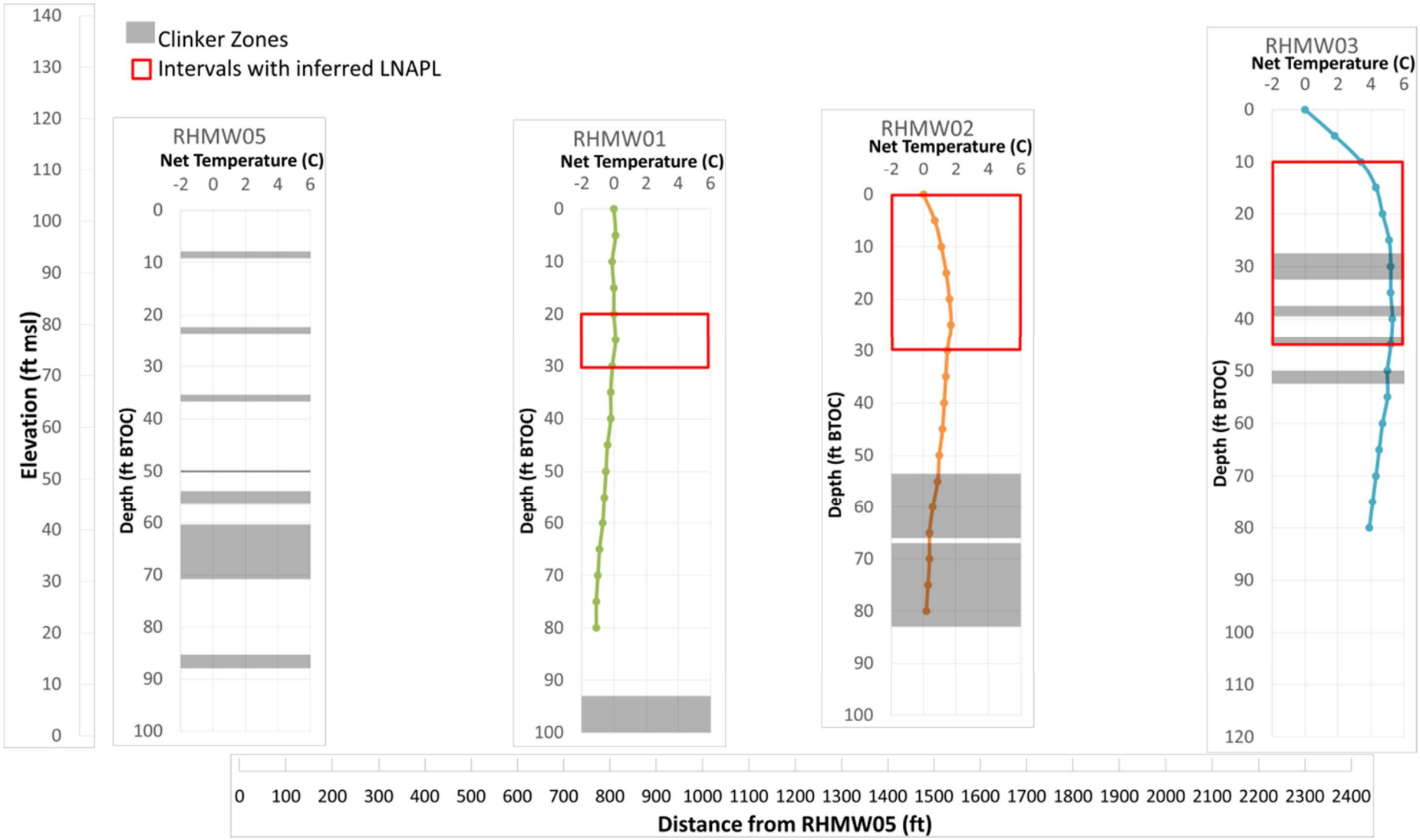

Figure 7-4
Net (Background Corrected) Temperature Profiles for Facility Wells (Well Air Temperatures Measurements), Highlighting Clinker Zones and Inferred LNAPL Intervals
Conceptual Site Model Rev. 01
Investigation and Remediation of Releases and Groundwater Protection and Evaluation
Red Hill Bulk Fuel Storage Facility
JBPHH, Oʻahu, Hawaiʻi

This page intentionally left blank

8. Module G: Exposure Model

The risk-based exposure model identifies the sources and migration routes of site COPCs and evaluates the exposure media and pathways for human receptors potentially exposed to these media (ecological exposures are not addressed in this CSM, as explained in Section 8.3.2). It is also referred to as a risk-based CSM (e.g., in the *Risk-Based Decision Criteria Development Plan*; DON 2017k). The exposure model is used to identify the potentially complete exposure pathways for human receptors evaluated in the human health risk assessment. Only potentially complete exposure pathways are evaluated quantitatively in the risk assessment, consistent with EPA (1989) guidance.

A complete exposure pathway includes all the following elements:

- Chemical source(s)
- Affected media
- Chemical release and transport mechanisms
- Routes of exposure
- Human and/or environmental receptors

The absence of any one of these elements results in an incomplete exposure pathway, which does not warrant further evaluation. The refined risk-based exposure model (Figure 8-1) visually depicts the potential current and future exposure pathways at the Facility.

Each identified exposure route has been assessed as potentially complete, potentially complete but insignificant, or incomplete in accordance with the following criteria:

- *Potentially complete:* exposure pathways that include all the above elements
- *Potentially complete but insignificant:* exposure pathways identified as potentially complete but the potential magnitude of exposure from the pathway is low relative to other pathways associated with the same medium and exposure route
- *Incomplete:* exposure pathways lacking at least one of the above elements are not complete and therefore will not affect human health

8.1 Chemical Sources and Releases

The Facility contains 18 active and 2 inactive underground fuel storage tanks operated by DLA. The tanks are accessed via a tunnel system that connects to Pearl Harbor. Kerosene-based jet fuels stored at the Facility have included JP-5, JP-8, and F-24. In January 2014, the Navy reported that JP-8 fuel was released from Tank 5 but did not exhibit a significant chemical impact on groundwater beneath the Facility above historical background levels; historical releases (prior to 2005) are considered to be the main source of impacts to groundwater at the Facility (see Section 7 and Appendix B). Other releases (e.g., spills or leaks elsewhere in the fuel system) may have occurred or may occur in the future, leading to possible environmental contamination.

8.2 Potentially Affected Media

Potentially contaminated media at the Facility site are unconsolidated materials, volcanic rock within the tunnels, soil vapor within the tunnels, tunnel air, and groundwater beneath the Facility.

Soil or rock may be contaminated directly by spills or leaks from the fuel tanks or associated components of the fuel system. Although the fuel tanks are constructed of steel-lined concrete, released fuels could migrate to the underlying soil if the integrity of the concrete containers is compromised. Volatile components of such releases could migrate as soil vapor and could affect the air in the tunnels.

As the Facility overlies the Waiawa System of the Pearl Harbor Aquifer Sector and the Moanalua System of the Honolulu Aquifer Sector (see Figure 2-6), fuel releases can migrate to groundwater beneath the Facility. The depth from ground surface to groundwater beneath the site and in downgradient areas ranges from approximately 80 ft bgs at Red Hill Shaft to as much as 400–500 ft bgs in the tank farm area. Water supply wells near the Facility are transport mechanisms in potentially complete groundwater exposure pathways. The Navy's Red Hill Shaft and the BWS municipal water supply wells Hālawa Shaft and Moanalua Wells represent the most significant pathways to human receptors due to their known or suspected pumping influence on the aquifer beneath the Facility, the size of their drinking water distribution system(s), and location relative to potential downgradient groundwater flow direction from the Facility. Water supply wells identified within the groundwater model domain are shown on Figure 2-7 and further discussed in Section 2.11.

As groundwater within the unconfined basalt aquifer at the Facility migrates toward the ocean, it dips below and becomes confined by overlying caprock. The confining action of the caprock produces artesian groundwater flow and creates numerous springs around Pearl Harbor, but not near the Facility.

The nearest surface water bodies, South Hālawa and Moanalua Streams, are approximately 600 ft and 1,800 ft away from the nearest tanks, respectively. However, these are both intermittent streams that lie at higher elevations than the basal aquifer and are not expected to receive groundwater discharge from the basal aquifer.

8.3 POTENTIAL RECEPTORS

8.3.1 Human Receptors

The human receptors that may contact onsite or offsite Facility-impacted media are Facility occupational workers, construction workers, and visitors, and offsite residents:

- Onsite occupational workers are people who work at the Facility. They are anticipated to spend their work day within the tunnels or on Facility grounds outside the tunnels.
- Construction workers also work at the Facility but are assumed to work in excavations at the Facility as part of tunnel construction or maintenance or in utility trenches. These work activities would expose construction workers to chemicals associated with soil or rock beneath the concrete floors of the tunnel system.
- Visitors to the Facility are assumed to have similar activities as occupational workers. They are anticipated to spend their work day within the tunnel system or on Facility grounds outside the tunnels.
- Offsite residents who use U.S. Navy Supply Well 2254-01 (Red Hill Shaft) (located approximately 2,600 ft west of the nearest underground fuel storage tank) as their tap water source are potential receptors for site chemicals that migrate via groundwater from Facility releases.
- Offsite residents who use BWS' Hālawa Shaft and/or Moanalua Wells as their tap water source are potential receptors for site chemicals that migrate via groundwater from Facility releases.

- Other offsite receptors may include people who might access groundwater discharge locations near Pearl Harbor.

8.3.2 Ecological Receptors

The potential receptors of primary interest are those potentially exposed to COPCs through water supply sources, in accordance with the AOC. These do not include ecological receptors. A preliminary risk assessment conducted as part of a previous Facility investigation concluded that there were no significant pathways for ecological receptors at the site (DON 2002). DON (2007) notes that both South Hālawa Stream and Moanalua Stream are impaired by nutrient inputs, pathogens, turbidity, and exotic species due to urban runoff, storm sewers, and other sources of disturbance. These streams do not support aquatic life. Further, groundwater occurs 80 ft beneath the stream beds and does not discharge to the streams. The artesian features near Pearl Harbor noted in Section 2.10 are considered too distant (Pearl Harbor is approximately 2.5 miles from the tank farm area) to pose a significant concern for any ecological receptor at those locations. For these reasons, ecological exposures are considered incomplete or insignificant and are not further evaluated for the Facility.

8.4 POTENTIALLY COMPLETE EXPOSURE PATHWAYS

The only contact with potentially contaminated soil would occur within the Facility tunnels. Incidental ingestion, dermal contact, inhalation of particulates, and inhalation of volatiles are potentially complete surface and subsurface soil exposure pathways for construction workers at the Facility.

Volatile components of fuels released to soil in the tunnels or released via spills or leaks in the active fuel systems may migrate to indoor air in the tunnels. All receptors in the tunnels are potentially exposed to these chemicals via inhalation of tunnel air. Although this pathway is considered potentially complete, the tunnels are well ventilated, which would limit buildup of volatile chemicals in air. Further, any potential vapor intrusion from soil releases into the tunnels could not be differentiated from other sources within the tank complex. Finally, because the Facility is an active work place, any potential occupational exposure to chemicals at the workplace is assumed to be covered under the Navy's Occupational Safety and Health Administration (OSHA) program.

Tap water at the Facility comes from the public water supply. Therefore, occupational workers, construction workers, and visitors that use tap water at the Facility could be exposed to chemicals via ingestion. The only dermal exposure to water at the Facility is from hand washing, as bathing is not a realistic scenario for onsite receptors; therefore, dermal exposure is considered an insignificant pathway.

Offsite residents that use the Red Hill Shaft water supply as their tap water source could be exposed to chemicals in tap water via direct ingestion and dermal contact. They may also be exposed to volatile chemicals via inhalation while showering/bathing and other household activities (e.g., dishwashing, clothes-washing).

8.5 INCOMPLETE OR INSIGNIFICANT PATHWAYS

Direct contact with surface and subsurface soil is not anticipated for occupational workers or visitors in the tunnels because the tunnels are concrete-lined and soil is not exposed.

Contact with tap water for all receptors in the tunnels is limited to direct ingestion. Dermal contact while washing hands is considered an insignificant pathway. Further, workers and visitors are not expected to shower at the site, and therefore inhalation and dermal contact while showering are not complete pathways.

Because the depth to groundwater precludes direct contact, all other direct groundwater exposure pathways are considered incomplete for Facility receptors. Even excavations in the tunnels would not be deep enough to contact groundwater at the Facility.

Vapor intrusion from groundwater at the site is possible but considered insignificant compared to other pathways because of the depth to groundwater.

The vapor intrusion pathway for nearby residents is also considered an insignificant pathway. This is due to the depth of groundwater in the residential areas adjacent to the Facility (at least 80 ft bgs), and the fact that the vast majority of the fuels stored at the Facility have very little volatile content.

Potential exposure to groundwater used as offsite irrigation water and at groundwater discharge locations near Pearl Harbor is considered insignificant. A quantitative evaluation of these supplementary, lower-exposure pathways is not warranted as the evaluation and protection of residential tap water exposures would also be protective of the other water-related pathways.

8.6 POTENTIAL EXPOSURE TO LNAPL

There is potential exposure to LNAPL by workers in the tunnels, but that is covered under the Navy's OSHA program. LNAPL migration is being evaluated as part of the AOC Statement of Work Section 3 TUA, and attenuation is being evaluated as part of the CSM. Finally, it is possible that LNAPL could reach Navy Supply Well 2254-01 (Red Hill Shaft), but contingencies would be put in place as described in the GWPP (DON 2014b) so that human health is protected in the event LNAPL impacts drinking water. (DON 2017i). New RBDC were proposed in the *Risk-Based Decision Criteria Development Plan* (DON 2017i, Table 5-1)

The DOH EAL approach considers the presence of LNAPL to represent a "free product" scenario and does not apply risk-based criteria to LNAPL-impacted media. However, the gross contamination EALs, which consider aspects of solubility and saturation limits, may be used for preliminary comparisons of LNAPL-related data.

8.7 UNCERTAINTIES

Various uncertainties are associated with the identification of potential sources, migration routes, receptors, and exposure pathways.

Although the 2014 fuel release from Tank 5 was detected, other releases may have occurred at the Facility where the types of chemicals that may have been released are unknown. The planned sentinel well network described in the *Sentinel Well Network Development Plan* (DON 2017j) will function as a tool to monitor past and potential releases from the Facility.

A pathway from the Facility to Red Hill Shaft has been identified as a possible chemical migration route. Uncertainty is associated with other possible migration routes to drinking water supply wells (e.g., Hālawa Shaft and Moanalua Wells) and other areas where groundwater might discharge. This uncertainty will be mitigated by the sentinel well monitoring network (DON 2017j).

Uncertainty is also associated with potential exposure via pathways that are considered insignificant. Because of the conservative nature of the evaluation of exposure and risk to residents, however, potential risks via these insignificant pathways are covered by the significant pathways that are evaluated.

Although land use at the Facility is not expected to change in the future, a land use change would warrant a re-evaluation of potential receptors and exposure pathways.

8.8 ADDRESSING UNCERTAINTIES

As described in Section 8.7, the main uncertainties with risk-based exposure model are those associated with the possibility of unidentified sources and migration routes. These are addressed by the groundwater flow and solute transport modeling, the extent of the planned sentinel groundwater monitoring network, especially where it is focused on the water supply wells (see Section 2.11), and by the conservative nature of the evaluation of residential exposures to tap water.

This page intentionally left blank

Contributing Source	Transport Mechanism & Exposure Medium	Exposure Route*	Receptors			
			Offsite Resident (Adult/Child)	Onsite Occupational Worker	Onsite Construction Worker	Onsite Visitor
Releases from Red Hill Fuel Storage Tanks						
Surface Soil	Direct Contact with Surface Soil [a]	Ingestion:	Incomplete	Incomplete	**Potentially Complete**	Incomplete
		Dermal:	Incomplete	Incomplete	**Potentially Complete**	Incomplete

Rationale: The only contact with potentially contaminated soil would occur within the Facility tunnels. There are no current (or anticipated future) residents within the tunnels, and the concrete foundation precludes any soil exposure for occupational workers or Facility visitors. For these receptors, the exposure pathway for surface soil is incomplete.

Within the Facility, only construction workers (utility workers) in an excavation would be potentially exposed to soil, which is otherwise inaccessible.

Subsurface Soil	Direct Contact with Subsurface Soil	Ingestion:	Incomplete	Incomplete	**Potentially Complete**	Incomplete
		Dermal:	Incomplete	Incomplete	**Potentially Complete**	Incomplete

Rationale: The only contact with potentially contaminated soil would occur within the Facility tunnels. There are no current (or anticipated future) residents within the tunnels, and the concrete walkways preclude any soil exposure for occupational workers or Facility visitors. For these receptors, the exposure pathway for surface soil is incomplete.

Within the Facility, only construction workers (utility workers) in an excavation would be potentially exposed to soil, which is otherwise inaccessible.

	Volatilization & Dispersion to Tunnel Air	Inhalation:	Incomplete	**Potentially Complete**	**Potentially Complete**	**Potentially Complete**

Rationale: Inhalation of soil vapor VOCs in ambient air is not a complete pathway for residents because any soil contamination is localized at the Facility, where there are no current residents and where future residential use is not likely.

Volatile components of fuels could migrate to indoor air within the Facility and inhalation inside contaminated tunnels is a potentially complete exposure pathway for these receptors. Because the Facility is an active workplace, however, any occupational exposures to volatile chemicals within the tunnels are assumed to be covered under the Navy's OSHA programs.

	Infiltration to Groundwater	Ingestion:	**Potentially Complete**	**Potentially Complete**	**Potentially Complete**	**Potentially Complete**
		Dermal:	**Potentially Complete**	Insignificant	Insignificant	Insignificant
		Inhalation (Bathing/Showering):	**Potentially Complete**	Incomplete	Incomplete	Incomplete
		Inhalation/ Vapor Intrusion:	Insignificant	Insignificant	Insignificant	Insignificant

Rationale: Direct exposure to chemicals in tap water (ingestion and dermal contact) and inhalation of VOCs while bathing are considered potentially complete pathways for residents that use groundwater in the area as a drinking water source.

All onsite receptors could potentially be exposed to drinking water at the Facility, due to the proximity of Red Hill Shaft downgradient of the Facility. Offsite receptors could be exposed to drinking water from Red Hill Shaft, Hālawa Shaft, and Moanalua Wells. Bathing, however, is not a realistic scenario for onsite receptors. Therefore, while dermal exposure (washing hands) is possible, the dermal pathway for onsite receptors is considered insignificant.

Due to the depth to groundwater across the site (between 400–500 ft bgs at the tank farm and approximately 80 ft bgs at Red Hill Shaft), there is not a complete exposure pathway for construction workers in an excavation.

Inhalation of indoor or outdoor air is considered insignificant because groundwater is too deep for any appreciable migration of VOCs to indoor or outdoor air to occur; any such exposure is expected to be insignificant compared to exposure via the direct use of tap water for residents and insignificant for people in the tunnels compared to VOC inputs to tunnel air from releases to soil and current Facility operations.

	Groundwater Discharge to Surface Water	All Pathways:	Incomplete	Incomplete	Incomplete	Incomplete

Rationale: In the Facility vicinity, there are no known surface water bodies that receive groundwater discharges. Although there might be groundwater discharge locations close to Pearl Harbor, any potential exposure to offsite receptors at these locations is considered insignificant as Pearl Harbor is approximately 2.5 miles from the tank farm area.

	Use of Groundwater for Irrigation	All Pathways:	Insignificant	Incomplete	Incomplete	Incomplete

Rationale: Groundwater could be used to irrigate gardens at local residences. Ingestion of or dermal contact with irrigation water is expected to be minimal, and exposure to volatile COPCs in groundwater would be limited given the expected high rate of volatilization to outdoor air during irrigation. Further, exposure to volatile or non-volatile components of COPCs is expected to be insignificant for residential gardeners compared to direct contact of groundwater as a drinking water source. There is not a complete relevant pathway for onsite receptors.

* A potentially complete exposure pathway includes all the following elements:
- Sources and type of chemicals present
- Affected media
- Chemical release and transport mechanisms
- Known and potential routes of exposure
- Known or potential human receptors

Insignificant exposure pathway: pathway is potentially complete, but not likely to pose a potential for adverse effects to human health.
Incomplete exposure pathway: pathway is not complete and therefore will not affect human health.

Figure 8-1
Human Health Exposure Pathway Evaluation

This page intentionally left blank

9. References

Asmuth, J., and M. Knotters. 2004. "Characterising Groundwater Dynamics Based on a System Identification Approach." *Journal of Hydrology* 296: 118–134. https://doi.org/10.1016/j.jhydrol.2004.03.015.

ASTM International. 2014a. *Standard Guide for Developing Conceptual Site Models for Contaminated Sites*. E1689-95 (Reapproved 2014). West Conshohocken, PA.

———. 2014b. *Standard Guide for Development of Conceptual Site Models and Remediation Strategies for Light Nonaqueous-Phase Liquids Released to the Subsurface*. E2531-06(2014). West Conshohocken, PA.

Atlas Geotechnical (Atlas), Eastern Research Group ERG Inc. (ERG), PEMY Consulting (PEMY) PEMY, and Powers Engineering and Inspection PEI Inc. (PEI). 2017. *Underground Storage Tank System Evaluation Final Report, Red Hill Bulk Fuel Storage Facility, Joint Base Pearl Harbor-Hickam*. Submitted to: U.S. Environmental Protection Agency, Region 9. June.

Belcher, W. R., P. E. Elliot, and A. L. Geldon. 2001. *Hydraulic-Property Estimates for Use With a Transient Ground-Water Flow Model of the Death Valley Regional Ground-Water Flow System, Nevada and California*. Water-Resources Investigations Report 01-4120. U.S. Geological Survey.

Bohling, G. C., W. Jin, and J. J. Butler. 2011. *Kansas Geological Survey Barometric Response Function Software User's Guide*. Kansas Geological Survey Open-File Report 2011-10. Lawrence, KS: University of Kansas.

Bouwer, H., and R. C. Rice. 1976. "A Slug Test for Determining Hydraulic Conductivity of Unconfined Aquifers with Completely or Partially Penetrating Wells." *Water Resources Research* 12 (3): 423–428. https://doi.org/10.1029/WR012i003p00423.

Box, G. E. P., and G. M. Jenkins. 1970. *Time Series Analysis Forecasting and Control*. San Francisco: Holden Day.

Bruno, B. C., G. J. Taylor, S. K. Rowland, P. G. Lucey, and S. Self. 1992. "Lava Flows Are Fractals." *Geophysical Research Letters* 19 (3): 305–308.

Buscheck, T. E., and C. M. Alcantar. 1995. "Regression Techniques and Analytical Solutions to Demonstrate Intrinsic Bioremediation." In *Intrinsic Bioremediation (Proceedings from the Third International In Situ and On-Site)*. Columbus, OH: Battelle Press.

Board of Water Supply, City and County of Honolulu (BWS). 2016. *2016 Water Master Plan*. Prepared by CDM Smith. October.

Cooper, H. H., J. D. Bredehoeft, and I. S. Papadopulos. 1967. "Response of a Finite-Diameter Well to an Instantaneous Charge of Water." *Water Resources Research* 3 (1): 263–269. https://doi.org/10.1029/WR003i001p00263.

Cooper, H. H., Jr., and C. E. Jacob. 1946. "A Generalized Graphical Method for Evaluating Formation Constants and Summarizing Well Field History." *Transactions, American Geophysical Union* 27 (4).

Commission on Water Resource Management (CWRM). 2001. *Well Completion Report, Oahu (Halawa) Deep Monitor Well 2253-03*. State of Hawaii Department of Land and Natural Resources. October 11.

Dale, R. H. 1978. *A Ground-Water Inventory of the Waialua Basal-Water Body, Island of Oahu, Hawaii*. Open-File Report 78-24. Prepared in cooperation with Board of Water Supply, City and County of Honolulu, Honolulu, Hawaii. U.S. Geological Survey.

Dames & Moore. 1991. *Site Characterization, Halawa Medium Security Facility, Halawa Valley, Oahu, Hawaii*. D&M Job Number 0314-147-037. October 25.

Department of Health, State of Hawaii (DOH). 2017. *Evaluation of Environmental Hazards at Sites with Contaminated Soil and Groundwater, Hawai'i Edition*. Hazard Evaluation and Emergency Response. Revised 2017. Fall.

———. 2018. *Technical Guidance Manual for the Implementation of the Hawaii State Contingency Plan*. Interim Final. Honolulu, HI: Hazard Evaluation and Emergency Response Office. April.

———. Letter from M. K. Miyasaka, Hazard Evaluation and Emergency Response Office, to D. Ige, Naval Facilities Engineering Command, Pacific. 2005. "Subject: Request for No Further Action Determination for the Red Hill Oily Waste Disposal Facility," April 11, 2005.

Doherty, J. L. 2000. *PEST: Model Independent Parameter Estimation, Preface to the 4th Edition*. Watermark Numerical Computing.

Department of the Navy (DON). 1943. *Log of Formations in Tank Excavation, Tank Barrels 1–20 [1941–1943]*. Pacific Naval Air Bases.

———. 1996a. *Phase I Remedial Investigation Report, Red Hill Oily Waste Disposal Facility, Fleet and Industrial Supply Center, Pearl Harbor, Oahu, Hawaii*. Prepared by Ogden Environmental and Energy Services Co., Inc., Honolulu, HI. Pearl Harbor, HI: Naval Facilities Engineering Command, Pacific. January.

———. 1996b. *Final Remediation Verification Report, Closure and Removal of Red Hill Stilling Basin, Fleet and Industrial Supply Center - Pearl Harbor, Red Hill, Hawaii*. Prepared by OHM Remediation Services Corp., Pleasanton, CA. Pearl Harbor, HI: Naval Facilities Engineering Command, Pacific. February.

———. 1999. *Initial Phase II Site Characterization Report, Fleet Industrial Supply Center Bulk Fuel Storage Facility at Red Hill*. Prepared by Ogden Environmental and Energy Services Co., Inc., Honolulu, HI. Pearl Harbor, HI: Naval Facilities Engineering Command, Pacific. March.

———. 2000. *Remedial Investigation Phase II, Red Hill Oily Waste Disposal Facility, Halawa, Oahu, Hawaii*. Prepared by Earth Tech, Inc., Honolulu, HI. Volume I, Technical Report. Pearl Harbor, HI: Naval Facilities Engineering Command, Pacific. September.

———. 2002. *Red Hill Bulk Fuel Storage Facility Investigation Report (Final) for Fleet Industrial Supply Center (FISC), Oahu, Hawaii*. Prepared by AMEC Earth & Environmental, Inc., Huntsville, AL. Pearl Harbor, HI: Naval Facilities Engineering Command, Pacific. August.

———. 2005. *Red Hill Bulk Fuel Storage Facility Work Plan, Pearl Harbor, Hawaii*. Prepared by The Environmental Company, Inc. (TEC), Honolulu, HI; and AMEC Earth & Environmental, Inc., Honolulu, HI. Pearl Harbor, HI: Naval Facilities Engineering Command, Pacific. June.

———. 2007. *Red Hill Bulk Fuel Storage Facility Final Technical Report, Pearl Harbor, Hawaii*. Prepared by TEC, Inc. Pearl Harbor, HI: Naval Facilities Engineering Command, Pacific. August.

———. 2008a. *Monthly Soil Vapor Monitoring Reports, Red Hill Bulk Fuel Storage Facility*. 2008–Present. Prepared for Naval Facilities Engineering Command, Hawaii, JBPHH, HI.

———. 2008b. *Red Hill Bulk Fuel Storage Facility Final Groundwater Protection Plan, Pearl Harbor, Hawaii*. Prepared by TEC Inc. Includes December 2009 Revisions to the Red Hill Groundwater Protection Plan. Pearl Harbor, HI: Naval Facilities Engineering Command, Pacific. January.

———. 2008c. *Tank 17 Removal Action Report, Red Hill Fuel Storage Facility, Pearl Harbor, Oahu, Hawaii*. Prepared by TEC Inc., Honolulu, HI. Pearl Harbor, HI: Commander, Navy Region Hawaii, Environmental Department, Code N45. September.

———. 2010. *Type 1 Letter Report – Re-Evaluation of the Tier 3 Risk Assessment/Groundwater Model & Proposed Course of Action Red Hill Bulk Fuels Storage Facility, Pearl Harbor, HI*. Prepared by TEC Inc. Prepared for Naval Fleet Engineering Service Center and Pearl Harbor Naval Base Fleet Industrial Supply Center. May 4.

———. 2012. *FY11SRM Repair of Red Hill Fuel Tunnel, Geotechnical Data Report*. Prepared by URS Corporation. August 3.

———. 2014a. *Tank 5 Initial and Quarterly Release Response Reports, Red Hill Bulk Fuel Storage Facility, JBPHH, Oahu, Hawaii*. April 2014–Present. Prepared by Commander Navy Region Hawaii Environmental Department, Code N45, JBPHH, HI.

———. 2014b. *Interim Update, Red Hill Bulk Fuel Storage Facility Final Groundwater Protection Plan, Pearl Harbor, Hawaii. (January 2008)*. Pearl Harbor, HI: Naval Facilities Engineering Command, Pacific. August.

———. 2015a. *Draft Monitoring Well Installation Report, Red Hill Bulk Fuel Storage Facility, Joint Base Pearl Harbor-Hickam, Hawaii*. Prepared by Battelle, Columbus, OH; and Parsons, South Jordan, UT. JBPHH HI: Naval Facilities Engineering Command, Hawaii. March.

———. 2015b. *Final Archaeological Inventory Survey of the Red Hill Fuel Facility, Joint Base Pearl Harbor-Hickam, O'ahu, Hawai'i. Tax Map Key (TMK): (1) 1-1-012:003 and 004 (Both, Portions); and TMK (1) 9-9-010:001, 006, 026 (All, Portions), and 050*. Prepared by International Archaeology, LLC, Honolulu, HI. Pearl Harbor, HI: Naval Facilities Engineering Command, Pacific. August.

———. 2015c. *Work Plan/Sampling and Analysis Plan, Long-Term Groundwater and Soil Vapor Monitoring, Red Hill Bulk Fuel Storage Facility, Joint Base Pearl Harbor-Hickam, Oahu, Hawaii*. Prepared by Element Environmental, LLC, Aiea, HI. JBPHH HI: Naval Facilities Engineering Command, Hawaii. September.

———. 2015d. *Red Hill Tank Complex, Soil Vapor Sampling Results for August 2015*. Letter Report from A. Y. Poentis, Navy Region Hawaii, Regional Environmental Department; to: R. Takaba, Hawaii State Department of Health, Environmental Management Division, Solid and Hazardous Waste Branch, Underground Storage Tank Section. September 8.

———. 2016a. *3.2 Tank Upgrade Alternatives (TUA), Scope of Work Outline Final Submission, Red Hill Fuel Storage Facility, NAVSUP FLC Pearl Harbor, HI (PRL), Joint Base Pearl Harbor-Hickam*. Administrative Order on Consent In the Matter of Red Hill Bulk Fuel Storage Facility EPA Docket No. RCRA 7003-R9-2015 01 DOH Docket No. 15-UST-EA-01. Prepared by Enterprise Engineering, Inc., Freeport, ME. JBPHH HI: Naval Facilities Engineering Command, Pacific. September.

———. 2016b. *Monitoring Well Installation Work Plan, Red Hill Bulk Fuel Storage Facility, Joint Base Pearl Harbor-Hickam, O'ahu, Hawai'i; August 29, 2016*. Prepared by AECOM Technical Services, Inc., Honolulu, HI. Prepared for Defense Logistics Agency Energy, Fort Belvoir, VA, under Naval Facilities Engineering Command, Hawaii, JBPHH HI.

———. 2017a. *Work Plan / Scope of Work, Investigation and Remediation of Releases and Groundwater Protection and Evaluation, Red Hill Bulk Fuel Storage Facility, Joint Base Pearl Harbor-Hickam, O'ahu, Hawai'i; January 4, 2017, Revision 02*. Prepared by AECOM Technical

Services, Inc., Honolulu, HI. Prepared for Defense Logistics Agency Energy, Fort Belvoir, VA, under Naval Facilities Engineering Command, Hawaii, JBPHH HI.

———. 2017b. *Existing Data Summary and Evaluation Report for Groundwater Flow and Contaminant Fate and Transport Modeling, Red Hill Bulk Fuel Storage Facility, Joint Base Pearl Harbor-Hickam, O'ahu, Hawai'i; March 5, 2017, Revision 00*. Prepared by AECOM Technical Services, Inc., Honolulu, HI. Prepared for Defense Logistics Agency Energy, Fort Belvoir, VA, under Naval Facilities Engineering Command, Hawaii, JBPHH HI.

———. 2017c. *Groundwater Flow Model Progress Report 01, Red Hill Bulk Fuel Storage Facility, Joint Base Pearl Harbor-Hickam, O'ahu, Hawai'i; April 5, 2017, Revision 00*. Prepared by AECOM Technical Services, Inc., Honolulu, HI. Prepared for Defense Logistics Agency Energy, Fort Belvoir, VA, under Naval Facilities Engineering Command, Hawaii, JBPHH HI.

———. 2017d. *Data Gap Analysis Report, Investigation and Remediation of Releases and Groundwater Protection and Evaluation, Red Hill Bulk Fuel Storage Facility, Joint Base Pearl Harbor-Hickam, O'ahu, Hawai'i; April 25, 2017, Revision 00*. Prepared by AECOM Technical Services, Inc., Honolulu, HI. Prepared for Defense Logistics Agency Energy, Fort Belvoir, VA, under Naval Facilities Engineering Command, Hawaii, JBPHH HI.

———. 2017e. *Groundwater Flow Model Progress Report 02, Red Hill Bulk Fuel Storage Facility, Joint Base Pearl Harbor-Hickam, O'ahu, Hawai'i; August 4, 2017, Revision 00*. Prepared by AECOM Technical Services, Inc., Honolulu, HI. Prepared for Defense Logistics Agency Energy, Fort Belvoir, VA, under Naval Facilities Engineering Command, Hawaii, JBPHH HI.

———. 2017f. *Monitoring Well Installation Work Plan Addendum 02, Investigation and Remediation of Releases and Groundwater Protection and Evaluation, Red Hill Bulk Fuel Storage Facility, Joint Base Pearl Harbor-Hickam, O'ahu, Hawai'i; August 25, 2017, Revision 00*. Prepared by AECOM Technical Services, Inc., Honolulu, HI. Prepared for Defense Logistics Agency Energy, Fort Belvoir, VA, under Naval Facilities Engineering Command, Hawaii, JBPHH HI.

———. 2017g. *Attenuation Evaluation Plan, Investigation and Remediation of Releases and Groundwater Protection and Evaluation, Red Hill Bulk Fuel Storage Facility, Joint Base Pearl Harbor-Hickam, O'ahu, Hawai'i; September 1, 2017, Revision 00*. Prepared by AECOM Technical Services, Inc., Honolulu, HI. Prepared for Defense Logistics Agency Energy, Fort Belvoir, VA, under Naval Facilities Engineering Command, Hawaii, JBPHH HI.

———. 2017h. *Groundwater Model Evaluation Plan, Investigation and Remediation of Releases and Groundwater Protection and Evaluation, Red Hill Bulk Fuel Storage Facility, Joint Base Pearl Harbor-Hickam, O'ahu, Hawai'i; September 8, 2017, Revision 00*. Prepared by AECOM Technical Services, Inc., Honolulu, HI. Prepared for Defense Logistics Agency Energy, Fort Belvoir, VA, under Naval Facilities Engineering Command, Hawaii, JBPHH HI.

———. 2017i. *Risk-Based Decision Criteria Development Plan, Investigation and Remediation of Releases and Groundwater Protection and Evaluation, Red Hill Bulk Fuel Storage Facility, Joint Base Pearl Harbor-Hickam, O'ahu, Hawai'i; December 11, 2017, Revision 00*. Prepared by AECOM Technical Services, Inc., Honolulu, HI. Prepared for Defense Logistics Agency Energy, Fort Belvoir, VA, under Naval Facilities Engineering Command, Hawaii, JBPHH HI.

———. 2017j. *Sentinel Well Network Development Plan, Investigation and Remediation of Releases and Groundwater Protection and Evaluation, Red Hill Bulk Fuel Storage Facility, Joint Base Pearl Harbor-Hickam, O'ahu, Hawai'i; December 11, 2017, Revision 00*. Prepared by AECOM Technical Services, Inc., Honolulu, HI. Prepared for Defense Logistics Agency Energy, Fort Belvoir, VA, under Naval Facilities Engineering Command, Hawaii, JBPHH HI.

———. 2018a. *Well Elevation Survey Report, Red Hill Bulk Fuel Storage Facility, Joint Base Pearl Harbor-Hickam, O'ahu, Hawai'i; Revision 00*. Prepared by AECOM Technical Services, Inc., Honolulu, HI. Prepared for Defense Logistics Agency Energy, Fort Belvoir, VA, under Naval Facilities Engineering Command, Hawaii, JBPHH HI. January.

———. 2018b. *Technical Memorandum, Testing and Verification of Packer Integrity at RHMW11, Red Hill Bulk Fuel Storage Facility, Joint Base Pearl Harbor-Hickam, O'ahu, Hawai'i; February 9, 2018*. JBPHH HI: Naval Facilities Engineering Command, Hawaii. February.

———. 2018c. *Seismic Profiling to Map Hydrostratigraphy in the Red Hill Area, Red Hill Bulk Fuel Storage Facility, Joint Base Pearl Harbor-Hickam, O'ahu, Hawai'i; March 30, 2018, Revision 00*. Prepared by Lee Liberty and James St. Claire, Boise State University, Boise, ID, for AECOM Technical Services, Inc., Honolulu, HI. Boise State University Technical Report BSU CGISS 18-01. Prepared for Defense Logistics Agency Energy, Fort Belvoir, VA, under Naval Facilities Engineering Command, Hawaii, JBPHH HI.

———. 2018d. *Technical Memorandum, Gyroscopic Survey Results and Calculated Correction Factors for Groundwater Monitoring Network Wells at the Red Hill Bulk Fuel Storage Facility, Joint Base Pearl Harbor-Hickam, O'ahu, Hawai'i*. JBPHH HI: Naval Facilities Engineering Command, Hawaii. May.

———. 2018e. *Well Elevation Surveys for Red Hill Monitoring Well RHMW11 and Navy 'Aiea Halawa Shaft 2255-032, Honolulu, O'ahu, Hawai'i*. Prepared by AECOM Technical Services, Inc., Honolulu, HI. Letter Report. Prepared for Naval Facilities Engineering Command, Hawaii, JBPHH HI. May.

———. 2018f. *Final First Quarter 2018 - Quarterly Groundwater Monitoring Report, Red Hill Bulk Fuel Storage Facility, Joint Base Pearl Harbor-Hickam, O'ahu, Hawai'i*. Prepared by AECOM Technical Services, Inc. JBPHH HI: Naval Facilities Engineering Command, Hawaii. July.

———. 2018g. *Conceptual Site Model, Red Hill Bulk Fuel Storage Facility, Joint Base Pearl Harbor-Hickam, O'ahu, Hawai'i; July 27, 2018, Revision 00*. Prepared by AECOM Technical Services, Inc., Honolulu, HI. Prepared for Defense Logistics Agency Energy, Fort Belvoir, VA, under Naval Facilities Engineering Command, Hawaii, JBPHH HI.

———. 2018h. *Groundwater Protection and Evaluation Considerations for the Red Hill Bulk Fuel Storage Facility, Joint Base Pearl Harbor-Hickam, O'ahu, Hawai'i; July 27, 2018, Revision 00*. Prepared by AECOM Technical Services, Inc., Honolulu, HI. Prepared for Defense Logistics Agency Energy, Fort Belvoir, VA, under Naval Facilities Engineering Command, Hawaii, JBPHH HI.

———. 2019. *Final First Quarter 2019 - Quarterly Groundwater Monitoring Report, Red Hill Bulk Fuel Storage Facility, Joint Base Pearl Harbor-Hickam, O'ahu, Hawai'i*. Prepared by AECOM Technical Services, Inc. JBPHH HI: Naval Facilities Engineering Command, Hawaii. May.

Driscoll, F. G. 1986. *Groundwater and Wells*. 2nd ed. St. Paul, MN: Johnson Screens.

Duffield, G. M. 2007. *AQTESOLV for Windows, Version 4.5*. Reston, VA: HydroSOLVE, Inc. http://www.aqtesolv.com.

Environmental Chemical Corporation (ECC). 2000. *Removal of Underground Storage Tank TAMC 137-4, Building 137, Tripler Army Medical Center, Oahu, Hawaii*. Prepared for Department of Army Headquarters, United States Army Garrison, Hawaii. September.

Edward K. Noda and Associates, Inc. (EKNA). 1999. *Closure Report: Halawa Medium Security Facility, Existing UST Closure Actions, 99-902 Moanalua Road, Aiea, Hawaii, 96701.* Prepared

for State of Hawaii, Department of Accounting and General Services Division of Public Works. June 11.

———. 2000. *Addendum to Closure Report: Halawa Medium Security Facility, Underground Storage Tank Actions, Honolulu, Oahu Hawaii*. Prepared for DMT Consulting Engineers, Honolulu, HI. April 4.

Engott, J. A., A. G. Johnson, M. Bassiouni, and S. K. Izuka. 2015. *Spatially Distributed Groundwater Recharge for 2010 Land Cover Estimated Using a Water-Budget Model for the Island of O'ahu, Hawai'i*. Scientific Investigations Report 2015–5010. Prepared in cooperation with the State of Hawai'i Commission on Water Resource Management and the City and County of Honolulu Board of Water Supply. U.S. Geological Survey.

Environmental Protection Agency, United States (EPA). 1989. *Risk Assessment Guidance for Superfund, Volume I: Human Health Evaluation Manual (Part A)*. Interim Final. EPA/540/1-89/002. Office of Emergency and Remedial Response. December.

———. 1995. *Light Nonaqueous Phase Liquids*. Ground Water Issue. EPA/540/S-95/500. Washington, DC: Office of Research and Development, Office of Solid Waste and Emergency Response. July.

———. 1999. *Use of Monitored Natural Attenuation at Superfund, RCRA Corrective Action, and Underground Storage Tank Sites*. OSWER 9200.4-17P. Office of Solid Waste and Emergency Response. April.

———. 2011. *Environmental Cleanup Best Management Practices: Effective Use of the Project Life Cycle Conceptual Site Model*. Quick Reference Fact Sheet. EPA 542-F-11-011. Office of Solid Waste and Emergency Response. July.

———. 2019. *Regional Screening Levels for Chemical Contaminants at Superfund Sites*. EPA Office of Superfund. May.

Environmental Protection Agency, United States, Region 9; and Department of Health, State of Hawaii (EPA Region 9 and DOH). 2015. *Administrative Order on Consent In the Matter of Red Hill Bulk Fuel Storage Facility, EPA Docket No: RCRA 7003-R9-2015-01; DOH Docket No: 15-UST-EA-01*. September.

———. 2016. "Final Scoping for AOC SOW Sections 6 and 7, and Navy's Proposed Chemical of Potential Concern (COPC) Recommendations," February 4, 2016. Letter from Bob Pallarino, EPA Red Hill Project Coordinator, and Steven Chang, DOH Red Hill Project Coordinator, to: James A. K. Miyamoto, Naval Facilities Engineering Command, Hawaii, Joint Base Pearl Harbor-Hickam.

Eyre, P. R. 1983. *The Effects of Pumpage, Irrigation Return, and Regional Ground-Water Flow on the Water Quality at Waiawa Water Tunnel, Oahu, Hawaii*. Water-Resources Investigations Report 83–4097. U.S. Geological Survey.

Eyre, P. R., C. Ewart, and P. J. Shade. 1986. *Hydrology of the Leeward Aquifers, Southeast Oahu, Hawaii: Regional Analysis of the Southern Oahu Ground-Water Flow System*. Water-Resources Investigations Report 85-4270. U.S. Geological Survey.

Garg, S., C. J. Newell, P. R. Kulkarni, D. C. King, D. T. Adamson, M. I. Renno, and T. Sale. 2017. "Overview of Natural Source Zone Depletion: Processes, Controlling Factors, and Composition Change." *Groundwater Monitoring & Remediation* 37 (3): 62–81. https://doi.org/10.1111/gwmr.12219.

Gingerich, S. B., and D. S. Oki. 2000. "Ground Water in Hawaii." Report 126–00. Fact Sheet. U.S. Geological Survey.

Gingerich, S. B., and C. I. Voss. 2005. "Three-Dimensional Variable-Density Flow Simulation of a Coastal Aquifer in Southern Oahu, Hawaii, USA." *Hydrogeology Journal* 13 (2): 436–450. https://doi.org/10.1007/s10040-004-0371-z.

Historic American Engineering Record (HAER). 2015. *U.S. Naval Base, Pearl Harbor, Red Hill Underground Fuel Storage System: Photographs, Written Historical and Descriptive Data*. HAER HI-123. Washington, DC: National Park Service.

Hantush, M. S. 1956. "Analysis of Data from Pumping Tests in Leaky Aquifers." *Eos, Transactions American Geophysical Union* 37 (6): 702–714. https://doi.org/10.1029/TR037i006p00702.

Hantush, M. S., and R. G. Thomas. 1966. "A Method for Analyzing a Drawdown Test in Anisotropic Aquifers." *Water Resources Research* 2 (2): 281–285. https://doi.org/10.1029/WR002i002p00281.

Honolulu Authority for Rapid Transportation (HART). 2014. *Geotechnical Data Reports for Honolulu Rail Transit Project, 2014–2016*. Aloha Stadium Station, Pearl Highlands Station, Pearl Highlands Station, Ramp H2R2, Kalihi Station, Kapalama Station, Roadway Pavement from Halawa Drive to Dillingham Boulevard and TPSS #28, Aiea to Middle Street, Middle Street to Ala Moana Center, Pearl Harbor Naval Base Station, Lagoon Drive Station, Honolulu International Airport Station, Middle Street Station, City Center Section Utilities and Guideway, Airport Section Guideway - 7-Pier Construction. Prepared by: Anil Verma Associates, Inc.; Shannon & Wilson, Inc.; Yogi Kwong Engineers, LLC; and Geolabs, Inc.

Hem, J. D. 1985. *Study and Interpretation of the Chemical Characteristics of Natural Water*. Water-Supply Paper 2254. 3rd Ed. U.S. Geological Survey.

Hillel, D. 1982. *Introduction to Soil Physics*. San Diego, CA: Academic Press.

Hua, Q., M. Barbetti, and A. Z. Rakowski. 2013. "Atmospheric Radiocarbon for the Period 1950–2010." *Radiocarbon* 55 (4): 2059–72.

Hunt Jr., C. D. 1996. *Geohydrology of the Island of Oahu, Hawaii*. Professional Paper 1412-B. Regional Aquifer-System Analysis—Oahu, Hawaii. U.S. Geological Survey.

Huntley, D., and G. D. Beckett. 2002. *Evaluating Hydrocarbon Removal from Source Zones and Its Effect on Dissolved Plume Longevity and Magnitude*. API Publication 4715. American Petroleum Institute, Regulatory Analysis and Scientific Affairs Department.

Hutcheson, M. S., D. Pedersen, N. D. Anastas, J. Fitzgerald, and D. Silverman. 1996. "Beyond TPH: Health-Based Evaluation of Petroleum Hydrocarbon Exposures." *Regulatory Toxicology and Pharmacology* 24 (1): 85–101. https://doi.org/10.1006/rtph.1996.0066.

Hvorslev, M. J. 1951. "Time Lag and Soil Permeability in Ground-Water Observations." Bulletin No. 36. Vicksburg, MS: Waterways Experiment Station, Corps of Engineers, U.S. Army. April.

Isobe, K. 2016. "Navy Intensifies Modernization of Red Hill Bulk Fuel Storage Facility." *Currents—The Navy's Energy and Environmental Magazine*, Fall 2016.

Interstate Technology & Regulatory Council (ITRC). 2008. *LNAPL Training Part 2: LNAPL Characterization and Recoverability – Improved Analysis*. ITRC Internet-Based Training Program. Co-sponsored by the EPA Office of Superfund Remediation and Technology Innovation.

———. 2009a. *Evaluating Natural Source Zone Depletion at Sites with LNAPL*. LNAPL-1. Prepared by the ITRC LNAPLs Team. April.

———. 2009b. *Evaluating LNAPL Remedial Technologies for Achieving Project Goals*. Washington, DC: Technical/Regulatory Guidance. December.

———. 2018. *Light Non-Aqueous Phase Liquid (LNAPL) Site Management: LCSM Evolution, Decision Process, and Remedial Technologies*. LNAPL-3. Washington, DC: LNAPL Update Team. March.

Izuka, S. K. 1992. *Geology and Stream Infiltration of North Halawa Valley, Oahu, Hawaii*. Prepared in cooperation with the State of Hawaii Department of Transportation. Honolulu, HI. Water-Resources Investigations Report 91-4197. U.S. Geological Survey.

Izuka, S. K., J. A. Engott, K. Rotzoll, M. Bassiouni, A. G. Johnson, L. D. Miller, and A. Mair. 2018. *Volcanic Aquifers of Hawai'i—Hydrogeology, Water Budgets, and Conceptual Models*. Ver. 2.0, March 2018. Scientific Investigations Report 2015–5164. Water Availability and Use Science Program. U.S. Geological Survey.

Juturna LLC. 2014. *Letter Report: Summary of Well Sampling Activities, BWS DH-43 No. 2253-02 and CWRM Halawa Deep Monitoring Well No. 2253-03, Red Hill Fuel Tank Facility Groundwater Contamination Evaluation*. Prepared for Kennedy/Jenks Consultants, Honolulu, HI. November 16.

Kao, C. M., W. Y. Huang, L. J. Chang, T. Y. Chen, H. Y. Chien, and F. Hou. 2006. "Application of Monitored Natural Attenuation to Remediate A Petroleum-Hydrocarbon Spill Site." *Water Science & Technology* 53 (2): 321–328.

Kimura, Kimura International, Inc. (Kimura). 2000. *Release Response Report: City & County of Honolulu, Halawa Bus Facility, 99-999 Iwaena Street, Honolulu, Hawaii*. Prepared for Fuel Oil Polishing Company, Inc. August.

Landmeyer, J. E., F. H. Chapelle, M. D. Petkewich, and P. M. Bradley. 1998. "Assessment of Natural Attenuation of Aromatic Hydrocarbons in Groundwater Near A Former Manufactured-Gas Plant, South Carolina, USA." *Environmental Geology* 34 (4): 279–292.

Langenheim, V. M., and D. A. Clague. 1987. "The Hawaiian-Emperor Volcanic Chain, Part II, Stratigraphic Framework of Volcanic Rocks of the Hawaiian Islands." In *Volcanism in Hawaii*, v. 1, chap. 1, pp. 55–84. Professional Paper 1350. U.S. Geological Survey.

Macdonald, G. A. 1941. *Geology of the Red Hill and Waimalu Areas, Oahu, in Relation to the Underground Fuel Storage Project of the U.S. Navy*. February 21, 1941 Report Attachment to Letter from H. T. Stearns, U.S. Geological Survey Geologist in Charge, Hawaiian Ground-Water Investigations, to: Capt. H. F. Bruns, Public Works Office, Pearl Harbor, February 26, 1941. Honolulu, HI: U.S. Geological Survey.

McCoy, K., J. Zimbron, T. Sale, and M. Lyverse. 2014. "Measurement of Natural Losses of LNAPL Using CO_2 Traps." *Groundwater* 53: 658–667.

Mink, John F. 1980. *State of the Groundwater Resources of Southern Oahu*. Honolulu, HI: Board of Water Supply, City and County of Honolulu.

Mink, John F., and L. Stephen Lau. 1990. *Aquifer Identification and Classification for Oahu: Groundwater Protection Strategy for Hawaii*. Technical Report No. 179. Honolulu, HI: University of Hawaii, Water Resources Research Center. November 1987; rev. February 1990.

Mitchell, J. N., and D. S. Oki. 2018. *Groundwater-Level, Groundwater-Temperature, and Barometric-Pressure Data, July 2017 to February 2018, Hālawa Area, O'ahu, Hawai'i*. Open-File Report 2018–1147. Prepared in Cooperation with the U.S. Navy. Reston, VA: U.S. Geological Survey.

Mutch, Jr., R. D. 2005. "A Distance-Drawdown Aquifer Test Method for Aquifers with Areal Anisotropy." *Ground Water* 43 (6): 935–938. https://doi.org/10.1111/j.1745-6584.2005.00105.x.

Naval Facilities Engineering Command, Engineering and Expeditionary Warfare Center (NAVFAC EXWC). 2016. *Red Hill Facility Tank Inspection, Repair, and Maintenance Report, Administrative*

Order on Consent (AOC) Statement of Work (SOW), Section 2.2. Site Specific Report SSR-NAVFAC EXWC-CI-1655. 11 October.

Ng, G.-H. C., B. A. Bekins, I. M. Cozzarelli, M. J. Baedecker, P. C. Bennett, and R. T. Amos. 2014. "A Mass Balance Approach to Investigating Geochemical Controls on Secondary Water Quality Impacts at a Crude Oil Spill Site Near Bemidji, MN." *Journal of Contaminant Hydrology* 164: 1–15. https://doi.org/10.1016/j.jconhyd.2014.04.006.

Ng, G.-H. C., B. A. Bekins, I. M. Cozzarelli, M. J. Baedecker, P. C. Bennett, R. T. Amos, and W. N. Herkelrath. 2015. "Reactive Transport Modeling of Geochemical Controls on Secondary Water Quality Impacts at a Crude Oil Spill Site Near Bemidji, MN." *Water Resources Research* 51: 4156–183. https://doi.org/10.1002/2015WR016964.

Nichols, W. D., P. J. Shade, and C. D. Hunt Jr. 1996. *Summary of the Oahu, Hawaii, Regional Aquifer-System Analysis*. Professional Paper 1412-A. Regional Aquifer-System Analysis—Oahu, Hawaii. U.S. Geological Survey.

Oki, D. S. 1998. *Geohydrology of the Central Oahu, Hawaii, Ground-Water Flow System and Numerical Simulation of the Effects of Additional Pumping*. Water-Resources Investigations Report 97–4276. Prepared in Cooperation with the Honolulu Board of Water Supply. U.S. Geological Survey.

———. 2005. *Numerical Simulation of the Effects of Low-Permeability Valley-Fill Barriers and the Redistribution of Ground-Water Withdrawals in the Pearl Harbor Area, Oahu, Hawaii*. Scientific Investigations Report 2005-5253. U.S. Geological Survey.

———. 2017. *Synoptic Groundwater-Level Survey, November 18, 2016, Hālawa Area, O'ahu, Hawai'i.*

Oki, D. S., and A. Brasher. 2003. *Environmental Setting and the Effects of Natural and Human-Related Factors on Water Quality and Aquatic Biota, Oahu, Hawaii*. Water-Resources Investigations Report 03-4156. Honolulu, HI: U.S. Geological Survey.

Oki, D. S., S. B. Gingerich, and R. L. Whitehead. 1999. "Hawaii." In *Ground Water Atlas of the United States: Segment 13 - Alaska, Hawaii, Puerto Rico and the U.S. Virgin Islands*. HA 730-N. U.S. Geological Survey.

Oki, D. S., W. R. Souza, E. I. Bolke, and G. R. Bauer. 1996. *Numerical Analysis of Ground-Water Flow and Salinity in the Ewa Area, Oahu, Hawaii*. Open-File Report 96-442. Prepared in Cooperation with the State of Hawaii Commission on Water Resource Management. U.S. Geological Survey.

Okuhata, B., A. El-Kadi, H. Dulai, D. Oki, and B. Carr. 2017. "Development of a Model to Identify Local Hydrogeology and Simulate Groundwater Injection in Nuuanu and Kalihi Aquifer Systems, Oahu, Hawaii." Geology and Geophysics Master of Science thesis, December: University of Hawaii.

Pankiwskyj, K. A. 1972. "Geology of the Salt Lake Area, Oahu, Hawaii." *Pacific Science* 26 (2): 242–253.

Pacific Geotechnical Engineers, Inc. (PGE). 2015. *0 to 35% Design, FY15 DLA MILCON P-205, Red Hill Fire Suppression and Ventilation System, Joint Base Pearl Harbor-Hickam, Red Hill Fuel Storage Facility, Hawaii*. PGE Job No. 3773-008.

Presley, T. K., J. M. Sinton, and M. Pringle. 1997. "Postshield Volcanism and Catastrophic Mass Wasting of the Waianae Volcano, Oahu, Hawaii." *Bulletin of Volcanology* 58 (8): 597–616. https://doi.org/10.1007/s004450050165.

Red Hill Fuel Storage Facility Task Force, State of Hawai'i (RHSF Task Force). 2014. *Report to the Twenty-Eighth Legislature, State of Hawaii, 2015, Pursuant To Senate Concurrent Resolution 73 Requesting the Department of Health to Convene a Task Force to Study the Effects of the January 2014 Fuel Tank Leak at the Red Hill Fuel Storage Facility*. December.

Rockhold, M. L., R. R. Yarwood, and J. S. Selker. 2004. "Coupled Microbial and Transport Processes in Soils." *Vadose Zone J.* 3: 368–383. https://doi.org/10.2113/3.2.368.

Rosenau, J. C., E. R. Lubke, and R. H. Nakahara. 1971. *Water Resources of North-Central Oahu, Hawaii*. Geological Survey Water-Supply Paper 1899-D. Prepared in cooperation with the State of Hawaii, Department of Land and Natural Resources, Division of Water and Land Development. U.S. Geological Survey.

Rotzoll, K. 2012. *Numerical Simulation of Flow in Deep Open Boreholes in a Coastal Freshwater Lens, Pearl Harbor Aquifer, O'ahu, Hawai'i*. Scientific Investigations Report 2012-5009. Prepared in Cooperation with the Honolulu Board of Water Supply. Reston, VA: U.S. Geological Survey.

Rotzoll, K., and A. I. El-Kadi. 2007. *Numerical Ground-Water Flow Simulation for Red Hill Fuel Storage Facilities, NAVFAC Pacific, Oahu, Hawaii*. Prepared for The Environmental Company (TEC). Appendix L in: Department of the Navy (2007), *Red Hill Bulk Fuel Storage Facility Final Technical Report, Pearl Harbor, Hawaii*; Naval Facilities Engineering Command, Pacific. Honolulu, HI: University of Hawaii, Water Resources Research Center. August.

Rotzoll, K., A. I. El-Kadi, and S. B. Gingerich. 2007. "Estimating Hydraulic Properties of Volcanic Aquifers Using Constant-Rate and Variable-Rate Aquifer Tests." *JAWRA Journal of the American Water Resources Association* 43 (2): 334–345. https://doi.org/10.1111/j.1752-1688.2007.00026.x.

Shaw, Shaw Environmental, Inc. (Shaw). 2009. *Technical Report: Demolish JP-5 Slop Tank at the Red Hill Fuel Facility Fleet and Industrial Supply Center Pearl Harbor, Hawaii*. Rev. 0. Brooks City-Base, TX: Air Force Center for Engineering and the Environment. April.

Sherrod, D. R., J. M. Sinton, S. E. Watkins, and K. M. Brunt. 2007. "Geologic Map of the State of Hawai'i, Sheet 3—Island of O'ahu." Open-File Report 2007-1089.

Sohn, Y. K., and K. H. Park. 2005. "Composite Tuff Ring/Cone Complexes in Jeju Island, Korea: Possible Consequences of Substrate Collapse and Vent Migration." *Journal of Volcanology and Geothermal Research* 141: 157–175.

Soroos, R. L. 1973. *Determination of Hydraulic Conductivity of Some Oahu Aquifers with Step-Drawdown Test Data*. M.S. Thesis, Univ. of Hawaii, Honolulu, HI.

Souza, W. R., and C. I. Voss. 1987. "Analysis of an Anisotropic Coastal Aquifer System Using Variable-Density Flow and Solute Transport Simulation." *Journal of Hydrology* 92 (1–2): 17–41.

Stearns, H. T. 1939. *Geologic Map and Guide of the Island of Oahu, Hawaii*. Bulletin 2. Prepared in cooperation with the Geological Survey. Honolulu: Hawaii (Terr.) Department of Public Lands, Division of Hydrography.

———. 1943. "Letter from H. T. Stearns, Senior Geologist, U.S. Geological Survey, to: O. E. Meinzer, Division of Ground Water, U.S. Geological Survey, Washington, DC," January 18, 1943.

———. 1978. *Quaternary Shorelines in the Hawaiian Islands*. Bernice P. Bishop Museum Bulletin 237. Honolulu, HI: Bishop Museum Press.

Stearns, H. T., and T. K. Chamberlain. 1967. "Deep Cores of Oahu, Hawaii and Their Bearing on the Geologic History of the Central Pacific Basin." *Pacific Science* 21 (2): 153–165.

Stearns, H. T., and K. N. Vaksvik. 1935. *Geology and Groundwater Resources of the Island of Oahu, Hawaii*. Bulletin 1. Prepared in cooperation with the Geological Survey. Honolulu: Hawaii (Terr.) Department of Public Lands, Division of Hydrography.

Takasaki, K. J., and S. Valenciano. 1969. *Water in the Kahuku Area, Oahu, Hawaii*. Water Supply Paper 1874. U.S. Geological Survey.

Unitek. 1988. *Halawa Medium Security Facility Borings by P.R. Drilling/Kenton Beal for Wells 8067-001 to -005.* Reproduced in App. G of Dames & Moore 1991: Site Characterization, Halawa Medium Security Facility, Halawa Valley, Oahu, Hawaii (D&M Job Number 0314-147-037).

United States Department of Agriculture, Soil Conservation Service (USDA SCS). 1972. *Soil Survey of Islands of Kauai, Oahu, Maui, Molokai, and Lanai, State of Hawaii*. In cooperation with the University of Hawaii Agricultural Experiment Station. Washington, DC. August. https://www.nrcs.usda.gov/wps/portal/nrcs/surveylist/soils/survey/state/?stateId=HI.

United States Geological Survey (USGS). 2003. *Environmental Settings and Effects of Natural and Human-Related Factors on Water Quality and Aquatic Biota, Oahu, Hawaii*. Water Resources Investigation Report 03-4156.

———. 2017a. *National Water Information System - Moanalua Precipitation Gauge*. Https://Nwis.Waterdata.Usgs.Gov/Nwis/Inventory/?Site_no=212359157502601&agency_cd=USGS. Accessed October 2017.

———. 2017b. *National Water Information System - North Halawa Valley Precipitation Gauge*. Https://Nwis.Waterdata.Usgs.Gov/Nwis/Inventory/?Site_no=212428157511201&agency_cd=USGS. Accessed October 2017.

———. 2017c. *USGS 212304157542201 771.9 N Halawa Rain Gage Nr Honolulu, Oahu, HI*. Https://Waterdata.Usgs.Gov/Nwis/Dv?Cb_00045=on&format=html&site_no=212304157542201&referred_module=sw&period=&begin_date=2005-01-01&end_date=2017-07-07. Accessed July 2017.

———. 2017d. *USGS 212346157533701 772.1 N Halawa Rain Gage Nr Aiea, Oahu, HI*. Https://Waterdata.Usgs.Gov/Nwis/Dv?Cb_00045=on&format=html&site_no=212346157533701&referred_module=sw&period=&begin_date=2005-01-01&end_date=2017-07-06. Accessed July 2017.

———. 2017e. *Final Synoptic Water Level Study Work Plan, Hālawa Area, O'ahu, Hawai'i*. Honolulu, HI: Pacific Islands Water Science Center. August 10.

Visher, F. N., and J. F. Mink. 1964. *Ground-Water Resources in Southern Oahu, Hawaii*. Geological Survey Water Supply Paper 1778. Prepared in Cooperation with the State of Hawaii, Department of Land and Natural Resources, Division of Water and Land Development. U.S. Geological Survey.

Vitturi, M. D. M., and S. Tarquini. 2018. "MrLavaLoba: A New Probabilistic Model for the Simulation of Lava Flows as a Settling Process." *Journal of Volcanology and Geothermal Research* 349: 323–334.

Walker, G. P. L. 1990. "Geology and Volcanology of the Hawaiian Islands." *Pacific Science* 44 (4): 315–347.

Wentworth, C. K. 1938. *Geology and Ground Water Resources of the Palolo-Waialae District*. Honolulu, HI: Board of Water Supply.

———. 1951. *Geology and Groundwater Resources of the Honolulu-Pearl Harbor Area, Oahu, Hawaii*. Honolulu, HI: City and County of Honolulu, Board of Water Supply.

Wentworth, C. K., and G. A. MacDonald. 1953. *Structures and Forms of Basaltic Rocks in Hawaii*. Geological Survey Bulletin 994. U.S. Geological Survey.

White, J. D. L., and P. S. Ross. 2011. "Maar-Diatreme Volcanoes: A Review." *Journal of Volcanology and Geothermal Research* 201: 1–29.

Whittier, R. B. 2018. "Re: RHSF Monitoring Well Observations," June 26, 2018. Email communication from Bob Whittier/Hawai'i Department of Health to John Kronen/AECOM, cc: various AOC Parties.

Whittier, R. B., K. Rotzoll, S. Dhal, A. I. El-Kadi, C. Ray, and D. Chang. 2010. "Groundwater Source Assessment Program for the State of Hawaii, USA: Methodology and Example Application." *Hydrogeology Journal* 18 (3): 711–723. https://doi.org/10.1007/s10040-009-0548-6.

Whittier, R. B., K. Rotzoll, S. Dhal, A. I. El-Kadi, C. Ray, G. Chen, and D. Chang. 2004. *Hawaii Source Water Assessment Report*. Prepared for the Hawai'i Department of Health, Safe Drinking Water Branch. University of Hawai'i, Water Resources Research Center.

Wiedemeier, T. H., H. S. Rifai, C. J. Newell, and J. T. Wilson. 1999. *Natural Attenuation of Fuels and Chlorinated Solvents in the Subsurface*. New York: John Wiley & Sons, Inc.

Wiedemeier, T. H., J. T. Wilson, D. H. Kampbell, R. N. Miller, and J. E. Hansen. 1999a. *Technical Protocol for Implementing Intrinsic Remediation with Long-Term Monitoring for Natural Attenuation of Fuel Contamination Dissolved in Groundwater. Vols. I & II*. San Antonio, TX: Air Force Center for Environmental Excellence, Technology Transfer Division. March.

———. 1999b. *Technical Protocol for Implementing Intrinsic Remediation with Long-Term Monitoring for Natural Attenuation of Fuel Contamination Dissolved in Groundwater. Volume II.* San Antonio, TX: Air Force Center for Environmental Excellence, Technology Transfer Division. March.

Williams, J. A., and R. L. Soroos. 1973. *Evaluation of Methods of Pumping Test Analyses for Application to Hawaiian Aquifers*. Technical Report No. 70. Submitted to Board of Water Supply, City and County of Honolulu, Honolulu, HI.

Woodbury, D. O. 1946. *Builders For Battle: How the Pacific Naval Air Bases Were Constructed*. New York: E. P. Dutton and Co. Inc.

Appendix A:
Cumulative Historical Groundwater Monitoring Results and COPC Concentration Graphs (DON 2019)

Appendix A.1 Cumulative Groundwater COPC Results

- Attached to this PDF as a Microsoft Excel file due to table size.
  Click to:

- Show Appendix A.1 Excel attachment
- Show PDF bookmarks

Appendix A.1 file contents:

- Table A.1-1: Cumulative Groundwater COPC Results
- Table A.1-2: Cumulative Groundwater Results - Total Petroleum Hydrocarbons
- Table A.1-3: Cumulative Groundwater Results - Volatile Organic Compounds
- Table A.1-4: Cumulative Groundwater Results - Polynuclear Aromatic Hydrocarbons
- Table A.1-5 Cumulative Groundwater Results - Lead and Lead Scavengers
- Table A.1-6: Cumulative Groundwater Results - Semivolatile Organic Compounds and Fuel Additive Compounds
- Table Notes

This page intentionally left blank

RHMW2254-01

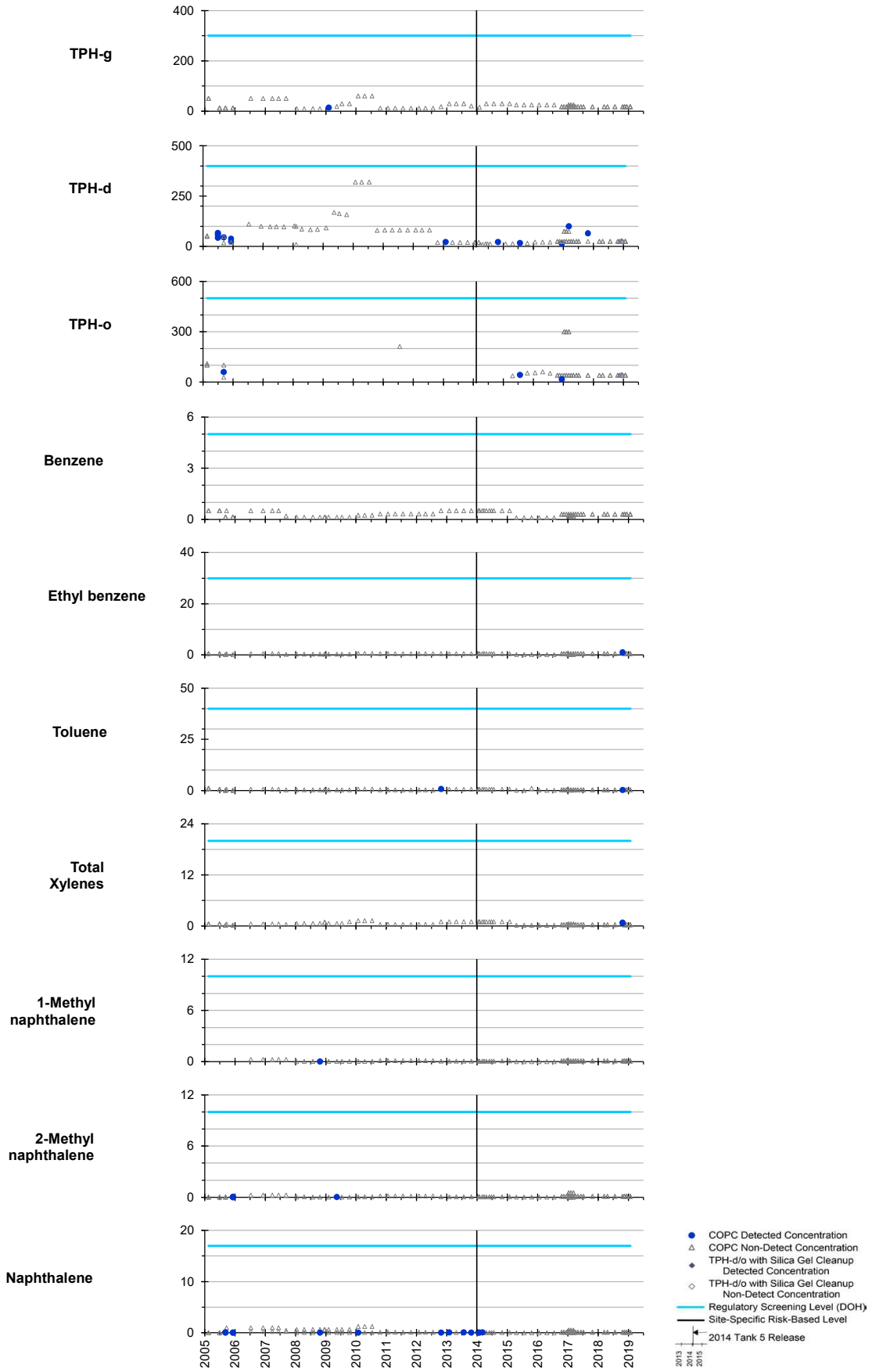

All results in micrograms per liter (µg/L or parts per billion).

EPA Region 9 Laboratory split sampling data from First to Third Quarters 2017 included in the graphs.

RHMW01

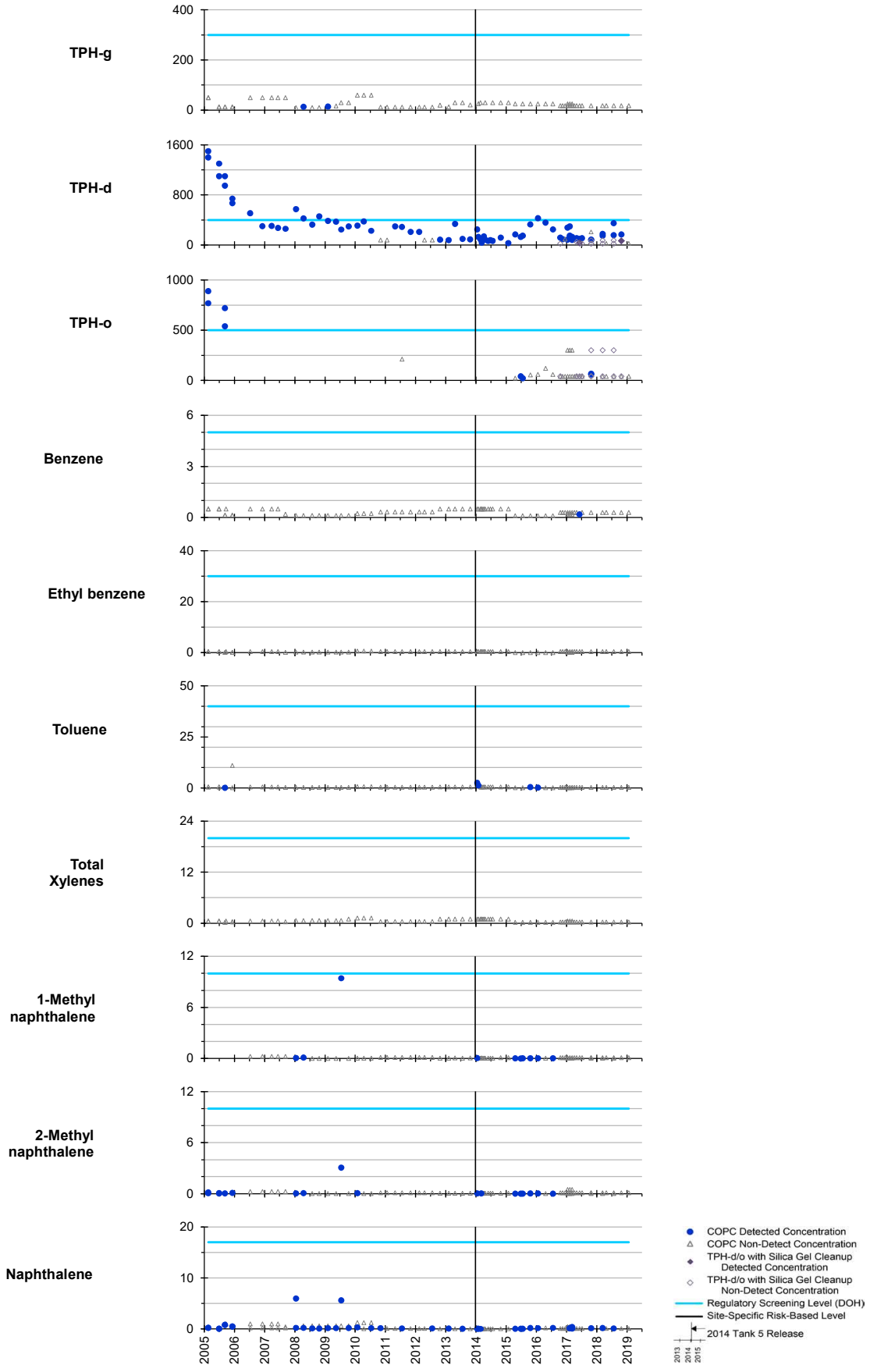

All results in micrograms per liter (µg/L or parts per billion).

EPA Region 9 Laboratory split sampling data from First to Fourth Quarters 2017, First Quarter 2018, and Third Quarter 2018 included in the graphs.

RHMW02

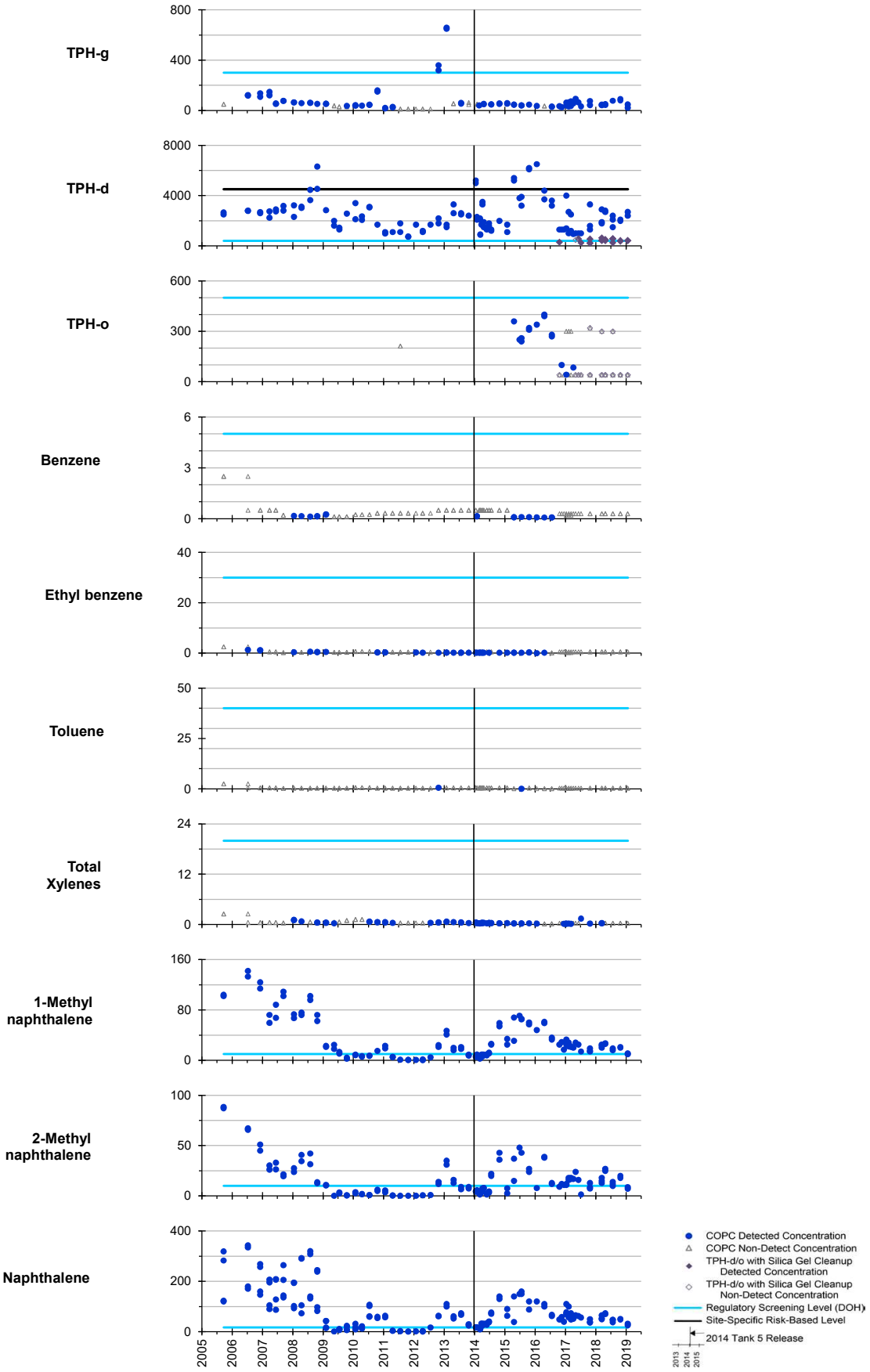

All results in micrograms per liter (µg/L or parts per billion).

EPA Region 9 Laboratory split sampling data from First to Fourth Quarters 2017, First Quarter 2018, and Third Quarter 2018 included in the graphs.

RHMW03

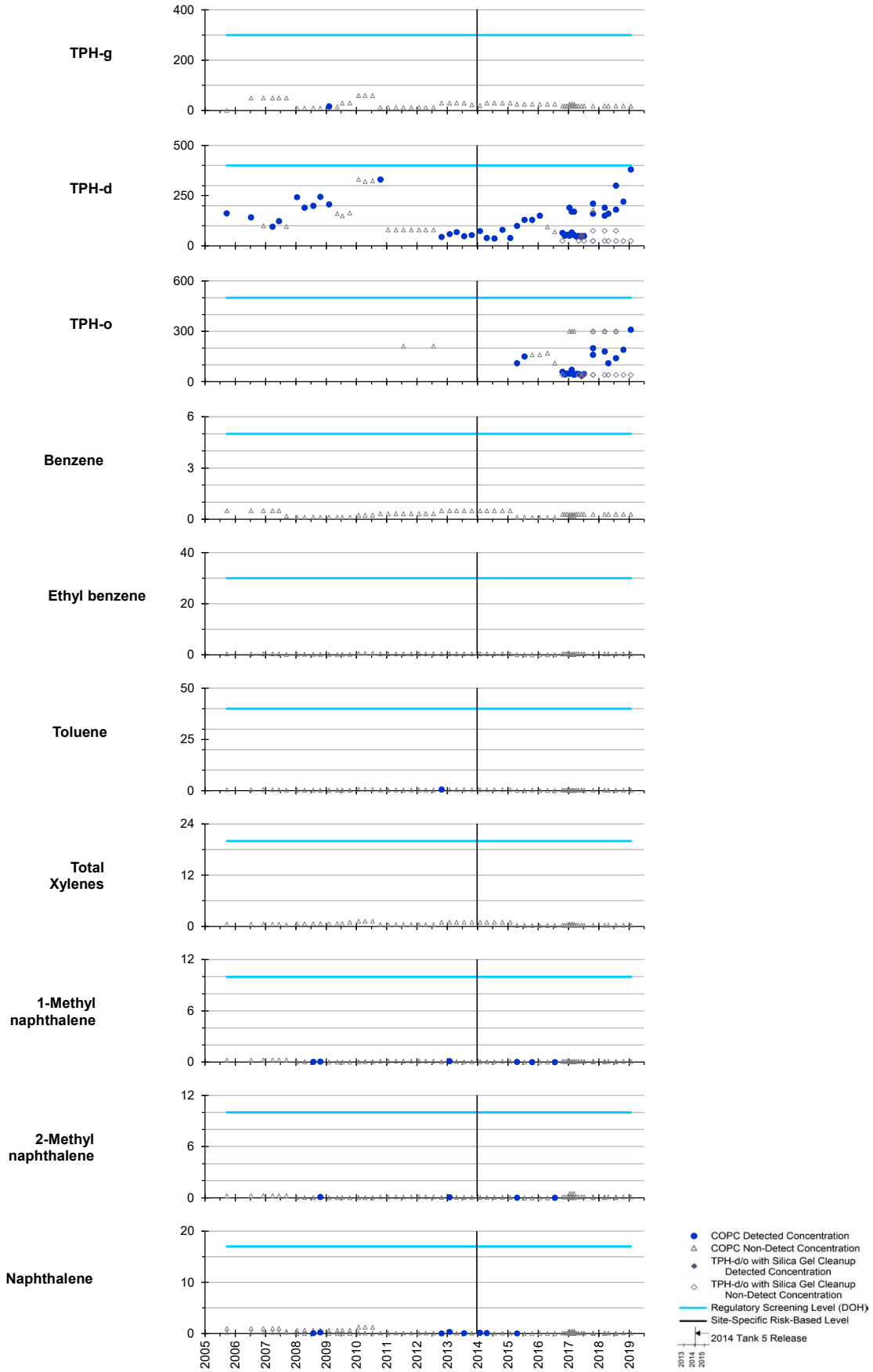

All results in micrograms per liter (µg/L or parts per billion).

EPA Region 9 Laboratory split sampling data from First to Fourth Quarters 2017, First Quarter 2018, and Third Quarter 2018 included in the graphs.

RHMW04

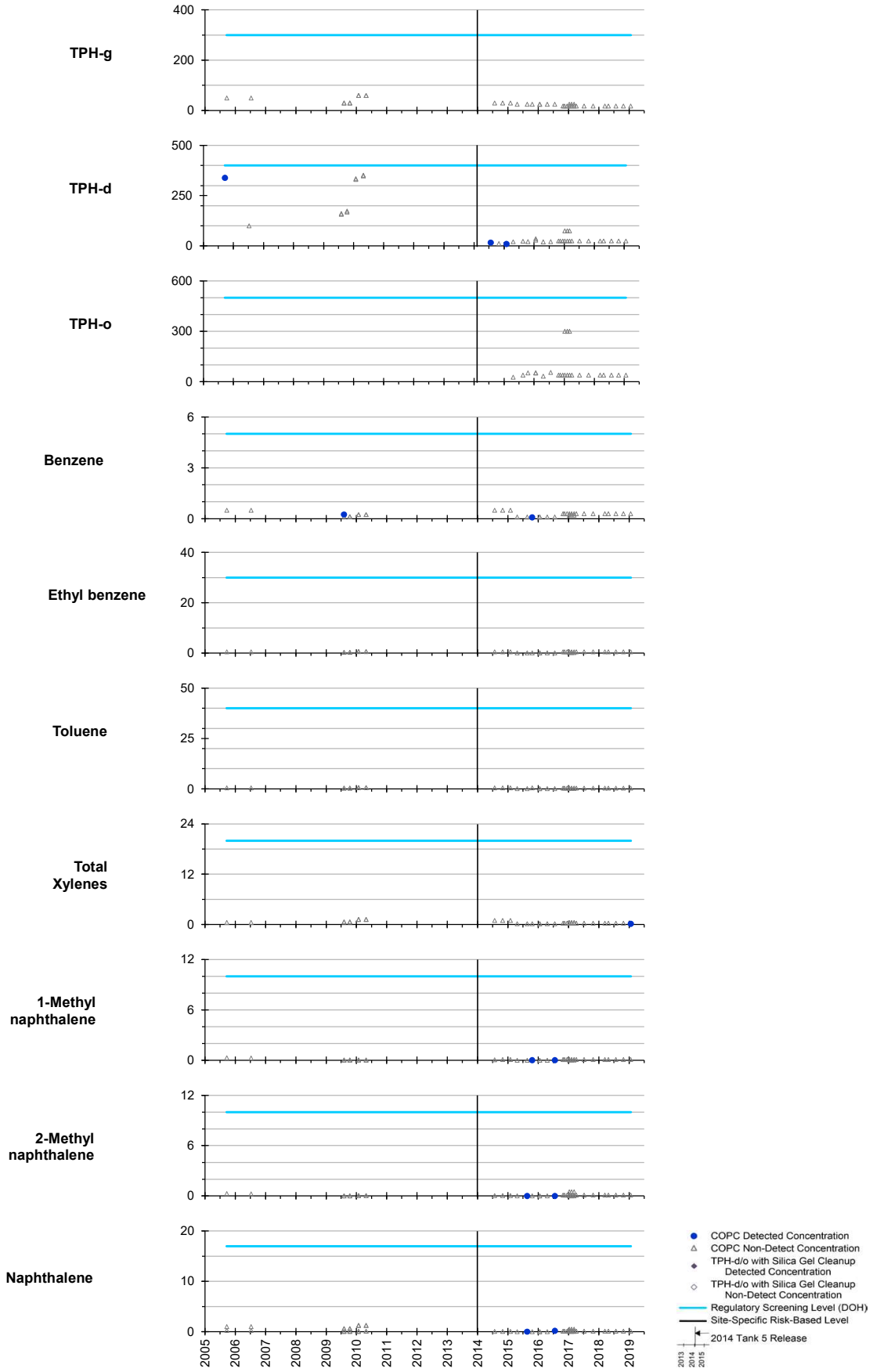

All results in micrograms per liter (µg/L or parts per billion).

EPA Region 9 Laboratory split sampling data from First to Third Quarters 2017 included in the graphs.

RHMW05

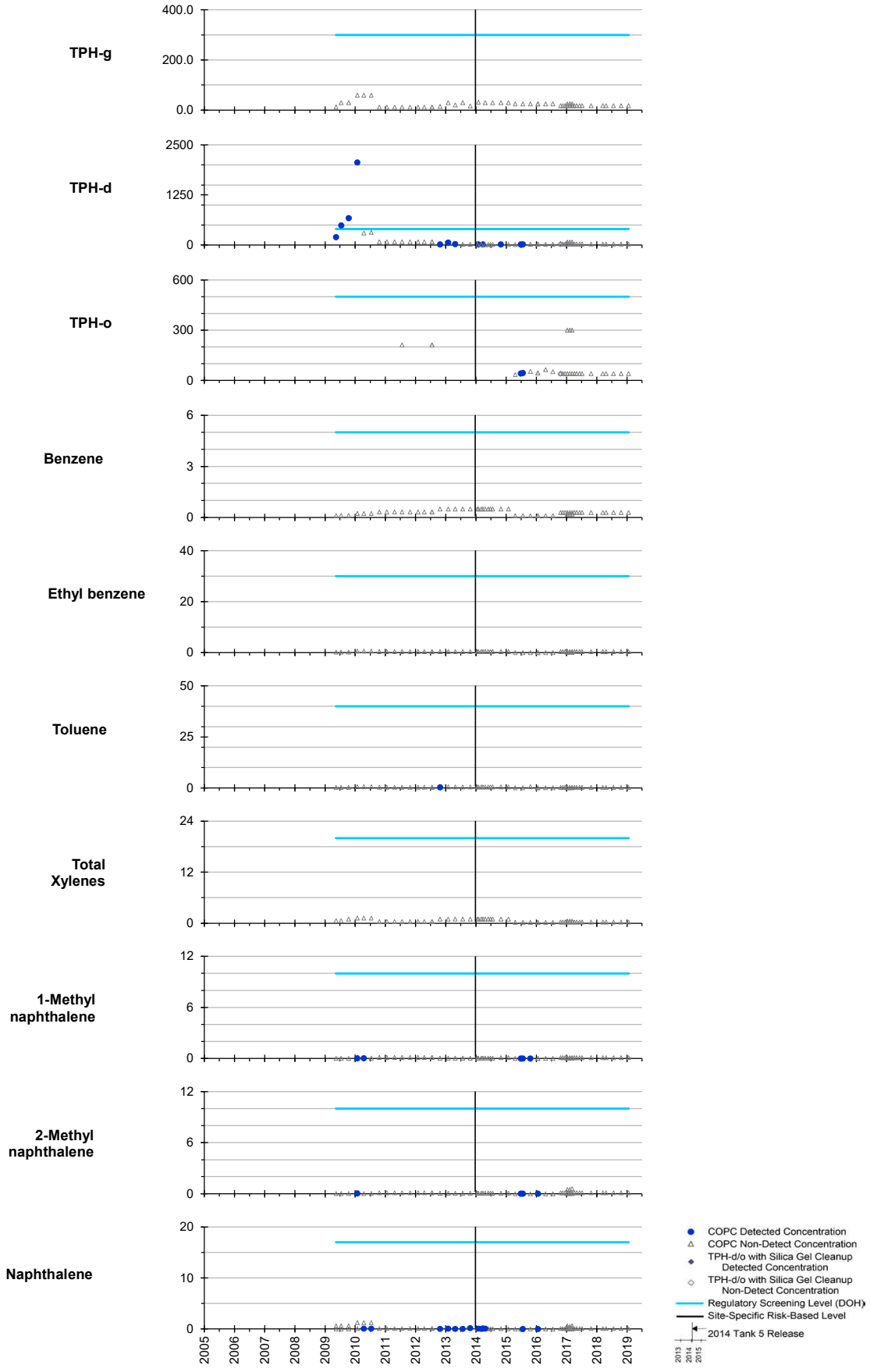

All results in micrograms per liter (µg/L or parts per billion).

EPA Region 9 Laboratory split sampling data from First to Third Quarters 2017 included in the graphs.

RHMW06

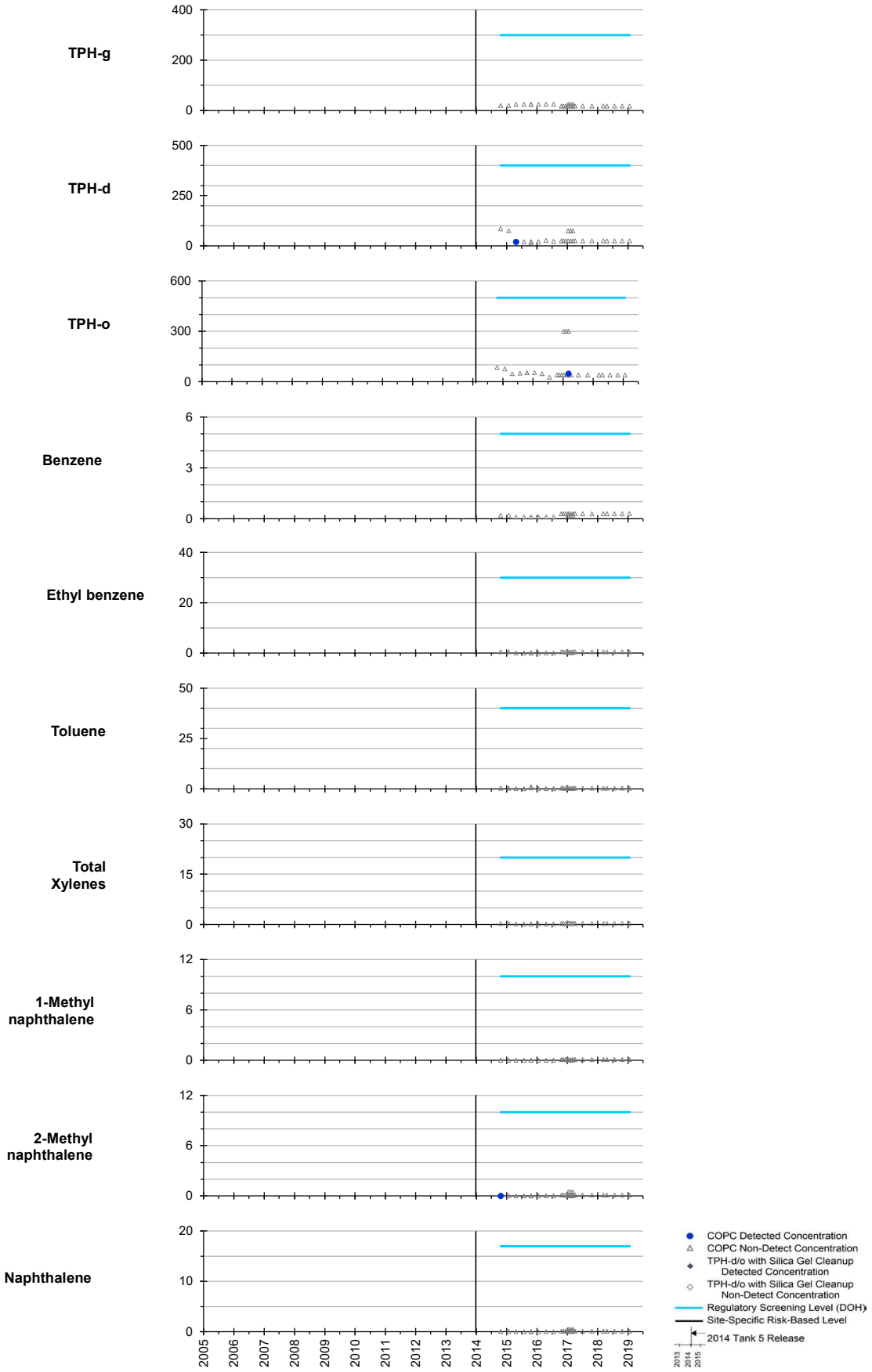

All results in micrograms per liter (µg/L or parts per billion).

EPA Region 9 Laboratory split sampling data from First to Third Quarters 2017 included in the graphs.

RHMW07

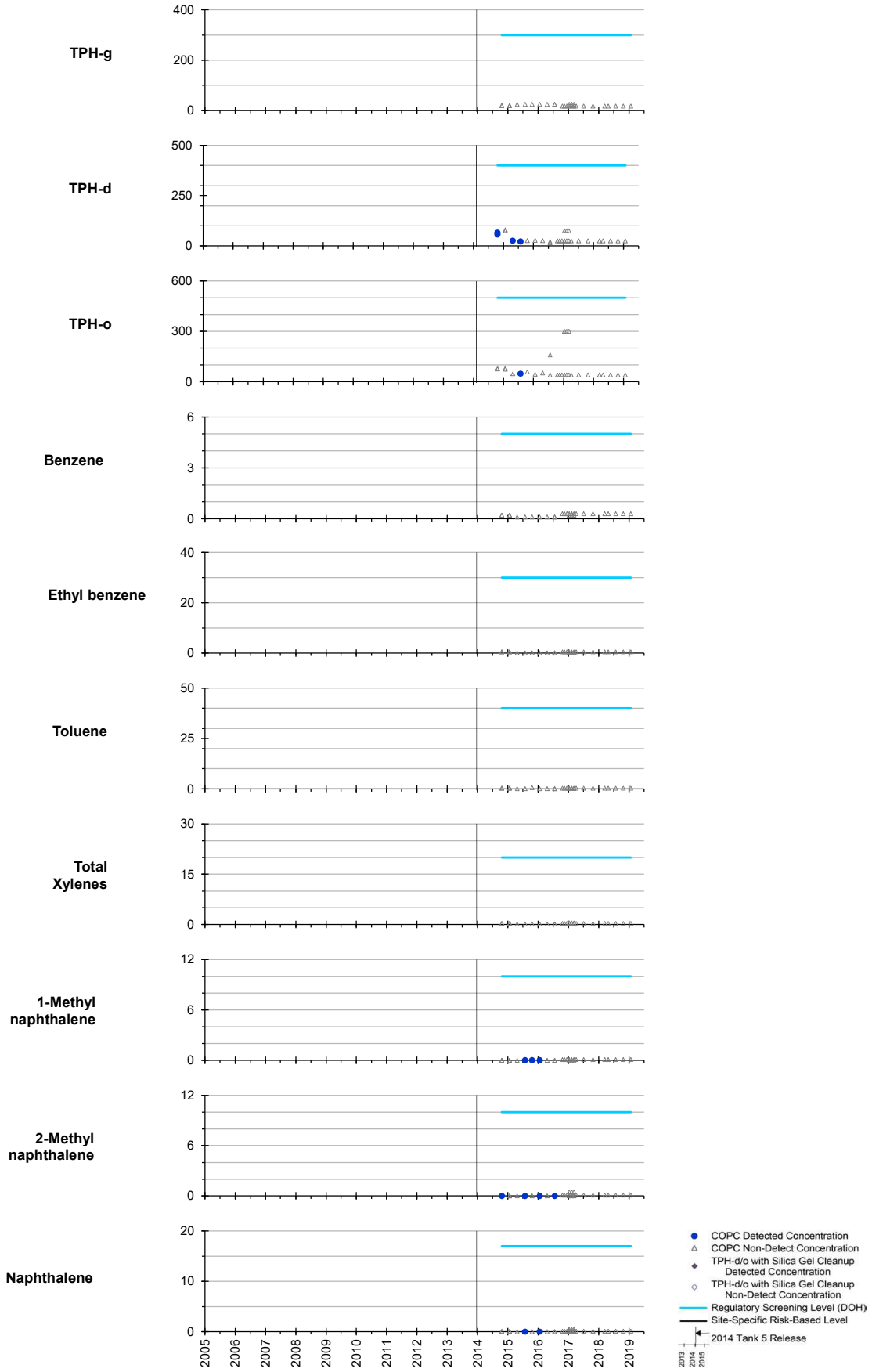

All results in micrograms per liter (µg/L or parts per billion).

EPA Region 9 Laboratory split sampling data from First to Third Quarters 2017 included in the graphs.

RHMW08

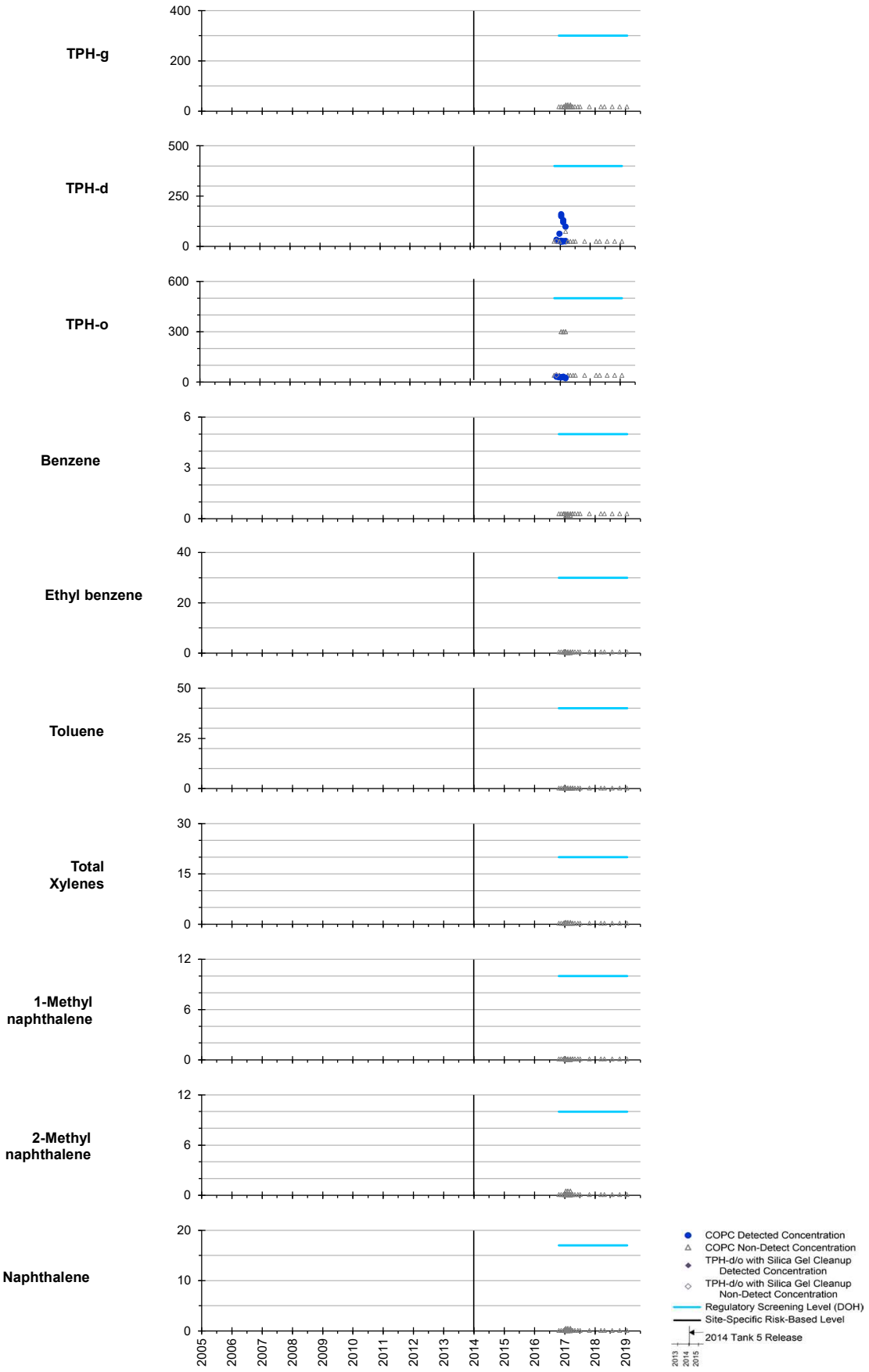

All results in micrograms per liter (µg/L or parts per billion).

EPA Region 9 Laboratory split sampling data from First to Third Quarters 2017 included in the graphs.

RHMW09

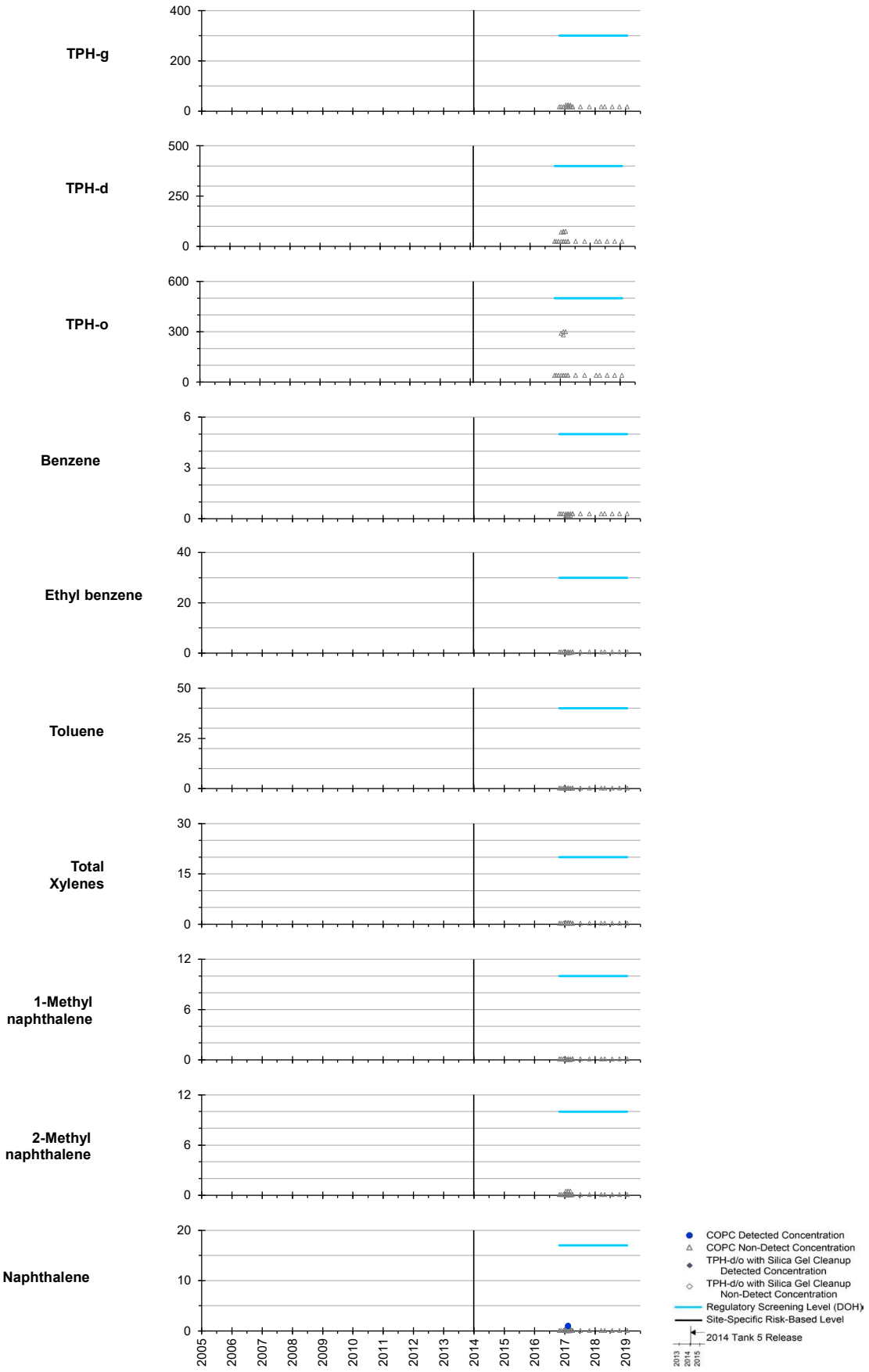

All results in micrograms per liter (µg/L or parts per billion).

EPA Region 9 Laboratory split sampling data from First to Third Quarters 2017 included in the graphs.

RHMW10

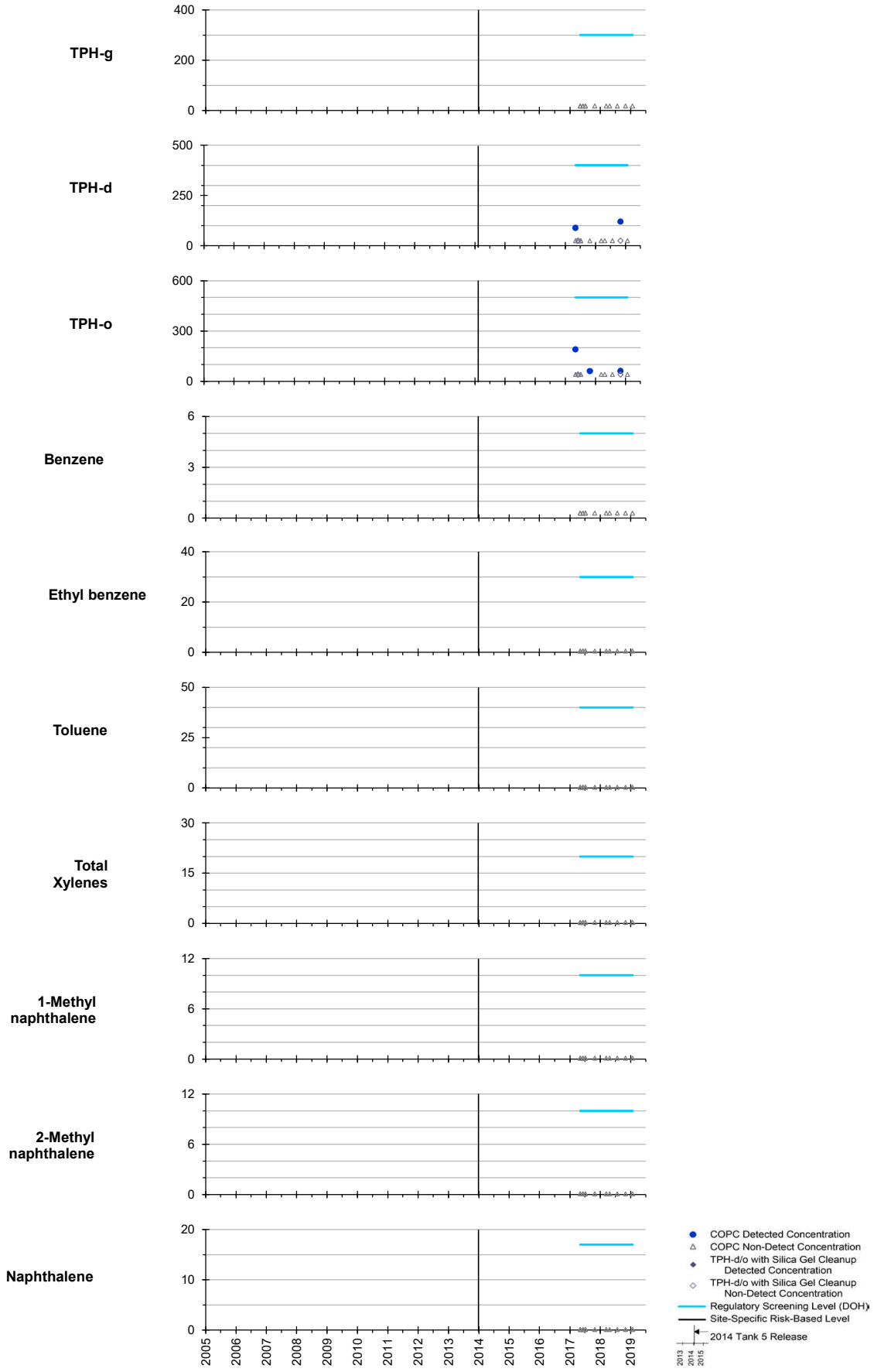

All results in micrograms per liter (µg/L or parts per billion).

RHMW11 Zone 1

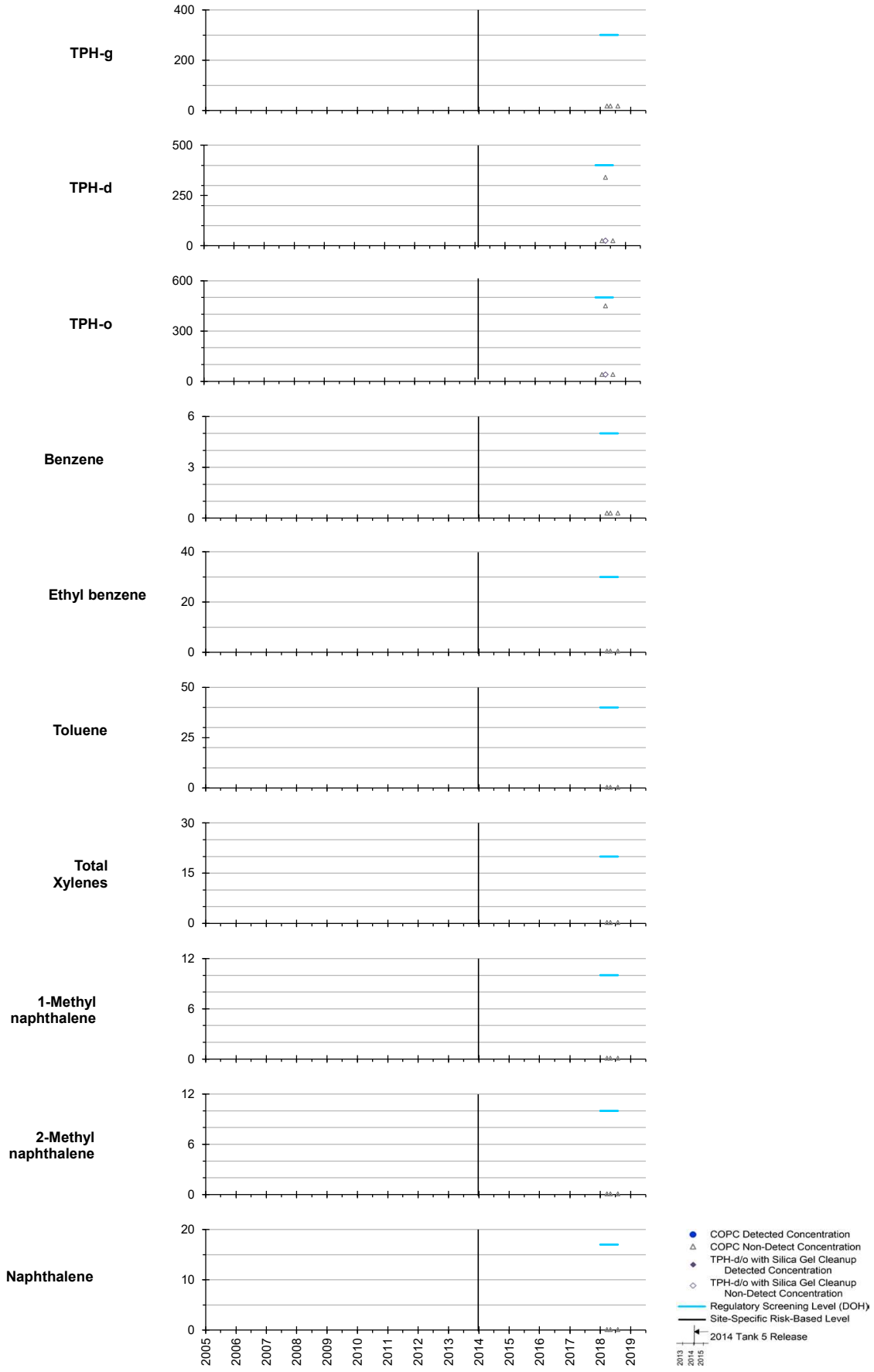

All results in micrograms per liter (µg/L or parts per billion).

RHMW11 Zone 2

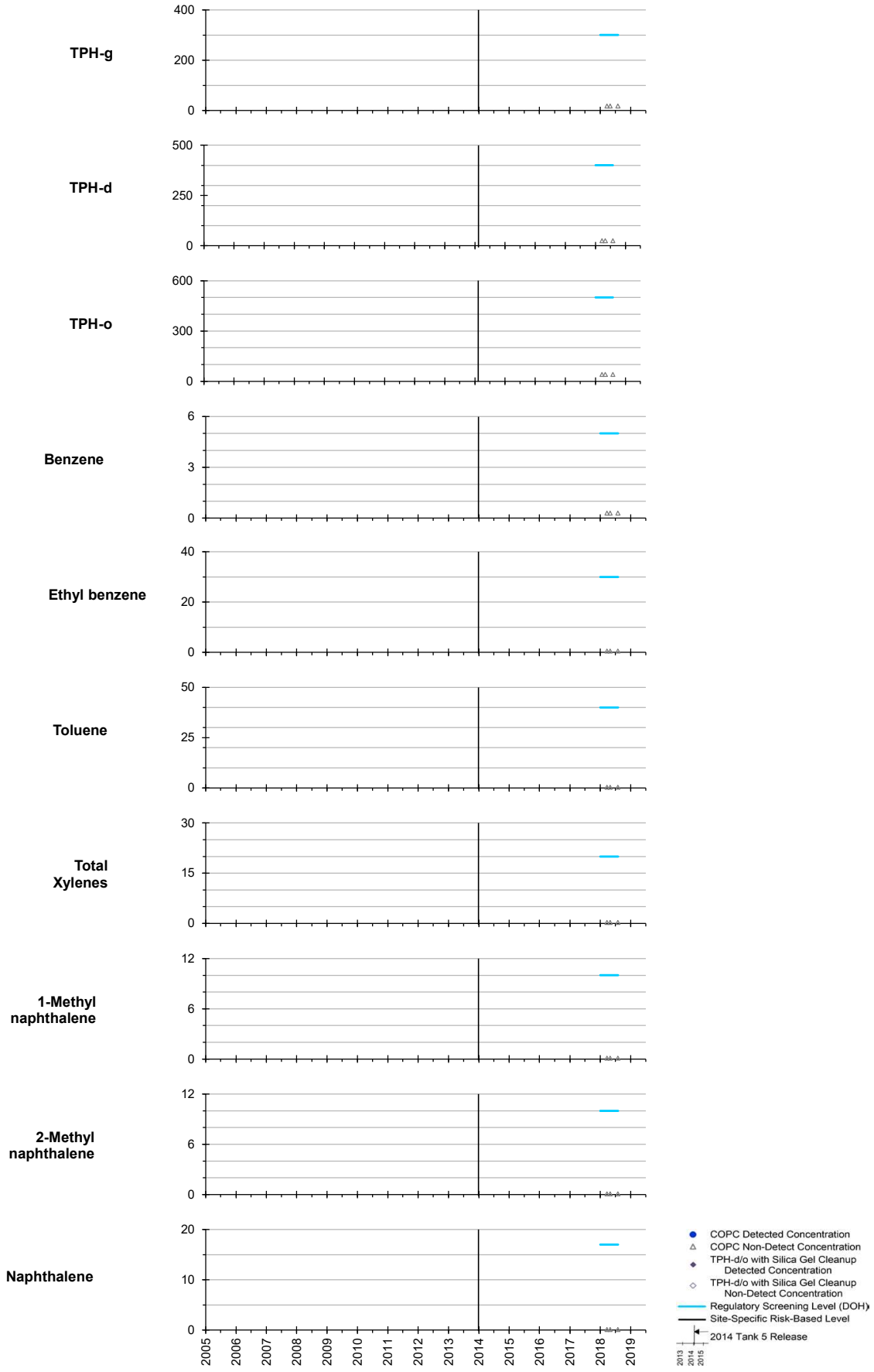

All results in micrograms per liter (µg/L or parts per billion).

RHMW11 Zone 3

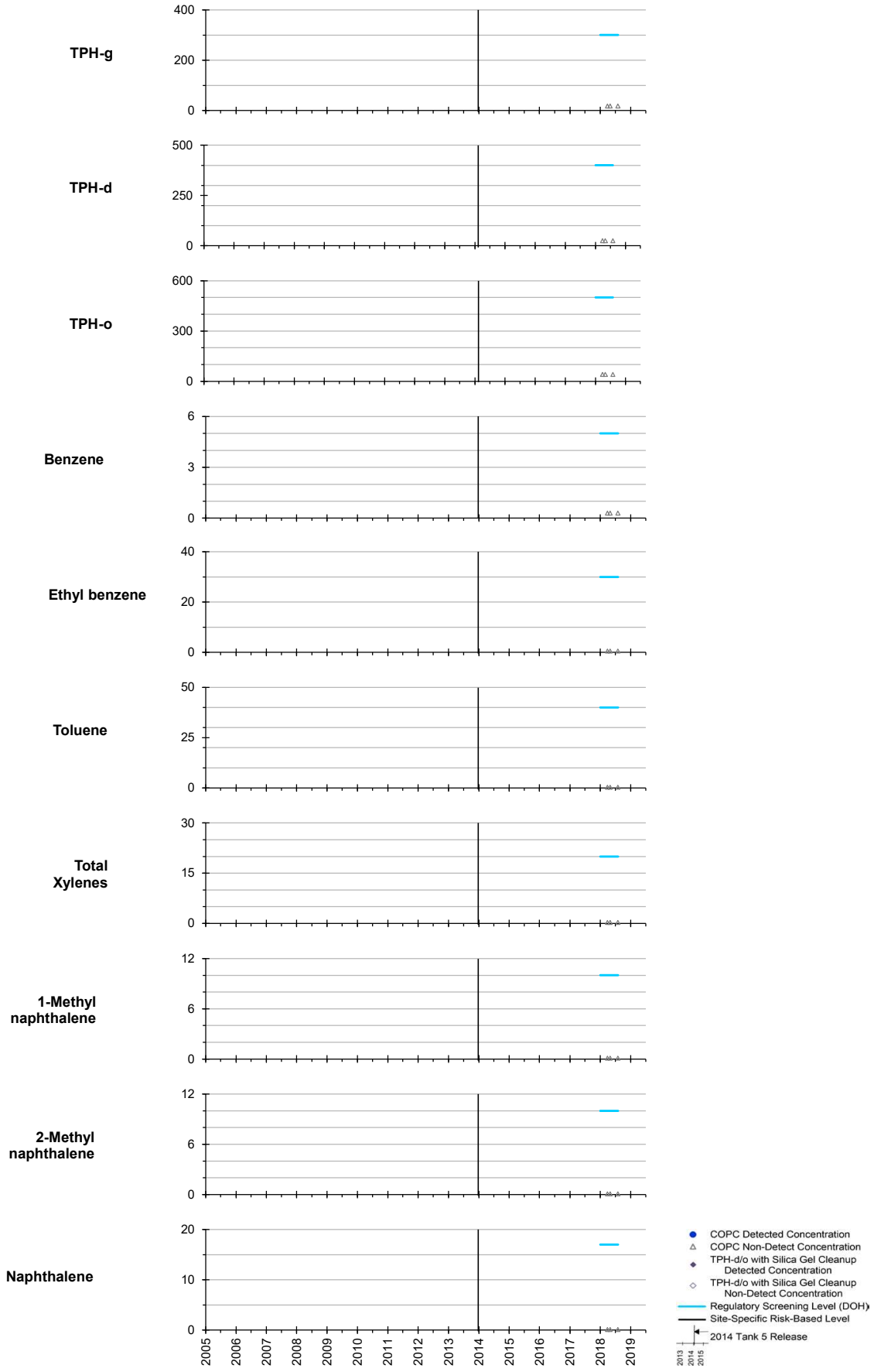

All results in micrograms per liter (µg/L or parts per billion).

RHMW11 Zone 4

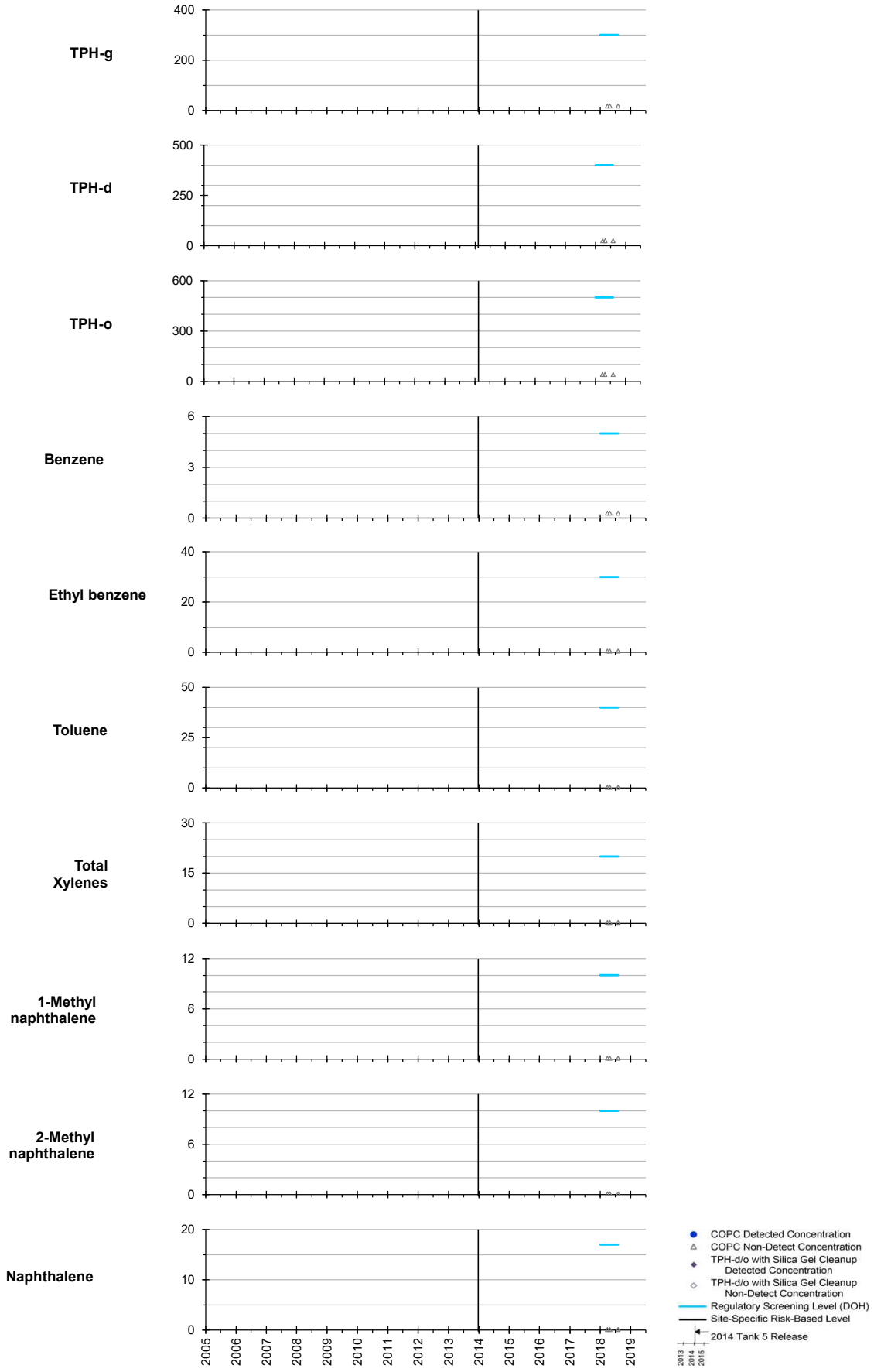

All results in micrograms per liter (µg/L or parts per billion).

RHMW11 Zone 5

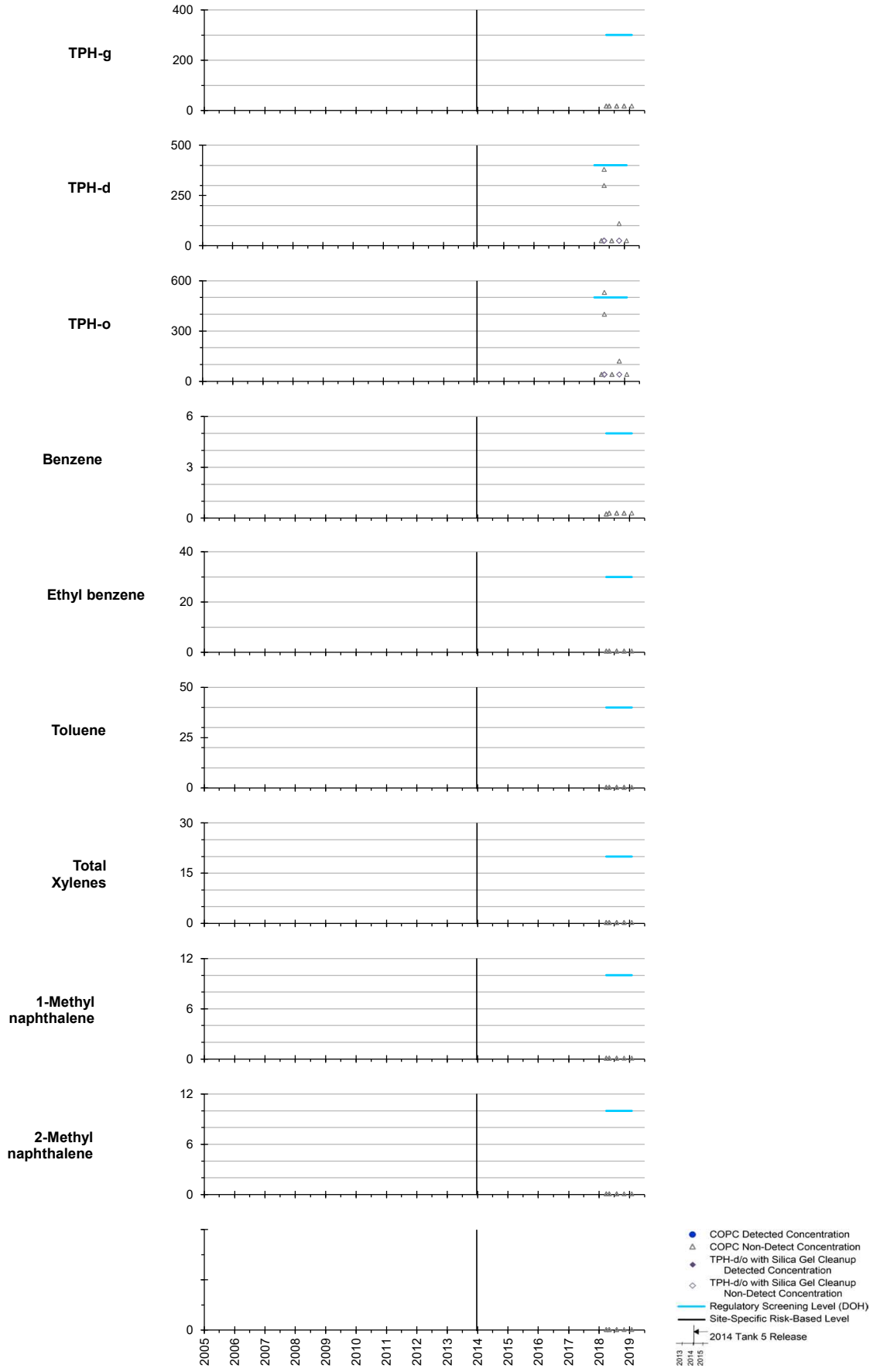

All results in micrograms per liter (µg/L or parts per billion).

HDMW2253-03

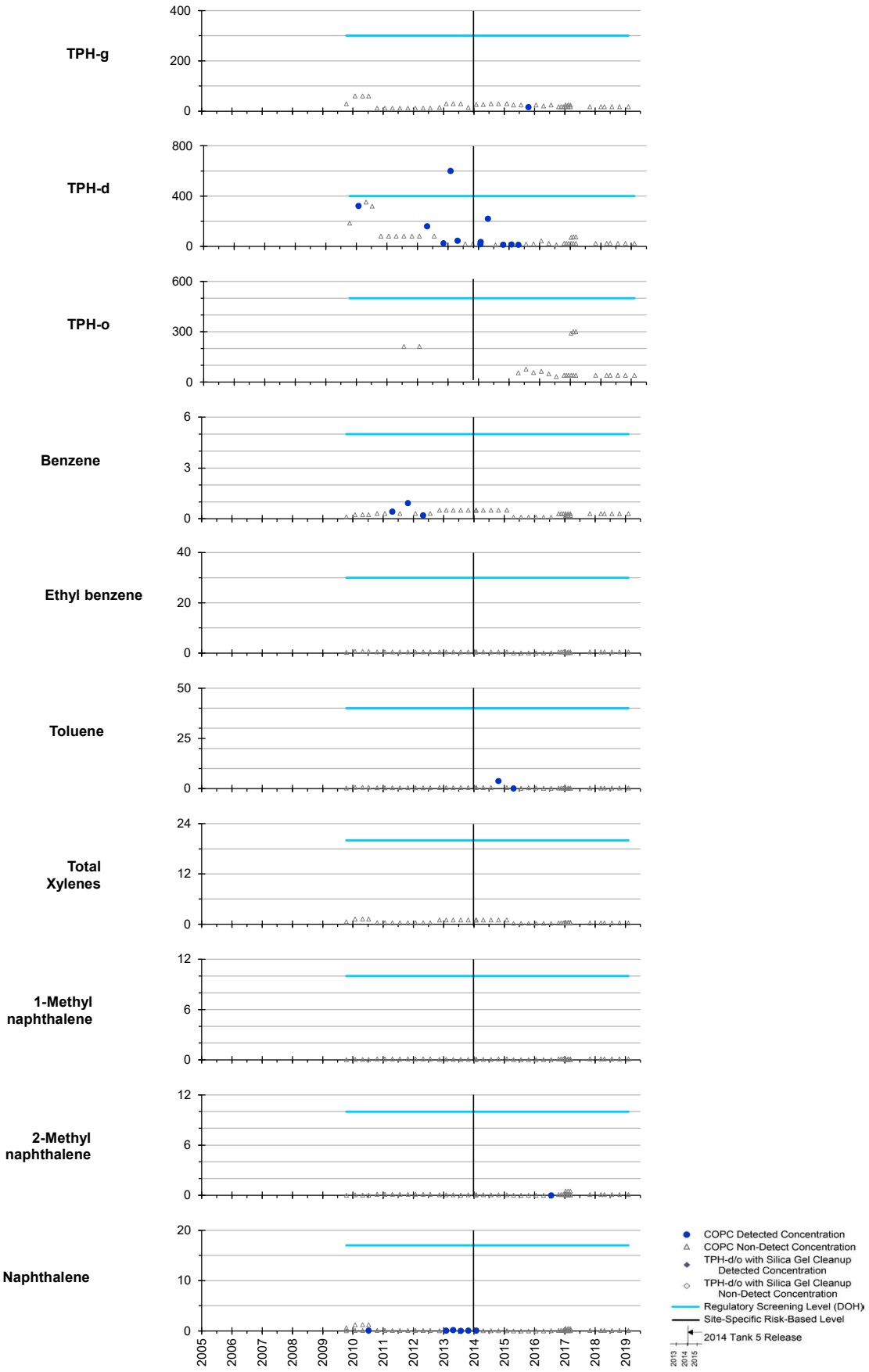

All results in micrograms per liter (µg/L or parts per billion).

EPA Region 9 Laboratory split sampling data from First to Third Quarters 2017 included in the graphs.

OWDFMW01

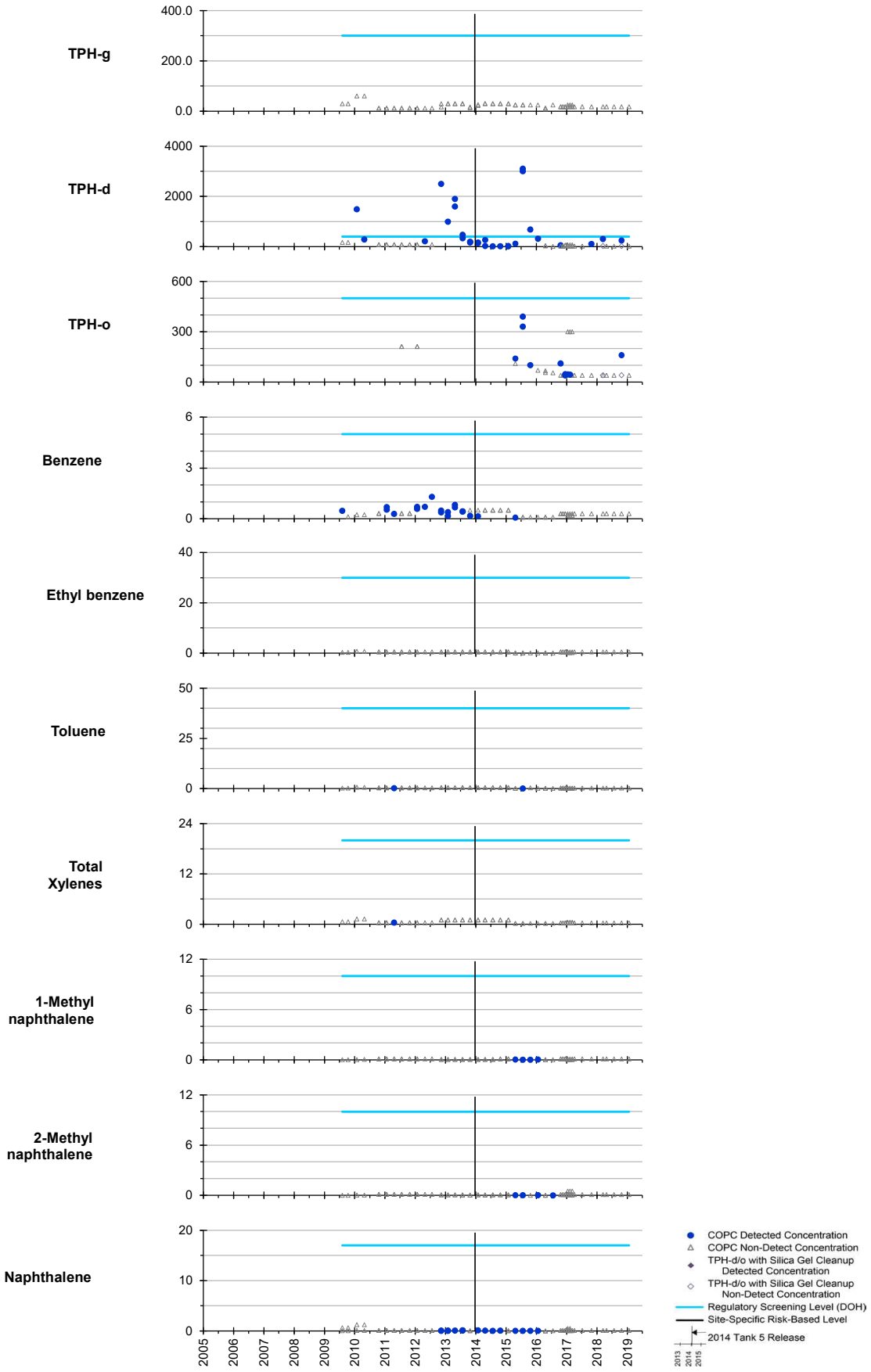

All results in micrograms per liter (µg/L or parts per billion).

EPA Region 9 Laboratory split sampling data from First to Third Quarters 2017 included in the graphs.

Appendix B:
Fate and Transport Analyses

B.1: Thermal NSZD Analysis

B.2: Carbon Trap NSZD Analysis

B.3: Soil Vapor Analysis (2017 Study)

B.4: MNA Primary Lines of Evidence and Rate Calculations

B.5: MNA Secondary Lines of Evidence

B.6: Microcosm Study and Microbial Parameter Analysis

B.7: Forensics and Data Evaluation - Groundwater

B.8: Comprehensive Evaluation of Groundwater Chemistry

This page intentionally left blank

Appendix B.1:
Thermal NSZD Analysis

CONTENTS

Acronyms and Abbreviations iv

1. Introduction 1-1

1.1 Technical Background 1-1
1.2 Study Objectives 1-1
1.3 Selection of Monitoring Wells for NSZD Study 1-1
1.4 Measurement Protocols 1-3
1.4.1 Measurement Protocol 1: Well Air Temperature Measurements 1-3
1.4.2 Measurement Protocol 2: Wall Temperature Measurements 1-4
1.5 Background Location 1-7

2. NAPL Distribution Inferred from Temperature Data 2-1

3. NSZD Rates 3-1

3.1 Calculation Method 1: Background-Corrected Net Temperatures 3-1
3.1.1 Net Temperature Profiles 3-1
3.1.2 NSZD Calculations for Method 1 3-1
3.2 Calculation Method 2: Model-Corrected Thermal Profiles 3-4
3.2.1 NSZD Calculations for Method 2 3-5
3.3 Agreement Between Calculation Method 1 and Calculation Method 2 NSZD Rates 3-7
3.4 Calculation Method 3: Groundwater Temperatures (only Accounts for Downward Heat Flux) 3-7

4. Conclusions 4-1

5. References 5-1

ATTACHMENTS

B.1.1 Thermal Monitoring Data

FIGURES

1-1 Location of Temperature Profile Wells in Relation to Tank Farm 1-2

1-2 Pipe Test-Ball Plug (left) and Inflated Plug Inside Well (right) 1-4

1-3 Design of Wall Temperature Measurements Device (Protective Mesh Around Test Ball and Weight Not Shown) 1-4

1-4 Polyethylene Mesh Netting Used to Secure Thermocouple Tip to Test Ball 1-5

1-5 Comparison of Raw (Uncorrected) Thermal Profiles for Well Air Temperature and Wall Temperature Measurements 1-6

1-6 Raw (Uncorrected) Thermal Profiles for Facility Wells 1-7

2-1 Net (Background-Corrected) Temperature Profiles for Facility Wells (Well Air Temperature Measurements) 2-1

2-2 Conceptualization of Vapor Transport-Related NSZD Processes at a Typical Petroleum Release Site, Where Heat Generation Occurs above NSZD Zone 2-2

2-3 Conceptualization of Vapor Transport-Related NSZD Processes at the Facility, Where Heat Generation Occurs in NSZD Zone 2-3

2-4 Net (Background-Corrected) Temperature Profiles for Facility Wells (Well Air Temperature Measurements) 2-4

2-5 Net (Background-Corrected) Temperature Profiles for Facility Wells (Well Air Temperature Measurements), Highlighting Clinker Zones (Identified from Boring Logs) and LNAPL Intervals 2-6

3-1 Area Encompassed by Tank Farm 3-4

3-2 Calculation Method 2 (Model-Correction) Thermal Profiles for Facility Wells (Well Air Temperature Measurements) 3-5

4-1 Soil Contamination at Tank Farm Observed During 1998–2002 Environmental Investigation 4-3

TABLES

1-1 Summary of Details for Monitoring Wells Used for NSZD Study 1-2

1-2 Average Temperatures in Honolulu, HI 1-3

2-1 Inferred LNAPL-Containing Intervals Indicated by Net (Background-Corrected) Temperature Profiles from Three Facility Monitoring Wells 2-4

3-1 Calculation of Top and Bottom Heat Fluxes for NSZD Using Well Air Temperature Measurements and Calculation Method 1 (Background-Correction) 3-2

3-2 Calculation Method 1(Background-Correction) Conversion from W/m^2 to gal/acre/yr of NSZD 3-2

3-3 Calculation Method 1 (Background-Correction) NSZD Rates for Facility Wells (Well Air Temperature Measurements) 3-3

3-4 Calculation Method 1 (Background-Correction) NSZD Rates for Facility Wells (Average of Well Air Temperature Measurements and Well Wall Temperature Measurements) 3-3

3-5 Calculation of Top and Bottom Heat Fluxes for NSZD Using Well Air Temperature Measurements and Calculation Method 2 (Model-Correction) 3-6

3-6 Calculation Method 2 (Model-Correction) NSZD Rates for Facility Wells (Well Air Temperature Measurements) 3-6

3-7 Calculation Method 2 (Model-Correction) NSZD Rates for Facility Wells (Average of Well Air Temperature and Wall Temperature Measurements) 3-7

3-8 Water Temperatures at RHMW03 and RHMW05 3-8

3-9 Calculation of Mass of Water Flow from RHMW03 to RHMW05 3-9

3-10 Calculation Method 3: Biodegradation Affecting Groundwater Temperature 3-9

3-11 The Bottom Heat Flux NSZD Rate (i.e., Associated with Downward Heat Transfer) for the Three Calculation Methods 3-10

4-1 Summary of Total NSZD Rates (Gallons per Year) from the Tank Farm 4-1

ACRONYMS AND ABBREVIATIONS

btoc	below top of casing
°C	degree Celsius
cal/yr	calories per year
cal/g/°C	calorie per gram per degree Celsius
CSM	conceptual site model
DAWT	directly above the water table
ft	foot/feet
gal	gallon
gal/acre/yr	gallons per acre per year
gal/yr	gallons per year
ITRC	Interstate Technology and Regulatory Council
J	joule
K	Kelvin
kg	kilogram
L	liter
LNAPL	light non-aqueous-phase liquid
m^2	square meter
m^3	cubic meter
MJ	megajoule
msl	mean sea level
NSZD	natural source-zone depletion
W	watt
yr	year

1. Introduction

This subappendix is summarized in Section 7.3.1.4 of the Conceptual Site Model (CSM) main document.

1.1 TECHNICAL BACKGROUND

NSZD is the active process whereby light non-aqueous-phase liquid (LNAPL) is degraded in the subsurface by biodegradation and other naturally occurring processes. For this document, LNAPL consists of petroleum hydrocarbons in the form of various fuels. NSZD rates have been measured at many LNAPL sites and can be quantified by measuring the magnitude and distribution of subsurface temperatures and then calculating the net heat flux being generated by biodegradation processes.

Natural source-zone depletion (NSZD) is a well-accepted technology described by hundreds of technical papers, guidance documents, and patents. The Interstate Technology and Regulatory Council (ITRC), a state environmental regulator-directed industry group, issued the first NSZD guidance in 2009 and updated this to represent new technologies, including thermal NSZD in 2018. Key publications summarizing this technology include *Overview of Natural Source Zone Depletion: Processes, Controlling Factors, and Composition Change* (Garg et al. 2017) and *Light Non-Aqueous Phase Liquid (LNAPL) Site Management: LCSM Evolution, Decision Process, and Remedial Technologies, Appendix B—Natural Source Zone Depletion (NSZD)*(ITRC 2018).

1.2 STUDY OBJECTIVES

In this study, the objectives were to determine if temperature profiles in monitoring wells in the Red Hill tank farm area can be used to:

1. Assess the vertical distribution of LNAPL based on depths with elevated temperatures.
2. Quantify the rate of NSZD based on temperature profile measurements.

Temperature profiles were collected in five existing monitoring wells at the site: RHMW01, RHMW02, RHMW03, RHMW04, and RHMW05.

1.3 SELECTION OF MONITORING WELLS FOR NSZD STUDY

The temperature profiles were measured at the Red Hill Bulk Fuel Storage Facility ("the Facility") from the surface to the bottom of the well. Data for existing monitoring wells were reviewed to select several suitable wells with dissolved-phase constituents (RHMW01, RHMW02, and RHMW03, all installed inside the lower tunnel), as well as two possible background wells: RHMW04 located outside the tunnel and RHMW05 located inside the lower tunnel. Although RHMW04 showed no evidence of LNAPL impact, it was clear that the profile for RHMW04 was very different from the profiles for wells inside the lower tunnel and, as a result, RHMW04 was not suitable for use as a background well (e.g., RHMW04 was a surface well that was much deeper than any of the wells drilled from the tunnel and had very different thermal characteristics from the tunnel wells). It is highly unlikely that the different thermal characteristics at RHMW04 are related to biodegradation of contaminants because the available data show no indication of LNAPL or groundwater contamination at RHMW04 that could affect the temperature profile. Rather, the different temperature profile at RHMW04 is attributable to different geologic materials, geothermal heat flow, and greater depth of RHMW04 compared to conditions beneath the tank farm. Recent thermal profiles measured in monitoring wells in April 2019 outside the tank farm area may provide additional insights and are currently under evaluation. The raw

temperature data from RHMW04 are presented in Attachment B.1.1 along with the raw data for the other wells; however, RHMW04 is not discussed further in this subappendix.

Well construction details, measured groundwater levels, and measured borehole depths are summarized in Table 1-1, as provided in the *Existing Data Summary and Evaluation Report for Groundwater Flow and Contaminant Fate and Transport Modeling, Red Hill Bulk Fuel Storage Facility* (DON 2017) dated March 5, 2017 and measured in the field. The locations of these wells are shown on Figure 1-1. RHMW05 was chosen as the background well because it is the furthest from the tank farm of all the wells and therefore is likely to have no impact from LNAPL in the unsaturated zone.

Table 1-1: Summary of Details for Monitoring Wells Used for NSZD Study

Well	Lower Tunnel Floor Surface (ft msl)	Top of Casing (ft msl)	Groundwater Surface as of March 5, 2017 (ft btoc)	Groundwater Surface as of March 5, 2017 (ft msl)	Borehole Depth (ft btoc)	Borehole Depth (ft msl)	Ambient Air Temperature at Time of Measurement (October 2017) (°C)
RHMW01	101.94	102.0	83.7	18.3	100.00	2.0	26.6
RHMW02	105.25	104.6	86.4	18.2	102.85	1.75	26.4
RHMW03	121.62	120.9	102.6	18.3	117.28	3.62	26.9
RHMW05 (Background)	101.78	101.3	83.0	18.3	124.22	-22.92	26.8

°C degree Celsius
btoc below top of casing
ft foot/feet
msl mean sea level

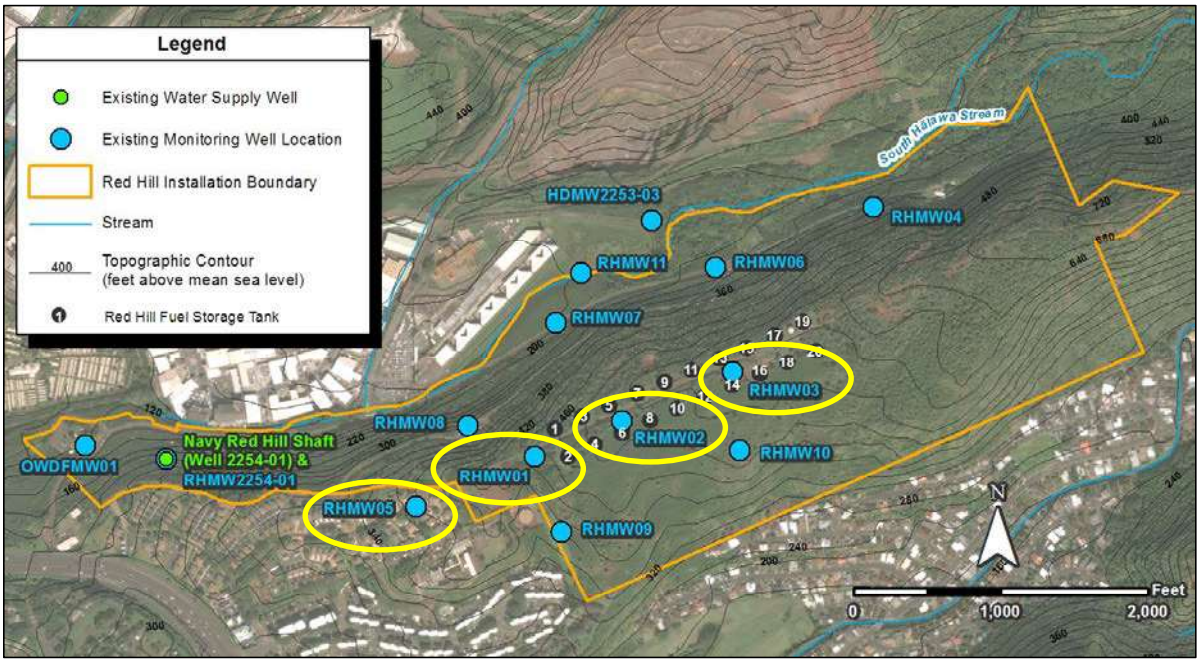

Figure 1-1: Location of Temperature Profile Wells in Relation to Tank Farm

The ambient temperatures inside the tunnels at the time of measurement were fairly similar to typical temperatures in Honolulu (Table 1-2). This is likely because the air in the tunnels is in relative equilibrium with the ambient air because of tunnel ventilation.

Table 1-2: Average Temperatures in Honolulu, HI

Month	Average Temperature (°C)	
	Typical Year (Multi-Year Average)	2017
January	22.9	23.1
February	22.8	23.2
March	23.6	24.6
April	24.5	25.4
May	25.4	25.8
June	26.8	26.7
July	27.3	27.6
August	27.7	27.7
September	27.5	27.6
October	26.7	26.7
November	25.3	—
December	23.8	—
Overall	25.4	—

Source: (U.S. Climate Data 2018)
— no data

1.4 MEASUREMENT PROTOCOLS

Temperature measurements were obtained using high accuracy Type-T thermocouples, calibrated on July 20, 2017. Both Well Air Temperature and Wall Temperature Measurements were collected because of concern that the temperature of the well air might differ from the temperature of the well wall and the subsurface due to the complicated setting at the site. For example, due to temperature variations within the well air column, either circulation or stratification of the air was considered possible. Also, it was hypothesized that open space in the wells might be subject to air flow from open screen intervals near the water table to the lower pressure tunnel environment, which might distort the formation of a temperature signal in the thermocouple. Therefore, wells were capped for several days before Well Air Temperature Measurements were collected and Wall Temperature Measurements were also collected to reduce the impacts of this confounding factor if it occurred. As explained below, however, little to no difference was seen between the thermal profiles for both protocols.

1.4.1 Measurement Protocol 1: Well Air Temperature Measurements

In this configuration, the thermocouple was fed through a hole in a well plug, a weight was attached to a line attached to the end of the thermocouple, and the assembly was fed down the well. The weight ensured the thermocouple wire stayed taut as temperature measurements were taken at 5-ft intervals down to the water table, then at the top, middle, and bottom of the water column. The weight and thermocouple were decontaminated with Alconox and water between each well, and a new line was used for each well. This protocol had the advantage of simplicity but could potentially be impacted by circulation or stratification or air flowing up the well.

1.4.2 Measurement Protocol 2: Wall Temperature Measurements

In the Wall Temperature Measurements configuration, the thermocouple was attached to a pipe test ball plug (Figure 1-2 and Figure 1-3), which was fed down the well and inflated using a bicycle tire pump at the surface up to a specific inflation pressure. A protective mesh netting was placed around the test ball and thermocouple tip to hold the tip in place next to the test ball (Figure 1-4). The inflated test ball ensured that the measurement tip of the thermocouple was pressed against the well casing, to potentially increase the accuracy of subsurface temperature readings.

Figure 1-2: Pipe Test-Ball Plug (left) and Inflated Plug Inside Well (right)

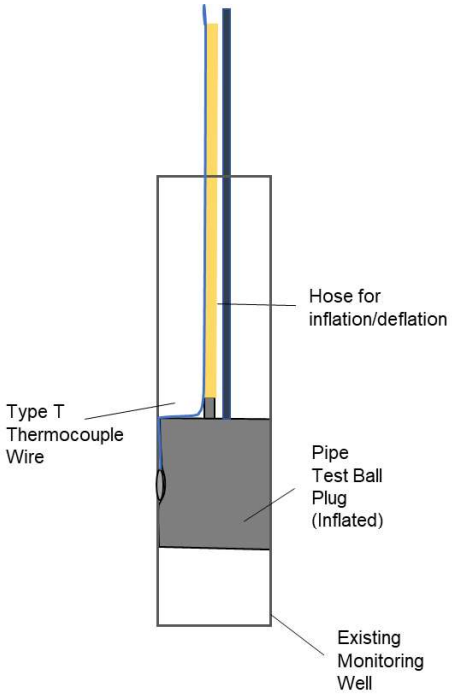

Figure 1-3: Design of Wall Temperature Measurements Device (Protective Mesh Around Test Ball and Weight Not Shown)

Figure 1-4: Polyethylene Mesh Netting Used to Secure Thermocouple Tip to Test Ball

As the thermocouple, inflatable plug, and inflation/deflation hose were lowered from ground surface into the monitoring well, the assembly remained straight using a weight attached to the end of the downhole assembly.

Similar to the Well Air Temperature Measurements, Wall Temperature Measurements were taken at 5-ft intervals. Measurements were taken down to no less than 5 ft above the water table. Note that the assembly for Wall Temperature Measurements was not lowered into the water table in the wells to avoid cross contamination from the rubber material used in the test ball.

After evaluating the temperature readings for both protocols, however, little to no difference was seen between the temperature profiles from Well Air Temperature and Wall Temperature Measurements (Figure 1-5). Therefore, both measurement protocols are deemed valid for performing NSZD calculations.

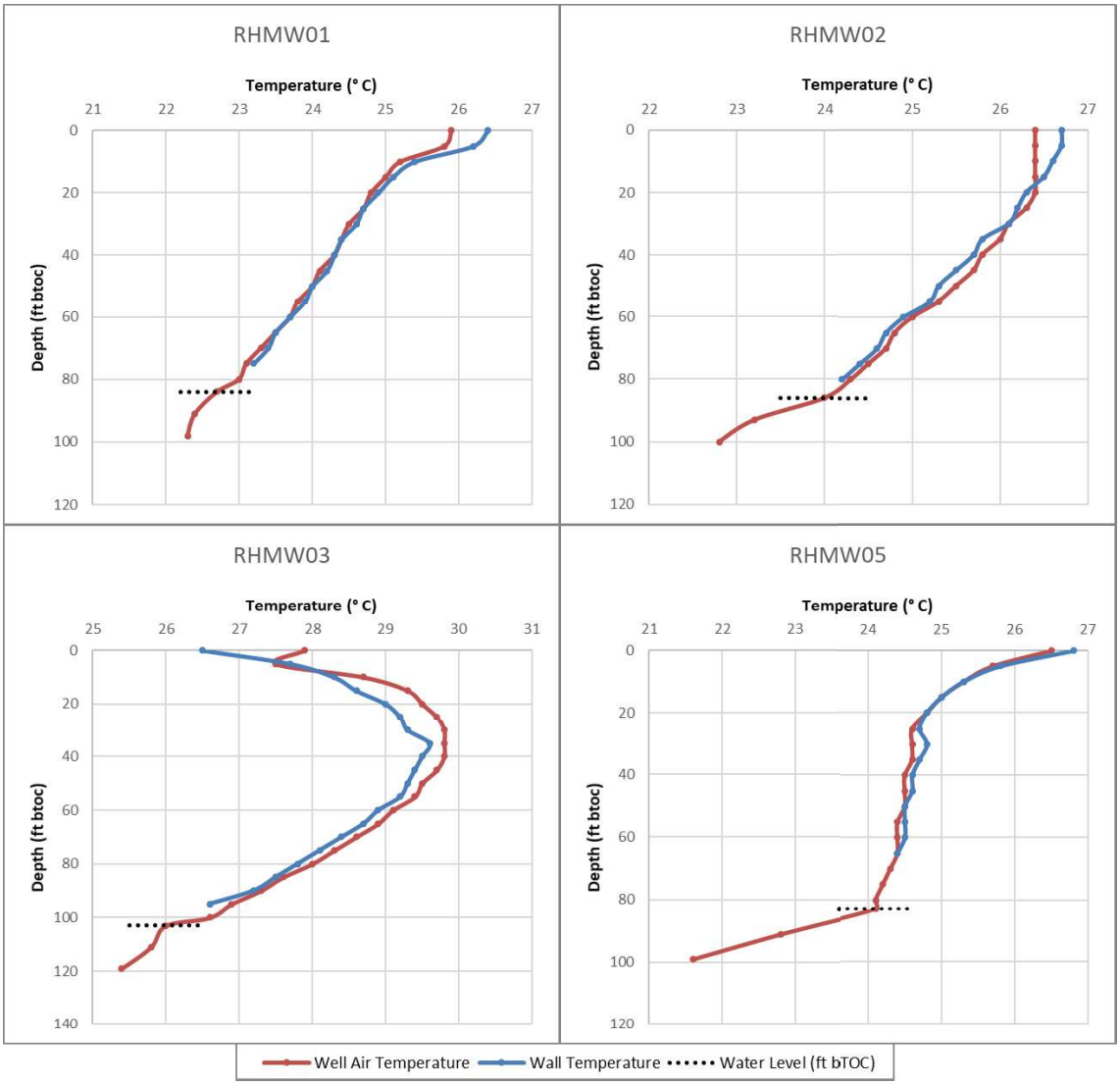

Figure 1-5: Comparison of Raw (Uncorrected) Thermal Profiles for Well Air Temperature and Wall Temperature Measurements

The thermal profiles in RHMW01, RHMW02, and RHMW03 showed a temperature response indicative of heat generation within a defined elevation interval associated LNAPL biodegradation. The calculations of NSZD rates were performed using both the Well Air Temperature and Wall Temperature Measurements, and then those rates were averaged to arrive at final NSZD rates. Section 1.4 provides a detailed discussion on the measurement protocols with similar outcomes. Consequently, to present a more concise evaluation, calculations (Sections 3.1.2 and 3.2.1) are shown using only the Well Air Temperature Measurements. The data for all the wells using both protocols are shown on Figure 1-6 and in Attachment B.1.1.

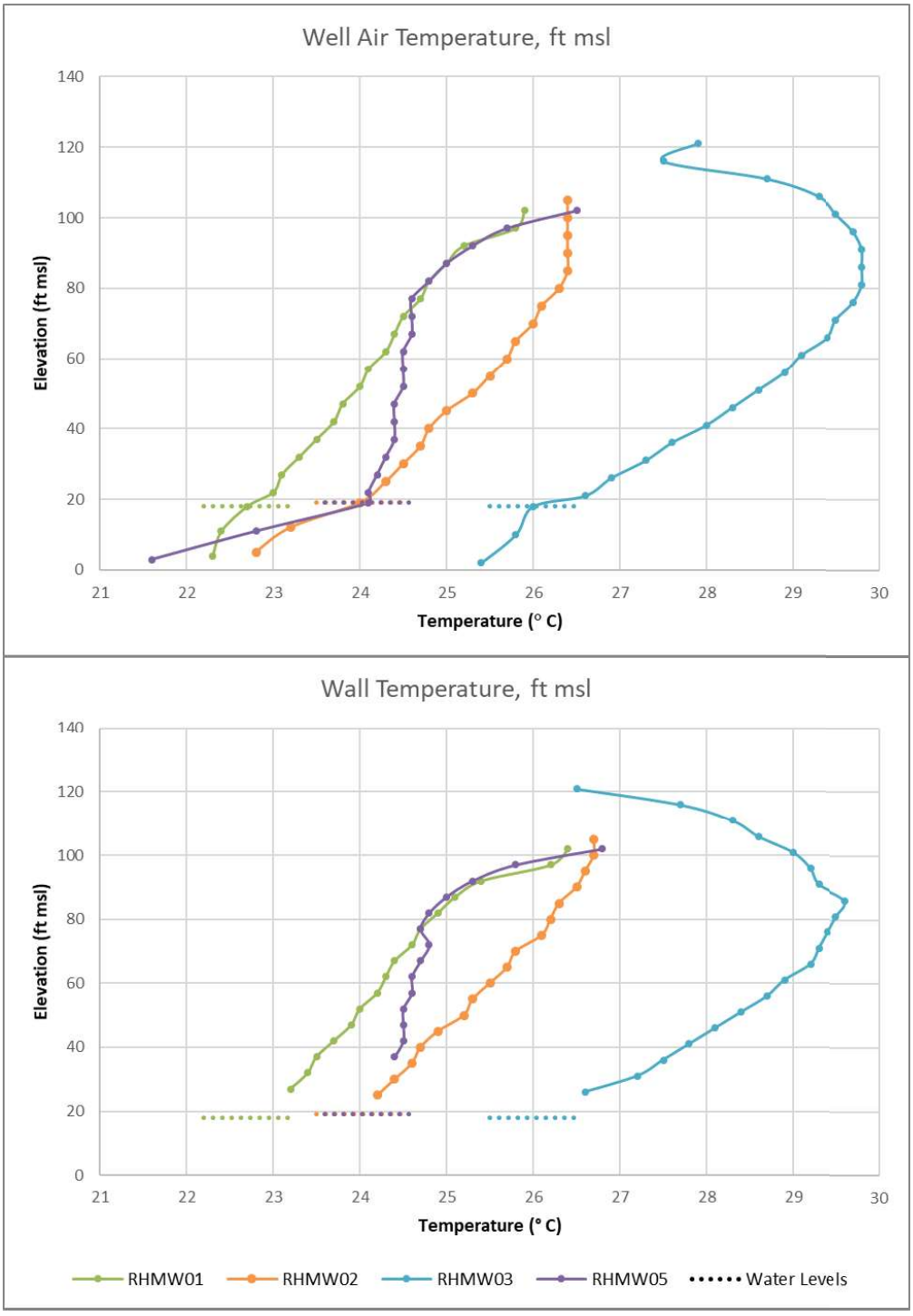

1 **Figure 1-6: Raw (Uncorrected) Thermal Profiles for Facility Wells**

2 1.5 BACKGROUND LOCATION

3 RHMW05 was chosen as the background well location for net temperature calculations for multiple
4 reasons: 1) it showed the least evidence of heat generation associated with biodegradation, 2) there is

no indication of LNAPL in the groundwater sample data at the well, and 3) it is the furthest from the tank farm of all the wells installed in the lower tunnel. This can easily be seen in the graph of temperature vs. depth for RHMW05 on Figure 1-5. The upper approximately 20 ft below top of casing (btoc) at RHMW05 show decreasing temperatures with depth consistent with the expected late summer/fall season shallow temperature profile. However, from approximately 20 ft btoc down to the water table, the ground temperature is fairly constant. This indicates that no heat generation is occurring within this interval, and thus no NSZD is occurring. The sharp decrease in temperature that is seen at the bottom of the graph (below 83 ft btoc) occurs once the thermocouple entered the groundwater and shows the temperature decrease that occurs within the shallow aquifer.

2. NAPL Distribution Inferred from Temperature Data

The temperature profiles were used to assess where the LNAPL is in the subsurface near each of the temperature profile monitoring wells, which correspond with previously observed LNAPL distributions, as discussed near the end of this section. This was done by looking at the net (background-corrected) temperature profiles to remove the background temperature seasonal signals while preserving the temperature signal associated with LNAPL biodegradation. Net temperatures are the difference between the raw temperature recorded at each depth for a well minus the raw temperature calculated at the same depth for the background well (RHMW05), which is expected to show no effect of LNAPL in the unsaturated zone and no groundwater contamination. These net temperature profiles are shown on Figure 2-1. In the background-corrected temperature profile, the peak temperature occurs within the LNAPL biodegradation zone. The temperature gradients (i.e., change in temperature with depth) above and below this peak are used to quantify the magnitude of LNAPL biodegradation.

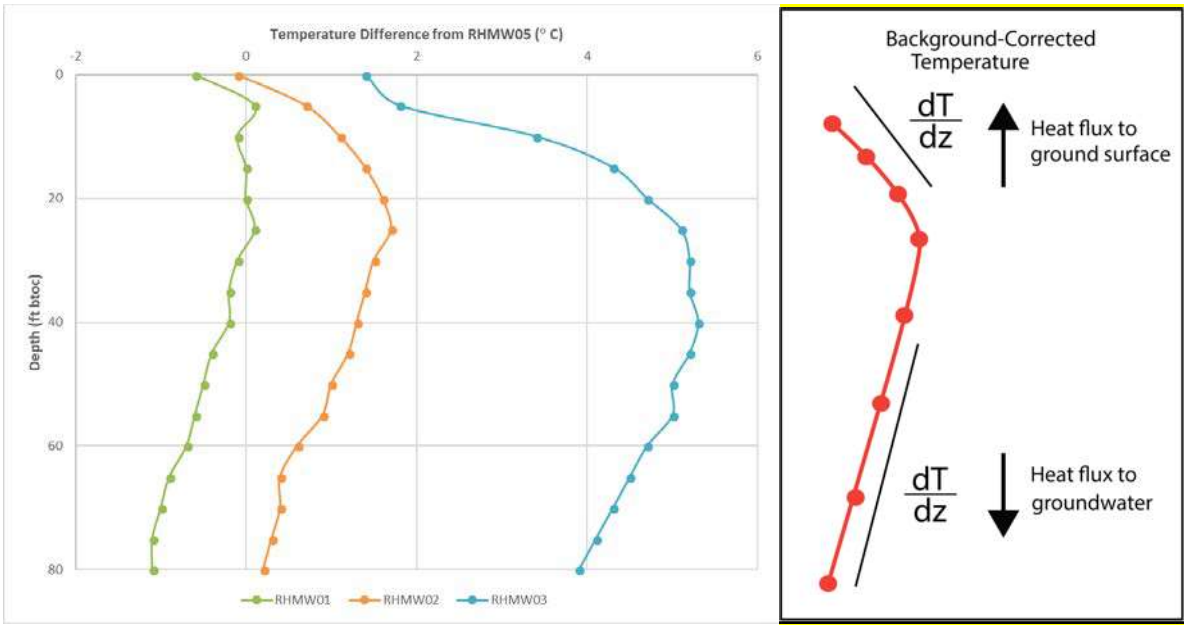

Notes:
1. The net temperature profile for RHMW05 is not shown because it is the background well (i.e., temperature difference equals zero).
2. Net (background-corrected) temperature profiles are shown for temperature data from the top of casing to 80 ft btoc because that was the deepest measurement taken for RHMW05 above the water table.
3. The net (background-corrected) temperature at 0 ft btoc is typically set to be 0°C for the purposes of NSZD calculations. The net (background-corrected) temperature profiles shown on Figure 2-1 do not reflect this procedure; however, this will be assumed going forward.
4. Depths to water for the wells shown are as follows: RHMW01: 83.7 ft btoc; RHMW02: 86.4 ft btoc; RHMW03: 102.6 ft btoc.

Figure 2-1: Net (Background-Corrected) Temperature Profiles for Facility Wells (Well Air Temperature Measurements)

Using the net (background-corrected) temperature data, the interval of biological heat generation at each well location was determined. Within the interval of heat generation, the vertical (upwards or downwards) heat flux is increasing. This is reflected in the net (background-corrected) temperature profile through an increasing negative slope (for upward heat flux) or an increasing positive slope (for downward heat flux). Outside of the heat generation interval, the heat flux is relatively constant

resulting in a relatively constant slope in the net (background-corrected) temperature vs. elevation profile.

At many NSZD sites, anaerobic LNAPL biodegradation at or near the water table produces methane that diffuses toward the surface. This methane, in turn, is biodegraded within the unsaturated zone when it mixes with downward diffusing oxygen from the ground surface. At these sites, the bulk of the heat generation occurs in the methane degradation zone vertically removed from the LNAPL-impacted zone (Figure 2-2).

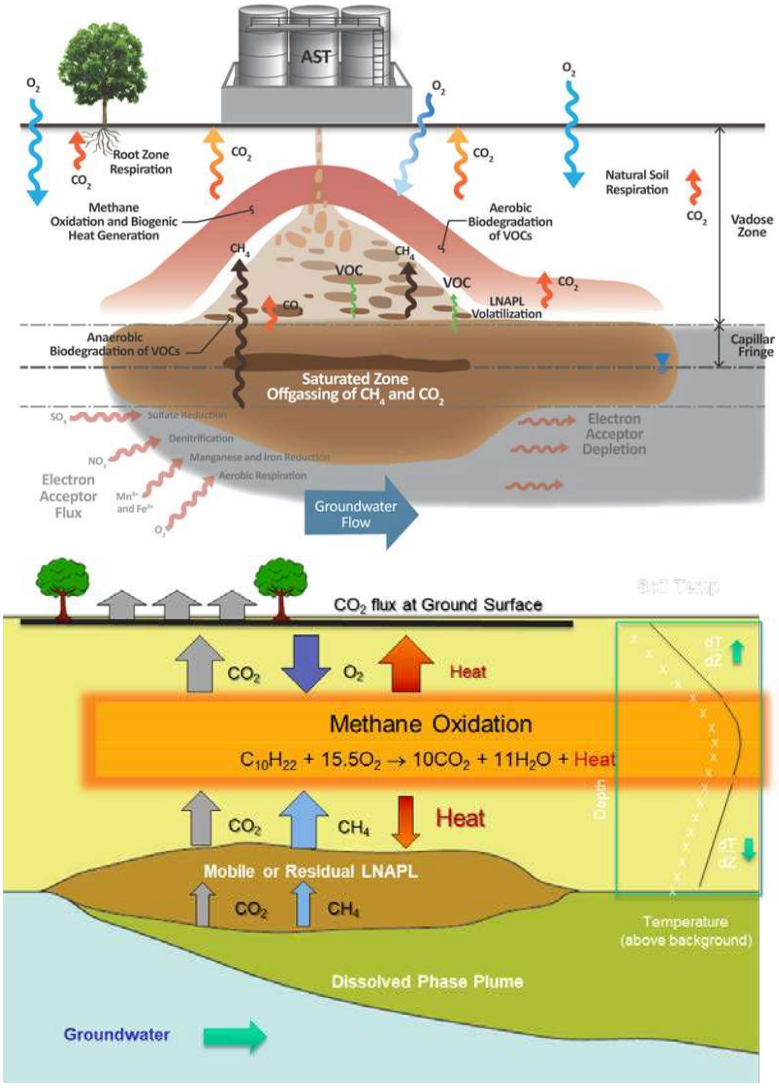

(Palaia and Fitzgibbons 2018)

Figure 2-2: Conceptualization of Vapor Transport-Related NSZD Processes at a Typical Petroleum Release Site, Where Heat Generation Occurs above NSZD Zone

However, at the Facility, high oxygen concentrations (generally >19%) were observed at all unsaturated zone measurement locations, including well headspace samples collected in close proximity to the water table and soil gas wells installed 10–30 ft below the base of the fuel tanks. In

addition, no methane was detected in any unsaturated zone measurement locations (see CSM Appendix B.3). The vapor sample data indicate aerobic conditions throughout the unsaturated zone with little or no methane production/transport. Therefore, unsaturated-zone heat generation appears to be attributable to the direct aerobic biodegradation of petroleum, and the interval of heat generation is assumed to indicate the interval containing residual LNAPL (Figure 2-3).

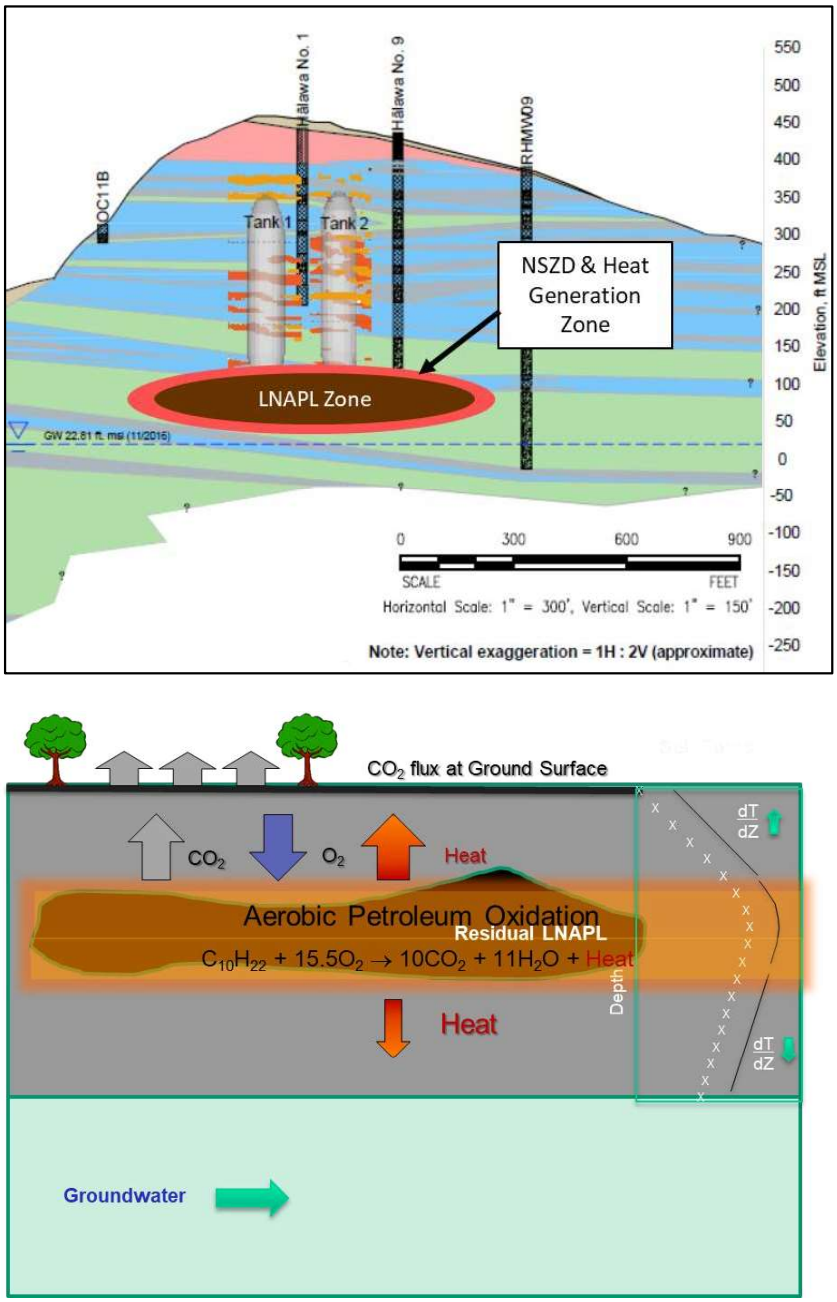

Figure 2-3: Conceptualization of Vapor Transport-Related NSZD Processes at the Facility, Where Heat Generation Occurs in NSZD Zone

This is highlighted on Figure 2-4, which shows the net temperature profile for each of the three wells, assuming an identical surface temperature (i.e., net temperature of 0 at the floor of the lower tunnel). The intervals in each profile that have constant slopes (i.e., no LNAPL) are highlighted with dashed lines, and the areas with changing slopes (due to heat generation associated with biodegradation of petroleum) are shaded. For each temperature profile, the depth intervals with constant slopes (no LNAPL) and the depth interval with changing slope (LNAPL) were identified using professional judgement based on visual inspection of the temperature profile. These intervals are shown in Table 2-1.

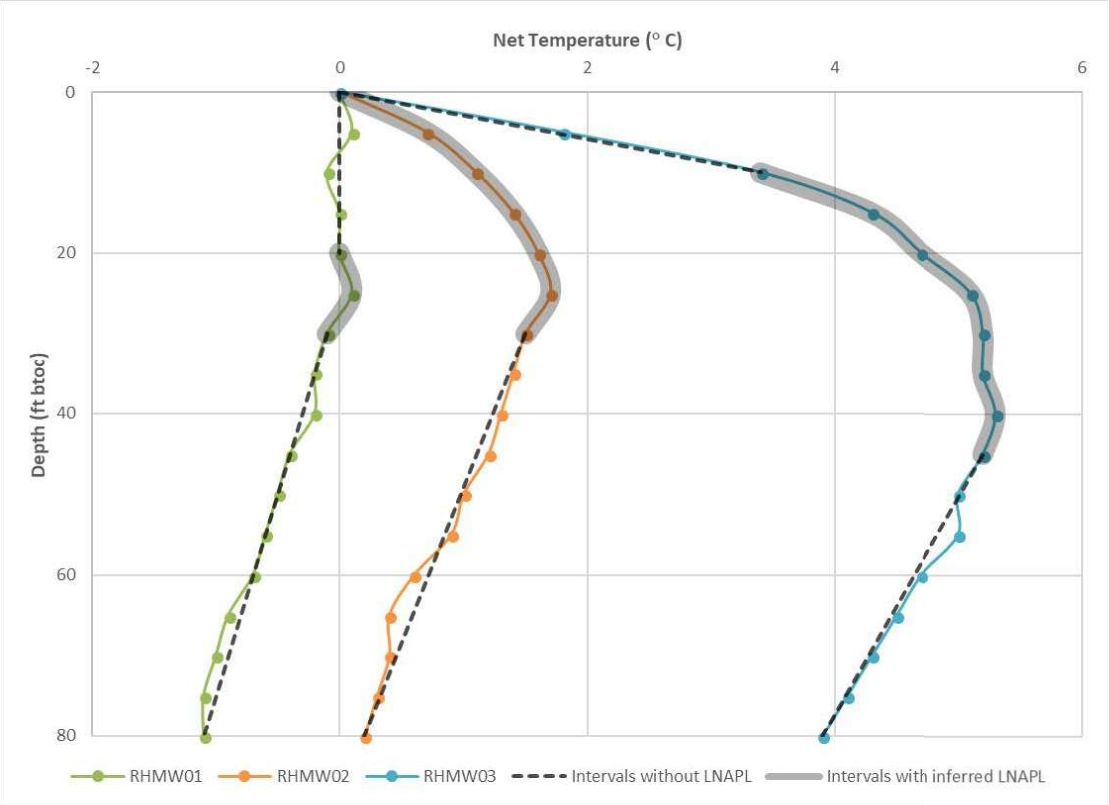

Notes:
1. Grey shading shows interval of heat generation indicating presence of LNAPL within this interval.
2. Depths to water for the wells shown are as follows: RHMW01: 83.7 ft btoc; RHMW02: 86.4 ft btoc; RHMW03: 102.6 ft btoc.

Figure 2-4: Net (Background-Corrected) Temperature Profiles for Facility Wells (Well Air Temperature Measurements)

Table 2-1: Inferred LNAPL-Containing Intervals Indicated by Net (Background-Corrected) Temperature Profiles from Three Facility Monitoring Wells

Monitoring Well	Top of Casing Elevation (ft msl)	Approximate Top of LNAPL (ft btoc)	Approximate Bottom of LNAPL (ft btoc)	Approximate Top of LNAPL (ft msl)	Approximate Bottom of LNAPL (ft msl)
RHMW01	102.00	20	30	82	72
RHMW02	104.60	0	30	105	75
RHMW03	120.90	10	45	111	76

Note: All three wells are installed in the lower tunnel of the Facility.

Note that the LNAPL distribution shown at RHMW03, between 10 and 45 ft below the tunnel (76–111 ft mean sea level [msl]), corresponds to the observed LNAPL distribution below Tank 14 observed in the 2000 timeframe, where LNAPL was observed between 88.83 and 98.15 ft msl in angle boring B-14, as shown in CSM Appendix B.2 Figure 4-3. This suggests that the thermal NSZD method is a robust approach to delineating vertical LNAPL distributions in the aerobic system.

The net (background-corrected) temperature signal at RHMW02, measured from 0 to 30 ft below the lower tunnel floor, is consistent with a release of LNAPL from Tank 5 in 2014 that did not make it down to the water table.

As shown on Figure 2-5, the location of the LNAPL does not correspond directly with the location of the clinker zones at these locations. This indicates that other geologic media, such as thin pāhoehoe layers, is likely transmitting and holding LNAPL.

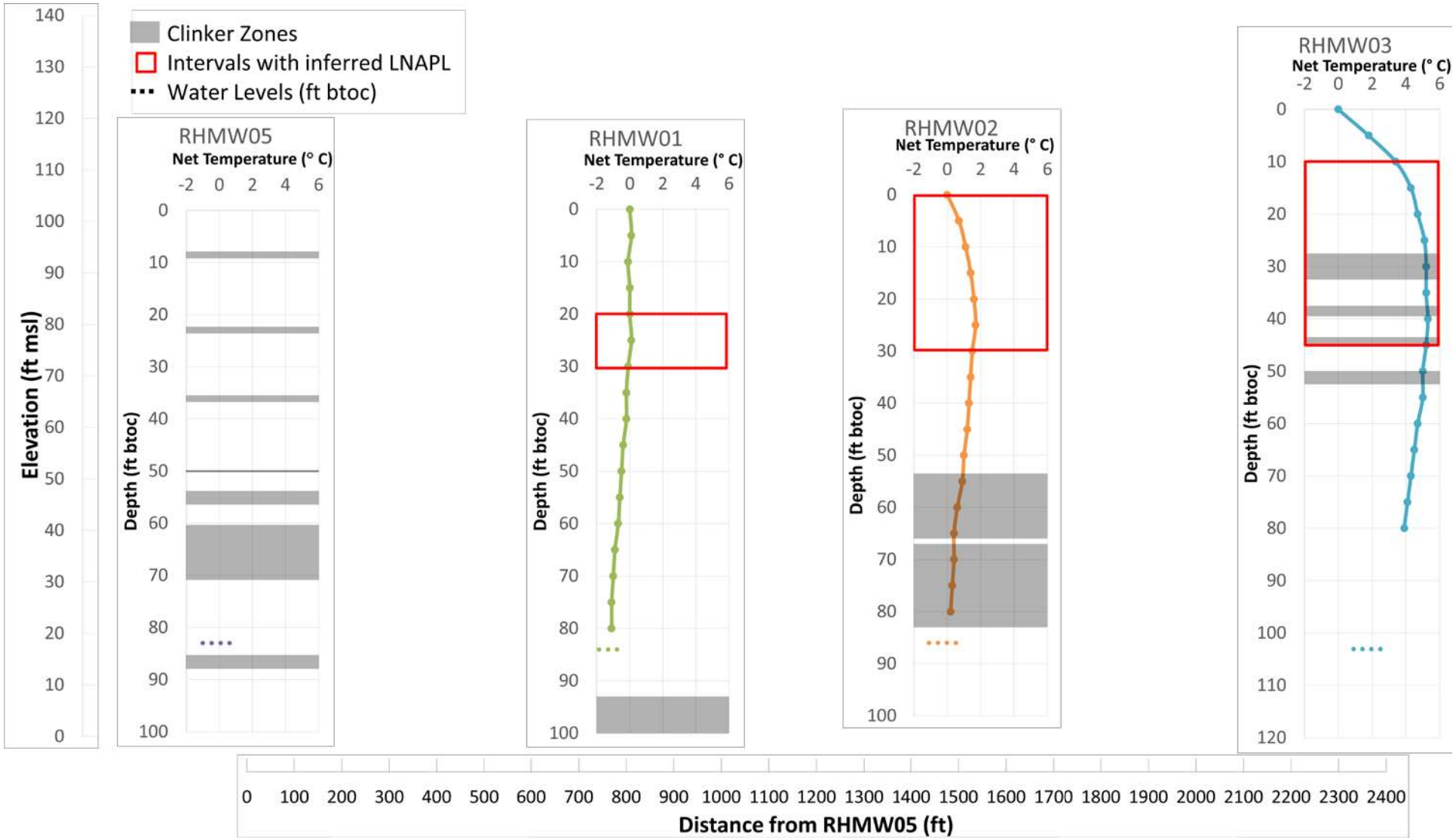

Note: Each scale shows depth below the tunnel floor, with the elevation scale (ft msl) on the far left.

Figure 2-5: Net (Background-Corrected) Temperature Profiles for Facility Wells (Well Air Temperature Measurements), Highlighting Clinker Zones (Identified from Boring Logs) and LNAPL Intervals

3. NSZD Rates

Three methods are used for calculating NSZD rates. Calculation Method 1 is considered the primary method and uses the net (background-corrected) temperature vertical profiles. Calculation Method 2 uses the Hillel (1982) model-corrected thermal profiles, rather than the net (background-corrected) temperature profiles and is considered an alternative method for calculating NSZD rates. Calculation Method 3 uses differences in groundwater temperatures to calculate a bulk biodegradation rate for the entire tank farm. All three methods were employed for this assessment and are detailed in the following subsections.

3.1 CALCULATION METHOD 1: BACKGROUND-CORRECTED NET TEMPERATURES

3.1.1 Net Temperature Profiles

The primary method for calculating NSZD rates uses the net (background-corrected) temperature vertical profiles. These are shown on Figure 2-4, and the calculations are detailed below.

3.1.2 NSZD Calculations for Method 1

To calculate the rate of NSZD occurring in the subsurface at each well, the downward heat flux going from the unsaturated zone to the water table and the upward heat flux going to the atmosphere were calculated. This was done by determining a temperature gradient from the net (background-corrected) temperatures, then calculating a heat flux, and finally using the heat flux to calculate the NSZD rate. The temperature gradient above the heat generation interval was used to calculate the upward heat flux to the atmosphere, and the temperature gradient below the heat generation interval was used to calculate the downward heat flux to the water table. In theory, the net (background-corrected) temperature gradients above and below the heat generation interval should be constant; however, limitations in background correction can result in small variations in the measured temperature gradient. As a result, the temperature gradient is generally estimated using as many measurement points as possible from outside the heat generation interval. Two points is the minimum number needed for this calculation, but using additional points when available provides more confidence in the result.

To obtain the value for the temperature gradient going downward toward the water table, the slope of a linear regression of all the net (background-corrected) temperature values between 50 and 80 ft btoc (seven points) was calculated to get an average "dT/dz" value in degrees Celsius (°C) per ft. The depth of 50 ft btoc was chosen as the top of the interval for the regression because this depth is below the interval of heat generation (i.e., below the biodegradation zone), indicating a constant, and therefore reliable heat flux. Here, 80 ft btoc was chosen as the bottom of the interval for the regression because this depth was the deepest measurement taken for RHMW05 above the water table.

The dT/dz value for the heat flux going up into the atmosphere was obtained by dividing the net temperature at 15 ft btoc by 15. This is because the average temperature at 0 ft btoc (i.e., at the base of the lower access tunnel) for all wells is assumed to have a net (background-corrected) temperature of 0°C. A simple two-point line was used to determine this gradient, rather than a linear regression, because seasonal and daily variations in temperature within the top 30 ft can cause the slope of a regression to vary significantly from the average temperature gradient going into the atmosphere, and these variations are removed when using a simple two-point line and assuming an identical temperature at 0 ft btoc. The depth 15 ft btoc was chosen as the bottom of the interval for the gradient calculation because it is a good compromise between having a bottom depth near the top of or above the zone of heat generation/biodegradation (for the sake of an accurate gradient) and having a bottom depth far enough below the ground surface (to remove seasonal and daily surface temperature variations). For

RHMW02 (and possibly RHMW03) the 15-ft depth is likely within the biodegradation zone. As a result, the calculated NSZD rate likely underestimates the actual degradation rate.

The dT/dz values were then multiplied by the thermal conductivity of the soil or rock (basalt in this case, with a thermal conductivity of 1.69 W/m-K) (Eppelbaum, Kutasov, and Pilchin 2014) to obtain heat fluxes into the groundwater and atmosphere in Watts per square meter (W/m^2). The calculations are shown in Table 3-1.

Table 3-1: Calculation of Top and Bottom Heat Fluxes for NSZD Using Well Air Temperature Measurements and Calculation Method 1 (Background-Correction)

Well	Net Temp. at 50 ft btoc (°C)	Net Temp. at 80 ft btoc (°C)	Bottom dT/dz from Regression Using 7 Points (°C/ft)	Bottom Heat Flux (W/m^2)	Net Temp. at 15 ft btoc (°C)	dT/dz (°C/ft)	Top Heat Flux (W/m^2)
RHMW01	-0.5	-1.1	0.02	0.12	0.0	0.00	0.00
RHMW02	1.0	0.2	0.03	0.15	1.4	0.09	0.52
RHMW03	5.0	3.9	0.04	0.22	4.3	0.29	1.59

Note: Values are rounded. Calculations were performed using unrounded values.

These two heat fluxes were then added together and that value converted to gallons per acre per year (gal/acre/yr) of NSZD, using the conversion from W/m^2 to gal/acre/yr, as calculated in Table 3-2.

Table 3-2: Calculation Method 1(Background-Correction): Conversion from W/m^2 to gal/acre/yr of NSZD

Parameter	Value	Reasoning
Conversion from W to J/sec	1 J/sec-W	Known
Conversion from sec to yrs	3.2×10^7 sec/yr	Known
Conversion from m^2 to ac	4,047 m^2/ac	Known
Heat of Combustion of Jet Fuel	4.7×10^7 J/kg	(Martínez 2017)
Density of Jet Fuel	800 kg/m^3	(Martínez 2017)
Conversion from m^3 to L	1,000 L/m^3	Known
Conversion from L to gal	0.26 gal/L	Known
Conversion from W/m^2 to gal/acre/yr	898 (gal/acre/yr)/(W/m^2)	Calculation

Note: Values are rounded. Calculations were performed using unrounded values.
J joule
gal gallon
kg kilogram
L liter
m^3 cubic meter
yr year

Following this process, the following NSZD rates were calculated (Table 3-3 and Table 3-4):

Table 3-3: Calculation Method 1 (Background-Correction) NSZD Rates for Facility Wells (Well Air Temperature Measurements)

Well	Total Heat Flux (W/m^2)	NSZD Rate (gal/acre/yr)
RHMW01	0.12	110
RHMW02	0.67	600
RHMW03	1.81	1,622

Note: Values are rounded. Calculations were performed using unrounded values.

Table 3-4: Calculation Method 1 (Background-Correction) NSZD Rates for Facility Wells (Average of Well Air Temperature Measurements and Well Wall Temperature Measurements)

Well	NSZD Rate from Well Air Temperature Measurements (gal/acre/yr)	NSZD Rate from Wall Temperature Measurements (gal/acre/yr)	Average NSZD Rate (gal/acre/yr)
RHMW01	110	173	**141**
RHMW02	600	677	**638**
RHMW03	1,622	1,374	**1,498**

Note: Values are rounded. Calculations were performed using unrounded values.

Assuming the three NSZD measurements are representative samples of NSZD within the tank farm, an average NSZD rate for the entire tank farm was calculated in gallons per year (gal/yr). Note that it is assumed that all NSZD is occurring underneath the tank farm because there is no evidence of extensive migration out of the tank farm area. This would not necessarily be the case for a large, sudden release. Taking an average of all the NSZD rates (759 gal/acre/yr) and multiplying this by the area encompassed by the tank farm (13.1 acres; Figure 3-1), the total NSZD rate comes to 9,935 gal/year or about 10,000 gal/yr.

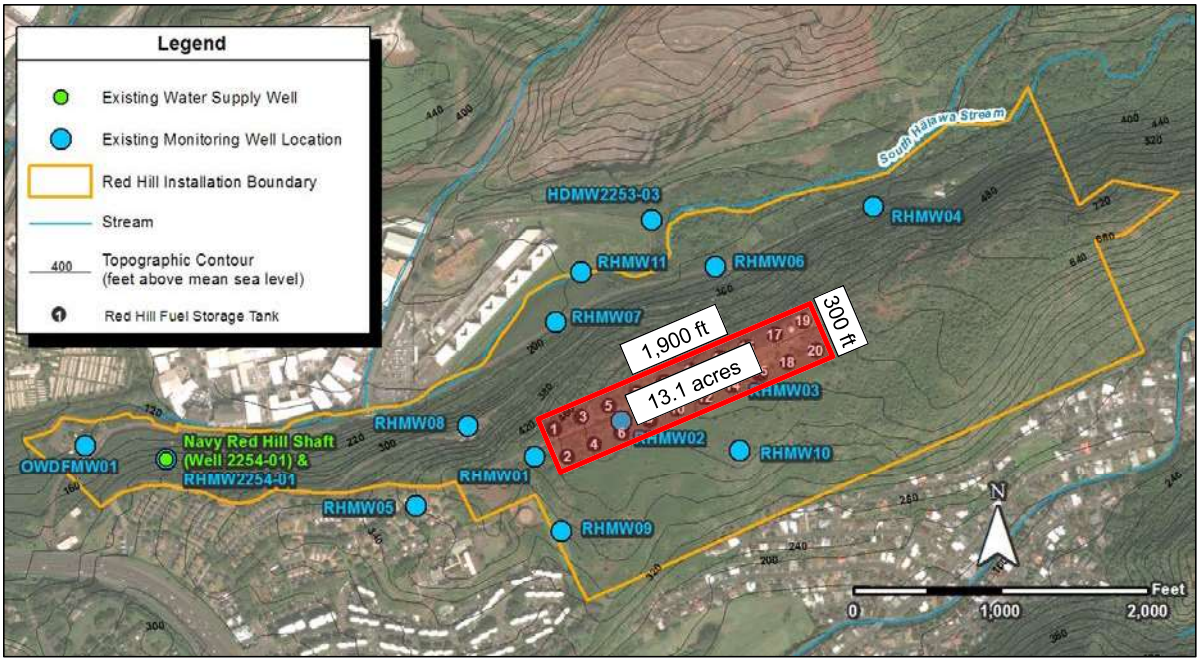

Figure 3-1: Area Encompassed by Tank Farm

3.2 CALCULATION METHOD 2: MODEL-CORRECTED THERMAL PROFILES

The accuracy of NSZD rates calculated using Calculation Method 1 (Background-Correction) depends on the suitability of the background location used for the background correction. If the temperature profile at the background location is not representative of the LNAPL-impacted locations, then the use of this location for background correction can result in an over-estimation or under-estimation of the true NSZD rates. An alternative method for calculating NSZD rates is to use Hillel (1982) model-corrected thermal profiles, rather than the net (background-corrected) temperature profiles. In this method, it is assumed that enough heat flux is going into the groundwater and into the atmosphere that it can be seen in the raw thermal profiles, which are then corrected for seasonal variations in temperature using the Hillel (1982) model. This alternative calculation method was done to evaluate the accuracy of Calculation Method 1 (Background-Correction). Attainment of similar NSZD rates using the two methods provides increased confidence in the accuracy of both methods.

To correct for seasonal variations in temperature, the temperature values from the raw thermal profiles were altered by the amount that a soil column would be expected to vary from average Honolulu air temperatures as calculated by Nofziger and Wu (2003) using the Hillel (1982) formula. The average temperature used for the model average annual air temperature in Honolulu (25.4°C) (Table 1-2) minus 0.9°C to account for the lower average air temperature at the elevation of the air intake for the tunnels (approximately 300 ft). This comes from the assumption that air temperatures cool by the "dry adiabatic lapse rate" of approximately 3°C for every 1,000 ft increase in elevation (Boubel et al. 1994). These corrected profiles are shown on Figure 3-2.

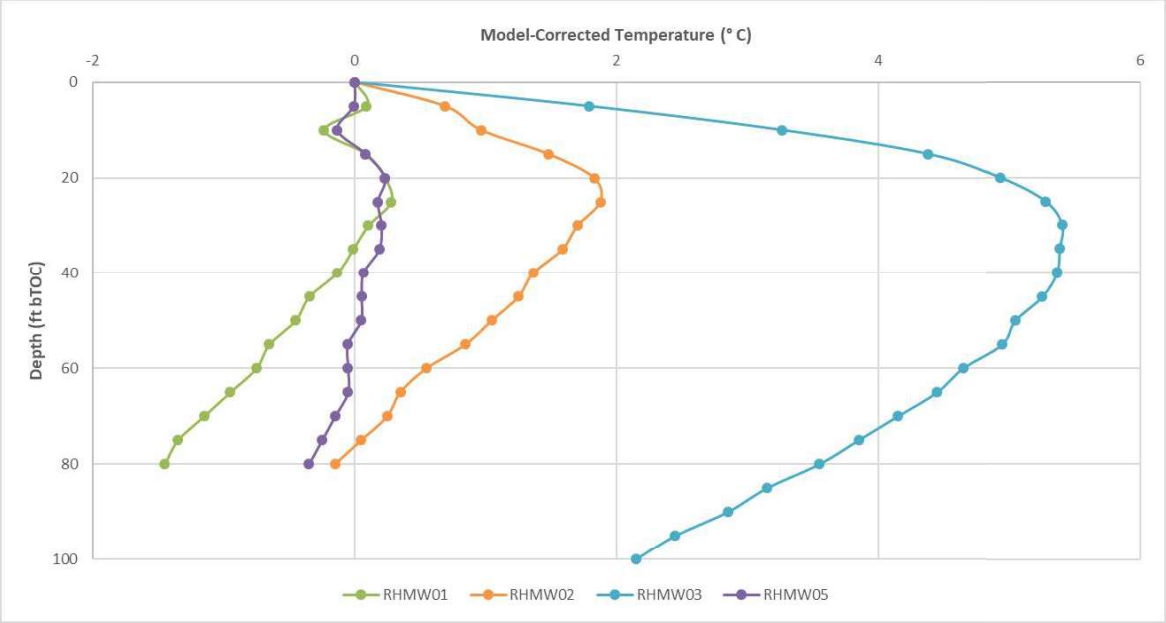

Note: Depths to water for the wells shown are as follows: RHMW01: 83.7 ft btoc; RHMW02: 86.4 ft btoc; RHMW03: 102.6 ft btoc.

Figure 3-2: Calculation Method 2 (Model-Correction) Thermal Profiles for Facility Wells (Well Air Temperature Measurements)

Also, because seasonal and daily effects cause uncertainty for the temperature measurements at the top of subsurface raw thermal profiles, and the tunnel ventilation system likely introduces a seasonal temperature signal to the basalt in the Facility, the model-corrected temperature at 0 ft btoc was assumed to be 0°C for all wells for the purpose of calculating NSZD rates.

3.2.1 NSZD Calculations for Method 2

To calculate the rate of NSZD occurring in the subsurface at each well, after correcting the profiles using the Hillel (1982) formula, the downward heat flux going from the unsaturated zone to the water table and the upward heat flux going to the atmosphere were calculated. This was done by determining a temperature gradient from the model-corrected thermal profiles, and then calculating a heat flux and thus a NSZD rate. The temperature gradient above the heat generation interval was used to calculate the upward heat flux to the atmosphere, and the temperature gradient below the heat generation interval was used to calculate the downward heat flux to the water table.

The dT/dz values for Calculation Method 2 (Model-Correction) were calculated similarly as for Calculation Method 1 (Background-Correction). For the bottom gradient, the slope of a linear regression of all the model-corrected temperature values between 50 ft btoc and the temperature directly above the water table (DAWT) (seven or eleven points, depending on the well) was calculated to get an average "dT/dz" value in degrees Celsius (°C) per ft. For the top of the interval for the regression, 50 ft btoc was chosen because this depth is below the interval of heat generation (i.e., below the biodegradation zone), indicating a relatively constant, and therefore reliable, heat flux. The value DAWT was chosen as the bottom of the interval for the regression, rather than 80 ft btoc, because RHMW03 was a deeper well than the other wells. For the upper gradient, the dT/dz value for the heat flux going into the atmosphere was obtained by dividing the model-corrected temperature at 15 ft btoc by 15. This is because the average temperature at 0 ft btoc (i.e., at the base of the lower access tunnel)

for all wells is assumed to have a model-corrected temperature of 0°C. A simple two-point line was used in this case, rather than a linear regression, because seasonal and daily variations in temperature within the top 30 ft can cause the slope of a regression to vary significantly from the average temperature gradient going into the atmosphere, and these variations are muted when using a simple two-point line and assuming an identical temperature at 0 ft btoc. The depth 15 ft btoc was chosen as the bottom of the interval for the gradient calculation because it represented a good compromise between having a bottom depth near the top of or above the zone of biodegradation (for the sake of an accurate gradient) and having a bottom depth far enough below the ground surface (to remove seasonal and daily surface temperature variations). For RHMW02 (and possibly RHMW03), the 15-ft depth is likely within the biodegradation zone. As a result, the calculated NSZD rate likely underestimates the actual degradation rate.

Both lower and upper dT/dz values were then multiplied by the thermal conductivity of the soil (1.69 W/m-K) (Eppelbaum, Kutasov, and Pilchin 2014) to obtain heat fluxes into the groundwater and atmosphere in W/m^2. The calculations are shown in Table 3-5.

Table 3-5: Calculation of Top and Bottom Heat Fluxes for NSZD Using Well Air Temperature Measurements and Calculation Method 2 (Model-Correction)

Well	Model-Corrected Temp. at 50 ft btoc (°C)	Model-Corrected Temp. DAWT (°C)	dT/dz from Regression (°C/ft) [Number of Points Used]	Bottom Heat Flux (W/m^2)	Model-Corrected Temp. at 15 ft btoc (°C)	dT/dz (°C/ft)	Top Heat Flux (W/m^2)
RHMW01	-0.5	-1.4	0.03 [7]	0.19	0.1	0.01	0.03
RHMW02	1.0	-0.1	0.04 [7]	0.22	1.5	0.10	0.55
RHMW03	5.0	3.6	0.05 [11]	0.33	4.4	0.29	1.62
RHMW05	0.0	-0.3	0.01 [7]	0.07	0.1	0.01	0.03

Note: Values are rounded. Calculations were performed using unrounded values.

These two heat fluxes were then added together, and that value converted to gal/acre/yr of NSZD, using the conversion from Watts/m^2 to gal/acre/yr, as calculated in Table 3-2. The calculated NSZD rates are shown in Table 3-6 and Table 3-7.

Table 3-6: Calculation Method 2 (Model-Correction) NSZD Rates for Facility Wells (Well Air Temperature Measurements)

Well	Total Heat Flux (W/m^2)	NSZD Rate (gal/acre/yr)
RHMW01	0.22	197
RHMW02	0.76	687
RHMW03	1.95	1,753
RHMW05	0.10	87

Note: Values are rounded. Calculations were performed using unrounded values.

Table 3-7: Calculation Method 2 (Model-Correction) NSZD Rates for Facility Wells (Average of Well Air Temperature and Wall Temperature Measurements)

Well	NSZD Rate from Well Air Temperature Measurements (gal/acre/yr)	NSZD Rate from Wall Temperature Measurements (gal/acre/yr)	Average NSZD rate (gal/acre/yr)
RHMW01	197	222	**210**
RHMW02	687	709	**698**
RHMW03	1,753	1,513	**1,633**
RHMW05	87	57	**72**

Note: Calculations were performed using unrounded values.

Assuming NSZD is happening only underneath the tank farm, an average NSZD rate was calculated in gal/yr. Note that it is assumed that all NSZD is occurring underneath the tank farm because there is no evidence of extensive migration out of the tank farm area. This would not necessarily be the case for a large, sudden release. Taking an average of the NSZD rates for RHMW01, RHMW02, and RHMW03 (ignoring the background well) gave a value of 847 gal/acre/yr. This value was multiplied by the area encompassed by the tank farm (13.1 acres; Figure 3-1), yielding a total NSZD rate of 11,000 gal/yr, fairly close to that calculated using Calculation Method 1 (Background-Correction)(Section 3.1.2).

3.3 AGREEMENT BETWEEN CALCULATION METHOD 1 AND CALCULATION METHOD 2 NSZD RATES

NSZD rates were calculated using two different calculation methods: Method 1 (Background-Correction) and Method 2 (Model-Correction):

1. RHMW05 is the farthest of the four monitoring wells from the tank farm. For Calculation Method 1 (Background-Correction), RHMW05 was assumed to be unaffected by LNAPL and was used as the background location to generate net temperature profiles for the remaining locations. For Calculation Method 2 (Model-Correction) (which does not require a background location), the temperature profile for RHMW05 was processed using the same calculation procedures applied to the other locations. The very low NSZD rate calculated for RHMW05 using Calculation Method 2 (72 gal/acre/yr) is likely an artifact of small measurement errors or natural temperature variations at this location. The extremely low NSZD rate measured at RHMW05 using Calculation Method 2 confirms it was a suitable well to serve as a background well for Calculation Method 1.
2. At the three locations within the tank area (RHMW01, RHMW02, and RHMW03), the NSZD rates calculated using the two methods were similar, providing increased confidence in the accuracy of the results (i.e., the resulting rates are not an artifact of assumptions associated with a specific calculation method). For the three locations, the average difference in NSZD rates for the two methods was only 90 gal/acre/yr. For the two locations with the highest NSZD rates (RHMW02 and RHMW03), the difference in rates between the two methods was only 9%.

3.4 CALCULATION METHOD 3: GROUNDWATER TEMPERATURES (ONLY ACCOUNTS FOR DOWNWARD HEAT FLUX)

The groundwater temperature in the monitoring wells within the tank area (i.e., RHMW02 and RHMW03) is elevated relative to the background well (RHMW05). Elevated groundwater

temperatures have been observed at other NSZD sites (e.g., Kimmel and Braids 1980). To evaluate whether the downward convection of heat associated with the observed vadose zone biodegradation is consistent with the observed increase in groundwater temperature within this area, a third method for calculating NSZD was conducted based on the heat required to heat the groundwater flowing through this area. In this method, the difference in groundwater temperatures was measured between RHMW01, RHMW02, and RHMW03 and RHMW05. The reason for this temperature difference is likely due to NSZD in the unsaturated zone, which is causing a heat flux into the groundwater that is increasing the water temperature above the temperature of the background groundwater. This method yields a partial NSZD rate that accounts only for the downward heat flux from the unsaturated zone to the groundwater. It does not account for upward heat loss from the unsaturated zone to the atmosphere. However, the results from this method are comparable to the downward heat flux portion of the unsaturated temperature profile NSZD methods.

The calculation was conducted for a range of elevated groundwater temperatures based on (1) the difference between the temperature at RHMW03 (the well with the highest temperature) and RHMW05 (the background well) and (2) the difference between the average temperature of the groundwater for RHMW01, RHMW02, and RHMW03 vs. RHMW05. The groundwater temperatures are shown in Table 3-8. The average temperature of the groundwater for RHMW01 is approximately the same temperature as the average temperature of the groundwater for RHMW05 (cooler by approximately 0.3°C), which is in line with the vadose zone temperature profile at RHMW01 that indicates only minor amounts of NSZD at this location. The average temperature of the groundwater for the other two wells had higher temperatures than RHMW05.

Table 3-8: Water Temperatures at RHMW03 and RHMW05

Well	Temp. at Top of Water Column (°C)	Temp. at Middle of Water Column (°C)	Temp. at Bottom of Water Column (°C)	Average Water Temp. (°C)
RHMW01	22.7	22.4	22.3	22.5
RHMW02	24.0	23.2	22.8	23.3
RHMW03	26.0	25.8	25.4	25.7
			Average of RHMW01, RHMW02, & RHMW03	23.8
RHMW05	24.1	22.8	21.6	22.8
			Difference	1.0 – 2.9

Note: The temperature difference range is based on (1) the difference between RHMW03 and RHMW05 and (2) the difference of the average of RHMW01, RHMW02, and RHMW03 vs. RHMW05.

Also, the mass of groundwater that would be affected by this temperature change was calculated. Note that a range of seepage velocities was used based on preliminary particle tracking model results conducted for the investigation's interim groundwater flow modeling effort reflecting the range between base model and the base model with clinker zone. This calculation is shown in Table 3-9.

Table 3-9: Calculation of Mass of Water Flow from RHMW03 to RHMW05

Parameter	Value	Reasoning
Width of Groundwater Flow	300 ft	Width of tank farm
Thickness of Heated Zone	15 ft	Screened intervals
Darcy Velocity	1.63 – 13 ft/day	Based on interim groundwater flow modeling
Volume of Groundwater Flow Per Year	2.7×10^6 – 2.1×10^7 ft^3/yr 7.6×10^7 – 6.0×10^8 L/yr	Calculation (300 ft × 15 ft x 1.63 ft/day × 365 days/yr; 300 ft × 15 ft × 13 ft/day × 365 days/yr) (1 ft^3 = 28.3 L)
Density of Water	1 kg/L	Known
Mass of Groundwater Flow Per Year	7.6×10^7 – 6.0×10^8 kg/yr 7.6×10^{10} – 6.0×10^{11} g/yr	Calculation (7.6×10^7 L/yr × 1 kg/L; 6.0×10^8 L/yr × 1 kg/L) (1 kg = 1,000 g)

Note: Values are rounded. Calculations were performed using unrounded values.

Using these data, a rate of biodegradation in the groundwater (in gallons of fuel per year) was calculated, as shown in Table 3-10.

Table 3-10: Calculation Method 3: Biodegradation Affecting Groundwater Temperature

Parameter	Value	Reasoning
Heat Capacity of Water	1 cal/g/°C	Known
Total Heat Generated (1.0°C difference)	7.7×10^{10} – 6.1×10^{11} cal/yr 320,531 – 2.6×10^6 MJ/yr	Calculation (7.6×10^7× 1.0°C × 1 cal/g/°C; 6.0×10^{11} g/yr × 1.0°C × 1 cal/g/°C) (1 MJ = 239,006 cal)
Total Heat Generated (2.9°C difference)	2.2×10^{11} – 1.8×10^{12} cal/yr 919,325 – 7,3 x 10^6 MJ/yr	Calculation (7.6×10^7 × 2.9°C × 1 cal/g/°C; 6.0×10^{11} g/yr × 2.9°C × 1 cal/g/°C) (1 MJ = 239,006 cal)
Heat Combustion of Jet Fuel	47 MJ/kg	Martinez (2017)
Amount of Biodegradation (1.0°C difference)	6,820 – 54,391 kg/yr **2,255 – 17,986 gal/yr**	Calculation (320,531 MJ/yr / 47 MJ/kg); 2.6×10^6MJ/yr / 47 MJ/kg) (1 kg Jet Fuel = 0.33 gal Jet Fuel)
Amount of Biodegradation (2.9°C difference)	19,560 – 156,001 kg/yr **6,468 – 51,588 gal/yr**	Calculation (919,325 MJ/yr / 47 MJ/kg); 7.3×10^{10} MJ/yr / 47 MJ/kg) (1 kg Jet Fuel = 0.33 gal Jet Fuel)

Note: Calculations were performed using unrounded values.
cal/yr calories per year
cal/g/°C calories per gram per degrees Celsius

Therefore, the heat flux going into the groundwater from NSZD in the unsaturated zone is coming from the degradation of approximately 2,300–51,600 gallons of fuel per year. Comparing this to the average Bottom NSZD rate (the only heat flux that would go into the groundwater) from Calculation Method 1 (Background-Correction) and Calculation Method 2 (Model-Correction) (average for each method), the two average Bottom NSZD rates are similar to the lower range, providing additional confidence that the elevated groundwater temperatures in these wells are attributable to the vadose zone NSZD (Table 3-11).

The high-end NSZD estimate of 51,600 gallons of LNAPL biodegraded per year was derived using groundwater flow data from the clinker-based groundwater flow model and is about 20 times higher than the results from Method 1 and Method 2 NSZD results (2,000 and 2,800 gal/yr, respectively). While other factors support use of the clinker-based groundwater flow model, the NSZD results alone

suggests that the baseline groundwater flow model may be closer to representing site conditions near RHMW03 rather than the clinker-based model.

Table 3-11: The Bottom Heat Flux NSZD Rate (i.e., Associated with Downward Heat Transfer) for the Three Calculation Methods

Method	Bottom Heat Flux NSZD Rate (gal/yr)
Calculation Method 1(Background-Correction)	2,000 gal/yr
Calculation Method 2 (Model-Correction)	2,800 gal/yr
Calculation Method 3 (Groundwater Temperatures)	2,300 – 51,600 gal/yr

Note: Values are rounded. Calculations were performed using unrounded values.

In conclusion, Calculation Method 3 (Groundwater Temperatures), an independent method that did not rely on vertical temperature profiles in the unsaturated zone, yielded results that match the corresponding part of the NSZD calculations from Calculation Method 1 (Background-Correction) and Calculation Method 2 (Model-Correction)(i.e., downward heat flux parts), especially when using the baseline groundwater flow model, thereby increasing the confidence in those methods.

4. Conclusions

Two protocols were used in the field to measure vertical temperature profiles in wells in the Facility with both producing similar data. These data were used to determine the general vertical location of LNAPL at each location (shown in Table 2-1) and the corresponding NSZD rates for that LNAPL.

The NSZD rates were calculated using three different methods: Method 1 (Background-Correction), Method 2 (Model-Correction), and Method 3 (Groundwater Temperatures). Calculation Method 3 (Groundwater Temperatures) accounts for only downward heat flux from the bottom of the LNAPL zone to groundwater. The Calculation Method 3 results serve to confirm the reasonableness of Calculation Method 1 (Background-Correction) and Calculation Method 2 (Model-Correction) results, but Calculation Method 3 does not provide an estimate of the total NSZD rates at the Facility. Despite some differences between these methods, each produced fairly consistent NSZD rates among the three locations. Total NSZD rates in units of gal/yr are shown in Table 4-1.

Table 4-1: Summary of Total NSZD Rates (Gallons per Year) from the Tank Farm

Well	Calculation Method 1 (Background-Correction)	Calculation Method 2 (Model-Correction)	Calculation Method 3 (Groundwater Temperatures)
Bottom Heat Flux NSZD Rate (gal/yr)			
RHMW01	1,600	2,200	N/A
RHMW02	2,100	2,500	N/A
RHMW03	2,500	3,900	N/A
Average	*2,000*	*2,800*	*2,300–51,600*
Top Heat Flux NSZD Rate (gal/yr)			
RHMW01	220	600	N/A
RHMW02	6,300	6,700	N/A
RHMW03	17,000	17,500	N/A
Average	*7,900*	*8,200*	*N/A*
Total NSZD Rate (gal/yr)			
RHMW01	1,900	2,700	N/A
RHMW02	8,400	9,100	N/A
RHMW03	20,000	21,400	N/A
Average	*9,900*	*11,100*	*N/A*

Note: Values are rounded. Calculations were performed using unrounded values.
N/A not applicable

The NSZD rates using Calculation Method 1 (Background-Correction) (see Table 3-4) are shown below. These are considered the most accurate calculations for NSZD rates of all the methods.

- RHMW01: 140 gal/acre/yr of NSZD
- RHMW02: 640 gal/acre/yr of NSZD
- RHMW03: 1,500 gal/acre/yr of NSZD

The calculated NSZD rates at the three locations are consistent with the understanding of historical LNAPL releases at the Facility:

1. RHMW01 is the farthest of the three monitoring wells from the tank farm and therefore was expected to be the location least impacted by LNAPL releases. The low NSZD rate (140 gal/acre/yr) is consistent with limited LNAPL impacts.
2. RHMW02 has a relatively high NSZD rate (640 gal/acre/yr), which is expected due a known release of 27,000 gallons of fuel that occurred in early 2014 from Tank 5.
3. RHMW03 has the highest NSZD rate (1,500 gal/acre/yr). This is consistent with results of the 1998–2002 angle borings investigation (Figure 4-1) that indicated historical releases from three adjacent tanks; Tank 13, Tank 14, and Tank 16 (DON 1999, 2002; see main CSM document, Section 4.1).

The thermal NSZD analysis confirms that biodegradation of LNAPL in the vadose zone is an important NSZD process at the Facility. In addition, the downward heat flux associated with this NSZD is sufficient to explain the elevated groundwater temperatures observed in RHMW03 and RHMW02.

As part of the concurrently published interim environmental analysis document (DON 2018), the calculated NSZD rate will be used to evaluate the LNAPL assimilative capacity at the Facility. This assimilative capacity will be used for the evaluation of hypothetical future release scenarios. To establish a range of values for the total NSZD at the tank farm, the standard deviation of the total NSZD rate of all three wells using Calculation Method 1 (Background-Correction) was calculated. This standard deviation is 7,300 gal/yr.

Thus, the best estimate for the total NSZD rate at the tank farm is 9,900 gal/yr, with a likely range of 2,600–17,300 gal/yr.

Based on recent literature (Garg et al. 2017), NSZD rates may be relatively constant over time, such as since 1998 when angle borings indicated historical releases near Tank 13, Tank 14, and Tank 16. If the measured NSZD rate from this study is assumed to be constant between 1998 and 2018 (a 20-year period), then approximately 50,000–350,000 gallons of fuel has been degraded via NSZD (with a best estimate of approximately 200,000 gallons).

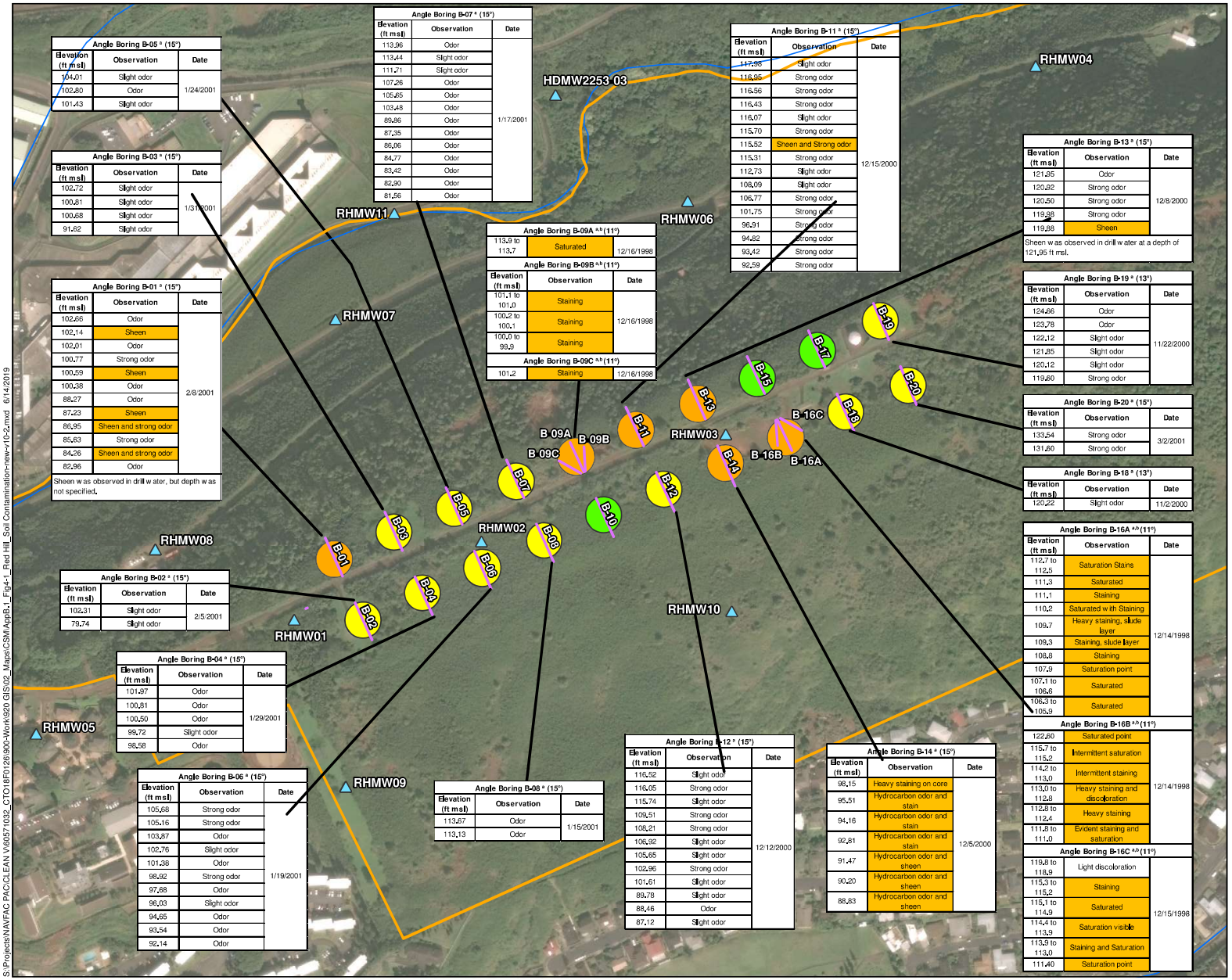

Angle Boring B-05 ª (15°)

Elevation (ft msl)	Observation	Date
104.01	Slight odor	1/24/2001
102.80	Odor	
101.43	Slight odor	

Angle Boring B-03 ª (15°)

Elevation (ft msl)	Observation	Date
102.72	Slight odor	1/31/2001
100.81	Slight odor	
100.68	Slight odor	
91.62	Slight odor	

Angle Boring B-01 ª (15°)

Elevation (ft msl)	Observation	Date
102.66	Odor	2/8/2001
102.14	Sheen	
102.01	Odor	
100.77	Strong odor	
100.59	Sheen	
100.38	Odor	
88.27	Odor	
87.23	Sheen	
86.95	Sheen and strong odor	
85.63	Strong odor	
84.26	Sheen and strong odor	
82.96	Odor	

Sheen was observed in drill water, but depth was not specified.

Angle Boring B-02 ª (15°)

Elevation (ft msl)	Observation	Date
102.31	Slight odor	2/5/2001
79.74	Slight odor	

Angle Boring B-04 ª (15°)

Elevation (ft msl)	Observation	Date
101.97	Odor	1/29/2001
100.81	Odor	
100.50	Odor	
99.72	Slight odor	
98.58	Odor	

Angle Boring B-06 ª (15°)

Elevation (ft msl)	Observation	Date
105.68	Strong odor	1/19/2001
105.16	Strong odor	
103.87	Odor	
102.76	Slight odor	
101.38	Odor	
98.92	Strong odor	
97.68	Odor	
96.03	Slight odor	
94.65	Odor	
93.54	Odor	
92.14	Odor	

Angle Boring B-07 ª (15°)

Elevation (ft msl)	Observation	Date
113.96	Odor	1/17/2001
113.44	Slight odor	
111.71	Slight odor	
107.26	Odor	
105.55	Odor	
103.48	Odor	
89.86	Odor	
87.35	Odor	
86.06	Odor	
84.77	Odor	
83.42	Odor	
82.90	Odor	
81.56	Odor	

Angle Boring B-08 ª (15°)

Elevation (ft msl)	Observation	Date
113.67	Odor	1/15/2001
113.13	Odor	

Angle Boring B-09A ª,b (11°)

113.9 to 113.7	Saturated	12/16/1998

Angle Boring B-09B ª,b (11°)

Elevation (ft msl)	Observation	Date
101.1 to 101.0	Staining	12/16/1998
100.2 to 100.1	Staining	
100.0 to 99.9	Staining	

Angle Boring B-09C ª,b (11°)

101.2	Staining	12/16/1998

Angle Boring B-11 ª (15°)

Elevation (ft msl)	Observation	Date
117.98	Slight odor	12/15/2000
116.95	Strong odor	
116.56	Strong odor	
116.43	Strong odor	
116.07	Slight odor	
115.70	Strong odor	
115.52	Sheen and Strong odor	
115.31	Strong odor	
112.73	Slight odor	
108.09	Slight odor	
106.77	Strong odor	
101.75	Strong odor	
96.91	Strong odor	
94.82	Strong odor	
93.42	Strong odor	
92.59	Strong odor	

Angle Boring B-12 ª (15°)

Elevation (ft msl)	Observation	Date
116.52	Slight odor	12/12/2000
116.05	Strong odor	
115.74	Slight odor	
109.51	Strong odor	
108.21	Strong odor	
106.92	Slight odor	
105.65	Slight odor	
102.96	Strong odor	
101.61	Slight odor	
89.78	Slight odor	
88.46	Odor	
87.12	Slight odor	

Angle Boring B-14 ª (15°)

Elevation (ft msl)	Observation	Date
98.15	Heavy staining on core	12/5/2000
95.51	Hydrocarbon odor and stain	
94.16	Hydrocarbon odor and stain	
92.81	Hydrocarbon odor and stain	
91.47	Hydrocarbon odor and sheen	
90.20	Hydrocarbon odor and sheen	
88.83	Hydrocarbon odor and sheen	

Angle Boring B-13 ª (15°)

Elevation (ft msl)	Observation	Date
121.95	Odor	12/8/2000
120.92	Strong odor	
120.50	Strong odor	
119.88	Strong odor	
119.38	Sheen	

Sheen was observed in drill water at a depth of 121.95 ft msl.

Angle Boring B-19 ª (13°)

Elevation (ft msl)	Observation	Date
124.66	Odor	11/22/2000
123.78	Odor	
122.12	Slight odor	
121.85	Slight odor	
120.12	Slight odor	
119.60	Strong odor	

Angle Boring B-20 ª (15°)

Elevation (ft msl)	Observation	Date
133.54	Strong odor	3/2/2001
131.60	Strong odor	

Angle Boring B-18 ª (13°)

Elevation (ft msl)	Observation	Date
120.22	Slight odor	11/2/2000

Angle Boring B-16A ª,b (11°)

Elevation (ft msl)	Observation	Date
112.7 to 112.5	Saturation Stains	12/14/1998
111.3	Saturated	
111.1	Staining	
110.2	Saturated with Staining	
109.7	Heavy staining, slude layer	
109.3	Staining, slude layer	
108.8	Staining	
107.9	Saturation point	
107.1 to 106.6	Saturated	
106.3 to 105.9	Saturated	

Angle Boring B-16B ª,b (11°)

122.60	Saturated point	12/14/1998
115.7 to 115.2	Intermittent saturation	
114.2 to 113.0	Intermittent staining	
113.0 to 112.8	Heavy staining and discoloration	
112.8 to 112.4	Heavy staining	
111.8 to 111.0	Evident staining and saturation	

Angle Boring B-16C ª,b (11°)

119.8 to 118.9	Light discoloration	12/15/1998
115.3 to 115.2	Staining	
115.1 to 114.9	Saturated	
114.4 to 113.9	Saturation visible	
113.9 to 113.0	Staining and Saturation	
111.40	Saturation point	

Key Map

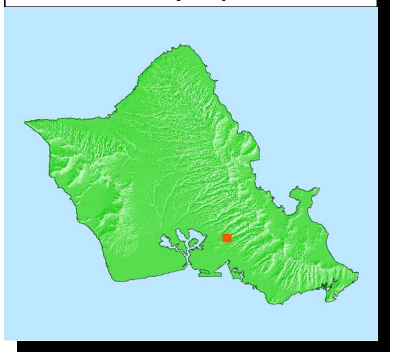

Legend

- Red Hill Fuel Storage Tank- Fuel Odor Noted in Boring Log
- Red Hill Fuel Storage Tank- Sheen or Staining Observed in Boring Log
- Red Hill Fuel Storage Tank- No Evidence of Contamination Observed in Boring Log
- Groundwater Monitoring Well
- Angle Boring
- Groundwater Model Domain
- Red Hill Facility Boundary
- Stream

Notes

1. Map projection: NAD 1983 Hawaii State Plane Zone 3 feet
2. DigitalGlobe, Inc. (DG) and NRCS.
   Publication_Date: 2015
3. References:
   a. Boring logs from DON 2002. Red Hill Bulk Fuel Storage Facility Investigation Report (Final) for Fleet Industrial Supply Center (FISC), Oahu, Hawaii. Prepared by AMEC Earth and Environmental, Inc. for NAVFAC Pacific. August.
   b. Boring logs from DON 1999. Initial Phase II Site Characterization Report, Fleet Industrial Supply Center Bulk Fuel Storage Facility at Red Hill. Prepared by Ogden Environmental and Energy Services Co., Inc. for NAVFAC Pacific. March.

* Elevations presented as "~100" are approximations made based on boring logs and notes in the text.

N

0 200 400 800 Feet

Appendix B.1 Figure 4-1
Soil Contamination at Tank Farm Observed During 1998–2002 Environmental Investigation
Conceptual Site Model Rev. 01
Red Hill Bulk Fuel Storage Facility
JBPHH, O'ahu, Hawai'i

S:\Projects\NAVFAC PAC\CLEAN V\60571032_CTO18F0126\900-Work\920 GIS\02_Maps\CSM\AppB.1_Fig4-1_Red Hill_Soil Contamination-new-v10-2.mxd 6/14/2019

5. References

Boubel, R. W., D. L. Fox, D. B. Turner, and A. C. Stern. 1994. *Fundamentals of Air Pollution*. 3rd ed. Academic Press.

Department of the Navy (DON). 1999. *Initial Phase II Site Characterization Report, Fleet Industrial Supply Center Bulk Fuel Storage Facility at Red Hill*. Prepared by Ogden Environmental and Energy Services Co., Inc., Honolulu, HI. Pearl Harbor, HI: Naval Facilities Engineering Command, Pacific. March.

———. 2002. *Red Hill Bulk Fuel Storage Facility Investigation Report (Final) for Fleet Industrial Supply Center (FISC), Oahu, Hawaii*. Prepared by AMEC Earth & Environmental, Inc., Huntsville, AL. Pearl Harbor, HI: Naval Facilities Engineering Command, Pacific. August.

———. 2017. *Existing Data Summary and Evaluation Report for Groundwater Flow and Contaminant Fate and Transport Modeling, Red Hill Bulk Fuel Storage Facility, Joint Base Pearl Harbor-Hickam, O'ahu, Hawai'i; March 5, 2017, Revision 00*. Prepared by AECOM Technical Services, Inc., Honolulu, HI. Prepared for Defense Logistics Agency Energy, Fort Belvoir, VA, under Naval Facilities Engineering Command, Hawaii, JBPHH HI.

———. 2018. *Groundwater Protection and Evaluation Considerations for the Red Hill Bulk Fuel Storage Facility, Joint Base Pearl Harbor-Hickam, O'ahu, Hawai'i; July 27, 2018, Revision 00*. Prepared by AECOM Technical Services, Inc., Honolulu, HI. Prepared for Defense Logistics Agency Energy, Fort Belvoir, VA, under Naval Facilities Engineering Command, Hawaii, JBPHH HI.

Eppelbaum, L., I. Kutasov, and A. Pilchin. 2014. *Applied Geothermics*. 1st ed. Springer-Verlag Berlin Heidelberg.

Garg, S., C. J. Newell, P. R. Kulkarni, D. C. King, D. T. Adamson, M. I. Renno, and T. Sale. 2017. "Overview of Natural Source Zone Depletion: Processes, Controlling Factors, and Composition Change." *Groundwater Monitoring & Remediation* 37 (3): 62–81. https://doi.org/10.1111/gwmr.12219.

Hillel, D. 1982. *Introduction to Soil Physics*. San Diego, CA: Academic Press.

Interstate Technology & Regulatory Council (ITRC). 2018. *Light Non-Aqueous Phase Liquid (LNAPL) Site Management: LCSM Evolution, Decision Process, and Remedial Technologies*. LNAPL-3. Washington, DC: LNAPL Update Team. March.

Kimmel, G. E., and O. C. Braids. 1980. *Leachate Plumes in Ground Water From Babylon and Islip Landfills, Long Island, New York*. Professional Paper 1085. Prepared in cooperation with the Suffolk County Department of Environmental Control: U.S. Geological Survey.

Martínez, I. 2017. *Fuel Data for Combustion with Air*. Departamento de Motopropulsión y Termofluidodinámica, Universidad Politecnica, Madrid, Spain. http://webserver.dmt.upm.es/~isidoro/dat1/eCombus.pdf.

Nofziger, D. L., and J. Wu. 2003. *Soil Temperature Changes with Time and Depth*. http://soilphysics.okstate.edu/software/SoilTemperature/document.pdf.

Palaia, T., and J. Fitzgibbons. 2018. *Natural Source Zone Depletion (NSZD)*. Retrieved 28 March 2019. https://www.enviro.wiki/index.php?title=Natural_Source_Zone_Depletion_(NSZD).

U.S. Climate Data. 2018. *Climate Honolulu – Hawaii and Weather Averages Honolulu*. https://www.usclimatedata.com/climate/honolulu/hawaii/united-states/ushi0026.

Attachment B.1.1:
Thermal Monitoring Data

GSI ENVIRONMENTAL

ATTACHMENT B.1.1: THERMAL MONITORING DATA
Conceptual Site Model, Investigation and Remediation of Releases and Groundwater Protection and Evaluation
Red Hill Bulk Fuel Storage Facility, JBPHH, O'ahu, HI

Ambient Temperature (C)				
RHMW01	RHMW02	RHMW03	RHMW04	RHMW05
26.60	26.40	26.90	19.80	26.80

	Temperature (C)									
	Well Air Temperature, ft bTOC					Wall Temperature, ft bTOC				
Depth (ft bTOC)	RHMW01	RHMW02	RHMW03	RHMW04	RHMW05	RHMW01	RHMW02	RHMW03	RHMW04	RHMW05
0	25.90	26.40	27.90	20.60	26.50	26.40	26.70	26.50	24.80	26.80
5	25.80	26.40	27.50	23.70	25.70	26.20	26.70	27.70	25.20	25.80
10	25.20	26.40	28.70	25.20	25.30	25.40	26.60	28.30	25.00	25.30
15	25.00	26.40	29.30	25.00	25.00	25.10	26.50	28.60	24.70	25.00
20	24.80	26.40	29.50	24.40	24.80	24.90	26.30	29.00	24.10	24.80
25	24.70	26.30	29.70	24.20	24.60	24.70	26.20	29.20	23.80	24.70
30	24.50	26.10	29.80	23.90	24.60	24.60	26.10	29.30	23.70	24.80
35	24.40	26.00	29.80	23.70	24.60	24.40	25.80	29.60	23.40	24.70
40	24.30	25.80	29.80	23.60	24.50	24.30	25.70	29.50	23.50	24.60
45	24.10	25.70	29.70	23.40	24.50	24.20	25.50	29.40	23.30	24.60
50	24.00	25.50	29.50	23.30	24.50	24.00	25.30	29.30	23.20	24.50
55	23.80	25.30	29.40	23.20	24.40	23.90	25.20	29.20	23.30	24.50
60	23.70	25.00	29.10	23.10	24.40	23.70	24.90	28.90	23.10	24.50
65	23.50	24.80	28.90	23.00	24.40	23.50	24.70	28.70	23.00	24.40
70	23.30	24.70	28.60	22.90	24.30	23.40	24.60	28.40	23.00	
75	23.10	24.50	28.30	22.80	24.20	23.20	24.40	28.10	23.00	
80	23.00	24.30	28.00	22.80	24.10		24.20	27.80	22.90	
83					24.10					
84	22.70									
85			27.60	22.70				27.50	22.80	
86		24.00								
88										
90			27.30	22.60				27.20	22.80	
91	22.40				22.80					
93		23.20								
95			26.90	22.60				26.60	22.70	
96										
98	22.30									
99					21.60					
100		22.80	26.60	22.50					22.60	
103			26.00							
105				22.50					22.60	
110				22.40					22.60	
111			25.80							
115				22.40					22.50	
119			25.40							
120				22.30					22.50	
125				22.30					22.50	
130				22.20					22.40	
135				22.20					22.40	
140				22.10					22.30	
145				22.10					22.30	
150				22.10					22.20	
155				22.00					22.20	
160				22.00					22.10	
165				22.00					22.10	
170				22.00					22.00	
175				22.00					22.00	
180				21.90					22.10	
185				21.90					22.00	
190				21.80					21.90	
195				21.80					22.10	
200				21.80					21.90	
205				21.70					21.60	
210				21.70					21.70	
215				21.60					21.70	
220				21.60					21.70	
225				21.60					21.60	
230				21.50					21.60	
235				21.50					21.60	
240				21.40					21.60	
245				21.40					21.50	
250				21.30					21.50	
255				21.30					21.50	
260				21.30					21.40	
265				21.20					21.40	
270				21.20					21.30	
275				21.10					21.30	
280				21.10					21.20	
285				21.00					21.20	
289				20.90						
297				20.90						
310				20.90						

Appendix B.2:
Carbon Trap NSZD Analysis

CONTENTS

Acronyms and Abbreviations iii

1. Introduction 1-1

2. NSZD Rate Based on Tunnel Carbon Dioxide Flux 2-1

2.1 Carbon Cartridges 2-1

2.1.1 Reason for Difference in NSZD Rates Between Tunnels 2-5

2.2 Carbon Traps 2-6

3. NSZD Rate Based on Ground Surface Carbon Dioxide Flux 3-1

4. Conclusions 4-1

5. References 5-1

ATTACHMENTS

B.2.1 E-Flux Laboratory Reports

FIGURES

2-1 Diagram Showing Carbon Dioxide Measurement Points in the Exhaust Tunnels (E1 and E2) and the Inlet Location (I1) 2-2

2-2 Diagram Showing Carbon Trap Locations in Tunnels 2-7

3-1 Carbon Trap Receiver, Trap (in Uncapped Mode), Rubber Connector, and Rain Cover 3-1

3-2 Locations for Eight Ground Surface Carbon Trap Deployments at Facility with Results in gal/acre/yr 3-2

3-3 Area Encompassed by Traps and Tank Farm for Ground Surface NSZD Calculation 3-3

4-1 Conceptual Illustration of Carbon Dioxide Flux to Ground Surface and Tunnels 4-1

TABLES

2-1 Carbon Cartridge Results 2-1

2-2 Calculation of Upper-Bound NSZD Rate from Unadjusted Carbon Cartridge Results in Upper Tunnel 2-3

2-3 Calculation of Upper-Bound NSZD Rate from Unadjusted Carbon Cartridge Results in Lower Tunnel 2-4

2-4 Total Upper-Bound NSZD Rate Calculated from Unadjusted Carbon Cartridge Results 2-4

2-5 Calculation of Lower-Bound NSZD Rate from Adjusted Carbon Cartridge Results in Upper Tunnel 2-4

2-6 Calculation of Lower-Bound NSZD Rate from Adjusted Carbon Cartridge Results in Lower Tunnel 2-5

2-7 Total Lower-Bound NSZD Rate Calculated from Adjusted Carbon Cartridge Results 2-5

2-8 Results from Tunnel Carbon Traps 2-6

3-1 Results from Ground Surface Carbon Traps 3-2

4-1 Calculation of Tunnel-Induced Ventilation of the Unsaturated Zone Required to Sustain Aerobic Conditions 4-2

ACRONYMS AND ABBREVIATIONS

^{14}C	carbon-14
cm^3	cubic centimeter
CO_2	carbon dioxide
ft^3	cubic foot
g	gram
gal	gallon
L	liter
LNAPL	light non-aqueous-phase liquid
min	minute
mol	mole
NSZD	natural source-zone depletion
O_2	oxygen
yr	year

1. Introduction

This subappendix is summarized in Section 7.3.1.4 of the Conceptual Site Model main document.

Natural source-zone depletion (NSZD) is the active process whereby light non-aqueous-phase liquid (LNAPL) is degraded in the subsurface by biodegradation and other naturally occurring processes. For this report, LNAPL consists of petroleum hydrocarbons in the form of various fuels. NSZD is now emerging as an important remediation approach for petroleum hydrocarbon sites (Garg et al. 2017). As described in Garg et al. (2017), a variety of methods have been used to obtain NSZD rates.

One such method is the carbon dioxide efflux method (or "carbon trap" method). This method measures the amount of carbon dioxide being generated through the biodegradation of LNAPL. The carbon dioxide is captured using two carbon dioxide sorbent elements comprised of soda lime (consisting primarily of calcium hydroxides), which are contained in a canister, over LNAPL zones (McCoy et al. 2014). The carbon dioxide generated by LNAPL biodegradation is transported to the surface by diffusion, and in some cases advection, and is trapped in one sorbent element. Another sorbent element prevents atmospheric carbon dioxide from being captured by the first sorbent element. Traps are typically deployed in receivers in the field for 14 days and then sent to the laboratory. The carbon-14 fraction (^{14}C correction) is also measured in the laboratory so that "modern carbon" (e.g., carbon dioxide generated from biodegradation of recent plant material) can be separated from "ancient carbon" (carbon dioxide associated with the biodegradation of fossil fuel). The efflux rate of ancient carbon is used to calculate a NSZD rate in units of gallons per acre per year (gal/acre/yr). Due to the unique construction of the Facility, conventional carbon traps were used to measure carbon dioxide flux at the ground surface and modified carbon cartridges were used to measure carbon dioxide flux into the tunnels.

2. NSZD Rate Based on Tunnel Carbon Dioxide Flux

2.1 CARBON CARTRIDGES

The ventilation system in the tunnels creates a negative pressure gradient within the tank access tunnels (i.e., a pressure gradient from the basalt into the tunnel), so that advective gas flow is from the vadose zone into the tunnels (see CSM Appendix B.3). As a result, the tunnels act like a soil vapor extraction system and can capture ancient (i.e., petrogenic) carbon dioxide generated through biological NSZD occurring in the vadose zone. This reduces the carbon dioxide captured by any traps installed on the top and sides of the tank farm (Figure 3-2; Section 3). It was unknown beforehand whether this gas flow is mostly via fractures in the concrete/gunite lined tunnels or from the permeability of the concrete/gunite (competent concrete permeability to gas flow is low but measurable).

To measure any NSZD-related carbon dioxide pulled into the tunnels in this manner, a custom measurement procedure was deployed in the exhaust tunnels of the tank farm (Figure 2-1) at several locations including E1 near exhaust fan 1-A in the upper tunnel, E2 near exhaust fan 2-A in the lower tunnel, and I1 near the inlet fan at Adit 6. Carbon dioxide concentrations in the tunnels were measured through the collection of 24-hour air samples pumped through carbon trap cartridges.

The results from the carbon cartridges are shown in Table 2-1. The carbon dioxide mass sorbed on the sorbent element was corrected to remove the modern carbon signal using ^{14}C measurements (Attachment B.2.1). The unadjusted fossil fuel carbon dioxide (CO_2) (ancient carbon) calculation used a standard fraction of modern carbon in contemporary living material of 1.05 (Hua, Barbetti, and Rakowski 2013). However, the measurements from the inlet showed some non-zero fossil fuel CO_2 values, so the fraction of modern carbon in contemporary living material was altered to 1.038, so that the average of the fossil fuel CO_2 values from the inlet (I1) would be zero in the adjusted values.

The volume of air forced through the trap was then used to provide an ancient carbon concentration. This concentration of ancient carbon in the exhaust gas was multiplied by the design air flow rate of the ventilation system at the various sampling locations (Figure 2-1) to obtain an ancient carbon mass discharge rate. The mass discharge rate was then converted to a NSZD rate in units of gallons per year (gal/yr).

Table 2-1: Carbon Cartridge Results

Cartridge ID	Unadjusted Fossil Fuel CO_2 (g)	Adjusted Fossil Fuel CO_2 (g)	Pumping Rate (L/min)	Sample Time (min)	Sample Volume (L)
E1a	0.02	0.01	1.06	1,335	1,415
E1b	0.04	0.02	1.06	1,447	1,534
E2a	0.09	0.07	1.06	1,322	1,401
E2b	0.08	0.06	1.06	1,453	1,540
I1a	0.03	0.02	1.06	1,397	1,481
I1b	Non-detect	Non-detect	1.06	1,328	1,408

g gram
L liter
min minute

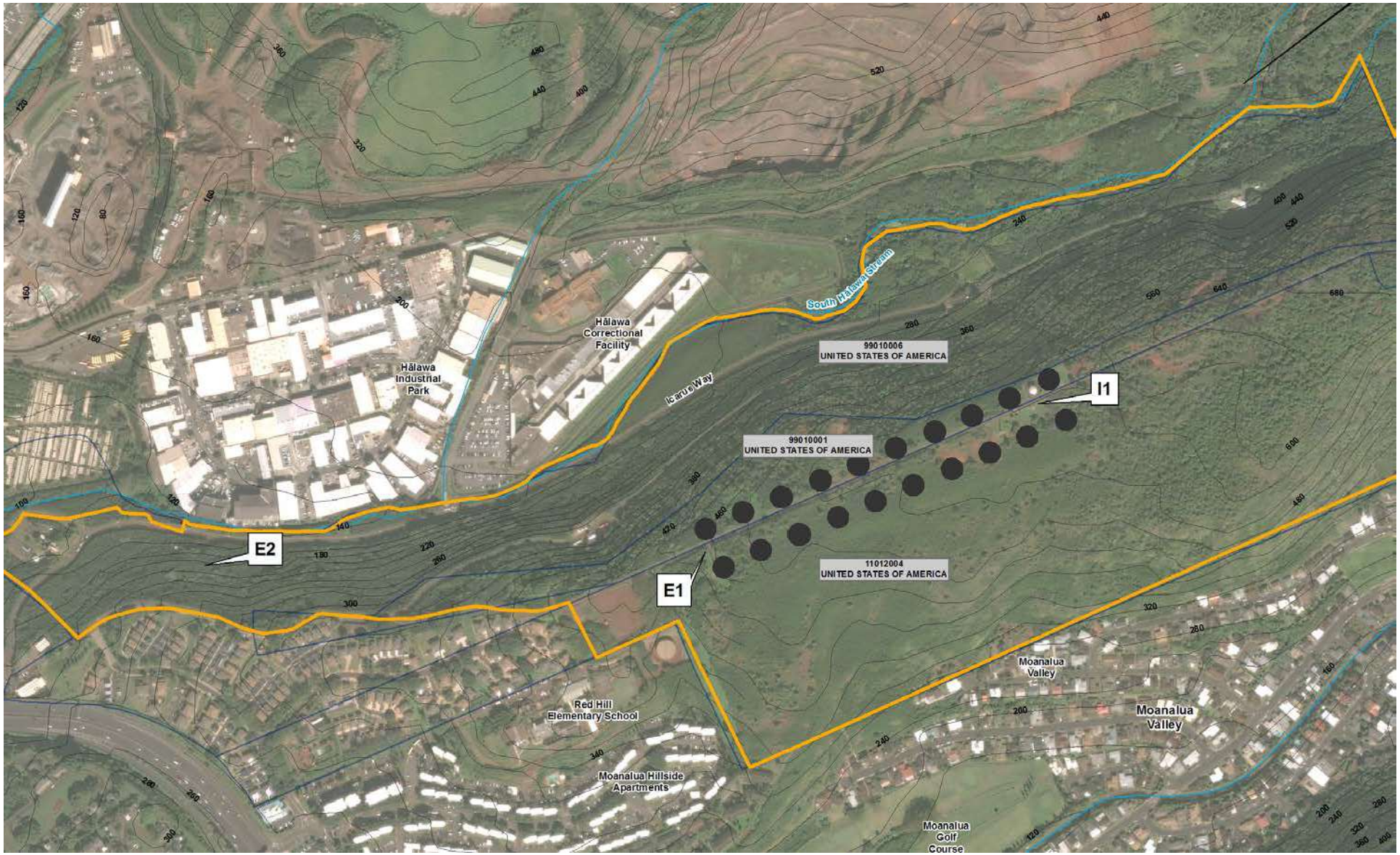

1 **Figure 2-1: Diagram Showing Carbon Dioxide Measurement Points in the Exhaust Tunnels (E1 and E2) and the Inlet Location (I1)**

The calculations using unadjusted fossil fuel CO_2 values are shown in Table 2-2, Table 2-3, and Table 2-4. This provides an upper bound for the NSZD rate based on carbon dioxide flowing into the tunnels. A lower bound was calculated by running the same calculations but using the adjusted values and assuming a lesser air flow rate through the tunnels. Based on communications with the Navy (pers. comm., December 5, 2017, email message from John Floyd to Curtis C. Stanley, GSI Environmental, "RE: 4671 Tunnel Ventilation Questions for Navy"), for 14 hours per day (58% of each day) during this sampling, air flows in the tunnels may have decreased by 50%, so, as a conservative estimate, all flows were decreased by 29% (50% decrease for 58% of the time). The calculations using adjusted fossil fuel CO_2 values and decreased flow rates are shown in Table 2-5, Table 2-6, and Table 2-7.

Table 2-2: Calculation of Upper-Bound NSZD Rate from Unadjusted Carbon Cartridge Results in Upper Tunnel

Parameter	Value	Reasoning
Average E1 Fossil Fuel CO_2	0.03 g CO_2	Calculation [(0.02 g CO_2 + 0.04 g CO_2) / 2] (Table 2-1)
Average E1 Sample Volume	1,474 L air	Calculation [(1,415 L + 1,534 L) / 2] (Table 2-1)
Average Fossil Fuel CO_2 Concentration	2.0×10^{-5} g CO_2/L air 5.8×10^{-4} g CO_2/ft^3 air	Calculation (0.03 g CO_2 / 1,474 L) 1 L = 0.0353 ft^3
Air Flow Rate in Upper Tunnel	16,000 ft^3 air/min	Red Hill Mechanical New Airflow Diagram - Scheme 3 (InSynergy Engineering 2013)
CO_2 Flow Rate in Upper Tunnel	9.2 g CO_2/min 0.2 mol CO_2/min	Calculation (5.8×10^{-4} g CO_2/ft^3 air × 16,000 ft^3 air/min) Mol weight of CO_2 = 44 g/mol
Stoichiometric Ratio of CO_2 to Jet Fuel	11 mol CO_2/mol fuel	Taken from degradation equation: $C_{11}H_{24} + 17O_2 \rightarrow 11CO_2 + 12H_2O$
Jet Fuel NSZD Rate (Upper Tunnel)	0.02 mol fuel/min 3.0 g fuel/min	Calculation (0.2 mol CO_2/min / 11 mol CO_2/mol fuel) Mol weight of fuel = 156 g/mol
Density of Jet Fuel	0.78 g fuel/cm^3 fuel	Tien et al. (2015)
Jet Fuel NSZD Rate (Upper Tunnel)	3.8 cm^3 fuel/min 0.001 gal fuel/min **529 gal fuel/yr**	Calculation (3.0 g fuel/min / 0.78 g fuel/cm^3 fuel) 1 cm^3 = 0.000264 gal 525,600 min = 1 year

cm^3 cubic centimeter
ft^3 cubic foot
gal gallon
L liter
mol mole
yr year

Table 2-3: Calculation of Upper-Bound NSZD Rate from Unadjusted Carbon Cartridge Results in Lower Tunnel

Parameter	Value	Reasoning
Average E2 Fossil Fuel CO_2	0.085 g CO_2	Calculation [(0.09 g CO_2 + 0.08 g CO_2) / 2] (Table 2-1)
Average E2 Sample Volume	1,471 L air	Calculation [(1,401 L + 1,540 L) / 2] (Table 2-1)
Average Fossil Fuel CO_2 Concentration	5.8×10^{-5} g CO_2/L air 1.6×10^{-3} g CO_2/ft^3 air	Calculation (0.085 g CO_2 / 1,471 L) 1 L = 0.0353 ft^3
Air Flow Rate in Lower Tunnel	63,000 ft^3 air/min	Red Hill Mechanical New Airflow Diagram - Scheme 3 (InSynergy Engineering 2013)
CO_2 Flow Rate in Lower Tunnel	103 g CO_2/min 2.3 mol CO_2/min	Calculation (1.6×10^{-3} g CO_2/ft^3 air × 63,000 ft^3 air/min) Mol weight of CO_2 = 44 g/mol
Stoichiometric Ratio of CO_2 to Jet Fuel	11 mol CO_2/mol fuel	Taken from degradation equation: $C_{11}H_{24} + 17O_2 \rightarrow 11CO_2 + 12H_2O$
Jet Fuel NSZD Rate (Lower Tunnel)	0.21 mol fuel/min 33 g fuel/min	Calculation (2.3 mol CO_2/min / 11 mol CO_2/mol fuel) Mol weight of fuel = 156 g/mol
Density of Jet Fuel	0.78 g fuel/cm^3 fuel	Tien et al. (2015)
Jet Fuel NSZD Rate (Lower Tunnel)	43 cm^3 fuel/min 0.01 gal fuel/min **5,916 gal fuel/yr**	Calculation (33 g fuel/min / 0.78 g fuel/cm^3 fuel) 1 cm^3 = 0.000264 gal 525,600 min = 1 year

Table 2-4: Total Upper-Bound NSZD Rate Calculated from Unadjusted Carbon Cartridge Results

Location	NSZD Rate (gal/year)
Upper Tunnel	529
Lower Tunnel	5,916
Both Tunnels (Total)	**6,445**

Table 2-5: Calculation of Lower-Bound NSZD Rate from Adjusted Carbon Cartridge Results in Upper Tunnel

Parameter	Value	Reasoning
Average E1 Fossil Fuel CO_2	0.015 g CO_2	Calculation [(0.01 g CO_2 + 0.02 g CO_2) / 2] (Table 2-1)
Average E1 Sample Volume	1,474 L air	Calculation [(1,415 L + 1,534 L) / 2] (Table 2-1)
Average Fossil Fuel CO_2 Concentration	1.0×10^{-5} g CO_2/L air 2.9×10^{-4} g CO_2/ft^3 air	Calculation (0.015 g CO_2 / 1,474 L) 1 L = 0.0353 ft^3
Air Flow Rate in Upper Tunnel	11,300 ft^3 air/min	Red Hill Mechanical New Airflow Diagram - Scheme 3 (InSynergy Engineering 2013). Air flow rate reduced by 29% as described in text above.
CO_2 Flow Rate in Upper Tunnel	3.3 g CO_2/min 0.074 mol CO_2/min	Calculation (2.9×10^{-4} g CO_2/ft^3 air × 11,300 ft^3 air/min) Mol weight of CO_2 = 44 g/mol
Stoichiometric Ratio of CO_2 to Jet Fuel	11 mol CO_2/mol fuel	Taken from degradation equation: $C_{11}H_{24} + 17O_2 \rightarrow 11CO_2 + 12H_2O$
Jet Fuel NSZD Rate (Upper Tunnel)	0.0067 mol fuel/min 1.1 g fuel/min	Calculation (0.074 mol CO_2/min / 11 mol CO_2/mol fuel) Mol weight of fuel = 156 g/mol
Density of Jet Fuel	0.78 g fuel/cm^3 fuel	Tien et al. (2015)
Jet Fuel NSZD Rate (Upper Tunnel)	1.3 cm^3 fuel/min 3.6×10^{-4} gal fuel/min **187 gal fuel/yr**	Calculation (1.1 g fuel/min / 0.78 g fuel/cm^3 fuel) 1 cm^3 = 0.000264 gal 525,600 min = 1 year

Table 2-6: Calculation of Lower-Bound NSZD Rate from Adjusted Carbon Cartridge Results in Lower Tunnel

Parameter	Value	Reasoning
Average E2 Fossil Fuel CO_2	0.065 g CO_2	Calculation [(0.07 g CO_2 + 0.06 g CO_2) / 2] (Table 2-1)
Average E2 Sample Volume	1,471 L air	Calculation [(1,401 L + 1,540 L) / 2] (Table 2-1)
Average Fossil Fuel CO_2 Concentration	4.4×10^{-5} g CO_2/L air 1.3×10^{-3} g CO_2/ft^3 air	Calculation (0.065 g CO_2 / 1,471 L) 1 L = 0.0353 ft^3
Air Flow Rate in Lower Tunnel	44,600 ft^3 air/min	Red Hill Mechanical New Airflow Diagram - Scheme 3 (InSynergy Engineering 2013). Air flow rate reduced by 29% as described in text above.
CO_2 Flow Rate in Lower Tunnel	56 g CO_2/min 1.3 mol CO_2/min	Calculation (1.3×10^{-3} g CO_2/ft^3 air × 44,600 ft^3 air/min) Mol weight of CO_2 = 44 g/mol
Stoichiometric Ratio of CO_2 to Jet Fuel	11 mol CO_2/mol fuel	Taken from degradation equation: $C_{11}H_{24} + 17O_2 \rightarrow 11CO_2 + 12H_2O$
Jet Fuel NSZD Rate (Lower Tunnel)	0.12 mol fuel/min 18 g fuel/min	Calculation (1.3 mol CO_2/min / 11 mol CO_2/mol fuel) Mol weight of fuel = 156 g/mol
Density of Jet Fuel	0.78 g fuel/cm^3 fuel	Tien et al. (2015)
Jet Fuel NSZD Rate (Lower Tunnel)	23 cm^3 fuel/min 0.0061 gal fuel/min **3,205 gal fuel/yr**	Calculation (18 g fuel/min / 0.78 g fuel/cm^3 fuel) 1 cm^3 = 0.000264 gal 525,600 min = 1 year

Table 2-7: Total Lower-Bound NSZD Rate Calculated from Adjusted Carbon Cartridge Results

Location	NSZD Rate (gal/year)
Upper Tunnel	187
Lower Tunnel	3,205
Both Tunnels (Total)	**3,392**

From these calculations, then, the NSZD rate from carbon dioxide entering the tunnels is between 3,400 and 6,400 gal/yr.

2.1.1 Reason for Difference in NSZD Rates Between Tunnels

In both the upper-bound and lower-bound calculations, the calculated NSZD rate for the lower tunnel was much higher (more than 10 times as large) than the calculated NSZD rate for the upper tunnel. This is because much more ancient carbon dioxide entered the lower tunnel from the basalt compared to the upper tunnel, as seen by the calculations for CO_2 flow rates through each tunnel in Table 2-2, Table 2-3, Table 2-5, and Table 2-6.

The higher rate of ancient carbon dioxide influx in the lower tunnel is caused by a combination of factors: (1) more LNAPL in the basalt is likely to be near the low portion of the tanks and below, which allows more carbon dioxide to enter the lower tunnel than the upper tunnel and (2) the lower tunnel's much higher flow rate (about four times as large) than the upper tunnel. Because of these two factors, significantly more ancient CO_2 flows through the lower tunnel than the upper tunnel, and, thus, the calculated NSZD rate from the carbon cannisters in the lower tunnel is much higher than the calculated NSZD rate from the carbon cannisters in the upper tunnel.

2.2 CARBON TRAPS

Two carbon traps (with a trip blank) were also sealed onto the tunnel floor at locations shown in Figure 2-2 as follows: F1 (between tanks T5 and T6 in the upper access tunnel) and F2 (between tanks T5 and T-6 in the lower access tunnel). A silicon sealer/grout was used to determine if there was a measurable carbon dioxide flux through the tunnel walls/floor. The grout was placed to allow any gas migrating directly through the concrete/gunite but not allow any transport from the tunnel air into the trap. The specific locations for trap deployment were selected to minimize the potential for disturbance during the sample period. A trip blank was placed at F2; any ancient carbon dioxide detected in the trip blank is subtracted from the ancient carbon detected in the exposed samples before calculating NSZD rates. The results from these tunnel traps are shown in Table 2-8.

Table 2-8: Results from Tunnel Carbon Traps

Trap ID	NSZD Rate (gal/acre/yr)
F1	0
F2	10

Attachment B.2.1 explains the process of developing these values from the carbon trap measurements. The NSZD rates measured indicate that some carbon dioxide is flowing into the tunnels through the competent concrete/gunite, but at very low to zero rates. Because of their low values, the carbon dioxide flow rate through the tunnel floor is likely low. Most of the carbon dioxide flow rate into the tunnels, therefore, must be occurring through various cracks in the tunnel and not directly through the concrete/gunite.

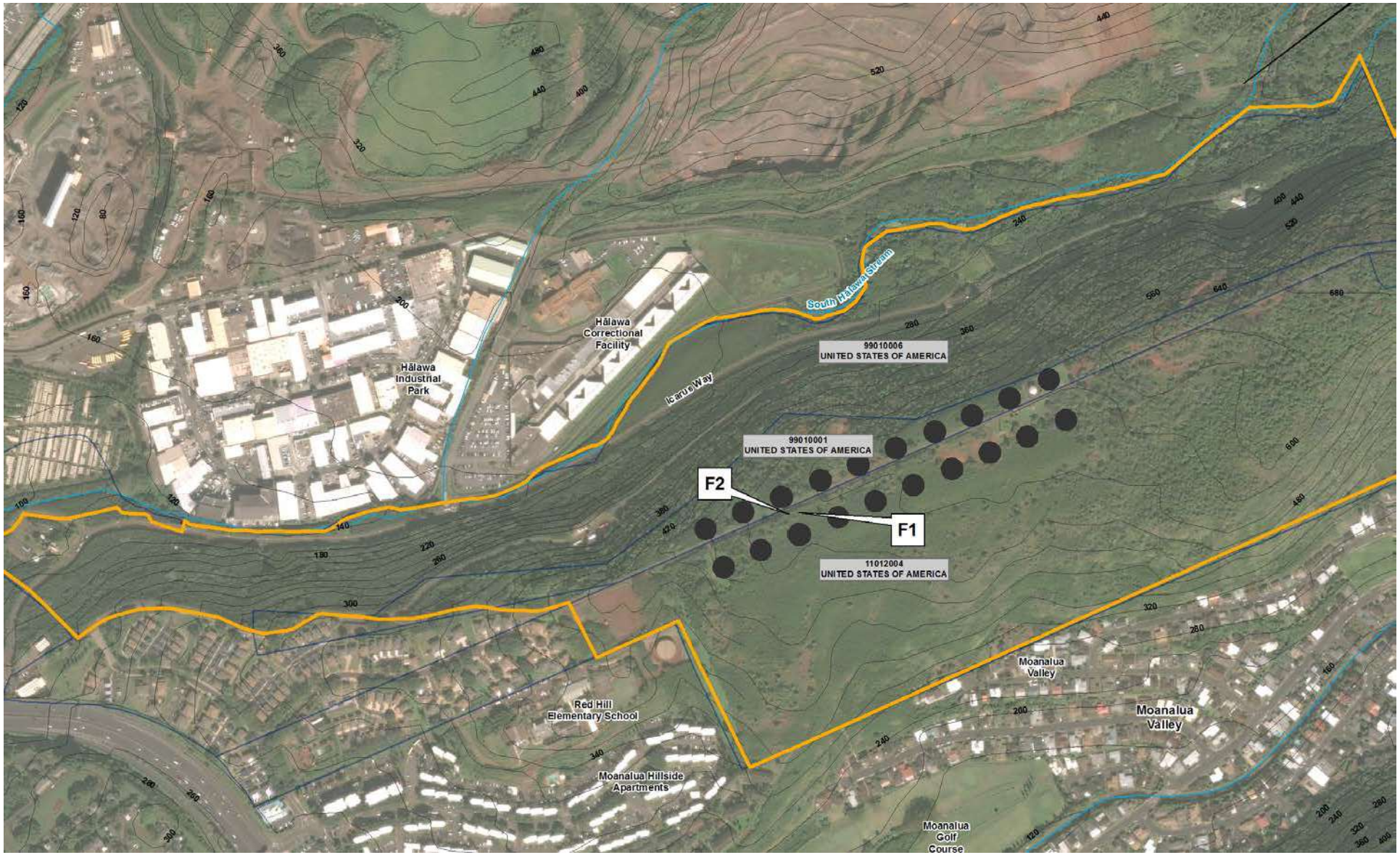

Figure 2-2: Diagram Showing Carbon Trap Locations in Tunnels

3. NSZD Rate Based on Ground Surface Carbon Dioxide Flux

Eight carbon traps (with a trip blank) were deployed for 14 days on the top and sides of the tank farm to measure carbon dioxide efflux in the conventional manner assuming that the carbon dioxide being generated by NSZD might diffuse upwards and/or sideways out of the tank farm (E-Flux, 3185-A Rampart Road, #250D Fort Collins, CO 80521 970-492-4360). Installing carbon traps involves installing a trap receiver, placing the trap into the receiver, inserting a diffusion cap, and placing a rain cover on the entire assembly (Figure 3-1).

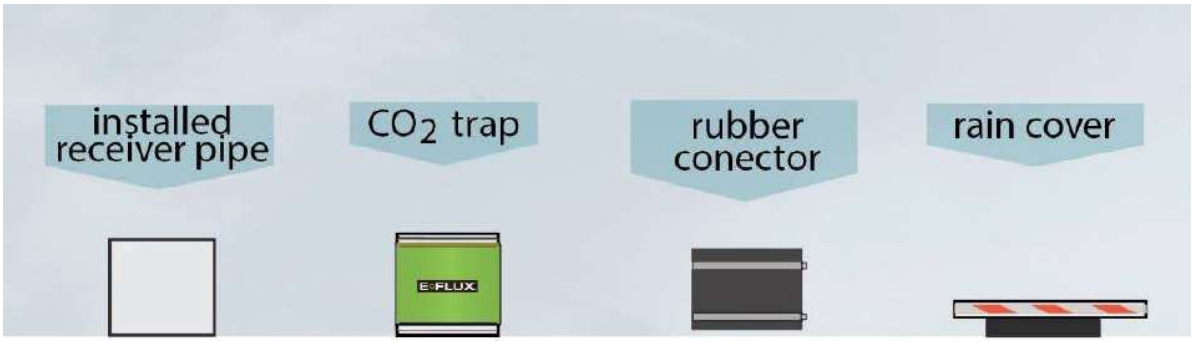

Figure 3-1: Carbon Trap Receiver, Trap (in Uncapped Mode), Rubber Connector, and Rain Cover

Eight traps were deployed on the top and sides of the tank farm using E-Flux standard operating procedures. Locations are summarized below and shown on Figure 3-2:

- A line of four traps (T1 to T4) was placed transverse to the tank farm, with one on the north side, one on the south side, and two near the top of the tank farm near Tanks 5 and 6, which is a known impact area based on soil vapor data. T1 and T4 were placed on clinker zone outcrops on the side of the tank farm. A trip blank was placed at T2; any ancient carbon dioxide detected in the trip blank is subtracted from the ancient carbon detected in the exposed samples before calculating NSZD rates.
- A second line of four traps was placed transverse to the tank farm, with one on the north side, one on the south side, and two near the top of the tank farm near Tanks 11 and 12, which is a zone with potentially less LNAPL impacts based on soil vapor data. T5 and T8 were placed on clinker zone outcrops on the side of the tank farm.

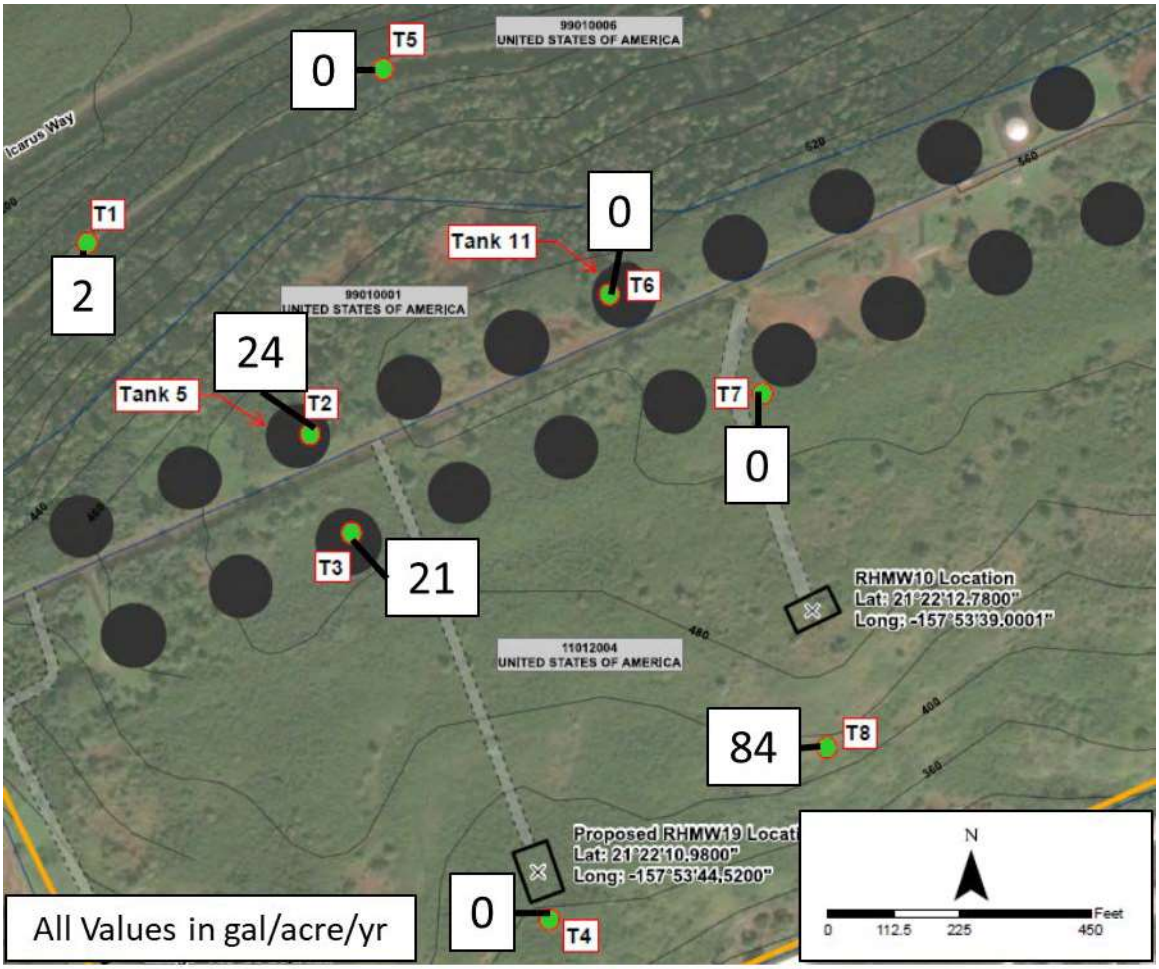

Figure 3-2: Locations for Eight Ground Surface Carbon Trap Deployments at Facility with Results in gal/acre/yr

The results from the analysis of these traps are shown in Table 3-1.

Table 3-1: Results from Ground Surface Carbon Traps

Trap ID	NSZD Rate (gal/acre/yr)
T1	2
T2	24
T3	21
T4	0
T5	0
T6	0
T7	0
T8	84

Attachment B.2.1 explains the process of developing these values from the carbon trap measurements. The rates measured by these traps were fairly low and in some cases zero, indicating that ancient

carbon flux to the ground surface is low and variable. It is worth noting, however, that the largest rate measured was in one of the traps that was placed on a clinker outcrop. This suggests that the carbon dioxide from the NSZD does indeed preferentially flow laterally through the clinker zones to the surface. Assuming the ancient carbon flux from NSZD that was measured by these traps is happening in the area encompassed by the traps and the tank farm, an average NSZD rate was calculated in gal/yr (a collective rate over the area, rather than an individual rate in gal/acre/yr). This was done by taking an average of all the NSZD rates (16 gal/acre/year) and multiplying this by the area encompassed by the traps and the tank farm (61.1 acres; Figure 3-3). The total NSZD rate attributable to ground surface ancient carbon flux from top and sides of the tank farm from this calculation comes to about 1,000 gal/yr.

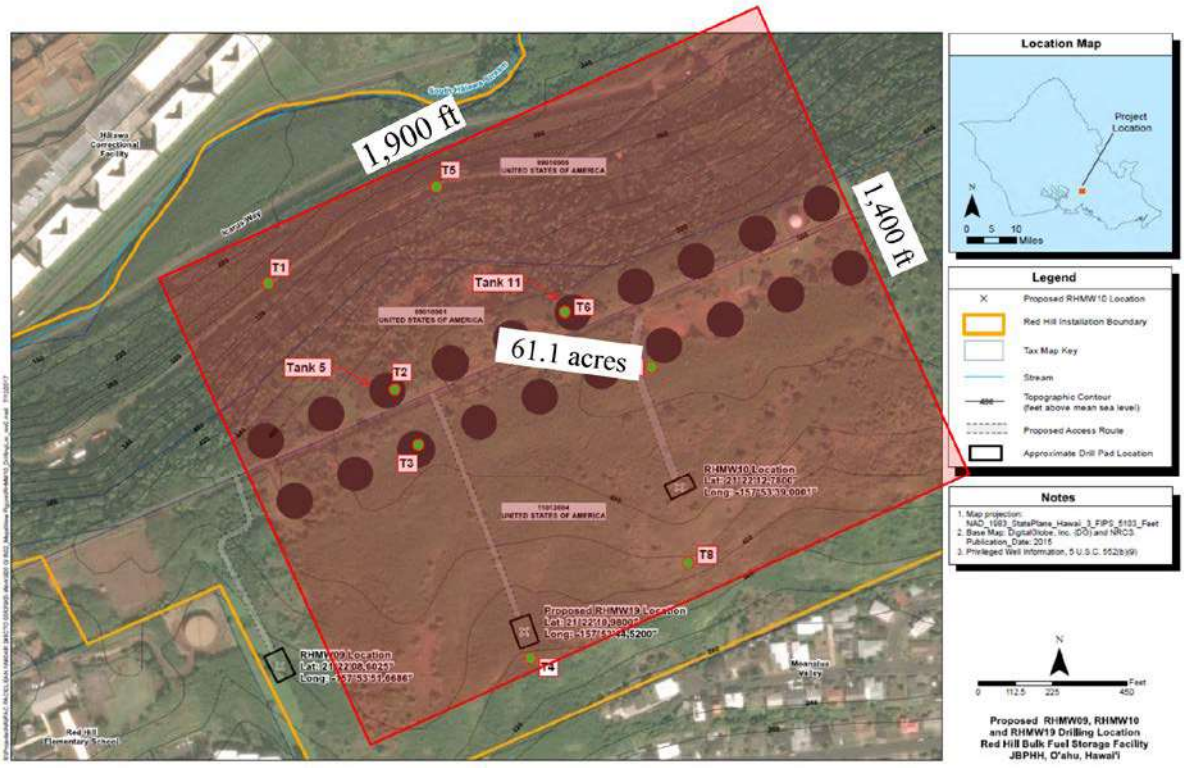

Figure 3-3: Area Encompassed by Traps and Tank Farm for Ground Surface NSZD Calculation

4. Conclusions

Carbon cartridges and traps were installed within the tunnels and on the top and sides of the tank farm. Based on the mass of ancient carbon sorbed to these cartridges and traps, an approximate NSZD rate was determined.

From the cartridges, a range of 3,400–6,400 gal/yr was calculated. Little to no NSZD was seen in the tunnel traps set on the tunnel floor, indicating that the carbon dioxide within the tunnels was mostly entering through cracks, not directly through the concrete/gunite. From the ground surface traps, a value of 1,000 gal/yr outside the tunnels was calculated.

Therefore, the majority of the NSZD is from the tunnel acting like a partial soil vapor extraction system (Figure 4-1), pulling carbon dioxide from the basalt into the tunnels. The two NSZD rates (tunnel and hill top) are additive, however, so, the total NSZD rate in the tank farm is between 4,400 and 7,400 gal/yr.

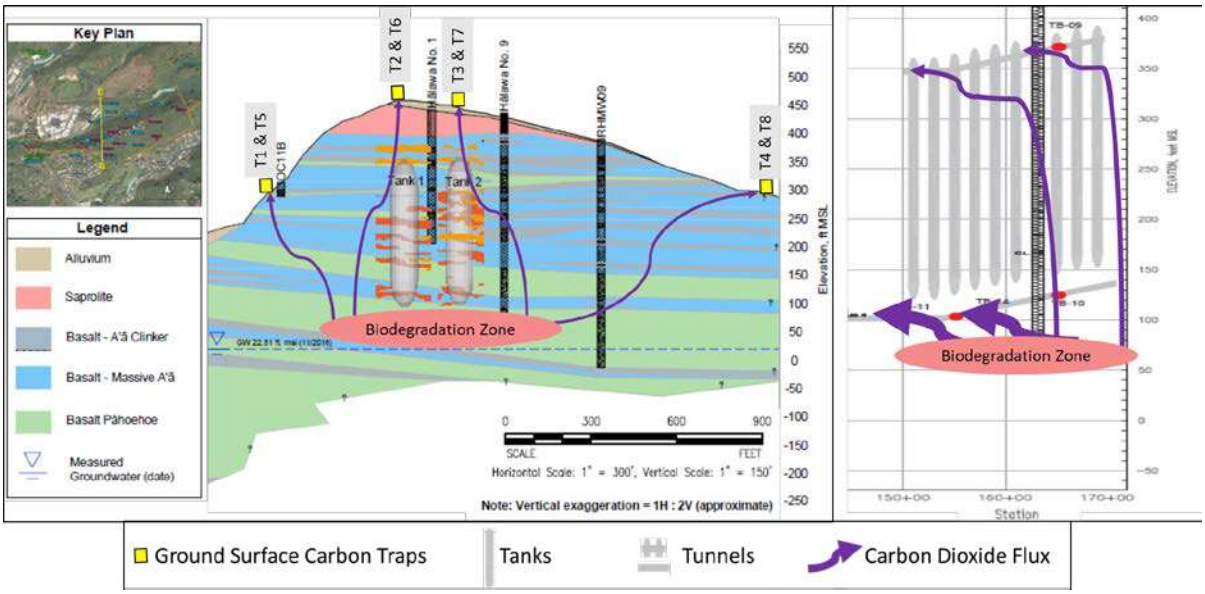

Notes: Thicker arrows indicate greater flux. Location of tanks, traps, and biodegradation zones are approximate.

Figure 4-1: Conceptual Illustration of Carbon Dioxide Flux to Ground Surface and Tunnels

Furthermore, if less than 0.5% of air flow through the tunnel originates from the vadose zone (rather than the tunnel entrances), then the resulting ventilation of the vadose zone would be sufficient to provide 100% of the oxygen needed to support the observed NSZD while maintaining vadose zone oxygen concentrations above 19% (Table 4-1). Thus, only a small amount of leakage from the unsaturated zone into the tunnels through the tunnel walls is required to provide sufficient air flow through the unsaturated zone to sustain aerobic biodegradation.

Table 4-1: Calculation of Tunnel-Induced Ventilation of the Unsaturated Zone Required to Sustain Aerobic Conditions

Parameter	Value	Reasoning
NSZD Rate	6,400 gal fuel/yr 2.4 x10^7 cm^3 fuel/yr	Upper Bound NSZD Rate (Table 2-4) 1 cm^3 = 0.000264 gal
Density of Jet Fuel	0.78 g fuel/cm^3 fuel	Tien et al. (2015)
NSZD Rate	1.9 x10^7 g fuel/yr	Calculation (2.4×10^7 cm^3 fuel/yr × 0.78 g fuel/cm^3 fuel)
Molecular Weight of Jet Fuel	156 g fuel/mol fuel	Assume that Jet Fuel is $C_{11}H_{24}$
NSZD Rate	121,100 mol fuel/yr	Calculation (1.9 x10^7 g fuel/yr / 156 g fuel/mol fuel)
Stoichiometric Ratio of O_2 to Jet Fuel	17 mol O_2/mol fuel	Taken from degradation equation: $C_{11}H_{24} + 17O_2 \rightarrow 11CO_2 + 12H_2O$
O_2 Consumption Rate	2.1 x10^6 mol O_2/yr	Calculation (121,100 mol fuel/yr × 17 mol O_2/mol fuel)
Molecular Weight of O_2	32 g O_2/mol O_2	Known
O_2 Consumption Rate	6.6 x10^7 g O_2/yr	Calculation (2.1 x10^6 mol O_2/yr × 32 g O_2/mol O_2)
Density of O_2	1.43 g O_2/L O_2	Known
O_2 Consumption Rate	4.6 x10^7 L O_2/yr	Calculation (6.6 x10^7 g O_2/yr / 1.43 g O_2/LO_2)
Percentage of O_2 in Air	21%	Known
Air flow rate to sustain aerobic conditions in basalt	2.2 x10^8 L air/yr 7.8 x10^6 ft^3 air /yr	Calculation (4.6 x10^7 L O_2/yr / 21%) 1 L = 0.0353 ft^3
Current Air Flow Rate in Tunnels	79,000 ft^3 air/min 4.2 x10^{10} ft^3 air/yr	Sum of Upper and Lower Tunnel Flow Rates 525,600 min = 1 year
Percentage of Current Air Flow Rate in Tunnel Required to Sustain Aerobic Conditions in Basalt	0.02%	Calculation (7.8 x10^6 ft^3 air/yr / 4.2 x10^{10} ft^3 air/yr)

Note: As reported in CSM Appendix B.3, an oxygen (O_2) concentration of 19% was seen in the unsaturated zone, suggesting that only 10% of the available O_2 is being utilized for biodegradation. Thus, up to 10 times as much air flow through the basalt might be required to sustain an average oxygen concentration of 19% in the basalt (i.e., 0.2% of the air flow through the tunnel).

5. References

Garg, S., C. J. Newell, P. R. Kulkarni, D. C. King, D. T. Adamson, M. I. Renno, and T. Sale. 2017. "Overview of Natural Source Zone Depletion: Processes, Controlling Factors, and Composition Change." *Groundwater Monitoring & Remediation*, July. https://doi.org/10.1111/gwmr.12219.

Hua, Q., M. Barbetti, and A. Z. Rakowski. 2013. "Atmospheric Radiocarbon for the Period 1950–2010." *Radiocarbon* 55 (4): 2059–072.

InSynergy Engineering. 2013. *Red Hill Mechanical New Airflow Diagram - Scheme 3*.

McCoy, K., J. Zimbron, T. Sale, and M. Lyverse. 2014. "Measurement of Natural Losses of LNAPL Using CO_2 Traps." *Groundwater* 53: 658–667.

Tien, C-J., Y-Y. Shu, S-R. Ciou, and C. S. Chen. 2015. "Partitioning of Aromatic Constituents into Water from Jet Fuels." *Arch Environ Contam Toxicol* 69: 153–162. https://doi.org/10.1007/s00244-015-0154-7.

Attachment B.2.1:
E-Flux Laboratory Reports

ATTACHMENT B.2.1: E-FLUX LAB REPORTS
Conceptual Site Model, Investigation and Remediation of Releases and Groundwater Protection and Evaluation
Red Hill Bulk Fuel Storage Facility, JBPHH, Oʻahu, HI

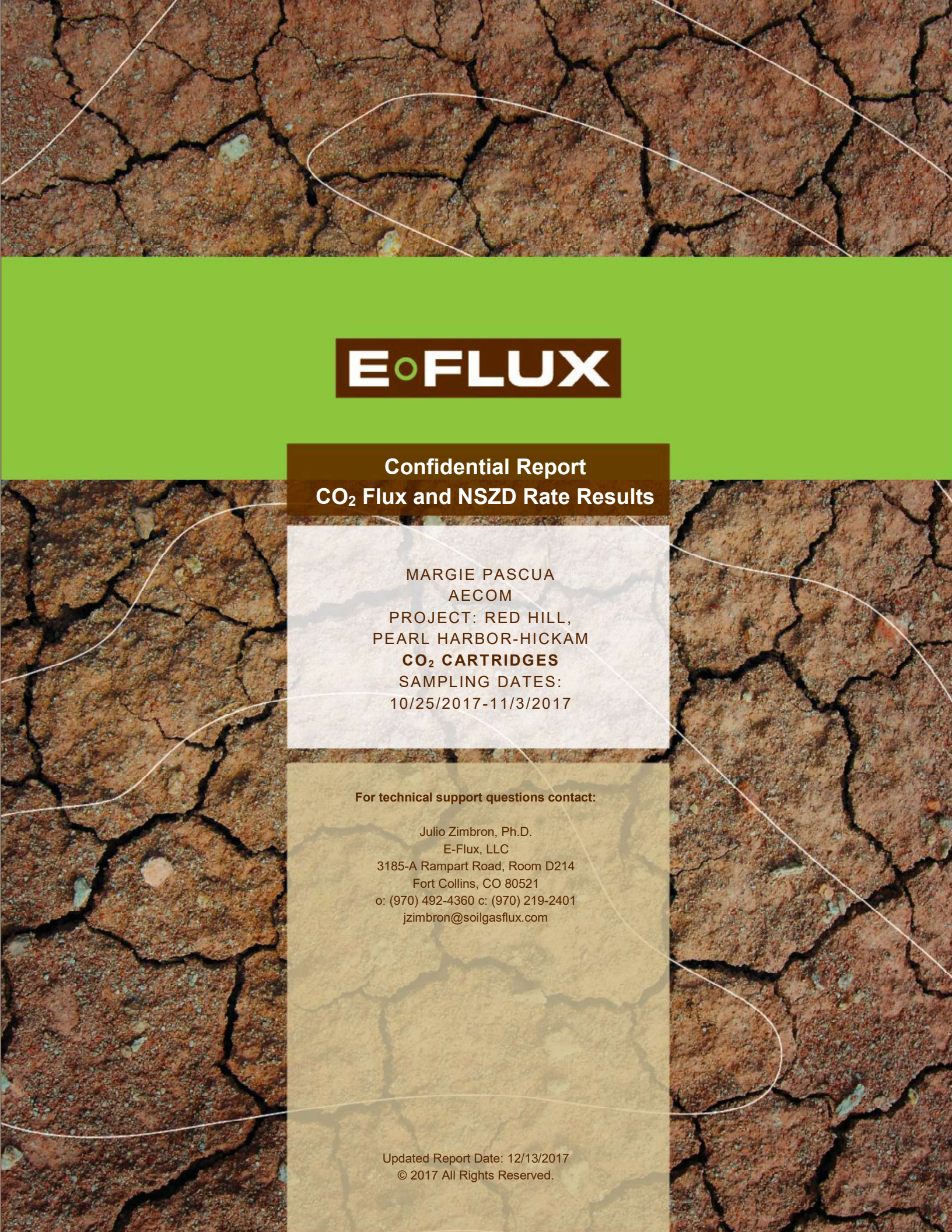

Confidential Report
CO_2 Flux and NSZD Rate Results

MARGIE PASCUA
AECOM
PROJECT: RED HILL,
PEARL HARBOR-HICKAM
CO_2 CARTRIDGES
SAMPLING DATES:
10/25/2017-11/3/2017

For technical support questions contact:

Julio Zimbron, Ph.D.
E-Flux, LLC
3185-A Rampart Road, Room D214
Fort Collins, CO 80521
o: (970) 492-4360 c: (970) 219-2401
jzimbron@soilgasflux.com

Updated Report Date: 12/13/2017
© 2017 All Rights Reserved.

This report is for measurement of the mass of fossil fuel-derived CO_2 using cartridges. The purpose of this document is to provide sample calculations of the results reported here and to explain the basis for differentiating petroleum hydrocarbon-derived CO_2 (i.e., fossil fuel CO_2) from modern CO_2 interferences. The following topics are addressed:

- The Value of ^{14}C Analysis
- Site Specific Study Results and Applicable Notes
- Calculation Explanations
- References

The Value of the ^{14}C Analysis

How to differentiate petroleum hydrocarbon-derived CO_2 from modern CO_2 interferences.

Unimpacted soils have natural CO_2 flux generation rates, due to microbial root zone activity and/or the degradation of natural organic matter (NOM). Thus, the total CO_2 flux measured at an impacted location is the sum of both natural soil respiration processes and those related to LNAPL degradation (Sihota et al, 2011).

This report uses carbon isotopic analysis (14C) to determine the contributions to an environmental sample sorbed into CO2 cartridges from both modern and fossil fuel sources, using ASTM Method D6686-12.

Carbon Isotope Analysis Methodology

Sampling was done using CO_2 cartridges loaded with a predetermined mass of CO_2 sorbent. Upon retrieval and shipment to the lab, the samples were homogenized and analyzed for total CO_2 and ^{14}C using methods described before (McCoy et al, 2015).

Unstable isotopic analysis has been previously used to differentiate anthropogenic (due to fossil fuel-burning) and natural sources of atmospheric CO, CO_2 and methane (for example, Klouda and Connolly, 1995; Levin et al, 1995; Avery et al, 2006). Such findings are the basis of ASTM Method D6686-12, Determining the Biobased Content in Solids, Liquids and Gases Using Radiocarbon Analysis (ASTM, 2012). The technique relies on the analysis of ^{14}C, an unstable carbon isotope (with a half-life of approximately 5600 years) that is generated by cosmic rays in the atmosphere. Thus, contemporary (modern) organic carbon is ^{14}C-rich, while fossil fuel carbon is completely ^{14}C-depleted. Furthermore, contemporary samples and atmospheric samples have the same characteristic amount of ^{14}C. The detection limit of ^{14}C by accelerator mass spectrometry enables dating of samples younger than 60,000 years, while older samples (such as fossil fuels) have non-detectable ^{14}C activity (Stuiver and Polach, 1977).

For a sample that contains carbon from both modern and fossil fuel carbon sources, measurement of the ^{14}C enables quantitation of both source contributions. The fossil fuel fraction of the sample, ff_{sample}, and the remaining non-fossil fuel or contemporary fraction ($1- ff_{sample}$), are related by the following two-component mass balance:

©2017 All Rights Reserved

$$Fm_{sample} = ff_{sample}\left(Fm_{ff}\right) + \left(1 - ff_{sample}\right)\left(Fm_{atm}\right)$$

In this formula, Fm_{sample} is the measured modern fraction of the sample, Fm_{ff} is the fraction of modern carbon in fossil fuel ($Fm_{ff} = 0$), and Fm_{atm} is the fraction of modern carbon in contemporary living material ($Fm_{atm} = 1.05$) (Hua et al., 2013). By convention, the reporting of carbon isotope analysis is based on a 1950 NBS oxalic acid standard, synthesized when the ^{14}C atmospheric levels were lower than current ones due to nuclear tests. Thus, Fm_{sample} is reported as if the analysis was done in 1950, and Fm_{atm} is counter-intuitively larger than 1.

Expected Results and Recommendations

The fossil-fuel carbon content on the unexposed sorbent is non-zero (typically around 35%). This might be the result of either a background fossil fuel signature of the sorbent (due to processing of the chemical or mineral sources), or due to material handling (i.e., exposure to fossil fuel fumes). Although the fossil fuel CO_2 mass is very small, this error is adjusted by a travel blank correction procedure. This consists of subtracting the fossil fuel CO_2 mass from an unexposed trap (a travel blank) from those measured on the traps deployed in the field. The ^{14}C analysis is done on CO_2 sorbent subsamples, after homogenization.

©2017 All Rights Reserved

Study Results

The report and results below are based on proprietary technology to measure the fossil fuel content of an environmental sample using E-Flux CO_2 cartridges. All information contained in this report is strictly confidential to the customer. The chemical analysis is based on methods ASTM 4373-02 (Rapid Determination for Carbonate Content in Soils) and ASTM D6686-12 (Determining the Biobased Content in Solids, Liquids and Gases Using Radiocarbon Analysis).

The site specific results and interpretation are as follows:

E◦FLUX
Easy set-up. Expert results.

Project: Red Hill, Pearl Harbor-Hickam CO_2 Traps

Customer: AECOM

Customer Contact: Margie Pascua, (808) 356-5373

Updated Report Date: 13-Dec-17

Sample ID	Deployment Dates			Raw Results (not blank corrected)					Blank Corrected Results[a] and ^{14}C Analysis (Fossil Fuel)					
	Deployed	Retrieved	Days	Moisture	Dry Sorbent Mass (g)	Num. of Reps.[b]	Avg CO_2[b]	CV CO_2[c]	Carbon Content[d] %	Carbon Content[d] (g)	Modern Carbon, As Reported[e]	Std. Dev. Modern	Adjusted Fossil Fuel Carbon[f]	Grams Of Fossil Fuel CO_2 (g)
PHHI-C1-CO2-TB	NA	NA	0.00	20.6%	4.136	2	0.91%	7.22%	-	-	65.3%	0.30%	37.1%	-
PHHI-C1-CO2-01	10/25/17 10:05	10/26/17 8:20	0.93	3.1%	4.858	2	25.92%	0.57%	25.0%	1.22	101.8%	0.40%	1.9%	0.01
PHHI-C1-CO2-02	10/26/17 8:26	10/27/17 8:33	1.00	3.0%	4.882	2	25.40%	0.77%	24.5%	1.20	100.5%	0.33%	3.1%	0.02
PHHI-C1-CO2-03	10/30/17 9:56	10/31/17 7:58	0.92	3.0%	5.005	2	28.41%	0.03%	27.5%	1.38	97.4%	0.32%	6.1%	0.07
PHHI-C1-CO2-04	10/31/17 8:00	11/1/17 8:13	1.01	2.9%	5.101	2	30.29%	0.07%	29.4%	1.50	98.3%	0.33%	5.3%	0.06
PHHI-C1-CO2-05	11/1/17 8:45	11/2/17 8:02	0.97	4.4%	4.877	2	25.57%	0.08%	24.7%	1.20	100.8%	0.30%	2.8%	0.02
PHHI-C1-CO2-06	11/2/17 8:07	11/3/17 6:15	0.92	3.0%	4.817	2	23.62%	0.99%	22.7%	1.09	104.0%	0.50%	ND	ND

This report contains Confidential Information and is to be delivered only to the Customer indicated above.

See following page for assumptions, project specific quality assurance/quality control information, and notes.

The Following Assumptions and General Notes apply for CO_2 fossil fuel analysis:

a. Results are travel blank corrected but not background location corrected.
Blank Corrected Results = Raw Results - Travel Blank

b. Number of Replicates: Carbon analysis was conducted in duplicate if CV ≤ 5%. If CV > 5%, carbon analysis was conducted with triplicates (see Quality Assurance/Quality Control notes). Avg % refers to the percent of CO_2 in the dry sorbent mass before blank corrected.

c. CV is coefficient of variation, equal to the ratio of the standard deviation over the average.

d. If the cartridge carbon content is not larger than travel blank, results are reported as ND. Expressed as CO_2 not pure carbon.

e. "As reported" refers to % modern carbon at the time of development of the test (1950).

f. Adjusted fossil fuel carbon has been transformed from the "As reported" basis (1950) to present ^{14}C levels.

g. Note that for this report a value of 1.038 was used in place of 1.05 so that the average grams of fossil fuel carbon for samples PHHI-C1-CO2-05 and PHHI-C1-CO2-06 equaled 0.

NA means Not Applicable.

Quality Assurance / Quality Control Notes:

- The Travel Blank (**PHHI-C1-CO2-TB**) concentration for this report was **0.91%**. Typical Travel Blank concentration is <2%.
- Cartridge tops were not saturated with CO_2, but some had appreciable CO_2 contents. The mass sorbed in the top element was up to 20% of the total mass sorbed in the whole cartridge. Because of the configuration of these cartridges, this could indicate CO_2 breakthrough from the bottom element, and total carbon may be underestimated by these results. Maximum measured top concentration was **8.20%** (sample **PHHI-C1-CO2-02.1**). Sorbent saturation is 30%.
- ASTM 4373-02 QA/QC criteria does not provide acceptable variability (CV) standards. Similar methods (for example the carbonates in water, such as ASTM 513.02) provide typical error ≤20%. E-Flux practice is that a CV ≤5% is acceptable. *Sample **PHHI-C1-CO2-TB** had a CV of **7.22%**; this could not be brought down to acceptable levels, as there was not enough sample mass.*

Calculation Explanations

Conversion of Modern C to Fossil Fuel C

Reported modern carbon content (from carbon dating or ^{14}C analysis) is by convention at the ^{14}C levels as of the time of development of the test (1950). Due to higher current levels of ^{14}C in the environment resulting from atomic testing, current (contemporary) levels are approximately 5% higher than in 1950 (Hua et al., 2013). Thus, fossil fuel C can be found with the following conversions:

$$\%\ Modern\ C_{contemporary} = \frac{\%\ Modern\ C_{1950}}{1.05}$$

$$Contemporary\ fossil\ fuel\ C\ \% = 1 - \%\ Modern\ C_{contemporary} = 1 - \frac{\%\ Modern\ C_{1950}}{1.05}$$

Note that for this report a value of 1.038 was used in place of 1.05 so that the average grams of fossil fuel carbon for samples PHHI-C1-CO2-05 and PHHI-C1-CO2-06 equaled 0.

Calculating Grams of Fossil Fuel CO_2

Calculating grams of fossil fuel (ff) CO_2 is based on the travel blank corrected percent fossil fuel carbon in the sample (the difference between total fossil fuel CO_2 in the sample and that of the travel blank). This is done as follows:

$$g\ CO_{2(ff)} = g\ sorbent * \left((Avg\ sample\ \%\ CO_2 * ff\ sample\ \%\ C) - (Avg\ TB\ \%\ CO_2 * ff\ TB\ \%\ C)\right)$$

N/A

References

ASTM (2012), Method D6686-12, Determining the Biobased Content in Solids, Liquids and Gases Using Radiocarbon Analysis.

ASTM (2002), Method D4373-02, Standard Test Method for Rapid Determination of Carbonate Content of Soil.

Avery et al, (2006). Carbon isotopic characterization of dissolved organic carbon in rainwater: Terrestrial and marine influences. Atmos. Environ. p. 7539-7545.

Bauer, H.P.; Beckett, P.H.; and Bie, S.W. (1972). A Rapid Gravimetric Method for Estimating Calcium Carbonate in Soils, Plant and Soil, Vol 37, p. 689-690.

Hua, Q.; Barbetti, M.; and Rakowski, A.Z. (2013). Atmospheric Radiocarbon for the Period 1950-2010. Radiocarbon. 55(4), p. 2059-2072.

Klouda and Connolly, (1995). Radiocarbon (14C) Measurements to Quantify Sources of Atmospheric Carbon Monoxide in Urban Air. Atmos. Environ. p. 3309-3318.

Levin, I. R. Graul, Ne. Trivett. (1995). Long-term observations of atmospheric CO_2 and carbon isotopes at continental sites in Germany. Tellus., 47B, p. 23-34.

McCoy, K., Zimbron, J., Sale, T. and Lyverse, M. (2015), Measurement of Natural Losses of LNAPL Using CO2 Traps. Groundwater, 53: p. 658–667. doi:10.1111/gwat.12240.

Stuiver and Polach, (1977). Discussion. Reporting of ^{14}C data. Radiocarbon 19(3), p. 355–363.

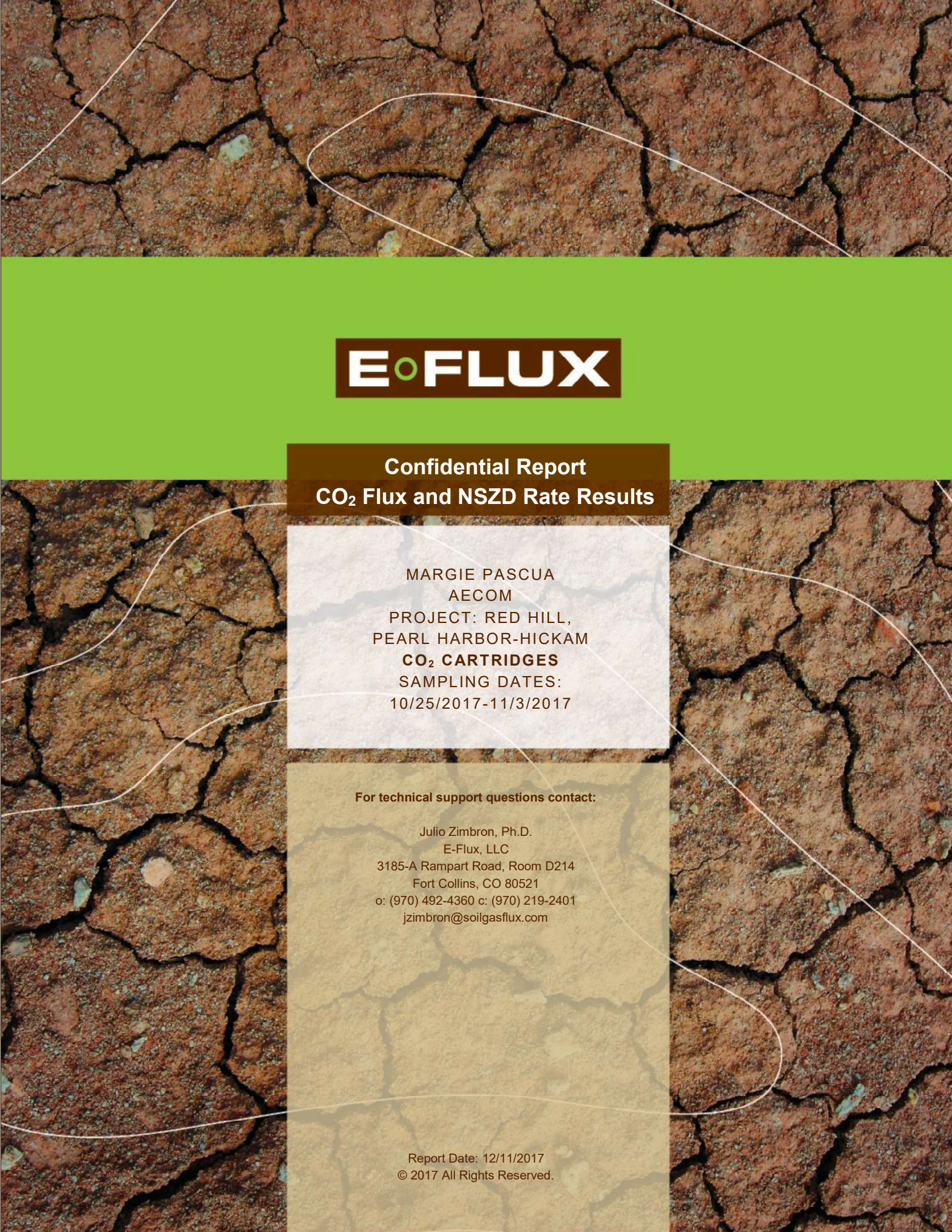

Confidential Report
CO_2 Flux and NSZD Rate Results

MARGIE PASCUA
AECOM
PROJECT: RED HILL,
PEARL HARBOR-HICKAM
CO_2 CARTRIDGES
SAMPLING DATES:
10/25/2017-11/3/2017

For technical support questions contact:

Julio Zimbron, Ph.D.
E-Flux, LLC
3185-A Rampart Road, Room D214
Fort Collins, CO 80521
o: (970) 492-4360 c: (970) 219-2401
jzimbron@soilgasflux.com

Report Date: 12/11/2017
© 2017 All Rights Reserved.

©2017 All Rights Reserved

This report is for measurement of the mass of fossil fuel-derived CO_2 using cartridges. The purpose of this document is to provide sample calculations of the results reported here and to explain the basis for differentiating petroleum hydrocarbon-derived CO_2 (i.e., fossil fuel CO_2) from modern CO_2 interferences. The following topics are addressed:

- The Value of ^{14}C Analysis
- Site Specific Study Results and Applicable Notes
- Calculation Explanations
- References

The Value of the ^{14}C Analysis

How to differentiate petroleum hydrocarbon-derived CO_2 from modern CO_2 interferences.

Unimpacted soils have natural CO_2 flux generation rates, due to microbial root zone activity and/or the degradation of natural organic matter (NOM). Thus, the total CO_2 flux measured at an impacted location is the sum of both natural soil respiration processes and those related to LNAPL degradation (Sihota et al, 2011).

This report uses carbon isotopic analysis (14C) to determine the contributions to an environmental sample sorbed into CO2 cartridges from both modern and fossil fuel sources, using ASTM Method D6686-12.

Carbon Isotope Analysis Methodology

Sampling was done using CO_2 cartridges loaded with a predetermined mass of CO_2 sorbent. Upon retrieval and shipment to the lab, the samples were homogenized and analyzed for total CO_2 and ^{14}C using methods described before (McCoy et al, 2015).

Unstable isotopic analysis has been previously used to differentiate anthropogenic (due to fossil fuel-burning) and natural sources of atmospheric CO, CO_2 and methane (for example, Klouda and Connolly, 1995; Levin et al, 1995; Avery et al, 2006). Such findings are the basis of ASTM Method D6686-12, Determining the Biobased Content in Solids, Liquids and Gases Using Radiocarbon Analysis (ASTM, 2012). The technique relies on the analysis of ^{14}C, an unstable carbon isotope (with a half-life of approximately 5600 years) that is generated by cosmic rays in the atmosphere. Thus, contemporary (modern) organic carbon is ^{14}C-rich, while fossil fuel carbon is completely ^{14}C-depleted. Furthermore, contemporary samples and atmospheric samples have the same characteristic amount of ^{14}C. The detection limit of ^{14}C by accelerator mass spectrometry enables dating of samples younger than 60,000 years, while older samples (such as fossil fuels) have non-detectable ^{14}C activity (Stuiver and Polach, 1977).

For a sample that contains carbon from both modern and fossil fuel carbon sources, measurement of the ^{14}C enables quantitation of both source contributions. The fossil fuel fraction of the sample, ff_{sample}, and the remaining non-fossil fuel or contemporary fraction ($1- ff_{sample}$), are related by the following two-component mass balance:

©2017 All Rights Reserved

$$Fm_{sample} = ff_{sample}\left(Fm_{ff}\right) + \left(1 - ff_{sample}\right)\left(Fm_{atm}\right)$$

In this formula, Fm_{sample} is the measured modern fraction of the sample, Fm_{ff} is the fraction of modern carbon in fossil fuel ($Fm_{ff} = 0$), and Fm_{atm} is the fraction of modern carbon in contemporary living material ($Fm_{atm} = 1.05$) (Hua et al., 2013). By convention, the reporting of carbon isotope analysis is based on a 1950 NBS oxalic acid standard, synthesized when the ^{14}C atmospheric levels were lower than current ones due to nuclear tests. Thus, Fm_{sample} is reported as if the analysis was done in 1950, and Fm_{atm} is counter-intuitively larger than 1.

Expected Results and Recommendations

The fossil-fuel carbon content on the unexposed sorbent is non-zero (typically around 35%). This might be the result of either a background fossil fuel signature of the sorbent (due to processing of the chemical or mineral sources), or due to material handling (i.e., exposure to fossil fuel fumes). Although the fossil fuel CO_2 mass is very small, this error is adjusted by a travel blank correction procedure. This consists of subtracting the fossil fuel CO_2 mass from an unexposed trap (a travel blank) from those measured on the traps deployed in the field. The ^{14}C analysis is done on CO_2 sorbent subsamples, after homogenization.

©2017 All Rights Reserved

Study Results

The report and results below are based on proprietary technology to measure the fossil fuel content of an environmental sample using E-Flux CO_2 cartridges. All information contained in this report is strictly confidential to the customer. The chemical analysis is based on methods ASTM 4373-02 (Rapid Determination for Carbonate Content in Soils) and ASTM D6686-12 (Determining the Biobased Content in Solids, Liquids and Gases Using Radiocarbon Analysis).

The site specific results and interpretation are as follows:

E◦FLUX
Easy set-up. Expert results.

Project: Red Hill, Pearl Harbor-Hickam

Customer: AECOM

Customer Contact: Margie Pascua, (808) 356-5373

Report Date: 11-Dec-17

Sample ID	Deployment Dates			Raw Results (not blank corrected)					Blank Corrected Results[a] and ^{14}C Analysis (Fossil Fuel)					
	Deployed	Retrieved	Days	Moisture	Dry Sorbent Mass (g)	Num. of Reps.[b]	Avg CO_2[b]	CV CO_2[c]	Carbon Content[d] %	Carbon Content[d] (g)	Modern Carbon, As Reported[e]	Std. Dev. Modern	Adjusted Fossil Fuel Carbon[f]	Grams Of Fossil Fuel CO_2 (g)
PHHI-C1-CO2-TB	NA	NA	0.00	20.6%	4.136	2	0.91%	7.22%	-	-	65.3%	0.30%	37.8%	-
PHHI-C1-CO2-01	10/25/17 10:05	10/26/17 8:20	0.93	3.1%	4.858	2	25.92%	0.57%	25.0%	1.22	101.8%	0.40%	3.1%	0.02
PHHI-C1-CO2-02	10/26/17 8:26	10/27/17 8:33	1.00	3.0%	4.882	2	25.40%	0.77%	24.5%	1.20	100.5%	0.33%	4.3%	0.04
PHHI-C1-CO2-03	10/30/17 9:56	10/31/17 7:58	0.92	3.0%	5.005	2	28.41%	0.03%	27.5%	1.38	97.4%	0.32%	7.2%	0.09
PHHI-C1-CO2-04	10/31/17 8:00	11/1/17 8:13	1.01	2.9%	5.101	2	30.29%	0.07%	29.4%	1.50	98.3%	0.33%	6.4%	0.08
PHHI-C1-CO2-05	11/1/17 8:45	11/2/17 8:02	0.97	4.4%	4.877	2	25.57%	0.08%	24.7%	1.20	100.8%	0.30%	4.0%	0.03
PHHI-C1-CO2-06	11/2/17 8:07	11/3/17 6:15	0.92	3.0%	4.817	2	23.62%	0.99%	22.7%	1.09	104.0%	0.50%	0.9%	ND

This report contains Confidential Information and is to be delivered only to the Customer indicated above.

See following page for assumptions, project specific quality assurance/quality control information, and notes.

The Following Assumptions and General Notes apply for CO_2 traps:

a. Results are travel blank corrected but not background location corrected.
Blank Corrected Results = Raw Results - Travel Blank

b. Number of Replicates: Carbon analysis was conducted in duplicate if CV ≤ 5%. If CV > 5%, carbon analysis was conducted with triplicates (see Quality Assurance/Quality Control notes). Avg % refers to the percent of CO_2 in the dry sorbent mass before blank corrected.

c. CV is coefficient of variation, equal to the ratio of the standard deviation over the average.

d. If the cartridge carbon content is not larger than travel blank, results are reported as ND. Expressed as CO_2 not pure carbon.

e. "As reported" refers to % modern carbon at the time of development of the test (1950).

f. Adjusted fossil fuel carbon has been transformed from the "As reported" basis (1950) to present ^{14}C levels.

NA means Not Applicable.

Quality Assurance / Quality Control Notes:

- The Travel Blank (**PHHI-C1-CO2-TB**) concentration for this report was **0.91%**. Typical Travel Blank concentration is <2%.
- Cartridge tops were not saturated with CO_2, but some had appreciable CO_2 contents. The mass sorbed in the top element was up to 20% of the total mass sorbed in the whole cartridge. Because of the configuration of these cartridges, this could indicate CO_2 breakthrough from the bottom element, and total carbon may be underestimated by these results. Maximum measured top concentration was **8.20%** (sample **PHHI-C1-CO2-02.1**). Sorbent saturation is 30%.
- **PHHI-C1-CO2-06** showed non-detectable fossil fuel carbon (ND).
- ASTM 4373-02 QA/QC criteria does not provide acceptable variability (CV) standards. Similar methods (for example the carbonates in water, such as ASTM 513.02) provide typical error ≤20%. E-Flux practice is that a CV ≤5% is acceptable. *Sample **PHHI-C1-CO2-TB** had a CV of **7.22%**; this could not be brought down to acceptable levels, as there was not enough sample mass.*

Calculation Explanations

Conversion of Modern C to Fossil Fuel C

Reported modern carbon content (from carbon dating or ^{14}C analysis) is by convention at the ^{14}C levels as of the time of development of the test (1950). Due to higher current levels of ^{14}C in the environment resulting from atomic testing, current (contemporary) levels are approximately 5% higher than in 1950 (Hua et al., 2013). Thus, fossil fuel C can be found with the following conversions:

$$\%\ Modern\ C_{contemporary} = \frac{\%\ Modern\ C_{1950}}{1.05}$$

$$Contemporary\ fossil\ fuel\ C\ \% = 1 - \%\ Modern\ C_{contemporary} = 1 - \frac{\%\ Modern\ C_{1950}}{1.05}$$

Calculating Grams of Fossil Fuel CO_2

Calculating grams of fossil fuel (ff) CO_2 is based on the travel blank corrected percent fossil fuel carbon in the sample (the difference between total fossil fuel CO_2 in the sample and that of the travel blank). This is done as follows:

$$g\ CO_{2(ff)} = g\ sorbent * \left((Avg\ sample\ \%\ CO_2 * ff\ sample\ \%\ C) - (Avg\ TB\ \%\ CO_2 * ff\ TB\ \%\ C)\right)$$

N/A

©2017 All Rights Reserved

References

ASTM (2012), Method D6686-12, Determining the Biobased Content in Solids, Liquids and Gases Using Radiocarbon Analysis.

ASTM (2002), Method D4373-02, Standard Test Method for Rapid Determination of Carbonate Content of Soil.

Avery et al, (2006). Carbon isotopic characterization of dissolved organic carbon in rainwater: Terrestrial and marine influences. Atmos. Environ. p. 7539-7545.

Bauer, H.P.; Beckett, P.H.; and Bie, S.W. (1972). A Rapid Gravimetric Method for Estimating Calcium Carbonate in Soils, Plant and Soil, Vol 37, p. 689-690.

Hua, Q.; Barbetti, M.; and Rakowski, A.Z. (2013). Atmospheric Radiocarbon for the Period 1950-2010. Radiocarbon. 55(4), p. 2059-2072.

Klouda and Connolly, (1995). Radiocarbon (14C) Measurements to Quantify Sources of Atmospheric Carbon Monoxide in Urban Air. Atmos. Environ. p. 3309-3318.

Levin, I. R. Graul, Ne. Trivett. (1995). Long-term observations of atmospheric CO_2 and carbon isotopes at continental sites in Germany. Tellus., 47B, p. 23-34.

McCoy, K., Zimbron, J., Sale, T. and Lyverse, M. (2015), Measurement of Natural Losses of LNAPL Using CO2 Traps. Groundwater, 53: p. 658–667. doi:10.1111/gwat.12240.

Stuiver and Polach, (1977). Discussion. Reporting of ^{14}C data. Radiocarbon 19(3), p. 355–363.

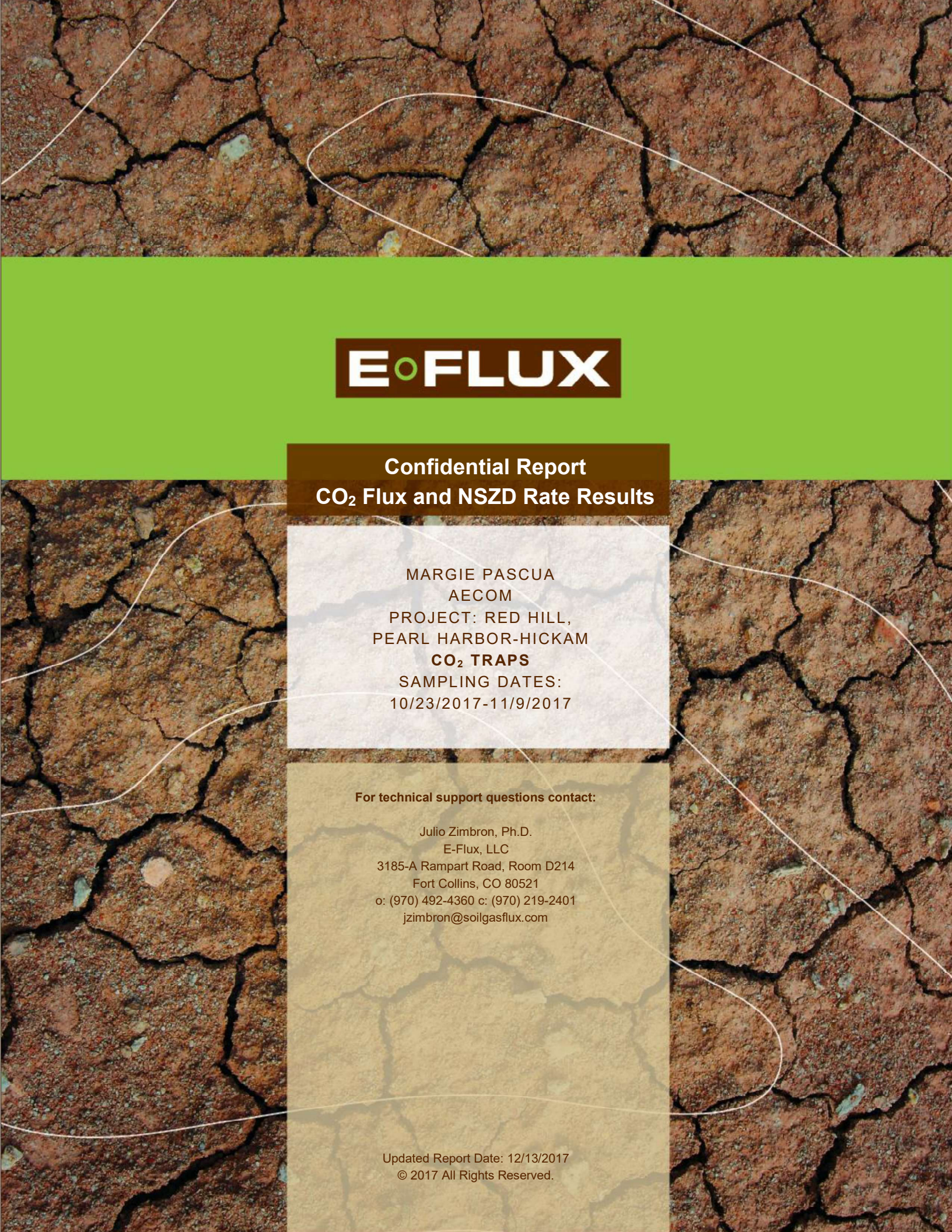

Confidential Report
CO_2 Flux and NSZD Rate Results

MARGIE PASCUA
AECOM
PROJECT: RED HILL,
PEARL HARBOR-HICKAM
CO_2 TRAPS
SAMPLING DATES:
10/23/2017-11/9/2017

For technical support questions contact:

Julio Zimbron, Ph.D.
E-Flux, LLC
3185-A Rampart Road, Room D214
Fort Collins, CO 80521
o: (970) 492-4360 c: (970) 219-2401
jzimbron@soilgasflux.com

Updated Report Date: 12/13/2017
© 2017 All Rights Reserved.

©2017 All Rights Reserved

The purpose of this document is to provide sample calculations of the results reported here and to explain the basis for differentiating petroleum hydrocarbon-derived CO_2 (i.e., fossil fuel CO_2) from modern CO_2 interferences. The following topics are addressed:

- The Value of ^{14}C Analysis
- Site Specific Study Results and Applicable Notes
- Calculation Explanations
- References

The Value of the ^{14}C Analysis

How to differentiate petroleum hydrocarbon-derived CO_2 from modern CO_2 interferences using CO_2 flux traps.

Unimpacted soils have natural CO_2 flux generation rates, due to microbial root zone activity and/or the degradation of natural organic matter (NOM). Thus, the total CO_2 flux measured at an impacted location is the sum of both natural soil respiration processes and those related to LNAPL degradation (Sihota et al, 2011).

The CO_2 flux due to natural soil respiration can be estimated by measuring CO_2 fluxes at unimpacted locations, and subtracting such rates from the total CO_2 fluxes at LNAPL impacted locations in order to estimate CO_2 flux due to LNAPL degradation (Sihota et al, 2012). This is known as the "background correction" and assumes that the rates of natural soil respiration (i.e., modern carbon CO_2 fluxes) are similar for both impacted and unimpacted locations.

The difficulties of this approach are: a) at many industrial facilities it is difficult to find unimpacted locations, and b) the unimpacted locations have very different vegetation to that at the impacted locations. This document provides the basis to use carbon isotope analysis as a location specific correction to the total carbon CO_2 fluxes, designed to overcome the limitations of the background correction.

Carbon Isotope Analysis Methodology

Upon sampling and analysis of the samples by the methods described before (McCoy et al, 2015), the analysis for carbon isotopes is conducted on the homogenized solid samples from the CO_2 flux traps.

Unstable isotopic analysis has been previously used to differentiate anthropogenic (due to fossil fuel-burning) and natural sources of atmospheric CO, CO_2 and methane (for example, Klouda and Connolly, 1995; Levin et al, 1995; Avery et al, 2006). Such findings are the basis of ASTM Method D6686-12, Determining the Biobased Content in Solids, Liquids and Gases Using Radiocarbon Analysis (ASTM, 2012). The technique relies on the analysis of ^{14}C, an unstable carbon isotope (with a half-life of approximately 5600 years) that is generated by cosmic rays in the atmosphere. Thus, contemporary (modern) organic carbon is ^{14}C-rich, while fossil fuel carbon is completely ^{14}C-depleted. Furthermore, contemporary samples and atmospheric samples have the same characteristic amount of ^{14}C. The detection limit of ^{14}C by accelerator mass spectrometry enables dating of samples younger than 60,000

years, while older samples (such as fossil fuels) have non-detectable ^{14}C activity (Stuiver and Polach, 1977).

For a sample that contains carbon from both modern and fossil fuel carbon sources, measurement of the ^{14}C enables quantitation of both source contributions. The fossil fuel fraction of the sample, ff_{sample}, and the remaining non-fossil fuel or contemporary fraction ($1- ff_{sample}$), are related by the following two-component mass balance:

$$Fm_{sample} = ff_{sample}\left(Fm_{ff}\right)+\left(1-ff_{sample}\right)\left(Fm_{atm}\right)$$

In this formula, Fm_{sample} is the measured modern fraction of the sample, Fm_{ff} is the fraction of modern carbon in fossil fuel ($Fm_{ff} = 0$), and Fm_{atm} is the fraction of modern carbon in contemporary living material ($Fm_{atm} = 1.05$) (Hua et al., 2013). By convention, the reporting of carbon isotope analysis is based on a 1950 NBS oxalic acid standard, synthesized when the ^{14}C atmospheric levels were lower than current ones due to nuclear tests. Thus, Fm_{sample} is reported as if the analysis was done in 1950, and Fm_{atm} is counter-intuitively larger than 1.

Expected Results and Recommendations

Our results suggest that the ^{14}C-based technique offers a built-in, location specific correction for fossil fuel as an alternative to the background correction often done at these sites. Earlier data on a limited amount of samples suggested that results using the ^{14}C-correction were equivalent to the background correction (McCoy et al, 2015; Sihota et al, 2012). However, a recent compilation at 4 sites comparing results from the background correction to the ^{14}C-correction suggests that modern carbon fluxes can vary over a factor of 5x for different locations within the same site (Zimbron and Kasyon, 2015). The resulting difference between the background-corrected estimates and the fossil-fuel carbon corrected data can be up to one order of magnitude (depending on the location).

This finding suggests that the assumption implied by the background correction that the modern carbon flux is constant for an entire site might introduce large errors in the correction for petroleum-biodegradation derived CO_2 fluxes. Contrary to the background correction, the ^{14}C-based correction is collocated with the measurement, and thus spatially unbiased by uncertainties related to differences with respect to background location(s) (i.e., due to different vegetation and lithology, unknown impacts, different gas transport regimes, high sensitivity to soil moisture, etc).

The fossil-fuel carbon content on the unexposed sorbent is non-zero (typically around 30%). This might be the result of either a background fossil fuel signature of the sorbent (due to processing of the chemical or mineral sources), or due to material handling (i.e., exposure to fossil fuel fumes). Although the fossil fuel CO_2 mass is very small, this error is adjusted by a travel blank correction procedure. This consists of subtracting the fossil fuel CO_2 mass from an unexposed trap (a travel blank) from those measured on the traps deployed in the field. The ^{14}C analysis is done on CO_2 sorbent subsamples, after homogenization.

©2017 All Rights Reserved

Study Results

The report and results below are based on proprietary technology to measure the soil gas efflux. All information contained in this report is strictly confidential to the customer. The chemical analysis is based on methods ASTM 4373-02 (Rapid Determination for Carbonate Content in Soils) and ASTM D6686-12 (Determining the Biobased Content in Solids, Liquids and Gases Using Radiocarbon Analysis).

The site specific results and interpretation are as follows:

EoFLUX
Easy set-up. Expert results.

Project: Red Hill, Pearl Harbor-Hickam CO_2 Traps

Customer: AECOM

Customer Contact: Margie Pascua, (808) 356-5373

Updated Report Date: 13-Dec-17

Sample ID	Deployment Dates			Raw Results (not blank corrected)					Blank Corrected Results[a] and ^{14}C Analysis (Fossil Fuel)								
	Deployed	Retrieved	Days	Moisture	Dry Sorbent Mass (g)	Num. of Reps.[b]	Avg CO_2[b]	CV CO_2[c]	Carbon Content[d] %	Carbon Content[d] (g)	CO_2 Flux[e] (microM/ m^2.sec)	Modern Carbon, As Reported[g]	Std. Dev. Modern	Modern CO_2 Flux (microM/ m^2.sec)	Adjusted Fossil Fuel Carbon[h]	Grams Of Fossil Fuel CO_2 (g)	Fossil Fuel CO_2 Flux (microM/ m^2.sec)	Equivalent Fossil Fuel-Based NAPL Loss Rate (gallons/ acre.yr)
PHHI-R1-CO2-TB	NA	NA	0.00	19.4%	42.099	2	0.92%	1.21%	-	-	-	64.6%	0.21%	-	37.8%	0	-	-
PHHI-R1-CO2-01	10/26/17 8:20	11/9/17 10:25	14.09	16.9%	42.991	2	1.01%	1.95%	0.1%	0.04	0.1	66.5%	0.24%	0.1	36.0%	0.01	0.0	9
PHHI-R1-CO2-02	10/23/17 13:40	11/6/17 12:20	13.94	25.7%	41.747	2	3.66%	4.35%	2.7%	1.14	2.7	93.9%	0.26%	2.7	9.6%	0.00	0.0	2
PHHI-R1-CO2-03	10/24/17 11:10	11/7/17 12:57	14.07	21.0%	44.178	2	5.08%	1.42%	4.2%	1.84	4.2	98.5%	0.29%	4.3	5.1%	ND	ND	ND
PHHI-R1-CO2-04	10/24/17 16:00	11/7/17 11:15	13.80	25.7%	41.937	2	2.48%	1.42%	1.6%	0.65	1.5	89.9%	0.26%	1.6	13.4%	ND	ND	ND
PHHI-R1-CO2-05	10/24/17 15:10	11/7/17 11:22	13.84	20.7%	44.826	2	5.54%	4.55%	4.6%	2.07	4.9	98.3%	0.34%	4.9	5.3%	ND	ND	ND
PHHI-R1-CO2-06	10/23/17 14:35	11/6/17 12:32	13.91	21.6%	44.412	2	4.76%	0.15%	3.8%	1.71	4.0	97.6%	0.26%	4.0	6.0%	ND	ND	ND
PHHI-R1-CO2-07	10/23/17 11:30	11/6/17 12:05	14.02	24.6%	43.589	2	7.56%	2.15%	6.6%	2.90	6.7	99.6%	0.28%	6.7	4.1%	ND	ND	ND
PHHI-R1-CO2-08	10/25/17 13:20	11/8/17 9:40	13.85	21.5%	45.130	2	5.97%	4.41%	5.0%	2.28	5.3	96.6%	0.27%	5.3	7.0%	0.03	0.1	45
PHHI-R1-CO2-09	10/25/17 12:30	11/8/17 10:00	13.90	23.7%	41.666	2	3.26%	0.23%	2.3%	0.98	2.3	94.1%	0.28%	2.3	9.4%	ND	ND	ND
PHHI-R1-CO2-10	10/26/17 8:50	11/9/17 10:55	14.09	17.8%	42.199	2	0.94%	4.78%	0.0%	0.01	0.0	68.2%	0.26%	0.0	34.3%	ND	ND	ND
PHHI-R1-CO2-TBB	NA	NA	0.00	21.0%	42.595	2	0.97%	0.61%	-	-	-	70.2%	0.21%	-	33.1%	-	-	-

This report contains Confidential Information and is to be delivered only to the Customer indicated above.

See following page for assumptions, project specific quality assurance/quality control information, and notes.

The Following Assumptions and General Notes apply for CO_2 traps:

a. Results are travel blank corrected but not background location corrected.
Blank Corrected Results = Raw Results - Travel Blank

b. Number of Replicates: Carbon analysis was conducted in duplicate if CV ≤ 5%. If CV > 5%, carbon analysis was conducted with triplicates. Avg % refers to the percent of CO_2 in the dry sorbent mass before blank corrected.

c. CV is coefficient of variation, equal to the ratio of the standard deviation over the average.

d. If trap carbon content is not larger than travel blank, results are reported as ND. Expressed as CO_2 not pure carbon.

e. Trap cross sectional area is **8.11×10^{-3}** m^2 (i.e., equivalent to a **4in** receiver pipe).

f. The flux equivalence is 1 microMole/(m^2.sec) equals **625** gallons/(acre.yr). This assumes a hydrocarbon density of **0.77** g/mL and a formula of **C_8H_{18}**.

g. "As reported" refers to % modern carbon at the time of development of the test (1950).

h. Adjusted fossil fuel carbon has been transformed from the "As reported" basis (1950) to present ^{14}C levels.

NA means Not Applicable.

Quality Assurance / Quality Control Notes:

- The Travel Blank (PHHI-R1-CO2-TB) concentration for this report was **0.92%.** Typical Travel Blank concentration is <2%. The additional travel blank (PHHI-R1-CO2-TBB) had a concentration of **0.97%.** Carbon contents were blank-corrected using **PHHI-R1-CO2-TB**.
- Trap tops were not saturated with CO_2. Maximum measured top concentration was **1.85%** (sample **PHHI-R1-CO2-01.1**). Sorbent saturation is 30%.
- Modern carbon fluxes represent the contribution of plant and microbial activity to the total carbon flux that the ^{14}C analysis corrects for. Average modern CO_2 flux was **3.20** microMole/m^2.s, with a coefficient of variation of **70%**.
- **PHHI-R1-CO2-03, PHHI-R1-CO2-04, PHHI-R1-CO2-05, PHHI-R1-CO2-06, PHHI-R1-CO2-07, PHHI-R1-CO2-09**, and **PHHI-R1-CO2-10** showed non-detectable fossil fuel CO_2 flux (ND). The totality of the CO_2 flux should be considered modern. Such samples are not included in the modern CO_2 flux average or coefficient of variation calculations.
- ASTM 4373-02 QA/QC criteria does not provide acceptable variability (CV) standards. Similar methods (for example the carbonates in water, such as ASTM 513.02) provide typical error ≤20%. E-Flux practice is that a CV ≤5% is acceptable.

Calculation Explanations

Conversion of grams CO_2 to CO_2 Flux

Calculating the CO_2 flux from grams of CO_2 involves the cross-sectional area of the trap as well as the number of days that the trap was deployed in the field. The cross-sectional area of the trap is 8.11 x 10^{-3} m^2 (for a 4in receiver). The molecular weight of CO_2 is 44 g/mol. Converting g of CO_2 to CO_2 flux is as follows:

$$\frac{\left(g\ CO_2 * \left(\frac{1\ mol\ CO_2}{44\ g\ CO_2}\right) * \left(\frac{1{,}000{,}000\ micromol\ CO_2}{mol\ CO_2}\right) * \left(\frac{1}{8.11 * 10^{-3}\ m^2}\right)\right)}{days\ in\ the\ field * \frac{24\ hr}{day} * \frac{3600\ sec}{hr}} = \frac{micro\ mol\ CO_2}{m^2 * sec}$$

Conversion of Modern C to Fossil Fuel C

Reported modern carbon content (from carbon dating or ^{14}C analysis) is by convention at the ^{14}C levels as of the time of development of the test (1950). Due to higher current levels of ^{14}C in the environment resulting from atomic testing, current (contemporary) levels are approximately 5% higher than in 1950 (Hua et al., 2013). Thus, fossil fuel C can be found with the following conversions:

$$\%\ Modern\ C_{contemporary} = \frac{\%\ Modern\ C_{1950}}{1.05}$$

$$Contemporary\ fossil\ fuel\ C\ \% = 1 - \%\ Modern\ C_{contemporary} = 1 - \frac{\%\ Modern\ C_{1950}}{1.05}$$

Note that for this report a value of 1.038 was used in place of 1.05 so that the average grams of fossil fuel carbon for samples PHHI-C1-CO2-05 and PHHI-C1-CO2-06 equaled 0.

Calculating Grams of Fossil Fuel CO_2

Calculating grams of fossil fuel (ff) CO_2 is based on the travel blank corrected percent fossil fuel carbon in the sample (the difference between total fossil fuel CO_2 in the sample and that of the travel blank). This is done as follows:

$$g\ CO_{2(ff)} = g\ sorbent * \left((Avg\ sample\ \%\ CO_2 * ff\ sample\ \%\ C) - (Avg\ TB\ \%\ CO_2 * ff\ TB\ \%\ C)\right)$$

Calculation to Convert Carbon Flux to Equivalent LNAPL Loss Rate

The intermediate reactions for LNAPL mineralization include methanogenesis (production of methane and CO_2) and the subsequent aerobic oxidation of methane (into CO_2):

$$C_8H_{18} + 3.5\ H_2O \rightarrow 6.25\ CH_4 + 1.75\ CO_2$$

$$6.25\ CH_4 + \ 12.5\ O_2 \ \rightarrow 6.25\ CO_2 + 12.5\ H_2O$$

The overall reaction (the summation of both reactions), is:

$$C_8H_{18} + 12.5\ O_2 \rightarrow \ 9H_2O + 8\ CO_2$$

For C_8H_{18}, the molecular weight is 114.23 g/mole. Assuming an LNAPL density of 0.77 g/mL (in the upper range of gasoline, for a conservative estimate), the following unit conversion results:

$$1\frac{\mu Mole\ CO_2}{m^2\ s}$$
$$= \frac{\mu Mole\ CO_2}{m^2\ s} \times \left(\frac{1\ \mu Mole\ C_8H_{18}}{8\ \mu Mole\ CO_2}\right) \times \left(\frac{Mole}{1 \times 10^6 \mu Mole}\right) \times \left(\frac{4{,}046\ m^2}{1\ acre}\right) \times \left(\frac{3600\ s}{1\ h}\right) \times \left(\frac{24\ h}{1\ d}\right) \times \left(\frac{365\ d}{1\ yr}\right)$$
$$\times \left(\frac{114\ g\ C_8H_{18}}{1\ Mole\ C_8H_{18}}\right) \times \left(\frac{1\ mL\ C_8H_{18}}{0.77\ g\ C_8H_{18}}\right) \times \left(\frac{1\ L}{1000 mL}\right) \times \left(\frac{1\ gallon}{3.785\ L}\right) = 625\frac{gallon\ C_8H_{18}}{acre.yr}$$

Note that both the LNAPL formula and its density are assumed, and thus subject to uncertainty. If available, site specific data can be used.

Alternative assumptions on the LNAPL formula and its corresponding density generally result in slightly different conversion factors, within 10-15% of the value shown here. Thus, such uncertainty still results in an acceptable estimate.

©2017 All Rights Reserved

References

ASTM (2012), Method D6686-12, Determining the Biobased Content in Solids, Liquids and Gases Using Radiocarbon Analysis.

ASTM (2002), Method D4373-02, Standard Test Method for Rapid Determination of Carbonate Content of Soil.

Avery et al, (2006). Carbon isotopic characterization of dissolved organic carbon in rainwater: Terrestrial and marine influences. Atmos. Environ. p. 7539-7545.

Bauer, H.P.; Beckett, P.H.; and Bie, S.W. (1972). A Rapid Gravimetric Method for Estimating Calcium Carbonate in Soils, Plant and Soil, Vol 37, p. 689-690.

Hua, Q.; Barbetti, M.; and Rakowski, A.Z. (2013). Atmospheric Radiocarbon for the Period 1950-2010. Radiocarbon. 55(4), p. 2059-2072.

Klouda and Connolly, (1995). Radiocarbon (14C) Measurements to Quantify Sources of Atmospheric Carbon Monoxide in Urban Air. Atmos. Environ. p. 3309-3318.

Levin, I. R. Graul, Ne. Trivett. (1995). Long-term observations of atmospheric CO_2 and carbon isotopes at continental sites in Germany. Tellus., 47B, p. 23-34.

McCoy, K., Zimbron, J., Sale, T. and Lyverse, M. (2015), Measurement of Natural Losses of LNAPL Using CO2 Traps. Groundwater, 53: p. 658–667. doi:10.1111/gwat.12240.

Sihota, N. and U. Mayer. (2012). Characterizing vadose zone hydrocarbon biodegradation using CO2-effluxes, isotopes, and 2 reactive transport modeling. Vadose Zone Journal. Accepted for publication.

Stuiver and Polach, (1977). Discussion. Reporting of ^{14}C data. Radiocarbon 19(3), p. 355–363.

Zimbron, J. and E. Kasyon, (2015). Combined Use of Isotope Analysis and Passive CO_2 Flux Traps to Estimate Field Rates of Hydrocarbon Degradation. Battelle Remediation Conference. Miami FL, May 18-21.

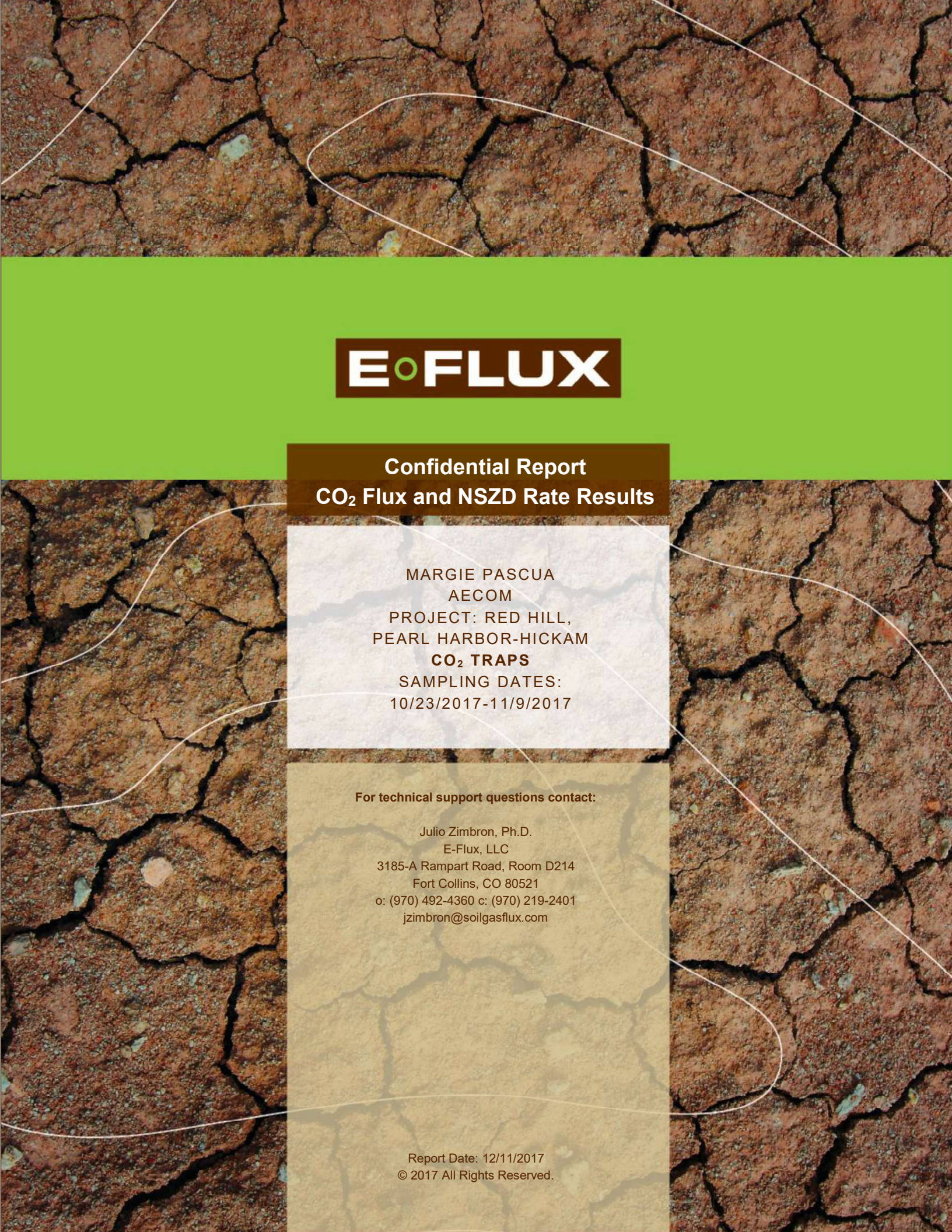

Confidential Report
CO_2 Flux and NSZD Rate Results

MARGIE PASCUA
AECOM
PROJECT: RED HILL,
PEARL HARBOR-HICKAM
CO_2 TRAPS
SAMPLING DATES:
10/23/2017-11/9/2017

For technical support questions contact:

Julio Zimbron, Ph.D.
E-Flux, LLC
3185-A Rampart Road, Room D214
Fort Collins, CO 80521
o: (970) 492-4360 c: (970) 219-2401
jzimbron@soilgasflux.com

Report Date: 12/11/2017
© 2017 All Rights Reserved.

©2017 All Rights Reserved

The purpose of this document is to provide sample calculations of the results reported here and to explain the basis for differentiating petroleum hydrocarbon-derived CO_2 (i.e., fossil fuel CO_2) from modern CO_2 interferences. The following topics are addressed:

- The Value of ^{14}C Analysis
- Site Specific Study Results and Applicable Notes
- Calculation Explanations
- References

The Value of the ^{14}C Analysis

How to differentiate petroleum hydrocarbon-derived CO_2 from modern CO_2 interferences using CO_2 flux traps.

Unimpacted soils have natural CO_2 flux generation rates, due to microbial root zone activity and/or the degradation of natural organic matter (NOM). Thus, the total CO_2 flux measured at an impacted location is the sum of both natural soil respiration processes and those related to LNAPL degradation (Sihota et al, 2011).

The CO_2 flux due to natural soil respiration can be estimated by measuring CO_2 fluxes at unimpacted locations, and subtracting such rates from the total CO_2 fluxes at LNAPL impacted locations in order to estimate CO_2 flux due to LNAPL degradation (Sihota et al, 2012). This is known as the "background correction" and assumes that the rates of natural soil respiration (i.e., modern carbon CO_2 fluxes) are similar for both impacted and unimpacted locations.

The difficulties of this approach are: a) at many industrial facilities it is difficult to find unimpacted locations, and b) the unimpacted locations have very different vegetation to that at the impacted locations. This document provides the basis to use carbon isotope analysis as a location specific correction to the total carbon CO_2 fluxes, designed to overcome the limitations of the background correction.

Carbon Isotope Analysis Methodology

Upon sampling and analysis of the samples by the methods described before (McCoy et al, 2015), the analysis for carbon isotopes is conducted on the homogenized solid samples from the CO_2 flux traps.

Unstable isotopic analysis has been previously used to differentiate anthropogenic (due to fossil fuel-burning) and natural sources of atmospheric CO, CO_2 and methane (for example, Klouda and Connolly, 1995; Levin et al, 1995; Avery et al, 2006). Such findings are the basis of ASTM Method D6686-12, Determining the Biobased Content in Solids, Liquids and Gases Using Radiocarbon Analysis (ASTM, 2012). The technique relies on the analysis of ^{14}C, an unstable carbon isotope (with a half-life of approximately 5600 years) that is generated by cosmic rays in the atmosphere. Thus, contemporary (modern) organic carbon is ^{14}C-rich, while fossil fuel carbon is completely ^{14}C-depleted. Furthermore, contemporary samples and atmospheric samples have the same characteristic amount of ^{14}C. The detection limit of ^{14}C by accelerator mass spectrometry enables dating of samples younger than 60,000

years, while older samples (such as fossil fuels) have non-detectable ^{14}C activity (Stuiver and Polach, 1977).

For a sample that contains carbon from both modern and fossil fuel carbon sources, measurement of the ^{14}C enables quantitation of both source contributions. The fossil fuel fraction of the sample, ff_{sample}, and the remaining non-fossil fuel or contemporary fraction ($1- ff_{sample}$), are related by the following two-component mass balance:

$$Fm_{sample} = ff_{sample}\left(Fm_{ff}\right)+\left(1-ff_{sample}\right)\left(Fm_{atm}\right)$$

In this formula, Fm_{sample} is the measured modern fraction of the sample, Fm_{ff} is the fraction of modern carbon in fossil fuel ($Fm_{ff} = 0$), and Fm_{atm} is the fraction of modern carbon in contemporary living material ($Fm_{atm} = 1.05$) (Hua et al., 2013). By convention, the reporting of carbon isotope analysis is based on a 1950 NBS oxalic acid standard, synthesized when the ^{14}C atmospheric levels were lower than current ones due to nuclear tests. Thus, Fm_{sample} is reported as if the analysis was done in 1950, and Fm_{atm} is counter-intuitively larger than 1.

Expected Results and Recommendations

Our results suggest that the ^{14}C-based technique offers a built-in, location specific correction for fossil fuel as an alternative to the background correction often done at these sites. Earlier data on a limited amount of samples suggested that results using the ^{14}C-correction were equivalent to the background correction (McCoy et al, 2015; Sihota et al, 2012). However, a recent compilation at 4 sites comparing results from the background correction to the ^{14}C-correction suggests that modern carbon fluxes can vary over a factor of 5x for different locations within the same site (Zimbron and Kasyon, 2015). The resulting difference between the background-corrected estimates and the fossil-fuel carbon corrected data can be up to one order of magnitude (depending on the location).

This finding suggests that the assumption implied by the background correction that the modern carbon flux is constant for an entire site might introduce large errors in the correction for petroleum-biodegradation derived CO_2 fluxes. Contrary to the background correction, the ^{14}C-based correction is collocated with the measurement, and thus spatially unbiased by uncertainties related to differences with respect to background location(s) (i.e., due to different vegetation and lithology, unknown impacts, different gas transport regimes, high sensitivity to soil moisture, etc).

The fossil-fuel carbon content on the unexposed sorbent is non-zero (typically around 30%). This might be the result of either a background fossil fuel signature of the sorbent (due to processing of the chemical or mineral sources), or due to material handling (i.e., exposure to fossil fuel fumes). Although the fossil fuel CO_2 mass is very small, this error is adjusted by a travel blank correction procedure. This consists of subtracting the fossil fuel CO_2 mass from an unexposed trap (a travel blank) from those measured on the traps deployed in the field. The ^{14}C analysis is done on CO_2 sorbent subsamples, after homogenization.

©2017 All Rights Reserved

Study Results

The report and results below are based on proprietary technology to measure the soil gas efflux. All information contained in this report is strictly confidential to the customer. The chemical analysis is based on methods ASTM 4373-02 (Rapid Determination for Carbonate Content in Soils) and ASTM D6686-12 (Determining the Biobased Content in Solids, Liquids and Gases Using Radiocarbon Analysis).

The site specific results and interpretation are as follows:

EoFLUX
Easy set-up. Expert results.

Project: Red Hill, Pearl Harbor-Hickam CO_2 Traps

Customer: AECOM

Customer Contact: Margie Pascua, (808) 356-5373

Report Date: 11-Dec-17

Sample ID	Deployment Dates			Raw Results (not blank corrected)					Blank Corrected Results[a] and ^{14}C Analysis (Fossil Fuel)								
	Deployed	Retrieved	Days	Moisture	Dry Sorbent Mass (g)	Num. of Reps. [b]	Avg CO_2[b]	CV CO_2[c]	Carbon Content[d] %	Carbon Content[d] (g)	CO_2 Flux[e] (microM/ m^2.sec)	Modern Carbon, As Reported[g]	Std. Dev. Modern	Modern CO_2 Flux (microM/ m^2.sec)	Adjusted Fossil Fuel Carbon [h]	Grams Of Fossil Fuel CO_2 (g)	Fossil Fuel CO_2 Flux (microM/ m^2.sec)	Equivalent Fossil Fuel-Based NAPL Loss Rate (gallons/ acre.yr)
PHHI-R1-CO2-TB	NA	NA	0.00	19.4%	42.099	2	0.92%	1.21%	-	-	-	64.6%	0.21%	-	38.5%	-	-	-
PHHI-R1-CO2-01	10/26/17 8:20	11/9/17 10:25	14.09	16.9%	42.991	2	1.01%	1.95%	0.1%	0.04	0.1	66.5%	0.24%	0.1	36.7%	0.01	0.0	10
PHHI-R1-CO2-02	10/23/17 13:40	11/6/17 12:20	13.94	25.7%	41.747	2	3.66%	4.35%	2.7%	1.14	2.7	93.9%	0.26%	2.6	10.6%	0.01	0.0	21
PHHI-R1-CO2-03	10/24/17 11:10	11/7/17 12:57	14.07	21.0%	44.178	2	5.08%	1.42%	4.2%	1.84	4.2	98.5%	0.29%	4.3	6.2%	ND	ND	ND
PHHI-R1-CO2-04	10/24/17 16:00	11/7/17 11:15	13.80	25.7%	41.937	2	2.48%	1.42%	1.6%	0.65	1.5	89.9%	0.26%	1.5	14.4%	0.00	0.0	2
PHHI-R1-CO2-05	10/24/17 15:10	11/7/17 11:22	13.84	20.7%	44.826	2	5.54%	4.55%	4.6%	2.07	4.9	98.3%	0.34%	4.9	6.4%	ND	ND	ND
PHHI-R1-CO2-06	10/23/17 14:35	11/6/17 12:32	13.91	21.6%	44.412	2	4.76%	0.15%	3.8%	1.71	4.0	97.6%	0.26%	4.0	7.0%	ND	ND	ND
PHHI-R1-CO2-07	10/23/17 11:30	11/6/17 12:05	14.02	24.6%	43.589	2	7.56%	2.15%	6.6%	2.90	6.7	99.6%	0.28%	6.7	5.2%	0.02	0.0	24
PHHI-R1-CO2-08	10/25/17 13:20	11/8/17 9:40	13.85	21.5%	45.130	2	5.97%	4.41%	5.0%	2.28	5.3	96.6%	0.27%	5.2	8.0%	0.06	0.1	84
PHHI-R1-CO2-09	10/25/17 12:30	11/8/17 10:00	13.90	23.7%	41.666	2	3.26%	0.23%	2.3%	0.98	2.3	94.1%	0.28%	2.3	10.4%	ND	ND	ND
PHHI-R1-CO2-10	10/26/17 8:50	11/9/17 10:55	14.09	17.8%	42.199	2	0.94%	4.78%	0.0%	0.01	0.0	68.2%	0.26%	0.0	35.0%	ND	ND	ND
PHHI-R1-CO2-TBB	NA	NA	0.00	21.0%	42.595	2	0.97%	0.61%	-	-	-	70.2%	0.21%	-	33.1%	-	-	-

This report contains Confidential Information and is to be delivered only to the Customer indicated above.

See following page for assumptions, project specific quality assurance/quality control information, and notes.

The Following Assumptions and General Notes apply for CO_2 traps:

a. Results are travel blank corrected but not background location corrected.
Blank Corrected Results = Raw Results - Travel Blank

b. Number of Replicates: Carbon analysis was conducted in duplicate if CV ≤ 5%. If CV > 5%, carbon analysis was conducted with triplicates. Avg % refers to the percent of CO_2 in the dry sorbent mass before blank corrected.

c. CV is coefficient of variation, equal to the ratio of the standard deviation over the average.

d. If trap carbon content is not larger than travel blank, results are reported as ND. Expressed as CO_2 not pure carbon.

e. Trap cross sectional area is **8.11×10^{-3}** m^2 (i.e., equivalent to a **4in** receiver pipe).

f. The flux equivalence is 1 microMole/(m^2.sec) equals **625** gallons/(acre.yr). This assumes a hydrocarbon density of **0.77** g/mL and a formula of **C_8H_{18}**.

g. "As reported" refers to % modern carbon at the time of development of the test (1950).

h. Adjusted fossil fuel carbon has been transformed from the "As reported" basis (1950) to present ^{14}C levels.

NA means Not Applicable.

Quality Assurance / Quality Control Notes:

- The Travel Blank (PHHI-R1-CO2-TB) concentration for this report was **0.92%.** Typical Travel Blank concentration is <2%. The additional travel blank (PHHI-R1-CO2-TBB) had a concentration of **0.97%.** Carbon contents were blank-corrected using **PHHI-R1-CO2-TB**.
- Trap tops were not saturated with CO_2. Maximum measured top concentration was **1.85%** (sample **PHHI-R1-CO2-01.1**). Sorbent saturation is 30%.
- Modern carbon fluxes represent the contribution of plant and microbial activity to the total carbon flux that the ^{14}C analysis corrects for. Average modern CO_2 flux was **3.16** microMole/m^2.s, with a coefficient of variation of **70%**.
- **PHHI-R1-CO2-03, PHHI-R1-CO2-05, PHHI-R1-CO2-06, PHHI-R1-CO2-09**, and **PHHI-R1-CO2-10** showed non-detectable fossil fuel CO_2 flux (ND). The totality of the CO_2 flux should be considered modern. Such samples are not included in the modern CO_2 flux average or coefficient of variation calculations.
- ASTM 4373-02 QA/QC criteria does not provide acceptable variability (CV) standards. Similar methods (for example the carbonates in water, such as ASTM 513.02) provide typical error ≤20%. E-Flux practice is that a CV ≤5% is acceptable.

Calculation Explanations

Conversion of grams CO_2 to CO_2 Flux

Calculating the CO_2 flux from grams of CO_2 involves the cross-sectional area of the trap as well as the number of days that the trap was deployed in the field. The cross-sectional area of the trap is 8.11 x 10^{-3} m^2 (for a 4in receiver). The molecular weight of CO_2 is 44 g/mol. Converting g of CO_2 to CO_2 flux is as follows:

$$\frac{\left(g\ CO_2 * \left(\frac{1\ mol\ CO_2}{44\ g\ CO_2}\right) * \left(\frac{1{,}000{,}000\ micromol\ CO_2}{mol\ CO_2}\right) * \left(\frac{1}{8.11 * 10^{-3}\ m^2}\right)\right)}{days\ in\ the\ field * \frac{24\ hr}{day} * \frac{3600\ sec}{hr}} = \frac{micro\ mol\ CO_2}{m^2 * sec}$$

Conversion of Modern C to Fossil Fuel C

Reported modern carbon content (from carbon dating or ^{14}C analysis) is by convention at the ^{14}C levels as of the time of development of the test (1950). Due to higher current levels of ^{14}C in the environment resulting from atomic testing, current (contemporary) levels are approximately 5% higher than in 1950 (Hua et al., 2013). Thus, fossil fuel C can be found with the following conversions:

$$\%\ Modern\ C_{contemporary} = \frac{\%\ Modern\ C_{1950}}{1.05}$$

$$Contemporary\ fossil\ fuel\ C\ \% = 1 - \%\ Modern\ C_{contemporary} = 1 - \frac{\%\ Modern\ C_{1950}}{1.05}$$

Calculating Grams of Fossil Fuel CO_2

Calculating grams of fossil fuel (ff) CO_2 is based on the travel blank corrected percent fossil fuel carbon in the sample (the difference between total fossil fuel CO_2 in the sample and that of the travel blank). This is done as follows:

$$g\ CO_{2(ff)} = g\ sorbent * \left((Avg\ sample\ \%\ CO_2 * ff\ sample\ \%\ C) - (Avg\ TB\ \%\ CO_2 * ff\ TB\ \%\ C)\right)$$

Calculation to Convert Carbon Flux to Equivalent LNAPL Loss Rate

The intermediate reactions for LNAPL mineralization include methanogenesis (production of methane and CO_2) and the subsequent aerobic oxidation of methane (into CO_2):

$$C_8H_{18} + 3.5\ H_2O \rightarrow 6.25\ CH_4 + 1.75\ CO_2$$

$$6.25\ CH_4 + 12.5\ O_2 \rightarrow 6.25\ CO_2 + 12.5\ H_2O$$

The overall reaction (the summation of both reactions), is:

$$C_8H_{18} + 12.5\ O_2 \rightarrow\ 9H_2O + 8\ CO_2$$

For C_8H_{18}, the molecular weight is 114.23 g/mole. Assuming an LNAPL density of 0.77 g/mL (in the upper range of gasoline, for a conservative estimate), the following unit conversion results:

$$1\frac{\mu Mole\ CO_2}{m^2\ s}$$
$$= \frac{\mu Mole\ CO_2}{m^2\ s} \times \left(\frac{1\ \mu Mole\ C_8H_{18}}{8\ \mu Mole\ CO_2}\right) \times \left(\frac{Mole}{1 \times 10^6 \mu Mole}\right) \times \left(\frac{4{,}046\ m^2}{1\ acre}\right) \times \left(\frac{3600\ s}{1\ h}\right) \times \left(\frac{24\ h}{1\ d}\right) \times \left(\frac{365\ d}{1\ yr}\right)$$
$$\times \left(\frac{114\ g\ C_8H_{18}}{1\ Mole\ C_8H_{18}}\right) \times \left(\frac{1\ mL\ C_8H_{18}}{0.77\ g\ C_8H_{18}}\right) \times \left(\frac{1\ L}{1000 mL}\right) \times \left(\frac{1\ gallon}{3.785\ L}\right) = 625\frac{gallon\ C_8H_{18}}{acre.yr}$$

Note that both the LNAPL formula and its density are assumed, and thus subject to uncertainty. If available, site specific data can be used.

Alternative assumptions on the LNAPL formula and its corresponding density generally result in slightly different conversion factors, within 10-15% of the value shown here. Thus, such uncertainty still results in an acceptable estimate.

©2017 All Rights Reserved

References

ASTM (2012), Method D6686-12, Determining the Biobased Content in Solids, Liquids and Gases Using Radiocarbon Analysis.

ASTM (2002), Method D4373-02, Standard Test Method for Rapid Determination of Carbonate Content of Soil.

Avery et al, (2006). Carbon isotopic characterization of dissolved organic carbon in rainwater: Terrestrial and marine influences. Atmos. Environ. p. 7539-7545.

Bauer, H.P.; Beckett, P.H.; and Bie, S.W. (1972). A Rapid Gravimetric Method for Estimating Calcium Carbonate in Soils, Plant and Soil, Vol 37, p. 689-690.

Hua, Q.; Barbetti, M.; and Rakowski, A.Z. (2013). Atmospheric Radiocarbon for the Period 1950-2010. Radiocarbon. 55(4), p. 2059-2072.

Klouda and Connolly, (1995). Radiocarbon (14C) Measurements to Quantify Sources of Atmospheric Carbon Monoxide in Urban Air. Atmos. Environ. p. 3309-3318.

Levin, I. R. Graul, Ne. Trivett. (1995). Long-term observations of atmospheric CO_2 and carbon isotopes at continental sites in Germany. Tellus., 47B, p. 23-34.

McCoy, K., Zimbron, J., Sale, T. and Lyverse, M. (2015), Measurement of Natural Losses of LNAPL Using CO2 Traps. Groundwater, 53: p. 658–667. doi:10.1111/gwat.12240.

Sihota, N. and U. Mayer. (2012). Characterizing vadose zone hydrocarbon biodegradation using CO2-effluxes, isotopes, and 2 reactive transport modeling. Vadose Zone Journal. Accepted for publication.

Stuiver and Polach, (1977). Discussion. Reporting of ^{14}C data. Radiocarbon 19(3), p. 355–363.

Zimbron, J. and E. Kasyon, (2015). Combined Use of Isotope Analysis and Passive CO_2 Flux Traps to Estimate Field Rates of Hydrocarbon Degradation. Battelle Remediation Conference. Miami FL, May 18-21.

Appendix B.3:
Soil Vapor Analysis (2017 Study)

CONTENTS

Acronyms and Abbreviations iv

1. Introduction 1-1

1.1 Technical Background 1-1
1.2 Study Objectives 1-2

2. Field Methods and Procedures 2-1

2.1 Selection of Sample Locations for Analysis 2-1
2.2 Installation of Shallow Soil Vapor Points 2-1
2.3 Installation of Soil Vapor Probes (Vapor Pins) through Tunnel Walls 2-3
2.4 Soil Vapor Sampling Procedures 2-3
2.5 Monitoring Well Headspace Sampling Procedures 2-4
2.6 Laboratory Analysis 2-6

3. Investigation Results 3-1

3.1 Laboratory Analysis of VOCs in Soil Vapor Samples 3-1
3.1.1 Magnitude of Petroleum Vapors 3-1
3.1.2 Composition of Petroleum Vapors 3-3
3.1.3 Tentatively Identified Compounds in Soil Vapor Samples 3-6
3.1.4 Evaluation of FID Chromatograms 3-6
3.2 Field Measurements 3-8
3.2.1 PID Readings 3-8
3.2.2 Oxygen, Carbon Dioxide, and Methane 3-8
3.2.3 Differential Pressure 3-9
3.3 Correlation between Field Measurements and Laboratory Results 3-9
3.3.1 Field PID Readings vs. Laboratory Total Quantified VOC Concentrations 3-9
3.3.2 Field vs. Laboratory Oxygen, Carbon Dioxide, and Methane Concentrations 3-11

4. Discussion of Soil Vapor Investigation Results 4-1

5. Gradient Method for Measuring NSZD 5-1

5.1 Technical Background 5-1
5.2 Gradient Method Data Collection 5-1
5.3 Soil Vapor Carbon Dioxide and Gradient Profiles 5-2
5.4 Reasons for Complex Soil Vapor Oxygen Profiles at the Facility 5-3
5.4.1 Horizontal Oxygen Migration 5-3
5.4.2 Tunnel System Acting Like Soil Vapor Extraction (SVE) System 5-4
5.5 Gradient Method Conclusions 5-5

6. References 6-1

ATTACHMENTS

B.3.1 Fingerprint Charts for Soil Vapor and Groundwater Monitoring Well Headspace Samples

B.3.2 FID Chromatograms for Soil Vapor and Groundwater Monitoring Well Headspace Samples

B.3.3 Soil Vapor Field Monitoring Results

B.3.4 Soil Vapor and Groundwater Monitoring Well Headspace Sample Analytical Results

B.3.5 LNAPL Indications from Drilling Fluids and Boring Logs for Borings Completed Below Fuel Storage Tanks (Most Borings Completed 1998–2001)

B.3.6 Laboratory Report and EDD for Soil Vapor Samples Analyzed by Alpha Analytical; Laboratory Job Number L1740493

FIGURES

1-1 Facility Tank Farm 1-1

1-2 Typical Soil Vapor Monitoring Point Construction Details 1-2

2-1 Locations of Shallow Soil Vapor Points Installed on Top of Red Hill near Carbon Trap Locations T2 and T6 2-2

2-2 Illustration of Connection between Soil Vapor Point and Summa Canister 2-4

2-3 Illustration of Vapor Sample Collection from Monitoring Well 2-6

3-1 Total Concentration of Quantified VOCs in Soil Vapor Samples 3-2

3-2 Distribution of Alkanes in Soil Vapor Samples for All Samples Except Tank 5 3-4

3-3 Distribution of Alkanes in Soil Vapor Samples for Tank 5 3-5

3-4 FID Chromatograms from Representative Samples Showing Range of Unresolved Hump 3-7

3-5 Correlation between PID Readings and Laboratory Total Target Analytes Plus TICs 3-10

3-6 Correlation between Field- and Laboratory-Measured Oxygen Concentration 3-12

3-7 Correlation between Field- and Laboratory-Measured Oxygen Concentration Excluding Two Low-Biased Laboratory Measurements 3-13

3-8 Correlation between Field- and Laboratory-Measured Carbon Dioxide Concentration 3-14

4-1 Top: LNAPL Indications from Drilling Fluids; Bottom: LNAPL Indications from Boring Logs 4-3

4-2 Linear Scale Graph of Monthly PID Monitoring Results for Below-Tank Soil Vapor Points 4-5

4-3 Monthly PID Monitoring Results for Below-Tank Soil Vapor Monitoring Points 4-7

4-4 Log Scale Graph of Average Monthly PID Monitoring Results across All Below-Tank Soil Vapor Points. Note log-scale for Y-axis. 4-8

5-1 Oxygen vs. Elevation Data Collected at the Facility 5-2

5-2 Left: Soil Vapor Data Collected at Oil Field Site; Right: Actual Data from 5-1 vs. Expected Pattern if Gradient Method Conditions Were Met 5-3

5-3 Vertical Location of Tank 5 in North-South Cross Section between Tanks 5 and 6 5-4

TABLES

2-1 Petroleum VOC Analyte List for TO-15 PIANO Analysis 2-7

4-1 Study Question 1: Is There Evidence of Recent or Historical Fuel Releases at One or More of the Tanks? 4-1

4-2 Study Question 2: Is LNAPL Present below the Tanks? 4-2

4-3 Study Question 3: Is NSZD Occurring? 4-4

4-4 Study Question 4: Can Vapor Monitoring Help Detect New LNAPL Fuel Releases? 4-4

4-5 Study Question 5: Can Vapor Monitoring Be Used to Track NSZD Progress Over Time? 4-6

4-6 Study Question 6: Are Vadose-Zone Petroleum Vapors a Significant Source of Impacts In the Tunnels? 4-9

4-7 Summary of PID Measurements in the Tunnels 4-10

ACRONYMS AND ABBREVIATIONS

bgs	below ground surface
cfm	cubic feet per minute
CSM	conceptual site model
ENV	Environmental Protection Agency, United States
FID	flame ionization detector
ft	foot/feet
GC	gas chromatograph/chromatograph
Hg	mercury
L	liter
LNAPL	light non-aqueous-phase liquid
mbar	millibar
mL	milliliter
MS	mass spectrum
msl	mean sea level
NAPL	non-aqueous-phase liquid
NSZD	natural source-zone depletion
PIANO	paraffins, isoparaffins, aromatics, naphthenes, and olefins
PID	photoionization detector
ppbv	parts per billion by volume
ppm	parts per million
ppmv	parts per million by volume
ppt	parts per thousand
SOP	standard operating procedure
SVE	soil vapor extraction
SVMP	soil vapor monitoring point
TIC	tentatively identified compound
TPH	total petroleum hydrocarbons
UCM	unresolved complex mixture
VOC	volatile organic compound

1. Introduction

This subappendix, summarized in Section 7.3.1.4 of the Conceptual Site Model (CSM) main document, describes vapor monitoring relative to evaluation of natural source-zone depletion (NSZD) and potential release detection.

1.1 TECHNICAL BACKGROUND

The Red Hill Bulk Fuel Storage Facility (the "Facility") tank farm is a complex of 20 petroleum storage tanks constructed inside Red Hill (Figure 1-1).

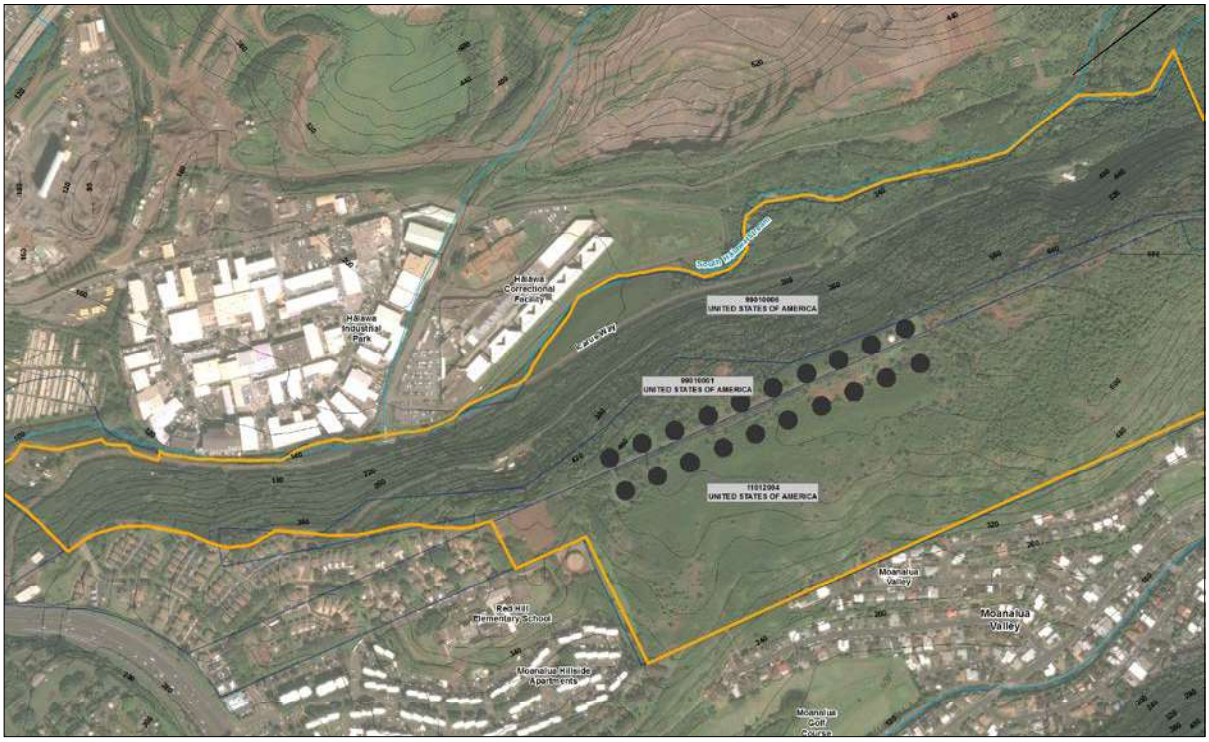

Figure 1-1: Facility Tank Farm

The 20 fuel storage tanks have been used mostly for storage of jet fuel such as JP-5 and JP-8 and to a lesser extent marine diesel fuel, fuel oil, and gasoline. Because of the predominance of jet fuel in the tanks and in the January 2014 release, this subappendix uses jet fuel as the primary reference fuel for the evaluation of the soil vapor data.

Section 3 of the CSM main document provides more detailed background information on the Facility. From 1998 to 2002, angle borings were installed below each tank. In 2006, soil vapor monitoring points (SVMPs) were constructed inside these existing boreholes below each tank except for Tank 1 and Tank 19, which were already permanently out of service. Two to three SVMPs were installed in each of the existing boreholes (Figure 1-2). This yielded a robust network of 47 SVMPs below active tanks.

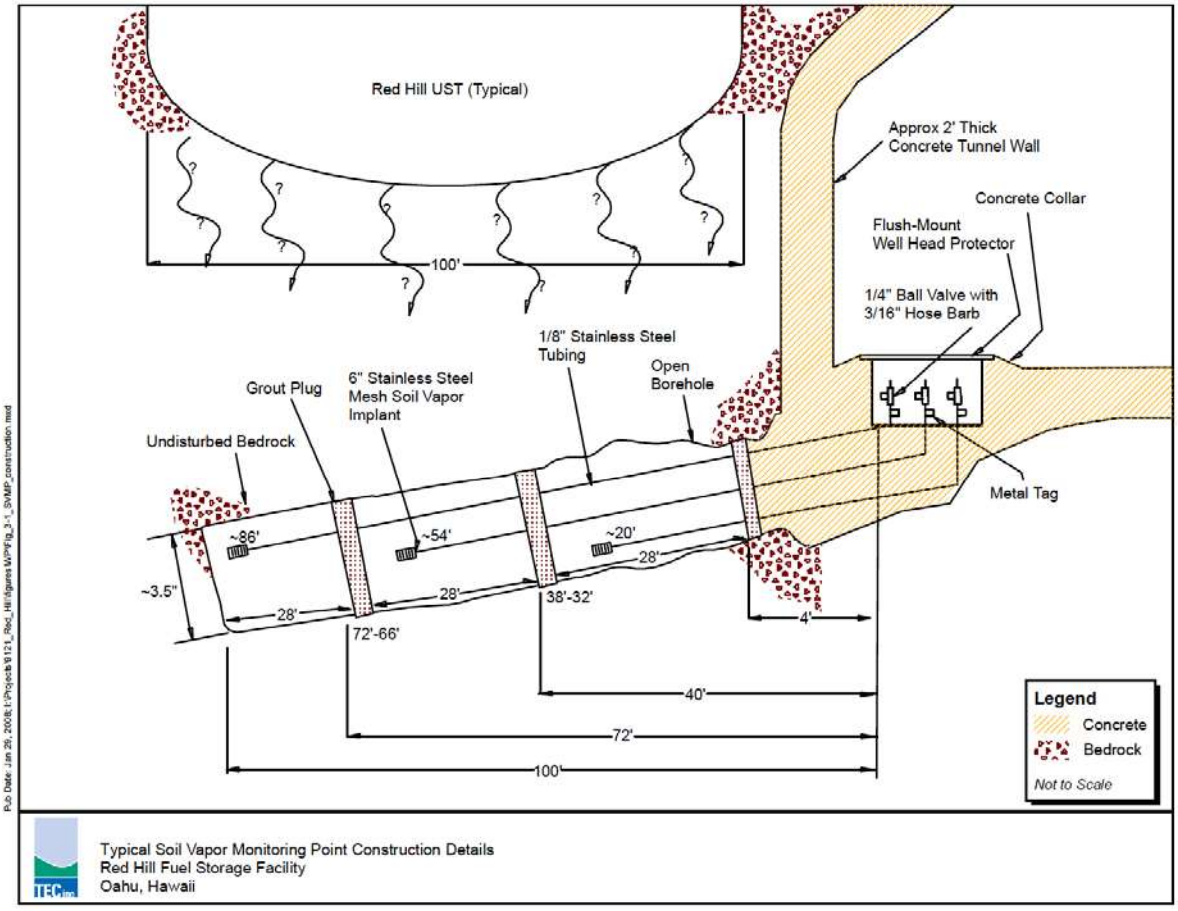

Source: TEC 2010.

Figure 1-2: Typical Soil Vapor Monitoring Point Construction Details

Historically, a small number of soil vapor samples had been collected for laboratory analysis of volatile organic compounds (VOCs) and total petroleum hydrocarbons (TPH). More recently, the soil vapor points have been used for field screening (TEC 2010). Most of these vapor points are monitored monthly using a field portable photoionization detector (PID) to measure total VOC concentrations. Despite the technical analysis presented in TEC (2010), PID readings alone provide little or no ability to distinguish between dissolved and light non-aqueous-phase liquid (LNAPL) petroleum contamination. Additional data may provide an improved ability to characterize sources and interpret temporal variations in PID readings.

1.2 STUDY OBJECTIVES

The vapor sampling program described in this sub-appendix was completed to (1) provide a better understanding of recent and historical fuel releases at the Facility, (2) support assessment of the natural source-zone depletion (NSZD) whereby LNAPL is degraded in the subsurface by biodegradation and other naturally occurring processes, and (3) assess how vapor monitoring might aid in detection of potential future LNAPL fuel releases at the Facility.

2. Field Methods and Procedures

Field measurements and collection of samples for laboratory analysis were completed between October 25 and November 2, 2017. Activities included the following:

- Field measurements and soil vapor sampling from the existing soil vapor points below the fuel tanks
- Installation of and field measurements at two shallow soil vapor points on top of the tank farm
- Installation of and field measurements at two Cox-Colvin Vapor Pin locations in the upper tunnel
- Field measurements and well headspace vapor sampling from monitoring wells RHMW01, RHMW02, RHMW03, and RHMW04

2.1 Selection of Sample Locations for Analysis

Existing and newly installed soil vapor points and monitoring wells were selected for field measurements. This included the following:

- Forty-seven existing below-tank soil vapor points at 18 tanks. Tanks 2–18 and Tank 20 have soil vapor monitoring points. Tanks 1 and 19 are no longer in service and do not have soil vapor monitoring points. All the remaining tanks have three soil vapor monitoring points except for Tanks 6, 10, 11, and 18, which each have two soil vapor monitoring points. No field screening or soil vapor sampling was conducted at Tank 17 because a physical structure constructed for tank maintenance blocked access to the soil vapor monitoring points at the time of the field investigation.
- Two shallow soil vapor points installed on top of the tank farm above Tank 5 and Tank 11.
- Two new Vapor Pin points installed in the upper tunnel (at Tank 5 and Tank 11).
- Monitoring wells RHMW01, RHMW02, RHMW03, and RHMW04 were selected for collection of well headspace samples.

2.2 Installation of Shallow Soil Vapor Points

Shallow soil vapor sample points were installed above Tanks 5 and 11 near locations T2 and T6 (Figure 2-1). First, a hand auger was used to drill a hole to a depth of 5 feet (ft) below ground surface (bgs). 1/8-inch outside diameter nylon tubing with a porous sampling point at the end was lowered into the hole and the porous point was emplaced within 6 inches of sand (3 inches below and 3 inches above). One foot of dry bentonite was poured above the sand, and the rest of the hole was filled with hydrated bentonite in a stepwise fashion (a small amount of dry bentonite poured in, then water poured in to hydrate the bentonite; this process was repeated to the top of the hole). At the surface, a three-way valve was connected to the nylon tubing using Masterflex tubing and set so that the below-ground tubing was isolated from the atmosphere.

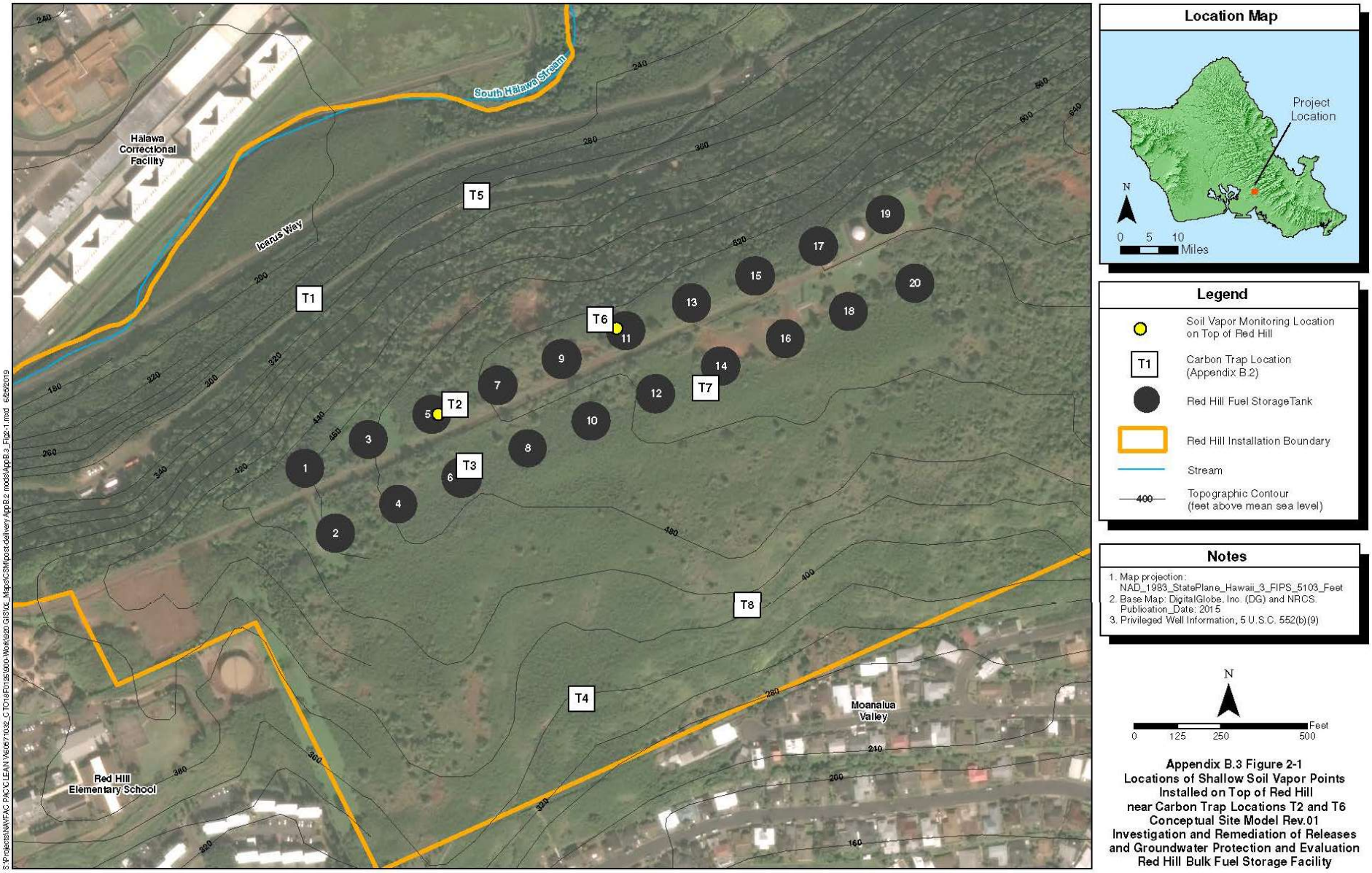

Appendix B.3 Figure 2-1
Locations of Shallow Soil Vapor Points
Installed on Top of Red Hill
near Carbon Trap Locations T2 and T6
Conceptual Site Model Rev.01
Investigation and Remediation of Releases
and Groundwater Protection and Evaluation
Red Hill Bulk Fuel Storage Facility

Figure 2-1: Locations of Shallow Soil Vapor Points Installed on Top of Red Hill near Carbon Trap Locations T2 and T6

2.3 INSTALLATION OF SOIL VAPOR PROBES (VAPOR PINS) THROUGH TUNNEL WALLS

Two Cox-Colvin Vapor Pins were installed in the upper tunnel: one near Tank 5 and one near Tank 11. Two additional potential Vapor Pin locations were planned at the top of the access ladders at the top of Tank 5 and Tank 11. However, site maintenance activities prevented access to the Tank 5 ladder. At Tank 11, it was determined that the required equipment could not safely be transported up the access ladder for installation of the Vapor Pin at that location.

To install each Vapor Pin, a hammer drill with an 18-inch × 5/8-inch drill bit was used to drill a hole through the tunnel wall at a height of approximately 3 ft above the floor. The drill bit was used to create a 16-inch-deep hole. The gunite wall over the native basalt was estimated to be approximately 4 inches thick based on a subtle color and texture contrast in the drill cuttings between the gunite and the basalt. For flush-mounted completion, a 1½-inch drill bit was used to over-drill the hole to a depth of 1¾ inches. The Vapor Pin was installed in accordance with the Cox-Colvin Vapor Pin installation Standard Operating Procedure (SOP) (Cox-Colvin 2016). After installation, the Vapor Pin was capped with a protective cover to prevent air flow when not sampling.

2.4 SOIL VAPOR SAMPLING PROCEDURES

Field instruments were calibrated every morning in accordance with manufacturers' instructions. Field screening was conducted at all soil vapor points (i.e., the new shallow soil vapor points, the new upper tunnel Vapor Pins, and the existing tank soil vapor monitoring points). Samples for laboratory analysis were collected only from the existing tank soil vapor points.

Field Screening: A minimum of 1 liter (L) of gas was purged from each soil vapor point prior to field screening. Purging was performed using either the pump in the PID or a separate pump.

- Total VOC Concentration: Total VOC concentrations were measured in the field using a ppb RAE PID. The PID was connected directly to the soil vapor point, and the meter reading was monitored for a minimum of 1 minute until a stable reading was obtained. If the meter had not stabilized after 5 minutes, the reading at 5 minutes was recorded and the lack of stabilization was noted in the field notes.
- Oxygen, Carbon Dioxide, and Methane: Following completion of PID measurements, a syringe pump was used to pump 750 mL soil vapor into a Tedlar bag. A GEM5000 Landfill Gas Meter was used to measure oxygen, carbon dioxide, and methane concentrations in the bag. The meter reading typically stabilized after approximately 1 minute (500 milliliters [mL]), and the reading was recorded when the bag was almost emptied by the meter. A charcoal filter cartridge was installed in the sample line between the water filter and the Tedlar bag to prevent false positive methane readings associated with petroleum vapors in the samples. No methane was detected in any sample.
- **Differential Pressure:** Following completion of the fixed gas readings, differential pressure was measured by connecting the GEM5000 directly to the soil vapor point.

Sample Collection: At each tank, a sample was collected from the vapor monitoring point with the highest PID reading. Samples were collected into batch clean-certified 2.7-L Summa canisters (with 200 mL/min flow controller). The sample collection setup is illustrated on Figure 2-2. The sampling was completed as follows:

- **Leak Check:** The absence of leaks between the Summa and the ball valve on the soil vapor point was verified by using a syringe to induce a vacuum. The vacuum was maintained for a minimum of 10 seconds. If any air entered the system (as evidenced by the syringe plunger not returning to the base of the syringe when the plunger was released), then the connections were tightened, and a second leak test was performed. During the field program, one Summa canister was rejected because the flow controller did not pass the leak test even after tightening the connections.

Summa Canister Sample: After passing the leak test, the syringe was used to remove air from the sample line running from the 3-way valve to the Summa canister and the 3-way valve was set to isolate the syringe while connecting the Summa to the sample point. The ball valve on the soil vapor point was opened and then the valve on the Summa canister was opened. The valves were kept open until the canister vacuum fell to less than 4 inches mercury (Hg) and were then closed. All Summas filled over a period of 10–12 minutes. A field duplicate sample was collected from soil vapor point RHSV05S below Tank 5.

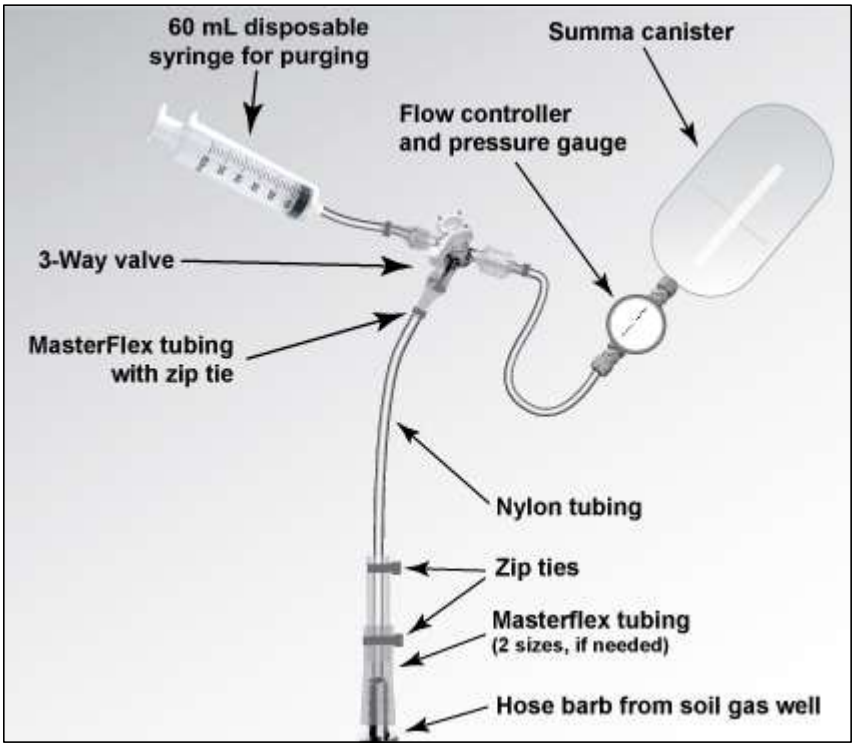

Figure 2-2: Illustration of Connection between Soil Vapor Point and Summa Canister

2.5 MONITORING WELL HEADSPACE SAMPLING PROCEDURES

Well headspace field measurement and samples were collected from four groundwater monitoring wells: RHMW01, RHMW02, RHMW03, and RHMW04 (background).

Sample Collection: At each monitoring well, a vapor sample was collected into a batch clean-certified 2.7-L Summa canister (with 200 mL/min flow controller) as follows:

1. **Well Plugging:** At least 18 hours prior to sample collection, the vented well cap was replaced with a rubber stopper that formed a gas-tight seal and prevented gas flow through the well.
2. **Sampling Equipment:** A sample line was constructed to extend to a depth of 2 ft above the water level in the well. As shown on Figure 2-3, the 1/8-inch nylon sample line was deployed through a second rubber stopper. This second stopper had a small hole for the sample line and served to minimize vertical gas flow in the well during sample line deployment and sample collection. After the sample line was deployed to the correct depth, modeling clay was used to seal the small opening around the sample line.
3. **Sample Line Purge and Leak Check:** A disposable syringe was used to purge three line volumes of gas from the sample line. 1/8-inch tubing has a line volume of approximately 2.4 mL/ft. Following the purge, the Summa was connected, and the syringe was used to create a vacuum between the Summa and the 3-way valve to check for leaks. If leakage was detected, the hardware was tightened, and the leak check was performed again.
4. **Sample Collection:** After passing the leak test, the syringe was used to remove air from the sample line connecting the Summa canister to the 3-way valve and the 3-way valve was set to isolate the syringe while connecting the Summa to the well. The valve was opened on the Summa canister and kept open until the canister vacuum fell to less than 4 in Hg. All Summas filled over a period of 10–12 minutes.

Field Screening: At each monitoring well, after Summa sample collection, field screening was conducted using the field instruments (PID and Landfill Gas Meter).

1. **Total VOC Concentration:** The PID was connected directly to the nylon sample line and the meter was monitored for a minimum of 1 minute until a stable reading was obtained. If the meter had not stabilized after 5 minutes, the reading at 5 minutes was recorded and the lack of stabilization was noted in the field notes.
2. **Oxygen, Carbon Dioxide, and Methane:** Following completion of PID measurements, a syringe pump was used to pump 750 mL of headspace vapor into a Tedlar bag. The GEM5000 Landfill Gas Meter was used to measure oxygen, carbon dioxide, and methane concentrations in the bag. The meter reading typically stabilized after approximately 1 minute (500 mL), and the reading was recorded when the bag was almost emptied by the meter. A charcoal filter cartridge was installed in the sample line between the water filter and the Tedlar bag to prevent false positive methane readings associated with petroleum vapors in the samples. No methane was detected in any sample.
3. **Differential Pressure:** Following completion of the fixed gas readings, differential pressure was measured by connecting the GEM 5000 directly to the nylon sample line installed inside the groundwater monitoring well.

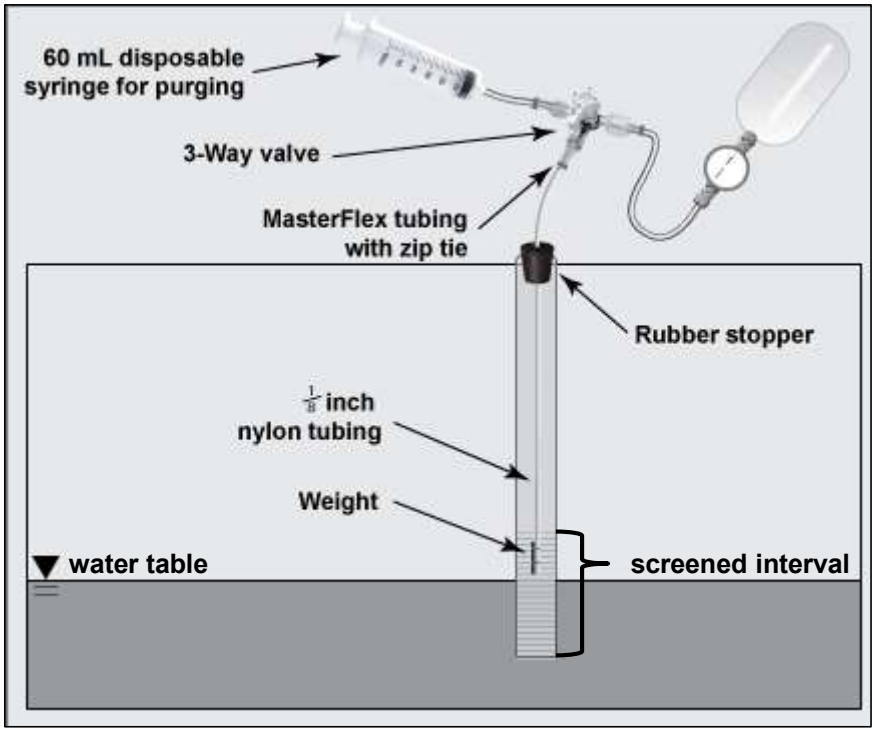

Figure 2-3: Illustration of Vapor Sample Collection from Monitoring Well

2.6 LABORATORY ANALYSIS

The Summa canister samples were shipped at ambient temperature under chain of custody control to Alpha Analytical Laboratory, Westborough, MA for analysis of volatile petroleum hydrocarbons by U.S. Environmental Protection Agency (EPA) Method TO-15 PIANO (see Table 2-1 for analyte list) and fixed gases (oxygen, carbon dioxide, methane, and nitrogen) by EPA Method 3C. Additionally, the laboratory was requested to report tentatively identified compounds (TICs).

Table 2-1: Petroleum VOC Analyte List for TO-15 PIANO Analysis

1-Decene	1,2,4,5-Tetramethylbenzene	3-Ethylhexane	Methylcyclopentane
1-Ethyl-1-Methylcyclopentane	1,3-Butadiene	3-Methylheptane	MMT
1-Heptene	1,3-Dimethyl-2-Ethylbenzene	3-Methylhexane	n-Butylbenzene
1-Hexene	1,3-Dimethyl-4-Ethylbenzene	3-Methylpentane	n-Hexane
1-Methyl-2-Ethylbenzene	1,3-Dimethyl-5-Ethylbenzene	3-Methylthiophene	N-Pentylbenzene
1-Methyl-2-Isopropylbenzene	1,3,5-Trimethylbenzene	Benzene	n-Propylbenzene
1-Methyl-2-N-Propylbenzene	1,4-Dimethyl-2-Ethylbenzene	Benzothiophene	Naphthalene
1-Methyl-3-Ethylbenzene	2-Ethylthiophene	cis-2-Pentene	Nonane (C9)
1-Methyl-3-Isopropylbenzene	2-Methyl-1-Butene	Cyclohexane	o-Xylene
1-Methyl-3-N-Propylbenzene	2-Methylheptane	Cyclopentane	Octane
1-Methyl-4-Ethylbenzene	2-Methylhexane	Decane (C10)	p/m-Xylene
1-Methyl-4-Isopropylbenzene	2-Methylnaphthalene	Dodecane (C12)	Pentane
1-Methyl-4-N-Propylbenzene	2-Methylpentane	Ethyl-Tert-Butyl-Ether	sec-Butylbenzene
1-Methylnaphthalene	2-Methylthiophene	Ethylbenzene	Styrene
1-Nonene	2,2-Dimethylpentane	Heptane	Tertiary Butanol
1-Octene	2,3-Dimethylbutane	Indane	Tertiary-Amyl Methyl Ether
1-Pentene	2,3-Dimethylhexane	Indene	Thiophene
1,2-Dibromoethane	2,3-Dimethylpentane	Isooctane	Toluene
1,2-Dichloroethane	2,3,3-Trimethylpentane	Isopentane	trans-2-Pentene
1,2-Diethylbenzene	2,3,4-Trimethylpentane	Isopropyl Ether	Tridecane
1,2-Dimethyl-3-Ethylbenzene	2,4-Dimethylhexane/ 2,2,3-Trimethylpentan	Isopropylbenzene	Undecane
1,2-Dimethyl-4-Ethylbenzene	2,4-Dimethylpentane	Methyl tert butyl ether	
1,2,4-Trimethylbenzene	2,5-Dimethylhexane	Methylcyclohexane	

3. Investigation Results

3.1 LABORATORY ANALYSIS OF VOCS IN SOIL VAPOR SAMPLES

Soil vapor samples for laboratory analysis were collected from the soil vapor points below each fuel tank with the highest PID reading and from the headspace of RHMW01, RHMW02, RHMW03, and RHMW04. A table of laboratory analytical results for the soil vapor points and well headspace samples is provided as Attachment B.3.4. The magnitude and chemical composition of soil vapor samples can be used to evaluate the occurrence of recent and historical releases of fuel from the fuel tanks and weathering of these releases.

3.1.1 Magnitude of Petroleum Vapors

Each vapor sample was analyzed for 83 petroleum constituents and seven petroleum additives (four oxygenates, two lead scavengers, and one octane booster). Seventy-four petroleum constituents and five additives (four oxygenates and one lead scavenger) were detected in one or more samples. In addition, for each sample, the laboratory estimated the concentration and used mass spectrum matching software to identify TICs with the most prominent gas chromatogram (GC) peaks that were not on the standard sample analyte list. As discussed in Section 3.1.3, the TICs included a variety of petroleum and non-petroleum compounds. The TIC concentrations were estimated based on the instrument response relative to an internal standard and, therefore, these concentrations are more uncertain than the concentrations reported for the target analytes.

The magnitude of quantified VOCs in soil vapor samples (i.e., the total concentration of target analytes and TICs) can be used to evaluate the likely presence of LNAPL below each tank. The total concentration of quantified analytes is summarized on Figure 3-1. Siloxane and silanol compounds were excluded from the TICs because these compounds are commonly associated with the laboratory equipment and were likely not present in the original samples (http://analyteguru.com/gc-gc-ms-troubleshooting-part-ii-siloxane-peak-contamination/).

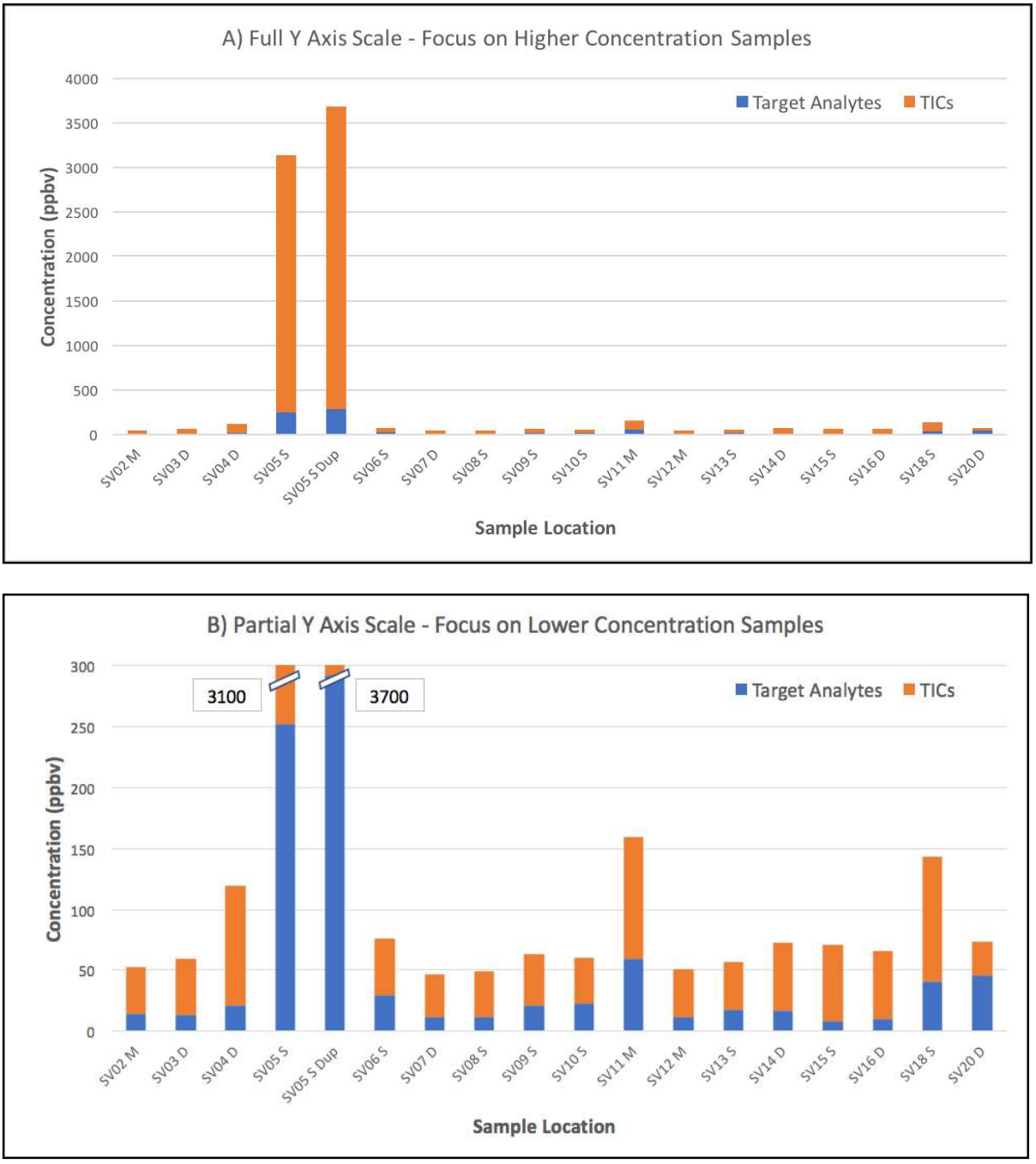

ppbv parts per billion by volume

Figure 3-1: Total Concentration of Quantified VOCs in Soil Vapor Samples

At equilibrium between liquid fuel and vapor, the vapor pressure defines the total petroleum vapor concentration in the vapor phase. The vapor pressure of fresh jet fuel is approximately 2–4 millibars (mbar) (https://www.ncbi.nlm.nih.gov/books/NBK231234/; Shepard et al. 2000). At equilibrium, this represents a petroleum vapor concentration of 2,000–4,000 parts per million by volume (ppmv) of fresh jet fuel (i.e., 1 mbar is approximately equal to 1 part per thousand [ppt]) or 1,000 parts per million [ppm]). However, the vapor pressure of fuel decreases with weathering as the more volatile components are depleted from the liquid fuel (Shepard et al. 2000).

Total VOC concentrations measured in soil vapor samples rarely approach concentrations predicted by equilibrium partitioning (McHugh and McAlary 2009). In a study evaluating soil vapors at 24 contaminated groundwater sites, the measured soil vapor concentrations ranged from 0.002% to 10% of that predicted by Henry's law, with a mean of 0.66% (Fitzpatrick and Fitzgerald 1996). Similar non-equilibrium conditions are expected at LNAPL sites because similar vapor attenuation processes (diffusion, advection, and biodegradation) prevent full equilibration in bulk soil vapor.

As shown on Figure 3-1, the magnitude of VOCs detected in the samples for the soil vapor points varied over a relatively small range (46–160 parts per billion by volume [ppbv]) except for the duplicate samples collected from the shallow soil vapor point below Tank 5 (3,138 and 3,682 ppbv). The total concentration of target analytes plus TICs in Tank 5 (i.e., 3 ppmv and 4 ppmv) samples was equal to approximately 0.1% of the expected equilibrium vapor concentration of fresh jet fuel (2,000–4,000 ppmv). After accounting for the effects of weathering on decreasing the vapor pressure of jet fuel, the likely presence of unquantified petroleum compounds in the samples, and non-equilibrium conditions in soil vapor, the total VOC concentrations measured below Tank 5 (i.e., 0.1% of equilibrium with fresh jet fuel) are likely consistent with the presence of weathered jet fuel LNAPL in the vicinity of the sample collection point. The total VOC concentrations measured below all the other tanks (i.e., < 0.01% of equilibrium with fresh jet fuel) are too low to be indicative of LNAPL containing a significant volatile fraction. However, as discussed in Section 3.1.4, many of these samples contained an unresolved "hump" of less-volatile constituents visible on the flame ionization detector (FID) chromatogram that may indicate the presence of heavily weathered LNAPL in the vicinity of these tanks.

Finding: The magnitude of quantified petroleum vapors in samples from the below-tank soil vapor points indicates the presence of weathered LNAPL below Tank 5. Although the quantitative laboratory results from the other tanks are not indicative of LNAPL below these other tanks, other lines of evidence do suggest the presence of heavily weathered LNAPL below other tanks.

3.1.2 Composition of Petroleum Vapors

The mixture of petroleum compounds detected in each soil vapor sample can be used to evaluate the weathering state of the source fuel. Specifically, the distribution of alkanes provides a good marker for biological weathering. C8–C12 n-alkanes are the most prominent components of vapors from unweathered jet fuel, with lower concentrations of branched alkanes and cycloalkanes (Pleil, Smith, and Zelnick 2000, Figure 4). However, under either aerobic conditions (Kaplan et al. 1997) or anaerobic conditions (Baedecker et al. 2011), n-alkanes are readily biodegraded while branched alkanes are more slowly degraded and cycloalkanes exhibit the slowest degradation rates. As a result, branched alkanes and cycloalkanes are more dominant in vapors from more weathered fuel.

"Fingerprint" graphs for each sample are provided as Attachment B.3.1.

The distribution of alkanes in samples collected from the soil vapor points is provided on Figure 3-2 and Figure 3-3. The distribution Figure 3-2 is consistent with unweathered or lightly weathered jet fuel; the distribution on Figure 3-3 is consistent with weathered jet fuel.

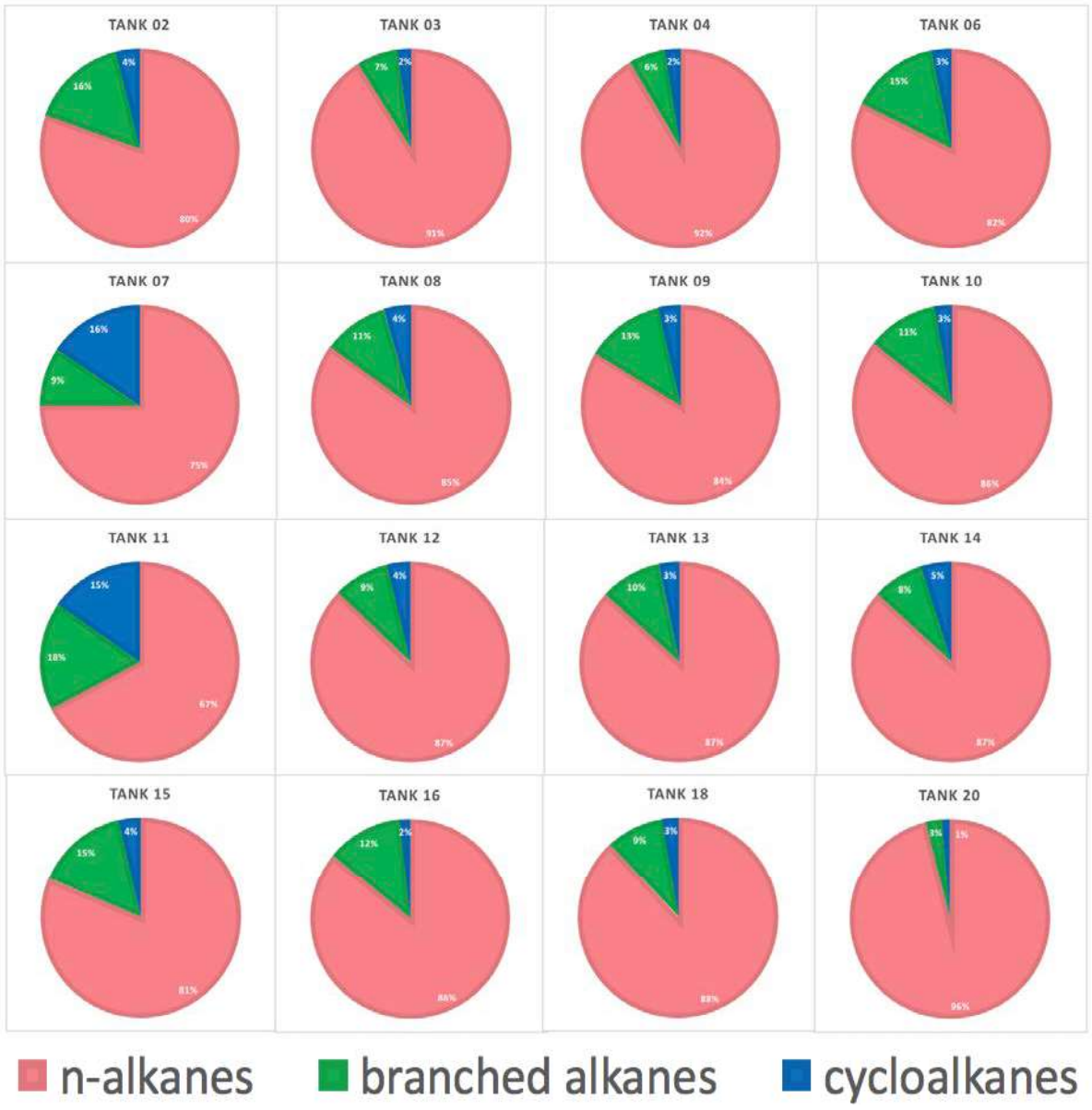

Figure 3-2: Distribution of Alkanes in Soil Vapor Samples for All Samples Except Tank 5

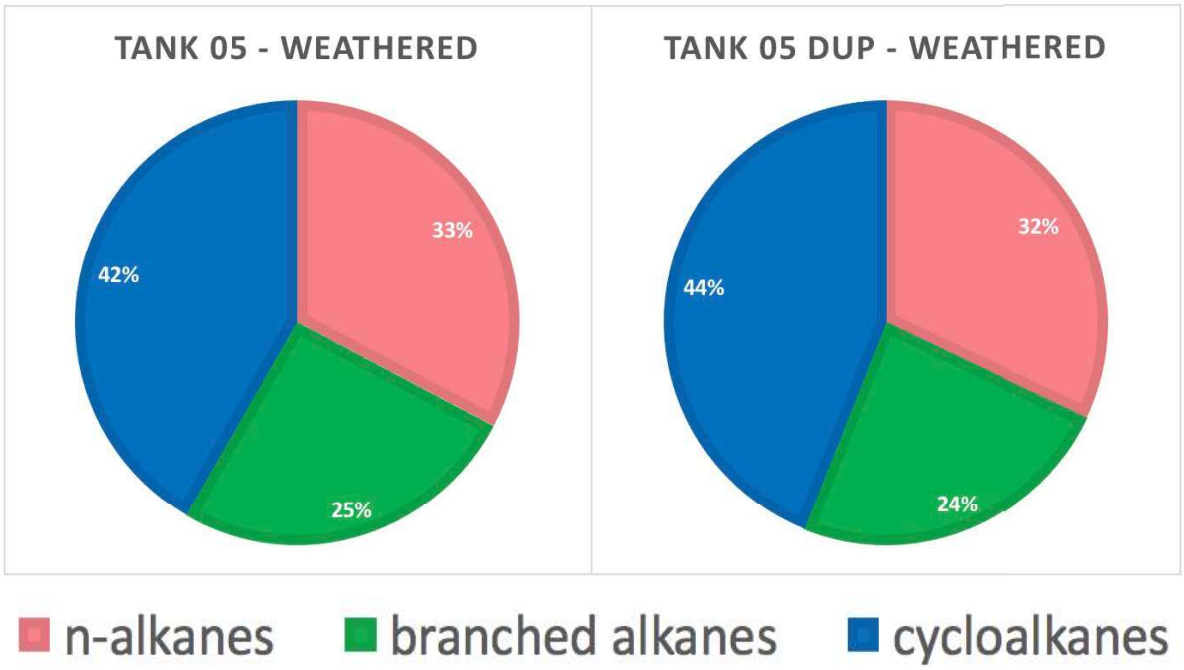

Figure 3-3: Distribution of Alkanes in Soil Vapor Samples for Tank 5

As shown on Figure 3-2, except for Tank 5, the quantified target analytes for the samples from the soil vapor points shown an alkane distribution consistent with little or no weathering of the fuel (Kaplan et al. 1997). These samples are dominated by n-alkanes (67–96%) with much smaller percentages of branched alkanes (3–18%) and cycloalkanes (1–16%). In addition, as shown in Attachment B.3.1, most of these samples exhibit a normal distribution of n-alkanes within the range of C9 (nonane) to C13 (tridecane), consistent with the profile observed in fresh diesel vapors (e.g., Figure 4A from Pleil, Smith, and Zelnick 2000; Figure 3A from Gregg et al. 2007). Fresh diesel vapors are similar in composition to fresh jet fuel vapors.

Based on low total VOC concentration (Section 3.1.1) and the composition consistent with unweathered jet fuel, the petroleum vapors in these samples likely reflect low-level vapor-phase releases of petroleum rather than LNAPL releases. Aside from Tank 5, the total target analyte plus TIC concentration was very low (ranging from 46 ppbv to 160 ppbv); several orders of magnitude below the equilibrium vapor concentration associated with fresh jet fuel LNAPL. In addition, aside from Tank 5, the concentrations of all individual petroleum constituents (except naphthalene) were below EPA Regional Screening Levels for industrial indoor air. In other words, even undiluted, the individual VOCs detected in the below-tank soil vapor samples would not pose an indoor air exposure risk. Although the specific source(s) of these vapors were not identified through this study, low-level vapor releases at fuel storage facilities are not unexpected. Vapor releases can occur through joints, valves, and gaskets as well as during tank filling and fuel transfer operations. These types of small vapor-phase releases are difficult to completely eliminate.

In contrast to the samples from below the other tanks, the normal and duplicate vapor samples collected from below Tank 5 (Figure 3-3) exhibited a smaller percentage of n-alkanes (32–33%) and a higher percentage of branched alkanes (24–25%) and cycloalkanes (42–44%). This distribution is consistent with biologically weathered jet fuel (Kaplan et al. 1997; Baedecker et al. 2011).

Finding: Considering both the concentration and composition of petroleum vapors detected in the below-tank soil vapor points, the results from Tank 5 are consistent with a LNAPL release that has undergone significant biological weathering, and the results from the other tanks are consistent with low level vapor-phase releases typical of any fuel storage operation.

3.1.3 Tentatively Identified Compounds in Soil Vapor Samples

An evaluation of the TICs provides additional support for the evaluation of the Tank 5 sample as weathered LNAPL. For Tank 5, all the TICs that could be tentatively identified by the laboratory were cycloalkanes or branched alkanes with estimated concentrations in the range of 200–400 ppbv. As discussed above, the cycloalkanes and branched alkanes biodegrade more slowly than the n-alkanes and, therefore, become more predominant as the LNAPL weathers. For the other tanks, the TICs were mostly a mixture of petroleum hydrocarbons, alcohols, and ketones with much lower estimated concentrations of 1–20 ppbv.

3.1.4 Evaluation of FID Chromatograms

Middle distillate fuels such as jet fuel contain a complex mixture of petroleum compounds many of which cannot be completely separated in a laboratory GC column. As a result, an unresolved "hump" (also called an "unresolved complex mixture," UCM) is often visible at the end of the chromatogram (Tran et al. 2010). As the fuel weathers in the environment, this unresolved hump often becomes more prominent. Compounds in this unresolved hump are not quantified as either target analytes or TICs.

For each soil vapor sample, the FID chromatogram was reviewed to evaluate the presence of an unresolved hump indicative of compounds not quantified as either target analytes or TICs. For this purpose, the FID chromatogram rather than the mass spectrum (MS) detector chromatogram was used because the FID response is more consistent across petroleum compounds. Representative FID chromatograms are provided on Figure 3-4, and the full set of FID chromatograms are provided in Attachment B.3.2.

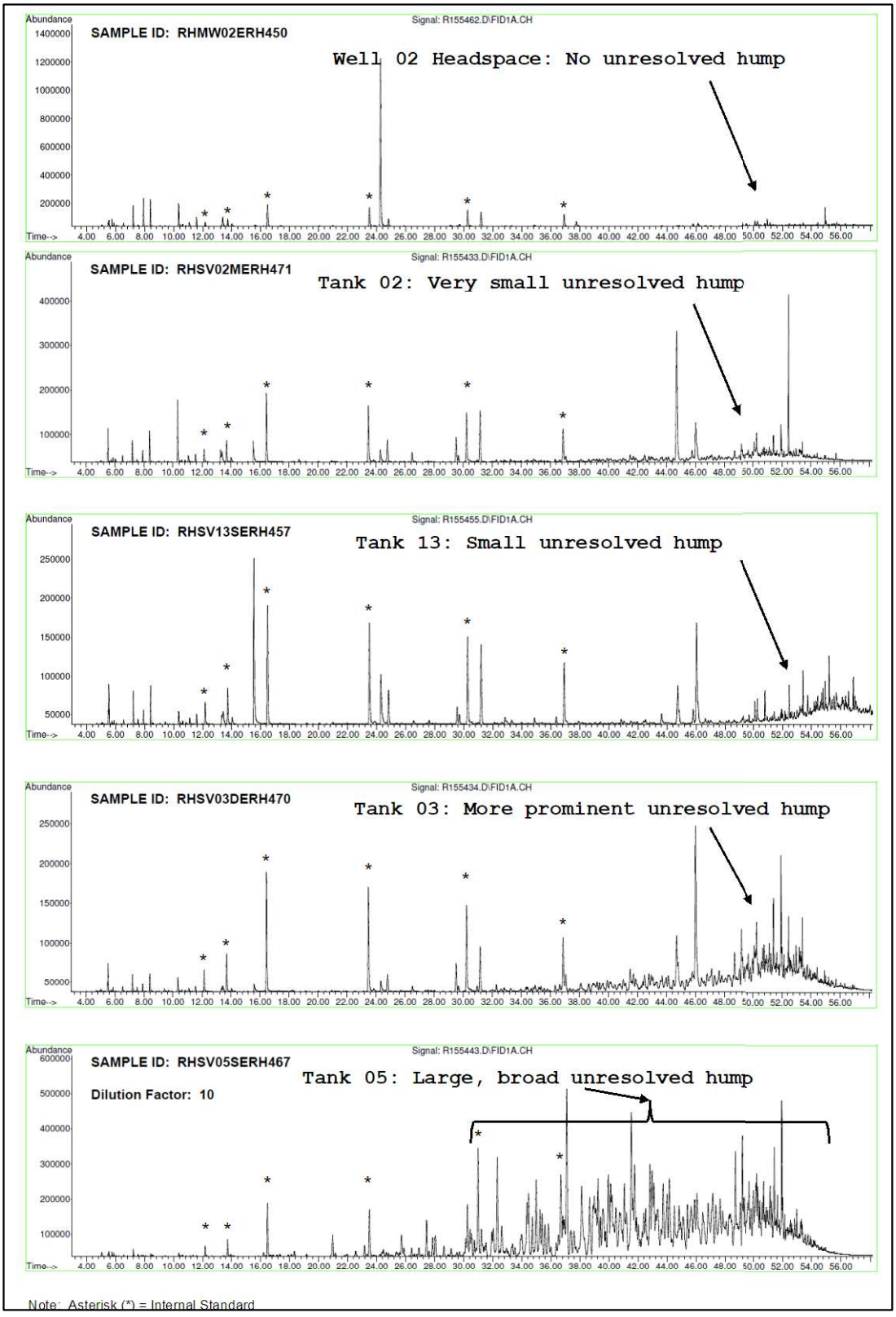

Figure 3-4: FID Chromatograms from Representative Samples Showing Range of Unresolved Hump

All samples collected from the below-tank soil vapor points contained a visible unresolved hump at the end of the FID chromatogram indicating the presence of at least some unquantified lower volatility compounds in these samples. In contrast, none of the four well headspace samples contained a visible unresolved hump. For the below-tank samples, the size of this hump varied between samples indicating differing amounts of the unquantified compounds:

- **Tank 5:** The shape and magnitude of the unresolved hump is consistent with the presence of weathered LNAPL. This is consistent with the analysis of target analytes and TICs in Sections 3.1.1–3.1.3.
- **Tanks 3, 4, 7, and 18:** The shape and magnitude of the unresolved hump is consistent with the presence of heavily weathered LNAPL. For these tanks, the analysis of target analytes and TICs indicates low-level vapor-phase releases likely associated with ongoing Facility operations. Thus, the samples collected from these soil vapor points likely consist of a mixture of unweathered (or slightly weathered) vapor releases and vapors from heavily weather petroleum LNAPL.
- **Tanks 2, 6, 9, 10, 11, 12, 13, 14, 15, 16, and 20:** The shape and magnitude of the unresolved hump is mostly consistent with fresh jet fuel vapors with contributions from heavily weathered LNAPL apparent in some of the samples. For these tanks, the analysis of target analytes and TICs is consistent with unweathered or lightly weathered jet fuel indicating likely low-level vapor-phase releases associated with ongoing Facility operations. Thus, the samples collected from these soil vapor points likely consist of unweathered (or slightly weathered) vapor releases with a smaller component of vapors from heavily weathered petroleum LNAPL.

3.2 FIELD MEASUREMENTS

Field measurements were conducted at existing and new soil vapor points, plus RHMW01, RHMW02, RHMW03, and RHMW04 headspace. In addition, ambient readings were recorded for the tunnel and outdoor air. Field measurements included total VOC concentration by PID, and oxygen, carbon dioxide, methane concentrations and differential pressure by Landfill Gas Meter. All field measurements are presented in Attachment B.3.3.

3.2.1 PID Readings

PID readings at the soil vapor points ranged from 44 to 40,000 ppbv. Readings above 10,000 ppbv were recorded at seven locations (RHMW01 headspace and soil vapor points below Tanks 5, 6, 11, 12 [two points], and 18). However, as discussed in Section 3.3, there was a poor correlation between PID readings and the total VOC concentration measured in samples collected for laboratory analysis. Specifically, the PID reading was often much higher than the laboratory-measured total VOC concentration.

3.2.2 Oxygen, Carbon Dioxide, and Methane

High oxygen and low carbon dioxide concentrations were recorded at almost all measurement locations. For the below-tank soil vapor points, oxygen concentrations ranged from 13.7% to 20.6%, with only two readings below 18%. Carbon dioxide concentrations ranged from 0.1% to 3.2%, with most readings less than 1%. For the well headspace samples, oxygen was 17–21% and carbon dioxide was 0.1–2.1% except for RHMW02, where oxygen was 6.6% and carbon dioxide was 8.5%. Methane was not detected in any measurement location. These results indicate an aerobic

environment throughout the vadose zone. The results for the individual sample points are provided in Attachment B.3.3.

3.2.3 Differential Pressure

For 39 of the 46 below-tank soil vapor points tested, both of the two upper-tunnel Vapor Pin points, and three of four monitoring wells, the differential pressure measurements showed a positive pressure relative to the tunnel (i.e., a pressure gradient indicating gas flow from the vadose zone into the tunnel). At most of these locations, the differential pressure was greater than 0.1 inch H_2O (i.e., > 25 pascals). For comparison, a differential pressure of 0.02 inch H_2O (5 pascals) is typically considered sufficient to support advective flow in the context of vapor intrusion mitigation (i.e., sufficient for effective sub-slab depressurization systems). These results indicate that advective air flow is from the vadose zone into the tunnels.

3.3 Correlation between Field Measurements and Laboratory Results

The correlations between field measurements and laboratory analytical results were evaluated to determine the utility of field measurements for ongoing screening and monitoring activities.

3.3.1 Field PID Readings vs. Laboratory Total Quantified VOC Concentrations

All below-tank soil vapor points have been screened monthly using a PID since 2008. To evaluate the utility of this screening for tracking petroleum vapor concentrations going forward, the correlation between the October/November 2017 field PID readings and the collocated laboratory measured total VOC concentrations was evaluated (Figure 3-5).

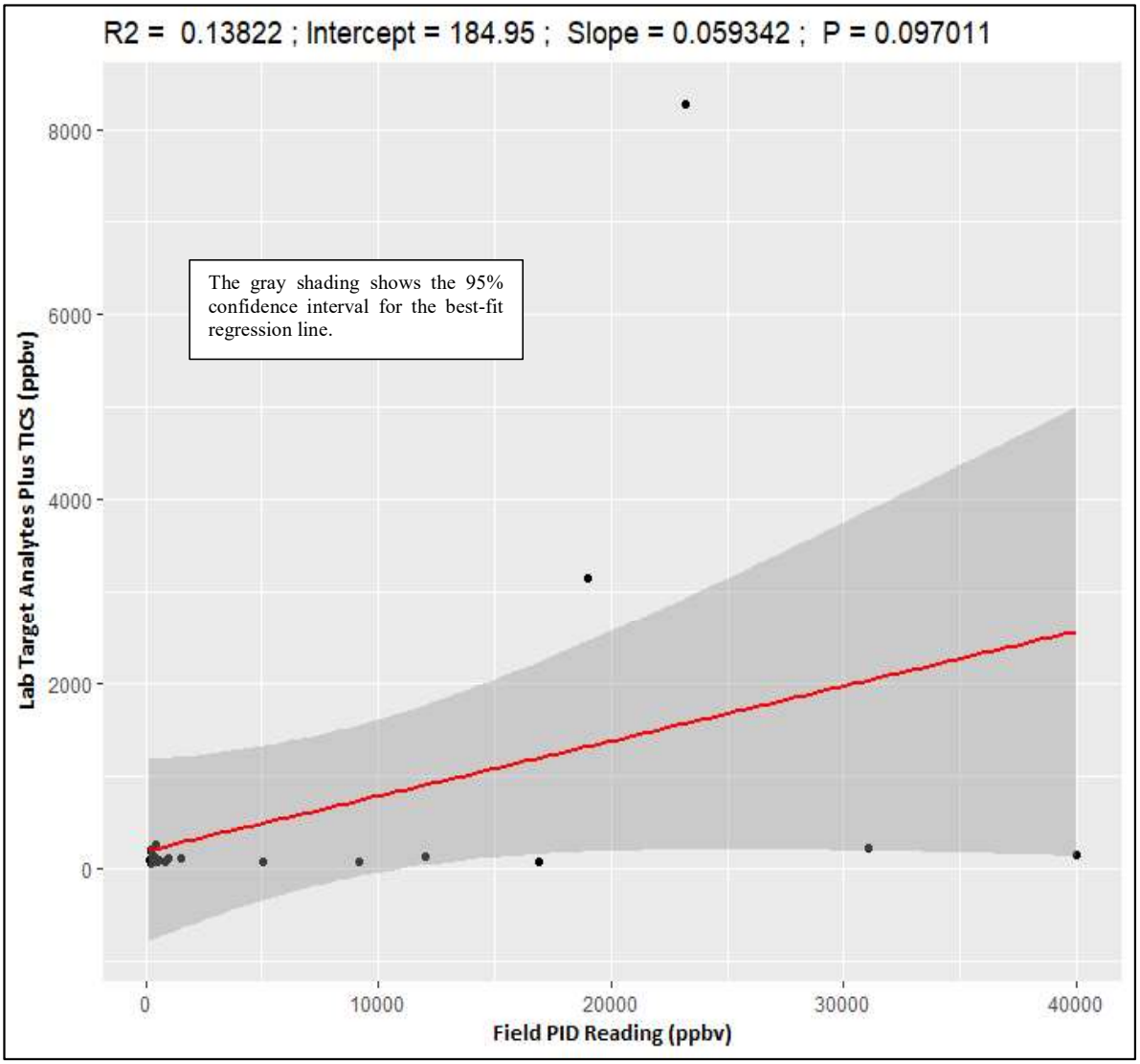

Figure 3-5: Correlation between PID Readings and Laboratory Total Target Analytes Plus TICs

As shown on Figure 3-5, a poor correlation was observed between PID readings and laboratory-measured total VOC concentrations (Slope = 0.06, R^2 = 0.14). For Tank 5 (PID = 19,000; Laboratory = 3,100) and MW01 Headspace (PID = 23,200; Laboratory = 8,300), the sum of target analytes and TICs was in reasonable agreement with the PID reading. However, for the remaining paired measurements, the sum of target analytes and TICs ranged from 46 to 254 ppbv while the PID readings ranged from 160 to 40,000 ppbv. In addition to Tank 5, six other locations yielded PID readings above 10,000 ppbv. However, the sum of target analytes and TICs at these six locations was 254 ppbv or lower. Thus, the PID appeared to have a large false-positive rate, commonly yielding PID readings of greater than 10,000 ppbv at locations without high concentrations of laboratory measured petroleum or other VOCs. The cause(s) of these high PID readings was not determined.

Although a poor correlation between PID readings and laboratory-quantified VOCs was observed during the single monitoring event, this dataset did not allow evaluation of the utility of changes in PID readings over time for detection of new releases. As discussed in Section 4 (Question 5), for

individual monitoring locations, changes in PID readings over time do appear to provide an indication of possible new LNAPL fuel releases.

3.3.2 Field vs. Laboratory Oxygen, Carbon Dioxide, and Methane Concentrations

In addition to field measurement at all locations, oxygen, carbon dioxide, and methane concentrations were measured by EPA Method 3C in all samples collected for laboratory analysis. Methane was not detected in any sample by field measurement or laboratory analysis. To evaluate the accuracy of the field measurements, the correlation between the field measurement and the laboratory measurement was evaluated.

Oxygen Concentration: As shown on Figure 3-6, a relatively poor correlation was observed between the field and laboratory measured oxygen concentrations. However, this poor correlation is attributable to two locations where the laboratory measured oxygen concentration was much lower than the field measured concentration. For both of these locations the laboratory and field-measured carbon dioxide concentrations were low (0.2–0.4%). Because low oxygen in soil vapor samples is typically accompanied by elevated carbon dioxide levels, these results suggest erroneous laboratory results for these two samples. When these two data points are removed from the dataset, a very high correlation is observed (Slope = 1.01; $R^2 = 0.98$, Figure 3-7). This analysis indicates high accuracy for the field measured oxygen concentrations.

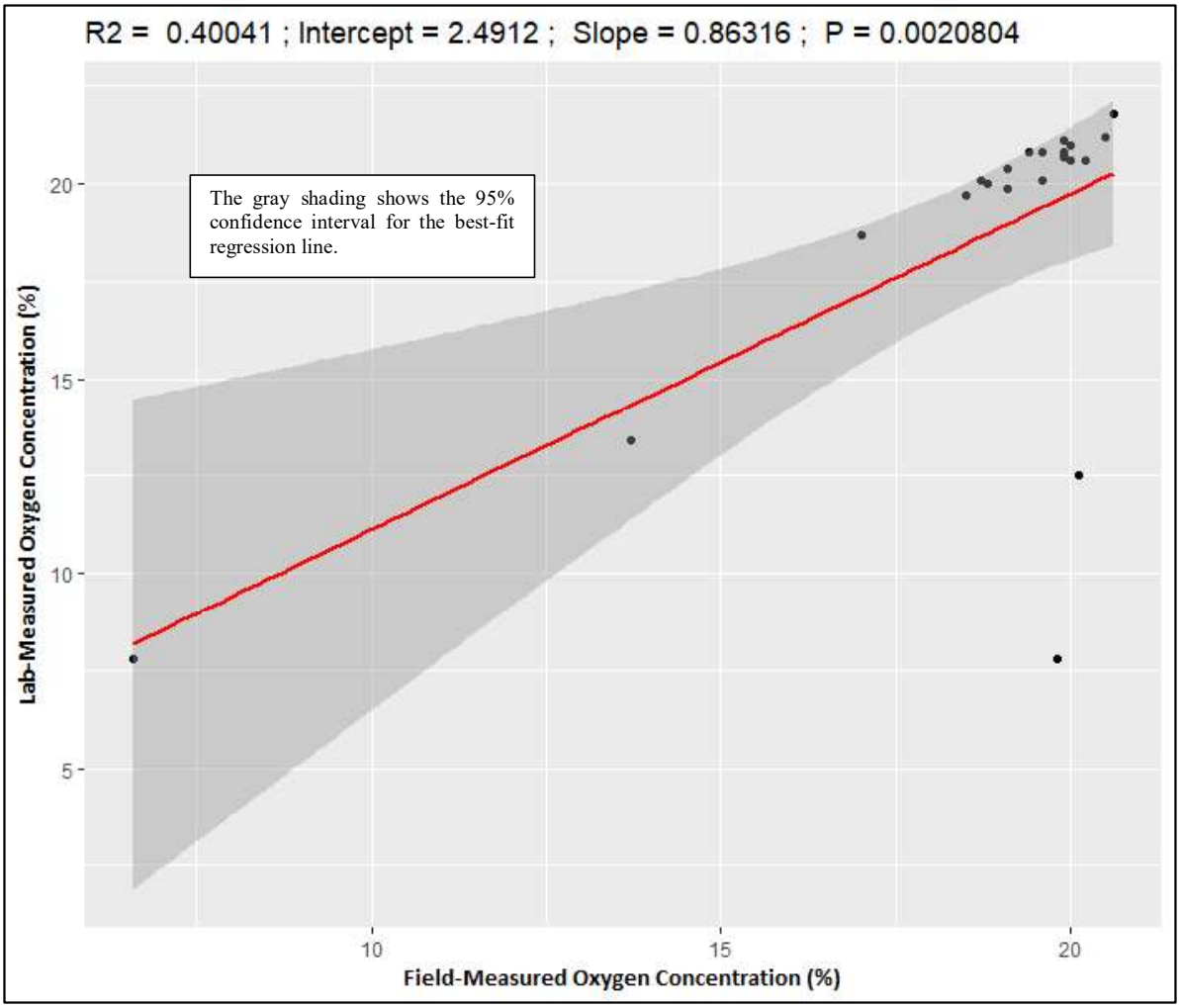

Figure 3-6: Correlation between Field- and Laboratory-Measured Oxygen Concentration

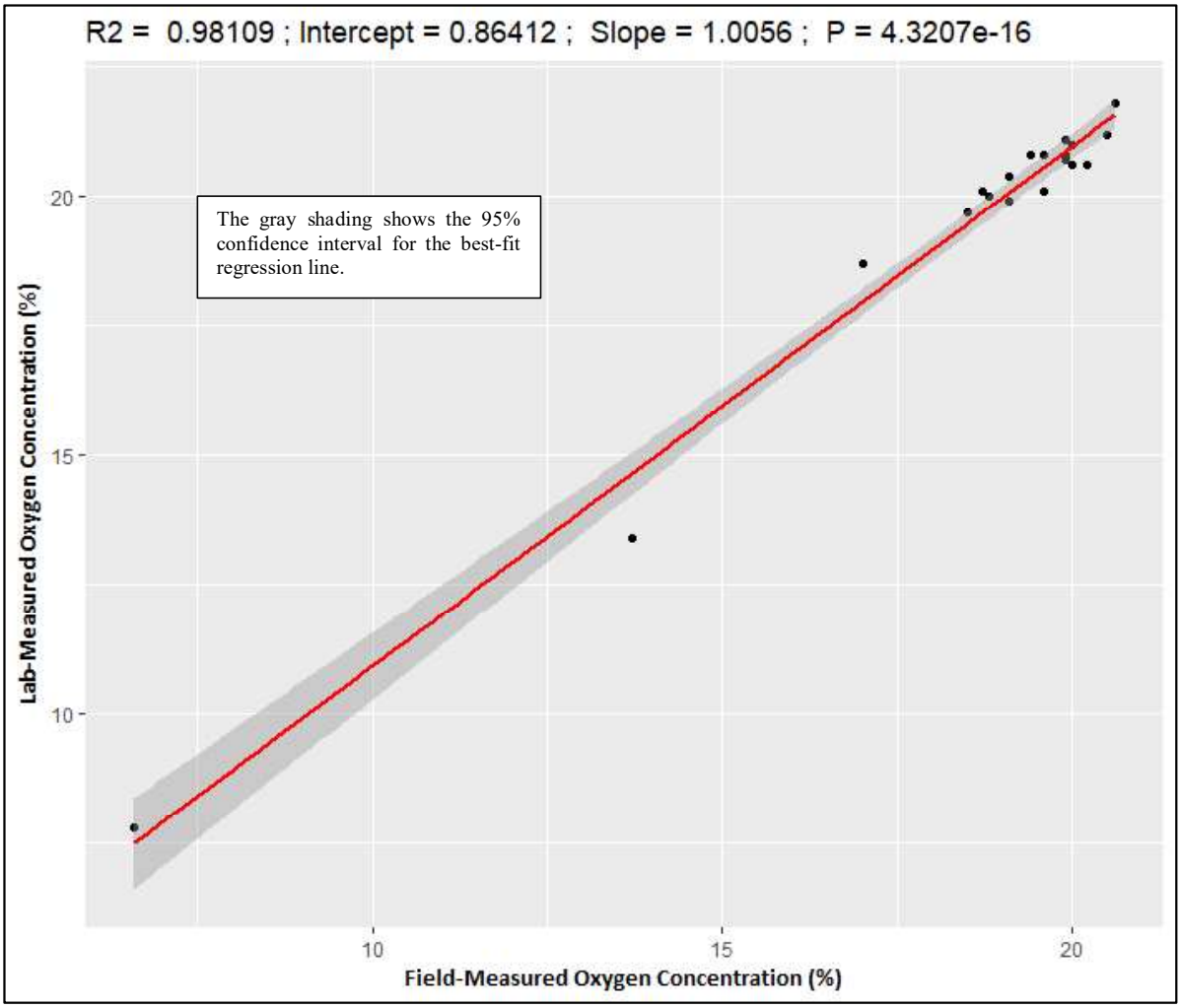

Figure 3-7: Correlation between Field- and Laboratory-Measured Oxygen Concentration Excluding Two Low-Biased Laboratory Measurements

Carbon Dioxide Concentration: As shown on Figure 3-8, a good correlation was observed between the field and laboratory carbon dioxide concentrations (Slope = 1.08; $R^2 = 0.99$). This indicates high accuracy for the field-measured carbon dioxide concentrations.

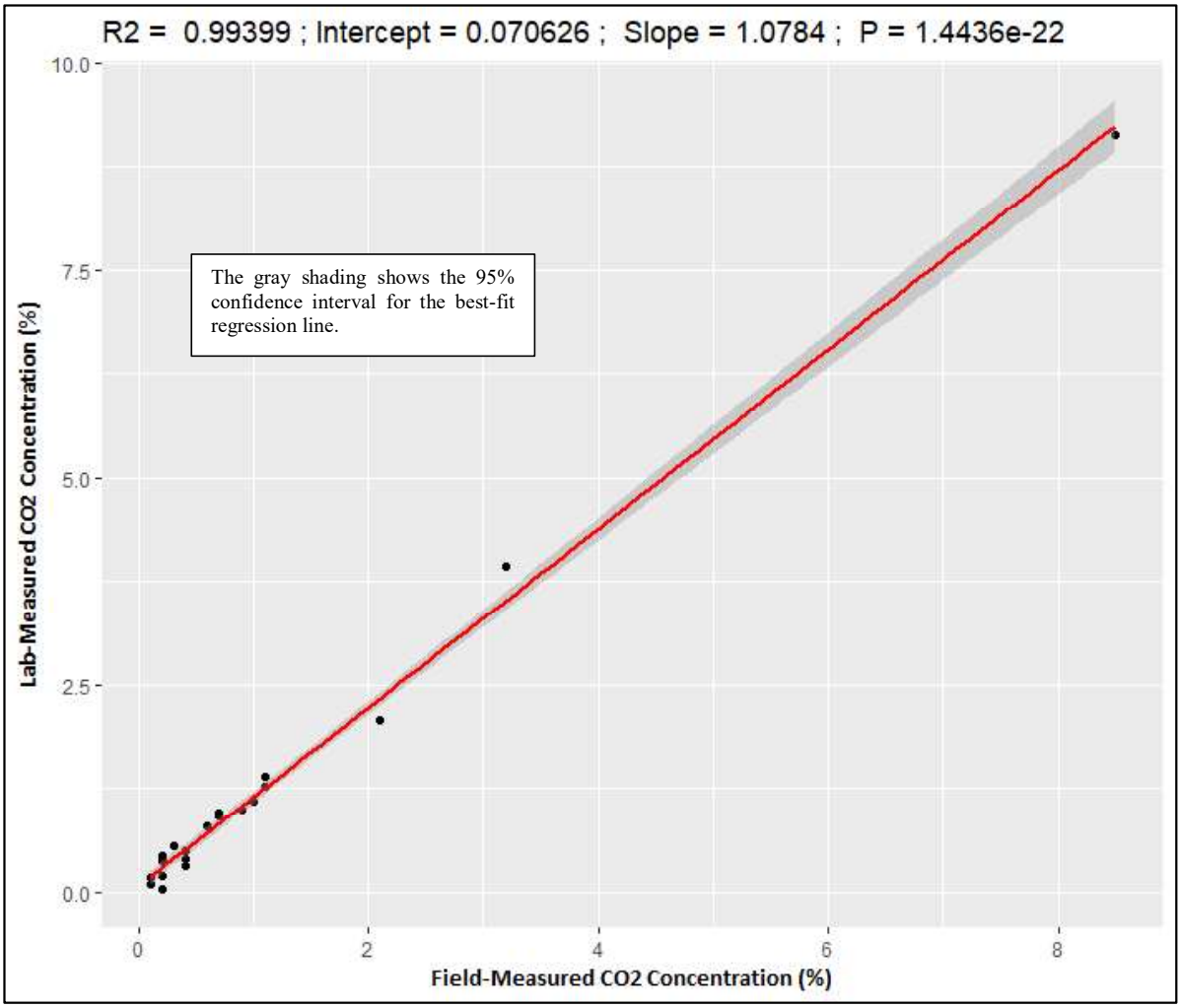

Figure 3-8: Correlation between Field- and Laboratory-Measured Carbon Dioxide Concentration

4. Discussion of Soil Vapor Investigation Results

The purpose of the soil vapor investigation was to help address the following questions:

1. Is there evidence of recent or historical fuel releases at one or more of the tanks?
2. Is LNAPL present below the tanks?
3. Is NSZD occurring?
4. Can vapor monitoring help detect potential future LNAPL fuel releases?
5. Can vapor monitoring be used to track NSZD progress over time?
6. Are vadose zone petroleum vapors a significant source of impacts in the tunnels?

Findings are presented in Table 4-1 – Table 4-6.

Table 4-1: Study Question 1: Is There Evidence of Recent or Historical Fuel Releases at One or More of the Tanks?

Finding	Discussion
YES, the soil vapor results suggest an historical release of LNAPL fuel at Tank 5 and, at the other tanks, low-level vapor-phase releases associated with ongoing Facility operations.	The analysis of soil vapor samples indicates a LNAPL fuel release at Tank 5. The total VOC (i.e., sum of target analytes plus TICs) concentration in the two soil vapor samples from below Tank 5 (3 and 4 ppmv) were approximately 0.1% of equilibrium vapor concentrations for fresh jet fuel (2,000–4,000 ppmv). Accounting for non-equilibrium conditions typically observed in the subsurface and the expected reduction in vapor pressure associated with the weathering of jet fuel, the concentration of VOC vapors measured below Tank 5 is consistent with the presence of weathered jet fuel LNAPL in this area. The alkanes in this sample were predominately cycloalkanes and branched alkanes, compounds that are more resistant to biodegradation, with a lower percentage of readily biodegradable n-alkanes (Figure 3-3). This composition suggests that the LNAPL is weathered. The analysis of soil vapor samples from below the other tanks does not indicate the presence of fresh or weathered LNAPL containing measureable levels of VOCs. The total VOC concentrations at these locations (0.05–0.16 ppmv) is less than 5% of the concentration at Tank 5. In addition, the alkanes in these samples are dominated by the readily degradable n-alkanes (67–96%; Figure 3-2) indicating little or no weathering of the fuel. The low VOC concentration combined with the absence of weathering suggests low-level vapor-phase releases of fuel near these tanks are likely associated with ongoing Facility operations.

Table 4-2: Study Question 2: Is LNAPL Present below the Tanks?

Finding	Discussion
YES, the soil vapor results suggest the presence of weathered LNAPL fuel below Tank 5. Borings completed below some of the other tanks provided visual evidence of LNAPL at the time the borings were installed (1998-2012). For these other tanks, the presence of LNAPL is not reflected in the quantitative analysis soil vapor samples collected in October/November 2017; however, many of the FID chromatograms show an unresolved hump of less-volatile compounds potentially consistent with the presence of highly weathered LNAPL (see Attachment B.3.2).	The total VOC concentration and alkane composition in the soil vapor samples collected from below Tank 5 are consistent with the presence of weathered LNAPL in this area. These results suggest that significant weathering has occurred since the documented Tank 5 fuel release in 2014. Angle borings completed below the fuel tanks from 1998 to 2012 suggested the presence of LNAPL below several additional tanks, such as Tanks 1, 9, 13, 14, 16, and 17 (Figure 4-1; Attachment B.3.5). The 2017 soil vapor samples collected from below all tanks (except Tank 5) contained low concentrations of target VOCs and TICs. The distribution of alkanes in these samples (i.e., mostly n-alkanes) was consistent with unweathered or lightly weathered jet fuel likely associated with vapor-phase releases from ongoing Facility operations. However, all these samples contained unresolved humps at the end of the FID chromatograms indicating the presence of less volatile compounds in these samples that were not quantified as target analytes or TICs (see Attachment B.3.2). The greatest amount of this material was observed in the samples from below Tanks 3, 4, 7, and 18. These results suggest that the LNAPL observed below the tanks in the 1998–2012 borings has weathered to the point that most or all of the volatile constituents have been depleted.

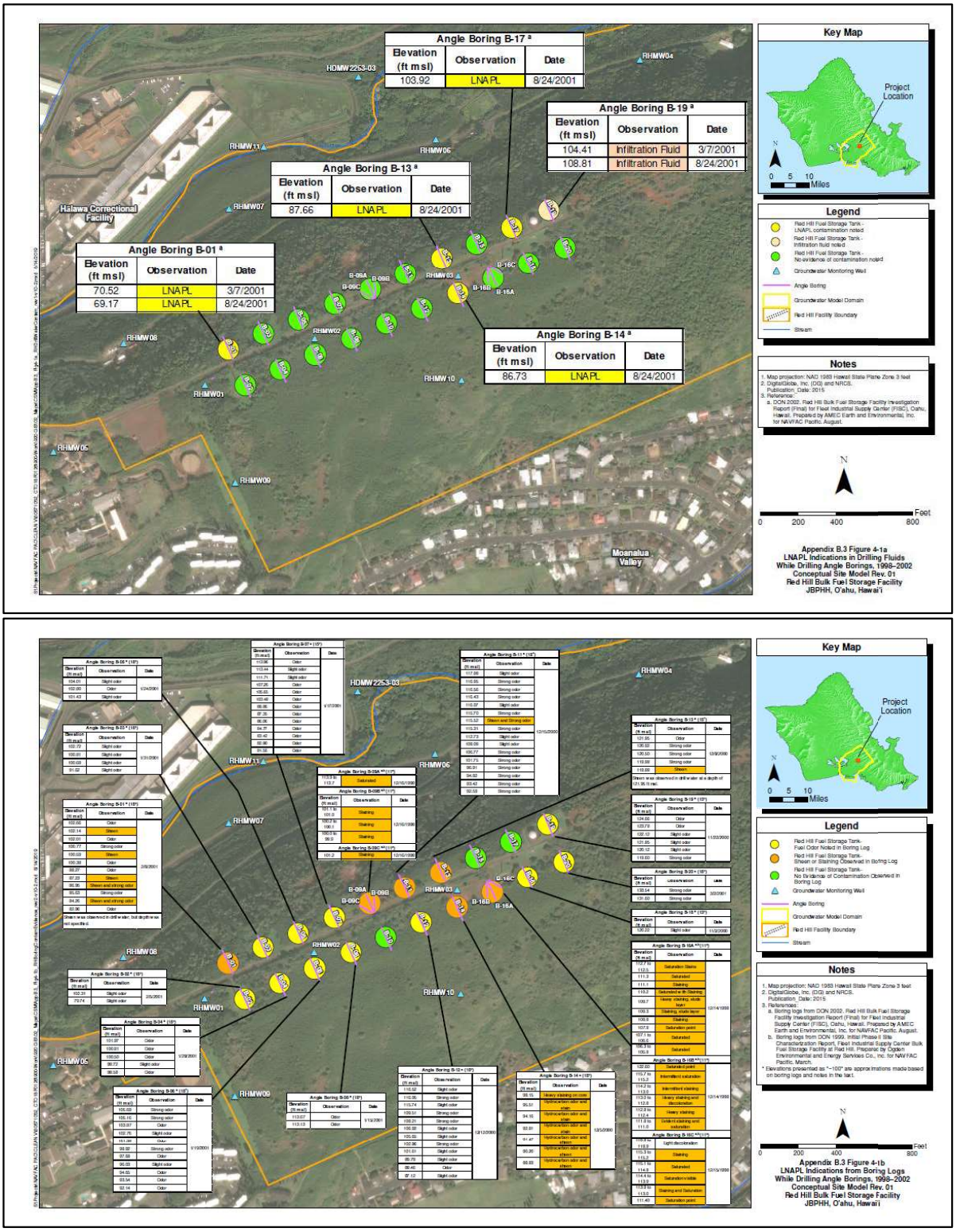

1 Most data from 1998–2001; see Attachment B.3.5 for full-size figures.

2 **Figure 4-1: Top: LNAPL Indications from Drilling Fluids; Bottom: LNAPL Indications from Boring Logs**

Table 4-3: Study Question 3: Is NSZD Occurring?

Finding	Discussion
YES, as discussed above, the soil vapor results suggest that significant biological weathering of the LNAPL below Tank 5 has occurred since the 2014 release. This is consistent with other lines of evidence supporting biological NSZD.	The conclusion of biological weathering of LNAPL releases is supported by the following observations: • The petroleum vapor fingerprint from below Tank 5 is consistent with weathered LNAPL associated with the 2014 release. • The vapor testing below other tanks indicates that the LNAPL visually observed in borings completed below these tanks in 1998 to 2002 is depleted in VOCs. • Field monitoring and laboratory analysis indicate high oxygen concentrations (13.7–20.6%) and non-detect levels of methane (<0.1%) in all the below-tank soil vapor points, supporting aerobic biodegradation. Carbon dioxide concentrations are low (0.1–3.2%), but above atmospheric levels (0.04%). • Thermal monitoring indicates ongoing biological NSZD (see CSM Appendix B.1). • Carbon trap data provide an additional, independent line of evidence on ongoing biological NSZD (see CSM Appendix B.2).

Table 4-4: Study Question 4: Can Vapor Monitoring Help Detect New LNAPL Fuel Releases?

Finding	Discussion
YES. Monthly PID screening of the soil vapor points with laboratory confirmation for those with elevated PID readings is likely to be a reliable method for detecting any new LNAPL releases of jet fuel.	Although a poor correlation was observed between PID readings and laboratory measured total VOC concentrations across soil vapor points during a single monitoring event, changes in PID readings over time do appear to provide useful information regarding possible new releases of LNAPL jet fuel. As shown on Figure 4-2, PID readings at the Tank 5 soil vapor points spiked rapidly from less than 100 ppbv in December 2013 to greater than 200,000 ppbv in January 2014 corresponding to the 2014 Tank 5 release event. PID readings at Tank 5 peaked at 450,000 ppbv May 2014 and have then decreased over time consistent with biological weathering and other NSZD processes. In contrast, PID readings from below other tanks have rarely exceeded 100,000 ppbv since 2008. The PID monitoring results suggest that rapid increases in PID readings below a fuel tank may indicate a new release of LNAPL fuel. If a rapid increase is observed in future monitoring, laboratory analysis by TO-15 PIANO (i.e., TO-15 analysis with 90+ petroleum VOC analyte list) can be used to provide confirmation that the spike is associated with a new release. The January 2014 release event from Tank 5 resulted in PID readings >100,000 ppbv in all three soil vapor points below Tank 5. In addition, the release event caused elevated PID readings (i.e., >25,000 ppbv) in soil vapor points below all three adjacent tanks (i.e., in one of three soil vapor points below Tank 3, two of two soil vapor points below Tank 6, and three of three soil vapor points below Tank 7). Although these readings were smaller in magnitude and shorter in duration than those observed in the Tank 5 soil vapor points, they were clearly elevated relative to baseline (pre-release) PID readings. Thus, following the release event, elevated PID readings were observed in a total of nine soil vapor points. This indicated that the soil vapor monitoring network is very robust with a higher monitoring point density than needed to detect releases on the magnitude of thousands of gallons. The PID monitoring results further suggest that a large release event (i.e., thousands of gallons) results in a sustained increase in PID readings below the tank that persists for months to years. Following the January 2014 release event of 27,000 gallons at Tank 5, PID readings for the soil vapor points below Tank 5 remained above 100,000 ppbv for approximately 30 months (i.e., until June 2016). The absence of similar sustained elevated PID readings for the soil vapor points below the other tanks suggests that no large release events have occurred from these tanks during the period of PID monitoring (i.e., 2008 to present).

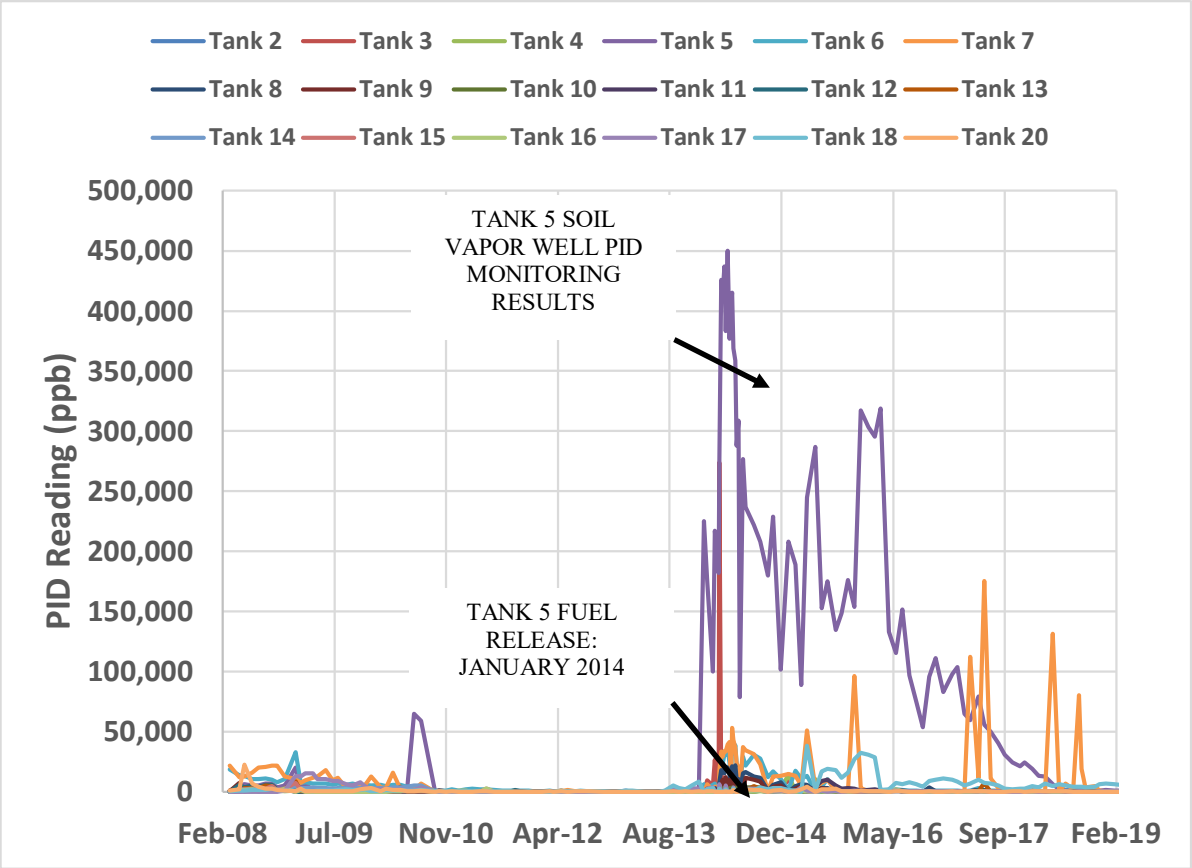

Figure 4-2: Linear Scale Graph of Monthly PID Monitoring Results for Below-Tank Soil Vapor Points

Table 4-5: Study Question 5: Can Vapor Monitoring Be Used to Track NSZD Progress Over Time?

Finding	Discussion
YES, monthly PID monitoring appears to track decreases in petroleum vapor concentration over time associated with weathering of LNAPL releases. The TO-15 PIANO analysis provides detailed information on the petroleum VOC vapor composition that can be used to evaluate the degree of biological weathering.	Monthly PID monitoring of the below-tank soil vapor points has been conducted since 2008 (Figure 4-3 and Figure 4-4). These monitoring data document below-tank petroleum impacts that pre-date the initiation of PID monitoring resulting in 2008 PID readings generally in the range of 1,000 ppbv to 10,000 ppbv. As shown on Figure 4-3 and Figure 4-4, these PID readings generally decreased over time from 2008 through 2013 consistent with NSZD of the historical fuel impacts. In early 2014, PID readings for the Tank 5 soil vapor points increased above 200,000 ppbv corresponding with the January 2014 release from Tank 5. Smaller PID reading increases were observed for soil vapor points below tanks adjacent to Tank 5. From 2014 to 2017, PID readings again showed a gradual decrease over time consistent with NSZD of the 2014 release. In November 2017, TO-15 PIANO analysis documented the occurrence of biological weathering of the LNAPL below Tank 5 and indicated that any LNAPL present below the other tanks is heavily weathered. Aside from the elevated PID readings associated with the Tank 5 release event in early 2014, the monthly SVMP PID monitoring has rarely shown a PID reading above 10,000 ppbv. Since August 2015, only SVMPs at Tank 5, Tank 7, and Tank 18 have exhibited PID readings above 10,000 ppbv. Tank 5 PID readings have decreased over time since 2014 consistent with natural attenuation of the 2014 LNAPL release and have been below 10,000 ppbv since April 2018. For Tank 18, the SVMP PID readings exhibited an abrupt increase from around 2,000 ppbv to 38,000 ppbv in April 2015. From April 2015 to May 2017, 12 of the 26 monthly PID readings were above 10,000 ppbv; however, the monthly PID readings have been below 10,000 ppbv since June 2017. For Tank 7, monthly PID readings since August 2015 have generally been less than 1,000 ppbv. However, six large 1-month spikes have been observed: 51,000 ppbv in April 2015, 96,000 ppbv in Nov 2015, 112,000 ppbv in April 2017, 176,000 ppbv in June 2017, 131,000 ppbv in April 2018, and 81,000 in August 2018. For the four Tank 7 spikes since April 2017, the PID readings at Tank 7 were much higher than the readings at Tank 5, suggesting that the Tank 7 readings were not associated with the 2014 Tank 5 release. For both Tank 7 and Tank 18, the laboratory analysis of vapor samples collected in late October 2017 did not show evidence of recent (i.e., 2017) LNAPL releases from these tanks. For both tanks, the total concentrations of target analytes plus TICs were much lower than observed at Tank 5, and the FID chromatograms were not indicative of fresh jet fuel vapors. However, the timing of this field sampling program (late October/early November 2017) did not correspond to the period of elevated PID readings at Tank 7 and Tank 18. Laboratory analysis of a vapor sample collected coincidently with the observation of an elevated PID reading would provide a better understanding of the cause of that elevated PID reading. When averaged across all the soil vapor monitoring points, the monthly PID readings show a clear decreasing trend over time (expect for the rapid increase in PID readings associated with the January 2014 Tank 5 release), see Figure 4-4. This decreasing trend over time provides further evidence of 1) no significant releases of fuel from the tanks outside of the January 2014 Tank 5 release and 2) ongoing NSZD of the historical fuel releases.

Tank	1	3	5	7	9	11	13	15	17	19
	2	4	6	8	10	12	14	16	18	20
Max ppm	3.8	274	383	176	12.6	10.2	8.8	7.7	38.4	22.7

2008	T1–2	T3–4	T5–6	T7–8	T9–10	T11–12	T13–14	T15–16	T17–18	T19–20
24-Mar		579	1,295	21,667	405	419	1,195	600	—	
	—	827	18,567	428	246	231	347	195	662	1,133
6-May		668	5,441	12,433	7,644	2,770	640	831	—	
	252	1,235	13,733	4,266	5,368	6,055	2,302	1,521	1,162	2,045
29-May		685	6,523	12,867	878	1,507	3,108	2,082	—	
	1,785	681	13,333	607	521	3,915	2,056	1,576	1,224	22,667
3-Jul		1,504	5,195	16,000	4,238	2,318	3,464	1,541	—	
	1,090	898	10,560	1,764	3,212	5,374	2,816	2,395	1,844	6,976
31-Jul		1,313	5,190	20,367	1,024	1,409	3,469	2,349	—	
	728	1,144	10,502	804	855	4,420	2,204	936	1,679	4,201
2-Sep		1,645	6,905	21,067	1,949	3,459		2,585	—	
	754	1,270	11,416	1,605	1,410	5,948	2,325	1,300	1,792	2,709
29-Sep		4,425	7,149	22,100	2,714	3,157	4,872	4,746	—	
	553	1,454	10,456	2,397	2,266	5,794	2,101	1,461	2,515	2,796
23-Oct		1,423	3,690	21,733	1,458	1,234	1,504	1,905	—	
	555	1,321	8,337	1,358	1,043	2,237	2,477	788	1,481	1,609
25-Nov		1,417	5,221	12,867	2,142	1,238	2,961	2,886	980	
	3,396	893	10,683	2,780	1,825	2,066	2,666	2,594	1,262	1,208
2009										
14-Jan		4,658	20,567	10,667	4,851	2,123	8,757	7,650	13,567	
	329	1,138	32,867	7,153	5,568	11	4,798	361	996	714
5-Feb		1,756	1,824	7,718	786	425	815	1,892	12,933	
	264	746	7,624	1,263	957	226	3,042	1,738	2,099	2,553
26-Feb		2,616	7,015	9,532	930	298	713	605	15,567	
	1,912	1,920	7,936	1,289	798	463	3,080	176	915	674
1-Apr		611	1,179	12,033	241	117	362	249	15,633	
	195	608	6,857	416	194	149	3,971	87	820	645
20-Apr		573	1,326	12,700	361	333	492	351	11,000	
	704	695	6,872	484	241	245	3,385	238	963	798
27-May		568	1,123	18,233	326	210	452	251	10,567	
	1,473	740	6,940	367	194	162	3,392	86	1,146	627
29-Jun		665	1,131	9,743	425	364	516	882	8,982	
	2,141	796	6,161	491	312	274	2,912	256	1,122	663
20-Jul		1,272	1,582	11,667	704	462	667	977	9,093	
	1,360	1,354	7,120	727	424	510	3,312	245	1,597	729
28-Aug		703	1,776	3,078	515	403	622	711	6,506	
	564	751	5,901	563	352	360	3,080	269	2,156	473
24-Sep		860	1,906	2,213	708	763	791	759	5,345	
	488	846	6,917	752	539	680	3,903	356	1,549	762
29-Oct		902	1,724	6,121	710	734	1,016	708	8,051	
	999	931	5,430	762	546	675	3,199	326	1,888	2,259
19-Nov		740	2,715	5,342	928	744	1,622	673	5,115	
	305	788	6,129	877	751	1,058	3,249	327	2,209	2,789
16-Dec		800	3,418	12,633	1,410	1,142	2,026	541	2,840	
	356	726	5,549	1,382	1,141	311	3,417	301	776	3,545
2010										
28-Jan		575	1,227	4,079	510	396	542	779	2,497	
	684	616	5,721	621	356	336	3,550	288	888	666
22-Feb		641	2,234	3,519	877	619	792	442	2,846	
	364	713	4,841	840	711	104	2,795	209	1,631	2,599
25-Mar		919	1,484	16,200	670	847	863	806	1,865	
	394	761	5,709	612	815	569	4,006	707	1,222	1,625
28-Apr		733	1,532	2,365	858	738	4,463	599	2,072	
	385	683	5,905	756	695	444	3,617	447	1,575	1,597
26-May		621	1,147	3,244	543	880	600	608	1,637	
	374	618	4,483	560	420	439	4,383	1,633	1,190	746
28-Jun		645	64,900	1,786	627	444	637	592	1,773	
	400	626	4,800	609	440	383	5,258	1,144	1,299	898
28-Jul		528	59,433	6,775	630	440	661	623	3,745	
	332	588	4,347	610	994	397	5,447	1,112	1,485	1,191
Aug		—	—	—	—	—	—	—	—	
	—	—	—	—	—	—	—	—	—	—
29-Sep		259	—	372	377	321	382	328	—	
	224	318	1,090	352	288	283	334	359	580	284
18-Oct		876	—	839	923	720	737	677	—	
	577	843	1,084	1,221	686	722	597	576	839	602
16-Nov		581	—	701	607	326	626	605	—	
	424	644	1,142	740	625	252	438	467	778	365
14-Dec		732	—	369	633	198	572	556	—	
	416	335	2,043	657	385	272	452	327	725	484

2011	T1–2	T3–4	T5–6	T7–8	T9–10	T11–12	T13–14	T15–16	T17–18	T19–20
14-Jan		627	—	451	668	418	878	625	—	
	651	633	1,282	862	501	333	604	923	512	306
15-Feb		542	—	550	586	343	565	552	—	
	298	609	2,245	541	310	357	525	1,348	662	361
15-Mar		350	—	296	312	224	434	367	—	
	221	471	2,542	304	246	339	311	331	515	368
18-Apr		401	—	333	365	260	501	368	—	
	327	475	2,412	489	297	285	550	230	518	540
18-May		840		900	1,102	920	1,915	2,864	—	
	980	983	2,343	1,263	1,077	1,005	1,767	2,985	742	752
22-Jun		386	—	475	223	183	370	314	—	
	205	356	1,558	412	216	278	306	330	551	347
27-Jul		127	—	342	181	145	159	193	—	
	101	187	909	320	88	132	158	470	380	305
26-Aug		146	—	135	122	86	207	192	—	
	—	205	924	180	97	134	254	765	382	252
22-Sep		346	—	443	302	333	390	136	—	
	318	373	1,385	309	301	1,631	112	219	367	240
27-Oct		294	—	537	271	290	361	199	—	
	270	281	1,155	338	245	256	236	214	358	263
22-Nov		338	—	431	243	183	394	230	—	
	235	356	1,098	355	195	303	257	245	403	334
16-Dec		274	—	424	379	75	860	94	—	
	408	799	651	211	141	185	156	121	327	361
2012										
20-Jan		223	—	356	148	272	229	101	—	
	239	141	537	340	224	297	105	198	233	88
23-Feb		190	—	213	135	135	201	271	—	
	167	436	943	222	139	148	180	195	326	393
13-Mar		341	—	782	360	144	282	117	—	
	222	146	816	391	387	423	514	282	373	236
16-Apr		230	—	708	1,212	157	161	832	—	
	149	241	756	485	323	123	222	1,280	402	424
15-May		196	—	1,877	137	66	233	153	—	
	146	253	699	157	87	130	190	247	594	176
19-Jun		422	—	686	626	347	382	570	—	
	292	464	498	466	319	315	406	570	875	383
10-Jul		265	—	638	325	252	369	454	—	
	206	289	373	325	353	345	292	340	1,425	563
14-Aug		410	—	680	350	342	334	303	—	
	389	358	476	296	225	285	237	344	853	494
Sep	—	—	—	—	—	—	—	—	—	—
	—	—	—	—	—	—	—	—	—	—
24-Oct		246		552	335	303	195	146	—	
	166	221	474	400	164	153	157	166	752	264
26-Nov		139	—	100	78	121	59	19	—	
	110	187	—	76	51	34	13	92	215	106
18-Dec		109	—	—	87	35	42	10	—	
	106	99	—	—	36	23	5	28	171	39
2013										
31-Jan		54	—	—	66	10	3	4	—	
	966	423	—	—	11	8	6	13	1,423	223
28-Feb		215	—	—	133	100	44	85	—	
	47	87	—	—	91	98	518	77	913	296
28-Mar		52	—	—	47	14	32	13	—	
	12	24	—	—	23	16	16	21	572	263
25-Apr		39	—	—	59	44	43	25	—	
	18	39	—	—	40	62	29	36	293	182
30-May		160	221	—	226	158	40	—	—	
	204	135	—	—	301	73	112	56	307	95
27-Jun		35	233	676	47	27	44	59	274	
	15	26	378	402	301	44	280	51	264	137
25-Jul		179	322	583	184	138	148	90	876	
	316	130	742	176	100	101	124	76	1,197	332
29-Aug		13	161	173	39	784	255	710	3,069	
	165	192	1,066	28	1,621	270	862	—	5,326	581
26-Sep		49	114	253	3	52	3	14	1,716	
	306	18	566	15	3	8	12	20	3,190	323
24-Oct		277	250	396	200	321	206	181	648	
	285	295	1,485	2,013	191	221	170	173	2,333	454
21-Nov		150	120	191	133	471	83	46	3,349	
	186	159	322	88	76	140	75	163	5,227	350
23-Dec		17	794	8	13	14	11	18	3,023	
	61	14	39	6	12	11	—	6	8,679	787

2014	T1–2	T3–4	T5–6	T7–8	T9–10	T11–12	T13–14	T15–16	T17–18	T19–20
30-Jan		9,444	176,000	6,539	2,408	374	1,109	1,025	2,980	
	11	165	3,046	2,952	483	270	—	139	2,116	697
24-Feb		5,290	100,000	1,187	330	307	116	65	4,069	
	135	163	6,165	601	165	215	—	65	3,241	571
25-Mar		274,000	271,000	17,300	5,465	53	332	372	6,391	
	146	11,800	2,169	7,880	1,148	66	261	388	2,545	242
22-Apr		2,442	383,000	33,500	12,600	167	575	623	5,221	
	739	948	31,100	21,000	3,381	290	349	302	2,082	561
27-May		1,536	369,000	43,000	10,200	959	1,615	1,071	3,827	
	697	817	31,900	15,100	2,850	810	697	348	2,856	1,451
23-Jun		3,530	78,700	495	22	17	727	260	3,138	
	183	1,233	2,747	133	10	374	824	169	2,050	1,271
21-Jul		1,215	237,000	34,900	12,000	240	1,191	1,321	2,804	
	527	735	21,900	16,800	3,640	290	634	552	2,823	2,213
27-Aug		1,050	222,000	31,400	10,200	3,218	4,638	1,916	2,954	
	199	296	31,200	12,700	3,650	2,769	1,376	1,026	1,478	1,618
25-Sep		1,298	208,000	23,000	8,583	3,185	2,562	3,159	2,056	
	1,028	614	28,000	11,600	4,093	2,338	1,295	1,226	3,679	1,561
29-Oct		254	180,000	540	185	154	205	—	257	
	409	194	12,600	1,196	117	144	127	—	2,008	283
20-Nov		919	229,000	12,800	4,102	1,182	1,208	754	998	
	309	409	17,100	5,894	2,124	1,147	678	458	3,404	983
23-Dec		2,004	102,000	13,500	5,213	1,261	1,621	886	1,319	
	811	1,483	10,900	7,996	2,225	1,075	654	470	3,421	1,516
2015										
28-Jan		10,300	208,000	15,000	87	99	85	71	282	
	3,808	14,800	2,051	237	74	63	85	63	1,762	101
27-Feb		2,231	189,000	13,200	2,689	1,056	1,309	956	877	
	160	370	17,700	4,689	1,187	609	648	333	1,398	898
26-Mar		554	88,900	5,280	4,885	2,294	2,562	1,585	3,938	
	360	814	11,500	6,634	104	1,203	1,088	884	—	2,211
20-Apr		436	245,000	51,300	2,410	835	1,145	651	952	
	164	339	13,300	5,860	1,175	728	434	393	38,400	4,586
28-May		6,657	287,000	3,740	2	4,184	—	—	268	
	1,285	10,500	763	—	—	—	—	—	1,191	29
25-Jun		435	153,000	7,341	3,074	9,065	1,594	1,239	955	
	248	295	4,536	3,323	959	897	986	531	17,200	2,456
21-Jul		880	175,000	10,200	2,383	10,200	1,431	927	275	
	243	385	11,000	3,430	823	940	500	93	19,100	1,994
27-Aug		576	135,000	1,025	859	5,595	659	1,126	1,045	
	270	406	731	549	363	1,047	892	777	13,000	2,673
23-Sep		2,316	148,667	113	44	2,584	59	193	358	
	341	460	486	—	71	64	148	477	11,625	455
20-Oct		619	176,267	569	476	3,045	286	277	439	
	323	627	1,881	412	380	584	320	289	16,280	697
18-Nov		469	153,867	96,503	103	2,714	125	253	1,082	
	—	425	—	93	103	207	161	735	27,153	556
17-Dec		506	317,400	3,086	420	1,071	393	338	612	
	904	323	1,620	538	403	541	418	432	32,387	1,010
2016										
20-Jan		963	308,367	719	703	1,534	707	633	810	
	739	602	1,548	644	667	630	589	580	31,047	427
17-Feb		888	295,600	832	591	2,316	615	530	765	
	671	617	1,763	633	574	616	543	705	28,737	724
15-Mar		841	319,000	956	662	947	407	551	818	
	565	520	1,797	599	608	465	532	607	1,699	840
20-Apr		855	138,033	626	951	1,133	451	451	726	
	454	428	1,347	810	535	456	371	371	2,154	344
23-May		1,382	115,567	1,403	1,797	1,271	1,233	1,668	1,033	
	856	1,093	2,122	1,691	1,342	1,008	877	2,147	7,787	813
21-Jun		763	151,600	796	701	968	436	479	766	
	473	622	1,668	632	595	675	441	576	6,715	584
22-Jul		740	96,967	427	347	522	292	253	520	
	519	575	1,176	309	298	346	296	353	8,082	322
23-Aug		518	74,483	889	526	498	392	306	417	
	396	387	1,312	629	479	312	319	298	6,230	252
21-Sep		646	53,800	428	379	273	295	234	375	
	516	660	621	293	295	321	196	273	4,441	178
19-Oct		727	95,847	900	698	409	316	308	730	
	426	751	1,322	3,981	567	293	238	236	9,297	539
17-Nov		540	111,200	904	469	353	307	306	536	
	289	306	1,379	671	485	235	277	304	10,427	259
20-Dec		802	82,860	657	579	630	474	511	838	
	543	552	1,234	602	576	568	522	463	11,247	262

2017	T1–2	T3–4	T5–6	T7–8	T9–10	T11–12	T13–14	T15–16	T17–18	T19–20
31-Jan		618	98,227	329	434	411	231	263	507	
	477	407	1,091	390	333	333	340	299	10,312	646
22-Feb		454	103,867	557	554	302	299	284	492	
	679	351	1,350	485	495	338	335	356	8,613	211
24-Mar		458	64,780	320	342	827	511	353	534	
	323	343	781	304	290	318	355	322	5,366	626
20-Apr		480	59,747	112,600	388	491	720	293	398	
	472	529	1,074	509	322	361	319	235	6,817	434
28-May		1,628	79,537	11,877	1,840	918	846	484	446	
	1,646	1,746	3,201	1,645	682	1,541	492	376	10,253	411
25-Jun		699	55,877	175,533	1,078	1,415	7,761	519	519	
	624	568	1,815	966	973	1,213	615	362	7,718	422
21-Jul		731	50,333	11,383	733	731	—	418	343	
	604	637	1,135	770	500	461	324	268	7,241	262
27-Aug		608	40,520	3,551	862	692	—	344	404	
	519	596	1,187	775	708	297	313	245	5,694	358
23-Sep		412	31,050	966	410	354	796	289	238	
	296	315	662	355	283	324	227	134	2,567	200
20-Oct		373	24,613	772	712	399	695	434	348	
	297	318	746	664	558	369	335	280	2,304	745
18-Nov		345	21,623	395	365	226	323	561	276	
	269	281	747	195	193	196	286	222	2,849	545
18-Dec		410	24,693	469	310	346	327	271	357	
	310	323	685	258	280	290	278	329	2,585	306
2018										
31-Jan		242	19,520	436	383	390	1,261	379	480	
	158	158	912	362	341	357	383	360	4,773	896
22-Feb		361	13,307	421	377	356	375	229	372	
	410	339	1,037	299	391	341	347	371	3,994	403
24-Mar		540	13,113	470	444	535	365	355	820	
	412	397	701	387	482	779	414	389	6,908	602
20-Apr		456	6,616	131,367	324	308	260	226	450	
	356	302	757	282	321	357	314	305	5,112	388
28-May		558	2,149	593	573	758	273	262	487	
	340	307	1,190	406	426	329	343	245	6,588	553
20-Jun		621	1,772	7,277	619	349	367	373	519	
	707	443	1,259	512	338	392	394	412	5,366	436
25-Jul		440	2,003	1,986	423	312	253	343	315	
	384	359	1,069	319	283	251	306	322	4,631	195
21-Aug		436	1,482	80,667	479	291	363	235	410	
	400	316	1,047	267	281	256	277	302	4,210	295
30-Aug		589	1,768	19,037	578	333	357	344	461	
	441	463	1,255	518	311	292	298	343	4,597	273
18-Sep		450	1,211	3,852	159	84	153	123	313	
	267	202	480	149	66	148	68	197	3,657	133
30-Oct		391	802	4,646	186	157	297	113	356	
	280	214	402	169	158	176	216	152	4,625	232
20-Nov		461	1,415	1,126	429	337	453	201	452	
	394	381	717	329	259	276	218	392	6,500	227
18-Dec		482	1,628	786	373	354	440	344	620	
	438	451	714	291	318	361	364	563	7,163	218
2019										
24-Jan		694	1,348	491	285	243	486	301	592	
	531	494	682	308	243	308	336	397	6,658	198

Parts per Billion by Volume (ppbv)

—	no data
1	< 50
2	51 – 100
3	101 – 500
4	501 – 1,000
5	1,001 – 2,000
6	2,001 – 5,000
7	5,001 – 10,000
8	10,001 – 20,000
9	20,001 – 50,000
10	50,001 – 100,000
11	100,001 – 200,000
12	200,001 – 450,000
	not monitored; Tanks 1 & 19 = inactive

Appendix B.3 Figure 4-3: Monthly PID Monitoring Results for Below-Tank Soil Vapor Monitoring Points
Conceptual Site Model Rev. 01
Red Hill Bulk Fuel Storage Facility
JBPHH, O'ahu, Hawai'i

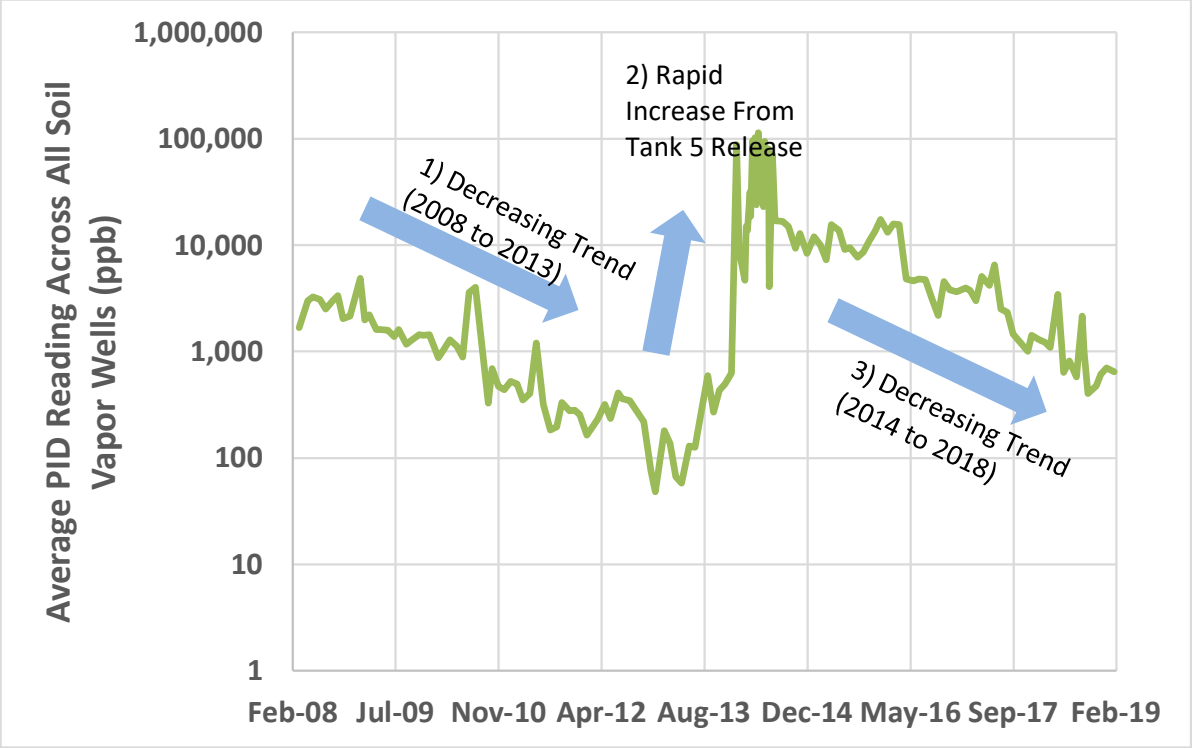

Figure 4-4: Log Scale Graph of Average Monthly PID Monitoring Results across All Below-Tank Soil Vapor Points. Note log-scale for Y-axis.

Table 4-6: Study Question 6: Are Vadose-Zone Petroleum Vapors a Significant Source of Impacts In the Tunnels?

Finding	Discussion
NO. Facility operations are the primary source of petroleum vapors in the tunnels. Any soil vapors entering the tunnel are highly diluted by the tunnel ventilation system. The magnitude and sources of petroleum vapors in the tunnels were evaluated using PID readings and qualitative observations. These data suggest that: • Petroleum vapor concentrations in the tunnels are higher than in outdoor air. • Although vapor flow is from the vadose zone into the tunnel, any soil vapors entering the tunnels are highly diluted by ambient air from the tunnel ventilation system. • The primary source of the petroleum vapors in the tunnels is active operations at the Facility.	**Relative to outdoors, PID readings are elevated in the tunnels and in the soil vapor points.** The PID readings showed similar petroleum vapor concentrations in the tunnels and soil vapor points below the tanks (Table 4-7). The median PID readings in the lower tunnel and the soil vapor points were almost identical and the maximum soil vapor point PID reading was equal to the maximum PID reading from the upper tunnel (i.e., both 40,000 ppb). In addition, as discussed in Section 3, laboratory analysis of soil vapor samples collected from the below-tank soil vapor points suggested that elevated PID readings at these soil vapor points are not always associated with the presence of petroleum vapors. Although PID readings above 10,000 ppbv were observed in soil vapor points at six of the 17 tanks tested, the laboratory analysis of samples collected from these soil vapor points indicated high petroleum vapors only at Tank 5. At the other locations, the high PID readings do not appear to be associated with elevated petroleum VOC concentrations. These results suggest that the primary source of petroleum vapors in the tunnels is not petroleum vapors in the basalt. **Any vadose zone vapors entering the tunnels are highly diluted by the tunnel ventilation system.** The tunnel ventilation system is designed to maintain a combined air flow through the upper (16,000 cubic feet per minute [cfm]) and lower (63,000 cfm) tunnels in the vicinity of the fuel tanks of 79,000 cfm (see CSM Appendix B.2, Figure 2-1). As discussed in Section 3.2.3, the tunnels have a negative pressure relative to the vadose zone such that any gas flow is from the vadose zone into the tunnels. However, the large volume of outdoor air pumped though the tunnels results in significant dilution of any soil vapors entering the tunnels. The vadose zone to tunnel dilution factor was estimated using two independent datasets: 1) oxygen concentration measurements and thermal NSZD rates, and 2) ancient carbon (carbon dioxide associated with the biodegradation of fossil fuel) concentrations in the tunnels. These calculations are provided in CSM Appendix B.2. Both calculations indicated that less than 0.5% of the air in the tunnels originates from the vadose zone. In other words, any vapors entering the tunnels are diluted by > 100× with outdoor air provided by the ventilation system (i.e., an attenuation factor of < 0.01). Applying this attenuation factor to the average PID reading for the soil vapor points (4,335 ppbv × 0.01 = 43 ppb) suggests that vadose zone soil vapors account for less than 10% of the average PID reading in the tunnels (660 ppb). **The primary source of petroleum vapors in the tunnels is Facility operations.** The observed Facility operations and distribution of petroleum vapors in the tunnels suggest that ongoing Facility operations are the primary source of petroleum vapors in the tunnels. On the first day of soil vapor point sampling (October 27, 2017), fuel was being transferred from Tank 20 using a flexible hose. The Facility personnel suggested that work be deferred in that area because disconnection of the hose would result in elevated petroleum vapors in the tunnels. As a result, sample collection at Tank 20 was deferred until three days later (October 30); even at this later date, PID readings at Tank 20 were 2,400 ppb, almost twice as high as any other locations within the lower tunnel. Note that Tanks 19 and 20 are located within a "dead end" section of the lower tunnel (i.e., beyond the Adit 6 ventilation system) and are less highly ventilated compared to the other sections of the lower tunnel. Observations and readings in the upper tunnel also suggested that the Facility operations could be a source of petroleum vapors to the tunnels. The top of each tank can be accessed from the upper tunnel by a fixed set of ladder stairs at the end of the lateral tank access tunnels. These ladder stairs are accessed directly from the upper tunnel without any door or other enclosure. During the field program, access to the top of Tank 6 was attempted for the purpose of installing a soil vapor sample point. Approximately one-third of the way up the ladder, the multigas meter being used for safety monitoring showed a petroleum vapor reading of 40 ppmv (i.e., 40,000 ppbv) and rising. A petroleum vapor concentration of 40 ppmv is –2% of the equilibrium vapor concentration for fresh jet fuel (2,000–4,000 ppmv). Based on the reading, the ladder was exited and measurements of the maximum petroleum vapor concentration in this area were not attempted. Taken together, the observations of petroleum vapors at Tank 20 in the lower tunnel and Tank 6 in the upper tunnel suggest that ongoing Facility operations are the primary source of petroleum vapors in tunnels.

Table 4-7: Summary of PID Measurements in the Tunnels

Parameter	Outdoor Air	Upper Tunnel [a]	Lower Tunnel	Soil Vapor Points [b]
Number of Readings	2	2	17	46
Minimum (ppb)	0	180	85	44
Median (ppb)	NC	NC	581	594
Average (ppb)	78	340	660	4,335
Maximum (ppb)	155	40,000	2,400	40,000

Notes:
[a] Table includes a reading of 40,000 ppbv taken using as multigas meter approximately one-third of the way up the access ladder to the top of Tank 6. Excluding this value, the maximum PID reading within the upper tunnel was 500 ppb.
[b] Two or three soil vapor points are installed below each of the 18 active fuel storage tanks.
NC not calculated

5. Gradient Method for Measuring NSZD

5.1 TECHNICAL BACKGROUND

Based on the results of the soil vapor sampling program (Table 4-3 and Table 4-4), NSZD is occurring at the Facility. Under certain conditions, NSZD rates can be obtained by using the gradient method by measuring the oxygen gradient from the surface (oxygen concentration of 21% of air) to a point in the subsurface where the oxygen is completely consumed. When this vertical oxygen gradient is multiplied by an effective diffusion coefficient, and if certain other conditions hold, a NSZD rate can be obtained (e.g., Johnson, Lundegard, and Liu 2006; Lundegard and Johnson 2006). The diffusive flux can be converted to a NSZD rate in units of gallons per acre per year.

The key assumptions required to apply the gradient method to calculate NSZD rates are:

- Oxygen and/or carbon dioxide concentrations in the air phase in the unsaturated zone migrate via one dimensional diffusion from the source of these compounds (for oxygen, the source is ground surface; for carbon dioxide, the location where methane/hydrocarbons are oxidized) to the sink of these compounds (for oxygen, the sink is the location where methane/hydrocarbons are oxidized; for carbon dioxide, it is the ground surface).
- Relatively uniform soil conditions in the soil column and over time so that a one-dimensional diffusion model can be applied.
- No advective source of vapor flow in the subsurface.

As the data collection activities described in the *Attenuation Evaluation Plan* (DON 2017) progressed, it became more obvious that the key assumptions above were not valid for the Facility system. This section describes applicability of the gradient method at the Facility and issues with the underlying assumptions.

5.2 GRADIENT METHOD DATA COLLECTION

The gradient method was employed using data from the following vapor measurement points designed to collect vapor samples from the surrounding basalt at different elevations:

- Bottom of the tanks using the existing soil vapor points.
- Through the sidewall of the upper tunnel near Tanks 5 and 11 (Vapor Pin sample locations). These two locations represent a range of possible conditions from likely impacted (Tank 5) to a location with a potentially smaller impact in the middle of the tank farm (Tank 11).
- In shallow soil vapor points above/near Tanks 5 and 11.
- In the atmosphere, where ambient oxygen concentrations are 21% and carbon dioxide concentrations are about 400 ppbv.

In addition, vapor samples were also collected from the screened intervals in the two nearest monitoring wells (RHMW02 and RHMW03) to Tanks 5 and 11, respectively. Because these sample locations were below any LNAPL accumulation in the unsaturated zone they were not originally intended to be used for the gradient method calculations. Data were collected at these locations principally to better understand the distribution of LNAPL below the tank farm and help interpret the site attenuation data.

A GEM5000 Landfill Gas Meter was used to collect all the oxygen and carbon dioxide data from the sampling points except for the ambient concentration in the atmosphere where literature values were used.

5.3 SOIL VAPOR CARBON DIOXIDE AND GRADIENT PROFILES

Oxygen vs. elevation data were plotted as an initial screen to determine if the gradient method could be applied at the Facility (Figure 5-1) to determine NSZD rates. In general, if the key conditions necessary to apply the gradient method are present, the oxygen vs. elevation data will plot in a relatively straight line with a negative slope (e.g., Lundegard and Johnson 2006).

The oxygen values at the lowest elevation are from two monitoring wells: RHMW02 for Tank 5 and RHMW03 for Tank 11 (note that RHMW03 is actually over 100 ft distant from Tank 11).

The oxygen levels near 100 ft above mean sea level (msl) elevation are from the soil vapor points underlying the tanks, where the elevations were estimated using the general design of the probes and the angle of the borings.

The oxygen levels at about 380 ft msl correspond to Vapor Pins drilled into the sides of the upper access tunnel. The two highest elevation data points represent shallow soil vapor points installed about 5 ft into the soil at the top of the tank farm and ambient atmospheric conditions at ground surface.

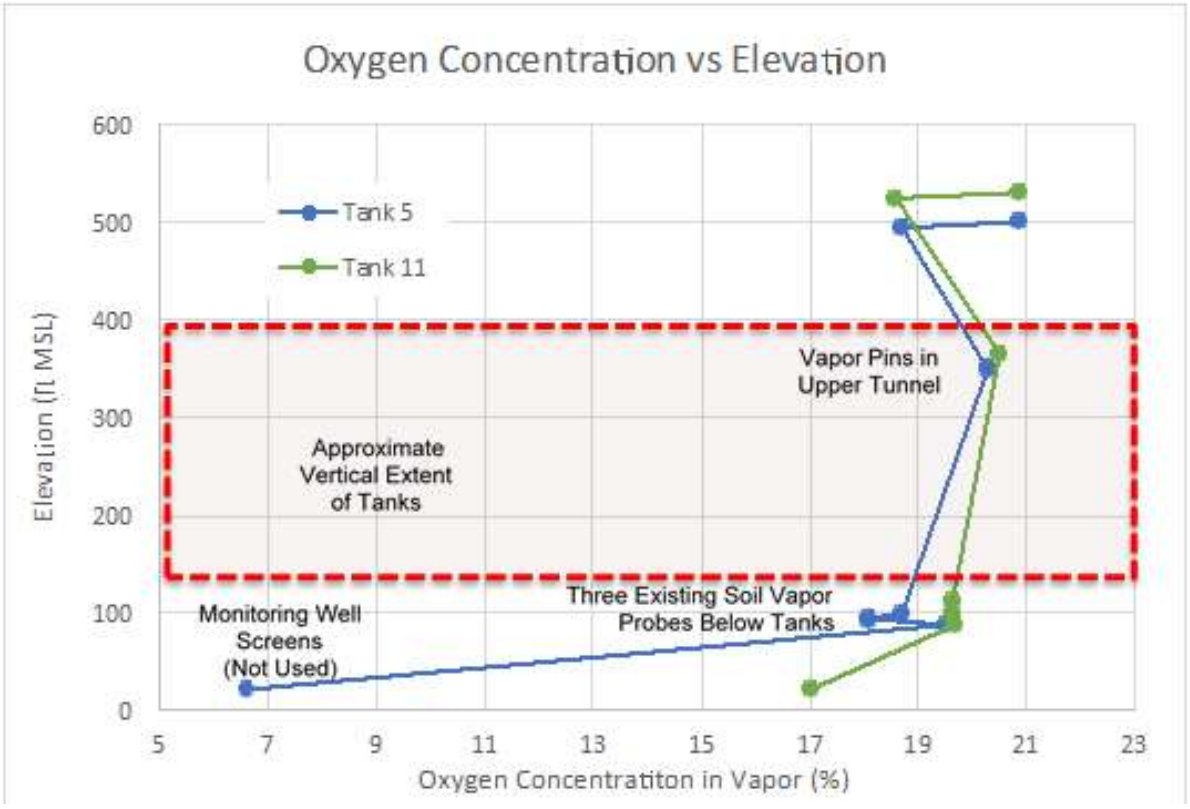

Figure 5-1: Oxygen vs. Elevation Data Collected at the Facility

At most sites where the gradient is applied successfully, a relatively constant oxygen gradient is observed in the unsaturated zone above the LNAPL body (Figure 5-2).

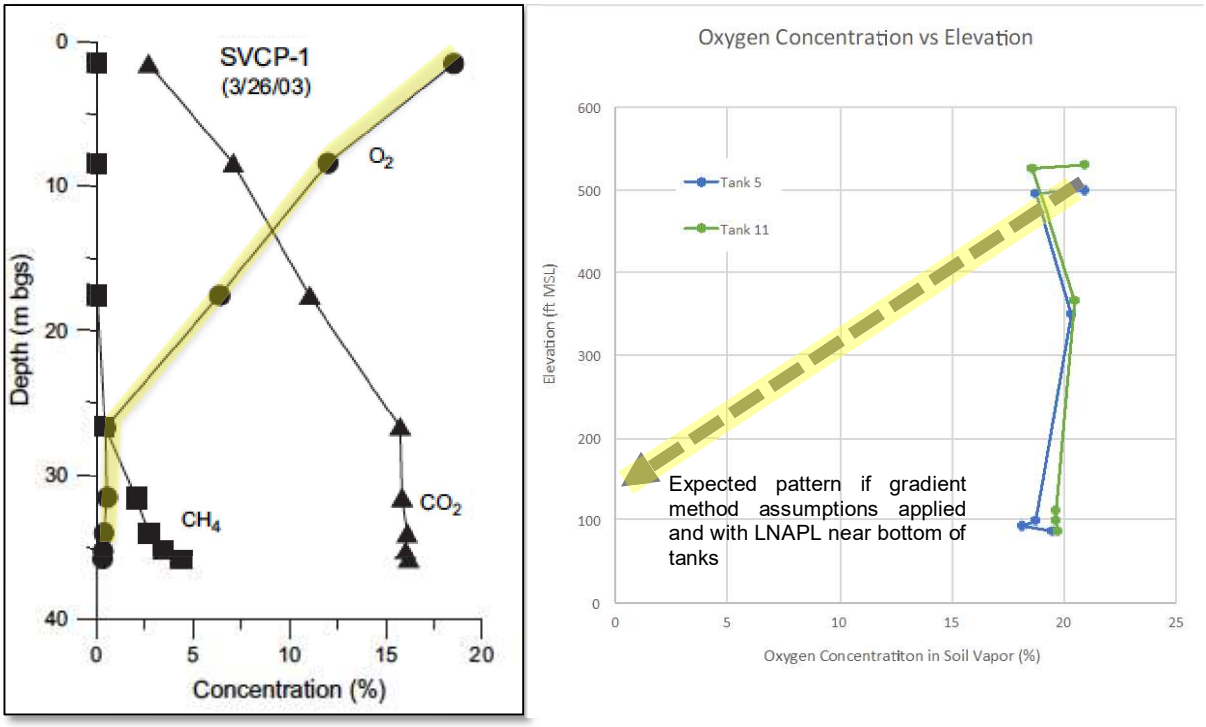

Source (left panel): Lundegard and Johnson 2006.
Yellow highlight shows oxygen gradient in unsaturated zone above the LNAPL body that is appropriate for applying the gradient method.

Figure 5-2: Left: Soil Vapor Data Collected at Oil Field Site; Right: Actual Data from Figure 5-1 vs. Expected Pattern if Gradient Method Conditions Were Met

5.4 REASONS FOR COMPLEX SOIL VAPOR OXYGEN PROFILES AT THE FACILITY

As shown on Figure 5-2 (right side), the non-linear oxygen gradient at both Tank 5 and Tank 11 locations suggests that the gradient method is not applicable at the Facility. Several confounding processes are present:

- The presence of horizontal pathways for oxygen delivery, thereby violating the assumption of a purely vertical diffusion process.
- The ventilation system within the Facility tunnel system that acts as a partial soil vapor extraction system, thereby violating the diffusion-only requirement.

5.4.1 Horizontal Oxygen Migration

The shallow vapor point data show oxygen concentrations in the 18–19% range, lower than the 20.9% atmosphere and lower than the oxygen concentrations in the upper tunnel Vapor Pins (about 20.5% oxygen). This suggests that the soils these shallow vapor points are screened in likely: (1) have low permeability that restricts the influx of oxygen from the surface; and/or (2) are affected by natural organic sources decaying and are thereby removing oxygen.

The relatively high oxygen concentrations in the upper tunnel near atmospheric conditions (about 20.4% oxygen) indicate that there is an influx of oxygen in this location. This may be from high-permeability clinker zones or thin pāhoehoe zones that have preferential pathways and/or very high air-filled porosity that is allowing oxygen to diffuse in from the sides of the tank farm. As shown on Figure 5-3, there are clinker and pāhoehoe units in the vertical intervals where the tanks are located. On the figure, yellow arrows indicate geologic pathways that appear to be delivering oxygen horizontally to the tank farm.

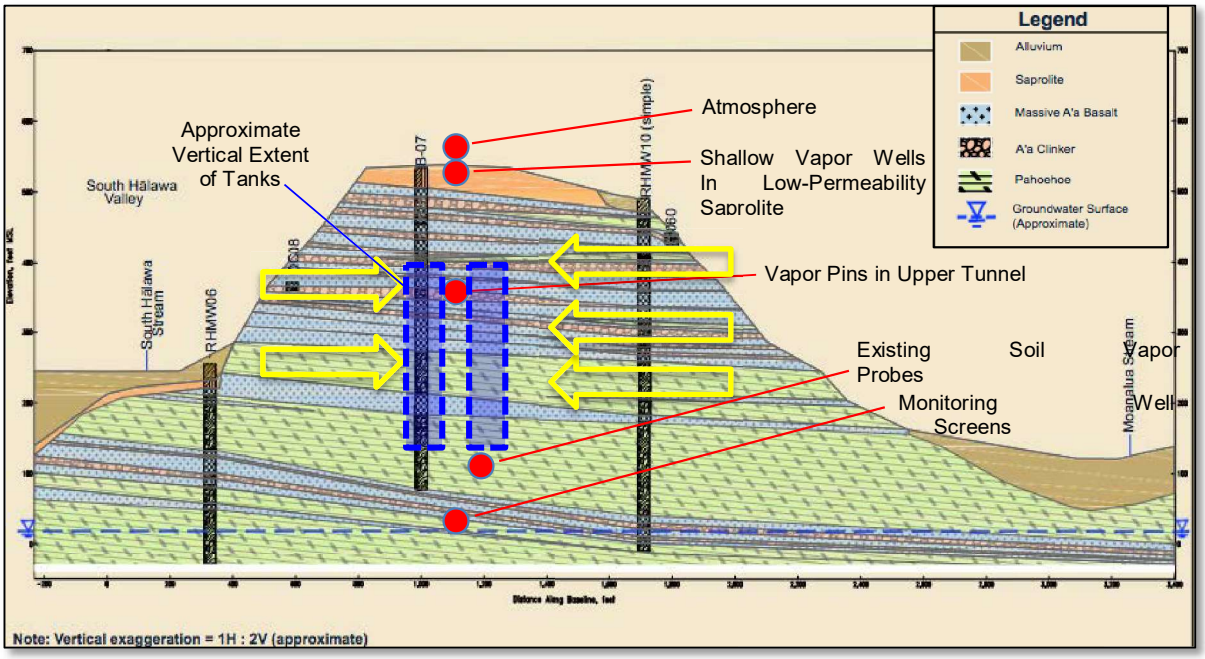

Location of tanks and sample points are approximate. Yellow arrows indicate geologic pathways that appear to be delivering oxygen horizontally to the tank farm, thereby violating the gradient method assumptions.

Figure 5-3: Vertical Location of Tank 5 in North-South Cross Section between Tanks 5 and 6

Planning-level diffusion calculations show the horizontal pathways likely have similar capacity (within an order of magnitude) to diffuse oxygen in from the sides of the tank farm as from the vertical pathways from the top of the tank farm. Note that the presence of fine-grained material in the weathered a'ā clinker zones would reduce the ability of the clinker to transmit gas by diffusion, but only by a relatively small amount compared to the reduction in hydraulic conductivity. Consequently, the presence of fine-grained material does not likely impede the diffusion of gases significantly compared to its effect on the advection of gases and water through this material.

5.4.2 Tunnel System Acting Like Soil Vapor Extraction (SVE) System

The highly oxygenated vapor throughout the Facility oxygen profiles indicates there is a significant influx of air due to advection. As discussed in Section 3.2.3, the tunnel ventilation system results in the tunnels being kept at a lower pressure than ambient air in the basalt. Therefore, there is a net inflow of air into tunnels from the basalt. In addition to the differential pressure measurements, carbon trap data indicate that, while there is some air migration through the floor of the tunnel, most is from small cracks and fractures (see CSM Appendix B.2). Overall, the carbon trap data show:

- A small fraction of the tunnel air (less than 0.5%) (see CSM Appendix B.2) is likely drawn from the basalt via cracks and fractures in the tunnel walls/floor.
- The signal of "ancient carbon" (carbon dioxide associated with the biodegradation of fossil fuel) shows that some of the carbon dioxide leaving the tunnels originated in fossil fuels (which are depleted in carbon-14 due to their age).
- The amount of ancient carbon can be converted to a NSZD rate, and this rate is within the NSZD rate estimated by the thermal NSZD analysis (see CSM Appendix B.1).
- The tunnel is acting like a relatively inefficient SVE system, but one that efficient enough to draw air from the atmosphere to the LNAPL zones.

Because of the tunnel system acting as a SVE system, the movement of oxygen near the tank farm violates the gradient method's assumption of oxygen transport by vertical gas-phase diffusion only.

5.5 GRADIENT METHOD CONCLUSIONS

Soil vapor oxygen concentrations were collected at elevations near Tanks 5 and Tank 11 in order to apply the gradient method to estimate NSZD rates. Certain geologic and contaminant transport conditions were required to apply the gradient method. The presence or absence of these conditions at the Facility was not known prior to the field investigation.

When the vertical oxygen profile data were analyzed along with carbon trap data and other attenuation data, it became clear that two of the key assumptions necessary to apply the gradient method are not found at the Facility:

- It is unlikely that oxygen transport between the surface and near the biodegradation zone is via one-dimensional gas-phase diffusion. Within the tank farm, horizontal oxygen migration pathways are likely present, thereby invalidating the one-dimensional vertical diffusion assumption.
- It is very likely that the ventilation system with the Facility tunnels is acting like a SVE system, drawing air through small cracks and fractures in the tunnel walls/floor and thereby introducing oxygen by advection. This also invalidates the one-dimensional vertical diffusion assumption. The SVE-like behavior of the tunnel system is supported by multiple lines of evidence, including:
  - Carbon trap data on the hillside are much lower than typical hydrocarbon release sites.
  - Carbon trap data in the tunnels shows high concentrations of "ancient carbon" in the carbon dioxide leaving the tunnel. This ancient carbon in the form of carbon dioxide confirms LNAPL biodegradation is ongoing, and significant amounts of the carbon dioxide is being captured by the tunnel ventilation system.
  - Soil vapor data shows the geologic media around the tanks is surprisingly high in oxygen content, indicating an active mechanism for delivering oxygen to the tanks.
  - Soil measurements show the air pressure outside the tunnels is higher than the air pressure within the tunnels.
  - Calculations show only a small amount of air leakage (< 0.5%; see CSM Appendix B.2) from the basalt into the tunnels can explain all the biodegradation being measured at the Facility.

6. References

Baedecker, M. J., R. P. Eganhouse, B. A. Bekins, and G. N. Delin. 2011. "Loss of Volatile Hydrocarbons from an LNAPL Oil Source." *Journal of Contaminant Hydrology* 126: 140–152.

Cox-Colvin, Cox-Colvin & Associates, Inc. 2016. *Standard Operating, Procedure Installation and Extraction of the Vapor Pin®*. Plain City, OH: Updated September 16.

Department of the Navy (DON). 2017. *Attenuation Evaluation Plan, Investigation and Remediation of Releases and Groundwater Protection and Evaluation, Red Hill Bulk Fuel Storage Facility, Joint Base Pearl Harbor-Hickam, O'ahu, Hawai'i; September 1, 2017, Revision 00*. Prepared by AECOM Technical Services, Inc., Honolulu, HI. Prepared for Defense Logistics Agency Energy, Fort Belvoir, VA, under Naval Facilities Engineering Command, Hawaii, JBPHH HI.

Fitzpatrick, N. A., and J. J. Fitzgerald. 1996. *An Evaluation of Vapor Intrusion into Buildings Through a Study of Field Data*. In: Proceedings of the 11th Annual Conference on Contaminated Soils, University of Massachusetts at Amherst, October 1996.

Gregg, S. D., J. L. Campbell, J. W. Fisher, and M. G. Bartlett. 2007. "Methods for the Characterization of Jet Propellent-8: Vapor and Aerosol." *Biomedical Chromatography* 21: 463–472.

Johnson, P., P. Lundegard, and Z. Liu. 2006. "Source Zone Natural Attenuation at Petroleum Hydrocarbon Spill Sites: I. Site-Specific Assessment Approach." *Groundwater Monitoring & Remediation* 26: 82–92.

Kaplan, I., Y. Galperin, S. T. Lu, and R. P. Lee. 1997. "Forensic Environmental Geochemistry: Differentiation of Different Fuel Types, Their Sources and Release Times." *Org. Geochem.* 27: 289–317.

Lundegard, P. D., and P. C. Johnson. 2006. "Source Zone Natural Attenuation at Petroleum Hydrocarbon Spill Sites: II. Application to a Former Oil Field." *Groundwater Monitoring & Remediation* 26 (4): 93–106. https://doi.org/10.1111/j.1745-6592.2006.00115.x.

McHugh, T. E., and T. McAlary. 2009. *Important Physical Processes For Vapor Intrusion: A Literature Review*. In: Proceedings of AWMA Vapor Intrusion Conference (San Diego, CA, January 28–30, 2009).

Pleil, J. D., L. B. Smith, and S. D. Zelnick. 2000. "Personal Exposure to JP-8 Jet Fuel Vapors and Exhaust at Air Force Bases." *Environmental Health Perspectives* 108 (3): 183–192.

Shepard, J. E., C. D. Nuyt, J. J. Lee, and J. E. Woodrow. 2000. *Flash Point and Chemical Composition of Aviation Kerosene (Jet A)*. In Collaboration with ARCO Products Company, Carson, CA and J. E. Woodrow Center for Environmental Sciences and Engineering, University of Nevada. Explosion Dynamics Laboratory Report FM99-4. Pasadena, CA: California Institute of Technology, Graduate Aeronautical Laboratories. April 2, Revised May 26.

TEC, Inc. (TEC). 2010. *Final Soil Vapor Sampling Monitoring Analysis Letter Report*. From Robert Whittier, Senior Hydrogeologist, to: Greg Yamasaki, Supervisory General Engineer, FISC Pearl Harbor. Contract No. N47408-04-D-8514, Task Order 054.

Tran, T. C., G. A. Logan, E. Grosjean, D. Ryan, and P. J. Marriott. 2010. "Use of Comprehensive Two-Dimensional Gas Chromatography/Time-of-Flight Mass Spectrometry for the Characterization of Biodegradation and Unresolved Complex Mixtures in Petroleum." *Geochimica et Cosmochimica Acta* 74: 6468–484.

Attachment B.3.1:
Fingerprint Charts for Soil Vapor and
Groundwater Monitoring Well Headspace Samples

GSI ENVIRONMENTAL

ATTACHMENT B.3.1: FINGERPRINT CHARTS FOR SOIL VAPOR AND GROUNDWATER MONITORING WELL HEADSPACE SAMPLES
Red Hill Bulk Fuel Storage Facility, Joint Base Pearl Harbor-Hickam, O'ahu, Hawai'i

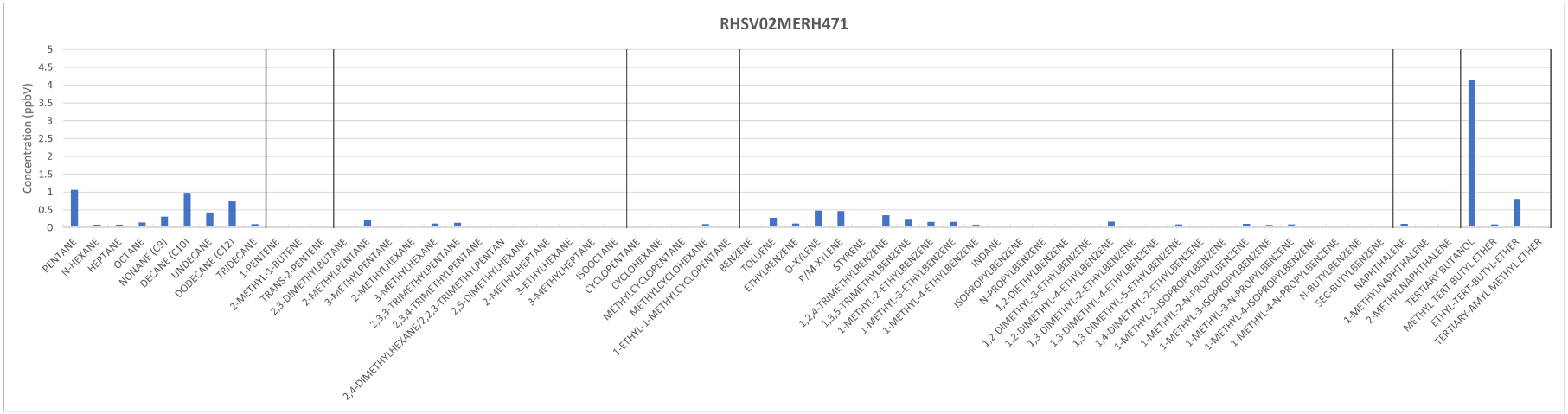

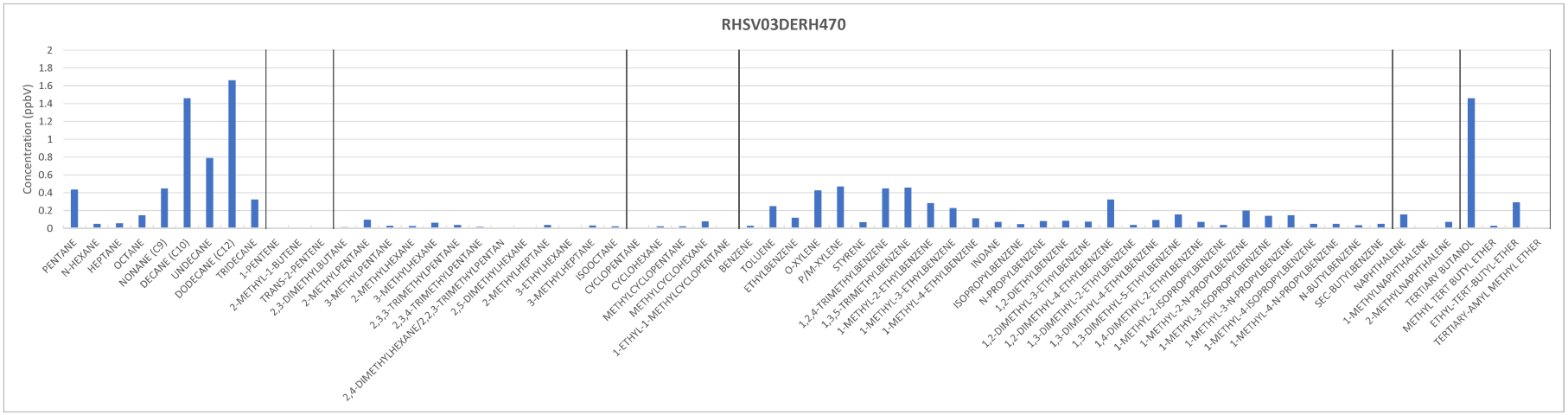

GSI ENVIRONMENTAL

ATTACHMENT B.3.1: FINGERPRINT CHARTS FOR SOIL VAPOR AND GROUNDWATER MONITORING WELL HEADSPACE SAMPLES
Red Hill Bulk Fuel Storage Facility, Joint Base Pearl Harbor-Hickam, O'ahu, Hawai'i

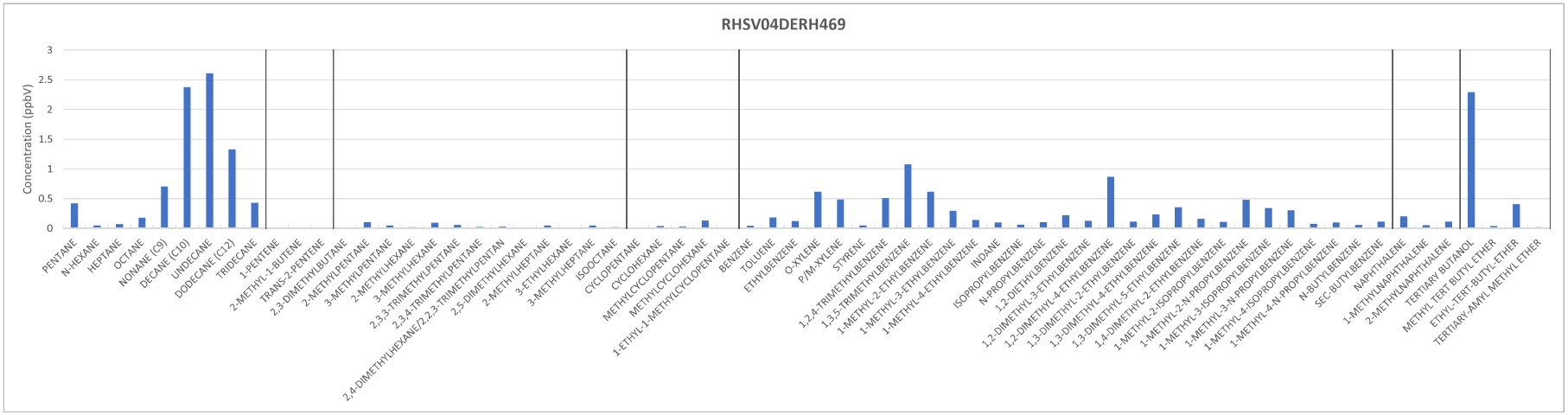

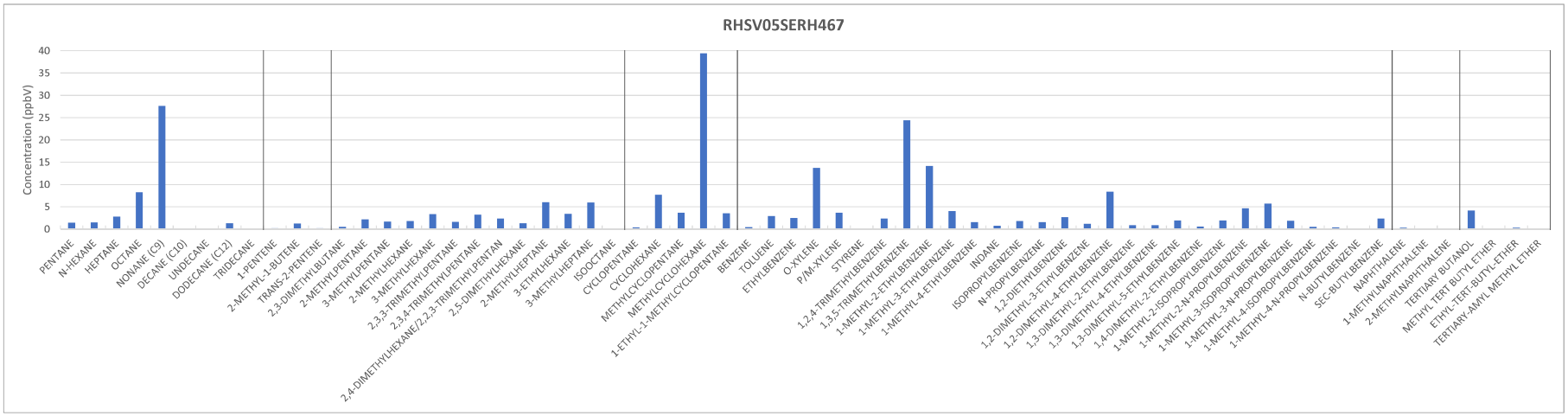

GSI ENVIRONMENTAL

ATTACHMENT B.3.1: FINGERPRINT CHARTS FOR SOIL VAPOR AND GROUNDWATER MONITORING WELL HEADSPACE SAMPLES
Red Hill Bulk Fuel Storage Facility, Joint Base Pearl Harbor-Hickam, O'ahu, Hawai'i

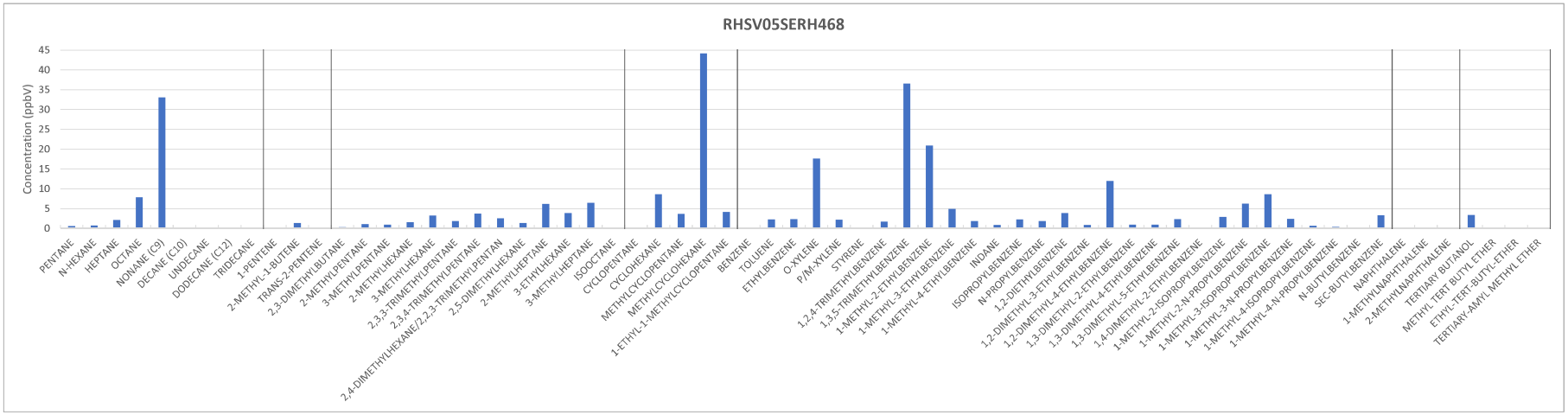

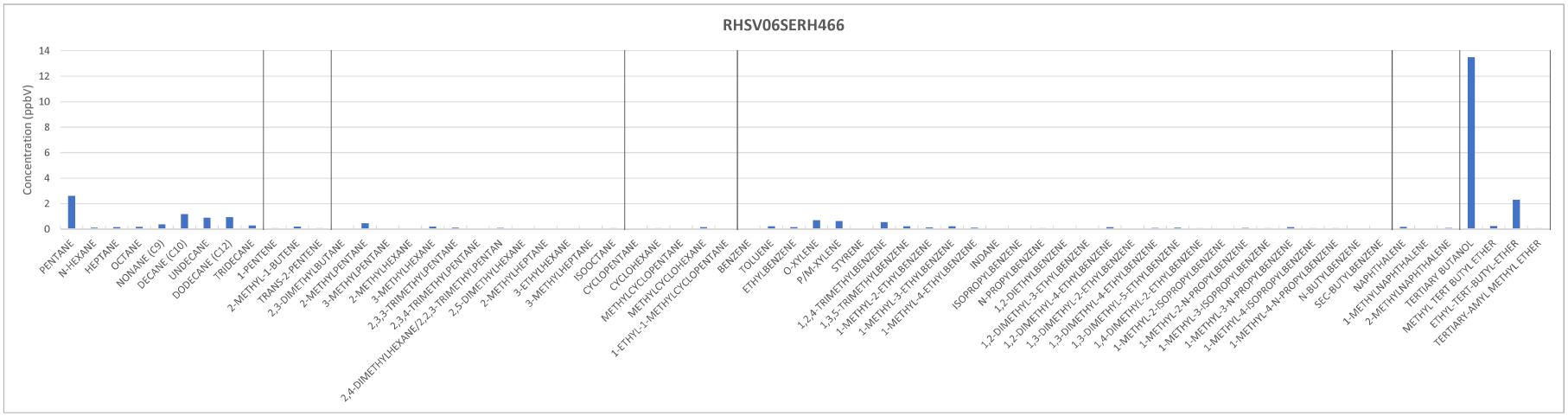

GSI ENVIRONMENTAL

ATTACHMENT B.3.1: FINGERPRINT CHARTS FOR SOIL VAPOR AND GROUNDWATER MONITORING WELL HEADSPACE SAMPLES
Red Hill Bulk Fuel Storage Facility, Joint Base Pearl Harbor-Hickam, O'ahu, Hawai'i

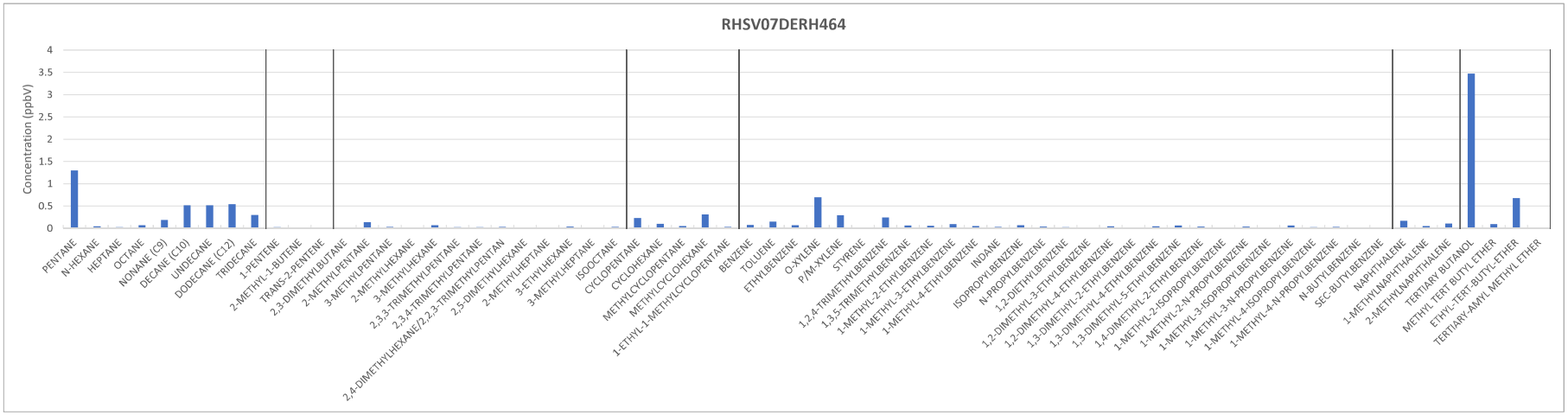

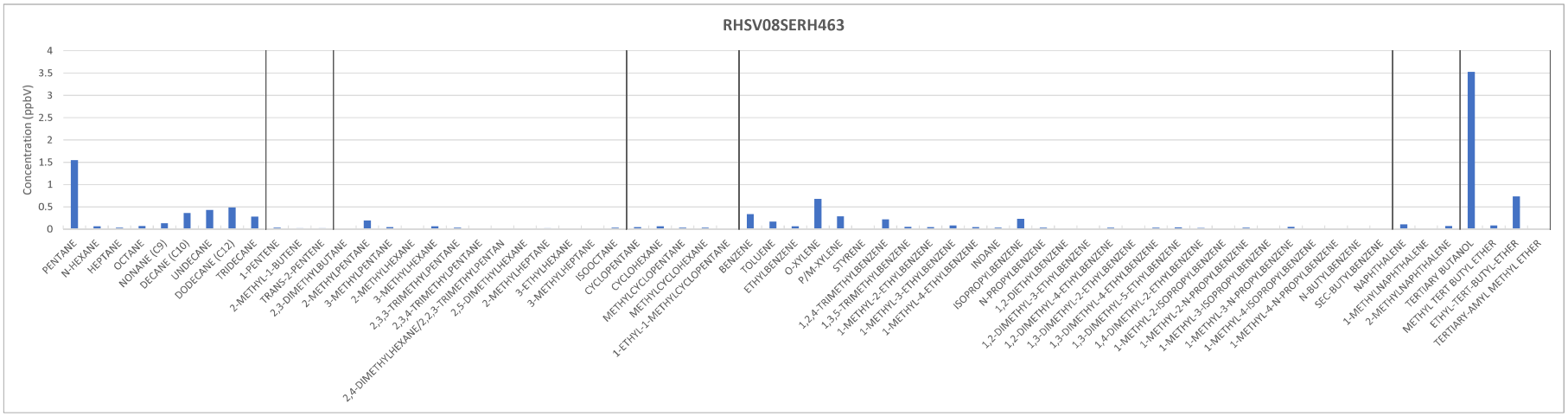

ATTACHMENT B.3.1: FINGERPRINT CHARTS FOR SOIL VAPOR AND GROUNDWATER MONITORING WELL HEADSPACE SAMPLES
Red Hill Bulk Fuel Storage Facility, Joint Base Pearl Harbor-Hickam, O'ahu, Hawai'i

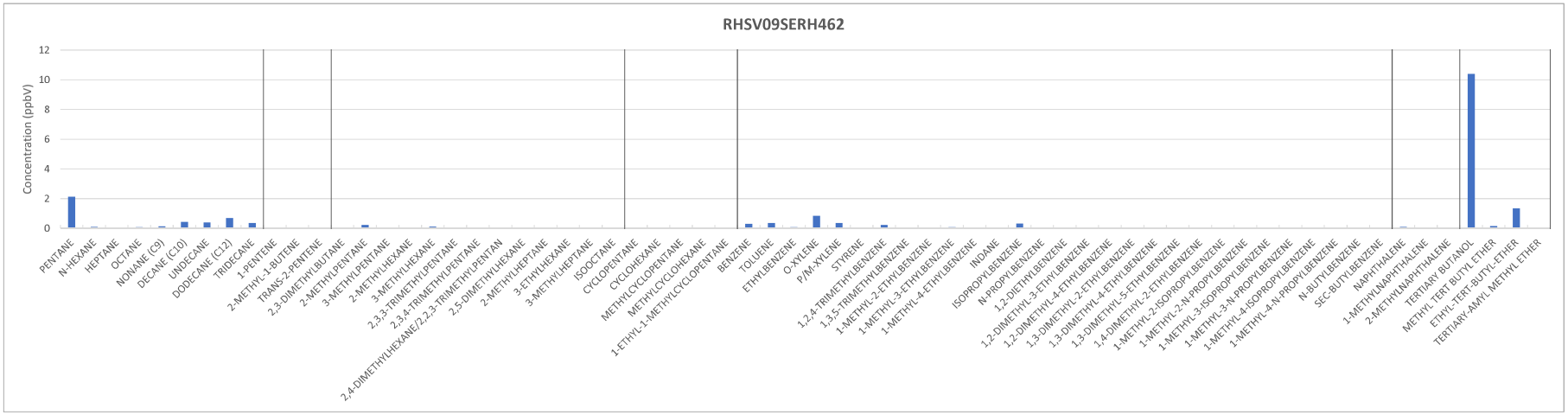

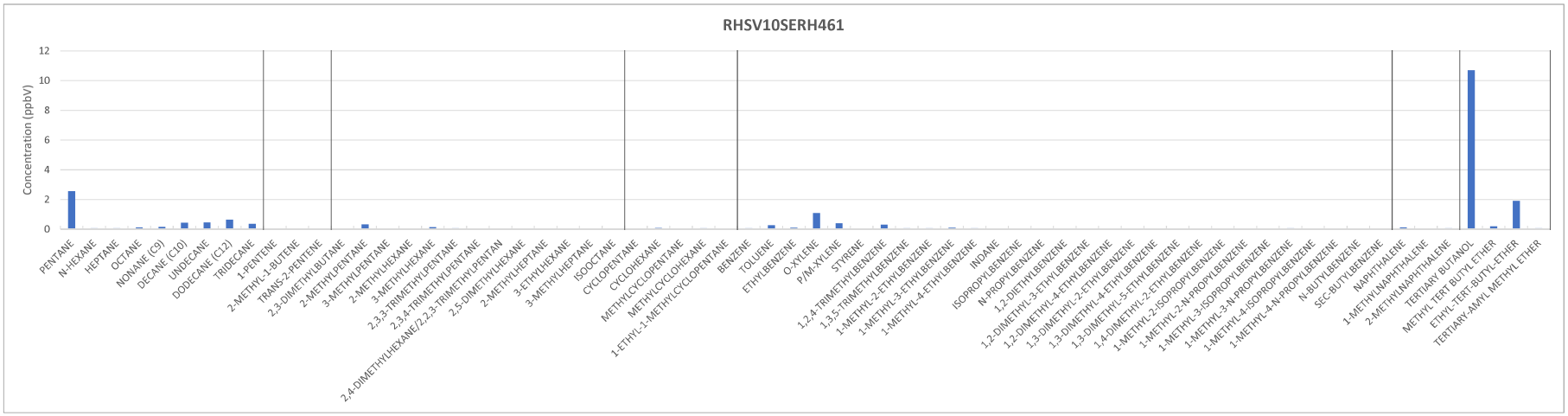

GSI ENVIRONMENTAL

ATTACHMENT B.3.1: FINGERPRINT CHARTS FOR SOIL VAPOR AND GROUNDWATER MONITORING WELL HEADSPACE SAMPLES
Red Hill Bulk Fuel Storage Facility, Joint Base Pearl Harbor-Hickam, O'ahu, Hawai'i

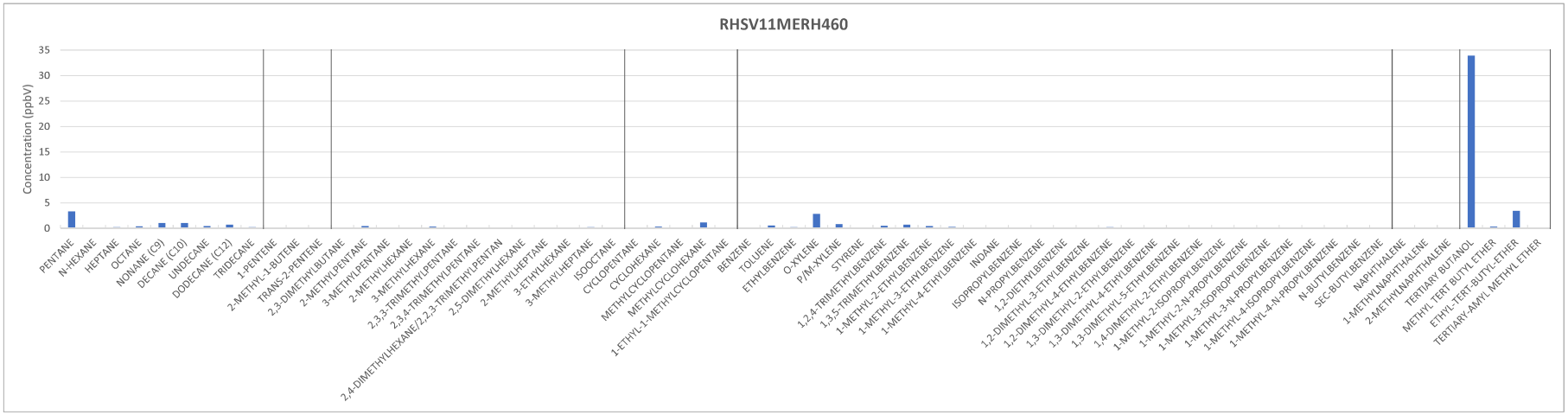

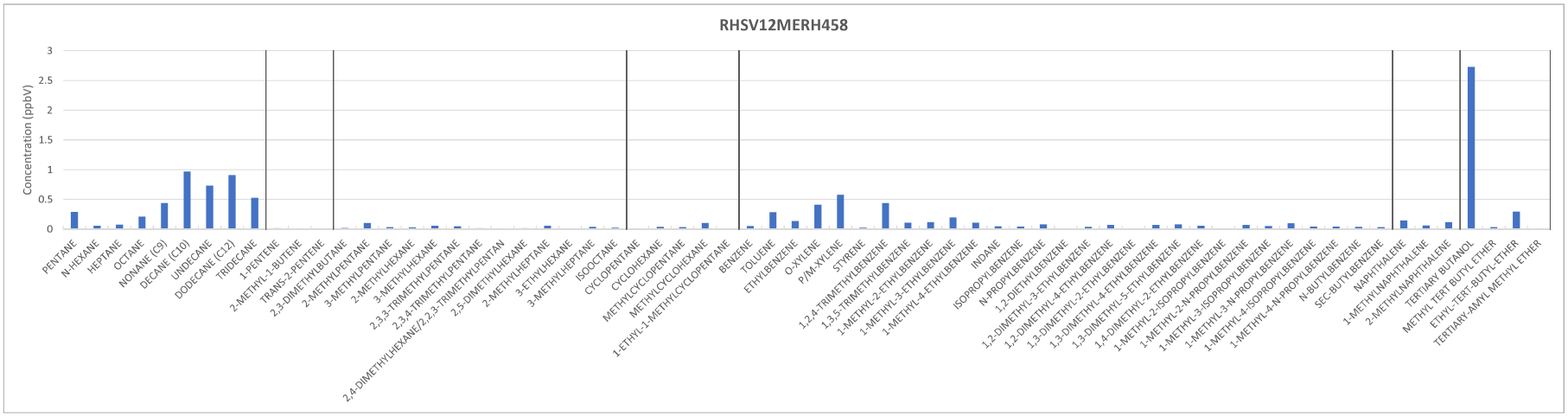

GSI ENVIRONMENTAL

ATTACHMENT B.3.1: FINGERPRINT CHARTS FOR SOIL VAPOR AND GROUNDWATER MONITORING WELL HEADSPACE SAMPLES
Red Hill Bulk Fuel Storage Facility, Joint Base Pearl Harbor-Hickam, O'ahu, Hawai'i

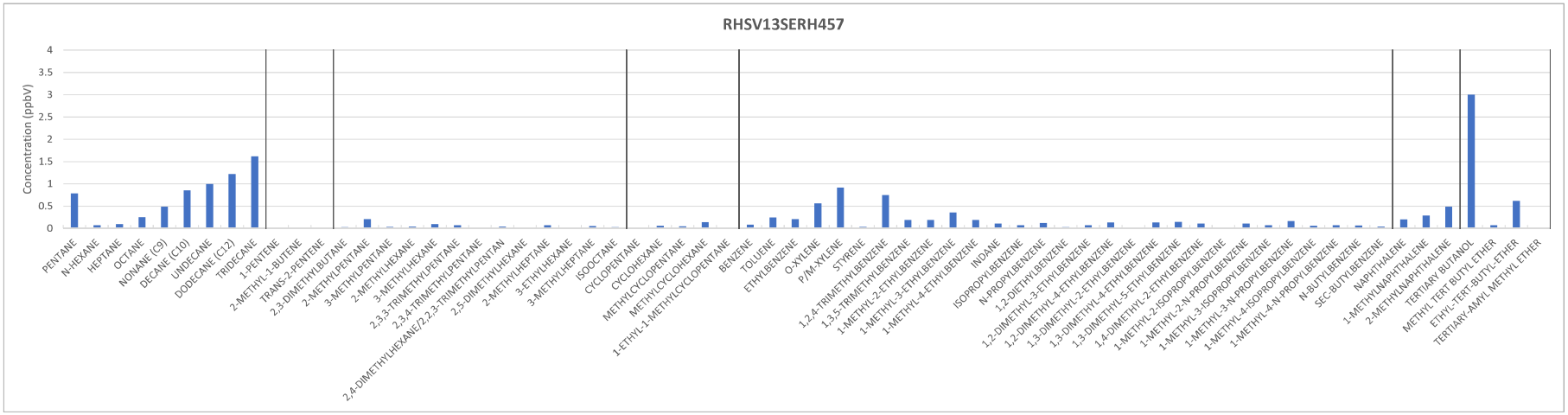

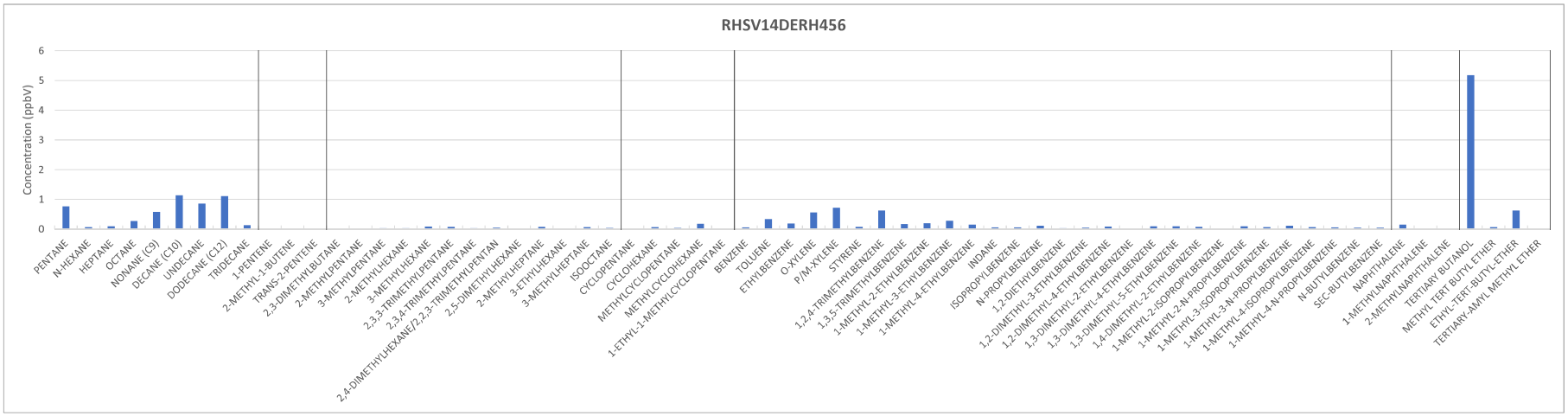

GSI ENVIRONMENTAL

ATTACHMENT B.3.1: FINGERPRINT CHARTS FOR SOIL VAPOR AND GROUNDWATER MONITORING WELL HEADSPACE SAMPLES
Red Hill Bulk Fuel Storage Facility, Joint Base Pearl Harbor-Hickam, O'ahu, Hawai'i

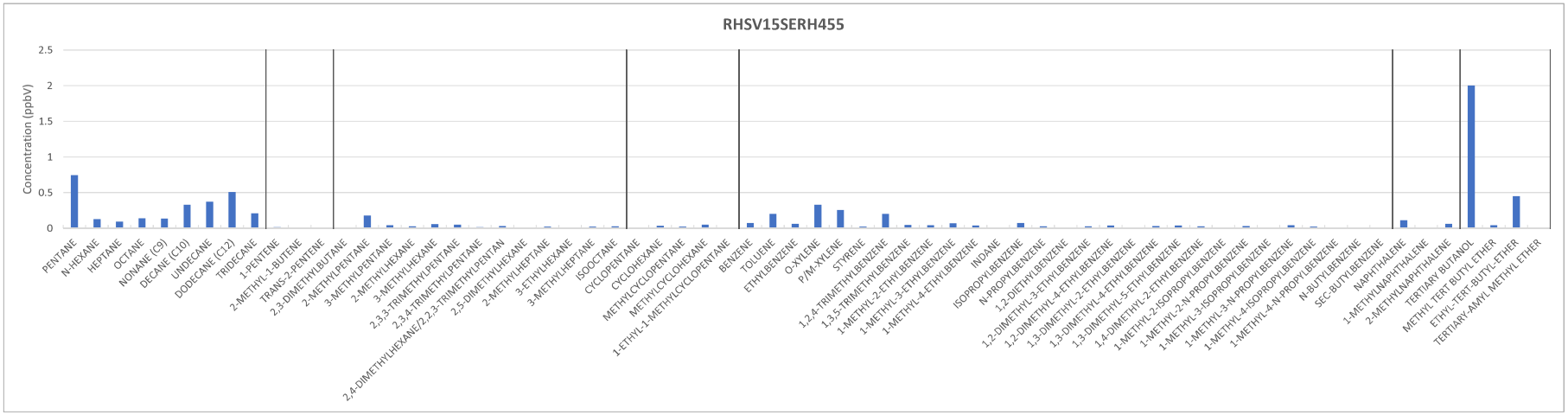

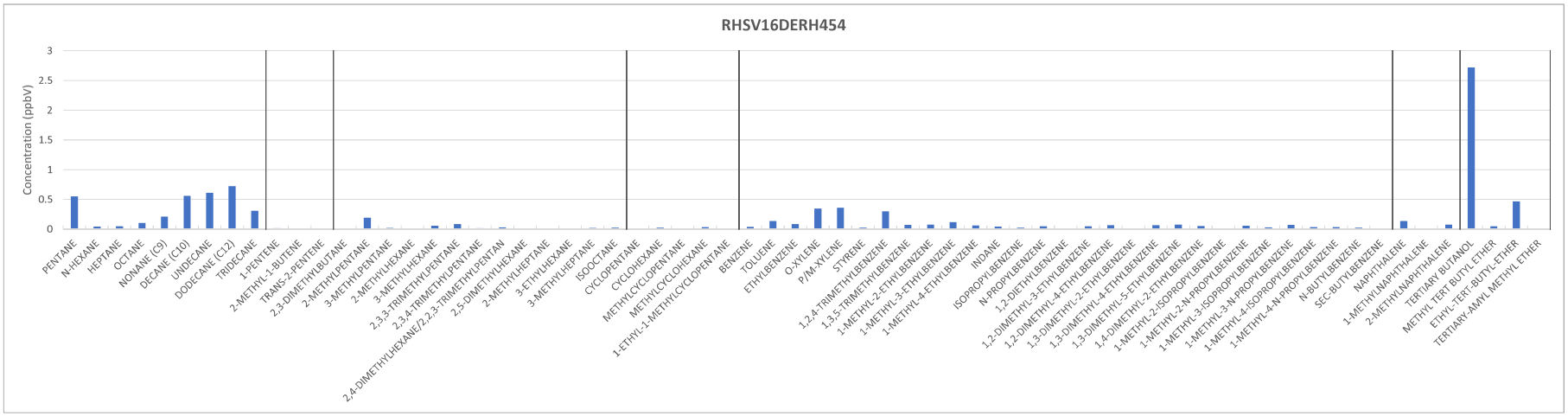

GSI ENVIRONMENTAL

ATTACHMENT B.3.1: FINGERPRINT CHARTS FOR SOIL VAPOR AND GROUNDWATER MONITORING WELL HEADSPACE SAMPLES
Red Hill Bulk Fuel Storage Facility, Joint Base Pearl Harbor-Hickam, O'ahu, Hawai'i

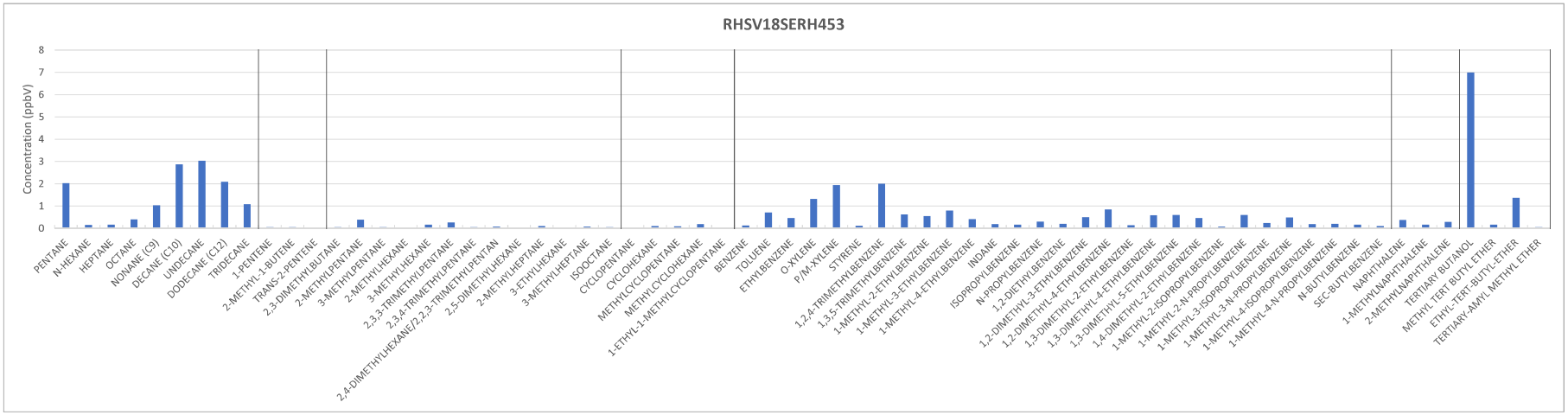

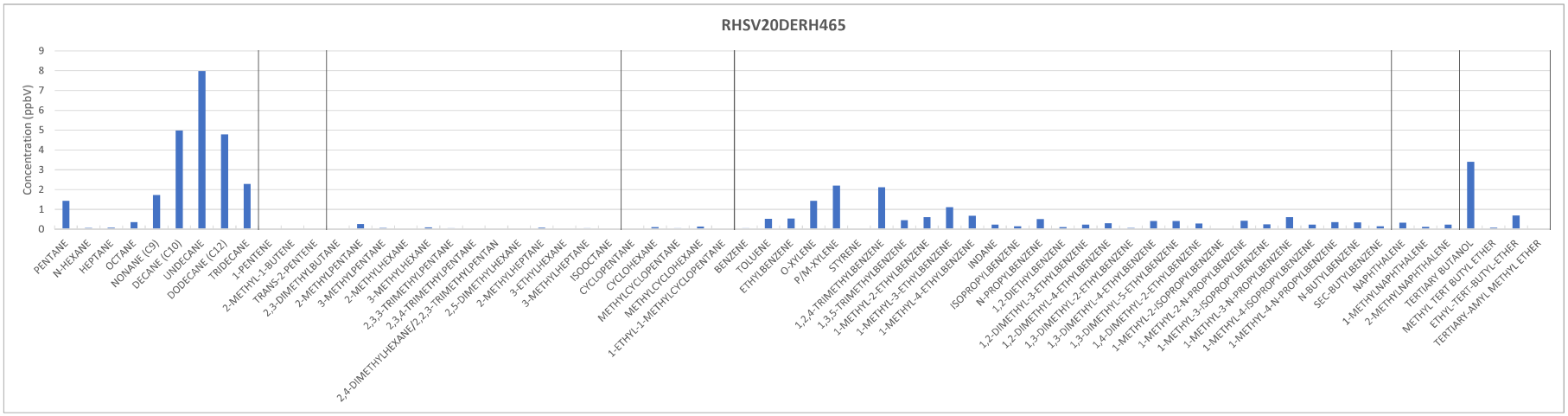

GSI ENVIRONMENTAL

ATTACHMENT B.3.1: FINGERPRINT CHARTS FOR SOIL VAPOR AND GROUNDWATER MONITORING WELL HEADSPACE SAMPLES
Red Hill Bulk Fuel Storage Facility, Joint Base Pearl Harbor-Hickam, O'ahu, Hawai'i

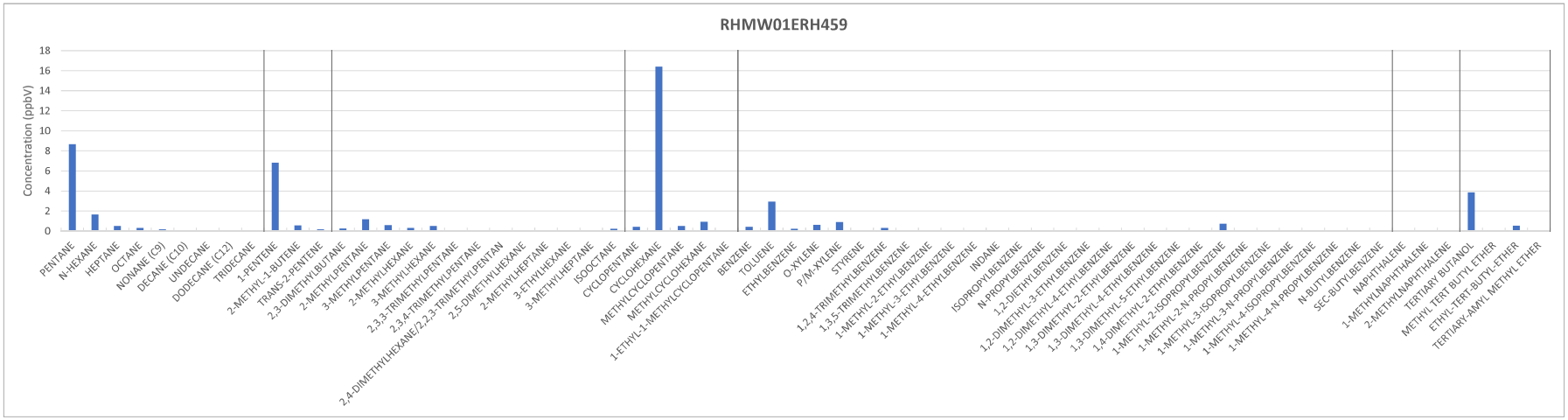

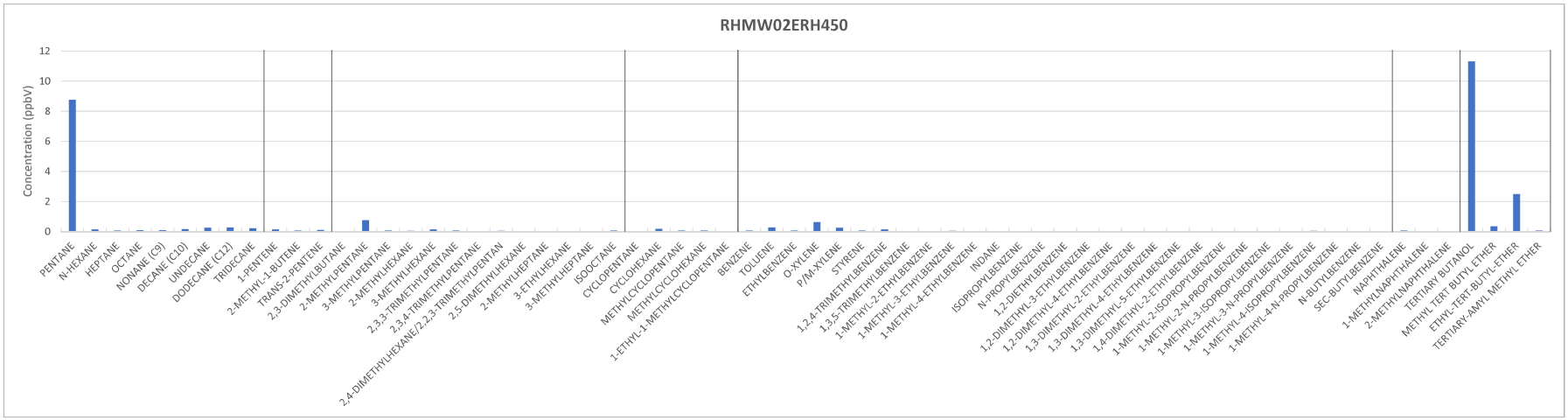

GSI ENVIRONMENTAL

ATTACHMENT B.3.1: FINGERPRINT CHARTS FOR SOIL VAPOR AND GROUNDWATER MONITORING WELL HEADSPACE SAMPLES
Red Hill Bulk Fuel Storage Facility, Joint Base Pearl Harbor-Hickam, O'ahu, Hawai'i

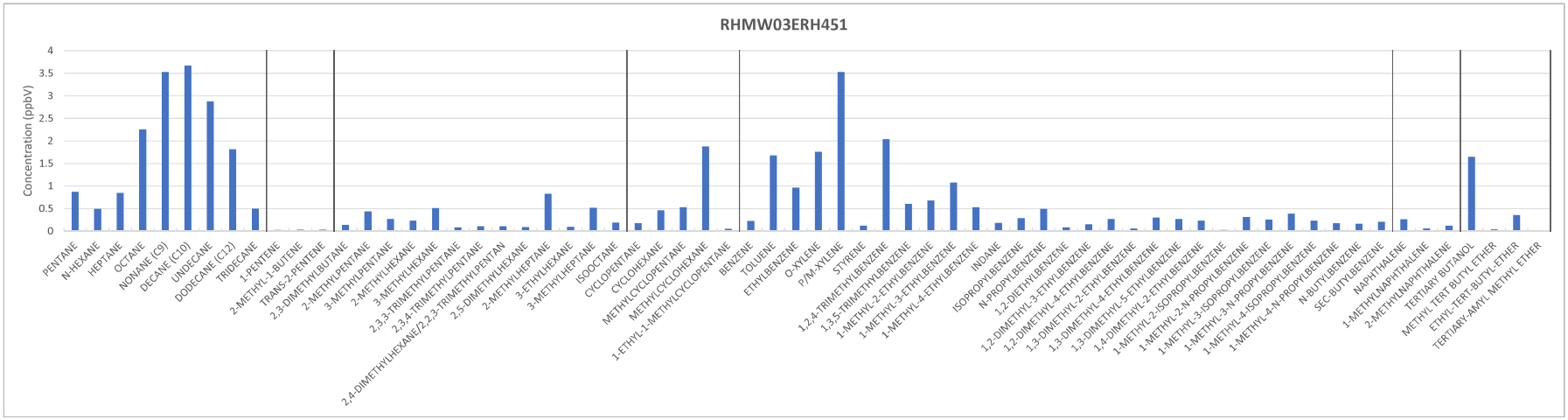

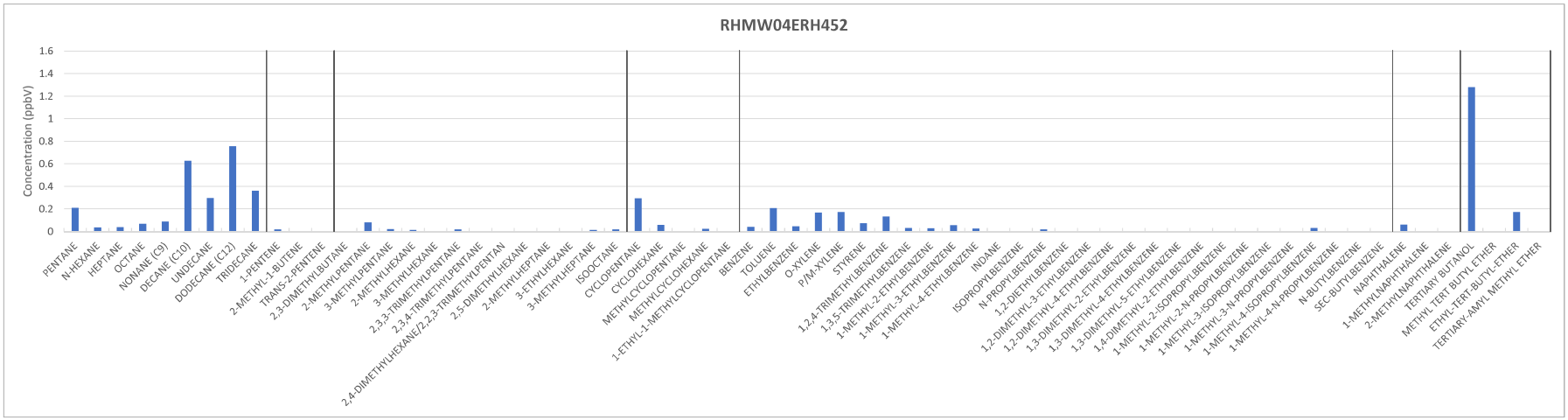

Attachment B.3.2:
FID Chromatograms for Soil Vapor and
Groundwater Monitoring Well Headspace Samples

GSI ENVIRONMENTAL

ATTACHMENT B.3.2: FID CHROMATOGRAMS FOR SOIL VAPOR AND GROUNDWATER MONITORING WELL HEADSPACE SAMPLES

Red Hill Bulk Fuel Storage Facility, Joint Base Pearl Harbor-Hickam, O'ahu, Hawai'i

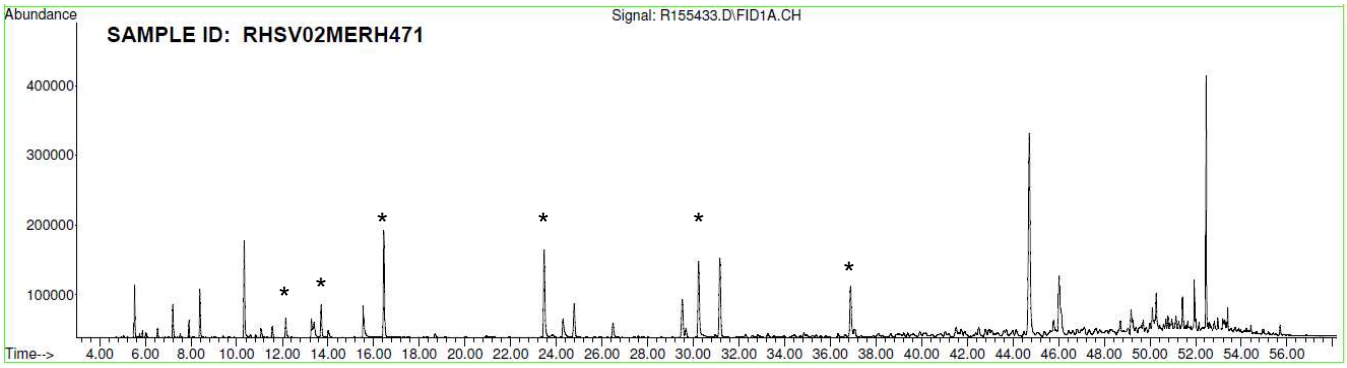

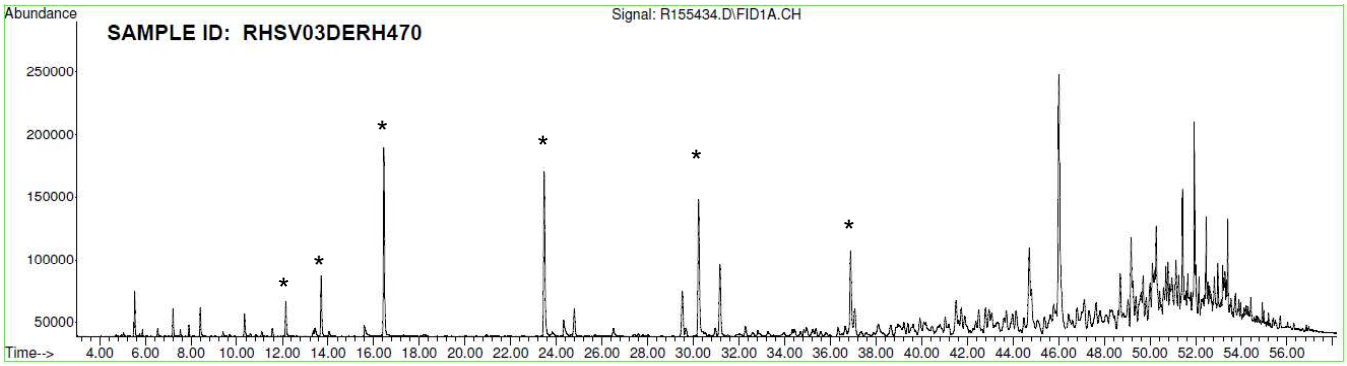

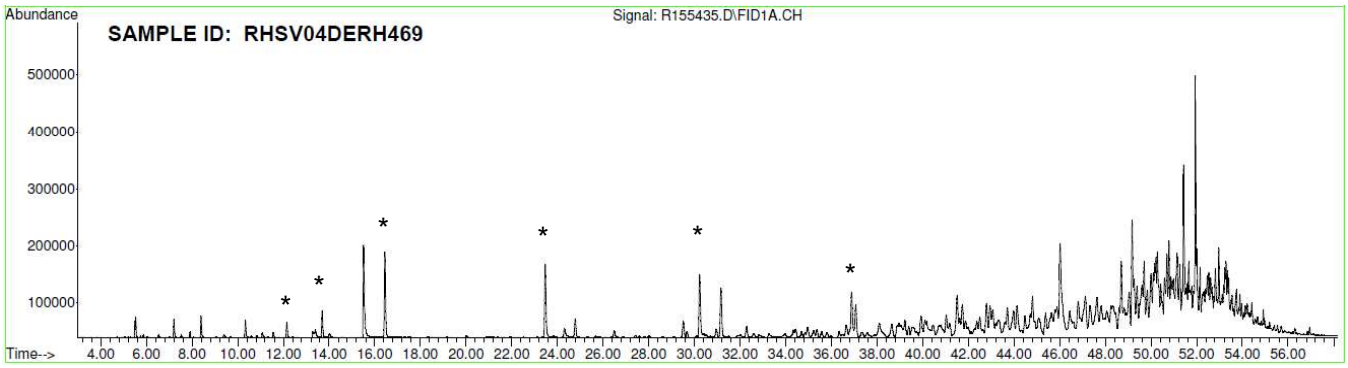

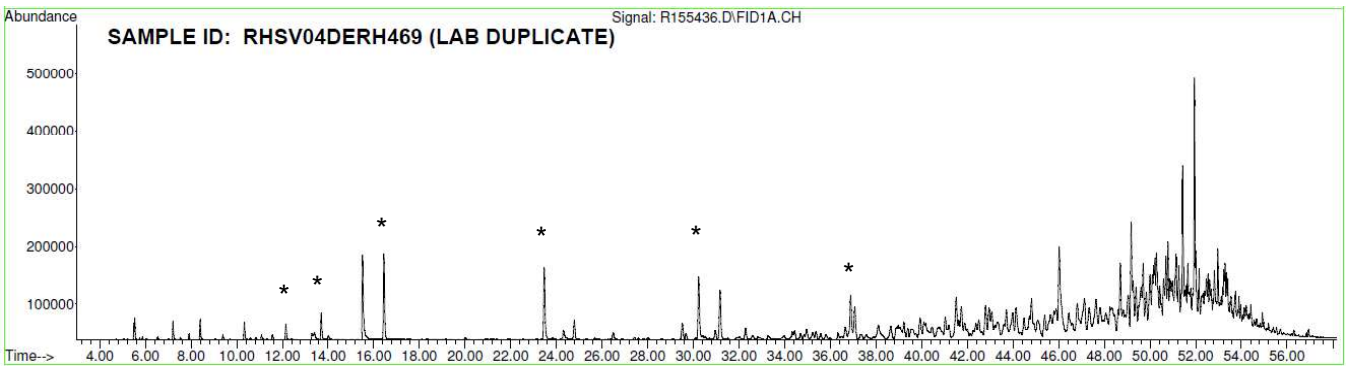

Note: Asterisk (*) = Internal Standard

GSI ENVIRONMENTAL

ATTACHMENT B.3.2: FID CHROMATOGRAMS FOR SOIL VAPOR AND GROUNDWATER MONITORING WELL HEADSPACE SAMPLES

Red Hill Bulk Fuel Storage Facility, Joint Base Pearl Harbor-Hickam, O'ahu, Hawai'i

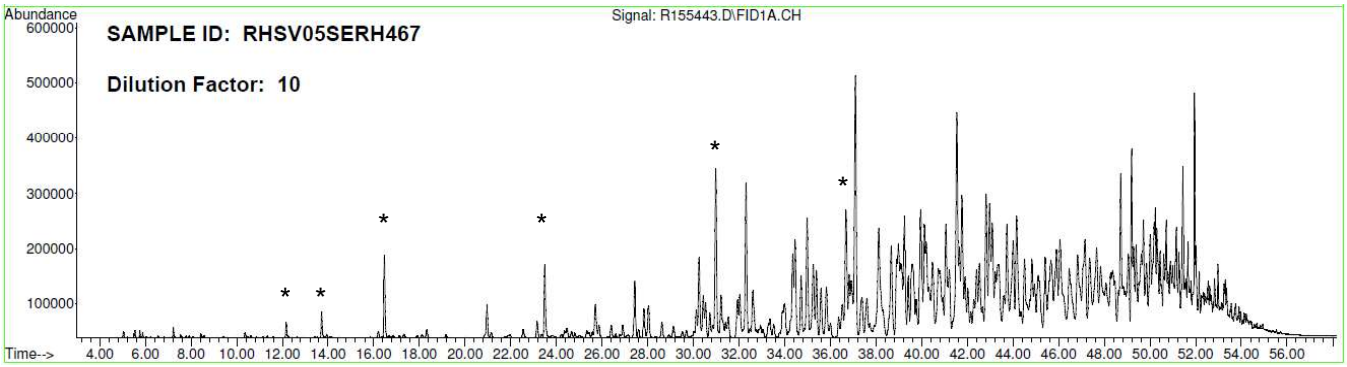

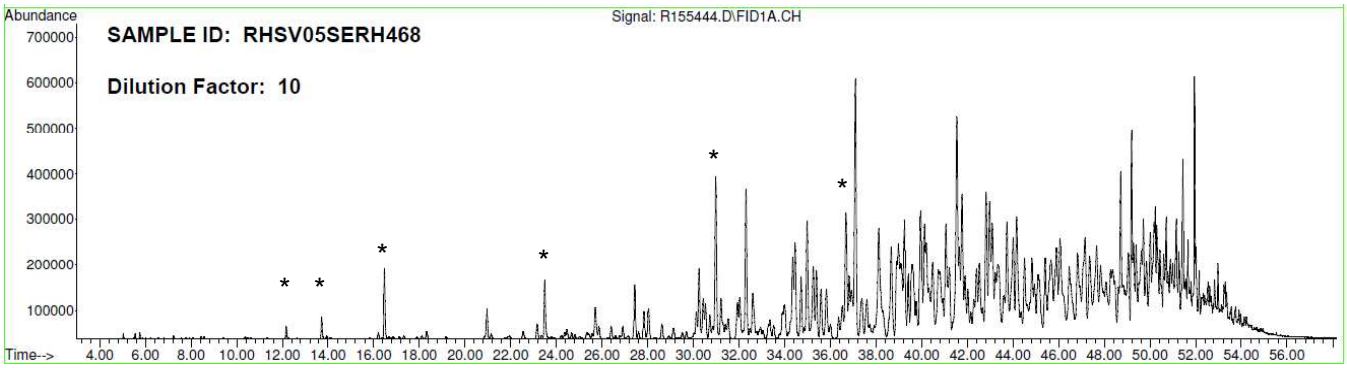

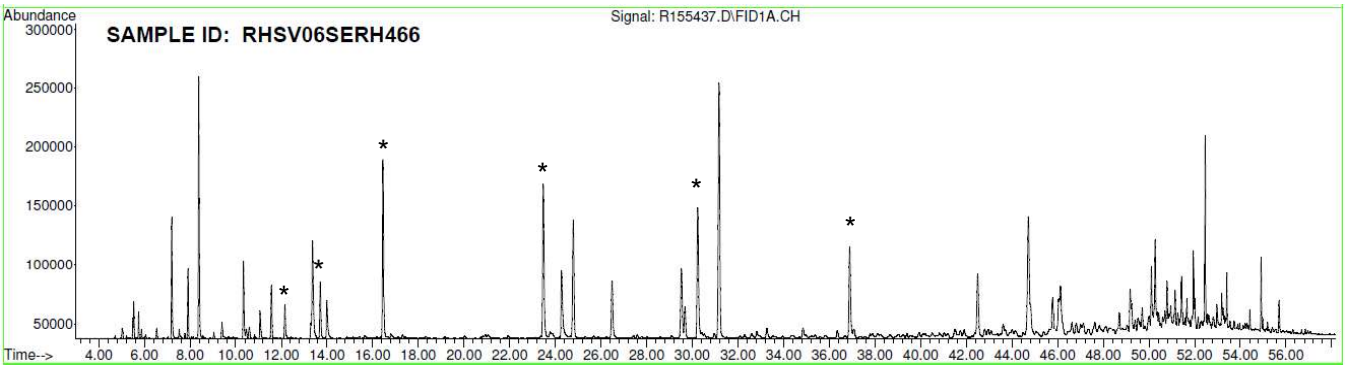

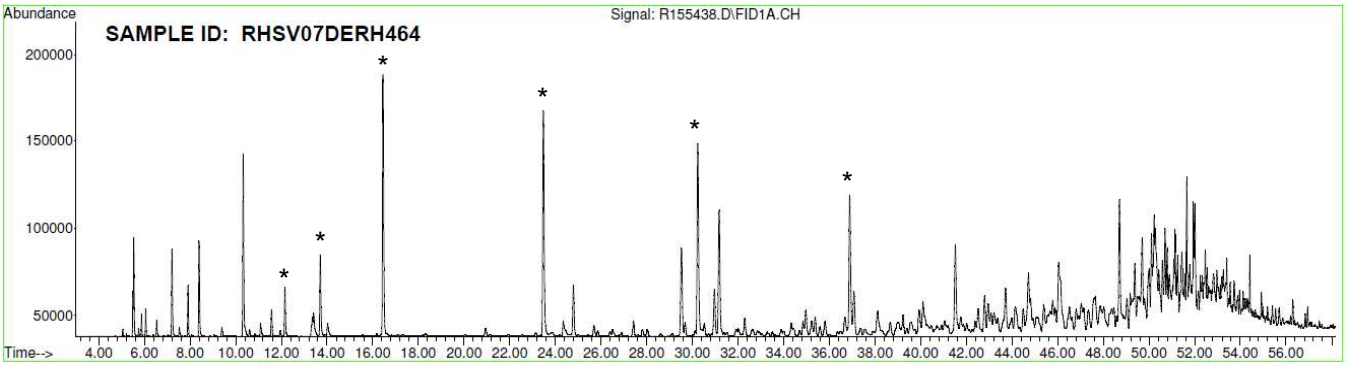

Note: Asterisk (*) = Internal Standard

GSI ENVIRONMENTAL

ATTACHMENT B.3.2: FID CHROMATOGRAMS FOR SOIL VAPOR AND GROUNDWATER MONITORING WELL HEADSPACE SAMPLES

Red Hill Bulk Fuel Storage Facility, Joint Base Pearl Harbor-Hickam, O'ahu, Hawai'i

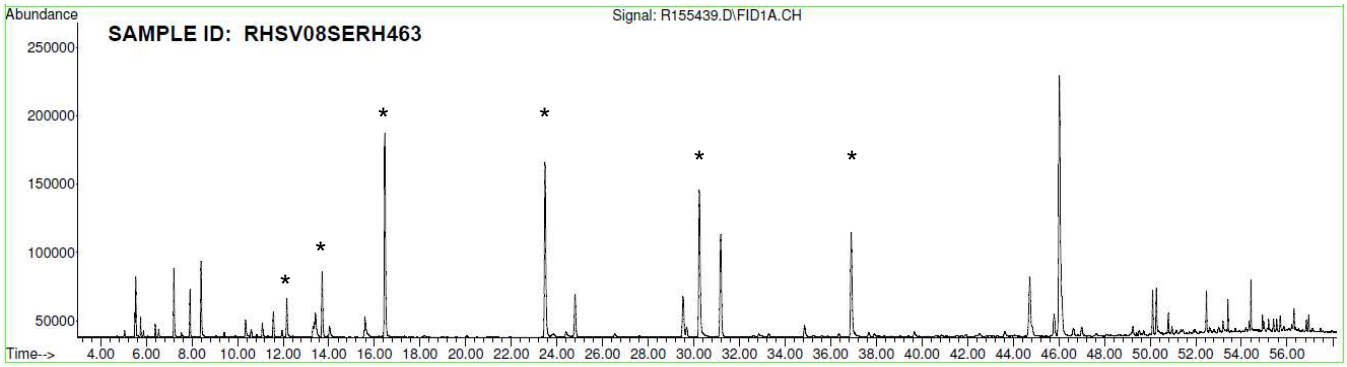

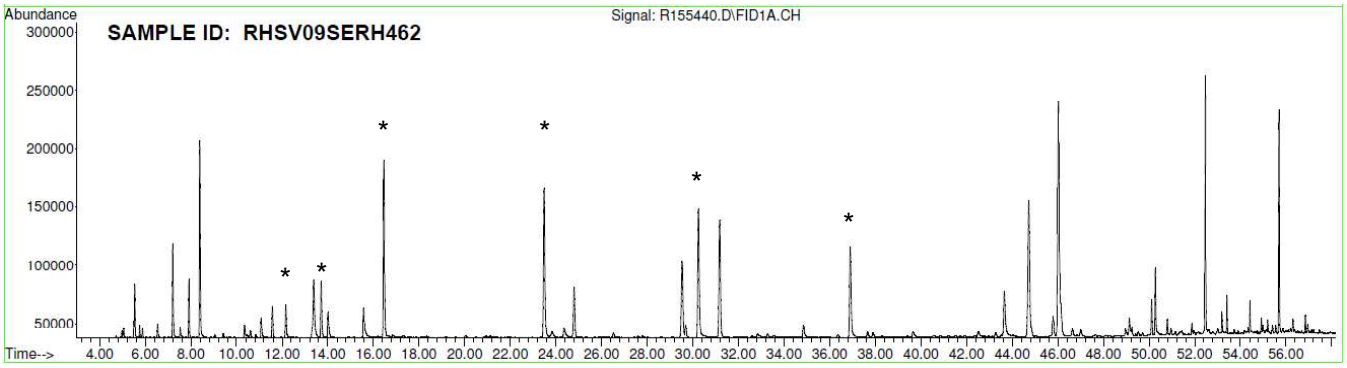

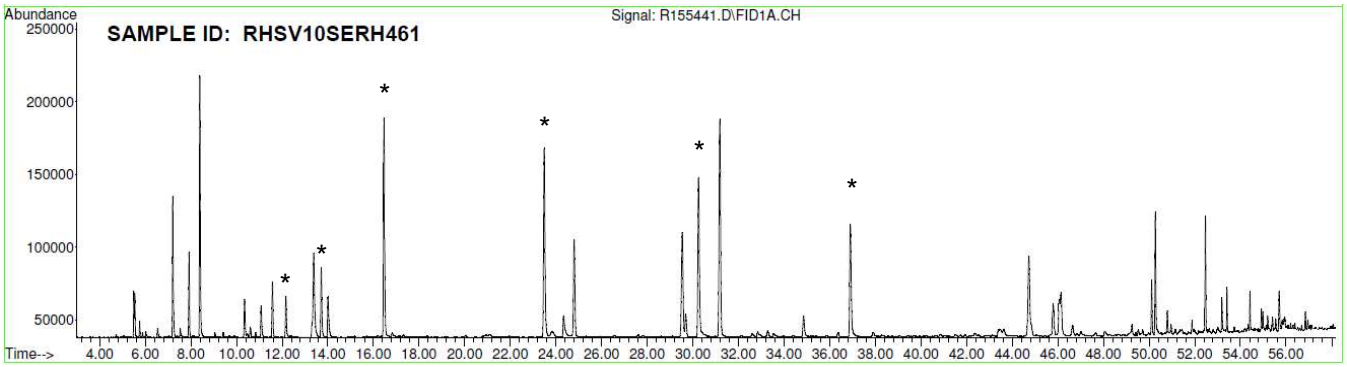

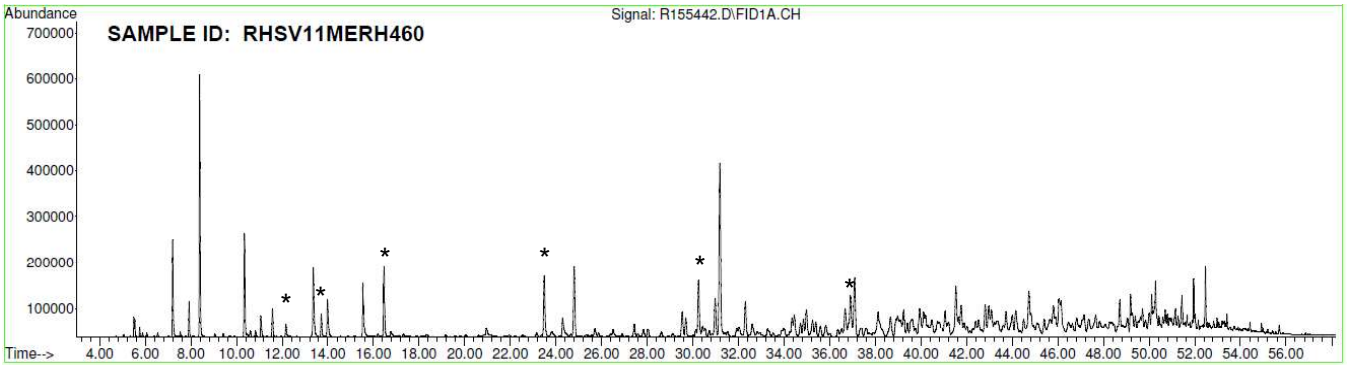

Note: Asterisk (*) = Internal Standard

GSI ENVIRONMENTAL

ATTACHMENT B.3.2: FID CHROMATOGRAMS FOR SOIL VAPOR AND GROUNDWATER MONITORING WELL HEADSPACE SAMPLES

Red Hill Bulk Fuel Storage Facility, Joint Base Pearl Harbor-Hickam, O'ahu, Hawai'i

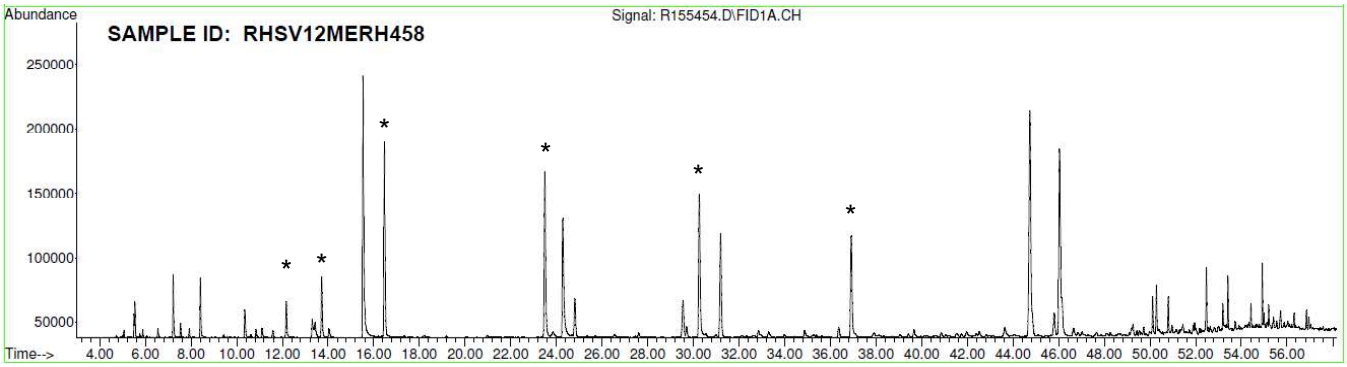

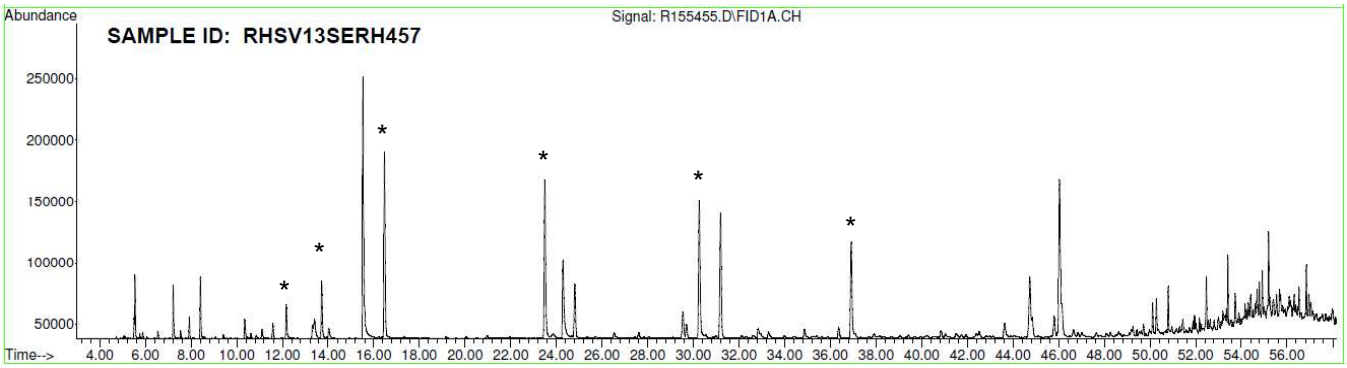

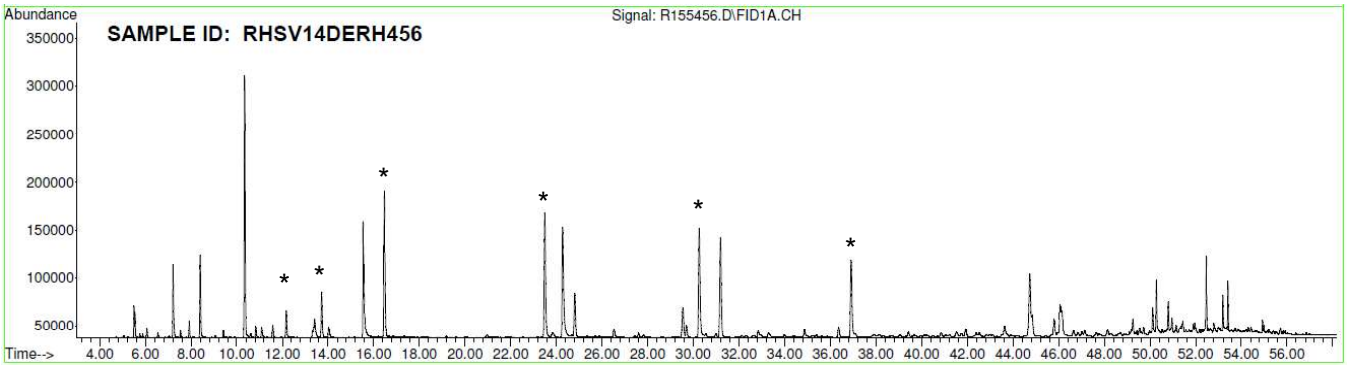

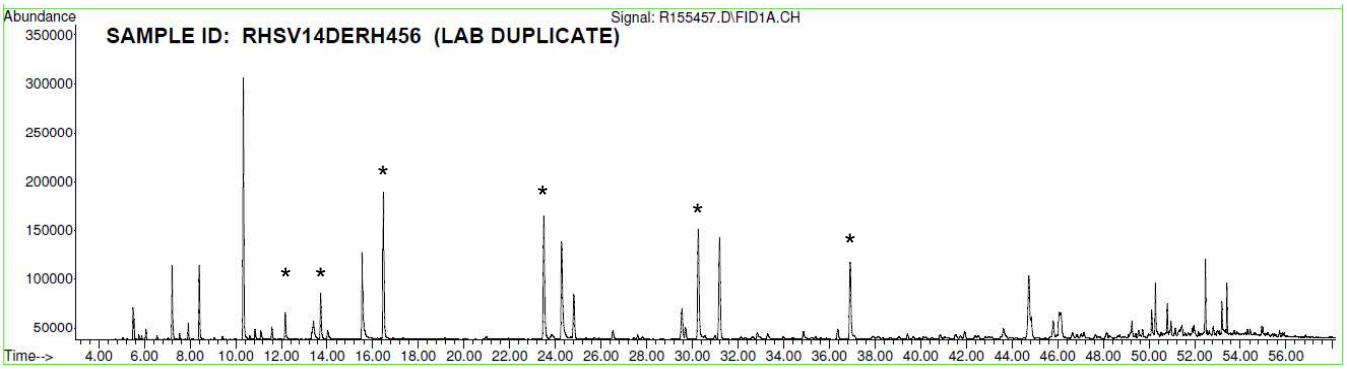

Note: Asterisk (*) = Internal Standard

GSI ENVIRONMENTAL

ATTACHMENT B.3.2: FID CHROMATOGRAMS FOR SOIL VAPOR AND GROUNDWATER MONITORING WELL HEADSPACE SAMPLES

Red Hill Bulk Fuel Storage Facility, Joint Base Pearl Harbor-Hickam, O'ahu, Hawai'i

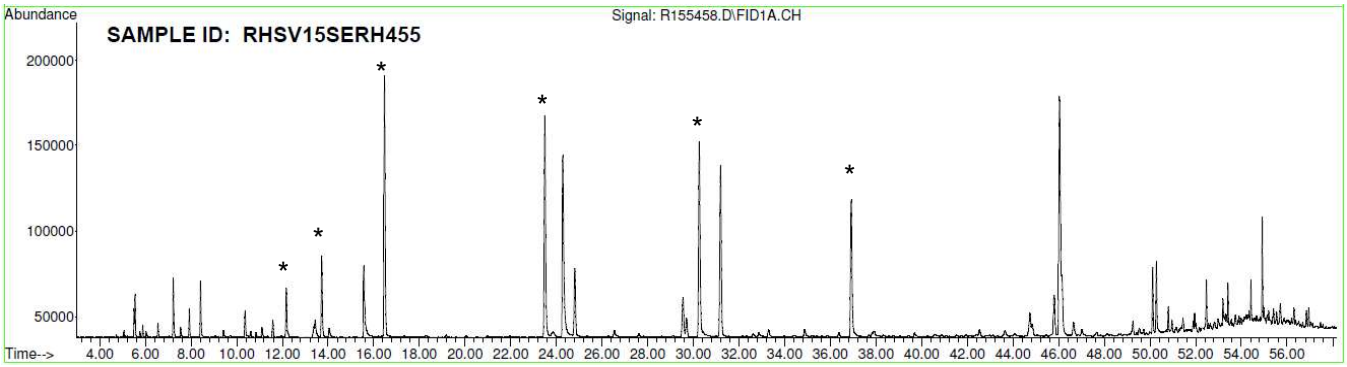

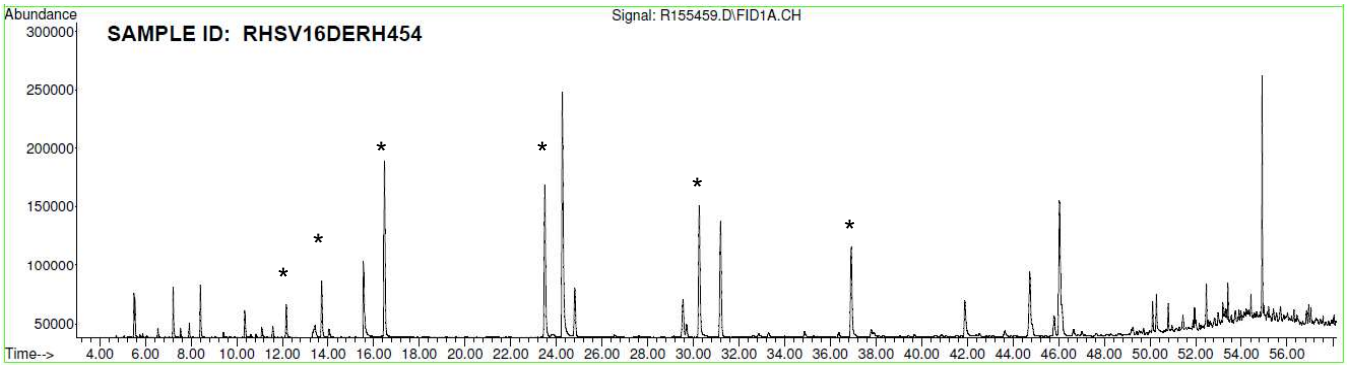

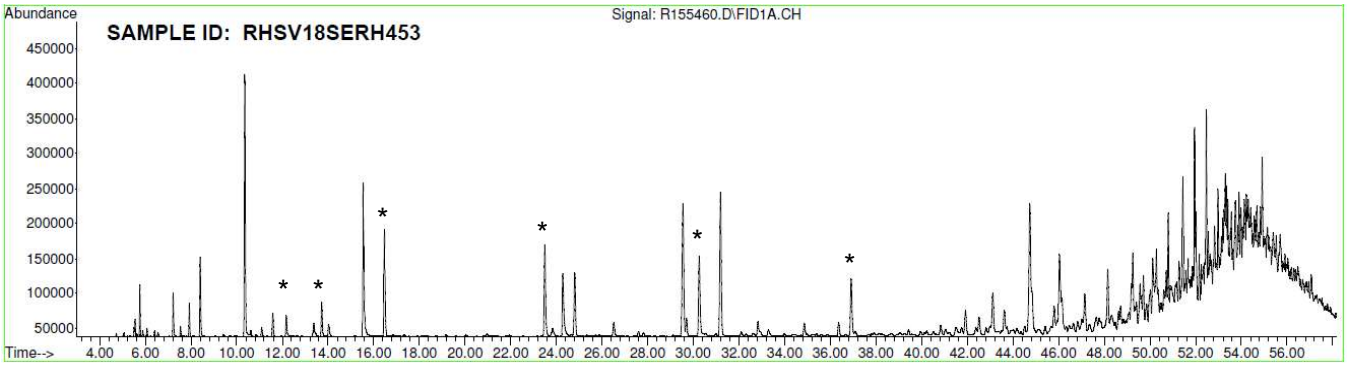

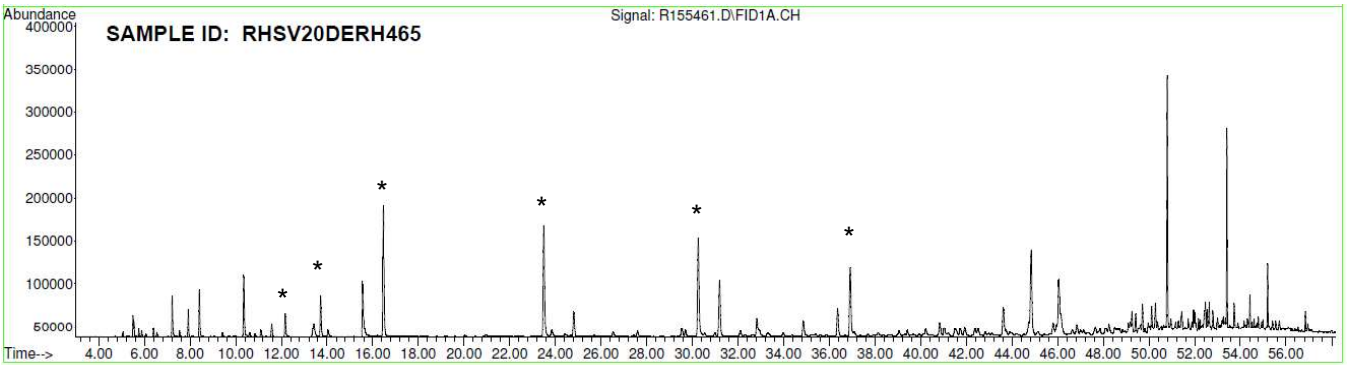

Note: Asterisk (*) = Internal Standard

GSI ENVIRONMENTAL

ATTACHMENT B.3.2: FID CHROMATOGRAMS FOR SOIL VAPOR AND GROUNDWATER MONITORING WELL HEADSPACE SAMPLES

Red Hill Bulk Fuel Storage Facility, Joint Base Pearl Harbor-Hickam, O'ahu, Hawai'i

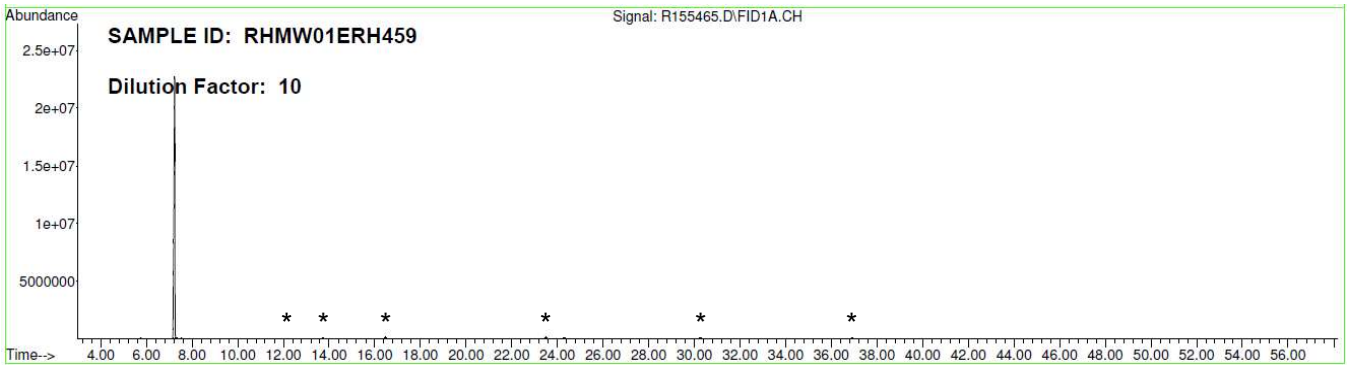

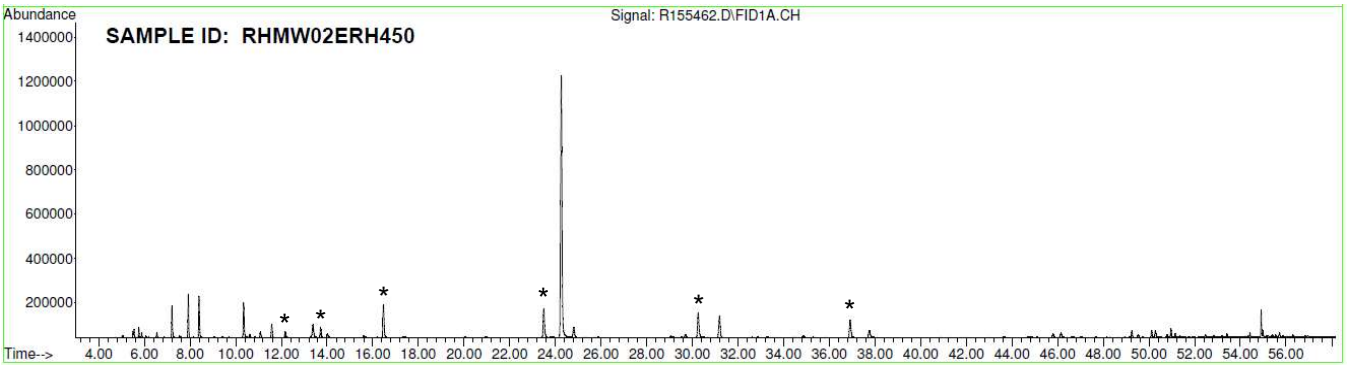

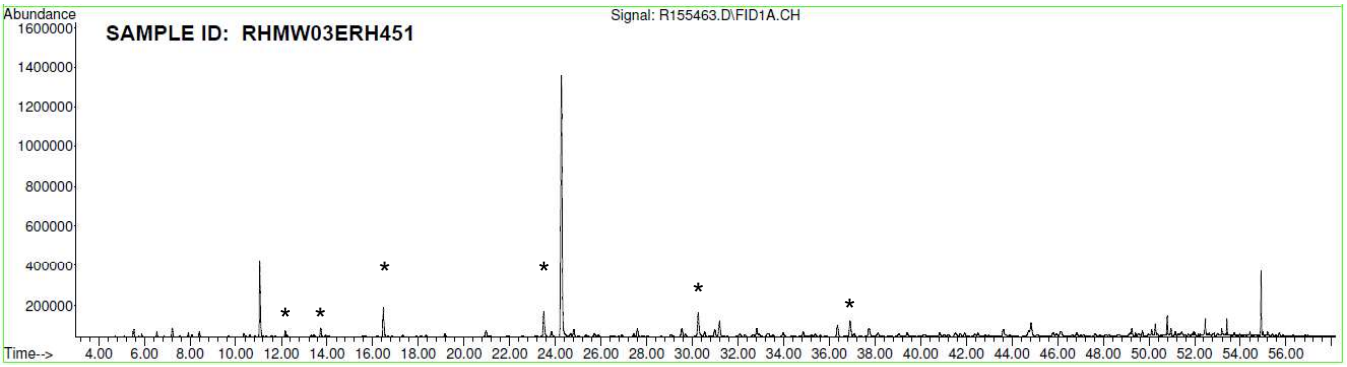

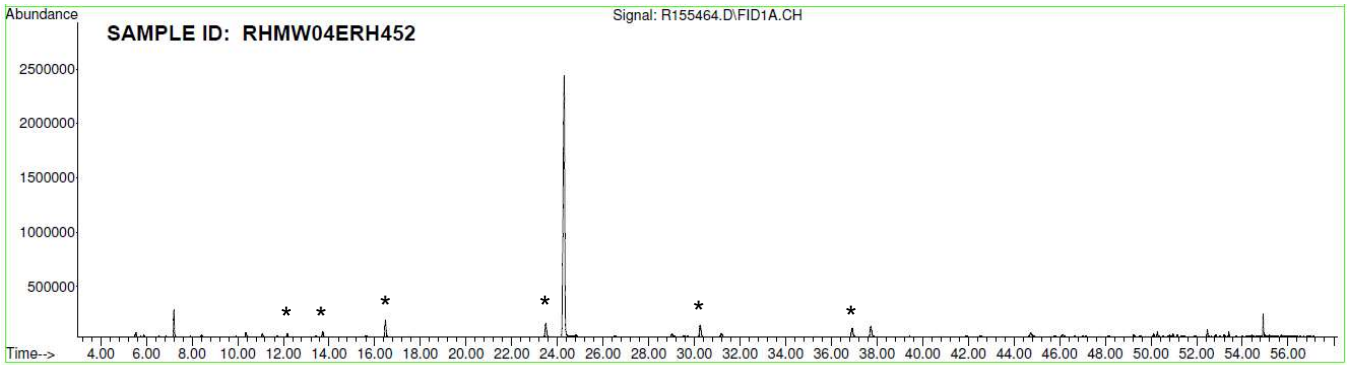

Note: Asterisk (*) = Internal Standard

ATTACHMENT B.3.2: FID CHROMATOGRAMS FOR
SOIL VAPOR AND GROUNDWATER MONITORING WELL HEADSPACE SAMPLES
Red Hill Bulk Fuel Storage Facility, Joint Base Pearl Harbor-Hickam, O'ahu, Hawai'i

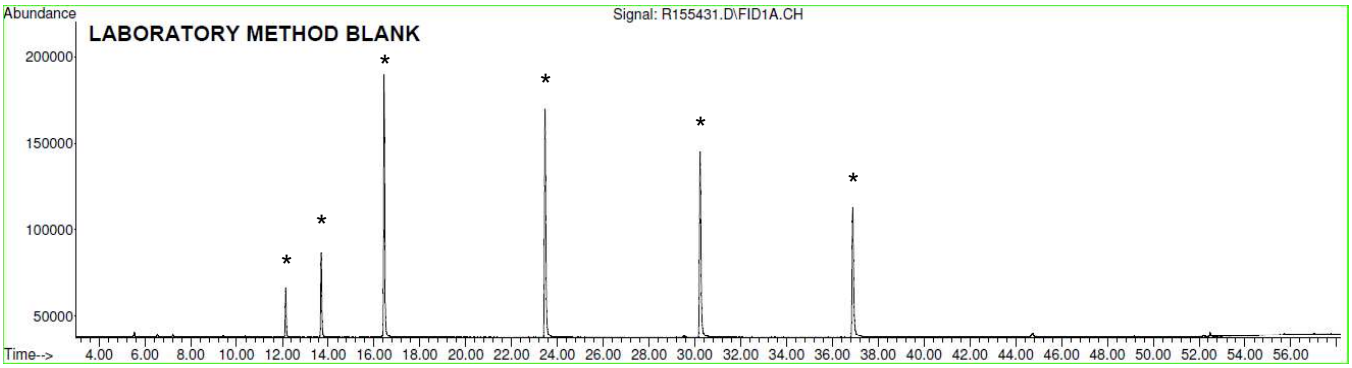

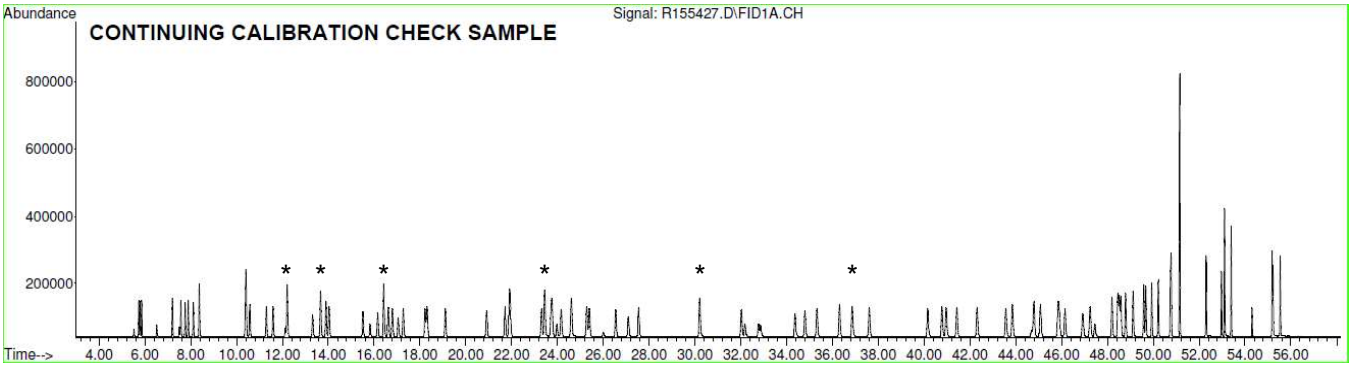

Note: Asterisk (*) = Internal Standard

Attachment B.3.3:
Soil Vapor Field Monitoring Results

GSI Job No. 4671
Issued: 22 December 2017

GSI ENVIRONMENTAL

ATTACHMENT B.3.3: SOIL VAPOR FIELD MONITORING RESULTS
Red Hill Bulk Fuel Storage Facility, Joint Base Pearl Harbor-Hickam, O'ahu, Hawai'i

	DATE	TIME	PID	OXYGEN	CO2	METHANE	BALANCE	DELTA P
LOCATION			ppb	%	%	%	%	in H20
SOIL VAPOR WELLS (Below Tanks)								
RHSV02 S	2017-10-31	11:30	608	19.5	0.7	0	79.8	0.176
RHSV02 M	2017-10-31	11:35	980	19.6	0.2	0	80.2	0.179
RHSV02 D	2017-10-31	11:40	405	19.4	0.8	0	79.8	0.164
RHSV03 S	2017-10-31	10:53	360	19	0.3	0	80.8	0.113
RHSV03 M	2017-10-31	10:57	365	20.2	0.1	0	79.7	0.225
RHSV03 D	2017-10-31	11:02	408	20.2	0.2	0	79.6	0.113
RHSV04 S	2017-10-31	10:10	340	19.5	0.7	0	79.9	0.116
RHSV04 M	2017-10-31	10:15	322	19.5	0.8	0	79.7	0.095
RHSV04 D	2017-10-31	10:20	340	19.4	0.9	0	79.7	0.095
RHSV05 S	2017-10-31	9:10	19000	18.7	0.9	0	80.5	0.035
RHSV05 M	2017-10-31	9:16	5300	18.1	1.3	0	80.6	-3.1
RHSV05 D	2017-10-31	9:27	9600	19.5	0.5	0	80	0.003
RHSV06 S	2017-10-31	8:40	12000	18.8	1.1	0	80.1	-0.036
RHSV06 M	2017-10-31	8:30	2500	19.3	0.6	0	80.1	-0.022
RHSV07 S	2017-10-30	13:58	240	20.2	0.3	0	79.5	-0.006
RHSV07 M	2017-10-30	14:01	250	19.7	0.4	0	79.9	-0.591
RHSV07 D	2017-10-30	14:07	468	13.7	3.2	0	83	0.006
RHSV08 S	2017-10-30	13:22	190	19.9	0.6	0	79.5	0.071
RHSV08 M	2017-10-30	13:25	122	19.8	0.7	0	79.5	0.016
RHSV08 D	2017-10-30	13:28	112	19.8	0.8	0	79.4	0.016
RHSV09 S	2017-10-30	12:40	1500	20	0.4	0	79.6	0
RHSV09 M	2017-10-30	12:50	385	19.8	0.6	0	79.7	0.03
RHSV09 D	2017-10-30	12:55	240	19.8	0.6	0	79.6	0.003
RHSV10 S	2017-10-30	11:15	580	19.9	0.3	0	79.8	0.019
RHSV10 M	2017-10-30	11:20	160	19.9	0.4	0	79.7	0.162
RHSV11 M	2017-10-30	10:32	31090	19.1	1	0	79.9	0.038
RHSV11 D	2017-10-30	10:43	9780	19.9	0.2	0	79.8	0.115
RHSV12 S	2017-10-27	13:41	1344	19.1	0.6	0	80.3	0.151
RHSV12 M	2017-10-27	13:48	16890	20.1	0.4	0	79.5	0.214
RHSV12 D	2017-10-27	13:56	10890	20.2	0.3	0	79.5	0.246
RHSV13 S	2017-10-27	13:00	495	19.6	0.7	0	79.8	0.204
RHSV13 M	2017-10-27	13:05	336	19.6	0.7	0	79.8	0.192
RHSV13 D	2017-10-27	13:12	396	19.7	0.6	0	79.8	0.199
RHSV14 S	2017-10-27	12:25	3286	16.4	1.5	0	82.1	0.031
RHSV14 M	2017-10-27	12:28	2938	15.7	2.4	0	81.9	0.165
RHSV14 D	2017-10-27	12:33	9154	19.8	0.4	0	79.8	0.245
RHSV15 S	2017-10-27	10:58	160	20	0.2	0	79.8	0.172
RHSV15 M	2017-10-27	11:00	Line plugged - no sample possible.					
RHSV15 D	2017-10-27	11:08	44	19.7	0.3	0	79.9	0.139
RHSV16 S	2017-10-27	10:12	1200	18.5	0.6	0	79.7	0.033
RHSV16 M	2017-10-27	10:25	2019	17.5	1.6	0	80.9	0.252
RHSV16 D	2017-10-27	10:28	5030	18.5	1.1	0	80.4	0.229
RHSV17 S	Not sampled. Access blocked by equipment.							
RHSV17 M	Not sampled. Access blocked by equipment.							
RHSV17 D	Not sampled. Access blocked by equipment.							
RHSV18 S	2017-10-27	9:15	40000	19.9	0.2	0	79.9	0.153
RHSV18 D	2017-10-27	9:11	5500	20	0.2	0	79.8	0.154
RHSV20 S	2017-10-30	14:44	580	20.6	0.1	0	79.3	0.14

GSI Job No. 4671
Issued: 22 December 2017

GSI ENVIRONMENTAL

ATTACHMENT B.3.3: SOIL VAPOR FIELD MONITORING RESULTS
Red Hill Bulk Fuel Storage Facility, Joint Base Pearl Harbor-Hickam, O'ahu, Hawai'i

	DATE	TIME	PID	OXYGEN	CO2	METHANE	BALANCE	DELTA P
LOCATION			**ppb**	**%**	**%**	**%**	**%**	**in H20**
RHSV20 M	2017-10-30	14:50	700	20.6	0.1	0	79.3	-0.007
RHSV20 D	2017-10-30	14:54	800	20.5	0.1	0	79.4	0.048
MONITORING WELL HEADSPACE								
RHMW01	2017-10-30	9:15	23200	19.1	0.7	0	80.2	0
RHMW02	2017-10-26	10:15	250	6.6	8.5	0	84.7	0.125
RHMW03	2017-10-26	11:40	200	17	2.1	0	NR	0.165
RHMW04	2017-10-26	15:10	400	20.6	0.1	0	79.3	0.47
UPPER TUNNEL VAPOR PINS								
RHVPT05	2017-10-26	12:25	75	20.3	0.3	0	79.4	0.185
RHVPT11	2017-10-26	12:37	1000	20.5	0.1	0	79.4	0.111
HILL TOP SOIL GAS POINTS								
T2 SGP	2017-10-31	12:56	329	18.7	1	0	80.3	NM
T6 SGP	2017-10-31	1:10	296	18.6	1.1	0	80.3	NM
AMBIENT AIR (mostly inside Lower Tunnel)								
Tank 2 Ambient	2017-10-31	11:30	600	20.4	0.1	0	79.5	NM
Tank 3 Ambient	2017-10-31	10:50	645	20.3	0.1	0	79.7	-0.001
Tank 4 Ambient	2017-10-31	10:07	660	20.3	0.2	0	79.5	0.002
Tank 5 Ambient	2017-10-31	9:04	970	20.1	0.4	0	79.5	0.013
Tank 6 Ambient	2017-10-31	8:35	350	20.2	0.1	0	79.7	-0.002
Tank 7 Ambient	2017-10-30	13:55	380	20.7	0.2	0	79.1	-0.002
Tank 8 Ambient	2017-10-30	13:20	220	20.6	0.2	0	79.2	-0.006
Tank 9 Ambient	2017-10-30	12:40	230	20.7	0.2	0	79.1	-0.001
Tank 10 Ambier	2017-10-30	11:11	175	20.5	0.1	0	79.4	0.004
Tank 11 Ambier	2017-10-30	10:31	267	20.3	0.3	0	79.3	0.002
Tank 12 Ambier	2017-10-27	13:37	581	20.6	0.1	0	79.3	NM
Tank 13 Ambier	2017-10-27	12:56	1125	20.6	0.1	0	79.3	NM
Tank 14 Ambier	2017-10-27	12:20	1300	20.8	0.1	0	79.1	NM
Tank 15 Ambier	2017-10-27	10:54	85	20.6	0.1	0	79.3	NM
Tank 16 Ambier	2017-10-27	10:13	235	20.4	0.1	0	79.7	NM
Tank 18 Ambier	2017-10-27	9:09	1000	20.5	0.1	0	79.4	-0.001
Tank 20 Ambier	2017-10-30	14:40	2400	20.7	0.2	0	79.1	NM
MW01 Ambient	2017-10-30	9:05	163	20.3	0.1	0	79.6	0
MW02 Ambient	2017-10-26	10:15	212	20.4	0.1	0	79.6	-0.001
MW03 Ambient	2017-10-26	11:40	38	20.3	0.9	0	78.8	-0.009
MW04 Ambient	2017-10-26	15:10	0	20.5	0	0	79.5	NM
Tank 5 UT Amb	2017-10-26	12:25	500	20.3	0.3	0	79.4	0.002
Tank 11 UT Am	2017-10-26	12:37	180	20.6	0.1	0	79.3	-0.007
T6 Ambient	2017-10-31	1:15	155	18.7	0	0	NR	

Attachment B.3.4:
Soil Vapor and Groundwater Monitoring Well Headspace Sample Analytical Results

GSI ENVIRONMENTAL

ATTACHMENT B.3.4: SOIL VAPOR AND GROUNDWATER MONITORING WELL HEADSPACE SAMPLE ANALYTICAL RESULTS
Red Hill Bulk Fuel Storage Facility, Joint Base Pearl Harbor-Hickam, O'ahu, Hawai'i

			Sample ID:	RHSV02MERH471	RHSV03DERH470	RHSV04DERH469	RHSV05SERH467	RHSV05SERH468	RHSV06SERH466
			Lab Sample ID:	L1740493-01	L1740493-02	L1740493-03	L1740493-04	L1740493-05	L1740493-06
			Sample Date/Time:	2017-10-31 12:00	2017-10-31 11:25	2017-10-31 10:43	2017-10-31 9:45	2017-10-31 10:00	2017-10-31 8:57
			Matrix:	SOIL_VAPOR	SOIL_VAPOR	SOIL_VAPOR	SOIL_VAPOR	SOIL_VAPOR	SOIL_VAPOR
FIXED GASES BY USEPA METHOD 3C									
Analyte		**Units**							
Carbon Dioxide		%		0.045 J	0.196 JD	0.989D	0.9D	0.992D	1.28D
Methane		%		<0.061	<0.061D	<0.075D	<0.068D	<0.054D	<0.066D
Oxygen		%		20.8	20.6D	20.8D	19.8D	20.1D	20D
VOCs BY USEPA METHOD TO-15 (TARGET ANALYTES)									
Analyte	**Class**	**Units**							
Decane (C10)	alkane	ppbV		0.975	1.46	2.38	<0.25	<0.25	1.17
Dodecane (C12)	alkane	ppbV		0.741	1.66	1.33	1.33D	<0.5	0.942
Heptane	alkane	ppbV		0.087	0.057	0.07	2.8D	2.12D	0.157
n-Hexane	alkane	ppbV		0.084	0.053	0.048	1.5D	0.75D	0.112
Nonane (C9)	alkane	ppbV		0.312	0.451	0.705	27.6D	33.1D	0.371
Octane	alkane	ppbV		0.146	0.146	0.18	8.26D	7.85D	0.178
Pentane	alkane	ppbV		1.06	0.435	0.42	1.45D	0.57D	2.61
Tridecane	alkane	ppbV		0.105 J	0.323 J	0.429 J	<0.5	<0.5	0.287 J
Undecane	alkane	ppbV		0.43	0.792	2.61	<0.25	<0.25	0.913
1,3-Butadiene	alkene	ppbV		<0.01	<0.01	<0.01	<0.1	<0.1	0.012 J
1-Decene	alkene	ppbV		<0.025	<0.025	<0.025	<0.25	<0.25	<0.025
1-Heptene	alkene	ppbV		<0.01	<0.01	0.055	<0.1	<0.1	0.04
1-Hexene	alkene	ppbV		<0.01	<0.01	<0.01	<0.1	<0.1	<0.01
1-Nonene	alkene	ppbV		<0.01	<0.01	<0.01	<0.1	<0.1	<0.01
1-Octene	alkene	ppbV		0.032	0.016 J	<0.01	<0.1	<0.1	<0.01
1-Pentene	alkene	ppbV		0.023 J	0.013 J	0.012 J	0.17 JD	0.19 JD	0.085
2-Methyl-1-Butene	alkene	ppbV		0.011 J	<0.01	<0.01	1.24D	1.35D	0.208
cis-2-Pentene	alkene	ppbV		<0.01	<0.01	<0.01	0.34D	0.34D	<0.01
trans-2-Pentene	alkene	ppbV		0.018 J	<0.01	<0.01	0.16 JD	0.15 JD	0.065
2,2-Dimethylpentane	branched alkane	ppbV		<0.01	<0.01	<0.01	0.2 JD	0.22 JD	<0.01
2,3,3-Trimethylpentane	branched alkane	ppbV		0.141	0.039	0.058	1.63D	1.83D	0.122
2,3,4-Trimethylpentane	branched alkane	ppbV		0.027	0.018 J	0.026	3.26D	3.76D	0.053
2,3-Dimethylbutane	branched alkane	ppbV		0.035	0.014 J	<0.01	0.5D	0.31D	0.049
2,3-Dimethylhexane	branched alkane	ppbV		0.099	<0.01	<0.01	3.28D	3.56D	<0.01
2,3-Dimethylpentane	branched alkane	ppbV		<0.01	<0.01	<0.01	2.25D	2.38D	<0.01
2,4-Dimethylhexane/2,2,3-Trimethylpentar	branched alkane	ppbV		0.042 J	<0.025	0.033 J	2.38D	2.56D	0.091
2,4-Dimethylpentane	branched alkane	ppbV		<0.01	<0.01	<0.01	0.66D	<0.1	<0.01
2,5-Dimethylhexane	branched alkane	ppbV		0.018 J	0.012 J	0.015 J	1.29D	1.34D	0.033
2-Methylheptane	branched alkane	ppbV		0.039	0.041	0.05	6.03D	6.23D	<0.01
2-Methylhexane	branched alkane	ppbV		0.028	0.026	0.024 J	1.83D	1.57D	0.023 J
2-Methylpentane	branched alkane	ppbV		0.217	0.096	0.105	2.2D	1.06D	0.463
3-Ethylhexane	branched alkane	ppbV		<0.01	<0.01	0.013 J	3.43D	3.91D	<0.01
3-Methylheptane	branched alkane	ppbV		0.032	0.033	0.048	6D	6.44D	0.043
3-Methylhexane	branched alkane	ppbV		0.118	0.065	0.095	3.38D	3.23D	0.202
3-Methylpentane	branched alkane	ppbV		0.041	0.029	0.049	1.64D	0.99D	0.04
Isooctane	branched alkane	ppbV		0.033	0.024 J	0.023 J	<0.1	<0.1	0.062
Isopentane	branched alkane	ppbV		<0.01	<0.01	<0.01	<0.1	<0.1	<0.01
1-Ethyl-1-Methylcyclopentane	cycloalkane	ppbV		<0.01	<0.01	0.014 J	3.56D	4.19D	<0.01
Cyclohexane	cycloalkane	ppbV		0.052	0.025	0.042	7.71D	8.69D	0.072
Cyclopentane	cycloalkane	ppbV		<0.01	<0.01	<0.01	0.36D	0.22 JD	<0.01
Methylcyclohexane	cycloalkane	ppbV		0.103	0.08	0.132	39.4D	44.2D	0.151
Methylcyclopentane	cycloalkane	ppbV		0.032	0.025	0.029	3.65D	3.66D	0.034
1,2,4,5-Tetramethylbenzene	aromatic	ppbV		<0.025	<0.025	0.056	<0.25	<0.25	<0.025
1,2,4-Trimethylbenzene	aromatic	ppbV		0.349	0.448	0.509	2.34D	1.7D	0.537
1,2-Diethylbenzene	aromatic	ppbV		0.042 J	0.085	0.221	2.68D	3.92D	0.029 J
1,2-Dimethyl-3-Ethylbenzene	aromatic	ppbV		0.043 J	0.076	0.13	1.23D	0.88D	0.031 J
1,2-Dimethyl-4-Ethylbenzene	aromatic	ppbV		0.169	0.326	0.871	8.41D	12D	0.16
1,3,5-Trimethylbenzene	aromatic	ppbV		0.25	0.458	1.08	24.4D	36.6D	0.229
1,3-Dimethyl-2-Ethylbenzene	aromatic	ppbV		<0.025	0.04 J	0.114	0.85D	1.01D	0.026 J
1,3-Dimethyl-4-Ethylbenzene	aromatic	ppbV		0.058	0.095	0.235	0.86D	0.95D	0.09
1,3-Dimethyl-5-Ethylbenzene	aromatic	ppbV		0.094	0.157	0.358	1.94D	2.41D	0.115
1,4-Dimethyl-2-Ethylbenzene	aromatic	ppbV		0.045 J	0.072	0.163	0.57D	<0.25	0.069
1-Methyl-2-Ethylbenzene	aromatic	ppbV		0.165	0.283	0.616	14.2D	20.9D	0.138
1-Methyl-2-Isopropylbenzene	aromatic	ppbV		<0.025	0.041 J	0.11	1.95D	2.92D	<0.025
1-Methyl-2-N-Propylbenzene	aromatic	ppbV		0.106	0.2	0.48	4.68D	6.26D	0.097
1-Methyl-3-Ethylbenzene	aromatic	ppbV		0.164	0.228	0.298	4.01D	4.99D	0.222
1-Methyl-3-Isopropylbenzene	aromatic	ppbV		0.078	0.142	0.343	5.71D	8.67D	0.084
1-Methyl-3-N-Propylbenzene	aromatic	ppbV		0.095	0.149	0.303	1.9D	2.44D	0.145
1-Methyl-4-Ethylbenzene	aromatic	ppbV		0.084	0.112	0.144	1.59D	1.84D	0.116
1-Methyl-4-Isopropylbenzene	aromatic	ppbV		0.039 J	0.052	0.076	0.49 JD	0.66D	0.084
1-Methyl-4-N-Propylbenzene	aromatic	ppbV		0.035 J	0.051	0.102	0.37 JD	0.4 JD	0.063
Benzene	aromatic	ppbV		0.054	0.029	0.044	0.45D	0.25D	0.057
Ethylbenzene	aromatic	ppbV		0.117	0.118	0.126	2.47D	2.35D	0.147
Indane	aromatic	ppbV		0.058	0.075	0.1	0.79D	0.92D	0.057
Indene	aromatic	ppbV		<0.025	<0.025	<0.025	<0.25	<0.25	<0.025
Isopropylbenzene	aromatic	ppbV		0.03	0.048	0.063	1.81D	2.27D	0.043
n-Butylbenzene	aromatic	ppbV		0.026 J	0.035 J	0.059	<0.25	<0.25	0.05
N-Pentylbenzene	aromatic	ppbV		<0.025	0.03 J	<0.025	<0.25	<0.25	<0.025
n-Propylbenzene	aromatic	ppbV		0.062	0.083	0.107	1.53D	1.84D	0.082
o-Xylene	aromatic	ppbV		0.484	0.426	0.621	13.7D	17.6D	0.691
p/m-Xylene	aromatic	ppbV		0.469	0.471	0.486	3.67D	2.22D	0.64
sec-Butylbenzene	aromatic	ppbV		0.028 J	0.053	0.114	2.33D	3.33D	0.05
Styrene	aromatic	ppbV		0.042	0.069	0.046	<0.1	<0.1	0.05
Toluene	aromatic	ppbV		0.277	0.252	0.183	2.91D	2.28D	0.237
1-Methylnaphthalene	naphthalene	ppbV		<0.05	<0.05	0.057 J	<0.5	<0.5	0.054 J
2-Methylnaphthalene	naphthalene	ppbV		<0.05	0.072 J	0.113 J	<0.5	<0.5	0.099 J
Naphthalene	naphthalene	ppbV		0.11	0.157	0.2	0.3 JD	<0.25	0.194
Tertiary Butanol	alcohol	ppbV		4.14	1.46	2.29	4.15D	3.37D	13.5
Ethyl-Tert-Butyl-Ether	ether	ppbV		0.806	0.294	0.408	0.34D	0.21 JD	2.3
Isopropyl Ether	ether	ppbV		<0.01	<0.01	<0.01	<0.1	<0.1	<0.01
Methyl tert butyl ether	ether	ppbV		0.091	0.031	0.04	<0.1	<0.1	0.241
Tertiary-Amyl Methyl Ether	ether	ppbV		0.031	<0.01	0.019 J	<0.1	<0.1	0.08
2-Ethylthiophene	thiophene	ppbV		<0.01	<0.01	<0.01	<0.1	<0.1	<0.01
2-Methylthiophene	thiophene	ppbV		<0.01	<0.01	<0.01	<0.1	<0.1	<0.01
3-Methylthiophene	thiophene	ppbV		<0.01	<0.01	<0.01	<0.1	<0.1	<0.01
Benzothiophene	thiophene	ppbV		<0.05	<0.05	<0.05	<0.5	<0.5	<0.05
Thiophene	thiophene	ppbV		<0.01	<0.01	<0.01	<0.1	<0.1	<0.01
1,2-Dibromoethane	other	ppbV		<0.01	<0.01	<0.01	<0.1	<0.1	<0.01
1,2-Dichloroethane	other	ppbV		<0.01	<0.01	<0.01	<0.1	<0.1	<0.01
MMT	other	ppbV		<0.05	<0.05	<0.05	<0.5	<0.5	<0.05

GSI ENVIRONMENTAL

ATTACHMENT B.3.4: SOIL VAPOR AND GROUNDWATER MONITORING WELL HEADSPACE SAMPLE ANALYTICAL RESULTS
Red Hill Bulk Fuel Storage Facility, Joint Base Pearl Harbor-Hickam, O'ahu, Hawai'i

			Sample ID:	RHSV02MERH471	RHSV03DERH470	RHSV04DERH469	RHSV05SERH467	RHSV05SERH468	RHSV06SERH466
			Lab Sample ID:	L1740493-01	L1740493-02	L1740493-03	L1740493-04	L1740493-05	L1740493-06
			Sample Date/Time:	2017-10-31 12:00	2017-10-31 11:25	2017-10-31 10:43	2017-10-31 9:45	2017-10-31 10:00	2017-10-31 8:57
			Matrix:	SOIL_VAPOR	SOIL_VAPOR	SOIL_VAPOR	SOIL_VAPOR	SOIL_VAPOR	SOIL_VAPOR
VOCs BY USEPA METHOD TO-15 (TENTATIVELY IDENTIFIED COMPOUNDS)									
1-Butanol	alcohol	ppbV		-	-	-	-	-	-
1-Hexanol, 2-ethyl-	alcohol	ppbV		6.84	17.3	-	-	-	-
Amylene Hydrate	alcohol	ppbV		-	-	-	-	-	-
Methyl Alcohol	alcohol	ppbV		4.38	-	-	-	-	-
Unknown	alcohol	ppbV		-	-	12.7	-	-	-
Unknown	alcohol	ppbV		-	-	-	-	-	-
Unknown	alcohol	ppbV		-	-	-	-	-	-
Unknown	alcohol	ppbV		-	-	-	-	269	-
unknown alcohol	alcohol	ppbV		-	-	-	-	-	-
unknown alcohol	alcohol	ppbV		-	-	-	-	-	-
Unknown	alcohol cycloalkane	ppbV		-	-	-	-	-	-
Propane	alkane	ppbV		-	-	-	-	-	-
Unknown	alkane	ppbV		-	-	-	-	-	-
Unknown	alkane	ppbV		-	-	-	-	-	-
unknown alkane	alkane	ppbV		-	-	-	-	-	-
unknown alkane	alkane	ppbV		-	-	-	-	-	-
1-Pentene, 2-methyl-	alkene	ppbV		-	-	-	-	-	-
2,4-Dimethyl-1-heptene	alkene	ppbV		-	4.45	-	-	-	-
Unknown	alkene	ppbV		-	-	-	-	-	-
Unknown	alkene	ppbV		-	-	-	-	-	-
Unknown	alkene	ppbV		-	-	-	-	282	-
Unknown	alkene	ppbV		-	4.18	-	-	-	-
Unknown	alkene	ppbV		-	-	-	-	-	-
Unknown	alkene	ppbV		-	-	-	-	233	-
Unknown	alkene	ppbV		-	-	-	-	-	-
Unknown	alkene	ppbV		-	-	-	-	-	-
Unknown	alkene	ppbV		9.21	-	7.34	-	-	17.4
Unknown	alkene	ppbV		-	-	-	-	-	-
Unknown	alkene	ppbV		-	-	-	-	-	-
Unknown	alkene	ppbV		-	-	-	-	280	-
Unknown	alkene	ppbV		-	-	-	-	-	4.2
Unknown	alkene	ppbV		-	-	-	-	-	-
Unknown	alkene	ppbV		-	-	-	223	266	-
Unknown	alkene	ppbV		-	-	-	194	-	-
unknown alkane	alkene	ppbV		-	3.76	-	-	-	-
unknown alkene	alkene	ppbV		-	-	-	-	-	4.43
unknown alkene	alkene	ppbV		-	-	-	-	-	-
Unknown	aromatic	ppbV		-	-	-	-	-	-
Unknown	aromatic	ppbV		-	-	-	224	-	-
Hexane, 2,3-dimethyl-	branched alkane	ppbV		-	-	-	-	-	10.4
Unknown	branched alkane	ppbV		-	-	-	-	-	-
Unknown	branched alkane	ppbV		-	-	-	-	-	-
Unknown	branched alkane	ppbV		-	-	-	-	-	-
Unknown	branched alkane	ppbV		-	-	-	-	-	-
unknown alkane	branched alkane	ppbV		5.26	-	-	-	-	-
unknown alkane	branched alkane	ppbV		-	-	-	-	-	-
unknown alkane	branched alkane	ppbV		-	-	-	-	-	-
Cyclohexane, 1,1,3-trimethyl-	cycloalkane	ppbV		-	-	-	296	335	-
Unknown	cycloalkane	ppbV		-	-	8.88	-	-	-
Unknown	cycloalkane	ppbV		-	-	8.34	-	-	-
Unknown	cycloalkane	ppbV		-	-	-	313	397	-
Unknown	cycloalkane	ppbV		-	-	-	-	-	-
Unknown	cycloalkane	ppbV		-	-	-	-	-	-
Unknown	cycloalkane	ppbV		-	-	-	218	256	-
Unknown	cycloalkane	ppbV		-	-	-	255	-	-
Unknown	cycloalkane	ppbV		-	-	11.6	-	-	-
Unknown	cycloalkane	ppbV		-	-	7.65	-	-	-
Unknown	cycloalkane	ppbV		-	-	-	238	-	-
Unknown	cycloalkane	ppbV		-	-	-	-	-	-
unknown alkane	cycloalkane	ppbV		-	-	-	232	-	-
unknown cycloalkane	cycloalkane	ppbV		-	-	-	-	268	-
unknown cycloalkane	cycloalkane	ppbV		-	-	-	476	-	-
unknown cycloalkane	cycloalkane	ppbV		-	-	-	-	565	-
unknown cycloalkane	cycloalkane	ppbV		-	-	-	-	-	-
Furan, tetrahydro-	furan	ppbV		2.98	-	-	-	-	-
2-Butanone	ketone	ppbV		-	-	-	-	-	-
Acetone	ketone	ppbV		-	-	-	-	-	5.55
Cyclohexanone	ketone	ppbV		-	-	-	-	-	-
Cyclopentanone	ketone	ppbV		-	-	-	-	-	5.53
Unknown	ketone	ppbV		-	-	-	-	-	-
Unknown	ketone	ppbV		-	-	-	-	-	-
Unknown	ketone	ppbV		-	6.24	-	-	-	-
Unknown	ketone	ppbV		-	-	-	-	-	-
Unknown	ketone cycloalkane	ppbV		3.11	-	-	-	-	-
Unknown	ketone cycloalkane	ppbV		-	2.95	-	-	-	-
Unknown	ketone cycloalkane	ppbV		-	-	7.13	-	-	-
Unknown	naphthalene	ppbV		3.77	7.54	20.4	217	239	-
Unknown	other	ppbV		-	-	-	-	-	-
Unknown	other	ppbV		-	-	-	-	-	-
Unknown	other	ppbV		-	-	-	-	-	-
Unknown	other	ppbV		3.01	-	-	-	-	-
Unknown	other	ppbV		-	-	-	-	-	-
Unknown	other	ppbV		-	-	-	-	-	-
Unknown	other	ppbV		-	-	-	-	-	-
Unknown	other	ppbV		-	-	-	-	-	-
Unknown	other	ppbV		-	-	-	-	-	-
Unknown	other	ppbV		-	-	-	-	-	-
Unknown	other	ppbV		-	-	-	-	-	-
Unknown	other	ppbV		-	-	-	-	-	-
Unknown	other	ppbV		-	-	-	-	-	-
Cyclotrisiloxane, Hexamethyl-	siloxane	ppbV		13.7	7.95	7.4	-	-	16.5
Silanol, Trimethyl-	siloxane	ppbV		17.1	-	-	-	-	8.16
Unknown	siloxane	ppbV		-	6.48	-	-	-	-
unknown siloxane	siloxane	ppbV		-	4.05	-	-	-	-
unknown siloxane	siloxane	ppbV		20.6	-	-	-	-	-
unknown siloxane	siloxane	ppbV		-	-	-	-	-	8.65
unknown siloxane	siloxane	ppbV		-	-	-	-	-	-
unknown siloxane	siloxane	ppbV		-	-	-	-	-	-
unknown siloxane	siloxane	ppbV		-	-	-	-	-	5.24

1. Samples collected by GSI and analyzed by Alpha Analytical.
2. Less than ("<") indicates the analyte was not found at the stated detection limit. J = estimated result between method detection limit and reporting limit.
   D = result from a dilution.

GSI ENVIRONMENTAL

ATTACHMENT B.3.4: SOIL VAPOR AND GROUNDWATER MONITORING WELL HEADSPACE SAMPLE ANALYTICAL RESULTS
Red Hill Bulk Fuel Storage Facility, Joint Base Pearl Harbor-Hickam, O'ahu, Hawai'i

			Sample ID:	RHSV07DERH464	RHSV08SERH463	RHSV09SERH462	RHSV10SERH461	RHSV11MERH460	RHSV12MERH458
			Lab Sample ID:	L1740493-07	L1740493-08	L1740493-09	L1740493-10	L1740493-11	L1740493-12
			Sample Date/Time:	2017-10-31 14:25	2017-10-31 13:44	2017-10-31 13:10	2017-10-31 11:36	2017-10-30 10:56	2017-10-27 14:11
			Matrix:	SOIL_VAPOR	SOIL_VAPOR	SOIL_VAPOR	SOIL_VAPOR	SOIL_VAPOR	SOIL_VAPOR
FIXED GASES BY USEPA METHOD 3C									
Analyte		**Units**							
Carbon Dioxide		%		3.94D	0.79D	0.495D	0.559D	1.09D	0.312D
Methane		%		<0.061D	<0.062D	<0.061D	<0.062D	<0.061D	<0.039D
Oxygen		%		13.4D	20.8D	21D	20.7D	20.4D	12.5D
VOCs BY USEPA METHOD TO-15 (TARGET ANALYTES)									
Analyte	**Class**	**Units**							
Decane (C10)	alkane	ppbV		0.516	0.365	0.437	0.438	1.05	0.97
Dodecane (C12)	alkane	ppbV		0.54	0.485	0.686	0.641	0.752	0.908
Heptane	alkane	ppbV		0.027	0.035	0.063	0.06	0.234	0.077
n-Hexane	alkane	ppbV		0.043	0.065	0.101	0.071	0.162	0.055
Nonane (C9)	alkane	ppbV		0.185	0.132	0.134	0.169	1.06	0.437
Octane	alkane	ppbV		0.071	0.07	0.089	0.119	0.42	0.211
Pentane	alkane	ppbV		1.3	1.55	2.14	2.55	3.36	0.29
Tridecane	alkane	ppbV		0.302 J	0.281 J	0.363 J	0.369 J	0.282 J	0.526 J
Undecane	alkane	ppbV		0.516	0.428	0.395	0.463	0.463	0.732
1,3-Butadiene	alkene	ppbV		<0.01	<0.01	<0.01	<0.01	<0.01	<0.01
1-Decene	alkene	ppbV		<0.025	<0.025	<0.025	<0.025	<0.025	<0.025
1-Heptene	alkene	ppbV		<0.01	<0.01	<0.01	<0.01	<0.01	<0.01
1-Hexene	alkene	ppbV		<0.01	<0.01	<0.01	<0.01	<0.01	<0.01
1-Nonene	alkene	ppbV		<0.01	<0.01	<0.01	<0.01	<0.01	<0.01
1-Octene	alkene	ppbV		<0.01	<0.01	0.017 J	0.024 J	<0.01	<0.01
1-Pentene	alkene	ppbV		0.025	0.033	0.046	0.048	0.073	0.012 J
2-Methyl-1-Butene	alkene	ppbV		0.013 J	0.02 J	0.027	0.023 J	0.07	<0.01
cis-2-Pentene	alkene	ppbV		<0.01	<0.01	<0.01	<0.01	0.085	<0.01
trans-2-Pentene	alkene	ppbV		0.02 J	0.024 J	0.04	0.042	0.064	<0.01
2,2-Dimethylpentane	branched alkane	ppbV		<0.01	<0.01	<0.01	<0.01	<0.01	<0.01
2,3,3-Trimethylpentane	branched alkane	ppbV		0.026	0.034	0.055	0.058	0.17	0.047
2,3,4-Trimethylpentane	branched alkane	ppbV		0.023 J	0.01 J	0.02 J	0.02 J	0.142	0.017 J
2,3-Dimethylbutane	branched alkane	ppbV		<0.01	<0.01	0.026	<0.01	<0.01	0.018 J
2,3-Dimethylhexane	branched alkane	ppbV		<0.01	0.01 J	<0.01	<0.01	<0.01	<0.01
2,3-Dimethylpentane	branched alkane	ppbV		<0.01	<0.01	<0.01	<0.01	0.085	<0.01
2,4-Dimethylhexane/2,2,3-Trimethylpentar	branched alkane	ppbV		0.032 J	<0.025	0.029 J	0.04 J	0.15	<0.025
2,4-Dimethylpentane	branched alkane	ppbV		<0.01	<0.01	<0.01	<0.01	<0.01	<0.01
2,5-Dimethylhexane	branched alkane	ppbV		0.014 J	<0.01	0.012 J	0.013 J	0.062	0.013 J
2-Methylheptane	branched alkane	ppbV		0.02 J	0.018 J	0.022 J	<0.01	0.165	0.058
2-Methylhexane	branched alkane	ppbV		<0.01	0.015 J	0.029	<0.01	<0.01	0.029
2-Methylpentane	branched alkane	ppbV		0.139	0.196	0.238	0.323	0.438	0.104 B
3-Ethylhexane	branched alkane	ppbV		0.04	<0.01	<0.01	<0.01	0.096	<0.01
3-Methylheptane	branched alkane	ppbV		0.016 J	0.011 J	0.026	0.023 J	0.22	0.039
3-Methylhexane	branched alkane	ppbV		0.068	0.067	0.111	0.136	0.369	0.057
3-Methylpentane	branched alkane	ppbV		0.033	0.045	0.05	<0.01	0.098	0.031
Isooctane	branched alkane	ppbV		0.031	0.03	0.051	0.047	0.114	0.026
Isopentane	branched alkane	ppbV		<0.01	<0.01	<0.01	<0.01	<0.01	<0.01
1-Ethyl-1-Methylcyclopentane	cycloalkane	ppbV		0.032	<0.01	<0.01	<0.01	0.1	<0.01
Cyclohexane	cycloalkane	ppbV		0.103	0.062	0.068	0.082	0.387	0.039
Cyclopentane	cycloalkane	ppbV		0.228	0.047	0.048	<0.01	<0.01	<0.01
Methylcyclohexane	cycloalkane	ppbV		0.309	0.032	0.037	0.056	1.16	0.104
Methylcyclopentane	cycloalkane	ppbV		0.05	0.036	0.033	0.02 J	0.111	0.035
1,2,4,5-Tetramethylbenzene	aromatic	ppbV		<0.025	<0.025	<0.025	<0.025	<0.025	<0.025
1,2,4-Trimethylbenzene	aromatic	ppbV		0.245	0.219	0.234	0.301	0.51	0.437
1,2-Diethylbenzene	aromatic	ppbV		0.025 J	<0.025	<0.025	<0.025	0.076	<0.025
1,2-Dimethyl-3-Ethylbenzene	aromatic	ppbV		<0.025	<0.025	<0.025	<0.025	0.033 J	0.038 J
1,2-Dimethyl-4-Ethylbenzene	aromatic	ppbV		0.043 J	0.034 J	0.032 J	0.04 J	0.248	0.071
1,3,5-Trimethylbenzene	aromatic	ppbV		0.066	0.05	0.052	0.067	0.729	0.11
1,3-Dimethyl-2-Ethylbenzene	aromatic	ppbV		<0.025	<0.025	<0.025	<0.025	0.028 J	<0.025
1,3-Dimethyl-4-Ethylbenzene	aromatic	ppbV		0.045 J	0.034 J	0.032 J	0.041 J	0.071	0.07
1,3-Dimethyl-5-Ethylbenzene	aromatic	ppbV		0.061	0.04 J	0.037 J	0.048 J	0.105	0.079
1,4-Dimethyl-2-Ethylbenzene	aromatic	ppbV		0.035 J	0.027 J	0.026 J	0.033 J	0.057	0.058
1-Methyl-2-Ethylbenzene	aromatic	ppbV		0.056	0.048 J	0.053	0.066	0.468	0.114
1-Methyl-2-Isopropylbenzene	aromatic	ppbV		<0.025	<0.025	<0.025	<0.025	0.052	<0.025
1-Methyl-2-N-Propylbenzene	aromatic	ppbV		0.041 J	0.031 J	0.032 J	0.037 J	0.158	0.071
1-Methyl-3-Ethylbenzene	aromatic	ppbV		0.094	0.083	0.091	0.114	0.289	0.198
1-Methyl-3-Isopropylbenzene	aromatic	ppbV		<0.025	<0.025	<0.025	0.027 J	0.178	0.051
1-Methyl-3-N-Propylbenzene	aromatic	ppbV		0.066	0.054	0.05	0.063	0.129	0.096
1-Methyl-4-Ethylbenzene	aromatic	ppbV		0.052	0.043	0.046	0.058	0.136	0.106
1-Methyl-4-Isopropylbenzene	aromatic	ppbV		0.026 J	<0.025	<0.025	0.027 J	0.09	0.044 J
1-Methyl-4-N-Propylbenzene	aromatic	ppbV		0.032 J	<0.025	<0.025	0.027 J	0.042 J	0.043 J
Benzene	aromatic	ppbV		0.076	0.34	0.304	0.062	0.09	0.053
Ethylbenzene	aromatic	ppbV		0.073	0.067	0.087	0.094	0.254	0.134
Indane	aromatic	ppbV		0.031 J	0.03 J	0.026 J	0.033 J	0.065	0.046 J
Indene	aromatic	ppbV		<0.025	<0.025	<0.025	<0.025	<0.025	<0.025
Isopropylbenzene	aromatic	ppbV		0.068	0.233	0.323	0.024 J	0.105	0.044
n-Butylbenzene	aromatic	ppbV		<0.025	<0.025	<0.025	<0.025	<0.025	0.041 J
N-Pentylbenzene	aromatic	ppbV		<0.025	<0.025	<0.025	<0.025	<0.025	<0.025
n-Propylbenzene	aromatic	ppbV		0.04	0.031	0.035	0.043	0.109	0.079
o-Xylene	aromatic	ppbV		0.699	0.681	0.847	1.1	2.82	0.411
p/m-Xylene	aromatic	ppbV		0.293	0.289	0.365	0.407	0.88	0.578
sec-Butylbenzene	aromatic	ppbV		<0.025	<0.025	<0.025	<0.025	0.08	0.034 J
Styrene	aromatic	ppbV		0.015 J	0.015 J	0.035	0.023 J	<0.01	0.026
Toluene	aromatic	ppbV		0.15	0.17	0.369	0.263	0.562	0.285
1-Methylnaphthalene	naphthalene	ppbV		0.052 J	<0.05	<0.05	<0.05	<0.05	0.061 J
2-Methylnaphthalene	naphthalene	ppbV		0.104 J	0.071 J	0.051 J	0.075 J	0.064 J	0.115 J
Naphthalene	naphthalene	ppbV		0.17	0.106	0.097	0.116	0.16	0.144 B
Tertiary Butanol	alcohol	ppbV		3.47	3.53	10.4	10.7	33.9	2.73
Ethyl-Tert-Butyl-Ether	ether	ppbV		0.678	0.739	1.35	1.91	3.44	0.297
Isopropyl Ether	ether	ppbV		<0.01	<0.01	<0.01	<0.01	<0.01	<0.01
Methyl tert butyl ether	ether	ppbV		0.092	0.083	0.144	0.193	0.335	0.032
Tertiary-Amyl Methyl Ether	ether	ppbV		<0.01	<0.01	0.048	0.069	0.141	<0.01
2-Ethylthiophene	thiophene	ppbV		<0.01	<0.01	<0.01	<0.01	<0.01	<0.01
2-Methylthiophene	thiophene	ppbV		<0.01	<0.01	<0.01	<0.01	<0.01	<0.01
3-Methylthiophene	thiophene	ppbV		<0.01	<0.01	<0.01	<0.01	<0.01	<0.01
Benzothiophene	thiophene	ppbV		<0.05	<0.05	<0.05	<0.05	<0.05	<0.05
Thiophene	thiophene	ppbV		<0.01	<0.01	<0.01	<0.01	<0.01	<0.01
1,2-Dibromoethane	other	ppbV		<0.01	<0.01	<0.01	<0.01	<0.01	<0.01
1,2-Dichloroethane	other	ppbV		<0.01	0.087	<0.01	<0.01	<0.01	<0.01
MMT	other	ppbV		<0.05	<0.05	<0.05	<0.05	<0.05	<0.05

ATTACHMENT B.3.4: SOIL VAPOR AND GROUNDWATER MONITORING WELL HEADSPACE SAMPLE ANALYTICAL RESULTS
Red Hill Bulk Fuel Storage Facility, Joint Base Pearl Harbor-Hickam, O'ahu, Hawai'i

			Sample ID:	RHSV07DERH464	RHSV08SERH463	RHSV09SERH462	RHSV10SERH461	RHSV11MERH460	RHSV12MERH458
			Lab Sample ID:	L1740493-07	L1740493-08	L1740493-09	L1740493-10	L1740493-11	L1740493-12
			Sample Date/Time:	2017-10-31 14:25	2017-10-31 13:44	2017-10-31 13:10	2017-10-31 11:36	2017-10-30 10:56	2017-10-27 14:11
			Matrix:	SOIL_VAPOR	SOIL_VAPOR	SOIL_VAPOR	SOIL_VAPOR	SOIL_VAPOR	SOIL_VAPOR
VOCs BY USEPA METHOD TO-15 (TENTATIVELY IDENTIFIED COMPOUNDS)									
1-Butanol	alcohol	ppbV		-	1.12	-	-	-	-
1-Hexanol, 2-ethyl-	alcohol	ppbV		-	17.7	17	-	-	11.8
Amylene Hydrate	alcohol	ppbV		-	-	-	2.99	7.73	-
Methyl Alcohol	alcohol	ppbV		-	2.6	2.74	-	-	-
Unknown	alcohol	ppbV		-	-	-	-	-	-
Unknown	alcohol	ppbV		3.44	-	-	-	-	-
Unknown	alcohol	ppbV		-	-	-	-	-	-
Unknown	alcohol	ppbV		-	-	-	-	-	-
unknown alcohol	alcohol	ppbV		-	-	3.25	-	-	-
unknown alcohol	alcohol	ppbV		-	-	-	-	-	-
Unknown	alcohol cycloalkane	ppbV		3.98	-	-	-	-	-
Propane	alkane	ppbV		-	-	-	-	-	-
Unknown	alkane	ppbV		-	-	-	-	-	-
Unknown	alkane	ppbV		-	-	-	-	-	-
unknown alkane	alkane	ppbV		-	-	-	-	-	-
unknown alkane	alkane	ppbV		-	-	-	-	-	-
1-Pentene, 2-methyl-	alkene	ppbV		-	-	-	2.95	-	-
2,4-Dimethyl-1-heptene	alkene	ppbV		-	5.82	-	-	-	-
Unknown	alkene	ppbV		-	-	-	-	-	-
Unknown	alkene	ppbV		6.69	-	-	-	-	-
Unknown	alkene	ppbV		-	-	-	-	-	-
Unknown	alkene	ppbV		-	-	2.95	4.47	-	-
Unknown	alkene	ppbV		-	-	-	-	9.32	-
Unknown	alkene	ppbV		-	-	-	-	-	-
Unknown	alkene	ppbV		-	-	-	-	-	-
Unknown	alkene	ppbV		-	-	-	-	-	-
Unknown	alkene	ppbV		5.84	-	7.76	12	34.1	6.27
Unknown	alkene	ppbV		-	-	-	-	-	-
Unknown	alkene	ppbV		-	-	-	-	-	-
Unknown	alkene	ppbV		-	-	-	-	-	-
Unknown	alkene	ppbV		-	-	-	-	-	-
Unknown	alkene	ppbV		-	1.9	-	-	-	-
Unknown	alkene	ppbV		-	-	-	-	-	-
Unknown	alkene	ppbV		-	-	-	-	-	-
unknown alkane	alkene	ppbV		-	-	-	-	-	-
unknown alkene	alkene	ppbV		-	-	-	-	-	-
unknown alkene	alkene	ppbV		-	-	-	-	-	-
Unknown	aromatic	ppbV		-	-	-	-	-	-
Unknown	aromatic	ppbV		-	-	-	-	-	-
Hexane, 2,3-dimethyl-	branched alkane	ppbV		-	-	-	-	17.4	-
Unknown	branched alkane	ppbV		-	-	-	-	-	-
Unknown	branched alkane	ppbV		-	-	-	-	-	-
Unknown	branched alkane	ppbV		-	-	4.44	-	-	-
Unknown	branched alkane	ppbV		-	-	-	-	-	-
unknown alkane	branched alkane	ppbV		-	3.33	-	-	-	3.29
unknown alkane	branched alkane	ppbV		-	-	-	-	-	-
unknown alkane	branched alkane	ppbV		-	-	-	7.27	-	-
Cyclohexane, 1,1,3-trimethyl-	cycloalkane	ppbV		-	-	-	-	8.03	-
Unknown	cycloalkane	ppbV		-	-	-	-	-	-
Unknown	cycloalkane	ppbV		3.53	-	-	-	-	-
Unknown	cycloalkane	ppbV		-	-	-	-	-	-
Unknown	cycloalkane	ppbV		-	-	-	-	-	2
Unknown	cycloalkane	ppbV		-	-	-	-	-	-
Unknown	cycloalkane	ppbV		-	-	-	-	-	-
Unknown	cycloalkane	ppbV		-	-	-	-	-	-
Unknown	cycloalkane	ppbV		-	-	-	-	-	-
Unknown	cycloalkane	ppbV		-	-	-	-	-	-
Unknown	cycloalkane	ppbV		-	-	-	-	-	-
Unknown	cycloalkane	ppbV		3.57	-	-	-	-	-
unknown alkane	cycloalkane	ppbV		-	-	-	-	-	-
unknown cycloalkane	cycloalkane	ppbV		-	-	-	-	-	-
unknown cycloalkane	cycloalkane	ppbV		-	-	-	-	-	-
unknown cycloalkane	cycloalkane	ppbV		-	-	-	-	-	-
unknown cycloalkane	cycloalkane	ppbV		-	-	-	-	12.8	-
Furan, tetrahydro-	furan	ppbV		-	-	-	-	-	1.56
2-Butanone	ketone	ppbV		-	-	-	2.13	-	-
Acetone	ketone	ppbV		3.21	2.92	4.68	5.51	12.1	2.7
Cyclohexanone	ketone	ppbV		-	-	-	-	-	-
Cyclopentanone	ketone	ppbV		-	-	-	-	-	9.1
Unknown	ketone	ppbV		-	-	-	-	-	2.21
Unknown	ketone	ppbV		-	-	-	-	-	-
Unknown	ketone	ppbV		-	-	-	-	-	-
Unknown	ketone	ppbV		-	1.48	-	-	-	-
Unknown	ketone cycloalkane	ppbV		-	-	-	-	-	-
Unknown	ketone cycloalkane	ppbV		-	-	-	-	-	-
Unknown	ketone cycloalkane	ppbV		-	-	-	-	-	-
Unknown	naphthalene	ppbV		-	-	-	-	-	-
Unknown	other	ppbV		-	-	-	-	-	-
Unknown	other	ppbV		-	-	-	-	-	-
Unknown	other	ppbV		4.48	-	-	-	-	-
Unknown	other	ppbV		-	-	-	-	-	-
Unknown	other	ppbV		-	-	-	-	-	-
Unknown	other	ppbV		-	-	-	-	-	-
Unknown	other	ppbV		-	-	-	-	-	-
Unknown	other	ppbV		-	-	-	-	-	-
Unknown	other	ppbV		-	-	-	-	-	-
Unknown	other	ppbV		-	-	-	-	-	-
Unknown	other	ppbV		-	-	-	-	-	-
Unknown	other	ppbV		-	-	-	-	-	-
Unknown	other	ppbV		-	-	-	-	-	-
Cyclotrisiloxane, Hexamethyl-	siloxane	ppbV		12.4	7.29	16.2	18.5	17.6	6.4
Silanol, Trimethyl-	siloxane	ppbV		14.3	-	-	3.08	29.6	-
Unknown	siloxane	ppbV		-	-	-	-	-	-
unknown siloxane	siloxane	ppbV		-	-	-	-	-	-
unknown siloxane	siloxane	ppbV		-	1.29	10.8	-	-	2.25
unknown siloxane	siloxane	ppbV		-	-	-	-	7.7	-
unknown siloxane	siloxane	ppbV		-	-	7.93	-	-	-
unknown siloxane	siloxane	ppbV		-	-	-	3.8	-	-
unknown siloxane	siloxane	ppbV		-	-	-	-	-	-

1. Samples collected by GSI and analyzed by Alpha Analytical.
2. Less than ("<") indicates the analyte was not found at the stated detection limit. J = estimated result between method detection limit and reporting limit.
D = result from a dilution.

ATTACHMENT C.3.4: SOIL VAPOR AND GROUNDWATER MONITORING WELL HEADSPACE SAMPLE ANALYTICAL RESULTS
Red Hill Bulk Fuel Storage Facility, Joint Base Pearl Harbor-Hickam, O'ahu, Hawai'i

			Sample ID:	RHSV13SERH457	RHSV14DERH456	RHSV15SERH455	RHSV16DERH454	RHSV18SERH453	RHSV20DERH465
			Lab Sample ID:	L1740493-13	L1740493-14	L1740493-15	L1740493-16	L1740493-17	L1740493-18
			Sample Date/Time:	2017-10-27 13:29	2017-10-27 12:48	2017-10-27 11:24	2017-10-27 10:46	2017-10-27 10:00	2017-10-30 15:08
			Matrix:	SOIL_VAPOR	SOIL_VAPOR	SOIL_VAPOR	SOIL_VAPOR	SOIL_VAPOR	SOIL_VAPOR
FIXED GASES BY USEPA METHOD 3C									
Analyte		**Units**							
Carbon Dioxide		%		0.951D	0.404D	0.428D	1.39D	0.368D	0.17 JD
Methane		%		<0.061D	<0.075D	<0.061D	<0.061D	<0.062D	<0.063D
Oxygen		%		20.1D	7.81D	20.6D	19.7D	21.1D	21.2D
VOCs BY USEPA METHOD TO-15 (TARGET ANALYTES)									
Analyte	**Class**	**Units**							
Decane (C10)	alkane	ppbV		0.855	1.14	0.331	0.559	2.88	4.98
Dodecane (C12)	alkane	ppbV		1.22	1.11	0.511	0.725	2.09	4.79
Heptane	alkane	ppbV		0.101	0.099	0.096	0.047	0.174	0.072
n-Hexane	alkane	ppbV		0.074	0.066	0.131	0.044	0.155	0.061
Nonane (C9)	alkane	ppbV		0.49	0.577	0.137	0.214	1.04	1.73
Octane	alkane	ppbV		0.253	0.272	0.142	0.106	0.406	0.362
Pentane	alkane	ppbV		0.787	0.769	0.746	0.552	2.03	1.43
Tridecane	alkane	ppbV		1.62	0.132 J	0.208 J	0.31 J	1.08	2.29
Undecane	alkane	ppbV		1	0.861	0.372	0.611	3.03	7.98
1,3-Butadiene	alkene	ppbV		<0.01	<0.01	<0.01	<0.01	<0.01	<0.01
1-Decene	alkene	ppbV		<0.025	<0.025	<0.025	<0.025	<0.025	<0.025
1-Heptene	alkene	ppbV		<0.01	<0.01	<0.01	<0.01	<0.01	<0.01
1-Hexene	alkene	ppbV		<0.01	<0.01	<0.01	<0.01	0.192	<0.01
1-Nonene	alkene	ppbV		<0.01	<0.01	<0.01	<0.01	<0.01	<0.01
1-Octene	alkene	ppbV		<0.01	<0.01	<0.01	0.043	<0.01	<0.01
1-Pentene	alkene	ppbV		0.014 J	0.019 J	0.017 J	0.013 J	0.052	0.026
2-Methyl-1-Butene	alkene	ppbV		0.025	0.018 J	0.01 J	<0.01	0.051	0.015 J
cis-2-Pentene	alkene	ppbV		<0.01	<0.01	<0.01	<0.01	<0.01	<0.01
trans-2-Pentene	alkene	ppbV		0.012 J	0.015 J	0.012 J	0.01 J	0.041	0.022 J
2,2-Dimethylpentane	branched alkane	ppbV		<0.01	<0.01	<0.01	<0.01	<0.01	<0.01
2,3,3-Trimethylpentane	branched alkane	ppbV		0.073	0.08	0.052	0.084	0.259	0.054
2,3,4-Trimethylpentane	branched alkane	ppbV		0.02 J	0.027	0.019 J	0.018 J	0.05	0.015 J
2,3-Dimethylbutane	branched alkane	ppbV		0.028	<0.01	<0.01	<0.01	0.052	<0.01
2,3-Dimethylhexane	branched alkane	ppbV		<0.01	<0.01	<0.01	<0.01	<0.01	0.018 J
2,3-Dimethylpentane	branched alkane	ppbV		<0.01	<0.01	<0.01	<0.01	<0.01	<0.01
2,4-Dimethylhexane/2,2,3-Trimethylpentar	branched alkane	ppbV		0.038 JB	0.045 JB	0.03 JB	0.03 JB	0.077 B	<0.025
2,4-Dimethylpentane	branched alkane	ppbV		<0.01	<0.01	<0.01	<0.01	<0.01	<0.01
2,5-Dimethylhexane	branched alkane	ppbV		0.021 J	<0.01	0.012 J	0.012 J	0.035	0.011 J
2-Methylheptane	branched alkane	ppbV		0.077	0.075	0.025	<0.01	0.1	0.068
2-Methylhexane	branched alkane	ppbV		0.044	0.036	0.027	<0.01	0.045	0.022 J
2-Methylpentane	branched alkane	ppbV		0.212	<0.01	0.178	0.196	0.39	0.251
3-Ethylhexane	branched alkane	ppbV		<0.01	<0.01	<0.01	<0.01	<0.01	<0.01
3-Methylheptane	branched alkane	ppbV		0.057	0.062	0.023 J	0.02 J	0.078	0.049
3-Methylhexane	branched alkane	ppbV		0.096	0.086	0.06	0.06	0.166	0.092
3-Methylpentane	branched alkane	ppbV		0.036	0.035	0.045	0.019 J	0.061	0.062
Isooctane	branched alkane	ppbV		0.027	0.038	0.028	0.022 J	0.057	0.032
Isopentane	branched alkane	ppbV		<0.01	<0.01	0.142	0.206	0.47	0.453
1-Ethyl-1-Methylcyclopentane	cycloalkane	ppbV		<0.01	<0.01	<0.01	<0.01	<0.01	<0.01
Cyclohexane	cycloalkane	ppbV		0.058	0.063	0.036	0.024 J	0.096	0.107
Cyclopentane	cycloalkane	ppbV		<0.01	<0.01	<0.01	<0.01	<0.01	<0.01
Methylcyclohexane	cycloalkane	ppbV		0.14	0.176	0.054	0.035	0.192	0.137
Methylcyclopentane	cycloalkane	ppbV		0.046	0.038	0.025	<0.01	0.089	0.057
1,2,4,5-Tetramethylbenzene	aromatic	ppbV		<0.025	<0.025	<0.025	<0.025	0.122	0.046 J
1,2,4-Trimethylbenzene	aromatic	ppbV		0.747	0.624	0.202	0.3	2	2.12
1,2-Diethylbenzene	aromatic	ppbV		0.033 J	0.03 J	<0.025	<0.025	0.205	0.099
1,2-Dimethyl-3-Ethylbenzene	aromatic	ppbV		0.073	0.054	0.027 J	0.048 J	0.503	0.237
1,2-Dimethyl-4-Ethylbenzene	aromatic	ppbV		0.137	0.089	0.039 J	0.07	0.854	0.305
1,3,5-Trimethylbenzene	aromatic	ppbV		0.194	0.173	0.047	0.073	0.626	0.46
1,3-Dimethyl-2-Ethylbenzene	aromatic	ppbV		0.025 J	<0.025	<0.025	<0.025	0.146	0.059
1,3-Dimethyl-4-Ethylbenzene	aromatic	ppbV		0.133	0.095	0.034 J	0.065	0.587	0.407
1,3-Dimethyl-5-Ethylbenzene	aromatic	ppbV		0.147	0.094	0.039 J	0.076	0.601	0.417
1,4-Dimethyl-2-Ethylbenzene	aromatic	ppbV		0.107	0.077	0.028 J	0.052	0.469	0.292
1-Methyl-2-Ethylbenzene	aromatic	ppbV		0.191	0.201	0.042 J	0.076	0.556	0.605
1-Methyl-2-Isopropylbenzene	aromatic	ppbV		<0.025	<0.025	<0.025	<0.025	0.072	0.03 J
1-Methyl-2-N-Propylbenzene	aromatic	ppbV		0.112	0.099	0.031 J	0.061	0.608	0.424
1-Methyl-3-Ethylbenzene	aromatic	ppbV		0.358	0.284	0.07	0.116	0.8	1.11
1-Methyl-3-Isopropylbenzene	aromatic	ppbV		0.07	0.066	<0.025	0.03 J	0.239	0.244
1-Methyl-3-N-Propylbenzene	aromatic	ppbV		0.163	0.117	0.042 J	0.071	0.491	0.613
1-Methyl-4-Ethylbenzene	aromatic	ppbV		0.189	0.146	0.038	0.063	0.419	0.681
1-Methyl-4-Isopropylbenzene	aromatic	ppbV		0.059	0.065	0.025 J	0.033 J	0.189	0.228
1-Methyl-4-N-Propylbenzene	aromatic	ppbV		0.071	0.057	<0.025	0.031 J	0.206	0.351
Benzene	aromatic	ppbV		0.084	0.06	0.072	0.042	0.122	0.054
Ethylbenzene	aromatic	ppbV		0.21	0.192	0.064	0.088	0.465	0.533
Indane	aromatic	ppbV		0.107	0.06	<0.025	0.045 J	0.195	0.223
Indene	aromatic	ppbV		<0.025	<0.025	<0.025	<0.025	<0.025	<0.025
Isopropylbenzene	aromatic	ppbV		0.074	0.055	0.076	0.024 J	0.171	0.158
n-Butylbenzene	aromatic	ppbV		0.064	0.044 J	<0.025	0.027 J	0.168	0.346
N-Pentylbenzene	aromatic	ppbV		0.06	<0.025	<0.025	<0.025	0.129	0.114
n-Propylbenzene	aromatic	ppbV		0.122	0.112	0.028	0.048	0.307	0.506
o-Xylene	aromatic	ppbV		0.565	0.563	0.331	0.348	1.32	1.44
p/m-Xylene	aromatic	ppbV		0.921	0.72	0.259	0.362	1.94	2.2
sec-Butylbenzene	aromatic	ppbV		0.039 J	0.047 J	<0.025	<0.025	0.11	0.154
Styrene	aromatic	ppbV		0.034	0.074	0.023 J	0.023 J	0.115	0.026
Toluene	aromatic	ppbV		0.247	0.337	0.202	0.134	0.708	0.525
1-Methylnaphthalene	naphthalene	ppbV		0.291 J	<0.05	<0.05	<0.05	0.16 J	0.126 J
2-Methylnaphthalene	naphthalene	ppbV		0.491 J	<0.05	0.064 J	0.076 J	0.289 J	0.226 J
Naphthalene	naphthalene	ppbV		0.201 B	0.148 B	0.113 B	0.135 B	0.384	0.328
Tertiary Butanol	alcohol	ppbV		3	5.18	2	2.72	6.99	3.41
Ethyl-Tert-Butyl-Ether	ether	ppbV		0.622	0.632	0.45	0.467	1.37	0.683
Isopropyl Ether	ether	ppbV		<0.01	<0.01	<0.01	<0.01	<0.01	<0.01
Methyl tert butyl ether	ether	ppbV		0.071	0.072	0.045	0.047	0.165	0.084
Tertiary-Amyl Methyl Ether	ether	ppbV		<0.01	<0.01	<0.01	<0.01	0.052	<0.01
2-Ethylthiophene	thiophene	ppbV		<0.01	<0.01	<0.01	<0.01	<0.01	<0.01
2-Methylthiophene	thiophene	ppbV		<0.01	<0.01	<0.01	<0.01	<0.01	<0.01
3-Methylthiophene	thiophene	ppbV		<0.01	<0.01	<0.01	<0.01	<0.01	<0.01
Benzothiophene	thiophene	ppbV		<0.05	<0.05	<0.05	<0.05	<0.05	<0.05
Thiophene	thiophene	ppbV		<0.01	<0.01	<0.01	<0.01	0.019 J	<0.01
1,2-Dibromoethane	other	ppbV		<0.01	<0.01	<0.01	<0.01	<0.01	<0.01
1,2-Dichloroethane	other	ppbV		<0.01	<0.01	<0.01	<0.01	0.12	<0.01
MMT	other	ppbV		<0.05	<0.05	<0.05	<0.05	<0.05	<0.05

ATTACHMENT B.3.4: SOIL VAPOR AND GROUNDWATER MONITORING WELL HEADSPACE SAMPLE ANALYTICAL RESULTS
Red Hill Bulk Fuel Storage Facility, Joint Base Pearl Harbor-Hickam, O'ahu, Hawai'i

			Sample ID:	RHSV13SERH457	RHSV14DERH456	RHSV15SERH455	RHSV16DERH454	RHSV18SERH453	RHSV20DERH465
			Lab Sample ID:	L1740493-13	L1740493-14	L1740493-15	L1740493-16	L1740493-17	L1740493-18
			Sample Date/Time:	2017-10-27 13:29	2017-10-27 12:48	2017-10-27 11:24	2017-10-27 10:46	2017-10-27 10:00	2017-10-30 15:08
			Matrix:	SOIL_VAPOR	SOIL_VAPOR	SOIL_VAPOR	SOIL_VAPOR	SOIL_VAPOR	SOIL_VAPOR
VOCs BY USEPA METHOD TO-15 (TENTATIVELY IDENTIFIED COMPOUNDS)									
1-Butanol	alcohol	ppbV		-	-	-	-	-	-
1-Hexanol, 2-ethyl-	alcohol	ppbV		10.2	-	17.2	-	-	-
Amylene Hydrate	alcohol	ppbV		-	2.49	-	1.69	-	1.87
Methyl Alcohol	alcohol	ppbV		3.23	-	-	2.16	-	-
Unknown	alcohol	ppbV		-	-	-	-	-	-
Unknown	alcohol	ppbV		-	-	-	-	-	-
Unknown	alcohol	ppbV		-	12	-	-	16.5	3.01
Unknown	alcohol	ppbV		-	-	-	-	-	-
unknown alcohol	alcohol	ppbV		-	-	-	-	-	-
unknown alcohol	alcohol	ppbV		-	-	-	-	-	-
Unknown	alcohol cycloalkane	ppbV		-	-	-	-	-	-
Propane	alkane	ppbV		-	2.26	-	-	-	-
Unknown	alkane	ppbV		-	-	-	1.93	5.14	-
Unknown	alkane	ppbV		-	-	-	-	-	-
unknown alkane	alkane	ppbV		-	2.04	-	-	-	-
unknown alkane	alkane	ppbV		2.04	-	-	-	-	-
1-Pentene, 2-methyl-	alkene	ppbV		-	-	-	-	-	-
2,4-Dimethyl-1-heptene	alkene	ppbV		-	-	-	-	-	-
Unknown	alkene	ppbV		-	-	-	-	-	1.39
Unknown	alkene	ppbV		-	-	-	-	-	-
Unknown	alkene	ppbV		-	-	-	-	-	-
Unknown	alkene	ppbV		-	-	-	-	-	-
Unknown	alkene	ppbV		-	-	3.04	-	-	-
Unknown	alkene	ppbV		-	-	-	-	-	-
Unknown	alkene	ppbV		-	-	-	-	8.16	-
Unknown	alkene	ppbV		-	-	3.56	-	-	-
Unknown	alkene	ppbV		8.02	-	12.7	-	-	-
Unknown	alkene	ppbV		-	-	-	-	12.3	-
Unknown	alkene	ppbV		-	-	-	-	-	-
Unknown	alkene	ppbV		-	-	-	-	-	-
Unknown	alkene	ppbV		-	-	-	-	-	-
Unknown	alkene	ppbV		-	-	-	-	-	-
Unknown	alkene	ppbV		-	-	-	-	-	-
Unknown	alkene	ppbV		-	-	-	-	-	-
unknown alkane	alkene	ppbV		-	-	-	-	-	-
unknown alkene	alkene	ppbV		-	-	-	-	-	-
unknown alkene	alkene	ppbV		-	6.15	-	5.99	-	3.7
Unknown	aromatic	ppbV		1.64	-	-	-	-	-
Unknown	aromatic	ppbV		-	-	-	-	-	-
Hexane, 2,3-dimethyl-	branched alkane	ppbV		-	-	-	-	-	-
Unknown	branched alkane	ppbV		-	-	-	-	7.35	-
Unknown	branched alkane	ppbV		-	-	-	-	-	1.54
Unknown	branched alkane	ppbV		-	-	-	-	-	-
Unknown	branched alkane	ppbV		-	-	-	2.09	-	1.76
unknown alkane	branched alkane	ppbV		4.69	-	6.68	-	-	-
unknown alkane	branched alkane	ppbV		-	-	-	-	14.7	-
unknown alkane	branched alkane	ppbV		-	7.45	-	7.01	-	4.83
Cyclohexane, 1,1,3-trimethyl-	cycloalkane	ppbV		-	-	-	-	-	-
Unknown	cycloalkane	ppbV		-	-	-	-	-	-
Unknown	cycloalkane	ppbV		-	-	-	-	-	-
Unknown	cycloalkane	ppbV		-	-	-	-	-	-
Unknown	cycloalkane	ppbV		-	-	-	-	-	-
Unknown	cycloalkane	ppbV		-	-	-	-	-	1.91
Unknown	cycloalkane	ppbV		-	-	-	-	-	-
Unknown	cycloalkane	ppbV		-	-	-	-	-	-
Unknown	cycloalkane	ppbV		-	-	-	-	-	-
Unknown	cycloalkane	ppbV		-	-	-	-	-	-
Unknown	cycloalkane	ppbV		-	-	-	-	-	-
Unknown	cycloalkane	ppbV		-	-	-	-	-	-
unknown alkane	cycloalkane	ppbV		-	-	-	-	-	-
unknown cycloalkane	cycloalkane	ppbV		-	-	-	-	-	-
unknown cycloalkane	cycloalkane	ppbV		-	-	-	-	-	-
unknown cycloalkane	cycloalkane	ppbV		-	-	-	-	-	-
unknown cycloalkane	cycloalkane	ppbV		-	-	-	-	-	-
Furan, tetrahydro-	furan	ppbV		-	-	-	-	-	-
2-Butanone	ketone	ppbV		-	-	-	-	-	-
Acetone	ketone	ppbV		2.42	-	-	-	-	-
Cyclohexanone	ketone	ppbV		-	-	-	-	-	-
Cyclopentanone	ketone	ppbV		6.47	-	16.4	-	-	-
Unknown	ketone	ppbV		-	-	4.14	-	-	-
Unknown	ketone	ppbV		-	-	-	-	-	-
Unknown	ketone	ppbV		-	-	-	-	-	-
Unknown	ketone	ppbV		-	-	-	-	-	-
Unknown	ketone cycloalkane	ppbV		-	-	-	-	-	-
Unknown	ketone cycloalkane	ppbV		-	-	-	-	-	-
Unknown	ketone cycloalkane	ppbV		-	-	-	-	-	-
Unknown	naphthalene	ppbV		-	-	-	-	-	-
Unknown	other	ppbV		-	-	-	2.58	8	-
Unknown	other	ppbV		-	-	-	11	9.96	5.73
Unknown	other	ppbV		-	-	-	-	-	-
Unknown	other	ppbV		-	-	-	-	-	-
Unknown	other	ppbV		-	1.69	-	-	-	-
Unknown	other	ppbV		-	-	-	-	7.15	-
Unknown	other	ppbV		-	-	-	-	-	-
Unknown	other	ppbV		-	10.9	-	19	8.49	-
Unknown	other	ppbV		-	6.9	-	1.41	-	1.55
Unknown	other	ppbV		-	2.37	-	1.43	5.21	1.52
Unknown	other	ppbV		-	-	-	-	-	-
Unknown	other	ppbV		-	-	-	-	-	-
Unknown	other	ppbV		-	2.61	-	-	-	-
Cyclotrisiloxane, Hexamethyl-	siloxane	ppbV		5.29	-	8.91	-	-	-
Silanol, Trimethyl-	siloxane	ppbV		-	-	1.55	-	-	-
Unknown	siloxane	ppbV		-	-	-	-	-	-
unknown siloxane	siloxane	ppbV		-	-	-	-	-	-
unknown siloxane	siloxane	ppbV		-	-	2.03	-	-	-
unknown siloxane	siloxane	ppbV		1.91	-	-	-	-	-
unknown siloxane	siloxane	ppbV		-	-	-	-	-	-
unknown siloxane	siloxane	ppbV		-	-	-	-	-	-
unknown siloxane	siloxane	ppbV		-	-	-	-	-	-

1. Samples collected by GSI and analyzed by Alpha Analytical.
2. Less than ("<") indicates the analyte was not found at the stated detection limit. J = estimated result between method detection limit and reporting limit.
D = result from a dilution.

ATTACHMENT B.3.4: SOIL VAPOR AND GROUNDWATER MONITORING WELL HEADSPACE SAMPLE ANALYTICAL RESULTS
Red Hill Bulk Fuel Storage Facility, Joint Base Pearl Harbor-Hickam, O'ahu, Hawai'i

			Sample ID:	RHMW01ERH459	RHMW02ERH450	RHMW03ERH451	RHMW04ERH452
			Lab Sample ID:	L1740493-19	L1740493-20	L1740493-21	L1740493-22
			Sample Date/Time:	2017-10-30 9:12	2017-10-26 10:03	2017-10-26 11:38	2017-10-26 15:03
			Matrix:	HEADSPACE	HEADSPACE	HEADSPACE	HEADSPACE
FIXED GASES BY USEPA METHOD 3C							
Analyte		**Units**					
Carbon Dioxide		%		0.908	9.13	2.08	0.094 J
Methane		%		<0.051	<0.057	<0.058	<0.058
Oxygen		%		19.9	7.8	18.7	21.8
VOCs BY USEPA METHOD TO-15 (TARGET ANALYTES)							
Analyte	**Class**	**Units**					
Decane (C10)	alkane	ppbV		<0.25	0.157	3.67	0.628
Dodecane (C12)	alkane	ppbV		<0.5	0.279	1.82	0.755
Heptane	alkane	ppbV		0.51D	0.066	0.851	0.039
n-Hexane	alkane	ppbV		1.65D	0.132	0.499	0.037
Nonane (C9)	alkane	ppbV		0.18 JD	0.083	3.53	0.089
Octane	alkane	ppbV		0.31D	0.081	2.26	0.07
Pentane	alkane	ppbV		8.69D	8.76	0.869	0.211
Tridecane	alkane	ppbV		<0.5	0.215 J	0.501 J	0.361 J
Undecane	alkane	ppbV		<0.25	0.247	2.88	0.297
1,3-Butadiene	alkene	ppbV		<0.1	<0.01	<0.01	<0.01
1-Decene	alkene	ppbV		<0.25	<0.025	<0.025	<0.025
1-Heptene	alkene	ppbV		<0.1	<0.01	<0.01	<0.01
1-Hexene	alkene	ppbV		3.28D	<0.01	<0.01	<0.01
1-Nonene	alkene	ppbV		<0.1	<0.01	<0.01	<0.01
1-Octene	alkene	ppbV		<0.1	<0.01	<0.01	<0.01
1-Pentene	alkene	ppbV		6.83D	0.151	0.031	0.019 J
2-Methyl-1-Butene	alkene	ppbV		0.57D	0.07	0.037	<0.01
cis-2-Pentene	alkene	ppbV		<0.1	<0.01	<0.01	<0.01
trans-2-Pentene	alkene	ppbV		0.19 JD	0.111	0.035	<0.01
2,2-Dimethylpentane	branched alkane	ppbV		<0.1	<0.01	<0.01	<0.01
2,3,3-Trimethylpentane	branched alkane	ppbV		<0.1	0.07	0.084	0.018 J
2,3,4-Trimethylpentane	branched alkane	ppbV		<0.1	0.017 J	0.111	<0.01
2,3-Dimethylbutane	branched alkane	ppbV		0.27D	<0.01	0.138	<0.01
2,3-Dimethylhexane	branched alkane	ppbV		<0.1	<0.01	<0.01	<0.01
2,3-Dimethylpentane	branched alkane	ppbV		<0.1	<0.01	0.205	<0.01
2,4-Dimethylhexane/2,2,3-Trimethylpentar	branched alkane	ppbV		<0.25	0.036 JB	0.112	<0.025
2,4-Dimethylpentane	branched alkane	ppbV		<0.1	<0.01	0.104	<0.01
2,5-Dimethylhexane	branched alkane	ppbV		<0.1	0.016 J	0.092	<0.01
2-Methylheptane	branched alkane	ppbV		<0.1	<0.01	0.829	<0.01
2-Methylhexane	branched alkane	ppbV		0.33D	0.044	0.236	0.014 J
2-Methylpentane	branched alkane	ppbV		1.19D	0.754	0.439	0.081 B
3-Ethylhexane	branched alkane	ppbV		<0.1	<0.01	0.099	<0.01
3-Methylheptane	branched alkane	ppbV		<0.1	0.025	0.52	0.013 J
3-Methylhexane	branched alkane	ppbV		0.52D	0.144	0.515	<0.01
3-Methylpentane	branched alkane	ppbV		0.61D	0.069	0.267	0.022 J
Isooctane	branched alkane	ppbV		0.24 JD	0.059	0.189	0.018 J
Isopentane	branched alkane	ppbV		<0.1	<0.01	1.14	<0.01
1-Ethyl-1-Methylcyclopentane	cycloalkane	ppbV		<0.1	<0.01	0.055	<0.01
Cyclohexane	cycloalkane	ppbV		16.4D	0.175	0.464	0.059
Cyclopentane	cycloalkane	ppbV		0.43D	<0.01	0.176	0.295
Methylcyclohexane	cycloalkane	ppbV		0.93D	0.08	1.88	0.025
Methylcyclopentane	cycloalkane	ppbV		0.52D	0.058	0.533	<0.01
1,2,4,5-Tetramethylbenzene	aromatic	ppbV		<0.25	<0.025	0.036 J	<0.025
1,2,4-Trimethylbenzene	aromatic	ppbV		0.31 JD	0.133	2.04	0.133
1,2-Diethylbenzene	aromatic	ppbV		<0.25	<0.025	0.085	<0.025
1,2-Dimethyl-3-Ethylbenzene	aromatic	ppbV		<0.25	<0.025	0.157	<0.025
1,2-Dimethyl-4-Ethylbenzene	aromatic	ppbV		<0.25	<0.025	0.27	<0.025
1,3,5-Trimethylbenzene	aromatic	ppbV		0.11 JD	0.03	0.605	0.032
1,3-Dimethyl-2-Ethylbenzene	aromatic	ppbV		<0.25	<0.025	0.061	<0.025
1,3-Dimethyl-4-Ethylbenzene	aromatic	ppbV		<0.25	<0.025	0.303	<0.025
1,3-Dimethyl-5-Ethylbenzene	aromatic	ppbV		<0.25	<0.025	0.274	<0.025
1,4-Dimethyl-2-Ethylbenzene	aromatic	ppbV		<0.25	<0.025	0.236	<0.025
1-Methyl-2-Ethylbenzene	aromatic	ppbV		<0.25	0.026 J	0.679	0.029 J
1-Methyl-2-Isopropylbenzene	aromatic	ppbV		0.73D	<0.025	0.032 J	<0.025
1-Methyl-2-N-Propylbenzene	aromatic	ppbV		<0.25	<0.025	0.316	<0.025
1-Methyl-3-Ethylbenzene	aromatic	ppbV		<0.25	0.047 J	1.08	0.055
1-Methyl-3-Isopropylbenzene	aromatic	ppbV		<0.25	<0.025	0.259	<0.025
1-Methyl-3-N-Propylbenzene	aromatic	ppbV		<0.25	<0.025	0.39	<0.025
1-Methyl-4-Ethylbenzene	aromatic	ppbV		<0.1	0.023 J	0.532	0.026
1-Methyl-4-Isopropylbenzene	aromatic	ppbV		<0.25	0.051	0.234	0.031 J
1-Methyl-4-N-Propylbenzene	aromatic	ppbV		<0.25	<0.025	0.179	<0.025
Benzene	aromatic	ppbV		0.44D	0.071	0.229	0.043
Ethylbenzene	aromatic	ppbV		0.24 JD	0.061	0.969	0.048
Indane	aromatic	ppbV		<0.25	<0.025	0.185	<0.025
Indene	aromatic	ppbV		<0.25	<0.025	<0.025	<0.025
Isopropylbenzene	aromatic	ppbV		0.1 JD	<0.01	0.289	<0.01
n-Butylbenzene	aromatic	ppbV		<0.25	<0.025	0.166	<0.025
N-Pentylbenzene	aromatic	ppbV		<0.25	<0.025	0.051	<0.025
n-Propylbenzene	aromatic	ppbV		<0.1	<0.01	0.495	0.019 J
o-Xylene	aromatic	ppbV		0.63D	0.612	1.76	0.167
p/m-Xylene	aromatic	ppbV		0.89D	0.24	3.53	0.174
sec-Butylbenzene	aromatic	ppbV		<0.25	<0.025	0.213	<0.025
Styrene	aromatic	ppbV		<0.1	0.063	0.125	0.074
Toluene	aromatic	ppbV		2.94D	0.266	1.68	0.208
1-Methylnaphthalene	naphthalene	ppbV		<0.5	<0.05	0.061 J	<0.05
2-Methylnaphthalene	naphthalene	ppbV		<0.5	<0.05	0.121 J	<0.05
Naphthalene	naphthalene	ppbV		<0.25	0.066 B	0.266	0.061 B
Tertiary Butanol	alcohol	ppbV		3.88D	11.3	1.65	1.28
Ethyl-Tert-Butyl-Ether	ether	ppbV		0.56D	2.48	0.361	0.173
Isopropyl Ether	ether	ppbV		<0.1	<0.01	<0.01	<0.01
Methyl tert butyl ether	ether	ppbV		<0.1	0.352	0.038	<0.01
Tertiary-Amyl Methyl Ether	ether	ppbV		<0.1	0.06	<0.01	<0.01
2-Ethylthiophene	thiophene	ppbV		<0.1	<0.01	<0.01	<0.01
2-Methylthiophene	thiophene	ppbV		<0.1	<0.01	<0.01	<0.01
3-Methylthiophene	thiophene	ppbV		<0.1	<0.01	<0.01	<0.01
Benzothiophene	thiophene	ppbV		<0.5	<0.05	<0.05	<0.05
Thiophene	thiophene	ppbV		<0.1	<0.01	<0.01	<0.01
1,2-Dibromoethane	other	ppbV		<0.1	<0.01	<0.01	<0.01
1,2-Dichloroethane	other	ppbV		<0.1	<0.01	<0.01	<0.01
MMT	other	ppbV		<0.5	<0.05	<0.05	<0.05

ATTACHMENT B.3.4: SOIL VAPOR AND GROUNDWATER MONITORING WELL HEADSPACE SAMPLE ANALYTICAL RESULTS
Red Hill Bulk Fuel Storage Facility, Joint Base Pearl Harbor-Hickam, O'ahu, Hawai'i

			Sample ID:	RHMW01ERH459	RHMW02ERH450	RHMW03ERH451	RHMW04ERH452
			Lab Sample ID:	L1740493-19	L1740493-20	L1740493-21	L1740493-22
			Sample Date/Time:	2017-10-30 9:12	2017-10-26 10:03	2017-10-26 11:38	2017-10-26 15:03
			Matrix:	HEADSPACE	HEADSPACE	HEADSPACE	HEADSPACE
VOCs BY USEPA METHOD TO-15 (TENTATIVELY IDENTIFIED COMPOUNDS)							
1-Butanol	alcohol	ppbV		-	-	-	-
1-Hexanol, 2-ethyl-	alcohol	ppbV		-	-	-	-
Amylene Hydrate	alcohol	ppbV		-	3.75	-	-
Methyl Alcohol	alcohol	ppbV		-	4.2	2.21	3.69
Unknown	alcohol	ppbV		-	-	-	-
Unknown	alcohol	ppbV		-	-	-	-
Unknown	alcohol	ppbV		-	-	-	-
Unknown	alcohol	ppbV		-	-	-	-
unknown alcohol	alcohol	ppbV		-	-	-	-
unknown alcohol	alcohol	ppbV		-	6.39	-	-
Unknown	alcohol cycloalkane	ppbV		-	-	-	-
Propane	alkane	ppbV		-	-	-	-
Unknown	alkane	ppbV		-	-	-	-
Unknown	alkane	ppbV		-	2.41	-	-
unknown alkane	alkane	ppbV		-	-	2.03	-
unknown alkane	alkane	ppbV		-	-	-	-
1-Pentene, 2-methyl-	alkene	ppbV		-	-	-	-
2,4-Dimethyl-1-heptene	alkene	ppbV		-	-	-	-
Unknown	alkene	ppbV		-	-	-	-
Unknown	alkene	ppbV		-	-	-	-
Unknown	alkene	ppbV		-	-	-	-
Unknown	alkene	ppbV		-	-	-	-
Unknown	alkene	ppbV		-	-	-	-
Unknown	alkene	ppbV		-	-	-	-
Unknown	alkene	ppbV		-	-	-	-
Unknown	alkene	ppbV		-	-	-	-
Unknown	alkene	ppbV		-	-	-	-
Unknown	alkene	ppbV		-	-	-	-
Unknown	alkene	ppbV		-	5.91	-	-
Unknown	alkene	ppbV		-	-	4.28	-
Unknown	alkene	ppbV		-	-	-	-
Unknown	alkene	ppbV		-	-	-	-
Unknown	alkene	ppbV		-	-	-	-
Unknown	alkene	ppbV		-	-	-	-
Unknown	alkene	ppbV		-	-	-	-
unknown alkane	alkene	ppbV		-	-	-	-
unknown alkene	alkene	ppbV		-	-	-	-
unknown alkene	alkene	ppbV		-	-	-	-
Unknown	aromatic	ppbV		-	-	-	-
Unknown	aromatic	ppbV		-	-	-	-
Hexane, 2,3-dimethyl-	branched alkane	ppbV		-	-	-	-
Unknown	branched alkane	ppbV		-	-	-	-
Unknown	branched alkane	ppbV		-	-	-	-
Unknown	branched alkane	ppbV		-	-	-	-
Unknown	branched alkane	ppbV		-	-	-	-
unknown alkane	branched alkane	ppbV		-	-	5.11	-
unknown alkane	branched alkane	ppbV		-	8.25	-	2.37
unknown alkane	branched alkane	ppbV		-	-	-	-
Cyclohexane, 1,1,3-trimethyl-	cycloalkane	ppbV		-	-	-	-
Unknown	cycloalkane	ppbV		-	-	-	-
Unknown	cycloalkane	ppbV		-	-	-	-
Unknown	cycloalkane	ppbV		-	-	-	-
Unknown	cycloalkane	ppbV		-	-	-	-
Unknown	cycloalkane	ppbV		-	7.71	1.94	-
Unknown	cycloalkane	ppbV		-	-	-	-
Unknown	cycloalkane	ppbV		-	-	-	-
Unknown	cycloalkane	ppbV		-	-	-	-
Unknown	cycloalkane	ppbV		-	-	-	-
Unknown	cycloalkane	ppbV		-	-	-	-
Unknown	cycloalkane	ppbV		-	-	-	-
unknown alkane	cycloalkane	ppbV		-	-	-	-
unknown cycloalkane	cycloalkane	ppbV		-	-	-	-
unknown cycloalkane	cycloalkane	ppbV		-	-	-	-
unknown cycloalkane	cycloalkane	ppbV		-	-	-	-
unknown cycloalkane	cycloalkane	ppbV		-	-	-	-
Furan, tetrahydro-	furan	ppbV		-	-	-	-
2-Butanone	ketone	ppbV		-	-	-	-
Acetone	ketone	ppbV		-	-	-	-
Cyclohexanone	ketone	ppbV		-	-	-	2.98
Cyclopentanone	ketone	ppbV		-	-	-	-
Unknown	ketone	ppbV		-	-	-	-
Unknown	ketone	ppbV		-	-	-	3.87
Unknown	ketone	ppbV		-	-	-	-
Unknown	ketone	ppbV		-	-	-	-
Unknown	ketone cycloalkane	ppbV		-	-	-	-
Unknown	ketone cycloalkane	ppbV		-	-	-	-
Unknown	ketone cycloalkane	ppbV		-	-	-	-
Unknown	naphthalene	ppbV		-	-	-	-
Unknown	other	ppbV		-	-	-	-
Unknown	other	ppbV		-	-	2.23	-
Unknown	other	ppbV		-	-	-	-
Unknown	other	ppbV		-	-	-	-
Unknown	other	ppbV		-	-	-	-
Unknown	other	ppbV		-	-	2.1	-
Unknown	other	ppbV		-	3.72	-	-
Unknown	other	ppbV		-	94.1	94.6	212
Unknown	other	ppbV		8220	13	39.8	20.6
Unknown	other	ppbV		-	2.29	2.29	-
Unknown	other	ppbV		-	-	2.31	-
Unknown	other	ppbV		-	-	-	3.3
Unknown	other	ppbV		-	-	-	-
Cyclotrisiloxane, Hexamethyl-	siloxane	ppbV		-	-	-	-
Silanol, Trimethyl-	siloxane	ppbV		-	-	-	-
Unknown	siloxane	ppbV		-	-	-	-
unknown siloxane	siloxane	ppbV		-	-	-	-
unknown siloxane	siloxane	ppbV		-	-	-	-
unknown siloxane	siloxane	ppbV		-	-	-	-
unknown siloxane	siloxane	ppbV		-	-	-	-
unknown siloxane	siloxane	ppbV		-	-	-	-
unknown siloxane	siloxane	ppbV		-	-	-	-

1. Samples collected by GSI and analyzed by Alpha Analytical.
2. Less than ("<") indicates the analyte was not found at the stated detection limit. J = estimated result between method detection limit and reporting limit. D = result from a dilution.

Attachment B.3.5:
LNAPL Indications from Drilling Fluids and Boring Logs
for Borings Completed Below Fuel Storage Tanks
(Most Borings Completed 1998–2001)

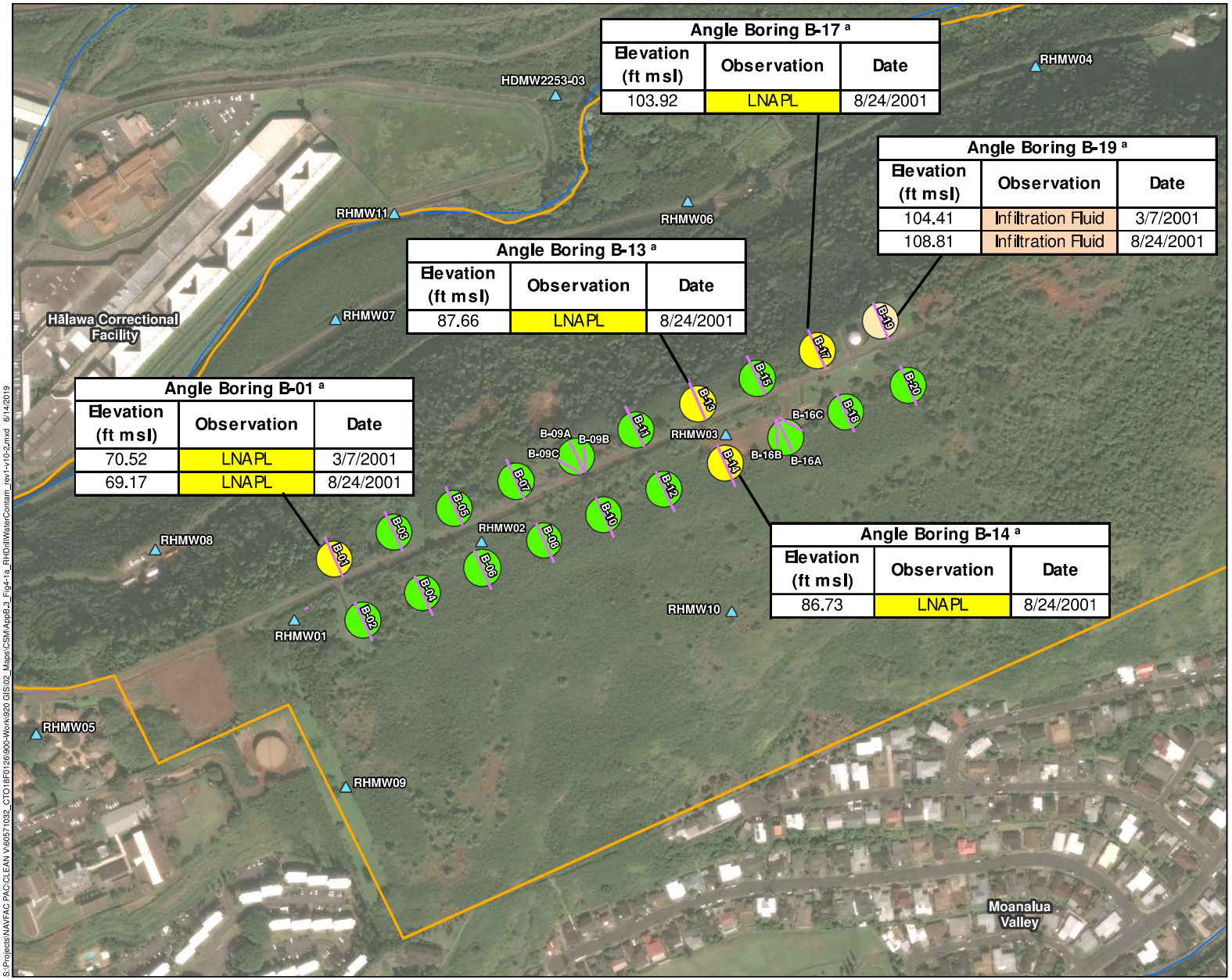

Key Map

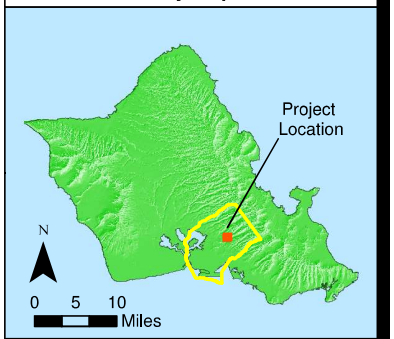

Legend

- Red Hill Fuel Storage Tank - LNAPL contamination noted
- Red Hill Fuel Storage Tank - Infiltration fluid noted
- Red Hill Fuel Storage Tank - No evidence of contamination noted
- Groundwater Monitoring Well
- Angle Boring
- Groundwater Model Domain
- Red Hill Facility Boundary
- Stream

Notes

1. Map projection: NAD 1983 Hawaii State Plane Zone 3 feet
2. DigitalGlobe, Inc. (DG) and NRCS. Publication_Date: 2015
3. Reference:
   a. DON 2002. Red Hill Bulk Fuel Storage Facility Investigation Report (Final) for Fleet Industrial Supply Center (FISC), Oahu, Hawaii. Prepared by AMEC Earth and Environmental, Inc. for NAVFAC Pacific. August.

N

0 200 400 800 Feet

Appendix B.3 Figure 4-1a
LNAPL Indications in Drilling Fluids While Drilling Angle Borings, 1998–2002
Conceptual Site Model Rev. 01
Red Hill Bulk Fuel Storage Facility
JBPHH, O'ahu, Hawai'i

S:\Projects\NAVFAC PAC\CLEAN V\60571032_CTO18F0126\900-Work\920 GIS\02_Maps\CSM\AppB-3_Fig4-1a_RHDrillWaterContam_rev1-v10-2.mxd 6/14/2019

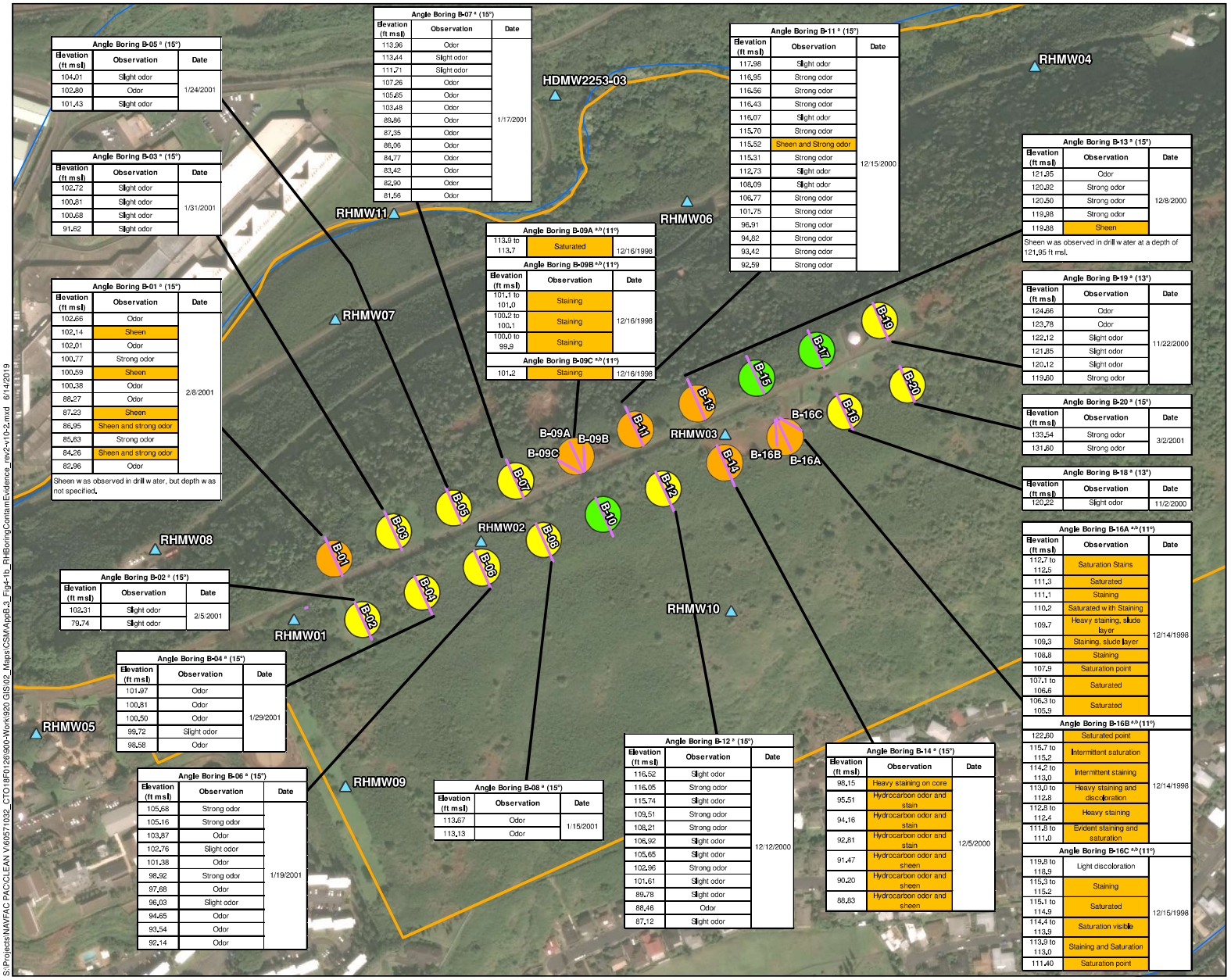

Key Map

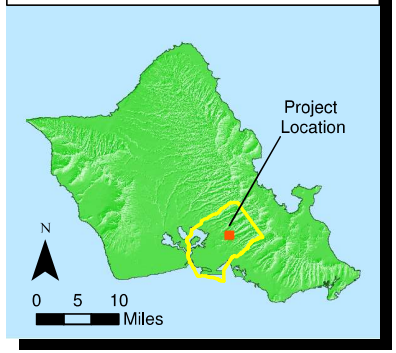

Legend

- Red Hill Fuel Storage Tank- Fuel Odor Noted in Boring Log
- Red Hill Fuel Storage Tank- Sheen or Staining Observed in Boring Log
- Red Hill Fuel Storage Tank- No Evidence of Contamination Observed in Boring Log
- Groundwater Monitoring Well
- Angle Boring
- Groundwater Model Domain
- Red Hill Facility Boundary
- Stream

Notes

1. Map projection: NAD 1983 Hawaii State Plane Zone 3 feet
2. DigitalGlobe, Inc. (DG) and NRCS. Publication_Date: 2015
3. References:
   a. Boring logs from DON 2002. Red Hill Bulk Fuel Storage Facility Investigation Report (Final) for Fleet Industrial Supply Center (FISC), Oahu, Hawaii. Prepared by AMEC Earth and Environmental, Inc. for NAVFAC Pacific. August.
   b. Boring logs from DON 1999. Initial Phase II Site Characterization Report, Fleet Industrial Supply Center Bulk Fuel Storage Facility at Red Hill. Prepared by Ogden Environmental and Energy Services Co., Inc. for NAVFAC Pacific. March.

* Elevations presented as "~100" are approximations made based on boring logs and notes in the text.

N

0 200 400 800 Feet

Appendix B.3 Figure 4-1b
LNAPL Indications from Boring Logs While Drilling Angle Borings, 1998–2002
Conceptual Site Model Rev. 01
Red Hill Bulk Fuel Storage Facility
JBPHH, O'ahu, Hawai'i

S:\Projects\NAVFAC PAC\CLEAN V\60571032_CTO18F0126\900-Work\920 GIS\02_Maps\CSM\AppB.3_Fig4-1b_RHBoringContamEvidence_rev2-v10-2.mxd 6/14/2019

Attachment B.3.6:
Laboratory Report and EDD for Soil Vapor Samples Analyzed by Alpha Analytical: Laboratory Job Number L1740493
(Available electronically by request from GSI Environmental, email Tom McHugh at temchugh@gsi-net.com)

This page intentionally left blank

Appendix B.4:
MNA Primary Lines of Evidence and Rate Calculations

CONTENTS

Acronyms and Abbreviations iii

1. Introduction 1-1

1.1 Technical Background 1-1
1.2 Study Objectives 1-1

2. Methods 2-1

2.1 Data Handling and Consolidation 2-1
2.2 Plume Duration: Point Attenuation (C vs. t) Rate Coefficient 2-2
2.3 Plume Attenuation: Bulk Attenuation (C vs. d) Rate Coefficient 2-2
2.4 Plume Attenuation: Biodegradation Rate Coefficient (λ) 2-4
2.5 Plume Attenuation: RHMW02 to Red Hill Shaft 2-5

3. Results 3-1

3.1 Plume Duration: Point Attenuation (C vs. t) Rate Coefficients 3-1
3.2 Plume Attenuation: Bulk Attenuation (C vs. d) Rate Coefficients 3-4
3.3 Plume Attenuation: Biodegradation Rate Coefficients 3-6
3.4 Plume Attenuation: RHMW02 to RHMW01 Attenuation Rate Coefficients for TPH-d with Silica Gel Cleanup 3-7
3.5 Plume Attenuation: RHMW02 to Red Hill Shaft 3-8

4. Conclusions 4-1

5. References 5-1

FIGURES

1-1 Location of RHMW01 and RHMW02 in Relation to Tank Farm 1-2

2-1 Concentration vs. Time Attenuation Rate Coefficient and Half-Life 2-2

2-2 Concentration vs. Distance Attenuation Rate Coefficient (k) and Half-Life 2-3

3-1 Linear and Natural Log Scale Plots of 1-Methylnaphthalene Concentrations from September 2005 to January 2019 at Monitoring Well RHMW02 3-2

3-2 Linear and Natural Log Scale Plots of 2-Methylnaphthalene Concentrations from September 2005 to January 2019 at Monitoring Well RHMW02 3-3

3-3 Linear and Natural Log Scale Plots of Naphthalene Concentrations from September 2005 to January 2019 at Monitoring Well RHMW02 3-4

TABLES

2-1 Appropriate Uses for Point (C vs. t), Bulk (C vs. d), and Biodegradation Attenuation Rate Coefficients 2-1

2-2 Number of COPC Data Pairs Used to Calculate C vs. d Rate Coefficients 2-4

3-1 C vs. t Coefficients, Half-Lives, and First-Order Model Fit Parameters for the COPCs at RHMW02 (September 2005 to January 2019) 3-1

3-2 C vs. d Bulk Attenuation Rate Coefficients and Half-Lives for the COPCs Along RHMW02–RHMW01 Transect (Includes Detected COPCs at Both Wells Only) 3-5

3-3 C vs. d Bulk Attenuation Rate Coefficients and Half-Lives for the COPCs Along RHMW02–RHMW01 Transect (Includes Detected COPCs at One or More Wells Only) 3-5

3-4 Biodegradation Rate Coefficients and Half-Lives for the COPCs along RHMW02–RHMW01 Transect (includes Detected COPCs at Both Wells Only) 3-6

3-5 Biodegradation Rate Coefficients and Half-Lives for the COPCs along RHMW02–RHMW01 Transect (includes Detected COPCs at One or More Wells Only) 3-6

3-6 C vs. d Rate Coefficients and Half-Lives for TPH-d, TPH-d (with silica gel cleanup), and TOC along RHMW02–RHMW01 Transect 3-7

3-7 Biodegradation Rate Coefficients and Half-Lives for TPH-d, TPH-d (with silica gel cleanup), and TOC along RHMW02–RHMW01 Transect 3-7

3-8 RHMW02 to Red Hill Shaft Attenuation Rate Coefficients Using All Naphthalene Detects at Red Hill Shaft (2005 to January 2019) 3-8

3-9 RHMW02 to Red Hill Shaft Attenuation Rate Coefficients Using Naphthalene Results from April 2015 to July 2016 3-9

ACRONYMS AND ABBREVIATIONS

α_x	longitudinal dispersivity
λ	biodegradation rate coefficient
µg/L	micrograms per liter
1-MeN	1-methylnaphthalene
2-MeN	2-methlynaphthalene
b	thickness of the LNAPL source area at the Facility
BTEX	benzene, toluene, ethylbenzene, and xylenes
C vs. d	concentration vs. distance
C vs. t	concentration vs. time
C	concentration of COPC at time t
C_o	concentration of COPC at t=0
COPC	chemical of potential concern
C_{RHMW02}	COPC concentration at RHMW02
C_{RHS-BD}	COPC concentration at Red Hill Shaft before dilution
CSM	conceptual site model
d	day
d^{-1}	per day
EPA	Environmental Protection Agency, United States
ft	foot/feet
ft/d	feet per day
ft^3/day	cubic feet per day
k	first-order rate coefficient
k/u	the negative of the slope of a line obtained from a log-linear plot of the (center-line) COPC concentration
k_{point}	concentration vs. time attenuation rate coefficient
LNAPL	light non-aqueous-phase liquid
LOD	limit of detection
LOQ	limit of quantitation
L_p	plume length
MDL	method detection limit
MGD	million gallons per day
MNA	monitored natural attenuation
n	number of samples
N	naphthalene
PAH	polynuclear aromatic hydrocarbon
Q_{RHS}	average pumping rate at Red Hill Shaft
R^2	coefficient of determination
RL	reporting limit
t	time
$t_{1/2}$	half-life for a given COPC
TOC	total organic carbon
TPH-d	total petroleum hydrocarbons – diesel-range organics
U.S.	United States
USGS	United States Geological Survey
v_{gw}	seepage velocity
w	width of the LNAPL source area at the Facility
yr	year
yr^{-1}	per year

1. Introduction

This subappendix is summarized in Section 7.3.2.4 of the Conceptual Site Model (CSM) main document.

1.1 TECHNICAL BACKGROUND

The United States (U.S.) Environmental Protection Agency (EPA) defines monitored natural attenuation (MNA) as:

> *... the reliance on natural attenuation processes (within the context of a carefully controlled and monitored clean-up approach) to achieve site-specific remedial objectives within a time frame that is reasonable compared to other methods. The "natural attenuation processes" that are at work in such a remediation approach include a variety of physical, chemical, or biological processes that, under favorable conditions, act without human intervention to reduce the mass, toxicity, mobility, volume, or concentration of contaminants in soil and ground water. These in-situ processes include, biodegradation, dispersion, dilution, sorption, volatilization, and chemical or biological stabilization, transformation, or destruction of contaminants* (EPA 1999).

A lines-of-evidence approach is commonly used to demonstrate that natural attenuation processes are occurring at a given site. Primary and secondary lines of evidence to evaluate MNA (EPA 1999; Newell et al. 2002; Wiedemeier, Wilson, et al. 1999; Wiedemeier, Rifai, et al. 1999) are:

- **Primary:** Rate of change in dissolved phase contaminant concentrations, both spatially and temporally, as a metric for plume behavior/status (i.e., stable, shrinking, expanding). Site-specific attenuation rate coefficient calculations can be used to evaluate the contribution of attenuation processes and estimate the time required to achieve remediation objectives.
- **Secondary:** Hydrogeologic and geochemical data as an indirect measure of active natural attenuation processes that support primary evidence/observations (e.g., decrease in parent contaminant concentrations). For example, changes in electron acceptor concentrations can be strong evidence for in-situ degradation of the parent compounds. Secondary lines of evidence are discussed in CSM Appendix B.5.

1.2 STUDY OBJECTIVES

The objective of this study was to evaluate natural attenuation processes at the Red Hill Bulk Fuel Storage Facility (the "Facility") using primary lines of evidence (i.e., temporal and spatial contaminant concentrations) from the Facility groundwater monitoring network. First-order rate coefficients and associated half-lives were calculated for the monitoring wells RHMW01 and RHMW02 at the Facility. Chemicals of potential concern (COPCs) considered for this study were diesel-range total petroleum hydrocarbons (TPH-d), 1-methylnaphthalene (1-MeN), 2-methylnaphthalene (2-MeN), and naphthalene (N). For TPH-d, concentration vs. time rate coefficients were not calculated due to issues with laboratory analysis for this parameter (discussed further in Section 2.2 and CSM Appendix B.7).

Benzene, toluene, ethylbenzene, and xylenes (BTEX) data were not analyzed in this study, given their low concentrations in Facility groundwater (mostly less than 1 microgram per liter [µg/L]) and/or limited data sets of detected results (i.e., the majority of BTEX concentrations were below respective detection limits) at wells RHMW01 and RHMW02. Beginning in 2017, the EPA co-sampled some

wells during the Navy sampling events. Because this co-sampling covers only a small portion of the monitoring timeframe, EPA analytical results have not been included in this analysis.

Figure 1-1 provides the locations of monitoring wells RHMW01 and RHMW02 in relation to the tank farm. Historical groundwater data from February 2005 to present (February 7, 2019) were used to calculate first-order rate coefficients and half-lives for the COPCs. Descriptions of the first-order attenuation calculations are provided in Section 2.

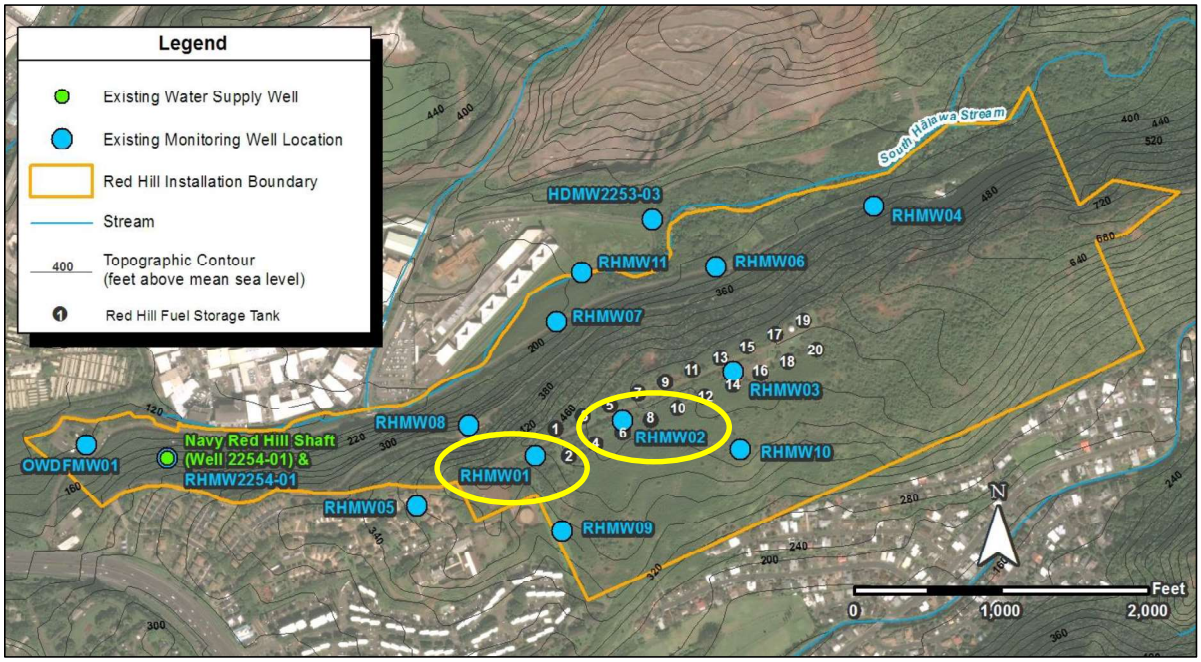

Figure 1-1: Location of RHMW01 and RHMW02 in Relation to Tank Farm

2. Methods

Three types of first-order attenuation rate coefficients were calculated to evaluate MNA processes at the Facility: Point attenuation rate (Concentration vs. Time [C vs. t]), Bulk attenuation rate (Concentration vs. Distance [C vs. d]), and Biodegradation rate coefficients (λ). The point attenuation (C vs. t) rate describes the *plume duration* at a single monitoring well location while the bulk attenuation rate (C vs. d) rate describes the *plume attenuation* (which includes both dispersion and biodegradation) and spatial distribution of COPCs from the source area at a given time. The biodegradation rate describes *plume attenuation* resulting from the effects of biodegradation only (exclusive of advection, dispersion and other attenuation mechanisms). Each is described further in Sections 2.2, 2.3, and 2.4, respectively.

Importantly, each rate coefficient describes a specific attenuation process and, as a result, estimated rates and half-lives cannot be directly compared to each other. Table 2-1 summarizes the significance of each rate coefficient and their appropriate application for assessing natural attenuation processes (Newell et al. 2002).

Table 2-1: Appropriate Uses for Point (C vs. t), Bulk (C vs. d), and Biodegradation Attenuation Rate Coefficients

Rate Coefficient	Method of Analysis	Significance	Use of Rate Constant		
			Plume Attenuation?	Plume Trends?	Plume Duration?
Point Attenuation Rate (k_{point}, time per year)	C vs. t Plot (Figure 2-1; Equation 1)	Reduction in contaminant concentration over time at a single point	NO*	NO*	YES
Bulk Attenuation Rate (k; time per year)	C vs. d Plot (Figure 2-2; Equations 2 & 3)	Reduction in dissolved contaminant concentration with distance from source due to dispersion + biodeg.	YES	NO*	NO
Biodegradation Rate (λ, time per year)	C vs. d Plot; Calculations (Equations 4 & 5)	Biodegradation rate for dissolved contaminants after leaving source, exclusive of advection, dispersion, etc.	YES	NO	NO

* Note: Although assessment of an attenuation rate constant at a single location does not yield plume attenuation information, or plume trend information, an assessment of general trends of multiple wells over the entire plume is useful to assess overall plume attenuation and plume trends.
(Source: Newell et al. 2002, Table 2-1)

2.1 DATA HANDLING AND CONSOLIDATION

To calculate these attenuation rates, historical data from 2005 to January/February 2019 were considered, with the following modifications to the data set:

- COPC concentrations reported by the laboratory as non-detect were assigned a concentration equal to the limit reported (e.g., < 0.1 µg/L = 0.1 µg/L). The limit may be the limit of detection (LOD), method detection limit (MDL), or reporting limit (RL). The type of limit reported for COPC concentrations is not known for all data. The LOD is a statistically derived concentration that can be distinguished from a blank with 99% confidence. The MDL is a statistically derived concentrations that can be distinguished from zero with 99% confidence (DoD and DOE 2017; DoD EDQW 2017).
- Qualified data (e.g., "J" flag) were assigned the reported COPC concentration (e.g., 12 J µg/L = 12 µg/L). Note that when a COPC is detected at a concentration below the limit of

quantitation (LOQ), the laboratory reports the result as detected, but the result is flagged with a "J" flag to indicate that the detected concentration was less than the LOQ.

- For sampling events where duplicates were collected, the average of the primary concentration and duplicate concentration was used.

2.2 PLUME DURATION: POINT ATTENUATION (C VS. T) RATE COEFFICIENT

The Point Attenuation (C vs. t) Rate Coefficient (k_{point}) describes the behavior of the COPC at one point in space and provides information regarding the potential plume duration at that location (Newell et al. 2002). This rate coefficient, expressed in units of inverse time (e.g., per year), is calculated from the slope of the natural logarithm (log) concentration vs. time curve measured at a selected monitoring location (Figure 2-1; Equation 1). The rate coefficient and half-life (Equation 1) provide information regarding the potential plume duration at the single monitoring location, largely due to changes in strength of the plume source. Note that a rate coefficient calculated from C vs. t data at a single location cannot be used to estimate the trend of an entire plume or bulk attenuation (Table 2-1).

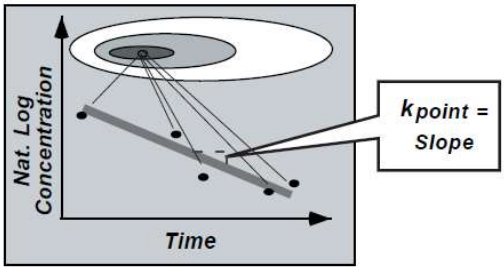

$$t = \frac{\ln(C/C_o)}{k_{point}};\ t_{1/2} = \frac{\ln(0.5)}{k_{point}} \quad (1)$$

where:
$t_{1/2}$ = Half-life for a given COPC (yr)
C = Concentration of COPC at time t (mg/L)
C_o = Concentration of COPC at t=0 (mg/L)
k_{point} = Concentration vs. time attenuation rate coefficient (yr^{-1})

(From Newell et al. 2002)

Figure 2-1: Concentration vs. Time Attenuation Rate Coefficient and Half-Life

C vs. t rate coefficients and half-lives were calculated for 1-MeN, 2-MeN, and N at RHMW02 only. For well RHMW01, the majority (> 50%) of concentration data for 1-MeN, 2-MeN, and N were below respective detection limits. For both wells, C vs. t rate coefficients were not calculated for TPH-d due to issues with the laboratory analysis for this parameter. As discussed in CSM Appendix B.7, during the monitoring period of 2005–2018, several different laboratories were used for analysis of groundwater samples. Some of the increases and decreases in TPH-d concentrations over time appear to be related to analytical differences between laboratories (see CSM Appendix B.7 for more information). As a result, a C vs. t attenuation rate for this parameter would not accurately reflect the true rate of COPC concentration change over time in individual monitoring wells.

For each COPC, natural log-transformed concentration data were plotted vs. time and fit to a linear trendline (using Microsoft Excel's built-in trendline and linear regression features) to estimate the first-order attenuation coefficient. The coefficient of determination (R^2) of the linear regression model and Mann Kendall p-value were used to evaluate the significance of the concentration trend with time. COPC half-lives were calculated using Equation 1.

2.3 PLUME ATTENUATION: BULK ATTENUATION (C VS. D) RATE COEFFICIENT

The C vs. d Rate Coefficient (k) (which includes both dispersion and biodegradation) describes the behavior of the COPC spatially within groundwater at one point in time (Newell et al. 2002). This rate coefficient, expressed in units of inverse time, is calculated by multiplying the slope of a line obtained

from a log-linear plot of COPC concentration vs. distance downgradient by the estimated groundwater seepage velocity (Figure 2-2; Equation 2). The rate coefficient and half-life (Equation 3) provide information on how quickly dissolved contaminants are attenuated within groundwater as they migrate from the source, indicating if a plume is expanding, showing relatively little change, or shrinking. As such, C vs. d attenuation rates are not directly comparable to C vs. t rates (which reflect the plume duration at a single location; see Section 2.2 and Table 2-1).

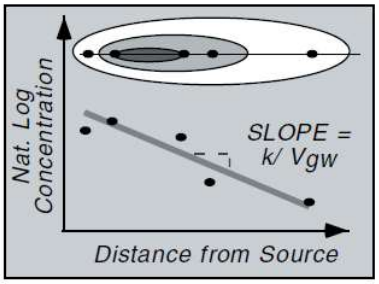

$$k = slope \times v_{gw} \quad (2)$$

$$t = \frac{\ln\left(C/C_o\right)}{k};\ t_{1/2} = \frac{\ln(0.5)}{k} \quad (3)$$

where:
k = Concentration vs. distance attenuation rate coefficient (d^{-1})
v_{gw} = Seepage velocity (ft/d)

(From Newell et al. 2002)

Figure 2-2: Concentration vs. Distance Attenuation Rate Coefficient (k) and Half-Life

For this study, data from monitoring wells RHMW01 and RHMW02 were used, based on the approximate west-southwesterly direction of groundwater flow through the tank farm and particle tracking indicating that these two monitoring wells fall along the same flow path. As the groundwater flow path between RHMW01 and RHMW02 is not precisely known (there is likely some amount of heterogeneity over short flow paths), there is some uncertainty in the calculated attenuation rates. Well RHMW05 was excluded from the analysis because preliminary particle tracking model results suggested that RHMW05 lies outside of the groundwater flow path connecting RHMW02 and RHMW01 (based on investigation's interim groundwater flow modeling). In addition, the majority of COPC concentrations were below respective detection limits at RHMW05. Wells RHMW02 and RHMW01 are located approximately 620 feet (ft) apart, with RHMW02 representing the area of highest COPC concentrations and RHMW01 representing the downgradient location. This analysis assumes that RHMW02 and RHMW01 are in the same flow path (i.e., the COPCs present in RHMW01 originated in the vicinity of RHMW02).

First-order rate coefficients and half-lives were calculated for TPH-d, 1-MeN, 2-MeN, and N using two modified data sets:

- **Detected COPCs at Both Wells:** a data set including only sampling events where concentrations of a COPC were detected at *both* RHMW01 and RHMW02.
- **Detected COPCs at One or Both Wells:** a data set including sampling events where concentrations of a COPC were detected at *one or both* wells. Non-detect samples were assigned a concentration equal to the reported limit (i.e., U-flagged value; see Section 2.1 for details on data handling).

The purpose of the two data sets was to assess the effect of including/excluding qualified data (non-detects) on the resulting attenuation rate coefficients and half-lives. For both data sets, the following data were excluded: (1) sampling events where a given COPC was below its reported limit at *both* wells and (2) sampling events where only one well was sampled (e.g., RHMW01 data collected before RHMW02 was installed). The numbers of data pairs for the COPCs for each data set are presented in Table 2-2.

Table 2-2: Number of COPC Data Pairs Used to Calculate C vs. d Rate Coefficients

COPC	Detected COPCs at *Both* Wells			Detected COPCs at *One or Both* Wells		
	No. of Data Pairs	No. of Non-detects		No. of Data Pairs	No. of Non-detects	
		RHMW01	RHMW02		RHMW01	RHMW02
TPH-d	58	0	0	65	7	0
1-Methylnaphthalene	10	0	0	64	54	0
2-Methylnaphthalene	13	0	0	65	52	0
Naphthalene	25	0	0	65	40	0
TPH-d (silica gel cleanup)				7	5	1
TOC				5	1	0

TOC total organic carbon

For each data pair, the slope of the natural log-linear plot of COPC concentration vs. distance was calculated using Microsoft Excel's built-in trendline feature. The average slope for each COPC was then multiplied by the estimated groundwater seepage velocity to calculate the first-order attenuation coefficient. COPC half-lives were calculated using Equation 3.

A groundwater seepage velocity of 40.8 ft/day for the Base Case model and 26 ft/day for the Clinker Model was used based on particle tracking model results conducted for the investigation's interim groundwater flow modeling effort.

Groundwater seepage velocity at the Facility is highly uncertain due to the complex geology and flat water table (i.e., very low hydraulic gradient). Efforts to develop an improved understanding of groundwater flow at the Facility are ongoing.

C vs. d attenuation rates were also calculated for variations of the TPH-d analysis (i.e., TPH-d with silica gel cleanup and total organic carbon [TOC]) to identify differences in attenuation rates for petroleum hydrocarbons vs. polar metabolites (Table 2-2). This information supports CSM Appendix B.7 and is discussed further in Section 3.4.

2.4 PLUME ATTENUATION: BIODEGRADATION RATE COEFFICIENT (Λ)

The Biodegradation Rate Coefficient (λ) describes the effect of biodegradation on COPC migration at one point in time and is expressed in units of inverse time. Biodegradation rate coefficients are generally smaller (and half-lives longer) than C vs. d attenuation rate coefficients, which reflect the combined effects of biodegradation, dispersion, and any other attenuation processes. For this study, biodegradation rate coefficients for each COPC were calculated using Equation 4 (Buscheck and Alcantar 1995) and Equation 5 (Xu and Eckstein 1995), as follows:

$$\lambda = (v_{gw}/4\alpha_x) \{[1 + 2\,\alpha_x(k/u)]^2 - 1\} \qquad (4)$$

$$\alpha_x = 2.72 \cdot [\log_{10}(L_p/3.28)]^{2.414} \qquad (5)$$

where:
λ = Biodegradation rate coefficient (d^{-1})
v_{gw} = Seepage velocity (ft/d)
α_x = Longitudinal dispersivity (ft)

k/u = The negative of the slope of a line obtained from a log-linear plot of the (center-line) COPC concentration versus distance downgradient along the flow path
L_p = Plume length (ft) (assumed to be the distance between RHMW01 and RHMW02)

Equation 4 (Buscheck and Alcantar 1995) assumes that (1) the plume is at steady-state, (2) monitoring wells are located along the centerline of groundwater flow, and (3) horizontal and vertical transverse dispersion are negligible. For purposes of this study, the distance between RHMW02 and RHMW01 (620 ft) was used as an estimate of plume length (L_p) to calculate longitudinal dispersivity. For a given COPC, the resulting biodegradation rate coefficient was calculated using the average slope of all data pairs and the estimated groundwater seepage velocity (12.4 ft per day; as discussed in Section 2.2). The same data pairs for each COPC (listed in Table 2-2) were used for this analysis. As with C vs. d rates, biodegradation rate coefficients were calculated for TPH-d (with silica gel cleanup) and TOC (Section 3.4).

2.5 PLUME ATTENUATION: RHMW02 TO RED HILL SHAFT

Similar to the analysis of COPC concentrations in RHMW02 and RHMW01, the change in COPC concentrations between RHMW02 and Red Hill Shaft can be used to estimate COPC attenuation rates (Equation 6). As Red Hill Shaft is a pumping well that induces flow, there is greater confidence in the flow path between RHMW02 and Red Hill Shaft than the flow path between RHMW01 and RHMW02 (note that particle tracking shows these well are on the same flowline, however). However, because Red Hill Shaft is a pumping well that captures groundwater flow from a large area, a modified evaluation method is required to account for dilution of COPCs caused by mixing of the plume with clean water. In addition, the attenuation rate is calculated based on travel time from RHMW02 to Red Hill Shaft rather than seepage velocity because the seepage velocity increases close to Red Hill Shaft (i.e., seepage velocity is not constant along the flow path). Groundwater seepage velocity and travel time at the Facility are highly uncertain due to the complex geology and flat water table (i.e., very low hydraulic gradient). Efforts to develop an improved understanding of groundwater flow at the Facility are ongoing. For a given concentration relationship, a shorter travel time yields a faster attenuation rate.

$$k = -\frac{Ln\left(C_{RHS-BD}/C_{RHMW02}\right)}{t} \quad (6)$$

where:
k = First-order attenuation rate coefficient (d^{-1})
C_{RHS-BD} = COPC concentration at Red Hill Shaft before dilution (Equation 7, µg/L)
C_{RHMW02} = COPC concentration at RHMW02 (µg/L)
t = Travel time from RHMW02 to Red Hill Shaft (Base case model = 64 days; Base with clinker model = 45 days, based on investigation's interim groundwater flow modeling)

The COPC concentration entering Red Hill Shaft before dilution due to mixing with clean groundwater can be estimated based on the volume of water pumped from Red Hill Shaft and the volume of water flowing through source area at the Facility (Equation 7):

$$C_{RHS-BD} = C_{RHS} \times \frac{Q_{RHS}}{V_a \times b \times W} \quad (7)$$

where:
C_{RHS-BD} = COPC concentration at Red Hill Shaft before dilution (µg/L)
C_{RHS} = Measured COPC concentration at Red Hill Shaft (i.e., after dilution, µg/L)

Q_{RHS} = Average pumping rate at Red Hill Shaft ([redacted])
V_d = Darcy velocity of groundwater in the Facility source area (1.63 ft/d for base model; 13 ft/d for base model with clinker; based on investigation's interim groundwater flow modeling)
b = Thickness of the light non-aqueous-phase liquid (LNAPL) source area at the Facility (2 m; 6.56 ft; assumed value from Connor, Newell, and Malander 1996)
W = Width of the LNAPL source area at the Facility (300 ft; assumed value based on width between rows of tanks)

In other words, the decrease in COPC concentration at Red Hill Shaft due to dilution with clean water is a function of the fraction of water that originates from the source area. Based on the input values used in Equation 7, 0.2% of the water captured by Red Hill Shaft flow through the source area at the Facility and the remaining 99.8% of the water does not contact the source area. This calculated estimate indicates N concentration in water entering Red Hill Shaft directly downgradient of RHMW02, before dilution by additional inflow along the tunnel may be about 620 times higher than the diluted N concentrations measured in diluted water samples collected for monitoring Red Hill Shaft.

3. Results

3.1 PLUME DURATION: POINT ATTENUATION (C VS. T) RATE COEFFICIENTS

Table 3-1 presents the C vs. t first-order attenuation coefficients, half-lives, number of data points, R^2 value, and the Mann Kendall p-value (significance level of 0.05) for the first-order model for each COPC at monitoring well RHMW02. At RHMW01, meaningful trend lines could not be developed for 1-MeN, 2-MeN, and N since the majority (> 50%) of concentration data were below respective detection limits.

Table 3-1: C vs. t Coefficients, Half-Lives, and First-Order Model Fit Parameters for the COPCs at RHMW02 (September 2005 to January 2019)

COPC	k (yr^{-1})	$t_{1/2}$ (yr)	n	R^2	p-value
1-Methylnaphthalene	-0.05	*	66	0.0167	0.916
2-Methylnaphthalene	0.04	**	66	0.0076	0.465
Naphthalene	0.03	**	66	0.0078	0.314

** Half-lives are not reported for 2-methylnaphthalene and naphthalene because attenuation rates were positive (Figure 3-2 and Figure 3-3). * Half-life for 1-methylnaphthalene is not reported because there is no statistically significant time trend.

k first-order rate coefficient
n number of samples
$t_{1/2}$ half-life
yr year
yr^{-1} per year

Figure 3-1 through Figure 3-3 present the linear and natural log scale plots for each COPC at monitoring well RHMW02. Concentrations of 1-MeN, 2-MeN, and N generally decreased during the initial 6 years of the monitoring period (2005–2011), followed by greater data scatter over the remainder. The observed scatter contributed to poor model fits and the resulting slopes were not statistically different than zero (p>0.05; Table 3-1); i.e., these COPCs show no statistically significant long-term concentration trend over the monitoring period.

The lack of a consistent trend in the C vs. t data for 1-MeN, 2-MeN, and N is not unexpected given the complexity of the light non-aqueous-phase liquid (LNAPL) source at the Facility. Since jet fuel is a complex mixture of aliphatic hydrocarbons (straight, branched, and cyclic alkanes), polynuclear aromatic hydrocarbons (PAHs, especially naphthalene and methylnaphthalenes), and heterocyclic compounds, each with different solubilities and biodegradation potential, it can be very difficult to clearly assess the rate of LNAPL depletion based solely on the C vs. t trends of individual components.

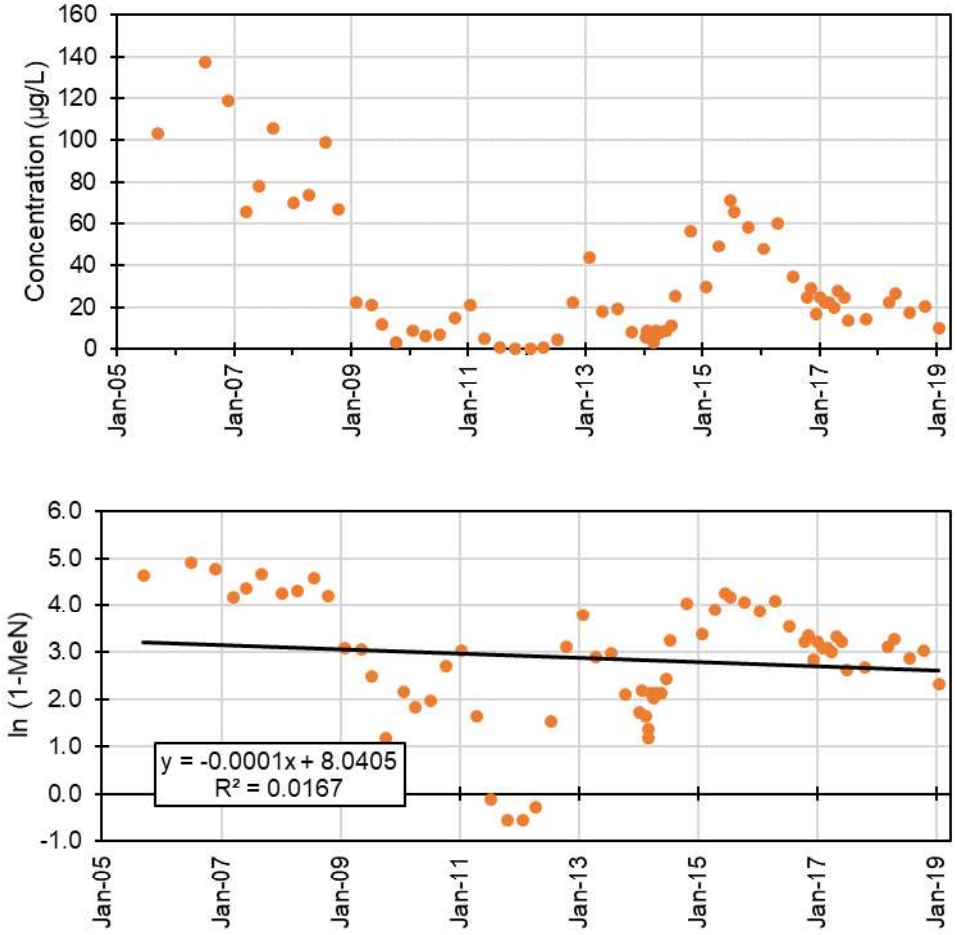

Figure 3-1: Linear and Natural Log Scale Plots of 1-Methylnaphthalene Concentrations from September 2005 to January 2019 at Monitoring Well RHMW02

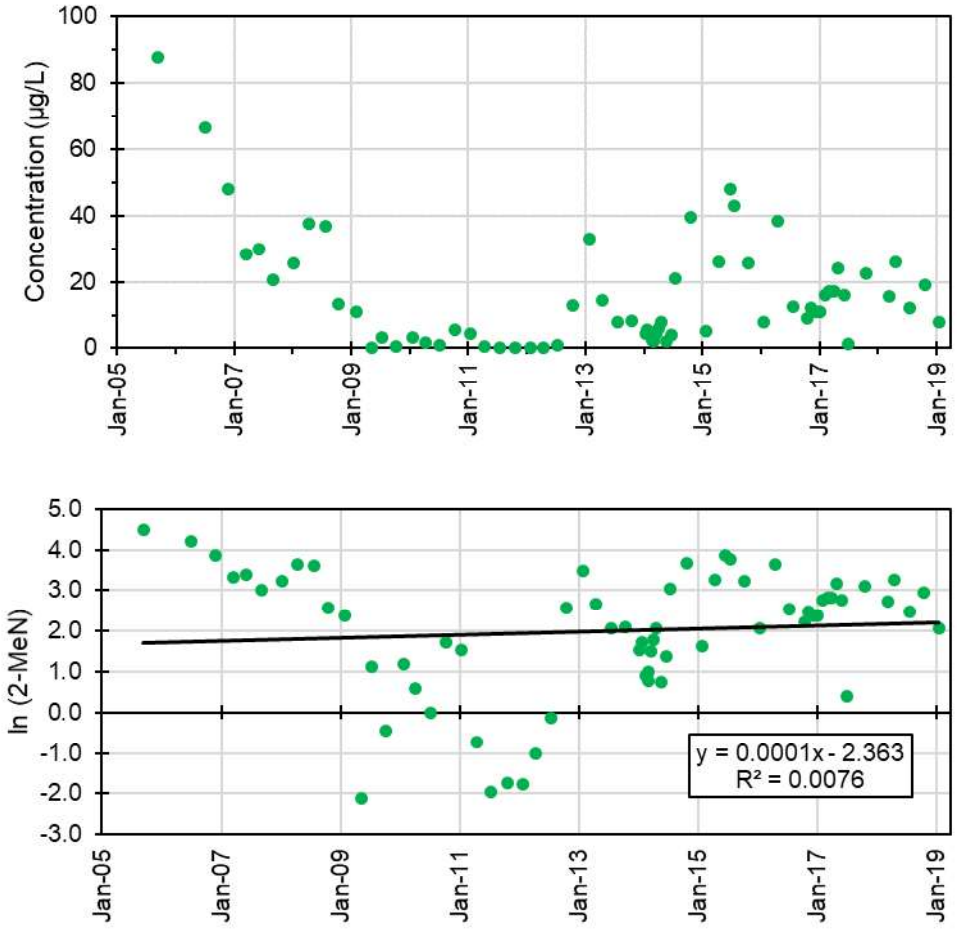

Figure 3-2: Linear and Natural Log Scale Plots of 2-Methylnaphthalene Concentrations from September 2005 to January 2019 at Monitoring Well RHMW02

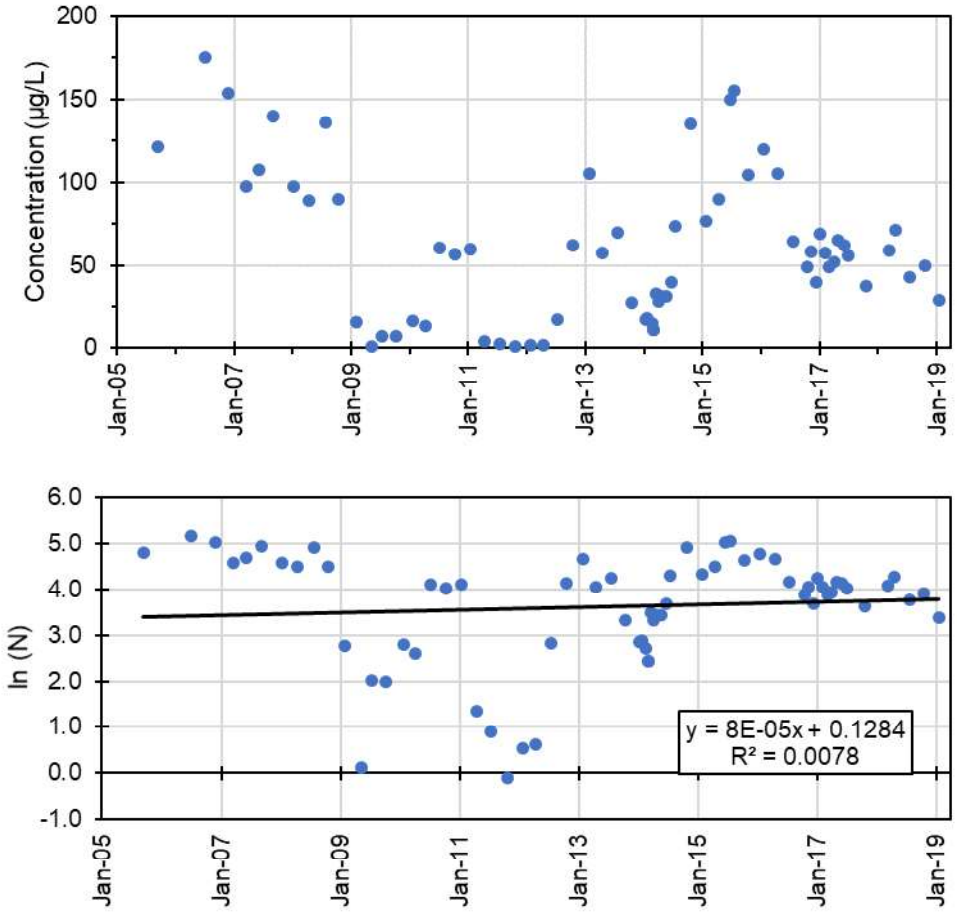

Figure 3-3: Linear and Natural Log Scale Plots of Naphthalene Concentrations from September 2005 to January 2019 at Monitoring Well RHMW02

3.2 PLUME ATTENUATION: BULK ATTENUATION (C VS. D) RATE COEFFICIENTS

A C vs. d attenuation rate was calculated for each data pair (i.e., each paired RHMW02–RHMW01 concentration measurement) for each COPC. Table 3-2 and Table 3-3 present the number of data pairs and the average first-order attenuation coefficient and corresponding half-life for each COPC. The results presented in Table 3-2 include data from sampling events where COPC concentrations above the detection limit were reported at *both* RHMW01 and RHMW02. The results presented in Table 3-3 include data from sampling events where COPC concentrations above the detection limit were reported at *one or both* of the wells. Attenuation rates and half-lives are reported in days in Table 3-2 and Table 3-3.

Table 3-2: C vs. d Bulk Attenuation Rate Coefficients and Half-Lives for the COPCs Along RHMW02–RHMW01 Transect (Includes Detected COPCs at Both Wells Only)

COPC	n	Base Case Model		Clinker Model	
		k (d^{-1}) *	$t_{1/2}$ (d)	k (d^{-1}) *	$t_{1/2}$ (d)
TPH-d	58	-0.16 ± 0.04	4.2	-0.11 ± 0.03	6.6
1-Methylnaphthalene	10	-0.44 ± 0.17	1.6	-0.28 ± 0.11	2.5
2-Methylnaphthalene	13	-0.40 ± 0.16	1.7	-0.25 ± 0.10	2.7
Naphthalene	25	-0.37 ± 0.12	1.9	-0.23 ± 0.08	3.0

* Attenuation rates are presented as mean ± standard deviation. Includes both dispersion and biodegradation effects.
d day
d^{-1} per day

Table 3-3: C vs. d Bulk Attenuation Rate Coefficients and Half-Lives for the COPCs Along RHMW02–RHMW01 Transect (Includes Detected COPCs at One or More Wells Only)

COPC	n	Base Case Model		Clinker Model	
		k (d^{-1}) *	$t_{1/2}$ (d)	k (d^{-1}) *	$t_{1/2}$ (d)
TPH-d	65	-0.17 ± 0.05	4.1	-0.11 ± 0.03	6.4
1-Methylnaphthalene	64	-0.36 ± 0.11	1.9	-0.23 ± 0.07	3.0
2-Methylnaphthalene	65	-0.32 ± 0.13	2.2	-0.20 ± 0.08	3.5
Naphthalene	65	-0.38 ± 0.10	1.8	-0.24 ± 0.06	2.8

* Attenuation rates are presented as mean ± standard deviation. Includes both dispersion and biodegradation effects.

Major findings/observations are summarized below:

1. C vs. d first-order bulk attenuation rate coefficients ranged from -0.11 d^{-1} to -0.44 d^{-1}, corresponding to half-lives of approximately 1.6–6.6 days (Table 3-2 and Table 3-3). As a result of the faster seepage velocity, higher attenuation rates and faster half-lives were calculated for the Base Case model compared to the Clinker model. These C vs. d rate coefficients (and associated half-lives) provide supporting evidence of COPC attenuation; however, these rates do reflect some uncertainty inherent in the calculations (e.g., limited number of well locations; uncertainty about the centerline of the plume and groundwater seepage velocity; uncertainty in flow path between RHMW01 and RHMW02).
2. Throughout the monitoring period, COPC concentrations at RHMW01 are 1–2 orders of magnitude (or more) lower than at RHMW02, suggesting that attenuation processes are potentially active and consistent along the groundwater flow path. This is also reflected in the relatively low variation in C vs. d attenuation rates over the monitoring period (i.e., small standard deviation). This observation suggests that the attenuation processes limiting migration of COPCs away from the area of RHMW02 have generally remained stable over the entire monitoring period (2005 to January 2019).
3. Bulk attenuation rate coefficients and associated half-lives for all COPCs were not appreciably different between the two data sets (i.e., excluding data pairs with one non-detect and including data pairs with one non-detect). This indicates that the C vs. d attenuation analysis is not sensitive to the laboratory analytical sensitivity for these COPCs.

These rates are based on methods presented in commonly used MNA protocols (e.g. Newell et al. 2002) and provide estimates of bulk attenuation processes that combine both the effects of dispersion and biodegradation. The results demonstrate that robust attenuation processes are ongoing in the aquifer. Biodegradation rates were calculated as discussed in Section 3.3.

3.3 PLUME ATTENUATION: BIODEGRADATION RATE COEFFICIENTS

Table 3-4 and Table 3-5 present the average first-order biodegradation rate coefficients, half-lives, and number of data pairs for the first-order model for each COPC along the RHMW02–RHMW01 transect. As discussed in Section 2.4, these biodegradation rates were calculated using the Buscheck and Alcantar (1995) method to separate the contributions of biodegradation and dispersion in the overall C vs. d attenuation rates. The results presented in Table 3-4 include data from sampling events where COPC concentrations above the detection limit were reported at *both* RHMW01 and RHMW02. The results presented in Table 3-5 include data from sampling events where COPC concentrations above the detection limit were reported at *one or both* of the wells. These rates are representative of aerobic biodegradation rates reported in literature (e.g., Suarez and Rifai 1999). The rates below can be used as starting point for calibration of the groundwater transport model.

Table 3-4: Biodegradation Rate Coefficients and Half-Lives for the COPCs along RHMW02–RHMW01 Transect (includes Detected COPCs at Both Wells Only)

		Base Case Model		Clinker Model	
COPC	n	λ (d^{-1}) *	$t_{1/2}$ (d)	λ (d^{-1}) *	$t_{1/2}$ (d)
TPH-d	58	-0.16 ± 0.04	4.6	-0.10 ± 0.03	7.2
1-Methylnaphthalene	10	-0.34 ± 0.18	2.0	-0.22 ± 0.11	3.2
2-Methylnaphthalene	13	-0.32 ± 0.17	2.2	-0.20 ± 0.11	3.4
Naphthalene	25	-0.30 ± 0.13	2.3	-0.19 ± 0.08	3.6

λ Biodegradation rate coefficient (d^{-1})

Table 3-5: Biodegradation Rate Coefficients and Half-Lives for the COPCs along RHMW02–RHMW01 Transect (includes Detected COPCs at One or More Wells Only)

		Base Case Model		Clinker Model	
COPC	n	λ (d^{-1}) *	$t_{1/2}$ (d)	λ (d^{-1}) *	$t_{1/2}$ (d)
TPH-d	65	-0.16 ± 0.05	4.5	-0.10 ± 0.03	7.0
1-Methylnaphthalene	64	-0.30 ± 0.12	2.3	-0.19 ± 0.07	3.6
2-Methylnaphthalene	65	-0.27 ± 0.14	2.6	-0.17 ± 0.09	4.1
Naphthalene	65	-0.31 ± 0.10	2.2	-0.20 ± 0.07	3.5

λ Biodegradation rate coefficient (d^{-1})

First-order biodegradation rate coefficients ranged from -0.10 d^{-1} to -0.34 d^{-1}, corresponding to half-lives of approximately 2–7.2 days (Table 3-4 and Table 3-5). The biodegradation rates for all COPCs were only slightly (8–21%) smaller than the respective C vs. d attenuation rates. This suggests that biodegradation is the primary attenuation process responsible for the reduction in COPC concentration from RHMW02 to RHMW01. As with the C vs. d attenuation rates, biodegradation rates were faster with the Base Case model compared to the Clinker Model.

3.4 PLUME ATTENUATION: RHMW02 TO RHMW01 ATTENUATION RATE COEFFICIENTS FOR TPH-D WITH SILICA GEL CLEANUP

The laboratory analytical method for TPH-d measures both diesel-range petroleum hydrocarbons and polar metabolites (see CSM Appendixes B.7 and B.8 for a more detailed discussion of issues associated with TPH-d analyses). In order to identify potential differences in attenuation rates for petroleum hydrocarbons vs. polar compounds/metabolites, C vs. d attenuation rates and biodegradation rates were determined for variations of the TPH-d analysis (Table 3-6 and Table 3-7):

- **TPH-d (65 paired measurements, 2005–2019):** The TPH-d analysis measures extractable organic matter that is measured by gas chromatography in the diesel range. It can include diesel-range petroleum hydrocarbons, polar compounds/metabolites and other naturally occurring organic matter.
- **TPH-d with Silica Gel Cleanup: (7 paired measurements, 2017–2019):** Silica gel cleanup removes the polar compounds/metabolites and other naturally occurring organic matter while retaining the diesel-range petroleum hydrocarbons.
- **Total Organic Carbon (TOC; 5 paired measurements, 2017–2019):** TOC measures all organic material in the sample including some polar compounds/metabolites and other naturally occurring organic matter that may not be extracted by the TPH-d extraction procedure or measurable by gas chromatography.

Table 3-6: C vs. d Rate Coefficients and Half-Lives for TPH-d, TPH-d (with silica gel cleanup), and TOC along RHMW02–RHMW01 Transect

COPC	n	k (d^{-1})	$t_{1/2}$ (d)
TPH-d	65	-0.05 ± 0.01	13.4
TPH-d (silica gel)	7	-0.05 ± 0.01	14.1
Total Organic Carbon	5	-0.04 ±0.01	19.7

		Base Case Model		Clinker Model	
COPC	n	k (d^{-1}) *	$t_{1/2}$ (d)	k (d^{-1}) *	$t_{1/2}$ (d)
TPH-d	65	-0.17 ± 0.05	4.1	-0.11 ± 0.03	6.4
TPH-d (silica gel)	64	-0.16 ± 0.03	4.3	-0.10 ± 0.02	6.7
TOC	65	-0.12 ± 0.03	6.0	-0.07 ± 0.02	9.4

Table 3-7: Biodegradation Rate Coefficients and Half-Lives for TPH-d, TPH-d (with silica gel cleanup), and TOC along RHMW02–RHMW01 Transect

COPC	n	λ (d^{-1})	$t_{1/2}$ (d)
TPH-d	65	-0.05 ± 0.01	14.6
TPH-d (silica gel)	7	-0.05 ± 0.01	15.3
Total Organic Carbon	5	-0.03 ± 0.01	20.9

		Base Case Model		Clinker Model	
COPC	n	λ (d^{-1}) *	$t_{1/2}$ (d)	λ (d^{-1}) *	$t_{1/2}$ (d)
TPH-d	65	-0.16 ± 0.05	4.5	-0.10 ± 0.03	7.0
TPH-d (silica gel)	64	-0.15 ± 0.03	4.6	-0.10 ± 0.02	7.3
TOC	65	-0.11 ± 0.03	6.4	-0.07 ± 0.02	10.0

As shown in Table 3-6 and Table 3-7, the C vs. d attenuation rates and the biodegradation rates are similar for the analyses that include or exclude the polar metabolites. This suggests that the diesel-range petroleum hydrocarbons and the polar metabolites are attenuating at similar rates within the groundwater at the Facility. The faster seepage velocity of the Base Case Model resulted in faster attenuation rates and shorter half-lives compared to the Clinker Model.

3.5 PLUME ATTENUATION: RHMW02 TO RED HILL SHAFT

The C vs. d attenuation rate coefficient for COPC migration from RHMW02 to Red Hill Shaft was evaluated only for NAPH because, to date, it has been the most commonly detected individual COPC at Red Hill Shaft (detections for 12 of 75 sampling events from 2005 to January 2019). The very low detection frequency for other COPCs results in too much uncertainty regarding COPC concentration. For NAPH, the average concentration over the monitoring period was used to determine the C vs. d attenuation rate coefficient. Use of the average concentration was considered appropriate because:

- The C vs. t analysis indicates little overall concentration trend at RHMW02 (slope of the trendline ≈ 0) over the monitoring period (Figure 3-3).
- The travel time from RHMW02 to Red Hill Shaft (95 days for the base model and 45 days for the base with clinker model, based on the investigation's interim groundwater flow modeling) makes it difficult to pair individual measurements at RHMW02 and Red Hill Shaft.
- During some parts of the monitoring period, the sampling frequency at RHMW02 has been higher than for Red Hill Shaft (e.g., 2014).

The average N concentration at Red Hill Shaft was used to determine the C vs. d attenuation rate coefficient. The average was calculated by averaging the detected results and ignoring the non-detect results (Average C = 0.049 µg/L). For RHMW02, N has been detected during all 66 sampling events from 2005 to January 2019 (Average C = 60 µg/L). Two attenuation rates were calculated based on two estimates of travel time from RHMW02 to Red Hill Shaft: (1) the travel time from the base case groundwater flow model (64 days) and (2) the travel time for the base case model including a clinker zone connecting the Facility source area to the Red Hill Shaft (45 days) (Table 3-8).

A second analysis of plume attenuation to Red Hill Shaft was conducted using data from the April 2015 to July 2016 period. During this period, all N results at Red Hill Shaft were non-detect with a MDL of 0.005 µg/L. The MDL was used as the proxy value for the N concentration at Red Hill Shaft. For RHMW02, N was detected during all six monitoring events during this period (Average C = 106 µg/L).

Table 3-8: RHMW02 to Red Hill Shaft Attenuation Rate Coefficients Using All Naphthalene Detects at Red Hill Shaft (2005 to January 2019)

COPC	n (RHMW02)	n (RH Shaft)	C_{RHMW02} (µg/L)	C_{RHS-BD} (µg/L)	t (d)	k (d^{-1})	$t_{1/2}$ (d)
Naphthalene (base case model)	66	12	60	31	95	0.03	24
Naphthalene (base model with clinker)	66	12	60	11	45	0.09	8

Note: The concentration entering Red Hill Shaft before dilution (C_{RHS-BD}) was calculated using Equation 7 above using the average measured naphthalene concentration in Red Hill Shaft for detected results of 0.049 µg/L.

Table 3-9: RHMW02 to Red Hill Shaft Attenuation Rate Coefficients Using Naphthalene Results from April 2015 to July 2016

COPC	n (RHMW02)	n (RH Shaft)	C_{RHMW02} (µg/L)	C_{RHS-BD} (µg/L)	t (d)	k (d^{-1})	$t_{1/2}$ (d)
Naphthalene (base case model)	6	6	106	3	95	0.07	9
Naphthalene (base model with clinker)	6	6	106	1.1	45	0.15	5

Note: The concentration entering Red Hill Shaft before dilution (C_{RHS-BD}) was calculated using Equation 7 above using the naphthalene method detection limit in Red Hill Shaft of 0.005 µg/L for the period of April 2015 to July 2016.

Based on this range of analyses, the plume attenuation half-life for N from RHMW02 to Red Hill Shaft was between 5 days (based the 2015–2016 monitoring period and travel time for the base case groundwater flow model with the clinker zone) and 24 days (based the N detects during the full monitoring period and travel time for the base case groundwater flow model without the clinker zone).

4. Conclusions

Groundwater monitoring data from the Facility over the monitoring period of 2005 to April 2018 were used to evaluate Plume Duration and Plume Attenuation. These evaluations support the following observations:

- **Plume Duration:** COPC concentrations at individual monitoring locations vary over time exhibiting both increases and decreases in concentration. At RHMW02, the monitoring location with the highest COPC concentrations, most of the COPCs show little or no long-term concentration trend due to high data variability over the monitoring period. The observed variability in COPC concentration reflects the complexity of the LNAPL source (i.e., complex mixture of individual compounds, each with different solubilities and biodegradation potential) and the changing composition of the LNAPL source over time.
- **Plume Attenuation:** COPC concentrations generally decrease from the source area (represented by RHMW02) to downgradient monitoring locations (RHMW01 and Red Hill Shaft). C vs. d bulk attenuation half-lives range from 2 to 7 days for the analysis of concentration changes from RHMW02 to RHMW01 while half-lives range from 5 to 24 days for the analysis of concentration changes from RHMW02 to Red Hill Shaft. Although both analyses support the conclusion that biodegradation is contributing to the natural attenuation of COPCs within groundwater, the estimated rate of attenuation varies by an order of magnitude depending on the data set and assumptions used. Both evaluations of C vs. d attenuation rates depend on important assumptions:
  - **RHMW02 to RHMW01:** This analysis assumes that RHMW02 and RHMW01 are in the same flow path (i.e., the COPCs present in RHMW01 originated in the vicinity of RHMW02) as indicated by the groundwater flow model. If the COPCs in RHMW01 actually originate from a different lower strength source (or a more distant source) than the analysis would overestimate the true attenuation rate.
  - **RHMW02 to Red Hill Shaft:** As a conservative measure, this analysis assumes that the very low N concentrations detected in Red Hill Shaft (i.e., <0.1 µg/L) reflect the actual N concentration in the Red Hill Shaft water rather than false-positive artifacts of laboratory analysis. For example, for a number of sample events in 2013 and 2014, low concentrations of N (<0.1 µg/L) were detected in most or all of the groundwater samples, including those from wells upgradient of the Facility source area (see CSM Appendix B.8 for additional discussion of the uncertainty associated with the low concentration detections of N). If the actual N concentrations in Red Hill Shaft are lower than those indicated by the laboratory detections, then the analysis would underestimate the true attenuation rate.
- **Groundwater Seepage Velocity:** Groundwater seepage velocity at the Facility is highly variable due to the heterogeneous geology and flat water table (i.e., very low hydraulic gradient). Efforts to develop an improved understanding of groundwater flow at the Facility are ongoing.

Taken together, analysis of RHMW02 to RHMW01 and RHMW02 to Red Hill Shaft represents an estimated range of plume bulk attenuation rates for COPCs in groundwater at the Facility (i.e., an attenuation half-life of 1.6–7.2 days or 5–24 days). These rate calculations demonstrate that robust attenuation processes are present in the groundwater underlying the Facility; they provide a starting point for the groundwater model and will be fine-tuned in the model.

5. References

Buscheck, T. E., and C. M. Alcantar. 1995. "Regression Techniques and Analytical Solutions to Demonstrate Intrinsic Bioremediation." In *Intrinsic Bioremediation (Proceedings from the Third International In Situ and On-Site)*. Columbus, OH: Battelle Press.

Connor, J. A., C. J. Newell, and M. W. Malander. 1996. *Parameter Estimation Guidelines for Risk-Based Corrective Action (RBCA) Modeling*. National Ground Water Association Petroleum Hydrocarbons Conference, Houston, TX, November.

Department of Defense and Department of Energy, United States (DoD and DOE). 2017. *Department of Defense (DoD) and Department of Energy (DOE) Consolidated Quality Systems Manual (QSM) for Environmental Laboratories*. DoD QSM Ver. 5.1; DOE Quality Systems for Analytical Services Ver. 3.1. Prepared by DoD Environmental Data Quality Workgroup and DOE Consolidated Audit Program Operations Team.

Department of Defense Environmental Data Quality Workgroup. 2017. *Fact Sheet: Detection and Quantification – What Project Managers and Data Users Need to Know*. October.

Department of the Navy (DON). 1999. *Initial Phase II Site Characterization Report, Fleet Industrial Supply Center Bulk Fuel Storage Facility at Red Hill*. Prepared by Ogden Environmental and Energy Services Co., Inc., Honolulu, HI. Pearl Harbor, HI: Naval Facilities Engineering Command, Pacific. March.

———. 2002. *Red Hill Bulk Fuel Storage Facility Investigation Report (Final) for Fleet Industrial Supply Center (FISC), Oahu, Hawaii*. Prepared by AMEC Earth & Environmental, Inc., Huntsville, AL. Pearl Harbor, HI: Naval Facilities Engineering Command, Pacific. August.

Environmental Protection Agency, United States (EPA). 1999. *Use of Monitored Natural Attenuation at Superfund, RCRA Corrective Action, and Underground Storage Tank Sites*. OSWER 9200.4-17P. Office of Solid Waste and Emergency Response. April.

Newell, C. J., H. S. Rifai, J. T. Wilson, J. A. Connor, J. A. Aziz, and M. P. Suarez. 2002. *Calculation and Use of First-Order Rate Constants for Monitored Natural Attenuation Studies*. Ground Water Issue. EPA/540/S-02/500. Cincinnati: EPA National Risk Management Research Laboratory. November.

Suarez, M. P., and H. S. Rifai. 1999. "Biodegradation Rates for Fuel Hydrocarbons and Chlorinated Solvents in Groundwater." *Bioremediation Journal* 3 (4): 337–362. https://doi.org/10.1080/10889869991219433.

Wiedemeier, T. H., H. S. Rifai, C. J. Newell, and J. T. Wilson. 1999. *Natural Attenuation of Fuels and Chlorinated Solvents in the Subsurface*. New York: John Wiley & Sons, Inc.

Wiedemeier, T. H., J. T. Wilson, D. H. Kampbell, R. N. Miller, and J. E. Hansen. 1999. *Technical Protocol for Implementing Intrinsic Remediation with Long-Term Monitoring for Natural Attenuation of Fuel Contamination Dissolved in Groundwater. Vols. I & II*. San Antonio, TX: Air Force Center for Environmental Excellence, Technology Transfer Division. March.

Xu, Moujin, and Yoram Eckstein. 1995. "Use of Weighted Least-Squares Method in Evaluation of the Relationship Between Dispersivity and Field Scale." *Ground Water* 33 (6): 905–8. https://doi.org/10.1111/j.1745-6584.1995.tb00035.x.

Appendix B.5:
MNA Secondary Lines of Evidence

CONTENTS

Acronyms and Abbreviations iii

1. Introduction 1-1

1.1 Technical Background 1-1
1.2 Study Objectives 1-1

2. Methods 2-1

2.1 Data Handling and Consolidation 2-1

3. Results 3-1

3.1 Spatial Concentrations of Geochemical Indicators 3-1
3.2 Temporal Concentrations of Geochemical Indicators 3-3
3.3 Key Relationships Between COPCs and Geochemical indicators 3-5

4. Conclusions 4-1

5. References 5-1

ATTACHMENTS

B.5.1 Time-Series Plots for Alkalinity, NO_3^-, SO_4^{2-}, Cl, Fe^{2+}, CH_4, DO, and ORP at All Monitoring Well Locations

B.5.2 X-Y Plots for Alkalinity, NO_3^-, SO_4^{2-}, Cl, Fe^{2+}, CH_4, DO, ORP, and COPCs at All Monitoring Well Locations

FIGURES

1-1 Location of the Facility Monitoring Wells in Relation to Tank Farm Area 1-2

3-1 Concentrations of O_2, NO_3^-, SO_4^{2-}, Fe^{2+}, CH_4, and ORP from the Facility Groundwater Monitoring Network on January 21 – February 7, 2019 3-2

3-2 Time-Series Plots of NO_3^- (Left Panel) and SO_4^{2-} (Right Panel) Concentrations at Monitoring Wells RHMW01, RHMW02, RHMW03, and RHMW05 3-4

3-3 Time-Series Plots of Fe^{2+} (Left Panel) and CH_4 (Right Panel) Concentrations at Monitoring Wells RHMW01, RHMW02, RHMW03, and RHMW05 3-4

3-4 Time-Series Plots of O2 (Left Panel) and ORP (Right Panel) Concentrations at Monitoring Wells RHMW01, RHMW02, RHMW03, and RHMW05 3-5

3-5 X-Y Plots for TPH-d Concentrations vs. NO_3^- (Left Panel) and SO_4^{2-} (Right Panel) Concentrations at Monitoring Wells RHMW01, RHMW02, RHMW03, and RHMW05 3-6

3-6 X-Y Plots for TPH-d Concentrations vs. Fe^{2+} (Left Panel) and CH_4 (Right Panel) Concentrations at Monitoring Wells RHMW01, RHMW02, RHMW03, and RHMW05 3-6

3-7 X-Y Plots for TPH-d Concentrations vs. DO Concentrations (Left Panel) and ORP (Right Panel) at Monitoring Wells RHMW01, RHMW02, RHMW03, and RHMW05 3-7

ACRONYMS AND ABBREVIATIONS

µg/L	micrograms per liter
1-MeN	1-methylnaphthalene
2-MeN	2-methlynaphthalene
CH_4	methane
CO_2	carbon dioxide
COPC	chemical of potential concern
CSM	conceptual site model
DL	detection limit
DO	dissolved oxygen
EPA	Environmental Protection Agency, United States
Fe^{2+}	ferrous iron
LOD	limit of detection
LOQ	limit of quantitation
MDL	method detection limit
mg/L	milligrams per liter
MNA	monitored natural attenuation
mV	millivolt
N	naphthalene
NO_3^-	nitrate as nitrogen
O_2	oxygen
ORP	oxidation-reduction potential
RL	reporting limit
SO_4^{2-}	sulfate
TEA	terminal electron acceptor
TPH-d	total petroleum hydrocarbons – diesel-range organics

1. Introduction

This subappendix is summarized in Section 7.3.2.4 of the Conceptual Site Model (CSM) main document.

1.1 TECHNICAL BACKGROUND

The United States Environmental Protection Agency (EPA) defines monitored natural attenuation (MNA) as:

> *...the reliance on natural attenuation processes (within the context of a carefully controlled and monitored clean-up approach) to achieve site-specific remedial objectives within a time frame that is reasonable compared to other methods. The "natural attenuation processes" that are at work in such a remediation approach include a variety of physical, chemical, or biological processes that, under favorable conditions, act without human intervention to reduce the mass, toxicity, mobility, volume, or concentration of contaminants in soil and ground water. These in-situ processes include, biodegradation, dispersion, dilution, sorption, volatilization, and chemical or biological stabilization, transformation, or destruction of contaminants* (EPA 1999).

A lines-of-evidence approach is commonly used to demonstrate that natural attenuation processes are occurring at a given site. Primary and secondary lines of evidence to evaluate MNA are:

- **Primary:** Rate of change in dissolved-phase contaminant concentrations, both spatially and temporally, as a metric for plume behavior/status (i.e., stable, shrinking, expanding). Site-specific attenuation rate coefficient calculations can be used to evaluate the contribution of attenuation processes and estimate the time required to achieve remediation objectives. Primary lines of evidence are discussed in CSM Appendix B.4.
- **Secondary:** Hydrogeologic and geochemical data as an indirect measure of active natural attenuation processes that support primary evidence/observations (e.g., decrease in parent contaminant concentrations). For example, changes in electron acceptor concentrations can be strong evidence for in-situ biodegradation of the parent compounds. Under aerobic conditions, oxygen serves as a terminal electron acceptor (TEA), while under anaerobic conditions, nitrate, sulfate, and carbon dioxide may serve as a TEA for the microbially mediated redox reactions (McCarty, Rittman, and Bouwer 1984).

1.2 STUDY OBJECTIVES

The objective of this study is to evaluate natural attenuation processes at the Red Hill Bulk Fuel Storage Facility (the "Facility") using secondary lines of evidence (e.g., geochemical data, electron acceptor concentrations) from the Facility groundwater monitoring network. The following analytes were considered in this study: total alkalinity, nitrate as nitrogen (NO_3^-), ferrous iron (Fe^{2+}), sulfate (SO_4^{2-}), and methane (CH_4). In addition, field measurements of dissolved oxygen (O_2) and oxidation-reduction potential (ORP) were incorporated. Chloride concentrations were also included as there is spatial variability at the site, additional discussion is provided in CSM Appendix B.8. Where sufficient data were available, relationships between electron acceptor concentrations (and field parameters) and concentrations of chemicals of potential concern (COPCs) were identified for all monitoring wells. COPCs include diesel-range total petroleum hydrocarbons (TPH-d), 1-methylnaphthalene (1-MeN), 2-methylnaphthalene (2-MeN), and naphthalene (N). Figure 1-1 provides the locations of the Facility

monitoring wells in relation to the tank farm. Data analysis/interpretation methods are described in Section 2.

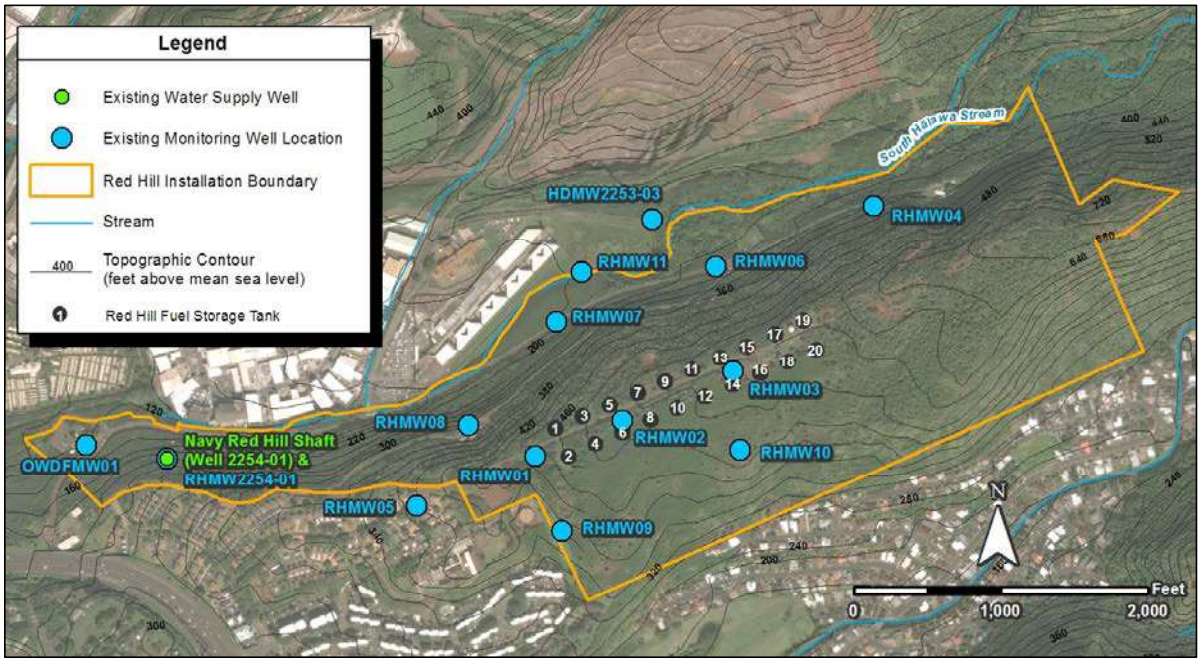

Figure 1-1: Location of the Facility Monitoring Wells in Relation to Tank Farm Area

2. Methods

Groundwater data from October 2016 to present (January/February 2019) were evaluated for all monitoring wells in the Facility network. Limited data from 2005 to 2007 were also included for monitoring wells RHMW01, RHMW02, RHMW03, and RHMW04, which were installed in 2001 (RHMW01) and 2005 (RHMW02, RHMW03, and RHMW04).

Two key lines of secondary evidence used to support MNA processes at the Facility, specifically biodegradation of COPCs, are summarized below (Beck and Mann 2010):

- **Depletion of TEAs:** Reduction of oxygen (O_2), nitrate (NO_3^-), and sulfate (SO_4^{2-}), in combination with declining COPC concentrations, provide strong evidence of COPC biodegradation, rather than simply attenuation by other mechanisms (e.g., volatilization, sorption, dilution).
- **Production of byproducts:** Detection and/or increasing concentrations of ferrous iron (Fe^{2+}), methane (CH_4), and carbon dioxide (CO_2; measured as alkalinity) provide supporting evidence of microbially mediated redox reactions. When all the soluble electron acceptors (i.e., dissolved oxygen, nitrate, ferric iron, and sulfate) are depleted, groundwater conditions become conducive to fermentation and methane is generated by methanogenesis. When evaluated alongside depressed TEA concentrations, the presence of methane is a strong line of evidence of anaerobic biodegradation.

Based on well-established MNA guidance (Newell, McLeod, and Gonzales 1996; EPA 1999; Wiedemeier, Wilson, et al. 1999; Wiedemeier, Rifai, et al. 1999), time-series plots and X-Y plots (COPC concentrations vs. TEA or byproduct concentrations) were developed to improve interpretation and analysis of the data set.

2.1 Data Handling and Consolidation

For this analysis, historical data from 2005 to January/February 2019 were considered, with the following modifications to the data set:

- COPC concentrations reported by the laboratory as non-detect were assigned a concentration equal to the limit reported (e.g., < 0.1 µg/L = 0.1 µg/L). The limit may be the limit of detection (LOD), method detection limit (MDL), or reporting limit (RL). The type of limit reported for COPC concentrations is not known for all data. The LOD is a statistically derived concentration that can be distinguished from a blank with 99% confidence. The MDL is a statistically derived concentrations that can be distinguished from zero with 99% confidence.
- Qualified data (e.g., "J" flag) were assigned the reported COPC concentration (e.g., 12 J µg/L = 12 µg/L). Note that when a COPC is detected at a concentration below the limit of quantitation (LOQ), the laboratory reports the result as detected, but the result is flagged with a "J" flag.
- For sampling events where duplicates were collected, the average of the primary concentration and duplicate concentration was used for each COPC.

Challenges with organic data interpretation must be considered when using the data to discuss trends. Issues with respect to sample analysis include: (1) analysis has been conducted by multiple labs with different reporting/detection limits, (2) analytical methodologies have also changed over time, and

(3) very low concentrations (for example, naphthalenes have had detection limits down to 0.005 µg/L) push laboratory abilities and may result in QA/QC issues. Issues with respect to field work and well installation may include: (1) comparing wells that were constructed differently (e.g., Hālawa Deep, RHMW11), or (2) installation of monitoring wells and routine site operations may intriduce low concentrations of chemicals to groundwater. These issues and more are discussed in detail in CSM Appendix B.8.

3. Results

3.1 SPATIAL CONCENTRATIONS OF GEOCHEMICAL INDICATORS

Figure 3-1 presents concentrations of electron acceptors (O_2, NO_3^-, SO_4^{2-}), metabolic byproducts (Fe^{2+}, CH_4), and ORP for the most recent groundwater sampling event (January 21 – February 7, 2019) at the Facility. Major findings/observations are summarized below:

- Spatial patterns observed for this most recent sampling event (January/February 2019) are consistent with those observed for prior sampling events for TEAs (O_2, NO_3^-, SO_4^{2-}) and metabolic byproducts (Fe^{2+}, CH_4). As shown on Figure 3-1, concentrations of O_2, NO_3^-, and SO_4^{2-} at monitoring wells RHMW01 and RHMW02 are much lower than concentrations in wells outside of the tank farm area. In addition, higher concentrations of Fe^{2+} and CH_4 are observed at these wells, relative to rest of the monitoring network. These observations strongly suggest that microbially mediated reactions are responsible for degradation of petroleum hydrocarbons (electron donor), depletion of available TEAs, and generation of anaerobic conditions (i.e., low O_2 and negative ORP values) at monitoring wells RHMW01 and RHMW02.
- For the most recent sampling event (January/February 2019), concentrations of O_2 were very low (< 1 milligram per liter [mg/L]) at RHMW01 and RHMW02 compared to the wells located outside of the tank farm area (where O_2 concentrations were generally greater than 5 mg/L). Likewise, ORP values consistent with mildly reducing conditions were reported at these wells. ORP values for wells located outside of the tank farm area were greater than 40 millivolts (mV), consistent with aerobic conditions. The three wells outside the tank farm area with the lowest O_2 (RHMW11-05, Hālawa Deep, RHMW07) are not representative of water table chemistry because of well construction (RHMW11-05), screened interval (Hālawa Deep), and hydraulic isolation (RHMW07). Also, water that has come into contact with saprolite (as is possible for these wells) is expected to have low dissolved oxygen (DO) (Hunt, Jr. 2004). This is discussed in more detail in CSM Appendix B.8.
- During the most recent sampling event (January/February 2019), the highest concentrations of Fe^{2+} and CH_4 and lowest concentrations of O_2, NO_3^-, and SO_4^{2-} were observed at RHMW02 (where COPC concentrations are greatest). A similar relationship (depletion of TEAs, increase in byproducts, presence of TPH-d) was observed at RHMW01. These observations are consistent with active hydrocarbon biodegradation in this area. Methane was not detected in soil vapor samples; the aerobic conditions of the vadose zone likely allow for rapid oxidation of methane to carbon dioxide. At RHMW03, depletion of TEAs and production of metabolic byproducts were not observed to the same extent (with the exception of low DO), despite the presence of detectable concentrations of TPH-d. This is potentially due to the influx of groundwater from upgradient of RHMW03.

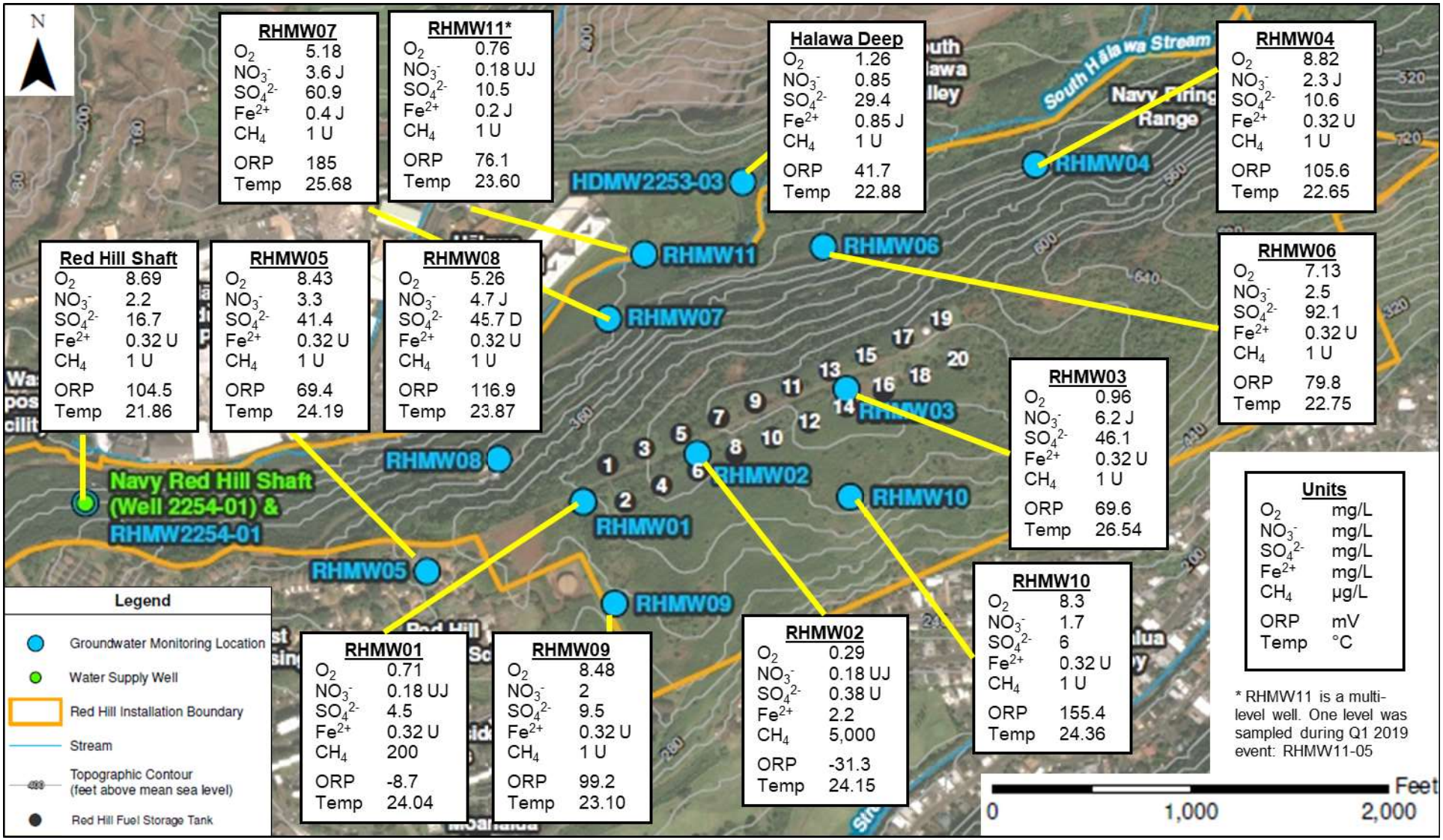

Figure 3-1: Concentrations of O_2, NO_3^-, SO_4^{2-}, Fe^{2+}, CH_4, and ORP from the Facility Groundwater Monitoring Network on January 21 – February 7, 2019

3.2 TEMPORAL CONCENTRATIONS OF GEOCHEMICAL INDICATORS

Attachment B.5.1 presents time-series plots for COPCs, electron acceptors, and metabolic byproducts at all Facility monitoring locations. For each analyte, three plots are presented: (1) all available data from February 2005 to January/February 2019 for all wells, (2) data from October 2016 to January/February 2019 for all wells, and (3) data from October 2016 to January/February 2019 for wells RHMW01, RHMW02, RHMW03, and RHMW05. In general, concentrations of electron acceptors and metabolic byproducts at each well have remained stable over the monitoring period (2016–2019), with a few exceptions (as discussed below).

Figure 3-2, Figure 3-3, and Figure 3-4 present NO_3^-, SO_4^{2-}, Fe^{2+}, CH_4, DO, and ORP from October 2016 to January/February 2019 for four monitoring wells RHMW01, RHMW02, RHMW03, and RHMW05, located within and in close proximity to, the tank farm area. Major findings/observations are summarized below:

- Concentrations of NO_3^-, Fe^{2+}, and SO_4^{2-} have remained fairly stable (with only minor fluctuations) at these monitoring wells from October 2016 to January/February 2019. Methane concentrations at RHMW01 and RHMW02 have decreased over the same period. Specifically, CH_4 concentrations at RHMW01 have decreased from 7,500 µg/L (November 2016) to 200 µg/L (January 2019); at RHMW02, concentrations have declined from 47,000 µg/L (October 2016) to 5,000 µg/L (January 2019). Methane concentrations were reported in 2007 for RHMW01 (811 µg/L) and RHMW02 (1140 and 1400 µg/L).
- As discussed in Section 3.1, concentrations of the electron acceptors NO_3^- and SO_4^{2-} are greatest at monitoring wells RHMW03 and RHMW05, located generally upgradient and downgradient respectively, of RHMW02. Dissolved oxygen is depleted at RHMW03, but is near saturation at RHMW05. Likewise, ORP values at RHMW03 and RHMW05 reflect generally aerobic conditions, while ORP at RHM02 and RHMW01 is consistent with mildly reducing conditions. These observations support that geochemical conditions are generally re-established along the presumed direction of groundwater flow within the tank farm area (i.e., toward Red Hill Shaft). Low to non-detect concentrations of Fe^{2+} and CH_4 (Figure 3-3) at these wells further support this conclusion.

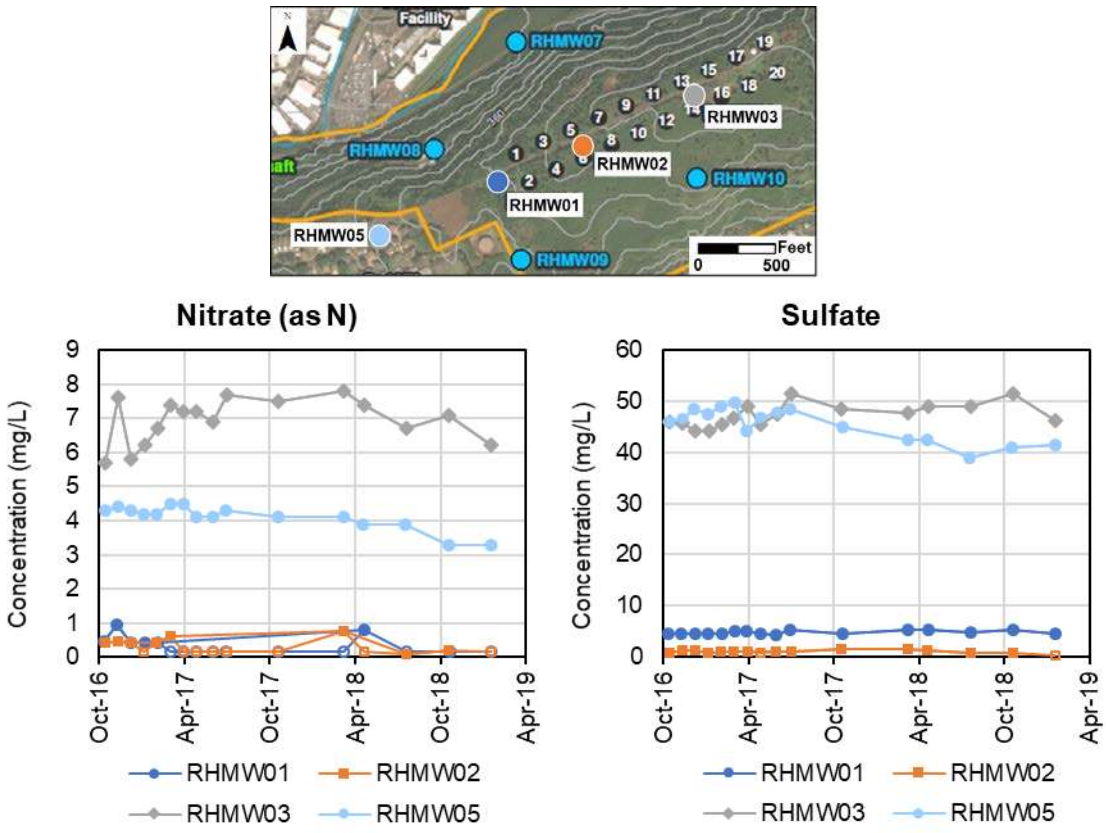

Note: Non-detect samples are shown as open markers.

Figure 3-2: Time-Series Plots of NO_3^- (Left Panel) and SO_4^{2-} (Right Panel) Concentrations at Monitoring Wells RHMW01, RHMW02, RHMW03, and RHMW05

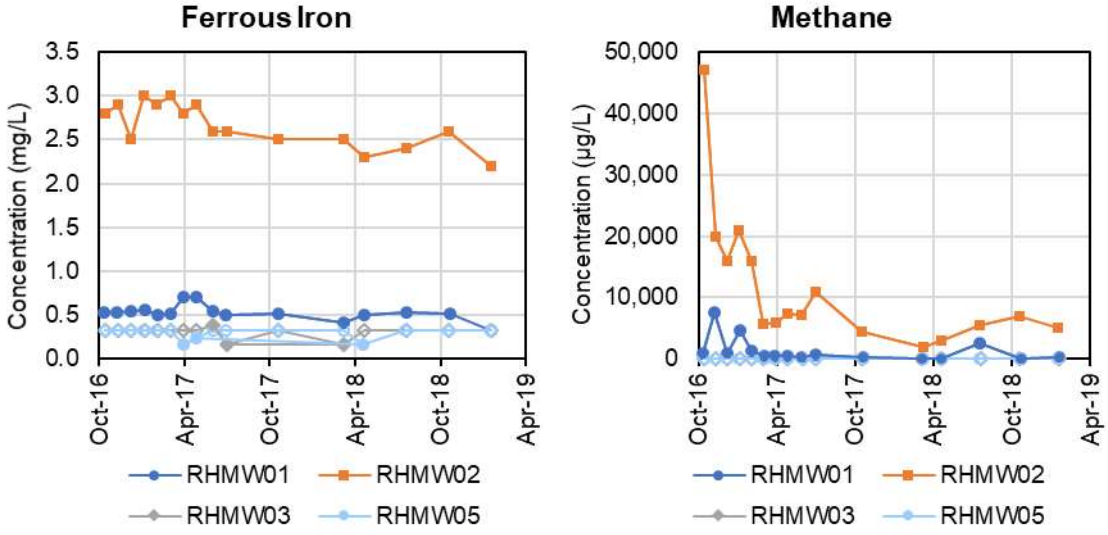

Note: Non-detect samples are shown as open markers.

Figure 3-3: Time-Series Plots of Fe^{2+} (Left Panel) and CH_4 (Right Panel) Concentrations at Monitoring Wells RHMW01, RHMW02, RHMW03, and RHMW05

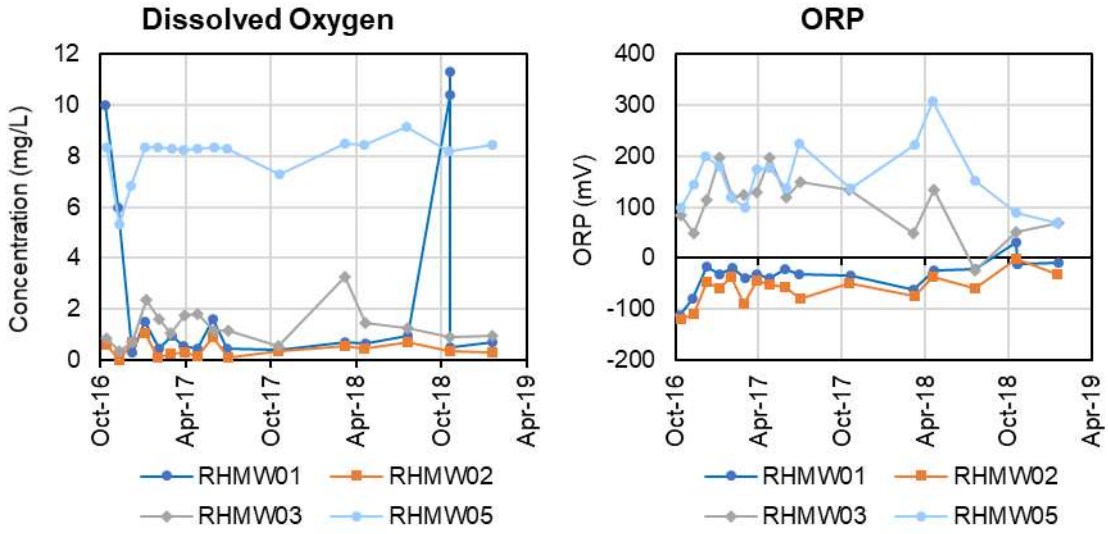

Figure 3-4: Time-Series Plots of O2 (Left Panel) and ORP (Right Panel) Concentrations at Monitoring Wells RHMW01, RHMW02, RHMW03, and RHMW05

3.3 KEY RELATIONSHIPS BETWEEN COPCS AND GEOCHEMICAL INDICATORS

Attachment B.5.2 presents X-Y plots for all COPCs (TPH-d, TPH-g, TPH-o, 1-MeN, 2-MeN, N) relative to concentrations of electron acceptors and metabolic byproducts at all Facility monitoring locations. For the X-Y graphs, the x-axis represents COPC concentrations; y-axis represents electron acceptor or metabolic byproduct concentrations. Since COPCs are detected primarily at RHMW02 (with some detections and qualified detections of select COPCs at RHMW01 and RHMW03) over the monitoring period, these X-Y plots clearly highlight the distinct difference in geochemistry and COPC concentrations at RHMW02 compared to the rest of the monitoring network (i.e., grouping of RHMW02 data stands apart from other wells). For cases where a COPC is also detected at RHMW01 and RHMW03 (i.e., TPH-d), some general trends are observed on the plots. For example, as shown on Figure 3-5, Figure 3-6, and Figure 3-7 the highest TPH-d concentrations (at RHMW02) are generally related to decreasing DO, NO_3^-, and SO_4^{2-} concentrations, increasing Fe^{2+} and CH_4 concentrations, and negative ORP. This finding is consistent with microbially mediated degradation of petroleum hydrocarbons (electron donor) within the tank farm. However, during the monitoring period 2005–2018, several different laboratories were used for analysis of groundwater samples. Some of the increases and decreases in TPH-d concentrations over time appear to be an artifact of analytical differences between laboratories (see CSM Appendixes B.7 and B.8 for further discussion). Due to the laboratory uncertainty associated with the TPH-d analysis, apparent changes in TPH-d concentration over time may not directly correlate with true changes in the magnitude of impact.

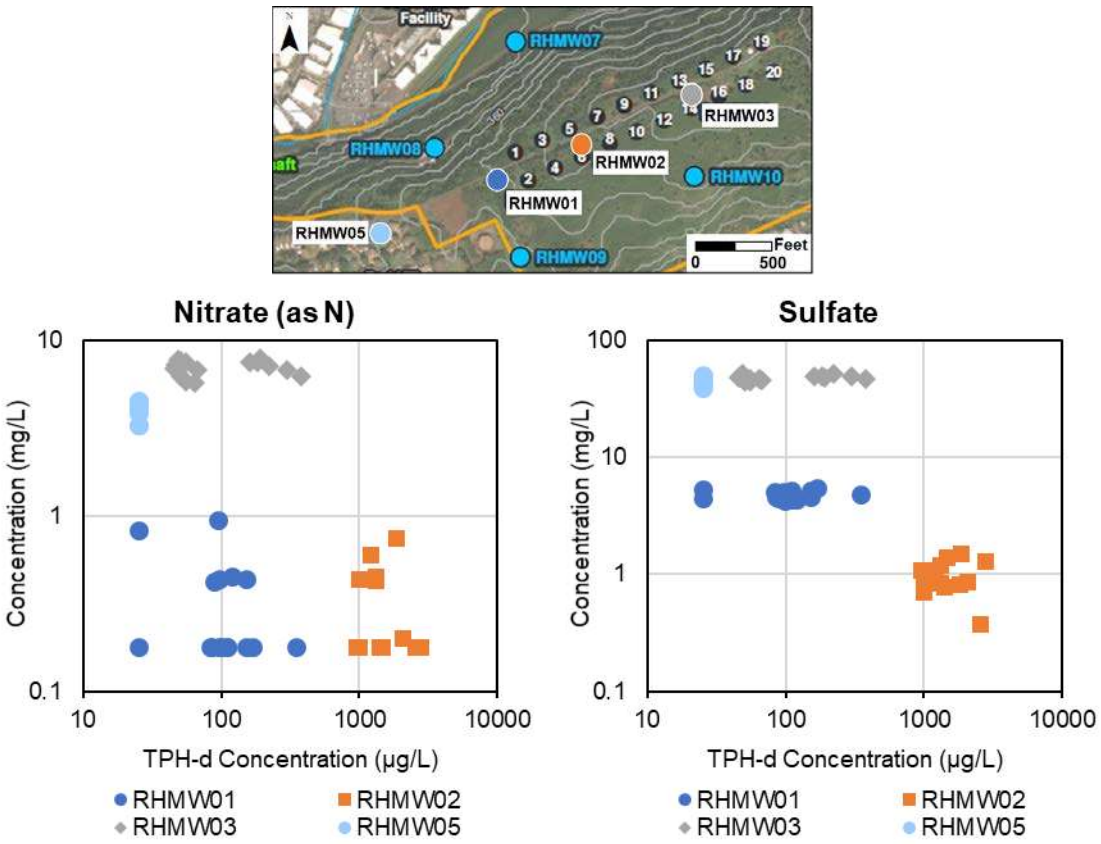

Note: Non-detect samples are plotted as the detection or reporting limit.

Figure 3-5: X-Y Plots for TPH-d Concentrations vs. NO_3^- (Left Panel) and SO_4^{2-} (Right Panel) Concentrations at Monitoring Wells RHMW01, RHMW02, RHMW03, and RHMW05

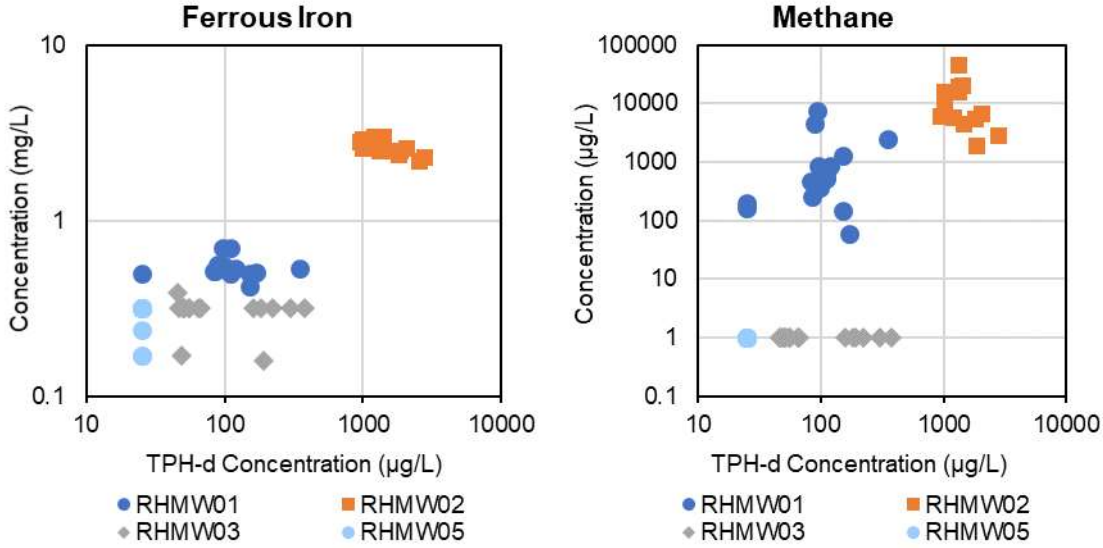

Note: Non-detect samples are plotted as the detection or reporting limit.

Figure 3-6: X-Y Plots for TPH-d Concentrations vs. Fe^{2+} (Left Panel) and CH_4 (Right Panel) Concentrations at Monitoring Wells RHMW01, RHMW02, RHMW03, and RHMW05

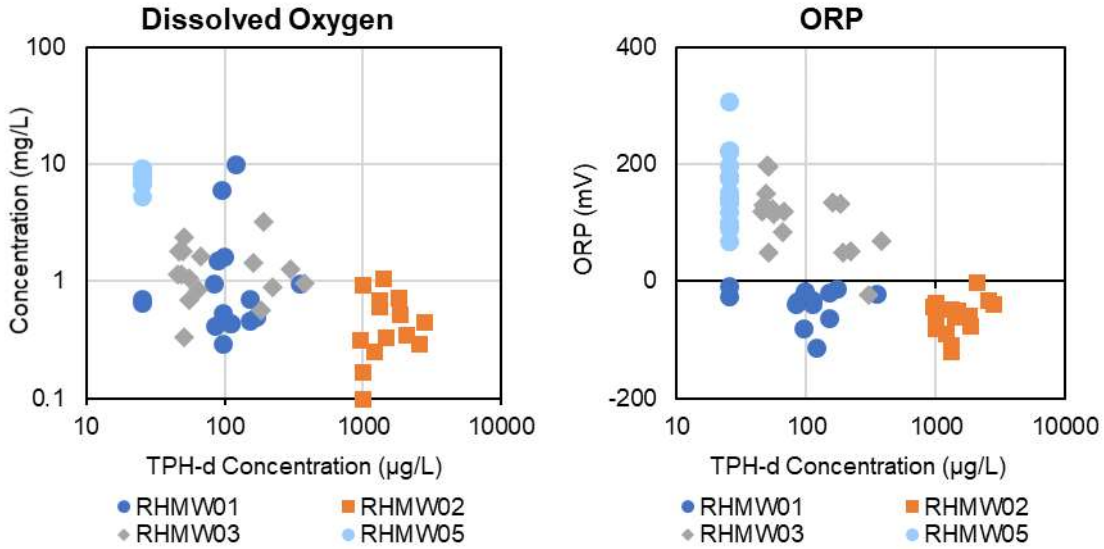

Note: Non-detect samples are plotted as the detection or reporting limit.

Figure 3-7: X-Y Plots for TPH-d Concentrations vs. DO Concentrations (Left Panel) and ORP (Right Panel) at Monitoring Wells RHMW01, RHMW02, RHMW03, and RHMW05

4. Conclusions

Time series and X-Y plots were developed to evaluate natural attenuation processes at the Facility using secondary lines of evidence (i.e., geochemical indicators, electron acceptor concentrations). Historical groundwater data from October 2016 to present (January/February 2019) were evaluated for all monitoring wells in the Facility network; limited data from 2005 and 2006 were also included for select monitoring wells.

Spatial and temporal concentration trends for TEAs (O_2, NO_3^-, SO_4^{2-}) and metabolic byproducts (Fe^{2+}, CH_4) provide strong evidence for aerobic and anaerobic petroleum hydrocarbon degradation within the tank farm. In the area of highest COPC concentration (RHMW02), electron acceptors (O_2, NO_3^-, SO_4^{2-}) are depleted (or have low concentrations) and concentrations of metabolic byproducts (Fe^{2+}, CH_4) are elevated relative to the monitoring locations outside of the tank farm area. Low DO concentrations and negative ORP values further support anaerobic conditions in this area. These secondary lines of evidence strongly indicate that active and robust biodegradation of COPCs is occurring within the tank farm.

5. References

Beck, P., and B. Mann. 2010. *A Technical Guide for Demonstrating Monitored Natural Attenuation Of Petroleum Hydrocarbons in Groundwater*. CRC CARE Technical Report No 15, CRC Contamination Assessment and Remediation of the Environment. Adelaide, Australia.

Environmental Protection Agency, United States (EPA). 1999. *Use of Monitored Natural Attenuation at Superfund, RCRA Corrective Action, and Underground Storage Tank Sites*. OSWER 9200.4-17P. Office of Solid Waste and Emergency Response. April.

Hunt, Jr., C. D. 2004. *Ground-Water Quality and Its Relation to Land Use on Oahu, Hawaii, 2000–01*. Water-Resources Investigations Report 03-4305. National Water-Quality Assessment Program. U.S. Geological Survey.

McCarty, P. L., B. E. Rittman, and E. J. Bouwer. 1984. "Microbial Processes Affecting Chemical Transformations in Groundwater." In *Groundwater Pollution Microbiology*. G. Britton and C. P. Gerba (Eds), Pp. 89–115. New York: John Wiley & Sons.

Newell, C. J., R. K. McLeod, and J. R. Gonzales. 1996. *BIOSCREEN Natural Attenuation Decision Support System User's Manual, Ver. 1.3.* Prepared for Air Force Center for Environmental Excellence (AFCEE) Technology Transfer Division at Brooks Air Force Base, by Groundwater Services, Inc., Houston.

Wiedemeier, T. H., H. S. Rifai, C. J. Newell, and J. T. Wilson. 1999. *Natural Attenuation of Fuels and Chlorinated Solvents in the Subsurface*. New York: John Wiley & Sons, Inc.

Wiedemeier, T. H., J. T. Wilson, D. H. Kampbell, R. N. Miller, and J. E. Hansen. 1999. *Technical Protocol for Implementing Intrinsic Remediation with Long-Term Monitoring for Natural Attenuation of Fuel Contamination Dissolved in Groundwater. Vols. I & II*. San Antonio, TX: Air Force Center for Environmental Excellence, Technology Transfer Division. March.

Attachment B.5.1:
Time-Series Plots for Alkalinity, NO_3^-, SO_4^{2-}, Cl, Fe^{2+}, CH_4, DO, and ORP at All Monitoring Well Locations

Attachment B.5.1: Time-Series Plots for Alkalinity, NO_3^-, SO_4^{2-}, Cl, Fe^{2+}, CH4, DO, and ORP at All Monitoring Well Locations

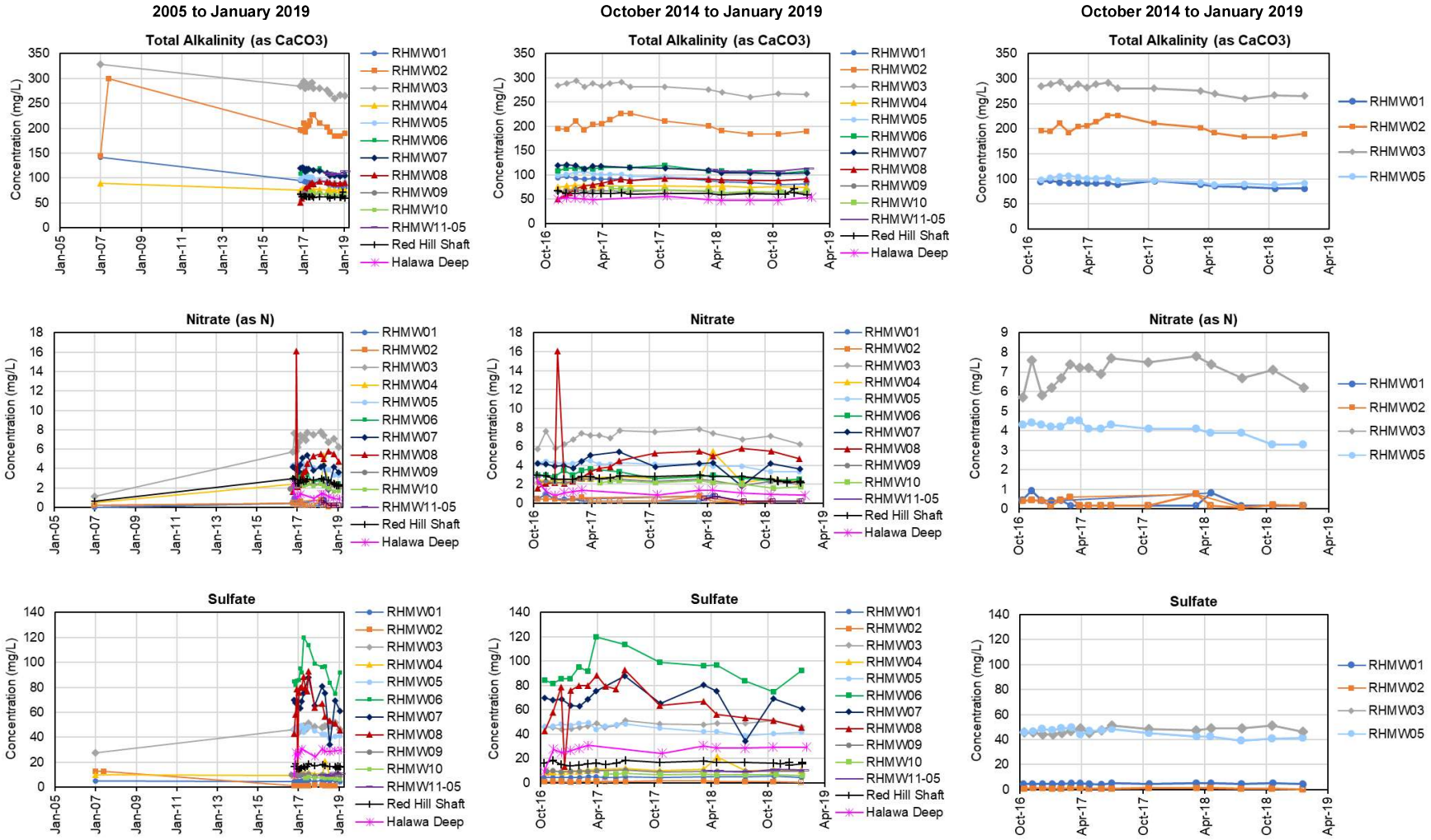

Attachment B.5.1: Time-Series Plots for Alkalinity, NO_3^-, SO_4^{2-}, Cl, Fe^{2+}, CH4, DO, and ORP at All Monitoring Well Locations (cont.)

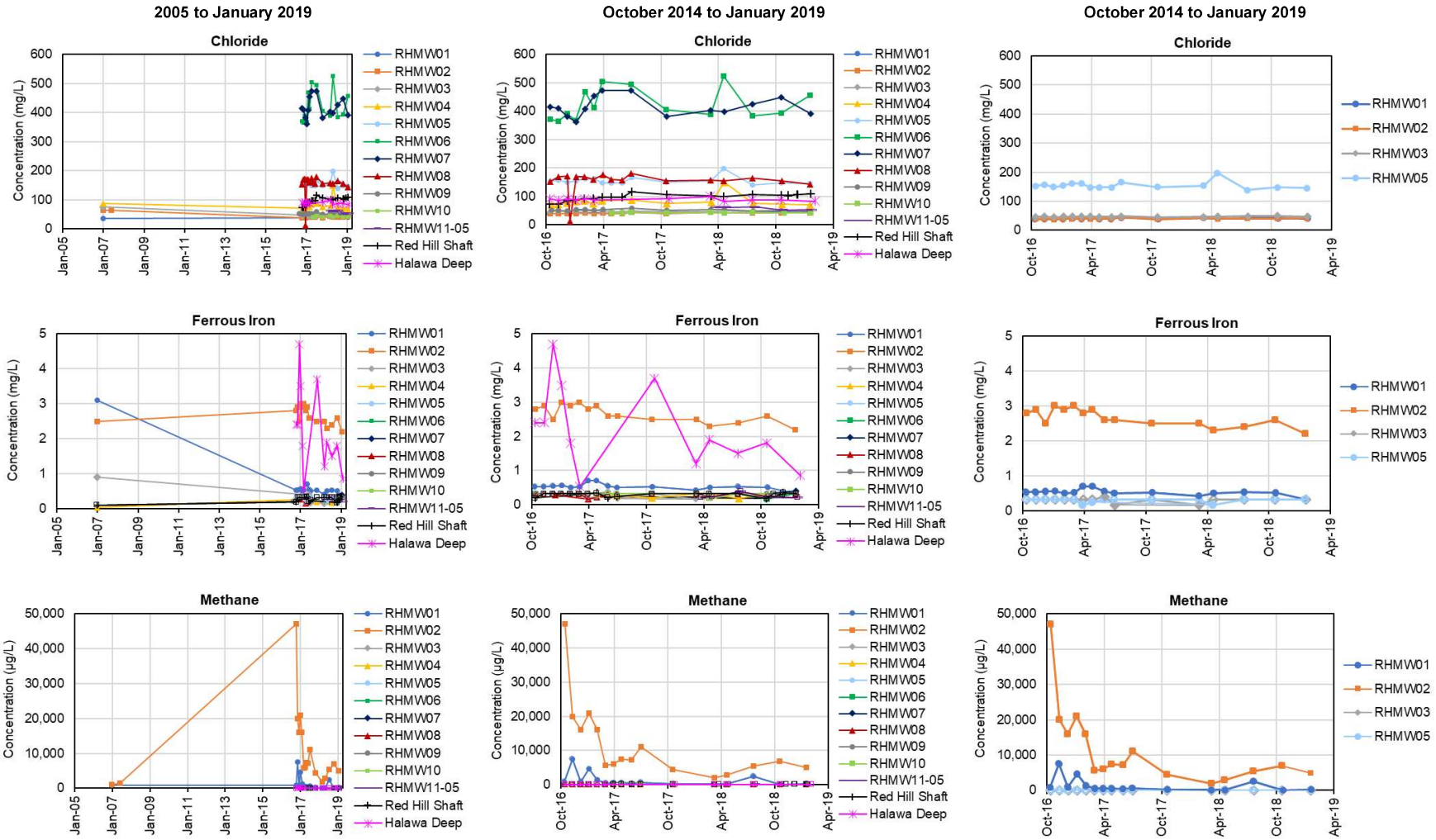

Attachment B.5.1: Time-Series Plots for Alkalinity, NO_3^-, SO_4^{2-}, Cl, Fe^{2+}, CH4, DO, and ORP at All Monitoring Well Locations (cont.)

2005 to January 2019

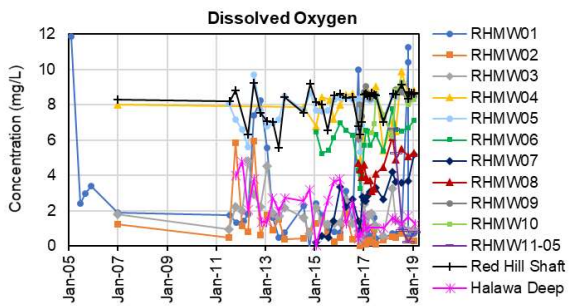

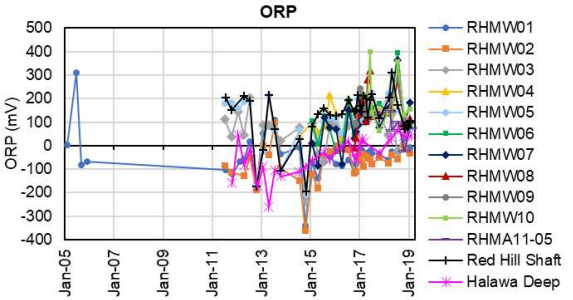

October 2014 to January 2019

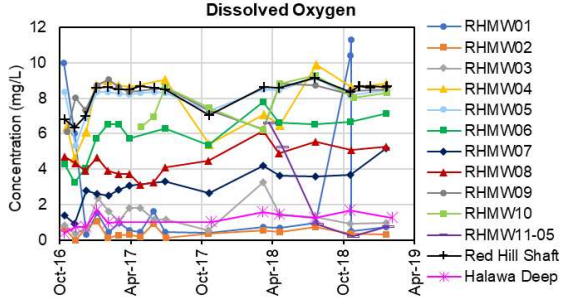

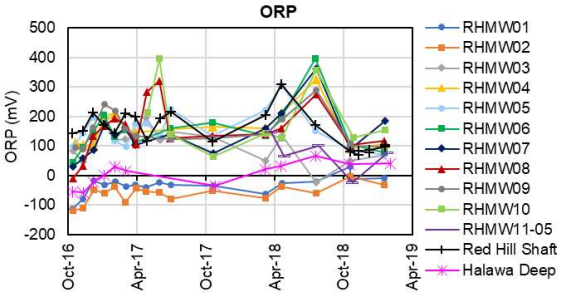

October 2014 to January 2019

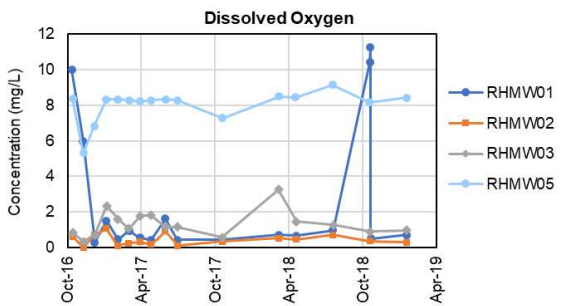

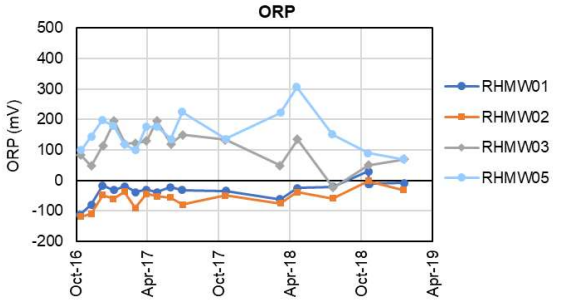

Note: Non-detect samples are plotted as open markers.

Attachment B.5.2:
X-Y Plots for Alkalinity, NO_3^-, SO_4^{2-}, Cl, Fe^{2+}, CH_4, DO, ORP, and COPCs at All Monitoring Well Locations

Attachment B.5.2: X-Y Plots for Alkalinity, NO_3^-, SO_4^{2-}, Cl, Fe^{2+}, CH_4, DO, ORP and COPCs at All Monitoring Well Locations

TPH-d

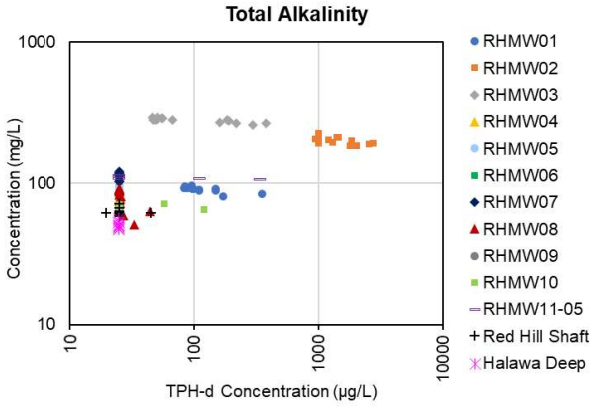

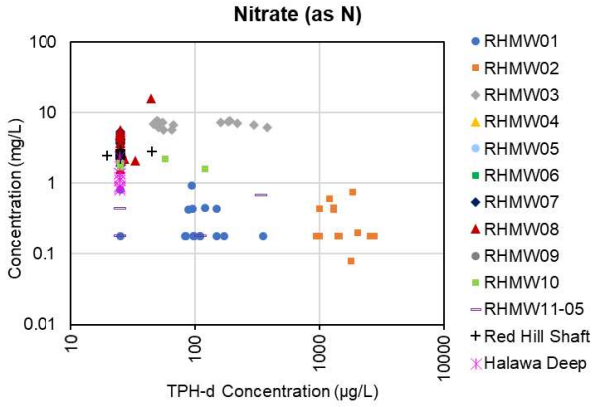

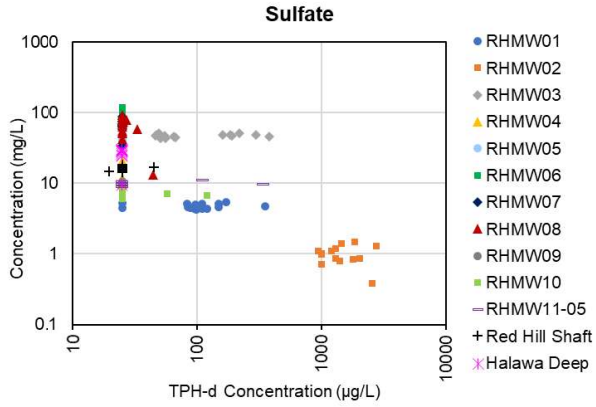

TPH-o

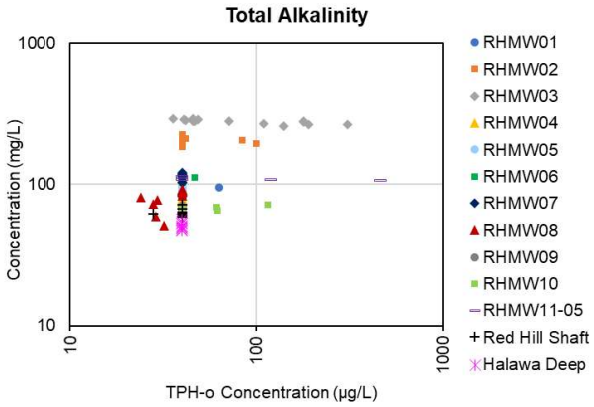

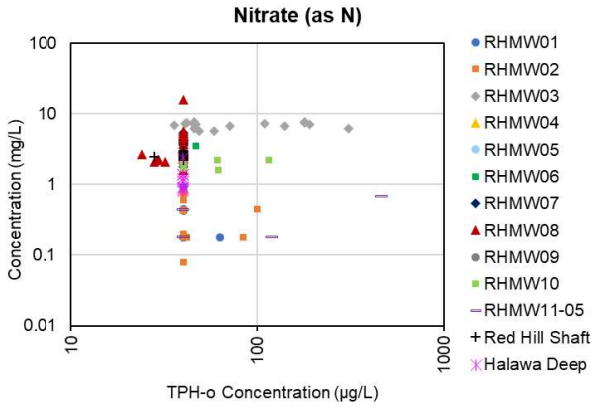

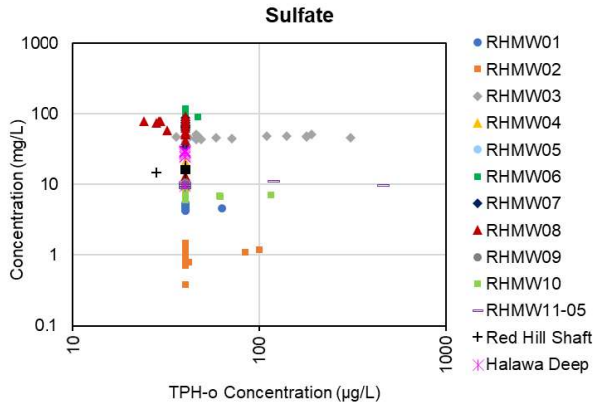

Attachment B.5.2: X-Y Plots for Alkalinity, NO_3^-, SO_4^{2-}, Cl, Fe^{2+}, CH_4, DO, ORP and COPCs at All Monitoring Well Locations (cont.)

TPH-d

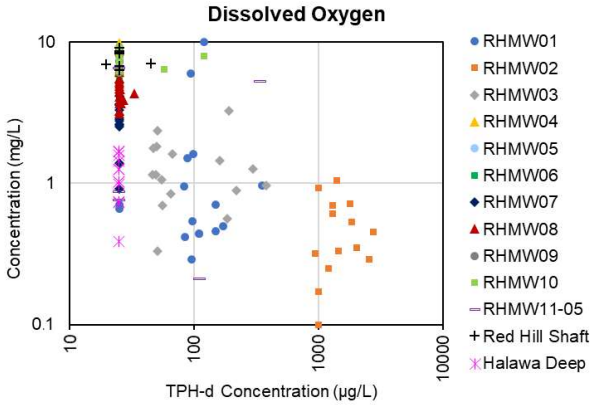

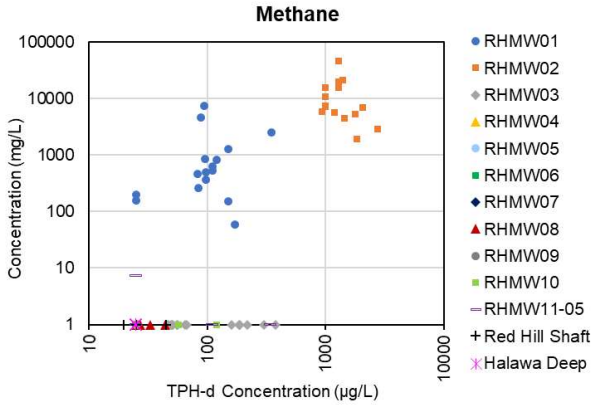

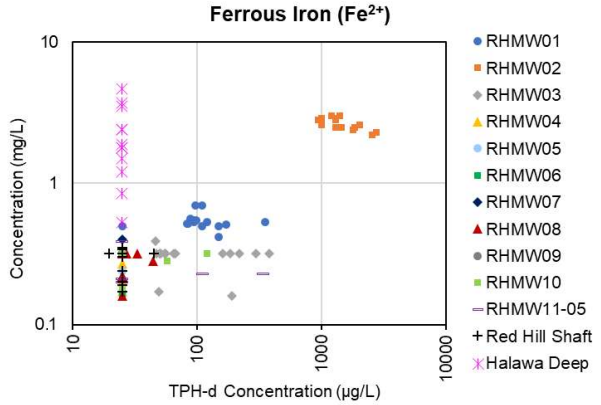

TPH-o

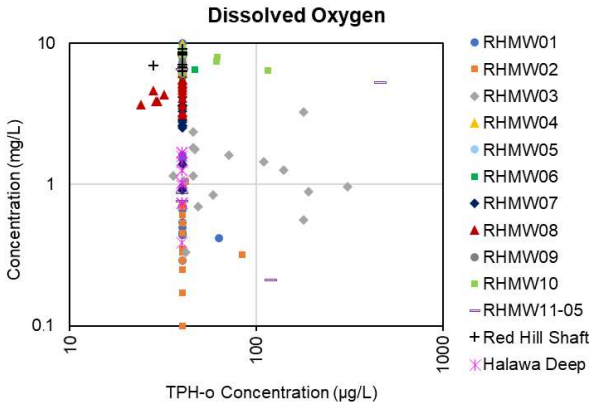

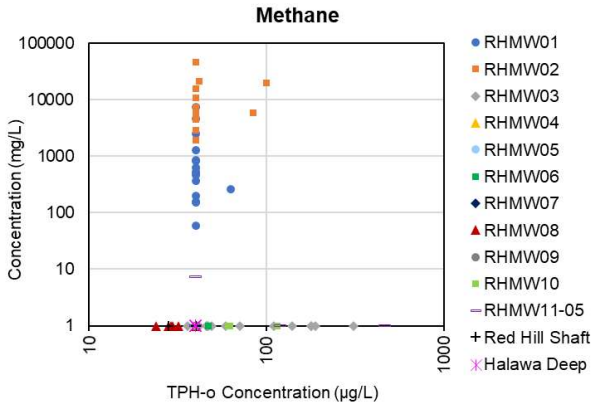

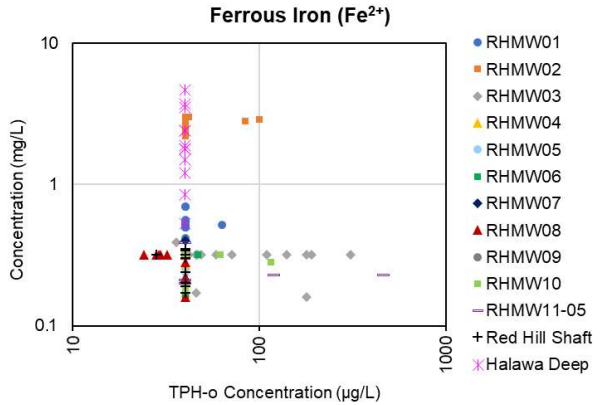

Attachment B.5.2: X-Y Plots for Alkalinity, NO_3^-, SO_4^{2-}, Cl, Fe^{2+}, CH_4, DO, ORP and COPCs at All Monitoring Well Locations (cont.)

TPH-d

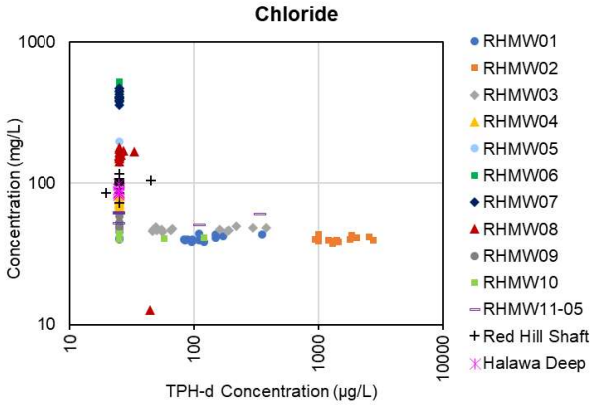

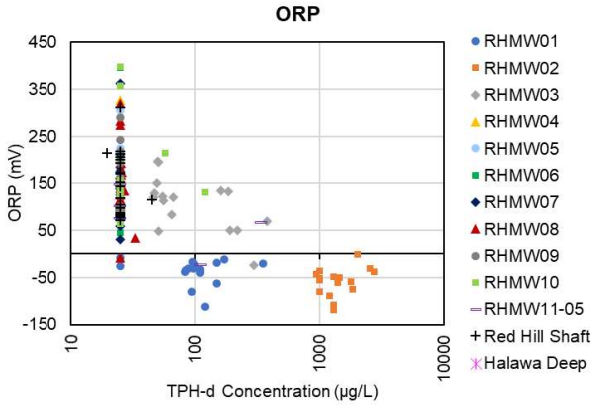

TPH-o

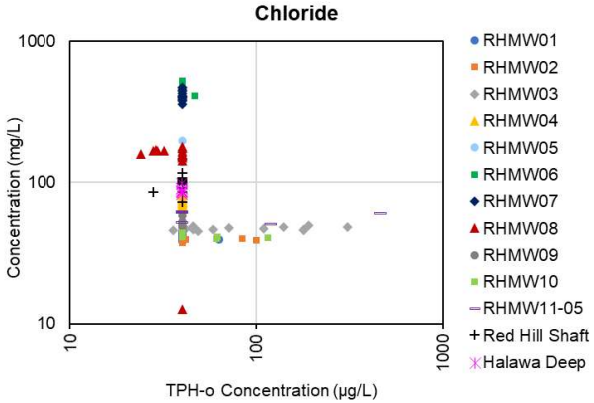

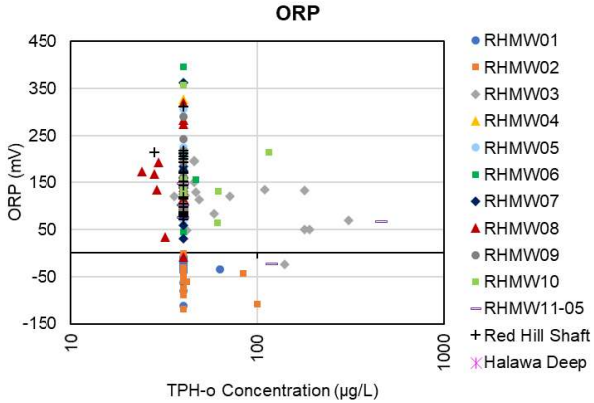

Attachment B.5.2: X-Y Plots for Alkalinity, NO_3^-, SO_4^{2-}, Cl, Fe^{2+}, CH_4, DO, ORP and COPCs at All Monitoring Well Locations (cont.)

TPH-g

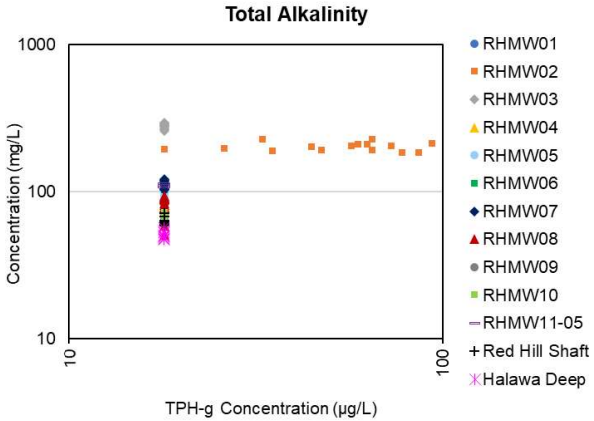

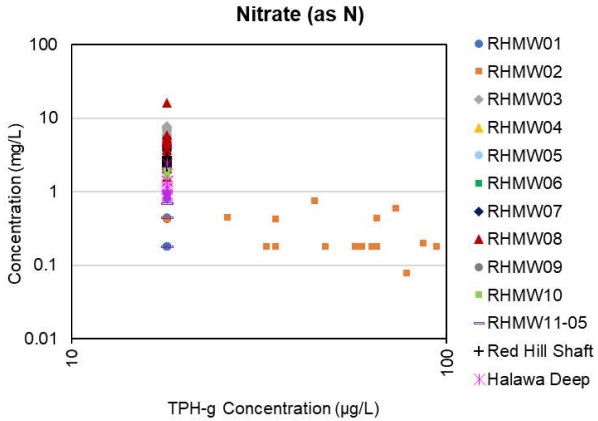

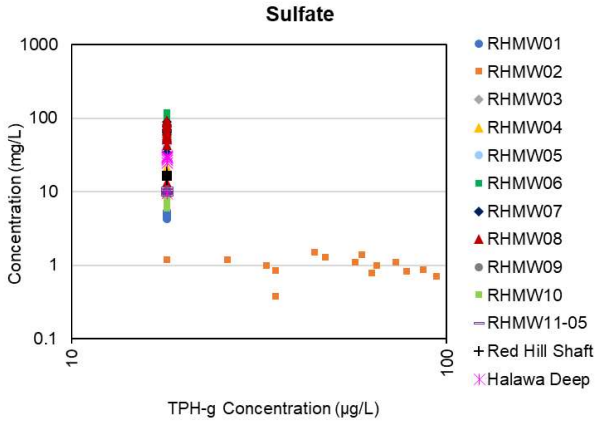

Naphthalene

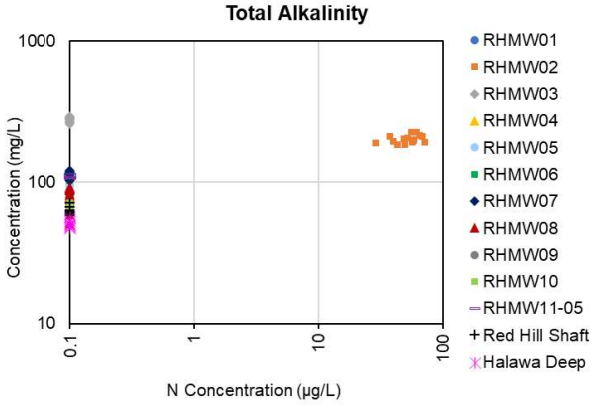

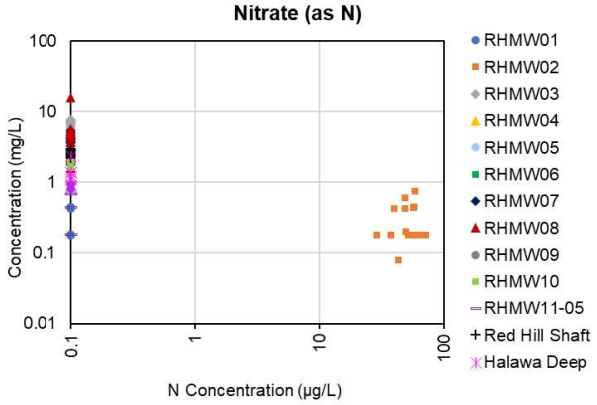

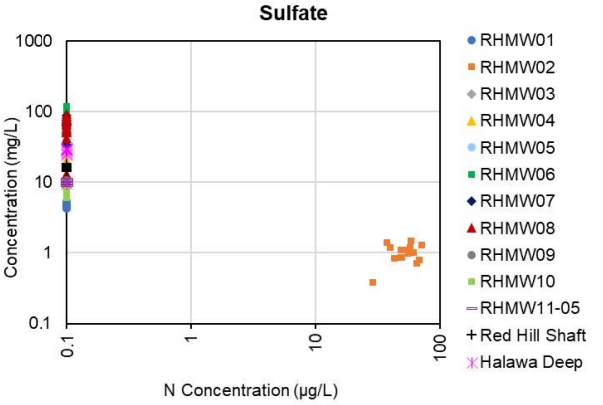

Attachment B.5.2: X-Y Plots for Alkalinity, NO_3^-, SO_4^{2-}, Cl, Fe^{2+}, CH_4, DO, ORP and COPCs at All Monitoring Well Locations (cont.)

TPH-g

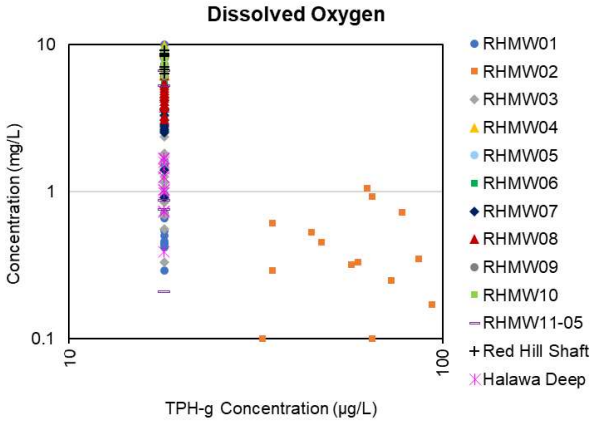

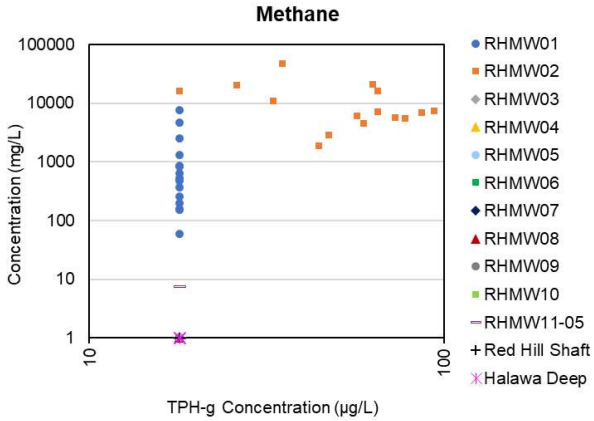

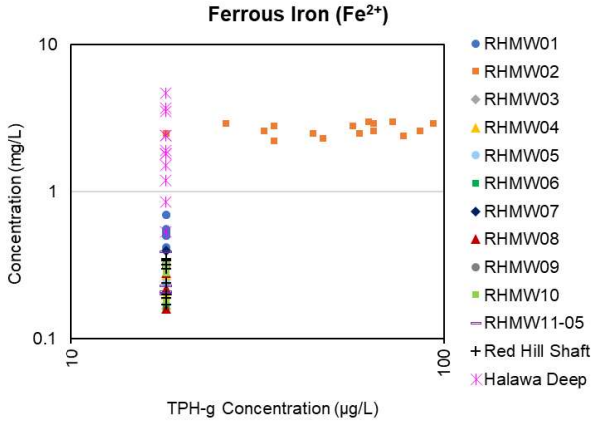

Naphthalene

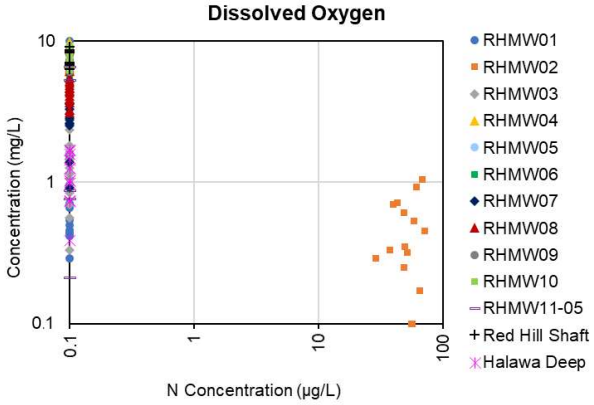

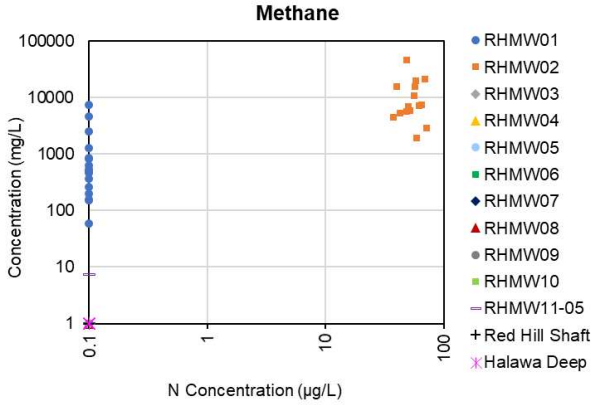

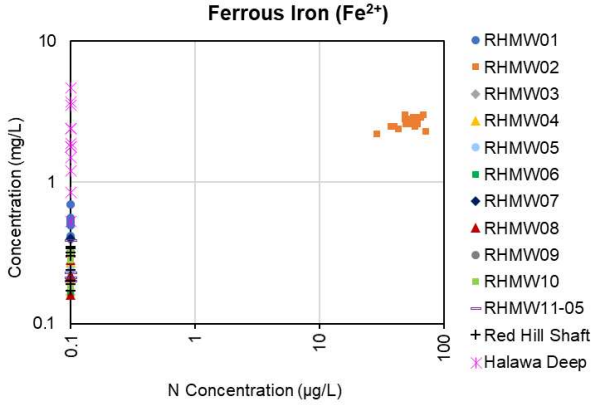

Attachment B.5.2: X-Y Plots for Alkalinity, NO_3^-, SO_4^{2-}, Cl, Fe^{2+}, CH_4, DO, ORP and COPCs at All Monitoring Well Locations (cont.)

TPH-g

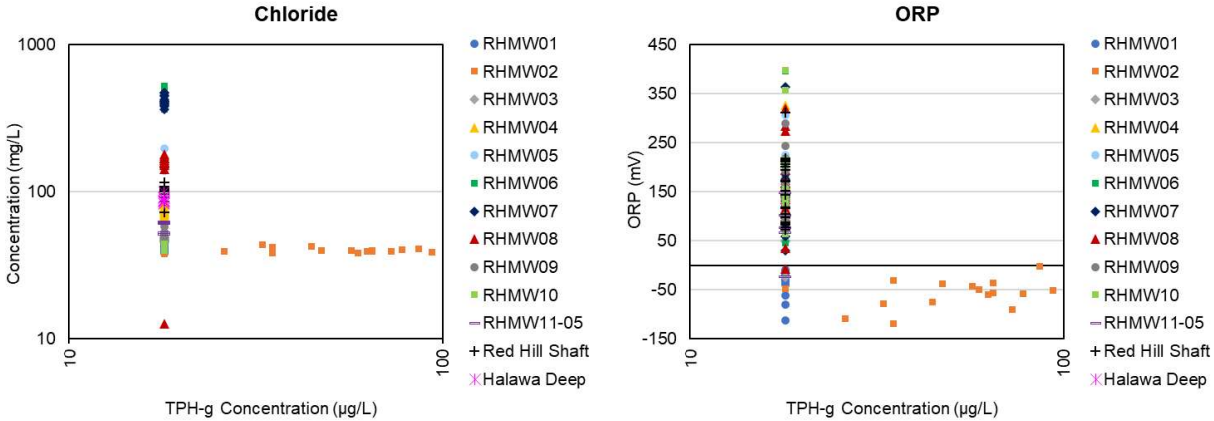

Naphthalene

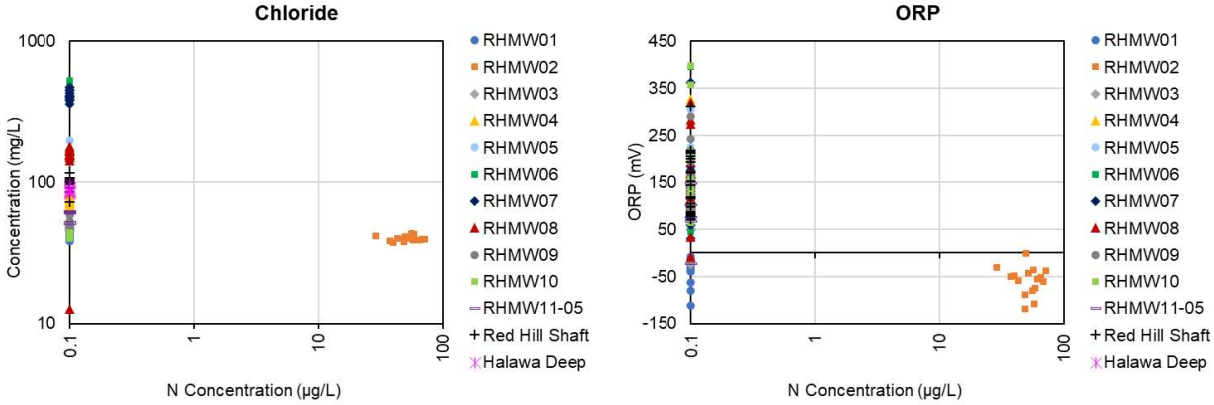

Attachment B.5.2: X-Y Plots for Alkalinity, NO_3^-, SO_4^{2-}, Cl, Fe^{2+}, CH_4, DO, ORP and COPCs at All Monitoring Well Locations (cont.)

1-Methylnaphthalene

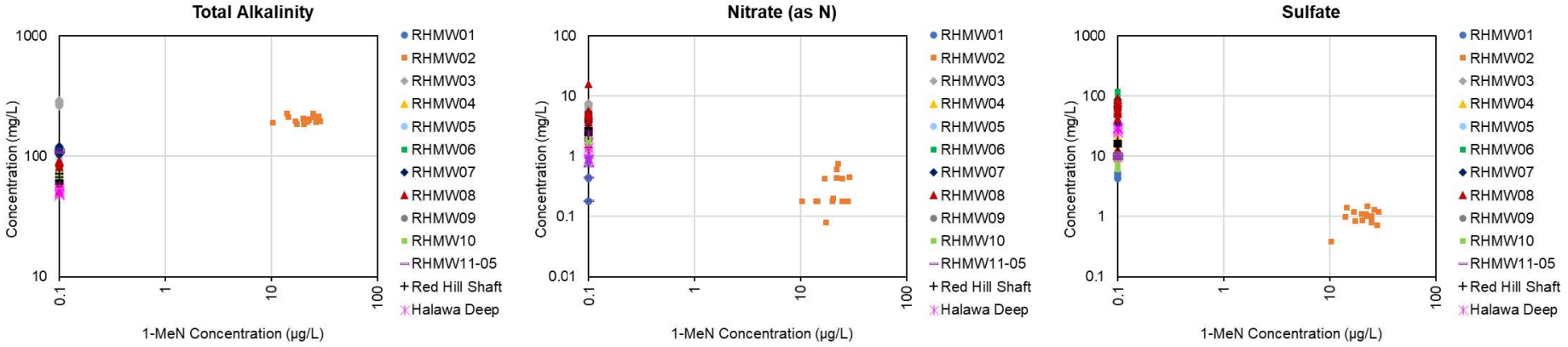

2-Methlynaphthalene

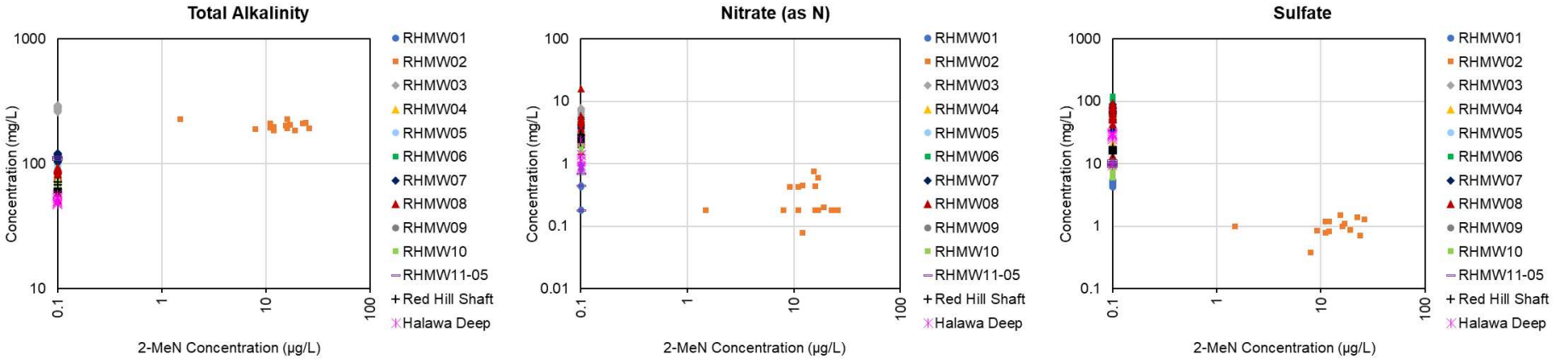

Attachment B.5.2: X-Y Plots for Alkalinity, NO_3^-, SO_4^{2-}, Cl, Fe^{2+}, CH_4, DO, ORP and COPCs at All Monitoring Well Locations (cont.)

1-Methylnaphthalene

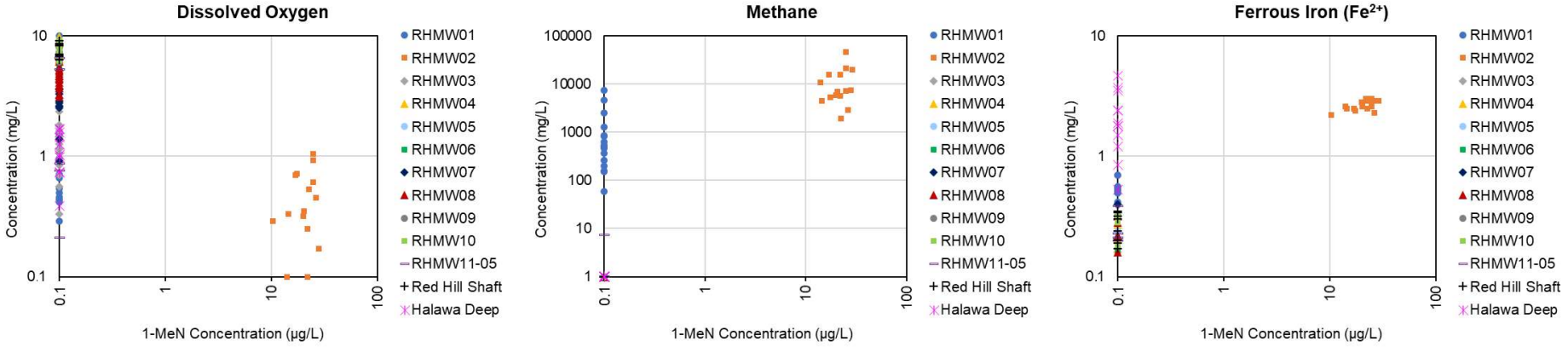

2-Methlynaphthalene

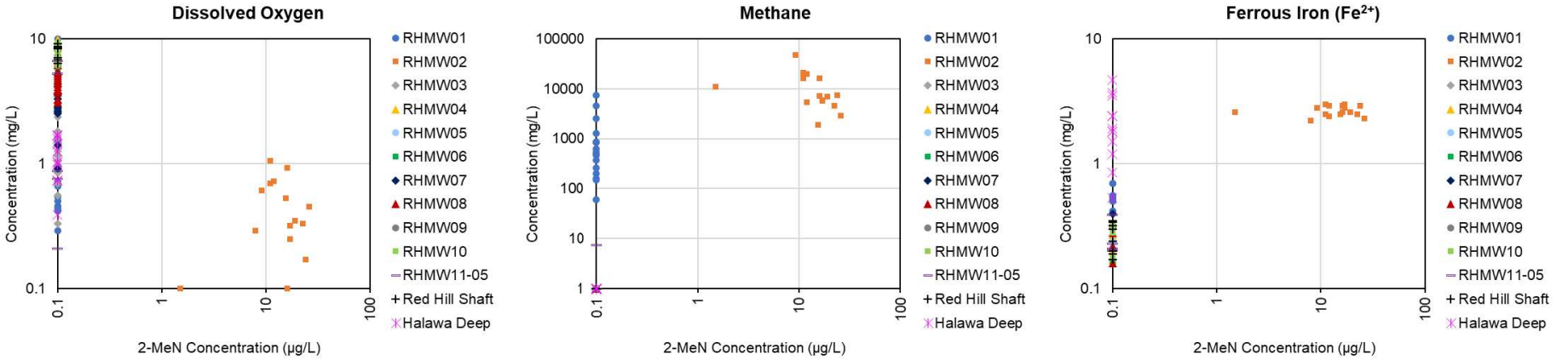

Attachment B.5.2: X-Y Plots for Alkalinity, NO_3^-, SO_4^{2-}, Cl, Fe^{2+}, CH_4, DO, ORP and COPCs at All Monitoring Well Locations (cont.)

1-Methylnaphthalene

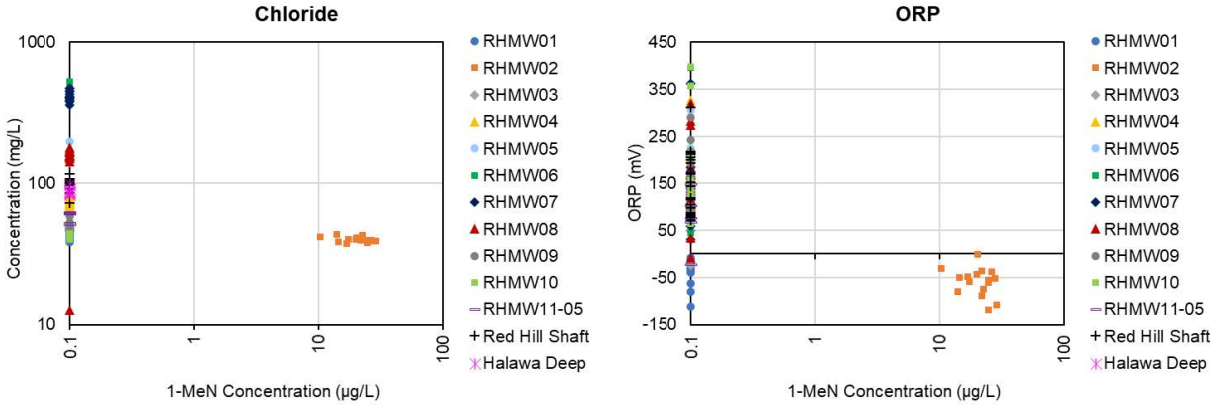

2-Methlynaphthalene

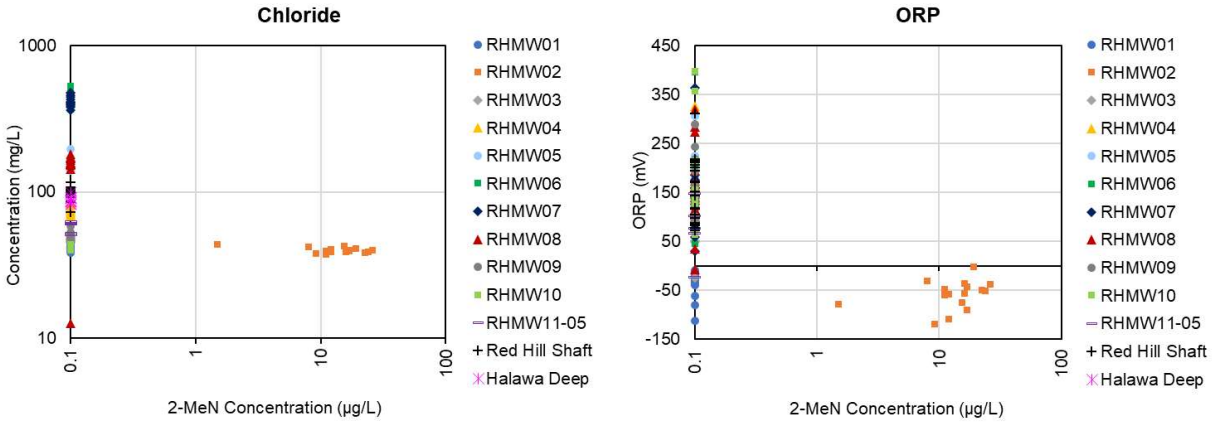

This page intentionally left blank

Appendix B.6:
Microcosm Study and Microbial Parameter Analysis

CONTENTS

Acronyms and Abbreviations ii

1. Introduction 1-1

2. Methods 2-1

2.1 Test Design 2-1
2.1.1 Microcosm Study 2-1
2.1.2 Microbial Parameters 2-2
2.2 Field Protocols for Sample Collection 2-3
2.2.1 Microcosm Study 2-3
2.2.2 Microbial Parameters 2-3
2.3 Laboratory Protocols for Analysis 2-4
2.3.1 Microcosm Study 2-4
2.3.2 Microbial Parameters 2-5

3. Results 3-1

3.1 Microcosm Study 3-1
3.2 Microbial Parameters 3-3

4. Conclusions 4-1

5. References 5-1

ATTACHMENTS

B.6.1 Summary of Current Data from Microcosm Study - Volatile Organic Compounds

B.6.2 Summary of Microbial Parameter Data

B.6.3 Laboratory Reports

FIGURES

2-1 Location of Facility Wells Included in Microcosm Study (White Circles) and Microbial Parameter Analysis (Yellow Circles) 2-2

2-2 Bio-filters Used During Sample Collection for Microbial Parameter Analysis 2-4

3-1 Results of Microcosm Study: Benzene and Toluene 3-5

3-2 Results of Microcosm Study: Xylenes 3-6

3-3 Results of Microcosm Study: 1,2,4-Trimethylbenzene and 1-Methylnaphthalene 3-7

3-4 Results of Microcosm Study: 2-Methylnaphthalene and Naphthalene 3-8

TABLES

2-1 Summary of Target Initial Concentrations for Microcosm Study 2-2

2-2 Treatments and Controls for Microcosm Study 2-5

3-1 Constituent-Specific Rate Coefficients Based on Data from Microcosm Study 3-1

ACRONYMS AND ABBREVIATIONS

µg/L	micrograms per liter
1,2,4-TMB	1,2,4-trimethylbenzene
ANAT	anaerobic natural attenuation treatment
BCR	benzoyl-coenzyme A reductase
BTEX	benzene, toluene, ethylbenzene, and xylenes
COPC	chemical of potential concern
DHG	dissolved hydrogen gases
LNAPL	light non-aqueous-phase liquid
mg/L	milligrams per liter
mL	milliliter
MTBE	methyl tert-butyl ether
mV	millivolt
NGS	Next Generation Sequencing
ONAT	oxygen-amended natural attenuation treatment
ORP	oxidation-reduction potential
PAH	polynuclear aromatic hydrocarbon
PCR	polymerase chain reaction
PHE	phenol hydroxylase
QA/QC	quality assurance / quality control
qPCR	quantitative polymerase chain reaction
RDEG	toluene monooxygenase 2
TOD	toluene dioxygenase
TPH	total petroleum hydrocarbons
TPH-d	total petroleum hydrocarbons – diesel-range organics
VOC	volatile organic compound

1. Introduction

This subappendix, summarized in Section 7.3.2.4 of the Conceptual Site Model main document, describes preliminary results from two studies that are being used to assess natural attenuation capacity at the Red Hill Bulk Fuel Storage Facility (the "Facility"):

- A ***microcosm study*** is being completed to provide an estimate of the bulk attenuation rate due to biodegradation for several constituents of concern under aerobic and anaerobic conditions. These are laboratory-based tests where the temporal concentrations of these constituents are monitored in bottles constructed using site material to understand the relative biodegradation kinetics. These tests started in October 2017 and monitoring continued over a several-month period.
- A series of ***microbial parameters***, including QuantArray-Petro and Next Generation Sequencing (NGS), have been employed to quantify particular biomarkers of petroleum hydrocarbon degradation. These tests involve analyses of site groundwater using quantitative polymerase chain reaction (qPCR)-based and other molecular techniques to provide a snapshot of the microbial community present at the Facility, including those capable of petroleum hydrocarbon degradation. Data from a single sampling event (October 25, 2017) are available and discussed within this subappendix.

Collectively, the results of these tests help to establish if key organisms are present, active, and degrading hydrocarbons at rates that help to limit migration. These data serve not only as a line of evidence for attenuation but also provide insight on rates.

2. Methods

2.1 TEST DESIGN

2.1.1 Microcosm Study

For the microcosm study, the primary design considerations were sampling locations, the test conditions, and the constituents to be monitored.

For the sampling locations, monitoring wells RHMW01 and RHMW02 were selected for further assessment (Figure 2-1). The primary rationale for this selection was that the recent monitoring data showed that these wells exhibited the highest concentrations of total petroleum hydrocarbon (TPH) constituents. Consequently, understanding biodegradation potential and rates at these locations is the highest priority and directly supports the decision-making process for the Facility. The concentration history at the locations also suggests that there is an active microbial community, and the microcosm study (as well as the molecular biological tests) serve as supporting evidence that biodegradation is a contributing factor to observed concentration trends.

Conditions tested during the microcosm study included both anaerobic and aerobic conditions. Anaerobic conditions were selected to provide measurements of intrinsic degradation activity without amendments. In general, the geochemical conditions around RHMW01 and RHMW02 are reducing, such that the anaerobic microcosms could be considered most representative of conditions in the immediate vicinity of the wells. However, groundwater containing small amounts of oxygen and other electron acceptors may flow into the areas around the wells, such that strictly anaerobic microcosms might underestimate activity. Consequently, a parallel set of aerobic microcosms were also included to assess biodegradation in conditions where oxygen availability was not limited. Because oxygen is supplied to maintain aerobic conditions in the microcosms, this set of tests provides a best-case scenario for natural attenuation in these wells. However, data from the aerobic microcosms were also designed to show how contaminants entering the downgradient portions of the aquifer—which are highly oxidizing—might be degraded.

Constituents that were included in the monitoring program for the microcosm study are listed in Table 2-1. These constituents were selected because each meets one or more of the following criteria: (1) it is a known or suspected constituent within the light non-aqueous-phase liquid (LNAPL) present at the Facility; (2) it has been detected in monitoring wells; and (3) the constituent is a potential risk driver (i.e., even if it is not currently detected). It is important to note that the initial concentrations of these constituents were either extremely low or below reporting limits in the samples collected from RHMW01 and RHMW02 for microcosm construction. Therefore, each of these constituents had to be added (spiked) to the microcosms. In this case, the goal was to achieve a concentration that was slightly below the effective solubility of each constituent assuming water was in equilibrium with JP-8 (i.e., a potential source material). These concentrations, which are listed in Table 2-1, were calculated using available literature studies, and the spiking procedure is described in Section 2.3.

Table 2-1: Summary of Target Initial Concentrations for Microcosm Study

Constituent	Target Concentration (µg/L)
Benzene	150
1,2,4-Trimethylbenzene	500
1-Methylnaphthalene	60
2-Methylnaphthalene	60
Naphthalene	60
Xylene, m,p-	1,000
Xylene, o-	500
Toluene	600

µg/L microgram per liter

2.1.2 Microbial Parameters

For the microbial parameters study, the primary design considerations were sampling locations and the type of molecular biological tools to be employed.

Samples from monitoring wells RHMW01, RHMW02, RHMW03, and RHMW04 were selected to be part of this assessment (Figure 2-1). These wells were chosen on the basis that they include the wells that exhibited the highest concentrations of TPH constituents during recent monitoring events (RHMW01 and RHMW02) but also several wells with low and/or non-detectable levels of TPH (RHMW03 and RHMW04). The former two wells can be used to establish the microbial community that is present within the plume core, while the latter two wells provide information on the microbial community in areas where current exposure to petroleum hydrocarbons is more limited. Note that RHMW04 is outside of the footprints of the tanks and thus is the most representative of background conditions (of the wells tested).

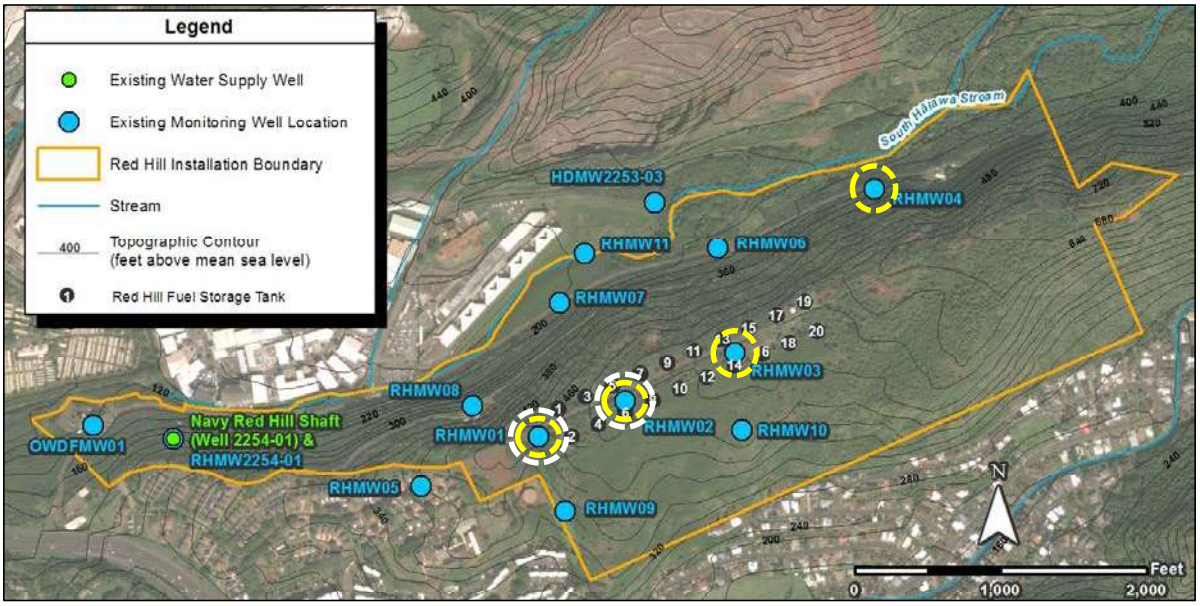

Figure 2-1: Location of Facility Wells Included in Microcosm Study (White Circles) and Microbial Parameter Analysis (Yellow Circles)

The two molecular biological tools that are part of the current microbial parameter analysis are QuantArray-Petro and NGS. QuantArray-Petro is a proprietary qPCR-based method (from Microbial Insights) that provides information on the abundance of specific biomarkers for petroleum hydrocarbon degradation. Genetic material (DNA) is extracted from environmental samples and then qPCR is used to amplify and quantify copies of specific target genes. Rapid quantification is aided by the use of plates containing grids of immobilized genetic material (microarrays) that bind to the genes of interest. NGS has a similar goal of providing information on community structure, but it generally provides a more comprehensive picture and does not require any previous knowledge of what populations may be present at a site. The method used for this study was developed by Microbial Insights and involves a step-wise procedure to fragment genetic material into a series of smaller identifying segments. Each of these segments can then be rapidly sequenced and quantified to relate to overall community structure. Use of another molecular biological tool (e.g., Stable Isotope Probing) is also planned but has not yet been performed.

2.2 FIELD PROTOCOLS FOR SAMPLE COLLECTION

The following subsection summarizes the field sampling protocols for the tests described in this sub-appendix. A comprehensive summary of methods (including quality assurance / quality control [QA/QC] procedures) is provided in Attachment B.6.3.

2.2.1 Microcosm Study

Site material (groundwater) from monitoring wells RHMW01 and RHMW02 was used to construct microcosms. Twelve liters of groundwater was collected from RHMW02 on September 19, 2017, and 9 liters of groundwater was collected from RHMW01 on September 26, 2017. In each case, samples were pumped from the well after surging to ensure that significant sediment was entrained in the groundwater. The inclusion of sediment helped ensure that sufficient initial biomass was available for the subsequent treatability tests. However, the amount of sediment was relatively small (<1% by volume) compared to amounts present in porous media. Samples were collected in polyethylene bottles with no headspace and no preservative per laboratory protocol. Samples were shipped in coolers on ice to the laboratory.

2.2.2 Microbial Parameters

Groundwater samples were collected from monitoring wells RHMW01, RHMW02, RHMW03, and RHMW04 during October 20–25, 2017 for microbial parameter analysis. In each case, 1–2 liters of groundwater were pumped from the well and then passed through a laboratory-supplied filter apparatus (bio-filter, Figure 2-2). The purpose of these filters is to collect and concentrate biomass from individual samples and thus eliminate the need to ship groundwater. Once filtering was complete, each bio-filter was capped, and the entire set shipped to the laboratory in coolers on ice.

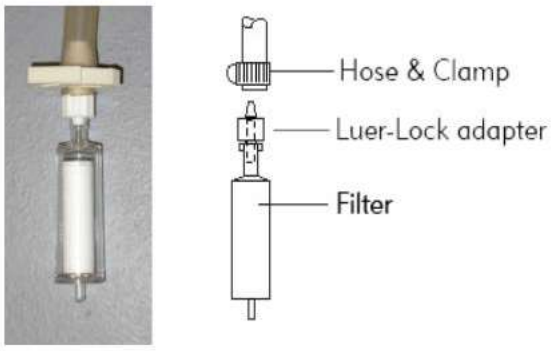

Figure 2-2: Bio-filters Used During Sample Collection for Microbial Parameter Analysis

2.3 LABORATORY PROTOCOLS FOR ANALYSIS

The following subsection summarizes the methodology used by the commercial laboratories that are performing this work. As noted above, a more comprehensive summary of these procedures for the microcosm study is provided in Attachment B.6.3.

2.3.1 Microcosm Study

A series of microcosms were constructed to assess degradation under various conditions (Table 2-2). Microcosm construction was initiated immediately after field samples were received by the laboratory (SiREM). Note that field samples from the two different site locations were handled separately. Each microcosm consisted of a 250-milliliter (mL) glass bottle filled with 200 mL of site groundwater. In addition, sediment that was collected with the field sample and then distributed in approximately equal amounts to each bottle. The bottles were sealed with Mininert valves to allow repetitive sampling of each microcosm, as well as the addition of oxygen in the aerobic treatments (labeled ONAT in Table 2-2). Given that the various analyses being included in the study required significant liquid volumes, sufficient sacrificial microcosms were constructed for each treatment condition.

Microcosms were constructed in disposable anaerobic glove bags to ensure that redox conditions within each bottle could be controlled during set up. This included a set of sterile control microcosms that were constructed using material from one location (RHMW02). The control bottles were autoclaved and amended with mercuric chloride and sodium azide to inhibit microbial activity. Anaerobic reactors (labeled ANAT in Table 2-2) and the sterile controls were then transferred to a permanent anaerobic chamber, while reactors intended for aerobic treatment were maintained on a benchtop.

Representative samples were collected prior the start of the test to determine the initial concentrations of specific chemicals of potential concern (COPCs). Concentrations of the majority were either below reporting limits or too low to reasonably test, and the decision was made to amend each reactor with representative petroleum hydrocarbons. Therefore, each reactor was spiked at the start of the study with an aliquot of neat solutions of saturated stock solutions of several hydrocarbons. In each case, the volume added was based on reaching the target concentrations listed in Table 2-1.

The ANAT and sterile control microcosms were incubated over a period of approximately 12 months. Aqueous samples were collected from the ANAT and sterile control microcosms at seven sampling events, approximately every 4–6 weeks for analysis of benzene, toluene, ethylbenzene and xylenes (BTEX), dissolved hydrogen gases (DHG; methane, ethene, ethane), anions (i.e., sulfate, nitrate, chloride, and phosphate), pH, and oxidation-reduction potential (ORP). Naphthalene, methylnaphthalene, and trimethylbenzene samples were collected from the sterile controls at the beginning and end of the study and from the ANAT microcosms at the beginning of the study, at least one point during the incubation period, and the end of the incubation period.

The ONAT microcosms were incubated over a shorter period of 2—3 months. Aqueous samples were collected over seven sampling events approximately every 1–3 weeks for analysis of BTEX, DHGs, anions, pH, and ORP. Naphthalene, methylnaphthalene, and trimethylbenzene analysis samples were collected at the beginning of the incubation period, during at least one point during the incubation period, and at the endpoint of the study. When a measurement for a particular constituent suggested that it had been completely degraded, bottles were respiked with that constituent to confirm continued biodegradation capacity. ONAT microcosms were also periodically re-amended with oxygen to sustain aerobic conditions throughout the test.

Naphthalene, methylnaphthalene, and trimethylbenzene analyses were completed at ALS Environmental in Waterloo, ON, Canada. All other analyses were completed by SiREM.

Table 2-2: Treatments and Controls for Microcosm Study

Condition	Number of Locations	Description	Number of Replicates for Location 1 (RHMW01)	Number of Replicates for Location 2 (RHMW02)
1. ONAT	2	Amended with gaseous oxygen and incubated aerobically	2	2
2. ANAT	2	No amendments and incubated anaerobically	2	2
3. Sterile Control	1	Autoclaved and amended with mercuric chloride and sodium azide	0	2

2.3.2 Microbial Parameters

A detailed description of laboratory procedures for QuantArray-Petro and NGS was not provided by the performing laboratory (Microbial Insights) because they involve proprietary techniques. However, the general approach used for this work are well-established and rely on identification and quantification of genetic material within samples. The laboratory report includes an interpretation of results, aided by information from their database of sample results from an unspecified number of other sites.

3. Results

3.1 MICROCOSM STUDY

The evaluation period for all microcosms started on October 24, 2017. As of this writing, data are available for the entire monitoring period (Attachment B.6.1). As noted above, the monitoring periods for the various treatments varied widely. Similarly, not all constituents were analyzed at each time point, in part because an external laboratory was used for certain analyses.

Rate coefficients were calculated for individual constituents using available time-series concentration data and assuming that degradation fit a first-order relationship. In other words, the rate coefficient is equal to the slope of the best fit regression line for concentration data plotted on a logarithmic axis (Figure 3-1 to Figure 3-4). For the purposes of this calculation, the reporting limit was used as a substitute value for any instance when the concentration fell below the reporting limit (note that this is a conservative assumption). These values are summarized in Table 3-1.

Table 3-1: Constituent-Specific Rate Coefficients Based on Data from Microcosm Study

Well Location	Condi-tion	Benzene (d^{-1})	Toluene (d^{-1})	Xylenes, o- (d^{-1})	Xylenes, m-, p- (d^{-1})	1,2,4-TMB (d^{-1})	1-Methyl-naphthalene (d^{-1})	2-Methyl-naphthalene (d^{-1})	Naphthalene (d^{-1})
RHMW01	OANT	0.029	0.06	0.072	0.088	0.080	0.114	0.227	0.204
	ANAT	0.0008	0.0032	0.0007	0.0004	0.0021	0.0013	0.0045	0.0068
RHMW02	OANT	0.111	0.196	0.184	0.195	0.26	0.268	0.80	0.67
	ANAT	0.00005	0.0014	0.0013	0.00005	0.0008	0.0002	0.0003	No degradation observed
	Sterile Control	No degradation observed	No degradation observed	No degradation observed	0.00006	No degradation observed	No degradation observed	0.00011	0.00012

Notes: (1) Rate coefficient for aerobic condition at RHMW02 includes data from the initial spike (Day 0–28), not the respike on Day 28; (2) "No degradation observed" is used for treatments where concentrations were unchanged or increased over the monitoring period.
1,2,4-TMB 1,2,4-trimethylbenzene

The major findings based on the results of the microcosm study are summarized below:

- Rapid biodegradation under aerobic conditions was observed in the microcosms from RHMW02. If the rate coefficients in Table 3-1 are converted to equivalent half-lives, then all constituents were degraded with half-lives of less than 1 week, and several were less than 1 day. The data indicate that strong degradation capacity can be stimulated at this location when oxygen is present.
- Slower biodegradation rates were observed in the aerobic microcosms from RHMW01, though all constituents exhibited a concentration decrease and have been completely removed by the end of current the monitoring period. Half-life estimates for the constituents included in the test range from 3 days (2-methylnaphthalenene) to 25 days (benzene). The slower rates observed in the microcosms from this well relative to RHMW02 are consistent with the molecular data discussed in the next section.
- Rapid biodegradation of naphthalene has been observed in aerobic microcosms from both RHMW01 (half-life of 3.4 days) and RHMW02 (half-life of 1.0 day).

- Relative to the rates observed under aerobic conditions, slower biodegradation was observed under anaerobic conditions in microcosms from both RHMW01 and RHMW02.
- In the anaerobic microcosm from RHMW01, the equivalent half-lives ranged from 216 to 1,732 days for benzene, toluene, and the xylenes, and from 101 to 533 days for 1,2,4-trimethylbenzene and the naphthalenes.
- In the anaerobic microcosm from RHMW02, degradation of toluene and o-xylene was established at an equivalent half-life of between 495 and 533 days. Similarly, degradation of 1,2,4-trimethylbenzene (half-life of 866 days), 1-methylnaphthalene (half-life of 3,466 days), and 2-methylnaphthalene (half-life of 2,310 days) at relatively slow rates could be established. Apparent degradation of benzene and m-xylene/p-xylene was very slow, and in the case of the latter, occurred at the same rate as the sterile control.
- Rates in anaerobic microcosms from RHMW01 were generally faster than rates for anaerobic microcosms from RHMW02. The opposite pattern was observed in the aerobic microcosms, and, as confirmed by the molecular data discussed in the next section, suggests minor differences in the microbial populations present at the two wells.
- Although slow degradation was eventually observed under anaerobic conditions, it also should be noted that little activity was observed during the first several months of monitoring. This likely reflected a lag period as the microbial cultures acclimated to the reactor conditions. While these microcosms were constructed in anaerobic conditions, the ORP measured at the start of the test (Day 0) was 155 millivolts (mV) for the RHMW01 microcosms and 166 mV for the RHMW02 microcosms. This reflects the introduction of oxygen during field sampling, which cannot be easily prevented. These oxidizing conditions are generally unfavorable for growth and activity of anaerobic organisms. However, the mass of oxygen and other oxidants in these bottles was relatively small, and utilization of oxygen was expected to eventually shift redox levels downwards. By Day 28, the ORP had dropped to -149 mV in the RHMW01 microcosms and -229 mV in the RHMW02 microcosms. These reducing conditions were more favorable for anaerobic activity, and this presumably led to more significant degradation of petroleum hydrocarbons in these microcosms during subsequent monitoring events.

Another factor that may have contributed to the relatively stable concentrations in the anaerobic microcosms was a low supply of electron acceptors to stimulate degradation. Degradation of petroleum hydrocarbons under anaerobic conditions is an oxidation reaction (i.e., releases electrons) that generally proceeds faster when electron acceptors such as nitrate or sulfate are available. Several of these parameters are included in the monitoring program for the microcosm study, and the data collected (to date) confirm that little sulfate (<0.07–4.0 milligrams per liter [mg/L]) and nitrate (< 0.09 mg/L) are present in the Facility groundwater. These geochemical conditions will limit the type of anaerobic degradation pathways (and rates) that can occur, particularly in microcosms with a finite amount of electron acceptors (as opposed to the aquifer underlying the Facility where rapid groundwater flow replenishes the supply of electron acceptors).

The biodegradation rate coefficients generated from the aerobic microcosms are generally comparable to published values for petroleum hydrocarbons. For example, Kao et al. (2006) evaluated natural attenuation of a petroleum hydrocarbon spill in an aquifer with a background oxygen concentration of 2.4 mg/L, and reported in situ first-order attenuation rates ranging from 0.051 per day (benzene) to 0.189 per day (1,2,4-trimethylbenzene). Xylenes and toluene were also evaluated and fell within this range. The range reported by Kao et al. (2006) is similar to the range

obtained for this same set of compounds in the microcosm for RHMW02 (0.11–0.18 per day). In a study of natural attenuation of aromatic hydrocarbons, Landmeyer et al. (1998) reported a much wider range for aerobic benzene and toluene biodegradation (0.03–0.84 per day), but notably was able to establish rapid aerobic biodegradation of naphthalene (0.88 per day) at a rate that was nearly identical to the RHMW02 microcosm (0.80 per day). Aerobic biodegradation rates from the RHMW01 microcosm were slightly slower than the rates from RHMW02 but are still comparable to the ranges of rates reported in these published studies. Collectively, these early microcosm results are consistent with literature studies and guidance documents that consider dissolved-phase petroleum hydrocarbons readily degradable under aerobic conditions (Chapelle 1999; EPA 1999; Das and Chandran 2011).

3.2 MICROBIAL PARAMETERS

Results from analysis of microbial parameters are available for a single sampling event (October 20–25, 2017). The QuantArray-Petro and NGS data are tabulated in Attachment B.6.2.

The major findings based on an interpretation of the data are summarized below:

- Samples from all wells showed evidence of aerobic and anaerobic petroleum hydrocarbon degrading capabilities. This is based on the presence of measurable levels of one or more functional genes associated with the aerobic and anaerobic degradation of BTEX, alkane, and/or polynuclear aromatic hydrocarbon (PAH) degradation.
- The abundance of most individual biomarkers that were detected was characterized as relatively low or moderate based on a comparison to other sample results from the laboratory's database. In part, this is attributable to the relatively low concentration of petroleum hydrocarbons (which are used to support growth of organisms expressing these enzymes) and redox conditions. Collectively, these conditions likely contributed to low levels of biomass overall that were observed in these tests (described below). In other words, the relatively low levels of biomarkers for petroleum hydrocarbons are primarily a reflection of low biomass at these locations.
- Based on the community analysis (NGS) and biomarker analysis, the data from RHMW01 and RHMW02 were highly similar, and RHMW04 was the most dissimilar to the other wells included in these tests. These relationships are consistent the relative locations of these wells at the Facility and their potential for exposure to petroleum hydrocarbons. However, there a few distinctions, as discussed below.
- RHMW02, RHMW03, and RHMW04 generally had the highest levels of biomarkers for aerobic degradation, including phenol hydroxylase (PHE), toluene dioxygenase (TOD), and toluene monooxygenase 2 (RDEG), all of which are associated with BTEX degradation. These functional genes are present at relatively low levels, consistent with the low level and/or sporadic detections of BTEX at these wells (particularly RHMW03 and RHMW04). RHMW04 is screened in an aerobic portion of the basalt aquifer based on the high dissolved oxygen levels (5.35 mg/L) observed in the October 2017 monitoring event. RHMW02 is screened in an apparently much more reducing portion of the basalt aquifer based on low dissolved oxygen levels (historically below 1 mg/L) and elevated methane levels (4.5 mg/L during the October 2017 monitoring event). In addition, the microcosm study showed that the RHMW02 microbial community could be easily stimulated to degrade petroleum hydrocarbons aerobically when oxygen was added to the bottles. Collectively, these data

indicate that a population of aerobic petroleum hydrocarbon degraders is present at RHMW02.

- RHMW01 generally had lower levels of most aerobic biomarkers than the other wells. This pattern is consistent with the existing geochemical data that suggest that the well is screened in groundwater zones that are more reducing, and the microcosm data that suggest that stimulating aerobic biodegradation took longer than in the sample from RHMW02.
- Samples from all four wells had moderate to high levels of BCR (benzoyl-coenzyme A reductase), which is a biomarker of an intermediate step in the anaerobic degradation of BTEX. However, biomarkers for other steps in anaerobic BTEX degradation were often low or missing from these sample locations.
- RHMW01 and RHMW02 had measurable levels of biomarkers associated with anaerobic PAH degradation (e.g., naphthalenes).
- RHMW01 and RHMW02 also had the highest levels of eubacteria, which can be used as a bulk indicator of microbial abundance. This is consistent with the diversity of aerobic and anaerobic biomarkers measured in samples from these wells. These levels were described as relatively low based on a percentile ranking within the laboratory's database (27th percentile for RHMW02 and 31st percentile for RHMW01). As a result, there is significant evidence that biodegradation of petroleum hydrocarbon can occur at these locations, but the rates may be controlled by the relatively low biomass concentrations.
- RHMW04 had the lowest levels of biomarkers for anaerobic petroleum hydrocarbon degradation of the four wells tested. This is consistent with the relatively oxidizing conditions in the groundwater at this location, as well as lower potential exposure to petroleum hydrocarbons (based on the historic groundwater monitoring data).
- The field blank also contained low but detectable levels of total eubacteria (a general bulk indicator of microbial abundance) and PM1 (a biomarker for BTEX and methyl tert-butyl ether [MTBE] degradation). The level of total eubacteria measured in the field blank (9,960 cells/mL) was only 6–20% of the levels measured in the four monitoring wells, confirming that the well samples contained significant biomass even after correcting for the levels in the field blank. The level of PM1 measured in the field blank (939 copies/mL) was similar or higher than the levels measured in samples from wells RHMW01 and RHMW03, meaning that the presence of elevated levels of this biomarker could not be confirmed in these wells. However, PM1 was present at 4× – 5× higher levels in samples from wells RHMW02 and RHMW04 relative to the field blank. These results are consistent with the other lines of evidence that suggest stronger aerobic biodegradation activity at wells RHMW02 and RHMW04.

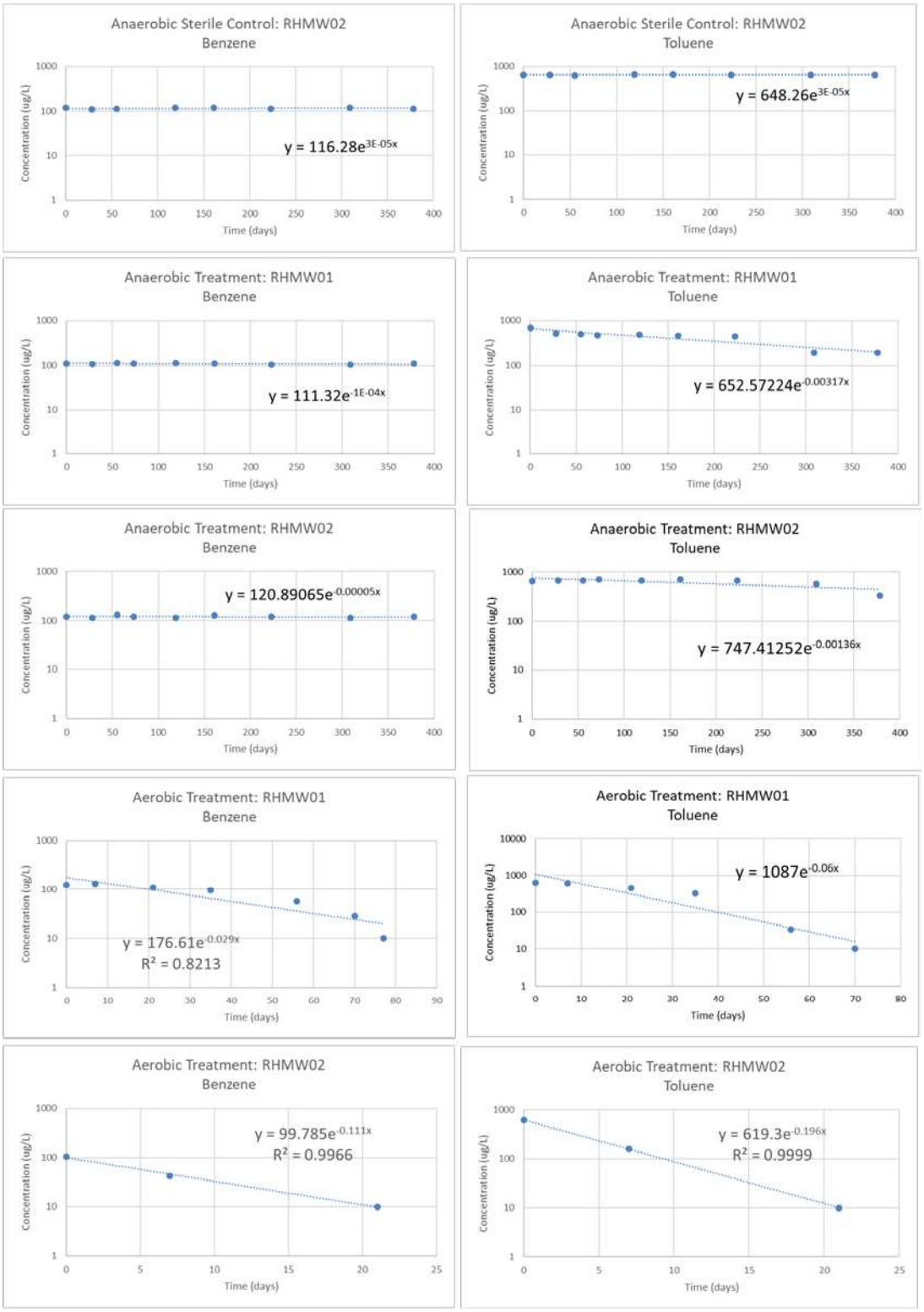

Note: In the regression equation for each set of data, the number in front of the x-variable represents the rate coefficient reported in Table 3-1.

Figure 3-1: Results of Microcosm Study: Benzene and Toluene

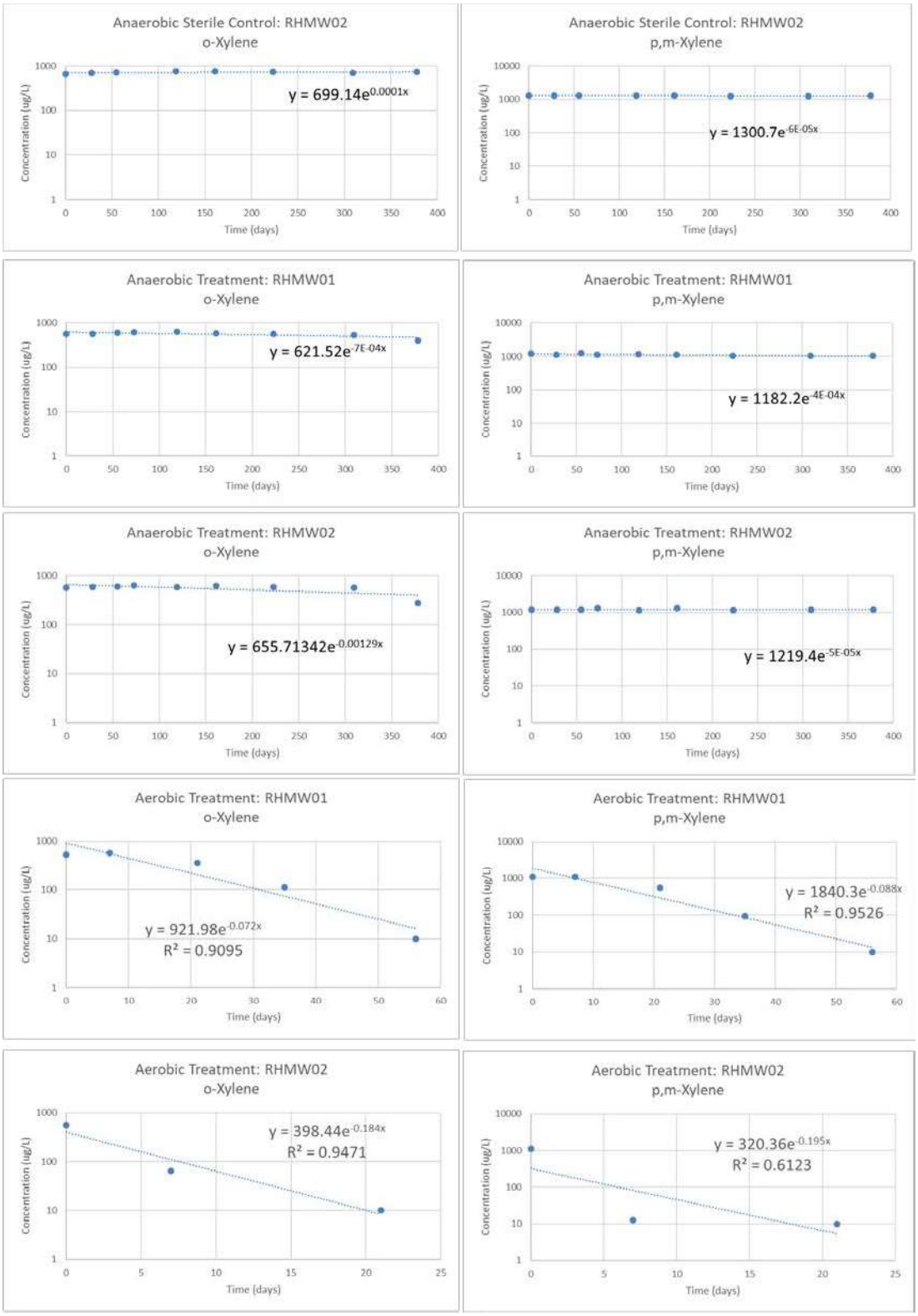

Note: In the regression equation for each set of data, the number in front of the x-variable represents the rate coefficient reported in Table 3-1.

Figure 3-2: Results of Microcosm Study: Xylenes

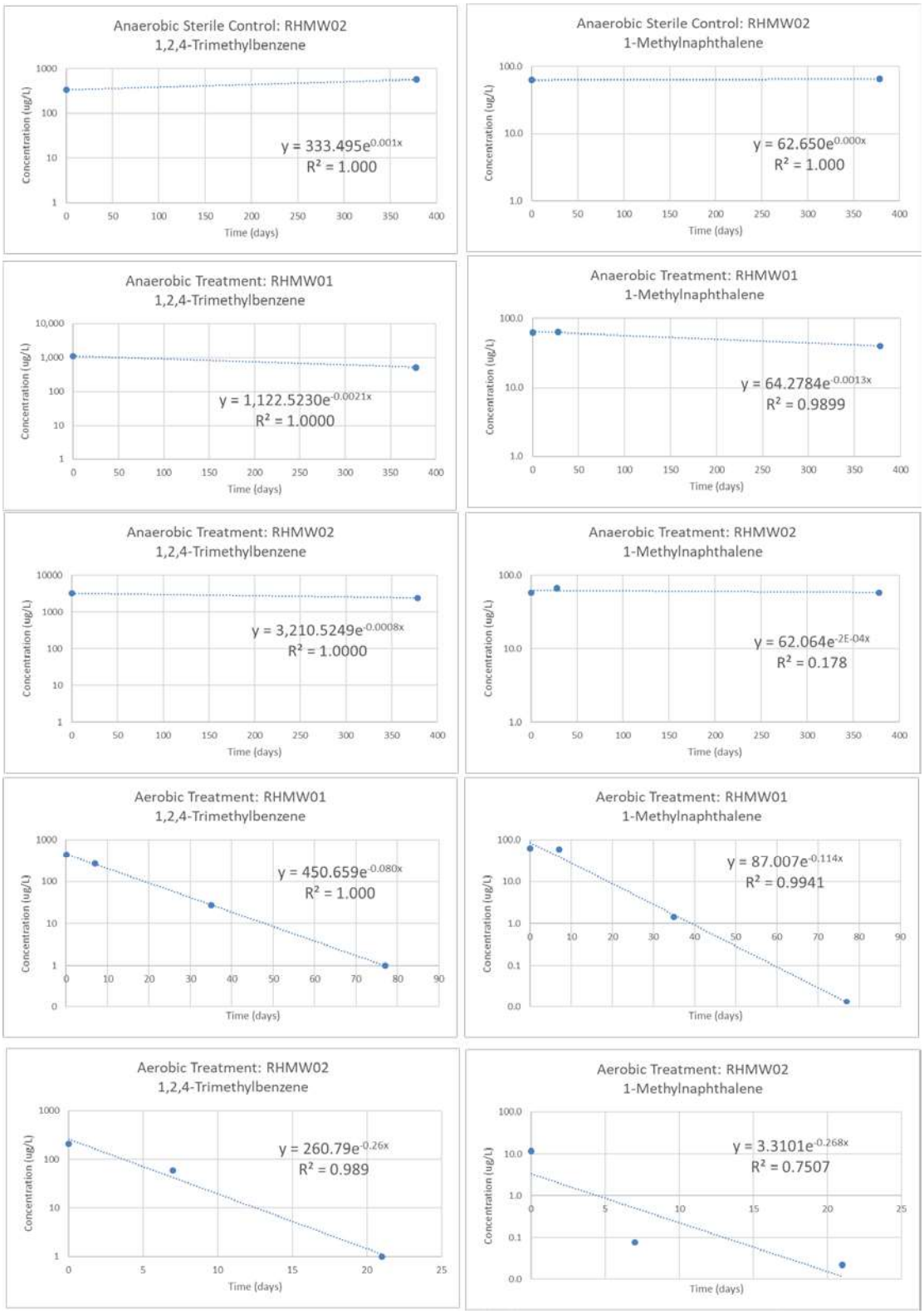

Note: In the regression equation for each set of data, the number in front of the x-variable represents the rate coefficient reported in Table 3-1.

Figure 3-3: Results of Microcosm Study: 1,2,4-Trimethylbenzene and 1-Methylnaphthalene

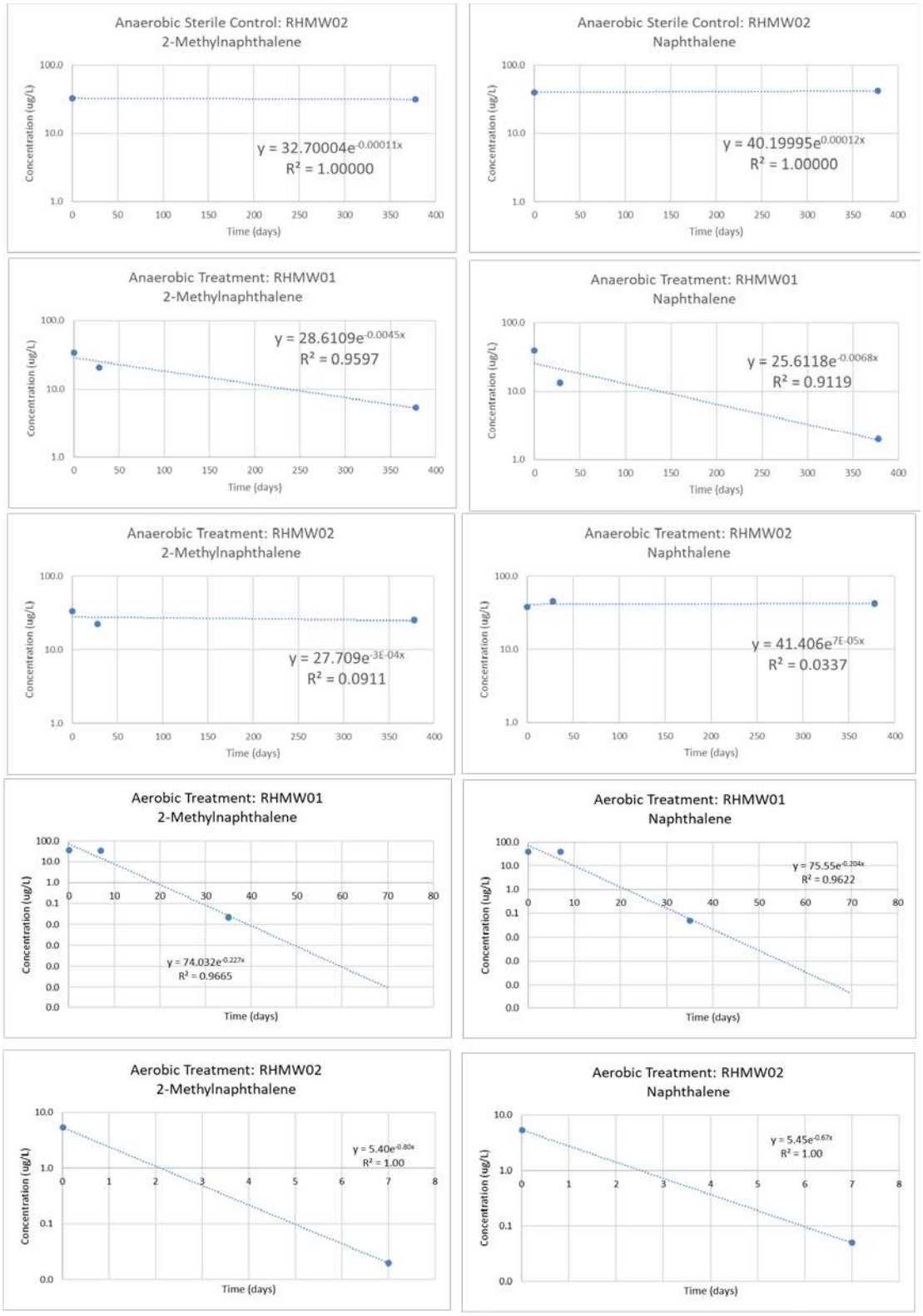

Note: In the regression equation for each set of data, the number in front of the x-variable represents the rate coefficient reported in Table 3-1.

Figure 3-4: Results of Microcosm Study: 2-Methylnaphthalene and Naphthalene

4. Conclusions

Results are presented from two different studies to better understand biodegradation potential at the Facility. The microcosm study was used to understand the biodegradation rates for selected petroleum hydrocarbons at RHMW01 and RHMW02, while molecular biological tools have been used to analyze for several microbial parameters in a larger set of wells.

In microcosms maintained under aerobic conditions, rapid degradation of all constituents was observed in RHMW02 (half-life < 7 days for all constituents, including benzene, toluene, xylenes, and PAHs). Slower aerobic degradation was observed in RHMW01 (half-lives currently on the order of 3–25 days).

Based on the microcosm results, degradation of these petroleum hydrocarbons is relatively slow under anaerobic conditions, with half-lives generally on the order of 63—>10,000 days. Slower anerobic degradation was observed in RHMW01 than RHMW02. Degradation of several compounds could not be established in RHMW01, and no degradation of benzene could be established in microcosms from either well. When degradation was observed under anaerobic conditions, it occurred after a lag period, indicating that native microbial populations were acclimating to the test conditions.

A suite of different functional genes associated with both aerobic and anaerobic petroleum hydrocarbon degradation was detected in samples from all four wells (RHMW01, RHMW02, RHMW03, and RHMW04). The presence of functional genes for degradation of petroleum hydrocarbons confirms that aerobic and anaerobic microorganisms are both present and active (i.e., the genes would not be expressed if the microorganisms were not active). These biomarkers appear to be present at relatively low to moderate concentrations, which is a function of the apparently low biomass measured at these locations.

The microbial data are largely consistent with concentration trends and geochemical conditions at the Facility. Specifically, the highest concentrations of petroleum hydrocarbon concentrations are generally measured at RHMW02 and then attenuate significantly moving away from this well. The molecular data suggest that a combination of anaerobic and aerobic processes is responsible for this attenuation, although the potential for rapid aerobic degradation (as observed in the microcosms) is restricted somewhat by the availability of oxygen. The degradation rates under aerobic conditions are apparently lower at RHMW01 based on the microcosm data, but the more rapid degradation under anaerobic conditions, as well as the molecular data, provide additional lines of evidence that biodegradation within the plume is contributing to the attenuation observed at the Facility.

RHMW03 and RHMW04 are located in areas with low or non-detectable levels of most petroleum hydrocarbon constituents. However, there is still biodegradation potential at these locations due to the presence of abundant dissolved oxygen and multiple biomarkers for aerobic and anaerobic degradation.

5. References

Chapelle, F. H. 1999. "Bioremediation of Petroleum Hydrocarbon-Contaminated Ground Water: The Perspectives of History and Hydrology." *Groundwater* 37 (1): 122–132.

Das, N., and P. Chandran. 2011. *Microbial Degradation of Petroleum Hydrocarbon Contaminants: An Overview*. DOI: 10.4061/2011/941810. Biotechnology Research International.

Environmental Protection Agency, United States (EPA). 1999. *Monitored Natural Attenuation of Petroleum Hydrocarbons*. EPA Remedial Technology Fact Sheet. EPA/600/F-98/021. May.

Kao, C. M., W. Y. Huang, L. J. Chang, T. Y. Chen, H. Y. Chien, and F. Hou. 2006. "Application of Monitored Natural Attenuation to Remediate A Petroleum-Hydrocarbon Spill Site." *Water Science & Technology* 53 (2): 321–328.

Landmeyer, J. E., F. H. Chapelle, M. D. Petkewich, and P. M. Bradley. 1998. "Assessment of Natural Attenuation of Aromatic Hydrocarbons in Groundwater Near A Former Manufactured-Gas Plant, South Carolina, USA." *Environmental Geology* 34 (4): 279–292.

Attachment B.6.1: Summary of Current Data from Microcosm Study - Volatile Organic Compounds

GSI Job No. G-4902
Issued: 30 June 2019

ATTACHMENT B.6.1: SUMMARY OF CURRENT DATA FROM MICROCOSM STUDY - VOLATILE ORGANIC COMPOUNDS
Red Hill Facility, Hawai'i

Treatment	Date	Day	Replicate	Bottle Set	SiREM: Volatile Organic Compounds						ALS: Volatile Organic Compounds				Comment
					Methane	CB	Benzene	Toluene	o-Xylene	p,m-Xylene	1,2,4-Trimethylbenzene	1-methylnaphthalene	2-methylnaphthalene	naphthalene	
					µg/L	µg/L	µg/L	µg/L	µg/L	µg/L	µg/L	µg/L	µg/L	µg/L	
Anaerobic															
Anaerobic Sterile Control	24-Oct-17	0													Poisoned wth mecuric chloride and sodium azide.
RHMW02															Amended the first replicate with 100 µL of resazurin.
															Spiked with BTX and naphthalene compounds.
			ANSC RHMW02-1	1	510	<10	120	650	620	1400	326	64.9	32.8	40.9	
			ANSC RHMW02-2	2	510	<10	120	640	690	1200	341	60.4	32.6	39.5	
			Average Concentration (µg/L)		**510**	**ND**	**120**	**645**	**655**	**1300**	**334**	**62.7**	**32.7**	**40.2**	
	21-Nov-17	28	ANSC RHMW02-1	1	410	<10	110	670	670	1400					
			ANSC RHMW02-2	2	430	<10	110	620	730	1200					
			Average Concentration (µg/L)		**420**	**ND**	**110**	**645**	**700**	**1300**					
	18-Dec-17	55	ANSC RHMW02-1	1	310	<10	110	650	650	1400					
			ANSC RHMW02-2	2	480	<10	120	610	760	1200					
			Average Concentration (mg/L)		398	**ND**	115	630	705	1300					
	20-Feb-18	119	ANSC RHMW02-1	1	250	<10	120	680	680	1400					
			ANSC RHMW02-2	2	370	<10	120	660	810	1200					
			Average Concentration (mg/L)		310	**ND**	120	670	745	1300					
	03-Apr-18	161	ANSC RHMW02-1	1	250	<20	120	690	710	1400					
			ANSC RHMW02-2	2	380	<20	120	660	810	1200					
			Average Concentration (mg/L)		315	**ND**	120	675	760	1300					
	04-Jun-18	223	ANSC RHMW02-1	1	210	<20	120	680	690	1400					
			ANSC RHMW02-2	2	300	<20	110	620	770	1100					
			Average Concentration (mg/L)		255	**ND**	115	650	730	1250					
	29-Aug-18	309	ANSC RHMW02-1	1	210	<20	120	680	650	1400					
			ANSC RHMW02-2	2	300	<20	120	620	740	1100					
			Average Concentration (mg/L)		255	**ND**	120	650	695	1250					
	06-Nov-18	378	ANSC RHMW02-1	1	220	<20	110	660	670	1400	573	63.3	30.7	41.1	
			ANSC RHMW02-2	2	320	<20	120	640	780	1200	560	65.8	32	43	
			Average Concentration (mg/L)		270	**ND**	115	650	725	1300	**567**	**64.6**	**31.4**	**42.1**	
Anaerobic Natural Attenuation Treatment	24-Oct-17	0													Amended the first replicate with 100 µL of resazurin.
RHMW01															Spiked with BTX and naphthalene compounds.
			ANAT RHMW01-1	3	110	<10	120	760	580	1200	355	64.7	34.1	38.6	
			ANAT RHMW01-2	4	120	<10	100	620	560	1200	1,890	60.6	34.7	40.1	
			Average Concentration (µg/L)		**115**	**ND**	**110**	**690**	**570**	**1200**	**1,123**	**62.7**	**34.4**	**39.4**	
	21-Nov-17	28	ANAT RHMW01-1	3	57	<10	95	410	520	1000		65.6	19.9	12.5	
			ANAT RHMW01-2	4	110	<10	120	600	600	1200		62.1	21.4	14.1	
			Average Concentration (µg/L)		**84**	**ND**	**107.5**	**510**	**560**	**1100**		**63.9**	**20.7**	**13.3**	
	18-Dec-17	55	ANAC RHMW01-1	3	91	<10	110	470	580	1300					
			ANAC RHMW01-2	4	110	<10	120	540	610	1200					
			Average Concentration (mg/L)		100	**ND**	115	505	595	1250					
	05-Jan-18	73	ANAC RHMW01-1	3	81	<10	110	430	620	1100					
			ANAC RHMW01-2	4	69	<10	110	510	600	1100					
			Average Concentration (mg/L)		75	**ND**	110	470	610	1100					
	20-Feb-18	119	ANAC RHMW01-1	3	98	<10	110	420	610	1100					
			ANAC RHMW01-2	4	140	<10	120	560	650	1200					
			Average Concentration (mg/L)		119	**ND**	115	490	630	1150					
	03-Apr-18	161	ANAC RHMW01-1	3	130	<20	100	380	560	970					
			ANAC RHMW01-2	4	190	<20	120	540	610	1200					
			Average Concentration (mg/L)		160	**ND**	110	460	585	1135					
	04-Jun-18	223	ANSC RHMW02-1	3	150	<20	99	370	550	940					
			ANSC RHMW02-2	4	220	<20	110	510	590	1100					
			Average Concentration (mg/L)		185	**ND**	105	440	570	1020					
	29-Aug-18	309	ANSC RHMW02-1	3	190	<20	99	370	520	940					
			ANSC RHMW02-2	4	300	<20	110	<20	560	1100					
			Average Concentration (mg/L)		245	**ND**	105	190	540	1020					
	06-Nov-18	378	ANSC RHMW02-1	3	200	<20	100	380	570	970	523	37.8	2.6	0.63	
			ANSC RHMW02-2	4	370	<20	120	<20	240	1100	511	41.9	8.1	3.41	
			Average Concentration (mg/L)		285	**ND**	110	190	405	1035	**517**	**39.9**	**5.4**	**2**	
Anaerobic Natural Attenuation Treatment	24-Oct-17	0													Amended the first replicate with 100 µL of resazurin.
RHMW02															Spiked with BTX and naphthalene compounds.
			ANAT RHMW02-1	5	370	<10	120	660	520	1200	5,730	56.7	31.2	38.9	
			ANAT RHMW02-2	6	340	<10	120	620	610	1200	691	59.1	35.5	37.6	
			Average Concentration (µg/L)		**350**	**ND**	**120**	**640**	**560**	**1200**	**3211**	**57.9**	**33.4**	**38.3**	
	21-Nov-17	28	ANAT RHMW02-1	5	400	<10	110	650	560	1200					
			ANAT RHMW02-2	6	520	<10	120	690	610	1300					
			Average Concentration (µg/L)		**460**	**ND**	**115**	**670**	**585**	**1200**					
	18-Dec-17	55	ANAC RHMW02-1	5	820	<10	140	640	520	1100					
			ANAC RHMW02-2	6	910	<10	120	690	660	1300					
			Average Concentration (mg/L)		865	**ND**	130	665	590	1200					
	05-Jan-18	73	ANAC RHMW02-1	5	860	<10	120	720	630	1300					
			ANAC RHMW02-2	6	890	<10	120	690	630	1300					
			Average Concentration (mg/L)		875	**ND**	120	705	630	1300					
	20-Feb-18	119	ANAC RHMW02-1	5	860	<10	110	640	540	1100					
			ANAC RHMW02-2	6	880	<10	120	690	610	1200					
			Average Concentration (mg/L)		870	**ND**	115	665	575	1150					
	03-Apr-18	161	ANAC RHMW02-1	5	920	<20	120	700	600	1300					
			ANAC RHMW02-2	6	880	<20	130	710	630	1300					

GSI Job No. G-4902
Issued: 30 June 2019

ATTACHMENT B.6.1: SUMMARY OF CURRENT DATA FROM MICROCOSM STUDY - VOLATILE ORGANIC COMPOUNDS
Red Hill Facility, Hawai'i

Treatment	Date	Day	Replicate	Bottle Set	SiREM: Volatile Organic Compounds						ALS: Volatile Organic Compounds				Comment
					Methane	CB	Benzene	Toluene	o-Xylene	p,m-Xylene	1,2,4-Trimethylbenzene	1-methylnaphthalene	2-methylnaphthalene	naphthalene	
					µg/L	µg/L	µg/L	µg/L	µg/L	µg/L	µg/L	µg/L	µg/L	µg/L	
			Average Concentration (mg/L)		900	**ND**	125	705	615	1300					
	04-Jun-18	223	ANSC RHMW02-1	5	800	<20	110	620	550	1100					
			ANSC RHMW02-2	6	860	<20	130	700	620	1200					
			Average Concentration (mg/L)		830	**ND**	120	660	585	1150					
	29-Aug-18	309	ANSC RHMW02-1	5	870	<20	110	650	590	1200					
			ANSC RHMW02-2	6	770	<20	120	480	550	1200					
			Average Concentration (mg/L)		820	**ND**	115	565	570	1200					
	06-Nov-18	378	ANSC RHMW02-1	5	850	<20	120	650	540	1200	2500	56.8	17.5	42.7	
			ANSC RHMW02-2	6	900	<20	120	<20	<20	1200	2290	59.3	32.9	41.9	
			Average Concentration (mg/L)		875	**ND**	120	330	275	1200	**2395**	**58.1**	**25.2**	**42.3**	
Aerobic															
Oxygen Amended Natural Attenuation Treatment RHMW01	24-Oct-17	0													Amended the first replicate with 100 µL of resazurin.
															Spiked with BTX and naphthalene compounds.
															Amended with neat oxygen gas to target a headspace of 21% oxygen.
			ONAT (RHMW01)-1	7	150	<10	130	630	500	1100	539	65	34.6	35.3	
			ONAT (RHMW01)-2	8	160	<10	120	620	560	1100	343	61.4	40.1	43	
			Average Concentration (µg/L)		**155**	**ND**	**125**	**625**	**530**	**1100**	**441**	**63.2**	**37.4**	**39.2**	
	31-Oct-17	7	ONAT (RHMW01)-1	7	100.00	<0.010	140	610	590	1100	263	62.6	34.6	41.9	
			ONAT (RHMW01)-2	8	99	<0.010	120	600	570	1100	276	55.7	36.5	40.0	
			Average Concentration (µg/L)		**100**	**ND**	**130**	**605**	**580**	**1100**	**270**	**59.2**	**35.6**	**41.0**	
															Amended with neat oxygen gas to target a headspace of 21% oxygen.
	14-Nov-17	21	ONAT (RHMW01)-1	7	80	<10	110	440	350	540					
			ONAT (RHMW01)-2	8	81	<10	110	470	370	560					
			Average Concentration (µg/L)		**80.5**	**ND**	**110**	**455**	**360**	**550**					
	28-Nov-17	35	ONAT (RHMW01)-1	7	36	<10	94	290	94	87	54.6	2.90	0.045	<0.050	
			ONAT (RHMW01)-2	8	58	<10	98	350	120	98	<1	<0.020	<0.020	<0.050	
			Average Concentration (µg/L)		**47**	**ND**	**96**	**320**	**112**	**92**	27	**1.45**	**0.023**	**ND**	
															Amended with neat oxygen gas to target a headspace of 21% oxygen.
	08-Dec-17	45													Amended with neat oxygen gas to target a headspace of 21% oxygen.
	19-Dec-17	56	ONAT (RHMW01)-1	7	10	<10	32	<10	<10	<10					
			ONAT (RHMW01)-2	8	47	<10	81	58	<10	<10					
			Average Concentration (mg/L)		**28.5**	**ND**	**56.5**	**34**	**ND**	**ND**					
	02-Jan-18	70	ONAT (RHMW01)-1	7	10	<10	<10	<10	<10	<10					
			ONAT (RHMW01)-2	8	33	<10	46	<10	<10	<10					
			Average Concentration (mg/L)		**22.5**	**ND**	**28**	**ND**	**ND**	**ND**					
															Amended with neat oxygen gas to target a headspace of 21% oxygen.
	09-Jan-18	77	ONAT (RHMW01)-1	7	13	<10	<10	<10	<10	<10	<1	0.027	<0.020	<0.050	
			ONAT (RHMW01)-2	8	34	<10	<10	<10	<10	<10	<1	<0.020	<0.020	<0.050	
			Average Concentration (mg/L)		**23.5**	**ND**	**ND**	**ND**	**ND**	**ND**	ND	**0.014**	**ND**	**ND**	
Oxygen Amended Natural Attenuation Treatment RHMW02	24-Oct-17	0													Amended the first replicate with 100 µL of resazurin.
															Spiked with BTX and naphthalene compounds.
															Amended with neat oxygen gas to target a headspace of 21% oxygen.
			ONAT (RHMW02)-1	9	320	<10	100	580	560	980	197	7.96	2.54	3.70	
			ONAT (RHMW02)-2	10	130	<10	110	640	570	1200	220	15.1	8.18	7.12	
			Average Concentration (µg/L)		**225**	**ND**	**105**	**610**	**565**	**1120**	**209**	**11.5**	**5.4**	**5.4**	
	31-Oct-17	7	ONAT (RHMW02)-1	9	16	<10	<10	<10	<10	<10	<2.0	0.059	<0.020	<0.050	
			ONAT (RHMW02)-2	10	11	<10	0.075	310	120	15	59	0.096	<0.020	<0.050	
			Average Concentration (µg/L)		**13.5**	**ND**	**8.75**	**160**	**65**	**12.5**	**59**	**0.078**	**ND**	**ND**	
															Amended with neat oxygen gas to target a headspace of 21% oxygen.
	14-Nov-17	21	ONAT (RHMW02)-1	9	13	<10	<10	<10	<10	<10	<1	0.021	<0.020	<0.050	
			ONAT (RHMW02)-2	10	12	<10	<10	<10	<10	<10	<1	0.023	<0.020	<0.050	
			Average Concentration (µg/L)		**12.5**	**ND**	**ND**	**ND**	**ND**	**ND**	ND	**0.022**	**ND**	**ND**	
	14-Nov-17	22													Prepared samples for external analysis.
	20-Nov-17	27													Re-Spiked with BTX and naphthalene compounds.
															Amended with neat oxygen gas to target a headspace of 21% oxygen.
	21-Nov-17	28	ONAT (RHMW02)-1	9	<10	<10	240	680	600	1200	<1	6.90	2.34	4.22	
			ONAT (RHMW02)-2	10	<10	<10	170	920	480	900	<1	4.26	1.32	2.82	
			Average Concentration (µg/L)		**ND**	**ND**	**205**	**800**	**540**	**1050**	ND	**5.58**	**1.83**	**3.52**	
	05-Dec-17	48	ONAT (RHMW02)-1	9	11	<10	<10	<10	<10	<10	<1	<0.020	<0.020	<0.050	
			ONAT (RHMW02)-2	10	10	<10	<10	<10	<10	<10	<1	<0.020	<0.020	<0.050	
			Average Concentration (µg/L)		**11**	**ND**	**ND**	**ND**	**ND**	**ND**	ND	**ND**	**ND**	**ND**	

Notes:
µL - microliters
ANAT - anaerobic natural attenuation treatment
ANSC - anaerobic sterile control
BTX - benzene, toluene and xylenes
CB - chlorobenzene
mg/L - milligrams per leter
mmoles - millimoles
ONAT - oxygen amended natural attenuation
o-xylene - ortho-xylene
p+m-xylene - para and meta xylene

Attachment B.6.2: Summary of Microbial Parameter Data

ATTACHMENT B.6.2: SUMMARY OF MICROBIAL PARAMETER DAT
Red Hill Facility, Hawai'i

	Sample ID	ERH438		ERH439		ERH440		ERH441		ERH406	
	Collected	2017-10-25		2017-10-23		2017-10-23		2017-10-24		2017-10-20	
	Sample Type	Biofilter		Biofilter		Biofilter		Biofilter		GW Equipment	
	Well Name	RHMW01		RHMW02		RHMW03		RHMW04		Field	
Analyte	**Units**	**Result**	**Q**	**Result**	**Q**	**Result**	**Q**	**Result**	**Q**	**Result**	**Q**
QuantArray-Petro Results											
- Aerobic BTEX&MTBE Degradation: Toluene/Benzene Dioxygenase [TOD]	cells/mL	< 2.5	U	**130**		**135**		**72.3**		< 1.3	U
- Aerobic BTEX&MTBE Degradation: Phenol Hydroxylase [PHE]	cells/mL	**202**		**213**		**919**		**407**		< 1.3	U
- Aerobic BTEX&MTBE Degradation: Toluene 2 Monooxygenase/Phenol Hyroxylase [RDEG]	cells/mL	**50**		**366**		**399**		**410**		< 1.3	U
- Aerobic BTEX&MTBE Degradation: Toluene Ring Hydroxylating Monooxygenases [RMO]	cells/mL	**0.087**	**J**	< 1.8	U	< 3.4	U	< 2.5	U	< 1.3	U
- Aerobic BTEX&MTBE Degradation: Xylene/Toluene Monooxygenase [TOL]	cells/mL	< 2.5	U	< 1.8	U	< 3.4	U	**18**		< 1.3	U
- Aerobic BTEX&MTBE Degradation: *Methylibium petroleiphilum* PM1 [PM1]	cells/mL	**1,000**		**4,200**		**628**		**4,490**		**939**	
- Other Aerobic BTEX&MTBE Degradation Markers	cells/mL	< 2.5	U	< 1.8	U	< 3.4	U	< 2.5	U	< 1.3	U
- Aerobic PAHs&Alkanes Degradation: Naphthalene-inducible Dioxygenase [Nid A]	cells/mL	< 2.5	U	< 1.8	U	< 3.4	U	**32.3**		< 1.3	U
- Aerobic PAHs&Alkanes Degradation: Phenanthrene Dioxygenase [PHN]	cells/mL	< 2.5	U	**96.4**		< 3.4	U	< 2.5	U	< 1.3	U
- Aerobic PAHs&Alkanes Degradation: Alkane Monooxygenase [ALK]	cells/mL	< 2.5	U	< 1.8	U	< 3.4	U	**65.4**		< 1.3	U
- Other Aerobic PAHs&Alkanes Degradation Markers	cells/mL	< 2.5	U	< 1.8	U	< 3.4	U	< 2.5	U	< 1.3	U
- Anaerobic BTEX Degradation: Benzoyl Coenzyme A Reductase [BCR]	cells/mL	**11,400**		**9,130**		**25,300**		**2,460**		< 1.3	U
- Anaerobic BTEX Degradation: Benzylsuccinate Synthase [BSS]	cells/mL	**63.8**		**89.9**		< 3.4	U	< 2.5	U	< 1.3	U
- Anaerobic BTEX Degradation: Benzene Carboxylase [ABC]	cells/mL	< 2.5	U	< 1.8	U	< 3.4	U	< 2.5	U	< 1.3	U
- Anaerobic PAHs&Alkanes Degradation: Naphthylmethylsuccinate Synthase [MNSSA]	cells/mL	**465**		**641**		< 3.4	U	< 2.5	U	< 1.3	U
- Other Anaerobic PAHs&Alkanes Degradation Markers	cells/mL	< 2.5	U	< 1.8	U	< 3.4	U	< 2.5	U	< 1.3	U
- Other: Total Eubacteria	cells/mL	**173,000**		**131,000**		**54,900**		**50,700**		**9,960**	
- Other: Sulfate Reducing Bacteria	cells/mL	**2,070**		**4,520**		**1,960**		< 2.5	U	< 1.3	U
Next Generation Sequencing (NGS) Results											
- Phylum: Actinobacteria	% Total Reads	3.5%		3.4%		4.0%		8.9%		0.3%	
- Phylum: Bacteroidetes	% Total Reads	–		2.7%		1.0%		3.6%		0.2%	
- Phylum: Chloroflexi	% Total Reads	2.3%		–		1.1%		–		–	
- Phylum: Cyanobacteria	% Total Reads	3.8%		7.4%		–		0.6%		0.1%	
- Phylum: DNA	% Total Reads	–		–		–		–		0.0%	
- Phylum: Euryarchaeota	% Total Reads	–		4.4%		–		–		–	
- Phylum: Firmicutes	% Total Reads	10.4%		9.3%		11.6%		4.5%		0.3%	
- Phylum: Nitrospirae	% Total Reads	–		–		4.6%		1.1%		–	
- Phylum: Planctomycetes	% Total Reads	–		–		1.7%		–		–	
- Phylum: Proteobacteria	% Total Reads	16.7%		20.4%		30.0%		44.5%		69.3%	
- Phylum: Spirochaetes	% Total Reads	3.4%		–		–		–		–	
- Phylum: Thermi	% Total Reads	–		–		–		–		0.0%	
- Phylum: Thermodesulfobacteria	% Total Reads	2.8%		3.0%		–		–		–	
- Phylum: Verrucomicrobia	% Total Reads	–		–		–		0.3%		–	
- Phylum: Unclassified at Phylum Level	% Total Reads	41.4%		36.0%		41.0%		35.0%		29.6%	
- Genus: Acinetobacter	% Total Reads	–		–		–		3.7%		–	
- Genus: Aquabacterium	% Total Reads	–		–		–		7.8%		–	
- Genus: Arcobacter	% Total Reads	–		–		–		–		0.2%	
- Genus: Bacillus	% Total Reads	–		–		1.2%		2.5%		–	
- Genus: Brevibacterium	% Total Reads	–		–		–		3.7%		–	
- Genus: Calothrix	% Total Reads	2.9%		6.3%		–		–		0.1%	
- Genus: Candidatus Scalindua	% Total Reads	–		–		1.5%		–		–	
- Genus: Caulobacter	% Total Reads	–		–		–		–		1.1%	
- Genus: Comamonas	% Total Reads	–		–		–		5.0%		–	
- Genus: Crenothrix	% Total Reads	–		1.4%		–		–		–	
- Genus: Dehalogenimonas	% Total Reads	1.4%		–		–		–		–	
- Genus: Desulfovibrio	% Total Reads	–		–		3.7%		–		–	
- Genus: Flavobacterium	% Total Reads	–		–		–		–		0.1%	
- Genus: Geobacillus	% Total Reads	1.2%		–		–		–		–	
- Genus: Hydrogenophaga	% Total Reads	–		–		–		–		0.1%	
- Genus: Marinospirillum	% Total Reads	–		–		4.2%		–		–	
- Genus: Methylobacterium	% Total Reads	–		–		–		–		67.7%	
- Genus: Microbacterium	% Total Reads	–		–		–		2.8%		–	
- Genus: Pelotomaculum	% Total Reads	1.5%		2.1%		3.4%		–		–	
- Genus: Pseudomonas	% Total Reads	–		–		2.2%		7.8%		–	
- Genus: Rastonia	% Total Reads	–		–		–		–		0.1%	
- Genus: Sulfuricurvum	% Total Reads	–		1.2%		–		–		–	
- Genus: Thermodesulfatator	% Total Reads	2.8%		3.0%		–		–		–	
- Genus: Thermodesulfovibrio	% Total Reads	2.0%		1.8%		3.8%		–		–	
- Genus: Treponema	% Total Reads	2.9%		2.4%		–		–		–	
- Genus: Unclassified at Genus Level	% Total Reads	55.2%		49.7%		50.3%		40.6%		30.0%	

Attachment B.6.3: Laboratory Reports

- Attached as a PDF file attachment.
  Click to:

  - Show Attachment B.6.3 PDF file attachment
  - Show PDF bookmarks

Appendix B.6 Attachment B.6.3 file contents:

- B.6.3a Microcosm Final Report
- B.6.3b QuantArray-Petro Report
- B.6.3c Next Generation Sequencing (NGS) Report

This page intentionally left blank

Appendix B.7: Forensics and Data Evaluation - Groundwater

CONTENTS

Acronyms and Abbreviations iii

1. Introduction 1-1

2. Jet Fuel Chemistry 2-1

- 2.1 General Jet Fuel Fingerprinting and Chemistry 2-1
- 2.2 Solubility of Jet Fuel in Water 2-4
  - 2.2.1 Calculated Effective Solubilities of Site COPCs 2-6
- 2.3 Biodegradation of Jet Fuel 2-11
  - 2.3.1 Polar Compounds/Metabolites 2-11
  - 2.3.2 Evidence of Biodegradation of Site Jet Fuel 2-13

3. Evaluation of Dissolved Material Measured as TPH-d in Groundwater – RHMW02 3-1

- 3.1 Composition of TPH-d in Groundwater and Evidence of Natural Attenuation – RHMW02 3-1
  - 3.1.1 Evaluation of Hydrocarbon and Polar Metabolite Concentrations in Groundwater – RHMW02 3-1
  - 3.1.2 Evaluation of Hydrocarbon and PAH Concentrations in Groundwater – RHMW02 3-4
- 3.2 Evaluation of Non-COPCs and Tentatively Identified Compounds in Groundwater – RHMW02 3-7
- 3.3 Natural Attenuation Parameters in Groundwater 3-9

4. Conclusions 4-1

5. References 5-1

ATTACHMENTS

B.7.1 Summary of Concentrations and Calculated Effective Solubilities

FIGURES

2-1 Primary Types of Hydrocarbon Compound Classes in Petroleum and Petroleum Products 2-1

2-2 Chromatograms of JP-5 and JP-8 and Jet-A 2-3

2-3 Comparison of Analysis of a Jet A Sample by (a) GC/MS and (b) HPLC 2-4

2-4 Water Solubilities of n-Octane and Xylenes 2-4

2-5 Normalized Relative Distribution of Hydrocarbon Types 2-6

2-6 Combined Calculated Ideal Effective Solubility Ranges from the Data Tabulated in 2-3 and Attachment B.7.1 2-8

2-7 Combined Calculated Ideal Effective Solubility Ranges from the Data Tabulated in 2-3 and Attachment B.7.1, including Two FISC JP-5 Samples 2-8

2-8 Petroleum Fraction Composition of JP-8 (Seven Samples) 2-10

2-9 Examples of Polar and Nonpolar Compounds 2-12

2-10 Examples of Degradation Pathways for Toluene, Ethylbenzene, Xylenes, n-Propylbenzene, Naphthalene, and 2-Methylnaphthalene 2-12

2-11 "Fingerprinting" of Fresh and Biodegraded Jet and Diesel—Comparison to a Site Groundwater Sample 2-14

3-1 % Polar Compounds/ Metabolites of TPH-d for Samples from RHMW02 3-3

3-2 Chromatographic Fingerprints of TPH-d Before and After SGC in Groundwater from RHMW02 3-4

3-3 Extended PAH Analysis of October 2017 Samples from RHMW02 3-5

3-4 Extended PAH Analysis of a Jet Fuel Sample 3-6

3-5 Relative Distribution of Naphthalenes Observed in RHMW02 and Theoretical Distribution of Naphthalenes in Water Equilibrated with JP-5, JP-8, and F-76 3-7

TABLES

2-1 Typical Distribution of Compound Classes for Jet A, JP-8, and JP-5 2-2

2-2 Analysis of Water-Soluble Fraction of Kerosene 2-5

2-3 Calculated Ideal Effective Solubility in Water of Selected Compounds in Jet Fuels, Diesel, and F-76 2-7

2-4 Solubility Properties of Hydrocarbon Fractions 2-9

3-1 TOC and TPH-d (Before and After SGC) for Select Samples of RHMW02 3-2

3-2 Ratios of Sum of Methylnaphthalenes to Naphthalene in Fuel and Calculated for Water 3-7

3-3 Detected Volatile and Semivolatile Organic Analytes in RHMW02 3-8

ACRONYMS AND ABBREVIATIONS

(n)	number of samples
µg/L	micrograms per liter
AFRL	Air Force Research Laboratory
API	American Petroleum Institute
BTEX	benzene, toluene, ethylbenzene, xylenes
CI/LI	corrosion inhibitor/lubricity improver
COPC	chemical of potential concern
CSM	conceptual site model
DL	detection limit
DOH	Department of Health, State of Hawai‘i
EAL	Environmental Action Level
EC	equivalent carbon number
EHE Guidance	*Evaluation of Environmental Hazards at Sites with Contaminated Soil and Groundwater*
EPA	Environmental Protection Agency, United States
F-76	Diesel Fuel-Marine
FISC	Fleet Industrial Supply Center
FSII	fuel system icing-inhibitor
g/g-mole	grams per gram-mole
GC/MS	gas chromatography with mass spectrometry detection
GCXGC	two-dimensional gas chromatography
HPLC	high-pressure liquid chromatography
J	estimated value
JP	Jet Fuel Propellant
LNAPL	light non-aqueous-phase liquid
LOD	limit of detection
mg/L	milligrams per liter
NAP	natural attenuation parameter
NATO	North Atlantic Treaty Organization
NIST	National Institute of Standards and Technology
PAH	polynuclear aromatic hydrocarbon
ppm	parts per million
SDA	static dissipater
SGC	silica gel cleanup
SVOC	semivolatile organic compound
TIC	tentatively identified compound
TOC	total organic carbon
TPH	total petroleum hydrocarbons
TPH-d	total petroleum hydrocarbons – diesel range organics
TPH-g	total petroleum hydrocarbons – gasoline range organics
TPH-o	total petroleum hydrocarbons – residual range organics (i.e., TPH-oil)
TPHCWG	Total Petroleum Hydrocarbon Criteria Working Group
UD	University of Dayton
USAF	United States Air Force
VOC	volatile organic compound
vol%	percent by volume
wt%	percent by weight

1. Introduction

This subappendix, summarized in the Conceptual Site Model (CSM) main document Sections 7.1 and 7.2, is intended to facilitate understanding of fuel chemistry as it relates to contaminants in the environment in order to facilitate a thorough understanding of petroleum forensics. Petroleum and petroleum-based products are unique in environmental site assessment and management because these are complex mixtures of compounds with wide-ranging physical and chemical properties. Following release into the environment, these complex mixtures are subject to change due to a multitude of processes commonly referred to as weathering (e.g., volatilization, dissolution, biodegradation, oxidation). Light-molecular-weight hydrocarbons can be lost from the original fuel release by evaporation. Depending on molecular structure, some compounds partition into water. Volatilization and biodegradation are the most important degradation mechanisms for middle distillates such as jet and diesel fuels, which are the main types of fuels stored at the site. Aerobic and anaerobic biodegradation produce intermediate metabolites that are more polar and thus more water-soluble than the parent hydrocarbon. Thus, evaluation or fingerprinting of contamination from fuel releases in the environment must take into consideration the fuel chemistry to assess potential source, degree of weathering, and composition of any dissolved or residual material in light non-aqueous-phase liquid (LNAPL), air, water, and soil.

One way to evaluate petroleum is through assessment of these mixtures in air, soil, and water is through the estimation of total petroleum hydrocarbons (TPH), an analytical parameter that is defined by the method used to measure it. The analytical methods are variable (e.g., different extraction solvents, extraction methods, calibration standards, and reported carbon ranges are variable and sometimes overlap). Non-petroleum materials may also be measured (ITRC 2018).

In accordance with the State of Hawai'i *Evaluation of Environmental Hazards at Sites with Contaminated Soil and Groundwater, Volume 1* ("EHE Guidance," DOH 2017), the term "TPH" is defined as the sum total of parent petroleum hydrocarbons, as well as petroleum hydrocarbon-related metabolites and other degradants. The latter includes alcohols, phenols, ketones, aldehydes, and organic acids (Mohler et al. 2013; Zemo et al. 2013, 2017). The toxicity of parent petroleum hydrocarbon compounds and related degradants is assumed to be similar for initial screening purposes (DOH 2017, Vol 1).

Understanding the properties of hydrocarbons is essential in sampling and analysis and fate and transport considerations for developing CSMs for appropriate management of TPH in environmental media.

This subappendix includes description of jet fuel composition, partitioning into water, and biodegradation, as well as an assessment of what composes the TPH in groundwater from monitoring location RHMW02, the only well with concentrations of TPH-d (hydrocarbons within the middle distillates or diesel range) exceeding State of Hawai'i Department of Health (DOH) Environmental Action Levels (EALs). This information is used to assess potential presence of LNAPL at or near the water table. A comprehensive evaluation of all available groundwater data for all wells is included in CSM Appendix B.8 using multiple lines of evidence to assess potential impact to groundwater after the 2014 Jet Fuel Propellant (JP)-8 release from Tank 5 and evidence of impact to outlying wells from fuel releases/site operations. CSM Appendix B.8 also includes discussions regarding limitations of TPH methods and data quality issues with extremely low level detections and the use of multiple laboratories.

In this study, the objectives were to assess the type of released fuel likely responsible for the observed dissolved groundwater plume, and the properties of chemicals of potential concern (COPCs) that are part of the Red Hill risk-based decision criteria (DON 2017b).

2. Jet Fuel Chemistry

2.1 GENERAL JET FUEL FINGERPRINTING AND CHEMISTRY

Kerosenes/jet fuels are middle distillates from crude oil. Middle distillates (e.g., kerosene, diesel, home heating fuel, JP-5, JP-8, Jet A) are characterized by a wide variety of aliphatic hydrocarbons (straight, branched, and cyclic alkanes), polynuclear aromatic hydrocarbons (PAHs, especially naphthalene and methylnaphthalenes), and heterocyclic compounds with carbon ranges of approximately nine carbons (C9) to C25. A small component of C5–C8 aliphatics and benzene, toluene, ethylbenzene, and xylene (BTEX) aromatics are also present (DOH 2017 Vol. 2, App. 1). The exact composition of chemicals in a fuel depends on the crude oil source and on the refinery processes used for production. Irrespective of this, kerosenes/jet fuels consist predominantly of hydrocarbons in the approximate C7–C18 range:

- Approximately 80% aliphatic hydrocarbons (paraffins or straight and branched alkanes and naphthenes or cycloalkanes)
- Approximately 20% aromatic hydrocarbons (mainly alkylbenzenes and alkylnaphthalenes)
- Less than 5% alkenes (olefins)

The primary types of hydrocarbon compound classes are shown on Figure 2-1.

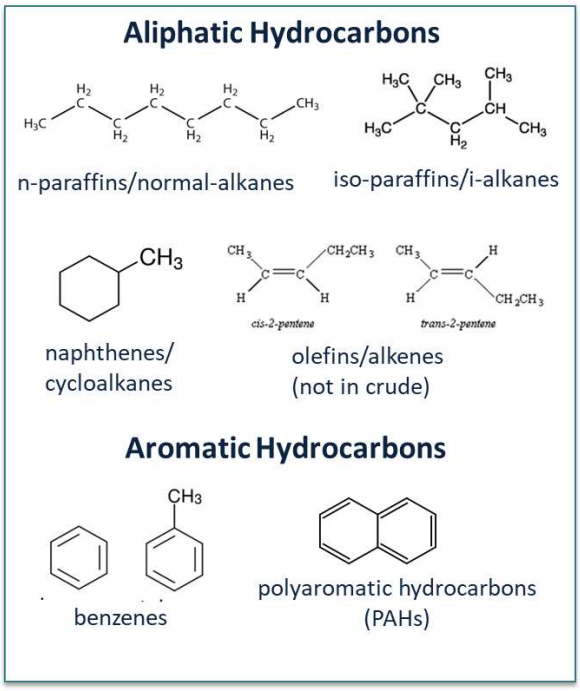

Figure 2-1: Primary Types of Hydrocarbon Compound Classes in Petroleum and Petroleum Products

Information on distribution of hydrocarbon types in Jet A, JP-8, and JP-5 is included in Table 2-1. Jet A is the primary kerosene-based fuel used by commercial airlines. It is governed by ASTM D1655, the standard specification for aviation turbine fuels. JP-8 (governed by military specifications document MIL-T-83139) is similar to Jet A except that JP-8 contains an additive package: static dissipater (SDA), fuel system icing-inhibitor (FSII), and corrosion inhibitor/lubricity improver (CI/LI). Both Jet A and JP-8 contain hydrocarbons in the C7–C18 range. Jet A with the additive package required by JP-8 can be designated as F-24 (governed by NATO Standard AFLP-3747). JP-5 is a higher-flash-point jet fuel developed by the Navy (MIL-T-5624) used on aircraft aboard ships, with hydrocarbons in the C8–C17 range. The data presented in Table 2-1 clearly show that Jet A, JP-8, and JP-5 are essentially equivalent in terms of hydrocarbon composition.

Table 2-1: Typical Distribution of Compound Classes for Jet A, JP-8, and JP-5

Compound Class	Unit	Jet A (n=13)	JP-8 (n=11)	JP-5 (n=2)
Total Saturates (Aliphatics)	vol%	80	79	78
Total Aromatics	vol%	20	21	22
- Monoaromatics (benzene and substituted benzenes)	*vol%*	*18*	*19*	*19*
- Diaromatics (naphthalene and substituted naphthalenes)	*vol%*	*3*	*2*	*3*

Source: CRC Report No. 647 (Hadaller and Johnson 2006).
vol% percent by volume
(n) number of samples

A small portion of the jet fuel, mainly the aromatic hydrocarbons, is water soluble with effective overall water solubility of approximately 5 milligrams per liter (mg/L) with about 3 mg/L from BTEX. Substituted benzenes, naphthalene, and substituted naphthalenes make up the rest of the dissolved components. See Section 2.2 for detailed discussion of solubility.

Most fuels are analyzed by gas chromatographic methods in a laboratory to fingerprint the fuel signature. Figure 2-2 shows the chromatographic profiles of fingerprints of JP-5, JP-8, and Jet A. It is evident that JP-5, JP-8, and Jet A are very similar. The large peaks in JP-5, JP-8, and Jet A profiles are primarily the n-alkanes that are the most abundant types of compounds in these fuels.

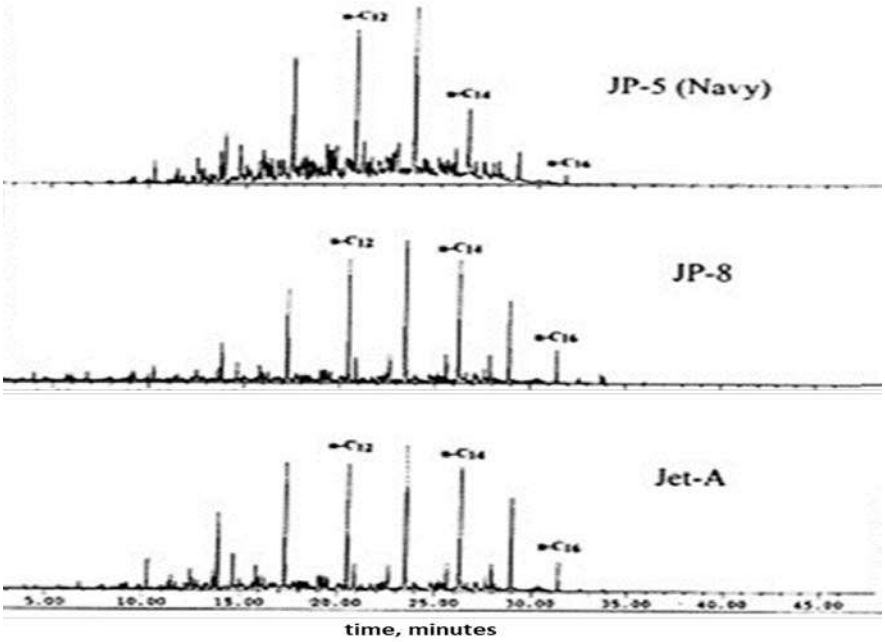

Source: Maurice et al. 2001.

Figure 2-2: Chromatograms of JP-5 and JP-8 and Jet-A

Hydrocarbon molecular structure is important in partitioning into water and weathering of the fuels once released to the environment (ITRC 2018). Examples of this importance include the following:

- The transport and dispersion of JP-5, JP-8, and Jet A fuels are dependent on the water solubility and volatility of the component hydrocarbon fractions.
- Lower-molecular-weight aliphatic hydrocarbons such as n-alkanes may volatilize relatively quickly from both water and soil, while larger aliphatics may be sorbed to organic particles in water or soil.
- Aromatic hydrocarbons will be dissolved in the aqueous phase in both vadose and saturated zones and may undergo some volatilization. Figure 2-3 shows the relative distribution of aromatics in Jet A (similar to JP-8). This figure illustrates the proportion of Jet A that is composed of saturates (aliphatics) and aromatics. The aromatic compounds are more water soluble.
- n-Alkanes can biodegrade under aerobic conditions and are essentially insoluble in water for molecules with greater than six carbons.
- Cycloalkanes are more resistant to biodegradation and are practically insoluble in water.
- Aromatics are more water-soluble, particularly ones with low molecular weight. These can be readily biodegraded.
- In general, the larger the number of carbons in a molecule, the less soluble and less volatile the molecule.

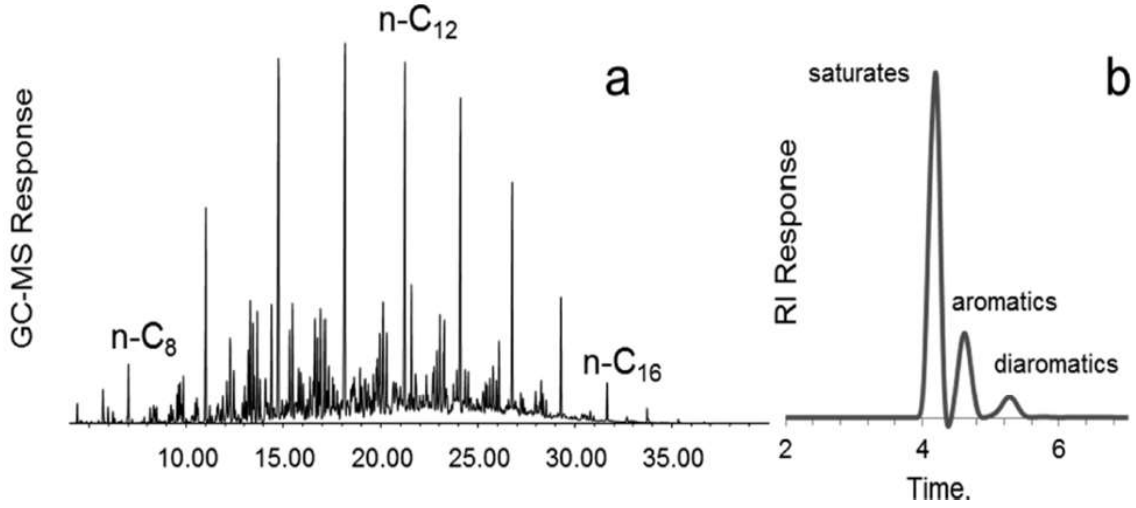

Source: CRC Report No. 647 (Hadaller and Johnson 2006).
GC/MS gas chromatography/mass spectrometry
HPLC high-pressure liquid chromatography

Figure 2-3: Comparison of Analysis of a Jet A Sample by (a) GC/MS and (b) HPLC

2.2 SOLUBILITY OF JET FUEL IN WATER

The main fuels currently stored at the Facility are the jet fuels JP-5 and F-24. Marine diesel fuels (i.e., F-76) are also stored at the Facility. As discussed in the previous section, the jet fuels are kerosene-type fuels with similar hydrocarbon composition.

Numerous studies indicate that kerosene-type fuels, which include Jet A, JP-5, and JP-8, have a water solubility of approximately 5,000 micrograms per liter (µg/L) (5 mg/L). Correspondingly, the EHE Guidance (DOH 2017) states that "*The solubility of diesel range and heavier fuels is assumed to be approximately 5,000 µg/L.*" The guidance also includes jet fuels as a subset of middle distillates and provides one set of regulatory criteria.

Water solubility values vary by orders of magnitude for the individual hydrocarbon constituents making up hydrocarbon-derived fuels. For individual compounds, both molecular weight and chemical structure influence the degree of solubility. Saturated/aliphatic hydrocarbons have relatively very low water solubility with respect to aromatic hydrocarbons. For instance, pure xylenes are greater than 200 times more soluble in water than pure n-octane (Figure 2-4). These compounds both have eight carbons, but the molecular structures are quite different.

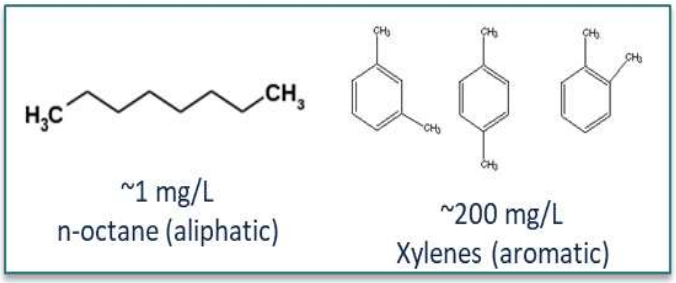

Figure 2-4: Water Solubilities of n-Octane and Xylenes

Aliphatic hydrocarbons in the jet fuel range are essentially insoluble in water, whereas aromatic hydrocarbons have pure compound solubilities ranging from 500 mg/L (toluene) to ~25 mg/L (methylnaphthalenes). Effective solubilities are even more variable, as these are proportional to the concentration of the individual aromatic hydrocarbons in the fuel, the average molecular weight of the fuel, and the inherent uncertainties with prediction of mole fraction in multicomponent fuels. Furthermore, component interactions within the organic phase result in deviations from ideality. Mixtures containing compounds that are different in structure (i.e., aliphatics and aromatics) deviate from ideal behavior, and the oil-to-water ratio has significant difference in the "effective solubility" (Bobra 1992). Furthermore, as the fuel weathers by evaporation, solubilization, and biodegradation, the remaining hydrocarbons have higher mole fractions and corresponding higher effective solubilities than the unweathered fuel (Baedecker et al. 2011, 2017). In summary, the effective solubility in groundwater of each component in fuels depends on the component structure, mole fraction in the fuel, loading rates of water to oil, and presence of other hydrocarbons, as well as temperature, ionic strength, and the amount of dissolved organic carbon in groundwater.

The ideal effective solubility in water of individual chemicals can be calculated from the mass fraction of the individual chemical in the fuel as follows:

Effective Solubility $C_w = x_o S$

C_w = *effective solubility*
x_o = *mole fraction (of chemical in fuel)*
S = *solubility*

Mole Fraction $x_o = MF_x MW_o / MW_x$

MF_x = *mass fraction of selected chemical in fuel*
MW_o = *average molecular weight of fuel*
MW_X = *molecular weight of selected chemical*

Table 2-2 and Figure 2-5 show the summary of a study by Coleman et al. (1984) on the partitioning of kerosene (the primary constituent of JP-5 and JP-8) into water. Although the Coleman et al. study used kerosene that as a whole product contained approximately 70% of aliphatic hydrocarbons (i.e., alkanes and cycloalkanes) and approximately 20% aromatic hydrocarbons (i.e., benzene, substituted benzenes, naphthalene and substituted naphthalenes), the water-soluble fraction contained primarily aromatic constituents (greater than 93%). This is expected, as aliphatic hydrocarbons with more than five carbons are essentially insoluble in water. In contrast, a wider range of aromatic hydrocarbons in the fuel have some water solubility, and these compounds partition into water depending on the effective solubility of the individual aromatic compound and its concentration in the fuel.

Table 2-2: Analysis of Water-Soluble Fraction of Kerosene

Kerosene Constituents	Estimated Weight % in Whole Product [a]	Water-Soluble Fraction [b]	
		0.5 hour	17 hours
Alkanes + Cycloalkanes	68.6	4.5	0.5
Benzene - Substituted Benzenes	13.7	63.5	53.2
Naphthalene + Substituted Naphthalenes	5.7	29.6	44.8

Source: Coleman et al. 1984.
[a] Estimated weight percent in unweathered kerosene.
[b] Estimated weight percent of constituents dissolved in water after 0.5 or 17 hours of incubation.

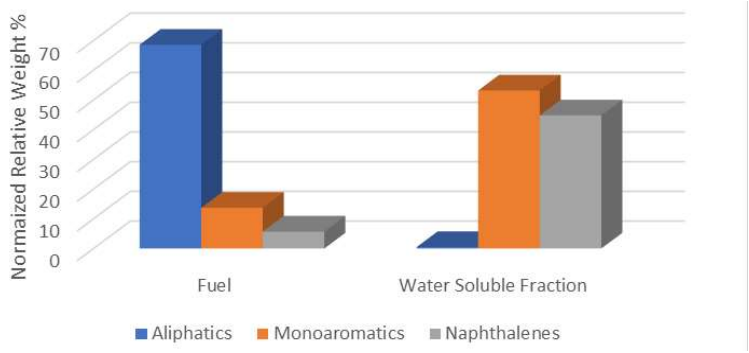

Source: Coleman et al. 1984.

Figure 2-5: Normalized Relative Distribution of Hydrocarbon Types

2.2.1 Calculated Effective Solubilities of Site COPCs

The main composition of the dissolved jet fuel from a recent release is primarly dissolved BTEX. As the fuel weathers by evaporation, solubilization, and biodegradation, the remaining residual fuel, in general, should be less water-soluble as the residual aromatics are larger molecules. However, the effective solubility of the remaining aromatic hydrocrabons would proportionally increase with increasing mole fractions (Baedecker et al. 2011, 2017). The absence of BTEX components, particularly the absence of xylenes, indicates no recent fuel releases and/or the active evaporation and biodegradation of released fuel.

Reliable data on the concentrations of individual fuel components are limited. Attachment B.7.1 presents the results from the analysis of benzene, naphthalene, 1-methylnaphthalene, and 2-methylnaphthalene for jet fuels (Jet A, JP-8, and JP-5), diesel, and F-76 from studies by the University of Dayton Research Instititute and the Air Force Research Laboratory (Shafer and Edwards 2011). These four compounds were analyzed by gas chromatography/mass spectrometry (GC/MS), a highly reliable method for identification and quantitation. Attachment B.7.1 also presents results from analysis of the same fuel types using two-dimensional gas chromatography (GCXGC), a group type analysis. Toluene is reported individually, but ethylbenzene and xylenes are combined as C2-benzenes. Individual concentrations for ethylbenzene and xylenes were estimated from assumed relative proportions of these compounds (pers. comm., J. T. Edwards, CIV USAF, Air Force Research Laboratory, January 2018). American Petroleum Institute (API) data for 14 Jet A samples and 12 diesel samples are also presented in Attachment B.7.1. These data were used to calculate effective solubilites for seven of the site COPCs.

Table 2-3 summarizes the calculated ideal effective solubilities from multiple sources. Table 2-3 includes information on maximum and minimum concentrations per fuel or combined fuels. Standard deviations were calculated for each COPC when possible (API data were available only as average, maximum, and minimum, thus it was not possible to calculate standard deviation). There is significant variability in effective solubilities for all compounds because of natural variability in concentration of individual components in the fuels. Nevertheless, the main difference among the jet fuels is the significantly lower benzene content in JP-5. This is expected for JP-5, since it is required to have less-volatile components because it is used on shipboard aircraft, where the risk of fire is an important consideration. Figure 2-6 clearly shows that all COPCs other than benzene in JP-5 are comparable for all jet fuels. Toluene, ethylbenzene, and xylenes may appear to be lower in JP-5, but data for these COPCs are limited to two samples.

Table 2-3: Calculated Ideal Effective Solubility in Water of Selected Compounds in Jet Fuels, Diesel, and F-76

Compound	Benzene (mg/L)	Naphthalene (mg/L)	1-Methyl-naphthalene (mg/L)	2-Methyl-naphthalene (mg/L)	Toluene (mg/L)	Ethylbenzene (mg/L)	Xylenes (mg/L)
Jet A & JP-8 - API & UD/AFRL	0.29	0.065	0.064	0.085	1.02	0.35	2.20
Number of Samples	*57*	*57*	*57*	*57*	*37*	*37*	*37*
Jet A - API	0.36	0.070	0.088	0.11	1.25	0.34	2.35
Number of Samples	*14*	*14*	*14*	*14*	*14*	*14*	*14*
Jet A (23), Jet A-1 (2) UD/AFRL	0.26 ± 0.24	0.067 ± 0.024	0.058 ± 0.015	0.081 ± 0.025	1.23 ± 0.74	0.29 ± 0.11	2.02 ± 0.73
Number of Samples	*25*	*25*	*25*	*25*	*13*	*13*	*13*
JP-8 UD/AFRL	0.27 ± 0.13	0.060 ± 0.021	0.053 ± 0.015	0.072 ± 0.024	0.93 ± 0.43	0.32 ± 0.13	2.21 ± 0.87
Number of Samples	*18*	*18*	*18*	*18*	*10*	*10*	*10*
JP-5 - UD/AFRL	0.028 ± 0.021	0.083 ± 0.045	0.068 ± 0.026	0.091 ± 0.040	0.27 ± 0.24	0.13 ± 0.07	0.88 ± 0.024
Number of Samples	*13*	*13*	*13*	*13*	*2*	*2*	*2*
FISC JP-5 - UD/AFRL	0.018	0.103	0.074	0.110	NA	NA	NA
FISC JP-5 - UD/AFRL	0.041	0.070	0.063	0.087	NA	NA	NA
Diesel on road <500ppm Sulfur - API	0.36	0.029	0.067	0.10	0.69	0.13	1.02
Number of Samples	*12*	*12*	*12*	*12*	*12*	*12*	*12*
Diesel - UD/AFRL	0.28 ± 0.13	0.021 ± 0.012	0.025 ± 0.016	0.044 ± 0.027	NA	NA	NA
Number of Samples	*39*	*39*	*39*	*39*	*NA*	*NA*	*NA*
F-76 - UD/AFRL	0.14 ± 0.077	0.076 ± 0.041	0.075 ± 0.032	0.118 ± 0.060	0.40 ± 0.13	0.10 ± 0.05	0.69 ± 0.31
Number of Samples	*18*	*18*	*18*	*18*	*9*	*9*	*9*
FISC F76 - UD/AFRL	0.080	0.030	0.047	0.061	NA	NA	NA
FISC F76 - UD/AFRL	0.204	0.028	0.049	0.060	NA	NA	NA

Notes: ppm: parts per million
UD/AFRL: University of Dayton and Air Force Research Laboratory (Shafer and Edwards 2011)
API samples: Analysis by GC/MS (ASTM D5769)
UD/AFRL samples: Analysis by GC/MS for benzene and all naphthalenes. Analysis by GCXGC for toluene, ethylbenzene, and xylenes. Data output is for C2-benzenes. Ethylbenzene and xylenes were calculated from the sum using 16% E and 84% X on advice from Tim Edwards, AFRL, Jan 2018 (emails).
Individual samples of JP-5 and F-76 from Pearl Harbor from Shafer and Edwards (2011) included for comparison to averaged data.
Effective Solubilities calculated by I. Rhodes, GSI Environmental.
Average molecular weight for JP-8 from GCXGC analysis (Striebich et al. 2014; pers. comm., J.T. Edwards, CIV USAF, Air Force Research Laboratory, January 2018): 160 g/mole.
Average molecular weight for JP-8 from GCXGC analysis (pers. comm., J. T. Edwards, CIV USAF, Air Force Research Laboratory, January 2018): 200 g/mole.
Solubility from TPHCWG Series, Vol. 3 (Gustafson, Tell, and Orem 1997).
Data sources: API (2010); API (2012); Shafer (2011); Striebich et al. (2014); pers. comm., J. T. Edwards, CIV USAF, Air Force Research Laboratory, January 2018.

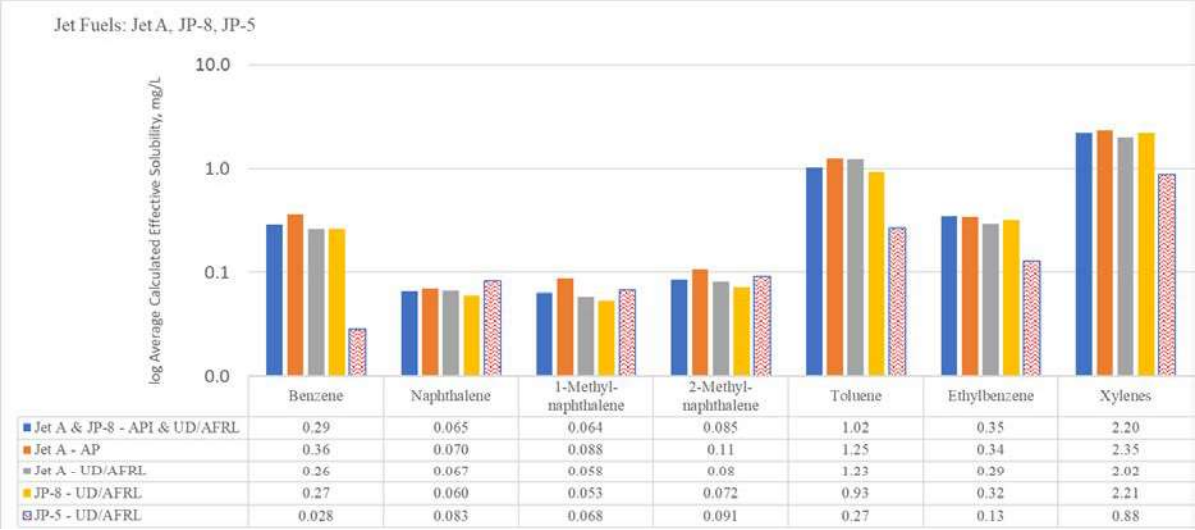

	Benzene	Naphthalene	1-Methyl-naphthalene	2-Methyl-naphthalene	Toluene	Ethylbenzene	Xylenes
Jet A & JP-8 - API & UD/AFRL	0.29	0.065	0.064	0.085	1.02	0.35	2.20
Jet A - AP	0.36	0.070	0.088	0.11	1.25	0.34	2.35
Jet A - UD/AFRL	0.26	0.067	0.058	0.08	1.23	0.29	2.02
JP-8 - UD/AFRL	0.27	0.060	0.053	0.072	0.93	0.32	2.21
JP-5 - UD/AFRL	0.028	0.083	0.068	0.091	0.27	0.13	0.88

Figure 2-6: Combined Calculated Ideal Effective Solubility Ranges from the Data Tabulated in Table 2-3 and Attachment B.7.1

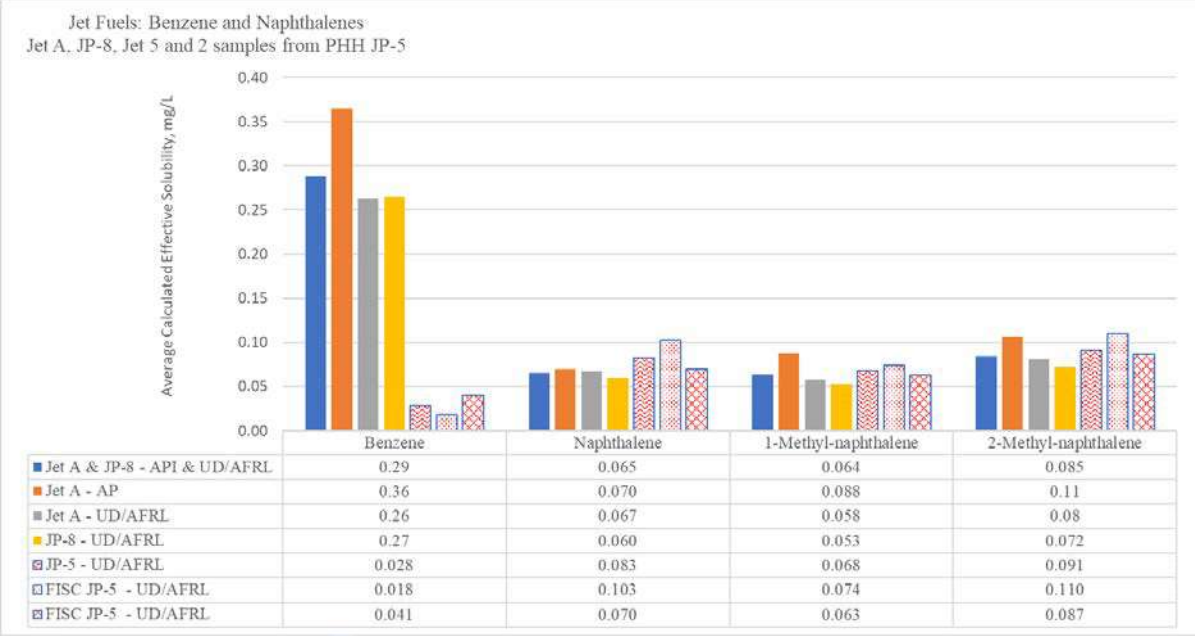

	Benzene	Naphthalene	1-Methyl-naphthalene	2-Methyl-naphthalene
Jet A & JP-8 - API & UD/AFRL	0.29	0.065	0.064	0.085
Jet A - AP	0.36	0.070	0.088	0.11
Jet A - UD/AFRL	0.26	0.067	0.058	0.08
JP-8 - UD/AFRL	0.27	0.060	0.053	0.072
JP-5 - UD/AFRL	0.028	0.083	0.068	0.091
FISC JP-5 - UD/AFRL	0.018	0.103	0.074	0.110
FISC JP-5 - UD/AFRL	0.041	0.070	0.063	0.087

Figure 2-7: Combined Calculated Ideal Effective Solubility Ranges from the Data Tabulated in Table 2-3 and Attachment B.7.1, including Two FISC JP-5 Samples

Table 2-3 also includes results from analysis of two samples of JP-5 and two samples of F-76 from the Fleet and Industrial Supply Center (FISC) Pearl Harbor (currently known as the NAVSUP Fleet Logistics Center Pearl Harbor). These samples are included in the averaged data. Results are shown individually for comparion to samples from throughout the United States. The two FISC JP-5 samples are included in the data set plotted on Figure 2-7 along with other jet fuels; these are plotted separately for comparison to the average results for all samples.

Additional concentration data and calculated effective solubilities for Jet A, JP-5, JP-8, diesel, and F-76 are included in Attachment B.7.1.

Other COPCs considered at the Facility include gasoline-, diesel-, and residual (oil)-range TPH (TPH-g, TPH-d, and TPH-o) (Section 3). These parameters are intended to be representative of gasoline, middle distillates (e.g., kerosene, jet, and diesel fuels), and heavy oils (e.g., motor oil). The results are dependent on the analytical methods used to measure them (ITRC 2018). A rough estimation of the effective solubility of these COPCs for jet fuel was done based on the data included in Table 2-4. Table 2-4 includes the estimated solubility of equivalent carbon number (EC) fractions of aliphatic and aromatic hydrocarbons defined by the *Total Petroleum Hydrocarbon Criteria Working Group* (TPHCWG) *Series*, Vol. 3 and Vol. 5 (Gustafson, Tell, and Orem 1997; Vorhees, Weisman, and Gustafson 1999) for risk assessment, as well as data from analysis of seven samples of JP-8. Jet fuels do not have hydrocarbons extending to the TPH-o range.

Only aromatic hydrocarbons in the fuel have significant solubility to partition into water. The types of compounds expected to be dissolved in groundwater are those indicated in Table 2-3, the aromatic fraction indicated in Table 2-4, and metabolites. The weight percentages from Figure 2-8 were visually estimated for use in the calculations in Table 2-4.

Table 2-4: Solubility Properties of Hydrocarbon Fractions

Equivalent Carbon Number Fraction (EC) [b]	EC	Molecular Weight (g/g-mole)	Solubility (mg/L)	Data for JP-8 (7 samples) - (wt% from Vorhees, Weisman, and Gustafson [1999], Figure 7, p. 11)		
				Average Aliphatic (wt%)	Average Aromatic (wt%)	Calculated Average Ideal Effective Solubility [a] (mg/L)
C5–C6 Aliphatic	5.5	80	36	1	—	0.72
>C6–C8 Aliphatic	7	100	5	2	—	0.16
>C8–C10 Aliphatic	9	130	0.4	13	—	0.064
>C10–C12 Aliphatic	11	160	0.03	39	—	0.012
>C12–C16 Aliphatic	14	200	8.00E-04	25	—	1.60E-04
>C16 Aliphatic	19	270	3.00E-06	4	—	7.10E-08
>C_6–C7 Aromatic [d]	6.5	78	1,780	—	0.0073	0.27
>C_7–C_8 Aromatic [e]	7.6	92	520	—	0.14	1.3
>C8–C10 Aromatic	9	120	65	—	2	1.7
>C10–C12 Aromatic	11	130	25	—	7	2.2
>C12–C16 Aromatic	14	150	6	—	6	0.38
>C16–C21 Aromatic	18.5	190	0.7	—	2	0.012
>C21 Aromatic	28	240	7.00E-03	—	3	0.00014
JP-8, Jet A	7 - 18	160[c]	—	—	—	—
Combined TPH Defined Equivalent Carbon Ranges [a,b]						
TPH-g (>C_6 to C_{10})						3.5
TPH-d (>C_{10} to C_{24})						2.6
TPH-o (C_{24+})						0

Source: TPHCWG Series, Vol. 5 (Vorhees, Weisman, and Gustafson 1999).
g/g-mole grams per gram-mole
Notes: Fraction composition data for JP-8 were used to calculate the effective solubility of the JP-8 fractions and estimate the effective solubility of TPH-g and TPH-d for JP-8 (Figure 2-7).

[a] Calculated by I. Rhodes, GSI Environmental.
[b] Equivalent Carbon Number (EC): Carbon number correlated with the retention time of constituents in a boiling point gas chromatography column, normalized to the n-alkanes.
[c] Average molecular weight for JP-8 from GCXGC analysis (Striebich et al. 2014; pers. comm., J.T. Edwards, CIV USAF, Air Force Research Laboratory, January 2018): 160 g/mole.
[d] Benzene is the only aromatic hydrocarbon in this range. Benzene average concentration from Shafer and Edwards (2011) 2011 (Attachment B.7.1).
[e] Toluene is the only aromatic hydrocarbon in this range. Toluene average concentration from Table 2-3.

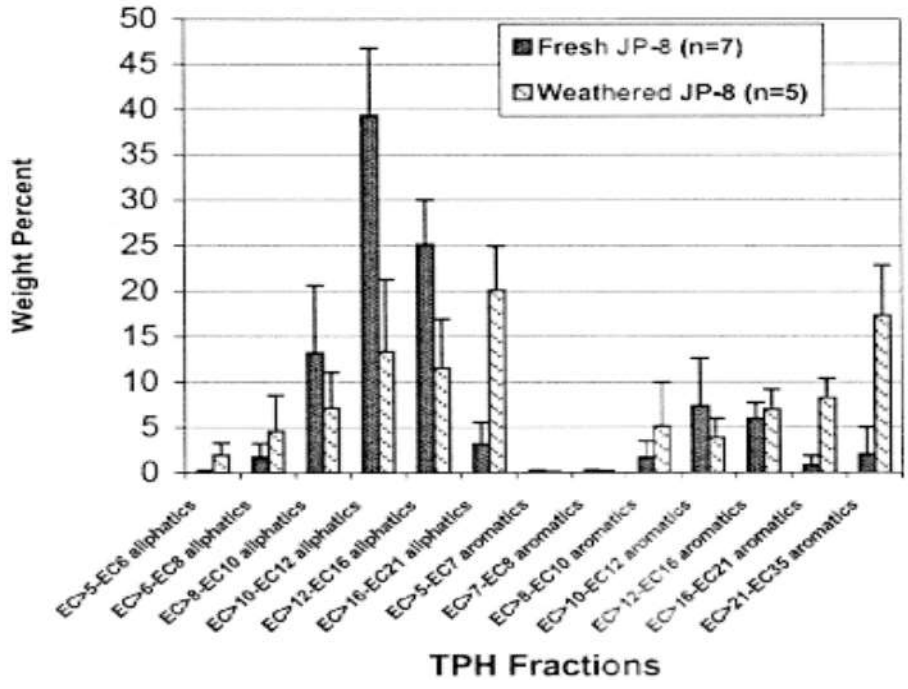

Source: TPHCWG Series, Vol. 5, pg. 11 (Vorhees, Weisman, and Gustafson 1999).

Figure 2-8: Petroleum Fraction Composition of JP-8 (Seven Samples)

The estimated ideal effective solubility in these studies is for fresh fuel. In general, it is not typical to analyze for individual compounds in groundwater beyond BTEX, naphthalenes, and selected PAHs. The concentration of dissolved fuel in water is usually measured as TPH-d (as further discussed in Section 3). It is possible to have dissolved TPH at concentrations exceeding the effective solubility of the fuel and not necessarily be indicative of the presence of free product. The TPH-d concentration may include both dissolved nonpolar hydrocarbons as well as metabolites from biodegradation of the dissolved aromatic components and from residual fuel. Metabolites are further discussed in Section 2.3.

The EHE Guidance (DOH 2017) indicates that the EAL for TPH-d assumes that petroleum-related compounds reported in this range will be dominated by non-volatile degradation compounds or "metabolites" of biogenic origin (Zemo et al. 2013, 2017). The resulting EAL is based on ingestion only and does not incorporate an inhalation pathway. Petroleum-related degradation compounds are assumed to have a similar toxicity as the parent hydrocarbon compounds for the purpose of this document, as it has not been otherwise demonstrated in a site-specific risk assessment (refer to EHE Guidance Vol. 1, Section 2.5.1 [DOH 2017]).

In summary, the compound types and the distribution of dissolved hydrocarbons in water from jet fuel releases are significantly different from the actual composition of the fresh and weathered jet fuel.

2.3 BIODEGRADATION OF JET FUEL

Biological weathering or biodegradation refers to chemical reactions catalyzed by microorganisms that alter and degrade hydrocarbons in the environment through actions of enzymes (biological catalysts). Enzymes are highly sensitive to the structure of the molecules they are binding and processing. Therefore, hydrocarbons with different structural elements (e.g., aliphatic, aromatic, cyclic/alicyclic, aromatic and/or aliphatic polycyclic, open-chain or branched) require different enzymes and microorganisms for biodegradation to occur. Hydrocarbons generally degrade most readily under aerobic conditions. Smaller aliphatic hydrocarbons are preferentially removed from the mixture by volatilization. Hydrocarbons can also biodegrade anaerobically. Anaerobic processes are predominant in the subsurface and in groundwater where biodegradation has depleted the available oxygen.

Different strains or types of microorganisms (e.g., bacteria, archaea, and fungi) differ in their ability to activate and/or process certain molecular features of hydrocarbons (e.g., position of functional groups or side chains, carbon chain length). That can explain, for example, why alkylbenzenes like toluene more readily degrade than a plain benzene molecule, or why a larger hydrocarbon (longer aliphatic chain) may be more degraded than a small one (Alvarez, Heathcote, and Powers 1998; Baedecker et al. 2011, 2017), or why there are differences in biodegradation rates of isomers of the same molecule. Factors that affect biodegradation include total mass of the release, oxygen levels, availability of other electron acceptors (especially in anaerobic conditions), water chemistry (pH, salinity, availability of nutrients), availability of hydrocarbons to microorganisms (affected by soil type and site geology), soil moisture, soil organic matter (competition for electron acceptors), and temperature.

Anaerobic biodegradation is quite complex. The most substantial differences in biodegradability of hydrocarbons are observed under anaerobic conditions. Under these conditions, some PAHs become almost impossible to degrade. For example, naphthalenes and alkylbenzenes can be recalcitrant when oxygen is not present.

Aerobic and anaerobic biodegradation produces intermediate metabolites that are more polar and thus more water-soluble than the parent hydrocarbon. Compared to aerobic degradation, anaerobic processes are both more diverse and more complex, thus anaerobic biodegradation occurs more slowly and is more prone to accumulation of metabolites (ITRC 2018).

2.3.1 Polar Compounds/Metabolites

Polar molecules are asymmetric molecules with electrons not shared equally in some of the bonds. Polar compounds can exist in nature as naturally occurring organic matter (e.g., humic material, organic acids) or these may also be formed by biodegradation of petroleum hydrocarbons (i.e., metabolites). Figure 2-9 illustrates polar versus nonpolar bonds.

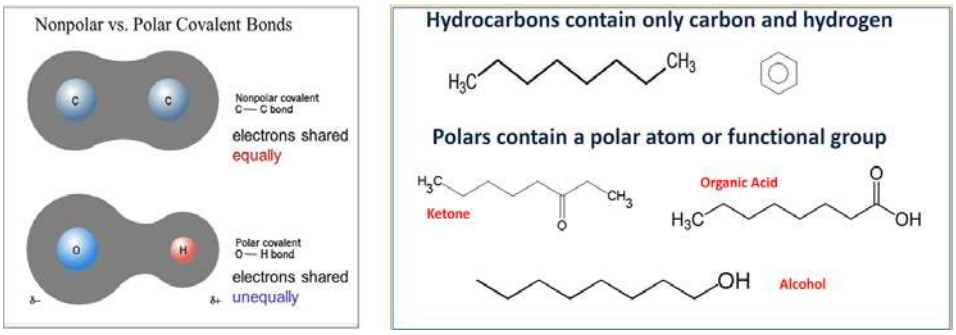

Figure 2-9: Examples of Polar and Nonpolar Compounds

Metabolites are polar molecules derived from chemicals that are undergoing or have undergone changes catalyzed by enzymes in living cells. Biodegradation of hydrocarbons is ubiquitous in soil and groundwater. Intermediate oxidation steps can result in acids/esters, alcohols, phenols, ketones, and aldehydes. These types of compounds are more soluble in water than the parent compound. For example, the intermediate compound for ethylbenzene indicated in Figure 2-10 (1-phenulethanol) is more than 100 times more soluble than ethylbenzene. Complete biodegradation ultimately converts hydrocarbons to carbon dioxide and water. Figure 2-10 shows examples of degradation pathways for several aromatic compounds common in jet fuels. These aromatic compounds partition into water from jet fuels and can biodegrade, resulting in formation of intermediate polar compounds or metabolites (Widdel and Rabus 2001); Figure 2-10 shows the bonds being broken and incorporation of oxygen into the molecules. The more polar intermediate biodegradation products have higher water solubility than the parent hydrocarbons.

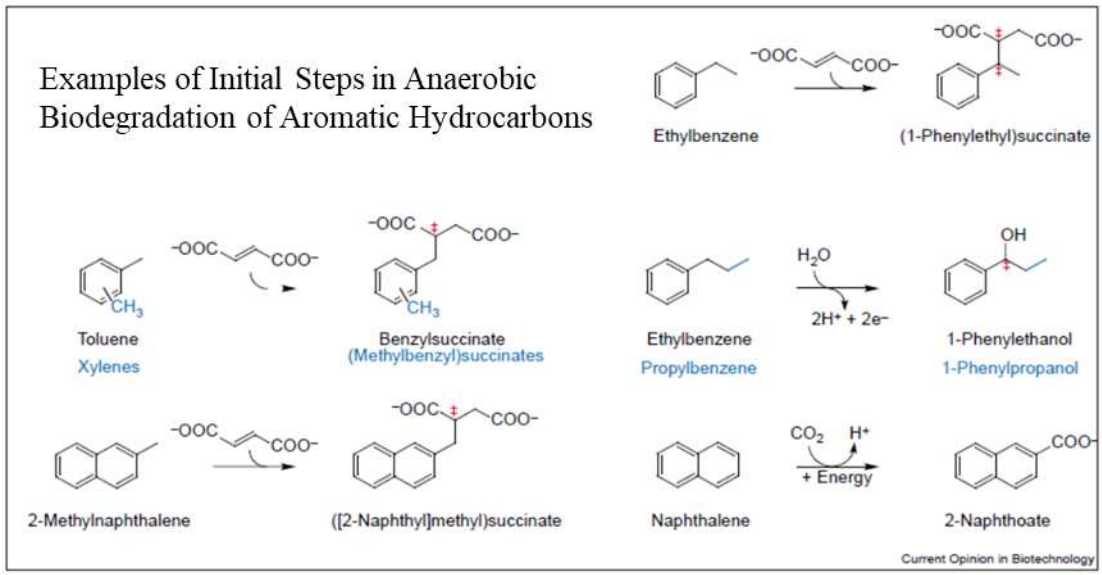

Source: Widdel and Rabus 2001.

Figure 2-10: Examples of Degradation Pathways for Toluene, Ethylbenzene, Xylenes, n-Propylbenzene, Naphthalene, and 2-Methylnaphthalene

2.3.2 Evidence of Biodegradation of Site Jet Fuel

Figure 2-11 shows the chromatograms from analysis of fresh and biodegraded jet and diesel fuels as well as the chromatogram obtained from TPH-d analysis from a sample of groundwater from the Facility (from monitoring well RHMW02). As discussed in Section 2.1, the chromatographic profile or fingerprint of jet and diesel fuels show the predominance of n-alkanes (Figure 2-2 and Figure 2-11). The n-alkanes are relatively easy to biodegrade under aerobic conditions. The chromatograms from analysis of biodegraded jet and diesel fuels show profiles that are characteristic of fuels that have depleted n-alkanes and predominance of highly branched alkanes and cycloalkanes, which are seen as unevenly distributed discrete peaks and the unresolved complex mixture or "hump." In comparison, the chromatogram from the analysis of the extracted dissolved material from RHMW02 has a very different profile. It is dominated by a "hump" and a few resolved peaks. A significant portion of the "hump" in the RHMW02 groundwater sample is heavier than the biodegraded jet fuel "hump." This profile is indicative of aromatic hydrocarbons from dissolved jet fuel (resolved peaks) and metabolites. Analysis of selected target compounds for this sample indicates that the largest resolved peaks are naphthalene, the two isomers of methylnaphthalene (C1-naphthalenes) and isomers with higher number of alkyl side chains substitution (C2-naphthalenes, C3-naphthalenes). Analysis of the extract after silica gel cleanup (SGC) eliminates the "hump," confirming that it is due to polar metabolites or biogenic matter (discussed in Section 3 and shown on Figure 3-2 and Figure 3-3).

The chromatograms provide evidence that the dissolved TPH-d in RHMW02 is from a jet fuel release that has weathered based on the aromatic hydrocarbons found in the water and the predominance of metabolites.

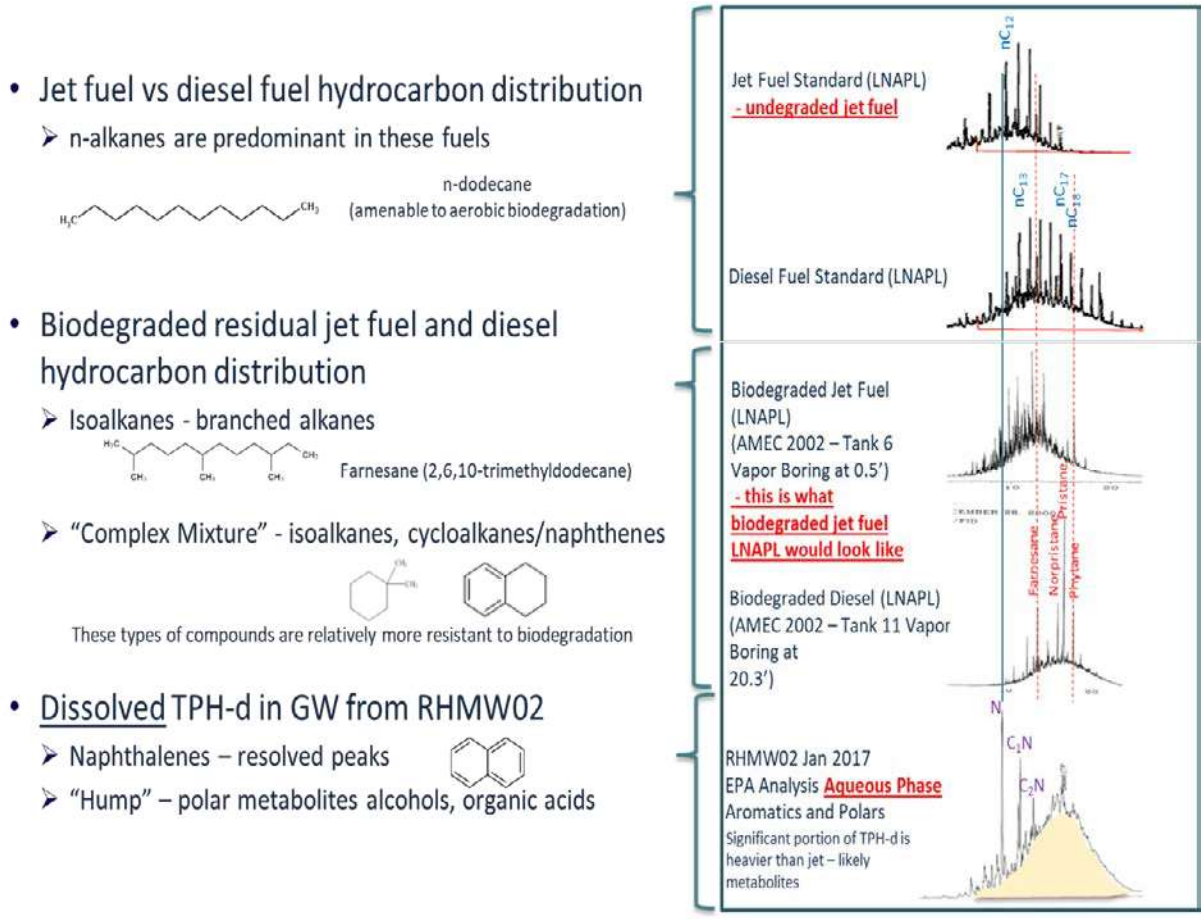

Figure 2-11: "Fingerprinting" of Fresh and Biodegraded Jet and Diesel—Comparison to a Site Groundwater Sample

3. Evaluation of Dissolved Material Measured as TPH-d in Groundwater – RHMW02

3.1 COMPOSITION OF TPH-D IN GROUNDWATER AND EVIDENCE OF NATURAL ATTENUATION – RHMW02

As discussed in more detail in CSM main document Section 7.1.2.1, for the available monitoring history to date, there has been no confirmed direct measurement of LNAPL in any Red Hill monitoring well. The focus of this evalution is to (1) characterize extractable organics in water inmonitoring well RHMW02, the only well with continuous TPH-d detections, and (2) correlate the TPH results to a type of source fuel.

As discussed in Section 2.2, the main components of jet fuels are aliphatic compounds that are not significantly water-soluble and are not expected in dissolved plumes. The aromatic compounds in jet fuels partition from the fuel into water based on the effective solubilities of the individual compounds in water. Therefore, the chromatographic profile or fingerprint of jet fuel is quite different from the corresponding fingerprint of dissolved jet fuel in water. Signficant changes in chromatographic profiles are expected as biodegradation progresses (ITRC 2018). Hydrocarbons biodegradation products are far more soluble in water than the parent hydrocarbons. For example, n-dodecane, a straight chain alkane relatively abundant in jet fuels, has water solubility of 4 µg/L and n-dodecanoic acid (a metabolite) has water solubility of 4,800 µg/L. Therefore, it is not uncommon to encounter TPH results that exceed the expected solubility of the corresponding undegraded fuels.

Per the EHE Guidance (DOH 2017), TPH-d is defined as anything that is extracted by an organic solvent from water, detected by gas chromatography with flame ionization eluting between nC10 and nC24, and quantitated with respect to a diesel standard. The method is not intended to detect all organic carbon-containing compounds but rather only those compounds that are amenable to the method as defined.

EHE Guidance Vol.1 (DOH 2017) states, "*The term "TPH" is defined for use in this guidance as the sum of total parent petroleum hydrocarbons as well as petroleum hydrocarbon-related metabolites and other degradants*." Furthermore, "*Petroleum-related degradation compounds are assumed to have similar toxicity as the parent hydrocarbon compounds for the purpose of this document, unless demonstrated in a site-specific risk assessment."* This means that reported TPH-d concentrations are not only the soluble components of the original fuel, but all detectable matter in the specified analysis window (nC10 to nC24), which would include the soluble components of the fuel plus metabolites of degradation of the dissolved aromatics and possible metabolites of degradation of aliphatic and aromatic hydrocarbons of any residual fuel in soil nearby.

3.1.1 Evaluation of Hydrocarbon and Polar Metabolite Concentrations in Groundwater – RHMW02

The relative concentrations of hydrocarbons in water vs. polar metabolites from TPH-d analysis can be evaluated using SGC methods to separate and remove polar compounds from environmental media extracts to minimize misidentification and inclusion of metabolites in the reported TPH concentration. Certain chemicals related to well construction and sampling equipment (e.g., grease used for the water pump used during drilling activities) may also contribute to TPH detections. Thus, the TPH chromatograms should be evaluated to determine if there are other sources of TPH than fuels or degraded fuels.

Results from analysis of total organic carbon (TOC) and TPH-d before and after SGC for samples from RHMW02 are summarized in Table 3-1.TOC measures the total organic carbon in the samples, whereas TPH measures what can be extracted from water with the solvent used for extraction, what is sufficiently volatile to be analyzed by gas chromatography, and what is within a carbon range as defined by the method used. It is evident that TPH-d is not measuring all carbon-containing compounds in groundwater since TOC is higher than TPH-d. The difference between these two types of measurements is also indicative of polar compounds/metabolites or naturally occurring organic matter present in the samples. It is also clear that the bulk of the organic compounds measured in RHMW02 as TPH-d is due to polar material, likely metabolites generated from biodegradation of dissolved petroleum compounds and potentially biodegradation of the source LNAPL. Variations in TPH-d results are expected since these methods rely on quantification of mixtures that spread over a relatively large retention time window and can be affected by baseline variationsIn addition, polar compounds are not very compatible with gas chromatographic techniques that rely on vaporization of the compounds. Polar compounds do not partition well between the vapor and liquid stationary phases of the chromatographic column, thus hampering the compound's ability to reach the detector. This leads to chromatograms showing unresolved humps (where polar metabolites do not give sharp peaks and tend to tail [i.e., appear in the chromatographic pattern as wide peaks or humps extending past the expected retention time window]), which make metabolites more difficult to quantify because these can have significantly different responses in the flame ionization detector compared to the diesel standard used to calibrate the gas chromatograph. Though not typically an issue with hydrocarbon analysis, samples analyzed later the same day may also have more peak tailing because more active sites may be present in the gas chromatograph injection system or instrument column due to nonvolatile residues from previous samples. Limitations of TPH measurements are further discussed in CSM Appendix B.8.

Table 3-1: TOC and TPH-d (Before and After SGC) for Select Samples of RHMW02

Date Sampled	Laboratory	Unit	TOC	TPH-d	TPH-d with Silica Gel Cleanup	TPH-d (Dup.)	TPH-d with Silica Gel Cleanup (Dup.)
May-17	APPL	µg/L	—	1,000	< 480 U	—	—
Jun-17	APPL	µg/L	—	1,000	570	—	—
Jul-17	APPL	µg/L	—	1,000	250	—	—
Oct-17	APPL	µg/L	6,900	1,300	230 J	1,600	230
	EPA	µg/L	—	3,300	550	—	—
Mar-18	APPL	µg/L	—	1,900	640	1,800	460
	EPA	µg/L	—	2,900	430	—	—
Apr-18	APPL	µg/L	4,700	2,700	510	2,800	420
Jul-18	APPL	µg/L	3,500	2,100	580	1,500	260
	EPA	µg/L	—	2,400	570	—	—
Oct-18	APPL	µg/L	4,130	2,000	370	2,100	430
Jan-19	APPL	µg/L	3,900	2,400	420	2,700	430

Notes: APPL non-detect results reported as < the limit of detection (< LOD U) in accordance with the Department of Defense *Quality Systems Manual*, Version 5.1 (DoD and DOE 2017). EPA non-detect results are reported as less than the detection limit (< DL U).
(Dup.) Duplicate Sample
J estimated value
U undetected

Results from split samples analyzed by the United States Environmental Protection Agency (EPA) Region 9 laboratory and the Navy-contracted laboratory (APPL) also showed how the unresolved polar metabolite hump led to different reported TPH-d concentrations between laboratories (see Table 3-1 and Figure 3-1) despite use of the same analytical method. Following evaluation of the split sampling results, APPL laboratory implemented changes to match EPA Region 9 extraction protocols. The low recovery of TPH-d at APPL laboratory is likely due to differences in extraction efficiency of polar metabolites.

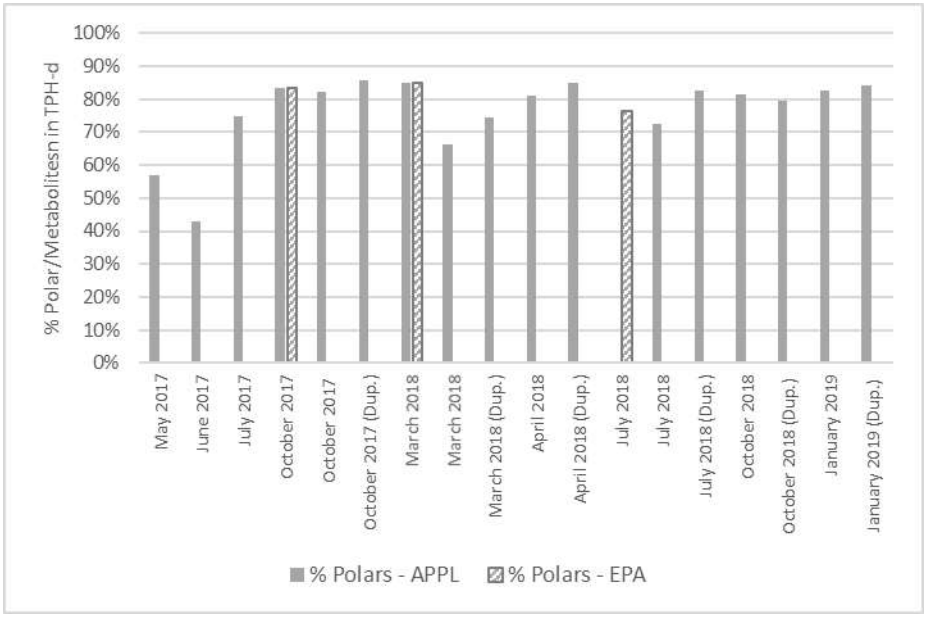

Figure 3-1: % Polar Compounds/ Metabolites of TPH-d for Samples from RHMW02

Figure 3-2 shows the typical chromatograms for analysis of dissolved material in RHMW02 for TPH-d before and after SGC. These chromatographic profiles are consistent with dissolved aromatic hydrocarbons in a weathered jet fuel, showing the presence of substituted benzenes (C3+), naphthalene, and substituted naphthalenes (C1+). The chromatographic profile of TPH-d before SGC shows the additional presence of metabolites.

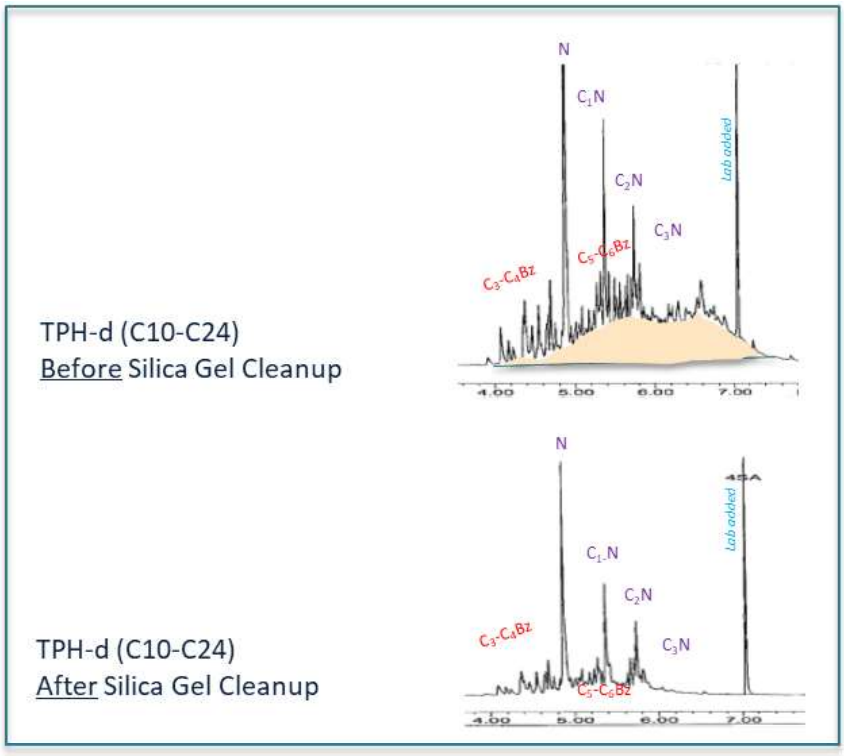

Figure 3-2: Chromatographic Fingerprints of TPH-d Before and After SGC in Groundwater from RHMW02

3.1.2 Evaluation of Hydrocarbon and PAH Concentrations in Groundwater – RHMW02

Changes in the TPH-d method in the second half of 2018 by the Navy-contracted laboratory (APPL) to better match the protocol used by the EPA Region 9 laboratory (CSM Appendix B.8) have resulted in comparable results as shown in Table 3-1. In general, groundwater samples from RHMW02 containon average approximately 80% of polar compounds/metabolites with the remainder TPH-d after removal of polar compounds/metabolites by SGC being hydrocarbons from fuel sources. The The concentrations of naphthalene, 1-methylnaphthalene, and 2-methylnaphthalene are quantified by EPA Method 8270, and, therefore, the contribution of these constituents to the TPH-d result are quantified directly. Based on these measurements and knowledge of other compounds in jet fuel, the likely estimated composition of hydrocarbons in "TPH-d" after removal of polar compounds is as follows:

- Naphthalene and methylnaphthalenes are approximately 1/5 of the TPH-d w/SGC
- C3+ benzenes and C2+ naphthalenes: remaining bulk of the TPH-d w/SGC result

Naphthalene concentrations in RHMW02 have at times exceeded naphthalene's effective solubility for unweathered fuel. The higher-than-expected concentrations of naphthalene are consistent with a weathered source that has lost lighter ends, such that naphthalene is likely a higher proportion in the residual fuel or LNAPL.

Naphthalene, 1-methylnaphthalene, and 2-methylnaphthalene are routinely analyzed in the groundwater samples from the Facility. The October 2017 samples for some of the Facility wells were also analyzed for an extended list of PAHs to better understand the composition of the

dissolved hydrocarbon portion of the TPH-d. Figure 3-3 shows the distribution of parent and alkylated PAHs for two samples from RHMW02. Visual comparison of the bar graph on Figure 3-3 and the bottom chromatogram shown on Figure 3-2 confirms the identity of heavier substituted naphthalenes (C2+) and indicates the presence of decalins and benzothiophenes in RHMW02.

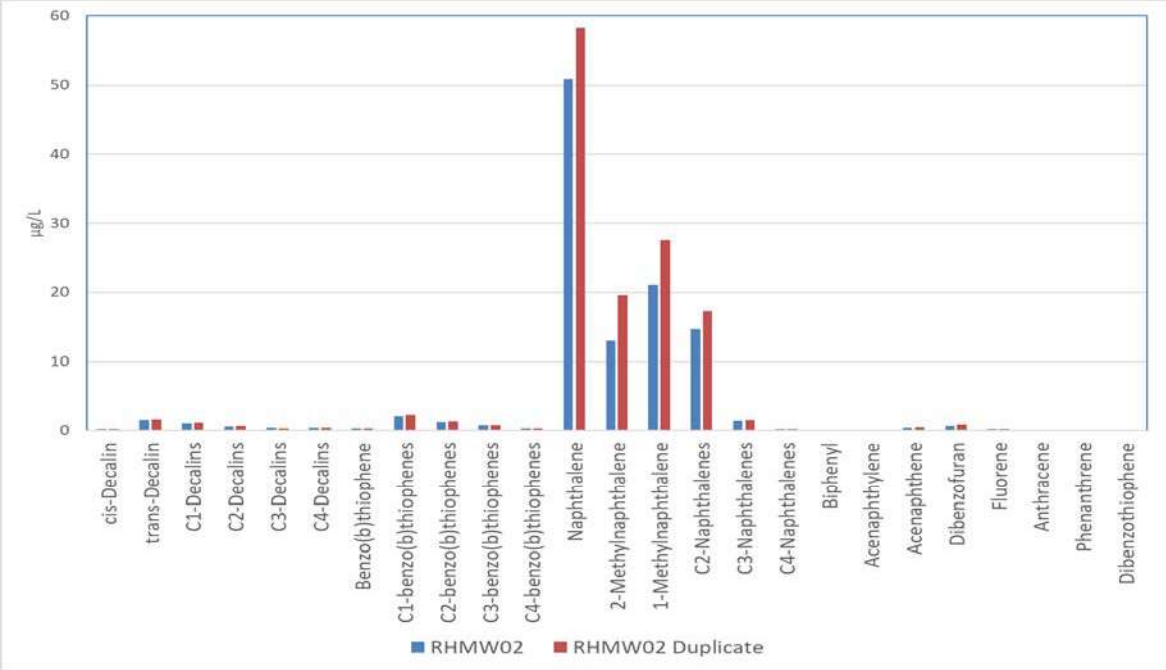

Figure 3-3: Extended PAH Analysis of October 2017 Samples from RHMW02

The distribution of naphthalenes in groundwater from RHMW02 is not consistent with the typical composition of jet fuel. Specifically, the methylnaphthalenes to naphthalene ratio in RHMW02 groundwater is much lower than expected. The RHMW02 naphthalene concentration is higher than the methylnaphthalenes, and 1-methylnaphthalene is higher than 2-methylnaphthalene. In contrast, unweathered petroleum-sourced fuels have alkylated naphthalenes that are more abundant than the parent naphthalene; furthermore, 2-methylnaphthalene is more abundant than 1-methylnaphthalene. A typical distribution of PAHs in JP-8 is shown in Figure 3-4. Naphthalene is less abundant than the methylnaphthalenes (Bernabei et al. 2003). The average concentrations of methylnaphthalene and naphthalene (Shafer and Edwards 2011 and Attachment B.7.1) for the types of fuels stored at the Facility are:

JP-5: methylnaphthalenes 0.54 wt%, naphthalene 0.21 wt%
JP-8: methylnaphthalenes 0.42 wt%, naphthalene 0.16 wt%
F-76: methylnaphthalenes 0.53 wt%, naphthalene 0.16 wt%

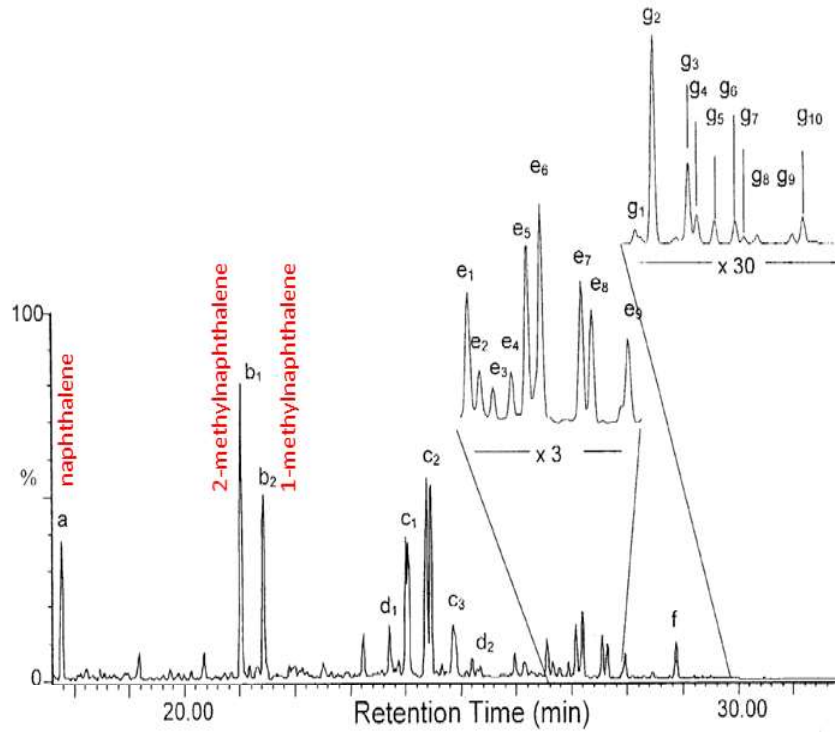

(a) naphthalene, (b) methylnaphthalenes, (c) dimethylnaphthalenes, (d) ethylnaphthalenes, (e) C_3-naphthalenes, (f) laboratory-added internal standard, (g) C_4-naphthalenes

Figure 3-4: Extended PAH Analysis of a Jet Fuel Sample

Although the samples used in the Shafer and Edwards 2011 study are not from the Facility, the average concentrations presented in the study are representative of the relative distribution of these compounds in JP-8 and of any petroleum-sourced middle distillates. Figure 3-5 displays the normalized relative distribution of the average of naphthalene, 1-methylnaphthalene, and 2-methylnaphthalene in RHMW02 from all monitoring events from 2005 to January 2019 compared to the normalized theoretical distribution expected in water in contact with JP-5, JP-8, and F-76 (from calculated ideal effective solubilities of these fuels summarized in Attachment B.7.1). It is clear that the COPC naphthalenes in RHMW02 are degraded with a distribution that has been significantly altered from what is expected from these types of middle distillate fuels from petroleum sources.

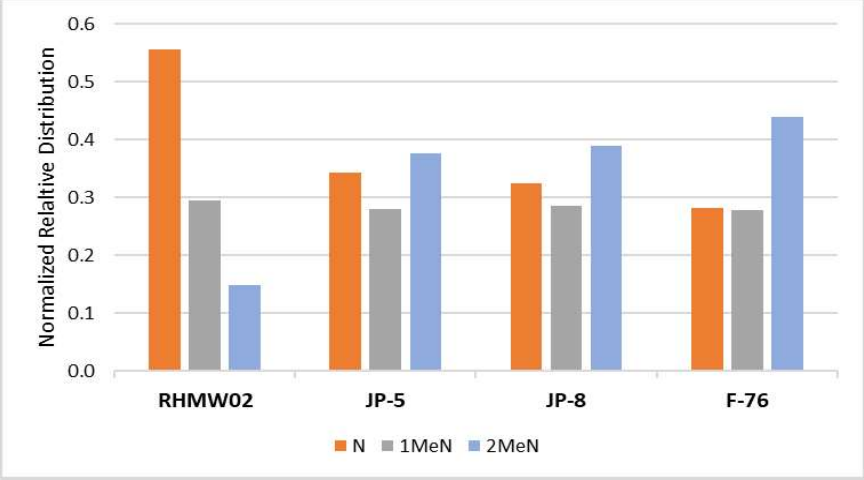

Figure 3-5: Relative Distribution of Naphthalenes Observed in RHMW02 and Theoretical Distribution of Naphthalenes in Water Equilibrated with JP-5, JP-8, and F-76

Forensics investigations often use ratios of target compounds rather than absolute concentrations to normalize sample variability and take advantage of properties and/or biodegradation differences among the different compounds that can be diagnostic of particular changes in the samples. Since the pure solubility of naphthalene (31 mg/L) and methylnaphthalenes (28–25 mg/L) are similar, the ratio of naphthalene to methylnaphthalene in fuel and in water should be relatively similar. Using the calculated ideal effective solubility estimates presented in Section 2.2.1, the ratio of the sum of methylnaphthalenes (1-methylnaphthalene and 2-methylnaphthalene) to naphthalene (Table 3-2) in the fuels and in water are approximately 2 for JP-8 (F-24), JP-5, and F-76 (diesel marine fuel). In contrast, the ratio of methylnaphthalenes to naphthalene in samples from RHMW02 is typically less than 1, further indicating that TPH-d in RHMW02 is from biodegraded fuel. This is discussed further in CSM Appendix B.8 Section 2.3.

Table 3-2: Ratios of Sum of Methylnaphthalenes to Naphthalene in Fuel and Calculated for Water

JP-5 (average, 13 samples)		JP-8 (average, 18 samples)		F-76 (average, 18 samples)	
Fuel	Water	Fuel	Water	Fuel	Water
2.5	1.9	2.7	2.1	3.3	2.5

In summary, the dissolved TPH-d in RHMW02 is composed of polar compounds/metabolites and aromatic hydrocarbons consistent with a jet fuel source that has undergone significant biological weathering. This is also consistent with the EHE Guidance (DOH 2017), which recommends to "*use SGC to assess petroleum degradation and to optimize remedial options*." The EHE Guidance also states that "*comparison of non-SGC data for groundwater indicates significant degradation of compounds outside of areas with LNAPL*."

3.2 EVALUATION OF NON-COPCS AND TENTATIVELY IDENTIFIED COMPOUNDS IN GROUNDWATER – RHMW02

In addition to analysis for COPCs like BTEX, naphthalene, and methylnaphthalenes that have specific EALs, some samples have been analyzed by the Navy and by EPA Region 9 for extended

lists of compounds as part of the split sampling and attenuation evaluation sampling conducted in 2017 (EPA 2017; DON 2017a). The analyses were done using EPA Method 8260 for volatile organic compounds (VOCs) and EPA Method 8270 for semivolatile organic compounds (SVOCs). Both methods use gas chromatograph and mass spectrometer to identify and quantify compounds. A list of detected target compounds that are quantitated against standards of those compounds is included as a summary in Table 3-3. Most of the detected compounds are aromatic hydrocarbons expected to partition from jet fuel to water and are consistent with the chromatographic patterns seen in the TPH analysis after SGC. The phthalate detected is likely a plasticizer from sampling equipment or lab contamination.

Table 3-3: Detected Volatile and Semivolatile Organic Analytes in RHMW02

Target Compounds	*Examples of Tentatively Identified Compounds (TICs)*
C2 Substituted Benzenes	**C4–C6 Substituted Benzenes**
Ethylbenzene [a]	*Tetramethylbenzenes*
Xylenes [a]	*Diethylbenzenes*
C3 Substituted Benzenes	*Ethyldimethylbenzenes*
i-Propylbenzene	*Methylpropylbenzenes*
n-Propylbenzene	*Dimethylstyrene*
C4 Substituted Benzenes	*Methylbytylbenzene*
tert-Butylbenzene	*Dimethylbutenylbenzene*
sec-Butylbenzene	**Naphthenobenzenes**
n-Butylbenzene	*Indane*
PAHs	*Methylindan*
Naphthalene [a]	*Ethylindan*
1-Methynaphthalene [a]	*Dimtheylindane*
2-Methylnapathalene [a]	*Tetralin, Methyltetralins*
Acynaphthalene	**C2 Substituted Naphthalenes**
Acenaphthene	*Dimethylnaphthalenes*
Fluorene	**Organic Acids**
Others	*Hexadecanoic Acid*
Dibenzofuran	*Octadecanoid Acid*
Bis(2-Ethtylhexyl)phthalate	*Naphthalenecarboxylic acid*

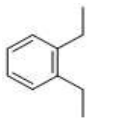

1,2-Diethylbenzene

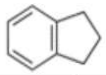

Indane

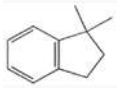

Dimethylindane

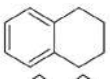

Tetralin

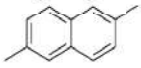

Dimethylnaphthalene

[a] Compounds with EALs.

Table 3-3 also includes a summary of tentatively identified compounds (TICs). Unlike target compounds that are identified and quantitated against standards, the identification of TICs is performed by doing a library search of the mass spectrum of each compound compared to those in the National Institute of Standards and Technology (NIST) Mass Spectrometry Data Center library. Mass spectrum detectors alone cannot differentiate isomers. For example, the mass spectra of ethylbenzene and the three isomers of xylenes are essentially the same. Most of those COPCs can be identified and quantitated individually because the actual compounds are included in the laboratory standards and have different retention times in the gas chromatograph, so that the analyst can verify the time of elution of each compound and report them. In the case of the TICs, the laboratory is identifying unknown peaks by performing a library search of the peak's mass spectrum. However, identification using mass spectra alone as well as quantitation without a calibration standard for the

specific compound results in a reported TIC concentration that is not reliable. Nevertheless, TICs can provide general information on the types of compounds that can also be present in the samples.

The TICs listed in Table 3-3 are also consistent with aromatic compounds that are present in jet fuels (Lovestead et al. 2016). Of particular significance is the identification of naphtheno-benzenes, such as indane and tetralin and some of their substituted homologues. These compounds are present in fuels at relatively low concentrations, but these become more abundant as the dissolved fuel components biodegrade. As shown in Table 3-3, naphtheno-benzenes are bi-cyclic compounds, with one benzene ring and the other non-aromatic ring attached to two carbons of the benzene ring. These types of compounds are relatively resistant to biodegradation. Some of the TICs also indicate organic acids that are likely metabolites. The presence of naphtheno-benzenes and organic acids provide additional evidence of natural attenuation.

A more in-depth evaluation of non-COPCs and TICs in all wells is included in CSM Appendix B.8.

3.3 NATURAL ATTENUATION PARAMETERS IN GROUNDWATER

Biodegradation depletes the groundwater of dissolved oxygen and other electron acceptors (e.g., nitrate, ferric iron, and sulfate), and subsequently increases ferrous iron and alkalinity concentrations of the groundwater. When all the soluble electron acceptors (i.e., dissolved oxygen, nitrate, ferric iron, and sulfate) are depleted, groundwater conditions become conducive to fermentation and methane is generated by methanogenesis. When evaluated alongside depressed dissolved oxygen concentrations, dissolved methane is a strong line of evidence of anaerobic biodegradation. Methane was not detected in soil vapor samples; the aerobic conditions of the vadose zone likely allows for rapid oxidation of methane to carbon dioxide. High levels of biodegradation are occurring in the vicinity of RHMW02, as key electron acceptors are depleted and high concentrations of dissolved methane are present (sometimes greater than 10 mg/L). Taken together, these data suggest the presence of weathered LNAPL (i.e., pre-2005 release) in the immediate vicinity of RHMW02 or within the saturated zone upgradient from this well. These natural attenuation parameters (NAPs) are indirect (or secondary) lines of evidence for biodegradation of COPCs and are discussed further in CSM Section 7.3 and Appendix B.5.

4. Conclusions

Fuels are complex mixtures of hydrocarbons with wide-ranging physical and chemical properties. In the environment, these complex mixtures change due to weathering processes. Chemistry, partitioning into water and biodegradation of jet fuel were assessed to better characterize the dissolved organic material in RHMW02, the only well with continuous TPH-d detections at the site.

The composition of the dissolved material measured as TPH-d in RHMW02 is consistent with a weathered jet fuel source.

The RHMW02 TPH-d chromatographic patterns show:

- Presence of naphthalene, C1-naphthalenes, as well as C2+naphthalenes. The chromatograms are consistent among the samples from RHMW02 and among kerosenes (JP-5 and JP-8 are kerosenes with special additives).
- Evidence of C3+benzenes from the analysis of TPH-g, VOCs, and TICs in both VOCs and SVOC analyses. Lighter components are partially lost in the extraction and concentration of the extract prior to analysis in TPH-d.
- Presence of a "hump" that extends beyond the end of the jet/kerosene carbon range (C16+). This is likely due to polar matter that are metabolites of biodegradation. SGC removes 43–86% of the TPH-d, indicating that the hydrocarbons in RHMW02 are degrading.
- Some of the compounds detected as TICs are more recalcitrant to biodegradation (naphtheno-benzenes, for example). These are typically low in concentration in the fuel, and the fact that these are detected as TICs indicates that they are relatively concentrated in the residual hydrocarbons more than in a fresh release. The presence of organic acids is also indicative of biodegradation.

Other indications of natural attenuation include:

- Dissolved methane in RHMW02. Methane was not detected in soil vapor samples; the aerobic conditions of the vadose zone likely allows for rapid oxidation of methane to carbon dioxide.
- Relative depletion of nitrate, sulfate, and dissolved oxygen in RHMW02 with respect to other wells.
- Relatively higher ferrous iron and alkalinity in RHMW02 with respect to other wells.

Taken together, the available data suggest the presence of weathered LNAPL (i.e., pre-2005 release) in the immediate vicinity of RHMW02 or within the saturated zone upgradient from this well. The data also indicate biodegradation of dissolved fuel constituents in groundwater is occurring. Based on the angle boring investigations conducted in 1998 to 2002, this LNAPL may have originated from Tank 9, 11, or 13. A continued discussion of the presence of LNAPL upgradient of RHMW02 is presented in CSM Appendix B.8 as part of a comprehensive analysis of groundwater chemistry.

5. References

Alvarez, P. J. J., R. C. Heathcote, and S. E. Powers. 1998. "Caution Against Interpreting Gasoline Release Dates Based on BTEX Ratios in Water." *Groundwater Monitoring & Remediation* 18 (4): 69–76. https://doi.org/10.1111/j.1745-6592.1998.tb00166.x.

American Petroleum Institute (API). 2010. *Kerosene/Jet Fuel Category Assessment Document*. API Petroleum HPV Testing Group. Submitted to the U.S. EPA. Consortium Registration # 1100997. September 21.

———. 2012. *Gas Oils Category Analysis Document and Hazard Characterization*. API Petroleum HPV Testing Group. High Production Volume (HPV) Chemical Challenge Program. Submitted to the U.S. EPA. Consortium Registration # 1100997. October 24.

Baedecker, M. J., R. P. Eganhouse, B. A. Bekins, and G. N. Delin. 2011. "Loss of Volatile Hydrocarbons from an LNAPL Oil Source." *Journal of Contaminant Hydrology* 126: 140–152.

Baedecker, M. J., R. P. Eganhouse, H. Qi, I. M. Cozzarelli, J. Trost, and B. A. Bekins. 2017. "Weathering of Oil in a Surficial Aquifer." *Groundwater*, [Epub ahead of print, Nov. 29]. https://doi.org/10.1111/gwat.12619.

Bernabei, M., R. Reda, R. Galiero, and G. Bocchinfuso. 2003. "Determination of Total Polycyclic Hydrocarbons in Aviation Jet Fuel." *Journal of Chromatography A*, January 24, 985 (1–2): 197–203.

Bobra, M. 1992. *Solubility Behaviour of Petroleum Oils in Water*. Study Funded by United States Minerals Management Service and Environment Canada, Emergencies Science Division. Ottawa: Consultchem.

Coleman, W. E., J. W. Munch, R. P. Streicher, H. P. Ringhand, and F. C. Kopfler. 1984. "The Identification and Measurement of Components in Gasoline, Kerosene, and No. 2 Fuel Oil That Partitions into the Aqueous Phase after Mixing." *Archives of Environmental Contamination and Toxicology* 13 (2): 171–178. https://doi.org/10.1007/BF01055874.

Department of Defense and Department of Energy, United States (DoD and DOE). 2017. *Department of Defense (DoD) and Department of Energy (DOE) Consolidated Quality Systems Manual (QSM) for Environmental Laboratories*. DoD QSM Ver. 5.1; DOE Quality Systems for Analytical Services Ver. 3.1. Prepared by DoD Environmental Data Quality Workgroup and DOE Consolidated Audit Program Operations Team.

Department of Health, State of Hawaii (DOH). 2017. *Evaluation of Environmental Hazards at Sites with Contaminated Soil and Groundwater, Hawai'i Edition*. Hazard Evaluation and Emergency Response. Revised 2017. Fall.

Department of the Navy (DON). 2017a. *Sampling and Analysis Plan Addendum 01, Investigation and Remediation of Releases and Groundwater Protection and Evaluation, Red Hill Bulk Fuel Storage Facility, Joint Base Pearl Harbor-Hickam, O'ahu, Hawai'i; September 1, 2017, Revision 00*. Prepared by AECOM Technical Services, Inc., Honolulu, HI. Prepared for Defense Logistics Agency Energy, Fort Belvoir, VA, under Naval Facilities Engineering Command, Hawaii, JBPHH HI.

———. 2017b. *Risk-Based Decision Criteria Development Plan, Investigation and Remediation of Releases and Groundwater Protection and Evaluation, Red Hill Bulk Fuel Storage Facility, Joint Base Pearl Harbor-Hickam, O'ahu, Hawai'i; December 11, 2017, Revision 00*. Prepared by AECOM Technical Services, Inc., Honolulu, HI. Prepared for Defense Logistics Agency Energy, Fort Belvoir, VA, under Naval Facilities Engineering Command, Hawaii, JBPHH HI.

Environmental Protection Agency, United States (EPA). 2017. *Split Sampling and Analysis Plan, Red Hill Fueling Facility, Honolulu, Hawai'i – Groundwater Monitoring, January 2017*. U.S. EPA Region 9 Land Division and Quality Assurance Office.

Gustafson, J. B., J. G. Tell, and D. Orem. 1997. *Total Petroleum Hydrocarbon Criteria Working Group Series, Volume 3: Selection of Representative TPH Fractions Based on Fate and Transport Considerations*. Amherst, MA: Amherst Scientific Publishers.

Hadaller, O. J., and J. M. Johnson. 2006. *World Fuel Sampling Program*. CRC Report No. 647. Alpharetta, GA: Coordinating Research Council, Inc. June.

Interstate Technology & Regulatory Council (ITRC). 2018. *TPH Risk Evaluation at Petroleum-Contaminated Sites*. TPHRisk-1. Washington, DC: ITRC, TPH Risk Evaluation Team. https://tphrisk-1.itrcweb.org.

Lovestead, T. M., J. L. Burger, N. Schneider, and T. J. Bruno. 2016. "Comprehensive Assessment of Composition and Thermochemical Variability by High Resolution GC/QToF-MS and the Advanced Distillation-Curve Method as a Basis of Comparison for Reference Fuel Development." *Energy & Fuels* 30 (12): 10029–044.

Maurice, L. Q., H. Lander, T. Edwards, and W. E. Harrison III. 2001. "Advanced Aviation Fuels: A Look Ahead via a Historical Perspective." *Fuel* 80 (5): 747–756. https://doi.org/10.1016/S0016-2361(00)00142-3.

Mohler, R. E., K. T. O'Reilly, D. A. Zemo, A. K. Tiwary, R. I. Magaw, and K. A. Synowiec. 2013. "Nontargeted Analysis of Petroleum Metabolites in Groundwater Using GC×GC–TOFMS." *Environ. Sci. & Technol.* 47 (18): 10471–476. https://doi.org/10.1021/es401706m.

Shafer, L. M., and T. Edwards. 2011. *Speciated Naphthalene Analysis in Liquid Transportation Fuels*. IASH 2011, The 12th International Conference on Stability, Handling and Use of Liquid Fuels, Sarasota, Florida USA, 16–20 October 2011.

Striebich, R. C., L. M. Shafer, R. K. Adams, Z. J. West, M. J. DeWitt, and S. Zabarnick. 2014. "Hydrocarbon Group-Type Analysis of Petroleum-Derived and Synthetic Fuels Using Two-Dimensional Gas Chromatography." *Energy & Fuels*, no. 28: 5696–706. https://doi.org/dx.doi.org/10.1021/ef500813x.

Vorhees, D. J., W. H. Weisman, and J. B. Gustafson. 1999. *Total Petroleum Hydrocarbon Criteria Working Group Series, Volume 5: Human Health Risk-Based Evaluation of Petroleum Release Sites: Implementing the Working Group Approach*. Amherst, MA: Amherst Scientific Publishers.

Widdel, Friedrich, and Ralf Rabus. 2001. "Anaerobic Biodegradation of Saturated and Aromatic Hydrocarbons." *Current Opinion in Biotechnology* 12 (3): 259–276. https://doi.org/10.1016/S0958-1669(00)00209-3.

Zemo, D. A., K. T. O'Reilly, R. E. Mohler, R. I. Magaw, C. E. Devine, S. Ahn, and A. K. Tiwary. 2017. "Life Cycle of Petroleum Biodegradation Metabolite Plumes, and Implications for Risk Management at Fuel Release Sites." *Integrated Environmental Assessment and Management* 13 (4): 714–727. https://doi.org/10.1002/ieam.1848.

Zemo, D. A., K. T. O'Reilly, R. E. Mohler, A. K. Tiwary, R. I. Magaw, and K. A. Synowiec. 2013. "Nature and Estimated Human Toxicity of Polar Metabolite Mixtures in Groundwater Quantified as TPHd/DRO at Biodegrading Fuel Release Sites." *Groundwater Monitoring & Remediation* 33 (4): 44–56. https://doi.org/10.1111/gwmr.12030.

Attachment B.7.1:
Summary of Concentrations and Calculated Effective Solubilities

Attachment B.7.1

Summary of Concentrations and Calculated Effective Solubilities

			Fuel	Water	Fuel	Water	Fuel	Water	Fuel	Water	Fuel	Water	Fuel	Water	Fuel	Water	Fuel
	~MW of Fuel[2,3]	Fuel Type	Benzene	Calculated Effective Solubility[1]	Naphthalene	Calculated Effective Solubility[1]	1-Methyl-naphthalene	Calculated Effective Solubility[1]	2-Methyl-naphthalene	Calculated Effective Solubility[1]	Toluene	Calculated Effective Solubility[1]	Ethyl-benzene	Calculated Effective Solubility[1]	Xylenes	Calculated Effective Solubility[1]	Density
	g/mole		ppmwt	mg/L	ppmwt	mg/L	ppmwt	mg/L	ppmwt	mg/L	ppmwt	mg/L	ppmwt	mg/L	ppmwt	mg/L	kg/L
MW[4]			78.1		128.2		142.2		142.2		92.1		106.2		106.2		
Solubility[4]			1780		31		28		25		515		152		200		
API Jet A																	
Avg	160	Jet A	100	0.36	1800	0.070	2800	0.088	3800	0.11	1400	1.25	1500	0.34	7800	2.35	0.810
Max	160		200	0.73	3000	0.12	3700	0.12	5700	0.16	5000	4.47	2600	0.60	17600	5.30	0.820
Min	160		ND	ND	700	0.027	1300	0.041	1800	0.051	600	0.54	800	0.18	3500	1.05	0.800
Count			14		14		14		14		14		14		14		14
UD/AFRL Jet A and Jet A-1																	
Avg	160	Jet A (23), Jet A-1 (2)	72	0.26	1731	0.067	1831	0.058	2878	0.081	1370	1.23	1280	0.29	6700	2.02	0.810
STDV	160		66	0.24	621	0.024	470.2	0.015	876	0.025	836	0.75	460	0.11	2420	0.73	0.016
Max	160		250	0.91	3292	0.13	2793	0.088	5219	0.15	3496	3.13	1930	0.44	10380	3.13	0.880
Min	160		2	0.007	695	0.027	870	0.027	1375	0.039	312	0.28	340	0.08	1770	0.53	0.796
Count			25		25		25		25		13		13		13		25
UD/AFRL JP-8																	
Avg	160	JP-8	73	0.27	1555	0.060	1674	0.053	2573	0.072	1038	0.93	1400	0.32	7330	2.21	0.805
STDV	160		35	0.13	540	0.021	488	0.015	861	0.024	484	0.43	551	0.13	2892	0.87	0.007
Max	160		124	0.452	2580	0.10	2430	0.077	4080	0.11	1713	1.53	2530	0.58	13600	4.10	0.822
Min	160		15	0.054	642	0.025	304	0.0096	710	0.020	358	0.32	50	0.01	280	0.08	0.79
Count			18		18		18		18		10		10		10		18
UD/AFRL JP-5																	
Avg	160	JP-5	7.8	0.028	2147	0.083	2147	0.068	3244	0.091	297	0.27	560	0.13	2920	0.88	0.816
STDV	160		5.8	0.021	1166	0.045	836	0.026	1434	0.040	269	0.24	292	0.067	1533	0.46	0.024
Max	160		21.1	0.077	3906	0.15	3144	0.099	5050	0.14	487	0.44	760	0.17	4100	1.24	0.893
Min	160		<1	ND	394	0.015	345	0.0109	502	0.014	106	0.09	350	0.08	1840	0.55	0.802
Count			13		13		13		13		2		2		2		11
UD/AFRL + API Jets Combined																	
Avg	160	JetA, JetA1, JP8,JP5	66	0.24	1777	0.069	2043	0.064	3052	0.086	1097	0.98	1461	0.33	7063	2.13	0.810
Max	160		250	0.91	3905	0.15	3700	0.12	5700	0.16	5000	4.47	2600	0.60	16950	5.11	0.893
Min	160		ND	ND	394	0.015	304	0.0096	502	0.014	106	0.09	50	0.01	280	0.08	0.79
Count			70		70		70		70		39		39		14		70
UD/AFRL + API Jets Combined MINUS JP-5																	
Avg	160	JetA, JetA1, JP8	79	0.29	1692	0.065	2019	0.064	3007	0.085	1140	1.02	1509	0.35	7287	2.20	0.808
Max	160		250	0.91	3292	0.13	2793	0.09	5219	0.15	5000	4.47	2600	0.60	17600	5.30	0.893
Min	160		ND	ND	642	0.025	304	0.0096	710	0.020	312	0.28	50	0.01	280	0.08	0.790
Count			57		57		57		57		37		37		37		57
API Diesel																	
Avg	200	Diesel, on-road, <500ppm Sulfur	80	0.36	600	0.029	1710	0.067	2750	0.097	620	0.69	470	0.13	2700	1.02	
STDV	200																
Max	200		250	1.14	1790	0.09	8240	0.32	14260	0.50	1780	1.99	700	0.20	9350	3.52	
Min	200		ND	ND	210	0.010	280	0.01	400	0.014	ND	ND	160	0.05	1010	0.38	
Count			12		12		12		12		12		12		12		
UD/AFRL Diesel																	
Avg	200	Diesel	62	0.28	430	0.021	639	0.025	1263	0.044							0.847
STDV	200		29	0.13	239	0.012	408	0.016	774	0.027							0.005
Max	200		124	0.56	1339	0.065	2538	0.100	4678	0.164							0.859
Min	200		8.8	0.040	102	0.005	116	0.005	184	0.006							0.837
Count			39		39		39		39								39
UD/AFRL + API Diesel Combined																	
Avg	200	Diesel	66	0.30	471	0.023	927	0.036	1620	0.057	620	0.69	470	0.13	2700	1.02	
Max	200		250	1.14	1790	0.087	8240	0.32	14260	0.501	1780	1.99	700	0.20	9350	3.52	
Min	200		ND	ND	102	0.005	116	0.005	184	0.006	ND	ND	160	0.05	1010	0.38	
Count			50		50		50		50		12		12		12		
UD/AFRL F-76 Only																	
Avg	200	F76	31	0.14	1568	0.076	1906	0.075	3346	0.118	355	0.40	346	0.10	1819	0.69	0.848
STDV	200		17	0.077	854	0.041	813	0.032	1767	0.062	118	0.13	159	0.046	833	0.31	0.007
Max	200		64	0.29	3537	0.171	4125	0.162	8472	0.298	519	0.58	569	0.16	3060	1.15	0.864
Min	200		3	0.014	480	0.023	678	0.027	1037	0.036	177	0.20	146	0.04	769	0.29	0.839
Count			18		18		18		18		9		9		9		16
UD/AFRL Data for Pearl Harbor Samples Only: JP-5																	
FISC Pearl Harbpr 4117506	160	JP-5	4.9	0.018	2651	0.103	2343	0.074	3921	0.110							0.811
FISC Pearl Harbpr 4117532	160	JP-5	11.2	0.041	1808	0.070	2000	0.063	3083	0.087							0.824
UD/AFRL Data for Pearl Harbor Samples Only: F-76																	
FISC Pearl Harbor 500065	200	F-76	17.5	0.080	611	0.030	1199	0.047	1723	0.061							0.859
FISC Pearl Harbor 4129218	200	F-76	44.8	0.204	575	0.028	1238	0.049	1698	0.060							0.848

UD/AFRL: University of Dayton and AirForce Research Laboratory, Shafer and Edwards 2011

1. Calculated by I. Rhodes
2. Average molecular weight for JP-8 from GCXGC analysis (Striebich 2014 and Edwards 2018): 160 g/mole
3. Average molecular weight for JP-8 from GCXGC analysis (Edwards 2018): 200 g/mole
4. Solubility from TPHCWG, Vol. 3, 1997

Ethylbenzene and Xylenes for USAF data: From GCXGC (wt%). Output is for C2-Benzenes. E and X were calcaulated from the sum using 16% E and 84% X on advices from Tim Edwards, AFRL, Jan 2018 (emails)

Data Sources:

API, 2010, API HPV Testing Group, Kerosene/Jet Fuel Category Assessment Document, #1100997, Report to USEPA 2010. http://www.petroleumhpv.org/petroleum-substances-and-categories/~/media/37A083A569294403AD230CB504AB17A6.ashx

API, 2012, High Production Volume (HPV) Chemical Challenge Program Gas Oils Category Analysis Document and Hazard Characterization, , Submitted to USEPA 2012. http://www.petroleumhpv.org/~/media/PetroleumHPV/Documents/2012_nov15_Gas%20Oils%20CAD%20Final%20Standard%2010_24_2012.pdf

UD/USAF, Shafer L.M. and Edwards T., Speciated Naphthalene Analysis in Liquid Transportation Fuels, IASH 2011, The 12th International Conference on Stability, Handling and Use of Liquid Fuels, Sarasota, Florida USA, 16-20 October 2011

UD/USAF, Striebich R.C., Shafer L.M., Adams R.K., West Z.J., DeWitt M.J., and Zabarnick S., Hydrocarbon Group-Type Analysis of Petroleum-Derived and Synthetic Fuels Using Two-Dimensional Gas Chromatography, Energy & Fuels, 2014, 28, 5696-5706, dx.doi.org/10.1021/ef500813x

Edwards J.T, (CIV USAF, Air Force Research Laboratory), personal communications with Ileana Rhodes (GSI Environmental), January 2018

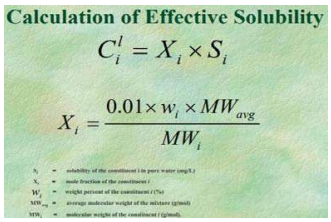

This page intentionally left blank

Appendix B.8:
Comprehensive Evaluation of Groundwater Chemistry

CONTENTS

Acronyms and Abbreviations iv

1. Introduction 1-1

1.1 Study Objectives 1-1
1.2 LNAPL Measurements in Monitoring Wells 1-1
1.3 Groundwater Monitoring Locations 1-2
1.4 Challenges with Organic Data Interpretation 1-4
1.5 Groundwater Chemistry as a Function of LNAPL Extent 1-5

2. Evaluation of COPCs 2-1

2.1 Fuel Additives and Lead 2-1
2.2 Evaluation of BTEX 2-1
2.2.1 BTEX in Near-Tank Wells 2-1
2.2.2 BTEX in Outlying Wells 2-4
2.3 Evaluation of Naphthalenes 2-4
2.3.1 Weathering of Naphthalenes 2-5
2.3.2 Naphthalenes in Near-Tank Wells 2-5
2.3.3 Naphthalenes in Outlying Wells 2-7
2.4 Evaluation of TPH 2-10
2.4.1 What Is Included in TPH-d Measurements 2-11
2.4.2 Variability in TPH-d Measurements 2-11
2.4.3 Low-Level TPH Measurements 2-13
2.4.4 TPH-d and TPH-o in Near-Tank Wells 2-14
2.4.5 TPH-d and TPH-o in Outlying Wells 2-15
2.5 Evaluation of Combined COPCs 2-18
2.5.1 Combined COPC Analysis in Near-Tank Wells 2-18
2.5.2 Combined COPC Analysis in Outlying Wells 2-18

3. Evaluation of Inorganic Geochemistry 3-1

3.1 Geochemical Trends 3-1
3.2 Principal Component Analysis 3-4
3.3 Groundwater Temperature 3-5
3.4 Isotopic Analysis 3-6
3.5 Geochemistry Summary 3-7

4. Evaluation of Non-COPCs 4-1

4.1 Non-COPC Detections 4-1
4.2 Hydrocarbon Non-COPC Analysis 4-2
4.3 Non-COPC Summary 4-6

5. Evaluation of TICs 5-1

6. Key Findings 6-1

6.1 Composition and Concentration of Dissolved Constituents in Near-Tank Wells 6-1
6.2 Composition and Concentration of Dissolved Constituents in Outlying Wells 6-2
6.3 2014 Tank 5 Release 6-3

6.4 Impacts to Outlying Wells 6-3
6.5 Summary of Lines of Evidence 6-4
7. References 7-1

ATTACHMENTS

B.8.1 Additional Figures
B.8.2 Analytical Tables – Non-COPCs and TICs
B.8.3 Statistical Methods

FIGURES

1-1 Site Location Map 1-3
2-1 Ethylbenzene Detections in RHMW02 2-2
2-2 Total Xylenes Detections in RHMW02 2-3
2-3 Toluene Detections in RHMW02 2-3
2-4 Benzene Detections in RHMW02 2-4
2-5 Naphthalenes Detections and Naphthalene Weathering Ratio in RHMW02 2-6
2-6 Naphthalenes Detections and Reporting Limits in RHMW01 2-7
2-7 Naphthalenes Detections and Reporting Limits in RHMW03 2-7
2-8 Sum of Naphthalenes in Outlying Wells 2-9
2-9 Detections and Reporting Limits of Naphthalene in Outlying Wells 2-10
2-10 TPH-d Results in RHMW02 with Laboratories Identified 2-12
2-11 RHMW04 TPH-d Chromatograms from July 2014 and January 2015 Samples 2-14
2-12 TPH-d in Near-Tank Wells 2-16
2-13 TPH-d in Outlying Wells 2-17
2-14 Combined COPC Detection Signature Charts for Near-Tank Wells 2-20
2-15 Combined COPC Detection Signature Charts for Outlying Wells 2-21
3-1 Geochemical Parameters a) dissolved oxygen, b) sulfate, c) nitrate, d) ferrous iron, e) methane, f) ORP, g) total alkalinity, h) chloride 3-2
3-2 Geochemical Results from First Quarter (January) 2019 Sampling Event 3-3
3-3 Results of Principal Component Analysis of Select Geochemical Data 3-4
3-4 Groundwater Temperature 3-6
3-5 Isotopic Analysis of δ15N and δ34S 3-7
4-1 Non-COPC Detections from 2005 to July 2018 4-2
4-2 Non-COPC Detections from October 2014 to July 2018 4-2
4-3 Hydrocarbon non-COPC Detections from 2005 to July 2018 4-3

4-4 Hydrocarbon Non-COPC Detections from October 2014 to July 2018 4-4

4-5 Priority Pollutant PAHs: Structure and Concentration Ranges in Fuels and Pure Compound Solubilities 4-5

4-6 Samples with Detections of Non-COPC non-Pyrogenic PAHs from 2005 to July 2018 4-6

5-1 TIC Detections by Compound Class 5-2

5-2 Hydrocarbon TIC Detections 5-3

TABLE

6-1 Summary of Lines of Evidence 6-4

ACRONYMS AND ABBREVIATIONS

µg/L	micrograms per liter
1-MeN	1-methylnaphthalene
2-MeN	2-methlynaphthalene
AOC	Administrative Order on Consent
bgs	below ground surface
BTEX	benzene, toluene, ethylbenzene, and xylenes
CFR	Code of Federal Regulations
COPC	chemical of potential concern
CSM	conceptual site model
DO	dissolved oxygen
DoD	Department of Defense, United States
DOE	Department of Energy, United States
DOH	Department of Health, State of Hawai‘i
DON	Department of the Navy, United States
EAL	Environmental Action Level
EPA	Environmental Protection Agency, United States
ft	foot/feet
J	estimated concentration
JP	Jet Fuel Propellant
LCS	laboratory control sample
LNAPL	light non-aqueous-phase liquid
LOD	limit of detection
LOE	line of evidence
LOQ	limit of quantitation
LTM	long-term monitoring
MDL	method detection limit
mg/L	milligrams per liter
ND	non-detect
non-COPC	non-constituent of potential concern—organic compounds that are targets of the analytical methods used to analyze for the COPCs but not required by the LTM program
NSZD	natural source-zone depletion
ORP	oxidation-reduction potential
PAH	polynuclear aromatic hydrocarbon
PCA	principal component analysis
ppb	parts per billion
PVC	polyvinyl chloride
QA/QC	quality assurance/quality control
QSM	*Quality Systems Manual*
SGC	silica gel cleanup
SIM	selected ion monitoring
TIC	tentatively identified compound
TPH	total petroleum hydrocarbons
TPH-d	total petroleum hydrocarbons – diesel range organics
TPH-g	total petroleum hydrocarbons – gasoline range organics
TPH-o	total petroleum hydrocarbons – residual range organics (i.e., TPH-oil)
VOC	volatile organic compound
δ15N	$^{14}C/^{15}C$-nitrogen

1	δ34S	$^{34}S/^{32}C$-sulfur

1. Introduction

This subappendix is summarized in Section 7.4 of the Conceptual Site Model (CSM) main document.

A comprehensive evaluation was conducted with all available groundwater data for all wells using multiple lines of evidence (LOEs) to assess two key issues:

- Potential impact to groundwater after the 2014 Jet Fuel Propellant (JP)-8 release from Tank 5
- Evidence of impact to Outlying Wells (see Section 1.3) from fuel releases/site operations

The data that was used for this evaluation are:

- Chemicals of potential concern (COPCs) that have specific EALs and are included in the Red Hill long-term monitoring (LTM) program conducted pursuant to the *Groundwater Protection Plan* (DON 2014)
- Inorganic groundwater chemistry parameters
- Organic compounds (referred to as non-COPCs) that are targets of the analytical methods used to analyze for the COPCs but not required by the LTM program
- Organic compounds (referred to as tentative identified compounds [TICs]) that are seen in the analysis of COPCs but are not target of the analytical method, thus have unconfirmed analyte identity and estimated concentrations. TICs are identified based on mass spectra.

Multiple LOEs utilizing temporal and spatial trends are presented to support the development of key findings

1.1 Study Objectives

- Evaluate all available Red Hill investigation and groundwater LTM chemistry data as an extension of prior chemistry analyses (see CSM Appendix A: Cumulative Historical Groundwater Monitoring Results).
- Evaluate whether the sporadic detections of various chemicals in Outlying Wells are associated with releases from the Red Hill Facility. This is also discussed in CSM Appendix I related to Multiple Impact Factor Analysis.
- Evaluate data with respect to potential LNAPL extent.
- Evaluate whether the 2014 Tank 5 fuel release contributed to groundwater contamination.
- Use multiple LOEs utilizing temporal and spatial trends to support development of Key Findings.

1.2 LNAPL Measurements in Monitoring Wells

The presence or absence of LNAPL in individual monitoring wells has been evaluated through (1) use of an oil/water interface probe during each monitoring well sampling event and (2) visual inspection of samples and purge water for a sheen or other evidence of LNAPL.

- Interface Probe: Interface probe measurements have never yielded definitive evidence of light non-aqueous phase liquid (LNAPL) in any monitoring well. In January 2008, the interface probe measurements at RHMW01 and RHMW02 were recorded as <0.01 foot [ft]; however,

this is believed to be a nomenclature issue (i.e., reflecting the detection limit of the probe [0.01 ft]) rather than an indication of a positive result from the probe.

- Visual Observation: Visual observation of samples and purge water has not provided clear indication of LNAPL in any of the monitoring wells prior to or since the January 2014 release. Discussion with DOH (Whittier 2018) indicate that yellow tint and naphthalene odors were noted in early sampling events for RHMW02 prior to the 2014 release.

In summary, for the available monitoring history to date, there has been no confirmed direct measurement of LNAPL in any monitoring well. Since LNAPL composition could not be analyzed or measured directly, the dissolved constituents in groundwater were evaluated in detail.

1.3 GROUNDWATER MONITORING LOCATIONS

Wells were divided into two groups (see Figure 1-1):

- Near-Tank Wells: RHMW01, RHMW02, RHMW03
- Outlying Wells: RHMW04, RHMW05, RHMW06, RHMW07, RHMW08, RHMW09, RHMW10, RHMW11, Red Hill Shaft (i.e., sampling point RHMW2254-01 located adjacent to the water supply pumps), Hālawa Deep Monitor Well (HDMW2253-03)

The Oily Waste Disposal Facility well (OWDFMW01) was not included in the analysis because water chemistry in this area has been impacted from past oily waste disposal operations not related to fuel releases from Red Hill and it is currently managed by Naval Facilities Engineering Command, Hawaii under the Comprehensive Long-Term Environmental Action Navy contract (nos. N62742-12-D-1829, N62742-12-D-1829).

Although RHMW07, RHMW11, and HDMW2253-03 are included in the analysis, these wells are not representative of water table chemistry. Well RHMW07 is screened in a less-permeable zone that may be affected by deeply penetrating saprolite, as well as being hydraulically isolated from the water table aquifer (discussed in CSM main document Section 6). RHMW11 is a multilevel monitoring well with eight monitoring zones: three within the saprolite layer and five well below the groundwater table within the basalt layer. Due to low hydraulic conductivity in the zones within the saprolite layer, groundwater analytical data were collected from zones within the basalt aquifer deeper below the elevation observed for the water table in other surrounding wells completed in the regional basal aquifer. Red Hill Shaft is a Navy water supply well with a long, horizontal shaft (the water development tunnel) that collects groundwater from near the water table aquifer and also from deeper portions of the aquifer because of vertical flow induced by pumping the shaft. HDMW2253-03 was not constructed as a typical monitoring well in the water table aquifer, but rather was designed and constructed to monitor the saltwater/freshwater interface which lies much deeper in the basalt aquifer. HDMW2253-03 has grout-sealed casing that extends down approximately 40 ft below the water table below which is an open borehole from 250 to 1,575 ft below ground surface (bgs). The RHMW07 and HDMW2253-03 well screens and the RHMW11 Zone 05 (RHMW11-05, the shallowest monitoring zone in the basalt layer) are located in or near the saprolite, which may affect dissolved oxygen concentrations (Hunt, Jr. 2004).

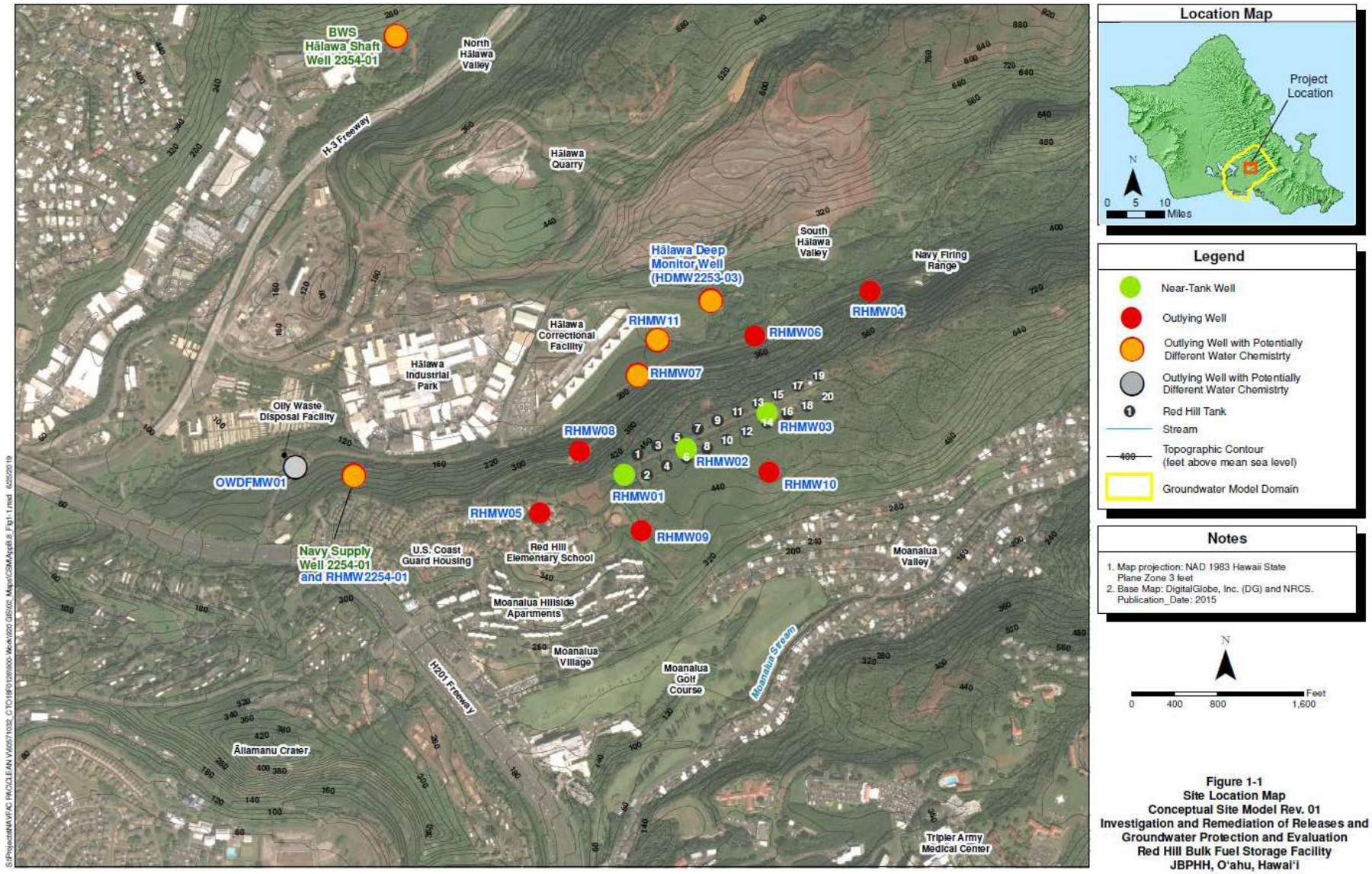

Figure 1-1
Site Location Map
Conceptual Site Model Rev. 01
Investigation and Remediation of Releases and Groundwater Protection and Evaluation
Red Hill Bulk Fuel Storage Facility
JBPHH, O'ahu, Hawai'i

Figure 1-1: Site Location Map

1.4 CHALLENGES WITH ORGANIC DATA INTERPRETATION

There are several concerns regarding the data quality and density with respect to interpretation of trends in organic constituents:

- Wells were installed at different times and have been sampled at different frequencies.
- Analytical laboratories and detection/reporting limits have varied throughout the monitoring program:
  a. Five different laboratories have been contracted by the Navy from 2005 to present. Two of them have been used twice.
  b. Additional analysis was conducted by the United States Environmental Protection Agency (EPA) Region 9 laboratory on split samples on some events (2017–2018).
  c. Analytical methodologies have changed over time.
  d. Laboratories reporting/detection limits (and methodologies) have changed over time. For example, reporting limits for naphthalenes have varied between 0.005 and 0.25 microgram per liter (µg/L).
- The analytical suite for non-COPCs has been inconsistent. For example, some volatile hydrocarbons (e.g., sec-butylbenzene and tert-butylbenzene) were analyzed for only in 2017 by the EPA Region 9 laboratory.
- TICs are available for only some events and some wells starting in August 2016.
- Very low concentrations push laboratory abilities and may result in laboratory quality assurance/quality control (QA/QC) issues. For example, field/laboratory contamination and inappropriate chemical/compound determination can result in "detections" that are not real as well as random instrument noise and carryover from previous analysis (see below for additional discussion).
- What is typically referred as "total petroleum hydrocarbons" (TPH) is defined by the analytical method used and might not be total, might not be entirely petroleum, and might not be entirely hydrocarbons, so careful examination of the meaning of the results is important. Reviewing chromatograms is useful for reducing the uncertainties inherent to TPH analysis (ITRC 2018).
- Groundwater in O'ahu and elsewhere has been impacted by various point and non-point sources unrelated to Red Hill, resulting in a background concentration of organic compounds in the environment (Rupert et al. 2014).
- Drilling and monitoring well installation activities and routine site operations may also introduce low concentrations of chemicals into groundwater. For example, at some well locations TPH was detected within 1 year of well installation, and not at any other time.

Evaluation of Low-Level Concentrations. The Department of Defense (DoD) *Quality Systems Manual* (QSM) (DoD and DOE 2017) requires three laboratory limits, compared to only two limits in most other regulatory programs. Under the DoD QSM, the laboratory must report detected concentrations between the method's limit of quantitation (LOQ, the smallest analyte concentration that produces a quantitative result with a known and recorded precision and bias) and the method's detection limit (DL, the smallest analyte concentration that can be demonstrated to be different from a zero concentration with a 99 percent confidence), while the laboratory must report non-detect concentrations (i.e., no positive identification of an analyte at the DL) to method's limit of detection

(LOD, the lowest concentration for reliable reporting of a non-detect with a false negative rate of 1 percent). For most other regulatory programs, analytical results below the reporting limit (RL, which is similar to the LOQ) and above the method detection limit (MDL, which is loosely similar to the DL) are reported as estimates and a "J" qualifier is assigned; non-detect results are reported as either less than the RL (< RL) or less than the MDL (< MDL), and there is no LOD equivalent.

This difference between reporting limits of DoD QSM and other regulatory programs is important to understand because of the level of confidence on an estimated detected concentration will vary between results reported to the DL versus results reported to the MDL; additionally, the level of confidence on a non-detect result will also vary between results reported as less than the LOD (< LOD) versus results reported as less than the MDL (< MDL).

MDLs are typically determined using reagent water or a method blank under ideal conditions. Therefore, although MDLs may be useful to compare the performance of different laboratories using the same method or different methods within the same laboratory using different instruments, MDLs may provide limited information about the method performance on real-world samples. The EPA MDL procedure as originally defined in 40 Code of Federal Regulations (CFR) Part 136 has been criticized as a poor estimator of the detection limit for numerous reasons including (DoD EDQW 2017):

- It is a single laboratory estimation that does not account for analytical bias, changing instrument conditions, or analyst skill.
- It does not account for changes in variance at different concentration levels as it assumes uniform variance across all possible spike concentrations.
- Laboratories can calculate MDLs that cannot be achieved in practice when very low spike levels are used.
- A laboratory has the option to pool data from multiple instruments to calculate one MDL that represents multiple instruments.
- There are no requirements for demonstration of the ability to detect an analyte at the calculated MDL.
- The MDLs are not reproducible from day-to-day, laboratory-to-laboratory and are typically not calculated more often than once per year.

Updates to the EPA MDL procedure (82 FR 40939 2017) have addressed some concerns such as: background contamination, multiple analysts and instruments, and have included verification requirements; however, the MDL calculation of spikes remains unchanged (DoD EDQW 2017; EPA 2017). Additional steps can be taken to document the uncertainty associated with measurements of low-level concentration data such as reviewing raw data (e.g., chromatograms) and comparing sample results to blanks (DoD EDQW 2017).

In summary, estimated concentrations down to MDLs should be considered with caution. Reviews of low-level detections of TPH and naphthalenes are provided in upcoming sections.

1.5 GROUNDWATER CHEMISTRY AS A FUNCTION OF LNAPL EXTENT

No conclusive evidence of measurable LNAPL has been detected in Red Hill wells (see Section 1.2). An analysis of dissolved-phase constituents can be used as LOEs to determine the presence and extent of LNAPL in the groundwater at the site. If LNAPL is present near a well, it would be expected to:

- Exhibit both an organic (e.g., consistent detections of COPCs and non-COPCs) and inorganic (e.g., low dissolved oxygen, presence of methane) footprint (as seen in RHMW02).
- Result in a continuing impact (i.e., chemical signature) to the well rather than random, sporadic, low-level detections.
- Exhibit an organic signature consistent with the fuel type (e.g., jet fuel) and representative of the dissolution and weathering of the LNAPL source over time.
- Exhibit an inorganic chemical signature demonstrating biodegradation (e.g., low dissolved oxygen).

Wells farther away from a LNAPL source would still see reduced concentrations of chemicals based on the factors mentioned above. The chemical signature would be significantly influenced by relative biodegradation of chemical constituents in the dissolved-phase plume. Even in this case, it is highly unlikely that the chemical signature would result in random sporadic detections.

2. Evaluation of COPCs

COPCs included in this analysis are: benzene, ethylbenzene, toluene, and total xylenes (BTEX); naphthalene, 1-methylnaphthalene, and 2-methlynaphthalene (collectively referred to as naphthalenes); and TPH.

2.1 Fuel Additives and Lead

Phenol and 2-[2-methoxyethoxy]-ethanol (fuel additives target compounds) data are also available but are not included in this study. 2-[2-methoxyethoxy]-ethanol has not been detected at the site. Phenol was detected only once in December 2016 at RHMW09 (DON 2017a).

Prior to 2016, analysis of lead scavengers 1,2-dibromoethane and 1,2-dichloroethanewas included for all wells as part of the full suite of volatile organic carbons (VOCs) analyzed for in the Red Hill LTM program; in 2016, the VOC list was scaled back to BTEX only based on evaluation of COPCs (EPA Region 9 and DOH 2016). However, these lead scavengers continue to be analyzed for in samples from newly installed monitoring wells for at least 1 year of sampling (at minimum) following well installation (DON 2017b); after that, lead scavenger analysis may be discontinued if sample results are below the screening levels established in the project's scoping completion letter (EPA Region 9 and DOH 2016). Lead scavengers were also included in the EPA split sampling program. 1,2-dibromoethane has not been detected at the site. 1,2-dichloroethane was detected only in RHMW08 in samples collected in January, February, and March of 2017 by the EPA Region 9 laboratory. 1,2-dichloroethane has had multiple uses including past use as fumigant and can be an impurity found in polyvinyl chloride (PVC).

Both lead scavengers were used in leaded gasoline, but only 1,2-dibromoethane was used in aviation gasoline. Leaded fuels were last stored at the Facility in 1968 in Tanks 17 and 18 (DON 2005, 2019).

Total and dissolved lead were analyzed for in most samples; however, lead is a naturally occurring element. Evidence of a leaded fuel release cannot be determined from lead concentrations in groundwater samples without careful consideration of the local range of background concentrations.

2.2 Evaluation of BTEX

During a fuel release, BTEX are typically the first compounds detected in groundwater near the release because they are the most abundant of the COPCs in undegraded jet and diesel fuels and are the most water-soluble components in jet fuels. Input from unweathered sources or recent releases are expected to increase BTEX concentrations in groundwater. The ideal effective solubilities of BTEX in the types of fuels stored at the Facility are summarized in CSM Appendix B.7.3. JP-8 equilibrated with water has an approximate average sum of BTEX of >3 milligrams per liter (mg/L).

Other than for RHMW02, there are few BTEX detections in all other Near-Tank and Outlying Wells.

2.2.1 BTEX in Near-Tank Wells

There are few detections of BTEX in RHMW01 and RHMW03. Benzene was detected once in RHMW01 (June 2017) and never in RHMW03. Toluene was detected three times in RHMW01 (September 2005 and twice in January 2014) and once in RHMW03 (October 2012). Ethylbenzene and xylenes have never been detected in RHMW01 or RMWH03.

At RHMW02, ethylbenzene and total xylenes have been detected consistently and with decreasing concentrations over time (Figure 2-1 and Figure 2-2, respectively). The small number and low concentrations of toluene detections in RHMW02 (Figure 2-3) compared to other BTEX compounds indicate a weathered LNAPL source. Fresh JP-8 would be expected to have higher concentrations of toluene than ethylbenzene based on the ideal effective solubilities of BTEX in fuel (CSM Appendix B.7 Table 3-3).

Benzene has been detected inconsistently in RHMW02 (Figure 2-4). The laboratory used from April 2015 to July 2016 (CAS/ALS) had a LOD that was five times lower than the previous laboratory (Calscience/Eurofins) and three times lower than the subsequent laboratory (APPL). This change in LOD, not a result of a new release, is likely the cause of the appearance of benzene, which was not observed in previous sampling events.

If a new fuel source was introduced, dissolved-phase BTEX concentrations should increase according to effective solubilities of fresh fuels. There is no apparent change in BTEX trends after the 2014 fuel release. The source of the nearby LNAPL is not the 2014 fuel release, as the detection trend extends further back than the 2014 fuel release.

The frequency of BTEX detections in Near-Tank Wells (RHMW01, RHMW02, and RHMW03) is discussed further in Section 2.5 along with the other COPCs.

<u>Key Point:</u> Overall, BTEX trends are consistent throughout the LTM program and do not show evidence of impact from the 2014 fuel release. However, LNAPL has likely impacted groundwater upgradient of RHMW02 prior to the 2014 fuel release.

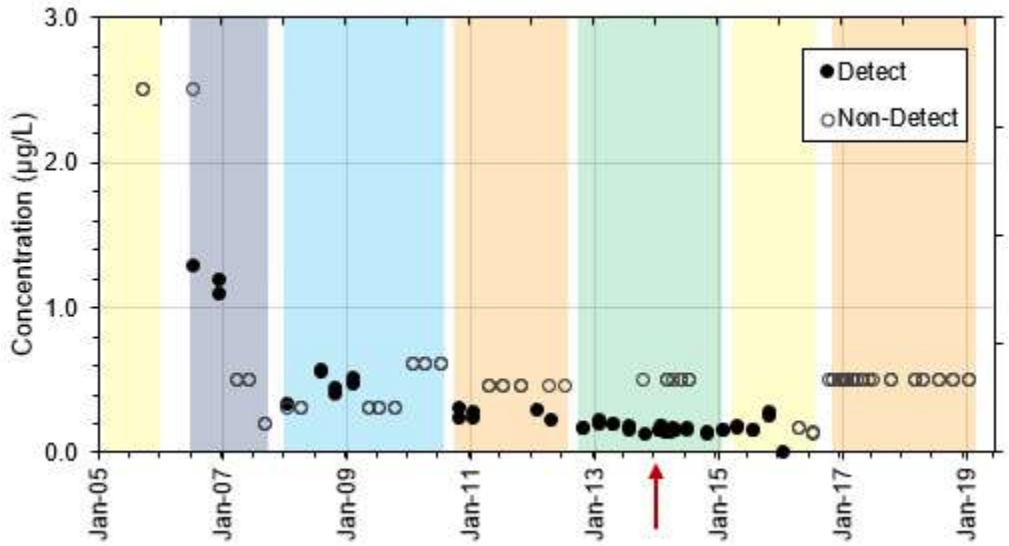

Notes: The red arrow indicates the Tank 5 fuel release date. The colored backgrounds highlight periods for different analytical laboratories: yellow = CAS and CAS/ALS, grey = Accutest, blue = SGS Alaska, orange = APPL, and green = Calscience/Eurofins.

Figure 2-1: Ethylbenzene Detections in RHMW02

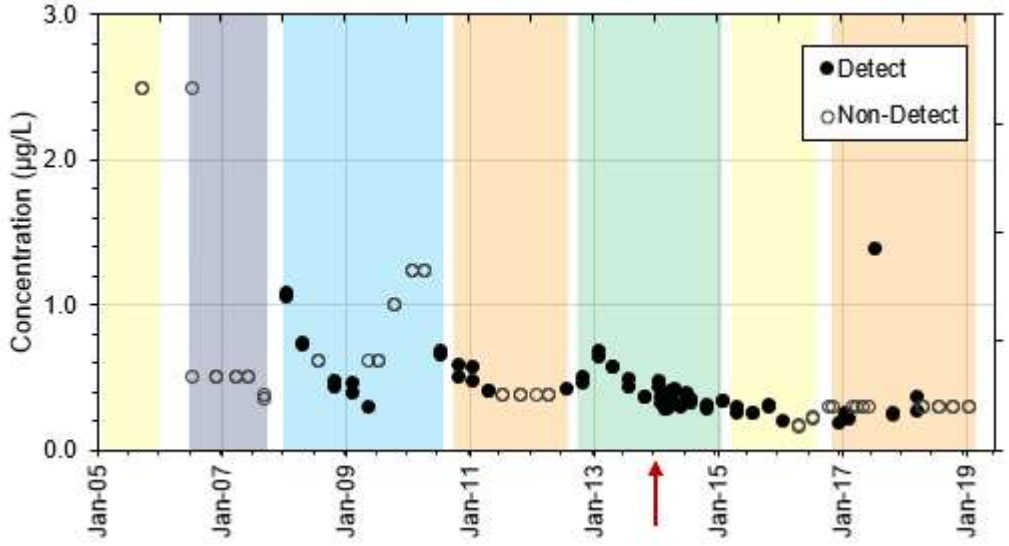

Notes: The red arrow indicates the Tank 5 fuel release date. The colored backgrounds highlight periods for different analytical laboratories: yellow = CAS and CAS/ALS, grey = Accutest, blue = SGS Alaska, orange = APPL, and green = Calscience/Eurofins.

Figure 2-2: Total Xylenes Detections in RHMW02

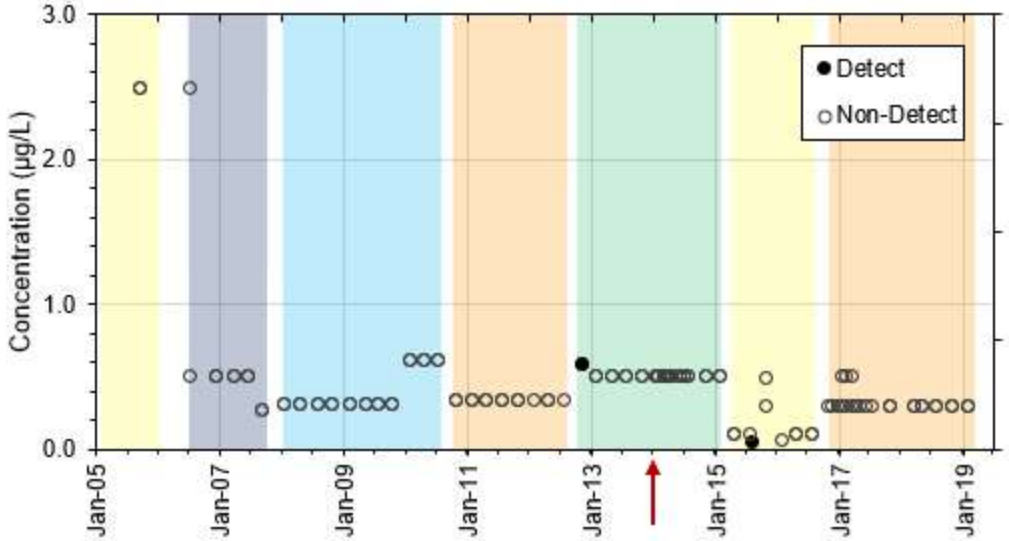

Notes: The red arrow indicates the Tank 5 fuel release date. The colored backgrounds highlight periods for different analytical laboratories: yellow = CAS and CAS/ALS, grey = Accutest, blue = SGS Alaska, orange = APPL, and green = Calscience/Eurofins.

Figure 2-3: Toluene Detections in RHMW02

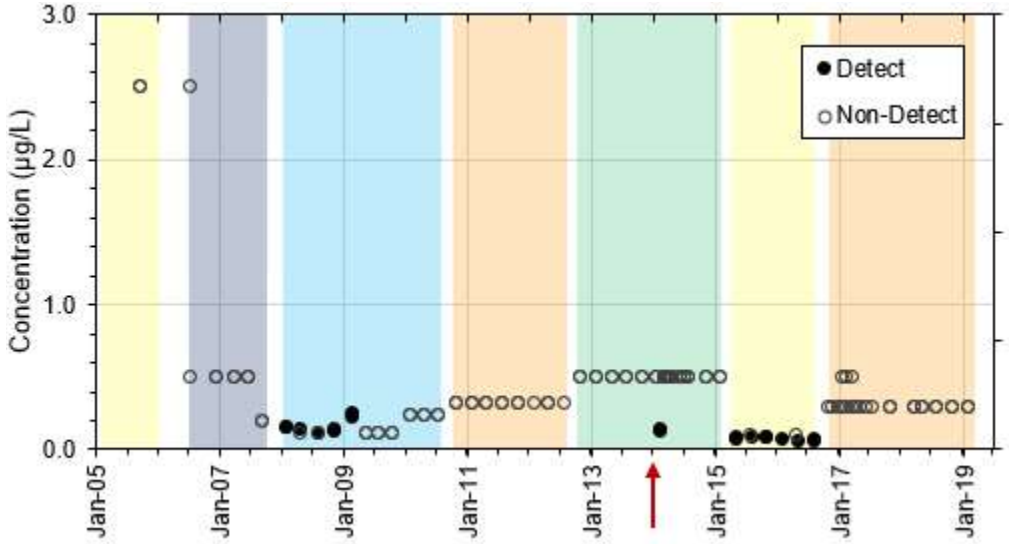

Notes: The red arrow indicates the Tank 5 fuel release date. The colored backgrounds highlight periods for different analytical laboratories: yellow = CAS and CAS/ALS, grey = Accutest, blue = SGS Alaska, orange = APPL, and green = Calscience/Eurofins.

Figure 2-4: Benzene Detections in RHMW02

2.2.2 BTEX in Outlying Wells

The frequency of BTEX detections in Outlying Wells is discussed further in Section 2.5 along with the other COPCs.

No BTEX were detected in RHMW06, RHMW07, RHMW08, RHMW09, RHMW10, and RHMW11. BTEX detections in RHMW04, RHMW05, Red Hill Shaft, and HDMW2253-03 are infrequent, and there are no BTEX hits in consecutive monitoring events.

Detections in RHMW04 occurred during three sampling events: August 2009 (benzene), October 2015 (benzene), and January 2019 (xylenes). RHMW05 had a single detection of toluene in a sample from October 2012. Detections in HDMW2253-03 of benzene occurred in three separate sampling events (April and October 2011 and April 2012). Toluene was reported in samples from October 2014 and April 2015.

Detections in Red Hill Shaft occurred during two sampling events: October 2012 (toluene) and October 2018 (toluene, ethylbenzene, xylenes). These detections may be due to field contamination or laboratory issues as these detections were not confirmed in the following sampling events.

***Key Point:** The sporadic BTEX detections in Outlying Wells are inconsistent with a nearby LNAPL source. BTEX detections in Outlying Wells show no apparent impact to groundwater in Outlying Wells from fuel releases or site operations.*

2.3 EVALUATION OF NAPHTHALENES

Naphthalene, 1-methlynaphthalene (1-MeN), and 2-methylnaphthalene (2-MeN)—collectively referred to herein as naphthalenes—are COPCs at Red Hill (EPA Region 9 and DOH 2016). Although most detections of naphthalenes occurred in Near-Tank Wells, specifically RHMW01 and RHMW02, low-level detections have also occurred in Outlying Wells. These low-level detections are susceptible

to interferences (e.g., laboratory/field contamination and instrument carryover) and are inherently more variable. Furthermore, analysis was done using mass spectrometry in selected ion monitoring (SIM) mode, which can be prone to potential false positives, particularly for laboratories that did not use the recommended 3-ion qualification for identification, as is currently required in QSM 5.1 (DoD and DOE 2017). The reporting limits have varied from the multiple laboratories used over the monitoring period, from 0.005 to 0.1 µg/L. Additional limitations of reporting concentrations down to MDLs are discussed in Section 1.4. Laboratories may calculate MDLs that cannot be achieved in practice and are not required to demonstrate ability to detect an analyte at the calculated MDL (DoD EDQW 2017; EPA 2017).

In general, there is lack of precision in the naphthalenes results in duplicate samples. The naphthalenes are extracted from water, and the extract is concentrated by evaporation before analysis using the EPA Method 8270 SIM analytical methodology. The DoD QSM (DoD and DOE 2017) lists wide acceptance criteria for laboratory control samples (LCSs) using this method (e.g., LCS acceptance criteria of 41–115% for the analyte 1-methylnaphthalene). The large acceptance criteria range indicate variability in the naphthalenes results, which may be due to partial loss in the concentration step as a result of naphthalenes' relative volatility. In contrast, analytical methods for VOCs do not require extraction, thus LCS control limits for BTEX are tighter, in the range of 78–121%. Additional issues with low-level detections of naphthalenes is discussed in Section 1.4

2.3.1 Weathering of Naphthalenes

Forensics investigations often use ratios of target compounds rather than absolute concentrations to normalize sample variability and take advantage of properties and/or biodegradation differences among the different compounds that can be diagnostic of particular changes in the samples. The relative distribution ratio of naphthalenes in groundwater in equilibrium with jet fuel can be used to evaluate weathering. The ratio is based on the abundance of naphthalenes in fuel and the ideal effective solubility of naphthalenes in water (additional discussion available in CSM Appendix B.7.3). The fuel signature in groundwater will show higher concentrations of methylnaphthalenes to naphthalene for a fresh source. The relative distribution ratio of naphthalenes of an unweathered source is approximately 2, with a ratio of less than 2 indicating a weathered source (see CSM Appendix B.7.4). The introduction of a new source to groundwater would be expected to change the relative distribution ratio, as the new source would likely have a different naphthalenes signature than what is currently present in the subsurface.

2.3.2 Naphthalenes in Near-Tank Wells

Naphthalenes were detected most frequently and at the highest concentrations in RHMW02. The concentrations of detected naphthalenes and the relative distribution ratio of naphthalenes for RHMW02 are presented on Figure 2-5. There are higher levels of naphthalenes before and after the Tank 5 release. Tank 5 was out of service from early 2011 to a short time before the 2014 release.

Dissolved-phase concentrations of naphthalene and methylnaphthalenes in RHMW02 are within a factor of 2 or less than their effective solubilities for unweathered jet fuel (CSM Appendix B.7 Table 3-3). It is possible that the relatively high concentrations of these constituents indicate: 1) a fuel source with higher than expected concentrations of naphthalenes and/or 2) a weathered source where the removal of other more soluble/biodegradable compounds results in the naphthalenes becoming relatively more concentrated in the residual LNAPL over time. The likelihood of a weathered source is more evident when diagnostic ratios of the naphthalenes are examined further (Figure 2-5). The weathering ratio is generally less than 1 for all samples and is less variable than the concentrations of

the individual compounds. The only exceptions where the ratio is greater than 2 are for a few samples in 2009 where the individual concentrations were low and the ratio calculation was unreliable. The fact that the ratio is consistently less than 2 strongly suggests that no new impact from unweathered fuels was observed at RHMW02 and, more specifically, no observed impact from the 2014 release event.

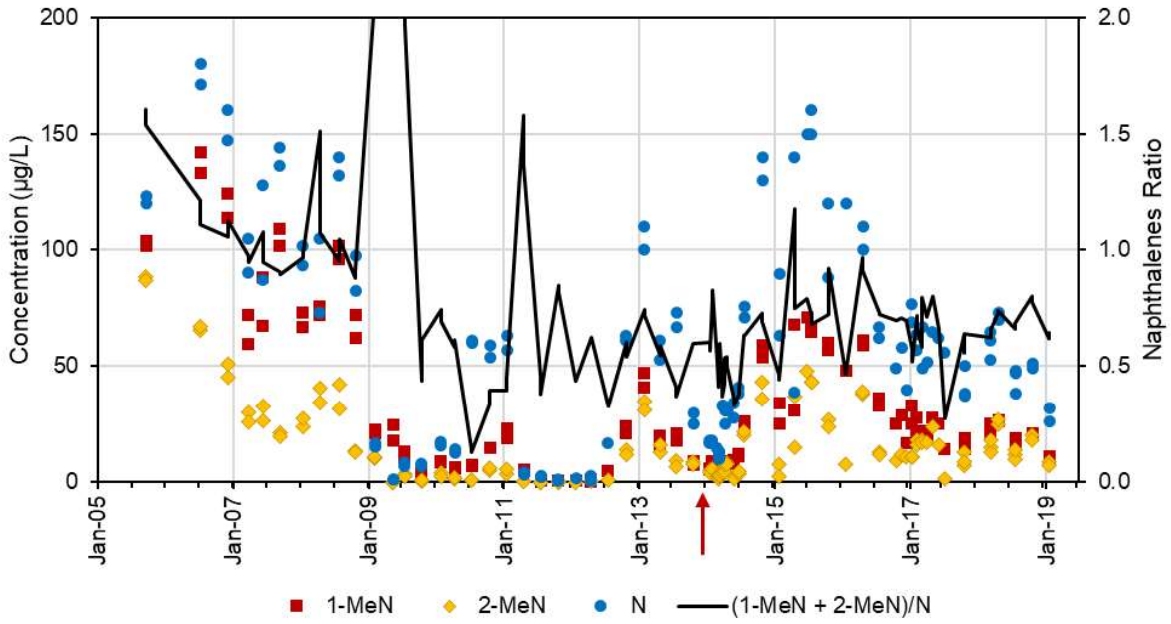

Note: The red arrow indicates the Tank 5 fuel release date.

Figure 2-5: Naphthalenes Detections and Naphthalene Weathering Ratio in RHMW02

The naphthalenes results for RHMW01 and RHMW03 are presented on Figure 2-6 and Figure 2-7. Naphthalenes are detected at lower concentrations in RHMW01 and RHMW03 compared to RHMW02. There are consistent naphthalene analyte detections in RHMW01, but coinciding detections of methylnaphthalenes are not as frequent as is seen in RHMW02. The naphthalenes detections at RHMW03 are noticeably less frequent than at RHMW01 or RHMW02.

Key Point: ***There was no change in the weathering ratio after the 2014 fuel release, which is inconsistent with a fresh fuel source resulting from the 2014 fuel release. Therefore, evidence of impact to groundwater from the 2014 release is not apparent.***

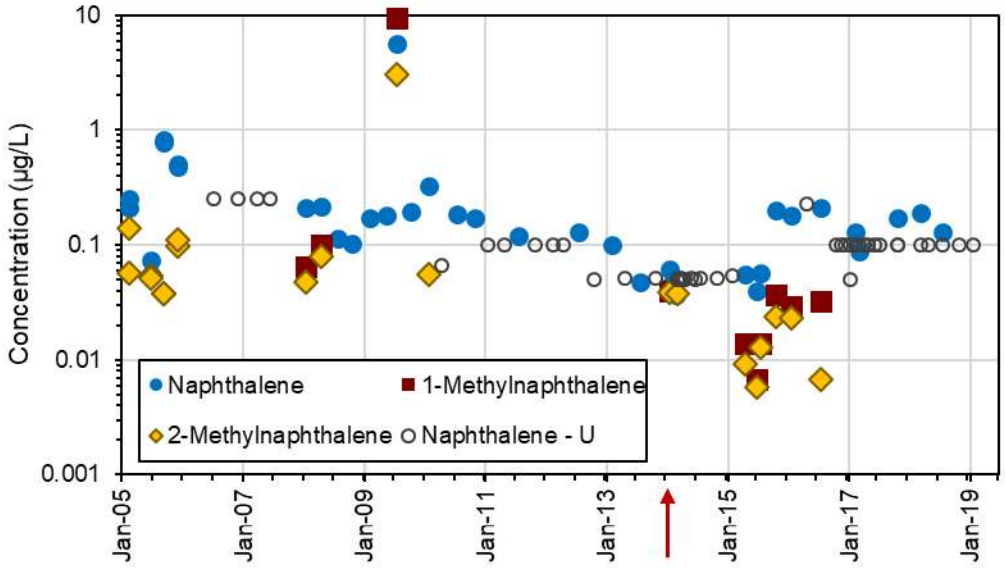

Note: The red arrow indicates the Tank 5 fuel release date.

Figure 2-6: Naphthalenes Detections and Reporting Limits in RHMW01

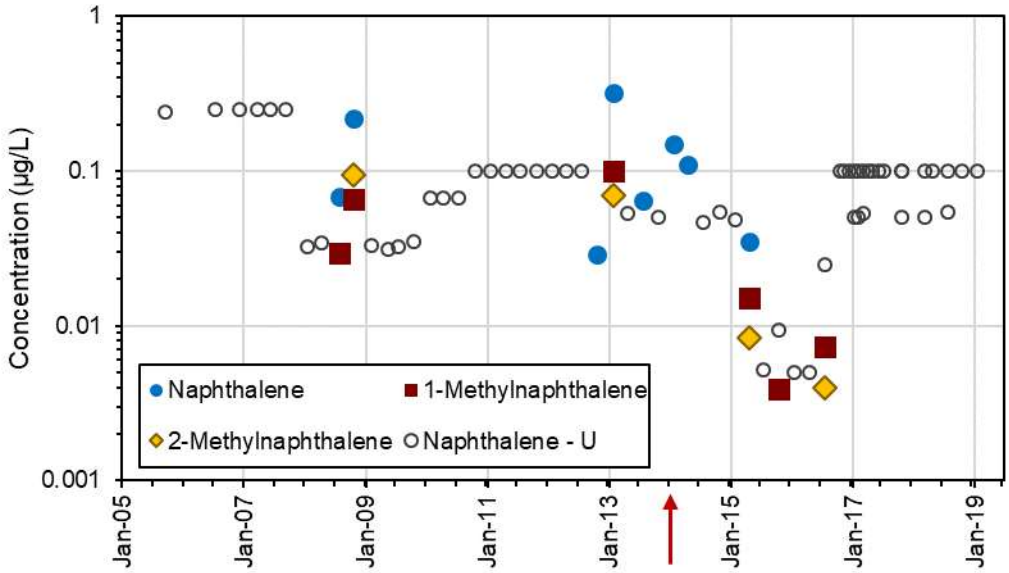

Note: The red arrow indicates the Tank 5 fuel release date.

Figure 2-7: Naphthalenes Detections and Reporting Limits in RHMW03

2.3.3 Naphthalenes in Outlying Wells

Detections of naphthalenes in Outlying Wells were sporadic and at concentrations below the DOH Environmental Action Levels (EALs). The sum of naphthalenes detections for RHMW04, RHMW05, RHMW06, RHMW07, Red Hill Shaft, and HDMW2253-03 are shown on Figure 2-8; wells with no detections are not shown. Detections appear to occur with similar frequency and at similar concentrations during the 2013–2015 period for RHMW05, Red Hill Shaft, and HDMW2253-03. As discussed in Section 1.3, these wells are constructed differently from each other (e.g., Red Hill Shaft

induces flow, which can result in substantial dilution). Considering the different construction but similar detection trends in these wells, the low-level naphthalenes detections by Calscience/Eurofins during this period are suspect.

Further analysis of the detections of the analyte naphthalene during the Calscience/Eurofins 2013–2015 period shows increased detection frequency from Fourth Quarter 2012 to Second Quarter 2014 followed be a period of no detections (Figure 2-9). The subsequent laboratory, CAS/ALS, did not detect naphthalene at the same frequency or at the same concentrations, even though the detection limit was an order of magnitude lower. These observations further support the conclusion that the naphthalene detections by Calscience/Eurofins are suspect.

Low-level detections of naphthalenes in Outlying Wells are not consistent with transport of LNAPL through either the vadose or saturated zones.

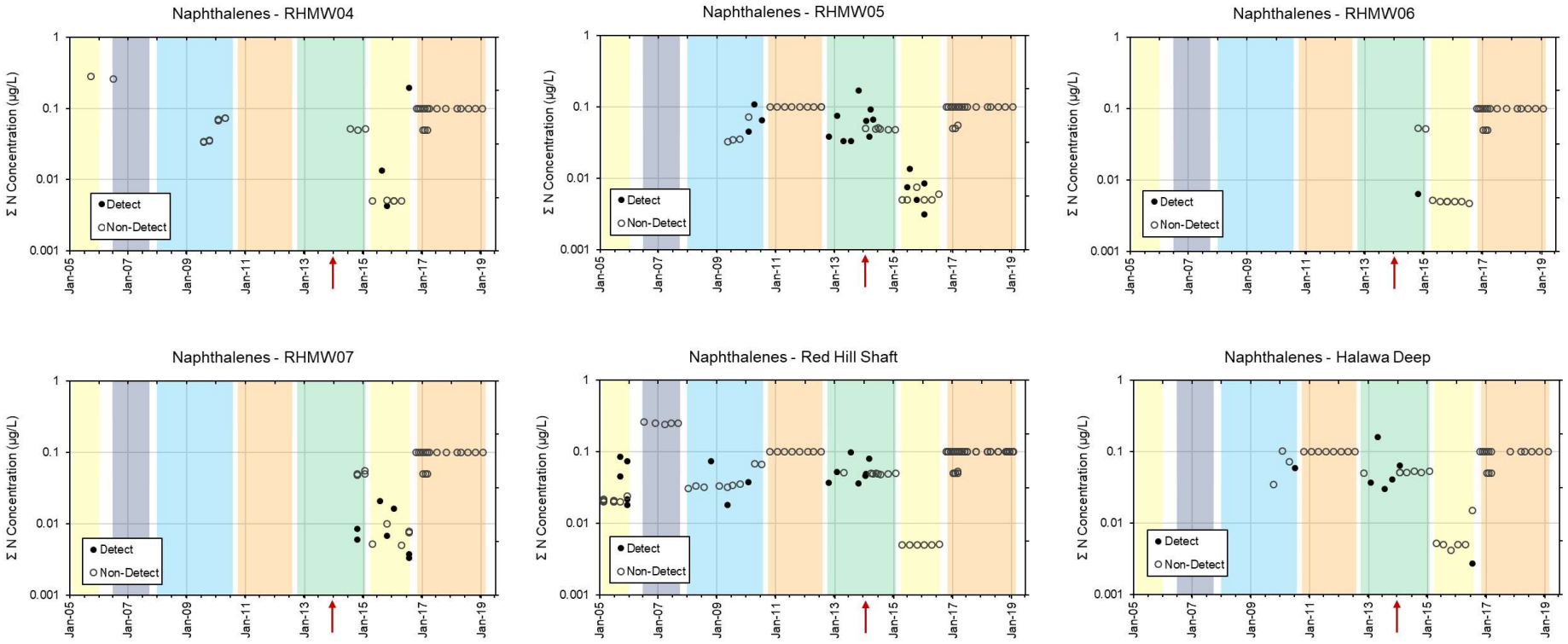

Notes: The red arrow indicates the Tank 5 fuel release date. The colored backgrounds highlight periods for different analytical laboratories: yellow = CAS and CAS/ALS, grey = Accutest, blue = SGS Alaska, orange = APPL, and green = Calscience/Eurofins.

Figure 2-8: Sum of Naphthalenes in Outlying Wells

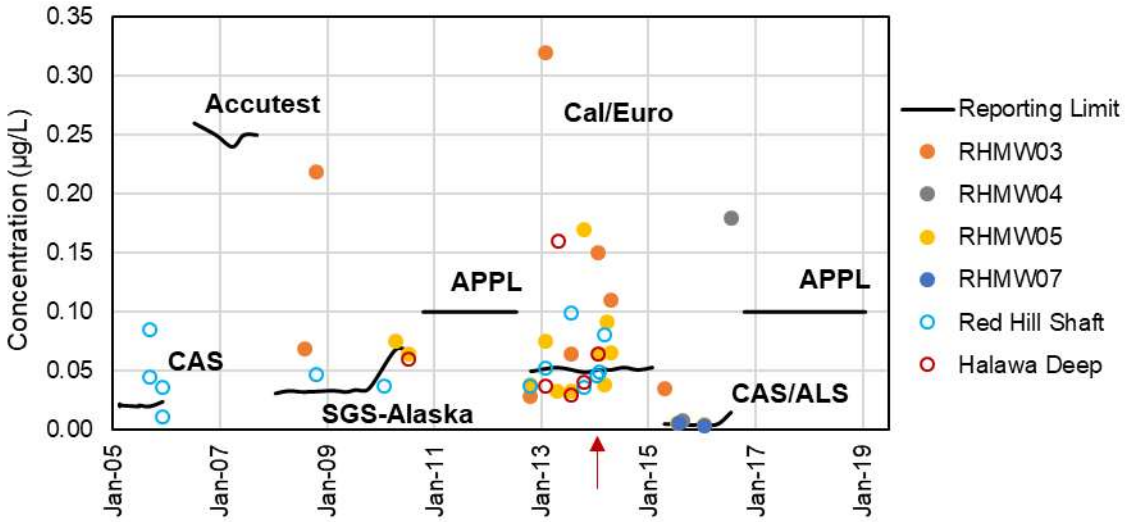

Note: The red arrow indicates the Tank 5 fuel release date.

Figure 2-9: Detections and Reporting Limits of Naphthalene in Outlying Wells

Key Point: ***The inconsistent and low-level detections of naphthalenes in Outlying Wells are not indicative of a nearby LNAPL source, and therefore evidence of impact to groundwater in Outlying Wells from fuel releases/site operations is not apparent.***

2.4 EVALUATION OF TPH

TPH measurements are defined in three carbon ranges intended to represent approximate carbon ranges of fuels, and each has a specific EAL: gasoline range organics (TPH-g), diesel range organics (TPH-d), and oil range organics (TPH-o). The focus of this section is TPH-d, which is the most commonly detected TPH carbon range and includes jet and diesel fuels. TPH-g and TPH-o are used as supporting details. A product type definition (e.g., gasoline range, diesel range) does not necessarily identify the presence of the specified product, but only that some of the measured material might fall in the compositional range of the named product. Expert evaluation of analysis results (including chromatograms) may help in assessing the product type, if any, as there are many possible organic interferences that will appear in the TPH portion of the chromatograms (ITRC 2018). Examples of interferences include biogenic naturally occurring compounds, solvents, and chlorinated compounds.

TPH is an analytical parameter defined by the method used to measure it (see CSM Appendix B.7 for additional discussion). The analytical methods are variable (e.g., different extraction solvents, extraction methods, calibration standards, and reported carbon ranges that sometimes overlap). Non-petroleum compounds may also be measured (ITRC 2018). As such, numerical results of dissolved TPH-d alone are not suitable as a diagnostic tool to assess the presence of LNAPL in groundwater.

TPH results are further complicated by biodegradation of the fuels, which produces polar compounds/metabolites that tend to be more water soluble than the aliphatic parent compounds (see detailed discussion in CSM Appendix B.7 Sections 3.3 and 4.1). Multiple LOEs should be evaluated to determine if an apparent change in TPH concentration based on previous results is due to a release and/or the presence of LNAPL, or is due to a result of changes in laboratory methods and inherent limitations of TPH measurement.

2.4.1 What Is Included in TPH-d Measurements

What is reported as TPH might not be total, might not be entirely petroleum, and might not be entirely hydrocarbons, so careful examination of the meaning of the numerical results is important. The numerical result may include petroleum hydrocarbons, petroleum hydrocarbon-related metabolites, and any other organic matter detected in the analysis. There are many possible organic interferences that may be measured and appear as TPH. The presence of polar material produced by biodegradation has a large impact on TPH results. Polar compounds are more soluble than the parent hydrocarbon and have significantly different responses to the detectors used to measure TPH-d (ITRC 2018).

In accordance with the State of Hawai'i *Evaluation of Environmental Hazards at Sites with Contaminated Soil and Groundwater, Volume 1* (DOH 2017), the term "TPH" is defined as the sum total of parent petroleum hydrocarbons, as well as petroleum hydrocarbon-related metabolites and other degradants. The latter includes alcohols, phenols, ketones, aldehydes, and organic acids (Mohler et al. 2013; Zemo et al. 2013, 2017). The toxicity of parent petroleum hydrocarbon compounds and related degradants is assumed to be similar for initial screening purposes (DOH 2017).

As discussed in CSM Appendix B.7 Section 4.1.1, the TPH-d measured in RHMW02 is 43–86% polar compounds/metabolites. This was determined by using silica gel cleanup (SGC), which is an additional step in TPH-d sample preparation that removes polar compounds/metabolites. This type of data is available for samples from 2017 to 2019. The TPH-d in RHMW02 is in the range of 1,000–3,300 µg/L before SGC but in the range of 230–640 µg/L after SGC (CSM Appendix B.7 Table 4-1).

The overall effective solubility of fresh diesel and jet fuels is approximately 5,000 µg/L, primarily from aromatic hydrocarbons (e.g., BTEX, alkylated benzenes, and naphthalenes). The presence of LNAPL can be inferred by comparing the concentrations of aromatic hydrocarbons, which are included in the measurement of TPH-d, in groundwater to the solubility of fresh fuels. However, TPH-d measurements also include polar compounds/metabolites, which are more soluble than parent hydrocarbons (ITRC 2018). As the source at Red Hill has been degraded and contains a substantial portion of polar compounds/metabolites (43–86%), it is more appropriate to compare the results of TPH-d after SGC to the effective solubility of jet and diesel fuels to infer the presence of LNAPL. The hydrocarbon portion (TPH-d after SGC) of TPH-d concentrations at RHMW02 is well below the jet and diesel fuel effective solubility.

***Key Point:** Polar compounds in RHMW02 are more soluble than the parent hydrocarbons; what is measured as TPH is not indicative of the presence of LNAPL from a fresh release but is indicative of an older nearby source*.

2.4.2 Variability in TPH-d Measurements

Fuels are complex mixtures of hydrocarbons with a range of physical and chemical properties that are subject to weathering by such processes as volatilization, dissolution, and biodegradation. Assessment of these mixtures is through the estimation of TPH, an analytical parameter that is defined by the method used to measure it. There are many methods and each method can vary from state to state and even laboratory to laboratory. There can be varied extraction solvents, instrument calibration protocols and standards, and reportable carbon ranges used in the procedures. Non-petroleum materials and metabolites are also measured as part of TPH. Considering these variables and uncertainties, numerical results and apparent trends should be interpreted with caution and with other LOEs.

The variability of TPH results is expected to be significantly higher than for single-component measurements like BTEX, similar to the naphthalene variability discussed in 2.3. This is reflected in

relatively wide ranges of acceptance criteria for laboratory controls and calibration standards. DoD QSM Version 5.1 specifies control limits for the TPH-d LCS of 36–132% of the expected value (DoD and DOE 2017). In comparison, the LCS control limits for BTEX are tighter, in the range of 78–121%. Performance testing TPH-d samples from vendors have acceptance criteria of 30–125% of the spiked concentrations.

The LCS is a laboratory control that is used to determine status of the calibration. For instance, if the LCS has an actual concentration of 100 parts per billion (ppb) and it is measured at 40 ppb on a given day, a field sample with the same concentration as the LCS may also be reported around 40 ppb. If another sample from the same well is analyzed on another day by the same laboratory but with the LCS measured at the time of analysis as 130 ppb, that sample may be also be measured as 130 ppb. Both results are acceptable and equivalent as the LCSs recovered within the control limits of 36–132%. Therefore, comparative analysis of hydrocarbon data should consider the large error inherent in TPH methods. In addition to lack of precision, variability in methods and polar/metabolites quantitation issues for TPH-d and TPH-o prevent valid trend analysis based on TPH alone. It is essential to understand what is really being measured as "TPH." Most site investigations focus on individual compounds, which are more definitive and reliable.

Switching to a different analytical laboratory also significantly affects evaluation of TPH on the basis of the numerical results alone. This is particularly important in determining trends with time.

TPH-d concentrations in RHMW02 over time separated by analytical laboratory are shown on Figure 2-10. There is clearly more variability on absolute TPH results depending on the laboratory than with time. These figures show that it is not feasible to evaluate trends on solely TPH without understanding the limitations of this parameter.

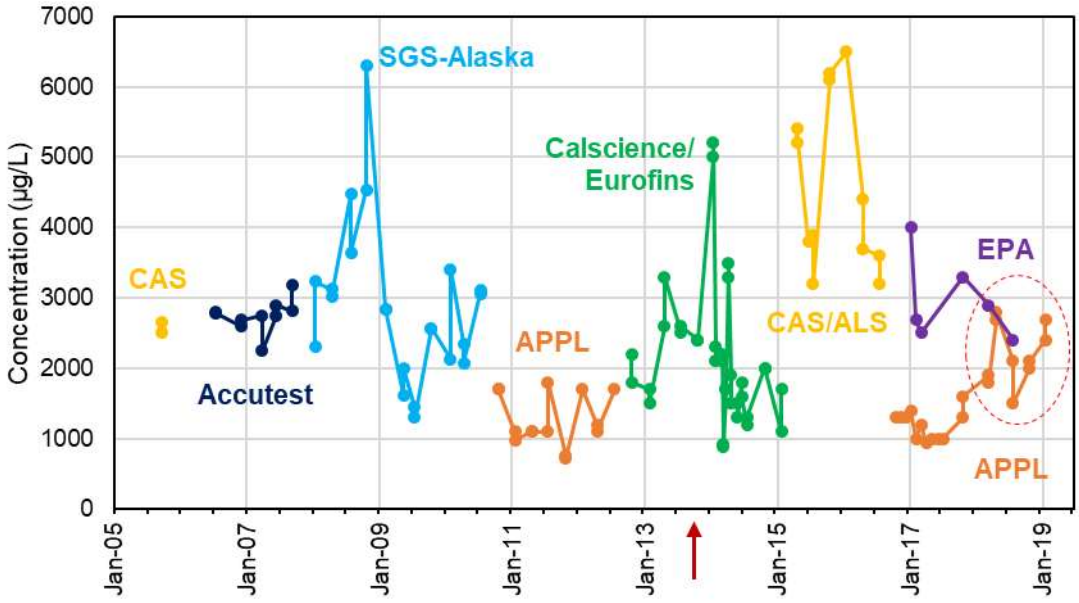

Note: The red arrow indicates the Tank 5 fuel release date. Samples analyzed by APPL after modifications to the analysis are indicated by the red circle.

Figure 2-10: TPH-d Results in RHMW02 with Laboratories Identified

Issues with TPH measurements are further illustrated when split samples from January, February, and March of 2017 were analyzed both by APPL (the current Navy laboratory for the Facility) and the EPA Region 9 laboratory for an extended suite of analytes including TPH-d and TPH-o. The Wilcoxon rank sum test was used to compare the TPH-d results of APPL and EPA for RHMW02 and RHMW01. There was a significant difference in the median between the two laboratories for both RHMW02 ($p = 0.003$) and RHMW01 ($p = 0.012$) (see Attachment B.8.3 for statistical method details). The differences were not random. Performance samples were analyzed by both laboratories, and it was evident that APPL was not extracting as much material from groundwater compared to the EPA laboratory. The issues were due to differences in extraction protocols (EPA Region 9 and DOH 2017; DON 2017c) exacerbated by the predominance of polar compounds/metabolites in the samples. As discussed in CSM Appendix B.7 Sections 3.3 and 4.1, polar compounds/metabolites are not hydrocarbons, are not the target of the TPH analysis, and are more susceptible to tailing in the gas chromatogram among other issues. In addition, TPH quantitation, as defined by the method, is with respect to a diesel standard, which is unweathered fuel and has a significantly different response in the detector used for quantitation than the polar/metabolites. APPL started modification of the extraction protocol toward the end of 2017. Figure 2-10 shows that the TPH-d results (in red circle) from APPL for the October 2017 to April 2018 samples are closer to EPA results. These higher results are not due to changing conditions in the groundwater at the Facility, but to changes in the laboratory's TPH extraction and analysis protocols.

2.4.3 Low-Level TPH Measurements

There are also significant issues with measuring TPH at low levels, as TPH is not a single peak like benzene, but a wide range of the chromatogram that is integrated and quantitated. Review of the chromatograms or "fingerprints" obtained from analysis of TPH is useful for reducing uncertainties inherent to the analysis (ITRC 2018). Review of chromatograms for low-concentration data is also suggested in a fact sheet from the DoD Environmental Quality Workgroup (2017). Analysis uncertainty is illustrated on Figure 2-11, which shows the chromatograms from analysis of the only detections for TPH-d for RHMW04.

TPH-d was detected by Calscience/Eurofins in RHMW04 in July 2014 and January 2015 at 17 J (J = estimated concentration) and 10 J µg/L, respectively. Review of the chromatograms reveals a series of discrete peaks in the July 2014 sample that do not resemble any type of fuel pattern, dissolved fuel components, or biodegraded matter. The sample from January 2015 shows over-integration of a very small signal at the LOD (Figure 2-11). These detections are likely false positives and do not support presence of fuels in RHMW04. Therefore, even though "detections" were reported, they are not petroleum hydrocarbons and are not indicative of fuels or metabolites. This additional review of the chromatograms decreases uncertainty in the significance of the TPH and may improve site characterization.

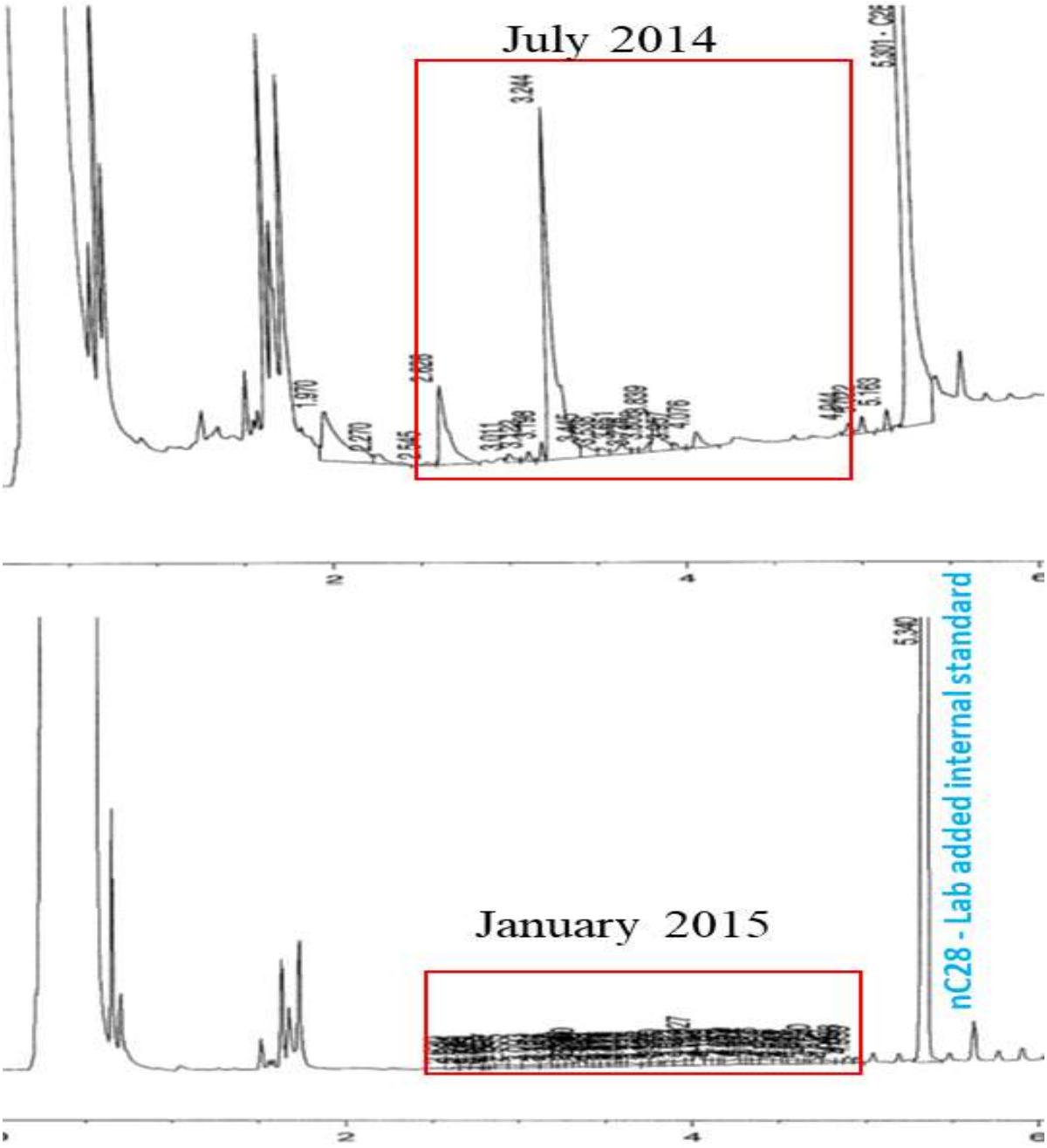

Figure 2-11: RHMW04 TPH-d Chromatograms from July 2014 and January 2015 Samples

Key Point: ***TPH trend analyses are challenging due to inconsistent methodology and laboratories, thus requiring data analysis of other constituents. TPH by itself is unreliable to use as evidence of impact from fuels to groundwater without review of chromatograms.***

2.4.4 TPH-d and TPH-o in Near-Tank Wells

RHMW02 has the highest TPH concentrations among the Facility monitoring wells (1,000–7,000 µg/L TPH-d and non-detect (ND) to 400 µg/L TPH-o) since the start of monitoring in 2005 (Figure 2-12

and Attachment B.8.1); however, there has been no direct evidence of LNAPL in this well. Much of the TPH concentrations (up to 86%) are in the form of polar compounds associated with the biodegradation of petroleum (see CSM Appendix B.7 Section 4 for an in-depth discussion of the composition of the TPH-d detected in RHMW02). The data suggest the presence of weathered LNAPL (i.e., pre-2005 release) in the immediate vicinity of RHMW02 or within the saturated zone upgradient from this well.

RHMW01 has had relatively consistent TPH-d detections (ND to 1,500 µg/L) with the concentrations showing a generally decreasing trend since the start of monitoring in 2005 (Figure 2-12). TPH-o was detected in 2005 but infrequently since then (Attachment B.8.1). RHMW03 has had relatively low (less than 500 µg/L) but consistent detections of TPH-d and TPH-o since 2005 (Figure 2-13 and Attachment B.8.1). Since May 2017, samples with TPH detections have also been analyzed after SGC. In all but one sample from RHMW03 and all but two samples from RHMW01, 100% of the TPH was removed (i.e., SGC samples were non-detect). The results show TPH-d and TPH-o in RHMW01 and RHMW03 contain mostly or entirely of polar compounds/metabolites. These data are consistent with the natural attenuation of dissolved constituents in groundwater and do not suggest the presence of LNAPL within the vicinity of RHMW01 or RHMW03.

Key Point: ***TPH data suggest the presence of weathered LNAPL (i.e., pre-2005 release) in the immediate vicinity of RHMW02 or within the saturated zone upgradient from this well. The data for RHMW01 and RHMW03 are consistent with the natural attenuation of dissolved constituents in groundwater and do not suggest the presence of LNAPL within the vicinity of these wells.***

2.4.5 TPH-d and TPH-o in Outlying Wells

In general, detections of TPH-d and TPH-o in Outlying Wells have been inconsistent and there have been no detections of these COPCs above DOH EALs (Figure 2-13 and Attachment B.8.1). Most (RHMW06 and RHMW10) or all (RHMW07 and RHMW08) TPH-d and TPH-o detections appear to occur in sampling events after well installation and afterward only infrequently and at relatively low levels. A comparison of TPH-d results between sampling events within 1 year of well installation and all times after was conducted for Outlying Wells. It was assumed that impacts from installation and/or well development would be similar for all wells (i.e., Outlying Wells behave similarly); therefore, Outlying Wells (excluding RHMW11, which has been sampled for only five quarters) were considered one population. The generalized Wilcoxon test was applied, and there was a significant difference ($p < 0.001$) in TPH-d results between sampling events within 1 year of installation and subsequent events.

There were no detections of TPH-d or TPH-o at RHMW09 and RHMW11 (in all five monitoring zones within the basalt layer). TPH-d detections in RHMW04 were discussed previously; one detection occurred immediately following installation and two other detections occurred in 2014 and 2015. Review of the 2014 and 2015 sample chromatograms showed these detections to likely be false positives and not indicative of fuels (see Section 2.4.3 for additional details).

TPH detections should be considered in the site evaluation, but the meaning of these detections must be carefully evaluated as TPH detection is not a direct indication of hydrocarbons in groundwater. Nevertheless, the TPH levels detected in these wells are not indicative of LNAPL or of impacts from Facility operations. TPH should be considered along with the occurrence of other COPCs and other LOEs when determining impacts to a site.

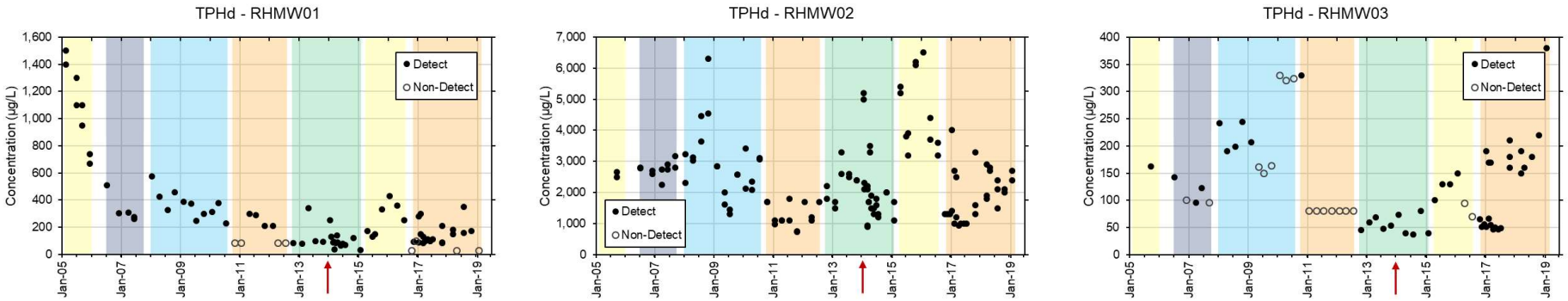

Notes: The red arrow indicates the Tank 5 fuel release date. The colored backgrounds highlight periods for different analytical laboratories: yellow = CAS and CAS/ALS, grey = Accutest, blue = SGS Alaska, orange = APPL, and green = Calscience/Eurofins.

Figure 2-12: TPH-d in Near-Tank Wells

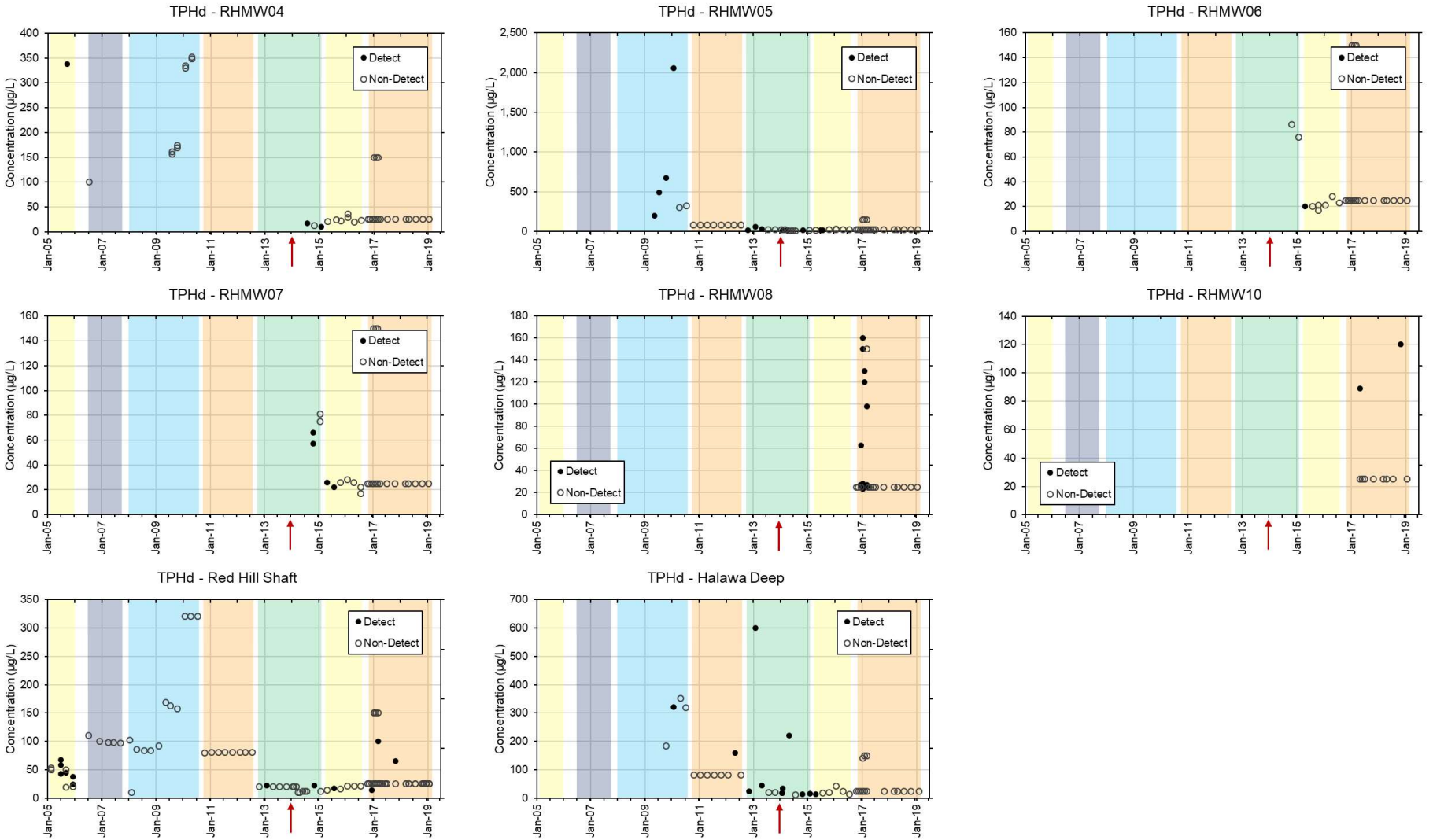

1 Notes: The red arrow indicates the Tank 5 fuel release date. The colored backgrounds highlight periods for different analytical laboratories: yellow = CAS and CAS/ALS, grey = Accutest, blue = SGS Alaska, orange = APPL, and green = Calscience/Eurofins.

2 **Figure 2-13: TPH-d in Outlying Wells**

2.5 EVALUATION OF COMBINED COPCS

Detection signature charts of COPCs are presented on Figure 2-14 and Figure 2-15. The detection signature charts show the number of detections of a given compound by quarter. These charts show detections of BTEX in green, naphthalenes in yellow, and TPH in blue. Quarters with detections are highlighted in different colors. Quarters in which the compounds were not analyzed are left blank. An increase in the number of detections from one quarter to the next does not indicate an increase in concentration, but simply that more samples were analyzed. For example, in RHMW02 there is an [apparent] increase in the number of ethylbenzene detections after the 2014 Tank 5 fuel release. This is due to the increased sampling frequency after the fuel release, and as shown on Figure 2-1 through Figure 2-4 did not correspond to an increase in the frequency of analyte detection. Typically, one set of duplicate samples from RHMW02 are analyzed quarterly, but in response to the Tank 5 release there were four sets of duplicate samples and a single sample collected from January to March 2014.

Consistent and coinciding detections of COPCs provide confidence in determining impact to groundwater because multiple LOEs (BTEX, naphthalenes, and TPH) are used to support conclusions.

2.5.1 Combined COPC Analysis in Near-Tank Wells

Consistent and coinciding detections of COPCs occurred in RHMW02 throughout the monitoring program (2005–2019) and to a lesser extent in RHMW01 and RHMW03. These detections support the conclusion that LNAPL has likely impacted groundwater near RHMW02 prior to the 2014 release. There is also some consistency between TPH-d and naphthalene detections in RHMW01. Although there are consistent detections of TPH-d in RHMW03, there are limited coinciding detections of naphthalenes.

2.5.2 Combined COPC Analysis in Outlying Wells

Wells impacted by a fuel release should show consistent agreement between multiple COPCs. For example, if naphthalene is detected in a sample, methylnaphthalenes and TPH is also expected to be detected. If BTEX are detected in a sample, TPH-d is also expected. There is greater confidence in conclusions that are drawn with multiple, concurring LOEs compared to an analysis of a single variable.

Detections of COPCs in Outlying Wells are sporadic and noncoincident. For example, throughout the monitoring program, at RHMW04 and RHMW06 there are no coincident detections of TPH with other COPCs. At RHMW08 and RHMW10, TPH has been detected but not naphthalenes or BTEX. In addition, there have been no detections of COPCs at RHMW09 or at RHMW11 (in all sampled monitoring zones). Kendall's tau analysis was used to determine if there was a correlation between TPH-d detections and other COPCs in Outlying Wells (as would be expected is detections were associated with a fuel release). Outlying Wells were combined and treated as one population. There was no significant correlation between TPH-d concentrations and naphthalene ($p = 0.787$), 1-MeN ($p = 0.965$), 2-MeN ($p = 0.934$), or dissolved oxygen ($p = 0.964$; dissolved oxygen is discussed in Section 3). As there has been discussion on some Outlying Wells not being representative of the water table (RHMW07, RHMW11, HDMW2253-03, Red Hill Shaft), the same analysis was conducted excluding these wells; no significant correlations were found (p-values of 1, 0.966, 0.957, 0.305 for naphthalene, 1-MeN, 2-MeN, and dissolved oxygen, respectively) (see Attachment B.8.3 for statistical method details).

Most, and in some cases all, TPH detections in Outlying Wells appear to occur in sampling events after well installation (not exceeding 1 year for detections), indicating that the TPH may be associated with well drilling and construction.

Sporadic detections of COPCs, with occasional detections of multiple COPCs in one quarter have occurred in RHMW05, RHMW07, Red Hill Shaft, HDMW2253-03. However, a closer review of the data shows similar detection signatures in 2013 and 2014 for Red Hill Shaft, HDMW2253-03, and RHMW05. These results are questionable considering the different construction of these wells: Red Hill Shaft is a pumping well with substantial dilution, HDMW2253-03 has an open borehole cased to approximately 40 ft below the regional aquifer, and RHMW05 is a standard monitoring well. It is more likely that these detections are a result of sampling or laboratory issues rather than presence of LNAPL. The suspect nature of the naphthalenes detections during this period is discussed in Section 2.3.3.

During the 2015–2016 period in which CAS/ALS was the analytical laboratory, there were similar concurrent detections of naphthalenes in multiple Outlying Wells (RHMW04, RHMW05, and RHMW07). It is unlikely that a LNAPL source reached each of these wells at the same time. Considering the very low detection level at the time (0.005 µg/L), these detections may be a result of laboratory or sampling issues.

In summary, COPC detections in Outlying Wells do not indicate a nearby LNAPL source. Detections may be a result of laboratory/method or sampling issues and uncertainties associated with low level detection and the use of different laboratories with time.

***Key Point*: Sporadic and noncoincident COPC detections in Outlying Wells are not indicative of a nearby LNAPL source. Therefore, evidence of impact to groundwater in Outlying Wells from fuel releases/site operations is not apparent.**

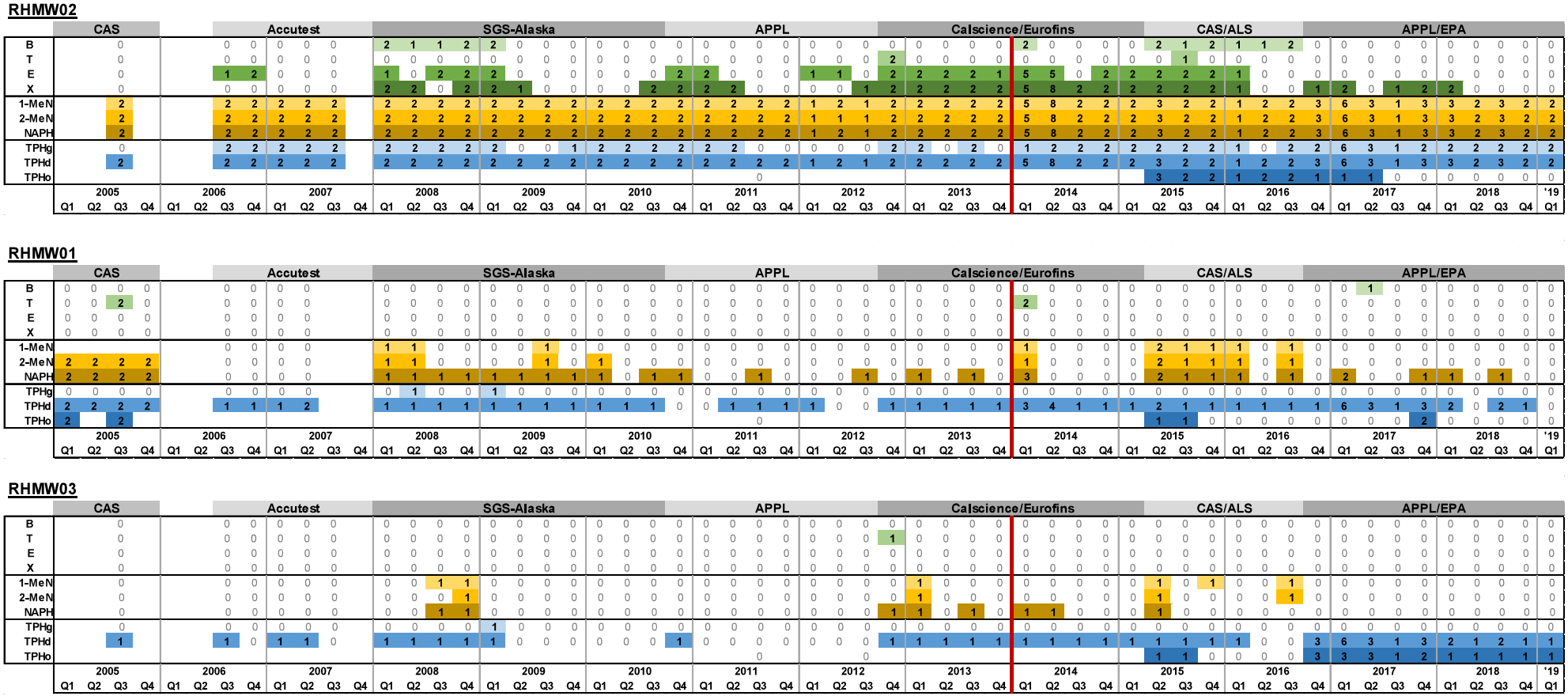

Notes: The red line indicates the Tank 5 fuel release date. The time periods for analytical laboratories are indicated at the top of each chart. The number of detections of a compound in a given quarter including duplicates are listed in the chart, quarters with no sample analyzed are blank. B = benzene, T = toluene, E = ethylbenzene, X = total xylenes, 1-MeN = 1-methlynaphthalene, 2-MeN = 2-methylnaphthalene, N = naphthalene.
Quarters with detections are highlighted in color, and each compound group is identified with a different color. The darker the color, the more detections that occurred in a given quarter.

Figure 2-14: Combined COPC Detection Signature Charts for Near-Tank Wells

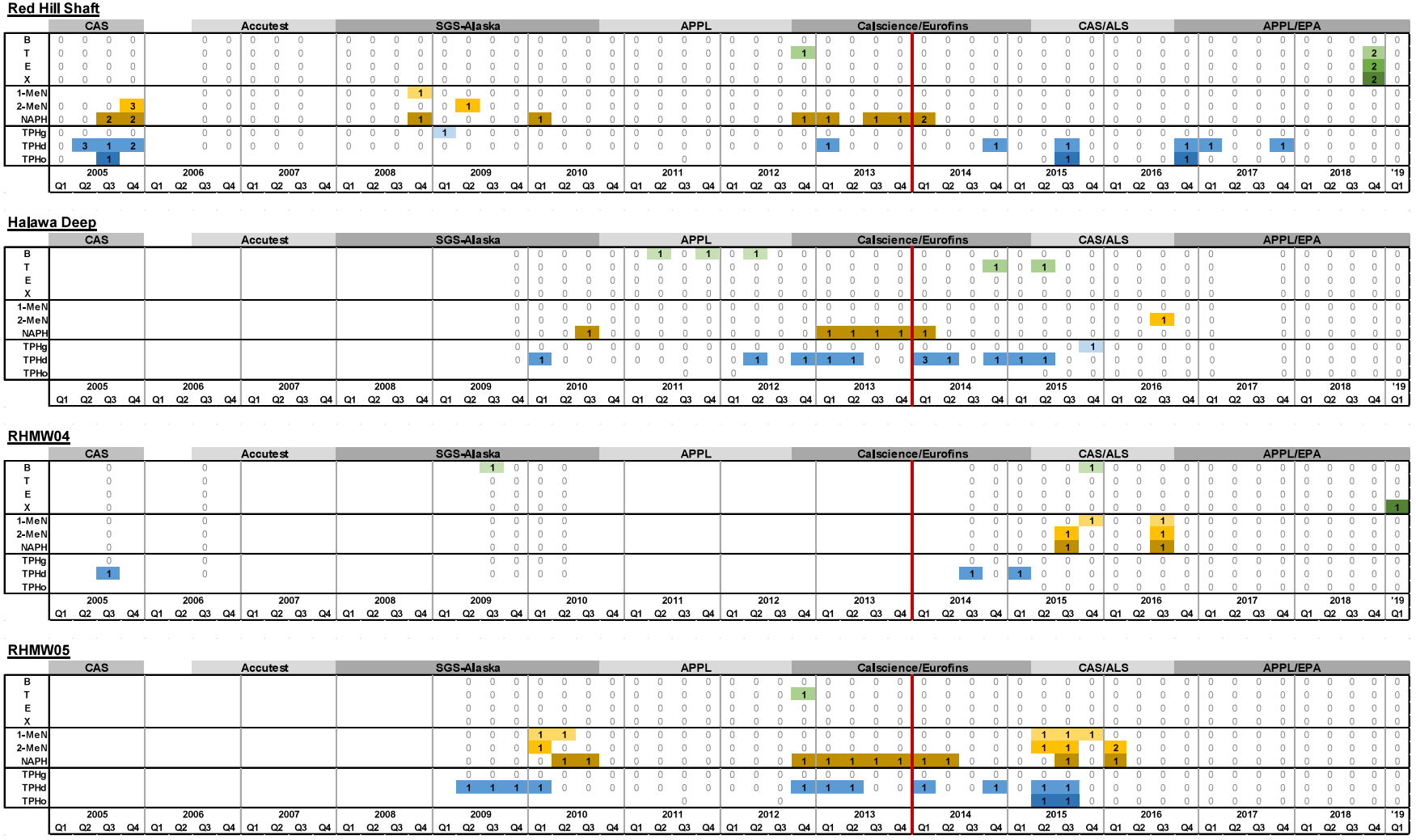

Figure 2-15: Combined COPC Detection Signature Charts for Outlying Wells
(page 1 of 2)

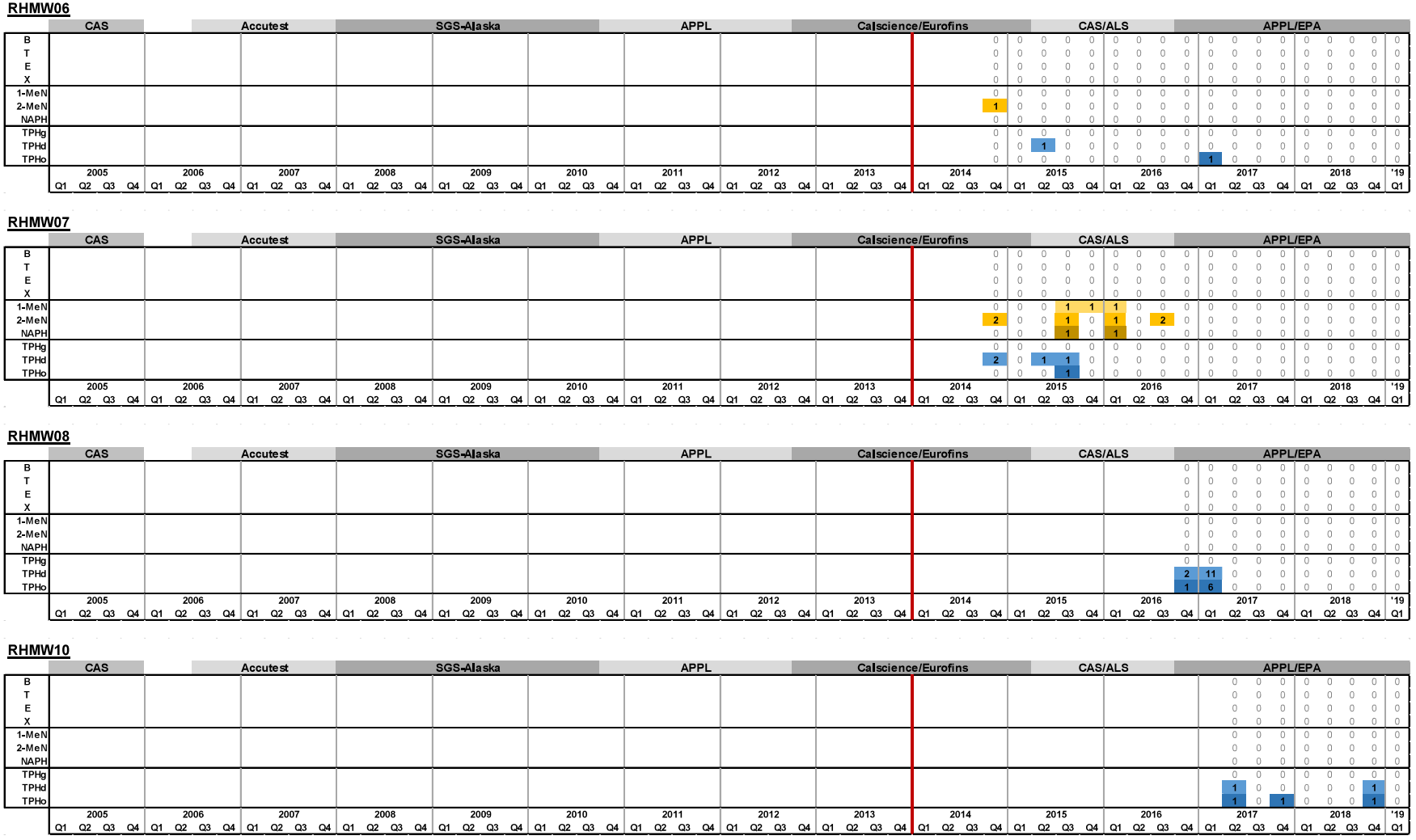

Notes: The red line indicates the Tank 5 fuel release date. The time periods for analytical laboratories are indicated at the top of each chart. The number of detections of a compound in a given quarter including duplicates are listed in the chart, quarters with no sample analyzed are blank. B = benzene, T = toluene, E = ethylbenzene, X = total xylenes, 1-MeN = 1-methlynaphthalene, 2-MeN = 2-methylnaphthalene, N = naphthalene.
Quarters with detections are highlighted in color, and each compound group is identified with a different color. The darker the color, the more detections that occurred in a given quarter.

Figure 2-15 (page 2 of 2): Combined COPC Detection Signature Charts for Outlying Wells

3. Evaluation of Inorganic Geochemistry

As discussed in CSM main document Section 7.3 and Appendixes B.4 and B.5, depletion of electron acceptors (dissolved oxygen, nitrate, and sulfate), generation of metabolic byproducts (ferrous iron and methane), and presence of reducing conditions (negative oxidation-reduction potential [ORP]) are key lines of evidence of biodegradation of COPCs. Consistent measurements of geochemical parameters have been collected at all existing site wells since October 2016, including dissolved oxygen, nitrate, sulfate, methane, ferrous iron, and ORP, were used for this analysis.

3.1 GEOCHEMICAL TRENDS

Geochemical parameters have been relatively stable over time, with outliers likely being due to field instrument and/or laboratory issues. For example, different field instruments (i.e., YSI, Horiba, or smarTROLL multiparameter water quality meters) can produce varying dissolve oxygen concentrations for the same groundwater sample volume. Figure 3-1 shows geochemical results from October 2016 to January 2019. Geochemical results for the most recent sampling event (January 2019) are presented on Figure 3-2. Wells that are not representative of water table chemistry (see discussion in Section 1.3) are shaded grey.

Groundwater samples from RHMW01 and RHMW02 consistently show the following trends: low concentrations of dissolved oxygen, nitrate, and sulfate; relatively high concentrations of methane and ferrous iron; and negative ORP. These data indicate biodegradation of a carbon source (e.g., petroleum fuels) upgradient of the wells.

RHMW03 has low dissolved oxygen, but the trends for other geochemical parameters show nitrate and sulfate are not depleted, metabolic byproducts are not detected, and ORP is positive. The relatively consistent detection of TPH-d, which could provide a carbon source for microorganisms, along with low dissolved oxygen provide indicators of biodegradation in RHMW03, but to a lesser extent than RHMW01 and RHMW02.

High alkalinity is associated with hydrocarbon biodegradation due to carbon dioxide production. The wells with the highest alkalinity are RHMW03 and RHMW02. This is consistent with the conclusions that biodegradation is occurring in RHMW02 and there are marginal indications of biodegradation in RHMW03. However, RHMW01, in which electron acceptors, metabolic byproducts, and ORP indicate biodegradation, does not have high alkalinity.

The trends for geochemical parameters at Outlying Wells that are representative of water table chemistry do not show the depletion of electron acceptors or the presence of metabolic byproducts, and have positive ORP. In January 2019, the dissolved oxygen concentrations in these wells ranged from 5.26 to 8.82 mg/L, the nitrate concentrations ranged from 1.7 to 6.2 J mg/L, the sulfate concentrations ranged from 6 to 92.1 mg/L, there were no detections of metabolic byproducts (e.g., ferrous iron or methane), and the ORP was positive. These geochemical trends, along with the infrequent detections of COPCs, indicate that biodegradation is not occurring at Outlying Wells that are representative of water table chemistry.

Lower dissolved oxygen in wells that are not representative of the groundwater table (RHMW07, RHMW11-05, and HDMW2253-03) may be a result of these wells being screened in or near the saprolite, which has been shown to lower dissolved oxygen (Hunt, Jr. 2004).

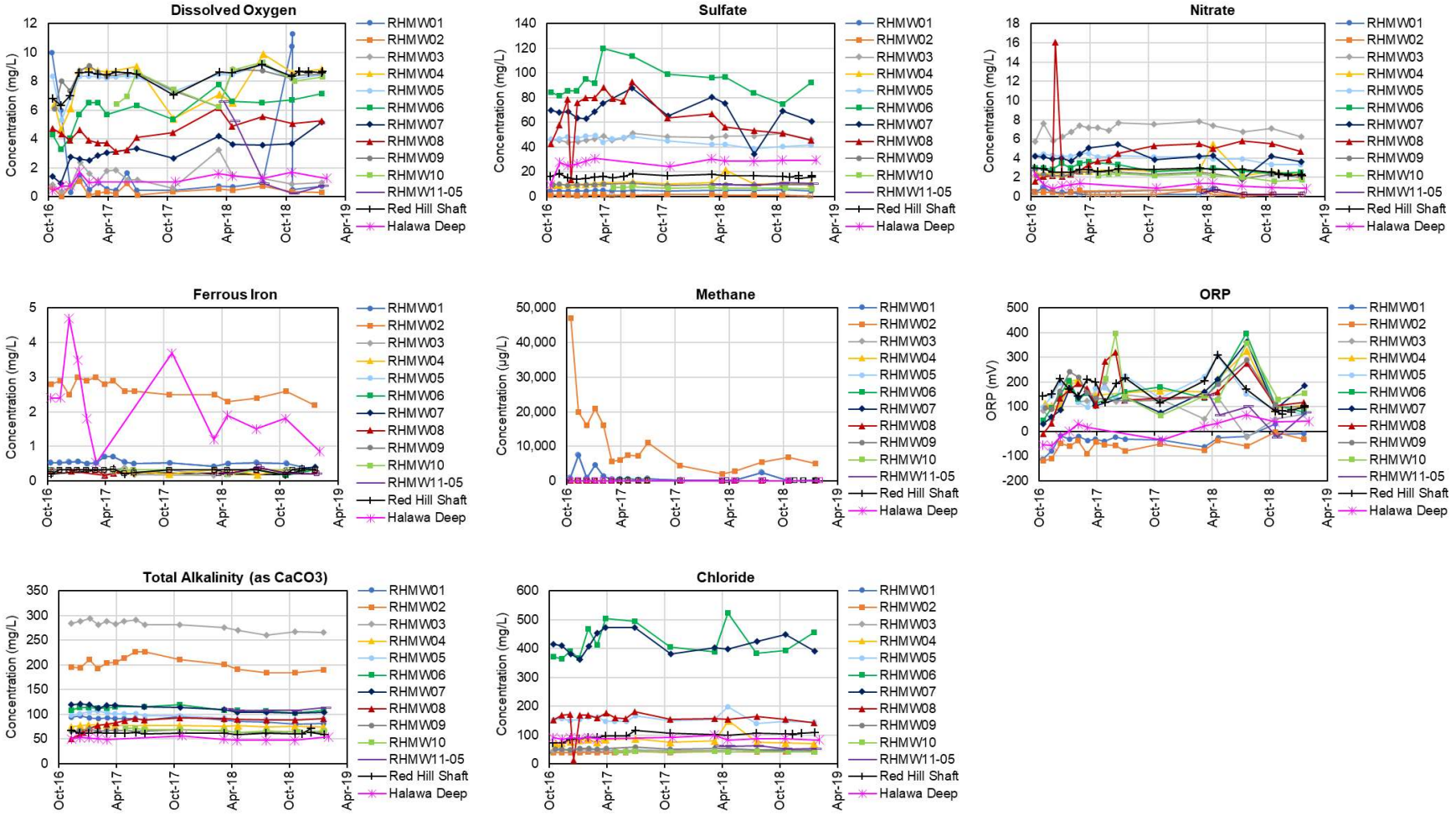

Note: Non-detect samples are identified with an open marker

Figure 3-1: Geochemical Parameters: a) dissolved oxygen, b) sulfate, c) nitrate, d) ferrous iron, e) methane, f) ORP, g) total alkalinity, h) chloride

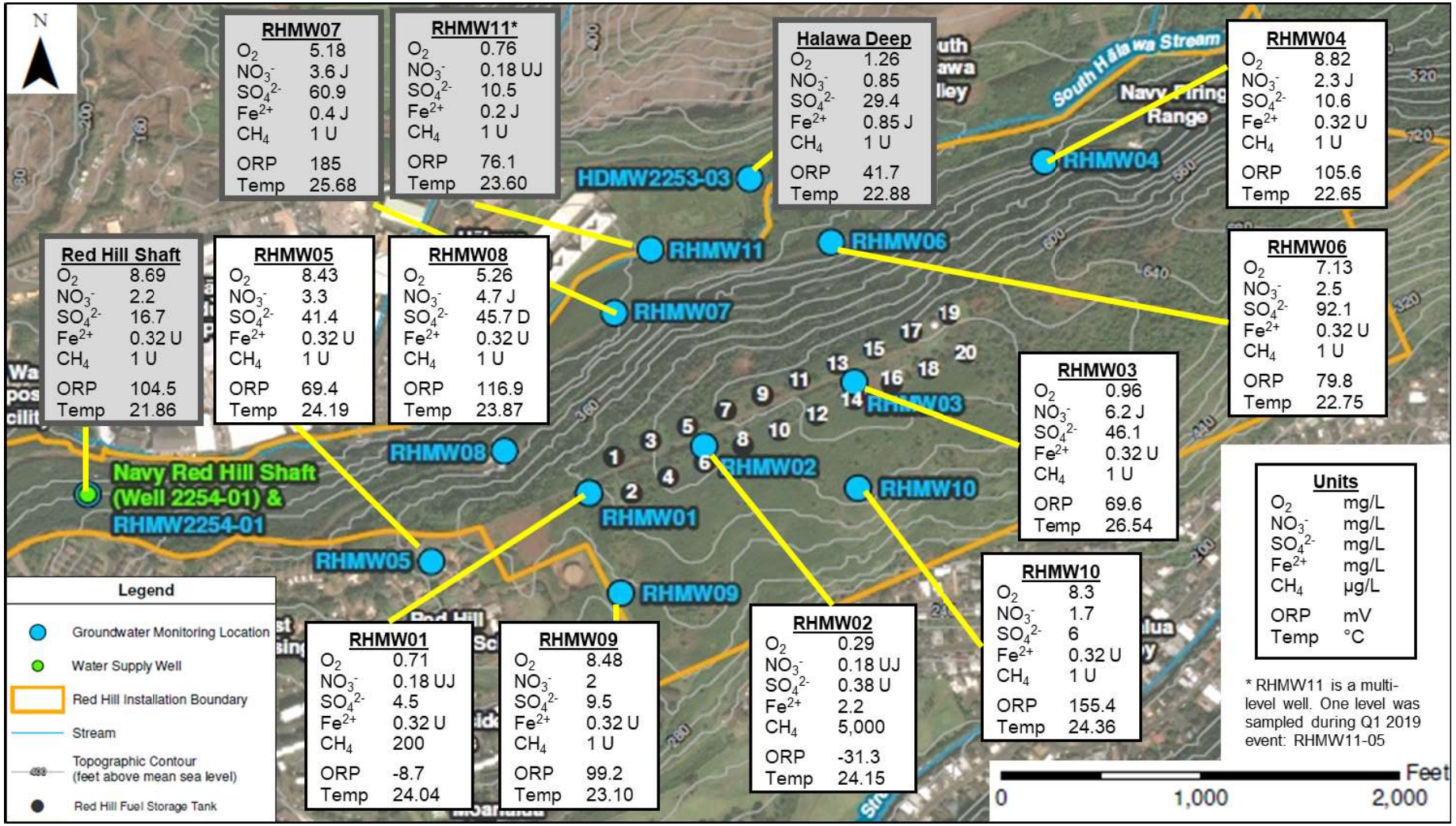

Note: Wells in grey may have water chemistry that differs from other water table wells because of local hydrogeologic factors, as discussed in Section 1.3

Figure 3-2: Geochemical Results from First Quarter (January) 2019 Sampling Event

Key Point 1: ***The presence of a source upgradient of RHMW02 is supported by indicators of biodegradation at RHMW02 and RHMW01. Evidence of biodegradation is also present at RHMW03, but to a lesser extent than RHMW01 and RHMW02.***

Key Point 2: ***Biodegradation indicators in Outlying Wells at the water table do not indicate the presence of a nearby LNAPL source and show no apparent evidence of impact to groundwater from fuel releases or site operations.***

As discussed above, the geochemistry supports to occurrence of biodegradation at RHMW01 and RHMW02. Low dissolved oxygen concentrations at RHMW03 along with regular detections of TPH-d at this well provide marginal indication of biodegradation.

3.2 PRINCIPAL COMPONENT ANALYSIS

Principal component analysis (PCA) was completed to visualize multiple dimensions of data (e.g., constituents) in a two-dimensional plot using new, calculated dimensions (i.e., components) that account for the largest data variance. The goal of conducting PCA is to the express the variability in the data with a few components without losing much information. The variables used to calculate components in this PCA are dissolved oxygen, nitrate, sulfate, alkalinity, chloride, and pH. Data from other wells on O'ahu from Hunt, Jr. et al. (2004) and the University of Hawai'i (2017) are included for comparison. The scores for components 1 and 2 (the components that account for the most variance in the data, 38% and 30%, respectively) are plotted on Figure 3-3.

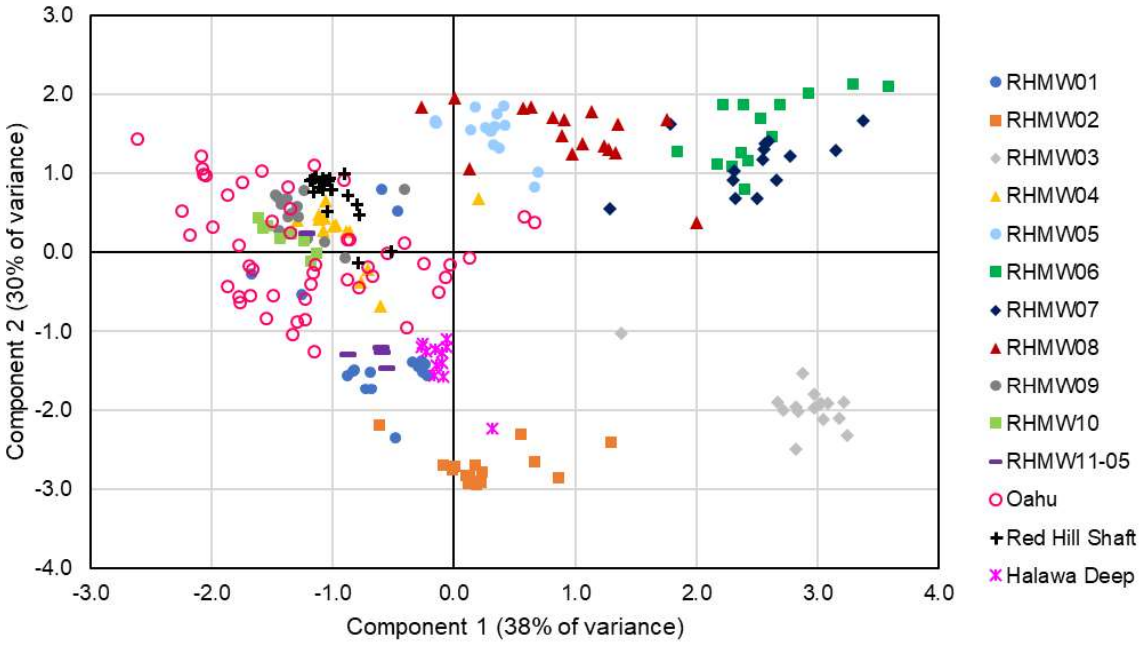

Figure 3-3: Results of Principal Component Analysis of Select Geochemical Data

Results of the PCA show groupings of different wells:

- RHMW06 and RHMW07 – The high chloride and sulfate concentrations separate these wells to the top right of the figure. The chemistry in these wells may related to the proximity of the saprolite.

- RHMW05 and RHMW08 – The relatively high chloride and sulfate concentrations also separate these wells, but the lower concentrations compared to RHMW06 and RHMW07 result in a slightly different location.
- RHMW03 – The high alkalinity and sulfate concentrations and low dissolved oxygen concentration separate this well. High alkalinity is associated with hydrocarbon biodegradation due to carbon dioxide production.
- RHMW01 and RHMW02 – The low concentrations of dissolved oxygen, nitrate, and sulfate separate these wells. The difference in alkalinity (higher in RHMW02) results in the wells showing different groupings.
- O'ahu wells – The overlap of some site wells (RHMW04, RHMW09, RHMW10, and Red Hill Shaft) with the O'ahu wells may indicate background conditions at these locations. Although RHMW11 also overlaps with the O'ahu wells, RHMW11 is the most recently installed well and has a limited data set; additional data may be useful before drawing conclusions about the geochemistry of this well.

Key Point 1: ***The dissolved inorganic parameters in groundwater at RHMW06 and RHMW07 differs from other wells, with notably higher chloride and sulfate concentrations. These differences indicate the geochemistry at RHMW06 and RHMW07 are not representative of the geochemistry at other Outlying Wells.***

Key Point 2: ***The inorganic parameters in groundwater at RHMW04, RHMW09, RHMW10, and Red Hill Shaft appear similar to other O'ahu wells and may represent background conditions, suggesting these wells are not impacted by fuel releases and/or site operations.***

3.3 GROUNDWATER TEMPERATURE

Groundwater temperature can be an indicator of biodegradation, as microbial activity can increase subsurface temperature. Groundwater temperature was measured at wells during groundwater monitoring events (Figure 3-4), and vertical temperature profiles were measured in Near-Tank Wells.

Groundwater temperature at RHMW03 is consistently higher than at other wells (Figure 3-4). The elevated temperatures are consistent with heat conduction from the vadose zone (i.e., natural source-zone depletion [NSZD] in the vadose zone is heating the shallow groundwater), which is confirmed by vertical temperature profiling data (see CSM Appendix B.1 for details).

Larger temperature variations are observed at Outlying Wells compared to Near-Tank Wells. This could be a result of different flow paths or sources of groundwater. Additional vertical temperature profiling at Outlying Wells was conducted in April 2019 to further assess the source of variability.

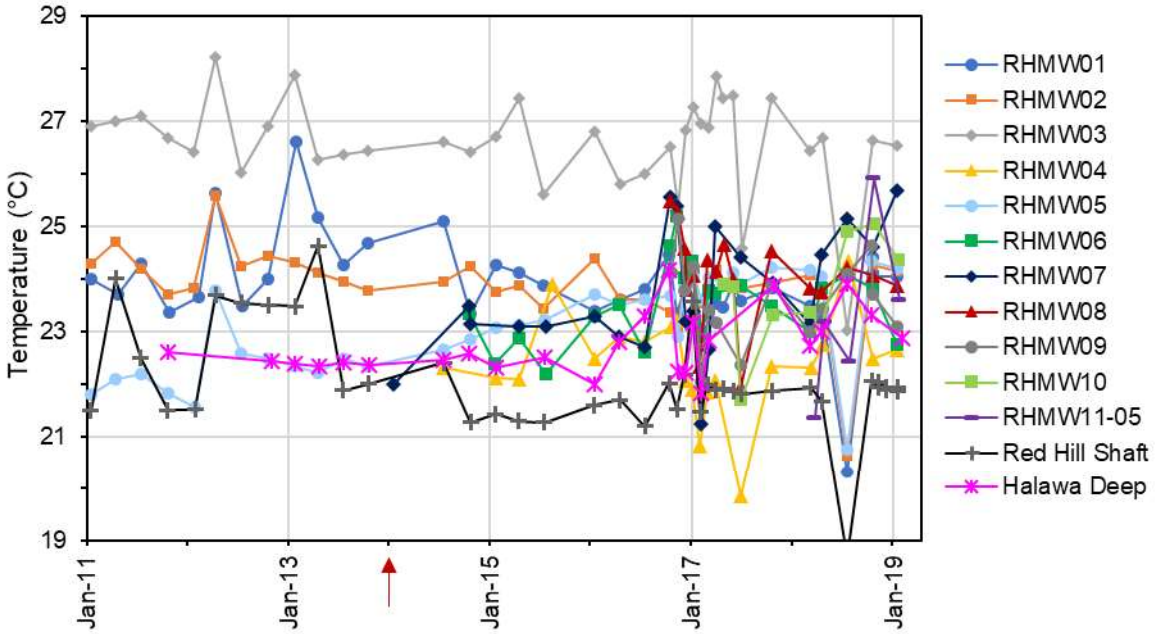

Note: The red arrow indicates the Tank 5 fuel release date.

Figure 3-4: Groundwater Temperature

3.4 ISOTOPIC ANALYSIS

Isotopic analysis of $^{14}C/^{15}C$-nitrogen (δ15N) and $^{34}C/^{32}C$-sulfur (δ34S) was conducted during the Fourth Quarter 2017 monitoring event. Enrichment of heavier isotopes of nitrogen and sulfur would be indicative of electron acceptor use during biodegradation. Trends were not conclusive, but a consistent grouping of RHMW04, RHMW09, RHMW10, and Red Hill Shaft is seen, similar to the PCA results (Figure 3-5).

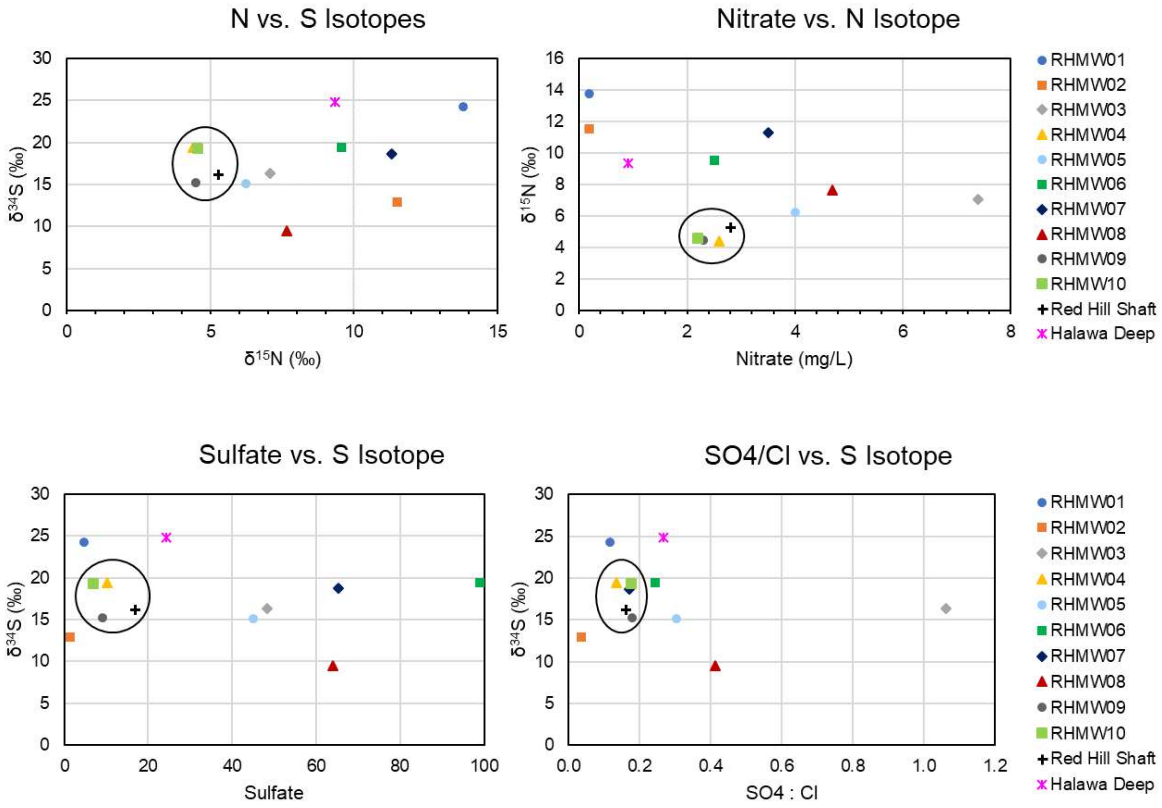

Figure 3-5: Isotopic Analysis of δ15N and δ34S

3.5 GEOCHEMISTRY SUMMARY

Electron acceptors and metabolic byproducts indicates biodegradation is occurring at RHMW02 and RHMW01. This is consistent with COPC detections in these wells. RHMW03 does not show depleted nitrate and sulfate, but there is relatively low dissolved oxygen. The low dissolved oxygen and frequent detections of TPH-d at RHMW03 provide marginal indicators that biodegradation is occurring there. Geochemical parameters do not indicate biodegradation at Outlying Wells.

Results of the PCA analysis show RHMW06 and RHMW07 grouped separately because of high chloride and sulfate concentrations in these wells compared to the other Outlying Wells. RHMW04, RHMW09, RHMW10, and Red Hill Shaft were grouped in the same area as other wells on O'ahu, which may indicate these wells are representative of background conditions. There was a similar grouping of RHMW04, RHMW09, RHMW10, and Red Hill Shaft when plotting δ15N and δ34S.

4. Evaluation of Non-COPCs

Non-COPCs are compounds that are analyzed with the same methods used for COPCs. Non-COPCs include compounds that are targets of specific EPA methods such as priority pollutant polynuclear aromatic hydrocarbons (PAHs), halogenated VOCs, and phthalates. These may be common field and laboratory contaminants potentially from well construction, maintenance, and sampling activities, historical land use, or background/regional contamination. Some of the non-COPCs may also be present in fuels. A complete list of non-COPCs is presented in Attachment B.8.2.

For ease of understanding and graphing purposes, non-COPCs are discussed as groups based on compound classes or categories:

- Hydrocarbons – Volatile hydrocarbons (i.e., substituted benzenes) and PAHs. Some of these compounds may be present in fuels.
- Phthalates – Solvents mainly used as wetting agents and plasticizers
- Halogenated VOCs – Compounds associated with water disinfections, manufacturing, soil fumigation, and laboratory contamination
- Oxygen-containing compounds – Including solvents for polymers, paints, varnishes, detergents, and emulsifiers
- Acetone – Common laboratory contaminant; graphed separately because the detection frequency was more consistent than for other oxygen-containing compounds

The list of non-COPCs analyzed by the different laboratories was not always consistent. Non-COPC data are available for all existing wells prior to reduction of the analyte list from First Quarter 2016 onward per the Administrative Order on Consent (AOC) Statement of Work Sections 6 and 7 scoping completion letter (EPA Region 9 and DOH 2016). There are a few additional sampling events with non-COPCs included for all wells in First Quarter 2017 and for some wells in Fourth Quarter 2017, First Quarter 2018, and Third Quarter 2018 (RHMW01, RHMW02, and RHMW03). RHMW10 and RHMW11 were not sampled before 2018 and therefore are not included in the discussion. RHMW10 and RHMW11 were evaluated for TICs, which are discussed in Section 5.

4.1 NON-COPC DETECTIONS

The total number of detections for compounds within each compound group are shown on Figure 4-1. The number of sampling events for non-COPCs for each well is shown at the top of the graph. The majority of hydrocarbon detections occurred in RHMW01 and RHMW02. Limited detections occurred in RHMW03 and Outlying Wells. A detailed discussion of non-COPCs in RHMW02 is included in CSM Appendix B.7 Section 4.2.

For a more consistent comparison between wells, detections from October 2014 to July 2018 are presented on Figure 4-2. Sampling of RHMW06 and RHMW07 began in October 2014, and more consistent sampling at RHMW04 occurred after this time. Plotting this shortened period results in a more comparable number of sampling events among the wells. The general trends remain the same, with hydrocarbon detections most frequent in RHMW01 and RHMW02.

Detections of phthalates, halogenated compounds, and oxygen-containing compounds occurred at most wells. These compounds are not related to fuels (see discussion of compound categories above); therefore, the focus of the rest of this section is on hydrocarbons that can be from fuel sources.

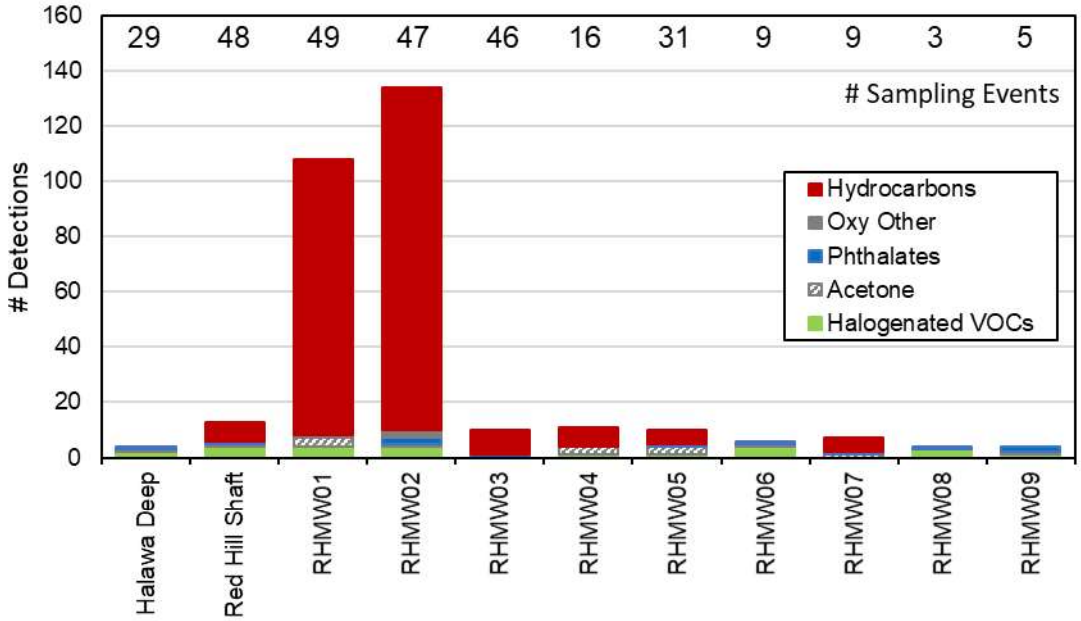

Figure 4-1: Non-COPC Detections from 2005 to July 2018

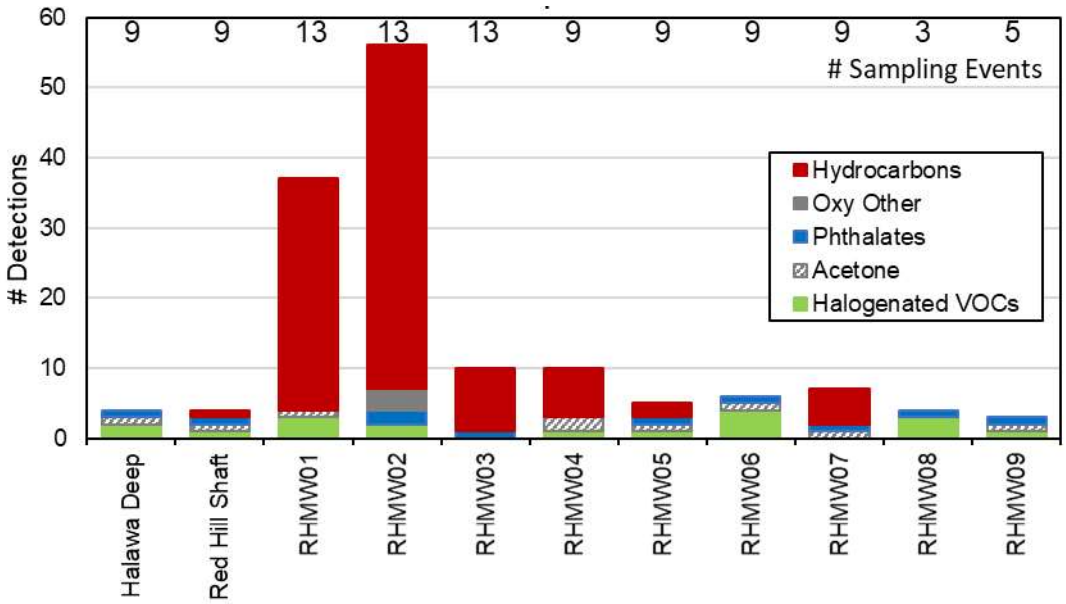

Figure 4-2: Non-COPC Detections from October 2014 to July 2018

<u>Key Point:</u> Phthalates, halogenated VOCs, and oxygen-containing non-COPCs detected in Outlying Wells are not related to fuel and therefore show no apparent evidence of impact to groundwater from fuel releases and/or site operations.

4.2 HYDROCARBON NON-COPC ANALYSIS

Detected hydrocarbon non-COPCs include volatile hydrocarbons (isopropylbenzene, n-butylbenzene, n-propylbenzene, sec-butylbenzene, tert-butylbenzene) and PAHs. The alkylated benzenes were

included in EPA Region 9 laboratory analysis in three sampling events (January, February, and March 2017) and were detected only in RHMW02. These alkylbenzenes are components of the fuels stored at the Facility.

PAHs were analyzed consistently by all laboratories until the analyte list was reduced from First Quarter 2016 onward per the AOC Statement of Work Sections 6 and 7 scoping completion letter (EPA Region 9 and DOH 2016). After this point, non-COPC PAHs (i.e., PAHs other than the naphthalenes) were occasionally analyzed for by the Navy laboratory APPL and the EPA Region 9 laboratory.

Hydrocarbon detections for all wells that were analyzed for non-COPCs are shown on Figure 4-3 and Figure 4-4. All data from 2005 to January 2019 are shown on Figure 4-3, while data from only October 2014 to January 2019 are presented on Figure 4-4 for comparison with more consistent number of sampling events among wells. The greatest number of PAH detections occurred in RHMW02 and RHMW01. No detections of non-COPC hydrocarbons occurred in HDMW2253-03, RHMW06, RHMW08, or RHMW09.

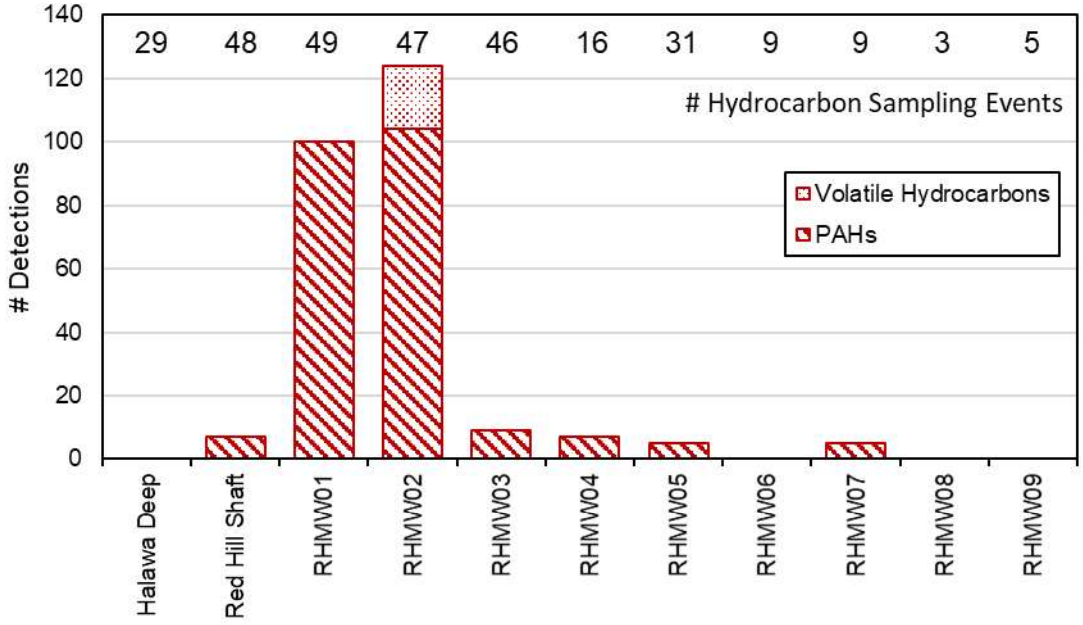

Figure 4-3: Hydrocarbon non-COPC Detections from 2005 to July 2018

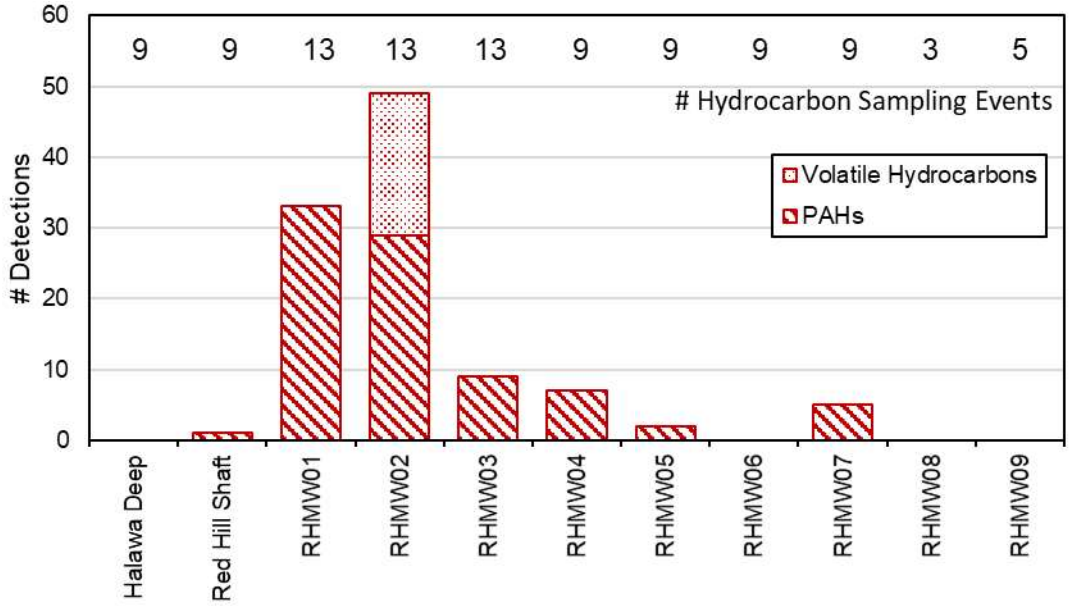

Figure 4-4: Hydrocarbon Non-COPC Detections from October 2014 to July 2018

PAH Non-COPC Analysis. Most sampling events from 2005 to 2016 include results for priority pollutant PAHs (Figure 4-5) in addition to the COPC PAHs (the naphthalenes). Therefore, PAHs are the most prevalent hydrocarbon class in the non-COPC data. As some PAHs may be associated with fuels, a more detailed evaluation of PAH detections was conducted. PAHs were divided into two categories: non-pyrogenic and pyrogenic. Non-pyrogenic PAHs, also called light PAHs or petrogenic PAHs, consist of two or three rings and are commonly found in petroleum. Two-ring PAHs include the naphthalenes, which are COPCs and have been discussed previously in Section 2.3. Pyrogenic PAHs, or heavy PAHs, consist of more than three rings and are associated with combusted materials, not fuels.

Jet and diesel fuels are distillation cuts from crude oil in which the most abundant PAHs are naphthalenes, typically < 3% by volume (Hadaller and Johnson 2006). PAHs with three rings are found in jet fuel in concentrations from non-detect to 0.05% by volume, and PAHs with four or more rings are at even lower concentrations (Figure 4-5). The distillation of crude oil cuts out heavy PAHs from fuels based on the temperature of the distillation end points for the specific fuel requirements. In general, PAHs heavier than fluorene should not be present in significant amounts in jet fuel, and PAHs heavier than phenanthrene should not be present in significant amounts in diesel fuel as their respective boiling points are above the end points of these fuels (API 2011). More details on the distribution of PAHs in a jet fuel is presented in CSM Appendix B.7 Section 4.1.2. PAHs have low solubility in water, particularly pyrogenic PAHs. This low solubility along with small or non-detectable concentrations in fuel should lead to very low concentrations (non-pyrogenic) or no detectable concentrations (pyrogenic) of PAHs in groundwater in contact with fuels. Since non-pyrogenic PAHs can be found in fuels, detections of non-COPC 3-ring (non-pyrogenic) PAHs are discussed further. Detections of heavier, pyrogenic PAHs are not discussed as these compounds are not related to fuels.

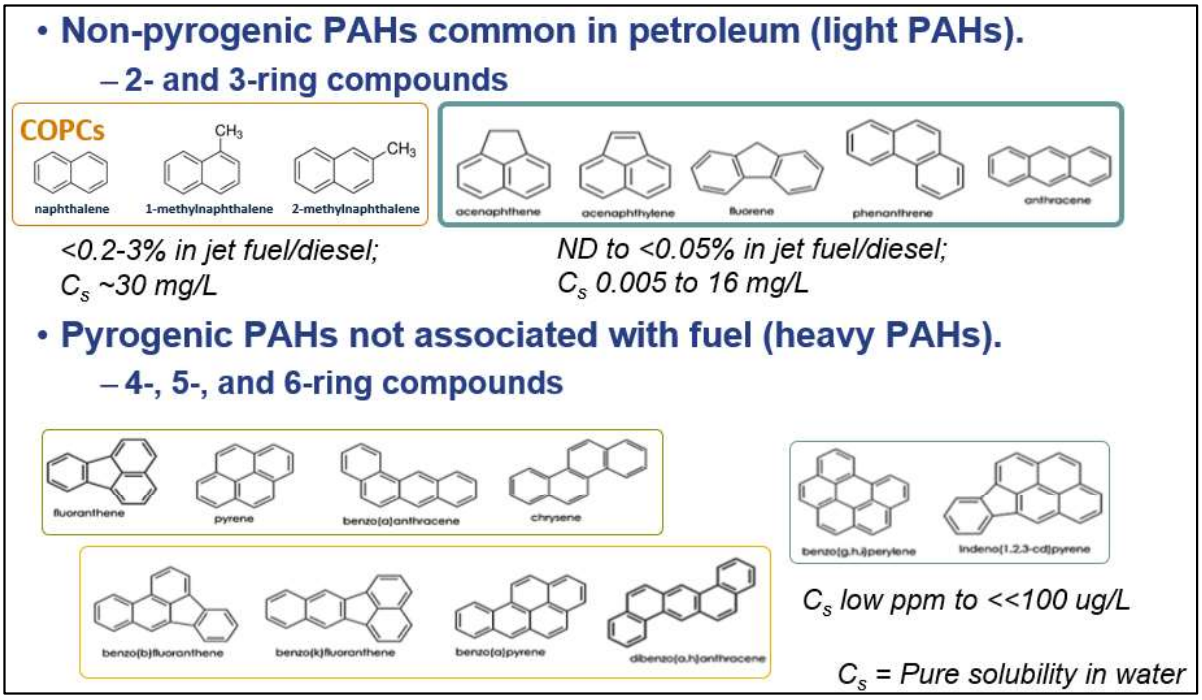

Figure 4-5: Priority Pollutant PAHs: Structure and Concentration Ranges in Fuels and Pure Compound Solubilities

The majority of non-pyrogenic PAHs occurred in RHMW02 and RHMW01 (Figure 4-6). Non-pyrogenic non-COPC PAH detections were infrequent in Outlying Wells, with detections occurring in only two samples each for RHMW05 and RHMW07 and one sample each for RHMW04 and Red Hill Shaft. The concentrations of non-pyrogenic non-COPC PAHs detected in Outlying Wells were low (0.0023–0.0182 J µg/L).

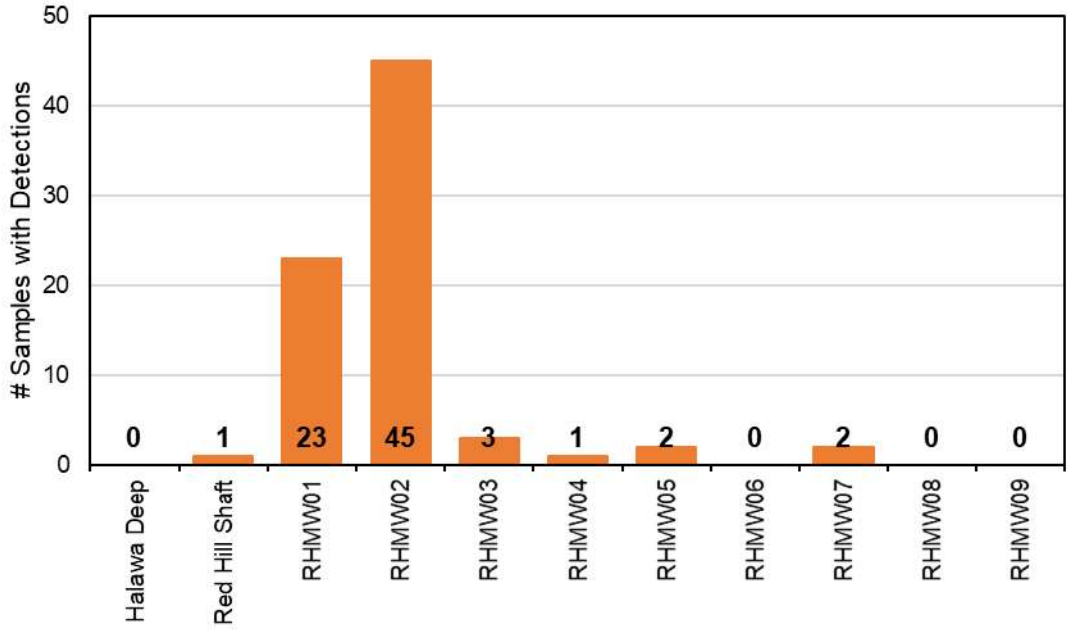

Figure 4-6: Samples with Detections of Non-COPC non-Pyrogenic PAHs from 2005 to July 2018

***Key Point*: The low-level and sporadic nature of non-pyrogenic PAH detections in Outlying Wells are not reliable as indicators of a nearby LNAPL source.**

4.3 NON-COPC SUMMARY

Non-pyrogenic non-COPC PAHs detections consistently occur at RHMW02, which aligns with the consistent COPC detections at this well (detection signature charts for non-COPCs grouped as classes are presented in Attachment B.8.1 Figures B.8.1-3 and B.8.1-4). Detections of five alkylated benzenes (volatile hydrocarbons) by the EPA Region 9 laboratory in three samples from this well also align with those results; alkylated benzenes are common components of the fuels stored at the Facility. Non-pyrogenic PAHs were fairly consistently detected in RHMW01, but detections were infrequent in RHMW03. This also matches with the COPC detection signatures in these wells (Section 2). Detections of phthalates, acetone, other oxygen-containing compounds, and halogenated VOCs did not coincide with non-pyrogenic PAH detections, as is consistent with these compounds not being related to fuel.

Inconsistent and sporadic detections of non-COPCs, including non-pyrogenic PAHs, occurred in Outlying Wells. The inconsistent detections support the conclusion that the detections are a result of field and/or laboratory contamination and limitations of detections down to MDLs (Section 1.4), and are not related to activities at the site.

A complete list of detected non-COPCs by well and the non-COPC analytical suite are included in Attachment B.8.2.

***Key Point*: Sporadic detections in PAHs in Outlying Wells are not associated with a fuel release from the Red Hill Facility and therefore there is no apparent evidence of impact to groundwater in Outlying Wells from fuel releases and/or site operations.**

5. Evaluation of TICs

TICs are peaks seen in the chromatogram of the analytical testing method but not a target compound for that method, thus are unknown. The TIC is identified by comparing the mass spectra of the unknown compound to a library of known compounds. This identification cannot distinguish between isomers and involves computer and analyst guesswork. Therefore, the identity of a TIC cannot be confirmed, or the concentration cannot be determined without comparison to a known standard. Because of the uncertainty of the identification of the TIC, the interpretation of these results is difficult (EPA 2006).

TIC data were collected starting in August of 2016, but analysis was inconsistent. Data ranged from 0 sampling events (RHMW11-02) to 11 sampling events (RHMW02).

As was done for non-COPCs (Section 4), TIC data are divided into compound groups for ease of comparison and plotting. Similar compound categories were used for some of the identified compounds: hydrocarbons, halogenated compounds, oxygen-containing compounds, and phthalates. However, the compound groups do not necessarily contain the same individual compounds. Also, additional compound groups were added including carboxylic acids and non-fuel-related olefins. As with most non-COPCs, the non-hydrocarbon TICs are not related to fuels. Some of the non-hydrocarbon compound classes reported as TICs are common anthropogenic compounds that are not present in jet fuel, but are found in groundwater near urban areas (Rupert et al. 2014) or are low-level laboratory contaminants. A list of TICs reported since August 2016 by well is included in Attachment B.8.2.

Hydrocarbon TICs that could be present in fuels were detected mainly in RHMW01 and RHMW02 (Figure 5-1), primarily alkylated benzenes, naphthalenes, and indenes. A detailed discussion of TICs in RHMW02 is included in CSM Appendix B.7 Section 4.2.

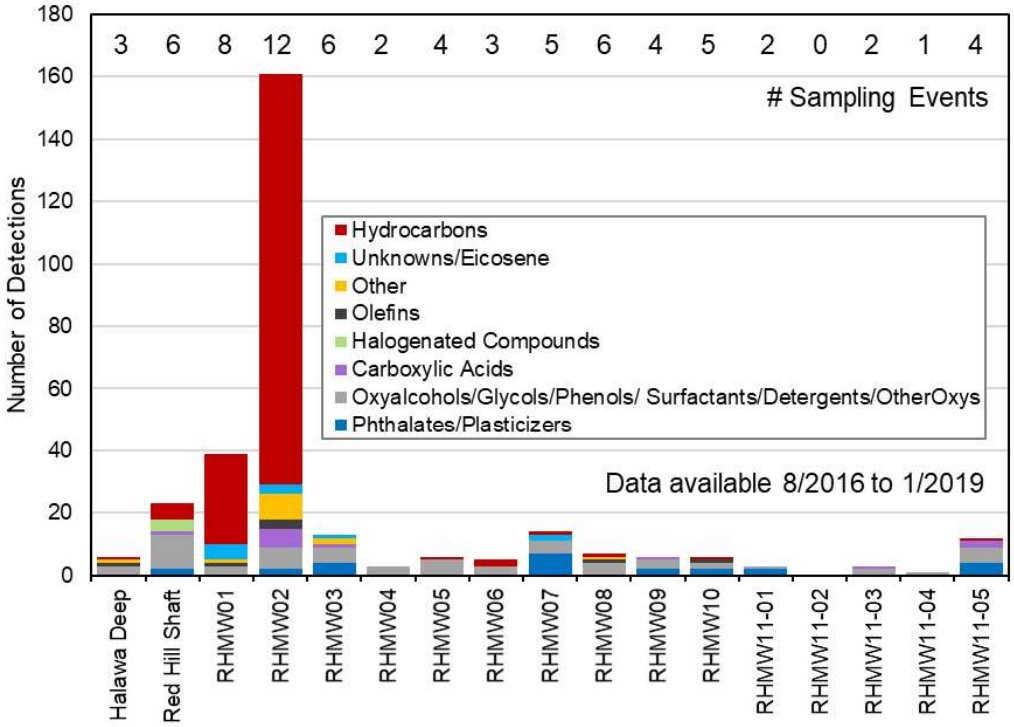

Figure 5-1: TIC Detections by Compound Class

The TIC detections in all Outlying Wells except for Red Hill Shaft consisted of only one or two detections of 1,2,4-trimetylbenzene and 1,3,5-trimethylbenzene (Figure 5-2). These two compounds were specifically analyzed as non-COPCs with EPA Method 8260 by Navy and/or EPA laboratories in multiple samples in 2017; however, they were not detected in in any of the wells analyzed, including RHMW01 and RHMW02. Therefore, the presence of these compounds is unconfirmed and likely inaccurate.

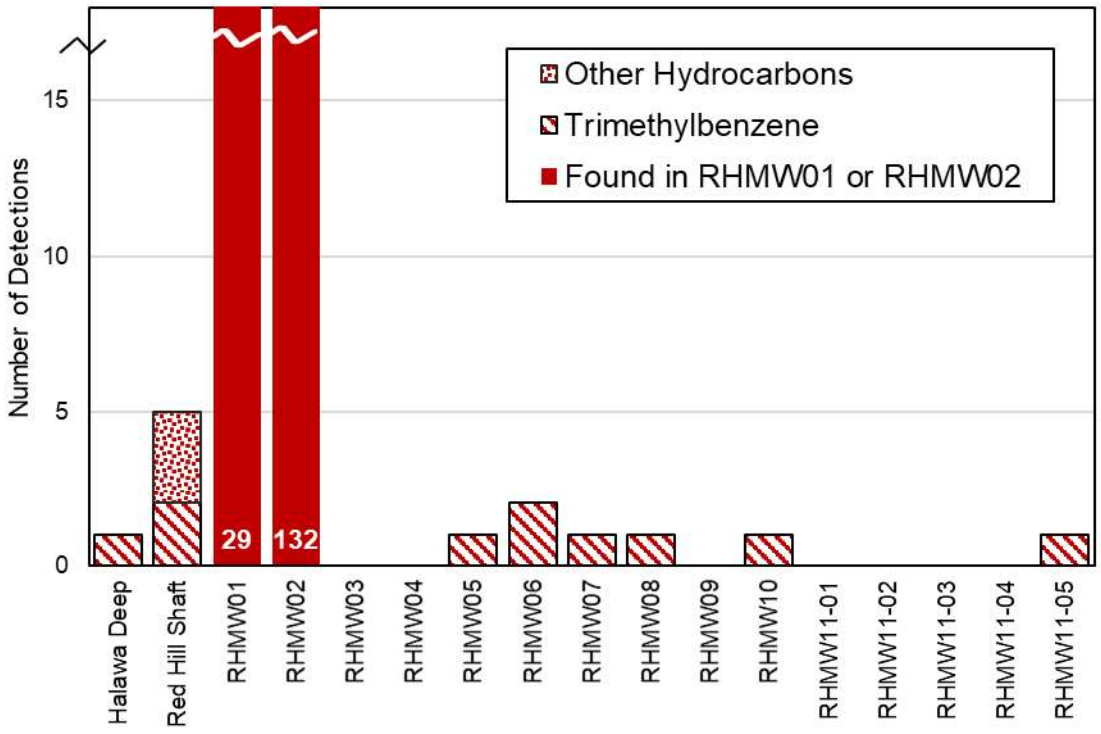

Figure 5-2: Hydrocarbon TIC Detections

Trimethylbenzenes can be misidentified for limonene, which is common in citrus fruit and is used in flavoring agents, fragrances, and cleaning products. If associated with fuel, these compounds would be expected to be detected along with other hydrocarbons. USGS has reported detections of 1,2,4-trimethylbenzene in O'ahu wells (Rupert et al. 2014).

Three other hydrocarbons were reported in Red Hill Shaft (two cycloalkanes in November 2018 and one olefin in December 2018). The TICs were not detected in the sample duplicates; therefore, those TICs are unconfirmed.

***Key Point 1:* Fuel-related hydrocarbons are specific to RHMW02 and RHMW01; other TIC compound classes (e.g., phthalates) are not associated with a fuel release.**

***Key Point 2:* TICs in Outlying Wells are inconsistent with RHMW01/RHMW02 and a fuel release; there is no apparent evidence to support impact to groundwater in Outlying Wells from fuel releases and/or site operations.**

TICs Summary. RHMW02 and RHMW01 had the greatest number of TIC detections, most of which were hydrocarbons. This is consistent with COPC detections and indicators of biodegradation in these wells. Most of the TICs detected in RHMW03 and Outlying Wells were not related to fuels or site activities. A closer look at the hydrocarbon TICs that were detected in Outlying Wells showed that none of those hydrocarbons were detected in RHMW01 or RHMW02. Further, the hydrocarbons that were detected in all Outlying Wells except Red Hill Shaft were trimethylbenzenes. Trimethylbenzenes were specifically analyzed for in 2017 and were not detected; therefore, those TIC detections are suspect.

6. Key Findings

Detection signature charts that incorporate all data discussed in this subappendix are presented for Near-Tank Wells and Outlying Wells in Attachment B.8.1 Figures B.8.1-5 and B.8.1-6. These signature charts combine all detections of organic compounds (COPCs, non-COPCs, and TICs) irrespective of concentration and level of certainty of the detections. These are discussed collectively in this section along with data from inorganic geochemistry parameters.

LOEs are summarized in Section 6.5.

6.1 Composition and Concentration of Dissolved Constituents in Near-Tank Wells

Monitoring well RHMW02 exhibits the highest total dissolved-phase fuel constituent concentrations among the Facility monitoring wells (approximately 1–7 mg/L since 2005). Much of these concentrations are in the form of polar compounds associated with the biodegradation of petroleum. At times, the concentrations of naphthalene, 1-MeN, and 2-MeN are equal to or greater than the expected concentration based on the effective solubilities of these compounds in jet fuel (see Appendix B.7 for discussion of effective solubilities). However, BTEX concentrations are very low (generally less than 1 µg/L). Detections of hydrocarbon TICs and low-level fuel-related non-COPCs (alkylated benzenes and non-pyrogenic PAHs) also occurred at RHMW02. Although COPC concentrations have varied over time, the observed concentration ranges are similar for the monitoring periods before and after the 2014 Tank 5 release. The geochemical results indicate high levels of biodegradation occurring in the vicinity of RHMW02, as key electron acceptors are depleted and high concentrations of dissolved methane are present (sometimes greater than 10 mg/L). Evaluated together, these data suggest the presence of weathered LNAPL (i.e., pre-2005 release) in the immediate vicinity of RHMW02 or within the saturated zone upgradient from this well. The groundwater monitoring data indicate it is likely that the 2014 Tank 5 release did not impact groundwater and more likely that impacts to groundwater are the result of historical leaks.

Monitoring well RHMW01 exhibits the next highest concentrations of dissolved-phase fuel constituents (not detected to approximately 0.1–1 mg/L since 2005); RHMW01 may have hydraulic connection to monitoring well RHMW02. Electron acceptors are depleted, and methane is present in the 0.2–7 mg/L range since 2005. Low-level detection of non-pyrogenic PAHs were somewhat consistent throughout the monitoring period. Hydrocarbon TICs were also detected in RHMW01, although not to the same extent as RHMW02. These data are consistent with the natural attenuation of dissolved constituents in groundwater and do not suggest the presence of LNAPL within the vicinity of RHMW01.

In monitoring well RHMW03, total dissolved-phase concentrations of fuel constituents are relatively low (less than 0.5 mg/L since 2005), with depressed dissolved oxygen concentrations and limited depletion of groundwater electron acceptors nitrate and sulfate, and no measurable methane production. Only one non-pyrogenic PAH (phenanthrene) was detected, and only during three sampling quarters at RHMW03 at very low (0.0057 J – 0.0074 J µg/L) concentrations. There were no detections of hydrocarbon TICs at this well. The groundwater data in this area suggest the presence of local low-concentration dissolved fuel constituents, potentially attributable to infiltration/leaching processes, and do not indicate the presence of LNAPL in the saturated zone in the vicinity of RHMW03.

6.2 COMPOSITION AND CONCENTRATION OF DISSOLVED CONSTITUENTS IN OUTLYING WELLS

A review of the historical data for Red Hill Shaft does not indicate that the well was impacted by the 2014 release and any impacts to groundwater are likely attributable to historical leaks. Very few COPCs were detected, and most detections were estimates below quantitation limits. Further, detections of TEX and naphthalenes did not correlate well with TPH detections (Figure 2-15). Analysis of the geochemical data shows Red Hill Shaft to be grouped with RHMW04, RHMW09, RHMW10, and other O'ahu wells, which indicates the groundwater quality is consistent with background from an inorganic geochemistry perspective. Fuel-related non-pyrogenic PAHs were detected during only one sampling event in 2005; non-COPC data do not support impact to Red Hill Shaft. Five hydrocarbon TIC detections have occurred at Red Hill Shaft; however, two of these detections were trimethylbenzene, which was not detected in 2017 when trimethylbenzenes were target analytes. The remaining hydrocarbon detections were compounds that were not detected in RHMW01 or RHMW02, indicating the Red Hill Shaft detections were not related to the fuel-associated detections in the Near-Tank Wells. Analysis of dissolved constituents at Red Hill Shaft does not support impact to this well.

HDMW2253-03 water chemistry differs from other monitor wells that collect groundwater from near the water table. This well is cased approximately 40 ft below the water table and has an open borehole from 250 to 1,575 ft bgs. HDMW2253-03 was not constructed as a typical water table monitoring well, but rather to monitor the saltwater/freshwater interface. Some historical lab analyses of samples from this deep monitor well have shown sporadic detections of TPH-d and naphthalene, along with infrequent detections of benzene and toluene (non-concurrently), and single detections of TPH-g and 2-methylnaphthalene. The majority (five of six) of naphthalene detections occurred while Calscience/Eurofins was doing the analysis; as previously discussed, these detections are suspect. The majority of TPH-d detections also occurred while Calscience/Eurofins was doing the analysis, and in that time the concentrations ranged over an order of magnitude. This inconsistency, even within the same laboratory, highlights the difficulties when assessing impacts with respect to TPH trends.

Some historical analyses of water samples from Well RHMW04 show inconsistent and noncoincident detections of COPCs (Figure 2-15). For example, for the three samples in which TPH was detected, no other COPC was co-detected. Furthermore, the highest TPH-d was reported immediately after well construction. The other two detections were at/near the LOD with no evidence of fuel impact after review of the two chromatograms. Naphthalenes were detected in RHMW04 by only one laboratory (CAS/ALS), and at low levels (0.0043 J – 0.18 µg/L). Non-pyrogenic PAHs were detected in one sample; however, no other COPCs were detected at that time. No hydrocarbon TICs were detected in RHMW04, and results of PCA analysis of inorganic geochemical parameters suggest that RHMW04 is representative of background conditions. Analysis of dissolved constituents at RHMW04 does not support impact to this well.

Some historical analyses of water samples from Well RHMW05 show inconsistent detections of fuel hydrocarbons at low concentrations (typically less than 0.05 mg/L). Naphthalenes were detected at this well; however, the majority of detections occurred during the suspect period when Calscience/Eurofins was conducting the analysis. The geochemical data do not support biodegradation. Two samples (First Quarter 2010 and Second Quarter 2015) had low-level detections of the non-pyrogenic PAH phenanthrene. There was one TIC detection of 1,2,4-trimethylbenzene; however, the EPA analyzed for 1,2,4- and 1,3,5-trimethylbenzene in three samples during 2017 and did not detect either compound, bringing the TIC detection into question. These data do not suggest the presence of LNAPL within the saturated zone between RHMW01 and RHMW05.

Well RHMW07 is screened in a less-permeable zone slightly above the water table aquifer, and the natural groundwater chemistry at this location may be affected by deeply penetrating saprolite, as well as being somewhat hydraulically isolated from the other wells on site, and therefore is not representative of water table chemistry. Historical detections of naphthalenes, TPH-d, and non-pyrogenic PAHs occurred almost entirely during the period when CAS/ALS was doing the analysis (Figure 2-15). As previously discussed, very low-level detections (CAS/ALS used a detection limit of 0.005 µg/L for PAHs) are questionable, as at these levels sampling or laboratory issues are more likely to impact results.

The infrequent and noncoincident COPC detections at RHMW06, RHMW08, and RHMW10 do not indicate impact to these wells. No COPCs have been detected at RHMW09 or RHMW11 (at all sampled monitoring zones).

6.3 2014 TANK 5 RELEASE

Elevated levels of some dissolved constituents detected at RHMW02 provide evidence of LNAPL in groundwater upgradient of RHMW02 released prior to 2005. The lower concentrations of COPCs at RHMW01 and RHMW03 compared to RHMW02 are not indicative of LNAPL in the vicinity of these two wells. The steady BTEX trends (Figure 2-1 to Figure 2-4) and unchanging naphthalenes weathering ratio (Figure 2-5) at RHMW02 before and after the 2014 fuel release do not support impact at RHMW02 from the 2014 fuel release. Similarly, there are no observable changes in COPC or non-COPC detections in site wells after the 2014 fuel release (Attachment B.8.1 Figure B.8.1-5).

A comprehensive evaluation of the entire monitoring data set does not indicate that the 2014 JP-8 release from Tank 5 impacted groundwater. The observed impacts to groundwater in some of the Near-Tank Wells are likely attributable to historical leaks.

6.4 IMPACTS TO OUTLYING WELLS

A wide variety of constituents was reported infrequently in Outlying Wells, including petroleum hydrocarbons, PAHs, phthalates, and halogenated compounds. Most of these compounds are not associated with fuels. The detections of COPCs and fuel-related non-COPCs are sporadic and at very low concentrations. There is also a similar detection pattern observed across a diverse set of wells (e.g., Red Hill Shaft, RHMW05, HDMW2253-03). Consistent detections of TPH were seen in almost all wells during the monitoring events following well construction. Most (RHMW06 and RHMW10), and in some cases all (RHMW07 and RHMW08) TPH-d and TPH-o detections occurred within 1 year of well construction, indicating the TPH detections may be associated with drilling and well installation.

Detection signatures at Outlying Wells are not consistent with fuel releases. There are inconsistent and noncoinciding detections of COPCs and fuel-related non-COPCs and TICs in Outlying Wells (Attachment B.8.1 Figure B.8.1-6). As mentioned in Section 1.5, the presence of LNAPL should result in continuing impact to wells.

A comprehensive evaluation of the entire monitoring data set does not indicate impacts to Outlying Wells associated with a nearby LNAPL source.

6.5 SUMMARY OF LINES OF EVIDENCE

Table 6-1: Summary of Lines of Evidence

1. NO EVIDENCE OF LNAPL NEAR OUTLYING WELLS	
Primary LOE	**Secondary LOEs**
1a. Naphthalene (by itself) is not a good indicator for the presence of LNAPL	i. The very low detection limits for naphthalenes (e.g., 0.005 µg/L by CAS/ALS) are susceptible to interferences/artifacts and are inherently more variable ii. There are sporadic detections of naphthalene at Outlying Wells. Incidence of detections correlates best with laboratories used rather than where detections occurred and at what concentrations. • Naphthalene detections during Fourth Quarter 2012 to First Quarter 2015 (Calscience/Eurofins) are suspect. – Frequent detections of naphthalene from Fourth Quarter 2012 to Third Quarter 2014, then all detections stopped from Cal/Euro. ▪ No coinciding detections of methylnaphthalenes – The laboratory that followed after Calscience (i.e., CAS/ALS) did not detect naphthalene at a similar frequencies or concentrations, even though the reporting limit was an order of magnitude lower. – Approximately 60% of naphthalene detections in Outlying Wells occurred during the suspect period of Cal/Euro analysis. The remaining detections are highly sporadic. – All naphthalenes were analyzed by EPA Method 8270 SIM at a time when only two ions were used to identify compounds. Three ions are required to have achieve robust identification.
1b. Electron acceptors are not depleted at Outlying Wells	i. Oxic conditions are present at Outlying Wells: • DO concentrations ranged from 5.09 to 9.31 mg/L (Fourth Quarter 2018) at Outlying Wells that are representative of water table chemistry. – RHMW07, RHMW11, and HDMW2253-03 are not representative of water table chemistry. – The range of DO in Red Hill Outlying Wells is generally consistent with observed DO in O'ahu wells. • Nitrate concentrations range from 2 to 5.5 mg/L (Fourth Quarter 2018) at Outlying Wells that are representative of water table chemistry, demonstrating that nitrate is not depleted. • Sulfate concentrations range from 6.9 to 51.3 mg/L (Fourth Quarter 2018) at Outlying Wells that are representative of water table chemistry, demonstrating that sulfate is not depleted. • Reducing conditions (ORP < 0 mV) are not present in Outlying Wells (Fourth Quarter 2018). • Apart from one sampling event at RHMW08, the ORP has been positive since Fourth Quarter 2016 at Outlying Wells representative of the water table.
1c. Metabolic by-products are not present at Outlying Wells	i. Methane has not been detected in Outlying Wells representative of water table chemistry since Fourth Quarter 2016 (no methane data prior to this quarter). ii. Ferrous iron was not detected in RHMW04, RHMW05, RHMW08, RHMW09, RHMW10, and was detected below the limit of quantitation at RHMW06 (0.16 J mg/L) (Fourth Quarter 2018). • Since Fourth Quarter 2016, ferrous iron has either been nondetect or below the limit of quantitation in Outlying Wells representative of water table chemistry.

1. NO EVIDENCE OF LNAPL NEAR OUTLYING WELLS

Primary LOE	Secondary LOEs
1d. There are not consistent coinciding detections of COPCs and non-COPCs (e.g., BTEX, methylnaphthalene, nonpyrogenic PAHs) with naphthalene	i. BTEX were not detected in RHMW06, RHMW07, RHMW08, RHMW09, RHMW10, or all levels of RHMW11. ii. BTEX were detected infrequently (1 to 5 times) at the remaining Outlying Wells over the monitoring period, which is more indicative of field/laboratory artifacts. • Concentrations were often below the limit of quantitation and ranged from 0.07 J to 3.8 µg/L. iii. Non-COPC detections in Outlying Wells consisted mainly of compounds that are not associated with fuel: phthalates, halogenated VOCs, acetone, oxygenated compounds, and pyrogenic PAHs. iv. Non-COPCs that can be present in fuels, such as non-pyrogenic PAHs, were detected infrequently in Outlying Wells; detections occurred in two samples each in RHMW05 and RHMW07, and one sample in RHMW04, indicating field/laboratory artifact issues. • Non-pyrogenic PAHs were not detected in RHMW06, RHMW08, or RHMW09.
1e. TPH should be assessed in the context of other COPCs and non-COPCs, as trend analyses are difficult because of inconsistent methodology and laboratories	i. TPH is a parameter defined by the method used. ii. TPH results can include hydrocarbons, metabolites/polar compounds and anything present that can be detected by the method. iii. TPH can be used as an indicator parameter for potential impact to groundwater, but the absolute values should be interpreted with caution. Changes can be method- and/or laboratory-related. • TPH detection is not a direct indication of hydrocarbons in groundwater.
1f. TICs are not a good indicator of the presence of LNAPL in Outlying Wells	i. TIC identification and concentrations cannot be confirmed without comparison to a known standard. ii. Majority of TIC detections are not associated with fuels: phthalates, halogenated compounds, oxygen-containing compounds. • These compounds are likely associated with field/laboratory contamination, well construction/maintenance, and/or historical or current activities at the site unrelated to fuel releases. iii. The only TIC hydrocarbon detections in Outlying Wells are trimethylbenzenes. • Trimethylbenzene are expected to be found with other hydrocarbons if coming from a fuel/LNAPL; trimethylbenzene was the only TIC detected in Outlying Well samples. • Trimethylbenzene was analyzed with Method 8260 in all Outlying Wells in 2017 and was not detected.
1g. Lead scavengers (1,2-dibromoethane and 1,2-dichloroethane) were not detected in Outlying Wells except for 1,2-dichloroethane in RHMW08 in 2017	i. 1,2-dichloroethane was used in motor gasoline (not aviation gasoline). Motor gasoline was stored in Tank 17 prior to 1968. It is likely the detections of 1,2-dichloroethane in RHMW08 are from either fumigants or PVC impurity rather than motor gasoline. ii. To adequately evaluate lead in the environment, careful consideration should be given to the local range of background concentrations as well as filtering of water samples, since lead is a naturally occurring element.
1A. No evidence of impact to Outlying Wells from 2014 fuel release (Red Hill discussed separately in LOE 2)	
1h. Continued sporadic detections of BTEX with no apparent increase in detection frequency after the 2014 fuel release	
1i. Continued sporadic detections of naphthalene with no apparent increase in detection frequency after 2014 fuel release	i. Apparent decrease in naphthalene detection frequency in Outlying Wells after the Fourth Quarter 2012 to Third Quarter 2014 period when Calscience/Eurofins stopped detecting naphthalene.

1

2. NO EVIDENCE OF LNAPL NEAR RED HILL SHAFT

Primary LOE	Secondary LOEs
2a. Naphthalene (by itself) is not a good indicator of the presence of LNAPL near Red Hill Shaft	i. There are sporadic detections of naphthalene at Red Hill Shaft. • Naphthalene detections during Fourth Quarter 2012 to First Quarter 2015 (Calscience/Eurofins) are suspect. – Frequent detections of naphthalene from Fourth Quarter 2012 to Third Quarter 2014, then all detections stopped from Cal/Euro, indicating field/laboratory artifacts. ▪ No coinciding detections of methylnaphthalenes. – The laboratory that followed Calscience (i.e., CAS/ALS) did not detect naphthalene at similar frequencies or concentrations even though the reporting limit was an order of magnitude lower. – The concentrations of naphthalene detected during Fourth Quarter 2012 to Third Quarter 2014 were similar to the concentrations detected in other Outlying Wells (e.g., HDMW2253-03, RHMW05). Similar concentrations would not be expected at these three wells with very different constructions: ▪ Red Hill Shaft – Induced flow ▪ HDMW2253-03 – Deep borehole with casing ~40 ft below the water table ▪ RHMW05 – Screened across the water table – All naphthalenes were analyzed by EPA Method 8270 SIM at a time when only two ions were used to identify compounds. Three ions are required to have achieve robust identification (DoD and DOE 2017). ii. The very low detection limits for naphthalenes (e.g., 0.005 µg/L by CAS/ALS) are susceptible to interferences/artifacts and are inherently more variable. iii. Naphthalene detections often do not coincide with 1- and 2-methylnaphthalene or TPH detections, as would be expected if the detections were due to a nearby LNAPL source.
2b. Electron acceptors are not depleted at Red Hill Shaft	i. Oxic conditions are present at Red Hill Shaft (DO = 8.7 mg/L during Fourth Quarter 2018 sampling event). ii. Nitrate was 2.3 mg/L during Fourth Quarter 2018 sampling event and is not depleted. iii. Sulfate was 15.6 mg/L during Fourth Quarter sampling event and is not depleted. iv. Reducing conditions (ORP < 0 mV) were not present.
2c. Metabolic byproducts (methane and ferrous iron) were not detected in Red Hill Shaft (Fourth Quarter 2018)	i. Methane has been non-detect in Red Hill Shaft since Fourth Quarter 2016 (no methane data prior to this quarter). ii. Ferrous iron has been most commonly non-detect in Red Hill Shaft since Fourth Quarter 2016, detected concentrations have ranged from 0.17 J to 0.34 mg/L.
2d. There are not consistent coinciding detections of COPCs and non-COPCs (e.g., BTEX, methylnaphthalene, nonpyrogenic PAHs) with naphthalene	i. BTEX have been detected in two samples (Fourth Quarter 2012 and Fourth Quarter 2018) and were not confirmed during the subsequent sampling events. ii. Non-COPC detections in Red Hill Shaft consisted mainly of compounds that are not associated with fuel: phthalates, halogenated VOCs, acetone, oxygenated compounds, and pyrogenic PAHs. iii. Non-COPCs related to fuel, non-pyrogenic PAHs, were detected in only one sample from Red Hill Shaft in Fourth Quarter 2005.
2e. TPH should be assessed in the context of other COPCs and non-COPCs as trend analysis is difficult because of inconsistent methodology and laboratories	i. TPH detections often did not coincide with detections of other COPCs. ii. TPH is a parameter defined by the method used. iii. TPH results can include hydrocarbons, metabolites/polar compounds, and anything present that can be detected by the method. iv. TPH can be used as an indicator parameter or potential impact to groundwater, but the absolute values should be interpreted with caution. Changes can be method- and/or laboratory-related. v. TPH detection is not a direct indication of hydrocarbons in groundwater.

2. NO EVIDENCE OF LNAPL NEAR RED HILL SHAFT

Primary LOE	Secondary LOEs
2f. TICs are not a good indicator of the presence of LNAPL in Outlying Wells	i. TIC identification and concentrations cannot be confirmed without comparison to a known standard. ii. The majority of TIC detections are not associated with fuel: phthalates, halogenated compounds, oxygen-containing compounds. • These compounds may be associated with field/laboratory contamination, well construction/maintenance, and/or historical or current activities at the site unrelated to fuel releases. iii. TIC hydrocarbon detections in Red Hill Shaft are of trimethylbenzene and two other hydrocarbons (1,2,3,4,5-pentamethyl-cyclopentane, and 3,5,5-trimethyl-2-hexene). • Trimethylbenzene would be expected to be found with other hydrocarbons if coming from a fuel/LNAPL; trimethylbenzene was the only TIC detected in Outlying Well samples. • Trimethylbenzene was analyzed for with Method 8260 in Red Hill Shaft in 2017 and was not detected. • The other TIC hydrocarbons were not detected in RHMW02 or RHMW01; detections are unlikely to be related to RHMW02.
2g. Lead scavengers (1,2-dibromoethane and 1,2-dichloroethane) have not been detected in Red Hill Shaft	

3. NO EVIDENCE OF GROUNDWATER IMPACT FROM 2014 FUEL RELEASE

Primary LOE	Secondary LOEs
3a. BTEX detection occurrences did not change in RHMW02 after the 2014 fuel release	
3b. The ratio of methylnaphthalenes to naphthalene in RHMW02 did not change after the 2014 fuel release	i. A fresh source of LNAPL in RHMW02 vicinity would change the ratio as fresh fuel has a different signature than degraded fuel. • In general, the parent PAH (COPC naphthalene) is less abundant than the sum of the corresponding alkylated PAHs (in this case, COPCs 1-methylnaphthalene and 2-methylnaphthalene, which are the two possible isomers of naphthalene with a methyl group substitution) from any petroleum sources.
3c. TPH alone not good indicator of changes in water chemistry at RHMW02 after 2014 release	i. TPH should be assessed in the context of other COPCs and non-COPCs, as trend analysis is difficult because of inconsistent methodology and laboratories. • EPA Method 8015 is a guidance method and is not prescriptive, which results in significant variation in analysis between laboratories. • Changes in analytical laboratory often coincide with sharp changes in detected TPH concentrations in RHMW02.
3d. Measured TPH concentrations in RHMW02 are not a good indicator of the presence of LNAPL	i. Results can include hydrocarbons, metabolites/polar compounds, and anything present detectable by the method. ii. Concentrations/presence of TPH metabolites/polar compounds can be determined by using SGC. iii. Polar compounds are more soluble than parent nonpolar compounds/hydrocarbons; therefore, the presence of polar compounds/metabolites can result in increased solubility of what is measured as TPH. iv. Polar compounds/metabolites in RHMW02 are more soluble than parent hydrocarbons; what is measured as TPH is not indicative of the presence of LNAPL from a fresh release, but is indicative of an older nearby source.
3e. COPC detection signature did not change in RHMW02 after the 2014 fuel release	i. The increased number of sampling events immediately following the 2014 fuel release results in an apparent increase in COPC detections. This is a result of more frequent sampling, not of an increase in TPH contamination in the groundwater.

7. References

American Petroleum Institute (API). 2011. *A Guide to Understanding, Assessment, and Regulation of PAHs in the Aquatic Environment*. Publication 4776.

Department of Defense and Department of Energy, United States (DoD and DOE). 2017. *Department of Defense (DoD) and Department of Energy (DOE) Consolidated Quality Systems Manual (QSM) for Environmental Laboratories*. DoD QSM Ver. 5.1; DOE Quality Systems for Analytical Services Ver. 3.1. Prepared by DoD Environmental Data Quality Workgroup and DOE Consolidated Audit Program Operations Team.

Department of Defense, Environmental Data Quality Workgroup (DoD EDQW). 2017. *Fact Sheet: Detection and Quantification – What Project Managers and Data Users Need to Know*. October. https://www.denix.osd.mil/edqw/documents/documents/revised-detection-and-quantitation-fact-sheet-october-2017/.

Department of Health, State of Hawaii (DOH). 2017. *Evaluation of Environmental Hazards at Sites with Contaminated Soil and Groundwater, Hawai'i Edition*. Hazard Evaluation and Emergency Response. Revised 2017. Fall.

Department of the Navy (DON). 2005. *Red Hill Bulk Fuel Storage Facility Work Plan, Pearl Harbor, Hawaii*. Prepared by The Environmental Company, Inc. (TEC), Honolulu, HI; and AMEC Earth & Environmental, Inc., Honolulu, HI. Pearl Harbor, HI: Naval Facilities Engineering Command, Pacific. June.

———. 2014. *Interim Update, Red Hill Bulk Fuel Storage Facility Final Groundwater Protection Plan, Pearl Harbor, Hawaii. (January 2008)*. Pearl Harbor, HI: Naval Facilities Engineering Command, Pacific. August.

———. 2017a. *Final First Quarter 2017 - Quarterly Groundwater Monitoring Report, Red Hill Bulk Fuel Storage Facility, Joint Base Pearl Harbor-Hickam, O'ahu, Hawai'i*. Prepared by AECOM Technical Services, Inc. JBPHH HI: Naval Facilities Engineering Command, Hawaii. April.

———. 2017b. *Sampling and Analysis Plan, Investigation and Remediation of Releases and Groundwater Protection and Evaluation, Red Hill Bulk Fuel Storage Facility, Joint Base Pearl Harbor-Hickam, O'ahu, Hawai'i; April 20, 2017, Revision 01*. Prepared by AECOM Technical Services, Inc., Honolulu, HI. Prepared for Defense Logistics Agency Energy, Fort Belvoir, VA, under Naval Facilities Engineering Command, Hawaii, JBPHH HI.

———. 2019. *Final First Quarter 2019 - Quarterly Groundwater Monitoring Report, Red Hill Bulk Fuel Storage Facility, Joint Base Pearl Harbor-Hickam, O'ahu, Hawai'i*. Prepared by AECOM Technical Services, Inc. JBPHH HI: Naval Facilities Engineering Command, Hawaii. May.

———. Letter from R. D. Hayes III to Bob Pallarino (EPA Region 9) and Steven Y. K. Chang (DOH). 2017c. "Navy's Response to Split Sampling Results from First Quarter 2017, Administrative Order on Consent Statement of Work Section 6 and Section 7, Red Hill Bulk Fuel Storage Facility (Red Hill), Joint Base Pearl Harbor-Hickam, Oahu, Hawaii," October 11, 2017.

Environmental Protection Agency, United States (EPA). 2006. *Tentatively Identified Compounds: What Are They and Why Are They Important?* TIC Frequently Asked Questions. Rev. No. 2.5. Region III Quality Assurance Team. February 17.

———. 2017. *Clean Water Act Analytical Methods: Method Detection Limit – Frequent Questions*. December 1. https://www.epa.gov/cwa-methods/method-detection-limit-frequent-questions.

Environmental Protection Agency, United States, Region 9; and Department of Health, State of Hawaii (EPA Region 9 and DOH). 2016. "Final Scoping for AOC SOW Sections 6 and 7, and Navy's Proposed Chemical of Potential Concern (COPC) Recommendations," February 4, 2016. Letter from Bob Pallarino, EPA Red Hill Project Coordinator, and Steven Chang, DOH Red Hill Project Coordinator, to: James A. K. Miyamoto, Naval Facilities Engineering Command, Hawaii, Joint Base Pearl Harbor-Hickam.

———. Letter from Bob Pallarino (EPA Region 9 Project Coordinator) and Steven Chang (DOH Project Coordinator) to: Mark Manfredi, Red Hill Project Coordinator, Naval Facilities Hawaii. 2017. "Split Sampling Results from First Quarter 2017," September 12, 2017.

Hadaller, O. J., and J. M. Johnson. 2006. *World Fuel Sampling Program*. CRC Report No. 647. Alpharetta, GA: Coordinating Research Council, Inc. June.

Helsel, D. R. 2012. *Statistics for Censored Environmental Data Using Minitab and R*. 2nd ed. Wiley Series in Statistics in Practice. Hoboken, N.J: Wiley.

Hunt, Jr., C. D. 2004. *Ground-Water Quality and Its Relation to Land Use on Oahu, Hawaii, 2000–01*. Water-Resources Investigations Report 03-4305. National Water-Quality Assessment Program. U.S. Geological Survey.

Interstate Technology & Regulatory Council (ITRC). 2018. *TPH Risk Evaluation at Petroleum-Contaminated Sites*. TPHRisk-1. Washington, DC: ITRC, TPH Risk Evaluation Team. https://tphrisk-1.itrcweb.org.

Mohler, R. E., K. T. O'Reilly, D. A. Zemo, A. K. Tiwary, R. I. Magaw, and K. A. Synowiec. 2013. "Nontargeted Analysis of Petroleum Metabolites in Groundwater Using GC×GC–TOFMS." *Environ. Sci. & Technol.* 47 (18): 10471–476. https://doi.org/10.1021/es401706m.

Rupert, M. G., C. D. Hunt, Jr., K. D. Skinner, L. M. Frans, and B. J. Mahler. 2014. *The Quality of Our Nation's Waters—Groundwater Quality in the Columbia Plateau and Snake River Plain Basin-Fill and Basaltic-Rock Aquifers and the Hawaiian Volcanic-Rock Aquifers, Washington, Idaho, and Hawaii, 1993–2005*. U.S. Geological Survey Circular 1359.

University of Hawai'i. 2017. "RedHill_NAWQA_geochem2Navy." Email communication from Dr. Nicole Lautze (Associate Specialist Faculty, Hawaii Institute of Geophysics and Planetology, Water Resources Research Center) to Ms. Tracy Saguibo (NAVFAC Hawaii). November 13.

Whittier, R. B. 2018. "Re: RHSF Monitoring Well Observations," June 26, 2018. Email communication from Bob Whittier/Hawai'i Department of Health to John Kronen/AECOM, cc: various AOC Parties.

Zemo, D. A., K. T. O'Reilly, R. E. Mohler, R. I. Magaw, C. E. Devine, S. Ahn, and A. K. Tiwary. 2017. "Life Cycle of Petroleum Biodegradation Metabolite Plumes, and Implications for Risk Management at Fuel Release Sites." *Integrated Environmental Assessment and Management* 13 (4): 714–727. https://doi.org/10.1002/ieam.1848.

Zemo, D. A., K. T. O'Reilly, R. E. Mohler, A. K. Tiwary, R. I. Magaw, and K. A. Synowiec. 2013. "Nature and Estimated Human Toxicity of Polar Metabolite Mixtures in Groundwater Quantified as TPHd/DRO at Biodegrading Fuel Release Sites." *Groundwater Monitoring & Remediation* 33 (4): 44–56. https://doi.org/10.1111/gwmr.12030.

Attachment B.8.1:
Additional Figures

Figure B.8.1-1: TPH-o in Near-Tank Wells

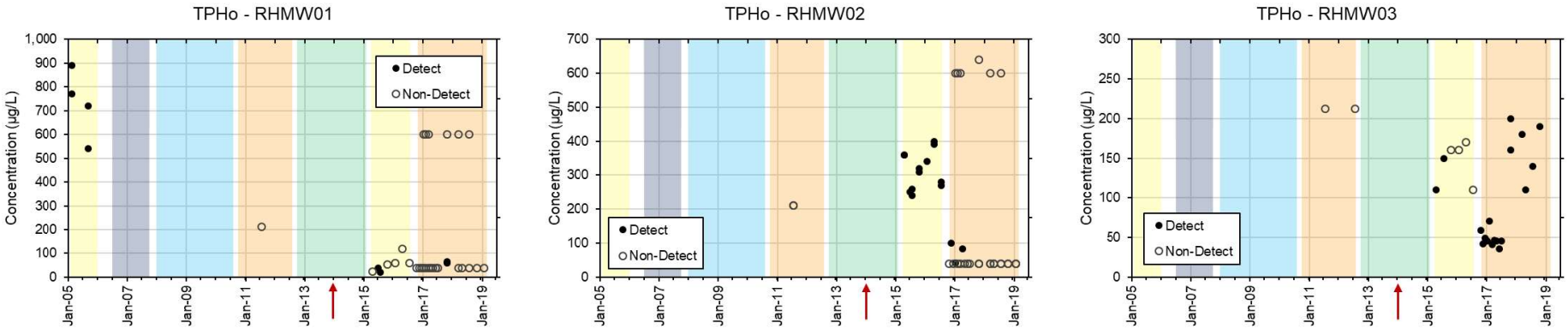

Notes: The red arrow indicates the Tank 5 fuel release date. The colored backgrounds highlight periods for different analytical laboratories: yellow = CAS and CAS/ALS, grey = Accutest, blue = SGS Alaska, orange = APPL, and green = Calscience/Eurofins.

Figure B.8.1-2: TPH-o in Outlying Wells

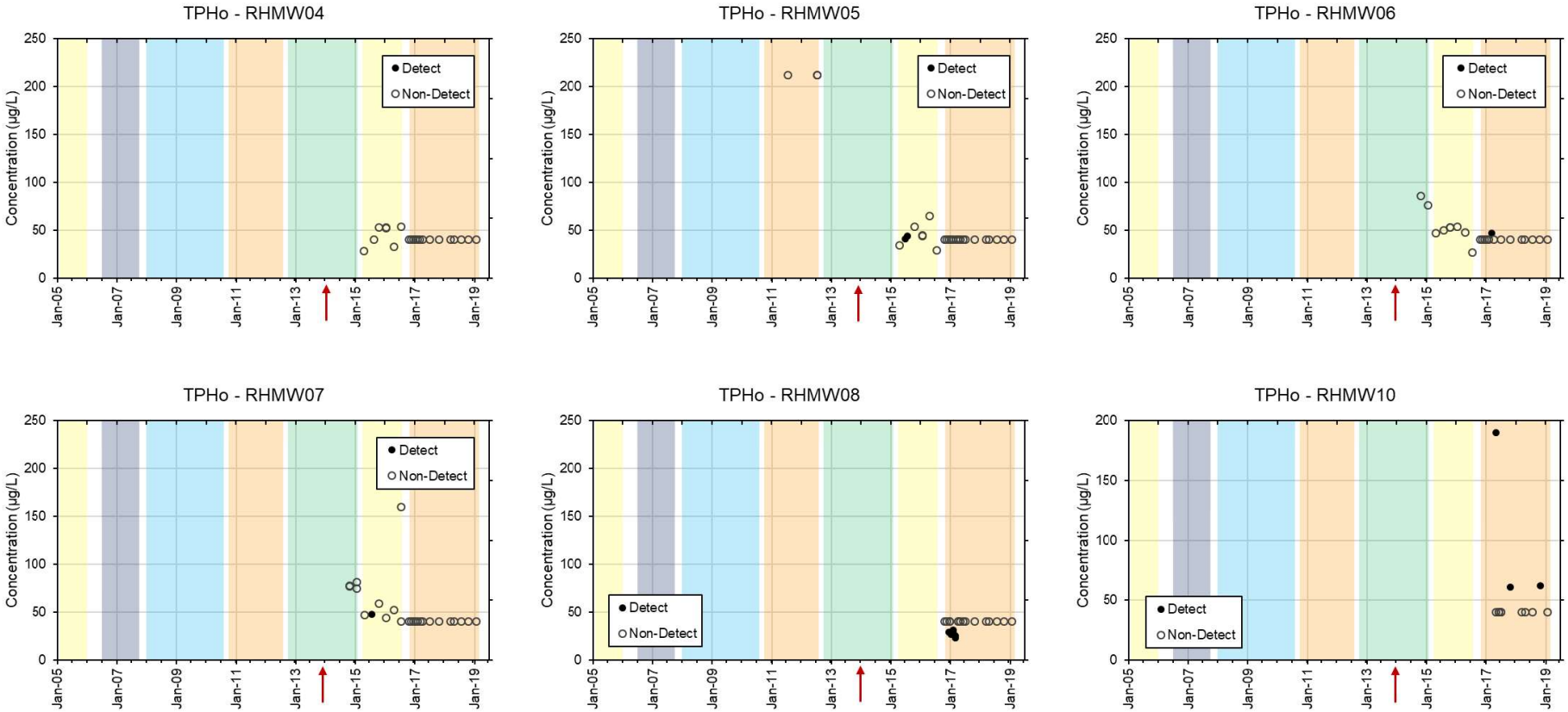

Notes: The red arrow indicates the Tank 5 fuel release date. The colored backgrounds highlight periods for different analytical laboratories: yellow = CAS and CAS/ALS, grey = Accutest, blue = SGS Alaska, orange = APPL, and green = Calscience/Eurofins.

Figure B.8.1-2: TPH-o in Outlying Wells (cont.)

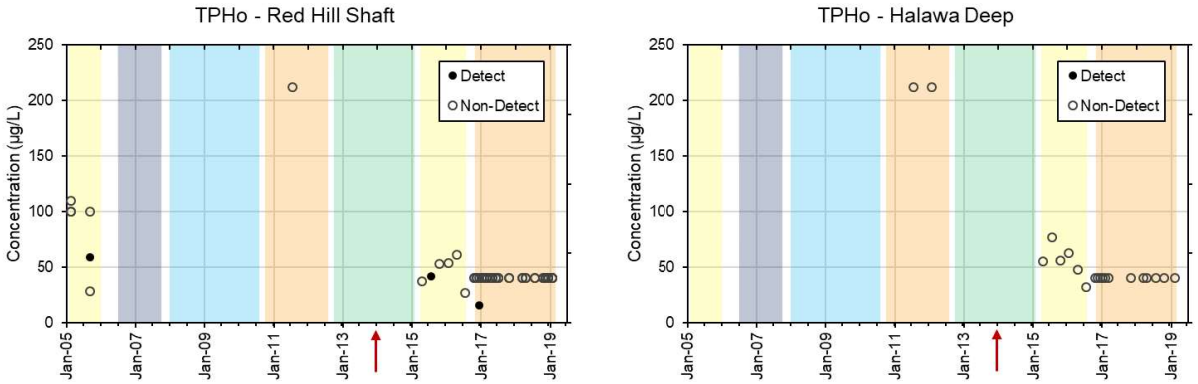

Notes: The red arrow indicates the Tank 5 fuel release date. The colored backgrounds highlight periods for different analytical laboratories: yellow = CAS and CAS/ALS, grey = Accutest, blue = SGS Alaska, orange = APPL, and green = Calscience/Eurofins.

Figure B.8.1-3: Non-COPC Detection Signature Charts for Near-Tank Wells

RHMW02

	CAS				Accutest				SGS-Alaska								APPL				Calscience/Eurofins				CAS/ALS				APPL/EPA							
	2005				2006				2007				2008				2009				2010				2011				2012				2013			
	Q1	Q2	Q3	Q4	Q1	Q2	Q3	Q4	Q1	Q2	Q3	Q4	Q1	Q2	Q3	Q4	Q1	Q2	Q3	Q4	Q1	Q2	Q3	Q4	Q1	Q2	Q3	Q4	Q1	Q2	Q3	Q4	Q1	Q2	Q3	Q4
Phthalates																																				
Acetone		0				0	0		0	0	0			0	0	0	1	0	0	0	0	0			0	0	0	0	0	0	0	0	0	0	0	0
Oxy Other		0				0	0		0	0	0		0	0	0	0	0	0	0	0	0	0	0	0	0	0	0	0	0	0	0	0	0	0	0	0
Halogenated		1				1	0		0	0	0		0	0	0	0	0	0	0	0	0	0	0	0	0	0	0	0	0	0	0	0	0	1	1	0
Pyro PAHs		2				0	0		0	0	0		0	0	0	0	0	0	3	0	1	0	0	0	0	0	0	0	0	0	0	0	0	1	0	0
nonPyro PAHs		0				2	2		2	2	2		2	2	2	2	0	1	3	2	2	2	2	3	3	3	3	2	3	2	1	2	2	2	2	2

	2014				2015				2016				2017				2018				'19
	Q1	Q2	Q3	Q4	Q1	Q2	Q3	Q4	Q1	Q2	Q3	Q4	Q1	Q2	Q3	Q4	Q1	Q2	Q3	Q4	Q1
Phthalates													1								
Acetone	0	0	0	0	0	0	0	0	0				0				0				
Oxy Other	0	0	0	0	0	0	0	0	0				1				0				
Halogenated	0	0	0	0	1	1	0	0					0				0				
Pyro PAHs	0	0	0	0	1	0	0	1					3				0	0	0		
nonPyro PAHs	2	0	0	1	2	3	2	3	2				3		2	1	2				

RHMW01

	CAS				Accutest				SGS-Alaska								APPL				Calscience/Eurofins				CAS/ALS				APPL/EPA							
	2005				2006				2007				2008				2009				2010				2011				2012				2013			
	Q1	Q2	Q3	Q4	Q1	Q2	Q3	Q4	Q1	Q2	Q3	Q4	Q1	Q2	Q3	Q4	Q1	Q2	Q3	Q4	Q1	Q2	Q3	Q4	Q1	Q2	Q3	Q4	Q1	Q2	Q3	Q4	Q1	Q2	Q3	Q4
Phthalates																																				
Acetone		0				0	0		0	0	0			0	0	0	0	0	0	0	1	0			0	0	0	0	0	0	0	0	0	0	0	0	0
Oxy Other		0				0	0		0	0	0		0	0	0	0	0	0	0	1	0	0	0	0	0	0	0	0	0	0	0	0	0	0	0	0
Halogenated		0				0	0		0	0	0		0	0	0	0	0	0	0	0	0	0	0	0	0	0	0	1	0	0	0	0	0	0	0	0
Pyro PAHs	5	9	4	9		0	0		0	0	0		0	0	0	0	0	0	3	0	0	0	0	0	0	0	0	0	0	0	0	1	0	0	0	0
nonPyro PAHs	3	3	3	4		0	0		0	0	0		2	2	1	1	1	2	3	2	3	2	2	0	0	0	0	0	0	0	0	0	0	0	0	0

	2014				2015				2016				2017				2018				'19
	Q1	Q2	Q3	Q4	Q1	Q2	Q3	Q4	Q1	Q2	Q3	Q4	Q1	Q2	Q3	Q4	Q1	Q2	Q3	Q4	Q1
Phthalates													0								
Acetone	1	0	0	0	0	0	0	0	0				1				0				
Oxy Other	0	0	0	0	0	0	0	0	0				0				0				
Halogenated	0	0	0	0	0	0	0	0					1				2				
Pyro PAHs	0	0	0	1	0	1	0	8					0				0	8	0		
nonPyro PAHs	2	0	0	0	4	3	2	4					1				1	1	0		

RHMW03

	CAS				Accutest				SGS-Alaska								APPL				Calscience/Eurofins				CAS/ALS				APPL/EPA							
	2005				2006				2007				2008				2009				2010				2011				2012				2013			
	Q1	Q2	Q3	Q4	Q1	Q2	Q3	Q4	Q1	Q2	Q3	Q4	Q1	Q2	Q3	Q4	Q1	Q2	Q3	Q4	Q1	Q2	Q3	Q4	Q1	Q2	Q3	Q4	Q1	Q2	Q3	Q4	Q1	Q2	Q3	Q4
Phthalates																																				
Acetone		0				0	0		0	0	0			0	0	0	0	0	0	0	0	0			0	0	0	0	0	0	0	0	0	0	0	0	0
Oxy Other		0				0	0		0	0	0		0	0	0	0	0	0	0	0	0	0	0	0	0	0	0	0	0	0	0	0	0	0	0	0
Halogenated		0				0	0		0	0	0		0	0	0	0	0	0	0	0	0	0	0	0	0	0	0	0	0	0	0	0	0	0	0	0
Pyro PAHs		0				0	0		0	0	0		0	0	0	0	0	0	0	0	0	0	0	0	0	0	0	0	0	0	0	0	0	0	0	0
nonPyro PAHs		0				0	0		0	0	0		0	0	0	0	0	0	0	0	0	0	0	0	0	0	0	0	0	0	0	0	0	0	0	0

	2014				2015				2016				2017				2018				'19
	Q1	Q2	Q3	Q4	Q1	Q2	Q3	Q4	Q1	Q2	Q3	Q4	Q1	Q2	Q3	Q4	Q1	Q2	Q3	Q4	Q1
Phthalates													1								
Acetone	0	0	0	0	0	0	0	0	0				0				0				
Oxy Other	0	0	0	0	0	0	0	0	0				0				0				
Halogenated	0	0	0	0	0	0	0	0					0				0				
Pyro PAHs	0	0	0	0	0	1	0	5					0				0	0	0		
nonPyro PAHs	0	0	0	0	1	1	0	1					0				0	0	0		

Notes: The red line indicates the Tank 5 fuel release date. The time periods for analytical laboratories are indicated at the top of each chart. The number of detections of a compound in a given quarter including duplicates are listed in the chart, quarters with no sample analyzed are blank. Oxy Other = oxygenated compounds apart from acetone, Pyro PAHs = pyrogenic PAHs, nonPyro PAHs = non-pyrogenic PAHs.
Quarters with detections are highlighted in color, and each compound group is identified with a different color. The darker the color, the more detections that occurred in a given quarter.

Figure B.8.1-4: Non-COPC Detection Signature Charts for Outlying Wells

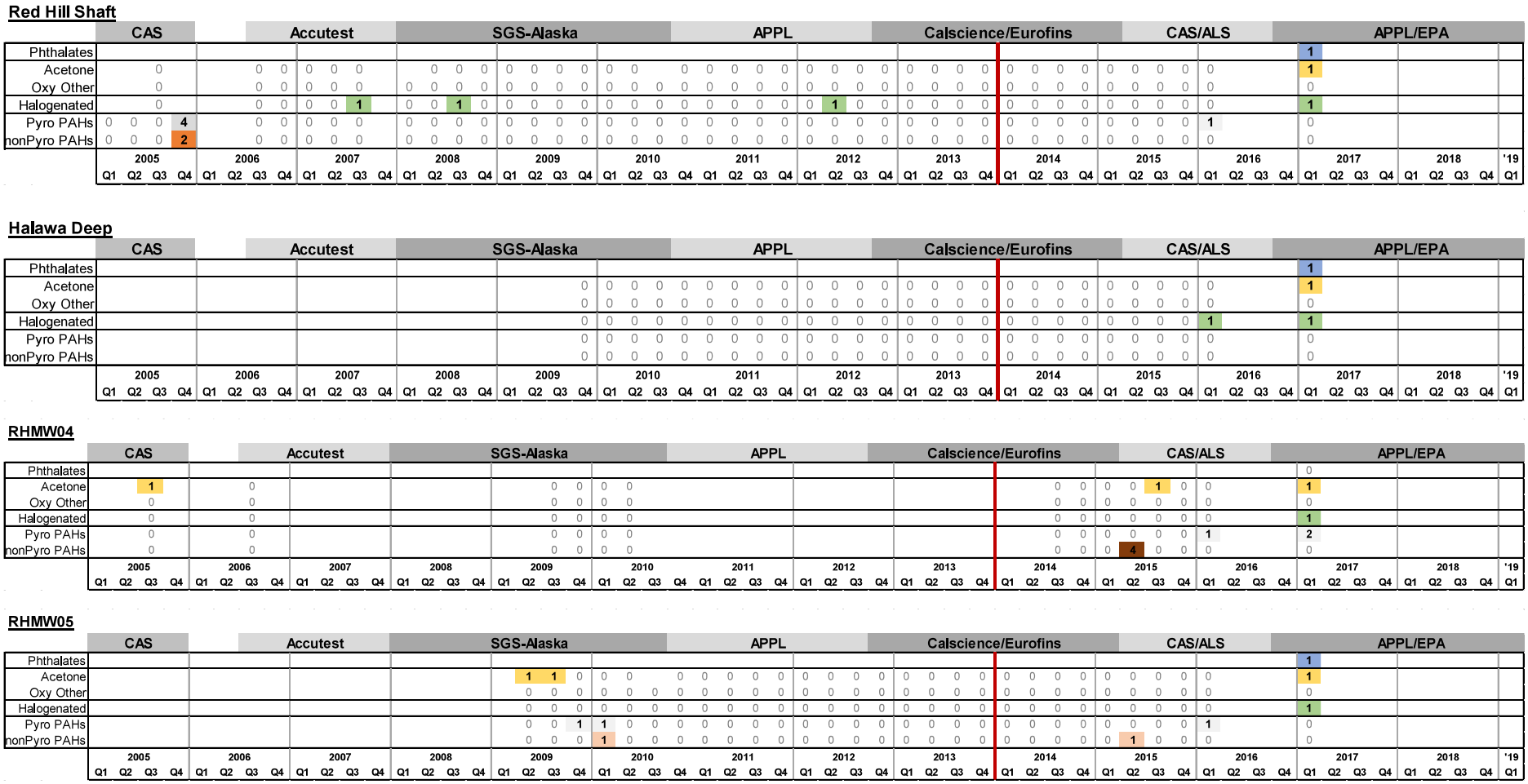

Notes: The red line indicates the Tank 5 fuel release date. The time periods for analytical laboratories are indicated at the top of each chart. The number of detections of a compound in a given quarter including duplicates are listed in the chart, quarters with no sample analyzed are blank. Oxy Other = oxygenated compounds apart from acetone, Pyro PAHs = pyrogenic PAHs, nonPyro PAHs = non-pyrogenic PAHs.
Quarters with detections are highlighted in color, and each compound group is identified with a different color. The darker the color, the more detections that occurred in a given quarter.

Figure B.8.1-4: Non-COPC Detection Signature Charts for Outlying Wells (cont.)

RHMW06

	CAS				Accutest				SGS-Alaska				APPL				Calscience/Eurofins				CAS/ALS				APPL/EPA			
	2005				2006				2007				2008				2009				2010				2011			
	Q1	Q2	Q3	Q4	Q1	Q2	Q3	Q4	Q1	Q2	Q3	Q4	Q1	Q2	Q3	Q4	Q1	Q2	Q3	Q4	Q1	Q2	Q3	Q4	Q1	Q2	Q3	Q4
Phthalates																												
Acetone																												
Oxy Other																												
Halogenated																												
Pyro PAHs																												
nonPyro PAHs																												

	2012				2013				2014				2015				2016				2017				2018				'19
	Q1	Q2	Q3	Q4	Q1	Q2	Q3	Q4	Q1	Q2	Q3	Q4	Q1	Q2	Q3	Q4	Q1	Q2	Q3	Q4	Q1	Q2	Q3	Q4	Q1	Q2	Q3	Q4	Q1
Phthalates																					1								
Acetone									0	0	0	0	0	0	0	0	0				1								
Oxy Other									0	0	0	0	0	0	0	0	0				0								
Halogenated									0	0	0	0	0	0	0	0	0				2								
Pyro PAHs									0	0	0	0	0	0	0	0	0				0								
nonPyro PAHs									0	0	0	0	0	0	0	0	0				0								

RHMW07

	CAS				Accutest				SGS-Alaska				APPL				Calscience/Eurofins				CAS/ALS				APPL/EPA			
	2005				2006				2007				2008				2009				2010				2011			
	Q1	Q2	Q3	Q4	Q1	Q2	Q3	Q4	Q1	Q2	Q3	Q4	Q1	Q2	Q3	Q4	Q1	Q2	Q3	Q4	Q1	Q2	Q3	Q4	Q1	Q2	Q3	Q4
Phthalates																												
Acetone																												
Oxy Other																												
Halogenated																												
Pyro PAHs																												
nonPyro PAHs																												

	2012				2013				2014				2015				2016				2017				2018				'19
	Q1	Q2	Q3	Q4	Q1	Q2	Q3	Q4	Q1	Q2	Q3	Q4	Q1	Q2	Q3	Q4	Q1	Q2	Q3	Q4	Q1	Q2	Q3	Q4	Q1	Q2	Q3	Q4	Q1
Phthalates																					1								
Acetone									1	0	0	0	0	0							0								
Oxy Other									0	0	0	0	0	0							0								
Halogenated									0	0	0	0	0	0							0								
Pyro PAHs									0	0	0	0	1								0								
nonPyro PAHs									0	0	2	2	0	0							0								

RHMW08

	CAS				Accutest				SGS-Alaska				APPL				Calscience/Eurofins				CAS/ALS				APPL/EPA			
	2005				2006				2007				2008				2009				2010				2011			
	Q1	Q2	Q3	Q4	Q1	Q2	Q3	Q4	Q1	Q2	Q3	Q4	Q1	Q2	Q3	Q4	Q1	Q2	Q3	Q4	Q1	Q2	Q3	Q4	Q1	Q2	Q3	Q4
Phthalates																												
Acetone																												
Oxy Other																												
Halogenated																												
Pyro PAHs																												
nonPyro PAHs																												

	2012				2013				2014				2015				2016				2017				2018				'19
	Q1	Q2	Q3	Q4	Q1	Q2	Q3	Q4	Q1	Q2	Q3	Q4	Q1	Q2	Q3	Q4	Q1	Q2	Q3	Q4	Q1	Q2	Q3	Q4	Q1	Q2	Q3	Q4	Q1
Phthalates																					1								
Acetone																					0								
Oxy Other																					0								
Halogenated																					2								
Pyro PAHs																					0								
nonPyro PAHs																					0								

RHMW09

	CAS				Accutest				SGS-Alaska				APPL				Calscience/Eurofins				CAS/ALS				APPL/EPA			
	2005				2006				2007				2008				2009				2010				2011			
	Q1	Q2	Q3	Q4	Q1	Q2	Q3	Q4	Q1	Q2	Q3	Q4	Q1	Q2	Q3	Q4	Q1	Q2	Q3	Q4	Q1	Q2	Q3	Q4	Q1	Q2	Q3	Q4
Phthalates																												
Acetone																												
Oxy Other																												
Halogenated																												
Pyro PAHs																												
nonPyro PAHs																												

	2012				2013				2014				2015				2016				2017				2018				'19
	Q1	Q2	Q3	Q4	Q1	Q2	Q3	Q4	Q1	Q2	Q3	Q4	Q1	Q2	Q3	Q4	Q1	Q2	Q3	Q4	Q1	Q2	Q3	Q4	Q1	Q2	Q3	Q4	Q1
Phthalates																					1	0							
Acetone																					0	1							
Oxy Other																					0	0							
Halogenated																					1	0							
Pyro PAHs																					0	0							
nonPyro PAHs																					0	0							

Notes: The red line indicates the Tank 5 fuel release date. The time periods for analytical laboratories are indicated at the top of each chart. The number of detections of a compound in a given quarter including duplicates are listed in the chart, quarters with no sample analyzed are blank. Oxy Other = oxygenated compounds apart from acetone, Pyro PAHs = pyrogenic PAHs, nonPyro PAHs = non-pyrogenic PAHs.
Quarters with detections are highlighted in color, and each compound group is identified with a different color. The darker the color, the more detections that occurred in a given quarter.

Figure B.8.1-5: Summary Detection Signature Charts for Near-Tank Wells

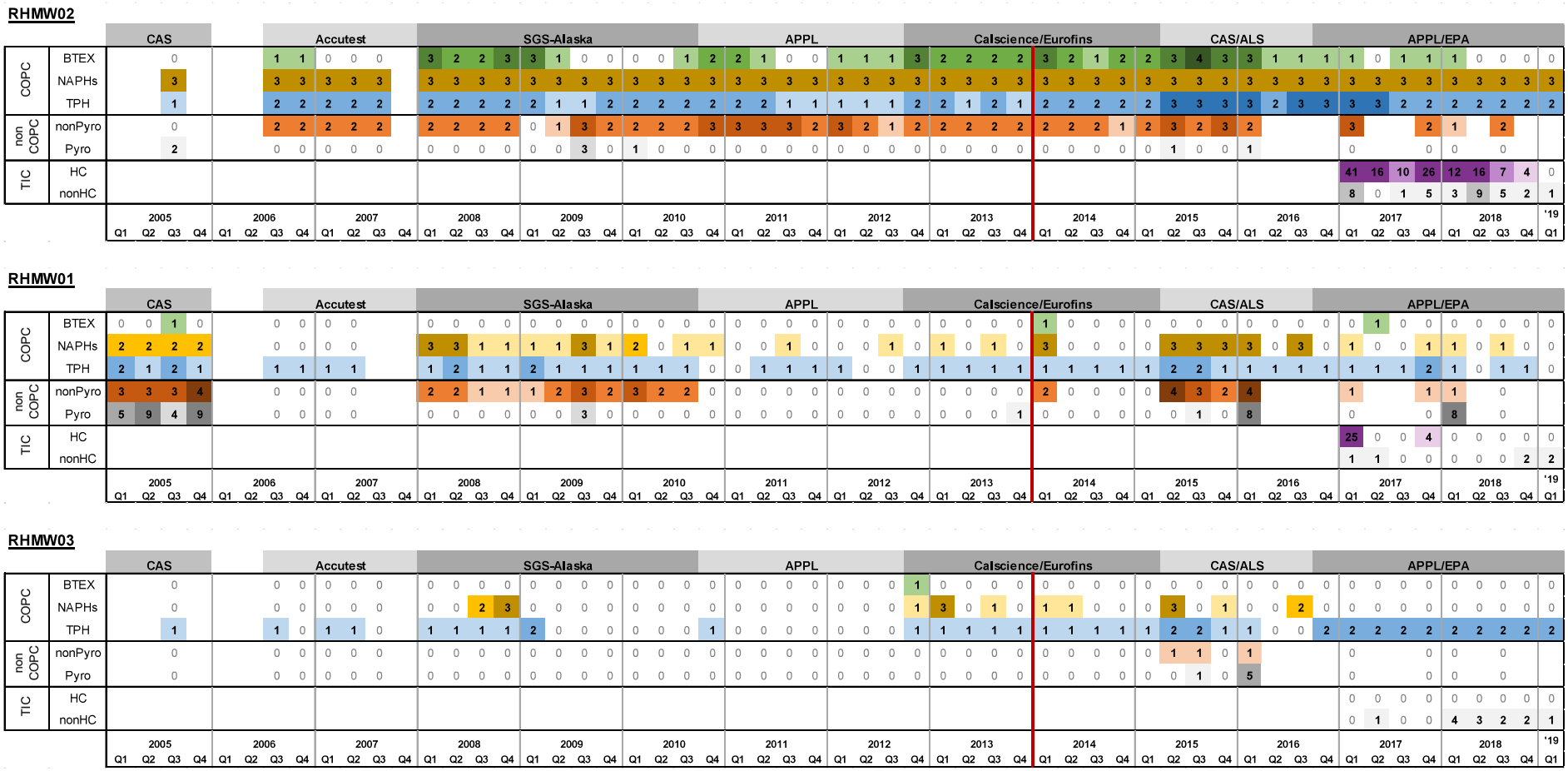

Notes: The red line indicates the Tank 5 fuel release date. The time periods for analytical laboratories are indicated at the top of each chart. The number of unique compounds detected within a given quarter is listed in the chart, quarters with no sample analyzed are blank. NAPHs = naphthalene, 1-methylnaphthalene, and 2-methylnaphthalene; TPH = TPH-g, TPH-d, and TPH-o, nonPyro = non-pyrogenic PAHs, Pyro = pyrogenic PAHs, HC = hydrocarbon.
Quarters with detections are highlighted in color, and each compound group is identified with a different color. The darker the color, the more detections that occurred in a given quarter.

Figure B.8.1-6: Summary Detection Signature Charts for Outlying Wells

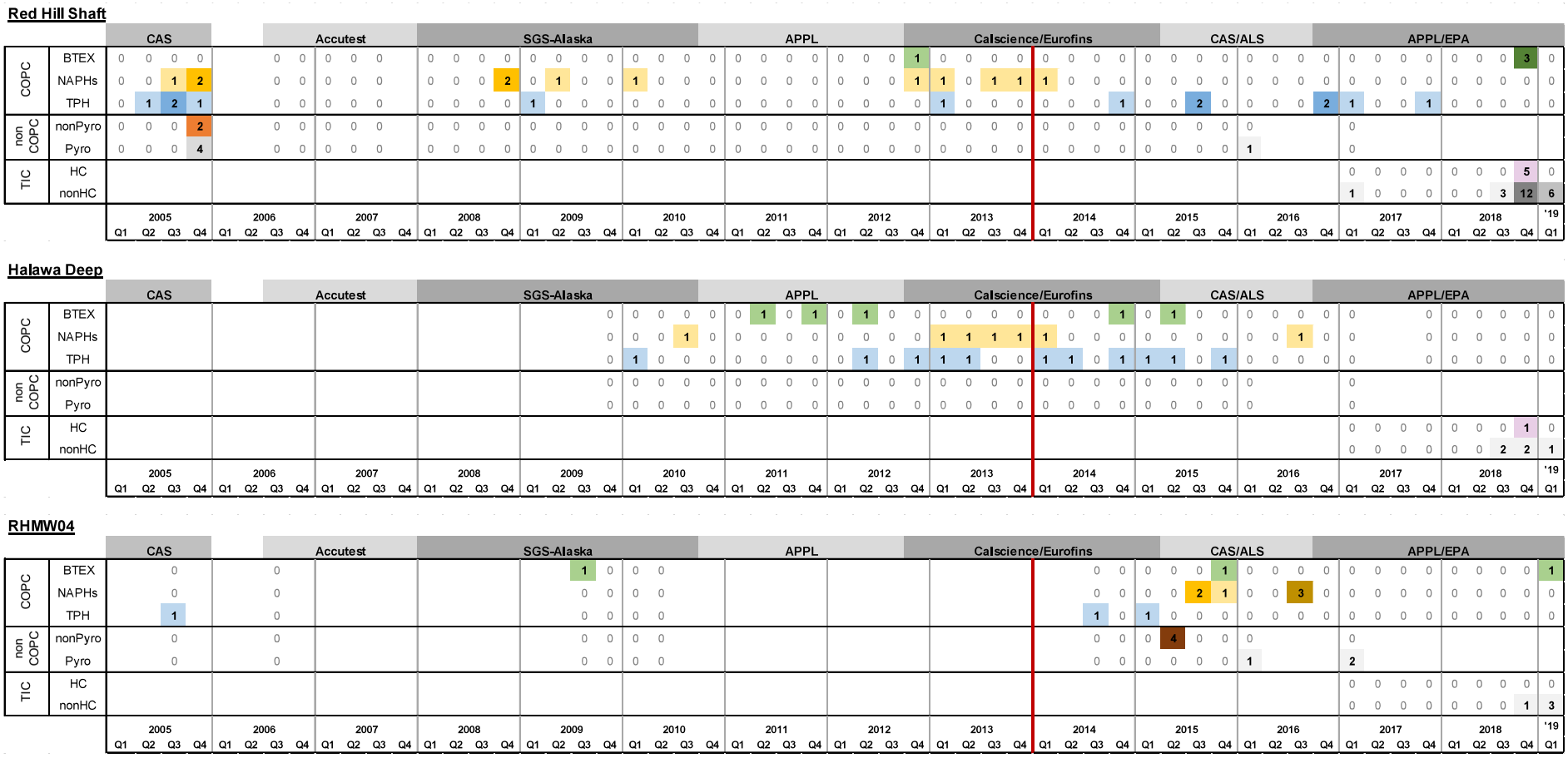

Notes: The red line indicates the Tank 5 fuel release date. The time periods for analytical laboratories are indicated at the top of each chart. The number of unique compounds detected within a given quarter is listed in the chart, quarters with no sample analyzed are blank. NAPHs = naphthalene, 1-methylnaphthalene, and 2-methylnaphthalene; TPH = TPH-g, TPH-d, and TPH-o, nonPyro = non-pyrogenic PAHs, Pyro = pyrogenic PAHs, HC = hydrocarbon.
Quarters with detections are highlighted in color, and each compound group is identified with a different color. The darker the color, the more detections that occurred in a given quarter.

Figure B.8.1-6: Summary Detection Signature Charts for Outlying Wells (cont.)

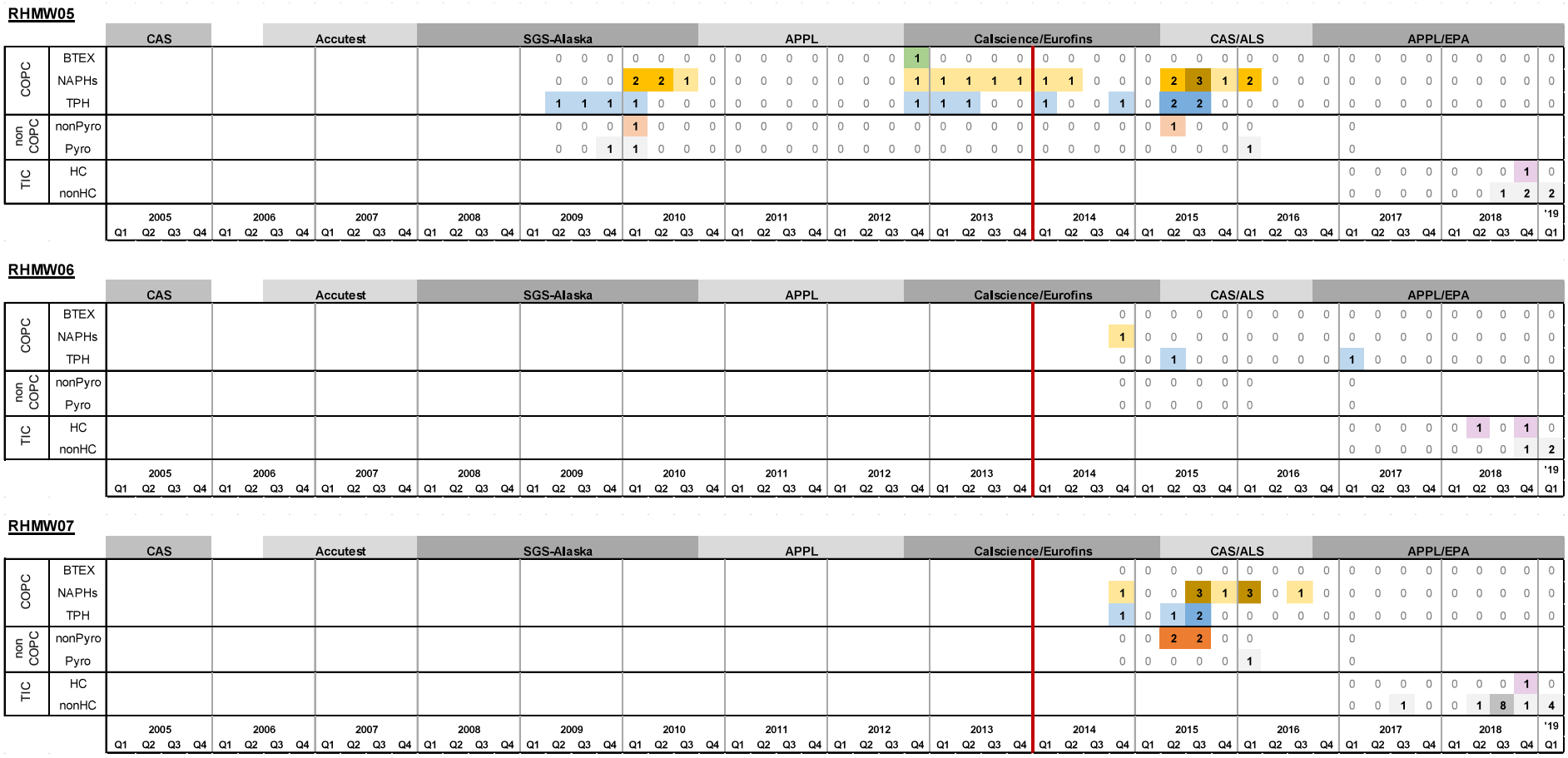

Notes: The red line indicates the Tank 5 fuel release date. The time periods for analytical laboratories are indicated at the top of each chart. The number of unique compounds detected within a given quarter is listed in the chart, quarters with no sample analyzed are blank. NAPHs = naphthalene, 1-methylnaphthalene, and 2-methylnaphthalene; TPH = TPH-g, TPH-d, and TPH-o, nonPyro = non-pyrogenic PAHs, Pyro = pyrogenic PAHs, HC = hydrocarbon.
Quarters with detections are highlighted in color, and each compound group is identified with a different color. The darker the color, the more detections that occurred in a given quarter.

Figure B.8.1-6: Summary Detection Signature Charts for Outlying Wells (cont.)

RHMW08

		CAS				Accutest				SGS-Alaska				APPL				Calscience/Eurofins				CAS/ALS				APPL/EPA																	
		2005				2006				2007				2008				2009				2010				2011				2012				2013				2014				2015			
		Q1	Q2	Q3	Q4	Q1	Q2	Q3	Q4	Q1	Q2	Q3	Q4	Q1	Q2	Q3	Q4	Q1	Q2	Q3	Q4	Q1	Q2	Q3	Q4	Q1	Q2	Q3	Q4	Q1	Q2	Q3	Q4	Q1	Q2	Q3	Q4	Q1	Q2	Q3	Q4	Q1	Q2	Q3	Q4
COPC	BTEX																																											
	NAPHs																																											
	TPH																																											
non COPC	nonPyro																																											
	Pyro																																											
TIC	HC																																											
	nonHC																																											

		2016				2017				2018				'19
		Q1	Q2	Q3	Q4	Q1	Q2	Q3	Q4	Q1	Q2	Q3	Q4	Q1
COPC	BTEX	0	0	0	0	0	0	0	0	0	0	0	0	0
	NAPHs	0	0	0	0	0	0	0	0	0	0	0	0	0
	TPH	2	2	0	0	0	0	0	0	0	0	0	0	0
non COPC	nonPyro					0								
	Pyro					0								
TIC	HC					0	0	0	0	0	1	0	0	0
	nonHC					0	2	0	0	0	0	1	3	2

RHMW09

		CAS				Accutest				SGS-Alaska				APPL				Calscience/Eurofins				CAS/ALS				APPL/EPA																	
		2005				2006				2007				2008				2009				2010				2011				2012				2013				2014				2015			
		Q1	Q2	Q3	Q4	Q1	Q2	Q3	Q4	Q1	Q2	Q3	Q4	Q1	Q2	Q3	Q4	Q1	Q2	Q3	Q4	Q1	Q2	Q3	Q4	Q1	Q2	Q3	Q4	Q1	Q2	Q3	Q4	Q1	Q2	Q3	Q4	Q1	Q2	Q3	Q4	Q1	Q2	Q3	Q4
COPC	BTEX																																											
	NAPHs																																											
	TPH																																											
non COPC	nonPyro																																											
	Pyro																																											
TIC	HC																																											
	nonHC																																											

		2016				2017				2018				'19
		Q1	Q2	Q3	Q4	Q1	Q2	Q3	Q4	Q1	Q2	Q3	Q4	Q1
COPC	BTEX	0	0	0	0	0	0	0	0	0	0	0	0	0
	NAPHs	0	0	0	0	0	0	0	0	0	0	0	0	0
	TPH	0	0	0	0	0	0	0	0	0	0	0	0	0
non COPC	nonPyro					0	0							
	Pyro					0	0							
TIC	HC					0	0	0	0	0	0	0	0	0
	nonHC					0	0	0	0	0	0	4	2	2

RHMW10

		CAS				Accutest				SGS-Alaska				APPL				Calscience/Eurofins				CAS/ALS				APPL/EPA																	
		2005				2006				2007				2008				2009				2010				2011				2012				2013				2014				2015			
		Q1	Q2	Q3	Q4	Q1	Q2	Q3	Q4	Q1	Q2	Q3	Q4	Q1	Q2	Q3	Q4	Q1	Q2	Q3	Q4	Q1	Q2	Q3	Q4	Q1	Q2	Q3	Q4	Q1	Q2	Q3	Q4	Q1	Q2	Q3	Q4	Q1	Q2	Q3	Q4	Q1	Q2	Q3	Q4
COPC	BTEX																																											
	NAPHs																																											
	TPH																																											
non COPC	nonPyro																																											
	Pyro																																											
TIC	HC																																											
	nonHC																																											

		2016				2017				2018				'19
		Q1	Q2	Q3	Q4	Q1	Q2	Q3	Q4	Q1	Q2	Q3	Q4	Q1
COPC	BTEX					0	0	0	0	0	0	0	0	0
	NAPHs					0	0	0	0	0	0	0	0	0
	TPH					2	0	1	0	0	0	2	0	
non COPC	nonPyro													
	Pyro													
TIC	HC					0	0	0	0	0	0	1	0	
	nonHC					1	0	0	3	0	1	0	0	

Notes: The red line indicates the Tank 5 fuel release date. The time periods for analytical laboratories are indicated at the top of each chart. The number of unique compounds detected within a given quarter is listed in the chart, quarters with no sample analyzed are blank. NAPHs = naphthalene, 1-methylnaphthalene, and 2-methylnaphthalene; TPH = TPH-g, TPH-d, and TPH-o, nonPyro = non-pyrogenic PAHs, Pyro = pyrogenic PAHs, HC = hydrocarbon.
Quarters with detections are highlighted in color, and each compound group is identified with a different color. The darker the color, the more detections that occurred in a given quarter.

Attachment B.8.2:
Analytical Tables – Non-COPCs and TICs

Table B.8.2-1
non-COPC Detections

Analyte	Compund Class	Halawa Deep	Red Hill Shaft	RHMW01	RHMW02	RHMW03	RHMW04	RHMW05	RHMW06	RHMW07	RHMW08	RHMW09
2-Butanone (MEK)	Oxy Other	--	--	Y	--	--	--	--	--	--	--	--
Acetone	Oxy Other	Y	Y	Y	Y	--	Y	Y	Y	Y	--	Y
Methylene chloride	Halogenated	--	--	--	Y	--	--	--	--	--	--	--
Dibenzofuran	Halogenated	--	--	--	Y	--	--	--	--	--	--	--
1,1,2,2-Tetrachloroethane	Halogenated	--	--	--	Y	--	--	--	--	--	--	--
1,2,3-Trichloropropane	Halogenated	--	--	--	Y	--	--	--	--	--	--	--
1,2,4-Trichlorobenzene	Halogenated	--	Y	--	--	--	--	--	--	--	--	--
Bromodichloromethane	Halogenated	--	--	--	--	--	--	--	Y	--	--	--
Bromomethane	Halogenated	--	Y	--	--	--	--	--	--	--	--	--
Chloroform	Halogenated	--	--	Y	--	--	--	--	--	--	--	--
Chloromethane	Halogenated	Y	Y	Y	--	--	Y	Y	Y	--	--	Y
cis-1,2-Dichloroethene	Halogenated	--	--	Y	--	--	--	--	--	--	--	--
Dibromochloromethane	Halogenated	--	--	--	--	--	--	--	--	--	Y	--
Trichloroethene	Halogenated	--	Y	Y	Y	--	--	--	--	--	--	--
Isopropylbenzene	Volatile Hydrocarbon	--	--	--	Y	--	--	--	--	--	--	--
n-Butylbenzene	Volatile Hydrocarbon	--	--	--	Y	--	--	--	--	--	--	--
n-Propylbenzene	Volatile Hydrocarbon	--	--	--	Y	--	--	--	--	--	--	--
sec-Butylbenzene	Volatile Hydrocarbon	--	--	--	Y	--	--	--	--	--	--	--
tert-Butylbenzene	Volatile Hydrocarbon	--	--	--	Y	--	--	--	--	--	--	--
Acenaphthene	PAH	--	--	Y	Y	--	--	--	--	--	--	--
Acenaphthylene	PAH	--	Y	Y	Y	--	Y	--	--	--	--	--
Anthracene	PAH	--	--	Y	--	--	Y	--	--	--	--	--
Benzo(a)anthracene	PAH	--	Y	Y	Y	Y	Y	Y	--	Y	--	--
Benzo(a)pyrene	PAH	--	--	Y	--	--	--	--	--	--	--	--
Benzo(b)fluoranthene	PAH	--	--	Y	Y	Y	Y	--	--	--	--	--
Benzo(ghi)perylene	PAH	--	--	Y	--	--	--	--	--	--	--	--
Benzo(k)fluoranthene	PAH	--	--	Y	--	--	--	--	--	--	--	--
Chrysene	PAH	--	Y	Y	Y	Y	Y	--	--	--	--	--
Dibenz(a,h)anthracene	PAH	--	--	Y	--	--	--	--	--	--	--	--
Fluoranthene	PAH	--	Y	Y	Y	--	--	Y	--	--	--	--
Fluorene	PAH	--	--	Y	Y	--	Y	--	--	Y	--	--
Indeno(1,2,3-cd)pyrene	PAH	--	--	Y	--	Y	--	--	--	--	--	--
Phenanthrene	PAH	--	Y	Y	Y	Y	Y	Y	--	Y	--	--

Notes: RHMW10 and RHMW11 were not analyzed for non-COPCs

Table B.8.2-2
non-COPC Analytical Suite

Halogenated Compounds

1,1,1,2-Tetrachloroethane
1,1,1-Trichloroethane
1,1,2,2-Tetrachloroethane
1,1,2-Trichloro-1,2,2-Trifluoroethane
1,1,2-Trichloroethane
1,1-Dichloroethane
1,1-Dichloroethylene
1,1-Dichloropropene
1,2,3-Trichlorobenzene
1,2,3-Trichloropropane
1,2,4-Tricholorobenzene
1,2-Dibromo-3- chloropropane
1,2-Dibromo-3- chloropropane
1,2-Dichlorobenzene
cis-1,2-Dichloroethylene
trans-1,2- Dichloroethylene
1,2-Dichloropropane
1,3-Dichlorobenzene
1,3-Dichloropropane
1,3-Dichloropropene (total of cis/trans)
1,4-Dichlorobenzene
2-Chloronaphthalene
2,2-Dichloropropane
2-Chlorotoluene
4-Chlorotoluene
Bromobenzene
Bromochloromethane
Bromodichloromethane
Bromoform
Bromomethane
Carbon Tetrachloride
Chlorobenzene
Chloroethane
Chloroform
Chloromethane
Dibromochloromethane
Dibromomethane
Dichlorodifluoromethane
Hexachlorobutadiene
Methylene chloride
Tetrachloroethylene
Trichloroethylene
Trichlorofluoromethane
Vinyl chloride
1,2,4-Trichlorobenzene
1,2-Dichlorobenzene
1,3-Dichlorobenzene
1,4-Dichlorobenzene
Hexachlorobenzene
Hexachlorobutadiene
Hexachlorocyclopentadiene
Hexachloroethane

Volatile Hydrocarbons

1,2,4-Trimethylbenzene
1,3,5-Trimethylbenzene
Cymene
Isopropylbenzene (Cumene)
n-Butylbenzene
n-Propylbenzene
sec-Butylbenzene
Styrene
tert-Butylbenzene

PAHs

Acenaphthene
Acenaphthylene
Anthracene
Benzo[a]anthracene
Benzo[g,h,i]perylene
Benzo[a]pyrene
Benzo[b]fluoranthene
Benzo[k]fluoranthene
Chrysene
Dibenz[a,h]anthracene
Fluoranthene
Fluorene
Indeno[1,2,3-cd]pyrene
Phenanthrene
Pyrene

Oxy Other

Acetone
2-Ethoxy-2-Methylpropane
2-Hexanone
2-Methoxy-2-Methylbutane
Isopropyl Ether
Methyl ethyl ketone (2-Butanone)
Methyl isobutyl ketone
Methyl tert-butyl Ether
tert-Butyl Alcohol
1,4-Dioxane (P-Dioxane)
2-Methylphenol (o-Cresol)
Benzyl Alcohol
Isophorone
Dibenzofuran
4-Bromophenyl Phenyl Ether
4-Chlorophenyl Phenyl Ether
Bis(2-Chloroethoxy) Methane
Bis(2-Chloroethyl) Ether

Phthalates

Benzyl Butyl Phthalate
Bis(2-Ethylhexyl) Phthalate
Diethyl Phthalate
Dimethyl Phthalate
Di-N-Butyl Phthalate
Di-N-Octylphthalate

Nitro Other

2,4-Dinitrotoluene
2,6-Dinitrotoluene
2-Nitroaniline
3,3'-Dichlorobenzidine
3-Nitroaniline
4-Chloroaniline
4-Nitroaniline
Carbazole
Diphenylamine
Nitrobenzene
N-Nitrosodi-N-Propylamine

Phenols

2,4,5-Trichlorophenol
2,4,6-Trichlorophenol
2,4-Dichlorophenol
2,4-Dimethylphenol
2,4-Dinitrophenol
2-Chlorophenol
2-Nitrophenol
3- And 4- Methylphenol (Total)
4,6-Dinitro-2-Methylphenol
4-Chloro-3-Methylphenol
4-Nitrophenol
Pentachlorophenol

Other Compounds

Carbon Disulfide

Notes: Compounds detected at Red Hill Shaft wells identified in red

Table B.8.2-3
Tentatively Identified Compounds Detected in RHMW02

Analyte	CAS	Compund Class	Number of Detections
Hexadecanoic Acid	57-10-3-TIC	Carboxylic Acid	1
Naphthalenecarboxylic acid	No CAS-TIC	Carboxylic Acid	2
Octadecanoic Acid	57-11-4-TIC	Carboxylic Acid	1
Pentenoic acid, phenyl-	No CAS-TIC	Carboxylic Acid	1
Propenoic acid, methylpheny	No CAS-TIC	Carboxylic Acid	1
(2-Methyl-2-Propenyl)-Benzene	3290-53-7-TIC	Hydrocarbon	1
[(E)-2-Methylbut-1-Enyl]Benzene	56253-64-6-TIC	Hydrocarbon	4
1,1'-Methylenebis-Benzene	101-81-5-TIC	Hydrocarbon	1
1,2,3,4-Tetrahydro-2-Methyl-Naphthalene	3877-19-8-TIC	Hydrocarbon	2
1,2,3,4-Tetramethylbenzene	488-23-3-TIC	Hydrocarbon	1
1,2,3,5-Tetramethylbenzene	527-53-7-TIC	Hydrocarbon	5
1,2-Diethylbenzene	135-01-3-TIC	Hydrocarbon	7
1,3-Diethyl Benzene	141-93-5-TIC	Hydrocarbon	2
1,3-Dimethylnaphthalene	575-41-7-TIC	Hydrocarbon	3
1,4-Diethyl Benzene	105-05-5-TIC	Hydrocarbon	1
1H-Indene, 2,3-Dihydro-1,1,3-Trimethyl-	2613-76-5-TIC	Hydrocarbon	1
1H-Indene, 2,3-Dihydro-1,1-Dimethyl-	4912-92-9-TIC	Hydrocarbon	4
1H-Indene, 2,3-Dihydro-1,3-Dimethyl-	4175-53-5-TIC	Hydrocarbon	3
1H-Indene, 2,3-Dihydro-1,6-Dimethyl-	17059-48-2-TIC	Hydrocarbon	3
1H-Indene, 2,3-Dihydro-4,7-Dimethyl-	6682-71-9-TIC	Hydrocarbon	1
1H-Indene,2,3,Dihydro-4-Methyl	824-22-6-TIC	Hydrocarbon	1
1-Methyl-2(2-Propenyl)-Benzene	1587-04-8-TIC	Hydrocarbon	2
1-Methyl-2-Propylbenzene	1074-17-5-TIC	Hydrocarbon	1
2,3-Dihydro-1H-Indene	496-11-7-TIC	Hydrocarbon	8
2,7-Dimethyl Naphthalene	582-16-1-TIC	Hydrocarbon	2
2-Ethenyl-1,4-Dimethylbenzene	2039-89-6-TIC	Hydrocarbon	6
2-Ethyl-1,3-Dimethyl Benzene	2870-04-4-TIC	Hydrocarbon	1
2-Ethyl-2,3-Dihydro-1H-Indene	56147-63-8-TIC	Hydrocarbon	1
5,6-Dimethylindan	1075-22-5-TIC	Hydrocarbon	1
Benzene, (3-Methyl-2-Butenyl)-	4489-84-3-TIC	Hydrocarbon	1
Benzene, 1,1'-(1-Ethenyl-1,3-Propanediyl)Bis	61141-97-7-TIC	Hydrocarbon	1
Benzene, 1-Methyl-2-(1-Methylethyl-	95660-61-0-TIC	Hydrocarbon	1
Benzene, 2,4-Dimethyl-1-(1-Methylethyl)-	4706-89-2-TIC	Hydrocarbon	1
Benzene, 2-Etheny-1,3-Dimethyl-	2039-90-9-TIC	Hydrocarbon	1
Benzene, butenyl	No CAS-TIC	Hydrocarbon	1
Benzene, diethyl	No CAS-TIC	Hydrocarbon	4
Benzene, ethenyldimethyl	No CAS-TIC	Hydrocarbon	3
Benzene, ethyl, dimethyl	No CAS-TIC	Hydrocarbon	4
Benzene, methyl-propyl	No CAS-TIC	Hydrocarbon	3
Benzene, propyl	No CAS-TIC	Hydrocarbon	1
Benzene, tetramethyl	No CAS-TIC	Hydrocarbon	2
Cyclohexylbenzene	827-52-1-TIC	Hydrocarbon	1
Cymene	99-87-6-TIC	Hydrocarbon	3
Dimethyl Naphthalene; 1,4-	571-58-4-TIC	Hydrocarbon	1
Dimethylstyrene	No CAS-TIC	Hydrocarbon	1
Ethyltetramethylcyclopentadiene	57693-77-3-TIC	Hydrocarbon	1
Indan, methyl	No CAS-TIC	Hydrocarbon	3
Indane	No CAS-TIC	Hydrocarbon	3
Indene, dihydrodimethy	No CAS-TIC	Hydrocarbon	6
m-Cymene	535-77-3-TIC	Hydrocarbon	2
Methylindane	767-58-8-TIC	Hydrocarbon	2
Naphthalene, 1,2,3,4-Tetrahydro-1-Methyl	1559-81-5-TIC	Hydrocarbon	4

Table B.8.2-3
Tentatively Identified Compounds Detected in RHMW02

Analyte	CAS	Compund Class	Number of Detections
Naphthalene, 1,2,3,4-Tetrahydro-5-Methyl	2809-64-5-TIC	Hydrocarbon	1
Naphthalene, 1,6-Dimethyl-	575-43-9.1-TIC	Hydrocarbon	4
Naphthalene, dimethyl-	No CAS-TIC	Hydrocarbon	4
Naphthalene, methyl	No CAS-TIC	Hydrocarbon	1
Naphthalene, tetrahydro	No CAS-TIC	Hydrocarbon	2
Phenylbutene	No CAS-TIC	Hydrocarbon	1
sec-Butylbenzene	135-98-8-TIC	Hydrocarbon	3
Tetralin	119-64-2-TIC	Hydrocarbon	2
Total hydrocarbon	No CAS-TIC	Hydrocarbon	2
Benzocycloheptatriene	No CAS-TIC	Olefin	2
Tetradecene	1120-36-1-TIC	Olefin	1
1-Methyl-2-Cyano-3-Ethyl-2-Piperideine	73657-67-7-TIC	Other	1
2-Cyano-1,3,4-Trimethyl-3-Piperidine	73657-70-2-TIC	Other	1
3,4-Dimethyl-1H-Pyrrolo[2,3-B]Pyridine	23612-70-6-TIC	Other	1
Sulfur Dioxide	7446-09-5-TIC	Other	1
1,3-Dimethylbicyclo[3.3.0] Oct-3-En-2-One	70640-02-7-TIC	Oxy/Other	1
2(1H)-Naphthalenone, 3,4-Dihydro-	530-93-8-TIC	Oxy/Other	1
2(1H)-Naphthalenone, Octahydro-, Trans-	16021-08-2-TIC	Oxy/Other	1
Benzaldehyde, 4-(1-Methylethyl)-	122-03-2-TIC	Oxy/Other	1
Diacetone Alcohol	123-42-2-TIC	Oxy/Other	1
Mesityl Oxide	141-79-7-TIC	Oxy/Other	1
1,2-Benzenedicarboxylic Acid, 1,2-Diisononyl Ester	28553-12-0-TIC	Phthalate/Plasticizers	1
Di-Isodecyl Phthalate	26761-40-0-TIC	Phthalate/Plasticizers	1
Bicyclo[3.2.1]Oct-2-Ene, 3-Methyl-4-Methylene-	49826-53-1-TIC	Rare	2
Bicyclotriene (01)	No CAS-TIC	Rare	2
Umbellulol	3310-03-0-TIC	Surfactant/Detergent	1

Appendix B.8
Attachment B.8.2

Table B.8.2-4
Tentatively Identified Counds Detected in RHMW01, RHMW03, and Outlying Wells

Analyte	CAS	Compund Class	Halawa Deep	Red Hill Shaft	RHMW01	RHMW03	RHMW04	RHMW05	RHMW06	RHMW07	RHMW08	RHMW09	RHMW10	RHMW11-01	RHMW11-02	RHMW11-03	RHMW11-04	RHMW11-05
2-Ethylhexanoic Acid	149-57-5-TIC	Carboxylic Acid	--	Y	--	--	--	--	--	--	--	--	--	--	--	--	--	--
Hexadecanoic Acid	57-10-3-TIC	Carboxylic Acid	--	--	--	--	--	--	--	--	--	Y	--	--	--	Y	--	Y
Octadecanoic Acid	57-11-4-TIC	Carboxylic Acid	--	--	--	Y	--	--	--	--	--	--	--	--	--	--	--	Y
3-Bromohexane	3377-87-5-TIC	Halogenated	--	Y	--	--	--	--	--	--	--	--	--	--	--	--	--	--
Dimethyl Benzidine Dihydrochloride; 3,3'-	612-82-8-TIC	Halogenated	--	Y	--	--	--	--	--	--	--	--	--	--	--	--	--	--
Propane, chloro	No CAS-TIC	Halogenated	--	Y	--	--	--	--	--	--	--	--	--	--	--	--	--	--
Tetrachloroethene	127-18-4-TIC	Halogenated	--	Y	--	--	--	--	--	--	--	--	--	--	--	--	--	--
1,2,3,4,5-Pentamethyl-Cyclopentane	33067-32-2-TIC	Hydrocarbon	--	Y	--	--	--	--	--	--	--	--	--	--	--	--	--	--
1,2,3-Trimethyl Benzene	526-73-8-TIC	Hydrocarbon	--	Y	--	--	--	--	Y	--	--	--	Y	--	--	--	--	--
1,2,4-Trimethylbenzene	95-63-6-TIC	Hydrocarbon	Y	Y	--	--	--	Y	Y	Y	--	--	--	--	--	--	--	Y
1,3,5-Trimethylbenzene (Mesitylene)	108-67-8-TIC	Hydrocarbon	--	--	--	--	--	--	--	--	Y	--	--	--	--	--	--	--
1,4-Ethanonaphthalene, 1,2,3,4-Tetrahydr	4715-52-4-TIC	Hydrocarbon	--	--	Y	--	--	--	--	--	--	--	--	--	--	--	--	--
1H-Indene, 2,3-Dihydro-1,1-Dimethyl-	4912-92-9-TIC	Hydrocarbon	--	--	Y	--	--	--	--	--	--	--	--	--	--	--	--	--
1H-Indene, 2,3-Dihydro-1,2-Dimethyl-	17057-82-8-TIC	Hydrocarbon	--	--	Y	--	--	--	--	--	--	--	--	--	--	--	--	--
1-Methyl-3-Propylcyclohexane	4291-80-9-TIC	Hydrocarbon	--	Y	--	--	--	--	--	--	--	--	--	--	--	--	--	--
2-Hexene, 3,5,5-Trimethyl-	26456-76-8-TIC	Hydrocarbon	--	Y	--	--	--	--	--	--	--	--	--	--	--	--	--	--
Adamantane	281-23-2-TIC	Hydrocarbon	--	--	Y	--	--	--	--	--	--	--	--	--	--	--	--	--
Benzene, hexamethyl	No CAS-TIC	Hydrocarbon	--	--	Y	--	--	--	--	--	--	--	--	--	--	--	--	--
Benzene, methylbutenyl	No CAS-TIC	Hydrocarbon	--	--	Y	--	--	--	--	--	--	--	--	--	--	--	--	--
Benzene, methylmethylethyl	No CAS-TIC	Hydrocarbon	--	--	Y	--	--	--	--	--	--	--	--	--	--	--	--	--
Benzene, pentenyl	No CAS-TIC	Hydrocarbon	--	--	Y	--	--	--	--	--	--	--	--	--	--	--	--	--
Indene, dihydrodimethy	No CAS-TIC	Hydrocarbon	--	--	Y	--	--	--	--	--	--	--	--	--	--	--	--	--
Indene, dihydrodimethyl	No CAS-TIC	Hydrocarbon	--	--	Y	--	--	--	--	--	--	--	--	--	--	--	--	--
Indene, dihydroimethy	No CAS-TIC	Hydrocarbon	--	--	Y	--	--	--	--	--	--	--	--	--	--	--	--	--
Indene, dihydrotrime (01)	No CAS-TIC	Hydrocarbon	--	--	Y	--	--	--	--	--	--	--	--	--	--	--	--	--
Indene,dihydrodimethy	No CAS-TIC	Hydrocarbon	--	--	Y	--	--	--	--	--	--	--	--	--	--	--	--	--
Naphthalene, 1,2,3,4-Tetrahydro-1,5-Dimethyl-	21564-91-0-TIC	Hydrocarbon	--	--	Y	--	--	--	--	--	--	--	--	--	--	--	--	--
Naphthalene, tetrahydro	No CAS-TIC	Hydrocarbon	--	--	Y	--	--	--	--	--	--	--	--	--	--	--	--	--
Total hydrocarbon	No CAS-TIC	Hydrocarbon	--	--	Y	--	--	--	--	--	--	--	--	--	--	--	--	--
Decamethyl-Cyclopentasiloxane	541-02-6-TIC	N/A	--	Y	--	--	--	--	--	Y	--	--	--	--	--	--	--	--
Hexamethylcyclotrisiloxane	541-05-9-TIC	N/A	--	--	--	--	--	--	--	Y	--	--	--	--	--	--	--	--
Octamethylcyclotetrasiloxane	556-67-2-TIC	N/A	--	Y	Y	--	Y	--	--	--	Y	Y	--	--	--	--	--	--
1-Hexadecene	629-73-2-TIC	Olefin	--	--	Y	--	--	--	--	--	Y	--	Y	--	--	--	--	--
2,3-Dimethyl-1-Pentene	3404-72-6-TIC	Olefin	Y	--	--	--	--	--	--	--	--	--	--	--	--	--	--	--
Ethyl Isothiocyanate	542-85-8-TIC	Other	Y	--	--	--	--	--	--	--	Y	--	--	--	--	--	--	--
Pentanamide	626-97-1-TIC	Other	--	--	--	Y	--	--	--	--	--	--	--	--	--	--	--	--
Tetradecanamide	638-58-4-TIC	Other	--	--	--	Y	--	--	--	--	--	--	--	--	--	--	--	--
1,2,2,3-Tetramethyl-3-Cyclopenten-1-OL	74055-14-4-TIC	Oxy/Other	Y	--	--	--	--	--	--	--	--	--	--	--	--	--	--	--
1-Heneicosyl Formate	77899-03-7-TIC	Oxy/Other	--	--	--	--	--	--	--	--	--	--	Y	--	--	--	--	--
2,2,4-Trimethyl-1,3-Dioxolane	1193-11-9-TIC	Oxy/Other	--	--	--	--	--	Y	--	--	--	--	--	--	--	--	--	--
4H-Pyran-4-One, Tetrahydro-	29943-42-8-TIC	Oxy/Other	--	--	--	--	--	--	--	--	Y	--	Y	--	--	--	--	--
Benzenemethanol, 4-Methyl-	589-18-4-TIC	Oxy/Other	--	--	--	--	--	--	--	--	--	--	--	--	--	--	--	Y
Benzenesulfonothioic Acid, S-Phenyl Ester	1212-08-4-TIC	Oxy/Other	--	Y	Y	Y	Y	Y	--	--	Y	Y	--	--	--	--	--	--
Diacetone Alcohol	123-42-2-TIC	Oxy/Other	Y	Y	--	--	Y	Y	--	Y	--	--	--	--	--	Y	Y	--
Di-Sec-Butyl Ether	6863-58-7-TIC	Oxy/Other	--	--	--	--	--	--	--	--	--	--	--	--	--	--	--	Y
Ethyl Acetate	141-78-6-TIC	Oxy/Other	--	Y	--	--	--	--	--	--	--	--	--	--	--	--	--	--
Hexanedioic Acid Dioctyl Ester	123-79-5-TIC	Oxy/Other	--	Y	Y	Y	--	--	Y	Y	Y	--	--	--	--	--	--	Y
Mesityl Oxide	141-79-7-TIC	Oxy/Other	Y	Y	Y	Y	Y	Y	Y	Y	--	Y	--	--	--	--	--	--
Pentanedioic Acid, Dimethyl Ester	1119-40-0-TIC	Oxy/Other	--	Y	--	--	--	Y	Y	--	--	--	--	--	--	--	--	--
Pentanol; 3-	584-02-1-TIC	Oxy/Other	--	--	--	Y	--	--	--	--	--	--	--	--	--	--	--	--
2-(2-Butoxyethoxy)Ethanol	112-34-5-TIC	OxyEthanol/Glycol/Alc	--	--	--	--	--	--	--	--	--	--	--	Y	--	--	--	Y
3-Penten-2-OL	1569-50-2-TIC	OxyEthanol/Glycol/Alc	--	Y	--	--	--	--	--	--	--	--	--	--	--	--	--	--

Appendix B.8
Attachment B.8.2

Table B.8.2-4
Tentatively Identified Counds Detected in RHMW01, RHMW03, and Outlying Wells

Analyte	CAS	Compund Class	Halawa Deep	Red Hill Shaft	RHMW01	RHMW03	RHMW04	RHMW05	RHMW06	RHMW07	RHMW08	RHMW09	RHMW10	RHMW11-01	RHMW11-02	RHMW11-03	RHMW11-04	RHMW11-05
Ethanol, 1-(2-Butoxyethoxy)-	54446-78-5-TIC	OxyEthanol/Glycol/Alc	--	--	--	--	--	--	--	--	--	--	--	--	--	Y	--	--
2,4-Dimethylphenol	105-67-9-TIC	Phenols	--	--	--	--	--	--	--	--	--	--	--	--	--	--	--	Y
1,2-Benzenedicarboxylic Acid, 1,2-Diisononyl Ester	28553-12-0-TIC	Phthalate/Plasticizers	--	Y	--	Y	--	--	--	Y	--	Y	--	--	--	--	--	Y
1,2-Benzenedicarboxylic Acid, Butyl 8-Methylnonyl Ester	89-18-9-TIC	Phthalate/Plasticizers	--	--	--	--	--	--	--	--	--	--	Y	--	--	--	--	--
1,2-Benzenedicarboxylic Acid, Diheptyl Ester	3648-21-3-TIC	Phthalate/Plasticizers	--	--	--	--	--	--	--	--	--	--	Y	--	--	--	--	--
1,2-Benzenedicarboxylic Acid, Dinonyl Ester	84-76-4-TIC	Phthalate/Plasticizers	--	--	--	--	--	--	--	--	--	Y	--	--	--	--	--	--
1,2-Benzenedicarboxylic Acid, Isodecyl Octyl Ester	1330-96-7-TIC	Phthalate/Plasticizers	--	--	--	--	--	--	--	Y	--	--	--	--	--	--	--	--
bis(2-Ethylhexyl) phthalate	117-81-7-TIC	Phthalate/Plasticizers	--	--	--	--	--	--	--	Y	--	--	--	--	--	--	--	--
Bis(4-Methyl-2-Pentanyl) Phthalate	146-50-9-TIC	Phthalate/Plasticizers	--	--	--	--	--	--	--	Y	--	--	--	--	--	--	--	--
Butyl benzyl phthalate	85-68-7-TIC	Phthalate/Plasticizers	--	--	--	--	--	--	--	--	--	--	--	Y	--	--	--	--
Butyl Isobutyl Phthalate	17851-53-5-TIC	Phthalate/Plasticizers	--	--	--	--	--	--	--	--	--	--	--	--	--	--	--	Y
Diisooctyl Phthalate	27554-26-3-TIC	Phthalate/Plasticizers	--	--	--	--	--	--	--	--	--	--	--	Y	--	--	--	--
Dimethyl phthalate	131-11-3-TIC	Phthalate/Plasticizers	--	--	--	Y	--	--	--	--	--	--	--	--	--	--	--	--
N-Ethyl-4-Methyl-Benzenesulfonamide	80-39-7-TIC	Phthalate/Plasticizers	--	--	--	Y	--	--	--	--	--	--	--	--	--	--	--	--
Phthalic Anhydride	85-44-9-TIC	Phthalate/Plasticizers	--	--	--	--	--	--	--	Y	--	--	--	--	--	--	--	--
Benzocycloheptene,dihydro	No CAS-TIC	Rare	--	--	Y	--	--	--	--	--	--	--	--	--	--	--	--	--
N-Tetradecanoic Acid Amide	TDCNAA-TIC	Surfactant/Detergent	--	--	--	Y	--	--	--	--	--	--	--	--	--	--	--	--
(E)-9-Eicosene	74685-29-3-TIC	Unknown/Eicosene	--	--	--	--	--	--	--	Y	--	--	--	--	--	--	--	--
3-Eicosene, (E)-	74685-33-9-TIC	Unknown/Eicosene	--	--	--	Y	--	--	--	--	--	--	--	--	--	--	--	--
5-Eicosene, (E)-	74685-30-6-TIC	Unknown/Eicosene	--	--	--	--	--	--	--	Y	--	--	--	--	--	--	--	--

Attachment B.8.3:
Statistical Methods

Methods

Two non-parametric statistical methods, the generalized Wilcoxon test and Kendall's tau test, were used to assess the statistical significance in chemical data when the U-flag data is encountered. For data sets that did not include U-flagged data, the Wilcoxon rank sum test (rather than the generalized Wilcoxon test) was performed. The available organic and inorganic chemical data include duplicate sample data, some of which are qualified with U, J, or UJ flag. The following procedure was taken to handle these duplicate sample data in the statistical analysis:

- Treated as no data (left as blank in the database) if the chemical data were not measured for both duplicate samples.
- Averaged duplicate sample results if the chemical data were measured without any flags.
- Chose the smallest value of the J-values and/or U-limits if the duplicate samples had the same flag of U or J or UJ.
- Used the detected value if only one of the duplicate samples was detected without any flag and the other had either U, J, or UJ flag.
- Chose J flag data if the other duplicate sample data had either U or UJ flag.
- Chose U flag data if the other duplicate sample data had UJ flag.

Generalized Wilcoxon test was performed to test whether two groups of chemical data with left-censored data are statistically different or similar (Helsel 2012). It was applied to support the evaluation of (1) the concentration reported by one laboratory versus the concentration by another laboratory or other laboratories for selected constituents, and (2) concentration after the installation of a monitoring well versus the concentration thereafter. This test was used because (1) it can handle left-censored chemical data with multiple reporting limits and (2) it does not require the data to follow a specific statistical distribution. Wilcoxon rank sum test was performed to test for those chemical data sets with all non-censored data. This test can also handle nonparametric data. The results of these tests are expressed as a p-value, which represents the probability that a null hypothesis is falsely rejected. The null hypothesis is that the two chemical data population are not statistically different. A p-value of 0.05 was selected as a threshold to test the null hypothesis. If the p-value is below 0.05, the two data populations are more likely to be different.

Kendall's tau test was applied to support the comparison the correlation between the concentrations of two constituents, such as TPH-d and another organic chemical including naphthalene, 1-methylnaphthalene, 2-methylnaphthalene, and dissolved oxygen for selected monitoring well(s). Kendall's tau is a rank-based nonparametric statistical method (Helsel 2012). It can handle censored data by giving concordant and discordant directions between two measured values. The null hypothesis is that the two concentration of the two constituents are not correlated. The Kendall's tau test result is expressed as a p-value, which represents the probability of falsely rejecting the hypothesis. A p-value threshold of 0.05 was adopted. A p-value smaller than 0.05 indicates that the correlation between two chemical data more likely to be statistically significant. In addition, Kendall's tau value ranges from -1 to 1 and it has a higher correlation as tau gets close to 1.0.

These statistical tests were calculated by established packages in R called NADA (Helsel 2012).

Reference

Helsel, D. R. 2012. *Statistics for Censored Environmental Data Using Minitab and R*. 2nd ed. Wiley Series in Statistics in Practice. Hoboken, N.J: Wiley.

This page intentionally left blank

Appendix C:
Strike and Dip Data

This page intentionally left blank

Gaussian Mixed Model Evaluation Coordinates

1	280	190	12	Halawa 1 pt		[190, 12],	21.375420	-157.890790
2	290	200	13	Halawa 1 pt		[200, 13],	21.374760	-157.892380
3	280	190	10	Halawa 1 pt		[190, 10],	21.375350	-157.891100
4	280	190	12	Halawa 1 pt		[190, 12],	21.375190	-157.891270
5	280	190	10	Halawa 1 pt		[190, 10],	21.374790	-157.892330
6	280	190	10	Halawa 1 pt		[190, 10],	21.370678	-157.900642
7	300	210	12	Halawa 1 pt		[210, 12],	21.370523	-157.901076
8	270	180	15	Halawa 1 pt		[180, 15],	21.373212	-157.895076
9	290	200	12	Halawa 1 pt		[200, 12],	21.373150	-157.896178
10	296	206	10	Halawa 1 pt		[206, 10],	21.373070	-157.896440
11	240	150	4	Halawa 1 pt		[150, 4],	21.373243	-157.896563
12	285	195	10	Halawa 1 pt		[195, 10],	21.373244	-157.896820
13	290	200	15	Halawa 1 pt		[200, 15],	21.373331	-157.896207
14	280	190	12	Halawa 1 pt		[190, 12],	21.373320	-157.896238
15	295	205	20	Halawa 1 pt		[205, 20],	21.372797	-157.897625
16	295	205	12	Halawa 1 pt		[205, 12],	21.372668	-157.897876
17	285	195	14	Halawa 1 pt		[195, 14],	21.372681	-157.898084
18	300	210	15	Halawa 1 pt		[210, 15],	21.371783	-157.899378
19	290	200	15	Halawa 1 pt		[200, 15],	21.371273	-157.901096
20	270	180	12	Halawa 1 pt		[180, 12],	21.370979	-157.902171
21	20	290	2	Moanalua 1 pt		[290, 2],	21.368495	-157.895831
22	300	210	10	Moanalua 1 pt		[210, 10],	21.365717	-157.895783
23	300	210	10	Moanalua 1 pt		[210, 10],	21.365783	-157.898400
25	320	230	10	Moanalua 1 pt		[230, 10],	21.365933	-157.898283
26	325	235	12	Moanalua 1 pt		[235, 12],	21.365933	-157.898283
27	290	200	5	Moanalua 1 pt		[200, 5],	21.368317	-157.896033
28	260	170	12	Moanalua 1 pt		[170, 12],	21.368317	-157.896033
29	280	190	12	Moanalua 1 pt		[190, 12],	21.368317	-157.896033
30	270	180	15	Moanalua 1 pt		[180, 15],	21.368300	-157.896133
31	265	175	8	Moanalua 1 pt		[175, 8],	21.368300	-157.896133
32	232	142	5	Moanalua Tunnel 1 pt		[142, 5],	04+45[1]	
33	265	175	8	Moanalua Tunnel 1 pt		[175, 8],	06+00[1]	
34	270	180	15	Moanalua Tunnel 1 pt		[180, 15],	10+25[1]	
35	390	300	30	Moanalua Tunnel 1 pt		[300, 30],	23+85[1]	
36	330	240	4.5	Moanalua Tunnel 1 pt		[240, 4.5],	25+65[1]	
45	310	220	4.5	Moanalua Tunnel 1 pt		[220, 4.5],	26+45[1]	
47	325	235	5.5	Moanalua Tunnel 1 pt		[235, 5.5],	28+38[1]	
48	275	185	13	Moanalua Tunnel 1 pt		[185, 13],	21.370741	-157.905226
49	272	182	20	Moanalua Tunnel 1 pt		[182, 20],	21.370741	-157.905226
50	307	217	3.085	Barrel log - Clinker Evaluation 2017 Weighted 5 pts		[217, 3.085],	n/a	n/a
51	307	217	3.085	Barrel log - Clinker Evaluation 2017 Weighted 5 pts		[217, 3.085],	n/a	n/a
52	307	217	3.085	Barrel log - Clinker Evaluation 2017 Weighted 5 pts		[217, 3.085],	n/a	n/a
53	307	217	3.085	Barrel log - Clinker Evaluation 2017 Weighted 5 pts		[217, 3.085],	n/a	n/a
54	307	217	3.085	Barrel log - Clinker Evaluation 2017 Weighted 5 pts		[217, 3.085],	n/a	n/a
55	309	219	2.732	Barrel log - Kriging Correlation 2018 Weighted 5 pts		[219, 2.732],	n/a	n/a
56	309	219	2.732	Barrel log - Kriging Correlation 2018 Weighted 5 pts		[219, 2.732],	n/a	n/a
57	309	219	2.732	Barrel log - Kriging Correlation 2018 Weighted 5 pts		[219, 2.732],	n/a	n/a
58	309	219	2.732	Barrel log - Kriging Correlation 2018 Weighted 5 pts		[219, 2.732],	n/a	n/a
59	309	219	2.732	Barrel log - Kriging Correlation 2018 Weighted 5 pts		[219, 2.732],	n/a	n/a

Gaussian Mixed Model Evaluation Coordinates (cont.)

60	299.311	209.311	2.779	Barrel log - Kriging Correlation T9-16 2018 Weighted 3 pts		[209.311, 2.779],	n/a	n/a
61	299.311	209.311	2.779	Barrel log - Kriging Correlation T9-16 2018 Weighted 3 pts		[209.311, 2.779],	n/a	n/a
62	299.311	209.311	2.779	Barrel log - Kriging Correlation T9-16 2018 Weighted 3 pts		[209.311, 2.779],	n/a	n/a
63	307	217	2.732	DOH Weighted 10 pts		[217, 2.732],	n/a	n/a
64	307	217	2.732	DOH Weighted 10 pts		[217, 2.732],	n/a	n/a
65	307	217	2.732	DOH Weighted 10 pts		[217, 2.732],	n/a	n/a
66	307	217	2.732	DOH Weighted 10 pts		[217, 2.732],	n/a	n/a
67	307	217	2.732	DOH Weighted 10 pts		[217, 2.732],	n/a	n/a
68	307	217	2.732	DOH Weighted 10 pts		[217, 2.732],	n/a	n/a
69	307	217	2.732	DOH Weighted 10 pts		[217, 2.732],	n/a	n/a
70	307	217	2.732	DOH Weighted 10 pts		[217, 2.732],	n/a	n/a
71	307	217	2.732	DOH Weighted 10 pts		[217, 2.732],	n/a	n/a
72	307	217	2.732	DOH Weighted 10 pts		[217, 2.732],	n/a	n/a
73	279.426	189.426	6	Quarry 10 pts		[189.426, 6],	n/a	n/a
74	284.347	194.347	6.017	Quarry 10 pts		[194.347, 6.017],	n/a	n/a
75	263.585	173.585	6.253	Quarry 10 pts		[173.585, 6.253],	n/a	n/a
76	274.772	184.772	6.025	Quarry 10 pts		[184.772, 6.025],	n/a	n/a
77	305.969	215.969	2.287	Quarry 10 pts		[215.969, 2.287],	n/a	n/a
78	296.366	206.366	3.838	Quarry 10 pts		[206.366, 3.838],	n/a	n/a
79	279.426	189.426	6	Quarry 10 pts		[189.426, 6],	n/a	n/a
80	284.347	194.347	6.017	Quarry 10 pts		[194.347, 6.017],	n/a	n/a
81	263.585	173.585	6.253	Quarry 10 pts		[173.585, 6.253],	n/a	n/a
82	274.772	184.772	6.025	Quarry 10 pts		[184.772, 6.025],	n/a	n/a
83	305.969	215.969	2.287	Quarry 10 pts		[215.969, 2.287],	n/a	n/a
84	296.366	206.366	3.838	Quarry 10 pts		[206.366, 3.838],	n/a	n/a
85	279.426	189.426	6	Quarry 10 pts		[189.426, 6],	n/a	n/a
86	284.347	194.347	6.017	Quarry 10 pts		[194.347, 6.017],	n/a	n/a
87	263.585	173.585	6.253	Quarry 10 pts		[173.585, 6.253],	n/a	n/a
88	274.772	184.772	6.025	Quarry 10 pts		[184.772, 6.025],	n/a	n/a
89	305.969	215.969	2.287	Quarry 10 pts		[215.969, 2.287],	n/a	n/a
90	296.366	206.366	3.838	Quarry 10 pts		[206.366, 3.838],	n/a	n/a
91	279.426	189.426	6	Quarry 10 pts		[189.426, 6],	n/a	n/a
92	284.347	194.347	6.017	Quarry 10 pts		[194.347, 6.017],	n/a	n/a
93	263.585	173.585	6.253	Quarry 10 pts		[173.585, 6.253],	n/a	n/a
94	274.772	184.772	6.025	Quarry 10 pts		[184.772, 6.025],	n/a	n/a
95	305.969	215.969	2.287	Quarry 10 pts		[215.969, 2.287],	n/a	n/a
96	296.366	206.366	3.838	Quarry 10 pts		[206.366, 3.838],	n/a	n/a
97	279.426	189.426	6	Quarry 10 pts		[189.426, 6],	n/a	n/a
98	284.347	194.347	6.017	Quarry 10 pts		[194.347, 6.017],	n/a	n/a
99	263.585	173.585	6.253	Quarry 10 pts		[173.585, 6.253],	n/a	n/a
100	274.772	184.772	6.025	Quarry 10 pts		[184.772, 6.025],	n/a	n/a
101	305.969	215.969	2.287	Quarry 10 pts		[215.969, 2.287],	n/a	n/a
102	296.366	206.366	3.838	Quarry 10 pts		[206.366, 3.838],	n/a	n/a
103	279.426	189.426	6	Quarry 10 pts		[189.426, 6],	n/a	n/a
104	284.347	194.347	6.017	Quarry 10 pts		[194.347, 6.017],	n/a	n/a
105	263.585	173.585	6.253	Quarry 10 pts		[173.585, 6.253],	n/a	n/a
106	274.772	184.772	6.025	Quarry 10 pts		[184.772, 6.025],	n/a	n/a
107	305.969	215.969	2.287	Quarry 10 pts		[215.969, 2.287],	n/a	n/a
108	296.366	206.366	3.838	Quarry 10 pts		[206.366, 3.838],	n/a	n/a
109	279.426	189.426	6	Quarry 10 pts		[189.426, 6],	n/a	n/a
110	284.347	194.347	6.017	Quarry 10 pts		[194.347, 6.017],	n/a	n/a

Gaussian Mixed Model Evaluation Coordinates (cont.)

111	263.585	173.585	6.253	Quarry 10 pts		[173.585, 6.253],	n/a	n/a
112	274.772	184.772	6.025	Quarry 10 pts		[184.772, 6.025],	n/a	n/a
113	305.969	215.969	2.287	Quarry 10 pts		[215.969, 2.287],	n/a	n/a
114	296.366	206.366	3.838	Quarry 10 pts		[206.366, 3.838],	n/a	n/a
115	279.426	189.426	6	Quarry 10 pts		[189.426, 6],	n/a	n/a
116	284.347	194.347	6.017	Quarry 10 pts		[194.347, 6.017],	n/a	n/a
117	263.585	173.585	6.253	Quarry 10 pts		[173.585, 6.253],	n/a	n/a
118	274.772	184.772	6.025	Quarry 10 pts		[184.772, 6.025],	n/a	n/a
119	305.969	215.969	2.287	Quarry 10 pts		[215.969, 2.287],	n/a	n/a
120	296.366	206.366	3.838	Quarry 10 pts		[206.366, 3.838],	n/a	n/a
121	279.426	189.426	6	Quarry 10 pts		[189.426, 6],	n/a	n/a
122	284.347	194.347	6.017	Quarry 10 pts		[194.347, 6.017],	n/a	n/a
123	263.585	173.585	6.253	Quarry 10 pts		[173.585, 6.253],	n/a	n/a
124	274.772	184.772	6.025	Quarry 10 pts		[184.772, 6.025],	n/a	n/a
125	305.969	215.969	2.287	Quarry 10 pts		[215.969, 2.287],	n/a	n/a
126	296.366	206.366	3.838	Quarry 10 pts		[206.366, 3.838],	n/a	n/a
127	279.426	189.426	6	Quarry 10 pts		[189.426, 6],	n/a	n/a
128	284.347	194.347	6.017	Quarry 10 pts		[194.347, 6.017],	n/a	n/a
129	263.585	173.585	6.253	Quarry 10 pts		[173.585, 6.253],	n/a	n/a
130	274.772	184.772	6.025	Quarry 10 pts		[184.772, 6.025],	n/a	n/a
131	305.969	215.969	2.287	Quarry 10 pts		[215.969, 2.287],	n/a	n/a
132	296.366	206.366	3.838	Quarry 10 pts		[206.366, 3.838],	n/a	n/a
133	268	178	3.079	Moanalua Side, Weighted 3 pts		[178, 3.079],	n/a	n/a
134	297.5	207.5	3.129	Moanalua Side, Weighted 3 pts		[207.5, 3.129],	n/a	n/a
135	273	183	8.208	Moanalua Side, Weighted 3 pts		[183, 8.208],	n/a	n/a
136	273	183	7.356	Moanalua Side, Weighted 3 pts		[183, 7.356],	n/a	n/a
137	273	183	4.437	Moanalua Side, Weighted 3 pts		[183, 4.437],	n/a	n/a
138	272.4	182.4	4.27	Moanalua Side, Weighted 3 pts		[182.4, 4.27],	n/a	n/a
139	271.7	181.7	4.051	Moanalua Side, Weighted 3 pts		[181.7, 4.051],	n/a	n/a
140	267.1	177.1	3.09	Moanalua Side, Weighted 3 pts		[177.1, 3.09],	n/a	n/a
141	284	194	8.004	Moanalua Side, Weighted 3 pts		[194, 8.004],	n/a	n/a
142	268	178	3.079	Moanalua Side, Weighted 3 pts		[178, 3.079],	n/a	n/a
143	297.5	207.5	3.129	Moanalua Side, Weighted 3 pts		[207.5, 3.129],	n/a	n/a
144	273	183	8.208	Moanalua Side, Weighted 3 pts		[183, 8.208],	n/a	n/a
145	273	183	7.356	Moanalua Side, Weighted 3 pts		[183, 7.356],	n/a	n/a
146	273	183	4.437	Moanalua Side, Weighted 3 pts		[183, 4.437],	n/a	n/a
147	272.4	182.4	4.27	Moanalua Side, Weighted 3 pts		[182.4, 4.27],	n/a	n/a
148	271.7	181.7	4.051	Moanalua Side, Weighted 3 pts		[181.7, 4.051],	n/a	n/a
149	267.1	177.1	3.09	Moanalua Side, Weighted 3 pts		[177.1, 3.09],	n/a	n/a
150	284	194	8.004	Moanalua Side, Weighted 3 pts		[194, 8.004],	n/a	n/a
151	268	178	3.079	Moanalua Side, Weighted 3 pts		[178, 3.079],	n/a	n/a
152	297.5	207.5	3.129	Moanalua Side, Weighted 3 pts		[207.5, 3.129],	n/a	n/a
153	273	183	8.208	Moanalua Side, Weighted 3 pts		[183, 8.208],	n/a	n/a
154	273	183	7.356	Moanalua Side, Weighted 3 pts		[183, 7.356],	n/a	n/a
155	273	183	4.437	Moanalua Side, Weighted 3 pts		[183, 4.437],	n/a	n/a
156	272.4	182.4	4.27	Moanalua Side, Weighted 3 pts		[182.4, 4.27],	n/a	n/a
157	271.7	181.7	4.051	Moanalua Side, Weighted 3 pts		[181.7, 4.051],	n/a	n/a
158	267.1	177.1	3.09	Moanalua Side, Weighted 3 pts		[177.1, 3.09],	n/a	n/a
159	284	194	8.004	Moanalua Side, Weighted 3 pts		[194, 8.004],	n/a	n/a

[1] station along tunnel alignment

n/a dip azimuth and magnitude are derived from common plane calculations using apparent dip measurements taken at multiple locations

Halawa Quarry Active Pit Mapping - Outcrops used for Common Plane Analysis

	Start		End	
Outcrop	Lat	Long	Lat	Long
1	21.376207	-157.897226	21.376114	-157.897448
2	21.376114	-157.897448	21.375881	-157.897504
3	21.375796	-157.897416	21.375848	-157.896856

*Coordinates from google earth

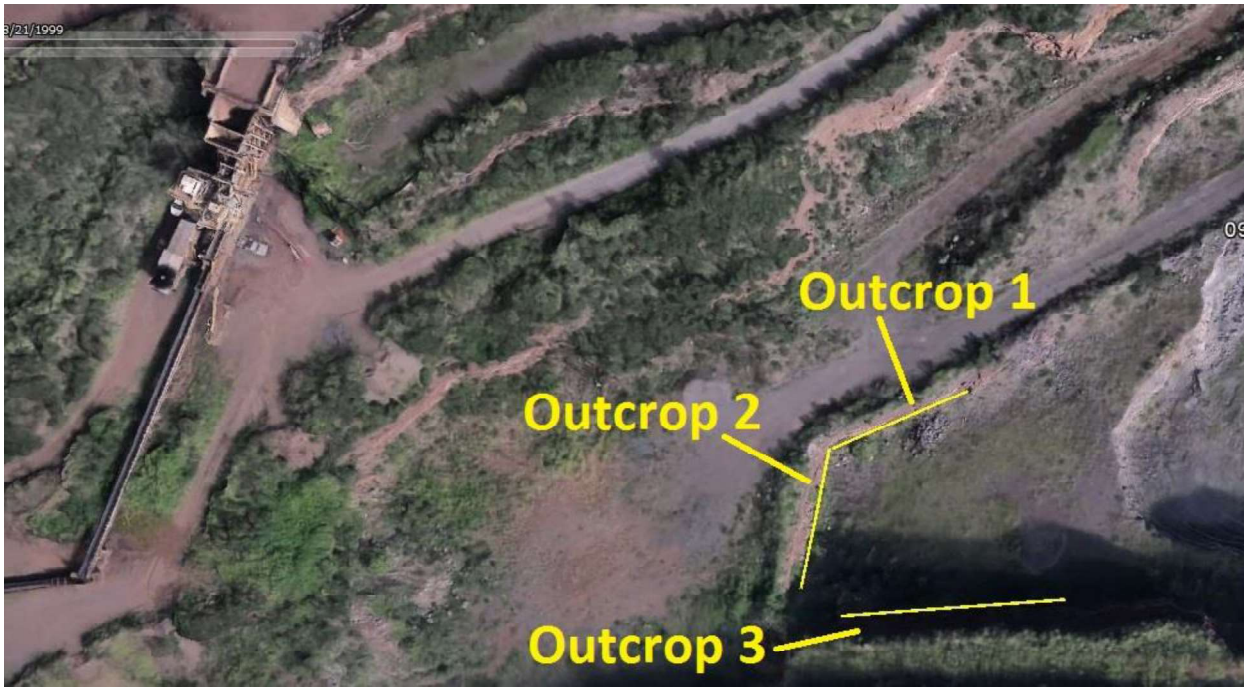

Halawa Quarry - Active Quarry Pit

Common Plane - Azimuth & Plunge Pairs	**Dip Direction**	**True Dip**	**Outcrop**
190º/6º and 265º/1.5º	189.426	6	2,3
190º/6º and 265º/2º	194.347	6.017	2,3
190º/6º and 245º/2º	173.585	6.253	2,1
190º/6º and 245º/3º	184.772	6.025	2,1
245º/2º and 265º/1.5º	215.969	2.287	1,3
245º/3º and 265º/2º	206.366	3.838	1,3
True Average:	**194.0775**	**5.07**	

Moanalua side of Red Hill from Tripler Ridge and in Moanalua Valley Mapping - Outcrops used for Common Plane Analysis

	Start		End	
Outcrop	Lat	Long	Lat	Long
A	21.369935	-157.893144	21.369962	-157.892368
B	21.375157	-157.883559	21.375654	-157.882614
C	21.37105	-157.889755	21.372091	-157.888742
D	21.377935	-157.875661	21.378232	-157.874895

*Coordinates from google earth

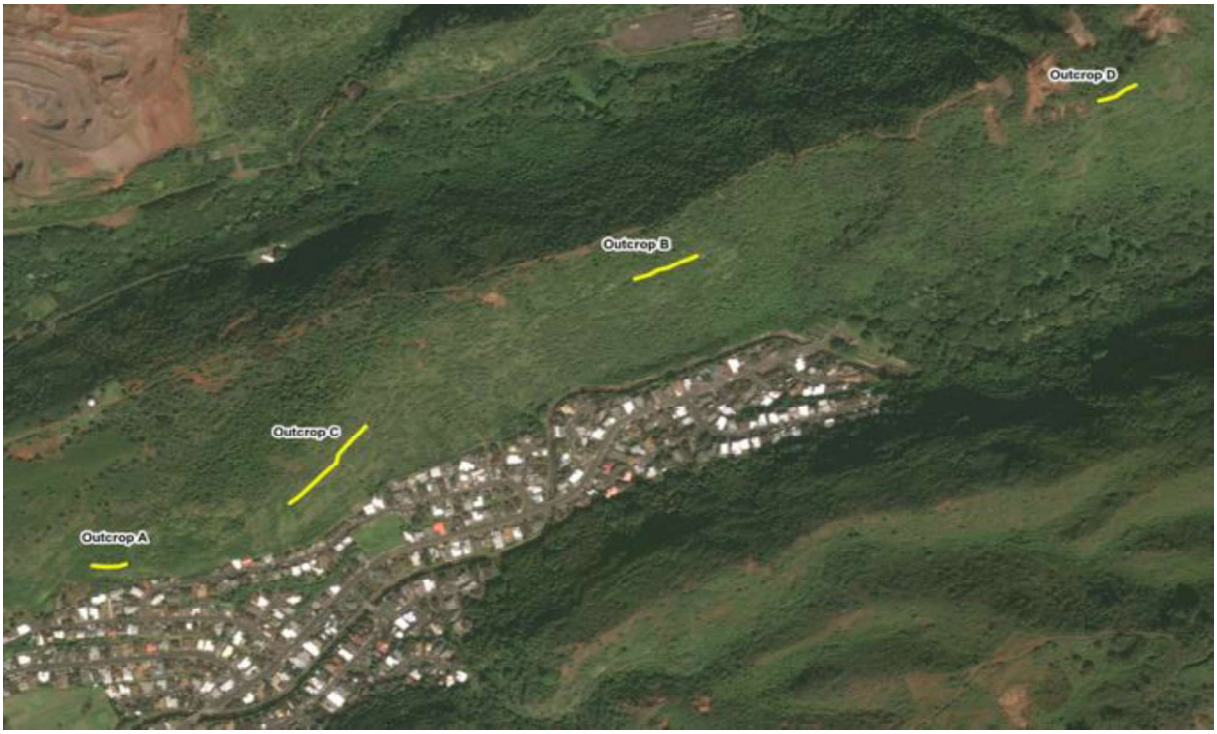

Data collected looking at Moanalua side of Red Hill from Tripler Ridge and in Moanalua Valley

	View Direction	Plane Direction (perpendicular to View Direction, i.e., azimuth)	App Dip	Outcrop
3 from Tripler	3	93	0	A
4 from Tripler	4	94	0	A
5 from Moanalua	5	95	0	B
16 from Tripler	16	106	1	B
255 from Moanalua	255	165	7	C
286 from Moanalua	286	196	8	B
281 from Tripler	281	191	3	C
293 from Tripler	293	203	4	C
314 from Tripler	314	224	3	C
358 from Tripler	358	268	0	D

Common Plane - Azimuth & Plunge Pairs	Dip Direction	True Dip	
191°/3 and 268°/0°	178	3.079	C, D
191°/3° and 224/3°	207.5	3.129	C, C
93°/0° and 196°/8°	183	8.208	A, B
93°/0° and 165°/7°	183	7.356	A, C
93°/0° and 106°/1°	183	4.437	A, B
106°/1° and 203°/4°	182.4	4.27	B, C
106°/1° and 224°/3°	181.7	4.051	B, C
106°/1° and 191°/3°	177.1	3.09	B, C
165°/7° and 196°/8°	194	8.004	C, B
True Average:	**185.5222**	**5.0693**	

Appendix D:
Evaluation of Potential Pāhoehoe Lava Flow Paths through Tank Farm Area

This page intentionally left blank

Evaluation of Potential Pāhoehoe Lava Flow Paths through Tank Farm Area

Random walk modeling was performed to evaluate the potential historical lava flow paths passing through the vicinity of the tanks. Lava flows were simulated using a probabilistic model recently developed by Vitturi and Tarquini (2018). The authors coded the model in Python. The software, named MrLavaLoba, is publicly available. The authors have applied the software to simulate the pāhoehoe lava flow during a Kilauea volcano eruption. The associated model parameters and input file to MrLavaLoba are provided as an example released with the software. The modeling for this evaluation was performed based on these parameters.

The downslope direction and angle were represented by an initial digital elevation model (DEM) generated based on dip orientation of azimuth of 213.6 degrees and dip angle of 2.9 degrees. The lava flow pathlines were simulated from a location upgradient from the tank farm. The starting locations were randomly generated along the yellow dashed line shown on Figure D-1. The extent of this line was selected to include possible lava flow paths through the tank farm area.

According to the study by Bruno et al. (1992), pāhoehoe lava flow paths show fractal characteristics, with fractal dimension ranging from 1.13 to 1.23. Since MrLavaLoba does not simulate fractal characteristics, the lava flow paths it generates might not fall within this fractal dimension range. Therefore, a Python code was developed for this evaluation to ignore the lava flow paths that have fractal dimension outside this range.

Figure D-1 shows examples of 20 simulated pathlines, the locations of the tanks, and the Red Hill Shaft footprint. A total of 10,000 Monte Carlo simulations of random pathlines were generated. Of these 10,000 simulated pathlines, 3,635 pathlines passed through the tank farm area and have fractal dimensions within the range of 1.13 to 1.23. None of the pathlines through the tank farm area also passed through the Red Hill Shaft area. Even if a pathline passes through the tank farm area and the Red Hill Shaft area, it might not pass through the elevation intervals of concern. In addition, a lava flow path does not imply a continuous channel that forms a chemical migration preferential pathway. Therefore, the results indicated that it is unlikely that a preferential pathway exists between the tank farm area and Red Hill Shaft area in relation to historical lava flows.

References

Bruno, B. C., G. J. Taylor, S. K. Rowland, P. G. Lucey, and S. Self. 1992. "Lava Flows Are Fractals." *Geophysical Research Letters* 19 (3): 305–308.

Vitturi, M. D. M., and S. Tarquini. 2018. "MrLavaLoba: A New Probabilistic Model for the Simulation of Lava Flows as a Settling Process." *Journal of Volcanology and Geothermal Research* 349: 323–334.

S:\Projects\NAVFAC PAC\CLEAN V\60571032_CTO18F0126\900-Work\920 GIS\02_Maps\CSM\AppD_FigD-1_PreferentialPathways.mxd 6/20/2019

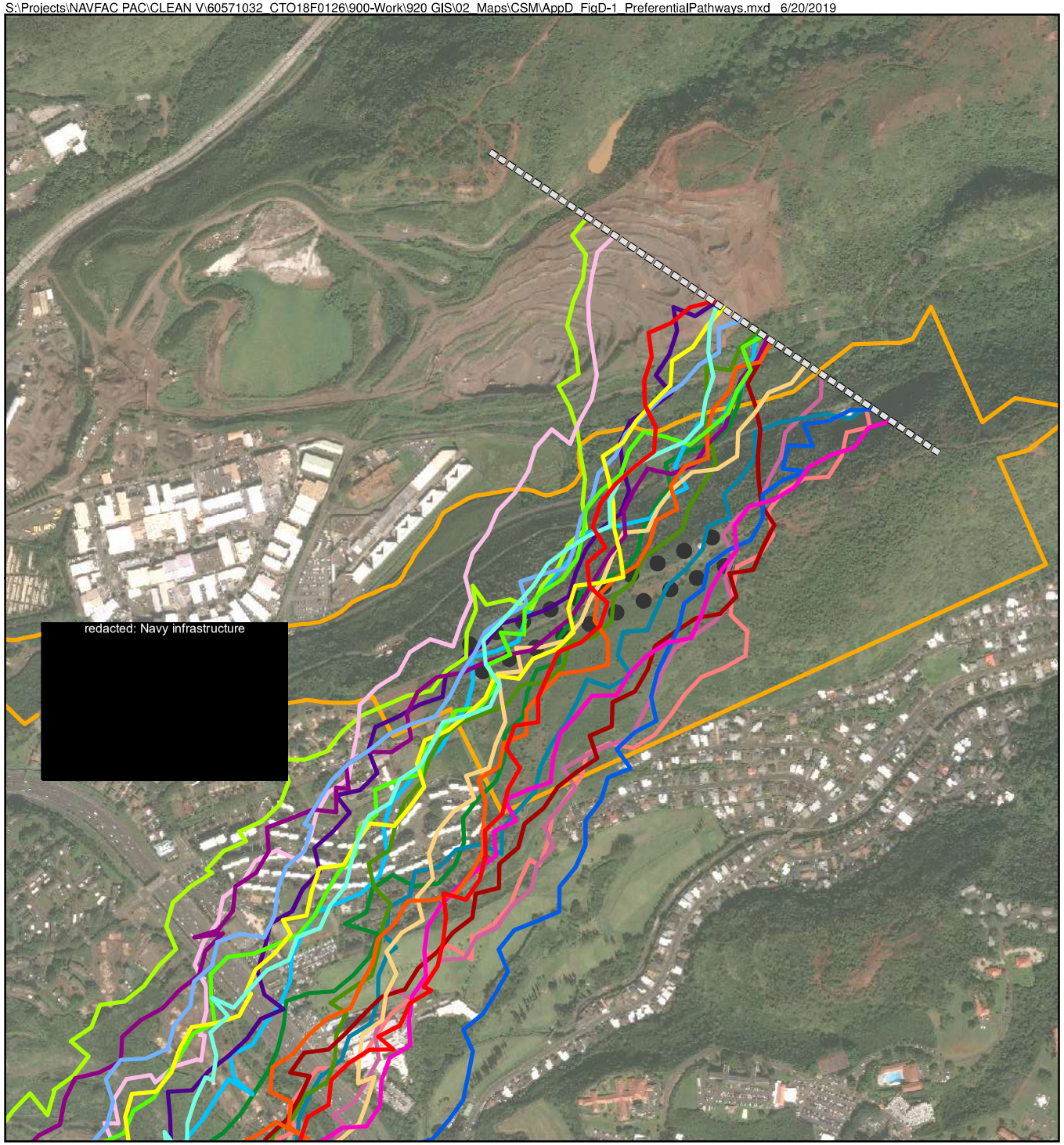

Location Map

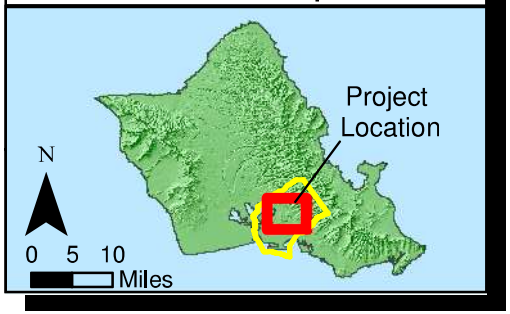

Legend

- Extent of Random Lava Flow Path Initiation
- Groundwater Model Domain
- Red Hill Facility Boundary and Fuel Storage Tanks

Notes

1. Map projection: NAD 1983 Hawaii State Plane Zone 3 feet.
2. DigitalGlobe, Inc. (DG) and NRCS. Publication_Date: 2015

N

0 500 1,000 2,000 Feet

Figure D-1
Preferential Pathways
Conceptual Site Model Rev. 01
Investigation and Remediation of Releases and Groundwater Protection and Evaluation
Red Hill Bulk Fuel Storage Facility
JBPHH, O'ahu, Hawai'i

Appendix E:
Geologic Framework Model

This page intentionally left blank

CONTENTS

Acronyms and Abbreviations E-ii

1. Red Hill Geologic Framework Model E-1

1.1 Saturated Clinker Evaluation E-3
1.2 Clinker/Pāhoehoe Volume Evaluation E-4

2. Three-Dimensional (3D) Regional Geologic Model E-6

2.1 Regional Geologic Model Data Sets E-6
2.1.1 USGS Caprock Thickness Data Sets E-6
2.1.2 Regional Geologic Cross Sections E-7
2.1.3 Geophysical Investigation E-7
2.1.4 Volcanic Tuff Mapping E-8
2.1.5 Marine Sediments E-10
2.1.6 South Hālawa Valley Base of Saprolite Interpretations E-10
2.2 Model Interpolation E-13

3. References E-13

ATTACHMENTS

E.1 Regional Geologic Cross Sections

FIGURES

E-1 Red Hill Geologic Cross Section Location Map E-1
E-2 External Grid (oblique view) E-2
E-3 Red Hill 3D Geologic Block Diagram E-3
E-4 Extent of Saturated Clinker (oblique view to the northeast) E-4
E-5 Scenario Zone Designations E-5
E-6 Extent of 3D Regional Geologic Model E-6
E-7 Regional Geologic Cross-Section Location Map E-7
E-8 Geophysical Investigation 3D Rendering E-8
E-9 Surface Tuff and Crater Rim Extent E-9
E-10 3D Block Diagram of Tuff Complex E-9
E-11 3D Block Diagram of Marine Sediments and Tuff Crater E-10
E-12 South Hālawa Valley Base of Saprolite (lower bound interpretation) E-11
E-13 South Hālawa Valley Base of Saprolite (upper bound interpretation) E-12
E-14 3D Regional Geologic Model Spatial Data Set E-13

TABLE

E-1 Clinker / Pāhoehoe Percent Volume Results E-5

ACRONYMS AND ABBREVIATIONS

3D	three-dimensional
EVS	Earth Volumetric Studio
ft	foot/feet
GIS	geographic information system
USGS	United States Geological Survey

1. Red Hill Geologic Framework Model

A geologic framework model was generated using CTECH's Earth Volumetric Studio (EVS) software. The lithologic information used to generate the model was derived from two primary sources and housed in a Microsoft Access database. The first data source came from available borehole lithology where lithologic contacts were pulled from borehole logs and tabulated in a simple flat-file format for inclusion into the lithology database. The second lithology source was derived from a series of geologic cross sections in the vicinity of Red Hill and several others throughout the groundwater flow model domain (Figure E-1). These cross sections were subdivided into a series of artificial boreholes with a horizontal spacing of 100–500 feet (ft). Lithologic contacts from these artificial boreholes were tabulated in a flat-file format and incorporated into the lithology database for interpolation.

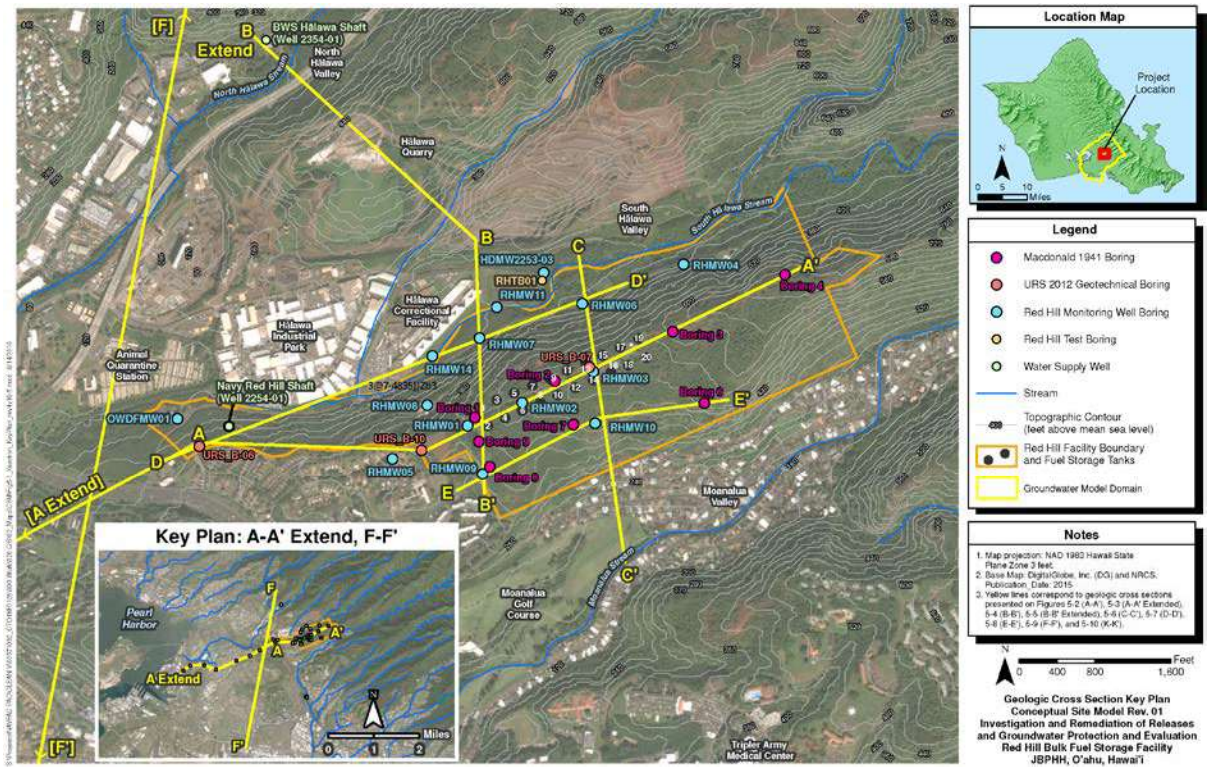

Figure E-1: Red Hill Geologic Cross Section Location Map

Interpolation of the lithologic contacts was achieved via adaptive indicator kriging. Adaptive indicator kriging applies kriging to a user-defined external grid and further refines it by splitting whole cells along boundaries between two or more materials to create smoother surfaces. The external grid used for the geologic framework model had an approximate horizontal cell size of 165 ft × 165 ft with 280 cells along the x-axis and 190 cells along the y-axis. Proportional gridding was used to establish the vertical thickness where a z-axis resolution of 100 was specified. Finally, the horizontal/vertical anisotropy was set at 100 (Figure E-2).

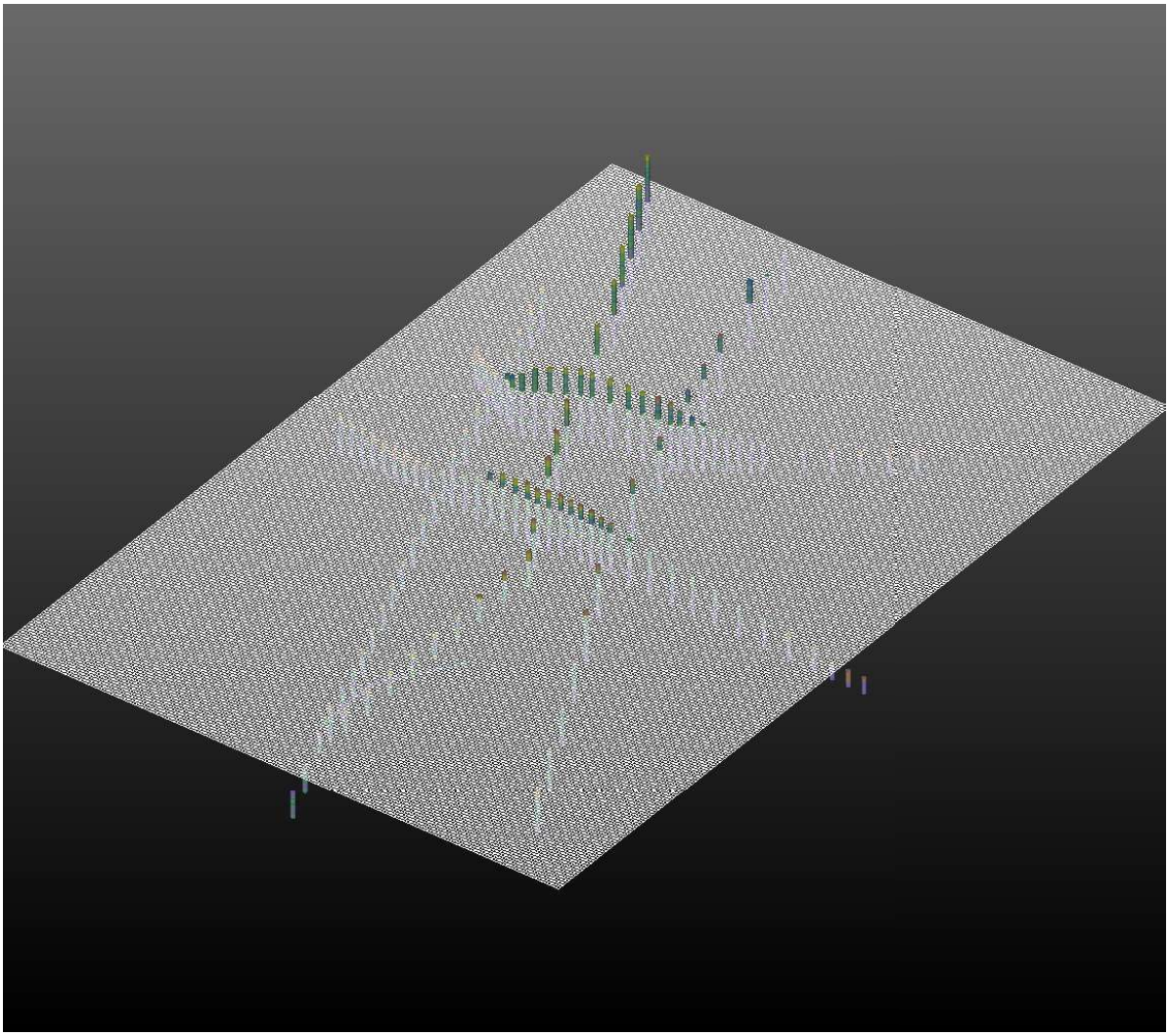

Figure E-2: External Grid (oblique view)

The resulting interpolation yielded a geologic block consisting of the following five primary soil/rock types: alluvium, saprolite, massive a'ā basalt, a'ā clinker, and pāhoehoe (Figure E-3).

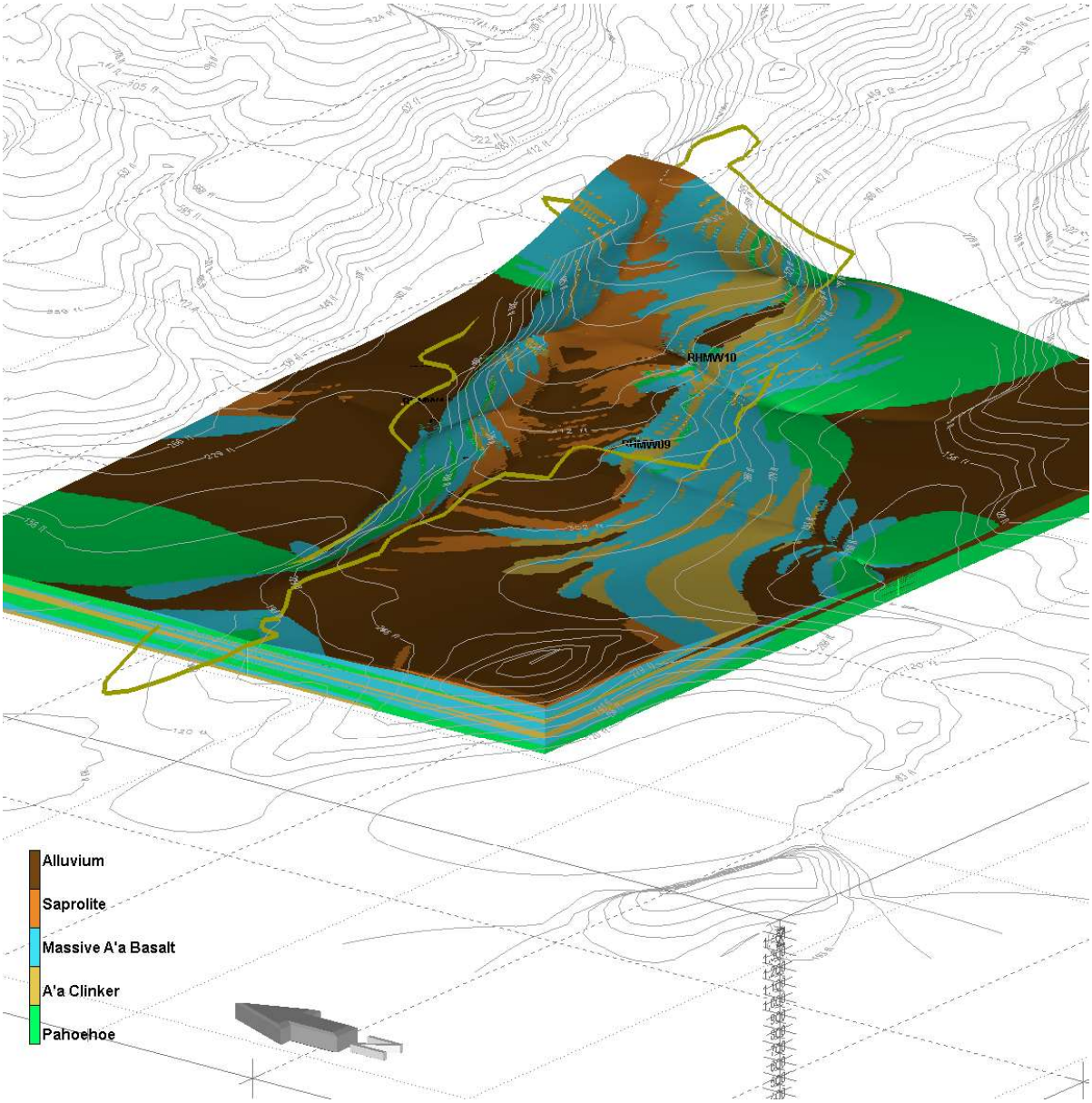

Figure E-3: Red Hill 3D Geologic Block Diagram

Various work products were developed from the geologic block. Specifically, fence diagrams in a variety of orientations along with volume calculations of specific material types from user-specified domains. A groundwater elevation surface was also introduced to visualize soil/rock types in the vadose zone versus saturated zone.

1.1 SATURATED CLINKER EVALUATION

The geologic framework model was used to visualize the extent of clinker beneath the water table. Groundwater data from the November 2016 synoptic gauging event was incorporated into the model to serve as an upper domain relative to the model's geologic block. The five soil/rock types that

compose the geologic block were turned off with exception of the clinker rock type to reveal its extent below the water table (Figure E-4).

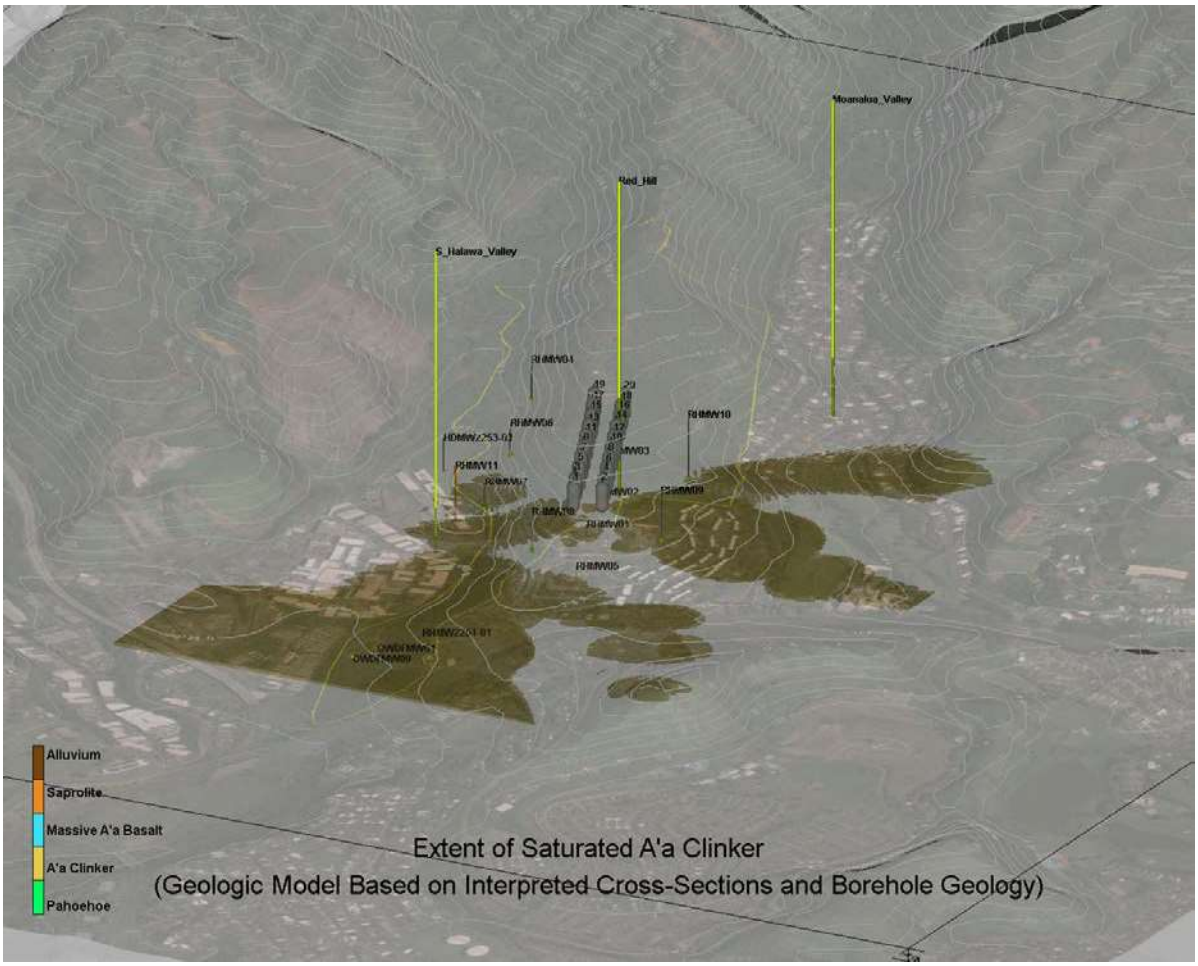

Figure E-4: Extent of Saturated Clinker (oblique view to the northeast)

1.2 CLINKER/PĀHOEHOE VOLUME EVALUATION

The geologic framework model was used to compute the estimated volume of clinker and pahoehoe within user specified domains. Two cells (1,600 ft × 1,600 ft and 720 ft × 720 ft) with specific elevation intervals (i.e., zones; Figure E-5) were specified domains for these volume computations. The EVS volumetric module was used to compute the volume of clinker and pāhoehoe within each zone against the overall geometric volume to achieve a percent total (see Table E-1). In addition to use for groundwater modeling, this geologic evaluation was also incorporated into the holding capacity analysis that was part of the *Groundwater Protection and Evaluation Considerations* report (DON 2018b).

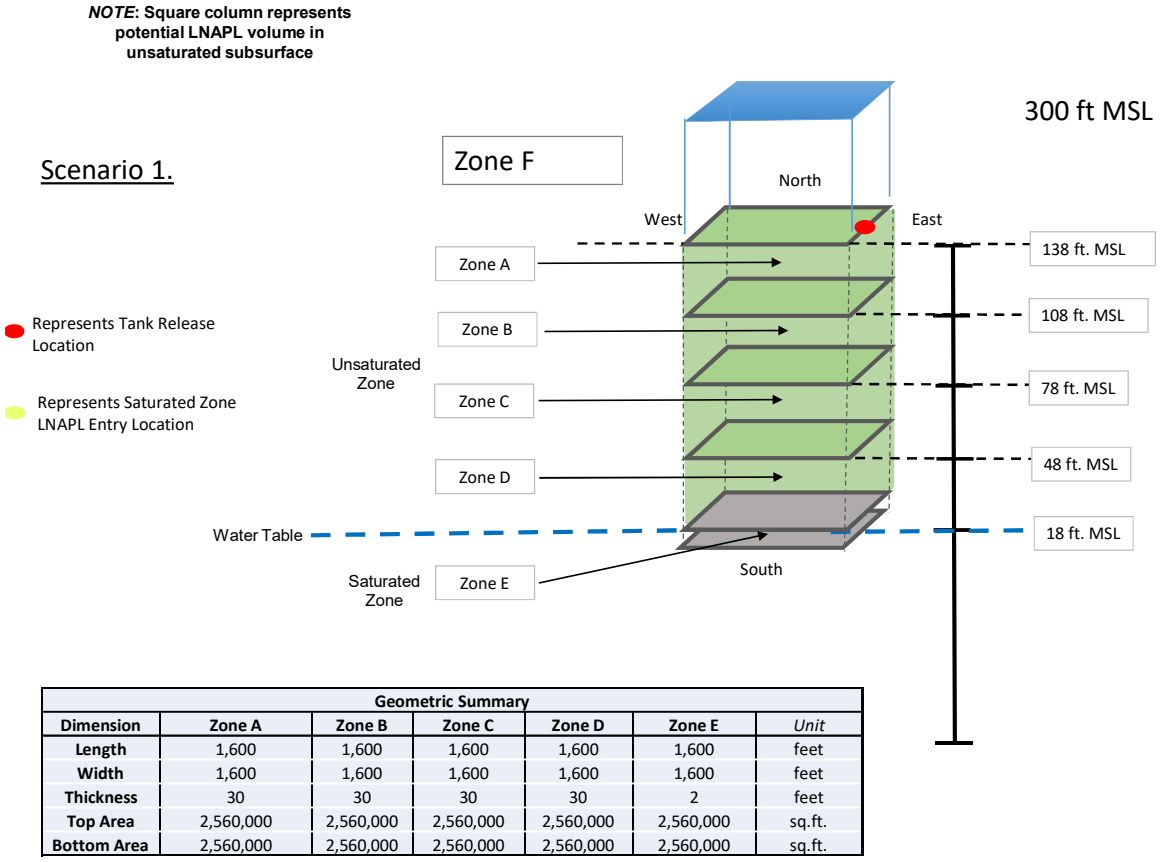

Geometric Summary						
Dimension	**Zone A**	**Zone B**	**Zone C**	**Zone D**	**Zone E**	*Unit*
Length	1,600	1,600	1,600	1,600	1,600	feet
Width	1,600	1,600	1,600	1,600	1,600	feet
Thickness	30	30	30	30	2	feet
Top Area	2,560,000	2,560,000	2,560,000	2,560,000	2,560,000	sq.ft.
Bottom Area	2,560,000	2,560,000	2,560,000	2,560,000	2,560,000	sq.ft.

1 **Figure E-5: Scenario Zone Designations**

2 **Table E-1: Clinker / Pāhoehoe Percent Volume Results**

Zone	Elevation Interval (ft)	Total Volume (cu. ft.)	Clinker Volume (cu. ft.)	Pāhoehoe Volume (cu. ft.)	% Clinker	% Pāhoehoe
Scenario 1 (1,600 ft × 1,600 ft Cell)						
F	300–138	4.15E+08	1.04E+08	4.54E+07	25%	11%
A	138–108	7.68E+07	9.93E+06	3.88E+07	13%	50%
B	108–78	7.68E+07	1.48E+06	4.43E+07	2%	58%
C	78–48	7.68E+07	1.94E+06	5.73E+07	3%	75%
D	48–18	7.68E+07	3.02E+06	6.40E+07	4%	83%
E	18–16	5.12E+06	5.68E+04	4.98E+06	1%	97%
Scenario 2 (720 ft × 720 ft Cell)						
F	300–138	8.40E+07	2.16E+07	8.82E+06	26%	11%
A	138–108	1.56E+07	1.11E+06	1.10E+07	7%	70%
B	108–78	1.56E+07	5.74E+03	9.78E+06	0.04%	63%
C	78–48	1.56E+07	2.49E+05	1.25E+07	2%	80%
D	48–18	1.56E+07	0.00E+00	1.45E+07	0%	93%
E	18–16	1.04E+06	0.00E+00	1.04E+06	0%	100%

2. Three-Dimensional (3D) Regional Geologic Model

In addition to the Red Hill-specific geologic model, a 3D regional geologic model was developed to provide stratigraphic support for the groundwater flow model. The model extent mirrored the extent of the groundwater flow model domain, which is approximately 9 miles along the northeast/southwest and approximately 6 miles in the northwest/southeast direction (Figure E-6).

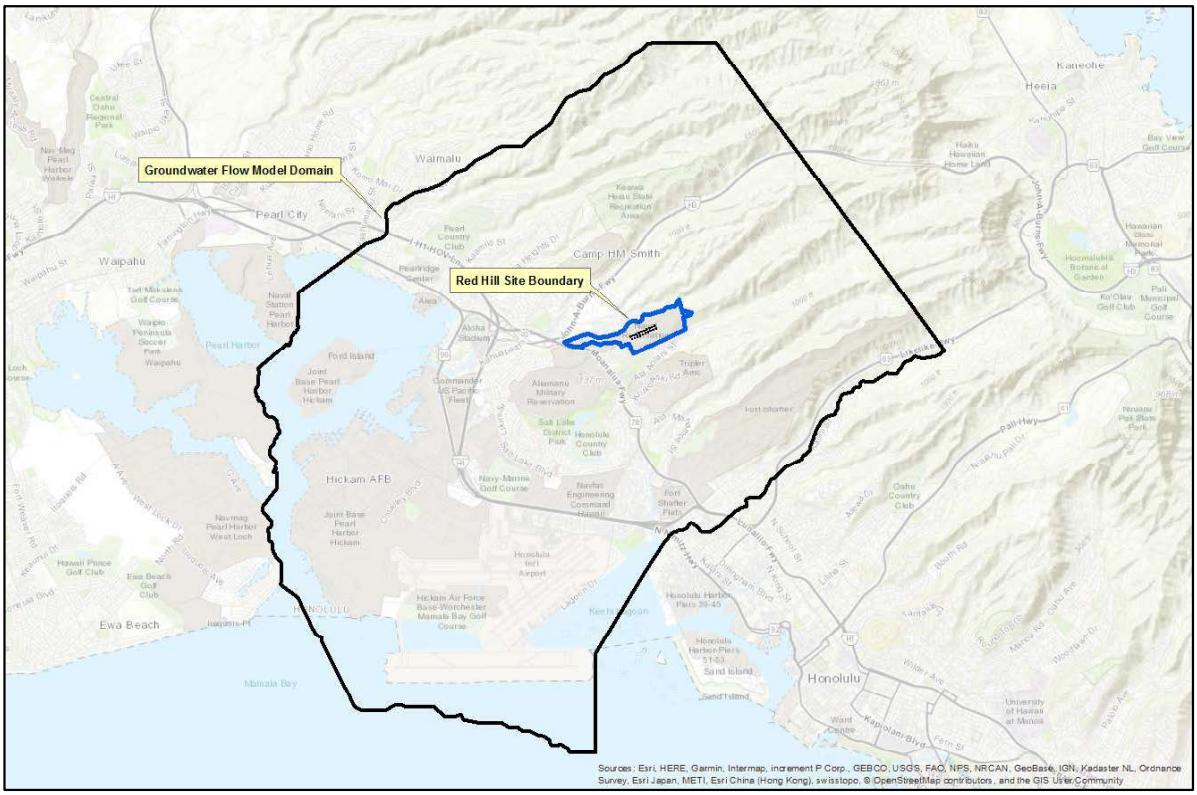

Figure E-6: Extent of 3D Regional Geologic Model

2.1 Regional Geologic Model Data Sets

Several data sources were used to develop the 3D regional geologic model. These sources included:

- United States Geological Survey (USGS) caprock thickness structural contour data sets
- Regional geologic cross sections
- Geophysical investigation study
- Volcanic tuff and pyroclastic mapping
- Marine sediment mapping
- South Hālawa Valley base of saprolite interpretations

2.1.1 USGS Caprock Thickness Data Sets

On July 20, 2017, the USGS provided the Navy with two preliminary spatial data sets depicting the thickness of the Caprock hydrogeological unit and the structural surface elevation contours of the

underlying undifferentiated basalt. These data sets were provided as geographic information system (GIS) shapefiles and served as the basis of the 3D regional geologic model as it relates to caprock thickness and surface elevation of the undifferentiated basalt.

2.1.2 Regional Geologic Cross Sections

Regional geologic cross sections were incorporated into the model to provide additional lithologic detail beyond what was provided in the USGS data sets. Cross-section locations are shown on Figure E-7; the cross-section diagrams are presented in Attachment E.1. Specifically, the geologic cross sections provided lithologic contact elevations for undifferentiated basalt, saprolite, alluvium, tuff, and marine deposits. These cross sections were subdivided into a series of artificial boreholes with a horizontal spacing of 500–1,000 ft. Lithologic contacts from these artificial boreholes were tabulated in a flat-file format and incorporated into the lithology database for interpolation.

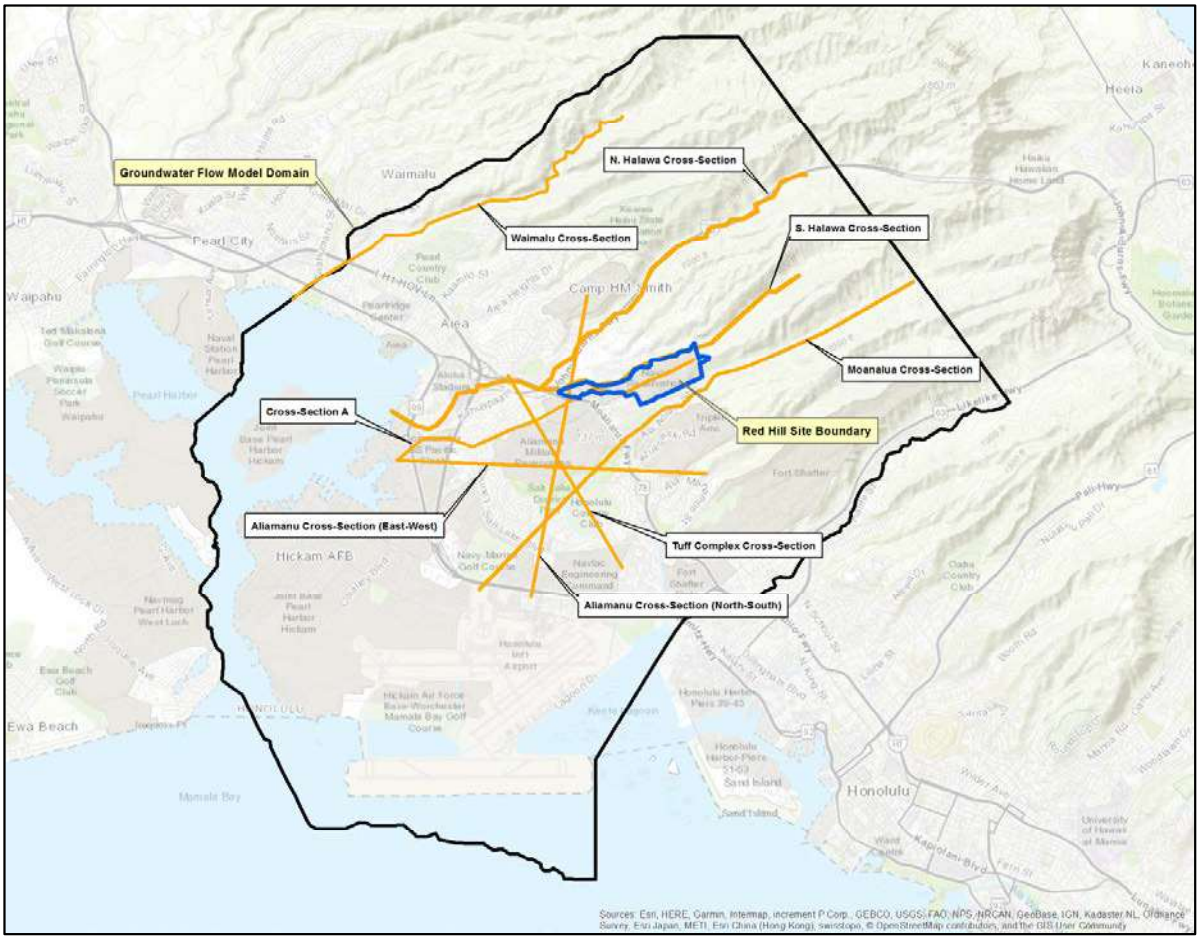

Figure E-7: Regional Geologic Cross-Section Location Map

2.1.3 Geophysical Investigation

A geophysical investigation was performed to better understand the extent of saprolite in the valleys adjacent to the Red Hill site. A seismic refraction and reflection survey was performed along a series of transects located on Red Hill and in North/South Hālawa and Moanalua Valleys. Findings from the

seismic study (DON 2018a) were incorporated into the regional geologic cross sections used in development of the 3D model (Figure E-8).

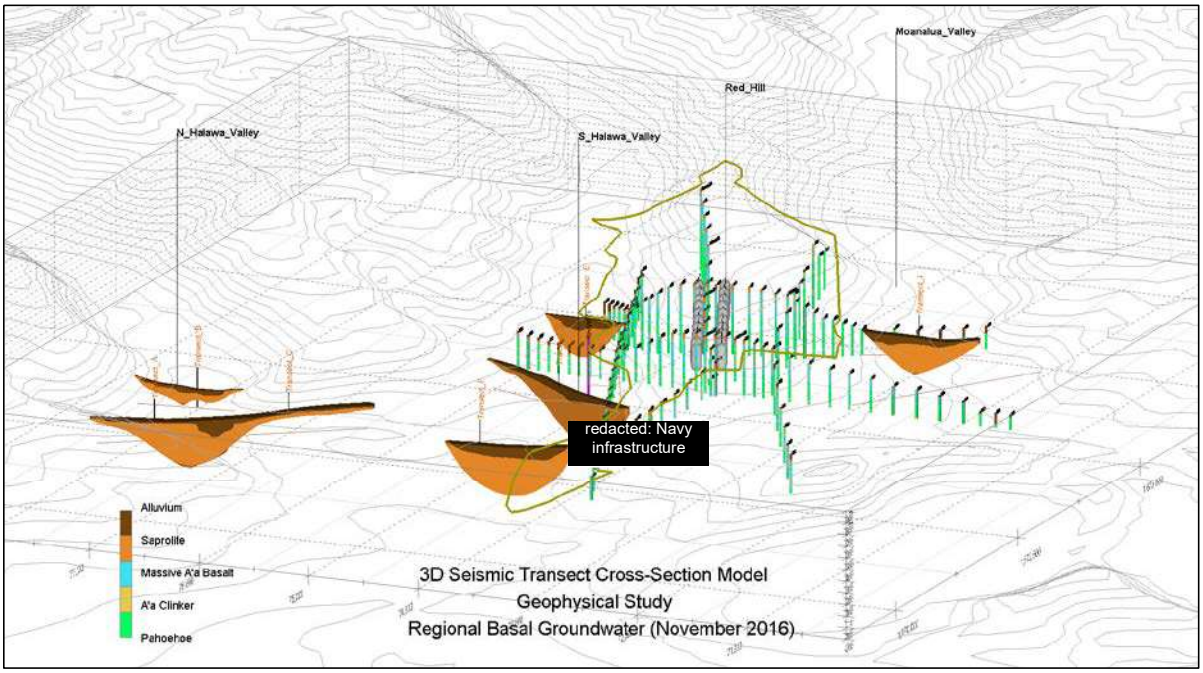

Figure E-8: Geophysical Investigation 3D Rendering

2.1.4 Volcanic Tuff Mapping

A series of pyroclastic craters and associated surface tuff deposits were incorporated into the 3D model based on a study of the Salt Lake Area by Pankiwskyj (1972). Figures from this study were used to delineate the crater rims and surface tuff extent through georeferencing in a GIS software platform. These features were then subsequently transferred into the 3D model for interpolation (Figure E-9 and Figure E-10).

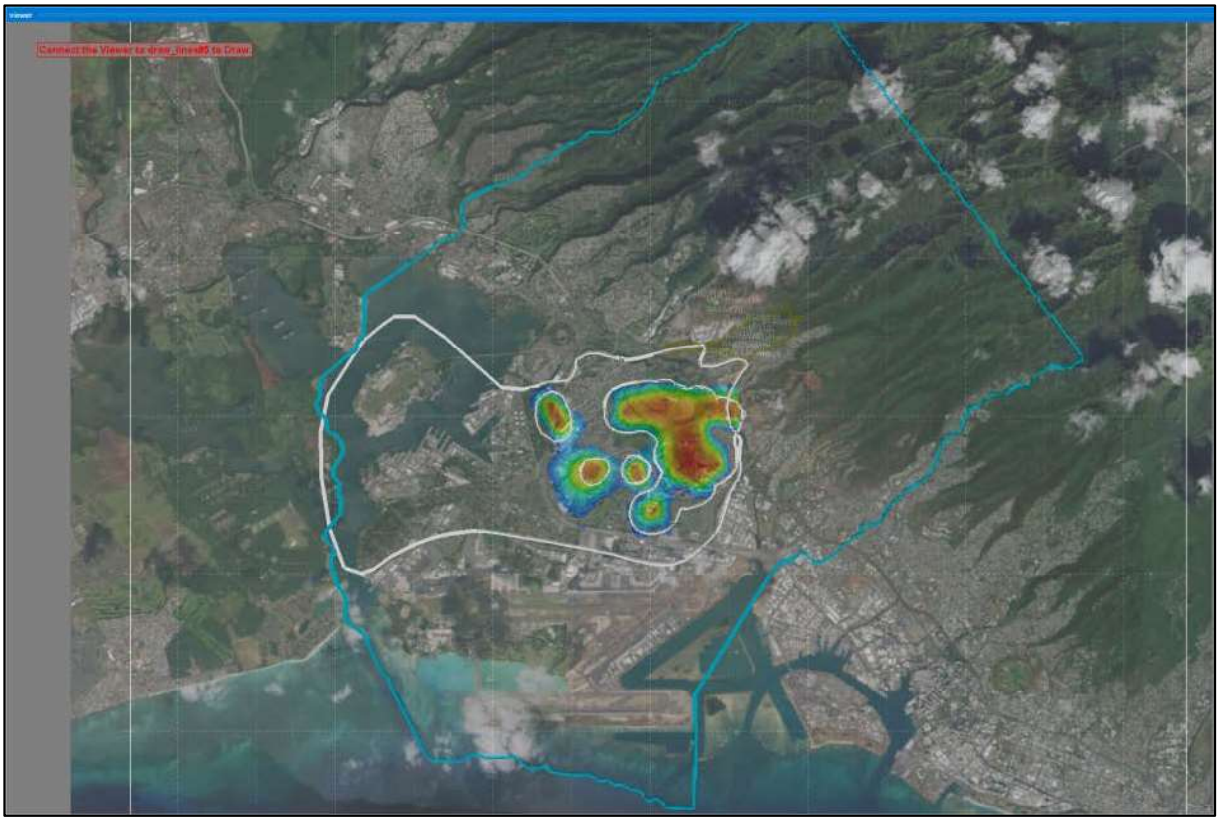

Figure E-9: Surface Tuff and Crater Rim Extent

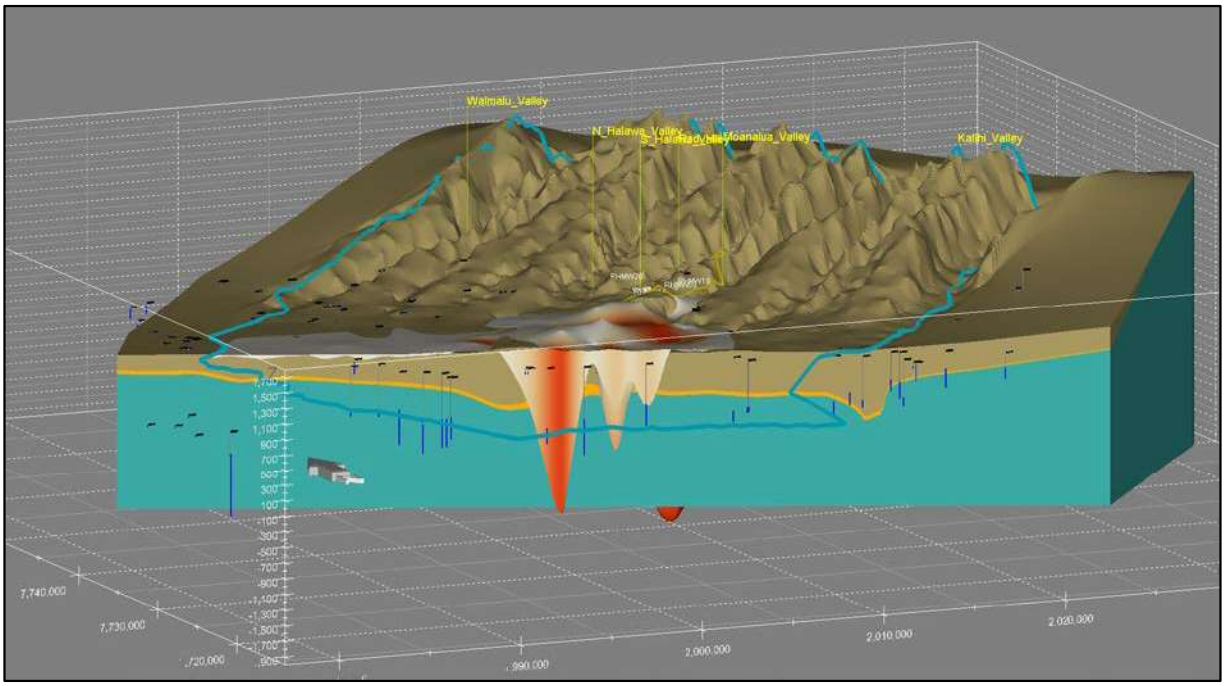

Figure E-10: 3D Block Diagram of Tuff Complex

2.1.5 Marine Sediments

Marine sediments were conceptually incorporated into the model and spatially situated based on available geologic mapping. The marine sediment lithology database and subsequent interpolation was generated in a fashion to show a transgression/regression pattern indicative of a coastal sediment depositional environment (Figure E-11).

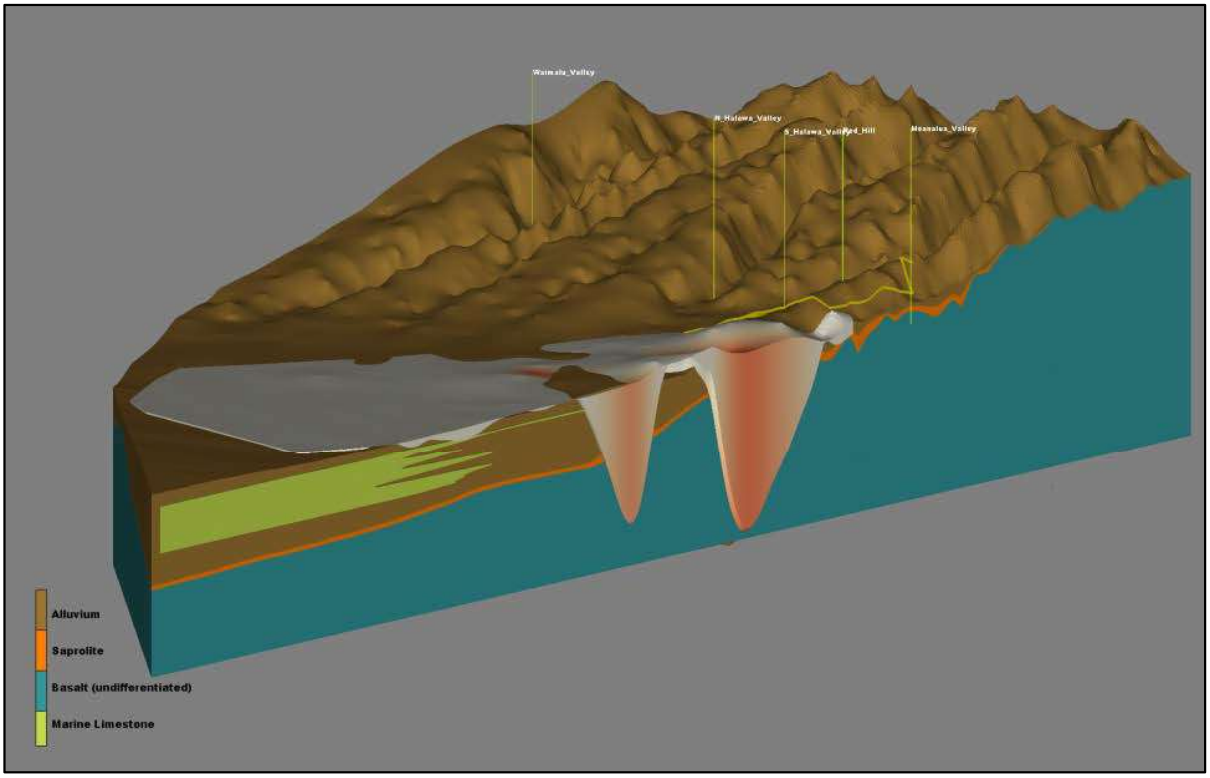

Figure E-11: 3D Block Diagram of Marine Sediments and Tuff Crater

2.1.6 South Hālawa Valley Base of Saprolite Interpretations

Two cross-section interpretations, an upper bound and a lower bound, situated along the South Hālawa Valley resulted in two versions of the 3D geologic model. These interpretations relate to the base of saprolite contact elevation with one version having a saprolite contact depth approximately 50 ft lower. As a result, two dedicated stand-alone geologic models were generated as the "Navy" and "DOH" interpretations (Figure E-12 and Figure E-13, respectively).

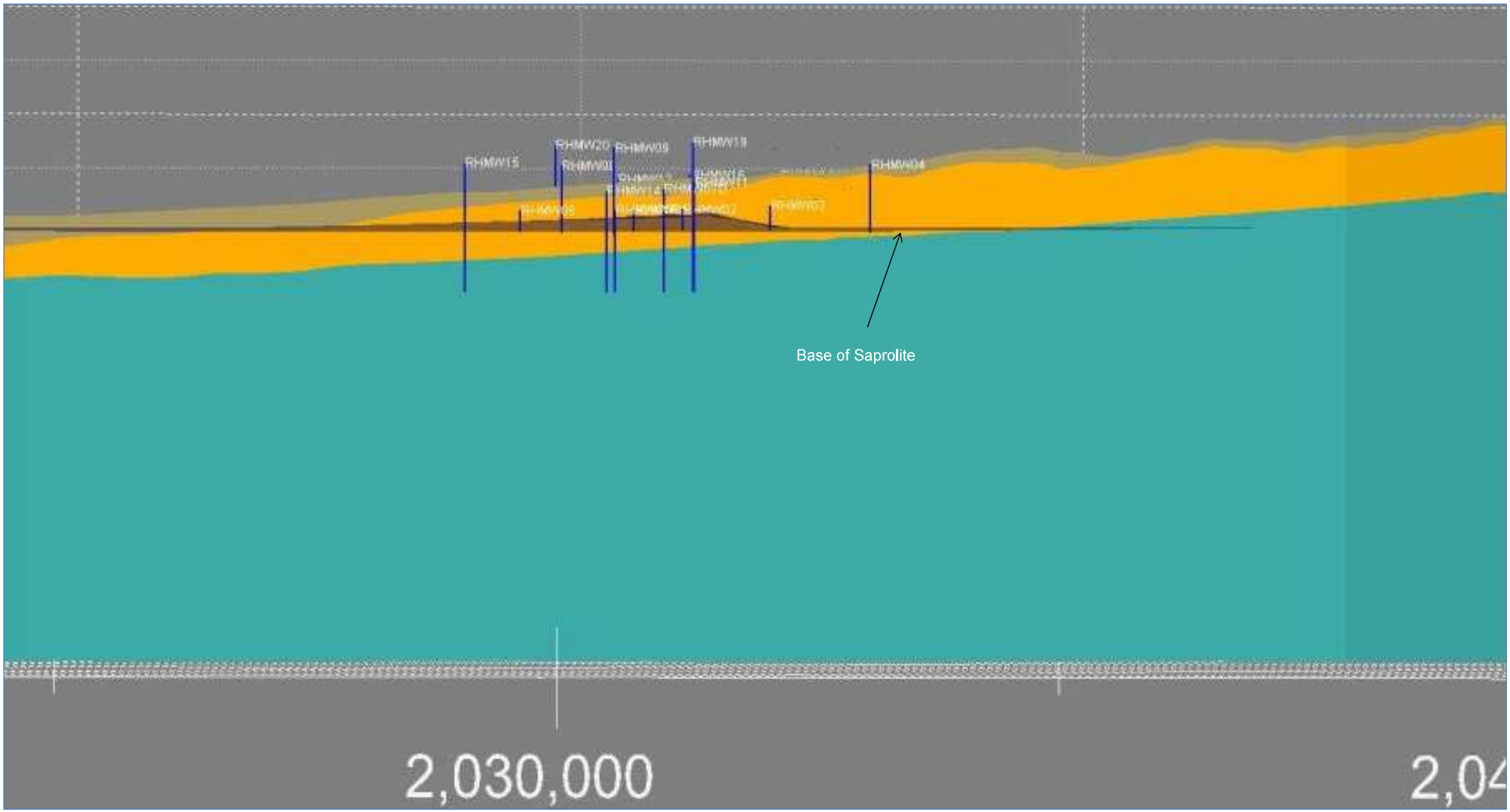

Figure E-12: South Hālawa Valley Base of Saprolite (lower bound interpretation)

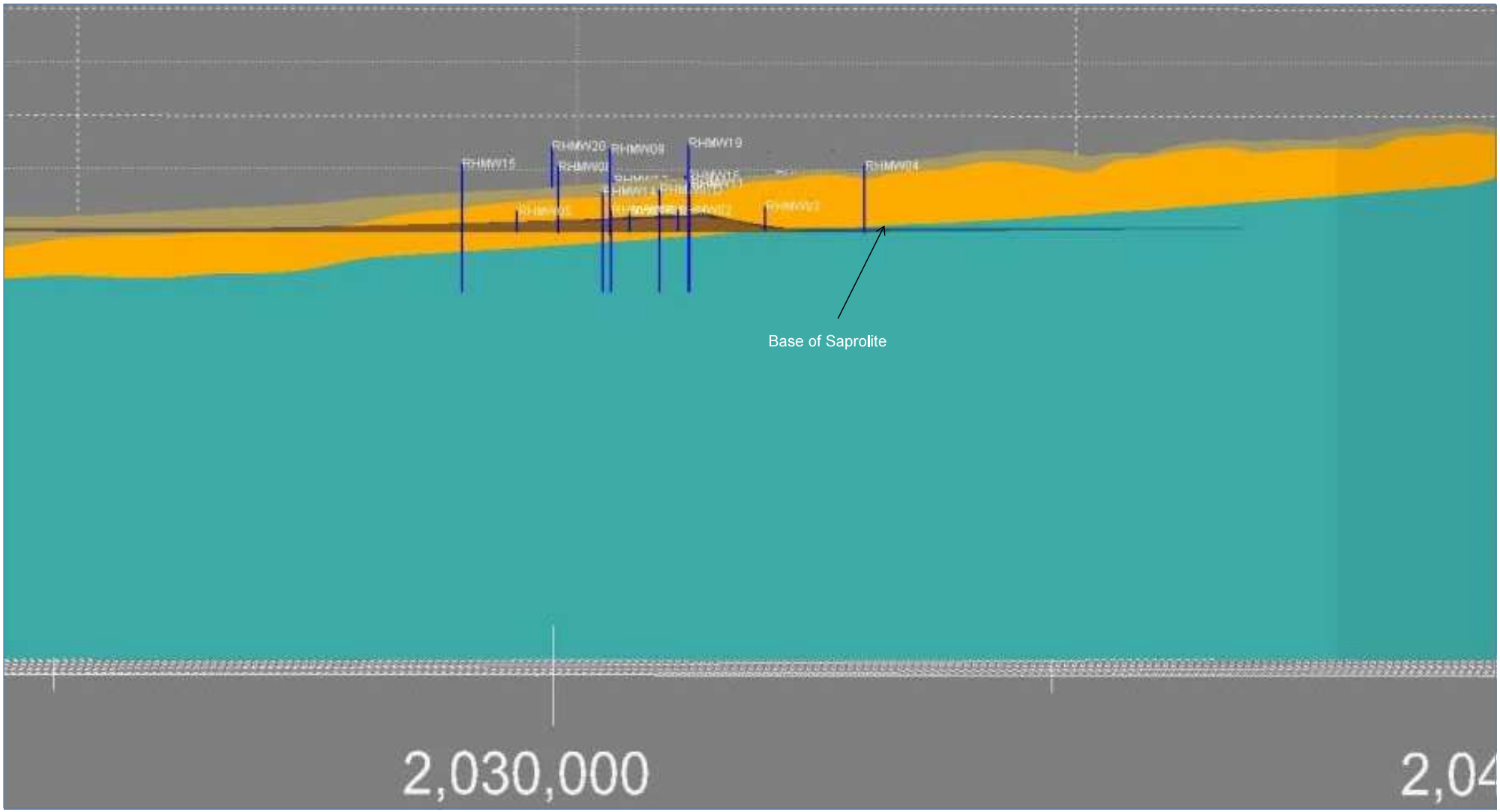

Figure E-13: South Hālawa Valley Base of Saprolite (upper bound interpretation)

2.2 MODEL INTERPOLATION

Pertinent geologic contacts from the aforementioned data sets were tabulated and housed in a Microsoft Access database consisting of 2,909 spatial data points. Each point represents the location of discrete geologic contacts (up to five depending on geology at that location). A higher concentration of data points resides in the nearby North/South Hālawa and Moanalua Valleys due to a variety of subsurface investigations in those areas (see Figure E-14). Interpolation of this spatial data set was performed in EVS via the krig_3D_geology module. This module interpolates data into a series of geologic horizons where each elevation represents a geologic surface at that point in space. Several kriging estimation methods within the krig_3D_geology module are available for use. The Natural Neighbors kriging estimation method was used to generate the 3D geologic block diagram.

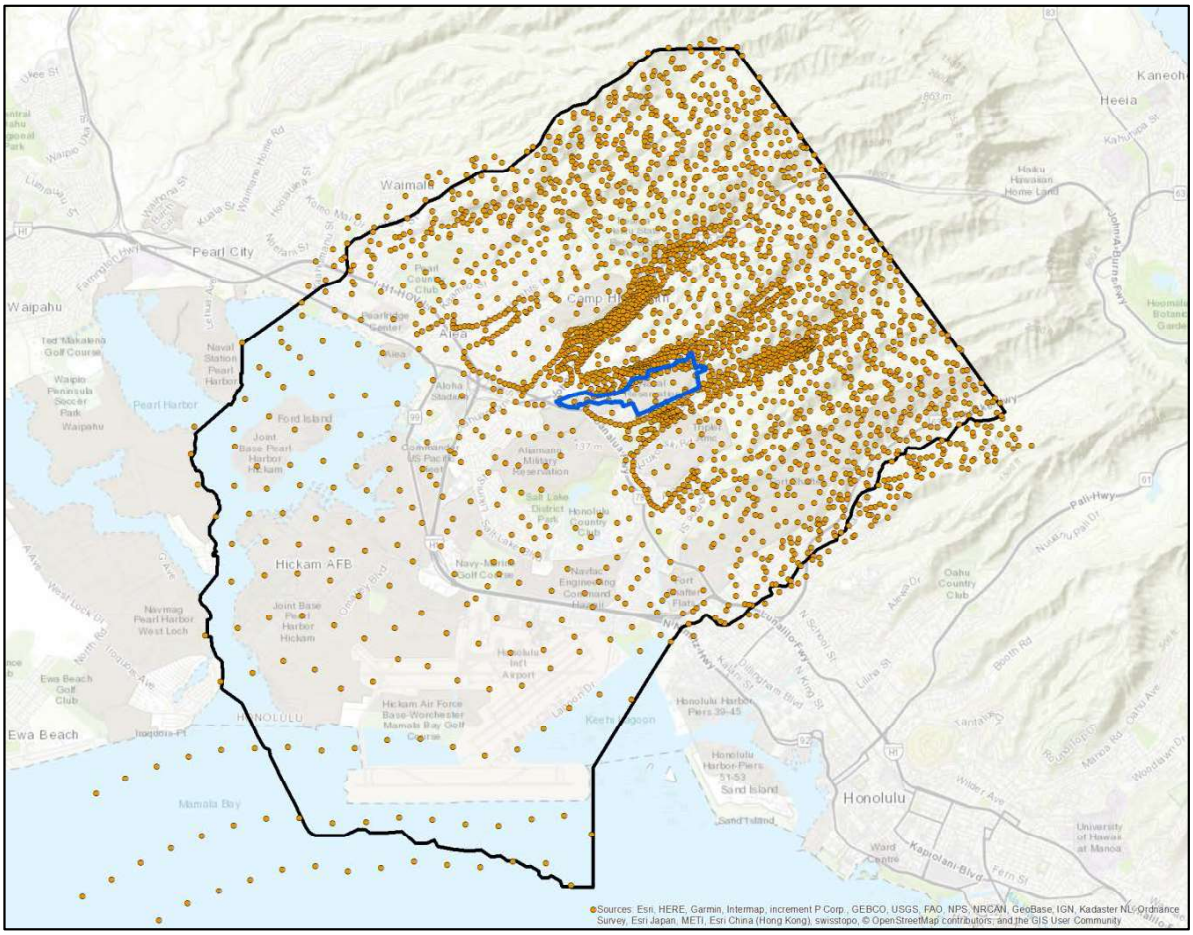

Figure E-14: 3D Regional Geologic Model Spatial Data Set

3. References

Department of the Navy (DON). 2018a. *Seismic Profiling to Map Hydrostratigraphy in the Red Hill Area, Red Hill Bulk Fuel Storage Facility, Joint Base Pearl Harbor-Hickam, O'ahu, Hawai'i; March 30, 2018, Revision 00.* Prepared by Lee Liberty and James St. Claire, Boise State University, Boise, ID, for AECOM Technical Services, Inc., Honolulu, HI. Boise State University Technical Report BSU CGISS 18-01. Prepared for Defense Logistics Agency Energy, Fort Belvoir, VA, under Naval Facilities Engineering Command, Hawaii, JBPHH HI.

———. 2018b. *Groundwater Protection and Evaluation Considerations for the Red Hill Bulk Fuel Storage Facility, Joint Base Pearl Harbor-Hickam, O'ahu, Hawai'i; July 27, 2018, Revision 00.* Prepared by AECOM Technical Services, Inc., Honolulu, HI. Prepared for Defense Logistics Agency Energy, Fort Belvoir, VA, under Naval Facilities Engineering Command, Hawaii, JBPHH HI.

Pankiwskyj, K. A. 1972. "Geology of the Salt Lake Area, Oahu, Hawaii." *Pacific Science* 26 (2): 242–253.

Attachment E.1:
Regional Geologic Cross Sections

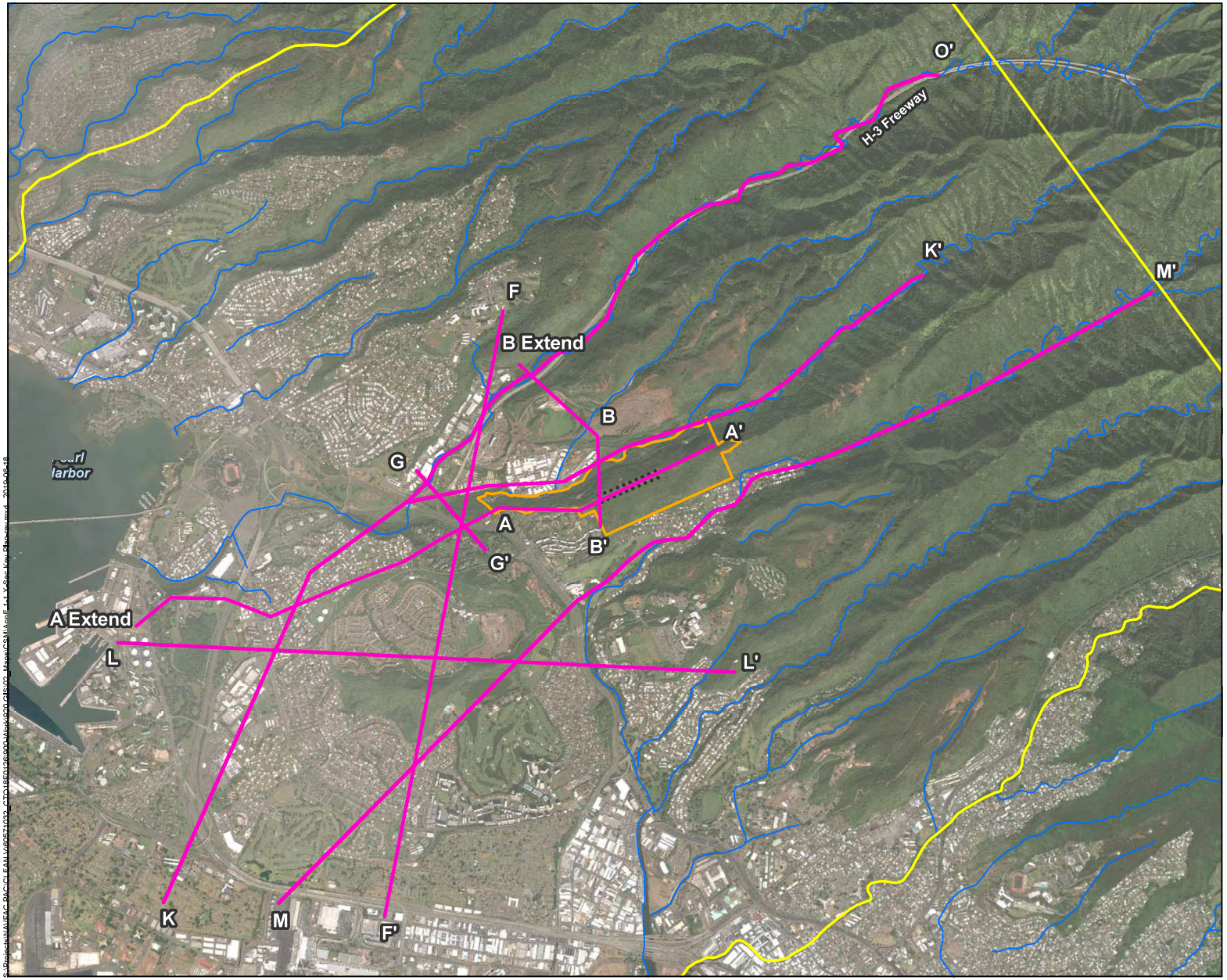

Location Map

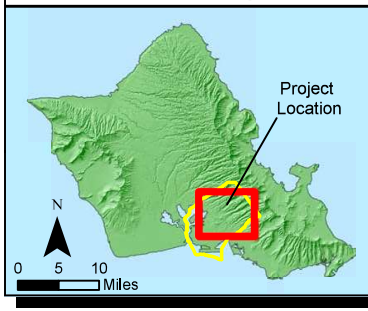

Legend

- Geologic Cross Section
- Groundwater Model Domain
- Red Hill Facility Boundary and Fuel Storage Tanks
- Stream

Notes

1. Map projection: NAD 1983 Hawaii State Plane Zone 3 feet
2. DigitalGlobe, Inc. (DG) and NRCS. Publication_Date: 2015

N

0 1,250 2,500 5,000 Feet

Figure E.1-1
Geologic Model Cross Section Key Plan
Conceptual Site Model Rev. 01
Investigation and Remediation of Releases and Groundwater Protection and Evaluation
Red Hill Bulk Fuel Storage Facility
JBPHH, O'ahu, Hawai'i

C:\Users\Mark.Higley\Documents\Autodesk\geomodel_180910.dwg 9/11/2018 7:39 AM Mark.Higley

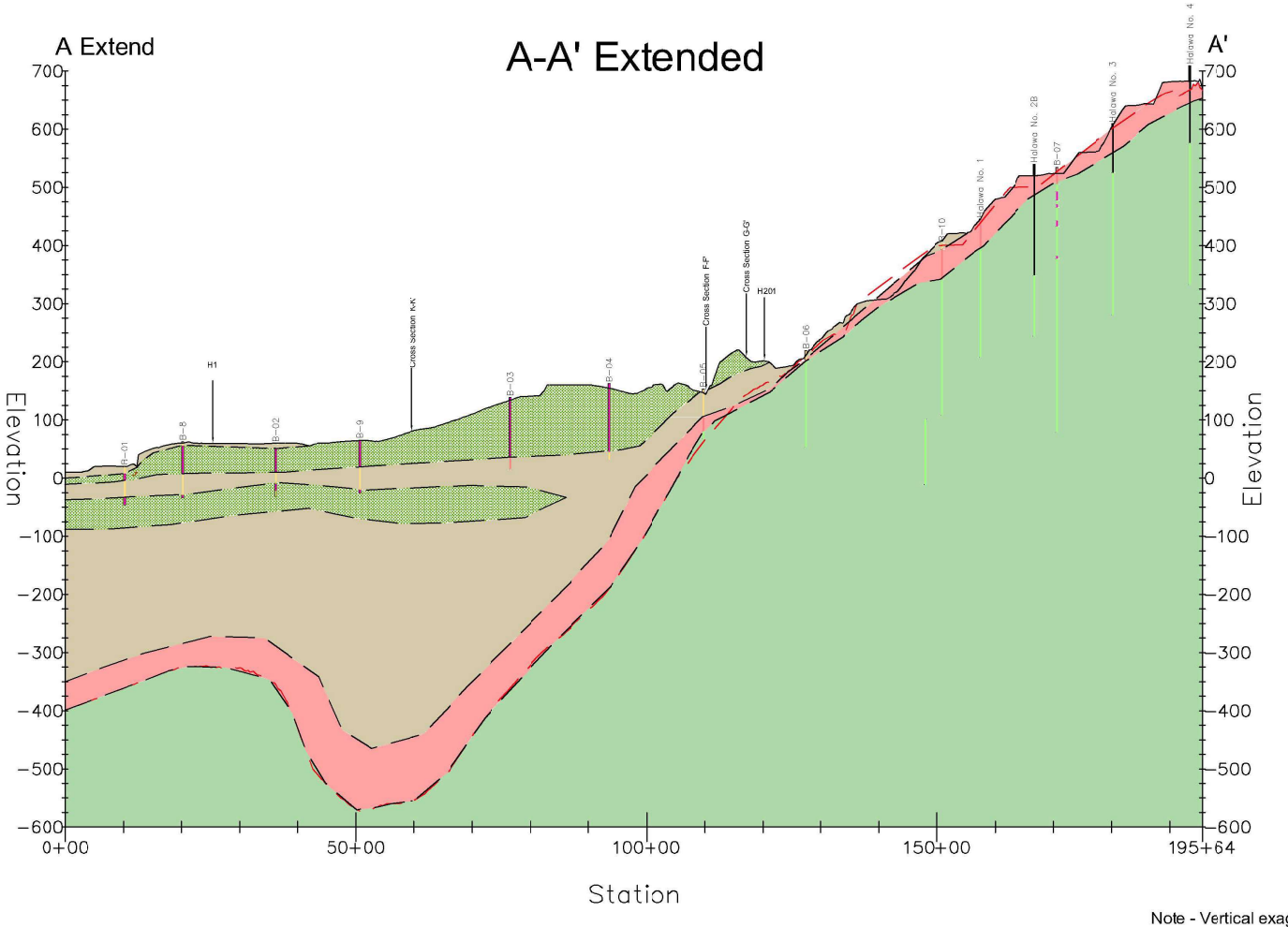

Note - Vertical exaggeration 10V/1H

LEGEND

- Alluvium
- Saprolite
- Basalt
- Basal Groundwater (approximate)
- Geologic Contact (approximate)
- Honolulu Volcanics - Tuff
- Top of Basalt (Izuka et al)

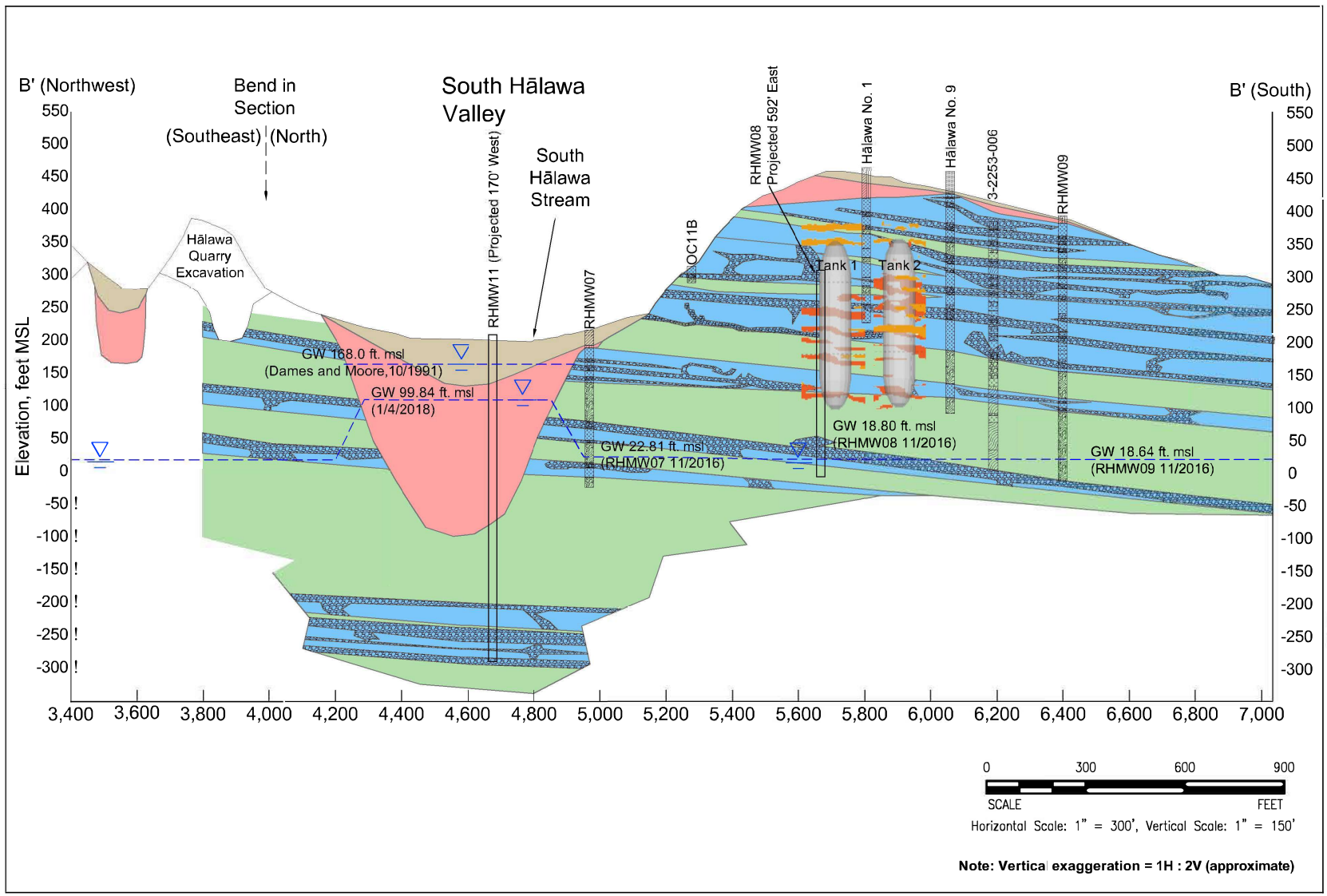

Key Plan

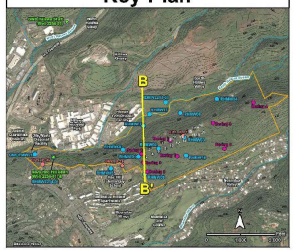

Legend

- Valley Fill 3
- Saprolite
- Basalt - A'ā Clinker
- Basalt - Massive A'ā
- Basalt Pāhoehoe
- Measured Groundwater (date)

Notes

1. RHMW07: DON 2015a
2. RHMW09: DON 2017e
3. Hālawa No.1, 9: Macdonald 1941
4. Outcrop OC11B: Field Notes 2017
5. As-Built Barrel Log: DON 1943
6. Westbay zone water levels in feet msl on 3/5/2018 (Table 6-1)

Cross Section B-B' (View Looking East)
Conceptual Site Model Revision 01
Investigation and Remediation of Releases and Groundwater Protection and Evaluation Red Hill Bulk Fuel Storage Facility, JBPHH, O'ahu, Hawai'i

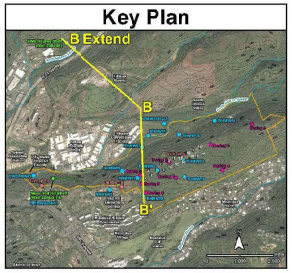

Legend

- Valley Fill
- Saprolite
- Basalt - A'ā Clinker
- Basalt - Massive A'ā
- Basalt Pāhoehoe
- Measured Groundwater (date)

Notes

1. RHMW07: DON 2015a
2. RHMW09: DON 2017e
3. Hālawa No.1, 9: Macdonald 1941
4. Outcrop OC11B: Field Notes 2017
5. As-Built Barrel Log: DON 1943

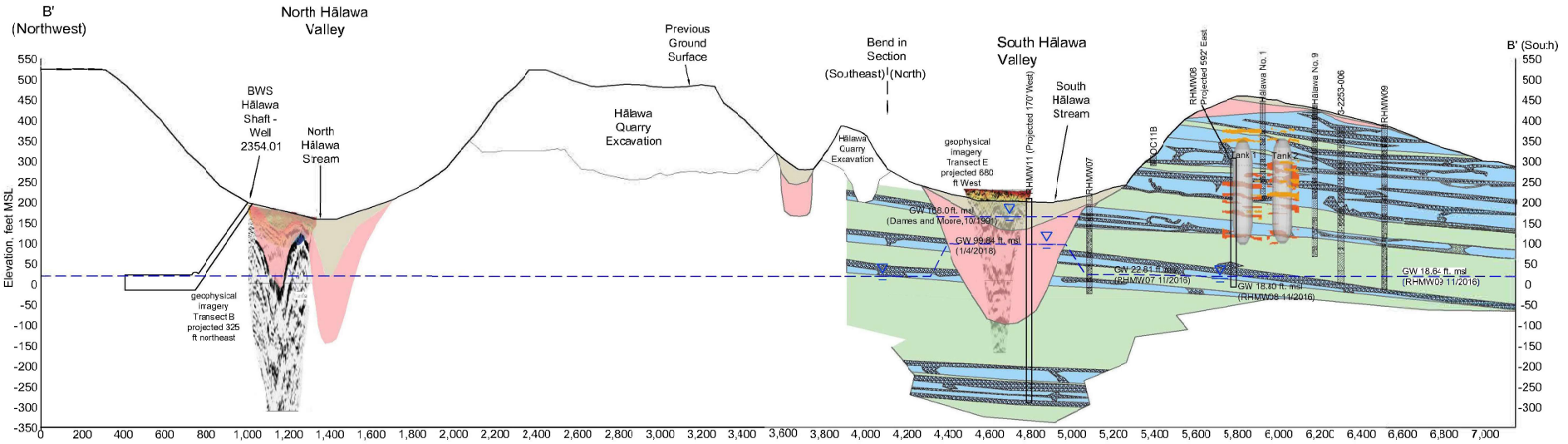

Note: Vertical exaggeration = 1H : 2V (approximate)

500' 0 500' 1000'

Horizontal Scale: 1" = 500', Vertical Scale: 1" = 250'

Cross Section B-B' Extended (View Looking East)
Conceptual Site Model Revision 01
Investigation and Remediation of Releases and Groundwater Protection and Evaluation
Red Hill Bulk Fuel Storage Facility, JBPHH, O'ahu, Hawai'i

Key Plan

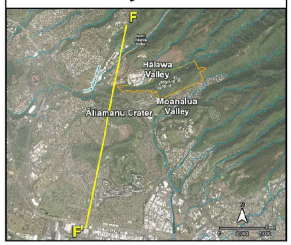

Legend

- Alluvium
- Saprolite
- Basalt (Undifferentiated)
- Honolulu Volcanics - Tuff
- Basal Groundwater (approximate)
- Geologic Contact (approximate)
- Top of Basalt (Izuka et al)

Notes

1. Stearns and Chamberlain, 1967
2. Hart Borings (2014-2016)
3. Izuka et. al., 2016
4. HDOT, 1988, I-H3-1(51)
5. HDOT, 1988, I-H3-1(54)
6. HDOT, 1987, I-H3-1 (3)

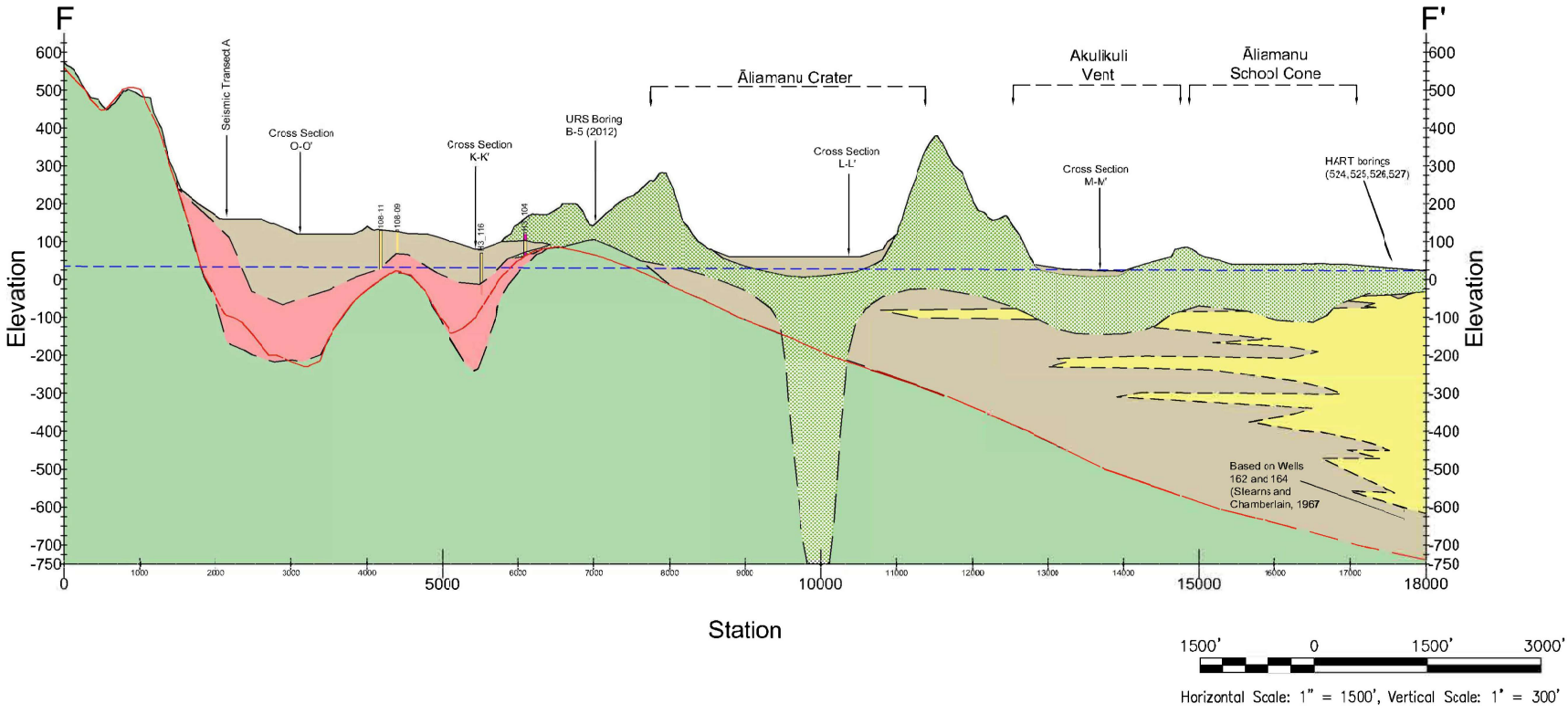

1500' 0 1500' 3000'

Horizontal Scale: 1" = 1500', Vertical Scale: 1" = 300'

Cross Section F-F' Āliamanu Crater Section
Conceptual Site Model Revision 01
Investigation and Remediation of Releases and Groundwater Protection and Evaluation
Red Hill Bulk Fuel Storage Facility, JBPHH, O'ahu, Hawai'i

G-G' - H3 interchange

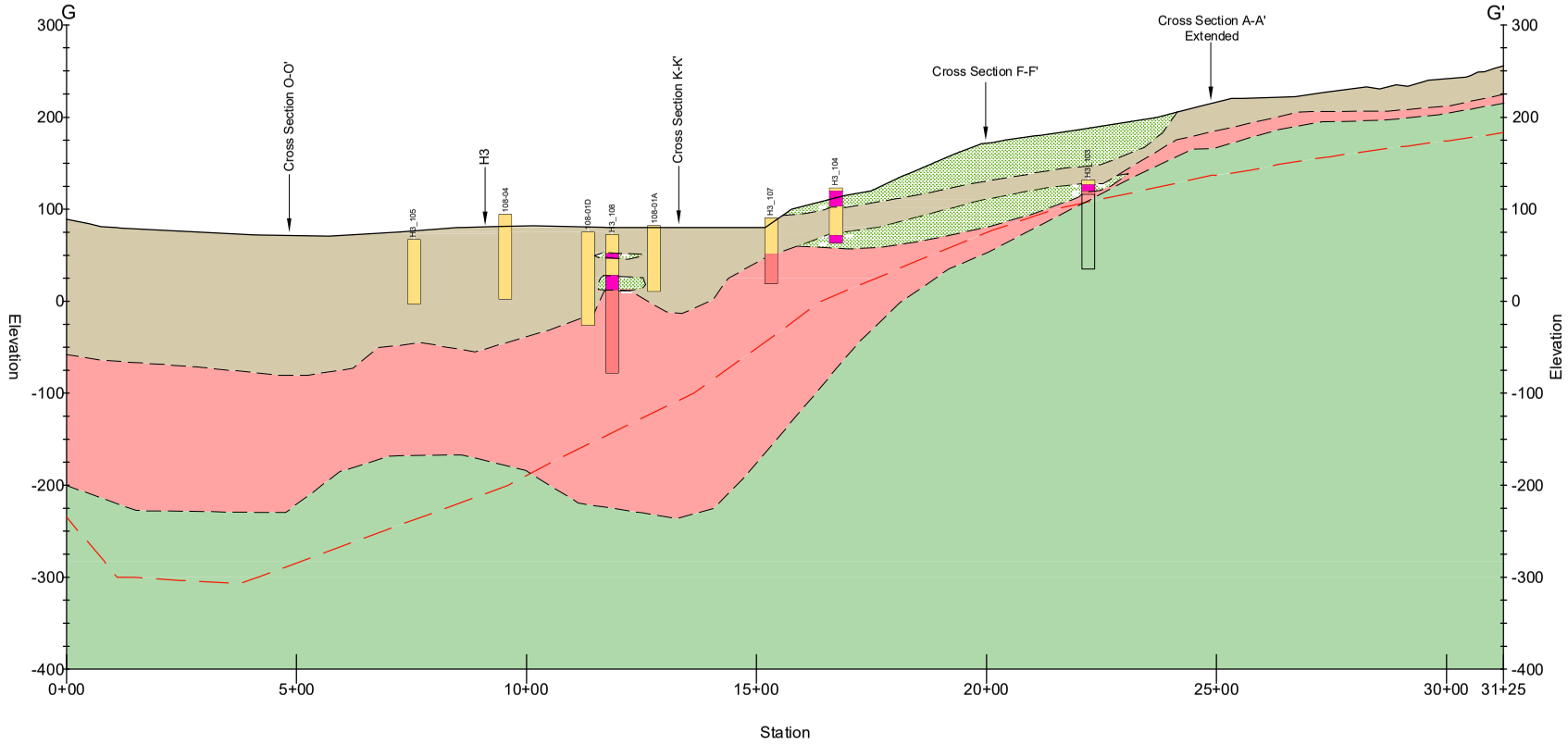

Note - Vertical exaggeration 2V/1H

LEGEND

- Alluvium
- Saprolite
- Basalt
- Basal Groundwater (approximate)
- Geologic Contact (approximate)
- Honolulu Volcanics - Tuff
- Top of Basalt (Izuka et al)

C:\Users\Mark.Higley\Documents\Autodesk\model area surface contours_180910.dwg 9/11/2018 7:39 AM Mark.Higley

K-K' - South Halawa Valley

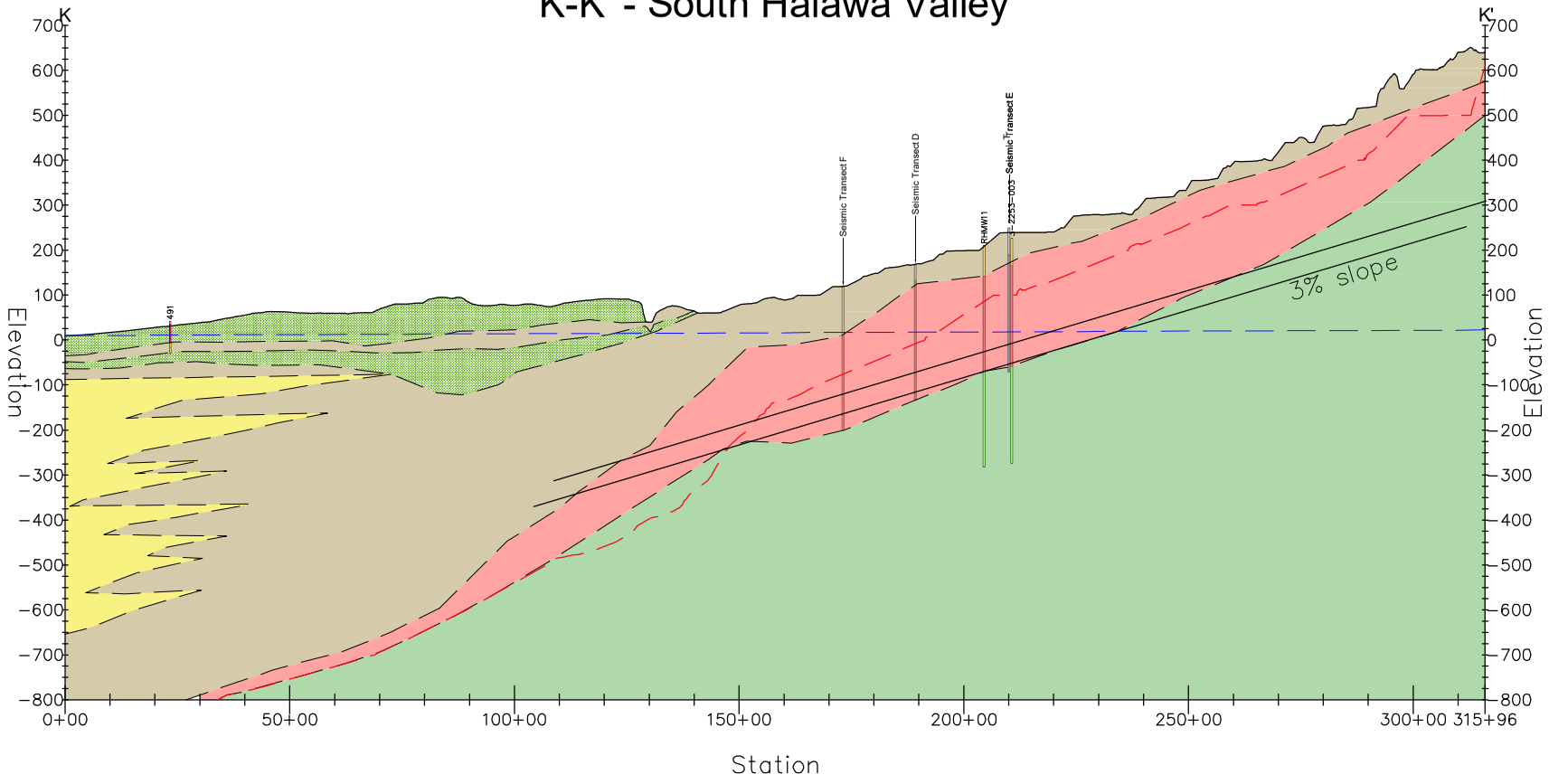

Note - Vertical exaggeration 10V/1H

LEGEND

- Alluvium
- Saprolite
- Basalt
- Basal Groundwater (approximate)
- Marine Deposits
- Honolulu Volcanics - Tuff
- Top of Basalt (Izuka et al)
- Geologic Contact (approximate)

C:\Users\Mark.Higley\Documents\Autodesk\geomodel_181106.dwg 11/6/2018 9:48 AM Mark.higley

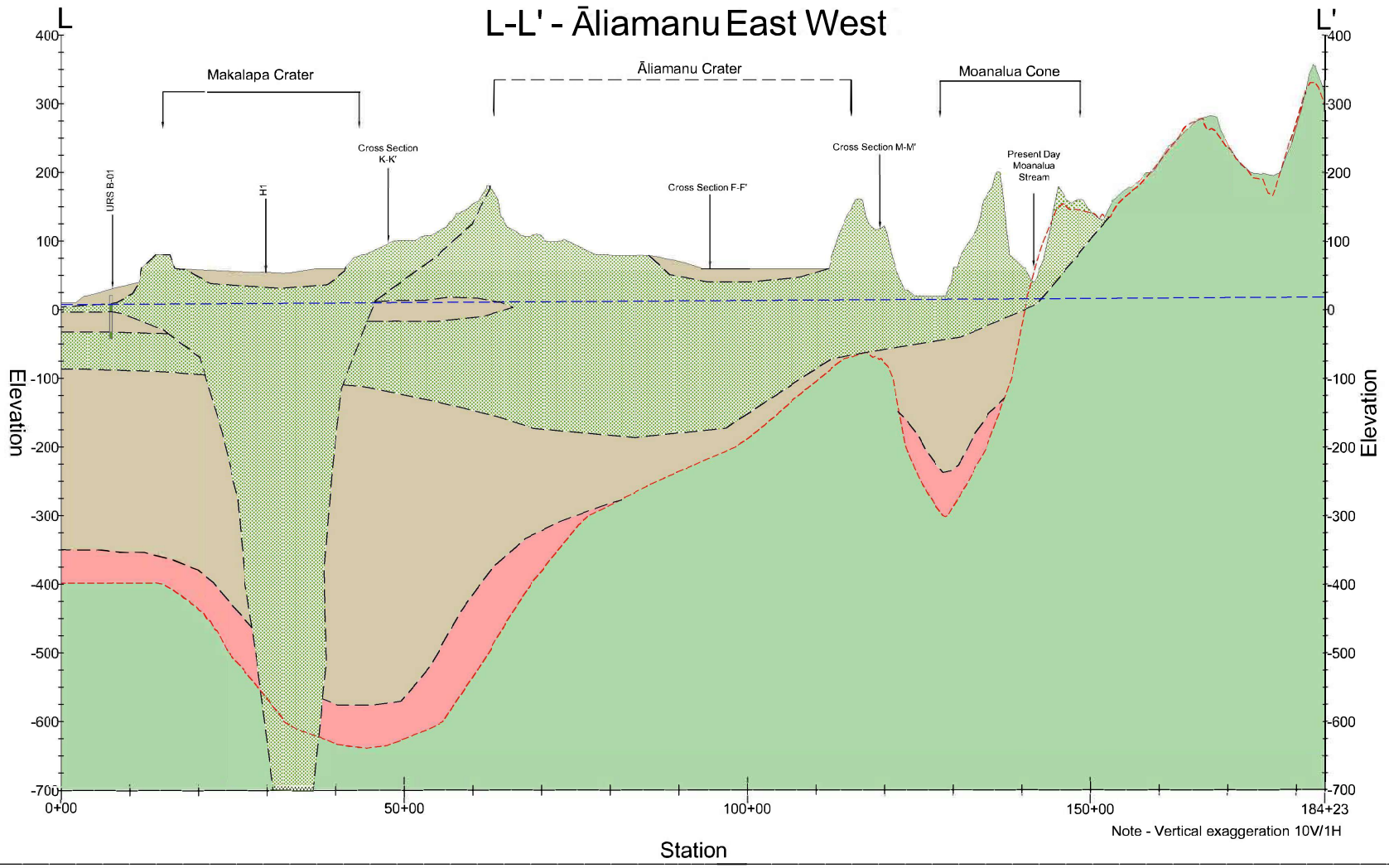

LEGEND

- Alluvium
- Saprolite
- Basalt
- Basal Groundwater (approximate)
- Geologic Contact (approximate)
- Honolulu Volcanics - Tuff
- Top of Basalt (Izuka et al)

C:\Users\Mark.Higley\Documents\Autodes dlmodel area s ce contours_180209 (2).dwg 9/11/2018 7:39 AM Mark.higley

M-M' - Moanalua Valley

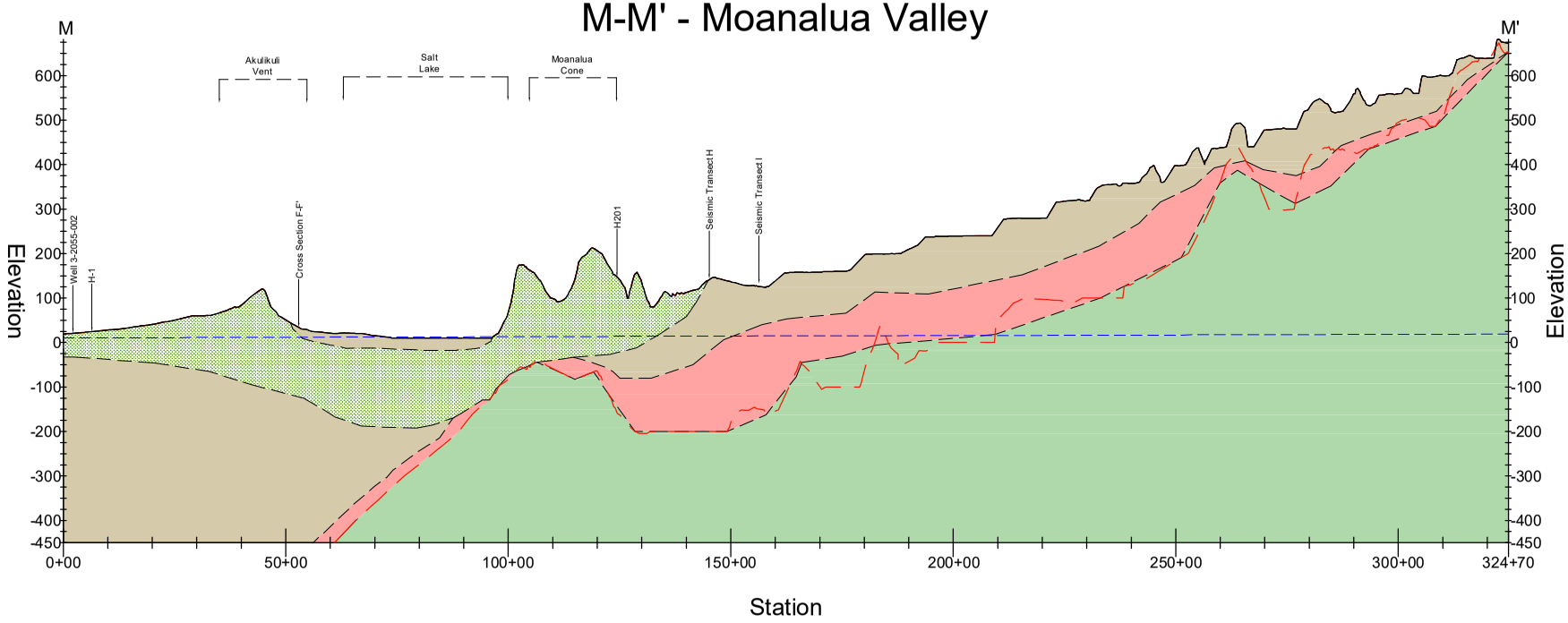

Note - Vertical exaggeration 10V/1H

LEGEND

- Alluvium
- Saprolite
- Basalt
- Measured Groundwater (date)
- Geologic Contact (approximate)
- Honolulu Volcanics - Tuff
- Top of Basalt (Izuka et al)

C:\Users\Mark.Higley\Documents\Autodesk\model area surface contours_180913.dwg 9/13/2018 2:18 PM Mark.higley

O-O' - North Halawa Valley

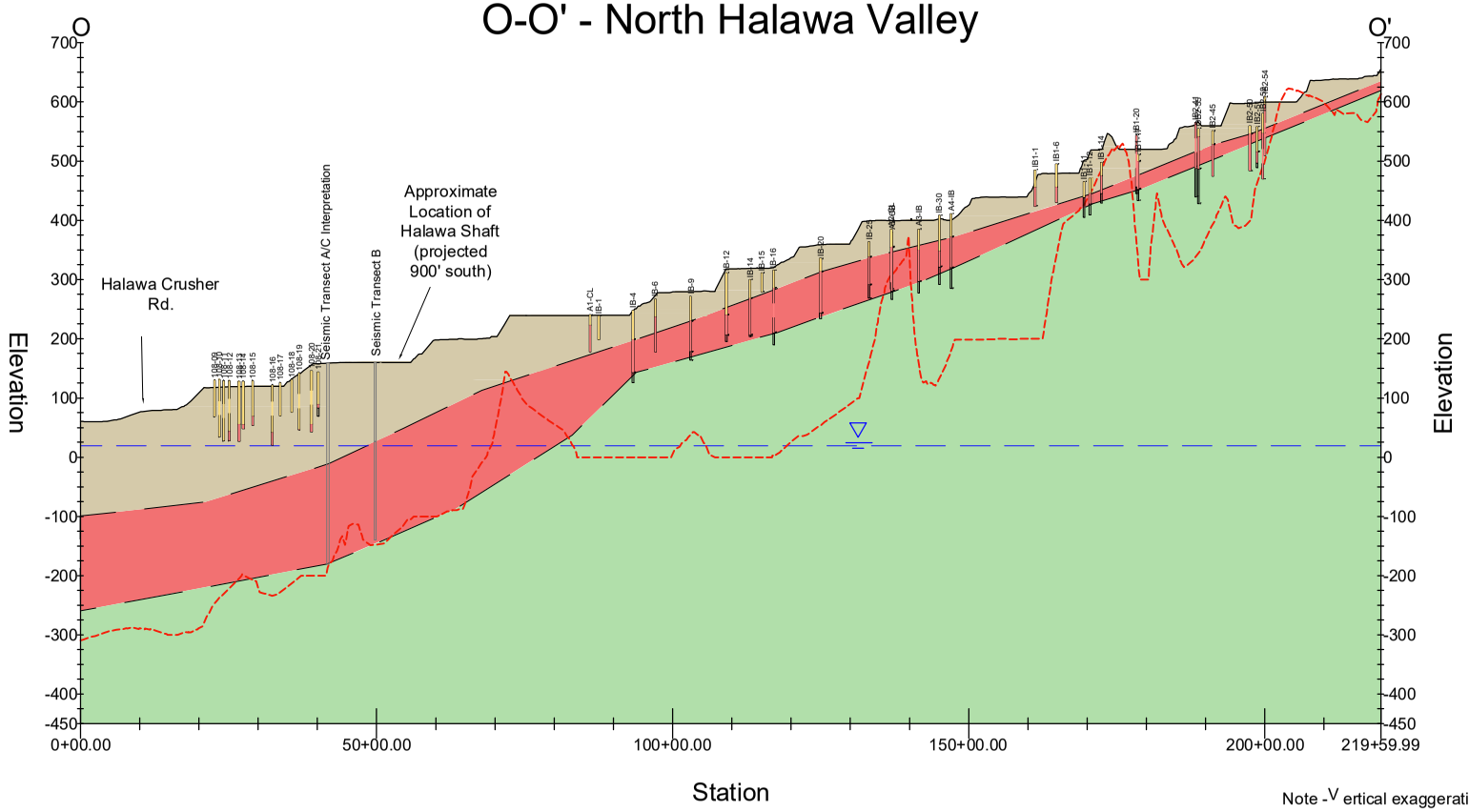

Note - Vertical exaggeration 10V/1H

LEGEND

- Alluvium
- Saprolite
- Basalt
- Basal Groundwater (approximate)
- Geologic Contact (approximate)
- Honolulu Volcanics - Tuff
- Top of Basalt (Izuka et al)

C:\Users\Mark.Higley\Documents\Autodesk\model area surface contours_180910.dwg 9/11/2018 7:39 AM Mark.Higley

This page intentionally left blank

Appendix F:
Petrographic Analytical Report

This page intentionally left blank

Mobility Data

Red Hill Bulk Fuel Storage Facility
Joint Base Pearl Harbor-Hickam
Oahu, Hawaii

Project No: 60571032

Performed for:

AECOM Technical Services, Inc.
1001 Bishop Street, Ste. 1600
Honolulu, HI 96831

October 2018

File: 1703942
Revision 1 December 18, 2018
Revision 2 January 23, 2019
Revision 3 May 1, 2019

Performed by:
Core Laboratories LP
3437 Landco Drive
Bakersfield, California 93308
(661) 325-5657

The analyses, opinions or interpretations contained in this report are based upon observations and material supplied by the client for whose exclusive and confidential use this report has been made. The interpretations or opinions expressed represent the best judgment of Core Laboratories. Core Laboratories assumes no responsibility and makes no warranty or representations, expressed or implied, as to the productivity, proper operations or profitableness, however, of any oil, gas, coal or other mineral, property, well or sand in connection with which such report is used or relied upon for any reason whatsoever.

Petroleum Services Division
3437 Landco Dr.
Bakersfield, California 93308
Tel: 661-325-5657
Fax: 661-325-5808
www.corelab.com

May 1, 2019

Margie Pascua
AECOM Technical Services, Inc.
1001 Bishop Street, Ste. 1600
Honolulu, HI 96831

Re: Petrophysical Properties
CL File No: 170349Rev2

Dear Ms. Pascua:

Enclosed are revised Residual Saturation and Fluid Properties Data for samples submitted from your Red Hill Bulk Fuel Storage Facility, Oahu, Hawaii.

Following data revisions were requested by Eric Wetzstein (April 19, 2019 email) and John Kronen (April 30, 2019 email).

- Appendix: Core Photographs – Natural Light

  - ERH 528: Change depth to 155.4-156.0, Depth (ft) 155.60
  - ERH 529: Change depth to 177.2-178.0, Depth (ft) 177.40
  - ERH 530: Change depth to 214.4-216.0, Depth (ft) 215.50
  - ERH 531: Change depth to 296.6-297.2, Depth (ft) 296.95
  - ERH 532: Change depth to 325.2-325.7, Depth (ft) 325.35

Thank you for this opportunity to be of service to AECOM Technical Services. Please do not hesitate to contact us (661-325-5657) if you have any questions regarding these results, or if we can be of any additional service.

Yours Sincerely,
Core Laboratories LP

Larry Kunkel
Area Manager - Western US

CLB Listed NYSE

This report is based entirely upon the core samples, soils, solids, liquids, or gases, together with related observational data, provided solely by the client. The conclusions, inferences, deductions and opinions rendered herein reflect the examination, study, and testing of these items, and represent the best judgment of Core Laboratories. Any reliance on the information contained herein concerning the profitability or productivity of any well, sand, or drilling activity is at the sole risk of the client, and Core Laboratories, neither extends nor makes any warranty or representation whatsoever with respect to same. This report has been prepared for the exclusive and confidential use of the client and no other party.

Petroleum Services Division
3437 Landco Dr.
Bakersfield, California 93308
Tel: 661-325-5657
Fax: 661-325-5808
www.corelab.com

January 23, 2019

Margie Pascua
AECOM Technical Services, Inc.
1001 Bishop Street, Ste. 1600
Honolulu, HI 96831

Re: Petrophysical Properties
CL File No: 170349Rev2

Dear Ms. Pascua:

Enclosed are revised Residual Saturation and Fluid Properties Data for samples submitted from your Red Hill Bulk Fuel Storage Facility, Oahu, Hawaii.

Data revisions per Eric Wetzstein's email dated January 4, 2019.

- Discussion
  - Add discussion regarding permeability re-runs
- Table 4 Basic Rock Properties
  - ERH512: re-run post-test permeability to air
  - ERH523: change description to welded a'a clinker
  - ERH522: re-run post-test permeability to air
  - ERH524: re-run post-test permeability to air
  - ERH531: re-run post-test permeability to air
  - ERH534: re-run post-test permeability to air
  - Add Core Lab air permeability check plug data

Thank you for this opportunity to be of service to AECOM Technical Services. Please do not hesitate to contact us (661-325-5657) if you have any questions regarding these results, or if we can be of any additional service.

Yours Sincerely,
Core Laboratories LP

Larry Kunkel
Area Manager - Western US

CLB Listed NYSE

This report is based entirely upon the core samples, soils, solids, liquids, or gases, together with related observational data, provided solely by the client. The conclusions, inferences, deductions and opinions rendered herein reflect the examination, study, and testing of these items, and represent the best judgment of Core Laboratories. Any reliance on the information contained herein concerning the profitability or productivity of any well, sand, or drilling activity is at the sole risk of the client, and Core Laboratories, neither extends nor makes any warranty or representation whatsoever with respect to same. This report has been prepared for the exclusive and confidential use of the client and no other party.

Petroleum Services Division
3437 Landco Dr.
Bakersfield, California 93308
Tel: 661-325-5657
Fax: 661-325-5808
www.corelab.com

December 18, 2018

Margie Pascua
AECOM Technical Services, Inc.
1001 Bishop Street, Ste. 1600
Honolulu, HI 96831

Re: Petrophysical Properties
CL File No: 170349Rev1

Dear Ms. Pascua:

Enclosed are revised Residual Saturation and Fluid Properties Data for samples submitted from your Red Hill Bulk Fuel Storage Facility, Oahu, Hawaii.

Data revisions per Jack Kronen's and Eric Wetzstein's emails dated December 17, 2018:

- Table 1 Mobility Summary
  - Add injection pressure
  - ERH509: change 56.7' to 65.7'
- Table 4 Basic Rock Properties
  - ERH509: change 56.7' to 65.7'
  - ERH510: change welded a'a clinker to massive a'a
  - ERH511: change massive a'a to pahoehoe
  - ERH513: change pahoehoe to welded a'a clinker
  - ERH514: change pahoehoe to massive a'a
  - ERH516: change massive a'a to pahoehoe
- Appendix 1 Test Plug Images
  - ERH528: move photos to ERH 531
  - ERH529: move photos to ERH 528
  - ERH530: move photos to ERH 532
  - ERH531: move photos to ERH 530
  - ERH532: move photos to ERH 529

Thank you for this opportunity to be of service to AECOM Technical Services. Please do not hesitate to contact us (661-325-5657) if you have any questions regarding these results, or if we can be of any additional service.

Yours Sincerely,
Core Laboratories LP

Larry Kunkel
Area Manager - Western US

CLB Limited NYSE

This report is based entirely upon the core samples, soils, solids, liquids, or gases, together with related observational data, provided solely by the client. The conclusions, inferences, deductions and opinions rendered herein reflect the examination, study, and testing of these items, and represent the best judgment of Core Laboratories. Any reliance on the information contained herein concerning the profitability or productivity of any well, sand, or drilling activity is at the sole risk of the client, and Core Laboratories, neither extends nor makes any warranty or representation whatsoever with respect to same. This report has been prepared for the exclusive and confidential use of the client and no other party.

Petroleum Services Division
3437 Landco Dr.
Bakersfield, California 93308
Tel: 661-325-5657
Fax: 661-325-5808
www.corelab.com

October 31, 2018

Margie Pascua
AECOM Technical Services, Inc.
1001 Bishop Street, Ste. 1600
Honolulu, HI 96831

Re: Petrophysical Properties
CL File No: 170349

Dear Ms. Pascua:

Enclosed are final Residual Saturation and Fluid Properties Data for samples submitted from your Red Hill Bulk Fuel Storage Facility, Oahu, Hawaii.

Twenty-three locations were selected from archived core to evaluate residual saturations to Jet Fuel (NAPL) by water drive. Initial NAPL saturations average 41% and following water drive residual NAPL averaged 34%. A data summary follows along with tabular data and test plug photographs.

Cores samples were shipped back to John (Jack) Kronen's attention at AECOM 1001 Bishop Street, Ste. 1600 Honolulu, HI 96831. NAPL samples were disposed through Core Laboratories non-chlorinated hydrocarbon waste stream.

Thank you for this opportunity to be of service to AECOM Technical Services. Please do not hesitate to contact us (661-325-5657) if you have any questions regarding these results, or if we can be of any additional service.

Yours Sincerely,
Core Laboratories LP

Larry Kunkel
Area Manager - Western US

CLB Listed NYSE

This report is based entirely upon the core samples, soils, solids, liquids, or gases, together with related observational data, provided solely by the client. The conclusions, inferences, deductions and opinions rendered herein reflect the examination, study, and testing of these items, and represent the best judgment of Core Laboratories. Any reliance on the information contained herein concerning the profitability or productivity of any well, sand, or drilling activity is at the sole risk of the client, and Core Laboratories, neither extends nor makes any warranty or representation whatsoever with respect to same. This report has been prepared for the exclusive and confidential use of the client and no other party.

Petroleum Services Division
3437 Landco Dr.
Bakersfield, California 93308
Tel: 661-325-5657
Fax: 661-325-5808
www.corelab.com

Company: AECOM Technical Services, Inc.
Project No: 60571032
Location: Oahu, Hawaii

Core Lab File No: 1703942Rev1
Date: October 2018

Summary

Twenty-three archived core sections from various borings of pahoehoe and a'a volcanic material were submitted for mobility analysis by water drive. AECOM personnel selected twenty-three test locations of which only twenty-two were suitable for testing. Ten gallons of Jet Fuel (NAPL) was supplied for saturating the samples along with viscosity, density and IFT analyses (Table 2-3).

Mobility by Water Drive

One, 1.5" diameter sample was obtained from each requested location and photographed under natural light to document lithology/structure of the ends and sides. Samples were sleeved using nickel foil (3mil thick) with 200 mesh screens place on each end. Sleeves were seated to the samples at 400psi net confining stress (NCS) to maintain sample integrity throughout the test sequence.

Samples were dried and basic properties of total porosity, permeability to air and grain density were determined (Table 4) at 250 psi NCS. Due to the nature of the core material there was a wide variation in sample properties. Permeability to air averaged 1496mD but ranged from a high of 11,716mD to a low of 0.018mD. Total porosity also had a wide variation with an average of 30.5%, a high of 51.3% and a low of 5.11%. Grain density was higher than typical sediments (2.65g/cc) but had a narrower range with an average of 3.02g/cc, a high of 3.08g/cc and a low of 2.94g/cc.

Samples were saturated using filtered (0.45micron) tap water and de-saturated by centrifuging to an irreducible or initial water saturation (S_{wi}). Samples were confined in a triaxial cell at 250psi NCS and saturated by injecting filtered (0.45micron) NAPL to complete the saturation. Initial saturations (Table 1) for water (S_{wi}) averaged 59% and 41% for NAPL (S_{Ni}).

Filtered (0.45micron) tap water was injected vertically upward at a head pressure equal to a maximum of 50ft-wtr through the sample producing mobile NAPL that was collected for material balance calculations. Higher permeability samples (#9, 13, 20, 23) used lower pressure due to the high flow rate that would be generated at 50ft-wtr. Injection continued for a minimum of one pore volume and a 99.9% producing water cut. At the conclusion of the test samples were unloaded from the cells and a saturated weight recorded. Residual pore fluids were extracted by Dean-Stark distillation (API RP40) for material balance calculations. Initial and residual volumes were converted to saturations using previously measured pore volumes (Table 4).

Table 1 summarizes the mobility saturation data. For eleven, of the twenty-two, samples the initial saturations are equal to residual or final fluid saturations due to permeability being too low for production at the requested injection pressure. Under these test conditions initial NAPL is considered residual NAPL. For the eleven samples that had production, initial NAPL saturation was reduced on the average ~17%.

This report is based entirely upon the core samples, soils, solids, liquids, or gases, together with related observational data, provided solely by the client. The conclusions, inferences, deductions and opinions rendered herein reflect the examination, study, and testing of these items, and represent the best judgment of Core Laboratories. Any reliance on the information contained herein concerning the profitability or productivity of any well, sand, or drilling activity is at the sole risk of the client, and Core Laboratories, neither extends nor makes any warranty or representation whatsoever with respect to same. This report has been prepared for the exclusive and confidential use of the client and no other party.

Petroleum Services Division
3437 Landco Dr.
Bakersfield, California 93308
Tel: 661-325-5657
Fax: 661-325-5808
www.corelab.com

Company: AECOM Technical Services, Inc.
Project No: 60571032
Location: Oahu, Hawaii

Core Lab File No: 1703942Rev2
Date: January 2019

1/23/19 Revision 2; Table 4: After data review and team discussion it was decided to re-run permeability to air on five samples due to high reported values. Samples were 512, 522, 524, 531 and 534 with pre-test permeabilities ranging from 3278md (512) to 11716md (534). Post-test permeabilities were re-run at 250psi confining stress and measured in both directions, A→B and B→A to check for directionality. Permeabilities were lower for 512 and 522, higher for 524 and 531. Sample 534 had the same permeability. Two Core Lab check samples were run to verify equipment performance.

End screens were removed from samples 512, 522, 524 and 531 had fines on the surface indicating possible pore throat plugging due to fines migration through the sample which could reduce permeability or, in the case of 524 and 531, increase permeability. Production of fines is usually attributed to dehydrating clays, loss of cementation or interaction with injected fluids.

Sample ID	Depth, ft.	Permeability to Air, md			AECOM Description
		Pre-Test	Post Test Re-Run		
			A->B	B->A	
ERH 512 105.9	106.10	3287	302	305	weathered a'a clinker
ERH 522 200.2-201	200.30	5371	632	614	weathered a'a clinker
ERH 524 248.8-249.5	249.00	7873	16543	16543	pahoehoe
ERH 531 296.6-297.2	296.95	3917	4529	4529	Pahoehoe - oxidized dark reddish brown, highly vesicular 50%, small vesicles
ERH 534 489.5-490.0	489.65	11716	11716	11716	Pahoehoe - sl. oxidized reddish brown, vesicular 25%, small to medium vesicles

Core Lab Check Samples		Assay	Measured	Diff, %	Description
CK D		131	132	+0.76	Sintered stainless steel check plug
CK E		928	949	+2.3	Sintered stainless steel check plug

Additional test programs should consider evaluating rock sensitivity to water salinity and use of fresh core samples is recommended.

This report is based entirely upon the core samples, soils, solids, liquids, or gases, together with related observational data, provided solely by the client. The conclusions, inferences, deductions and opinions rendered herein reflect the examination, study, and testing of these items, and represent the best judgment of Core Laboratories. Any reliance on the information contained herein concerning the profitability or productivity of any well, sand, or drilling activity is at the sole risk of the client, and Core Laboratories, neither extends nor makes any warranty or representation whatsoever with respect to same. This report has been prepared for the exclusive and confidential use of the client and no other party.

Petroleum Services Division
3437 Landco Dr.
Bakersfield, California 93308
Tel: 661-325-5657
Fax: 661-325-5808
www.corelab.com

Company: AECOM Technical Services, Inc.
Project No: 60571032
Location: Oahu, Hawaii

Core Lab File No: 1703942Rev1
Date: October 2018

Table of Contents

Description	Location
Mobility Data Summary	Table 1
NAPL Viscosity and Density Data	Table 2
Interfacial Tension Data	Table 3
Basic Rock Properties	Table 4
Core Plug Photographs – Natural Light	Appendix
Chain-of-Custody	Appendix

This report is based entirely upon the core samples, soils, solids, liquids, or gases, together with related observational data, provided solely by the client. The conclusions, inferences, deductions and opinions rendered herein reflect the examination, study, and testing of these items, and represent the best judgment of Core Laboratories. Any reliance on the information contained herein concerning the profitability or productivity of any well, sand, or drilling activity is at the sole risk of the client, and Core Laboratories, neither extends nor makes any warranty or representation whatsoever with respect to same. This report has been prepared for the exclusive and confidential use of the client and no other party.

Table 1
Free Product Mobility Data
Water Drive Method

Petroleum Services

AECOM Technical Services

Core Lab File No: 1703942

Project Name: Red Hill Bulk Fuel Storage Facility
Project No: 60481245
Project Location: Joint Base Pearl Harbor-Hickman, Oahu HI

		METHODS:	API RP 40		API RP 40	Core Lab, API RP40				
						Pore Fluid Saturations, frac pore volume				
			Density			Initial Fluid Saturations (2)		Injection	Final Fluid Saturations (2)	
Sample ID.	Depth ft.	Sample Orientation (1)	Bulk (Dry) g/cc	Grain g/cc	Total Porosity, frac	Water	NAPL (3)	Pressure, ft-wtr(4)	Water	NAPL (3)
ERH 509 65.7-66.4	65.90	V	1.70	2.94	0.418	0.711	0.289	50.0	0.861	0.139
ERH 510 81.0-81.7	81.10	V	2.70	3.00	0.051	0.436	0.564	50.0	0.436	0.564
ERH 511 155.2-155.9	155.30	V	1.80	3.05	0.412	0.639	0.361	50.0	0.693	0.307
ERH 512 105.9	106.10	V	1.66	2.98	0.447	0.750	0.250	50.0	0.871	0.129
ERH 513 133.0	133.20	V	2.12	2.99	0.289	0.574	0.426	50.0	0.778	0.222
ERH 514 162.8	162.95	V	2.40	3.04	0.211	0.367	0.633	50.0	0.644	0.356
ERH 515 181.5	Unable to obtain sufficient sample for testing									
ERH 516 242.6	242.70	V	1.76	3.05	0.409	0.707	0.293	50.0	0.707	0.293
ERH 517 341.3	341.40	V	1.77	3.06	0.429	0.241	0.759	4.6	0.415	0.585
ERH 521 171.0-171.8	171.35	V	1.89	3.05	0.374	0.574	0.426	50.0	0.576	0.424
ERH 522 200.2-201	200.30	V	1.80	2.95	0.390	0.849	0.151	50.0	0.849	0.151
ERH 523 218.2-219	218.80	V	2.45	3.00	0.176	0.511	0.489	50.0	0.781	0.219
ERH 524 248.8-249.5	249.00	V	1.58	3.00	0.483	0.644	0.356	4.6	0.644	0.356
ERH 525 289-289.8	289.25	V	2.11	3.08	0.299	0.630	0.370	50.0	0.827	0.173
ERH 526 108.5-109	108.70	V	2.12	3.02	0.294	0.805	0.195	50.0	0.805	0.195
ERH 527 137.6-138.4	137.80	V	2.55	3.00	0.133	0.556	0.444	50.0	0.556	0.444
ERH 528 155.4-156	155.60	V	2.22	3.00	0.262	0.699	0.301	50.0	0.699	0.301
ERH 529 177.2-178	177.40	V	2.10	3.07	0.292	0.694	0.306	50.0	0.694	0.306
ERH 530 214.4-216.0	215.50	V	2.58	2.99	0.118	0.523	0.477	50.0	0.523	0.477
ERH 531 296.6-297.2	296.95	V	1.51	3.02	0.513	0.556	0.444	11.5	0.619	0.381

Table 1
Free Product Mobility Data
Water Drive Method

Petroleum Services

AECOM Technical Services

Core Lab File No: 1703942

Project Name: Red Hill Bulk Fuel Storage Facility
Project No: 60481245
Project Location: Joint Base Pearl Harbor-Hickman, Oahu HI

		METHODS:	API RP 40		API RP 40	Core Lab, API RP40				
						Pore Fluid Saturations, frac pore volume				
			Density			Initial Fluid Saturations (2)		Injection	Final Fluid Saturations (2)	
Sample ID.	Depth ft.	Sample Orientation (1)	Bulk (Dry) g/cc	Grain g/cc	Total Porosity, frac	Water	NAPL (3)	Pressure, ft-wtr(4)	Water	NAPL (3)
ERH 532 325.2-325.7	325.35	V	2.30	3.01	0.233	0.481	0.519	50.0	0.481	0.519
ERH 533 393.5-394.2	393.60	V	2.56	3.00	0.133	0.364	0.636	50.0	0.364	0.636
ERH 534 489.5-490.0	489.65	V	1.97	3.04	0.351	0.624	0.376	2.3	0.673	0.327
		Max	2.70	3.08	0.513	0.849	0.759	50.0	0.871	0.636
		Min	1.51	2.94	0.051	0.241	0.151	2.3	0.364	0.129
		Avg	2.08	3.02	0.305	0.588	0.412	42.0	0.659	0.341

(1) V = vertical, H = horizontal
(2) NAPL Density = 0.8066 g/cc
(3) NAPL = Jet Fuel supplied by AECOM
(4) 50ft-wtr = 21.7psi

Table 2
VISCOSITY and DENSITY DATA
(METHODOLOGY: ASTM D445, ASTM D1481, API RP40)

PETROLEUM SERVICES

Company: **AECOM Technical Services**
Project Name: Red Hill Bulk Fuel Storage Facility
Project No: 60481245
Project Location: Joint Base Pearl Harbor-Hickman, Oahu HI

Core Lab File No: 1703942

Lab Sample No.	Project No.	Matrix	Sample Source	Sample Date	Analysis Date	Temperature °F	Density g/cc	°API	Viscosity	
									centistokes	centipoise
1703942-1	60481245	Jet Fuel	Client	N/A	8/17/18	60	0.8135	42.4	---	---
						76	0.8070		1.530	1.234
						80	0.8054		1.482	1.193
						91	0.8010		1.304	1.044

API measured by pycnometer
Viscosity measured by a Crossarm Viscometer

Table 3
INTERFACIAL / SURFACE TENSION DATA
(METHODOLOGY: DuNuoy Method - ASTM D971)

Phase Pair		Temp., °F	Interfacial Tension, Dynes/centimeter
Air	Water	60	69.9
Air	Jet Fuel	60	25.0
Water	Jet Fuel	60	15.7

Table 4
Basic Rock Properties

(METHODOLOGY: API RP40)

PETROLEUM SERVICES

AECOM Technical Services

Core Lab File No: 1703942EN

Project Name: Red Hill Bulk Fuel Storage Facility
Project No: 60481245
Project Location: Joint Base Pearl Harbor-Hickman, Oahu HI

Sample ID	Depth, ft.	Measured at 250psi Net Confining Stress*							Core Description Provided by AECOM
		Permeability to Air (Kair), md			Total Porosity %Vb	Helium Pore Volume cc	Helium Grain Volume cc	Grain Density g/cc	
		Pre-Test	Post Test Re-Run A --> B	Post Test Re-Run B --> A					
ERH 509 56.7-66.4	65.90	619			41.8	21.94	30.57	2.94	Weathered a'a clinker
ERH 510 81.0-81.7	81.10	0.018			5.11	3.04	56.38	3.00	welded a'a clinker
ERH 511 155.2-155.9	155.30	7.05			41.2	23.35	33.35	3.05	massive a'a
ERH 512 105.9	106.10	3287	302	305	44.7	18.33	22.69	2.98	Weathered a'a clinker
ERH 513 133.0	133.20	21.8			28.9	16.19	39.84	2.99	pahoehoe
ERH 514 162.8	162.95	0.097			21.1	11.93	44.70	3.04	pahoehoe
ERH 515 181.5	Unable to obtain sufficient sample for testing								Weathered a'a clinker
ERH 516 242.6	242.70	0.241			40.9	22.41	32.44	3.05	massive a'a
ERH 517 341.3	341.40	53.3			42.9	24.36	32.42	3.06	pahoehoe
ERH 521 171.0-171.8	171.35	1.77			37.4	21.67	36.29	3.05	pahoehoe
ERH 522 200.2-201	200.30	5371	632	614	39.0	19.67	30.80	2.95	Weathered a'a clinker
ERH 523 218.2-219	218.80	31.8			17.6	7.24	33.94	3.00	welded a'a clinker
ERH 524 248.8-249.5	249.00	7873	16543	16543	48.3	28.25	30.21	3.00	pahoehoe
ERH 525 289-289.8	289.25	0.380			29.9	16.28	38.10	3.08	pahoehoe
ERH 526 108.5-109	108.70	4.96			29.4	17.25	41.38	3.02	welded a'a clinker
ERH 527 137.6-138.4	137.80	0.050			13.3	5.64	36.81	3.00	massive a'a
ERH 528 155.4-156	155.60	2.65			26.2	15.99	45.12	3.00	Weathered a'a clinker
ERH 529 177.2-178	177.40	0.284			29.2	16.26	39.47	3.07	pahoehoe
ERH 530 214.4-216.0	215.50	0.089			11.8	7.32	54.60	2.99	massive a'a

*250 psi confining stress to minimize bypass around sample
Vb = Bulk Volume

Table 4
Basic Rock Properties

(METHODOLOGY: API RP40)

PETROLEUM SERVICES

AECOM Technical Services

Core Lab File No: 1703942EN

Project Name: Red Hill Bulk Fuel Storage Facility
Project No: 60481245
Project Location: Joint Base Pearl Harbor-Hickman, Oahu HI

Sample ID	Depth, ft.	Measured at 250psi Net Confining Stress*: Permeability to Air (Kair), md: Pre-Test	Post Test Re-Run: A --> B	Post Test Re-Run: B --> A	Total Porosity %Vb	Helium Pore Volume cc	Helium Grain Volume cc	Grain Density g/cc	Core Description Provided by AECOM
ERH 531 296.6-297.2	296.95	3917	4529	4529	51.3	30.08	28.60	3.02	Pahoehoe - oxidized dark reddish brown, highly vesicular 50%, small vesicles
ERH 532 325.2-325.7	325.35	0.098			23.3	13.35	44.01	3.01	Pahoehoe - gray, large vesicles 15%, some infilling in vesicles
ERH 533 393.5-394.2	393.60	0.149			13.3	7.70	49.99	3.00	Pahoehoe - gray, vesicular 25%, small to medium vesicles
ERH 534 489.5-490.0	489.65	11716	11716	11716	35.1	20.18	37.32	3.04	Pahoehoe - sl. oxidized reddish brown, vesicular 25%, small to medium vesicles
	Max	11716			51.3	30.1	56.4	3.08	
	Min	0.018			5.11	3.04	22.7	2.94	
	Avg	1496			30.5	16.7	38.1	3.02	

QC Check Samples	Assay, md	Measured, md	Diff %
Core Lab CK D	131	132	-0.76
Core Lab CK E	928	949	+0.76

*250 psi confining stress to minimize bypass around sample
Vb = Bulk Volume

Petroleum Services Division
3437 Landco Dr.
Bakersfield, California 93308
Tel: 661-325-5657
Fax: 661-325-5808
www.corelab.com

Company: AECOM Technical Services, Inc.
Project No: 60571032
Location: Oahu, Hawaii

Core Lab File No: 1703942Rev1
Date: October 2018

Appendix

This report is based entirely upon the core samples, soils, solids, liquids, or gases, together with related observational data, provided solely by the client. The conclusions, inferences, deductions and opinions rendered herein reflect the examination, study, and testing of these items, and represent the best judgment of Core Laboratories. Any reliance on the information contained herein concerning the profitability or productivity of any well, sand, or drilling activity is at the sole risk of the client, and Core Laboratories, neither extends nor makes any warranty or representation whatsoever with respect to same. This report has been prepared for the exclusive and confidential use of the client and no other party.

Appendix 1
Test Plug Images - Natural Light

Petroleum Services

AECOM Technical Services
Project Name: Red Hill Bulk Fuel Storage Facility
Project No: 60481245
Project Location: Joint Base Pearl Harbor-Hickman, Oahu HI

Core Lab File No: 1703942

ERH 509 56.7-66.4 Depth (ft): 65.90	ERH 510 81.0-81.7 Depth (ft): 81.10’	ERH 511 155.2-155.9 Depth (ft): 155.30’	ERH 512 105.9 Depth (ft): 106.10’	ERH 513 133.0 Depth (ft): 133.20’

Appendix 1
Test Plug Images - Natural Light

Petroleum Services

AECOM Technical Services
Project Name: Red Hill Bulk Fuel Storage Facility
Project No: 60481245
Project Location: Joint Base Pearl Harbor-Hickman, Oahu HI

Core Lab File No: 1703942

ERH 514 162.95 Depth (ft): 162.95	ERH 515 181.5 Depth (ft): 151.75	ERH 516 242.6 Depth (ft): 242.70	ERH 517 341.3 Depth (ft): 341.40	ERH 521 171.0-171.8 Depth (ft): 171.35

Appendix 1
Test Plug Images - Natural Light

Petroleum Services

AECOM Technical Services
Project Name: Red Hill Bulk Fuel Storage Facility
Project No: 60481245
Project Location: Joint Base Pearl Harbor-Hickman, Oahu HI

Core Lab File No: 1703942

ERH 522 200.2-201 Depth (ft): 200.30	ERH 523 218.2-219 Depth (ft): 218.80	ERH 524 248.8-249.5 Depth (ft): 249.00	ERH 525 289-289.8 Depth (ft): 289.25	ERH 526 108.5-109 Depth (ft): 108.70

Appendix 1
Test Plug Images - Natural Light

Petroleum Services

AECOM Technical Services
Project Name: Red Hill Bulk Fuel Storage Facility
Project No: 60481245
Project Location: Joint Base Pearl Harbor-Hickman, Oahu HI

Core Lab File No: 1703942

ERH 527 137.6-138.4 Depth (ft): 137.80	ERH 528 155.4-156 Depth (ft) 155.60	ERH 529 177.2-178 Depth (ft) 177.40	ERH 530 214.4-216.0 Depth (ft) 215.50	ERH 531 296.6-297.2 Depth (ft) 296.95

Appendix 1
Test Plug Images - Natural Light

Petroleum Services

AECOM Technical Services
Project Name: Red Hill Bulk Fuel Storage Facility
Project No: 60481245
Project Location: Joint Base Pearl Harbor-Hickman, Oahu HI

Core Lab File No: 1703942

ERH 532 325.2-325.7
Depth (ft) 325.35

ERH 533 393.5-394.2
Depth (ft): 393.60

ERH 534 489.5-490.0
Depth (ft): 489.65

CHAIN OF CUSTODY RECORD

Company	AECOM
Address	1001 Bishop St, Suite 1600 Honolulu, HI 96813
Project Manager	Jeff Johnson
Phone	808-356-5340
Project Name	CV 18F0126
Fax	808-523-8950
Project No.	60571032
Email	eric.wetzstein@aecom.com margie.pascua@aecom.com
Site Location	Red Hill
Sampler Signature	

ANALYSIS REQUEST

PO# 94992

Turnaround Time: 24 HR ☐ 48 HR ☐ 72 HR ☐ 5 Day ☐ Normal ☒

CL Bid No.

CL File No.

Sample ID	Date	Time	Depth, ft.	Number of Samples	SOIL: Vadose Zone Suite	Saturated Zone Suite	Pore Fluid Saturation Suite	Moisture Content: ASTM D2216	Porosity: Total, API RP40	Porosity: Effective, ASTM D425M	Bulk Density: API RP40 / ASTM D2937	Hydraulic Conductivity: API RP40	Grain Size Distribution: ASTM D422/D4464M	Atterberg Limits: ASTM D4318	TOC: Walkley-Black	FLUID: Fluid Properties Suite	Viscosity: ASTM D445	Density/Gravity: ASTM D1481	Pyro-Chromatography (Fingerprinting)	Comments
ERH 509	12/6/18	1200	165.7-166.4	1																TBD contact Eric Wetzstein
ERH 510	12/6/18	1205	81.0-81.7	1																TBD
ERH 511	12/6/18	1210	155.2-155.9	1																TBD
ERH 512	12/6/18	1215	105.9	1																TBD
ERH 513	12/6/18	1220	133.0	1																TBD
ERH 514	12/6/18	1225	162.8	1																TBD
ERH 515	12/6/18	1230	181.5	1																TBD
ERH 516	12/6/18	1235	242.6	1																TBD
ERH 517	12/6/18	1240	341.3	1																TBD

1. Relinquished By:	2. Received By:	2. Relinquished By:	2. Received By:
Mark Higley			
Company: AECOM	Company: Core Laboratories	Company:	Company:
Date: 12/20/18 Time: 1300	Date: 12/21/18 Time: 2:55pm	Date: Time:	Date: Time:

Core Lab

CORE LABORATORIES - 3437 Landco Dr. - Bakersfield, CA 93308 • Phone 661-325-5657 • Fax 661-325-5808

CHAIN OF CUSTODY RECORD

Company	AECOM
Address	1001 Bishop St, Suite 1600 Honolulu, HI 96813
Project Manager	Jeff Johnson
Phone	808-356-5340
Project Name	CV 18F0126
Fax	808-523-8950
Project No.	60571032
Email	eric.wetzstein@aecom.com margie.pascua@aecom.com
Site Location	Red Hill
Sampler Signature	

ANALYSIS REQUEST

PO# 94992

Turnaround Time: 24 HR ☐ 48 HR ☐ 72 HR ☐ 5 Day ☐ Normal ☒

CL Bid No.

CL File No.

Sample ID	Date	Time	Depth, ft.	Number of Samples	SOIL: Vadose Zone Suite	SOIL: Saturated Zone Suite	SOIL: Pore Fluid Saturation Suite	SOIL: Moisture Content: ASTM D2216	SOIL: Porosity: Total, API RP40	SOIL: Porosity: Effective, ASTM D425M	SOIL: Bulk Density: API RP40 / ASTM D2937	SOIL: Hydraulic Conductivity: API RP40	SOIL: Grain Size Distribution: ASTM D422/D4464M	SOIL: Atterberg Limits: ASTM D4318	SOIL: TOC: Walkley-Black	FLUID: Fluid Properties Suite	FLUID: Viscosity: ASTM D445	FLUID: Density/Gravity: ASTM D1481	FLUID: Pyro-Chromatography (Fingerprinting)	Comments
ERH 521	12/27/17	1220	171.5 - 171.5	1																TBD contact Eric Wetzstein
ERH 522	12/27/17	1225	200.2 - 201.0	1																TBD
ERH 523	12/27/17	1230	218.2 - 219	1																TBD
ERH 524	12/27/17	1235	248.3 - 249.5	1																TBD
ERH 525	12/27/17	1240	288.0 - 289.8	1																TBD
ERH 526	12/28/17	1225	108.5 - 109.0	1																TBD
ERH 527	12/28/17	1230	137.6 - 138.4	1																TBD
ERH 528	12/28/17	1235	155.4 - 156.0	1																TBD
ERH 529	12/28/17	1230	177.2 - 176.0	1																TBD

1. Relinquished By: Mark Higley	2. Received By:	2. Relinquished By:	2. Received By:
Company: AECOM	Company: Core Laboratories	Company:	Company:
Date: 12/20/18 Time: 1300	Date: 12/21/18 Time: 2:35pm	Date: Time:	Date: Time:

CHAIN OF CUSTODY RECORD

Company	AECOM
Address	1001 Bishop St, Suite 1600 Honolulu, HI 96813
Project Manager	Jeff Johnson
Phone	808-356-5340
Project Name	CV 18F0126
Fax	808-523-8950
Project No.	60571032
Email	eric.wetzstein@aecom.com margie.pascua@aecom.com
Site Location	Red Hill
Sampler Signature	

ANALYSIS REQUEST

PO# 94992

Turnaround Time: 24 HR ☐ 48 HR ☐ 72 HR ☐ 5 Day ☐ Normal ☒

CL Bid No.

CL File No.

Sample ID	Date	Time	Depth, ft.	Number of Samples	SOIL: Vadose Zone Suite	SOIL: Saturated Zone Suite	SOIL: Pore Fluid Saturation Suite	SOIL: Moisture Content: ASTM D2216	SOIL: Porosity: Total, API RP40	SOIL: Porosity: Effective, ASTM D425M	SOIL: Bulk Density: API RP40 / ASTM D2937	SOIL: Hydraulic Conductivity: API RP40	SOIL: Grain Size Distribution: ASTM D422/D4464M	SOIL: Atterberg Limits: ASTM D4318	SOIL: TOC: Walkley-Black	FLUID: Fluid Properties Suite	FLUID: Viscosity: ASTM D445	FLUID: Density/Gravity: ASTM D1481	FLUID: Pyro-Chromatography (Fingerprinting)	Comments
ERH 530	1/2/18	1220	214.4 - 216.0	1																TBD contact Eric Wetzstein
ERH 531	1/2/18	~~1220~~ 1225 (MH)	216.0 - 397.2	1																TBD
ERH 532	1/2/18	1230	325.2 - 325.7	1																TBD
ERH 533	1/2/18	1235	393.5 - 394.2	1																TBD
ERH 534	1/2/18	1240	489.5 - 490.0	1																TBD

1. Relinquished By:	Mark Higley	2. Received By:	
Company	AECOM	Company	Core Laboratories
Date / Time	12/20/18 1300	Date / Time	12/21/18 2:55pm
2. Relinquished By:		2. Received By:	
Company		Company	
Date / Time		Date / Time	

CHAIN OF CUSTODY RECORD

Company	AECOM
Address	1001 Bishop St, Suite 1600 Honolulu, Hawaii 96813
Project Manager	Jeff Johnson
Phone	808-356-5340
Project Name	CIV 53
Fax	808-523-8950
Project No.	60481245
Email	eric.wetzstein@aecom.com; margie.pascua@aecom.com
Site Location	Red Hill
Sampler Signature	

ANALYSIS REQUEST

PO# 94992

Turnaround Time: 24 HR [ ] 48 HR [ ] 72 HR [ ] 5 Day [ ] Normal [x]

CL Bid No.

CL File No.

Comments

Sample ID	Date	Time	Depth, ft.	Number of Samples	SOIL: Vadose Zone Suite	SOIL: Saturated Zone Suite	SOIL: Pore Fluid Saturation Suite	SOIL: Moisture Content: ASTM D2216	SOIL: Porosity: Total, API RP40	SOIL: Porosity: Effective, ASTM D425M	SOIL: Bulk Density: API RP40 / ASTM D2937	SOIL: Hydraulic Conductivity: API RP40	SOIL: Grain Size Distribution: ASTM D422/D4464M	SOIL: Atterberg Limits: ASTM D4318	SOIL: TOC: Walkley-Black	SOIL: Mobility Group-Centrifuge Method	SOIL: Mobility Group-Water Drive Method	SOIL: [unlabeled]	FLUID: Fluid Properties Suite	FLUID: Viscosity: ASTM D445	FLUID: Density/Gravity: ASTM D1481	FLUID: Pyro-Chromatography (Fingerprinting)	FLUID: Rock Core Slabbing	FLUID: Digital UV & White Light Core Imaging	FLUID: Core Viewing Interface and Data
ERH 530	1/2/18	12:20	214.4-216.0	1												X	X	J							
ERH 531	1/2/18	12:25	296.6-297.2	1												X	X	J							
ERH 532	1/2/18	12:30	325.2-325.7	1												X	X	J							
ERH 533	1/2/18	12:35	393.5-394.2	1												X	X	J							

1. Relinquished By:	Colleen Smith	2. Received By:	MIKE CARTER
Company	AECOM	Company	CORE LAB
Date / Time	1/17/18 10:30	Date / Time	1/18/18 1600
2. Relinquished By:	Bradley Bushoff	2. Received By:	
Company	Core Lab	Company	
Date / Time	12-5-18 0930	Date / Time	

CHAIN OF CUSTODY RECORD

Company	AECOM
Address	1001 Bishop St, Suite 1600 Honolulu, Hawaii 96813
Project Manager	Jeff Johnson
Phone	808-356-5340
Project Name	CIV 53
Fax	808-523-8950
Project No.	60481245
Email	eric.wetzstein@aecom.com; margie.pascua@aecom.com
Site Location	Red Hill
Sampler Signature	

PO# 94992

Turnaround Time

24 HR	
48 HR	
72 HR	
5 Day	
Normal	X

CL Bid No.

CL File No. 1703942.EN

Comments

ANALYSIS REQUEST

	Sample ID	Date	Time	Depth, ft.	Number of Samples	SOIL: Vadose Zone Suite	SOIL: Saturated Zone Suite	SOIL: Pore Fluid Saturation Suite	SOIL: Moisture Content: ASTM D2216	SOIL: Porosity: Total. API RP40	SOIL: Porosity: Effective, ASTM D425M	SOIL: Bulk Density: API RP40 / ASTM D2937	SOIL: Hydraulic Conductivity: API RP40	SOIL: Grain Size Distribution: ASTM D422/D4464M	SOIL: Atterberg Limits: ASTM D4318	SOIL: TOC: Walkley-Black	SOIL: Mobility Group-Centrifuge Method	SOIL: Mobility Group-Water Drive Method	SOIL:	FLUID: Fluid Properties Suite	FLUID: Viscosity: ASTM D445	FLUID: Density/Gravity: ASTM D1481	FLUID: Pryo-Chromatography (Fingerprinting)	FLUID: Rock Core Slabbing	FLUID: Digital UV & White Light Core Imaging	FLUID: Core Viewing Interface and Data
✓	ERH 509	12/6/17	12:00	0.65 7-60.4													X	X	✓							
✓	ERH 510	12/6/17	12:05	81.0-81.7													X	X	✓							
✓	ERH 511	12/6/17	12:10	155.2-155.9													X	X	✓							
✓	ERH 512	12/6/17	12:15	105.9													X	X	✓							
✓	ERH 513	12/6/17	12:20	133.0													X	X	✓							
✓	ERH 514	12/6/17	12:25	162.8													X	X	✓							
✓	ERH 515	12/6/17	12:30	181.5													X	X	✓							
✓	ERH 516	12/6/17	12:35	242.6													X	X	✓							
✓	ERH 517	12/6/17	12:40	341.3													X	X	✓							

1. Relinquished By:	Colleen Smith	2. Received By:	Tracey Bishop
Company	AECOM	Company	Core Lab
Date	12/8/17	Time	15:30
Date	12-11-17	Time	1116

2. Relinquished By:	Tracey Bishop	2. Received By:	
Company	Core Lab	Company	
Date	12/5/18	Time	0930
Date		Time	

CHAIN OF CUSTODY RECORD

Company	AECOM
Address	1001 Bishop St, Suite 1600 Honolulu, Hawaii 96813
Project Manager	Jeff Johnson
Phone	808-356-5340
Project Name	CIV 53
Fax	808-523-8950
Project No.	60481245
Email	eric.wetzstein@aecom.com; margie.pascua@aecom.com
Site Location	Red Hill
Sampler Signature	Smith, Colleen (Honolulu)

Digitally signed by Smith, Colleen (Honolulu)
DN: dc=com, dc=aecomnet, dc=ds, ou=AECOMUsers, ou=AMER, ou=US, cn=USPHNL1, cn=Smith, Colleen (Honolulu)
Date: 2018.01.18 14:51:57 -10'00'

ANALYSIS REQUEST

PO# 94992

Turnaround Time
- 24 HR
- 48 HR
- 72 HR
- 5 Day
- Normal: X

CL Bid No.

CL File No.

Sample ID	Date	Time	Depth, ft.	Number of Samples	SOIL: Vadose Zone Suite	SOIL: Saturated Zone Suite	SOIL: Pore Fluid Saturation Suite	SOIL: Moisture Content: ASTM D2216	SOIL: Porosity: Total, API RP40	SOIL: Porosity: Effective, ASTM D425M	SOIL: Bulk Density: API RP40 / ASTM D2937	SOIL: Hydraulic Conductivity: API RP40	SOIL: Grain Size Distribution: ASTM D422/D4464M	SOIL: Atterberg Limits: ASTM D4318	SOIL: TOC: Walkley-Black	SOIL: Mobility Group-Centrifuge Method	SOIL: Mobility Group-Water Drive Method	SOIL:	FLUID: Fluid Properties Suite	FLUID: Viscosity: ASTM D445	FLUID: Density/Gravity: ASTM D1481	FLUID: Pryo-Chromatography (Fingerprinting)	FLUID: Rock Core Slabbing	FLUID: Digital UV & White Light Core Imaging	FLUID: Core Viewing Interface and Data	Comments
ERH534	1/2/18	12:40	489.5 -490.0	1												X	X	✓								

1. Relinquished By:	Colleen Smith	2. Received By:	MEME CARTER
Company	AECOM	Company	CORE CAB
Date	1/17/2018	Time	10:30
Date	1/18/18	Time	1600

2. Relinquished By:	Stacey Bishop	2. Received By:	
Company	Core Lab	Company	
Date	12/5/18	Time	0930
Date		Time	

CHAIN OF CUSTODY RECORD

Company	AECOM
Address	1001 Bishop St, Suite 1600 Honolulu, Hawaii 96813
Project Manager	Jeff Johnson
Phone	808-356-5340
Project Name	CIV 53
Fax	808-523-8950
Project No.	60481245
Email	eric.wetzstein@aecom.com; margie.pascua@aecom.com
Site Location	Red Hill
Sampler Signature	

ANALYSIS REQUEST

PO# 94992

Turnaround Time: 24 HR [ ] 48 HR [ ] 72 HR [ ] 5 Day [ ] Normal [X]

CL Bid No.

CL File No.

Sample ID	Date	Time	Depth, ft.	Number of Samples	SOIL: Vadose Zone Suite	Saturated Zone Suite	Pore Fluid Saturation Suite	Moisture Content: ASTM D2216	Porosity: Total, API RP40	Porosity: Effective, ASTM D425M	Bulk Density: API RP40 / ASTM D2937	Hydraulic Conductivity: API RP40	Grain Size Distribution: ASTM D422/D4464M	Atterberg Limits: ASTM D4318	TOC: Walkley-Black	Mobility Group-Centrifuge Method	Mobility Group-Water Drive Method		FLUID: Fluid Properties Suite	Viscosity: ASTM D445	Density/Gravity: ASTM D1481	Pyro-Chromatography (Fingerprinting)	Rock Core Slabbing	Digital UV & White Light Core Imaging	Core Viewing Interface and Data	Comments
ERH521	12/27/17	12:20	171.0-171.8	1												X	X	V								
ERH522	12/27/17	12:25	200.2-201	1												X	X	V								
ERH523	12/27/17	12:30	218.2-219	1												X	X	V								
ERH524	12/27/17	12:35	248.8-249.5	1												X	X	V								
ERH525	12/27/17	12:40	289-289.8	1												X	X	V								
ERH526	12/28/17	12:25	108.5-109	1												X	X	V								
ERH527	12/28/17	12:20	137.6-138.4	1												X	X	V								
ERH528	12/28/17	12:35	155.4-156	1												X	X	V								
ERH529	12/28/17	12:30	177.2-178	1												X	X	V								

1. Relinquished By:	2. Received By:	2. Relinquished By:	2. Received By:
Colleen Smith	MIKE CARTER	Stacy Burns	
Company: AECOM	Company: CORE LAB	Company: CH2M Hill	Company:
Date: 1/17/18 Time: 10:30	Date: 1/18/18 Time: 1600	Date: 12/5/18 Time: 0930	Date: Time:

CHAIN OF CUSTODY RECORD

Company	AECOM
Address	1001 Bishop St, Suite 1600 Honolulu, Hawaii 96813
Project Manager	Jeff Johnson
Phone	808-356-5340
Project Name	CIV 53
Fax	808-523-8950
Project No.	60481245
Email	eric.wetzstein@aecom.com; margie.pascua@aecom.com
Site Location	Red Hill
Sampler Signature	

PO# 94992

Turnaround Time
- 24 HR
- 48 HR
- 72 HR
- 5 Day
- Normal [X]

CL Bid No. Q17-032

CL File No. 1703942

ANALYSIS REQUEST

Sample ID	Date	Time	Depth, ft.	Number of Samples	SOIL: Vadose Zone Suite	SOIL: Saturated Zone Suite	SOIL: Pore Fluid Saturation Suite	SOIL: Moisture Content: ASTM D2216	SOIL: Porosity: Total, API RP40	SOIL: Porosity: Effective, ASTM D425M	SOIL: Bulk Density API RP40 / ASTM D2937	SOIL: Hydraulic Conductivity: API RP40	SOIL: Grain Size Distribution: ASTM D422/D4464M	SOIL: Atterberg Limits: ASTM D4318	SOIL: TOC: Walkley-Black	FLUID: Fluid Properties Suite	FLUID: Viscosity: ASTM D445	FLUID: Density/Gravity: ASTM D1481	FLUID: Pyro-Chromatography (Fingerprinting)	Comments
Fuel Sample	12/18/17	0930	---	no analysis required, ten 1-gallon containers of fuel submitted																Disposed of per client request

1. Relinquished By:	2. Received By:	2. ~~Relinquished~~ By:	2. Received By:
WATSON TANJI		DISPOSED	
Company: AECOM	Company: CORE LAB	Company: CORE LAB	Company:
Date: 12/19/17 Time: 0930	Date: 12/20/17 Time: 1530	Date: 12/4/18 Time: 1130	Date: Time:

This page intentionally left blank

Appendix G:
Infiltration Study Report

This page intentionally left blank

GEOLABS, INC.
Geotechnical Engineering and Drilling Services

November 6, 2018
W.O. 7623-00

Ms. Allison Bolan
AECOM Technical Services, Inc.
1001 Bishop Street, Suite 1600
Honolulu, HI 96813

DOUBLE-RING INFILTROMETER TESTING
RED HILL BULK FUEL STORAGE FACILITY
JBPHH, OAHU, HAWAII
NAVY CLEAN N62742-12-D-1829, CTO 0053

Dear **Ms. Bolan:**

This report presents the results of our infiltration tests performed at the Red Hill Bulk Fuel Storage Facility of the Joint Base Pearl Harbor - Hickam (JBPHH) area on the Island of Oahu, Hawaii. The project location and general vicinity are shown on the Project Location Map (Plate 1) and Site Plan (Plate 2). The infiltration testing was conducted in general accordance with the scope of services outlined in our fee proposal dated October 9, 2017. The test results presented herein are subject to the limitations noted at the end of this report.

PROJECT CONSIDERATIONS

The project site is located at the Red Hill Bulk Fuel Storage Facility (RHBFSF) of the Joint Base Pearl Harbor -Hickam (JBPHH) area on the Island of Oahu, Hawaii. The RHBFSF is bordered on the north by the Halawa Correctional Facility and private industrial businesses, on the southwest by the U.S. Coast Guard reservation, on the south by residential neighborhoods, and on the east by Moanalua Valley. The Halawa quarry lies within one-quarter of a mile to the northwest.

Based on preliminary information from AECOM Technical Services, Inc. (AECOM), the RHBFSF encompasses approximately 144 acres of land with surface elevations ranging from about +200 to +600 feet Mean Sea Level (MSL). We understand that the infiltration test data collected at the three selected locations will be used to evaluate the infiltration characteristics of the near-surface soils in support of the Investigation and Remediation of Releases at the Red Hill Bulk Fuel Storage Facility.

PURPOSE AND SCOPE

The purpose of our work was to perform infiltration tests as requested by AECOM Technical Services, Inc. to evaluate the infiltration characteristics of the near-surface soils in support of the Investigation and Remediation of Releases at the Red Hill Bulk Fuel Storage Facility. To accomplish this, we performed a surface exploration and testing program consisting of the following tasks and work efforts:

1. Attendance of a brief meeting with AECOM prior to our field mobilization for coordination of the work efforts for the project.

2. Site visit to review the selected test locations by AECOM and coordination of utility clearance through Hawaii One-Call.

3. Preparation of an Activity Hazard Analysis document for review and approval prior to our field mobilization.

4. Procurement of base passes for access to the test site.

5. Mobilization and demobilization of a support truck with water tank, brush cutting and hand digging equipment with crew to and from the project site for clearing, excavation and backfilling of shallow test pits.

6. Mobilization and demobilization of double-ring infiltrometer testing equipment and laptop computer to and from the project site.

7. Clearing and grubbing of tall grass and shrub, excavation of three test pits to depths of about 6 to 18 inches below the existing ground surface, and setting up of the infiltration testing equipment.

8. Performance of one infiltration test using the double-ring infiltrometer at each test location by our field engineer and assistants.

9. Backfilling of the excavated test pits to the original grades after completion of the infiltration testing.

10. Performance of Atterberg Limits and moisture content tests on the near-surface soils obtained at each infiltration test location as an aid in classifying the materials and evaluating their engineering properties.

11. Preparation of this letter report summarizing the infiltration test data, laboratory test results, and calculated infiltration rates.

12. Coordination of our overall work on the project by our senior engineer.

13. Quality assurance of our work and client/design team consultation by our principal engineer.

14. Miscellaneous work efforts such as drafting, word processing, and clerical support.

GEOLOGIC CONDITIONS

The Island of Oahu encompasses approximately 604 square miles of land area that may be divided into four major geographic provinces. The geographic provinces include: 1) Koolau Range, 2) Waianae Range, 3) Schofield Plateau, and 4) Coastal Plains. The majority of the Island of Oahu was built by the extrusion of basaltic lava from two primary shield volcanoes known as Waianae and Koolau. The older Waianae Volcano is estimated to be middle to late Pliocene in geochronologic age and forms the bulk of the western third of the island. The younger Koolau Volcano is estimated to be late Pliocene to early Pleistocene (Ice Age) in age and forms the majority of the eastern two-thirds of the island.

The Waianae Volcano became extinct while the Koolau Volcano remained active; therefore, the westward flowing lava from the Koolau Volcano continued to bank against the weathered products of the Waianae Volcano to create the elevated area known as the Schofield Plateau, located between the two volcanoes.

Following the eruption of the bulk of the lavas, the coastal areas of Oahu were partially submerged and emerged cyclically due to large-scale sea-level fluctuations in response to periods of worldwide glaciation. In addition to the sea level fluctuations, the island mass was undergoing a gradual subsidence due to the island's mass and isostatic adjustment of the earth's crust beneath the island. As a result of the cyclic sea level fluctuations and the gradual subsidence of the island, the erosional baseline likewise, fluctuated, and major streams were drowned and buried and later emerged to renew their incision.

The lowering of the base level results in an increased stream gradient and consequently an increased rate of stream down cutting. The effect of changes in erosional baseline impact the evolution of landforms by influencing the rate of stream down cutting and sediment deposition in addition to changing the coastal exposure to ocean wave erosion. The combined effects are evidenced by the evolution of steep walled amphitheater-shape valleys, the filling of valleys to form broad, gently sloping alluvial floors, and the initiation of renewed stream dissection into the older alluvial deposits to form terraces at the bottom of the valley floors. This cyclic activity during the Pleistocene Epoch partially accounts for the present topography of today including the Ewa, Honolulu, and Kahuku sedimentary coastal plains and the coastal perimeter of the Island of Oahu.

Approximately 30 secondary volcanic vents have erupted on the Island of Oahu since the major Koolau valleys were dissected by erosion and partially filled with

alluvium. The younger eruptions are identified as the Honolulu Volcanic Series (Stearns and Vaksvik, 1938). The eruptions and resulting deposits occurred mainly on the southern portion of the Koolau Shield Volcano. The eruptions are believed to have occurred during the middle Pleistocene Epoch to the Recent Age. The vents are scattered near the ancient Koolau Shield's center of volcanic activity and generally spread outward along the southwest rift zone of the Koolau Volcano. The late stage eruptions are generally represented by pyroclastic materials, which include cinder, lava spatter, ash, tuff, and some lava flows.

The natural processes of erosion may be defined as the process of land denudation by the wearing away of soil and rock by both physical and chemical processes. The processes may include the weathering of rock to form soils, the mass wasting of blocks of earth materials, and the erosive activity of streams, waves, wind, and underground water on the soil and rock materials. In Hawaii, as well as other tropical regions, the processes of mass wasting combined with stream and ocean wave erosion are the most important forces acting to continually erode and stabilize landforms.

The project site is underlain by basaltic rock representing the weathered products of the Koolau Volcanic Series lavas. The basalt rock is prominently layered with alternating beds of basalt clinker sandwiched between hard basalt rock beds that represent individual lava flows of both a'a and pahoehoe type. As a result, the ground surface relief is somewhat irregular and "stepped" in character. The irregular hillslope surface is created by differential erosion between the weaker clinker layers and more indurated basalt rock layers representing the core of the lava flows. Therefore, periodic ledges of hard rock form greater relief in contrast to the more decomposed and low relief character of the bounding clinker layers. The steep rock cut slope at the bottom of the hillside is composed of alternating medium hard to very hard lava materials representing dense a'a lava core seams separated by weaker zones of cemented basaltic clinker (rocky rubble containing cobble and gravel size fragments welded by heat during deposition).

Based on our observations, the ground surfaces along the crest and upper slopes where our infiltration tests were conducted generally contain residual and alluvial soil accumulations overlying the basaltic rock formation. Based on our visual assessment of the existing ground surface conditions, the surface soils appear to be on the order of about 2 to 4 feet in thickness and may contain some embedded basaltic cobbles and boulders. Based on our visual reconnaissance, the cut slope face along the Lower Access Road is composed of medium hard to very hard, generally moderately weathered basaltic rock.

SITE DESCRIPTION

The project site is located at the Red Hill Bulk Fuel Storage Facility (RHBFSF) of the Joint Base Pearl Harbor-Hickam (JBPHH) area on the Island of Oahu, Hawaii. The RHBFSF is bordered on the north by the Halawa Correctional Facility and private

industrial businesses, on the southwest by the U.S. Coast Guard reservation, on the south by residential neighborhoods, and on the east by Moanalua Valley. The Halawa quarry lies within one-quarter of a mile to the northwest.

A service road (Icarus Way) winds its way uphill from the Halawa gate entrance and traverses from the lower southwest to the upper northeast ridge of Red Hill providing the only access to the test area. The site is generally covered with thick vegetation consisting of a variety of trees, including Haole Koa, Indian Plum, Cainito, Banyan trees, and a host of other tree species with an undergrowth of shrubs and tall reed grass. The ground elevations at the test area generally ranges between +500 and +580 feet MSL as shown on the Site Plan (Plate 2).

INFILTRATION TESTING

The water infiltration rates into the subsurface soils were tested by performing double-ring infiltrometer tests at the prepared test locations in general accordance with ASTM D3385. The tests were performed by driving two open concentric cylinders into the ground, partially filling the rings with water and maintaining a near-constant water level.

The double-ring infiltrometer test estimates the vertical movement of water through the bottom of the inner cylinder, while the outer ring helps to reduce the lateral movement of water in the soil. The volume of water added to the inner ring is measured as the infiltrated water volume. The tests were carried out in several increments until achieving a steady-state condition with a relatively constant water infiltration rate. Detailed test data and results are presented in Appendix A.

INFILTRATION TEST RESULTS

To characterize the water infiltration rates of the soils overlying the underground storage tanks at the project site, we conducted three double-ring infiltrometer tests at the locations identified and marked in the field by AECOM. The tests were conducted at the bottom of hand-excavated shallow pits/pads by Geolabs as summarized in the following table.

SUMMARY OF INFILTRATION TESTS

Test No.	Approximate Test Location		Final Infiltration Rate		Soil Classification
	Latitude	Longitude	(cm/hour)	(inch/hour)	(USCS)
IF-1	21° 22’22” N	157° 54’15” W	20.6	8.11	CH
IF-2	21° 22’16” N	157° 53’40” W	10.7	4.21	CH
IF-3	21° 22’20” N	157° 53’37” W	22	8.66	MH

Due to the divergent rates of flow between the inner and outer rings in Test Nos. IF-1 and IF-2, the final infiltration values of the inner ring were adopted in accordance with ASTM D3385 guidelines. The average infiltration rate for the tests is about 17.8 cm/hr. (7 in/hr.) It should be noted that Test Nos. IF-1 and IF-2 were performed in areas that were cleared of vegetation and excavated generally below the grass root line, approximately between 0.5 to 1 foot below the existing grade. On the other hand, Test No. IF-3 was performed on a levelled pad excavated near the toe of a barren saprolite outcrop. Laboratory Atterberg Limits tests conducted on the soil samples from each of the test locations indicate that the near-surface soils at Test Nos. IF-1 and IF-2 are classified as Silty Clay (CH), while the soil sample for Test No. IF-3 is classified as Clayey Silt (MH).

LIMITATIONS

The analyses submitted herein are based in part upon information obtained from our field exploration and infiltration tests conducted at the locations selected by AECOM. Variations of subsoil conditions may occur, and the nature and extent of these variations i.e.; thickness of the overburden soil, weathering and fracture conditions of the underlying rock, may not become evident until construction involving excavations into the subgrade below the tested zone is undertaken. If variations then appear evident, it may be necessary to re-evaluate the site infiltration characteristics presented herein.

This report has been prepared for the exclusive use of AECOM Technical Services, Inc. and their design consultants for specific application to the Investigation and Remediation of Releases at the Red Hill Bulk Fuel Storage Facility project in accordance with generally accepted geotechnical engineering principles and practices. No warranty is expressed or implied.

This report has been prepared solely for the purpose of gathering field infiltration measurements using the double-ring infiltrometer and water as a medium including limited surface soil characterization as requested by AECOM Technical Services, Inc. for hydrologic, environmental modelling and related purposes.

The infiltration testing conducted at the project site was not intended to investigate the potential presence of hazardous materials and/or archeological features existing at the site. It should be noted that the equipment, techniques, and personnel used to conduct a geo-environmental exploration differ substantially from those applied in geotechnical engineering.

CLOSURE

We appreciate the opportunity to be of service to you on this project. If you have questions or need additional information, please contact our office.

Respectfully submitted,

GEOLABS, INC.

By _____
Melchor Nolasco
Staff Engineer

By _____
Teddy S.T. Kwok, P.E.
Vice President

THIS WORK WAS PREPARED BY
ME OR UNDER MY SUPERVISION.

SIGNATURE

4-30-20
EXPIRATION DATE
OF THE LICENSE

TK:MN:as

Attachments: **PLATES**
Project Location Map, Plate 1
Site Plan, Plate 2

APPENDIX A
Field Infiltrometer Tests, Page A-1
Infiltrometer Test Data, Plates A-1.1 thru A-3.3

APPENDIX B
Laboratory Tests, Page B-1
Laboratory Test Data, Plates B-1 and B-2

h:\7600Series\7623-00.gs1

PLATES

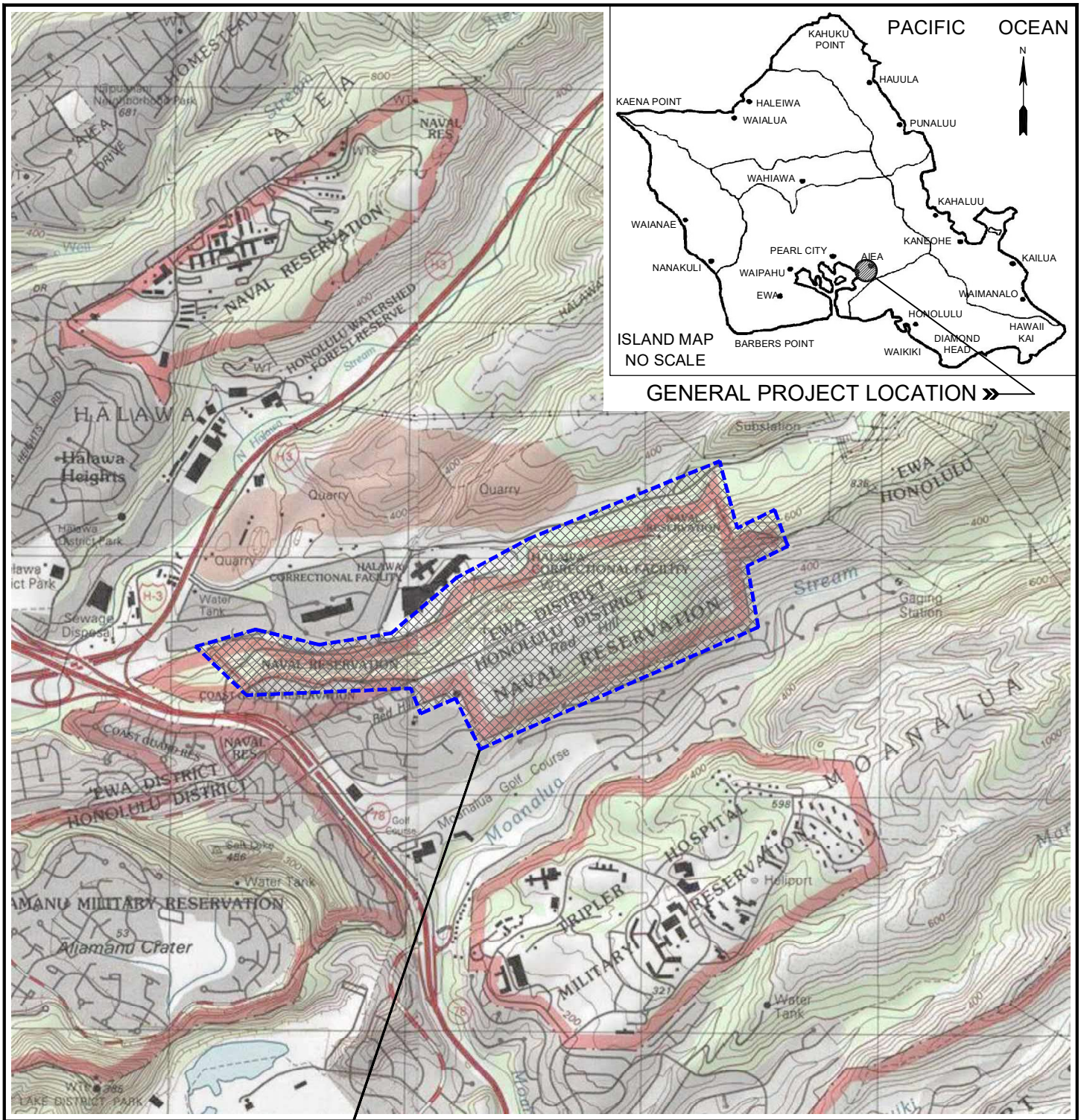

PROJECT LOCATION MAP

CIV 0053 DOUBLE-RING INFILTROMETER TESTING
RED HILL BULK FUEL STORAGE FACILITY
JBPHH, OAHU, HAWAII

2000 1000 0 2000 FT.

GRAPHIC SCALE

N

REFERENCE: MAP CREATED WITH TOPO!® ©2010 NATIONAL GEOGRAPHIC; ©2007 TELE ATLAS, REL. 1/2007.

GEOLABS, INC.
Geotechnical Engineering

DATE	DRAWN BY	PLATE
NOVEMBER 2017	ASP	1
SCALE	W.O.	
1" = 2,000'	7623-00	

CAD User: ASPASIONJR File Last Updated: November 13, 2017 5:43:43pm Plot Date: November 13, 2017 - 5:43:51pm
File: T:\Drafting\Working\7623-00RedHillBulkFuelStorageFacility\7623-00PLM.dwg\1.0 PLM
Plotter: DWG To PDF.pc3 Plotstyle: GEO-No-Dithering.ctb

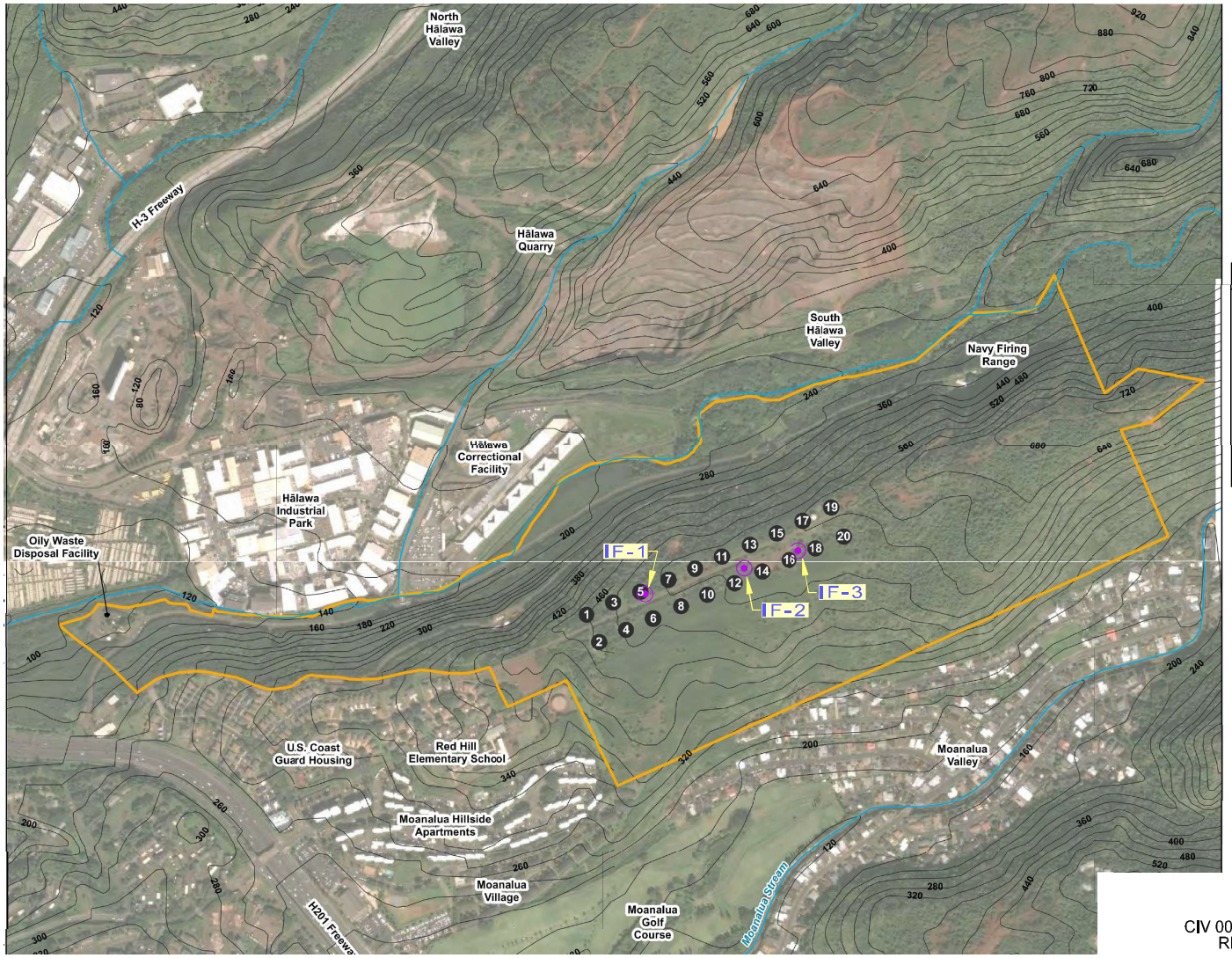

Legend

- Approximate Infiltrometer Test Location
- Red Hill Fuel Storage Tank
- Stream
- 400 Topographic Contour (feet above mean sea level)
- Red Hill Installation Boundary

0 375 750 1500 2250 FT.

GRAPHIC SCALE

N

REFERENCE: PLAN PROVIDED BY AECOM ENTITILED, "PROPOSED DOUBLE-RING INFILTROMETER SITES, RED HILL BULK FUEL STORAGE FACILITY, JBPHH, OAHU, HAWAII" DATED SEPTEMBER 25, 2017.

SITE PLAN

CIV 0053 DOUBLE-RING INFILTROMETER TESTING
RED HILL BULK FUEL STORAGE FACILITY
JBPHH, OAHU, HAWAII

GEOLABS, INC.
Geotechnical Engineering

DATE	DRAWN BY	PLATE
NOVEMBER 2018	KHN	2
SCALE	W.O.	
1" = 750'	7623-00	

CAD User: KIM File Last Updated: November 05, 2018 - 6:58:11pm Plot Date: November 05, 2018 - 6:59:35pm
File Name: C:\Working\Working\7623-00\Red_Hill_Storage_Facility\7623-00SitePlan.dwg
Plotted By: KIM on 36"x24" Plotstyle: GEO-NoShrinking-BlackAndWhite.ctb

APPENDIX A

A P P E N D I X A

Field Infiltrometer Tests

To measure the subsurface infiltration rates of the near-surface soils at the test locations, we conducted three infiltration tests using a double-ring infiltrometer at the bottom of each test pit in general accordance with the ASTM D3385. Results and graphic presentations of the infiltration tests are provided on Plates A-1.1 through A-3.3.

DOUBLE RING INFILTROMETER --- ASTM D3385-09

W.O. 7623-00

Project Name: Red Hill Bulk Storage Facility Infiltration Testing

Test ID: IF-1 Test Date: 10/15/18

Tested By: MN Liquid: Water pH:

Water Table Depth (feet) NA Ground Temp.:

Inner Ring Penetration (in) 4 Outer Ring Pen. (in) 6.0

Constants		Liquid depth	Liquid depth	Theoretical	Initial liq vol	Mariotte Tubes	
Area	(cm^2)	(in)	(cm)	(gal)	(gal)	No.	Vol/ΔH (cm^3/cm)
Inner Ring	707.0	6.0	15.2	2.8	0.83	1	54.0
Annular Space	2106.0	6.0	15.2	8.5	2.57	2	168.0

Liquid level maintained by: □ Flow Valve; □ Float Valve; ■ Mariotte Tube

Infiltration Test			Elapsed Time per Test	Total Elapsed Time	Flow Readings								Infiltration Rate			Remarks
					Inner Ring (MariotteTube 1)				Annular (MariotteTube 2)				Inner	Annular	Average	
No.	Start or End	Time hr:min	(min)	(min)	h_i (cm)	h_t (cm)	Δh (cm)	flow (cm^3)	h_i (cm)	h_t (cm)	Δh (cm)	flow, (cm^3)	(cm/h)	(cm/h)	(cm/h)	
1	Start	13:31	2	2	58.0	33.0	25.0	1350.0	58.0	25.0	33.0	5544	57.3	79.0	68.1	Water Temp =80°F
	End	13:33														
2	Start	13:36	2	7	58.0	45.0	13.0	702.0	58.0	45.0	13.0	2184	29.8	31.1	30.4	Refiled
	End	13:38														
3	Start	13:40	2	11	58.0	45.0	13.0	702.0	58.0	43.0	15.0	2520	29.8	35.9	32.8	Refiled
	End	13:42														
4	Start	13:45	2	16	58.0	48.0	10.0	540.0	58.0	43.0	15.0	2520	22.9	35.9	29.4	Refiled
	End	13:47														
5	Start	13:51	4	24	58.0	30.0	28.0	1512.0	58.0	23.0	35.0	5880	32.1	41.9	37.0	Refiled
	End	13:55														
6	Start	13:58	4	31	58.0	35.0	23.0	1242.0	58.0	24.0	34.0	5712	26.4	40.7	33.5	Refiled
	End	14:02														
7	Start	14:06	4	39	58.0	33.0	25.0	1350.0	58.0	23.0	35.0	5880	28.6	41.9	35.3	Refiled
	End	14:10														
8	Start	14:12	4	45	58.0	36.0	22.0	1188.0	58.0	27.0	31.0	5208	25.2	37.1	31.1	Refiled
	End	14:16														
9	Start	14:21	5	55	58.0	30.0	28.0	1512.0	58.0	22.0	36.0	6048	25.7	34.5	30.1	Refiled
	End	14:26														
10	Start	14:29	5	63	58.0	28.0	30.0	1620.0	58.0	24.0	34.0	5712	27.5	32.5	30.0	Refiled
	End	14:34														
11	Start	14:39	5	73	58.0	26.0	32.0	1728.0	58.0	16.0	42.0	7056	29.3	40.2	34.8	Refilled
	End	14:44														
12	Start	14:48	5	82	58.0	32.0	26.0	1404.0	58.0	17.0	41.0	6888	23.8	39.2	31.5	Refilled
	End	14:53														
13	Start	14:59	6	94	58.0	25.0	33.0	1782.0	58.0	10.0	48.0	8064	25.2	38.3	31.7	Refilled
	End	15:05														
14	Start	15:09	6	104	58.0	27.0	31.0	1674.0	58.0	12.0	46.0	7728	23.7	36.7	30.2	Refilled
	End	15:15														

DOUBLE RING INFILTROMETER --- ASTM D3385-09

W.O. 7623-00

Project Name: Red Hill Bulk Storage Facility Infiltration Testing

Test ID: IF-1 Test Date: 10/15/18

Tested By: MN Liquid: Water pH:

Water Table Depth (feet) NA Ground Temp.:

Inner Ring Penetration (in) 4 Outer Ring Pen. (in) 6.0

Constants		Liquid depth	Liquid depth	Theoretical	Initial liq vol	Mariotte Tubes	
Area	(cm^2)	(in)	(cm)	(gal)	(gal)	No.	Vol/ΔH (cm^3/cm)
Inner Ring	707.0	6.0	15.2	2.8	0.83	1	54.0
Annular Space	2106.0	6.0	15.2	8.5	2.57	2	168.0

Liquid level maintained by: □ Flow Valve; □ Float Valve; ■ Mariotte Tube

Infiltration Test			Elapsed Time per Test	Total Elapsed Time	Flow Readings								Infiltration Rate			Remarks
					Inner Ring (MariotteTube 1)				Annular (MariotteTube 2)				Inner	Annular	Average	
No.	Start or End	Time hr:min	(min)	(min)	h_i (cm)	h_t (cm)	Δh (cm)	flow (cm^3)	h_i (cm)	h_t (cm)	Δh (cm)	flow (cm^3)	(cm/h)	(cm/h)	(cm/h)	
15	Start	15:18	6	113	58.0	25.0	33.0	1782.0	58.0	13.0	45.0	7560	25.2	35.9	30.6	Refilled
	End	15:24														
16	Start	15:28	6	123	58.0	31.0	27.0	1458.0	58.0	12.0	46.0	7728	20.6	36.7	28.7	Refilled
	End	15:34														

Remarks: 1. Inner Infiltration Rate: $V_{IR} = \Delta V_{IR} / (A_{IR} * \Delta t)$ Annular space infiltration rate: $V_A = \Delta V_A / (A_A * \Delta t)$

2. Applicable to relatively UNIFORM FINE-GRAINED SOIL, with low to moderate ring penetration, and without fat clay and gravel-size particles.

3. Test should be conducted ABOVE ground water level.

4. NOT for very pervious or impervious soil (k should be within 10^{-6} to 10^{-2} cm/s). NOT for dry or stiff soil that fractures easily.

5. NOT able to determine coefficent of permeability *k* directly.

DOUBLE RING INFILTROMETER --- ASTM D3385-09

W.O. 7623-00

Project Name: Red Hill Bulk Storage Facility Infiltration Testing

Test ID: IF-1 Test Date: 10/15/18

Tested By: MN Liquid: Water pH:

Water Table Depth (feet) NA Ground Temp.:

Inner Ring Penetration (in) 4 Outer Ring Pen. (in) 6.0

Constants		Liquid depth	Liquid depth	Theoretical	Initial liq vol	Mariotte Tubes	
Area	(cm^2)	(in)	(cm)	(gal)	(gal)	No.	Vol/ΔH (cm^3/cm)
Inner Ring	707.0	6.0	15.2	2.8	0.83	1	54.0
Annular Space	2106.0	6.0	15.2	8.5	2.57	2	168.0

Liquid level maintained by: □ Flow Valve; □ Float Valve; ■ Mariotte Tube

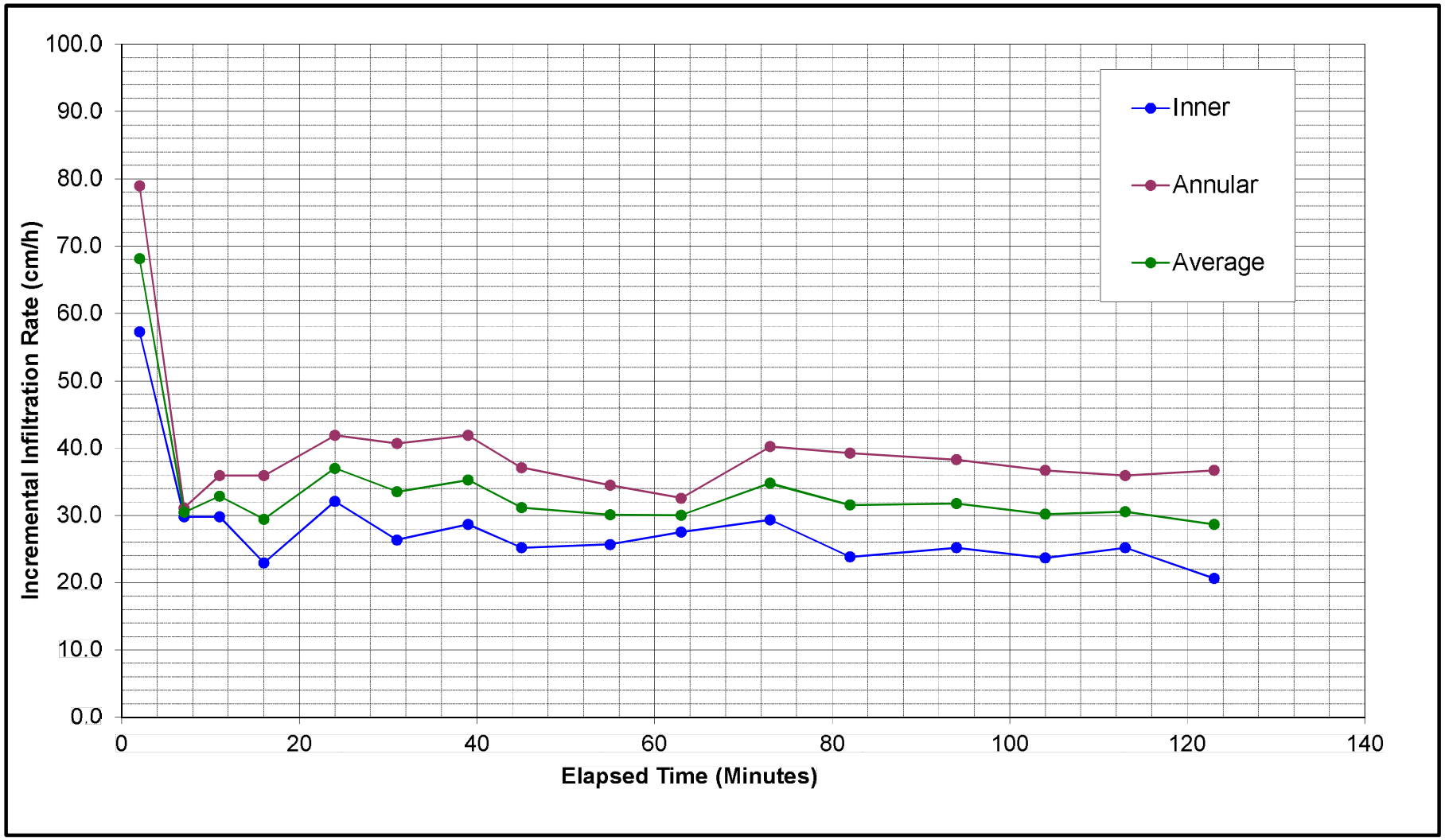

DOUBLE RING INFILTROMETER --- ASTM D3385-09

W.O. 7623-00

Project Name: Red Hill Bulk Storage Facility Infiltration Testing

Test ID: IF-2 Test Date: 10/17/18

Tested By: MN Liquid: Water pH: 8.2

Water Table Depth (feet) NA Ground Temp.:

Inner Ring Penetration (in) 3.5 Outer Ring Pen. (in) 4.0

Constants		Liquid depth	Liquid depth	Theoretical	Initial liq vol	Mariotte Tubes	
Area	(cm^2)	(in)	(cm)	(gal)	(gal)	No.	Vol/ΔH (cm^3/cm)
Inner Ring	707.0	5.0	12.7	2.4	0.83	1	54.0
Annular Space	2106.0	5.0	12.7	7.1	2.57	2	168.0

Liquid level maintained by: □ Flow Valve; □ Float Valve; ■ Mariotte Tube

Infiltration Test			Elapsed Time per Test	Total Elapsed Time	Flow Readings								Infiltration Rate			Remarks
					Inner Ring (MariotteTube 1)				Annular (MariotteTube 2)				Inner	Annular	Average	
No.	Start or End	Time hr:min	(min)	(min)	h_i (cm)	h_t (cm)	Δh (cm)	flow (cm^3)	h_i (cm)	h_t (cm)	Δh (cm)	flow, (cm^3)	(cm/h)	(cm/h)	(cm/h)	
1	Start	10:54	5	5	58.0	36.0	22.0	1188.0	58.0	29.0	29.0	4872	20.2	27.8	24.0	Water Temp =80°F
	End	10:59														
2	Start	11:07	5	18	58.0	41.0	17.0	918.0	58.0	34.0	24.0	4032	15.6	23.0	19.3	Refilled
	End	11:12														
3	Start	11:12	5	23	41.0	25.0	16.0	864.0	34.0	11.0	23.0	3864	14.7	22.0	18.3	
	End	11:17														
4	Start	11:21	5	32	58.0	39.0	19.0	1026.0	58.0	36.0	22.0	3696	17.4	21.1	19.2	Refilled
	End	11:26														
5	Start	11:29	10	45	58.0	19.0	39.0	2106.0	58.0	12.0	46.0	7728	17.9	22.0	19.9	Refilled
	End	11:39														
6	Start	11:56	10	72	58.0	25.0	33.0	1782.0	58.0	22.0	36.0	6048	15.1	17.2	16.2	Refilled
	End	12:06														
7	Start	12:08	10	84	58.0	34.0	24.0	1296.0	58.0	27.0	31.0	5208	11.0	14.8	12.9	Refilled
	End	12:18														
8	Start	12:25	10	101	58.0	31.0	27.0	1458.0	58.0	21.0	37.0	6216	12.4	17.7	15.0	Refilled
	End	12:35														
9	Start	12:44	10	120	58.0	32.0	26.0	1404.0	58.0	25.0	33.0	5544	11.9	15.8	13.9	Refilled
	End	12:54														
10	Start	12:58	15	139	58.0	20.0	38.0	2052.0	58.0	5.0	53.0	8904	11.6	16.9	14.3	Refilled
	End	13:13														
11	Start	13:19	15	160	58.0	22.0	36.0	1944.0	58.0	5.0	53.0	8904	11.0	16.9	14.0	Refilled
	End	13:34														
12	Start	13:39	15	180	58.0	22.0	36.0	1944.0	58.0	13.0	45.0	7560	11.0	14.4	12.7	Refilled
	End	13:54														

DOUBLE RING INFILTROMETER --- ASTM D3385-09

W.O. 7623-00

Project Name: Red Hill Bulk Storage Facility Infiltration Testing

Test ID: IF-2 Test Date: 10/17/18

Tested By: MN Liquid: Water pH: 8.2

Water Table Depth (feet) NA Ground Temp.:

Inner Ring Penetration (in) 3.5 Outer Ring Pen. (in) 4.0

Constants		Liquid depth	Liquid depth	Theoretical	Initial liq vol	Mariotte Tubes	
Area	(cm^2)	(in)	(cm)	(gal)	(gal)	No.	Vol/ΔH (cm^3/cm)
Inner Ring	707.0	5.0	12.7	2.4	0.83	1	54.0
Annular Space	2106.0	5.0	12.7	7.1	2.57	2	168.0

Liquid level maintained by: □ Flow Valve; □ Float Valve; ■ Mariotte Tube

Infiltration Test			Elapsed Time per Test	Total Elapsed Time	Flow Readings								Infiltration Rate			Remarks
					Inner Ring (MariotteTube 1)				Annular (MariotteTube 2)				Inner	Annular	Average	
No.	Start or End	Time hr:min	(min)	(min)	h_i (cm)	h_t (cm)	Δh (cm)	flow (cm^3)	h_i (cm)	h_t (cm)	Δh (cm)	flow, (cm^3)	(cm/h)	(cm/h)	(cm/h)	
13	Start	13:59	15	200	58.0	23.0	35.0	1890.0	58.0	14.0	44.0	7392	10.7	14.0	12.4	Refilled
	End	14:14														

Remarks: 1. Inner Infiltration Rate: $V_{IR} = \Delta V_{IR} / (A_{IR} * \Delta t)$ Annular space infiltration rate: $V_A = \Delta V_A / (A_A * \Delta t)$

2. Applicable to relatively UNIFORM FINE-GRAINED SOIL, with low to moderate ring penetration, and without fat clay and gravel-size particles.

3. Test should be conducted ABOVE ground water level.

4. NOT for very pervious or impervious soil (k should be within 10^{-6} to 10^{-2} cm/s). NOT for dry or stiff soil that fractures easily.

5. NOT able to determine coefficent of permeability *k* directly.

DOUBLE RING INFILTROMETER --- ASTM D3385-09

W.O. 7623-00

Project Name: Red Hill Bulk Storage Facility Infiltration Testing

Test ID: IF-2 Test Date: 10/17/18

Tested By: MN Liquid: Water pH: 8.2

Water Table Depth (feet) NA Ground Temp.:

Inner Ring Penetration (in) 3.5 Outer Ring Pen. (in) 4.0

Constants		Liquid depth	Liquid depth	Theoretical	Initial liq vol	Mariotte Tubes	
Area	(cm^2)	(in)	(cm)	(gal)	(gal)	No.	Vol/ΔH (cm^3/cm)
Inner Ring	707.0	5.0	12.7	2.4	0.83	1	54.0
Annular Space	2106.0	5.0	12.7	7.1	2.57	2	168.0

Liquid level maintained by: □ Flow Valve; □ Float Valve; ■ Mariotte Tube

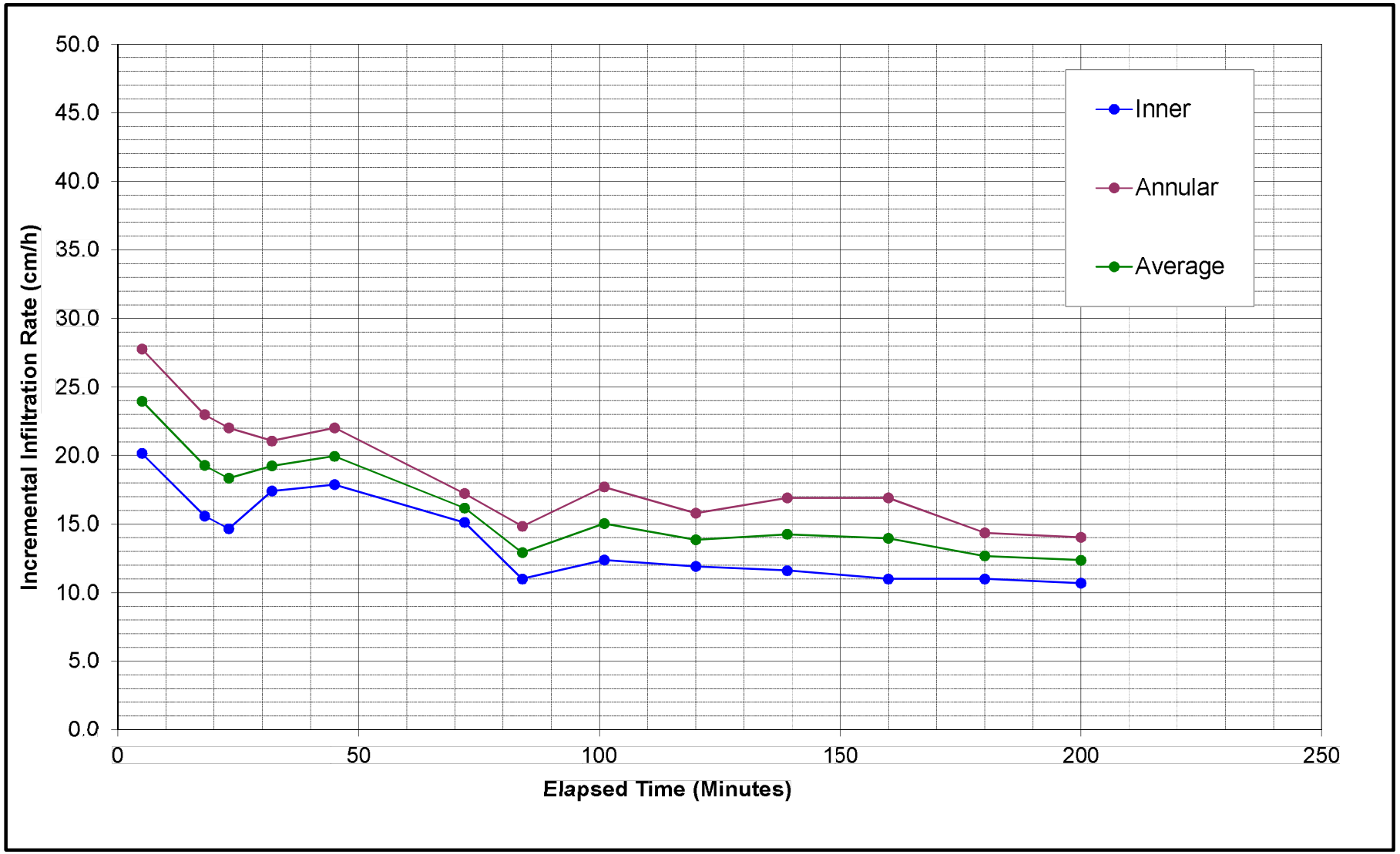

DOUBLE RING INFILTROMETER --- ASTM D3385-09

W.O. 7623-00

Project Name: Red Hill Bulk Storage Facility Infiltration Testing

Test ID: IF-3 Test Date: 10/16/18

Tested By: MN Liquid: Water pH: 8.2

Water Table Depth (feet) NA Ground Temp.:

Inner Ring Penetration (in) 3.5 Outer Ring Pen. (in) 4.0

Constants		Liquid depth	Liquid depth	Theoretical	Initial liq vol	Mariotte Tubes	
Area	(cm^2)	(in)	(cm)	(gal)	(gal)	No.	Vol/ΔH (cm^3/cm)
Inner Ring	707.0	5.0	12.7	2.4	0.83	1	54.0
Annular Space	2106.0	5.0	12.7	7.1	2.57	2	168.0

Liquid level maintained by: □ Flow Valve; □ Float Valve; ■ Mariotte Tube

Infiltration Test			Elapsed Time per Test	Total Elapsed Time	Flow Readings								Infiltration Rate			Remarks
					Inner Ring (MariotteTube 1)				Annular (MariotteTube 2)				Inner	Annular	Average	
No.	Start or End	Time hr:min	(min)	(min)	h_i (cm)	h_t (cm)	Δh (cm)	flow (cm^3)	h_i (cm)	h_t (cm)	Δh (cm)	flow, (cm^3)	(cm/h)	(cm/h)	(cm/h)	
1	Start	10:59	2	2	58.0	45.0	13.0	702.0	58.0	43.0	15.0	2520	29.8	35.9	32.8	Water Temp =80°F
	End	11:01														
2	Start	11:05	2	8	58.0	46.0	12.0	648.0	58.0	40.0	18.0	3024	27.5	43.1	35.3	Refilled
	End	11:07														
3	Start	11:09	2	12	58.0	46.0	12.0	648.0	58.0	42.0	16.0	2688	27.5	38.3	32.9	Refilled
	End	11:11														
4	Start	11:13	2	16	58.0	47.0	11.0	594.0	58.0	43.0	15.0	2520	25.2	35.9	30.6	Refilled
	End	11:15														
5	Start	11:16	4	21	58.0	32.0	26.0	1404.0	58.0	30.0	28.0	4704	29.8	33.5	31.6	Refilled
	End	11:20														
6	Start	11:23	4	28	58.0	34.0	24.0	1296.0	58.0	36.0	22.0	3696	27.5	26.3	26.9	Refilled
	End	11:27														
7	Start	11:29	4	34	58.0	37.0	21.0	1134.0	58.0	35.0	23.0	3864	24.1	27.5	25.8	Refilled
	End	11:33														
8	Start	11:34	4	39	58.0	38.0	20.0	1080.0	58.0	36.0	22.0	3696	22.9	26.3	24.6	Refilled
	End	11:38														
9	Start	11:40	6	47	58.0	27.0	31.0	1674.0	58.0	24.0	34.0	5712	23.7	27.1	25.4	Refilled
	End	11:46														
10	Start	11:48	6	55	58.0	28.0	30.0	1620.0	58.0	26.0	32.0	5376	22.9	25.5	24.2	Refilled
	End	11:54														
11	Start	11:54	8	63	58.0	15.0	43.0	2322.0	58.0	15.0	43.0	7224	24.6	25.7	25.2	Refilled
	End	12:02														
12	Start	12:07	8	76	58.0	20.0	38.0	2052.0	58.0	19.0	39.0	6552	21.8	23.3	22.6	Refilled
	End	12:15														
13	Start	12:17	8	86	58.0	19.0	39.0	2106.0	58.0	21.0	37.0	6216	22.3	22.1	22.2	Refilled
	End	12:25														
14	Start	12:29	8	98	58.0	17.0	41.0	2214.0	58.0	15.0	43.0	7224	23.5	25.7	24.6	Refilled
	End	12:37														

DOUBLE RING INFILTROMETER --- ASTM D3385-09

W.O. 7623-00

Project Name: Red Hill Bulk Storage Facility Infiltration Testing

Test ID: IF-3 Test Date: 10/16/18

Tested By: MN Liquid: Water pH: 8.2

Water Table Depth (feet) NA Ground Temp.:

Inner Ring Penetration (in) 3.5 Outer Ring Pen. (in) 4.0

Constants		Liquid depth	Liquid depth	Theoretical	Initial liq vol	Mariotte Tubes	
Area	(cm^2)	(in)	(cm)	(gal)	(gal)	No.	Vol/ΔH (cm^3/cm)
Inner Ring	707.0	5.0	12.7	2.4	0.83	1	54.0
Annular Space	2106.0	5.0	12.7	7.1	2.57	2	168.0

Liquid level maintained by: □ Flow Valve; □ Float Valve; ■ Mariotte Tube

Infiltration Test			Elapsed Time per Test	Total Elapsed Time	Flow Readings								Infiltration Rate			Remarks
					Inner Ring (MariotteTube 1)				Annular (MariotteTube 2)				Inner	Annular	Average	
No.	Start or End	Time hr:min	(min)	(min)	h_i (cm)	h_t (cm)	Δh (cm)	flow (cm^3)	h_i (cm)	h_t (cm)	Δh (cm)	flow, (cm^3)	(cm/h)	(cm/h)	(cm/h)	
15	Start	12:42	10	113	58.0	11.0	47.0	2538.0	58.0	13.0	45.0	7560	21.5	21.5	21.5	Refilled
	End	12:52														
16	Start	12:58	10	129	58.0	14.0	44.0	2376.0	58.0	11.0	47.0	7896	20.2	22.5	21.3	Refilled
	End	13:08														
17	Start	13:10	10	141	58.0	8.0	50.0	2700.0	58.0	13.0	45.0	7560	22.9	21.5	22.2	Refilled
	End	13:20														
18	Start	13:23	10	154	58.0	10.0	48.0	2592.0	58.0	12.0	46.0	7728	22.0	22.0	22.0	Refilled
	End	13:33														

Remarks:

1. Inner Infiltration Rate: $V_{IR} = \Delta V_{IR} / (A_{IR} * \Delta t)$ Annular space infiltration rate: $V_A = \Delta V_A / (A_A * \Delta t)$
2. Applicable to relatively UNIFORM FINE-GRAINED SOIL, with low to moderate ring penetration, and without fat clay and gravel-size particles.
3. Test should be conducted ABOVE ground water level.
4. NOT for very pervious or impervious soil (k should be within 10^{-6} to 10^{-2} cm/s). NOT for dry or stiff soil that fractures easily.
5. NOT able to determine coefficent of permeability *k* directly.

DOUBLE RING INFILTROMETER --- ASTM D3385-09

W.O. 7623-00

Project Name: Red Hill Bulk Storage Facility Infiltration Testing

Test ID: IF-3 Test Date: 10/16/18

Tested By: MN Liquid: Water pH: 8.2

Water Table Depth (feet) NA Ground Temp.:

Inner Ring Penetration (in) 3.5 Outer Ring Pen. (in) 4.0

Constants		Liquid depth	Liquid depth	Theoretical	Initial liq vol	Mariotte Tubes	
Area	(cm^2)	(in)	(cm)	(gal)	(gal)	No.	Vol/ΔH (cm^3/cm)
Inner Ring	707.0	5.0	12.7	2.4	0.83	1	54.0
Annular Space	2106.0	5.0	12.7	7.1	2.57	2	168.0

Liquid level maintained by: □ Flow Valve; □ Float Valve; ■ Mariotte Tube

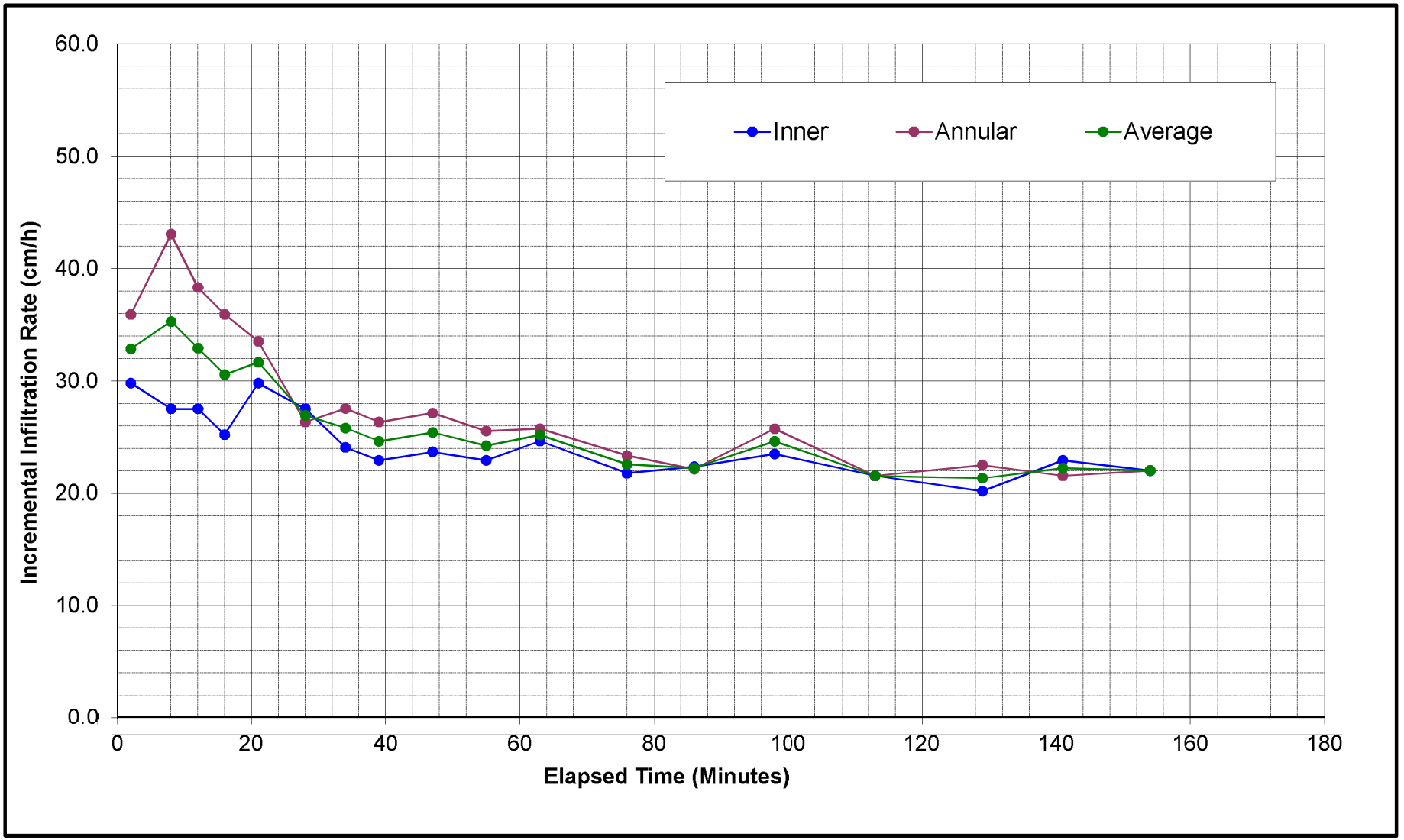

APPENDIX B

A P P E N D I X B

Laboratory Tests

Moisture Content (ASTM D2216) determinations were performed on a representative soil sample taken from each infiltrometer test location as an aid in the classification and evaluation of soil properties. The test results are presented on the Plate B-1.

Three Atterberg Limits tests (ASTM D4318) were performed on representative soil samples taken from each infiltrometer test location to evaluate the liquid and plastic limits of the soils as an aid in the classification and evaluation of soil the properties. Graphic presentation of the test results is provided on Plate B-2.

Location	Depth (feet)	Weight of Wet Soil & Cont. (g)	Weight of Cont. (g)	Length (in)	Diameter (in)	Weight of Wet Soil & Tare (g)	Weight of Dry Soil & Tare (g)	Weight of Tare (g)	Water Content (%)	Wet Density (pcf)	Dry Density (pcf)
IF1	0.5 - 1					202.7	169.2	50.9	**28.3**		
IF2	0.5 - 1					207.0	169.2	51.9	**32.2**		
IF3	0.5 - 1					234.8	189.4	51.7	**33.0**		

GEOLABS, INC.

GEOTECHNICAL ENGINEERING

W.O. 7623-00

WATER CONTENT & UNIT WEIGHT - ASTM D2216

RED HILL
BULK FUEL STORAGE FACILITY

Plate
B - 1

G_WC_U_WT 7623-00.GPJ GEOLABS.GDT 10/19/18

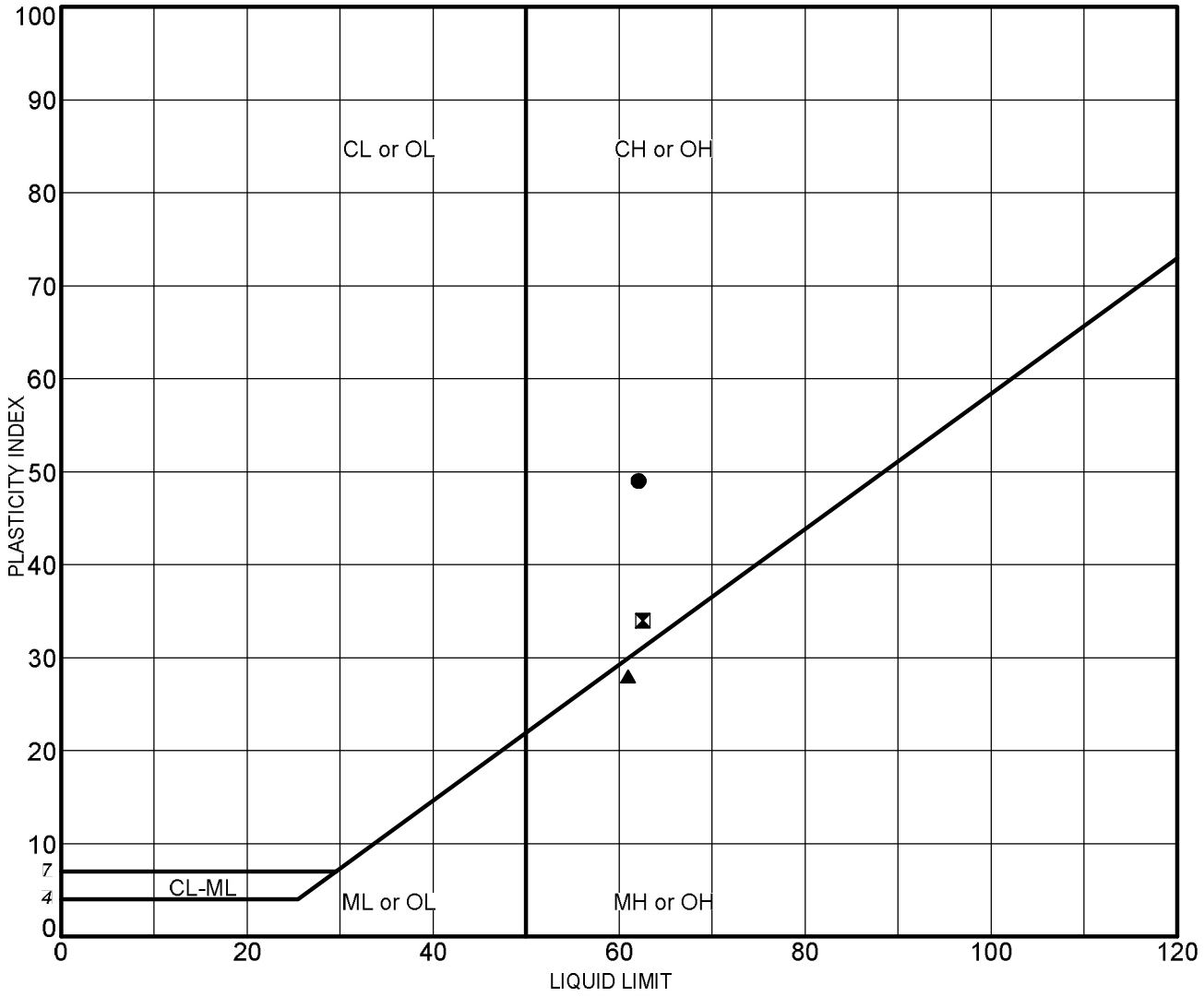

	Sample	Depth (ft)	LL	PL	PI	Description
●	IF1	0.5-1.0	62	13	49	Reddish brown silty clay (CH)
⧓	IF2	0.5-1.0	63	29	34	Reddish brown silty clay (CH)
▲	IF3	0.5-1.0	61	33	28	Reddish brown clayey silt (MH)

NP = NON-PLASTIC

GEOLABS, INC.
GEOTECHNICAL ENGINEERING

W.O. 7623-00

ATTERBERG LIMITS TEST RESULTS - ASTM D4318

RED HILL
BULK FUEL STORAGE FACILITY

Plate
B - 2

G_ATTERBERG_CONSTRUCTION_PHASE_7623-00.GPJ GEOLABS.GDT 10/25/18

This page intentionally left blank

Appendix H:
Transfer Function-Noise Analysis of 2017–2018 Synoptic Monitoring

This page intentionally left blank

CONTENTS

Acronyms and Abbreviations H-ii

1. Objectives H-1
2. Concept of TFN Model H-1
3. Initial Exploratory Data Analysis H-1
4. TFN Analysis Implementation H-2
5. References H-6

FIGURES

H-1 Time Series of Potentially Influential Sources H-7

H-2 Spectral Characteristics of Earth Tide, Barometric Pressure, and Red Hill Shaft Pumping Rate H-8

H-3 Strong Correlation of RHMW07 and Barometric Pressure Variation H-9

H-4 Empirical Step Response Function Response for RHMW05 H-10

H-5 Hantush (1956) versus Theis (1935) Step Response Functions H-11

H-6 TFN Analysis Results for RHMW08 H-12

H-7 Comparison of Observed and Computed Differences between Water Levels at RHMW05 and RHMW10 H-13

H-8 Examples of Unit Step Response Functions Associated with Red Hill Shaft Pumping H-14

H-9 Comparison of Transmissivity from TFN Analysis Associated with Red Hill Shaft Pumping with Hantush and Thomas (1966) H-15

TABLES

H-1 Equivalent Regional-Scale Aquifer Hydraulic Properties for Step Response Functions at Red Hill Monitoring Wells with Red Hill Shaft and Hālawa Shaft Pumping H-4

H-2 Transfer Function Values Associated with Step Response Functions at Red Hill Monitoring Wells H-5

ACRONYMS AND ABBREVIATIONS

EDA	exploratory data analyses
ft^2/day	square feet per day
mgd	million gallons per day
TFN	transfer function-noise

1. Objectives

The water level in a monitoring well changes with time in response to fluctuations in hydraulic stresses in the aquifer system. Hydraulic stresses affecting the 2017–2018 synoptic monitoring data are potentially caused by groundwater extraction, barometric pressure, tidal influences, recharge, and regional head changes. Transfer function-noise (TFN) modeling was applied to analyze selected 2017–2018 synoptic monitoring data to extract information for numerical groundwater model calibration. Specifically, the primary objective is to estimate the unit step response functions associated with Red Hill Shaft and Hālawa Shaft individually for direct use as model calibration targets. Individual contributions from groundwater extraction at these shafts, barometric pressure, and ocean/earth tides to the observed water level changes were simultaneously quantified and separated. The magnitude of the water level fluctuations that were not captured by TFN modeling (i.e., the residuals) were estimated.

2. Concept of TFN Model

TFN modeling is a well-established technique for estimating the source-response relationship of a linear system using time series data (e.g., Box and Jenkins 1970). It has been applied to many disciplines, including hydrology (e.g., Asmuth and Knotters 2004). A TFN model simulates the water level response to each hydraulic stress component through convolution integration of the hydraulic stress time series using a kernel function:

$$y_t = v_0 x_t + v_1 x_{t-1} + v_2 x_{t-2} + \cdots$$

where y_t is the water level response at time step t, x_{t-i} is a hydraulic stress source at i time steps prior to time step t, and v_i is the value of the associated kernel function. A convolution kernel function, v_i, represents the unit impulse response function representing the water level response at a monitoring well after i time steps after a unity impulse of hydraulic stress was applied. A hydraulic stress source time series is treated as a cumulation of impulses at individual time steps, x_t. The effect of an impulse at time step t is calculated by scaling the unit impulse response function by the magnitude of the impulse, as $v_i x_{t-i}$ at i time steps after the impulse. The contribution of the response due to the hydraulic stress time series is computed by superposition (i.e., addition) of the scaled responses of the impulses at all time steps (as $v_0 x_t + v_1 x_{t-1} + v_2 x_{t-2} + \cdots$). The total response to all sources is computed by superposition of their respective contributions. A unit impulse response function is related to a unit step response function, which is commonly used to represent drawdown response to pumping. A unit step increase in pumping rate is equivalent to the cumulative sum of all the responses due to impulses of hydraulic stress applied to all time steps from the time of the pumping rate increase. The value of step response function at a time step is equal to the sum of the impulse response function at prior time steps. The impulse function at a time step is the difference of the step response function between the time step and the prior time step.

3. Initial Exploratory Data Analysis

The TFN analysis was performed based on an hourly time step size. The time series data were aggregated based on hourly averaging. The sources of hydraulic stresses initially considered included (1) groundwater extraction from Red Hill Shaft, Hālawa Shaft, 'Aiea Hālawa Shaft, and Moanalua Wells; (2) barometric pressure; (3) rainfall; (4) ocean tide; and (5) earth tide. The rainfall data measured by rain gauge USC00516400 was used. The earth tide data were downloaded from a public website (http://geodesyworld.github.io/SOFTS/solid.htm).

Exploratory data analyses (EDA) were performed to examine the characteristics of the time series of the water levels in the monitoring wells and the known hydraulic stresses potentially impacting the water level responses. The time series plots of these sources are shown on Figure H-1. The characteristics examined included the power density spectra, auto-correlation functions, cross-correction functions, and signature/patterns. Figure H-2 shows the frequency amplitude spectra of the Red Hill Shaft pumping rates, barometric pressure, and earth tide, indicating the differences and similarities among them. The EDA results indicated that:

- The effect of the groundwater extraction at 'Aiea Hālawa Shaft and Moanalua Wells on the water levels at the monitoring wells is negligible.
- The ocean tide and earth tide time series are highly correlated with similar frequency characteristics; ocean tide data showed a few instantaneous drifts.
- Hourly time step size is reasonable since the predominant frequencies of variations are lower than approximately two cycles per day.
- The correlation between the water levels at the monitoring wells and daily rainfall is low. The correlation with weekly averaged rainfall is also low. The correlation with 30-day-averaged rainfall slightly increased.

Therefore, the TFN analysis included the hydraulic stresses due to groundwater extractions from Red Hill Shaft and Hālawa Shaft, barometric pressure, tidal influence, and rainfall. The earth tide time series was selected to be the surrogate representing the tidal influence. The 30-day-averaged rainfall was initially included as a source for consistency with the duration of the synoptic data period considered. The results of the initial analysis showed that the contribution from the 30-day-averaged rainfall is negligibly small, suggesting that there was no contribution from direct rainfall recharge in the vicinity of the monitoring well. The rainfall effect occurs at a time-scale much longer than 30 days, likely from delayed and extended response due to recharge from the significantly upgradient region. Therefore, the final TFN analysis was performed without the 30-day-averaged rainfall.

The TFN analysis was applied to the monitoring well data that show responses to Red Hill Shaft and Hālawa Shaft pumping. Figure H-3 shows the time series of the barometric pressure and the monitoring data at RHMW07 as well as a scatterplot of these time series. The figure shows the strong correlation and the dominant dependency of the monitoring data to barometric pressure. This well was excluded from the final TFN analysis.

4. TFN Analysis Implementation

The TFN analysis was implemented using the commercially available software MATLAB and its toolboxes. Several implementation variations were tested to examine the sensitivity of the analysis to:

- Different forms of the transfer functions, such as empirical (i.e., without presumptions of functional form) as well as the step response functions based on Hantush (1956), Theis (1935), and the analytical element software TTim (Bakker 2013).
- Transfer function estimation approaches, such as simultaneous calibration of all transfer functions using data from January 1 – February 28, 2018 versus sequential calibration of transfer functions associated with Red Hill Shaft and Hālawa Shaft pumping.
- Calibration objective functional forms, such as converted white noise, cross-correlation with sources, and root-mean-square errors.

As an example, Figure H-4 shows the step response function empirically derived from the monitoring data at RHMW05. The shape of this function resembles the step response function for a leaky aquifer analytical solution (Hantush 1956). Figure H-5 shows that a step response function based on Hantush (1956) simulated the water level response at RHMW05 in closer agreement with the observed data in comparison to the results from simulation using a step response function based on Theis (1935). Similarly, Figure H-5 also shows that the Hantush (1956) step response function produced better results in comparison to a step response function based on the TTim software (Bakker 2013).

An exploratory TFN analysis was performed to compute the transfer function empirically from data. The shapes of the empirically derived transfer functions resemble the analytical drawdown response solution based on Hantush (1956). Subsequently, the TFN analysis was performed using a Hantush (1956) functional form to represent the transfer functions. The actual locations of the pumping shafts and monitoring wells were used to calculate the distance used in the Hantush equation. In a heterogeneous and anisotropic aquifer, a monitoring well responds to pumping from a shaft as if the pumping is from an image location in an equivalent homogeneous and isotropic aquifer. It is analogous to an underwater object appearing to be shallower when it is viewed from above water. Therefore, in the final TFN analysis, the equivalent image location of the pumping center associated with each shaft was estimated by optimization to further improve TFN calibration to the observed water level time series. The optimized distances are generally less than 10 percent different from the actual geographical distance. In addition, the results of the preliminary analysis showed that the contribution from the 30-day-averaged rainfall is negligibly small, suggesting that there was no significant contribution from direct rainfall recharge in the vicinity of the monitoring wells during the analysis period. The rainfall effect likely occurred at a time-scale much longer than 30 days, as delayed and extended response to recharge from upgradient regions. Therefore, the final TFN analysis was performed without the 30-day-averaged rainfall.

As an example, Figure H-6 shows the results from the final TFN analysis of water level data at monitoring well RHMW08 for the Red Hill Shaft shutdown/restart period and the Hālawa Shaft shutdown/restart period, respectively. The simulated water level responses closely match the observed water level responses. The contribution of Hālawa Shaft pumping to the water level changes during the Red Hill Shaft shutdown/restart period from January 7 to 23, 2018 is small because the Hālawa Shaft pumping rate was steady. The time series plot of TFN residuals does not show correlation with shaft pumping, barometric pressure, or tidal fluctuations. Rather the TFN residuals are likely attributable to seasonal and background fluctuations caused by rainfall recharge in distal upgradient areas. Figure H-7 shows the observed and TFN model-simulated differences between the water levels at monitoring wells RHMW05 and RHMW10. They are in good agreement. The observed differential head time series do not show a trend, suggesting that the residuals from the TFN analysis for the selected wells are similar when Red Hill Shaft is off or on. Therefore, the impacts due to ambient fluctuation are spatially uniform, and the induced differential head is small. Differential head is dominated by the pumping influence of Red Hill Shaft. Figure H-8 shows several examples of the unit step response functions associated with Red Hill Shaft pumping for use as numerical model calibration targets.

TFN analysis was also applied to the water level data for Red Hill Shaft and Hālawa Shaft. In addition to the step response function based on Hantush (1956), a zero-lag (i.e., instantaneous response) term was added. The results indicated that ratios of the zero-lag terms to the total long-term drawdowns are approximately 2–4 percent for Red Hill Shaft and Hālawa Shaft. As an example, Figure H-9 shows the TFN results for Red Hill Shaft.

The equivalent regional-scale, homogeneous, and isotropic parameters (Hantush 1956) associated with the step response functions at different monitoring wells for Red Hill Shaft and Hālawa Shaft pumping are summarized in Table H-1. These parameters are consistent with the values estimated earlier based on the Theis and Cooper-Jacob analytical solutions. The transfer function values associated with the selected wells and Red Hill Shaft are presented in Table H-2.

Table H-1: Equivalent Regional-Scale Aquifer Hydraulic Properties for Step Response Functions at Red Hill Monitoring Wells with Red Hill Shaft and Hālawa Shaft Pumping

	Red Hill Shaft Pumping		Hālawa Shaft Pumping	
Monitoring Well	Effective Transmissivity (ft^2/day)	Apparent Storativity	Effective Transmissivity (ft^2/day)	Apparent Storativity
OWDFMW01	513,000	0.10	1,670,000	0.14
RHMW01	565,000	0.07	1,470,000	0.08
RHMW02	521,000	0.04	1,520,000	0.08
RHMW03	532,000	0.02	1,430,000	0.08
RHMW04	548,000	0.03	1,080,000	0.10
RHMW05	550,000	0.18	1,620,000	0.06
RHMW06	580,000	0.02	1,430,000	0.08
RHMW08	548,000	0.05	1,610,000	0.05
RHMW09	553,000	0.05	1,650,000	0.07
RHMW10	520,000	0.02	1,710,000	0.08
RHMW11 Z1	667,000	0.04	1,390,000	0.09
RHMW11 Z2	756,000	0.05	641,000	0.11
RHMW11 Z3	652,000	0.05	1,300,000	0.14
RHMW11 Z4	784,000	0.04	627,000	0.14
RHMW11 Z5	810,000	0.04	1,270,000	0.15

ft^2/day square feet per day

Table H-2: Transfer Function Values Associated with Step Response Functions at Red Hill Monitoring Wells

Time (days)	Drawdown (ft/mgd)														
	OWDF MW01	RHMW01	RHMW02	RHMW03	RHMW04	RHMW05	RHMW06	RHMW08	RHMW09	RHMW10	RHMW11 Z1	RHMW11 Z2	RHMW11 Z3	RHMW11 Z4	RHMW11 Z5
0.000	0.000	0.000	0.000	0.000	0.000	0.000	0.000	0.000	0.000	0.000	0.000	0.000	0.000	0.000	0.000
0.125	0.009	0.009	0.006	0.005	0.001	0.014	0.003	0.015	0.008	0.005	0.004	0.005	0.004	0.005	0.005
0.250	0.018	0.018	0.014	0.012	0.005	0.025	0.009	0.026	0.016	0.012	0.010	0.011	0.009	0.010	0.010
0.375	0.024	0.024	0.020	0.018	0.009	0.031	0.014	0.032	0.022	0.017	0.014	0.015	0.014	0.015	0.014
0.500	0.029	0.029	0.024	0.022	0.012	0.036	0.018	0.037	0.027	0.022	0.018	0.018	0.017	0.018	0.017
0.625	0.033	0.032	0.028	0.026	0.015	0.040	0.021	0.041	0.030	0.026	0.021	0.021	0.020	0.020	0.020
0.750	0.037	0.035	0.031	0.029	0.018	0.044	0.024	0.045	0.033	0.029	0.023	0.023	0.023	0.022	0.022
0.875	0.040	0.038	0.034	0.032	0.020	0.046	0.026	0.048	0.036	0.031	0.025	0.025	0.025	0.024	0.024
1.000	0.042	0.040	0.036	0.034	0.022	0.049	0.028	0.050	0.038	0.034	0.027	0.027	0.027	0.026	0.025
2.000	0.056	0.053	0.050	0.047	0.033	0.062	0.040	0.063	0.051	0.047	0.037	0.036	0.037	0.035	0.034
3.000	0.064	0.060	0.057	0.054	0.041	0.070	0.047	0.071	0.058	0.055	0.043	0.041	0.044	0.040	0.039
4.000	0.070	0.065	0.063	0.060	0.046	0.075	0.052	0.076	0.064	0.060	0.048	0.045	0.048	0.044	0.043
5.000	0.074	0.070	0.068	0.064	0.050	0.079	0.056	0.081	0.068	0.065	0.051	0.048	0.052	0.047	0.046
6.000	0.078	0.073	0.071	0.068	0.053	0.083	0.059	0.084	0.072	0.069	0.054	0.051	0.055	0.049	0.048
7.000	0.081	0.076	0.074	0.071	0.056	0.086	0.062	0.087	0.074	0.072	0.057	0.053	0.057	0.051	0.050
8.000	0.084	0.078	0.077	0.074	0.059	0.088	0.064	0.090	0.077	0.074	0.059	0.055	0.059	0.053	0.052
10.000	0.089	0.082	0.082	0.078	0.063	0.093	0.068	0.094	0.081	0.079	0.062	0.058	0.063	0.056	0.055

mgd million gallons per day

5. References

Asmuth, J., and M. Knotters. 2004. "Characterising Groundwater Dynamics Based on a System Identification Approach." *Journal of Hydrology* 296: 118–134. https://doi.org/10.1016/j.jhydrol.2004.03.015.

Bakker, M. 2013. "Semi-Analytic Modeling of Transient Multi-Layer Flow with TTim." *Hydrogeology Journal* 21 (4): 935–943.

Box, G. E. P., and G. M. Jenkins. 1970. *Time Series Analysis Forecasting and Control*. San Francisco: Holden Day.

Hantush, M. S. 1956. "Analysis of Data from Pumping Tests in Leaky Aquifers." *Eos, Transactions American Geophysical Union* 37 (6): 702–714. https://doi.org/10.1029/TR037i006p00702.

Hantush, M. S., and R. G. Thomas. 1966. "A Method for Analyzing a Drawdown Test in Anisotropic Aquifers." *Water Resources Research* 2 (2): 281–285. https://doi.org/10.1029/WR002i002p00281.

Theis, C. V. 1935. "The Relation between the Lowering of the Piezometric Surface and the Rate and Duration of Discharge of a Well Using Groundwater Storage." *Am. Geophys. Union Trans.* 16: 519–524.

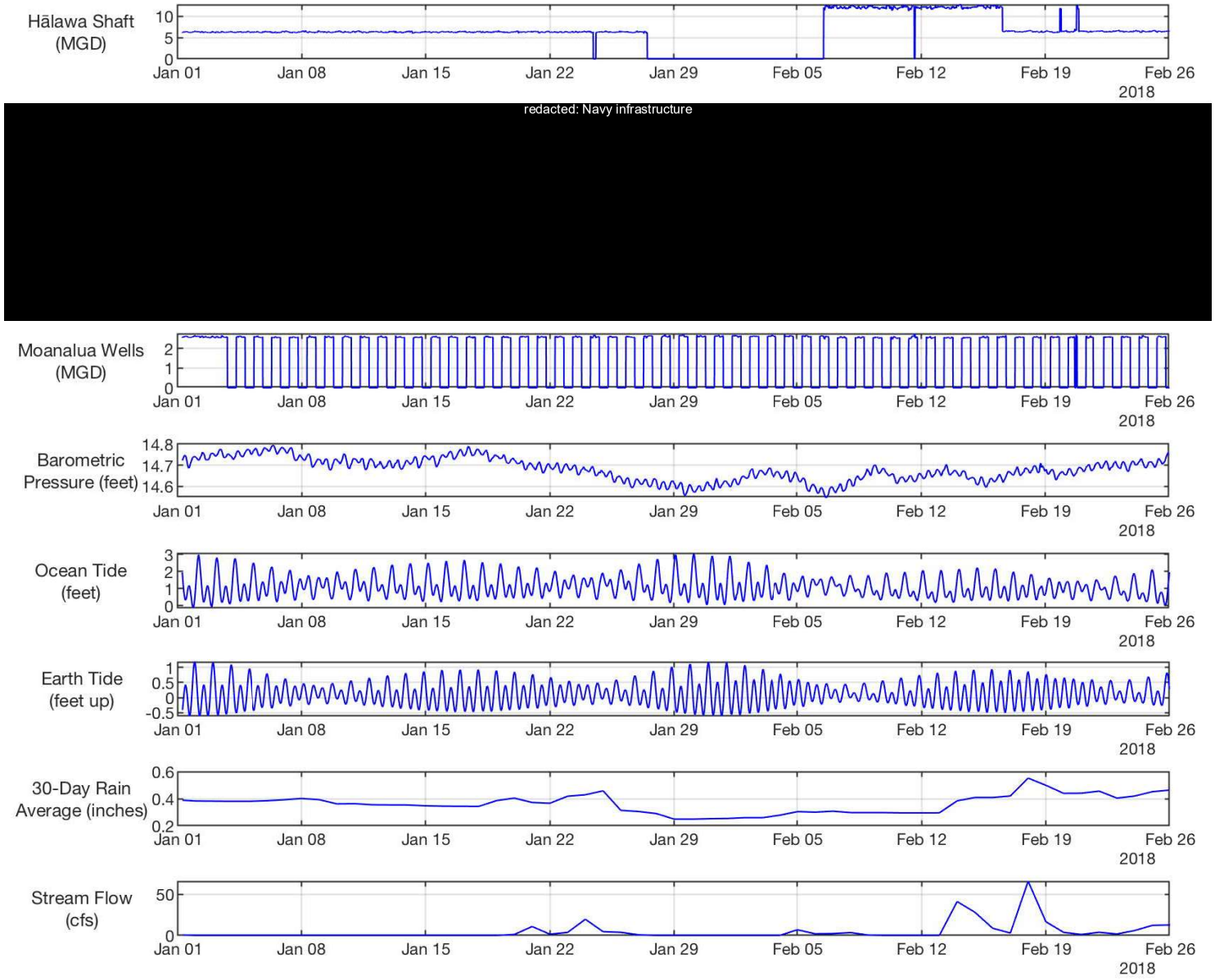

Figure H-1
Time Series of Potentially Influential Sources
Conceptual Site Model Rev. 01
Investigation and Remediation of Releases and Groundwater Protection and Evaluation
Red Hill Bulk Fuel Storage Facility
JBPHH, Oʻahu, Hawaiʻi

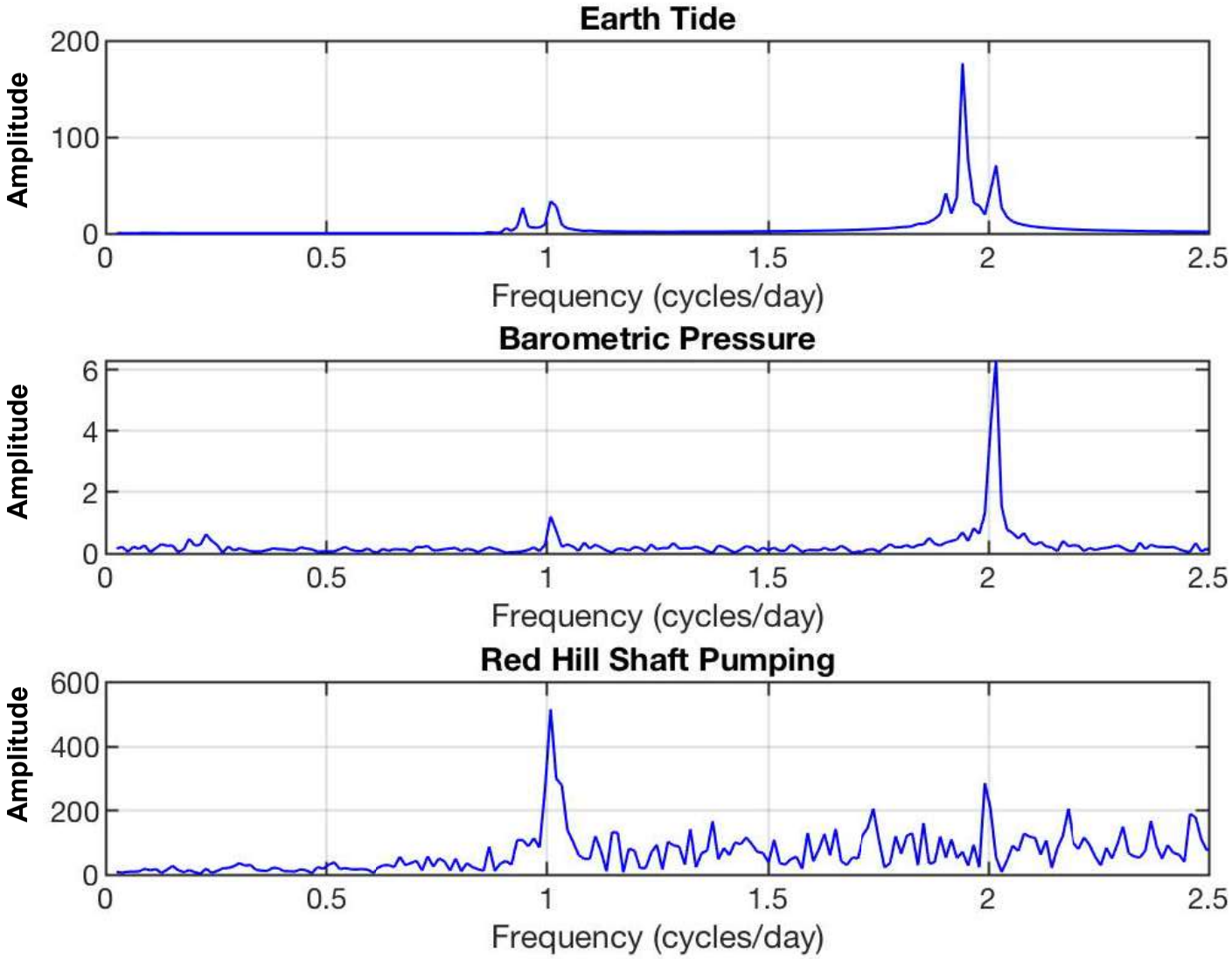

Figure H-2
Spectral Characteristics of Earth Tide, Barometric Pressure, and Red Hill Shaft Pumping Rate
Conceptual Site Model Rev. 01
Investigation and Remediation of Releases and Groundwater Protection and Evaluation
Red Hill Bulk Fuel Storage Facility
JBPHH, O‘ahu, Hawai‘i

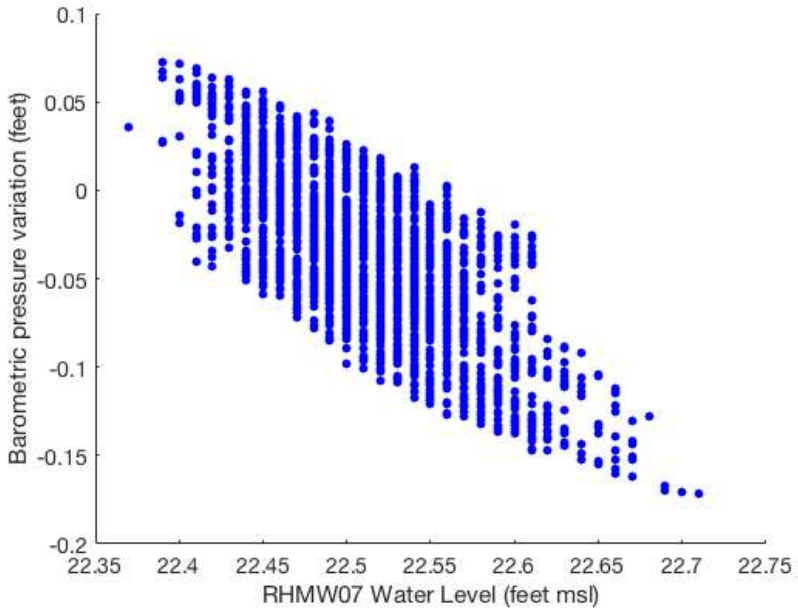

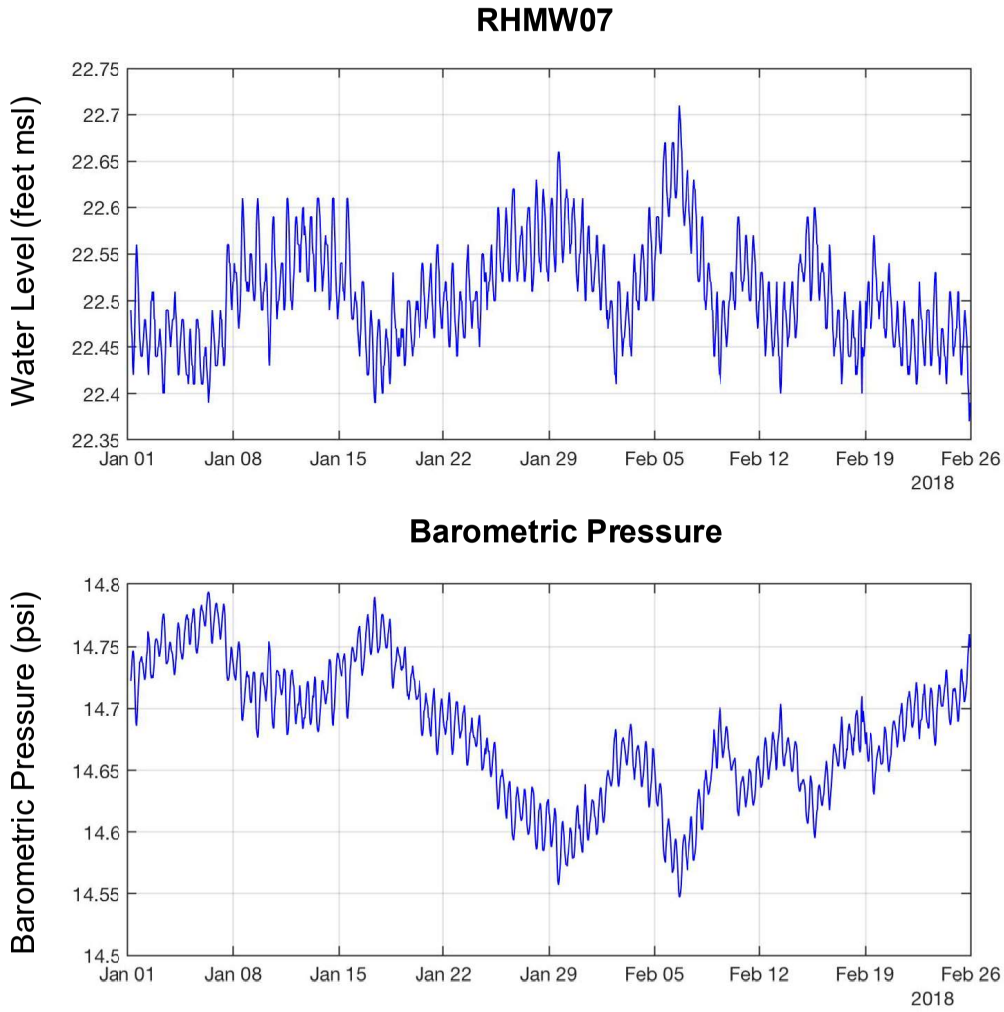

Figure H-3
Strong Correlation of RHMW07 and Barometric Pressure Variation
Conceptual Site Model Rev. 01
Investigation and Remediation of Releases and Groundwater Protection and Evaluation
Red Hill Bulk Fuel Storage Facility
JBPHH, O‘ahu, Hawai‘i

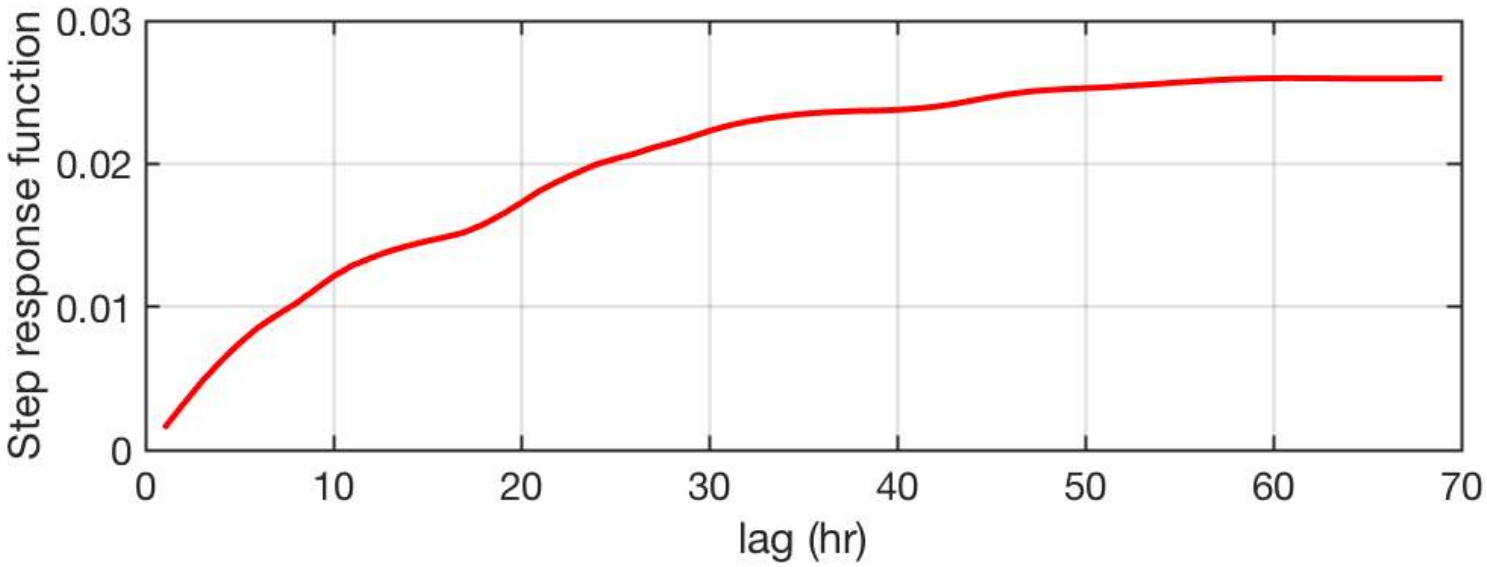

Note: Resembles Hantush leaky aquifer solution

Figure H-4
Empirical Step Response Function Response for RHMW05
Conceptual Site Model Rev. 01
Investigation and Remediation of Releases and Groundwater Protection and Evaluation
Red Hill Bulk Fuel Storage Facility
JBPHH, O‘ahu, Hawai‘i

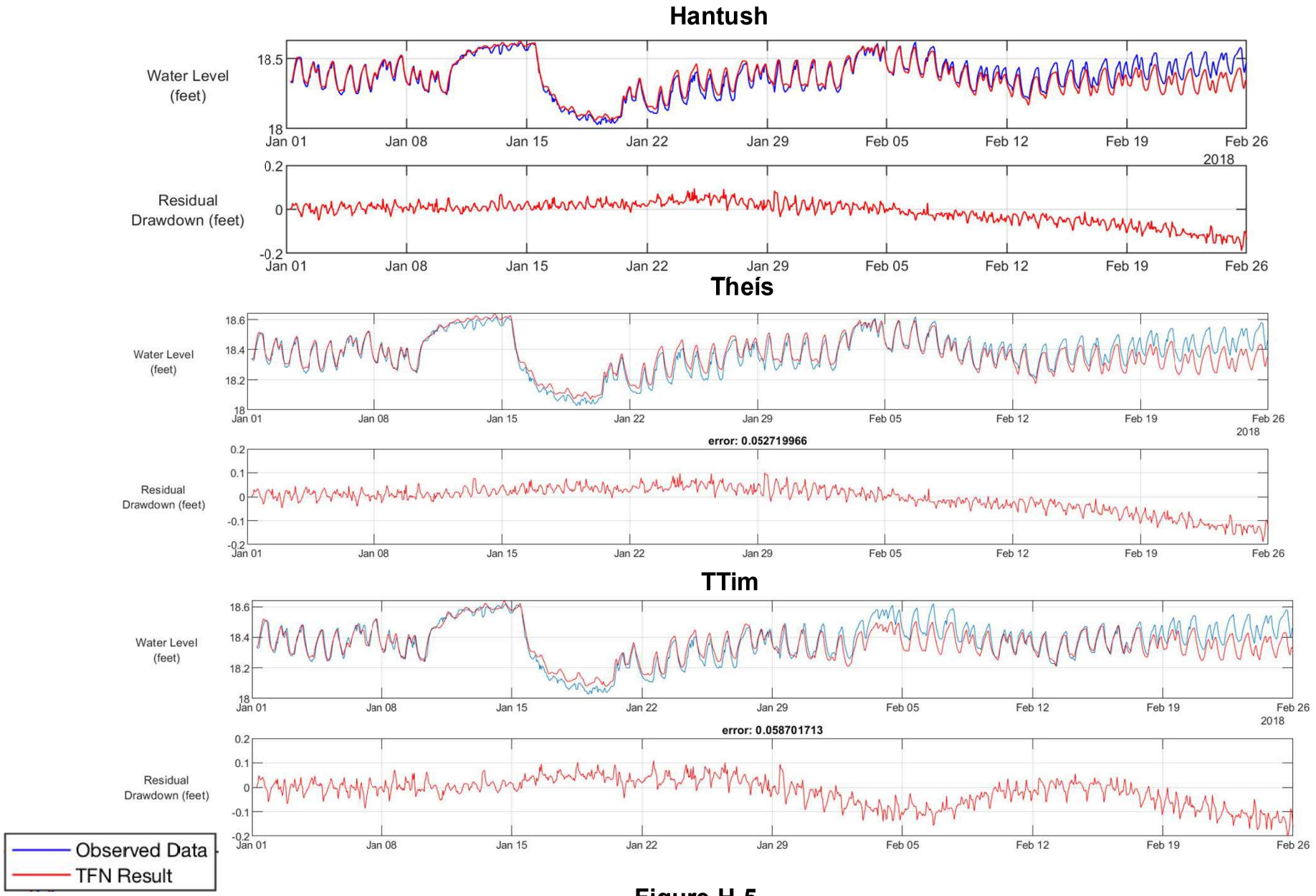

Figure H-5
Hantush (1956) versus Theis (1935) Step Response Functions
Conceptual Site Model Rev. 01
Investigation and Remediation of Releases and Groundwater Protection and Evaluation
Red Hill Bulk Fuel Storage Facility
JBPHH, O‘ahu, Hawai‘i

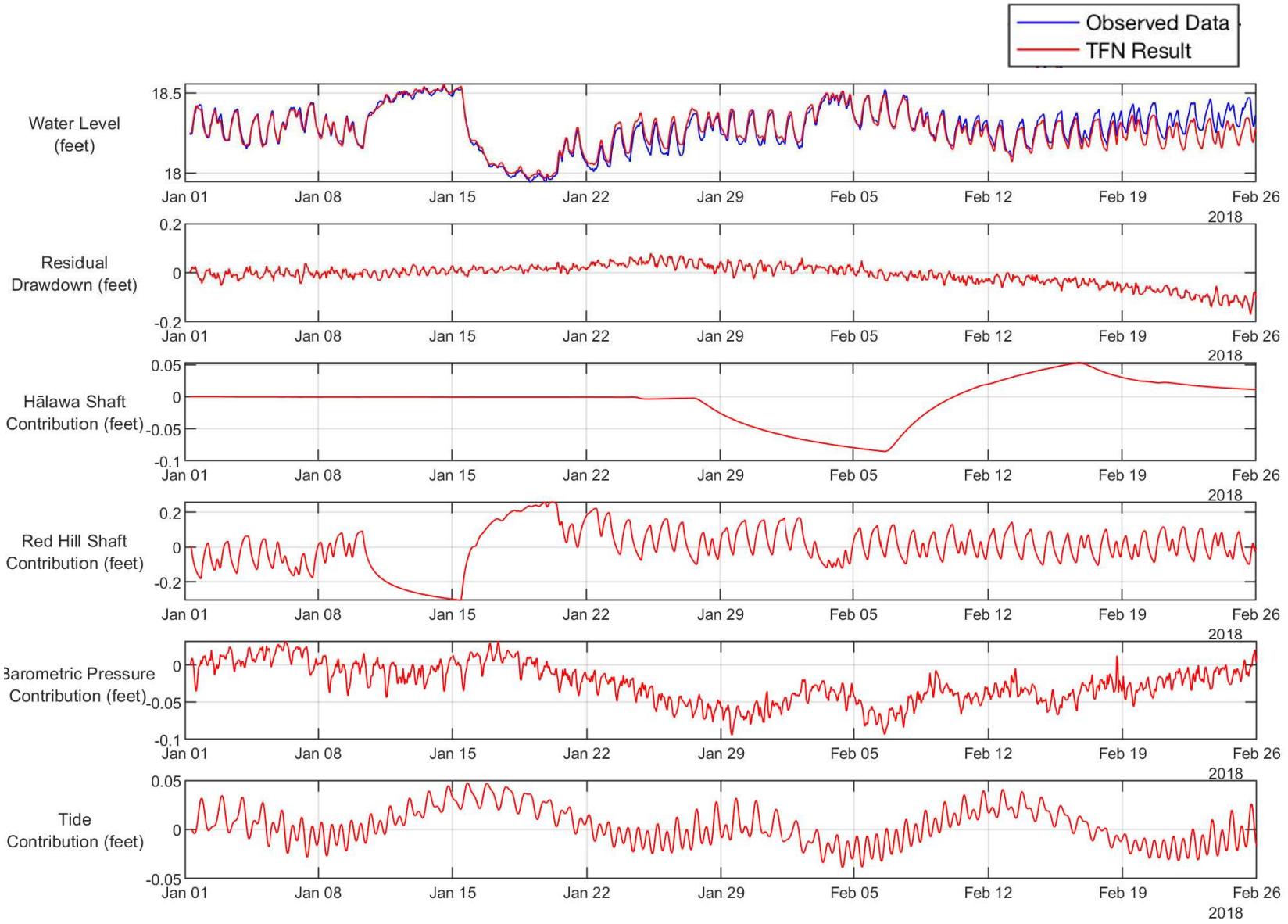

Figure H-6
TFN Analysis Results for RHMW08
Conceptual Site Model Rev. 01
Investigation and Remediation of Releases and Groundwater Protection and Evaluation
Red Hill Bulk Fuel Storage Facility
JBPHH, Oʻahu, Hawaiʻi

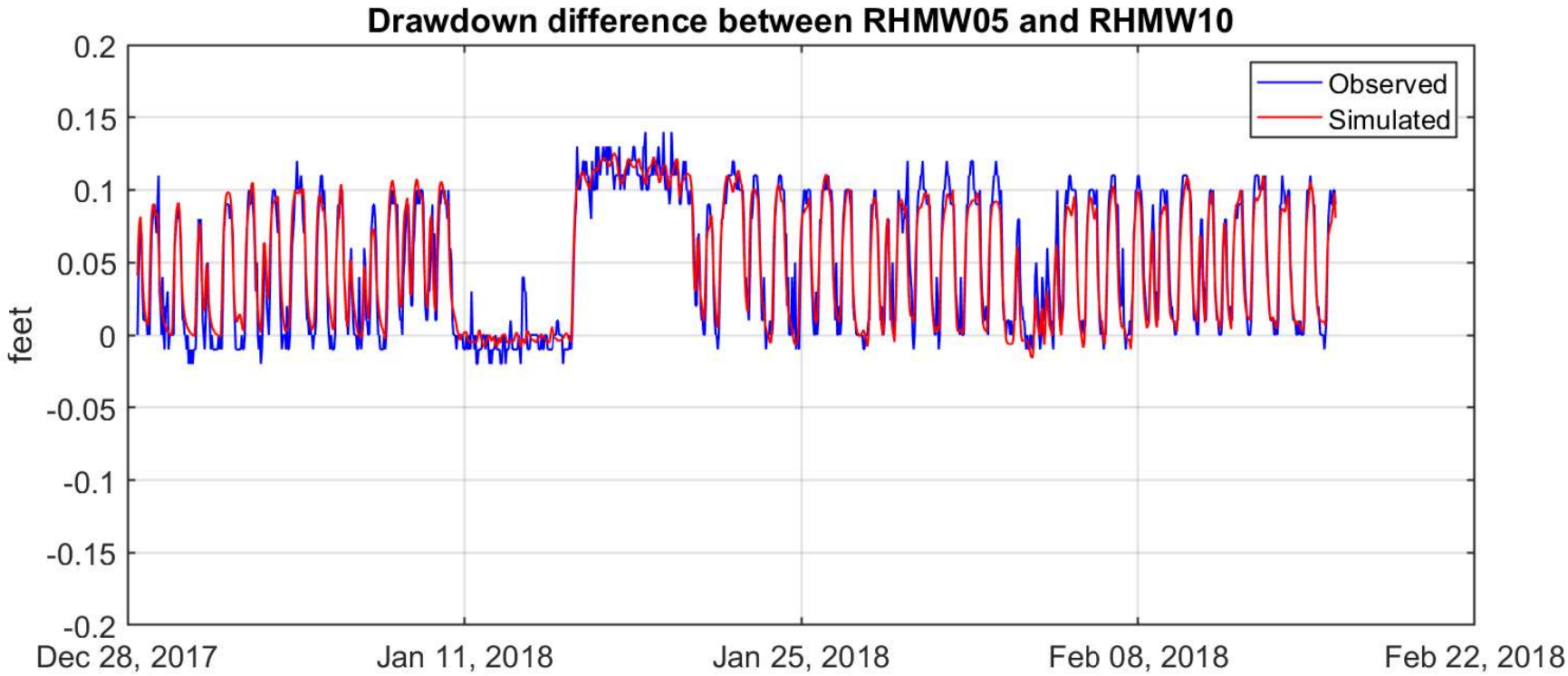

Figure H-7
Comparison of Observed and Computed Differences between Water Level at RHMW05 and RHMW10
Conceptual Site Model Rev. 01
Investigation and Remediation of Releases and Groundwater Protection and Evaluation
Red Hill Bulk Fuel Storage Facility
JBPHH, Oʻahu, Hawaiʻi

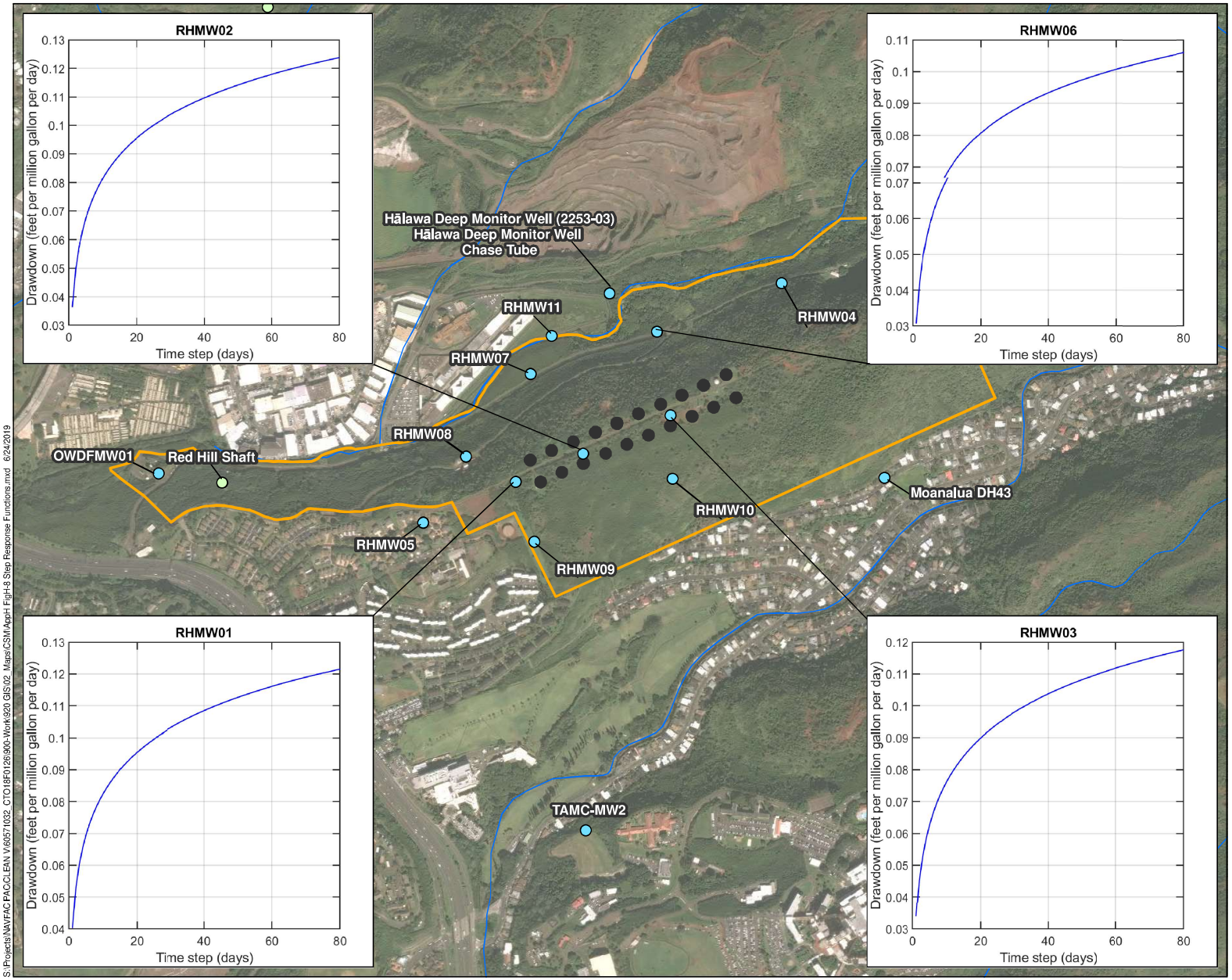

Location Map

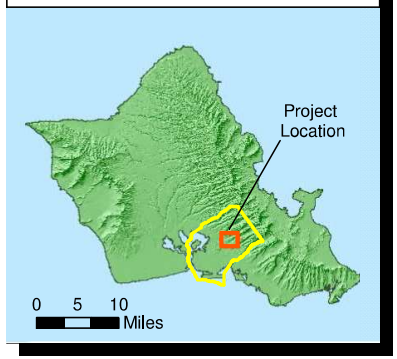

Legend

- Red Hill Fuel Storage Tank
- Supply Well
- Monitoring Well
- Groundwater Model Domain
- Red Hill Facility Boundary
- Stream

Notes

1. Map projection: NAD 1983 Hawaii State Plane Zone 3 (feet)
2. DigitalGlobe, Inc. (DG) and NRCS. Publication_Date: 2015

N

0 500 1,000 2,000 Feet

Figure H-8
Examples of Unit Step Response Functions Associated with Red Hill Shaft Pumping
Conceptual Site Model Rev. 01
Investigation and Remediation of Releases and Groundwater Protection and Evaluation
Red Hill Bulk Fuel Storage Facility
JBPHH, O'ahu, Hawai'i

S:\Projects\NAVFAC PACOM\CLEAN V\60571032_CTO18F0126\900-Work\920 GIS\02_Maps\CSM\AppH FigH-8 Step Response Functions.mxd 6/24/2019

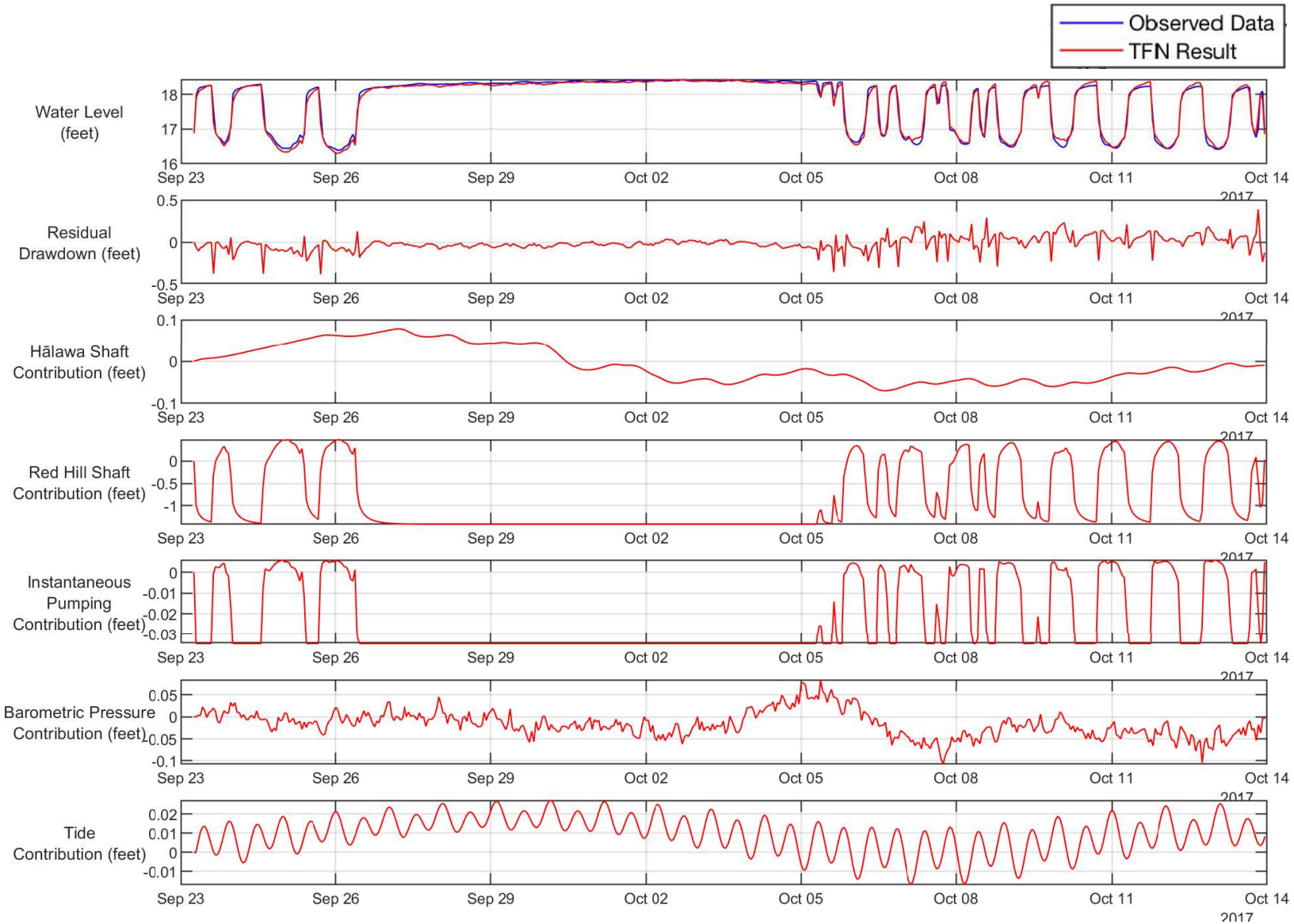

Figure H-9
TFN Analysis Results for Red Hill Shaft
Conceptual Site Model Rev. 01
Investigation and Remediation of Releases and Groundwater Protection and Evaluation
Red Hill Bulk Fuel Storage Facility
JBPHH, Oʻahu, Hawaiʻi

This page intentionally left blank

Appendix I:
Multiple Impact Factors

This page intentionally left blank

CONTENTS

1. Introduction 1-1
   - 1.1 Technical Background 1-1
   - 1.2 Study Objectives 1-1
2. Background Analysis – Dissolved Oxygen 2-1
   - 2.1 Comparison with Nationwide Background Dissolved Oxygen Data 2-1
   - 2.2 Comparison with Other Basalt Aquifers Dissolved Oxygen Data 2-3
   - 2.3 Comparison with O‘ahu Regional Shallow Groundwater Dissolved Oxygen Data 2-3
   - 2.4 Using Dissolved Oxygen Data to Detect Releases: Maui Case Study 2-6
   - 2.5 Processes that Can Cause Oxygen Depletion 2-7
   - 2.6 Nature of Oxygen Depletion in Other Facility Monitoring Wells 2-9
   - 2.7 Implications for Multiple Impact Factors Evaluation 2-9
3. Background Analysis – Total Petroleum Hydrocarbons 3-1
   - 3.1 LNAPL Impact or Drilling Contamination 3-1
   - 3.2 TPH-d Detections in Later Years in Monitoring Well RHMW04 3-4
   - 3.3 Implications for Multiple Impact Factors Evaluation 3-8
4. Multiple Impact Factors Analysis 4-1
   - 4.1 Overview of Network Data Analysis 4-1
   - 4.2 Data Selection 4-1
   - 4.3 Analysis Approach 4-1
   - 4.4 Analysis Results 4-4
5. Conclusions 5-1
6. References 6-1

ATTACHMENT

I-1 Analytical Results of Drilling “Make-Up” Water Samples

FIGURES

2-1 Location of 26 Monitored Natural Attenuation Studies with Background Groundwater Dissolved Oxygen Data (site list from Wiedemeier et al. 1999) 2-1

2-2 Screened Intervals for Public Water Supply Wells Used in Regional Groundwater Quality Study (Hunt Jr. 2004) vs. Screened Interval of Red Hill Monitoring Wells (depth below water surface) 2-4

2-3 Percent Detections of Man-Made but Non-Constituents of Potential Concern (Non-COPCs) in Outlying Monitoring Wells at the Facility 2-5

2-4 Groundwater Flow Direction and Location of Monitoring Wells, Central Maui Landfill Conceptual Site Model Study (CH2M Hill 2016) 2-6

2-5 Dissolved Oxygen Concentration vs. Time Since Installation for Three Facility Monitoring Wells Drilled Near Saprolite Zones 2-9

3-1 TPH-d Concentrations in Groundwater vs. Time Since Installation for Six Facility Monitoring Wells 3-1

3-2 Air Rotary Drilling Rig (DOH 2018b) 3-2

3-3 Excerpt from California Department of Toxic Substances Control's (1995) Guidance Regarding Use of Air Rotary Drilling for Environmental Investigations 3-3

3-4 Excerpt from California State Water Resources Control Board's (2012) *Leaking Underground Storage Tank Guidance Manual* Stressing the Importance of Not Assuming that Reported TPH Detections are Petroleum 3-5

3-5 Excerpt from San Francisco Bay Regional Water Quality Control Board's (2019) *User's Guide Derivation and Application of Environmental Screening Levels* Emphasizing the Non-Specific Nature of TPH Analysis and Need for Chromatogram Review 3-5

3-6 Excerpt from DOH's (2018a) *Collection and Use of Total Petroleum Hydrocarbon Data for the Risk-Based Evaluation of Petroleum Releases, Example Case Studies* Listing Data Usability Concerns, including TPH at Concentrations < 100 µg/L 3-6

3-7 Chromatograms from TPH-d Samples from RHMW04; Both Samples Were "J" Flag 3-8

4-1 Representative Indicator Values at Selected Wells (first-year data not used due to drilling artifacts) 4-3

4-2 Geographic Distribution of Five Monitoring Well Groups 4-4

4-3 Data Clustering Structure from Network Analysis Based on Representative Indicator Values at Selected Wells (first-year data not used due to drilling artifacts) 4-5

4-4 Data Clustering Structure from Network Analysis for Sensitivity Case 1 (all data) 4-6

4-5 Representative Indicator Values at Selected Wells for Sensitivity Case 1 (all data) 4-7

4-6 Data Clustering Structure from Network Analysis for Sensitivity Case 2 (first-year data not used due to drilling artifacts and data from Calscience/Eurofins laboratory not used) 4-8

4-7 Representative Indicator Values at Selected Wells for Sensitivity Case 2 (first-year data not used due to drilling artifacts and data from Calscience/Eurofins laboratory not used) 4-9

TABLES

2-1	Background Dissolved Oxygen Data from 26 Monitored Natural Attenuation Studies (Wiedemeier et al. 1999)	2-2
2-2	Dissolved Oxygen Data from Basalt Aquifers in Columbia Plateau (Steinkampf and Hearn Jr. 1996)	2-3
2-3	Background Dissolved Oxygen Data from 15 Upgradient, Far-Field Monitoring Wells	2-5
2-4	of Major Iron Chemistry, Conceptual Site Model Study of Central Maui Landfill (dissolved oxygen highlighting added) (CH2M Hill 2016)	2-7
2-5	Dissolved Oxygen Concentrations at Select Red Hill Wells vs. Monitoring Wells on O'ahu (Hunt Jr. 2004)	2-10
3-1	Various Laboratory Limits for TPH-d	3-7
4-1	Indicator Criteria Used for Multiple Impact Factor Analysis	4-2

ACRONYMS AND ABBREVIATIONS

µg/L	micrograms per liter
1-MeN	1-methylnaphthalene
2-MeN	2-methylnaphthalene
AOC	Administrative Order on Consent
B	benzene
BTEX	benzene, toluene, ethylbenzene, and xylene
CMLF	Central Maui Landfill
COPC	chemical of potential concern
CSM	conceptual site model
DL	detection limit
DO	dissolved oxygen
DoD	Department of Defense, United States
DOH	Department of Health, State of Hawai‘i
E	ethylbenzene
EPA	Environmental Protection Agency, United States
GAC	granular activated carbon
HOP	hydrocarbon oxidation product
J	estimated concentration
LNAPL	light non-aqueous-phase liquid
LOD	limit of detection
LOQ	limit of quantitation
MDL	method detection limit
mg/L	milligrams per liter
MNA	monitored natural attenuation
MSWLF	municipal solid waste landfill
N	naphthalene
NAWQA	National Water-Quality Assessment
NOC	natural organic compound
non-COPC	non-constituent of potential concern
PWS	public water supply
QL	quantitation limit
RL	reporting limit
T	toluene
TPH	total petroleum hydrocarbons
TPH-d	total petroleum hydrocarbons – diesel range organics
TPH-g	total petroleum hydrocarbons – gasoline range organics
TPH-o	total petroleum hydrocarbons – residual range organics (i.e., TPH-oil)
U	non-detect
UJ	estimated non-detect
USGS	United States Geological Survey
X	xylene

1. Introduction

This appendix is summarized in Section 7.2 of the Conceptual Site Model (CSM) main document.

1.1 TECHNICAL BACKGROUND

Understanding the spatial distribution of groundwater quality parameters is important for understanding the distribution and nature of chemical impacts due to historical releases from the Red Hill Bulk Fuel Storage Facility ("the Facility"). An important aspect of this evaluation is the differentiation of non-Facility related influences, such as laboratory and sampling issues, induced contamination from drilling and well installation, anthropogenic related contamination from past and current upgradient sources, and natural background water quality conditions, on the groundwater quality parameters. Selected chemical parameters were considered individually as impact factors that are indicative of potential contamination. Multiple impact factor analysis was suggested by the Administrative Order on Consent (AOC) Parties in discussions during March 2019 technical working group meetings as a method (in addition to the analyses presented in CSM Appendix B.8) to evaluate whether these impact indicators for the outlying wells (i.e., Red Hill groundwater monitoring wells other than in-tunnel wells RHMW01, RHMW02, and RHMW03) are consistently indicative of an impact associated with petroleum releases from the Facility.

1.2 STUDY OBJECTIVES

This appendix provides a holistic evaluation of multiple impact factors to provide additional independent lines of evidence regarding which groundwater monitoring wells at the Facility may have been impacted by historical releases. Two key parameters for determining impacted conditions, dissolved oxygen (DO) and total petroleum hydrocarbons (TPH) – diesel range organics (TPH-d) were evaluated in detail (Sections 1 and 3, respectively). Several parameters indicative of impacted conditions and several other natural constituents found in groundwater were evaluated as multiple impact factors. Then a network data analysis was performed with these impact factors to quantitatively (1) evaluate their consistency as indicators of impacted conditions, (2) group wells with similar impact factor characteristics, and (3) assess whether outlying wells are dissimilar to the wells within the Facility.

2. Background Analysis – Dissolved Oxygen

For an accurate multiple impact factor analysis, knowing what represents background (unimpacted by the Facility) conditions with respect to DO concentrations is important. One key question is whether or not background dissolved oxygen concentrations in shallow groundwater near the Facility should be expected to be near the theoretical solubility of DO in groundwater, i.e., "at saturation."

Groundwater quality in shallow monitoring wells is typically not found at near-saturation levels. Rose et al. (1988) states: *"However, if ground water samples are uniformly saturated (approach the maximum solubility of O_2 in water at a given salinity, temperature, and pressure), the sampling method might be considered suspect."* They also state that using production wells is *"a method of last resort"* for measuring DO in groundwater due to the chance of artificially introducing oxygen into the sample and the tendency to mix groundwater from different stratigraphic zones.

2.1 Comparison with Nationwide Background Dissolved Oxygen Data

Background DO concentrations are almost always collected in monitored natural attenuation (MNA) projects. Wiedemeier et al. (1999) compiled MNA data from 26 MNA studies of hydrocarbon sites shown on Figure 2-1; the data are presented in Table 2-1. Despite having colder groundwater temperatures on average than O'ahu groundwater and therefore higher DO solubility (colder water has higher oxygen solubility), the average background (unimpacted) groundwater monitoring wells had on average only 6.7 milligrams per liter (mg/L) of DO. When compared to the theoretical DO solubility of 9.8 mg/L, the average background monitoring well at these 26 sites was at only 68% saturation; i.e., 32% of the oxygen had been consumed in the subsurface by natural (non-contamination-related) factors.

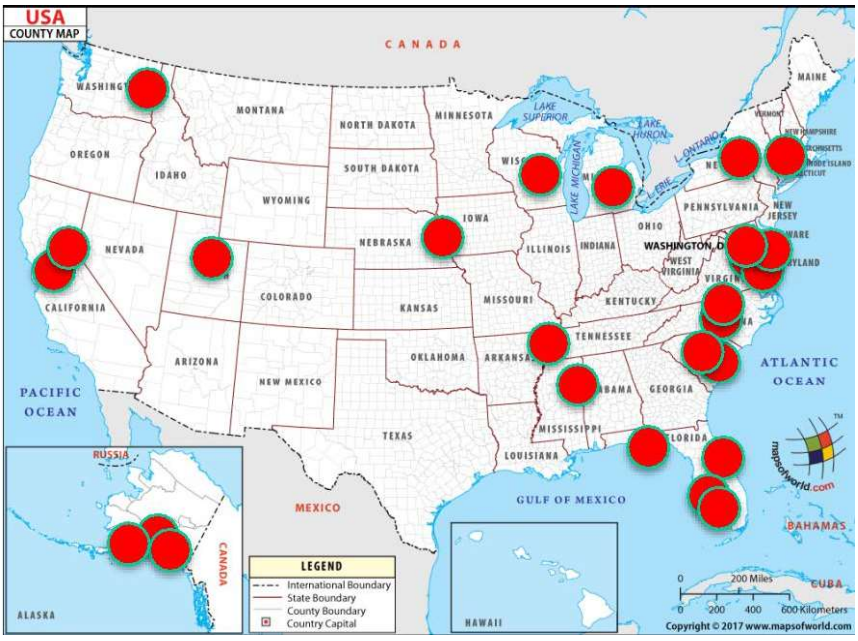

Figure 2-1: Location of 26 Monitored Natural Attenuation Studies with Background Groundwater Dissolved Oxygen Data (site list from Wiedemeier et al. 1999)

Table 2-1: Background Dissolved Oxygen Data from 26 Monitored Natural Attenuation Studies (Wiedemeier et al. 1999)

Month	Background DO Concentration (mg/L)	Groundwater Temperature (°C)	Theoretical DO Solubility (mg/L)	**% DO Saturation (%)**
Hill AFB, UT - Site 870	5.9	18.7	9.4	**63%**
Battle Creek ANGB, MI - Site 3	6.9	14.9	10.2	**68%**
Madison ANGB, WI	7.1	11.1	11.1	**64%**
Elmendorf AFB, AK - Hangar 10	0.8	6.9	12.3	**7%**
Elmendorf AFB, AK - ST-41	12.6	7.1	12.2	**103%**
King Salmon AFB, AK, SS-12	10.9	7.5	12.1	**90%**
Eglin AFB, FL - POL Facility	3.8	26	8.2	**46%**
Patrick AFB, FL - Gas Station	3.7	26.1	8.2	**45%**
MacDill AFB, FL - Site 56	2.4	25.2	8.4	**29%**
MacDill AFB, FL - Pump House 75	2.1	26.3	8.2	**26%**
Myrtle Beach, SC - POL Facility	1.9	17.2	9.7	**20%**
Langley AFB, VA - Site SS04	5.0	19.5	9.3	**54%**
Langley AFB, VA - Site SS16	6.5	26.7	8.2	**80%**
Griffis AFB, NY - Pumphouse 5	6.5	14.9	10.2	**64%**
Pope AFB, NC - FPTA #4	8.6	16.8	9.8	**88%**
Seymour Johnson AFB, NC - Bldg 470	9.0	17.4	9.7	**93%**
Fairchild AFB, WA, Bldg 1212	9.3	12.1	10.9	**86%**
Eaker AFB, AR - Gas Station	8.2	14.5	10.3	**80%**
Dover AFB, DL - Site SS27/XYZ	8.3	14	10.4	**80%**
Bolling AFB, D.C. - Car Care Center	7.5	20.3	9.1	**82%**
Offutt AFB, NE - Tank 349	6.8	22.2	8.8	**77%**
Westover AFB, MA - Christmas Tree FTA	11.2	13.4	10.6	**106%**
Columbus AFB, MS - ST-24	8.5	20.6	9.1	**94%**
Shaw AFB, SC - Bldg 1613	7.9	22.6	8.7	**90%**
Travis AFB, CA - Gas Station	3.7	21.7	8.9	**42%**
Beale AFB, CA - UST Site	8.4	17.6	9.6	**87%**
Average	*6.7*	*17.7*	*9.8*	***68%***

The subsurface environment supports both biological and geochemical processes that can consume and remove oxygen from the groundwater. Although the specific oxygen-consuming processes vary from site to site, the data from Wiedemeier et al. (1999) demonstrate that measurable oxygen depletion occurs at most sites. Thus, one should not expect typical background oxygen concentrations in groundwater to be at or near oxygen solubility. The United States Geological Survey (USGS) classifies any aquifer with more than 0.5 mg/L DO as being in the "oxic" redox category, with the predominant redox process being "oxygen reduction" (McMahon and Chapelle 2008).

Key Point: Although the specific oxygen-consuming processes vary from site to site, the data from Wiedemeier et al. (1999) demonstrate that measurable oxygen depletion occurs at most sites. DO in most groundwater is not found at saturation (the theoretical oxygen solubility) because of natural biological and geochemical reductants that will react with and deplete some of the oxygen.

2.2 COMPARISON WITH OTHER BASALT AQUIFERS DISSOLVED OXYGEN DATA

The USGS compiled geochemical analysis data from 425 wells in the Columbia Plateau, which is a basalt aquifer (Steinkampf and Hearn Jr. 1996). DO statistics were developed for three basalt hydrogeologic units (Table 2-2) and show average DO concentrations range from 2.6 to 6.4 mg/L. The report was not focused on any contaminated site or urban region.

Table 2-2: Dissolved Oxygen Data from Basalt Aquifers in Columbia Plateau (Steinkampf and Hearn Jr. 1996)

Basalt Hydrogeological Unit	DO Minimum (mg/L)	DO Maximum (mg/L)	DO Mean (mg/L)	Theoretical DO Saturation (mg/L)	**DO Saturation (%)**	Mean Groundwater Temperature (°C)	Number of Analyses
Saddle Mountains	0.5	10	6.39	9.8	**65%**	17	20
Wanapum	0.1	10.6	5.5	10.3	**53%**	14.4	266
Grande Ronde	0.1	10.2	2.6	9.5	**27%**	18.3	160

°C degrees Celsius

Key Point: A USGS study found that groundwater in three Columbia River Basalt aquifers exhibited oxygen depletion so that the DO was on average between 27% and 66% of the saturation value.

2.3 COMPARISON WITH O'AHU REGIONAL SHALLOW GROUNDWATER DISSOLVED OXYGEN DATA

The USGS (Hunt Jr. 2004) conducted a regional groundwater quality study as part of the USGS National Water-Quality Assessment (NAWQA). The O'ahu groundwater study was designed to meet the following objectives:

(a) *"Describe the occurrence and distribution of inorganic elements and organic compounds in Oahu ground water.*

(b) *Evaluate relationships between ground-water quality and land use.*

(c) *Determine whether land-use changes have caused changes in ground-water quality.*

(d) *Describe how the chemical composition of ground water is influenced by flow-system factors such as depth below the water table, proximity to recharge areas, and presence or absence of confining units."*

One key feature of this study was the inclusion of shallow monitoring wells in the study, because the 45 public water supply wells used in the study likely had a "clean bias" due to well depth and location within highly productive aquifer zones (Hunt Jr. 2004):

> *"Water following deep flowpaths in the aquifer originated as recharge in cool, forested uplands and is older, colder, and fresher than shallower water in the aquifer. Shallower water in downgradient parts of the aquifer contains young irrigation-return recharge with elevated concentrations of inorganic elements, nutrients, and organic compounds."*

To control for this deep pumping well "clean bias," the USGS incorporated 15 groundwater monitoring wells to better characterize shallow regional groundwater quality on O'ahu (Hunt Jr. 2004) (emphasis added):

> *"Recognizing this possible depth bias, a supplemental network of 15 monitoring wells was selected as a "Special Study" aimed at sampling shallower, younger ground water that is closed off from some of the public-supply wells (most monitoring wells are open at, or just beneath, the water table)…. **Although some of the selected monitoring wells originally were installed to investigate point-source contamination, only upgradient or "far-field" wells were selected so that results reflect regional water quality and not that of the point sources.** Unlike the random selection of the public-supply wells, the monitoring wells were selected arbitrarily, from a much smaller candidate list*."

The issue of "clean bias" is also relevant to the Facility because public wells in O'ahu (including several within a few miles of Red Hill) are screened much deeper (Figure 2-2) and within highly productive zones of the aquifer and are not representative of the groundwater sampled by the shallower Facility monitoring wells. Therefore, data from USGS upgradient/far-field monitoring wells should be used to determine the background conditions of shallow groundwater flowing into the Facility rather data from public water supply wells. (Hālawa Deep Monitor Well [HDMW2253-03] and RHMW11 are deep wells with low DO that appears to be unrelated to any possible releases from the Facility, and the geochemistry in these two wells is different from the water table monitoring wells at the Facility).

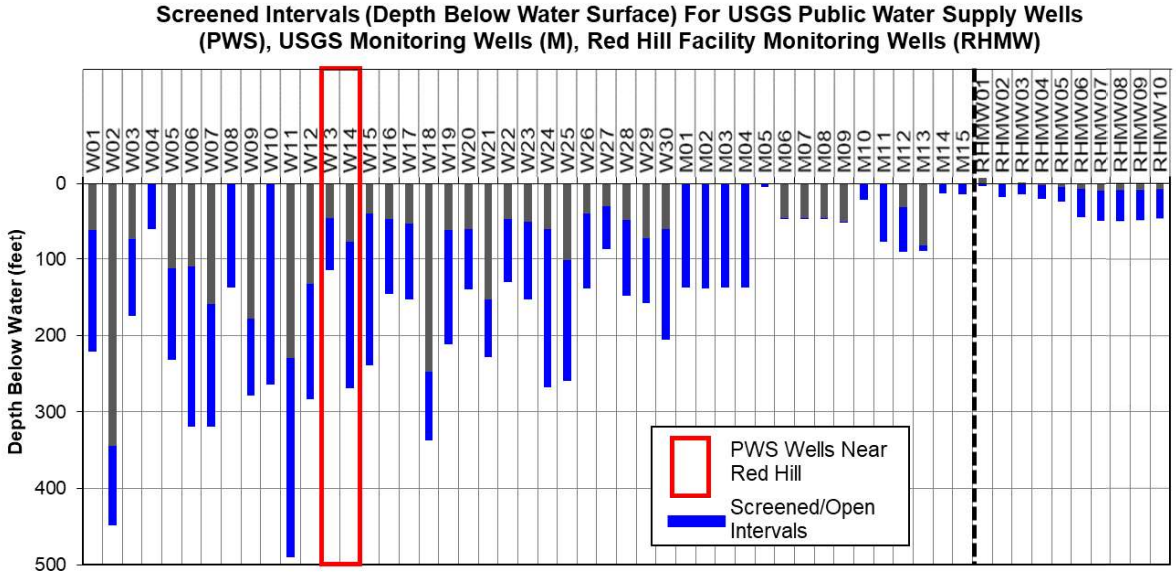

Note: The two public water supply wells closest to the Facility are outlined in red.

Figure 2-2: Screened Intervals for Public Water Supply Wells Used in Regional Groundwater Quality Study (Hunt Jr. 2004) vs. Screened Interval of Red Hill Monitoring Wells (depth below water surface)

The 15 groundwater monitoring wells used in the USGS study had an average of 6.7 mg/L DO, only 81% of the theoretical DO saturation. This is consistent with the conceptual understanding that shallow groundwater is less affected by the "clean bias" described by the USGS for deeper water supply wells. As described above, this finding of oxygen depletion in shallow groundwater is also supported by Rose et al. (1988), who state *"However, if ground water samples are uniformly saturated (approach the maximum solubility of O_2 in water at a given salinity, temperature, and pressure), the sampling method might be considered suspect."* Rose et al. (1988) also emphasized that using production wells for measuring DO in groundwater is *"a method of last resort."*

The USGS land use map (Hunt Jr. 2004) shows the Facility is located on "urban land" (which was formerly agricultural land). Detections of man-made chemicals that are not associated with the Facility (e.g., chlorinated volatile organic compounds) are observed in the Facility's outlying monitoring wells (Figure 2-3), thereby strongly supporting the conclusion that the shallow groundwater does not originate from completely unimpacted, pristine sources. Detections of acetone and phthalates may be a result of laboratory contamination.

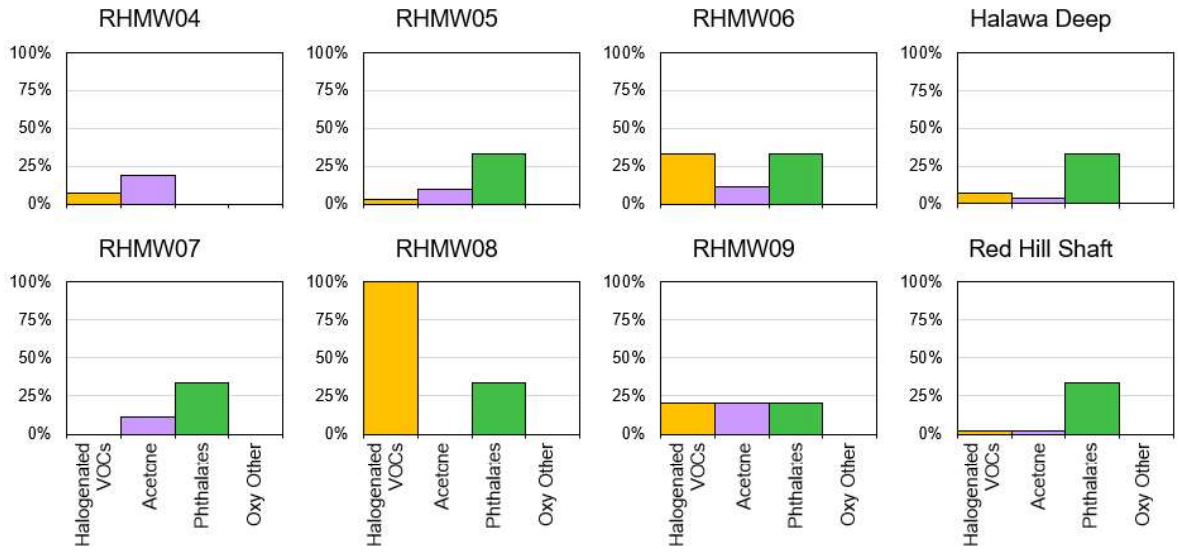

Halogenated VOCs: 1,1,2,2-tetrachloroethane,1,2,3-trichloropropane, 1,2,4-trichlorobenzene, bromodichloromethane, bromomethane, chloroform, chloromethane, cis-1,2-dichloroethene, dibromochloromethane, trichloroethene, methylene chloride
Phthalates: bis(2-Ethylhexyl) phthalate, dimethyl phthalate
Oxy Other: 2-butanone, dibenzofuran

Figure 2-3: Percent Detections of Man-Made but Non-Constituents of Potential Concern (Non-COPCs) in Outlying Monitoring Wells at the Facility

Table 2-3: Background Dissolved Oxygen Data from 15 Upgradient, Far-Field Monitoring Wells

USGS Upgradient, "Far Field" Monitoring Well	DO Concentration (mg/L)	**%DO Saturation (%)**
M01	6.5	77
M02	6.6	81
M03	4.7	57
M04	6.3	74
M05	6.8	82
M06	7.6	89
M07	7.2	86
M08	6.6	80
M09	6.8	83
M10	7.6	90
M11	7.6	94
M12	6.8	82
M13	7.1	85
M14	6.7	81
M15	6.1	73
Average	*6.7*	*81%*

Key Point: The USGS NAWQA found the average DO concentration in shallow groundwater in O'ahu was 6.7 mg/L, or only 81% of the DO saturation. The minimum DO value was 4.7 mg/L. None of these monitoring wells was measuring groundwater affected by point sources, but were upgradient, "far-field" monitoring wells representative of shallow groundwater in O'ahu. Based on the detection of man-made non-constituents of potential concern (non-COPCs) in outlying monitoring wells at the Facility, the shallow groundwater quality is more representative of an urban/agricultural land use than a pristine, forested land use. High DO concentrations at or near saturation are not expected in the monitoring wells at the Facility.

2.4 USING DISSOLVED OXYGEN DATA TO DETECT RELEASES: MAUI CASE STUDY

The County of Maui commissioned a study to develop a CSM for the Central Maui Landfill (CMLF) and evaluated groundwater quality to determine if there were any releases from the landfill (CH2M Hill 2016). Figure 2-4 shows the site layout with monitoring well locations, and Table 2-4 shows an excerpted table from the report.

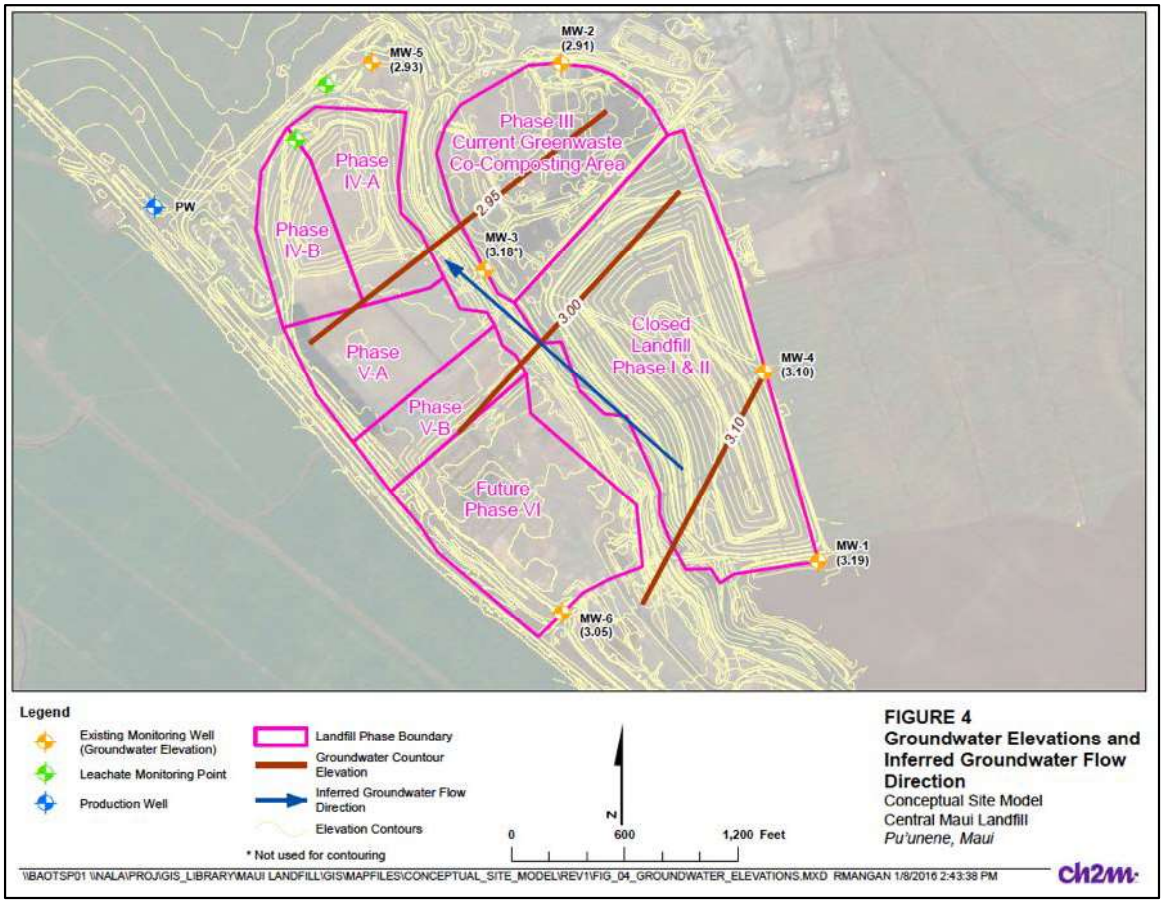

Figure 2-4: Groundwater Flow Direction and Location of Monitoring Wells, Central Maui Landfill Conceptual Site Model Study (CH2M Hill 2016)

Table 2-4: Table of Major Iron Chemistry, Conceptual Site Model Study of Central Maui Landfill (dissolved oxygen highlighting added) (CH2M Hill 2016)

Table 1. Major Ion Chemistry of CMLF Groundwater[a]
CMLF Conceptual Site Model

Constituent	MW-1[b]	MW-2	MW-3	MW-4	MW-5	MW-6
Nitrate	5.55	10	5.7	5.1	5.7	5.4
Total dissolved solids	663	870	705	710	735	650
Redox	159	195	132	102	69.1	81.6
Dissolved oxygen	6.09	7.30	5.31	4.44	5.86	5.25
pH	7.29	7.19	7.16	7.18	7.13	7.34

Notes
[a] Concentrations in milligrams per liter (mg/L) except for redox, which is in millivolts, and pH, which is the natural logarithm of the hydrogen ion activity.
[b] The December 2014 sample from MW-1 was analyzed twice, as a base sample and as a blind duplicate. The values noted are the arithmetic mean of the two values reported for the split sample.

Note: Average DO concentration is 5.7 mg/L.

With these data, the County of Maui report concluded that (emphasis added):

- *"If leachate were impacting groundwater, it would be expected that groundwater in the affected area* ***would exhibit more reduced (i.e. anaerobic) conditions than unaffected groundwater (i.e. background conditions).****"*
- *"Comparing the typical landfill effects and leachate quality to the groundwater quality data presented in Table 1 [Table 2-4],* ***no clear indication exists of landfill effects on groundwater quality at CMLF.****"*
- *"As reflected in Table 1 [Table 2-4], the presence of sulfate and nitrate above reporting limits in all wells,* ***the absence of dissolved iron, and aerobic nature of the groundwater (positive redox values and several mg/L of dissolved oxygen)*** *all suggest the lack of a water quality signature characteristic of releases from a MSWLF* [municipal solid waste landfill]*."*

Key Point: In a release study in Maui County, groundwater with DO between 4.4 and 7.3 mg/L and an average of 5.7 mg/L was used with other factors to unequivocally show that no release had occurred from this landfill. This supports the conclusion that oxygen depletion even well below the saturation level is not considered indicative of a release of contaminants.

2.5 PROCESSES THAT CAN CAUSE OXYGEN DEPLETION

In addition to contaminant-related processes (such as contaminant biodegradation), both natural biologic and natural geochemical processes (e.g., reactions with geologic media) can deplete oxygen from the subsurface. Natural organic matter (e.g., leaf litter, plant matter) can enter groundwater and be oxidized by oxygen consuming aerobic bacteria. A study of volcanic-rock aquifers performed by the USGS (Rupert et al. 2015) described how redox reactions work: *"The atmosphere is the source of the dissolved oxygen, so the redox conditions in an aquifer near where recharge occurs usually are oxic (defined here as having a concentration of dissolved oxygen of at least 0.5 mg/L). As groundwater moves through the aquifer along a flow path, the dissolved oxygen in the groundwater gradually is consumed by redox processes."*

Sawlan (2018) studied basalts in Columbia River flood basalt province and observed that these lavas had a large reservoir of reduced iron that drives oxidation reactions that consume DO. Lane, Jones, and West (1984) conducted laboratory experiments as part of a Nuclear Waste Repository study and demonstrated *"that basalt is effective in removing dissolved oxygen and in rapidly imposing reducing conditions on solutions."*

Geochemical oxygen depletion has been identified in Hawai'i as well. Hunt Jr. (2004) identified iron rich saprolites with anaerobic reducing conditions in perched groundwater:

> *"Some exposures of red saprolite in the study area contain greenish-gray bands where iron has been reduced from its ferric state (red) to its ferrous state (green). This suggests that anaerobic reducing conditions existed in the saprolite, most likely within perched water bodies."*

Finally, one deep monitoring well (HDMW2253-03) in the Facility vicinity was constructed as an open borehole to evaluate the deep fresh water/saltwater interface within the aquifer. This well shows oxygen depletion that is better explained by geochemical-induced reducing reactions, where geologic media serve as an electron donor, as opposed to contaminant-related oxygen depletion, where the hydrocarbon serves as the electron donor. (These geochemical reactions could involve non-contaminant microorganisms in a sequence of reactions.) In this well, the DO concentration averaged only 2.2 mg/L in 30 analyses conducted over an 8-year period from 2011 to 2019. Two factors confirm that contamination from the Facility could not have caused this DO depletion:

1. This well has an open borehole that begins about 25 feet below mean sea level, and about 45 feet below the piezometric surface of the regional basal aquifer, so that the groundwater extracted from this well is much deeper than groundwater that could be impacted by residual light non-aqueous-phase liquid (LNAPL) originating from the Facility (in addition, note the top ~35 feet of the open interval for this well is drilled through saprolite).
2. The alkalinity of this well has averaged only 50 mg/L for 12 samples collected from 2016 to 2019, indicating no excess carbon dioxide production from oxidation of hydrocarbons has occurred at this location, which would have been observed as increased alkalinity concentrations (i.e., the most highly impacted well at the Facility, RMHW02, has exhibited an average alkalinity concentration about four times higher, 200 mg/L).

In other words, if oxygen depletion has occurred but with no concurrent evidence of oxidation of hydrocarbon material, then the geochemical reactions induced by geologic media described in the basalt scientific literature has likely caused the oxygen depletion at HDMW2253-03.

One additional process could have also contributed to the observed oxygen depletion in Facility monitoring wells: the introduction of oxygen-depleting organics such as lubricating oils and drilling foams. Section 3.1 provides more information about lubricants and foams as part of the air rotary drilling process.

Key Point: The scientific literature confirms that basalt/saprolite can exert a geochemical oxygen demand on groundwater, and that slightly depleted DO by itself is not a reliable confirmatory marker of hydrocarbon contamination. Oxygen depletion from geochemical reactions is likely occurring at HDMW2253-03 and may have contributed to oxygen depletion in other monitoring wells at the Facility.

2.6 NATURE OF OXYGEN DEPLETION IN OTHER FACILITY MONITORING WELLS

The change in DO concentrations over time in some monitoring wells also supports the conclusion that geologic media can serve as the electron donor for oxygen depletion reactions rather than hydrocarbon contamination. As shown on Figure 2-5, the DO concentrations in three Facility monitoring wells drilled near saprolite zones were substantially depleted in DO in analyses conducted immediately after drilling but then showed a slow increase in DO over time.

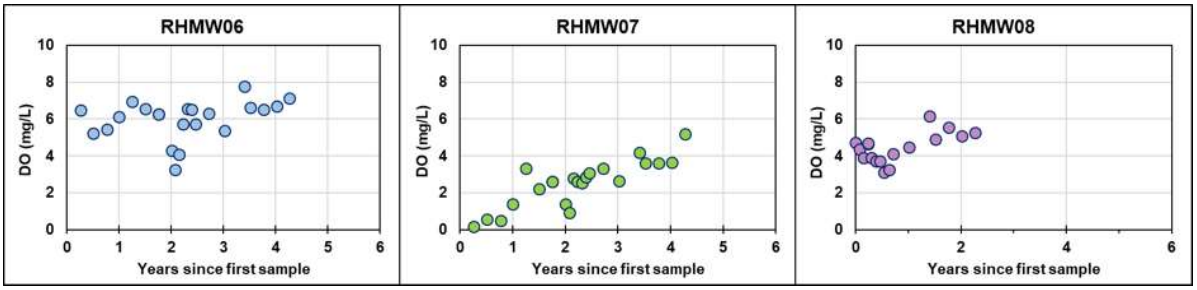

Note: RHMW06 and RMW07 were completed in Oct. 2014; RHMW08 in Oct. 2016.

Figure 2-5: Dissolved Oxygen Concentration vs. Time Since Installation for Three Facility Monitoring Wells Drilled Near Saprolite Zones

This slow increase in DO concentration is not consistent with an upgradient LNAPL source. The average alkalinity in these wells ranges between 80 and 100 mg/L. This is less than one-half of the alkalinity in the two monitoring wells located within the Facility tunnel that are nearly directly below the area of the tanks (RHMW02 and RHMW03) and is not indicative of carbon dioxide production from biodegradation reactions. In addition, concentrations of hydrocarbons in RHMW06, RHMW07, and RHMW08 have been very low or non-detect (see Section 2.7 for further detail).

In addition, low DO concentrations in some of the RHMW11 multilevel monitoring well zones may be related to the proximity to overlying saprolite.

One explanation is that drilling these wells exposed ferrous iron. Over time as groundwater flowed through the newly exposed geologic media near the well screen, this ferrous iron reacted with and consumed some of the DO. It is likely that this relatively small amount of newly exposed ferrous iron has been converted to its ferric state, which is not reactive with DO, reducing the amount of oxygen depletion and thereby slowly increasing the DO concentration.

Key Point: Facility monitoring wells near saprolite zones (RHMW06, RHMW07, and RHMW08) showed depleted DO concentrations immediately after installation, but then increasing concentrations over time. This pattern and other geochemical data are not consistent with an LNAPL source, but are consistent with exposing groundwater to more reactive ferrous iron in the newly drilled borehole wall with declining reaction rates thereafter. Over time, the abundance of oxygen-depleting ferrous iron has slowly declined because of exposure to more oxidizing flowing groundwater, thereby resulting in increasing DO concentrations.

2.7 IMPLICATIONS FOR MULTIPLE IMPACT FACTORS EVALUATION

Key Point: Based on national databases, geochemical analysis of basalt aquifers, a USGS regional groundwater quality study, and DO scientific literature, the background groundwater entering the Facility is likely partially depleted of DO because of biodegradation of naturally occurring compounds,

drilling-related contamination, and geochemical reactions with the basalt/saprolite. The DO concentration from 15 upgradient, "far-field" groundwater monitoring wells selected by the USGS to be representative of shallow regional conditions in O'ahu was never found near 100% saturation, but exhibited a minimum value of 4.7 mg/L and an average value of 6.7 mg/L. The DO in the USGS monitoring wells is compared to Red Hill monitoring wells in Table 2-5.

Table 2-5: Dissolved Oxygen Concentrations at Select Red Hill Wells vs. Monitoring Wells on O'ahu (Hunt Jr. 2004)

Well	DO Concentration (mg/L)			Notes
	Minimum	Maximum	Median	
RHMW04	4.62	9.9	8.36	—
RHMW05	5.32	9.7	8.29	—
RHMW06	3.26	7.77	6.28	Increasing trend with time, see Section 2.6 for discussion
RHMW07	0.18	5.18	2.63	Increasing trend with time, see Section 2.6 for discussion
RHMW08	3.12	6.16	4.46	Increasing trend with time, see Section 2.6 for discussion
RHMW09	6.1	9.06	8.38	—
RHMW10	6.22	9.31	8.03	—
USGS O'ahu Monitoring Wells	4.7	7.6	6.8	—

3. Background Analysis – Total Petroleum Hydrocarbons

TPH-d has been detected in the Facility's outlying monitoring wells RHMW04, RHMW06, RHMW07, RHMW08, and RHMW10. TPH is a non-specific parameter that is defined by whatever is "detected" within a specified analysis time window, but it is not necessarily total, petroleum or hydrocarbons. However, the temporal pattern of these detections is unusual: relatively high concentrations were detected during the first 2 years of sampling after drilling, then non-detect concentrations or very low estimated concentrations thereafter (Figure 3-1). The following multiple impact factor analysis has been developed to account for the nature of this unusual trend.

3.1 LNAPL Impact or Drilling Contamination

Overall, the early high concentration pattern indicates some type of drilling artifact or drilling-related contamination rather than nearby LNAPL contamination. As described below, this is a common occurrence related to induced low-level contamination associated with the type of drilling and monitoring well installation used in these wells. In the first year of sampling, 29% of the samples had detectable TPH-d with a maximum concentration of 338 micrograms per liter (µg/L), as shown on Figure 3-1. TPH-d detections in these five outlying wells became relatively rare following the first year after installation. Only 1 of the 24 samples (including duplicates) (4%) collected in the second year after installation had detections of TPH. In the subsequent years, the detections/samples were 0/27, 0/9, and 0/7, respectively (including duplicates).

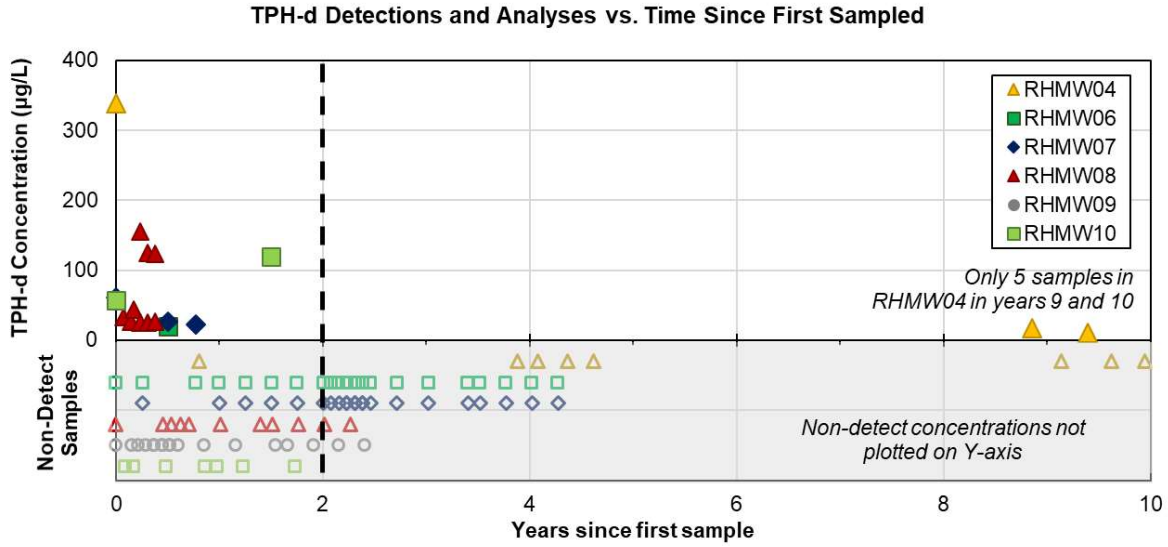

Notes: First 2 years of data shown with dashed line. Well completion dates: RHMW04, Sept. 2005; RHMW06 and RMW07, Oct. 2014; RHMW08 and RHMW09, Oct. 2016; RHMW10, May 2017.

Figure 3-1: TPH-d Concentrations in Groundwater vs. Time Since Installation for Six Facility Monitoring Wells

RHMW05 is not included in this analysis as it is located downgradient of the tank farm area. However, it does show the same TPH-d anomaly (unexpectedly high, short-lived TPH-d concentrations in the early part of the sampling record). During the first 2 years of sampling, 44% of the TPH-d samples had TPH-d detections, with a maximum concentration of 2,060 µg/L; in the subsequent 9 years, only 15% of the samples had TPH-d detections, with a maximum concentration of only 62 µg/L. As

discussed in Sections 3.2 and 3.3, TPH detections below 100 µg/L are not reliable indicators of petroleum contamination.

The relatively low-level TPH-d detections in the first year of sampling are not indicative of a long-term LNAPL source that is upgradient of all the monitoring wells. It would be extraordinary for all these wells to be impacted in this same way because these early TPH-d detections happened in different years for different wells, ranging from year 2005 for RHMW04 to year 2017 for RHMW10. In other words, the common factor for the higher-magnitude TPH detections is time since installation of the well, not calendar year.

The unique nature of this temporal signal, with five of six outlying monitoring wells showing high TPH-d concentrations in the first year of installation starting in 2005, 2014, 2016, and 2017, can be explained as an artifact of the drilling process. Air and mud rotary drilling techniques were used to ream out the monitoring wells through the basalt. This drilling procedure, common for hard rock applications, uses high volumes of compressed air and/or mud to remove the drilling cuttings from the borehole. This air is provided by a large rotary air compressor, which in turn requires oil for lubrication. Figure 3-2 shows an air rotary drilling rig depicted in State of Hawai'i Department of Health (DOH) environmental guidance and describes the function of the compressed air (DOH 2018b). Oil is also used to lubricate drill bits/hammers used in the air rotary drilling process.

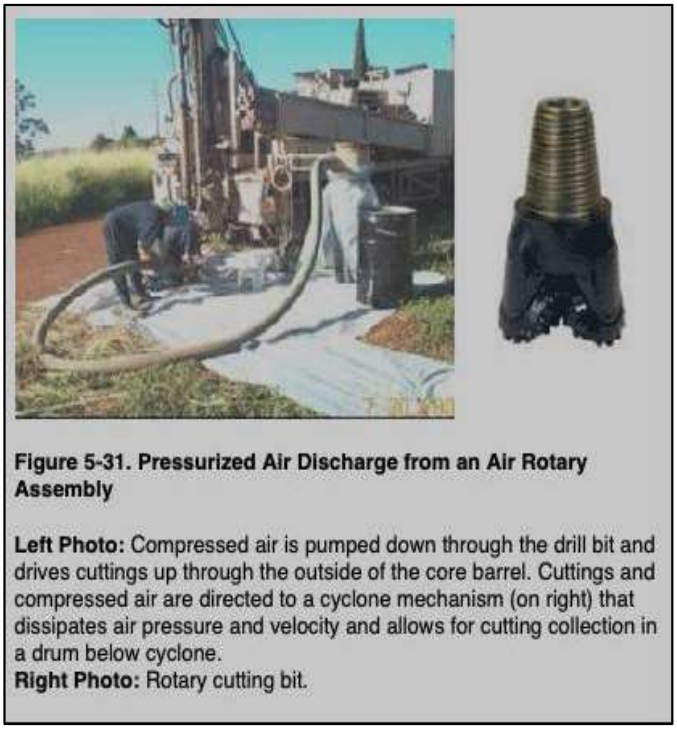

Figure 5-31. Pressurized Air Discharge from an Air Rotary Assembly

Left Photo: Compressed air is pumped down through the drill bit and drives cuttings up through the outside of the core barrel. Cuttings and compressed air are directed to a cyclone mechanism (on right) that dissipates air pressure and velocity and allows for cutting collection in a drum below cyclone.
Right Photo: Rotary cutting bit.

Figure 3-2: Air Rotary Drilling Rig (DOH 2018b)

The nature of this lubrication oil is described by a national drilling company newsletter and a state guidance document this way (emphasis added):

> *The air discharged from air compressors normally contain finely atomized lubricating oil. To help prevent this oil from contaminating monitoring well drill holes, compressor discharge*

> *filters must be installed (and maintained during regular intervals) on rigs used to drill monitoring wells. Air-discharge samples should be collected as reference samples for future comparison where hydrocarbon contamination is being studied.* ***These samples are a necessity in applications where lubrication of down-the-hole hammers or other tools is essential.*** (SD DENR 2003) (National Driller 2007)

Several environmental guidance documents and scientific literature citations caution about the potential for introducing oil into the formation when using air rotary. For example, Kostecki and Calabrese (1991) warned: *"The major limitations from a site assessment standpoint come from the potential for introduction of oils and contaminants into the well from poorly filtered air…."*

In a Final Order (NMED 2013), the State of New Mexico provided this insight about contamination risks with air rotary: *"One drawback of the down-the-hole hammer is that oil is required in the air stream to lubricate the hammer-actuating device, and this oil could potentially contaminate the soil in the vicinity of the borehole and the aquifer."*

Finally, California Department of Toxic Substances Control (1995) guidance explicitly describes the risk of oil contamination from air rotary drilling as shown on Figure 3-3 (highlight added).

> Unless an oil-less compressor is used, there is always the risk of introducing some quantity of compressor oil into the borehole. This can occur even when oil-removing filters are used, because their effectiveness depends on careful maintenance. At best, the issue of whether oil has been introduced into the aquifer will remain suspect. There is generally no way to tell when compressor filters need changing because most drilling equipment have safety bypass valves that route the air around plugged filters.

Figure 3-3: Excerpt from California Department of Toxic Substances Control's (1995) Guidance Regarding Use of Air Rotary Drilling for Environmental Investigations

Various issues related to oil induced drilling by air and mud rotary rigs used to drill monitoring wells at the Facility have been identified over time. For air rotary rigs, these issues include air compressor oil and lubrication of the drill pumps and drill string. Another issue for both air and mud rotary rigs is residual TPH from water truck tanks used to transport water from a source (e.g., municipal hydrant, driller baseyard) to the drill site. Especially high TPH concentrations were noted in the drilling "make-up" water during the installation of RHMW09 (data are provided in Attachment I-1) due to contamination from the water tank trucks and drill pumps. Thereafter, new procedures were developed to help minimize oil-induced contamination from drilling. Because of the issues mentioned above, inadvertent oil contamination had a high likelihood of occurring. It would be unlikely for most drillers to become aware that oil contamination from air rotary drilling occurred because: (1) drillers are not in the business of collecting and interpreting groundwater samples and therefore might not know about any subsequent TPH-d detections; (2) at some contaminated sites, drilling-related contamination would be revealed only by a rarely used low-level TPH-d analysis method; (3) drillers have rarely been observed to collect air discharge samples when using air rotary drilling to carefully monitor their filters; and (4) drilling guidance documents warn "at best" the issue of whether oil has been introduced into the aquifer will "remain suspect." With that said, the RHMW09 driller was aware of certain issues related to potential induced hydrocarbon contamination due to the new drilling procedures that were implemented to help address this issue. This included use of food-grade oil in place of petroleum-

based lubricants used in the water pumps in the drill rig and the integration of in-line granular activated carbon (GAC) systems to remove any oil or grease introduced from the pumps into the drilling "make-up" water flowed downhole. However, the driller was not informed of TPH concentrations in groundwater.

This lubrication oil would not produce a high-solubility dissolved-phase signal, but would likely generate low-concentration dissolution products and metabolic byproducts over time that would be detected only intermittently by sampling. Also, contamination of drilling "make-up" water is also an issue, as previously mentioned.

In addition, during the course of drilling RHMW09, TPH was discovered in the potable water that was used for drilling (see Attachment I-1). Efforts were taken to further identify potential sources for TPH in this water, and then actions were taken to attempt to isolate the problem. Since TPH was a factor during the drilling of RHMW09, it is likely that it also may have been a potential issue during the installation of earlier (as well as subsequent) monitoring wells. As an example, a review of the early TPH hits in RHMW10 clearly shows that the TPH is not fuel-related. These observations support the various analyses that conclude that early detections of TPH are likely due to drilling and well installation. Low-level detections of TPH related to drilling are not uncommon and are a known issue within the industry.

Finally, an organic, biodegradable chemical foam (Foamer ES by Matex Control Company) was used by the drillers at some of the Facility monitoring wells as part of the air rotary drilling process. This drilling foam, composed of sodium olefin sulphonate, is described this way by the vendor:

- FOAMER ES is a non-alcohol-based foam used for diamond and rotary drilling.
- FOAMER ES provides an environmentally acceptable foaming agent to be used in mineral exploration, oil and gas exploration, and water well drilling operations.
- FOAMER ES has an excellent half-life comparable to the leading foams on the market.

This chemical foam could also contribute to the observed TPH-d detections in the first 2 years after drilling.

This drilling-related contamination explains some of or all the early TPH-d detections in the outlying wells. Subsequent to the first 2 years after installation, TPH-d was detected only in two low-level samples from RHMW04; these detections are evaluated in detail in Section 3.2.

Key Point: TPH-d detections in the first and likely the second year after installation are most likely related to drilling or laboratory contamination and do not indicate an LNAPL release from the Facility.

3.2 TPH-D DETECTIONS IN LATER YEARS IN MONITORING WELL RHMW04

Two TPH-d detections at 17 J and 10 J µg/L were observed in RHMW04 a total of 8.8 and 9.1 years after the well was completed. Because of the long period after installation, these detections are not likely related to drilling-related contamination in the same way the TPH-d detections in the first 2 years after drilling are.

It is well known that because of the nature of the TPH analysis, anomalous detections of TPH in groundwater are a common concern, especially at low concentrations. Figure 3-4 shows an excerpt from the *California Leaking Underground Storage Tank Guidance Manual* (CWQCB 2012) that

stresses the importance of not assuming that reported detections are petroleum because of potential false positives such as chlorinated organics, laboratory contamination, and natural organics. Figure 3-5 shows an excerpt from San Francisco Bay Regional Water Quality Control Board's *Environmental Screening Levels User's Guide* (SFRWQCB 2019). This guidance also emphasizes the non-specific nature of TPH analytical methods and stresses the need to review TPH chromatograms to determine whether detected material consists of hydrocarbon, hydrocarbon oxidation products (HOPs), and/or natural organic compounds (NOCs). Figure 3-6 shows an excerpt from the Hawai'i DOH document *Collection and Use of Total Petroleum Hydrocarbon Data for the Risk-Based Evaluation of Petroleum Releases, Example Case Studies* (DOH 2018a), in which TPH concentrations < 100 µg/L are identified as having the potential issue of misinterpretation of chromatogram baseline noise.

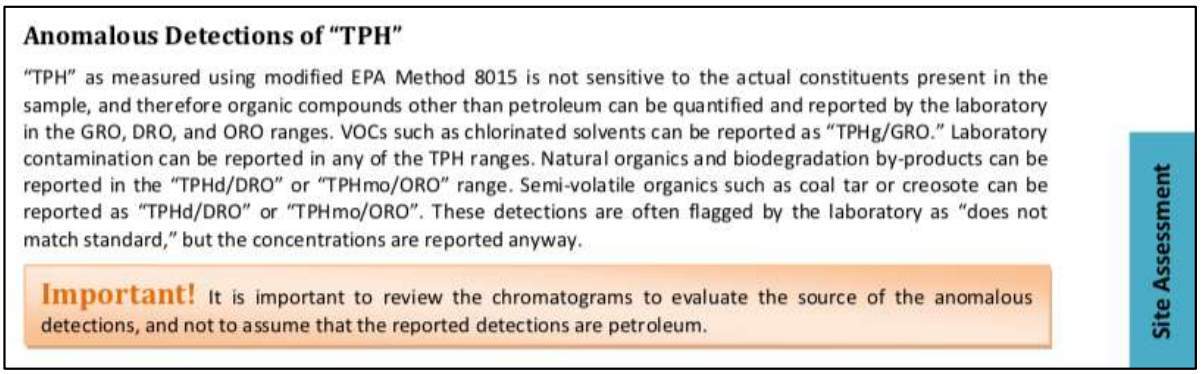

Figure 3-4: Excerpt from California State Water Resources Control Board's (2012) *Leaking Underground Storage Tank Guidance Manual* Stressing the Importance of Not Assuming that Reported TPH Detections are Petroleum

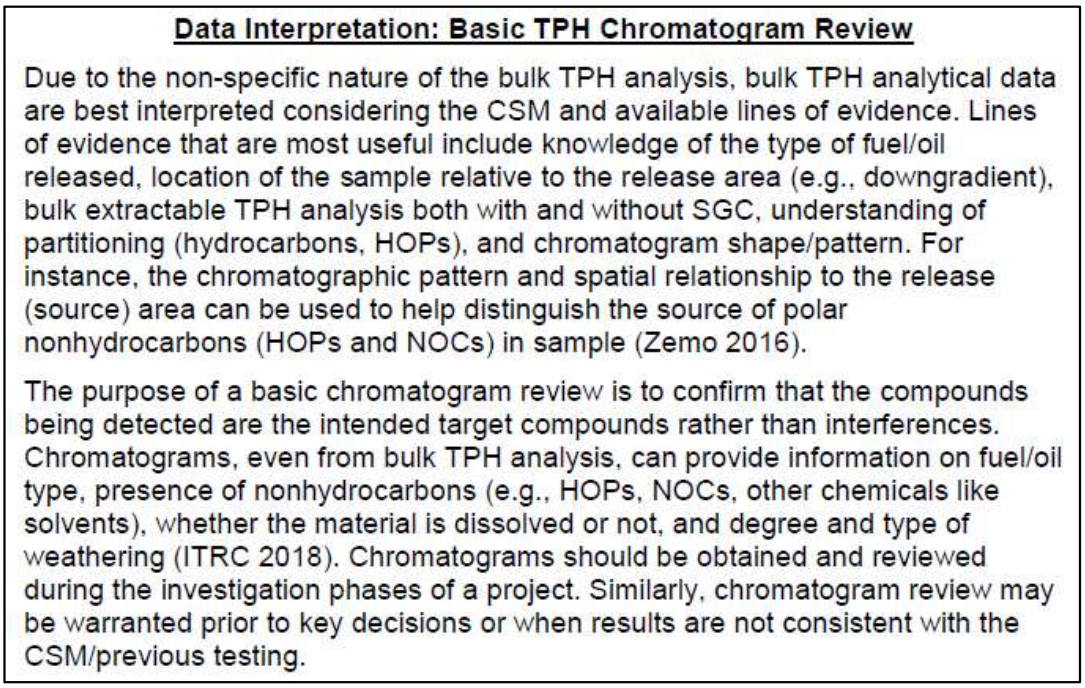

Figure 3-5: Excerpt from San Francisco Bay Regional Water Quality Control Board's (2019) *User's Guide: Derivation and Application of Environmental Screening Levels* Emphasizing the Non-Specific Nature of TPH Analysis and Need for Chromatogram Review

4 COMMON RISK ASSESSMENT PROBLEMS AND DATA LAPSES

As noted in the case studies, existing TPH data might or might not be adequate for risk-based assessment of potential environmental concerns at a petroleum-release site. Common types of data lapses and data usability issues include:

- Reliance on BTEXN and PAH data (i.e., indicator compounds) alone for decision making in the absence of TPH characterization data for all media (i.e., soil, sediment, water, soil vapor and/or indoor air);
- Failure to document nature, location and potential environmental concerns posed by residual contamination;
- Absence of a detailed CSM and consideration of all current or potential sources, pathways and receptors;
- Focus of initial risk assessment on human direct exposure and lack of data collection and assessment of other potential concerns, including leaching, vapor intrusion, impacts to aquatic habitats, gross contamination, and related environmental concerns;
- Inability to assess degradation state of petroleum in groundwater due to lack of silica gel cleanup data;
- Inability to assess potential environmental concerns posed by polar, TPH-related metabolites due to lack of groundwater data that excludes silica gel cleanup;
- Bias of existing TPH soil data due to presence of tree sap, pine needles and other non-petroleum, organic material in samples and inadequate processing and analysis at the laboratory;
- Bias of existing TPH groundwater or surface water data due to presence of algae, dissolved organic carbon, fish oils and other non-petroleum, organic material in samples and inadequate processing and analysis at laboratory;
- Misinterpretation of baseline noise in gas chromatograph signals below 100 µg/L as TPH in groundwater or surface water samples;
- Use and interpretation of data from different analytical methods (for example, method 8015 vs. state-specific methods); and
- Limitations of data use due to elevated detection limits and laboratory reporting errors.

Additional problems associated with the use of historic data at petroleum release sites are discussed in individual case studies.

Figure 3-6: Excerpt from DOH's (2018a) *Collection and Use of Total Petroleum Hydrocarbon Data for the Risk-Based Evaluation of Petroleum Releases, Example Case Studies* Listing Data Usability Concerns, including TPH at Concentrations < 100 µg/L

With these cautions in mind, note the RHMW04 detections also certainly relate to the extremely low method detection level used by the Navy-contracted laboratories for the Facility (see CSM Appendix B.8). For comparison, the United States Environmental Protection Agency's (EPA's) and other laboratories' various laboratory limits for TPH-d are shown in Table 3-1.

Table 3-1: Various Laboratory Limits for TPH-d

Laboratory	Laboratory Limit
Current (October 2016 to February 2019) Navy contracted laboratory MDL and LOD	13 and 25 µg/L
EPA Region 9 laboratory QL	150 µg/L
Typical routine Eurofins/Test America RL	100 µg/L
Historical Navy contract laboratories for the Facility monitoring DL	10–352 µg/L
Concentration below which misinterpretation of baseline noise may cause data usability issues (DOH 2018a)	**100 µg/L**
Two RHMW04 TPH-d Detections	*10 J – 17 J µg/L*

Notes: MDL = method detection limit; LOD = limit of detection; QL = quantitation limit; RL = reporting limit, DL = detection limit; J = estimated value

To illustrate the importance of these extremely low-level limits used at the Facility, two points can be made:

- These two RHWM04 samples would have been "non-detect" for TPH-d if the EPA Region 9 laboratory TPH-d quantitation limit (QL) or other laboratories' reporting limits (RLs) had been used.
- The EPA Region 9 laboratory has detected TPH-d only three times in the Facility's outlying wells (i.e., in the groundwater samples from RHMW08 in January, February, and March 2017, about 6 months after the well was completed).

A review of the chromatograms or "fingerprints" obtained from analysis of TPH is useful for reducing uncertainties inherent to the analysis (ITRC 2018). Review of chromatograms for low-concentration data is also recommended in a United States Department of Defense (DoD) Environmental Quality Workgroup fact sheet (DoD EDQW 2017). When the two chromatograms from these two RHMW04 samples (Figure 3-7) are evaluated, the uncertainty in these results is revealed:

- The series of discrete peaks in the July 2014 sample do not resemble any type of fuel pattern, dissolved fuel components, or biodegraded matter.
- The sample from January 2015 shows that when the chromatogram was quantified, there is obvious and often unavoidable over-integration of a very small signal at the limit of detection (LOD).

These detections are likely false positives inherent with attempting measurements near the method detection limits (MDLs) and do not support presence of fuels in RHMW04 during this period.

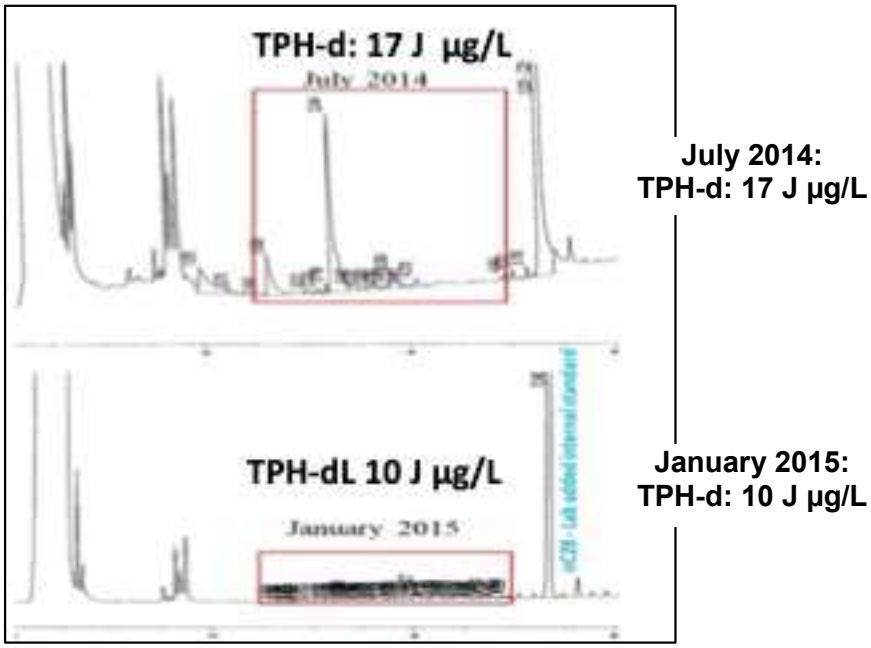

Figure 3-7: Chromatograms from TPH-d Samples from RHMW04; Both Samples Were "J" Flag

Key Point: Two low-level TPH-d detections in RHMW04, both less than 20 J µg/L, occurred about 9 years after installation and therefore are not likely related to drilling-related contamination. However, these two low level TPH-d detections are likely false positives due to analytical artifacts and therefore do not support the presence of fuels in RHMW04.

3.3 IMPLICATIONS FOR MULTIPLE IMPACT FACTORS EVALUATION

Key Point: When possible, the multiple factors analysis should not use the first and possibly the second year of data, or data below 150 µg/L (based on the EPA Region 9 laboratory's TPH-d QL) or below 100 µg/L (based on ITRC risk case studies posted in DOH [2018a]), or the analysis should compare results when these data are and are not used in the evaluation.

4. Multiple Impact Factors Analysis

Network data analysis was performed to quantitatively evaluate the similarity among the multiple impact factors at selected wells. Wells with similarity characteristics are grouped into clusters. The analysis simultaneously considered multiple factors and provides a holistic insight into the spatial distribution of potential chemical impacts due to a Facility release.

4.1 Overview of Network Data Analysis

In network data analysis, each data point consists of values of multiple attributes. Data points are referred to as "nodes." A group of nodes with similar characteristics are tightly connected and are referred to as a "community." The linkage between two nodes is referred to as "edge," and its length represents the similarities between the nodes. Network analysis is used to visualize the strength of complex relationships between the nodes as well as to identify the communities. In this analysis, cosine similarity was used as the metric to quantify the similarity between a pair of nodes. Cosine similarity is a commonly used metric in cluster analysis. The more similar the attributes of two nodes, the closer the cosine similarity value to 1. The pairwise cosine similarity measures were assembled into a similarity matrix associated with all the nodes. The matrix was depicted based on the strength of similarity, and the Louvain method was employed to detect the group of clusters in the network (e.g., Newman 2006).

4.2 Data Selection

The data considered in the network analysis include concentration values of petroleum hydrocarbons diesel range (TPH-d), gasoline range (TPH-g), and oil range (TPH-o), naphthalene (N), 1-methylnaphthalene (1-MeN), 2-methylnaphthalene (2-MeN), benzene (B), toluene (T), ethylbenzene (E), xylene (X), methane, sulfate (sulfate as SO4), nitrate (nitrate as nitrogen), and DO from samples collected between 2005 and 2019 at wells RHMW01–RHMW10, RHMW11 monitoring zones 1 to 5, Red Hill Shaft monitoring point (RHMW2254-01), and HDMW2253-03. They represent direct and indirect indicators of potential petroleum impacts.

The available chemical data include duplicate sample data, some of which are qualified with U (non-detect), J (estimated concentration), or UJ (estimated non-detect) flag. The following procedure was taken to handle these duplicate sample data in the analysis:

- Treated as no data (left as blank in the database) if the chemical data were not measured for both duplicate samples.
- Averaged duplicate sample results if the chemical data were measured without any flags.
- Used the lower value of duplicate samples if both samples have the same flag of U or J or UJ.
- Used the detected value (either with or without a J-flag) if only one of the duplicate samples had a detection.
- Chose U flag data if the other duplicate sample data had UJ flag.

4.3 Analysis Approach

The network data analysis was performed using an indicator approach such that the data for each considered constituent/factor are converted into a common scale between 0 and 1. A larger indicator value suggests a potentially greater petroleum impact. The data conversion to indicators for TPH-d, TPH-o, TPH-g, N, 1-MeN, 2-MeN, B, T, E, X, and methane was based on the following criteria:

- Any unflagged detected concentration values are treated as 1.
- All U or UJ flagged data are treated as 0.
- All J flagged data are treated as 0.5.

The indicator of DO reduction was assigned based on the following criteria:

- All values above 6.8 mg/L are treated as 0.
- All values below 4.7 mg/L as 1.
- All values between 4.7 – 6.8 mg/L are treated accordingly to a linear scale between 1 and 0.

The values of 4.7 mg/L and 6.8 mg/L are the lowest and median background concentrations, respectively, reported in a study by Hunt Jr. (2004) using data from unimpacted monitoring wells in O'ahu that were selected to reflect regional water quality.

Similar criteria were applied for sulfate and nitrate except that 12.80 mg/L and 1.94 mg/L are considered the respective lower thresholds, and all concentration values above them are considered as 0. Conversely, 3.90 mg/L and 0.18 mg/L are the respective upper thresholds for sulfate and nitrate, and all values below them are treated as 1.0. All values between the lower and upper thresholds are treated according to a linear scale between 1 and 0. The lower and upper thresholds are the lowest and median background concentrations, respectively, based on data from unimpacted monitoring wells in O'ahu (Hunt Jr. 2004). Indicator criteria for all analytes in summarized in Table 4-1.

Table 4-1: Indicator Criteria Used for Multiple Impact Factor Analysis

Analyte	Non-detect (U or UJ)	Estimated Value (J-flag)	Detected, Unflagged	> Median Background Concentration	Between Median and Minimum	< Minimum Background Concentration
COPCs [a]	0	0.5	1	—	—	—
DO	—	—	—	0 (6.8 mg/L)	Linear scale: 0 to 1	1 (4.7 mg/L)
Nitrate	—	—	—	0 (1.94 mg/L)	Linear scale: 0 to 1	1 (0.18 mg/L)
Sulfate	—	—	—	0 (12.80 mg/L)	Linear scale: 0 to 1	1 (3.90 mg/L)
Methane	0	0.5	1	—	—	—

[a] COPC chemical of potential concern (TPH, N, 1-MeN, 2-MeN, BTEX)

Due to the issues discussed in Section 3, all data within the first year of well installation were excluded in the analysis. In addition, generalized Wilcoxon statistical test results indicate that chemical data collected within the first year after installation of RHMW01, RHMW04, RHMW05, and RHMW07 are statistically different from the data collected in subsequent years (p value < 0.05), further supporting the exclusion of first-year data (a general statistical rule is if the p-value is less than 0.05, then a statistically significant difference does exist at a 95% confidence level). If there was more than one data value for a constituent within a quarter, the values were averaged to generate a quarterly averaged data value to avoid bias caused by more data within a quarter. To generate a representative indicator value for the constituent at a well, all quarterly averaged values were averaged. The resulting representative indicator value for each considered constituent at all selected wells is shown on Figure 4-1 and Figure 4-2.

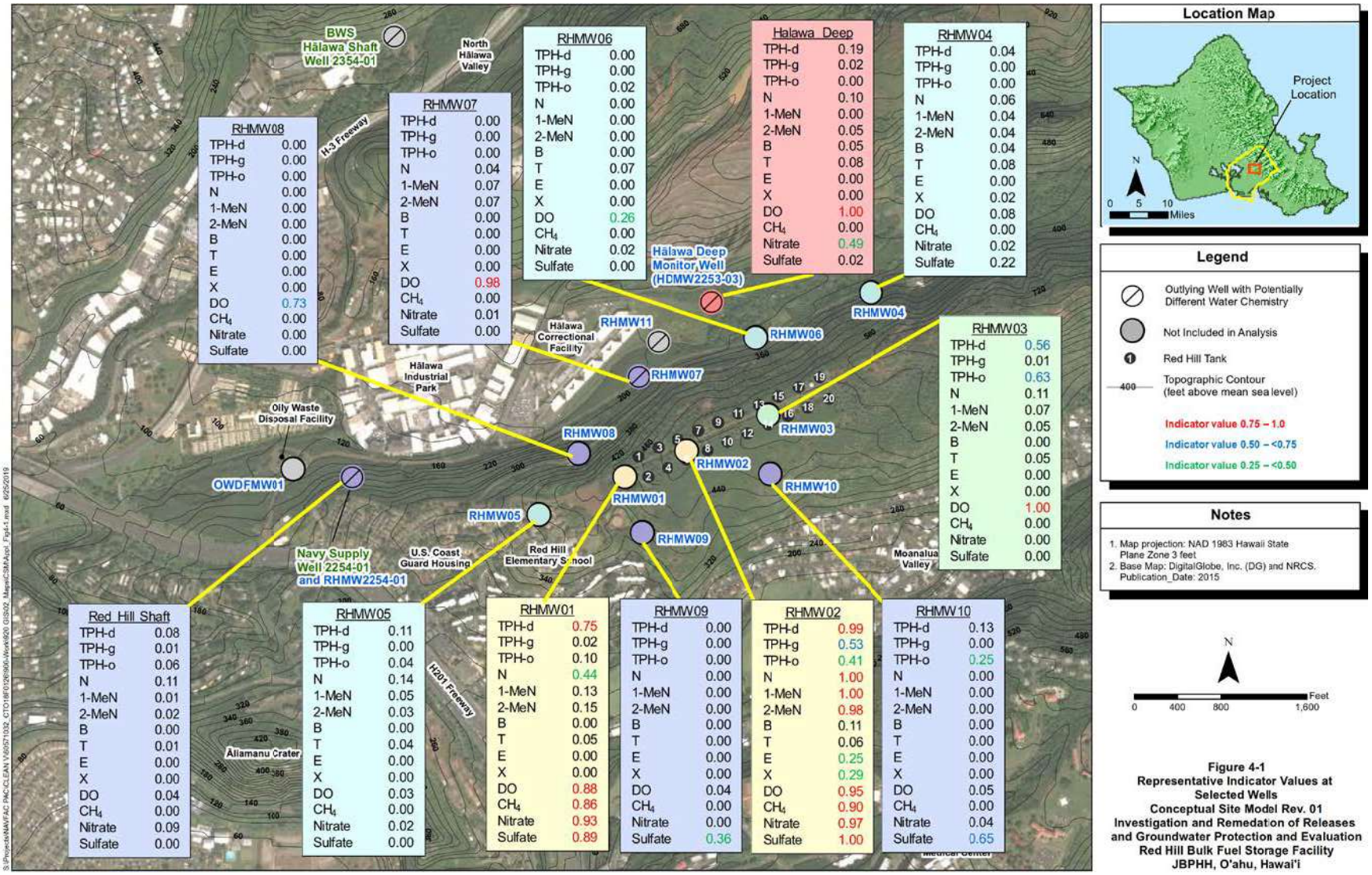

Figure 4-1
Representative Indicator Values at Selected Wells
Conceptual Site Model Rev. 01
Investigation and Remedation of Releases and Groundwater Protection and Evaluation
Red Hill Bulk Fuel Storage Facility
JBPHH, O'ahu, Hawai'i

Notes: Wells not included in analysis are: RHMW11 (only 1 year of data) and OWDFMW01 (water chemistry in this area has been impacted from past oily waste disposal operations not related to fuel releases from Red Hill). Outlying wells with potentially different water chemistry are discussed in more detail in CSM Appendix B.8 Section 1.3. Coloring of indicator boxes corresponds to cluster colors on Figure 4-3.

Figure 4-1: Representative Indicator Values at Selected Wells (first-year data not used due to drilling artifacts)

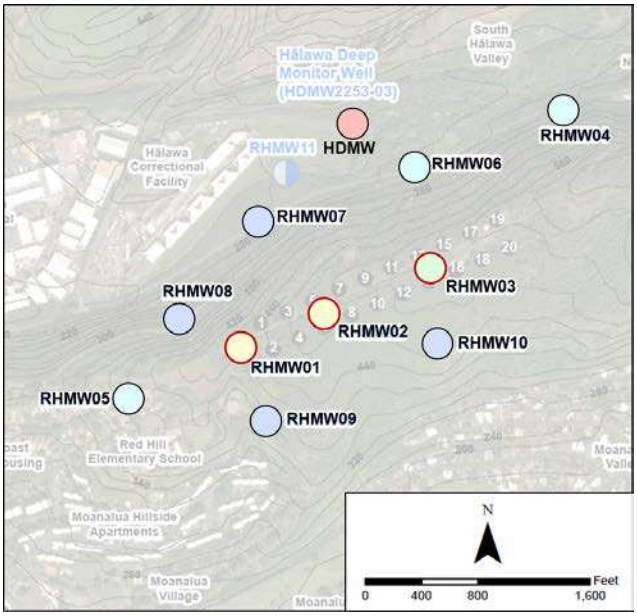

1 **Figure 4-2: Geographic Distribution of Five Monitoring Well Groups**

2 On Figure 4-1, the data box associated with each well is color-coded based on the results of network
3 clustering analysis presented in Section 4.4. Values between 0.75 and 1 are shown in red, indicating
4 the potential of petroleum impacts based on just one constituent/factor without considering its
5 consistency with other indicators/factors. Values between 0.5 and 0.75 are shown in blue. Values
6 between 0.25 and 0.5 are shown in green.

7 To evaluate the clustering structure of the multiple indicators associated with wells, network data
8 analysis was performed using the representative indicator values at the selected wells. Each well is
9 considered as a "node," and the representative indicator values at the well are treated as the attributes
10 associated with the node.

11 For comparison, sensitivity analysis was performed for the following two cases in addition to the base
12 case described above.

13 • Sensitivity Case 1: All data were included (i.e., without exclusion of first year of data at each
14 well).

15 • Sensitivity Case 2: In addition to exclusion of all data within the first year, naphthalene data
16 from Calscience/Eurofins laboratory (October 2012 to January 2015) were excluded in the
17 analysis. Generalized Wilcoxon test results show that the data from Calscience/Eurofins are
18 statistically different from the data from other laboratories (p value < 0.05).

19 ## 4.4 ANALYSIS RESULTS

20 Figure 4-3 graphically depicts clustering structure as "communities" in different colors. The results
21 indicate the following observations, by considering the representative indicators values of all
22 constituents/factors simultaneously:

- The chemical data at wells **RHMW01 and RHMW02** are relatively similar, likely due to impacts from the Facility. The TPH indicator value and other degradation indicator values are relatively high.
- The chemical data at **RHMW07, RHMW08, RHMW09, RHMW10, and Red Hill Shaft** are relatively similar. The indicator values for TPH, N, 1-MeN, and 2-MeN are low or zeroes. The indicator values for BTEX are zeroes. The indicator values for methane indicators are zeroes, and nitrate and sulfate are generally low, DO is low at RHMW09 and RHMW10, and there are no consistently high indicators at these wells.
- The chemical data at **RHMW04, RHMW05, and RHMW06** are relatively similar. The indicator values for TPH, N, 1-MeN, 2-MeN, and BTEX are low or zeroes. All methane indicators are zeroes. The indicator values for DO, nitrate, and sulfate are generally low.
- The chemical data at **RHMW03** are relatively more different from the three "communities" discussed above. The indicator values for TPH-d and TPH-o are moderate. The indicator values for TPH-g, N, 1-MeN, 2-MeN, and BTEX are low or zeroes. The indicator value for DO is high, while the indicator values for methane, nitrate, and sulfate are zeroes.
- The chemical data at **HDMW2253-03** (i.e., Hālawa Deep) are relatively different from the three "communities" discussed above. The indicator value for TPH-d is moderate. The indicator values for TPH-o, TPH-g, N, 1-MeN, 2-MeN, and BTEX are low or zeroes. However, the indicator value for DO is high, while the indicator value for nitrate is moderate. The indicator values for methane and sulfate are zero or almost zero.

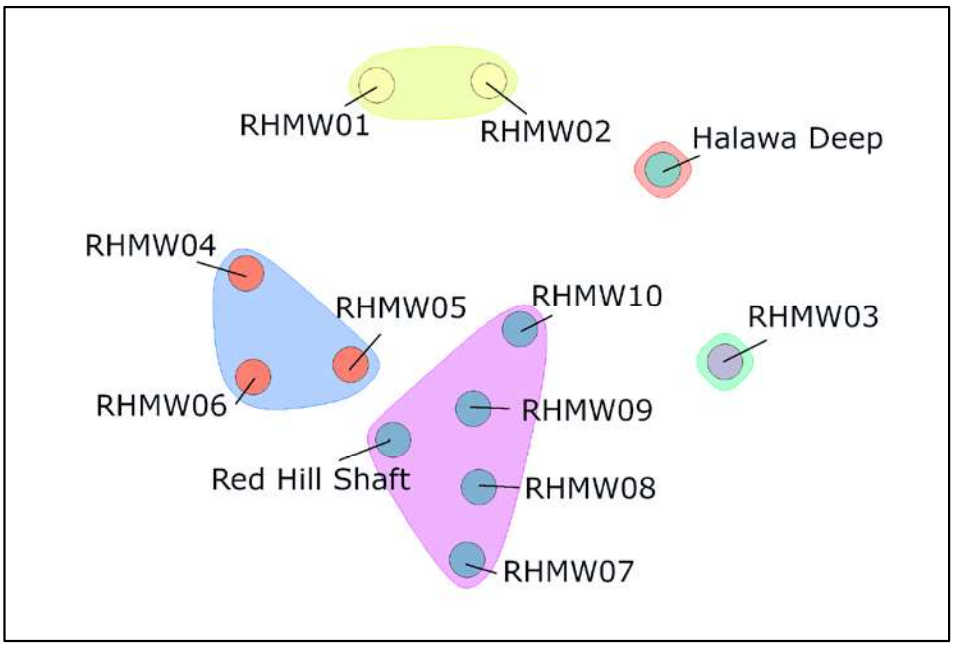

Figure 4-3: Data Clustering Structure from Network Analysis Based on Representative Indicator Values at Selected Wells (first-year data not used due to drilling artifacts)

For sensitivity comparison, Figure 4-4 depicts the clustering structure for Sensitivity Case 1 (all data included). The representative indicator values for various constituents in the selected wells are shown on Figure 4-5, indicating the impact of the first-year data in comparison to Figure 4-1. Due to the impact of the first-year data, the resulting higher TPH indicator values for RHMW07 and RHMW08

causes these two wells to be group as a separate "community." Although HDMW2253-03 is grouped into the same community as Red Hill Shaft, RHMW04, RHMW05, and RHMW06, it is farther away from them, suggesting a slightly less similarity.

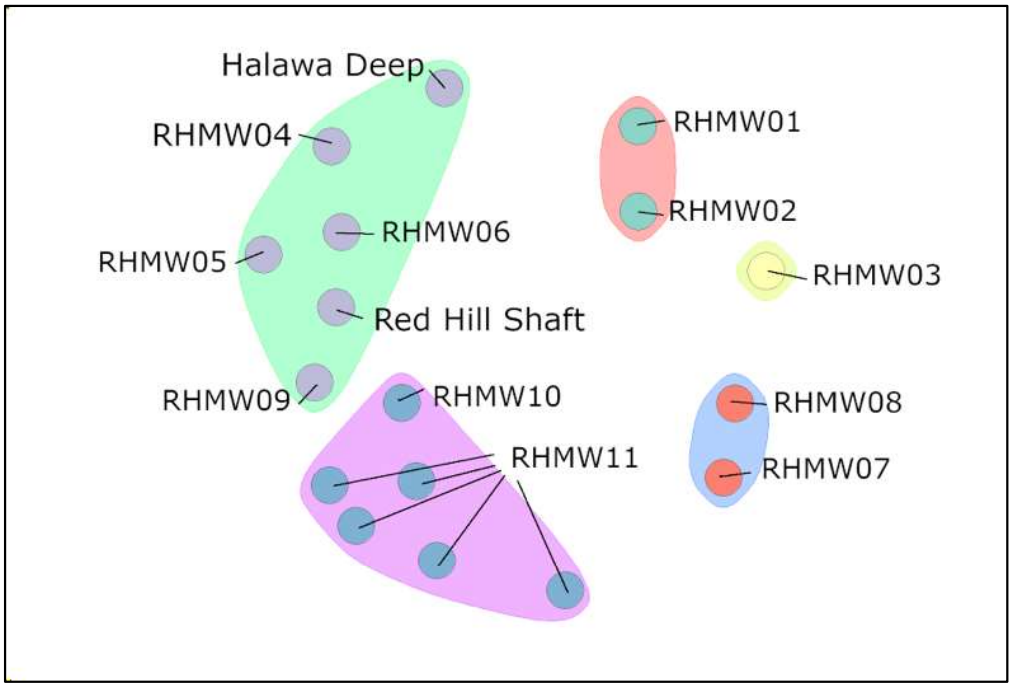

Figure 4-4: Data Clustering Structure from Network Analysis for Sensitivity Case 1 (all data)

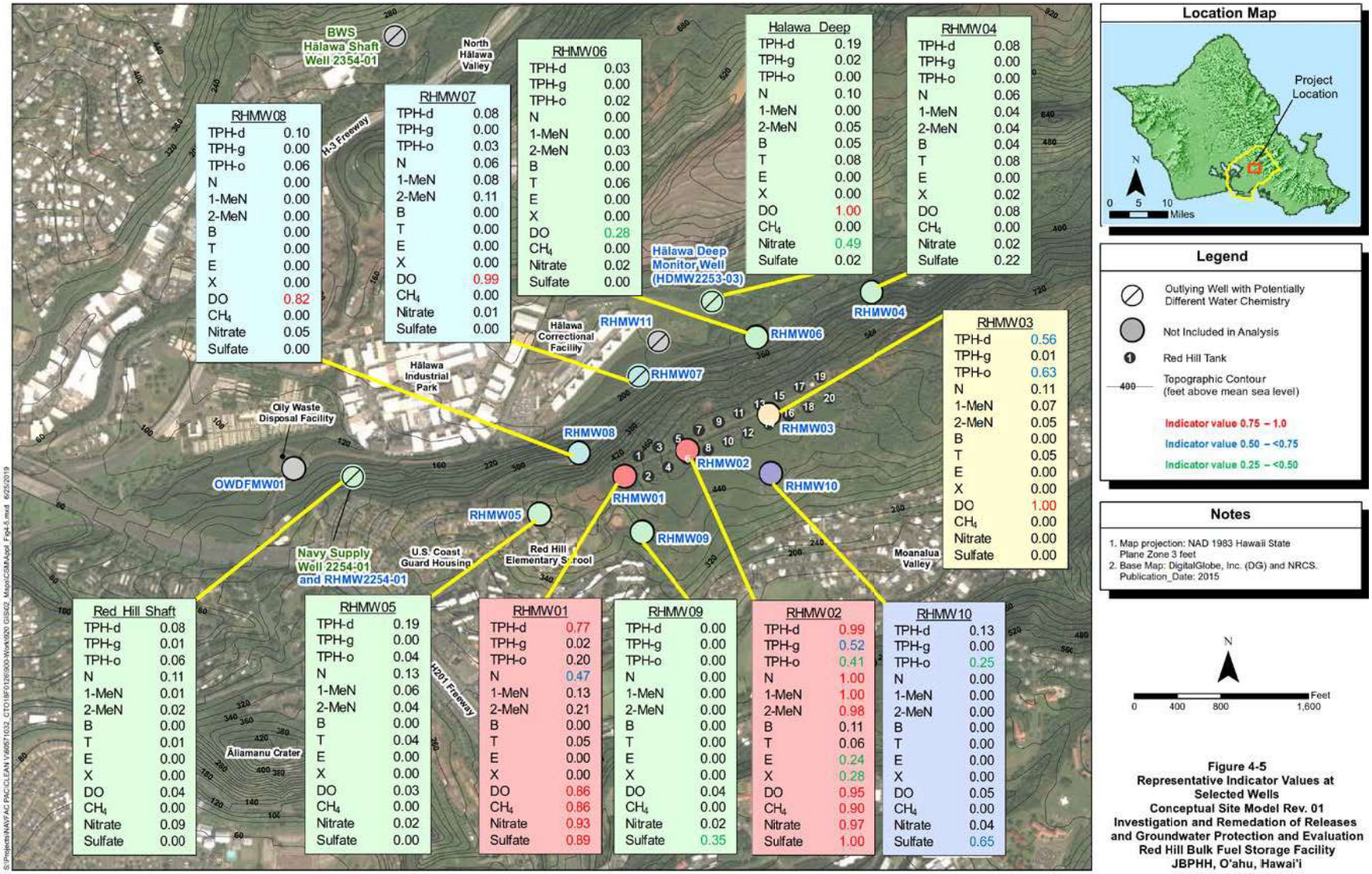

Figure 4-5
Representative Indicator Values at Selected Wells
Conceptual Site Model Rev. 01
Investigation and Remedation of Releases and Groundwater Protection and Evaluation
Red Hill Bulk Fuel Storage Facility
JBPHH, O'ahu, Hawai'i

Notes: Wells not included in analysis are: RHMW11 (only 1 year of data) and OWDFMW01 (water chemistry in this area has been impacted from past oily waste disposal operations not related to fuel releases from Red Hill). Outlying wells with potentially different water chemistry are discussed in more detail in CSM Appendix B.8 Section 1.3. Coloring of indicator boxes corresponds to cluster colors on Figure 4-4.

Figure 4-5: Representative Indicator Values at Selected Wells for Sensitivity Case 1 (all data)

Figure 4-6 depicts the clustering structure for Sensitivity Case 2. The clustering structure is the same as Figure 4-3, suggesting that the Calscience/ Eurofins data do not change the clustering structure. The representative indicator values for various constituents are shown on Figure 4-7.

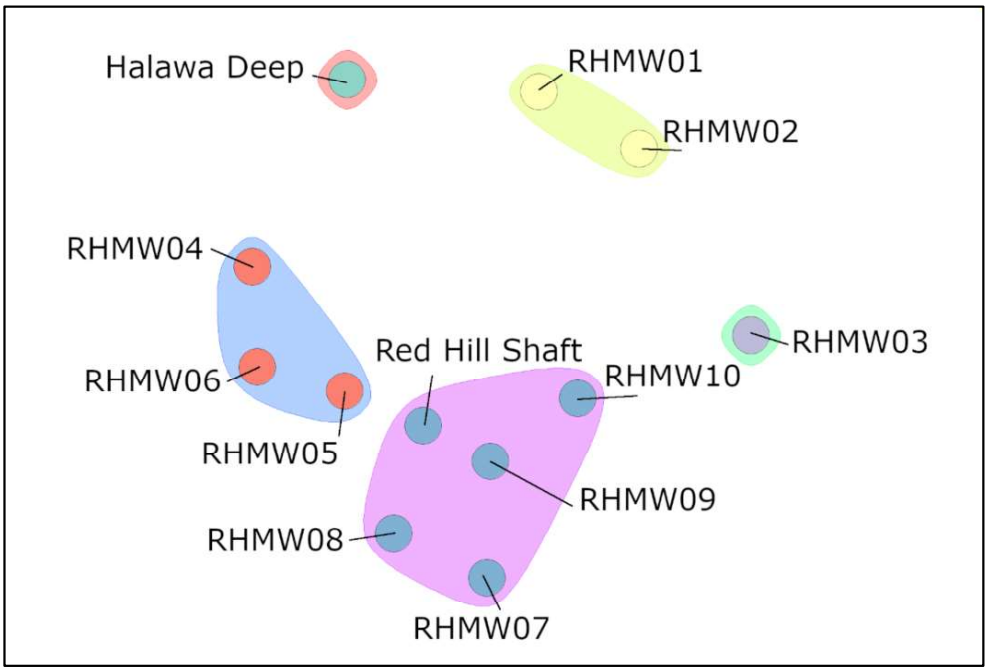

Figure 4-6: Data Clustering Structure from Network Analysis for Sensitivity Case 2 (first-year data not used due to drilling artifacts and data from Calscience/Eurofins laboratory not used)

The following structure is consistently observed in network data analysis and the sensitivity analysis based on wells as "nodes."

- RHMW01 and RHMW02 are in the same "community."
- RHMW04, RHMW05, and RHMW06 are in the same "community."

The other monitoring wells were grouped in different communities for the different scenarios.

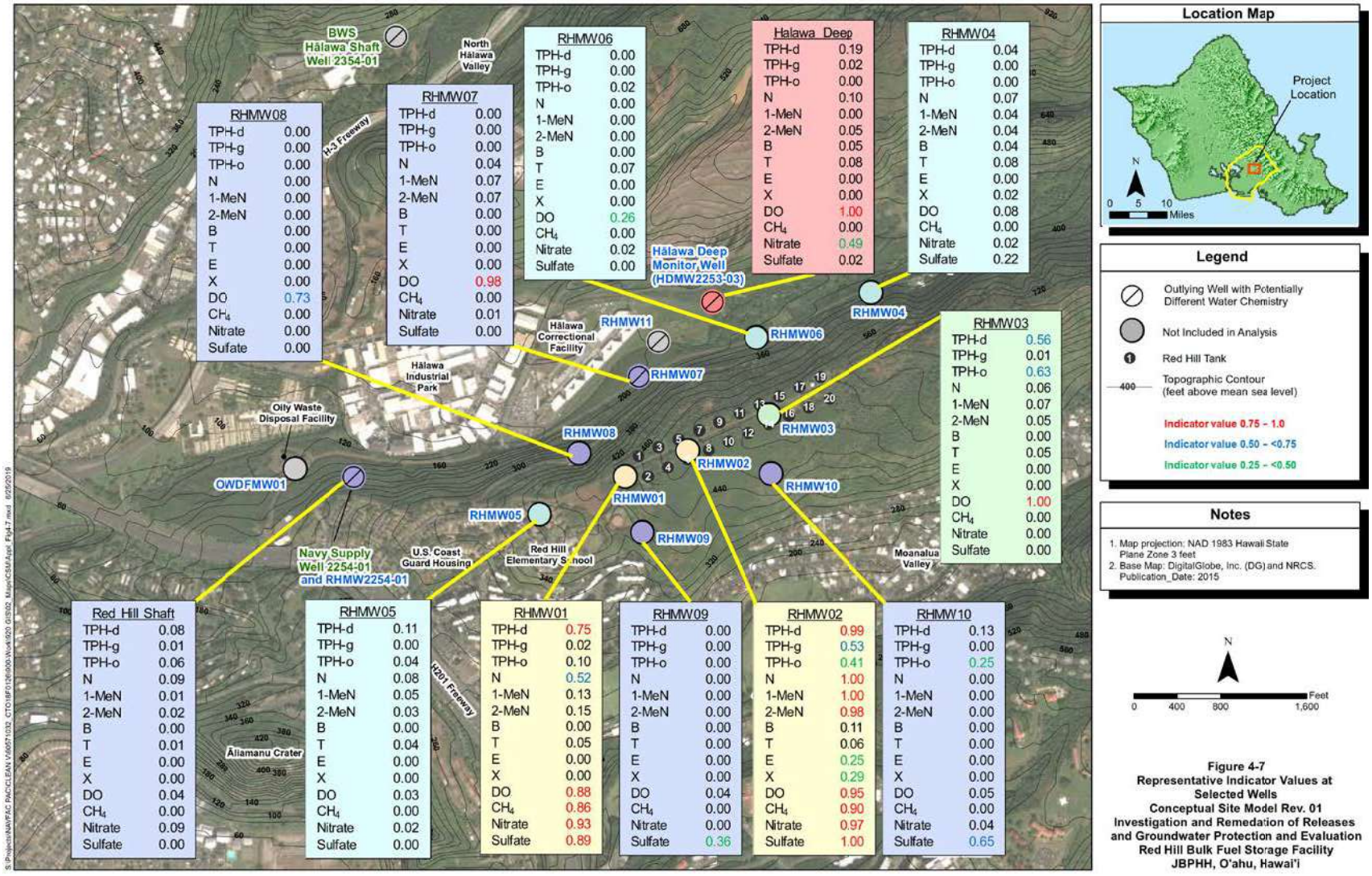

Figure 4-7
Representative Indicator Values at Selected Wells
Conceptual Site Model Rev. 01
Investigation and Remedation of Releases and Groundwater Protection and Evaluation
Red Hill Bulk Fuel Storage Facility
JBPHH, O'ahu, Hawai'i

Notes: Wells not included in analysis are: RHMW11 (only 1 year of data) and OWDFMW01 (water chemistry in this area has been impacted from past oily waste disposal operations not related to fuel releases from Red Hill). Outlying wells with potentially different water chemistry are discussed in more detail in CSM Appendix B.8 Section 1.3. Coloring of indicator boxes corresponds to cluster colors on Figure 4-6.

Figure 4-7: Representative Indicator Values at Selected Wells for Sensitivity Case 2 (first-year data not used due to drilling artifacts and data from Calscience/Eurofins laboratory not used)

5. Conclusions

A detailed analysis of DO and TPH measurements in groundwater showed:

- ***DO Measurements:*** DO concentrations in groundwater are typically less than theoretical saturation due to a variety of natural processes that consume DO from groundwater. The background groundwater entering the Facility is likely partially depleted of DO because of biodegradation of naturally occurring compounds, drilling related contamination, and geochemical reactions with the basalt/saprolite. The DO concentration from 15 upgradient, "far-field" groundwater monitoring wells selected by the USGS to be representative of shallow regional conditions in O'ahu was never found near 100% saturation, but exhibited a minimum value of 4.7 mg/L and an average value of 6.7 mg/L.
- ***TPH Measurements:*** Facility TPH-d data from the first year and likely the second year after a well is drilled should not be used to evaluate potential impacts from the Facility. In addition, TPH-d analysis with concentrations less than the EPA QL of 150 µg/L (or other commercial laboratories RLs of 100 µg/L) should be considered much less reliable than analyses at or above these QL or RLs. Consistent with the commercial laboratories' RLs, DOH (2018a) identified TPH concentrations less than 100 µg/L as potentially unreliable. If possible, the multiple factors analysis should not use the first and possibly the second year of data, or data below 150 µg/L, or the analysis should compare results when these data are and are not used in the evaluation.

A Multiple Impact Factors Analysis evaluated the similarity structures in the geochemical data from samples collected at selected wells based on their similarity characteristics. For context, Section 7.1.2.2 of the CSM main document describes the confirmed impacts of monitoring wells at the Facility this way (emphasis added):

- *"Monitoring well **RHMW02** exhibits the highest total dissolved-phase fuel constituent concentrations among the Facility monitoring wells (approximately 1–7 mg/L since 2005)."*
- *"Monitoring well **RHMW01** exhibits the next highest concentrations of dissolved-phase fuel constituents (not detected to approximately 0.1–1 mg/L since 2005)."*
- *"In monitoring well **RHMW03**, total dissolved-phase concentrations of fuel constituents are relatively low (less than 0.5 mg/L since 2005), with depressed dissolved oxygen concentrations and limited depletion of groundwater electron acceptors nitrate and sulfate, and no measurable methane production."*

At all outlying monitoring wells, impact indicators for TPH, N, 1-MeN, 2-MeN, and BTEX **are low or zero**, and impact indicator values for DO, nitrate, and sulfate **are generally low and methane is zero**. The multifactor network analysis introduced in Section 1.2 did not group any of the outlying Facility monitoring wells with the three impacted wells above, but rather separated the outlying wells into two or three other distinct groups (Figure 4-3, Figure 4-4, and Figure 4-5). All these groups were separate from the three impacted wells.

In conclusion:

- None of the outlying monitoring wells was similar to RHMW02, the well with highest dissolved fuel concentrations.

- None of the outlying monitoring wells was similar to RHMW01, the well with next-highest dissolved fuel concentrations.
- None of the outlying monitoring wells was similar to RHMW03, the well with relatively low dissolved fuel concentrations and limited depletion of electron acceptors.

Because no outlying wells were similar even to RHMW03 (the Facility well with relatively low dissolved fuel contamination), this analysis supports the conclusion that none of the outlying wells were impacted by fuel releases from the Facility.

6. References

California Environmental Protection Agency (CalEPA). 1995. *Drilling, Coring, Sampling and Logging at Hazardous Substance Release Sites*. Guidance Manual for Ground Water Investigations.

CH2M Hill Engineers, Inc. (CH2M Hill). 2016. *Conceptual Site Model, Central Maui Landfill, Puunene, Hawaii*. Prepared for The County of Maui Department of Environmental Management, Solid Waste Division. February.

California Water Quality Control Board (CWQCB). 2012. *Leaking Underground Fuel Tank Guidance Manual*. September.

Department of Defense, Environmental Data Quality Workgroup (DoD EDQW). 2017. *Fact Sheet: Detection and Quantification – What Project Managers and Data Users Need to Know*. October. https://www.denix.osd.mil/edqw/documents/documents/revised-detection-and-quantitation-fact-sheet-october-2017/.

Department of Health, State of Hawaii (DOH). 2018a. *Collection and Use of Total Petroleum Hydrocarbon Data for the Risk-Based Evaluation of Petroleum Releases: Example Case Studies*. R. Brewer, M. Nagaiah, and R. Keller, Authors. Honolulu, HI: Hazard Evaluation and Emergency Response Office. March.

———. 2018b. *Technical Guidance Manual for the Implementation of the Hawaii State Contingency Plan*. Interim Final. Honolulu, HI: Hazard Evaluation and Emergency Response Office. April.

Hunt Jr., C. D. 2004. "Ground-Water Quality and Its Relation to Land Use on Oahu, Hawaii, 2000-01." Report 2003–4305. Water-Resources Investigations Report. USGS Publications Warehouse. https://doi.org/10.3133/wri20034305.

Interstate Technology & Regulatory Council (ITRC). 2018. *TPH Risk Evaluation at Petroleum-Contaminated Sites*. TPHRisk-1. Washington, DC: ITRC, TPH Risk Evaluation Team. https://tphrisk-1.itrcweb.org.

Kostecki, P. T., and E. J. Calabrese, eds. 1991. *Hydrocarbon Contaminated Soils and Groundwater: Analysis, Fate, Environmental & Public Health Effects, & Remediation, Volume I*. 1st ed. Chelsea, MI: Lewis Publishers, Inc.

Lane, D. L., T. E. Jones, and M. H. West. 1984. "Preliminary Assessment of Oxygen Consumption and Redox Conditions in a Nuclear Waste Repository in Basalt." In *Geochemical Behavior of Disposed Radioactive Waste*, edited by G. S. Barney, J. D. Navratil, and W. W. Schulz, 181–195. ACS Symposium Series Vol. 246. Washington, DC: ACS.

McMahon, P. B., and F. H. Chapelle. 2008. "Redox Processes and Water Quality of Selected Principal Aquifer Systems." *Ground Water* 46 (2): 259–271.

National Driller. 2007. "Reverse-Air Rotary for Monitoring Wells." June 1, 2007. https://www.nationaldriller.com/articles/87151-reverse-air-rotary-for-monitoring-wells.

Newman, M.E.J. 2006. "Modularity and Community Structure in Networks." *Proceedings of the National Academy of Sciences* 103 (23): 8577–82. https://doi.org/10.1073/pnas.0601602103.

New Mexico Environment Department (NMED). 2013. *Stipulated Final Order, Transwestern Pipeline Company, L.L.C., Roswell Compressor Station*. March.

Rose, S., and A. Long. 1988. "Monitoring Dissolved Oxygen in Ground Water: Some Basic Considerations." *Groundwater Monitoring & Remediation* 8 (1): 93–97. https://doi.org/10.1111/j.1745-6592.1988.tb00981.x.

Rupert, M. G., C. D. Hunt Jr., K. D. Skinner, L. M. Frans, and B. J. Mahler. 2015. "The Quality of Our Nation's Waters: Groundwater Quality in the Columbia Plateau and Snake River Plain Basin-Fill and Basaltic-Rock Aquifers and the Hawaiian Volcanic-Rock Aquifers, Washington, Idaho, and Hawaii, 1993–2005." Report 1359. Circular. Reston, VA. https://doi.org/10.3133/cir1359.

Sawlan, M. G. 2018. "Alteration, Mass Analysis, and Magmatic Compositions of the Sentinel Bluffs Member, Columbia River Flood Basalt Province." *Geosphere* 14 (1): 286–303. https://doi.org/10.1130/GES01188.1.

State of South Dakota, Department of Environment & Natural Resources (SD DENR). 2003. *Drilling and Monitoring Well Installation at Hazardous Waste Sites in South Dakota*. SOP 2150. Version 2.0. March 18.

San Francisco Regional Water Quality Control Board (SFRWQCB). 2019. *User's Guide: Derivation and Application of Environmental Screening Levels (ESLs)*. Interim Final. https://www.waterboards.ca.gov/sanfranciscobay/water_issues/programs/esl.html.

Steinkampf, W.C., and P.P. Hearn Jr. 1996. "Ground-Water Geochemistry of the Columbia Plateau Aquifer System, Washington, Oregon, and Idaho." Open-File Report 95-467. U.S. Geological Survey. https://doi.org/10.3133/ofr95467.

Wiedemeier, T. H., H. S. Rifai, C. J. Newell, and J. T. Wilson. 1999. *Natural Attenuation of Fuels and Chlorinated Solvents in the Subsurface*. New York: John Wiley & Sons, Inc.

Attachment I-1
Analytical Results of Drilling "Make-Up" Water Samples

Table I-1: Analytical Results of Drilling "Make-Up" Water Samples

Well ID	Sample Date	Sampling Point	TPH-g µg/L	TPH-d µg/L	TPH-d SGC µg/L	TPH-o µg/L	TPH-o SGC µg/L	Benzene µg/L	Toluene µg/L	Ethylbenzene µg/L	Xylenes, Total µg/L	1-MeN µg/L	2-MeN µg/L	N µg/L
RHMW08	9/7/2016	Rig Outfall	< 18 U	**170 J**	—	**520 J**	—	< 0.30 U	< 0.30 U	< 0.50 U	< 0.30 U	< 0.10 U	< 0.10 U	< 0.10 U
RHMW08	9/29/2016	Rig Outfall	< 18 U	**85 J**	—	**160 J**	—	< 0.30 U	< 0.30 U	< 0.50 U	< 0.30 U	< 0.10 U	< 0.10 U	< 0.10 U
RHMW09	7/20/2016	Rig Outfall	< 18 U	**79**	—	**150**	—	< 0.30 U	< 0.30 U	< 0.50 U	< 0.30 U	< 0.10 U	< 0.10 U	< 0.10 U
RHMW09	7/26/2016	Water Truck Output	< 18 U	< 25 U	—	< 40 U	—	< 0.30 U	**0.24 J**	< 0.50 U	0.70 J	< 0.10 U	< 0.10 U	< 0.10 U
RHMW09	8/12/2019	Rig Outfall	< 15 U	< 25 U	—	**49**	—	< 0.30 U	< 0.30 U	< 0.50 U	< 0.30 U	< 0.10 U	< 0.10 U	< 0.10 U
RHMW09	1/6/1900	Municipal Hydrant	< 15 U	< 25 U	—	< 40 U	—	< 0.30 U	< 0.30 U	< 0.50 U	< 0.30 U	< 0.10 U	< 0.10 U	< 0.10 U
RHMW09	8/18/2016	Rig Outfall	< 15 U	**140 J**	—	**220 J**	—	< 0.30 U	< 0.30 U	< 0.50 U	< 0.30 U	< 0.10 U	< 0.10 U	< 0.10 U
RHMW09	8/22/2016	Water Truck Output	—	< 25 U	—	< 40 U	—	—	—	—	—	< 0.10 U	< 0.10 U	< 0.10 U
RHMW09	8/22/2016	Water Hose	—	< 25 U	—	< 40 U	—	—	—	—	—	< 0.10 U	< 0.10 U	< 0.10 U
RHMW09	8/22/2016	Rig Outfall	< 15 U	< 25 U	—	< 40 U	—	< 0.30 U	< 0.30 U	< 0.50 U	< 0.25 U	< 0.10 U	< 0.10 U	< 0.10 U
RHMW10	3/7/2017	Rig Outfall	< 18 U	**60**	—	**47**	—	< 0.30 U	< 0.30 U	< 0.50 U	< 0.30 U	< 0.10 U	< 0.10 U	< 0.10 U
RHMW10	3/28/2017	Rig Outfall	< 18 U	**180**	—	**480**	—	< 0.30 U	< 0.30 U	< 0.50 U	< 0.30 U	< 0.10 U	< 0.10 U	< 0.10 U
RHMW11	10/3/2017	Rig Outfall	< 18 U	< 25 UJ	—	< 40 UJ	—	< 0.30 U	< 0.30 U	< 0.50 U	< 0.30 U	< 0.10 U	< 0.10 U	< 0.10 U
RHMW14	1/11/2019	Municipal Hydrant	< 18 U	< 25 U	—	< 40 U	—	< 0.30 U	< 0.30 U	< 0.50 U	< 0.30 U	< 0.10 U	< 0.10 U	< 0.10 U
RHMW14	1/11/2019	Water Truck Output (pre-GAC)	< 18 U	< 25 U	—	< 40 U	—	< 0.30 U	< 0.30 U	< 0.50 U	< 0.30 U	< 0.10 U	< 0.10 U	< 0.10 U
RHMW14	1/11/2019	Rig Outfall (post-GAC)	< 18 U	**1,000**	< 25 U	**220**	< 40 U	< 0.30 U	< 0.30 U	< 0.50 U	< 0.38 U	< 0.10 U	< 0.10 U	< 0.10 U
RHMW14	1/22/2019	Water Hose (post-GAC)	< 18 U	**390**	< 25 U	**490**	< 40 U	< 0.30 U	< 0.30 UJ	< 0.50 U	< 0.30 U	< 0.10 U	< 0.10 U	< 0.10 U
RHMW14	1/22/2019	Rig Outfall (post-GAC)	< 18 U	**340**	< 25 U	**280**	< 40 U	< 0.30 U	< 0.30 UJ	< 0.50 U	< 0.30 U	< 0.10 U	< 0.10 U	< 0.10 U
RHMW14	2/18/2019	Water Hose (post-GAC)	< 18 U	< 25 U	—	< 40 U	—	< 0.30 U	< 0.30 U	< 0.50 U	< 0.30 U	< 0.10 U	< 0.10 U	< 0.10 U
RHMW14	2/18/2019	Rig Outfall (post-GAC)	< 18 UJ	< 25 U	—	< 40 U	—	< 0.30 UJ	< 0.30 UJ	< 0.50 UJ	< 0.30 UJ	< 0.10 U	< 0.10 U	< 0.10 U
RHMW15	12/1/2017	Rig Outfall	< 18 U	< 25 U	—	< 40 U	—	< 0.30 U	< 0.30 U	< 0.50 U	< 0.30 U	< 0.10 U	< 0.10 U	< 0.10 U
RHTB01	3/7/2019	Rig Outfall (post-GAC)	< 18 UJ	< 25 U	—	< 40 U	—	< 0.30 U	< 0.30 U	< 0.50 U	< 0.30 U	< 0.10 U	< 0.10 U	< 0.10 U

Notes:
Bold detected value
U The compound was analyzed for but not detected above the stated limit.
J estimated value
µg/L micrograms per liter
1-MeN 1-methylnaphthalene
2-MeN 2-methylnaphthalene
GAC granular activated carbon
N naphthalene
SGC silica gel cleanup
TPH-d total petroleum hydrocarbons – diesel range organics
TPH-g total petroleum hydrocarbons – gasoline range organics
TPH-o total petroleum hydrocarbons – residual range organics (i.e., TPH-oil)

Appendix J:
Regulatory Comments and Navy Responses

This page intentionally left blank

UNITED STATES ENVIRONMENTAL PROTECTION AGENCY
REGION IX
75 Hawthorne Street
San Francisco, CA 94105

STATE OF HAWAII
DEPARTMENT OF HEALTH
P. O. BOX 3378
HONOLULU, HI 96801-3378

OCT 29 2018

Captain Marc Delao
Regional Engineer
Navy Region Hawaii
850 Ticonderoga St. STE 110
Joint Base Pearl Harbor Hickam, Hawaii 96860

Re: Approval to revise schedule for deliverables 6.3- Investigation and Remediation of Releases Report and 7.1.3. - Groundwater Flow Model Report of the Red Hill Administrative Order on Consent ("AOC") Statement of Work ("SOW") and Comments on Interim Environmental Reports

Dear Captain Delao:

The U.S. Environmental Protection Agency ("EPA") and Hawaii Department of Health ("DOH"), collectively the "Regulatory Agencies", have received the U.S. Department of Navy's ("Navy's") letter dated October 12, 2018, and approve the Navy's request for a ten-month extension to the Red Hill AOC SOW (the "AOC") Sections 6.3 and 7.1.3 for the purpose of improving the quality of those deliverables. The Regulatory Agencies fully expect the Navy to utilize this extension to correct the deficiencies in the conceptual site model ("CSM") and groundwater flow model ("GFM") outlined in this letter and explained more fully in the enclosures. The CSM, GFM and other environmental work under the AOC was designed to inform ongoing and future planning decisions, and may be particularly relevant to those decisions related to AOC section 3 – Tank Upgrade Alternatives ("TUA"). The TUA Decision Document pursuant to section 3, is due to be submitted later this year. To the extent that the TUA Decision Document relies upon conclusions drawn from the substance of any of the environmental work being performed pursuant to other sections of the AOC, the quality of the TUA decision will necessarily depend on the quality of the underlying environmental work, or lack thereof, used to support that decision.

The Regulatory Agencies reviewed the *Groundwater Protection and Evaluation Considerations for the Red Hill Bulk Fuel Storage Facility* (dated July 27, 2018) and *Conceptual Site Model, Investigation and Remediation of Releases and Groundwater Protection and Evaluation, Red Hill Bulk Fuel Storage Facility* (dated July 27, 2018) developed by the Navy and its contractors. These interim documents detail the Navy's comprehensive understanding of the conceptual site

model representing the Red Hill Bulk Fuel Storage Facility ("Facility") and the surrounding environment, as well as a preliminary model of local and regional groundwater flow.

The Regulatory Agencies continue to believe that some of the interpretations and determinations made in the interim documents are premature or inappropriate after reviewing the supporting data and conducting independent analyses. During in-person meetings of August 14- 16, 2018, the Regulatory Agencies' consultants gave a presentation on issues of concern related to the interim information that had been made available at that time. We also acknowledge that the Navy has collected and compiled significant quality data for this effort, and the Navy's efforts continue to improve in this regard.

As summarized below, the Navy should use this extension to address several key aspects of the ongoing environmental investigation and interpretation work. Supporting materials developed by the Regulatory Agencies' consultants and subject matter experts are provided in the enclosure attached to this letter. As expanded upon more fully in the enclosures, the ten issues of greatest concern can be generally described as relating to the CSM, GFM and Fate and Transport.

Concerns with the Interim CSM

The CSM should explain all observed data in the field to the extent possible and data that are not incorporated into the model, even if qualified, should be thoughtfully considered. Conceptual and numerical models that best fit available data are critical for technical defensibility of the application of the model to evaluate flow paths and contaminant fate. In particular, the Regulatory Agencies continue to have concerns with the following aspects of the CSM:

1) Predominant strike and dip of basalt in the geologic model- The direction and magnitude as represented by the Navy thus far do not agree with the lava flow geometry independently evaluated by the Regulatory Agencies and provided to the Navy. This information is important because it will influence Navy's conclusions regarding groundwater flow paths and transport.

2) Saprolite extent in the interim model vs. depths inferred by seismic profiling- The extent of the modeled saprolite/basalt interface depths do not agree with the seismic profiling. In particular, the seismic profiling indicates that the saprolite layer depth in the upper reaches of the Halawa Valleys constitutes a much less protective barrier to northwest groundwater flow than the GFM indicates. This directly impacts the evaluation of risk to the Halawa Shaft.

3) Preferential pathways- The consideration and methods of incorporation of preferential pathways in both the CSM and the groundwater model are unclear. Although it is impracticable to precisely characterize these features, the influence that geologic structures, such as voids, fractures, lava tubes, and the permeable interface between lava flows, have on contaminant and groundwater transport should be explained conceptually in the CSM. The influence of these structures should also be incorporated into the GFM using appropriate and traceable mathematical representations. This directly impacts the Navy's ability to evaluate contaminant transport in the vadose zone and in the groundwater.

Concerns with the interim GFM

Outputs from the GFM do not comport with measured groundwater gradients in terms of their magnitude, direction, and variability. Several lines of evidence – including measured water

levels, organic and inorganic water quality sampling results – suggest occasional gradients, groundwater flow and contaminant migration toward the northwest from tanks located further up the ridge at the Facility. The Navy should address the following aspects of the GFM:

4) Representation of caprock, tuffs and sediments- These features are present in the Navy's narrative of the CSM but are not all incorporated within the interim GFM in a manner consistent with the CSM. Additional evaluation of how these features may affect gradients, groundwater flows, and transport, should be completed.

5) Drinking water shaft inflows- The GFM does not reproduce the documented distribution of inflows into the Red Hill drinking water shaft and tunnel system. Giving further consideration to conditions observed in Red Hill shaft may improve overall model calibration and reliability in the vicinity and downgradient of the facility.

6) Calibration to groundwater heads and gradients- The GFM does not closely reproduce measured heads and gradients. The final model should prioritize use of the best available groundwater level data reflecting the range of hydraulic gradients under reasonable pumping and non-pumping conditions.

7) Coastal marine boundary and discharge- The coastal discharge rates and patterns in the final GFM should be discussed with the groundwater modeling subject matter experts, as the over-determination of this boundary condition may reduce model sensitivity to other parameter changes.

Concerns with interim work related to Fate and Transport

The *Contaminant Fate and Transport Model Report* required by Red Hill AOC Statement of Work is not due until 180 days after the approval of the *GFM Report* and the *Investigation and Remediation of Releases Report*. Therefore, a *Contaminant Fate and Transport Report* is not anticipated to be completed until the middle of 2020 after our approval of this extension request. As a result, we are providing comments for your consideration in the CSM development and the Navy's longer-term development of the *Contaminant Fate and Transport Model Report*. In the short term, we expect conservative contaminant fate and transport considerations to be discussed as a component of the Navy's upcoming tank upgrade proposal at Red Hill.

The Navy's current CSM and statistical Non-Aqueous Phase Liquid ("NAPL") holding model do not adequately address potential impacts to groundwater from fuel releases, account for Light Non-Aqueous Phase Liquid ("LNAPL") migration processes, or explain lines of evidence for historical transport observed in the field. Although local characterization data indicates that substantial natural attenuation of hydrocarbons may be occurring, field characterization of the subsurface is highly challenging and impractical in some areas near and around the tanks at the Facility. Therefore, conservative assumptions bounding NAPL fate and transport or robust, dynamic fate and transport models are critical for long term environmental stewardship. The Navy should address the following issues:

8) Light Non-Aqueous Phase Liquid ("LNAPL") fate and transport- The CSM for LNAPL transport needs to more broadly consider potential rates, directions and distances of LNAPL transport and the primary features and processes affecting that potential transport. The Navy should present the Regulatory Agencies with an approach for developing modeling of

LNAPL fate and transport in this environmental setting. The final model should consider potential rates and directions of transport as a function of different types of releases, provide source terms to determine if releases can be captured through pumping, model cumulative effects of releases over time, and utilize incoming field results and new information to calibrate model outputs to observed conditions.

9) Groundwater data- Interpretations of groundwater data from before and following the time of the 2014 release do not adequately consider limited data density and the range of plausible interpretations, including the probability of northerly contaminant transport. Additionally, general water quality indicators including nitrate and dissolved oxygen should be closely examined as lines of evidence for transport and attenuation of past releases.

10) LNAPL and dissolved-phase distribution - The CSM presumes a specific distribution of LNAPL as an outcome of the 2014 release (and prior historical releases), without sufficient data to support this presumption (i.e., the Regulatory Agencies do not view the thermal profile interpretation as definitive). Vapor monitoring data from the time immediately following the release, as well as other historical data suggests other distributions may be possible. Based on the data that are currently available, the Regulatory Agencies believe that a range of possible LNAPL distributions is plausible and the Navy should more closely examine the data and consider the plausible range of migration pathways and timeframes.

Recommended Schedule for Navy's Extension

The Regulatory Agencies recommend the following schedule to address the issues detailed above. We anticipate that the Navy may want to provide additional opportunities for focused technical discussion remotely or in person, as needed. The Navy should also consider appropriate avenues and times for engaging external Subject Matter Experts.

Recommended Schedule for Navy Extension	
Date	**Task**
November 2018	Kickoff Meeting with Agencies
November – March 2019	Data Evaluation, CSM Updates and GFM, Fate and Transport (F&T) Updates
April 2019	Review with Regulatory Agencies and Subject Matter Experts, Updates to the CSM, Interim GFM, and F&T
May – June 2019	Continue GFM Updates and Predictive Simulations
July 2019	Presentation of Draft Deliverable to Subject Matter Experts
October 2019	Final Section 6.3 and 7.1.3 Deliverable Submittals

Response Requested

The Regulatory Agencies concur with the Navy that the deliverables required per Section 6.3 and 7.1 of the Red Hill AOC SOW shall be submitted to us no later than October 5, 2019. The Regulatory Agencies require that the Navy respond to this letter via letter or email by November 16, 2018 with a proposed schedule over the course of the extension and to confirm receipt of this extension approval. The Navy's schedule should include dates where it expects to seek agreement with the Regulatory Agencies on key issues prior to submitting the final deliverables.

Accounting for NAPL effects on groundwater and drinking water resources is important for the upcoming tank upgrade proposal and we would like to engage the Navy and its consultants in further discussion to resolve outstanding issues regarding NAPL fate and transport. The Regulatory Agencies also encourage the Navy to concurrently continue its efforts to install more groundwater monitoring wells to further improve its modeling efforts. We look forward to your response to this letter and the upcoming environmental work required as part of the AOC. Please let us know if you have any comments or concerns with the information in this letter.

Sincerely,

Omer Shalev
Project Coordinator
EPA Region 9 Land Division

Roxanne Kwan
Interim Project Coordinator
DOH Solid and Hazardous Waste Branch

Enclosures: Attachment 1- Navy letter to EPA Region 9 and DOH dated October 12, 2018
Attachment 2- Conceptual Site Model Topics
Attachment 3- Interim GFM
Attachment 4- Interim Fate and Transport Analyses
Attachment 5- Presentation Slideshow from August 2018

cc: Mr. Mark Manfredi, Navy (via email)
Mr. Aaron Poentis, Navy (via email)
Mr. Cory Waki, Navy (via email)

ATTACHMENTS

- Attachment 1 – Navy letter to EPA Region 9 and DOH dated October 12, 2018

- Attachment 2 – Conceptual Site Model Topics
    - 1. Basalt Strike and Dip
    - 2. Saprolite Extents
    - 3. Preferential pathways
    - Attachment 2 - Appendix

- Attachment 3 – Interim Groundwater Flow Model
    - 4. Caprock, tuffs, sediments
    - 5. Calibration - Red Hill tunnel inflows
    - 6. Calibration - heads and gradients
    - 7. Coastal submarine boundary

- Attachment 4 – Interim Fate and Transport Analyses
    - 8. Light Non-Aqueous Phase Liquid (LNAPL) Fate and Transport
    - 9. Groundwater Data
    - 10. LNAPL and Dissolved-Phase Plume Distribution

- Attachment 5 – Presentation Slideshow from August, 2018

ATTACHMENT 1

Navy Letter to EPA Region 9 and
DOH dated October 12, 2018

DEPARTMENT OF THE NAVY
COMMANDER
NAVY REGION HAWAII
850 TICONDEROGA ST STE 110
JBPHH, HAWAII 96860-5101

OCT 17 2018

5750
Ser N4/0627
12 OCT 2018

CERTIFIED NO: 7016 0910 0001 0891 9547

Mr. Omer Shalev
U.S. Environmental Protection Agency, Region IX
75 Hawthorne Street
San Francisco, CA 94105

CERTIFIED NO: 7016 0910 0001 0891 9554

Ms. Roxanne Kwan
State of Hawaii Department of Health
Solid and Hazardous Waste Branch
2827 Waimano Home Road
Pearl City, HI 96782

Dear Mr. Shalev and Ms. Kwan:

SUBJECT: REQUEST TO REVISE THE SCHEDULE FOR THE ADMINISTRATIVE ORDER ON CONSENT ("AOC") STATEMENT OF WORK ("SOW") SECTION 6.3 DELIVERABLE, INVESTIGATION AND REMEDIATION OF RELEASES REPORT, AND SECTION 7.1.3 DELIVERABLE, GROUNDWATER FLOW MODEL REPORT, RED HILL BULK FUEL STORAGE FACILITY ("FACILITY"), JOINT BASE PEARL HARBOR-HICKAM, OAHU, HAWAII

Thank you for the expedited review of the Conceptual Site Model and Groundwater Protection and Evaluation Considerations Reports submitted on July 27, 2018. These documents contain the results of the Navy/DLA's interim environmental analysis and present an initial framework and evaluation of potential environmental risks in preparation for the Investigation and Remediation of Releases Report and the Groundwater Flow Model Report currently due to the Regulatory Agencies by December 5, 2018.

The Navy/DLA greatly appreciate the technical comments and recommendations provided by your technical experts during meetings held the week of August 13, 2018 regarding the Navy/ DLA's interim environmental analysis and the upcoming Investigation and Remediation of Releases and Groundwater Flow Model Reports. Your technical comments and recommendations are integral in the development and eventual acceptance of these AOC SOW Section 6 and Section 7 deliverables with the primary goal of developing technically defensible tools to make more informed decisions regarding risk management and protection of drinking water.

As discussed during a teleconference held on September 14, 2018, time and effort are required to sufficiently address and incorporate the Regulatory Agencies' comments and recommendations into the upcoming Investigation and Remediation of Releases and

Groundwater Flow Model Reports. There are substantial changes required for the conceptual site model, groundwater flow model, and the evaluation of potential remedial alternatives. As developed, the current AOC SOW Section 6 and Section 7 schedule does not allot for time to address and incorporate the Regulatory Agencies' comments and recommendations; and additionally, does not allow for timely solicitation of technical feedback from stakeholders on those substantial changes which is critical to the development of AOC deliverables. Within the current schedule, the Navy/DLA have performed a significant amount of effort as outlined in our letter dated March 9, 2018 and showcased in our interim environmental analysis, such as the completion of an interim groundwater flow model ahead of the current December 5, 2018 submittal date in order to provide an advanced review of modeling process, development, and assumptions.

As such, the Navy/DLA respectfully request to revise the schedule for the AOC SOW Section 6.3 deliverable, Investigation and Remediation of Releases Report, and the AOC SOW Section 7.1.3 deliverable, the Groundwater Flow Model Report, to be submitted by October 5, 2019. This request assumes approval is received by October 31, 2018 which will allow for proper technical alignment on key issues. The revised schedule is required to complete the necessary updates to the conceptual site model, groundwater flow model, and hypothetical release scenarios for a more comprehensive evaluation of potential remedial alternatives. This revised schedule, however, does not consider time and effort for numerical light non-aqueous phase liquid (LNAPL) modeling based on previous agreements among the AOC Parties. During AOC SOW Section 6 and Section 7 Scoping Meetings and technical meetings held thereafter, it was agreed upon that potential LNAPL impacts would instead be reasonably bound utilizing conservative assumptions for all hypothetical future release scenarios. We look forward to continuing the evaluation of potential LNAPL impacts with the Regulatory Agencies.

The Navy/DLA appreciate the consideration of this request to revise the schedule for the Investigation and Remediation of Releases and the Groundwater Flow Model Reports. We are eager to continue the close technical engagement and dialogue with the Regulatory Agencies and stakeholders to develop technically defensible tools to make more informed decisions on risk management and protection of drinking water. If you have any questions, please contact Aaron Y. Poentis of our Regional Environmental Department at (808) 471-3858 or at aaron.poentis@navy.mil.

Sincerely,

M. R. DELAO
Captain, CEC, U.S. Navy
Regional Engineer
By direction of the
Commander

ATTACHMENT 2

Conceptual Site Model Topics

Item 1. Basalt Strike and Dip

The geometry of lava flows affects the transport of LNAPL, groundwater, and dissolved contaminants. This is particularly true for vadose zone transport of LNAPL. Characterizing the geometry of lava flows – in particular, the predominant strike and dip values and variations about these predominant values – is critical to assessing the risk the Red Hill facility poses to potential groundwater receptors.

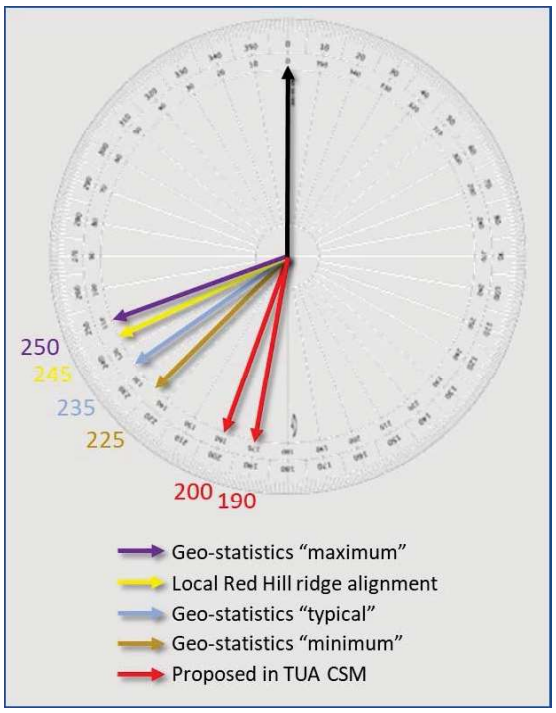

Figure 1.1 Estimated Dip Directions in and Around Red Hill

The values for the strike and dip of the lava flows reported by consultants to the Navy (CSM Report, page 5-2: "*True dip in the vicinity of Red Hill has been measured at angles of 10–12 degrees, with a strike of 190–205 degrees*") differ from values that were obtained independently by the regulator SMEs via field observation and measurement and geostatistical analysis of barrel log data, which consistently exhibit lower dip values of about 5 degrees and more westerly strike values (Inset Figure 1.1). Although these differences may appear subltle, they are consequential for groundwater flow and potential contaminant transport paths. This is illustrated in Inset Figure 1.2, which presents pathlines calculated using the interim groundwater model, with values for the direction of anisotropy that differ by 10 degrees (particles depicted in red were computed with a more westerly direction of anisotropy reflecting a more westerly assumed dip direction).

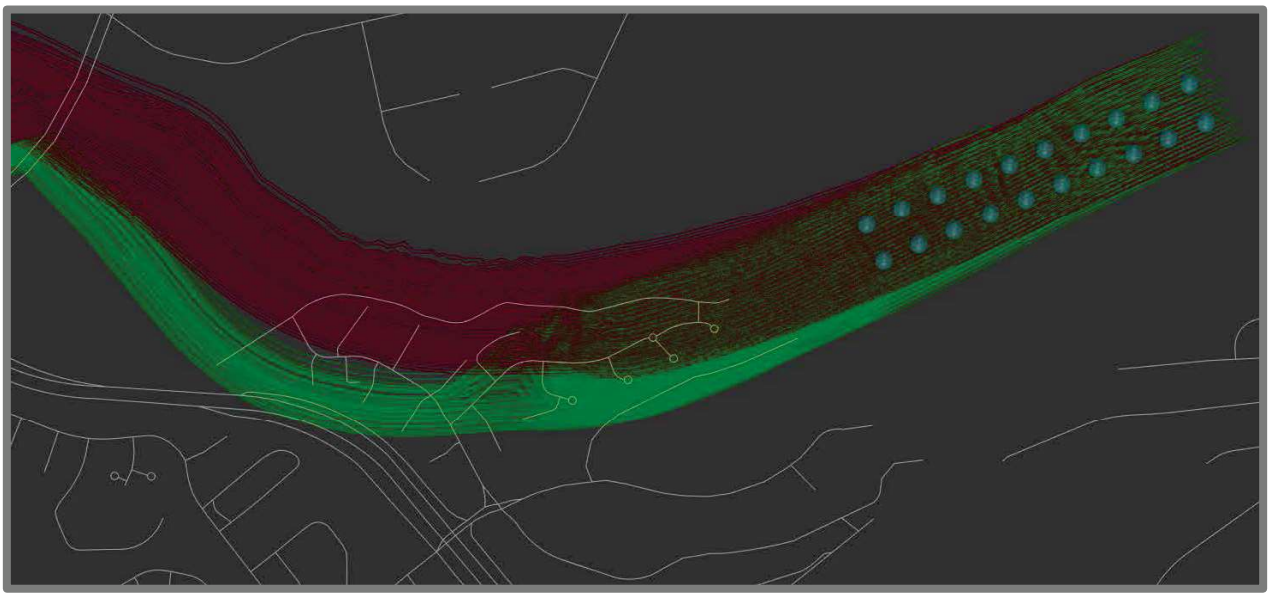

Figure 1.2 Illustration of Particle Path Sensitivity to Assumed Principal (Long-Axis) Direction of Anisotropy

Two difficulties are often encountered obtaining best estimates of dip and strike. First, measurements made at an outcrop face, where the scale is on the order of inches to feet, may not be directly applicable or accurate indicators at the scale over which fluid transport may occur, where distances of hundreds to thousands of feet must be considered. Second, there is likely to be variability in dip and strike values throughout an area, as a function of paleotopography, flow volume, and other factors.

Because there is a variety of data sources for dip and strike at Red Hill, it is appropriate to combine the data while considering their representative scales and quality to obtain a best-estimate at the scale of most interest to the fate-and-transport evaluation. Data sources at Red Hill include (a) close-quarters outcrop measurements such as obtained with a compass-clinometer, (b) surveys of visible outcrop from a distance that allow the geometry of a continuous bed-set to be followed for many tens or hundreds of feet, and (c) geostatistical analysis of the barrel log data. The resulting best-estimate derived from combining these lines of evidence can be to some extent corroborated by intersecting the derived plane with a digital elevation model for comparison with features observed in the field (Inset Figure 1.3).

Figure 1.3 Example of Extensive Correlatable Units Viewed from a Distance using a Theodolite Application for a Camera

References:

Conceptual Site Model, Investigation and Remediation of Releases and Groundwater Protection and Evaluation, Red Hill Bulk Fuel Storage Facility (dated July 27, 2018: "CSM Report")

Groundwater Protection and Evaluation Considerations for the Red Hill Bulk Fuel Storage Facility (dated July 27, 2018: "GPEC Report")

Item 2. Saprolite Extents

The saprolite (chemically and physically weathered basalt) is a critical hydrostratigraphic unit (HSU) that affects contaminant transport upon the water table and within groundwater. The saprolite typically exhibits a lower hydraulic conductivity than surrounding basalts and where present beneath the water table, it likely acts as a barrier to contaminant transport, causing groundwater and contaminants to migrate around or beneath it. The depth of the saprolite/basalt interface is important in many areas of the site, but the point up-valley where the saprolite/basalt interface rises above water table is a critical feature in assessing the risk the Red Hill facility poses to drinking water sources.

Review of the representation within the interim groundwater flow model files provided for courtesy review by the Navy of the saprolite/basalt interface depths and general trends (i.e., slopes) relative to the axis of the North and South Halawa Valleys suggests the saprolite is likely deeper down-valley and shallower up-valley than represented in the interim model. One consequence is that the point up-valley where the saprolite/basalt interface rises above water table may be more downslope than currently represented. If this is true, the role of the saprolite as a barrier to flow between valleys – particularly in up-slope areas – may be less protective than the current conceptual model indicates (Inset Figure 2.1).

There are at this time insufficient available data regarding the depth of the saprolite/basalt interface relative to the water table (particularly in North and South Halawa Valleys) to accurately and uniquely represent them in the model. Characterizing the three-dimensional (3D) extent and hydrogeological properties of the saprolite in each valley, including North and South Halawa Valleys, is difficult. Available data include a general CSM regarding basalt weathering and valley infilling; seismic geophysical analysis conducted along several transects; and a single detailed borehole geologic log that crosses the saprolite/basalt interface. Though the seismic data are very informative, ground-truthing is costly and only very localized. Available data from borings – such as the Halawa deep monitoring well – provide specific stratigraphic logs, but even these are accompanied by uncertainty regarding the appropriate depth to pick the interface (inset Figure 2.2). Consequently, uncertainty remains regarding the depth at which to represent the saprolite/basalt interface within North and South Halawa Valleys in particular, and regarding the protection afforded to Halawa Shaft by the saprolites acting as a barrier.

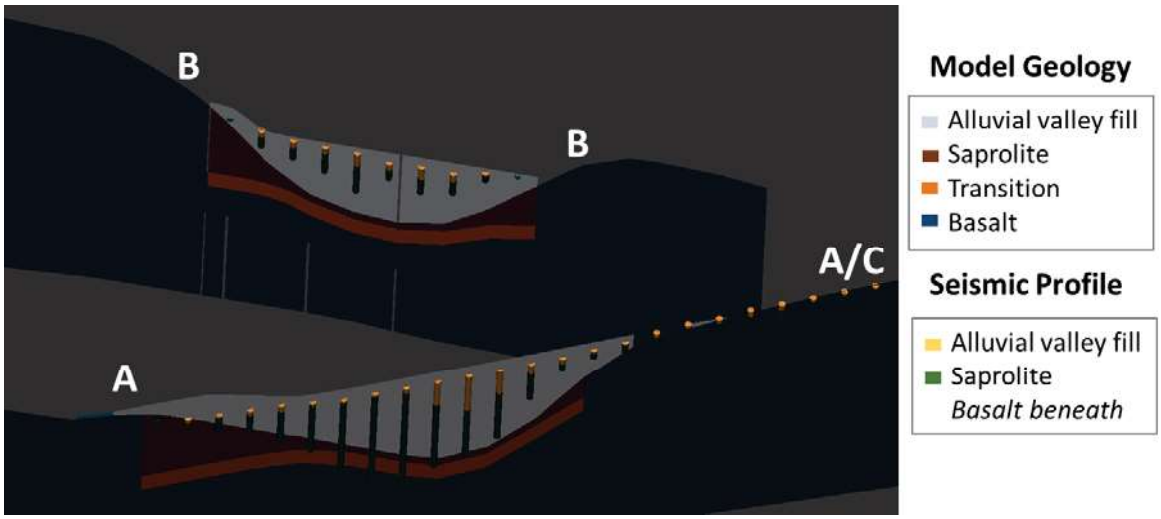

Figure 2.1 Example Comparison of Seismic Profiles and Representation in the Interim Model

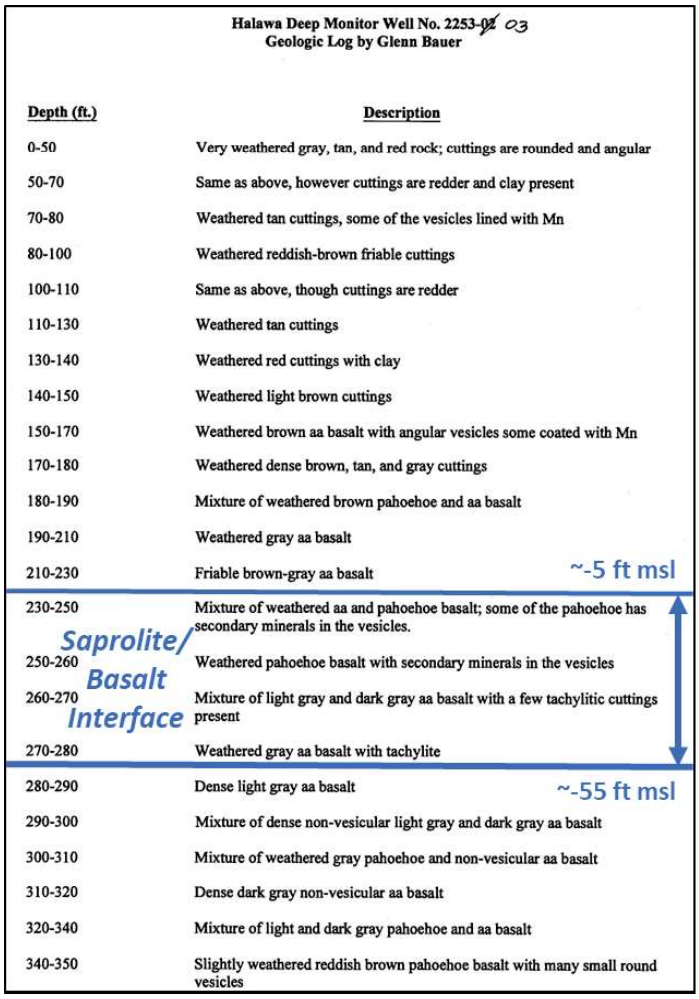

Halawa Deep Monitor Well No. 2253-~~02~~ 03
Geologic Log by Glenn Bauer

Depth (ft.)	Description
0-50	Very weathered gray, tan, and red rock; cuttings are rounded and angular
50-70	Same as above, however cuttings are redder and clay present
70-80	Weathered tan cuttings, some of the vesicles lined with Mn
80-100	Weathered reddish-brown friable cuttings
100-110	Same as above, though cuttings are redder
110-130	Weathered tan cuttings
130-140	Weathered red cuttings with clay
140-150	Weathered light brown cuttings
150-170	Weathered brown aa basalt with angular vesicles some coated with Mn
170-180	Weathered dense brown, tan, and gray cuttings
180-190	Mixture of weathered brown pahoehoe and aa basalt
190-210	Weathered gray aa basalt
210-230	Friable brown-gray aa basalt ~-5 ft msl
230-250	Mixture of weathered aa and pahoehoe basalt; some of the pahoehoe has secondary minerals in the vesicles.
250-260	Weathered pahoehoe basalt with secondary minerals in the vesicles
260-270	Mixture of light gray and dark gray aa basalt with a few tachylitic cuttings present
270-280	Weathered gray aa basalt with tachylite
280-290	Dense light gray aa basalt ~-55 ft msl
290-300	Mixture of dense non-vesicular light gray and dark gray aa basalt
300-310	Mixture of weathered gray pahoehoe and non-vesicular aa basalt
310-320	Dense dark gray non-vesicular aa basalt
320-340	Mixture of light and dark gray pahoehoe and aa basalt
340-350	Slightly weathered reddish brown pahoehoe basalt with many small round vesicles

Figure 2.2 Boring Log of Halawa Deep Monitoring Well

Available data which are overwhelmingly large scale and relatively low resolution (i.e., seismic profiles) must be interpreted in the context of the CSM and AOC to provide an appropriate representation for purposes of the flow and transport modeling. The solution to this problem likely lies in two parts: First, re-interpretation of the available data. When the currently seismic-inferred depths to the saprolite/basalt interface are compared to the CSM, the down-valley transects show a deeper interface depth than the current CSM would suggest while the up-valley transects suggest a shallower interface than currently believed. Interpolating between the down-valley and up-valley transects and extrapolating this trend up-slope from the most up-valley transect may help define where the saprolite is no longer beneath the water table and thus a barrier to flow and transport. Second, ground-truthing of the seismic data using test borings (this may already be planned as there is discussion of a test boring adjacent to Seismic Transect E near the Halawa Deep Monitoring Well [HDMW2253-03]). Additional ground-truthing is highly desirable, even though costly, in targeted areas with maximal information benefit to provide (a) seismic velocities needed to better constrain the depth to the saprolite/basalt reflector and (b) interface elevations at key boring locations to condition the geophysical results.

References:

Conceptual Site Model, Investigation and Remediation of Releases and Groundwater Protection and Evaluation, Red Hill Bulk Fuel Storage Facility (dated July 27, 2018: "CSM Report")

Groundwater Protection and Evaluation Considerations for the Red Hill Bulk Fuel Storage Facility (dated July 27, 2018: "GPEC Report")

Item 3. Preferential Pathways.

Voids, fractures, and related features in this shield volcanic setting will potentially allow for rapid transport of both LNAPL and dissolved-phase contaminants. These include lava tubes, bedding plane structures, fractures, etc. While mentioned in the CSM, there is no discussion or quantification of site specific facets. A good framing for hard rock and fractured systems is the ITRC fractured rock CSM schematic (e.g., Figure 3.1). Some of the more important factors are the orientation of these features, the wall roughness, dip, aperture ranges, continuity and density. While some of these aspects have been discussed in the CSM, none have been quantified (excepting dip, around which there are remaining questions), which would directly assist in considerations of contaminant F&T, particularly the LNAPL migration. For instance, based on the geologic barrel logging when the Red Hill tanks were installed, lava tubes are present beneath 13 of the 20 tanks; Tanks 1, 3, 4, 6, 8, 9, 13, 15, 16, 17, 18, 19, and 20. Lava tubes are expected to be a smooth-walled and distally continuous features (personal comm, Dr. Scott Rowland, U.H., 2018) that if intersected by LNAPL in the unsaturated zone would act as essentially an open-pipe transport conduits. In-filling, collapse and other post-deposition factors can affect how these conduits might behave, as noted in the Navy CSM. However, there is no site or area specific characterization of these important transport features in the CSM, absent which, little can be inferred regarding their potential effects on transport.

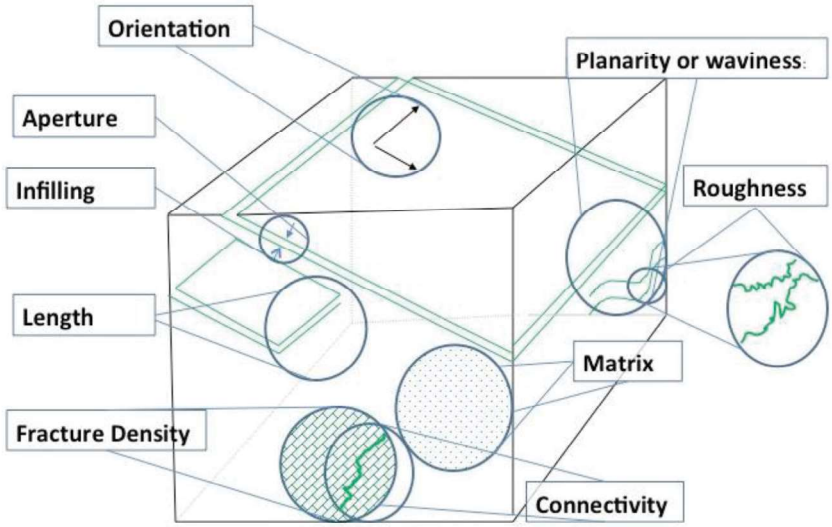

Figure 3.1 Key fracture/hard rock characteristics as defined by the Interstate Technology Regulatory Council (ITRC, December 2017). Of those shown, the most important factors are the orientation of these features, the wall roughness, dip, aperture ranges, continuity and feature density.

A portion of this issue is discussed in the bedding strike and dip discussion above. Based on the range of dip measurements by both the Navy and HDOH scientists, it is clear that there is significant variability in the dip and its azimuth. It also appears that there are changes in dip from the axis of the Red Hill Ridge to outlying areas. The Navy team does some good work in drawing analogies between current volcanic activity on the Big Island and past processes at work on O'ahu. We would simply note that on the Big

Island, recent flows have a much wider meander potential than the 30-45 degrees from the fall-line noted in the CSM. Maps of historically recent lava flows relative to the rift zone alignment show that flows can be in almost any downhill direction (Figure 3.2; USGS, 2018). Whether by preferential pathways or other mechanisms, the observed plume distribution noted previously is clearly not in the direction of the main bedding dip of 190 – 205 degrees stated in the CSM. This also affects the assumptions of the CSM LNAPL F&T evaluations discussed below.

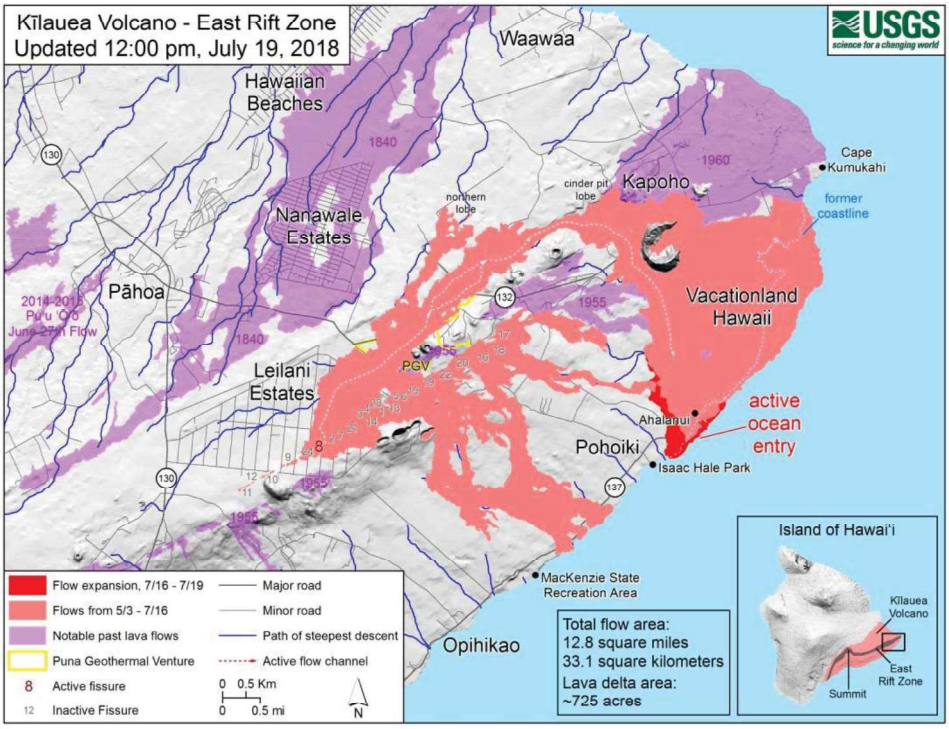

Figure 3.2 Geologic Map of recent lava flow directions from eruptions at the Kilauea Volcano, Hawaii. While the predominant downslope movement is roughly perpendicular to the East Rift Zone, there is significant variability in lava deposition pathways.

The agencies would like to see more thought and geologic features quantification with regard to preferential pathways in the CSM along with their potential effects on LNAPL and dissolved-phase F&T. We recommend such new evaluations be placed in context with the noted ITRC fractured rock framework with associated quantitative evaluations of these critical potential preferential pathways (along with other related technical literature). We also recognize that this system is not purely a fractured matrix, but rather one in which fractures, voids, bedding planes, clinker zones and other features interact as a continuum that will ultimately control LNAPL and dissolved-phase transport. Decisions regarding modeling methods, approaches, and conceptualizations will need to be made and described so the agencies can understand the assumptions and potential limitations therein.

We would also note that the Navy team may wish to consider some additional site data collection in this category using widely recognized fractured rock characterization techniques (e.g., Neumann, 2005). These include cross-hole pneumatic and hydraulic testing with tracers and a variety of other commonly

recognized field methods. Transport estimates, which are the backbone of risk evaluations will be much more reliable when coupled with these types of site specific observational data.

References:

API #4731, 2003. Light Non-Aqueous Phase Liquid (LNAPL) Parameters Database - Version 2.0 - User Guide.

Conceptual Site Model, Investigation and Remediation of Releases and Groundwater Protection and Evaluation, Red Hill Bulk Fuel Storage Facility (dated July 27, 2018: "CSM Report")

Fractured Bedrock Field Methods and Tools: Volume I, Main Report. Science Advisory Board for Contaminated Sites in British Columbia, authored by Golder & Associates, 2010.

Groundwater Protection and Evaluation Considerations for the Red Hill Bulk Fuel Storage Facility (dated July 27, 2018: "GPEC Report").

Hydrogeologic characterization of fractured rock masses intended for disposal of radioactive waste DM Reeves, R Parashar, Y Zhang - Radioactive Waste, 2012.

Huyakorn, P.S., Panday, S., Wu, Y.S., 1994. A Three Dimensional Multiphase Flow Model for Assessing NAPL Contamination in Porous and Fractured Media, 1. Formulation. Journal of Contaminant Hydrology, #16 (1994), pp 109-130.

Characterization and Remediation in Fractured Rocks. Online publication: https://fracturedrx-1.itrcweb.org/ ITRC, 2017.

Neuman, S. P., 2005. Trends, Prospects and Challenges In Quantifying Flow And Transport Through Fractured Rocks. Hydrogeology Journal, March 2005, Volume 13, Issue 1, pp 124–147.

Attachment 2 - Appendix

For Red Hill, the CSM would benefit by conceptualizing and quantifying key systemic features and their potential behavioral characteristics, as well as deciding on the transport framework that is most representative.

Figure 3. Representations of fractured media.

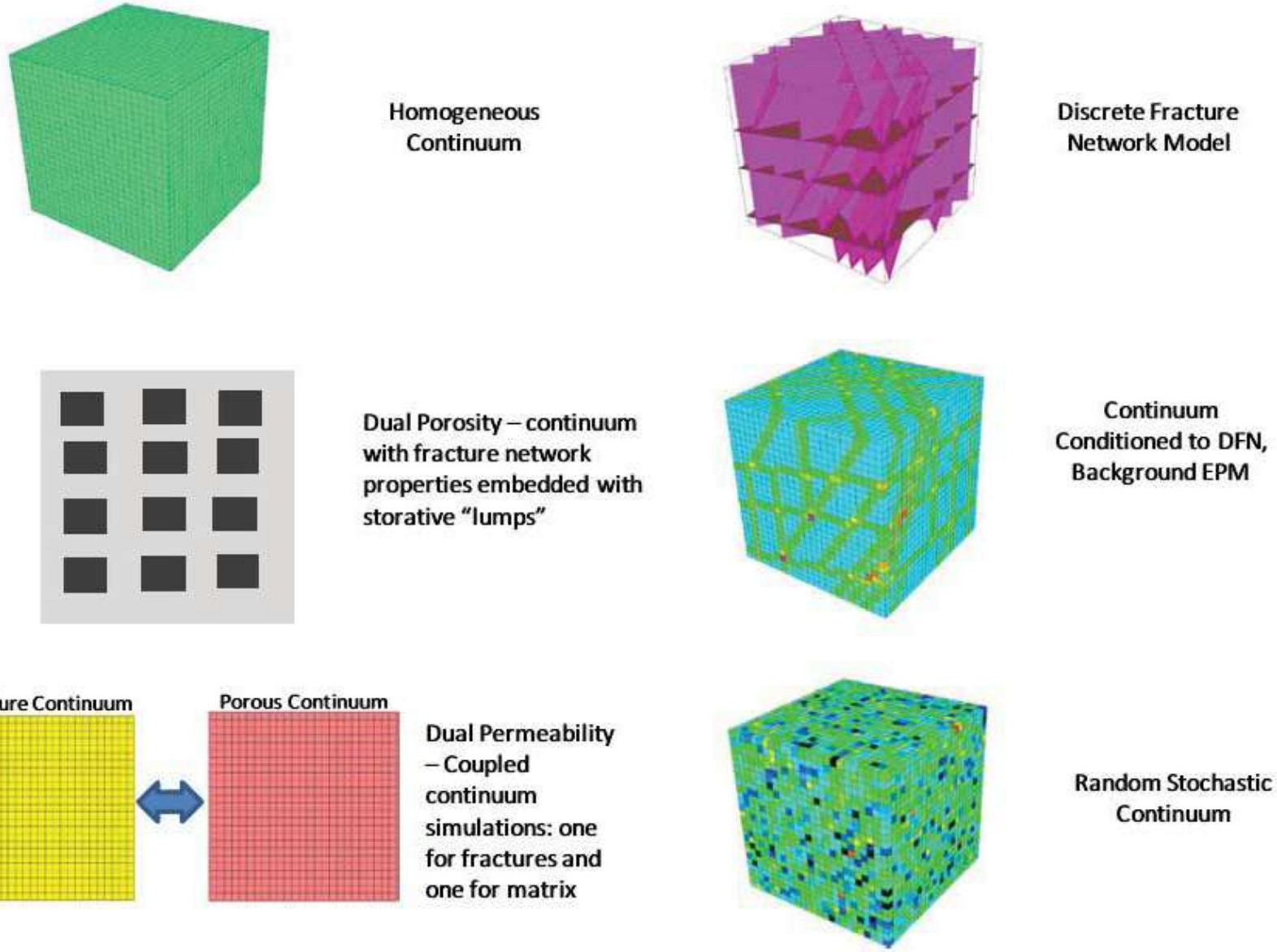

(source: Fractured Bedrock Field Methods and Analytical Tools, Volume 1, Main Report, Submitted to the Ministry of Environment Canada, April 2010.

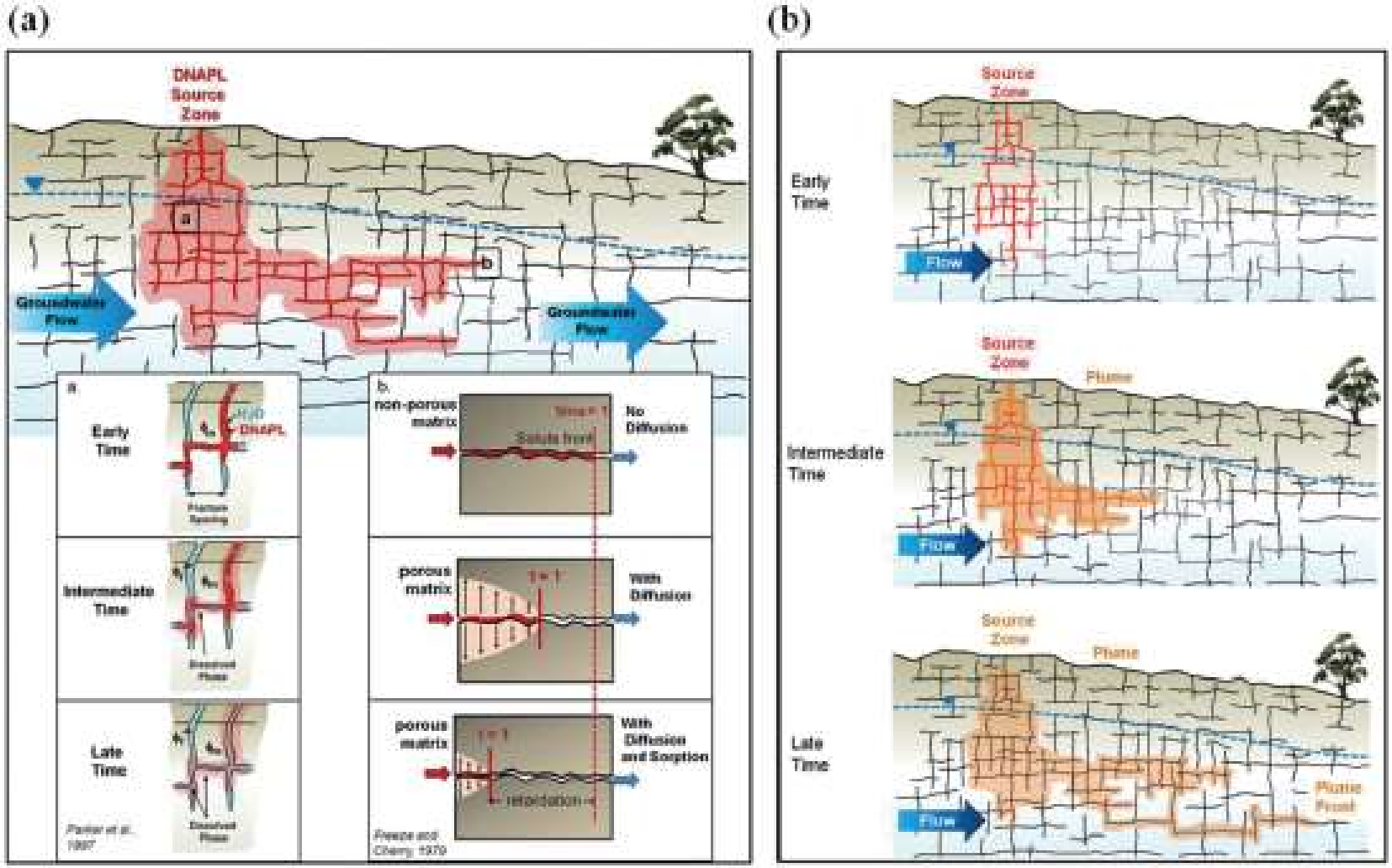

Fig. 1: *Conceptualization of source zone and plume evolution in fractured sedimentary rock: (a) schematic cross-section showing DNAPL release with formation of a downgradient plume, with insets showing source zone evolution (adapted from Parker et al., 1997) and diffusion effects on contaminant migration (adapted from Freeze and Cherry, 1979), and (b) conceptual stages of source zone and plume evolution (adapted from Parker et al., 2010).*

Similar to the Hunt (1996) lithologic schematic, these authors discuss the quantification of such a network for the purposes of understanding the nature of contaminant F&T. The features of Hunt's model need to be bounded by quantifying the various parametric apsects of those features and their impact on transport.

NAPL Distribution in a Fracture

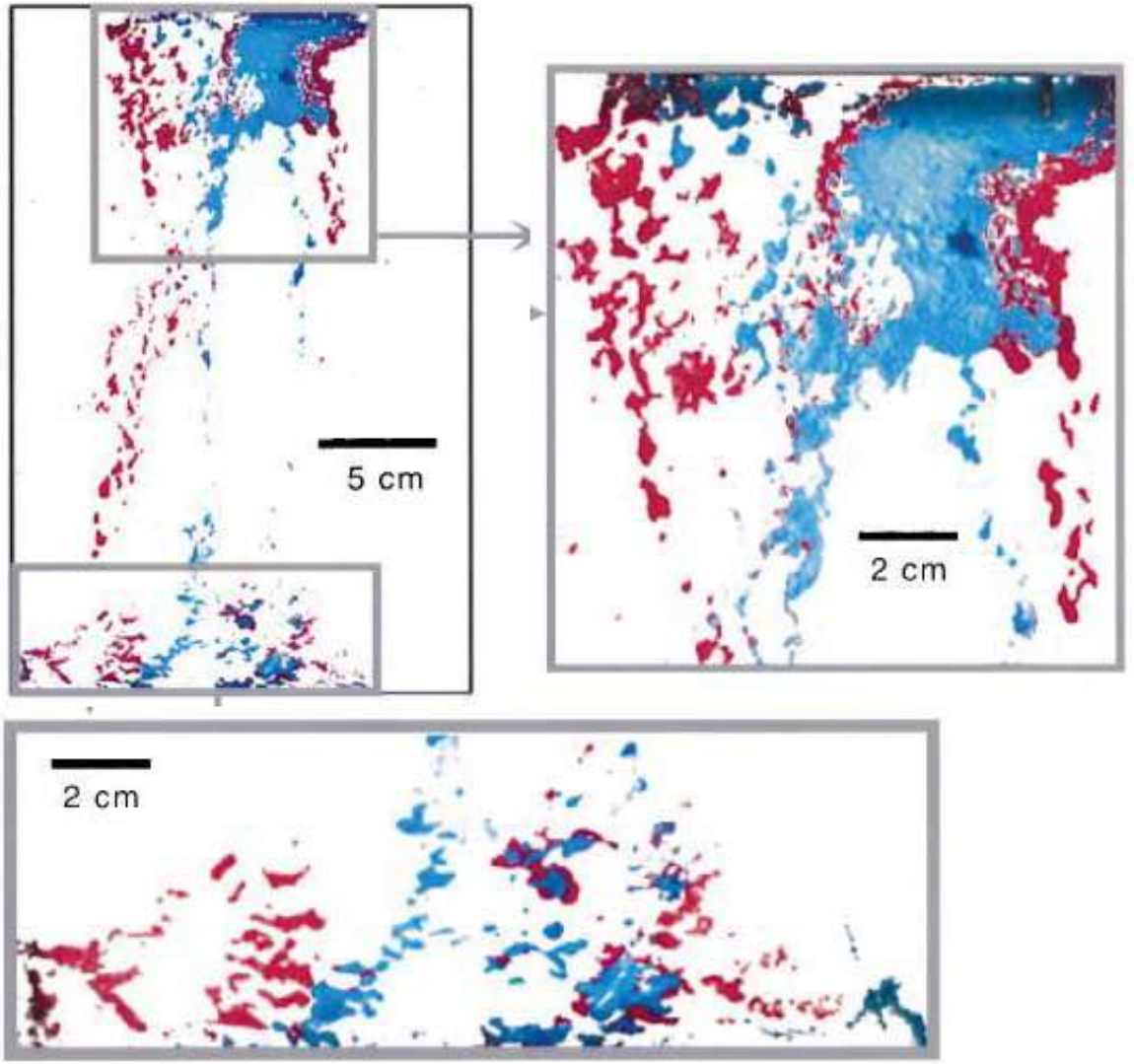

Geller et al., 2000

Heterogeneity of transport is the expected norm in a fractured/hard rock system such as Red Hill and the complexity of the LNAPL CSM needs to comport with the actual complexity of the system.

Just a Little Math... Cubic & Quintic Flow

$$Q = -\frac{\rho g}{12\mu} b^3 \partial h$$

$$K \quad \frac{2b^2 \rho g}{12\mu}$$

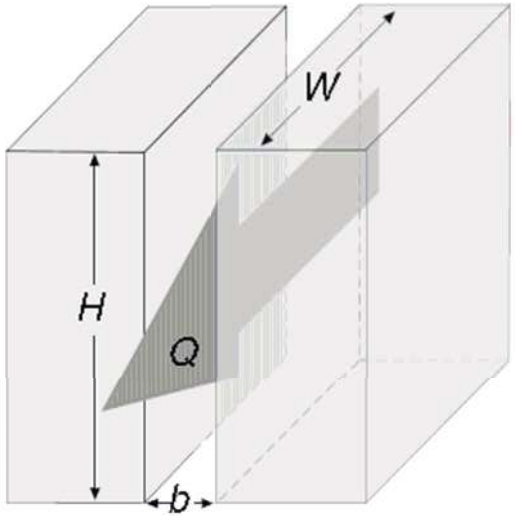

For "simple" fractures

Holy exponential cow!

Suggested for "real" fractures with aperture/length correlations

$$Q = -\frac{4\rho g}{3\mu(\pi\alpha)^2} b^5 \partial h$$

after Climczak et al., 2009

From a transport quantification point of view, fractures and voids of larger apertures and connectivity will allow for very rapid transport of LNAPL. These features need to be understood and quantified so the implications for transport may be understood and constrained.

ATTACHMENT 3

Interim Groundwater Flow Model

Item 4. Caprock, Tuffs and Sediments

The CSM that underlies the interim and final numerical groundwater and LNAPL models needs to represent, albeit in an approximate manner, the principle features and processes that affect groundwater flow and contaminant migration. The configuration and properties of the caprock, tuffs and sediments are collectively an important feature of the hydrogeologic system. The interim groundwater model terminates the saprolites a short distance down-valley of Red Hill; represents the caprock as a wide-reaching uniform and continuous layer; and does not appear to represent older Honolulu volcanics or surrounding finer sediments. These areas were evaporative "lakes" at one time, exhibiting strongly artesian fresh-water conditions, and they may form a barrier to flow influencing groundwater flow and contaminant transport.

Gradients simulated by the interim flow model, as presented in the GPEC Report and determined from the interim model files provided for courtesy review by the Navy, do not comport well with gradients determined from synoptic data in and around Red Hill facility. While this is in part related to conditions local to Red Hill, analyses conducted using the interim model exhibit high sensitivity to conditions downgradient of Red Hill - specifically, in the area broadly represented by the caprock (GPEC Report Section 5.9). This suggests that although uncertain, because there are insufficient data available to uniquely and accurately specify the distribution and properties of downgradient geologic units, it is important to represent the hydrostratigraphy downgradient of the Red Hill facility as accurately as possible, using as one basis the overarching CSM regarding the distribution and properties of these features (Inset Figure 3.1).

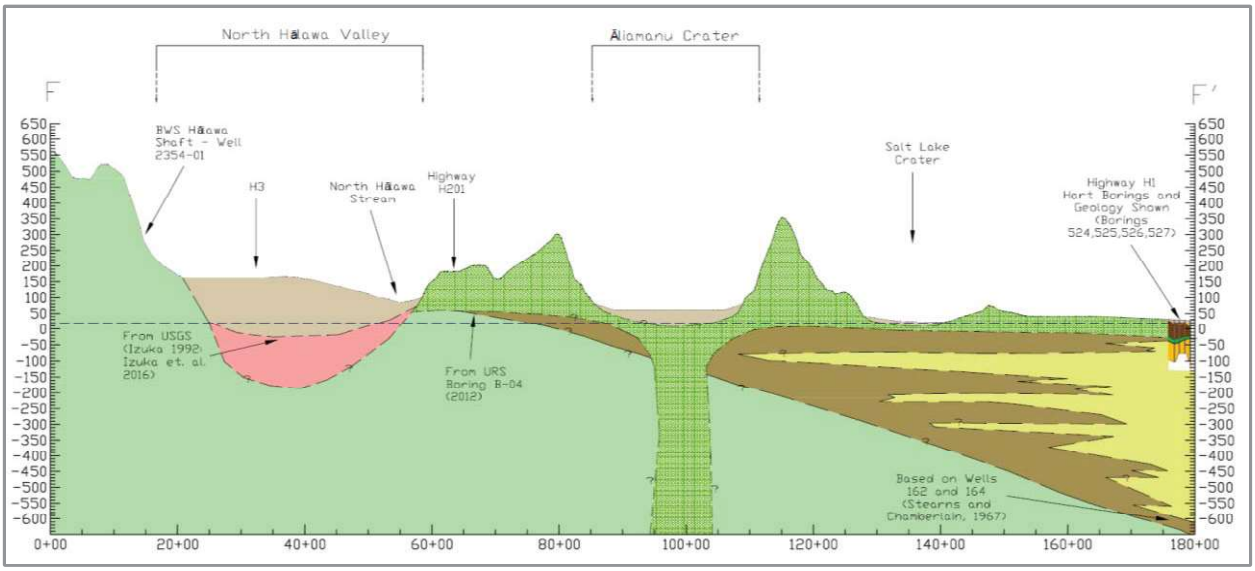

Figure 3.1 Example Figure Illustrating Hydrostratigraphic Features

Available information must be interpreted in the context of the CSM and AOC to provide an appropriate representation for flow and transport modeling. The solution to this problem likely lies in two parts: First, re-interpretation of the available data, and expanded use of sensitivity analysis and model calibration to help identify probable geometries and properties, including for example extending the saprolites down-valley, and differentiating Honolulu volcanics from surrounding sediments. Second, based on the anticipated results of sensitivity analyses conducted with this updated representation of

these features, consideration should be given to methods of data collection to better constrain the likely presence, extent and properties of these features. For example, other sources of information and data collection – such as airborne gravity surveys – may provide further evidence for the extents of some of these features.

References:

Conceptual Site Model, Investigation and Remediation of Releases and Groundwater Protection and Evaluation, Red Hill Bulk Fuel Storage Facility (dated July 27, 2018: "CSM Report")

Groundwater Protection and Evaluation Considerations for the Red Hill Bulk Fuel Storage Facility (dated July 27, 2018: "GPEC Report")

Item 5. Calibration – Tunnel Inflows

The role of Red Hill shaft as a mitigating hydraulic containment measure in the event of a contaminant release depends on its ability to develop a capture zone that encompasses the area impacted by a release. As a Hawaii-style water supply, Red Hill shaft does not function as a simple vertical well: it gains water via seepage along the quasi-horizontal tunnel that extends broadly eastward from the vertical shaft. One role of the interim and final groundwater models is to demonstrate the likely extent of capture (zone of contribution) of Red Hill shaft under a range of plausible conditions.

The interim groundwater flow model does represent Red Hill shaft as a linear quasi-horizontal feature rather than at a single vertical point, which is appropriate. However, the distribution of inflows to the eastern tunnel extension simulated by the interim model as determined from the model files provided for courtesy review by the Navy does not appear to match the inflow pattern encountered during tunnel construction (Inset Figure 5.1). During construction, a clinker zone was encountered that contributed more than 60% of the flow to the tunnel whereas the interim model simulates uniform inflow along the tunnel. This difference highlights two issues: first, there is heterogeneity present on a scale of many tens to hundreds of feet that is not well understood nor represented in the interim model; second, the extent of capture developed by the tunnel may be more head-dependent than represented in the interim model. That is, the capture zone under high water level conditions may be dominated by seepage from this clinker at the end of the east tunnel, but under low water level conditions may be dominated by drawdown within the vertical shaft itself. Sensitivity analyses conducted with the interim model indicate that the model exhibits sensitivity to the potential presence of a clinker zone (GPEC Report Section 5.9).

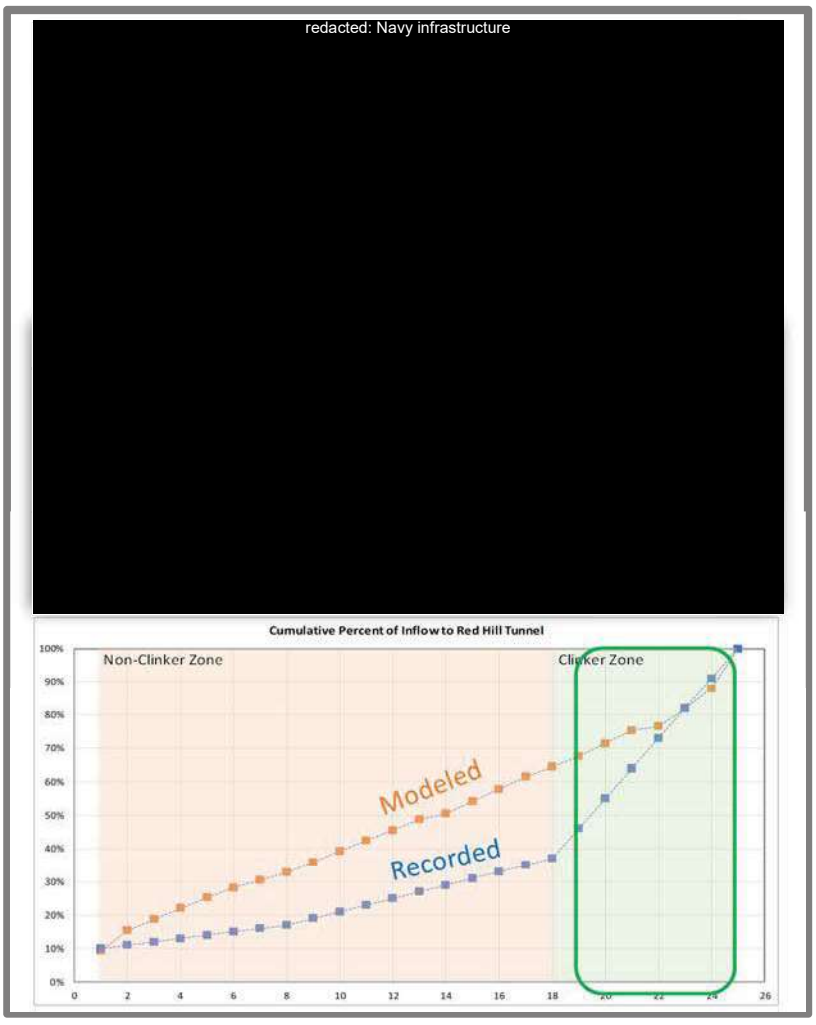

Figure 5.1 Schematic of Recorded and Simulated Inflows

The presence of large-scale heterogeneity is documented: however, the distribution and properties of these heterogeneities are not well known and cannot be perfectly represented in models. Despite this, consideration must be given to the role they may play in the

calibration of the groundwater model, and any inability to reasonably match heads and gradients; the zone of contribution to Red Hill shaft and tunnel system under different conditions; and, the transport and fate of constituents in groundwater.

The final CSM and model should make a greater effort to evaluate the possible role of these heterogeneities – in particular, as an illustrative example, the Red Hill tunnel clinker – on calibration, zones of contribution, and contaminant transport. This may be accomplished for example by evaluating the zone of contribution under high water level conditions dominated by tunnel seepage, and under low water level conditions dominated by active pumping at the Red Hill shaft.

References:

Conceptual Site Model, Investigation and Remediation of Releases and Groundwater Protection and Evaluation, Red Hill Bulk Fuel Storage Facility (dated July 27, 2018: "CSM Report")

Groundwater Protection and Evaluation Considerations for the Red Hill Bulk Fuel Storage Facility (dated July 27, 2018: "GPEC Report")

Item 6. Calibration Heads and Gradients

Groundwater flow and contaminant migration are, under most circumstances, determined or strongly influenced by hydraulic gradients. A groundwater model developed to predict the transport and fate of contaminants from a release should present reasonable correspondence with hydraulic gradients determined using site-specific measurements, to provide confidence the model will reasonably predict contaminant transport.

Hydraulic gradients determined from measured data are generally flat in and around Red Hill. On most occasions, gradients are to the southwest at a low slope, but occasionally they appear to be to the northwest and possibly north. The interim model outputs presented in the GPEC Report do not closely reproduce the magnitude or direction of these gradients. Flow in the calibrated interim model is dominantly Mauka-to-Makai, and most of the sensitivity-derived alternative models demonstrate flow toward Red Hill shaft at gradients that are 10 to 100 times higher than measured values. Although the sensitivity analyses do present a range of simulated gradients c(GPEC Report Section 5.9), the distribution of simulated gradients across all models that were provided for courtesy review by the Navy does not match closely values derived from the synoptic data (Inset Figure 6.1).

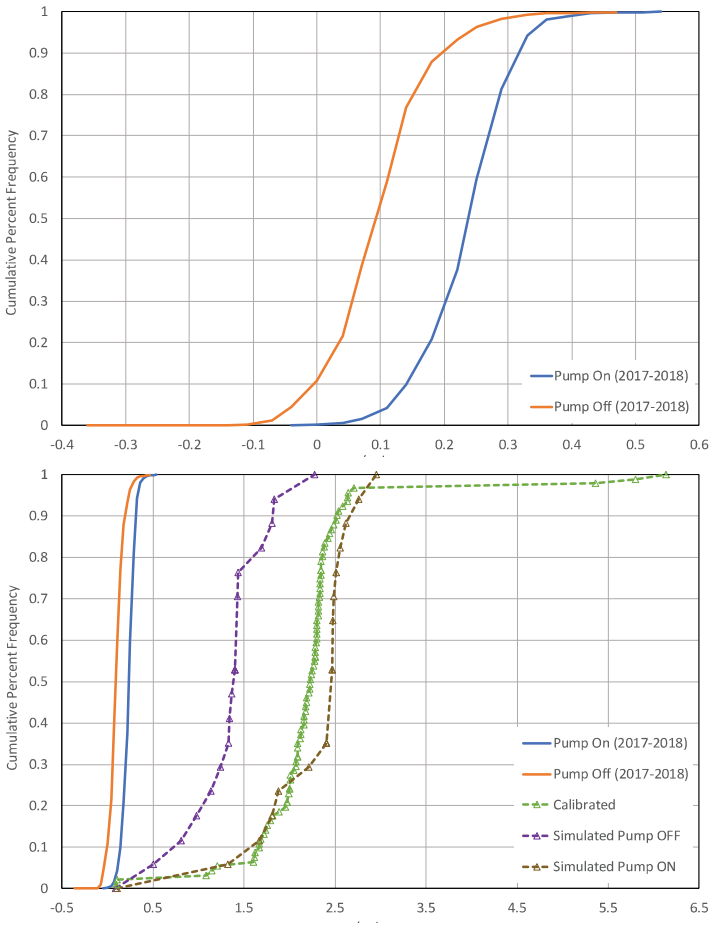

Figure 6.1 Example Comparison of Pairwise Head Differences from Synoptic Data with Simulate Head Differences from All Interim Models

Historical data had shortcomings (frequency, reference elevations, lack of pumping knowledge) that they were not easily amenable to rigorous analysis. Recent synoptic data provide improved frequency and quality. These data suggest that certain aspects of the CSM incorporated into the interim flow model may prevent the model from reproducing these gradients, including the saprolite distribution; basalt strike and dip; the "keying" of saprolites into down-valley Honolulu volcanics, older sediments and cap rock; and recharge distribution and rates.

The final CSM and model should focus on analyzing recent high-quality synoptic data to the extent possible, and down-weight analyses based on older data. Despite difficulties preparing water level maps, pairwise head-difference plots can show the effects of pumping on gradients and the frequency and magnitude of gradient reversals. Steady-state model calibration should focus on demonstrating a match

with regional patterns and with representative local gradients under pumping and non-pumping conditions. This combination is required to demonstrate that the model is useful for near-field transport to understand the available groundwater data, and for developing predictions of capture zones for Red Hill shaft and Halawa shaft to help evaluate risk and mitigating responses or strategies. Transient calibration will provide information on T, S, anisotropy, and possibly on the geometry of features such as the saprolite but is not a substitute for obtaining reasonable mean-centered correspondence to the measured gradients (or pairwise head differences).

References:

Conceptual Site Model, Investigation and Remediation of Releases and Groundwater Protection and Evaluation, Red Hill Bulk Fuel Storage Facility (dated July 27, 2018: "CSM Report")

Groundwater Protection and Evaluation Considerations for the Red Hill Bulk Fuel Storage Facility (dated July 27, 2018: "GPEC Report")

Item 7. Coastal Submarine Discharge

The CSM that underlies the interim numerical groundwater and LNAPL models and will underlie the final versions needs to represent the principle features and processes that affect groundwater flow and contaminant migration. There is uncertainty regarding the downgradient outflow boundary, which as currently represented in the model may lead to a bias toward discharge occurring in the northeast Pearl Harbor area. All groundwater that is not extracted by wells or discharged to streams or springs flows to the saline water bodies: how the model distributes groundwater between the Pearl Harbor Estuary and offshore (submarine) discharge areas can affect upslope flow patterns including the Red Hill area.

Gradients simulated by the interim flow model do not comport well with measured gradients in and around Red Hill facility. While this is in part related to conditions local to Red Hill, the interim model exhibit high sensitivity to conditions downgradient of Red Hill. The interim model represents the downgradient discharge (outflow) from the model to the saline water bodies (Pearl Harbor Estuary and offshore areas south of Pearl Harbor) via a general head boundary (GHB) with some areas exhibiting intervening high-conductivity cap rock (GPEC Report Section 4.4). The GHB allows flow based upon an ascribed elevation and an intervening resistance between the boundary and the aquifer. In this configuration, groundwater is simulated to preferentially flow to the eastern part of Pearl Harbor Estuary. However, muds and volcanic ash on the bottom of Pearl Harbor may impede flow leading to more flow from Moanalua Aquifer to the Waimalu Aquifer. Flow from the Moanalua Aquifer to the Waimalu Aquifer where spring systems and large pumping centers create significant drawdown could result in a flow path beneath the Red Hill facility to the northwest.

Thus, though there are insufficient available data regarding the distribution and properties of downgradient discharge outflow boundary to accurately and uniquely represent it in the groundwater model, sensitivity analyses indicate this area is important to regional flow patterns (GPEC Report Section 5.9). Therefore, available information must be interpreted in the context of the CSM and AOC to provide an appropriate representation for purposes of the flow and transport modeling.

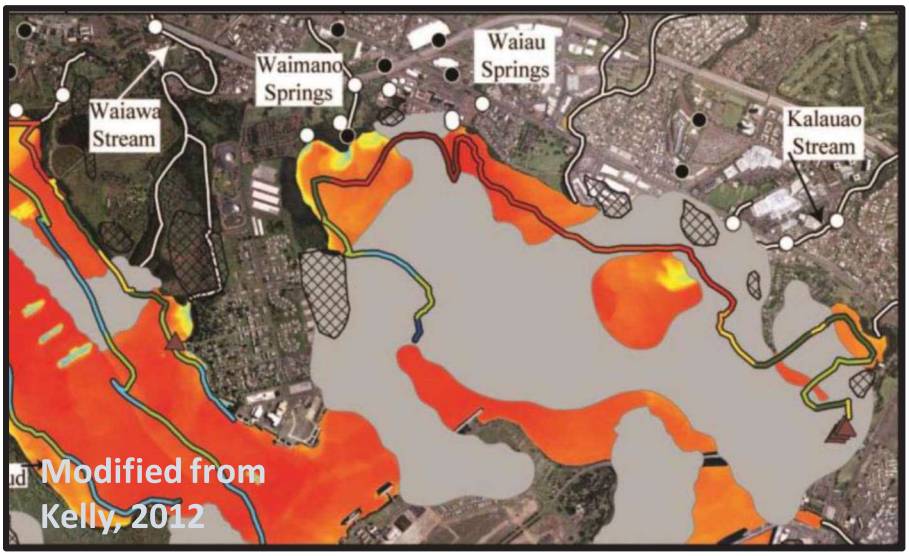

Figure 10.1 Example Figure Illustrating Variable Discharge to Pearl Harbor

The approach to simulating the groundwater flow to the Pearl Harbor Estuary and the southern offshore regions needs further work. Although uncertain in extent and character, it is important to represent the downgradient outflow conditions as accurately as possible, using as one basis the CSM regarding the distribution and properties of these features, and also other sources of information (Inset Figure 10.1).

The solution likely lies in two parts: First, re-interpretation of the available data, with expanded use of sensitivity analysis and model calibration to help identify probable geometries and properties. Model refinements may include using multiple layers to simulate the caprock and include older alluvial sediments and the muds and tuffs that blanket the floor of Pearl Harbor. Second, based on the anticipated results of sensitivity analyses conducted with this updated representation of these features, consideration should be given to methods of data collection to better constrain the likely presence, extent and properties of these features.

References:

Conceptual Site Model, Investigation and Remediation of Releases and Groundwater Protection and Evaluation, Red Hill Bulk Fuel Storage Facility (dated July 27, 2018: "CSM Report")

Groundwater Protection and Evaluation Considerations for the Red Hill Bulk Fuel Storage Facility (dated July 27, 2018: "GPEC Report")

ATTACHMENT 4

Interim Fate and Transport Analyses

8. LNAPL Fate and Transport.

The following set of comments pertain to the contaminant transport aspect of the CSM and related modeling and evaluation approaches taken by the Navy's technical team. Conceptually, contaminant transport will depend on a suite of facets starting with the LNAPL migration that will occur following its release to the subsurface and the cumulative effects of multiple releases over time. While the LNAPL is mobile and moving in the environment, it poses a potential threat to receptors as a free-phase contaminant. Once the LNAPL ceases to move, the residual along the transport pathways presents a longer-term source of contaminants to groundwater that may be transported some additional distance within the aquifer system. Combined, these two aspects of fuel F&T represent the primary threat pathways to the sole-source groundwater resource. The Navy team's conceptualization of these processes would benefit from additional technical work and data collection to be more consistent with observed site data discussed in prior comment sections.

It is unclear how the Navy's current CSM will effectively represent LNAPL transport as indicated in Section 7.4 of CSM document that states: *"..to estimate LNAPL migration for current and potential future releases, including the fraction expected to be immobilized in the vadose zone, and the fraction expected to reach groundwater. The modeling effort will also include an assessment of the potential migration of LNAPL within the saturated zone."* The primary component of the Navy's LNAPL current modeling approach is a "*statistical LNAPL holding model*" that accounts for only the residualization of some fraction of an assumed LNAPL release within an assumed release geometry. This results in a source zone for the dissolved phase transport model that is rather arbitrary in nature since no active LNAPL transport calculations have been done to account for primary and preferential pathways, pore volume already occupied by past releases or infiltrating water, or the characteristics of different release rates. While perhaps useful for some general framing, this non-dynamic form of LNAPL modeling cannot determine critical aspects of risk determinations and potential mitigation approaches. The Navy team's CSM and contaminant fate and transport evaluation should be able to address questions, such as:

- What range of LNAPL releases might reach groundwater (and how quickly) as a function of release rates, locations, fuel types, and other characteristics? Transport in each area of the tank farm can reasonably be expected to behave differently based on the boring and barrel logging of the ridge. How do geologic distribution differences affect the transport outcomes?
- How do chronic low-rate releases behave in comparison to large-scale sudden events? How can the release event ranges be confidently bracketed and what are those ranges?
- Related, what is the fraction of residual capacity already taken up by pre-existing releases or infiltrating water, and how can that be determined from existing data? If it cannot be determined from existing data, what conservative assumptions might be made?
- How fast and how far might LNAPL travel as a function of various release scenarios and in what directions? The approach discussed by the Navy teams assumes a southwest direction that does not seem to comport well with observed detections of petroleum related compounds and depletion of natural attenuation parameters to the northwest.
- How can hydraulic capture be achieved for LNAPL containment in context with the

estimated LNAPL transport rates and under what kinds of pumping regimes?

- How far would an LNAPL release need to propagate to create potential detections at the Halawa Shaft and/or other groundwater resource areas and with what release volume and scenario could that occur?

As the regulatory agencies SME's LNAPL screening modeling shows, a release that exceeds the formation's residualization capacity, which is presently undefined in the CSM or by any correlative data, could potentially reach the water table zone at a rapid rate. This rapid downward transport may result in LNAPL gradients that exceed the shallow groundwater gradient resulting in LNAPL migration in unexpected directions and distances. This is an area that needs more development prior to submitting a revision to the fate and transport model, since the area covered by LNAPL plumes is the source zone for the dissolved phase transport model.

Defining specific LNAPL transport parameters will be a significant challenge in this environment. The Navy should consider what additional efforts can be taken to characterize these parameters. Unfortunately, core-scale testing in petrophysical labs (CSM Chapter 5.2.3) may be of limited value. As evidenced through the results of the API LNAPL Parameters Database compilation (API 4731, 2003), capillary centrifuge testing has also been shown to be suspect where residual saturation is over-estimated compared to field studies and other soil properties databases (e.g. U.S. Salinity Lab and others). It has also been observed in work at the IDPP OU1-C area in Honolulu that the residual saturations determined in the lab are unreliable and non-conservative. The Navy needs to develop an approach to better constrain the residualization capacity of the formation. Briefly, in situ samples collected by continuous coring in free-phase LNAPL zones generally test at or below residual saturation values in site areas of significant free product LNAPL. Since LNAPL cannot flow into a well if it is below residual in the formation, these lab-derived values conflict with site LNAPL observations. The same limitations may be expected for the Red Hill petrophysical testing program and we recommend the Navy team develop alternate bench and field testing and data collection methods to more realistically constrain these important LNAPL F&T parameters.

Absent additional source zone characterization data, the LNAPL residual capacity will remain unconstrained along with other important elements to the LNAPL transport regime. As noted, this is one of several critical factors in the dynamic evaluation of LNAPL transport and potential risks to the groundwater system. Where measurements and data are absent, a greater degree of conservatism in the estimation approaches is necessary to allow for that uncertainty.

References:

API #4731, 2003. Light Non-Aqueous Phase Liquid (LNAPL) Parameters Database - Version 2.0 - User Guide.

Considerations on LNAPL Transport at the Navy Red Hill Facility, February 2018. G.D. Beckett, a presentation to interested Red Hill parties.

Conceptual Site Model, Investigation and Remediation of Releases and Groundwater Protection and Evaluation, Red Hill Bulk Fuel Storage Facility (dated July 27, 2018: "CSM Report")

Groundwater Protection and Evaluation Considerations for the Red Hill Bulk Fuel Storage Facility (dated July 27, 2018: "GPEC Report").

Nonaqueous-Phase-Liquid Dissolution in Variable-Aperture Fractures: Development Of A Depth-Averaged Computational Model With Comparison To A Physical Experiment. Detwiler, R.L., Rajaram, H., 2001. Water Resources Research, December 2001.

Neuman, S. P., 2005. Trends, Prospects and Challenges in Quantifying Flow and Transport Through Fractured Rocks. Hydrogeology Journal, March 2005, Volume 13, Issue 1, pp 124–147.

Item 9. Groundwater Data

Groundwater flow and contaminant migration pathways beneath the Red Hill facility are poorly understood. Analysis of groundwater chemistry data can help constrain flow paths. The interim and final groundwater flow models should present reasonable correspondence with available water level and gradient data, so they can underpin the transport model (developed to predict the fate of contaminants from potential releases) which in turn should present reasonable correspondence with available water quality data. This includes contaminant data and other data that may evidence groundwater impacts (e.g., terminal electron acceptors [TEAs]), or of migration directions and mixing of water from different sources (e.g., isotopic data and other quality indicators).

Interpretations of water quality data presented in the CSM Report and GPEC Report are in places non-conservative, and conflict with other lines of evidence and with conclusions reached by regulator SMEs. Example 1: The Navy consultants dismiss some detected results out of concerns for data quality (CSM Report Section 7.2 and Appendix B.7). Though in some instances justified, these concerns do not address all detected results, and from the regulatory perspective, any reported detections that are not qualified are evidence of impacts. Example 2: Independent analyses of TEA data presented and discussed in CSM Report Section 7.3.2 and Appendix B.4 and GPEC Report Figure 6.3 as indications of natural attenuation (e.g., Inset Figure 9.1), dissolved phase contaminant detection frequency and distribution (inset Figure 9.2), and hydraulic gradients, suggest transport occurred not just to the southwest but also to the northwest and possibly northeast of the facility. Example 3: The distribution and concentrations of general chemistry data (i.e. major ions, specific conductivity, and pH) show a poorly-mixed system inconsistent with the Navy CSM of robust flow from upslope recharge areas to Red Hill Shaft. The chemistry is highly variable with chloride concentrations spanning over an order of magnitude and is more suggestive of sluggish down-slope flow and compartmentalization (inset Figures 9.3 and 9.4).

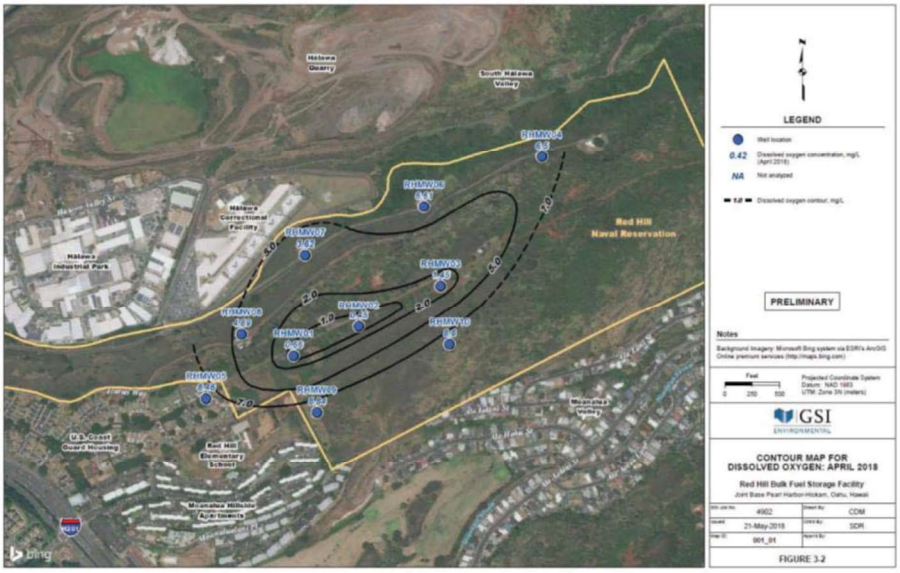

Figure 3-2: Contour Plot of O_2 Concentrations from the Facility Groundwater Monitoring Network (April 23–25, 2018)

Figure 9.1 Example Terminal Electron Acceptor (TEA) Map – Dissolved Oxygen

The relative absence of high-concentration detections within the small, widely-spaced, monitoring network around Red Hill is not proof of absence of impacts, but appears to be interpreted as such by the Navy consultants. Other data, including TEAs, TPH and individual fuel constituents suggest a broad area of impacts extending in various directions within a complex groundwater flow system that is not uniformly Mauka-to-Makai, with the possibility of LNAPL impacts at the water table as the cause.

Before developing the transport model, it is important that the CSM encompass reasonable interpretations of available water quality data. The CSM should, at this stage, allow for "alternative hypotheses" of at least equivalent likelihood of LNAPL impact to groundwater versus the current hypothesis of there having been no impacts. The final groundwater flow model, when it reasonably represents hydraulic gradient directions and magnitudes in the vicinity of Red Hill ridge, would be anticipated to underpin a contaminant transport model that demonstrates a reasonable match historical sample results (contaminants and TEAs, etc.), thereby demonstrating that the model is useful for near-field transport to understand the available groundwater data, and for developing predictions of contaminant transport and fate to help evaluate risk and mitigating responses or strategies.

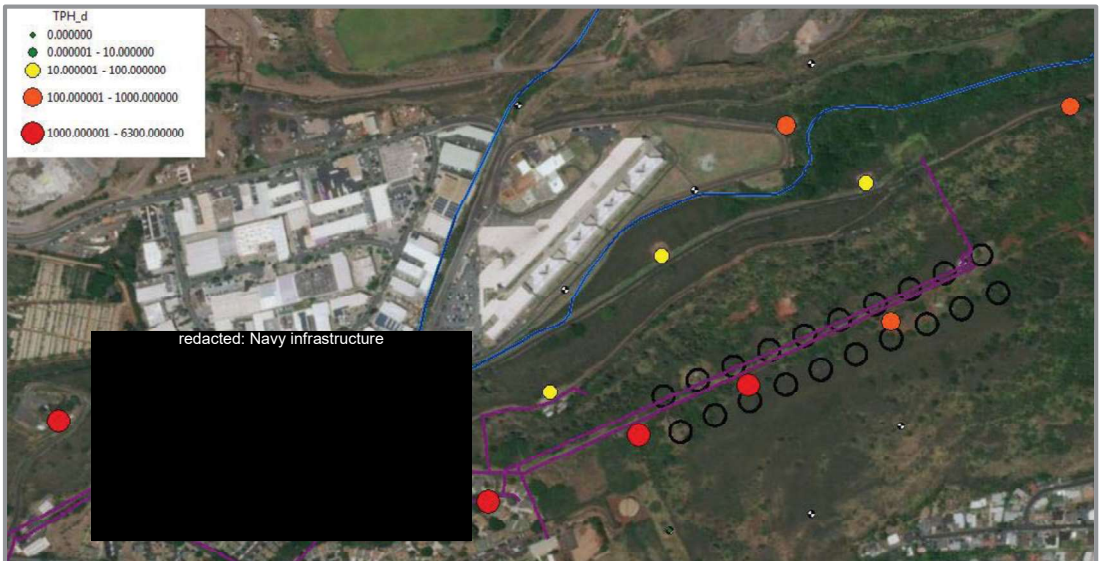

Figure 9.2 Example Map of TPH-D Detections

Figure 9.3 Image of Chloride Concentrations Sampled at Wells

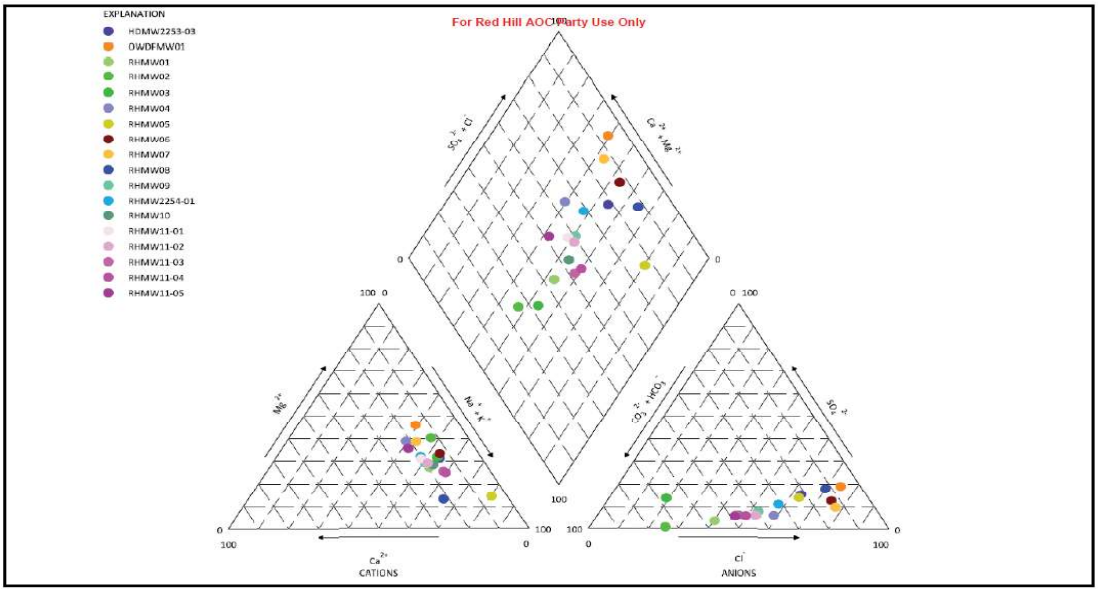

Figure 9.4 Example Piper Diagram

References:

Conceptual Site Model, Investigation and Remediation of Releases and Groundwater Protection and Evaluation, Red Hill Bulk Fuel Storage Facility (dated July 27, 2018: "CSM Report")

Groundwater Protection and Evaluation Considerations for the Red Hill Bulk Fuel Storage Facility (dated July 27, 2018: "GPEC Report")

10. **LNAPL and Dissolved-Phase Plume Distribution**:

The LNAPL and dissolved-phase plumes are potentially more widespread and in alternate directions than the Navy team's CSM suggests. This has direct implications to the estimation of potential risks. The CSM will benefit by consideration of these observations as representative and then accommodate those implications through more thorough evaluations and possibly additional data collection/demonstration. Site specifically, there are multiple data sets that indicate there have been historic detections of interest to the west and northwest. For example, the dissolved-oxygen depletion shown in Figure 9.1 closely parallels the observed historic detections of TPHd in groundwater, as expected based on the mechanisms of degradation and transport. The CoC distribution, elevated temperature distribution (Figure 10.1), and other natural attenuation parameters also support this historic transport direction.

Much less is known with respect to the potential LNAPL distribution in the subsurface that is the source of these groundwater impacts. Simplified transport estimates suggest that for a wide range of general site parametric conditions, the expected downgradient extent of these compounds is typically less than 100-ft away from the LNAPL source zone, particularly when attenuation rates are high. Naphthenic compounds, due to their transport properties, are not generally highly transportable in aquifers. This suggests the possibility of distal LNAPL impacts relative to the Tank Farm from cumulative historic releases that have left their signature in the groundwater system. Naphthenic compounds are frequently detected at several outlying monitoring locations at low concentrations (commonly J-flagged), but detections of petroleum related compounds and depletion of natural attenuation parameters (NAPs) occur predominantly in the tunnel and northwest wells.

With regard to the CSM interpretations about the outcome of the 2014 Tank 5 release, perhaps one of the most fundamental is the estimated release volume of 27,000 gallons. The regulatory agency SMEs have not been able to find the specific release volume calculations nor the certainty bounds on that value. In our experience, release volume estimates have significant uncertainty that would affect the assumptions and conclusions in the CSM, particularly given that the release occurred during both filling and draining of Tank 5. We believe the particular details of the release estimate need to be more fully discussed in the CSM and the implications of that range considered in the evaluations. If the estimate is relatively certain, that should be documented with the appropriate background so that related interpretations are appropriately bounded.

The CSM and the underlying available data cannot (at present) reliably place the LNAPL source zone(s) in context with the observed groundwater contaminant distribution. The underlying cause for this gap is the absence of characterization around the Tank Farm. The product staining indications in historic angled-core sampling beneath various Red Hill USTs are useful, but none of those investigatory locations were intended to be sampled to groundwater. Further, it is unclear whether wells RHMW01 through RHMW03 are directly within an area of vadose zone contamination or not. At the time of their installation there were no gross indications of vadose zone fuel impacts, but groundwater was impacted, suggesting a complex relationship between release transport pathways and groundwater impacts. In other words, LNAPL impacts in the vadose and water table regions sourcing these impacts are not delineated by the available investigatory locations. This key uncertainty is not adequately discussed in the CSM, but affects all the related F&T discussions and framing.

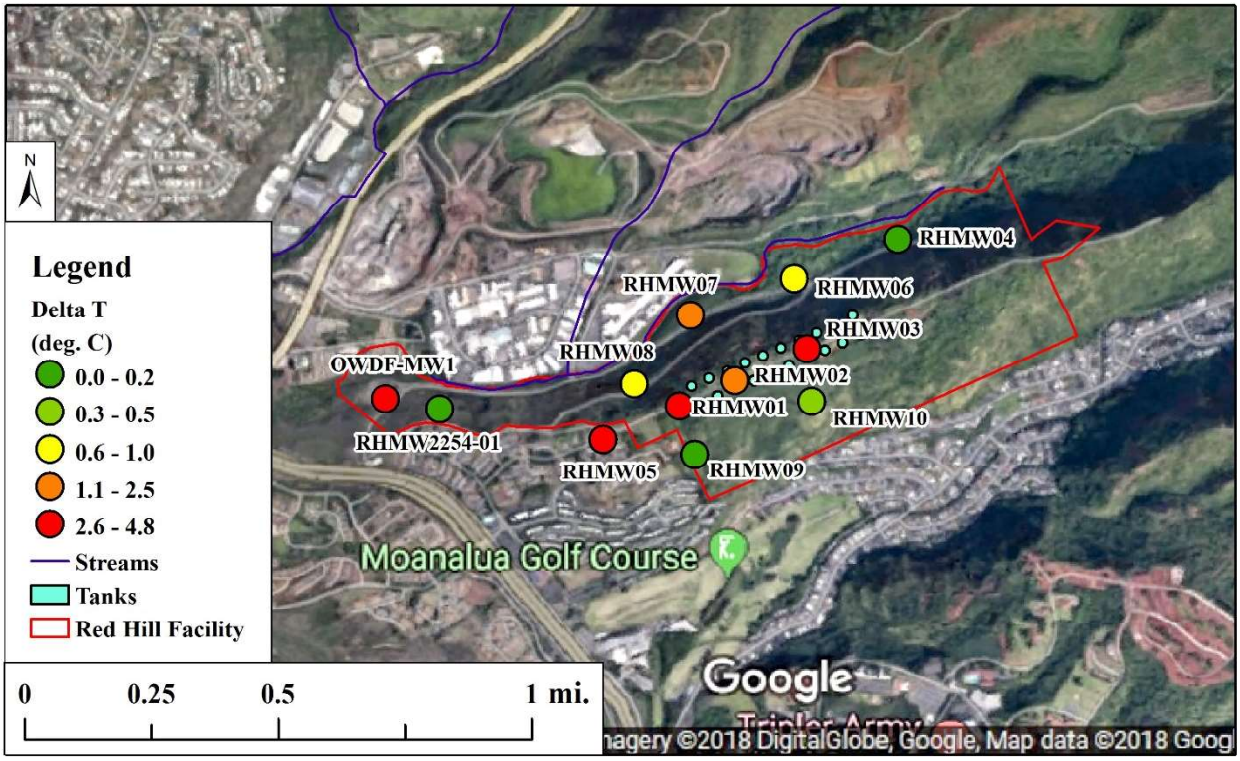

Figure 10.1 Net average temperature greater than the Red Hill Shaft (RHMW2254-01; in degrees Celsius). Like other MNA-related parameters, the elevated temperatures are generally along the Red Hill Ridge and to the west and north. Data source: USGS Synoptic Data, 2018.

The in situ vapor probe response around Tank 5 in the timeframe following the 2014 release can be interpreted as indicating that the primary vapor migration may have been to the northwest side of that tank and not in the direction of RHMW02 (see Figure 10.2 below). Actual LNAPL transport outcomes beneath Tank 5 in 2014 below the vapor probes is unknown; the conservative assumption based on this limited data is that transport was potentially to the northwest and is not represented with any certainty by the spatially limited monitoring well array.

In terms of the depth of migration of LNAPL from the Tank 5 release in 2014, the primary analysis relied upon in the CSM is the thermal profile at RHMW02, with backup support from chemistry considerations. A net positive temperature profile indicates the effects of exothermic biologic reactions and is affected by a variety of subsurface factors. In general, that relationship can be useful to infer lateral distributions of LNAPL biodegradation (e.g., Figure 10.1 above) but is highly uncertain with respect to the LNAPL vertical distribution. In many cases, as shown in the example thermal profile in our August 15, 2018 presentation (Slide 28), the LNAPL vertical mass distribution cannot be inferred from the temperature profile. A review of data in the 2007 Red Hill investigation report (DON, 2007) shows that the rock cores were evaluated for evidence of petroleum contamination by checking for odor and by screening with a photo-ionization detector. No evidence of petroleum contamination was found. The groundwater temperature in RHMW03 measured during sampling has remained unchanged at about 26.5 ^{o}C since first sampled in 2005 to the present, indicating that the temperature profile recently measured by the Navy likely existed when RHMW03 was first drilled. As a consequence, this locally-elevated temperature does not directly relate to the migration or distribution of LNAPL arising from the 2014 release but

relates (at least, predominantly) to past releases. Also, there has been no release of consequence since 2005 that would cause LNAPL to enter the zone indicated by the thermal anomaly in RHMW03. In summary, the Navy's contention that the thermal profiles in the tunnel wells show that the LNAPL is constrained above the water table is not supported by the available data. We believe the Navy technical team needs additional data to validate its interpretation of LNAPL transport around Tank 5 from the 2014 release, as it is a fundamental cornerstone to the remainder of the LNAPL F&T considerations. At a minimum, the Navy should include several Hawai'i or equivalent geology examples where the LNAPL source distribution has been definitively interpreted by this method and independently validated through subsurface data demonstrating that actual LNAPL source distribution (e.g., core sampling, downhole investigation, etc.). Alternatively, it would be useful to consider a site specific data collection program to verify the LNAPL source distribution around Tank 5 and possibly other key locations. By whatever approach, additional lines of evidence are needed to verify the assumptions relative to fate and transport of the 2014 release.

Lastly, CoC concentrations in groundwater at RHMW02 (and occasionally other locations) have been within the expected solubility ranges for jet, diesel and other fuels stored at the facility, suggesting that LNAPL may be in direct contact with the aquifer system somewhere in the vicinity. Robert Whittier, currently at DOH, visually observed LNAPL blebs at RHMW02 when this well was sampled using a bailer in 2009, indicating residual LNAPL in the vicinity of this well. Further indicating that LNAPL reached groundwater, was the distinct increase in several CoCs at this location immediately following the 2014 release that can be interpreted as a breakthrough curve (Figure 10.3). While the Navy Team's interpretation is of simple coincident data scatter, these data could be interpreted as a new arrival of LNAPL to groundwater in the general vicinity of RHMW02 in the timeframe associated with that release. The CSM would benefit from examining these potential viable working hypotheses, though it is acknowledged that this is a spatially sparse data set.

This alternate interpretation of LANPL reaching the groundwater table following the 2014 release is consistent with site data and transport processes. The chemical analyte ratio methods used in the CSM to suggest otherwise are unbounded by site specific data of fuel compositional variability and analyte transformations. Further, we believe where chemical ratios use TPHd values, those values should also consider the native totals (without silica gel cleanup) because the parent hydrocarbons are predominantly derived from the original petroleum source(s). We also recognize the value of having both native and silica gel cleanup values for interpretation for various aspects of this investigation such as biodegradation and attenuation.

Lastly, the current deployment design for the in-situ sampling pumps below the water table within the existing monitoring wells precludes the sampling of LNAPL or any direct observation of an LNAPL plume, if present. Such measurements could however be accomplished in these wells periodically either by resetting these pumps or removing them to allow direct sampling of the top of the water table.

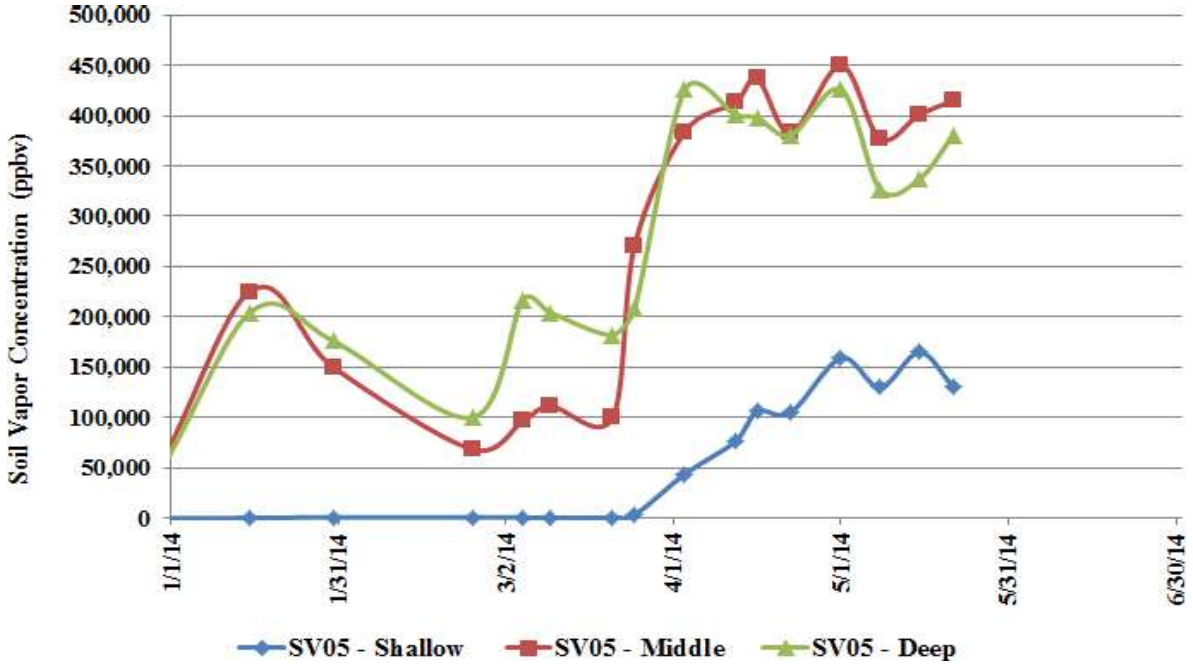

Figure 10.2 Soil vapor probe readings beneath Tank 5 following the January 2014 release. The deep probe is toward the outside of the tank corridor and the shallow probe closest to the tunnel. These data can be interpreted as initial release migration to the northwest of this Tank; note the shallow probe has low level detections that are not visible on a linear plot.

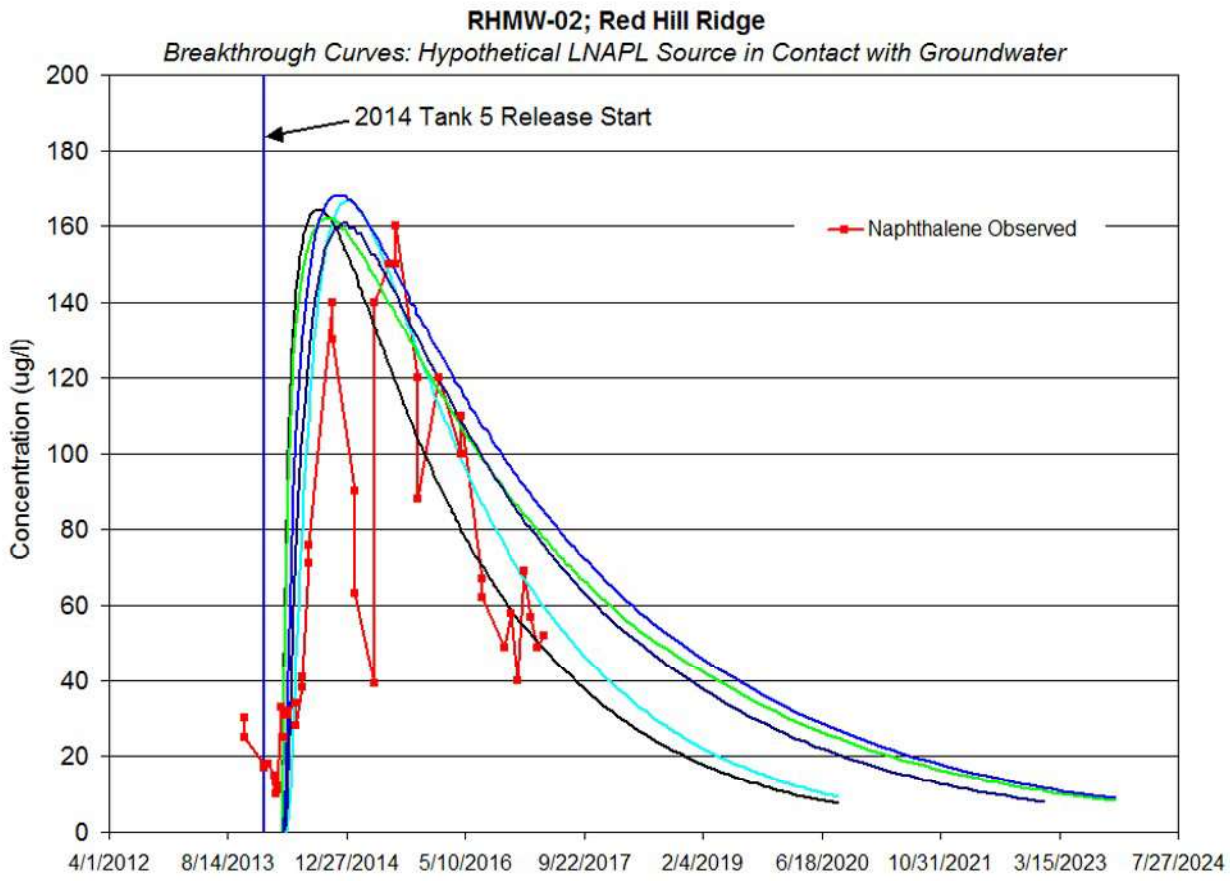

Figure 10.3 Observed naphthalene concentrations following the 2014 Tank 5 release and a family of conceptual contaminant transport breakthrough curves matching those data. Other interpretations are viable, as is the possibility of LANPL contacting groundwater near RHMW02 following that release.

References

Department of the Navy (DON), 2007. *Red Hill Bulk Fuel Storage Facility Final Technical Report, Pearl Harbor, Hawaii*. 12 Prepared by TEC Inc., Honolulu, HI. Pearl Harbor, HI: Naval Facilities Engineering Command, 13 Pacific. August

ATTACHMENT 5

Presentation Slideshow from August 2018

Comments on TUA Deliverables Red Hill Bulk Fuel Storage Are Oahu, Hawaii

Prepared for GWMG Meeting by:

Gary Beckett, Aquiver
Donald Thomas, SOEST
Matthew Tonkin, SSP&A
Robert Whittier, DOH

August 14, 2018

Overview

- Review summary
- Top ten (10) technical comments on TUA reports:
  - Ranked in consideration of priority, likely ease of reconciliation
  - Basis of difference identified
  - Basis of need to resolve comment
- Proposed path forward:
  - Anticipated approach and effort to resolve comment
- Discussion and illustration slides on each comment

Review Summary

Groundwater Protection and Evaluation Considerations for the Red Hill Bulk Fuel Storage Facility

- Organized deliverable reflecting the work presented previously
- Able to execute most sets of model files with minimal differences from received outputs (version check)
- Model provides foundation for final deliverables, with some refinements recommended here
- Presented path-line results are properly cast as “frequencies” or perhaps sensitivities, not probabilities due to lack of p(prior
  - Some caution also needed on variable grids

Conceptual Site Model, Investigation and Remediation of Releases and Groundwater Protection and Evaluation

- Large volume of high-quality data has been collected that was not previously available to characterize the site
- A great deal learned over the last 18-24 months from these data
- CSM report provides comprehensive documentation of most features and processes at the site, and much of the supporting data
- Some data that are used to support some conclusions don't seem to be presented clearly or comprehensively
- Some assumptions in the CSM may lead to difficulty simulating measured gradients and flowpaths

Top Ten Comments

Comment	Interpretive Difference	Basis of Need
1. Basalt strike-and-dip	• Direction and magnitude in question	• Flow paths, transport
2. Saprolite extents	• Modeled and measured depths up/down valley	• Flow paths, transport, calibration
3. Cap rock, tuffs, sediments	• Feature in CSM but not in interim model	• Flow paths, transport, calibration
4. Preferential pathways	• Incorporation / consideration unclear	• Flow paths, transport
5. Tunnel inflows	• Data reflecting heterogeneity	• Model corroboration
6. Calibration – heads, gradients	• Near-field directions and magnitudes	• Model corroboration
7. LNAPL F&T – vapor data	• Rapid heterogeneous transport vs CSM	• Predictive fate, transport
8. LNAPL F&T – temperature	• Temperature data do not constrain extent	• LNAPL fate, basalts capacity
9. Groundwater data	• Some data contradict CSM and flow paths	• Fate-and-transport
10. Coastal marine discharge	• Chosen boundary conditions may reduce model sensitivity to parameter changes	• Predictive reliability

Comment	Proposed Path Forward	Data Gap	Effort
1. Basalt strike-and-dip	• Collaborative SME review of available dip & strike data • Corresponding "base" model update	Unlikely	Moderate
2. Saprolite extents	• Collaborative SME review of geophysics and CSM • Targeted seismic ground-truthing • Corresponding "base" model update	Unlikely	Moderate
3. Cap rock, tuffs, sediments	• Collaborative SME review of CSM • Corresponding "base" model update	Partially	Small
4. Preferential pathways	• Suitable acknowledgement • Collaborative SME plan for representation in final F&T models	Yes*	Small
5. Tunnel inflows	• Model testing with predictive sensitivity analysis	Unlikely	Small
6. Calibration – heads, gradients	• Review of calibration following CSM revisions if made	Partially	Moderate
7. LNAPL F&T – vapor data	• Evaluation in context of 2014 and earlier releases • Constituent-specific sampling vs PID (release detection)	Unlikely	Moderate
8. LNAPL F&T – temperature	• Suitable acknowledgement • Evaluation of plausible alternative interpretations	Partially	Small
9. Groundwater data	• Comprehensive tabulation of COC data with qualifiers • Expanded interpretative analysis of NAP/TEA	Yes	Moderate
10. Coastal marine discharge	• Collaborative SME review of available boundary conditions	Partially	Moderate

Discussion of Comments

1. Strike and Dip

- Geo-statistics "maximum"
- Local Red Hill ridge alignment (topographic)
- Geo-statistics "typical"(similar to regional Red Hill ridge alignment)
- Geo-statistics "minimum"
- Proposed in TUA CSM

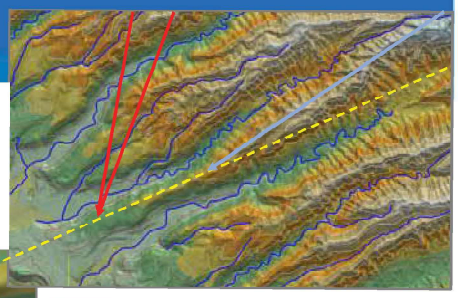

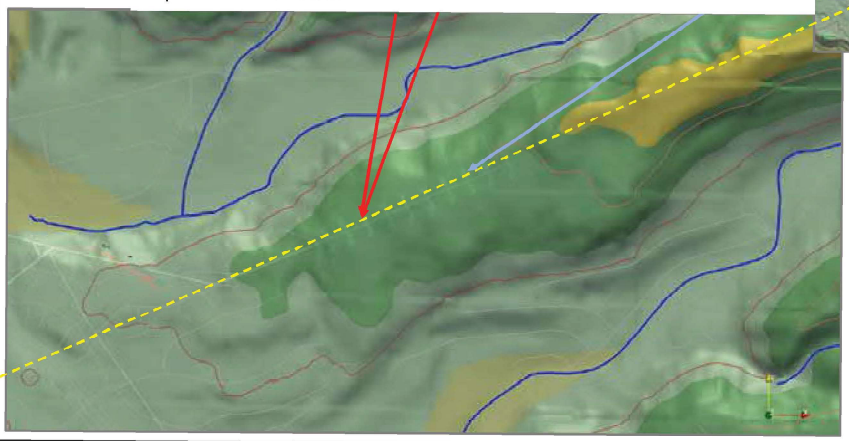

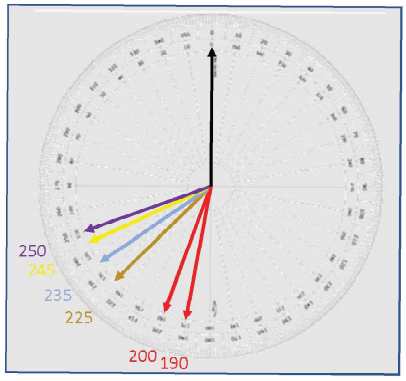

1. Strike and Dip

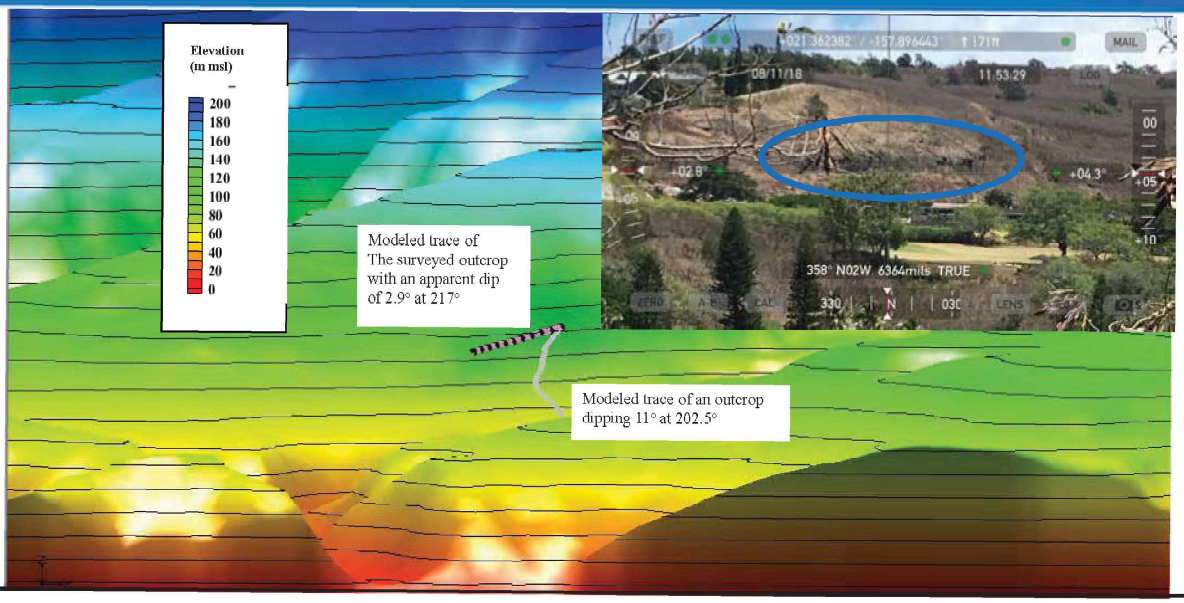

1. Strike and Dip

- Rudimentary tests - paths sensitive to assumed direction, magnitude
- Thorough testing or sensitivity analysis requires grid-realignment or full conductance tensor

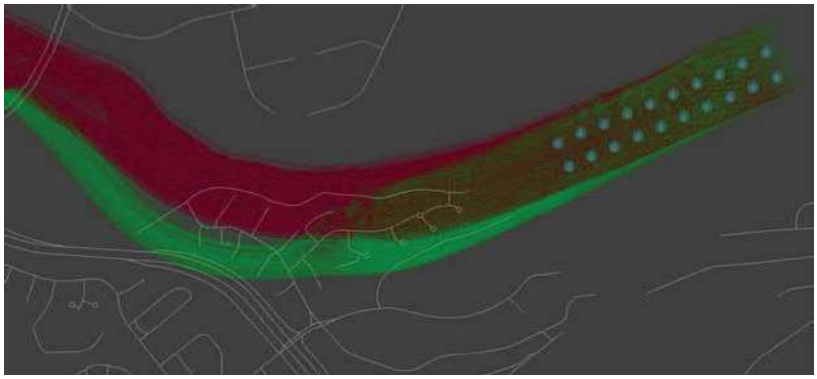

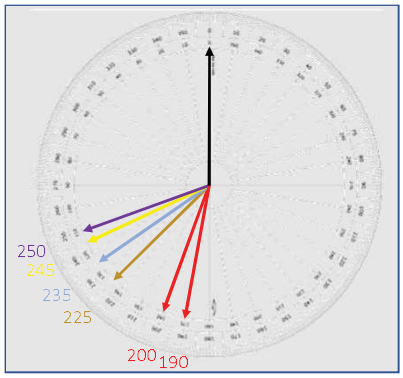

2. Saprolite Extents

- *"Key reflectors include the base of alluvium or top of saprolite, top of water saturated (possibly perched) sediments, and the contact between weathered basalt (saprolite) and unweathered basalt.*
- *Valley fill sediments are constrained to the upper 60 ft below land surface in all three valleys.*
- *Saturated and/or competent saprolite are mapped from surface to hundreds of feet bgs."*

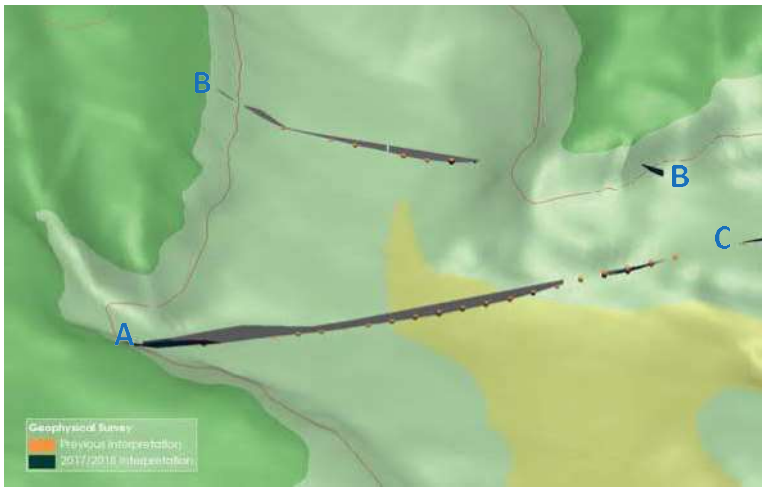

2. Saprolite Extents

- Valley alluvium thickness
- Systematic pattern of modeled saprolite depth
- Early termination of longitudinal extents of saprolite
- Layer elevations based on prior interpretations may require revision to accurately represent conditions

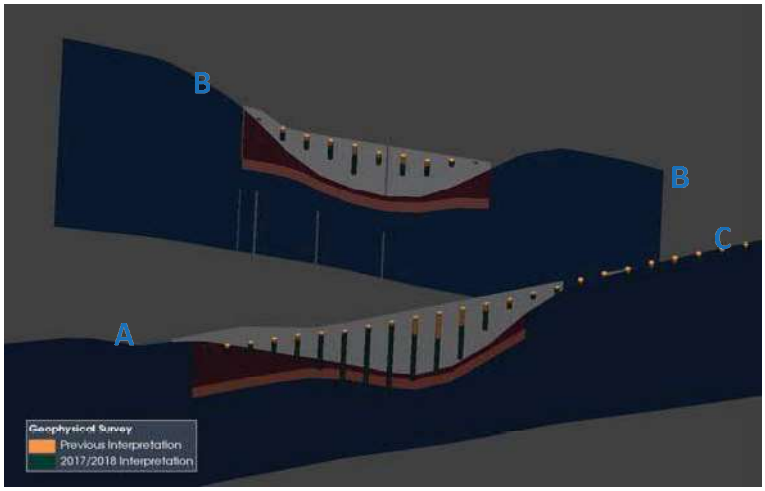

2. Saprolite Extents

- HDMW2253-03 as Ground-truth
  - Can we definitively define the saprolite/basalt interface from available data?
    - Geo-logs
    - Well construction
    - Water level in the HDMW Chase Tube
    - Groundwater elevation vs. RHMW11 Zone 7

2. Saprolite Extents

Halawa Deep Monitor Well No. 2253-05 03
Geologic Log by Glenn Bauer

Depth (ft.)	Description
0-50	Very weathered gray, tan, and red rock; cuttings are rounded and angular
50-70	Same as above, however cuttings are redder and clay present
70-80	Weathered tan cuttings, some of the vesicles lined with Mn
80-100	Weathered reddish-brown friable cuttings
100-110	Same as above, though cuttings are redder
110-130	Weathered tan cuttings
130-140	Weathered red cuttings with clay
140-150	Weathered light brown cuttings
150-170	Weathered brown aa basalt with angular vesicles some coated with Mn
170-180	Weathered dense brown, tan, and gray cuttings
180-190	Mixture of weathered brown pahoehoe and aa basalt
190-210	Weathered gray aa basalt
210-230	Friable brown-gray aa basalt
230-250	Mixture of weathered aa and pahoehoe basalt; some of the pahoehoe has secondary minerals in the vesicles.
250-260	Weathered pahoehoe basalt with secondary minerals in the vesicles
260-270	Mixture of light gray and dark gray aa basalt with a few tachylitic cuttings present
270-280	Weathered gray aa basalt with tachylite
280-290	Dense light gray aa basalt
290-300	Mixture of dense non-vesicular light gray and dark gray aa basalt
300-310	Mixture of weathered gray pahoehoe and non-vesicular aa basalt
310-320	Dense dark gray non-vesicular aa basalt
320-340	Mixture of light and dark gray pahoehoe and aa basalt
340-350	Slightly weathered reddish brown pahoehoe basalt with many small round vesicles

~-5 ft msl

Saprolite/Basalt Interface?

~-55 ft msl

17

- Chase tube either at base of saprolite or 50 feet above base of saprolite.
- Groundwater elevation in the chase is only slightly above that of RHMW06.
- Compare to RHMW11 Zone 7 where groundwater elevation is about 50 ft. above that in RHMW06.

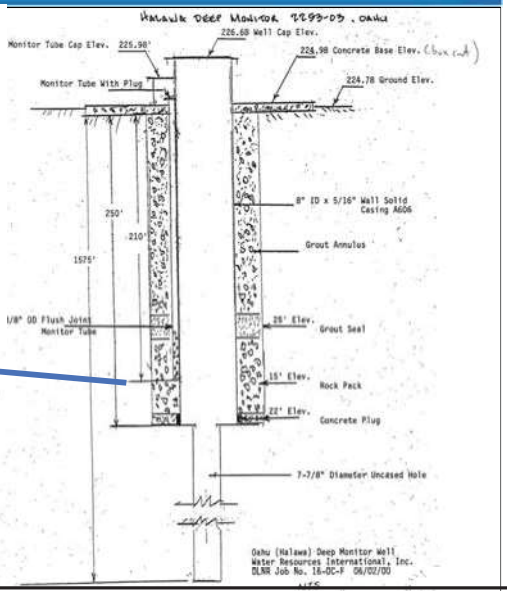

3. Cap Rock, Tuffs, Sediments

- Documented presence of tuffs and low-conductivity sediments
- Valley saprolites may "key-in" to these lower-conductivity sediments
- Resulting hydro-stratigraphic system may alter flow patterns as far up as Red Hill

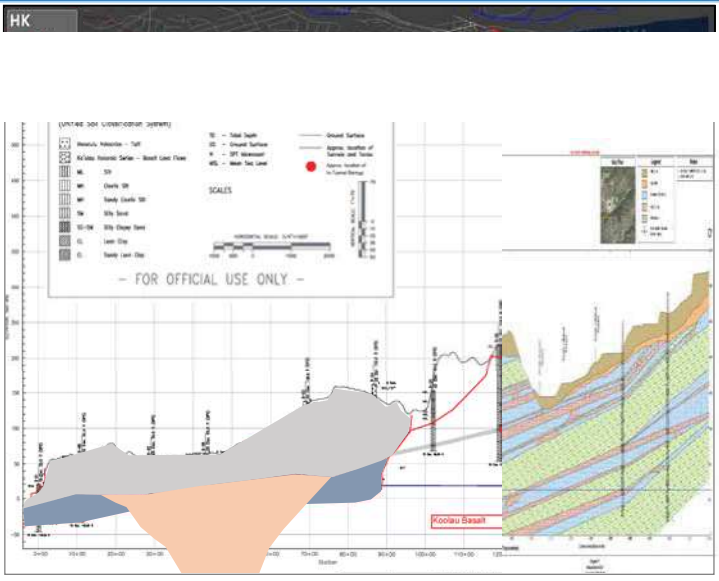

9/11/2018

3. Cap Rock, Tuffs, Sediments

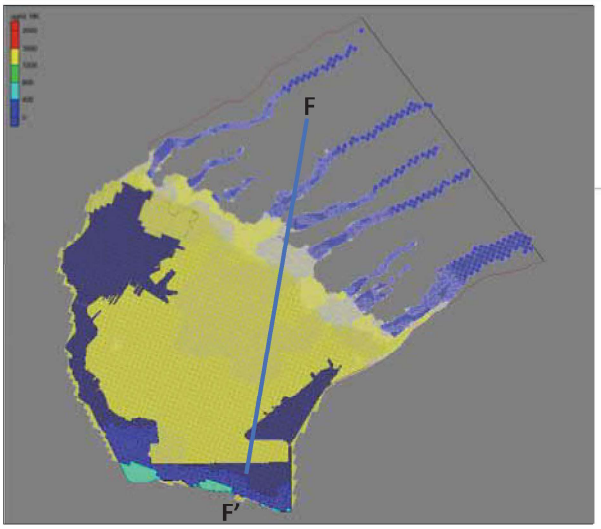

- &Model appears to lack the confining nature of older alluvium.
- &Expect bulk hydraulic conductivity of the caprock to be <<1,000 ft/d

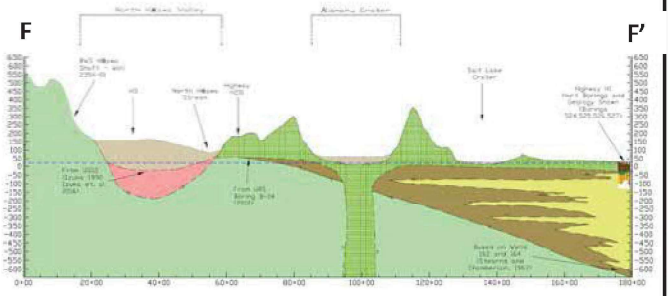

Figure 5-9 CSM

3. Cap Rock, Tuffs, Sediments

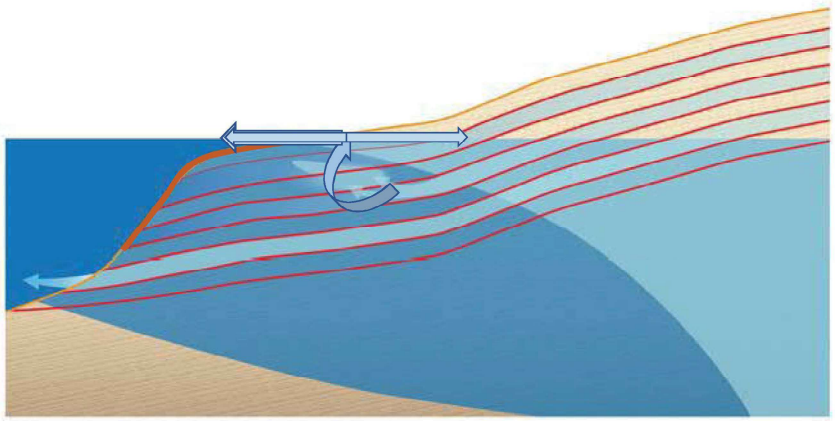

4. Preferential Pathways

Source: Iris Vanderzander, 2018

Source: Matt Tonkin, 2018

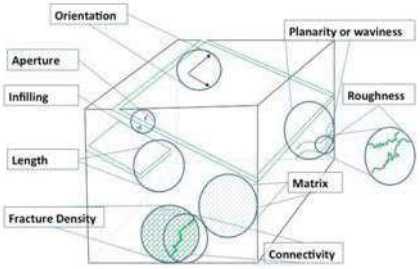

Source: ITRC, 2017

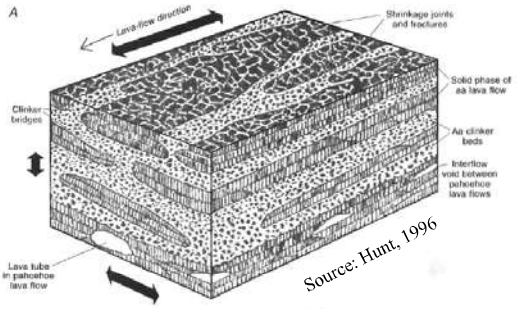

Source: Hunt, 1996

4. Preferential Pathways

- Thirteen of twenty tank barrel-log sets intercepted at least one lava tube:
  - Other areas of broken rock may represent collapsed lava tubes
- Connectivity, role in flow and transport, are uncertain

Table 6-2: RHMW11 Hydraulic Conductivity Estimates Derived from Pneumatic Testing and Laboratory Analyses

Slug Test Zone	K (Hvorslev 1951)		K (Bouwer & Rice 1976)		K (Cooper et al. 1967)		Date	Zone Geology / Feature
	ft/d	cm/sec	ft/d	cm/sec	ft/d	cm/sec		
Zone 8	9.2E-02	3.2E-05	1.0E-01	3.5E-05	7.1E-02	2.5E-05	12/13/2017	Saprolite
Zone 7	1.2E-01	4.2E-05	1.3E-01	4.6E-05	1.1E-01	3.8E-05	12/9/2017	Saprolitic clinker zone
Zone 7	2.6E-01	9.2E-05	2.8E-01	9.9E-05	2.7E-01	9.7E-05	12/11/2017	Saprolitic clinker zone
Zone 6	3.4E-01	1.2E-04	2.8E-01	9.9E-05	1.7E-01	6.0E-05	12/7/2017	Saprolite
Zone 5	—	—	—	—	—	—	—	Lava tube
Zone 4	—	—	—	—	—	—	—	Pāhoehoe
Zone 3	—	—	—	—	—	—	—	Pāhoehoe
Zone 2	—	—	—	—	—	—	—	Clinker zone
Zone 1	—	—	—	—	—	—	—	Clinker zone

5. Tunnel Inflows

redacted: Navy infrastructure

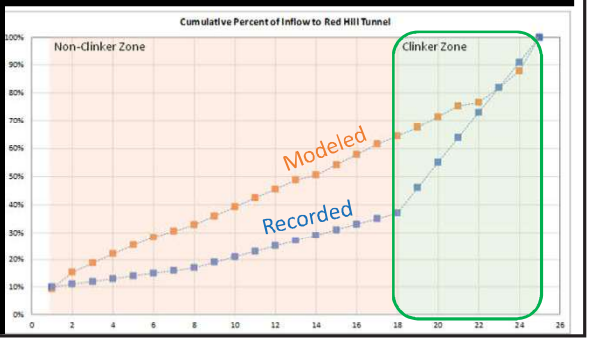

6. Calibration – Heads, Gradients

- Historic manual data infrequent, irregular
- Synoptic data improve CSM
  - Time-weighting
- Absolute head *vs.* gradients
- Systematic difference

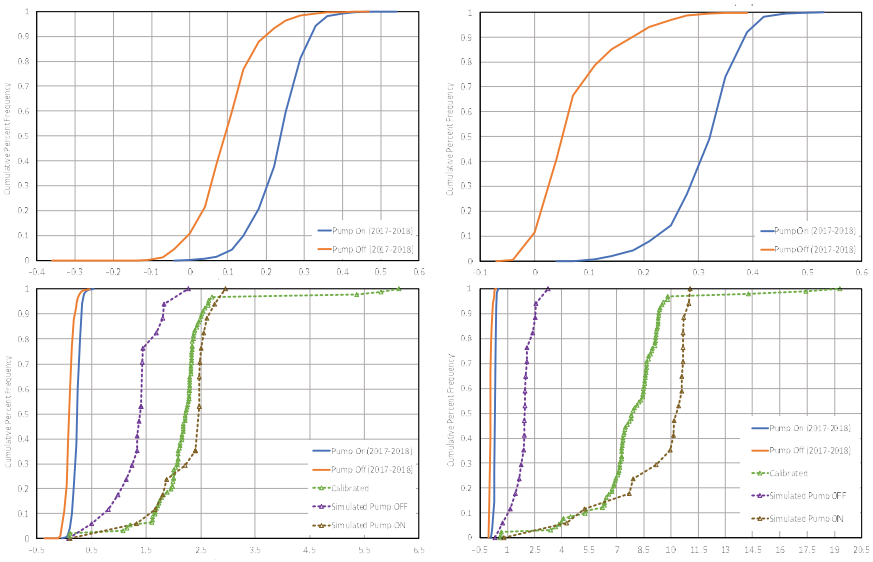

7. LNAPL F&T - Vapor Data

- Schematic of general vapor probe layout
- Angle boring, with deepest vapor port furthest from tunnel

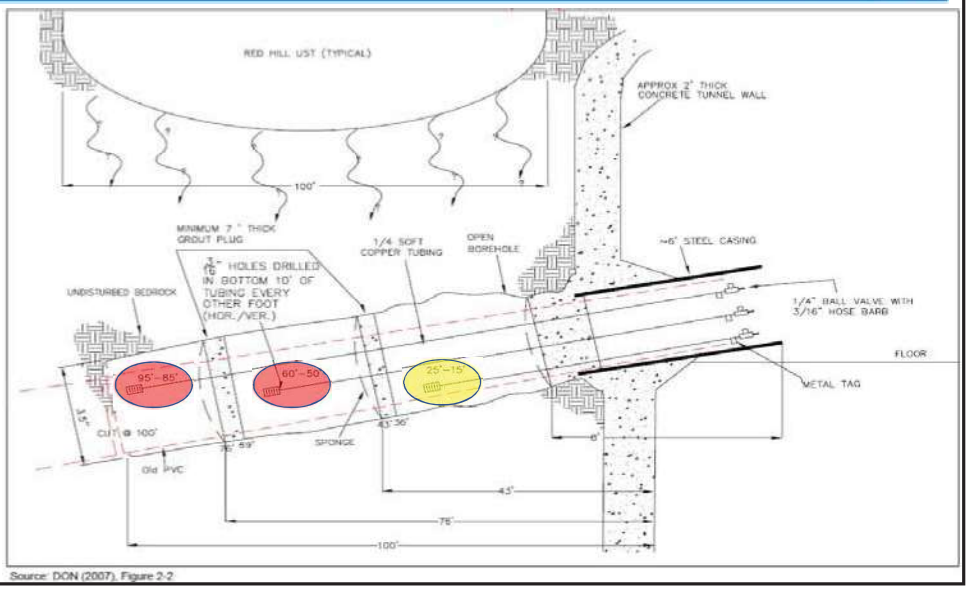

Source: DON (2007), Figure 2-2

7. LNAPL F&T - Vapor Data

- RHMW05 vapor behavior following 2014 release
- Shallow (interior) port slowest to respond, and response damped

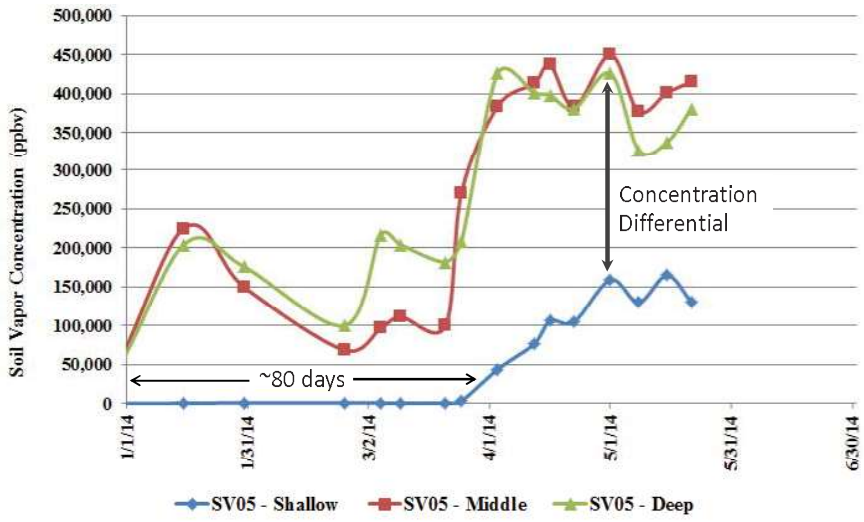

8. LNAPL F&T – Temperature

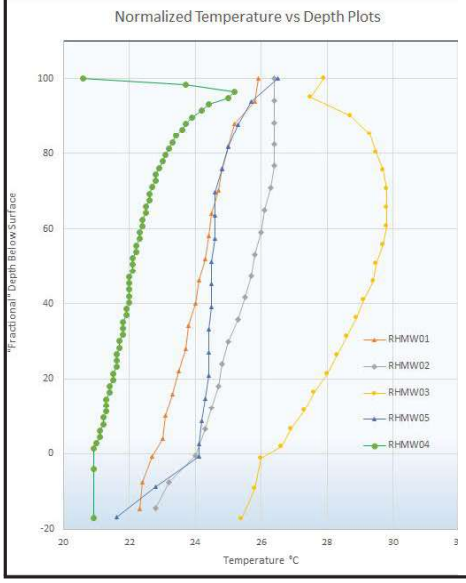

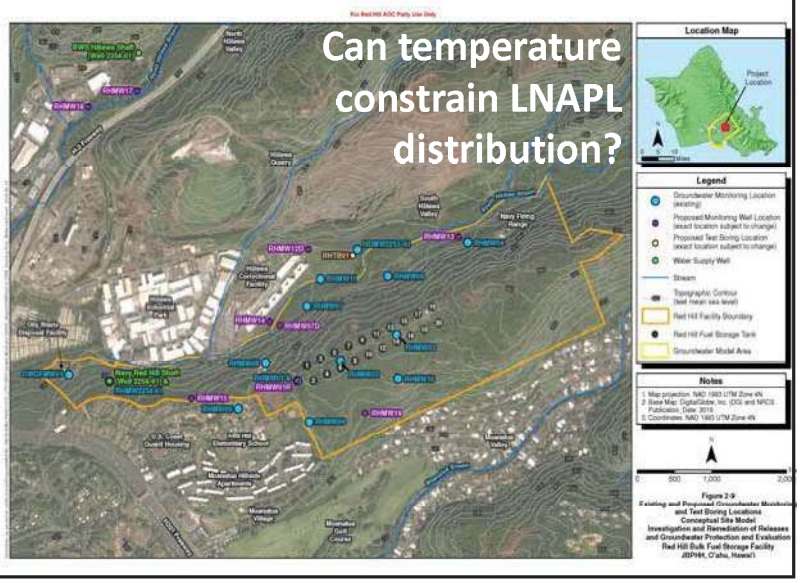

8. LNAPL F&T – Temperature

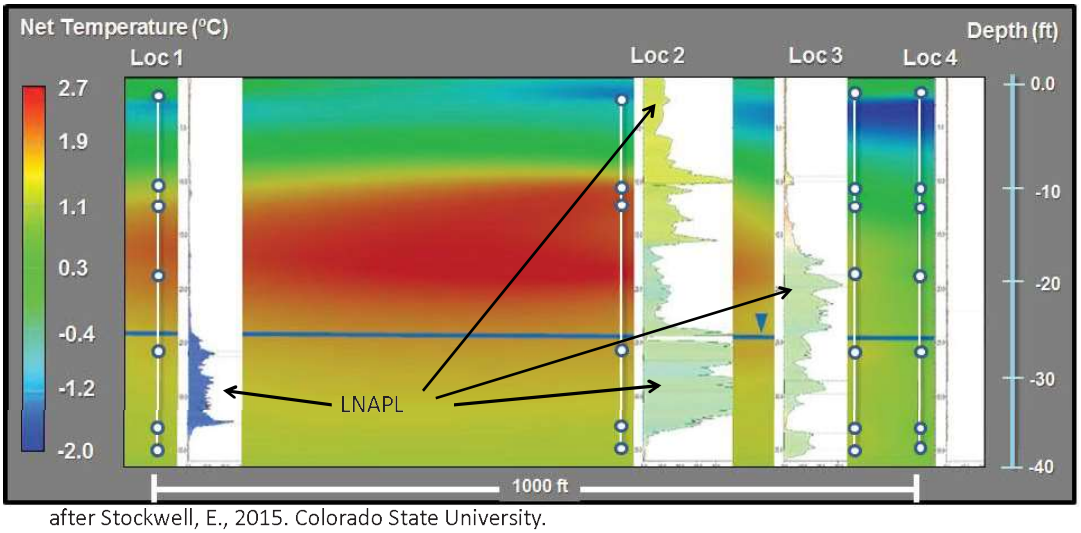

after Stockwell, E., 2015. Colorado State University.

8. LNAPL F&T – Example Animations

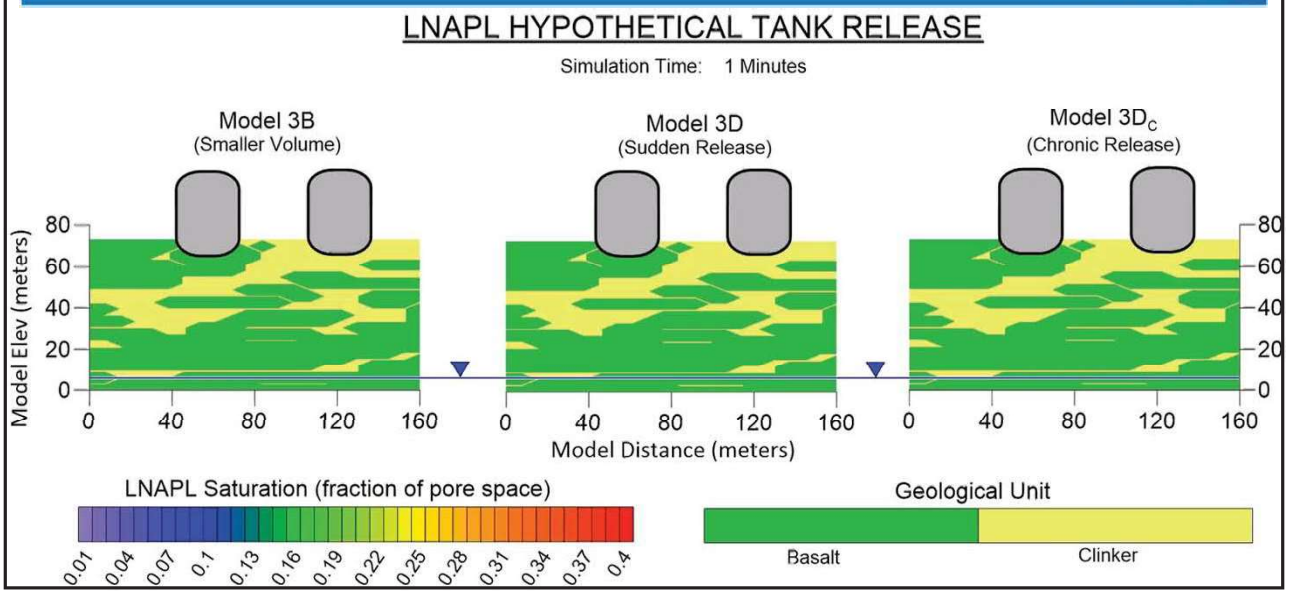

9. Groundwater Data

Distal detections at of TPH

(even recognizing some data should be qualified)

9. Groundwater Data

- Natural attenuation parameters describe a plume shadow:
  - Example shown is depleted O_2

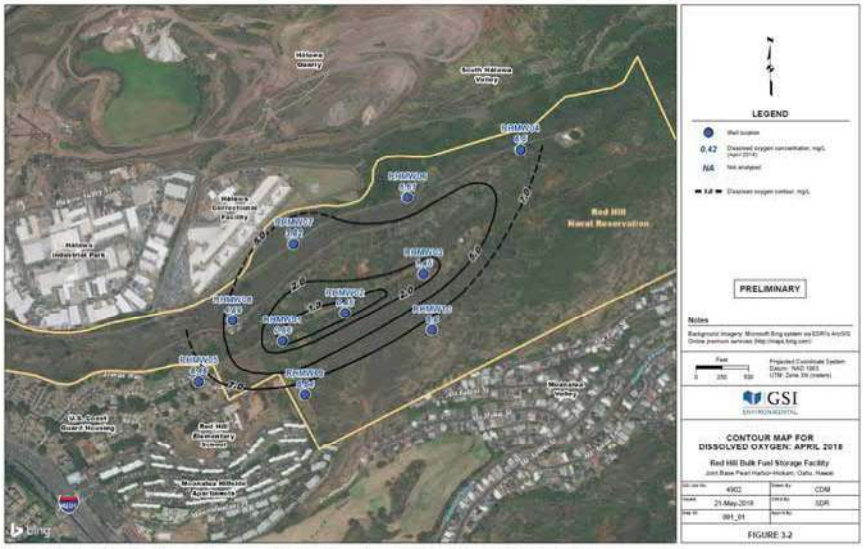

Figure 3-2: Contour Plot of O_2 Concentrations from the Facility Groundwater Monitoring Network (April 23–25, 2018)

9. Groundwater Data

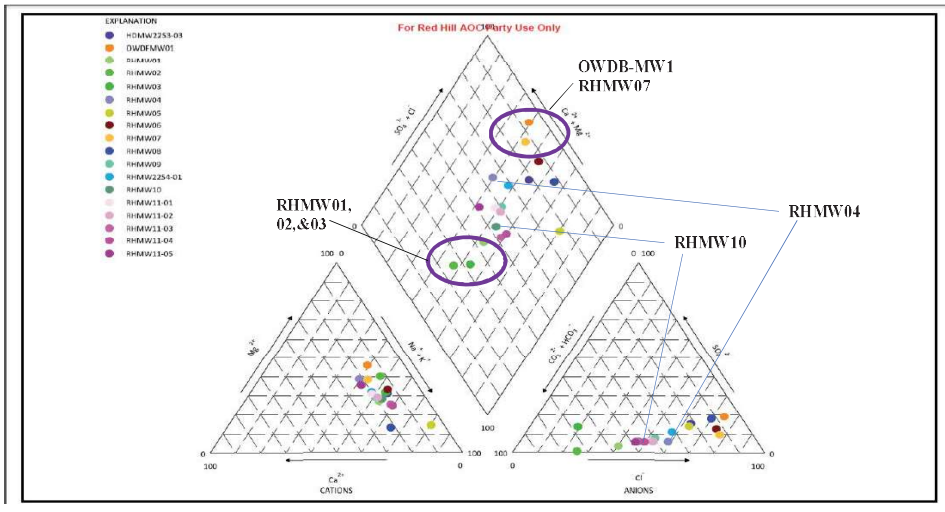

- Does the chemistry data show a flow path?
  - A potential mixing lines exists
  - However problems with spatial distribution
  - Possible more indicative of waters with contrasting chemistry

9. Groundwater Data

Chemistry shows indication of a poorly mixed system

- Chloride conc. vary from ~40->1000 mg/L
- Southeast very different from northwest
- Northwest chlorides still highly variable
- A large flux of groundwater down the Red Hill ridge should show better mixing

10. Coastal/Submarine Discharge

- Combination of high caprock K, GHB, and Pearl Harbor Embayment
- Likely results in model directing GW Flow into NE Pearl Harbor

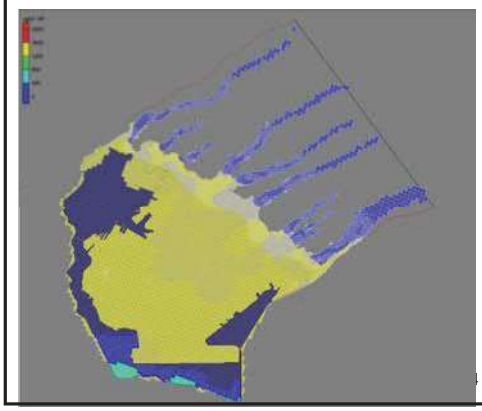

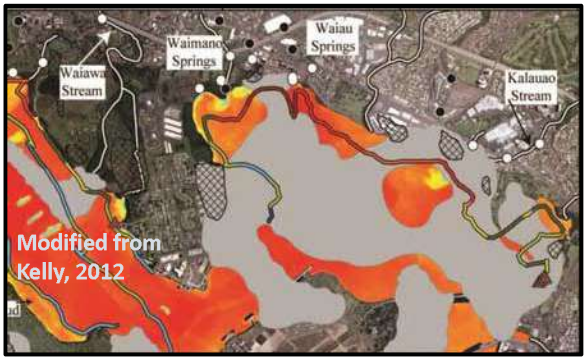

- Temperature (coolers colors indicate GW Flow) and
- Radon lines (red indicates GW Flow)
- Indicate little GW discharge into NE Pearl Harbor.

This page intentionally left blank

Regulatory Concerns with the CSM, Groundwater Flow Model, and Contaminant Fate and Transport Work and Navy Responses

Regulatory Concern [a]	Navy Response
Predominant strike and dip of basalt in the geologic model	The AOC Parties agreed upon 213.6 degrees as the dip azimuth and 2.9 degrees for the dip magnitude. This orientation has been incorporated into the new flow model grid.
Saprolite extent in the interim model vs. depths inferred by seismic profiling	A 3D geologic framework model was developed that describes the lateral and vertical extent of saprolite (as well as caprock, marine sediments, tuffs, and basalt) in the vicinity of Red Hill. This model is based on (a) the seismic study conducted by Boise State (DON 2018b), (b) previous geologic studies in the area, and (c) interpretation of boring logs from key well locations within the area. Two bounding interpretations of the Hālawa Deep Monitor Well (HDMW2253-03) boring log for the saprolite/basalt interface are presented here: (1) an upper bound interpretation of -5 ft msl and (2) a lower bound interpretation of -55 ft msl. The location where the surface of each saprolite/basalt interface would cross or intersect the air/groundwater interface (piezometric surface) of the regional basal aquifer in South Hālawa Valley was extrapolated by projecting the base of saprolite up-valley using a 3% slope, which is based on the Oki (2005) estimated projection for base of valley fill/saprolite in nearby valleys including North Hālawa and Waimalu Valleys.
Preferential pathways	The Navy recognizes that there are potential preferential pathways that can affect groundwater and contaminant flow at Red Hill. Regarding lava tubes, various evaluations conducted by the Navy and presented to the Regulatory Agencies demonstrated that it is highly unlikely that a lava tube could provide a complete preferential pathway between the Red Hill Facility and Hālawa Shaft. Per EPA recommendations, a random walk model was used to evaluate the potential for lava tubes to act as a preferential pathway between the tank farm and Red Hill Shaft. This analysis indicates that it is very unlikely that a lava tube preferential pathway exists between the tank farm and Red Hill Shaft. A sensitivity study as part of the interim modeling effort simulated a clinker zone beneath Red Hill to further evaluate preferential pathways related to highly permeable zones that could potentially impact Red Hill Shaft (and other areas). This type of approach will continue for the ongoing modeling efforts.
Representation of caprock, tuffs, and sediments	The Navy's 3D geologic model of the Red Hill area incorporates tuffs (associated with the Honolulu Volcanic Series), basalt, marine sediments, caprock, and saprolite. Interpretation of the marine limestone caprock geometry was based largely on borings from Stearns and Chamberlain (1967). The extent of ash deposits was based on a paper by Pankiwskyj (1972) as well as data from HART rail borings (HART 2014). The tuff cone vents were interpreted based on academic research papers on other similar Honolulu Volcanic Series tuff cones (Wentworth 1938) as well as tuff cones outside of Hawai'i (Sohn and Park 2005; White and Ross 2011). Marine sediments and tuffs will be modeled as separate zones as part of the ongoing modeling effort.
Drinking water shaft inflows	The Navy has evaluated conceptualization of the Red Hill and Hālawa water development tunnels for both the CSM and the ongoing groundwater modeling work. For the CSM, multiple analytical solutions were evaluated to define aquifer hydraulic properties for key synoptic monitoring periods. For these solutions, the location of the sink term was fixed, and was conceptualized as the last 200 feet of the Red Hill water development tunnel. This corresponds with the highest-producing portion of the tunnel as reported during construction (Stearns 1943). For the preliminary transfer function-noise (TFN) analysis, the residual was calculated using the analytical element software TTim (Bakker 2013), and it was inferior to the residual calculated allowing the development of an empirical solution, which resembled a leaky-confined aquifer solution as described by Hantush (1956). The current TFN analysis relied on an optimization process that did not include a fixed position for the water tunnels. The interim groundwater flow model results were insensitive to variability in the location of drinking water shaft inflows. For the current groundwater flow model, drinking water shaft inflows in the are represented using a connected linear feature (CLN) module. Variability in hydraulic conductivity along the length of that feature is being evaluated using various skin factors.

Regulatory Concern [a]	Navy Response
Calibration to groundwater heads and gradients	Previous groundwater models of the Red Hill area provided a wide range of water level gradients. Some of these groundwater contour maps and associated gradients were limited by sparse data sets and uncertain water level elevations due to measuring point accuracy issues. The Navy has conducted a Second Order, Class I survey to reduce uncertainty related to measuring point elevation accuracy (DON 2018a, 2018c). Interim modeling work used these older data sets, and calibration of the interim model was driven by, and potentially limited by, those data. However, calibration of the interim model was improved when a conceptual clinker zone was added to the model domain in the vicinity of Red Hill, suggesting that high hydraulic conductivity in localized zones contributed to flat gradients and variable orientations. The Navy, in cooperation with the USGS, has conducted a detailed synoptic survey of water levels with high data collection frequency to better evaluate groundwater levels under a wide range of pumping and non-pumping conditions. These more recently collected data, coupled with higher-resolution measuring point elevations at wells, have been used to produce a dense, long-term data set for evaluation of groundwater elevation conditions in the CSM. Using the recent synoptic data, a TFN analysis was used to develop well-specific step and impulse response functions, which will be used for ongoing groundwater flow model calibration.
Coastal marine boundary and discharge	The Navy has updated conceptualization of regional and local geologic features for both the CSM and the ongoing groundwater modeling. The Navy is explicitly representing various features in the model and is allowing the existing groundwater elevation data and defined ranges of aquifer properties to improve calibration of the model. The ranges of aquifer properties are either measured or based on literature values and will be allowed to vary during Parameter Estimation (PEST) simulations to define a range or realizations. A key update to the ongoing modeling is representation of the caprocks and tuffs associated with late-stage volcanic rejuvenation. Specific model layers and zones have been integrated into the model to account for and represent these features. Sensitivity to variability in the hydraulic properties of these features will be conducted using a multi-model approach.
Light Non-Aqueous Phase ("LNAPL") fate and transport	A simplified 3D LNAPL model has been developed by the Navy as part of an initial effort to help bound LNAPL flow in both the vadose zone and saturated zone related to potential future releases. This potential approach was presented to the AOC Parties (during a March 4, 2019 AOC Parties meeting). The Regulatory Agencies are currently developing a response, which the Navy will consider in determining if this LNAPL modeling effort goes forward.
Groundwater data	The Navy has evaluated all available groundwater quality data. In this regard, inorganic geochemistry data have been evaluated with consideration to MNA, DO, and TPH issues, and a multi-factor cluster analysis (as discussed and agreed to at the March 2019 AOC Parties Technical Meeting). All these analyses indicate that groundwater has been primarily impacted in the vicinity of RHMW02, with lesser impacts noted at RHMW01 and RHMW03. These analyses indicate that there is no indication of impacts from releases at Red Hill to outlying wells.
LNAPL and dissolved phase distribution	As previously stated and presented at AOC Party technical meetings, the Navy has thoroughly evaluated all groundwater quality data. As part of this analysis, jet fuel chemistry and TPH analyses were evaluated. In addition, COPC, non-COPC, and TIC water quality chemistry was thoroughly evaluated. As part of this analysis, the following conclusions are based on independent, multiple LOEs: 1) No evidence of LNAPL near outlying wells – 7 Primary LOEs 2) No evidence of impacts to the outlying wells from the 2014 release – 2 Primary LOEs 3) No evidence of LNAPL near Red Hill Shaft – 7 Primary LOEs 4) No evidence of groundwater impacts from the 2014 fuel release – 5 Primary LOEs The Navy has requested that the Regulatory Agencies provide a detailed response if they disagree.

[a] Source: EPA Region 9 and DOH (2018). The title used to describe each of the ten Regulatory concerns is the same as was provided in the reference. Additional details are provided in both the referenced letter, as well as attachments to that letter, for each of the Regulatory concerns.

3D three-dimensional
AOC Administrative Order on Consent
COPC chemical of potential concern
CSM conceptual site model
DO dissolved oxygen
ft foot/feet
LOE line of evidence
MNA monitored natural attenuation
msl mean sea level
TIC tentatively identified compound
USGS United States Geological Survey

References:

Bakker, M. 2013. "Semi-Analytic Modeling of Transient Multi-Layer Flow with TTim." *Hydrogeology Journal* 21 (4): 935–943.

Department of the Navy (DON). 2018a. *Well Elevation Survey Report, Red Hill Bulk Fuel Storage Facility, Joint Base Pearl Harbor-Hickam, O'ahu, Hawai'i; Revision 00*. Prepared by AECOM Technical Services, Inc., Honolulu, HI. Prepared for Defense Logistics Agency Energy, Fort Belvoir, VA, under Naval Facilities Engineering Command, Hawaii, JBPHH HI. January.

———. 2018b. *Seismic Profiling to Map Hydrostratigraphy in the Red Hill Area, Red Hill Bulk Fuel Storage Facility, Joint Base Pearl Harbor-Hickam, O'ahu, Hawai'i; March 30, 2018, Revision 00*. Prepared by Lee Liberty and James St. Claire, Boise State University, Boise, ID, for AECOM Technical Services, Inc., Honolulu, HI. Boise State University Technical Report BSU CGISS 18-01. Prepared for Defense Logistics Agency Energy, Fort Belvoir, VA, under Naval Facilities Engineering Command, Hawaii, JBPHH HI.

———. 2018c. *Well Elevation Surveys for Red Hill Monitoring Well RHMW11 and Navy 'Aiea Halawa Shaft 2255-032, Honolulu, O'ahu, Hawai'i*. Prepared by AECOM Technical Services, Inc., Honolulu, HI. Letter Report. Prepared for Naval Facilities Engineering Command, Hawaii, JBPHH HI. May.

Environmental Protection Agency, United States, Region 9; and Department of Health, State of Hawaii (EPA Region 9 and DOH). 2018. "Approval to Revise Schedule for Deliverables 6.3- Investigation and Remediation of Releases Report and 7.1.3. - Groundwater Flow Model Report of the Red Hill Administrative Order on Consent ('AOC') Statement of Work ('SOW') and Comments on Interim Environmental Reports." Letter from Omer Shalev, EPA Project Coordinator, and Roxanne Kwan, DOH Interim Project Coordinator, to: Captain Marc Delao, Navy Region Hawaii. October 29.

Hantush, M. S. 1956. "Analysis of Data from Pumping Tests in Leaky Aquifers." *Eos, Transactions American Geophysical Union* 37 (6): 702–714. https://doi.org/10.1029/TR037i006p00702.

Honolulu Authority for Rapid Transportation (HART). 2014. *Geotechnical Data Reports for Honolulu Rail Transit Project, 2014–2016*. Aloha Stadium Station, Pearl Highlands Station, Pearl Highlands Station, Ramp H2R2, Kalihi Station, Kapalama Station, Roadway Pavement from Halawa Drive to Dillingham Boulevard and TPSS #28, Aiea to Middle Street, Middle Street to Ala Moana Center, Pearl Harbor Naval Base Station, Lagoon Drive Station, Honolulu International Airport Station, Middle Street Station, City Center Section Utilities and Guideway, Airport Section Guideway - 7-Pier Construction. Prepared by: Anil Verma Associates, Inc.; Shannon & Wilson, Inc.; Yogi Kwong Engineers, LLC; and Geolabs, Inc.

Oki, D. S. 2005. *Numerical Simulation of the Effects of Low-Permeability Valley-Fill Barriers and the Redistribution of Ground-Water Withdrawals in the Pearl Harbor Area, Oahu, Hawaii*. Scientific Investigations Report 2005-5253. U.S. Geological Survey.

Pankiwskyj, K. A. 1972. "Geology of the Salt Lake Area, Oahu, Hawaii." *Pacific Science* 26 (2): 242–253.

Sohn, Y. K., and K. H. Park. 2005. "Composite Tuff Ring/Cone Complexes in Jeju Island, Korea: Possible Consequences of Substrate Collapse and Vent Migration." *Journal of Volcanology and Geothermal Research* 141: 157–175.

Stearns, H. T. 1943. "Letter from H. T. Stearns, Senior Geologist, U.S. Geological Survey, to: O. E. Meinzer, Division of Ground Water, U.S. Geological Survey, Washington, DC," January 18, 1943.

Stearns, H. T., and T. K. Chamberlain. 1967. "Deep Cores of Oahu, Hawaii and Their Bearing on the Geologic History of the Central Pacific Basin." *Pacific Science* 21 (2): 153–165.

Wentworth, C. K. 1938. *Geology and Ground Water Resources of the Palolo-Waialae District*. Honolulu, HI: Board of Water Supply.

White, J. D. L., and P. S. Ross. 2011. "Maar-Diatreme Volcanoes: A Review." *Journal of Volcanology and Geothermal Research* 201: 1–29.